

# *Transportation Issues and Resolutions – Compilation of Laboratory Transportation Work Package Reports*

---

## Fuel Cycle Research & Development

*Prepared for  
U.S. Department of Energy  
Used Fuel Disposition Campaign  
Compiled by Paul McConnell  
Sandia National Laboratories  
September 30, 2012  
FCRD-UFD-2012-000342*



**DISCLAIMER**

This information was prepared as an account of work sponsored by an agency of the U.S. Government. Neither the U.S. Government nor any agency thereof, nor any of their employees, makes any warranty, expressed or implied, or assumes any legal liability or responsibility for the accuracy, completeness, or usefulness, of any information, apparatus, product, or process disclosed, or represents that its use would not infringe privately owned rights. References herein to any specific commercial product, process, or service by trade name, trade mark, manufacturer, or otherwise, does not necessarily constitute or imply its endorsement, recommendation, or favoring by the U.S. Government or any agency thereof. The views and opinions of authors expressed herein do not necessarily state or reflect those of the U.S. Government or any agency thereof.

**Sandia National Laboratories**

Sandia National Laboratories is a multi-program laboratory managed and operated by Sandia Corporation, a wholly owned subsidiary of Lockheed Martin Corporation, for the U.S. Department of Energy's National Nuclear Security Administration under contract DE-AC04-94AL85000.

## FCT Quality Assurance Program Document

### Appendix E FCT Document Cover Sheet

Name/Title of Deliverable/Milestone  
Work Package Title and Number  
Work Package WBS Number  
Responsible Work Package Manager

Transportation Issues and Resolutions – Compilation of  
Laboratory Transportation Work Package Reports

ST Transportation – SNL / FT-12SN081305 (Rev. 1)

**1.02.08.13**

Paul McConnell

(Name/Signature) 

Date Submitted

Quality Rigor Level for Deliverable/Milestone	<input checked="" type="checkbox"/> QRL-3	<input type="checkbox"/> QRL-2	<input type="checkbox"/> QRL-1	<input type="checkbox"/> N/A*
			<input type="checkbox"/> Nuclear Data	

This deliverable was prepared in accordance with

Sandia National Laboratories

(Participant/National Laboratory Name)

QA program which meets the requirements of

DOE Order 414.1       NQA-1-2000

**This Deliverable was subjected to:**

Technical Review

Peer Review

**Technical Review (TR)**

**Peer Review (PR)**

**Review Documentation Provided**

**Review Documentation Provided**

Signed TR Report or,

Signed PR Report or,

Signed TR Concurrence Sheet or,

Signed PR Concurrence Sheet or,

Signature of TR Reviewer(s) below

Signature of PR Reviewer(s) below

**Name and Signature of Reviewers**

Doug Ammerman



\*Note: In some cases there may be a milestone where an item is being fabricated, maintenance is being performed on a facility, or a document is being issued through a formal document control process where it specifically calls out a formal review of the document. In these cases, documentation (e.g., inspection report, maintenance request, work planning package documentation or the documented review of the issued document through the document control process) of the completion of the activity along with the Document Cover Sheet is sufficient to demonstrate achieving the milestone. QRL for such milestones may be also be marked N/A in the work package provided the work package clearly specifies the requirement to use the Document Cover Sheet and provide supporting documentation.

## ACKNOWLEDGEMENTS

Several authors have contributed to this compilation of FY12 Transportation Work Package Reports: Z.H. Han, V.N. Shah, Y.Y. Liu, and M.C. Billone from Argonne National Laboratory; D. Keith Morton of Idaho National Laboratory; W.J. Marshall and J.C. Wagner of Oak Ridge National Laboratory; Steven J. Maheras, Ralph E. Best, Steven B. Ross, Erik A. Lahti, and David J. Richmond of Pacific Northwest National Laboratory, and D.R. Leduc of Savannah River National Laboratory. The compiler and author of the Sandia National Laboratories report acknowledges these authors and their accomplishments.

All of the authors wish to acknowledge John Orchard, DOE-NE-53 Lead, Transportation, for his guidance and support.

## SUMMARY

This report compiles the Fiscal Year 2012 milestone reports from the national laboratories that have participated on the Used Fuel Disposition Campaign Storage and Transportation Work Packages (WBS 1.02.08.13): Argonne National Laboratory, Oak Ridge National Laboratory, Idaho National Laboratory, Pacific Northwest National Laboratory, Sandia National Laboratories, and Savannah River National Laboratory.

This report is a Level M2 report. The Level is higher than all of the individual laboratory Level M3 reports (except for the Oak Ridge National Laboratory Level M2 report) contained herein to give the Transportation Work Packages more visibility and to consolidate the work of the Transportation team.

The Transportation WP activities closely parallel the UFD Campaign Storage R&D Investigations Work Packages. Notably a report was issued in FY11 by the Storage R&D Investigations multi-laboratory Team. “Gap Analysis to Support Extended Storage of Used Nuclear Fuel.” This report identified the functional requirements for safe storage of UNF; 1) retrievability, 2) thermal performance, 3) confinement, 4) radiation protection, and 5) subcriticality. Furthermore, this report documented a gap analysis performed to identify data and modeling needs related to the structures, systems, and components inherent to storage of UNF. The gap analysis informs activities necessary to develop the desired technical bases which would permit extended storage and subsequent transportation of the UNF.

The Transportation Team identified the retrievability and subcriticality safety functions to be of primary importance to the transportation of UNF after extended storage and to transportation of high burnup fuel. Accordingly, the tasks performed under the Transportation Work Packages address issues related to retrievability and subcriticality; integrity of cladding (properties of embrittled, high burnup cladding and loads applied to cladding during transport), criticality analyses of failed UNF within transport packages, moderator exclusion concepts, and stabilization of cladding with canisters for criticality control. In addition, maintaining a detailed inventory of UNF in dry storage was an additional ongoing activity.

## CONTENTS

SUMMARY .....	v
1. INTRODUCTION .....	1
2. LABORATORY TASKS AND REPORTS .....	3
2.1 Argonne National Laboratory .....	3
2.1.1 Summary of Development of Closure Bolt Analysis Rules on Design of ASME Section III, Division 3 Containments.....	3
2.1.2 Summary of Cladding Embrittlement Concerns for Storage and Transportation of High-Burnup Fuel .....	4
2.2 Idaho National Laboratory .....	4
2.2.1 Summary of FY 2012 Used Fuel Disposition Campaign Transportation Task Report on INL Efforts Supporting the Moderator Exclusion Concept and Standardized Transportation .....	5
2.3 Oak Ridge National Laboratory .....	5
2.3.1 Summary of Consequences of Fuel Failure on Criticality Safety of Used Nuclear Fuel.....	6
2.4 Pacific Northwest National Laboratory .....	8
2.4.1 Summary of A Preliminary Evaluation of Using Fill Materials to Stabilize Used Nuclear Fuel During Storage and Transportation .....	9
2.5 Savannah River National Laboratory .....	10
2.5.1 Summary of Dry Storage of Used Fuel Transition to Transport.....	10
2.6 Sandia National Laboratories .....	10
2.6.1 Summary of Fuel-Assembly Shaker Test: Tests for Determining Loads on Used Nuclear Fuel under Normal Conditions of Transport .....	11
3. APPENDICES .....	12

APPENDIX A: Development of Closure Bolt Analysis Rules on Design of ASME Section III, Division 3 Containments

APPENDIX B: Cladding Embrittlement Concerns for Storage and Transportation of High-Burnup Fuel

APPENDIX C: FY 2012 Used Fuel Disposition Campaign Transportation Task Report on INL Efforts Supporting the Moderator Exclusion Concept and Standardized Transportation

APPENDIX D: Consequences of Fuel Failure on Criticality Safety of Used Nuclear Fuel

APPENDIX E A Preliminary Evaluation of Using Fill Materials to Stabilize Used Nuclear Fuel During Storage and Transportation

APPENDIX F: Summary of PNNL Transportation Activities for FY12 to Support the UFD Program

APPENDIX G: Dry Storage of Used Fuel Transition to Transport

APPENDIX H: Compilation of Transportation Issues and Resolutions – Tests for Determining Loads on Used Nuclear Fuel under Normal Conditions of Transport

## **TRANSPORTATION ISSUES AND RESOLUTIONS – Compilation of Laboratory Transportation Work Package Reports**

### **1. INTRODUCTION**

The Used Fuel Disposition (UFD) Campaign Transportation activity was initiated in Fiscal Year 2011. The objectives of the Transportation Work Packages (WPs) have been general, e.g., from the FY12 Work Packaging Planning document:

*The objectives of the transportation activities are to address identified high priority technical issues. This includes developing the technical basis for the transport of high burnup used nuclear fuel and the transport of all used nuclear fuel after long-term storage.*

The Transportation Work Package Team, consisting of staff from Argonne National Laboratory (ANL), Oak Ridge National Laboratory (ORNL), Idaho National Laboratory (INL), Pacific Northwest National Laboratory (PNNL), Sandia National Laboratories (SNL), and Savannah River National Laboratory (SRNL), and the United States (US) Department of Energy (DOE) Technical Lead for Transportation, identified specific tasks for the individual laboratory Work Packages that addressed various technical issues and which were aligned with the capabilities of the laboratories.

The Transportation Team identified a set of technical issues that were related to either near-term transportation or post-extended storage transportation, but included high burnup used nuclear fuel (UNF) issues within both timeframes. (See Figure 1.) In addition and as a result of a primary Blue Ribbon Commission recommendation, potential Transportation campaigns were identified for transport of UNF from existing Independent Spent Fuel Storage Installations, with particular emphasis on transportation from orphan sites (decommissioned reactors), transportation from interim storage sites (consolidated storage facilities – yet to be sited or licensed), and transportation to a disposal facility.

The Transportation WP activities align with the UFD Campaign Storage R&D Investigations Work Packages. Notably a report was issued in FY11 by the Storage R&D Investigations multi-laboratory Team, “Gap Analysis to Support Extended Storage of Used Nuclear Fuel.”<sup>a</sup> This report identified the functional requirements for safe storage of UNF: 1) retrievability, 2) thermal performance, 3) confinement, 4) radiation protection, and 5) subcriticality. Furthermore, this report documented a gap analysis performed to identify data and modeling needs related to the structures, systems, and components inherent to storage of UNF. The gap analysis informs activities necessary to develop the desired technical bases which would permit extended storage and subsequent transportation of the UNF.

The Transportation Team identified the retrievability and subcriticality safety functions to be of primary importance to the transportation of UNF after extended storage and to transportation of high burnup fuel. Accordingly, the tasks performed under the Transportation Work Packages address issues related to retrievability and subcriticality: integrity of cladding (properties of embrittled, high burnup cladding and loads applied to cladding during transport), criticality analyses of failed UNF within transport packages, moderator exclusion concepts, and stabilization of cladding within canisters for criticality control. Maintaining an inventory of UNF in dry storage was an additional ongoing activity.

---

<sup>a</sup> Brady Hanson, PNNL; Halim Alsaed, INL; Christine Stockman, SNL, David Enos, ENL; Ryan Meyer, PNNL; Ken Sorenson, SNL, June 30, 2011, FCRD-USCD-2011-000136. Note, a future revision of this report shall incorporate transportation gaps. This revision was supported by members of the PNNL Transportation WP Team as an FY12 activity.

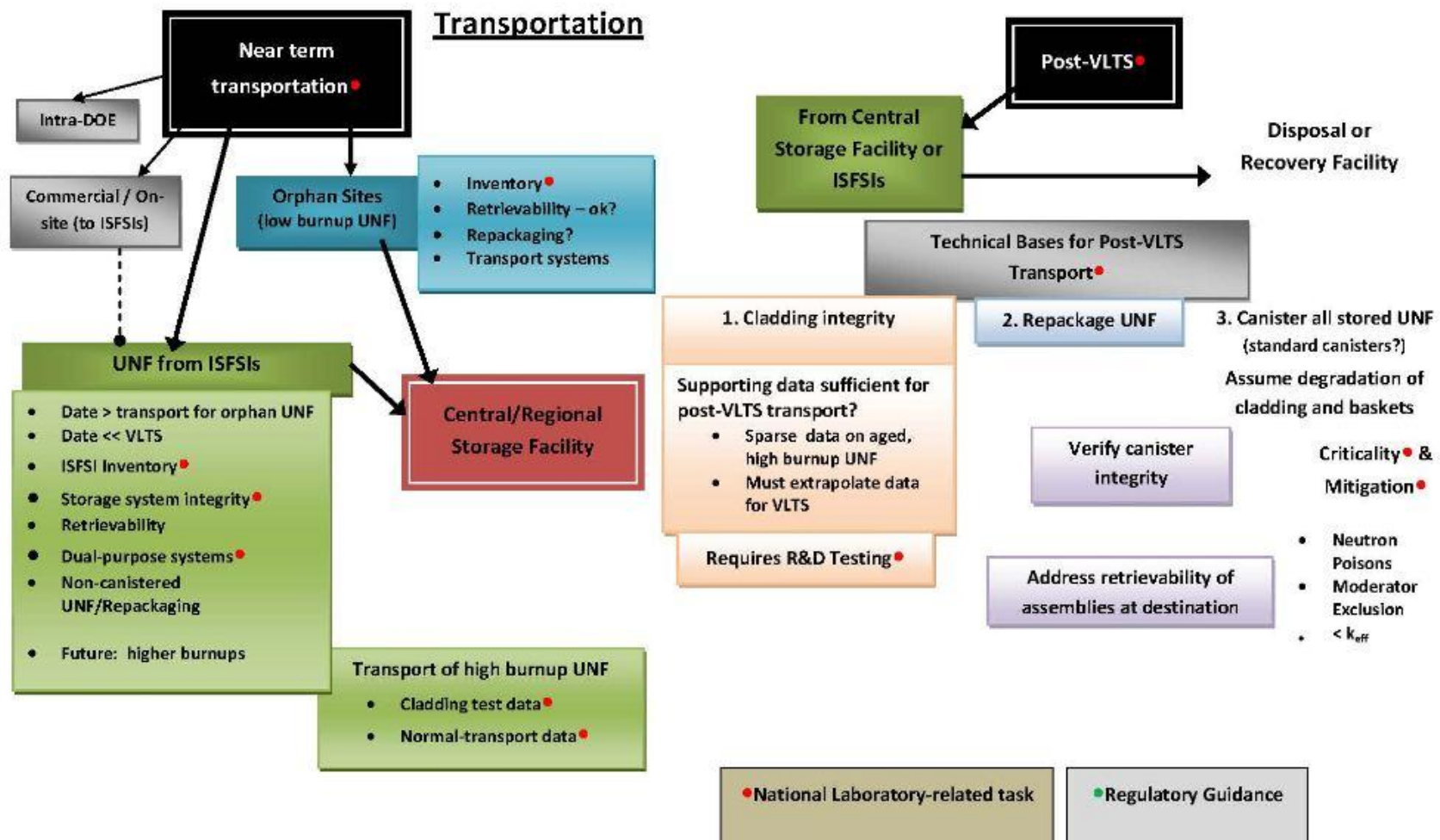


Figure 1. Transportation Campaigns and Related Technical Issues.

## 2. LABORATORY TASKS AND REPORTS

This document collates the laboratory reports from each laboratory for FY12. Each laboratory on the Transportation WP Team has been involved since FY11. These reports comprise Appendices A – H. Each of these reports has been submitted separately by the laboratory author, but this document collates the reports so that the Transportation activities can be readily referenced.

The activities described in the reports are varied, but all address issues relevant to the transportation of UNF and is aligned with the functional criteria. The activities of the Transportation Team ranged from cladding embrittlement of high burnup fuel to moderator exclusion and criticality analyses to storage canister stabilization to dry storage transportation issues to fuel assembly vibration testing.

### 2.1 Argonne National Laboratory

The ANL Transportation WP # is FT-12AN081301. The Scope of the ANL Transportation WP for FY12 is

ANL will support (1) gap analysis for transportation for long-term storage and high burnup assessment, (2) development of a test plan on fuel assembly in a cask under normal conditions of transport, (3) American Society of Mechanical Engineers (ASME) NUPACK, and (4) other transportation-related activities, as deemed necessary.

ANL issued two letter reports. These reports are in Appendices A and B. The first is “Development of Closure Bolt Analysis Rules on Design of ASME Section III, Division 3 Containments.” The second is “Cladding Embrittlement Concerns for Storage and Transportation of High-Burnup Fuel.”

#### 2.1.1 Summary of Development of Closure Bolt Analysis Rules on Design of ASME Section III, Division 3 Containments

The ASME Boiler and Pressure Vessel (BPV) Code Subcommittee responsible for Section III Division 3 is currently revising Subsections WB and WC and developing Subsection WD. Subsections WB and WC contain rules for the material, design, fabrication, examination, testing, marking, stamping, and preparation of reports by the Certificate Holder for Class TC transportation containments and Class SC storage containments, respectively, for spent nuclear fuel and high-level radioactive waste and materials. Subsection WD, which is under development, contains rules similar to those in Subsections WB and WC, but for internal supports inside the transportation and storage containments. The Working Group on the Design of Section III Division 3 Containments is addressing design issues, i.e., rules and/or guidance, for the bolted joints beyond the current Subsections WB and WC (and WD) limits. Further development of closure bolt analysis rules has been identified as a priority. As a member of the ASME BPV Code Subcommittee and the Working Group, Argonne National Laboratory has been tasked to assist in the further development of the closure bolt analysis rules.

Three tables have been created to compare the bolting rules between Subsections WB and WC, and between the rules in the mandatory Appendices XIII and XIV and Article WB-3000. The bolting rules in Subsections WB and WC are compared in Table 1 and the results were presented at the Working Group meeting in May 2012. The mandatory Appendices XIII and XIV to Section III Division 1 of the ASME BPV Code also contain bolting design analysis rules in Article XIII-1000, “Design Based on Stress Analysis,” and Article XIV-1000, “Design Based on Fatigue Analysis.” Although the rules in these two appendices are only applicable to the design of Class 2 vessels, they could be considered for use for containments meeting the requirements of WC-3200. The design rules and guidance in these two appendices are compared in Tables 2 and 3, respectively, against those in Subsection WB, for potential incorporation into Article WC-3000.

Subsection WB addresses the design stress limit for bolted closures under Level A and Level D service limits to ensure integrity of the bolted flange. Properly applied bolt preloads introduce clamping force in the bolted joint, ensuring leak-tightness of the transportation and storage casks. Work has begun in reviewing the bolting analysis rules in NUREG/CR-6007 “Stress Analysis of Closure Bolts for Shipping Casks” and the current practices for installing bolt preloads in the closure joints of transportation casks for hazardous and radioactive materials in ASME PCC-1, “Guidelines for Pressure Boundary Bolted Flange Joint Assembly.”

### **2.1.2 Summary of Cladding Embrittlement Concerns for Storage and Transportation of High-Burnup Fuel**

Structural analyses of high-burnup fuel require cladding mechanical properties and failure limits to assess fuel behavior during long-term dry cask storage and transportation. Pre-storage drying-transfer operations and early stage storage subject cladding to higher temperatures and much higher hoop stresses relative to in-reactor operation and pool storage. Under these conditions, radial hydrides may precipitate during slow cooling and provide an additional embrittlement mechanism as the cladding temperature decreases below the ductile-to-brittle transition temperature (DBTT).

In Interim Staff Guidance – 11, Revision 3 (ISG-11 Rev. 3), the Nuclear Regulatory Commission (NRC) recommends a peak cladding temperature limit of 400°C for drying-transfer operations and storage of used fuel in storage and transport casks containing high-burnup fuel. Limits are also placed on the number of drying cycles and the temperature drop per cycle. One concern for high-burnup cladding is the possible precipitation of radial hydrides, which could embrittle cladding in response to tensile hoop stress caused by the internal pressure loading. Limits established in ISG-11 Rev. 3 relied on data available prior to 2003, which were primarily for low-burnup and non-irradiated/pre-hydrided Zircaloy-4. At the time ISG-11 Rev. 3 was issued, NRC recognized that data for all high-burnup cladding alloys were needed to determine the extent of radial hydride embrittlement under conditions relevant to drying-transfer operations and storage. Data generated since 2003, mostly at Argonne, indicate that limits imposed by ISG-11 Rev. 3 do not protect high-burnup cladding from embrittlement due to radial hydrides. Recent NRC reviews of applications for license renewal of the Prairie Island ISFSI and Amendment 5 of the CoC for Transnuclear MP-197 have raised concerns for long-term storage and transportation of high-burnup fuel. The issues are summarized in “Compatibility of Requirements for Storage and Transportation of Spent Nuclear Fuel (Retrievability, Cladding Integrity, and Safe Handling),” — a summary paper presented at the NRC Public Meeting to obtain stakeholder feedback on enhancements to the licensing and inspection programs for spent fuel storage and transportation under 10 CFR Parts 71 and 72. A major concern is whether or not the high burnup fuel will maintain cladding integrity and be readily retrievable after more than 20 years of storage. License approvals for the transport of high-burnup fuel have been delayed because of a lack of data on high-burnup fuel cladding embrittlement after more than 20 years of storage, which corresponds to peak cladding temperatures of  $\approx$ 200°C or less.

## **2.2 Idaho National Laboratory**

The INL Transportation WP# is FT-12IN081302. The Scope of the INL Transportation WP for FY12 is

**Task #1:** This task is intended to take advantage of the current NRC review of extended storage aspects on its storage and transportation requirements. In SECY-11-0029, the NRC established plans to identify technical and regulatory needs to expand the basis for regulating the extended storage and transportation of used fuel. The staff plans to issue a gap assessment in November 2011 for comment and finalize it in April 2012. This effort is intended to bring the use of an inner containment forward to the NRC staff for their consideration of criticality safety by permitting the use of the requirement in 10 CFR Part 71.55(c) for both normal and hypothetical accident conditions for general designs. In

addition, to continue the efforts to promote this moderator exclusion concept, efforts will be made to present the concept to the Extended Storage Collaboration Program (ESCP) meetings as well as make a presentation at the upcoming Institute of Nuclear Materials Management (INMM) meeting scheduled for January 2012 or another appropriate venue.

**Task #2:** The inner containment will need to demonstrate a watertight barrier function. ASME BPV Section III, Division 3 committees are currently considering the incorporation of strain criteria for energy-limited events that would assure the leaktight performance of commonly used stainless steel base and weld materials (either 304/304L or 316/316L). These strain criteria would be applicable to the inner containment. An important aspect supporting the use of these strain criteria is the proper prediction of the strain responses. When performing inelastic analyses, strain rate effects need to be considered for accurate strain predictions. The first step needed is to determine what strain rate data is readily available for the base and weld materials of interest at the temperatures and strain rate levels associated with accidental drop events. This effort will establish a documented collection of strain rate data that is readily available. Having this gathered data would clarify future strain rate testing needs. This data could also support efforts to reduce the dependence on costly demonstration testing for hypothetical accident conditions.

INL issued a report (Appendix C) "FY 2012 Used Fuel Disposition Campaign Transportation Task Report on INL Efforts Supporting the Moderator Exclusion Concept and Standardized Transportation."

### **2.2.1 Summary of FY 2012 Used Fuel Disposition Campaign Transportation Task Report on INL Efforts Supporting the Moderator Exclusion Concept and Standardized Transportation**

Following the defunding of the Yucca Mountain Project, it is reasonable to assume that commercial used fuel will remain in storage for a longer time period than initially assumed. Previous transportation task work in FY 2011, under the Department of Energy's Office of Nuclear Energy, Used Fuel Disposition Campaign, proposed an alternative for safely transporting used fuel regardless of the structural integrity of the used fuel, baskets, poisons, or storage canisters after an extended period of storage. This alternative assures criticality safety during transportation by implementing a concept that achieves moderator exclusion (no in-leakage of moderator into the used fuel cavity). By relying upon a component inside of the transportation cask that provides a watertight function, a strong argument can be made that moderator intrusion is not credible and should not be a required assumption for criticality evaluations during normal or hypothetical accident conditions of transportation.

This Transportation Task report addresses the assigned FY 2012 work that supports the proposed moderator exclusion concept as well as a standardized transportation system. The two tasks assigned were to (1) promote the proposed moderator exclusion concept to both regulatory and nuclear industry audiences and (2) advance specific technical issues in order to improve American Society of Mechanical Engineers Boiler and Pressure Vessel Code, Section III, Division 3 rules for storage and transportation containments. The common point behind both of the assigned tasks is to provide more options that can be used to resolve current issues being debated regarding the future transportation of used fuel after extended storage.

## **2.3 Oak Ridge National Laboratory**

The ORNL Transportation WP# is FT-12INOR081302. The Scope of the ORNL Transportation WP for FY12 is

- Conduct a criticality safety assessment to mitigate the need for a complete set of clad materials data. (If criticality is not viable even with failed fuel, clad material properties become less important).
- Investigate options for dry transfer systems for used nuclear fuel in dry storage.

ORNL issued a Level 2 report entitled “Consequences of Fuel Failure on Criticality Safety of Used Nuclear Fuel” which is in Appendix D.

### **2.3.1 Summary of Consequences of Fuel Failure on Criticality Safety of Used Nuclear Fuel**

This report documents work performed for the Department of Energy’s Office of Nuclear Energy (DOE-NE) Fuel Cycle Technologies Used Fuel Disposition Campaign to assess the impact of fuel reconfiguration due to fuel failure on the criticality safety of UNF in storage and transportation casks. This work was motivated by concerns related to the potential for fuel degradation during extended storage (ES) periods and transportation following ES, but has relevance to other potential causes of fuel reconfiguration.

Commercial UNF in the United States is expected to remain in storage for longer periods than originally intended. Extended storage time and irradiation of nuclear fuel to high-burnup values ( $>45 \text{ GWd/t}$ ) may increase the potential for fuel failure during normal and accident conditions involving storage and transportation. Fuel failure, depending on the severity, can result in changes to the geometric configuration of the fuel, which has safety and regulatory implications for virtually all aspects of a UNF storage and transport system’s performance. The potential impact of fuel reconfiguration on the safety of UNF in storage and transportation is dependent on the likelihood and extent of the fuel reconfiguration, which is not well understood and is currently an active area of research. The objective of this work is to assess and quantify the impact of postulated failed fuel configurations on the criticality safety of UNF in storage and transportation casks. Although this work is motivated by the potential for fuel degradation during ES periods and transportation following ES, it has relevance to fuel reconfiguration due to the effects of high burnup. Regardless of the ultimate disposition path, UNF will need to be transported at some point in the future.

To investigate and quantify the impact of fuel reconfiguration on criticality safety limits, which are given in terms of the effective neutron multiplication factor,  $k_{\text{eff}}$ , a set of failed fuel configuration categories was developed and specific configurations were evaluated. The various configurations were not developed to represent the results of specific reconfiguration progressions; rather, they were designed to be bounding of any reconfiguration progressions that could occur. The configuration categories considered in this analysis include the following:

- clad thinning/loss – reduced cladding thickness up to the total removal of all cladding material
- rod failures – removal of one or more fuel rods from the assembly lattice
- loss of rod pitch control – rod pitch contraction and expansion within the storage cell
- loss of assembly position control – axial displacement of fuel assemblies
- gross assembly failure – rubblized fuel within the storage cells with varying degrees of moderation
- neutron absorber degradation – gaps of varying location and size; thinning of absorber panels

Within each category, a number of specific configurations were modeled to calculate the corresponding  $k_{\text{eff}}$  values and the associated consequences of those configurations relative to the reference intact configuration. The consequence of a given configuration is defined as the difference in the calculated  $k_{\text{eff}}$  values for the given configuration and the reference intact configuration, with a positive value indicating

an increase in  $k_{\text{eff}}$  as compared to the reference configuration. Several of the specific configurations are not considered credible but are included in the analyses for completeness (e.g., to fully understand trends and worst-case situations). Pending improved understanding of the various material degradation phenomenon, and subsequent determination and justification for what configurations are and are not credible, the assessment of the credibility of configurations provided herein is based on engineering judgment. The credibility of configurations and the impact of the configurations on criticality safety are dependent on many factors, including storage and transportation conditions, the fuel assembly characteristics, and the storage and/or transportation system characteristics. Therefore, the assessment and analysis of credible configurations for a specific cask system would need to be performed as part of the safety analysis for licensing that system.

Representative pressurized water reactor (PWR) and boiling water reactor (BWR) fuel assembly designs loaded in representative cask systems were considered in this report. The two fuel assembly designs selected for this analysis represent a large portion of the current inventory of discharged UNF and/or a significant portion of the fuel designs currently in use. The cask systems selected for this analysis are high-capacity 32-PWR-assembly general burnup credit cask (GBC-32) and 68-BWR-assembly multipurpose canister (MPC-68) cask designs based on the Holtec International HI-STAR 100 system.

The depletion conditions used in this analysis are considered representative of those used in a burnup credit criticality safety evaluation. The analysis focuses on typical discharge fuel conditions (e.g., fuel initial enrichment, discharge burnup, and post-irradiation decay time) that could be loaded into storage and transportation casks. Additional burnup and extended post-irradiation cooling times are considered in this analysis for both PWR and BWR fuel to establish the sensitivity of reconfiguration impacts to these parameters.

For the configurations judged by the authors to be potentially credible, the maximum increase in  $k_{\text{eff}}$  for the PWR cask system (GBC-32) was nearly 4%, corresponding to a nonuniform pitch expansion configuration due to a loss of fuel rod pitch control, and that for the BWR cask system (MPC-68) was 2.4%, corresponding to a configuration with multiple rod failures. It is important to emphasize that these results are contingent on the authors' judgment relative to the potential credibility of configurations, which includes not only whether a configuration category is credible but also whether the resulting configurations within a given category are credible for a specific cask system. For example, for the PWR cask system, axial assembly displacement such that assemblies extended more than 7.5 cm above or below the neutron absorber panel was not considered credible because of the presence of fuel assembly hardware and cask assembly spacers. If it were determined that such a configuration is credible, then that configuration and its specific characteristics may be limiting. Similarly, for the BWR cask system, the fuel assembly channel is assumed to be present and capable of constraining fuel rod pitch expansion. If the channel is not present or unable to constrain rod pitch expansion, then that configuration may be limiting. In addition to representative conditions for fuel burnup and post-irradiation decay time, the effects of higher burnup and longer cooling times were also investigated and found to be smaller than the reduction in  $k_{\text{eff}}$  associated with the higher burnup or cooling time.

Because a wide range of credible and non-credible configurations were analyzed, the calculated consequences also varied widely. For the PWR cask system (GBC-32), the calculated  $k_{\text{eff}}$  increase varied from 0.1% to almost 22.25%. For the BWR cask system (MPC-68), the calculated increase varied from 0.3% to as much as almost 36%. Some configurations in both cask systems result in decreases in  $k_{\text{eff}}$ . As the Nuclear Regulatory Commission (NRC) Standard Review Plans, which provide guidance for demonstrating compliance with the applicable regulations, recommend that  $k_{\text{eff}}$  should not exceed 0.95 under all credible conditions during storage and transportation, such large increases are concerning. However, as noted, a number of the configurations analyzed are not considered credible.

The magnitude of the potential increases in  $k_{\text{eff}}$  and the sensitivity of the potential increases in  $k_{\text{eff}}$  to the determination of the credibility of configurations highlight the importance of being able to determine and

justify which configurations are credible under a given set of conditions for a given cask system. It is anticipated, at least in the near term, that these determinations will be done on a case-by-case basis for each cask system and associated licensing conditions.

Given the establishment of a set of credible failed fuel configurations for a given cask system and assuming that one or more of the configurations result in an increase in  $k_{\text{eff}}$  (above the regulatory limit of 0.95), the consequence of this potential increase in  $k_{\text{eff}}$  must be addressed. There are a number of potential options, the viability of which depends on the magnitude of the increase in  $k_{\text{eff}}$ . For example, a cask design and/or fuel assembly loading conditions could be modified to ensure that the current  $k_{\text{eff}}$  limit of 0.95 is satisfied for all credible failed fuel configurations. Separate assembly loading criteria (e.g., loading curves) based on a reduced  $k_{\text{eff}}$  limit could be developed for fuel assemblies that may have questionable integrity. In the context of high-burnup fuel or ES durations, a separate loading curve based on a lower  $k_{\text{eff}}$  limit could be developed and applied to fuel assemblies with burnup greater than 45 GWd/MTU and/or with a post-irradiation storage period beyond some specified value. Alternatively, depending on the probability of fuel reconfiguration, it may be possible that a separate higher limit could be established to allow margin for the increased reactivity effect associated with fuel reconfiguration. This latter approach would be similar to the higher limit (i.e., 0.98) allowed for the unlikely optimum moderation condition in dry storage of fresh fuel under 10 CFR 50.68. In this case, the customary  $k_{\text{eff}}$  limit would still apply to all conditions involving intact fuel. Limits above 0.95 are also allowed in some facilities regulated by the NRC Fuel Cycle Safety and Safeguards Division, and hence precedents for this type of approach exist. For casks that have already been loaded prior to implementation of a generic mitigation strategy, the analysis basis may be extended to include or expand burnup credit, providing mitigation for potential consequences of fuel reconfiguration.

Although the results indicate that the potential impacts on subcriticality can be rather significant for certain configurations, it can be concluded that the consequences of credible fuel failure configurations from ES or transportation following ES are manageable. Some examples for how to address the potential increases in  $k_{\text{eff}}$  in a criticality safety evaluation were provided. Future work to further inform decision making relative to which configurations are credible, and therefore need to be considered in a safety evaluation, is recommended.

## 2.4 Pacific Northwest National Laboratory

The PNNL Transportation WP# is FT-12INPN081302. The Scope of the PNNL Transportation WP for FY12 is

1. Continued Analysis of Features, Events, and Processes (FEPs) for Transportation - FEPs for transportation have been identified and documented in the FY11 mid-year and year-end reports. Further work to consolidate the transportation FEPs with the storage FEPs is planned for FY12 to produce a consolidated document of all FEPs for storage and transportation.
2. Evaluation of Issues Related to Dry Repackaging of Bare UNF into Canisters or Transportation Containers - This work will involve the identification and evaluation of issues associated with the dry repackaging of bare used nuclear fuel into canisters or transportation containers. This fuel may arise from UNF in storage only (i.e., non-transportable) canisters, or failed/defective transportable storage casks. Emphasis will be placed on dry transfer capabilities that could be implemented at sites without operating nuclear reactors, i.e., where UNF storage/transportation canister and/or transportation cask handling facilities have been decommissioned. This task will be focused on identifying technical, programmatic, institutional, and regulatory issues that need to be addressed before repackaging could take place. These issues include 1) fuel and cladding integrity, 2) fuel handling infrastructure, and 3) canister or container selection.

3. Support UFD Campaign Efforts During FY12 - This effort will support UFD Program activities such as liaison with the security group, liaison with the decay heat management group, and preparation of the mid- and end-of-year transportation status reports.
4. Evaluation of Issues Associated with Canister Stabilization Feasibility - This work will involve evaluating the issues associated with stabilizing the contents of used nuclear fuel canisters. These issues would be examined with an eye towards end use of the used nuclear fuel, i.e., disposal in a repository, interim storage, or reprocessing. Potential issues to be addressed include 1) retrievability of the used fuel after stabilization, 2) weight, and 3) degradation during hypothetical accident conditions.

PNNL issued two reports entitled “A Preliminary Evaluation of Using Fill Materials to Stabilize Used Nuclear Fuel during Storage and Transportation” and “Summary of PNNL Transportation Activities for FY12 to Support the UFD Program” (Appendices E and F, respectively).

#### **2.4.1 Summary of A Preliminary Evaluation of Using Fill Materials to Stabilize Used Nuclear Fuel During Storage and Transportation**

The objective of the research described in this report was to conduct a preliminary evaluation of potential fill materials that could be used to fill void spaces in and around used nuclear fuel contained in dry storage canisters in order to stabilize the geometry and mechanical structure of the used nuclear fuel during extended storage and subsequent transportation. The use of fill material to stabilize used nuclear fuel is not considered to be a primary option for safely transporting used nuclear fuel after extended storage. However, the evaluation of potential fill materials, such as those described in this report, might provide the US Department of Energy UFD Campaign with an option that would allow continued safe storage and transportation if other options such as showing that the fuel remains intact or canning of used nuclear fuel do not prove to be feasible. As a first step in evaluating fill materials, previous work done in this area was summarized. This involved studies done by the Spent Fuel Stabilizer Materials Program, Allied-General Nuclear Services, the Canadian Nuclear Fuel Waste Management Program, the US Department of Energy, Spain, Sweden, and the Department of Energy’s Yucca Mountain Project. A wide variety of potential fill materials were evaluated in these studies, ranging from molten metal to particulates and beads to liquids and gases. The common element in the studies was that they were focused on the use of fill materials in waste packages for disposal, not in storage canisters or transportation casks. In addition, very few studies involved actual experiments that measured some physical property of the fill material to be used as a stabilizing material, and no studies were found that analyzed the performance of transportation casks containing fill material during the normal conditions of transport specified in 10 CFR 71.71 or under hypothetical accident conditions specified in 10 CFR 71.73. In addition, most studies did not address issues that would be associated with production-scale emplacement of fill material in canisters, as opposed to laboratory- or experimental-scale use of fill material. It is noteworthy that Sweden abandoned its plan to use fill materials to stabilize waste packages due to the complexity of emplacing the fill material.

A part of the evaluation of fill materials, conceptual descriptions of how canisters might be filled were developed with different concepts for liquids, particles, and foams. The requirements for fill materials were also developed. Elements of the requirements included criticality avoidance, heat transfer or thermodynamic properties, homogeneity and rheological properties, retrievability, material availability and cost, weight and radiation shielding, and operational considerations. Potential fill materials were grouped into 5 categories and their properties, advantages, disadvantages, and requirements for future testing were discussed. The categories were molten materials, which included molten metals and paraffin; particulates and beads; resins; foams; and grout. Based on this analysis, further development of fill materials to stabilize used nuclear fuel during storage and transportation is not recommended unless

options such as showing that the fuel remains intact or canning of used nuclear fuel do not prove to be feasible.

## 2.5 Savannah River National Laboratory

The SRNL Transportation WP# is FT-12INSR081302. The Scope of the SRNL Transportation WP for FY12 is

- Investigate options for dry transfer systems for canister based storage casks in dry storage
- Support used nuclear fuel storage/transportation database development and maintenance
- Investigate shipment in commerce of wet samples of used fuel. Wet samples are samples shipped with sufficient water to maintain the fuel sample surfaces in a fully wetted condition.
- Support standards committees and the EPRI ESCP

The SRNL report “Dry Storage of Used Fuel Transition to Transport” is in Appendix G.

### 2.5.1 Summary of Dry Storage of Used Fuel Transition to Transport

This report provides details of dry storage cask systems and contents in US for commercial light water reactor fuel. Section 2 contains details on the canisters used to store approximately 86% of assemblies in dry storage in the US. Transport cask details for both bare fuel, dual purpose casks and canister transport casks are included in Section 3. Section 4 details the inventory of those shutdown sites without any operating reactors. Information includes the cask type deployed, transport license and status as well as fuel types allowed in the specified cask system and allowable parameters. Section 5 contains details on the transfer casks used with each cask system including the current number of transfer casks of each type fabricated.

## 2.6 Sandia National Laboratories

The SNL Transportation WP# is FT-12INSN081302. The Scope of the SNNL Transportation WP for FY12 is

- The SNL Transportation FY12 work shall focus on planning and conducting normal transport tests using a truck cask containing an instrumented fuel assembly. An additional \$100k in funding was received in April 2012 because development of the test program required extensive engineering consultation and test concept changes as the program evolved. (The actual tests of the fuel assembly shall be performed in FY13.)
- The work shall also support ASME NUPACK, the International Atomic Energy Agency (IAEA) Dual-purpose Cask Working Group, EPRI/ESCP, and support to DOE/NE on an as-requested basis. The SNL Transportation Team Lead shall interact with the DOE/LV Oversight staff and the laboratory leads of the other Transportation WP Team members. The SNL Transportation Team Lead shall prepare a M2 report compiling the FY12 work of the Transportation WP Team.

In addition to this report, SNL issued a second report “Fuel-Assembly Shaker Test: Tests for Determining Loads on Used Nuclear Fuel under Normal Conditions of Transport” which is in Appendix H.

## 2.6.1 Summary of Fuel-Assembly Shaker Test: Tests for Determining Loads on Used Nuclear Fuel under Normal Conditions of Transport

This test plan is designed to capture the response of cladding in its representative configuration (i.e., *in-an-assembly-within-a-basket-within-a-cask-tied-to-a-transport-conveyance*) to actual loadings imposed during normal conditions of transport. Finite-element modeling after the normal transport tests are conducted will allow an estimate of the response irradiated rods would have experienced during the road tests based upon the test data from the surrogate rods. The assembly planned for the test is a Westinghouse 17x17 PWR assembly.

The rods to be used for the tests will not be actual irradiated zirconium-alloy/UO<sub>2</sub>-pellet rods. Surrogate rods shall be selected that have similar mass, stiffness, and natural frequency as the actual irradiated rods. Copper B280 alloy tubes filled with lead rods approximately meet the criteria for simulating Zircaloy-4/UO<sub>2</sub>-pellet rods. They shall be used for most of the positions with the assembly; Zircaloy-4/Pb rods shall be used for those assembly positions which will be instrumented for the test.

Finite-element modeling before the test shall provide information on which rod locations within the assembly should be instrumented and on which locations on those rods the instrumentation for measuring strains and accelerations should be placed. Finite-element modeling after the normal transport tests are conducted will allow an estimate of the response all the rods would have experienced during the road tests based upon the test data from the surrogate rods. The test data will also allow the finite element model to be benchmarked.

The test results will allow for an analytic assessment of the ability of aged, high burnup cladding to withstand normal transport loads by comparing the strength of the aged, high burnup cladding to the stresses imposed on the cladding during normal transport.

### **3. APPENDICES**

## **APPENDIX A**

### **Development of Closure Bolt Analysis Rules on Design of ASME Section III, Division 3 Containments**

# **Development of Closure Bolt Analysis Rules on Design of ASME Section III, Division 3 Containments**

Z.H. Han, V.N. Shah and Y.Y. Liu

Argonne National Laboratory

September 11, 2012

The ASME BPV Code Subcommittee responsible for Section III Division 3 is currently revising Subsections WB and WC and developing Subsection WD. Subsections WB and WC contain rules for the material, design, fabrication, examination, testing, marking, stamping, and preparation of reports by the Certificate Holder for Class TC transportation containments and Class SC storage containments, respectively, for spent nuclear fuel and high-level radioactive waste and materials. Subsection WD, which is under development, contains rules similar to those in Subsections WB and WC, but for internal supports inside the transportation and storage containments. The Working Group on the Design of Section III Division 3 Containments is addressing design issues, i.e., rules and/or guidance, for the bolted joints beyond the current Subsections WB and WC (and WD) limits. Further development of closure bolt analysis rules has been identified as a priority. As a member of the ASME BVP Code Subcommittee and the Working Group, Argonne National Laboratory has been tasked to assist in the further development of the closure bolt analysis rules.

Three tables have been created to compare the bolting rules between Subsections WB and WC, and between the rules in the mandatory Appendices XIII and XIV and Article WB-3000. The bolting rules in Subsections WB and WC are compared in Table 1 and the results were presented at the Working Group meeting in May 2012. The mandatory Appendices XIII and XIV to Section III Division 1 of the ASME BPV Code also contain bolting design analysis rules in Article XIII-1000, "Design Based on Stress Analysis," and Article XIV-1000, "Design Based on Fatigue Analysis." Although the rules in these two appendices are only applicable to the design of Class 2 vessels, they could be considered for use for containments meeting the requirements of WC-3200. The design rules and guidance in these two appendices are compared in Tables 2 and 3, respectively, against those in Subsection WB, for potential incorporation into Article WC-3000.

Subsection WB addresses the design stress limit for bolted closures under Level A and Level D service limits to ensure integrity of the bolted flange. Properly applied bolt preloads introduce clamping force in the bolted joint, ensuring leak-tightness of the transportation and storage casks. Work has begun in reviewing the bolting analysis rules in NUREG/CR-6007 "Stress Analysis of Closure Bolts for Shipping Casks" and the current practices for installing bolt preloads in the closure joints of transportation casks for hazardous and radioactive materials in ASME PCC-1, "Guidelines for Pressure Boundary Bolted Flange Joint Assembly."

## **Future Work**

Evaluation of the bolting analysis rules will continue, along with literature review of bolting analyses and practices for used fuel storage and transportation casks with bolted closures. Current practices for installing bolt preloads will be examined and finite-element analyses may need to be performed to determine preload uncertainties and scatters resulting from the different bolting-up methods.

The closure integrity of the storage and transportation casks in service is also affected by other factors such as aging and/or vibration during storage and transport, as well as the performance of seals. Aging effects on the bolted closure of storage and transportation casks could lead to a loss of preload due to

stress relaxation and self-loosening, or loss of bolting material due to corrosion and fatigue. Therefore, the impact of aging effects on the closure bolts and seals, and aging management programs and practices for bolted closures in storage and transportation casks should be evaluated.

Managing aging effects on the closure bolts of storage and transportation casks requires an aging management program (AMP) to prevent, mitigate, and detect aging effects, by condition and/or performance monitoring. One AMP titled “Bolted Canister Seal and Leakage Monitoring Program” has been developed for inclusion in Chapter IV of the report by O.K. Chopra, et al. [1]. The effectiveness of this AMP will be assessed against the operating experience from the storage and transportation casks with bolted closures in the future.

## **Reference**

- 1) O.K. Chopra, et al., *Managing Aging Effects on Dry Cask Storage Systems for Extended Long-Term Storage and Transportation of Used Fuel*, FCRD-USED-2012-000119 (ANL-12/29), June 30, 2012.

**Table 1 Comparison Matrix of Bolting Rules in Subsections WB and WC**

WB - BOLTING	WC - BOLTING	COMMENTS
ARTICLE WB-2000 MATERIAL	ARTICLE WC-2120 MATERIAL	
<b>WB-2100 GENERAL REQUIREMENTS FOR MATERIAL</b>	<b>WC-2100 GENERAL REQUIREMENTS FOR MATERIAL</b>	WB and WC are identical.
<b>WB-2120 CONTAINMENT MATERIAL</b>	<b>WC-2120 CONTAINMENT MATERIAL</b>	
<b>WB-2125 Bolting Material</b>  (a) Material for bolts and studs shall conform to the requirements of one of the specifications listed in Section II, Part D, Subpart 1, Table 4. Material for nuts shall conform to SA-194 or to the requirements of one of the specifications for nuts or bolting listed in Section II, Part D, Subpart 1, Table 4.  (b) The use of washers is optional. When used, they shall be made of wrought material with mechanical properties compatible with the nuts with which they are to be employed.	<b>WC-2128 Bolting Material</b>  (a) Material for bolts and studs shall conform to the requirements of one of the specifications listed in Table 4, Section II, Part D, Subpart 1. Material for nuts shall conform to SA-194 or to the requirements of one of the specifications for nuts or bolting listed in Table 4, Section II, Part D, Subpart 1.  (b) The use of washers is optional. When used, they shall be made of wrought material with mechanical properties compatible with the nuts with which they are to be employed.	
<b>WB-2200 MATERIAL TEST COUPONS AND SPECIMENS FOR FERRITIC STEEL MATERIAL AND DUCTILE CAST IRON</b>	<b>WC-2200 MATERIAL TEST COUPONS AND SPECIMENS FOR FERRITIC STEEL MATERIAL AND DUCTILE CAST IRON</b>	WB and WC have different requirements for test coupons and tests.
<b>WB-2220 PROCEDURE FOR OBTAINING TEST COUPONS AND SPECIMENS FOR QUENCHED AND TEMPERED MATERIAL AND FOR DUCTILE CAST IRON</b>	<b>WC-2220 PROCEDURE FOR OBTAINING TEST COUPONS AND SPECIMENS FOR QUENCHED AND TEMPERED MATERIAL AND FOR DUCTILE CAST IRON</b>	
<b>WB-2224 Location of Coupons</b>  (b) For bolting materials, test shall be made of either full-size bolts or test coupons are required by the base specification. The gauge length of the tension specimens and the area under the notch of Charpy specimens shall be at least one diameter or	<b>WC-2224 Bars and Bolting Material</b>  <b>WC-2224.3 Bolting Material</b>  For bolting material, the coupons shall be taken in conformance with the applicable material specification and with the	

WB - BOLTING	WC - BOLTING	COMMENTS
thickness from the heat treated end.	applicable material specification and with the midlength of the specimen at least one diameter or thickness from a heat treated end. When the studs, nuts, or bolts are not of sufficient length, the midlength of the specimen shall be at the midlength of the studs, nuts, or bolts. The studs, nuts, or bolts selected to provide test coupon material shall be identical with respect to the quenched contour and size except for length, which shall equal or exceed the length of the represented studs, nuts, or bolts.	
<p><b>WB-2300 FRACTURE TOUGHNESS REQUIREMENTS FOR MATERIAL</b></p> <p><b>WB-2310 MATERIAL TO BE TOUGHNESS TESTED</b></p> <p><b>WB-2311 Material for Which Toughness Testing Is Required</b></p> <p>(2) bolting, including studs, nuts, and bolts, with a nominal size of 1 in. (25 mm) and less;</p> <p><b>WB-2320 IMPACT TEST PROCEDURES</b></p> <p><b>WB-2322 Test Specimens</b></p> <p><b>WB-2322.1 Location of Test Specimens</b></p> <p>(a) ...When the studs, nuts, or bolts are not of sufficient length, the midlength of the specimen shall be at the midlength of the studs, nuts, or bolts. The studs, nuts, or bolts selected to provide test coupon material shall be identical with respect to the quenched contour and size except for length, which shall equal or exceed the length of the represented studs, nuts, or bolts.</p>	<p><b>WC-2300 FRACTURE TOUGHNESS REQUIREMENTS FOR MATERIAL</b></p> <p><b>WC-2310 MATERIAL TO BE IMPACT TESTED</b></p> <p><b>WC-2311 Material for Which Impact Testing Is Required</b></p> <p>(2) bolting, including studs, nuts, and bolts, with a nominal size of 1 in. (25 mm) and less;</p> <p><b>WC-2320 IMPACT TEST PROCEDURES</b></p> <p><b>WC-2322 Test Specimens</b></p> <p><b>WC-2322.1 Location of Test Specimens</b></p> <p>(a) ...When the studs, nuts, or bolts are not of sufficient length, the midlength of the specimen shall be at the midlength of the studs, nuts, or bolts. The studs, nuts, or bolts selected to provide test coupon material shall be identical with respect to the quenched contour and size except for length, which shall equal or exceed the length of the represented studs, nuts, or bolts.</p>	WB and WC are identical.
<b>WB-2330 TEST REQUIREMENTS AND ACCEPTANCE STANDARDS</b>	<b>WC-2330 TEST REQUIREMENTS AND ACCEPTANCE STANDARDS</b>	WB and WC are similar except for the test temperature.

WB - BOLTING	WC - BOLTING	COMMENTS																								
<b>WB-2333 Bolting Material</b>  For bolting material, including studs, nuts, and bolts, test three $C_v$ specimens at a temperature no higher than the preload temperature or the lowest service temperature, whichever is less. All three specimens shall meet the requirements of Table WB-2333-1.  Table WB-2333-1 Required $C_v$ Values for Bolting Material	<b>WC-2332.3 Bolting Material</b>  For bolting material, including nuts, studs, and bolts, a Charpy V-notch test shall be performed. The tests shall be performed at or below the Lowest Service Metal Temperature, and all three specimens shall meet the requirements of Table WC-2332.3-1.  Table WC-2332.3-1 Required $C_v$ Values for Bolting Material Tested in Accordance with WC-2332.3																									
<table border="1"> <thead> <tr> <th>Nominal Diameter, in. (mm)</th> <th>Lateral Expansion, mils (mm)</th> <th>Absorbed Energy, ft-lb (J)</th> </tr> </thead> <tbody> <tr> <td>1 (25) or less</td> <td>No test required</td> <td>No test required</td> </tr> <tr> <td>Over 1 to 4 (25 to 100), incl.</td> <td>25 (0.64)</td> <td>No requirements</td> </tr> <tr> <td>Over 4 (100)</td> <td>25 (0.64)</td> <td>45 (61)</td> </tr> </tbody> </table>	Nominal Diameter, in. (mm)	Lateral Expansion, mils (mm)	Absorbed Energy, ft-lb (J)	1 (25) or less	No test required	No test required	Over 1 to 4 (25 to 100), incl.	25 (0.64)	No requirements	Over 4 (100)	25 (0.64)	45 (61)	<table border="1"> <thead> <tr> <th>Nominal Diameter, in. (mm)</th> <th>Lateral Expansion, mils (mm)</th> <th>Absorbed Energy, ft-lb (J)</th> </tr> </thead> <tbody> <tr> <td>1 (25) or less</td> <td>No test required</td> <td>No test required</td> </tr> <tr> <td>Over 1 through 4 (25 through 100)</td> <td>25 (0.64)</td> <td>No requirements</td> </tr> <tr> <td>Over 4 (100)</td> <td>25 (0.64)</td> <td>45 (61)</td> </tr> </tbody> </table>	Nominal Diameter, in. (mm)	Lateral Expansion, mils (mm)	Absorbed Energy, ft-lb (J)	1 (25) or less	No test required	No test required	Over 1 through 4 (25 through 100)	25 (0.64)	No requirements	Over 4 (100)	25 (0.64)	45 (61)	
Nominal Diameter, in. (mm)	Lateral Expansion, mils (mm)	Absorbed Energy, ft-lb (J)																								
1 (25) or less	No test required	No test required																								
Over 1 to 4 (25 to 100), incl.	25 (0.64)	No requirements																								
Over 4 (100)	25 (0.64)	45 (61)																								
Nominal Diameter, in. (mm)	Lateral Expansion, mils (mm)	Absorbed Energy, ft-lb (J)																								
1 (25) or less	No test required	No test required																								
Over 1 through 4 (25 through 100)	25 (0.64)	No requirements																								
Over 4 (100)	25 (0.64)	45 (61)																								
<b>WB-2340 NUMBER OF TOUGHNESS TESTS REQUIRED</b>  <b>WB-2345 Bolting Material</b>  One test shall be made for each lot of material where a lot is defined as one heat of material heat treated in one charge or as one continuous operation, not to exceed the following:	<b>WC-2340 NUMBER OF IMPACT TESTS REQUIRED</b>  <b>WC-2345 Bolting Material</b>  One test shall be made for each lot of material where a lot is defined as one heat of material heat treated in one charge or as one continuous operation, not to exceed the following:	WB and WC are identical.																								
<table> <thead> <tr> <th>Diameter</th> <th>Weight</th> </tr> </thead> <tbody> <tr> <td>1-3/4 in. (44 mm) and less</td> <td>1,500 lb (680 kg)</td> </tr> <tr> <td>Over 1-3/4 in. to 2-1/2 in. (44 mm to 64 mm)</td> <td>3,000 lb (1350 kg)</td> </tr> <tr> <td>Over 2-1/2 in. to 5 in. (6 mm to 127 mm)</td> <td>6,000 lb (2700 kg)</td> </tr> <tr> <td>Over 5 in. (127 mm)</td> <td>10,000 lb (4500 kg)</td> </tr> </tbody> </table>	Diameter	Weight	1-3/4 in. (44 mm) and less	1,500 lb (680 kg)	Over 1-3/4 in. to 2-1/2 in. (44 mm to 64 mm)	3,000 lb (1350 kg)	Over 2-1/2 in. to 5 in. (6 mm to 127 mm)	6,000 lb (2700 kg)	Over 5 in. (127 mm)	10,000 lb (4500 kg)	<table> <thead> <tr> <th>Diameter</th> <th>Weight</th> </tr> </thead> <tbody> <tr> <td>1-3/4 in. (44 mm) and less</td> <td>1,500 lb (680 kg)</td> </tr> <tr> <td>Over 1-3/4 in. to 2-1/2 in. (44 mm to 64 mm)</td> <td>3,000 lb (1350 kg)</td> </tr> <tr> <td>Over 2-1/2 in. to 5 in. (6 mm to 127 mm)</td> <td>6,000 lb (2700 kg)</td> </tr> <tr> <td>Over 5 in. (127 mm)</td> <td>10,000 lb (4500 kg)</td> </tr> </tbody> </table>	Diameter	Weight	1-3/4 in. (44 mm) and less	1,500 lb (680 kg)	Over 1-3/4 in. to 2-1/2 in. (44 mm to 64 mm)	3,000 lb (1350 kg)	Over 2-1/2 in. to 5 in. (6 mm to 127 mm)	6,000 lb (2700 kg)	Over 5 in. (127 mm)	10,000 lb (4500 kg)					
Diameter	Weight																									
1-3/4 in. (44 mm) and less	1,500 lb (680 kg)																									
Over 1-3/4 in. to 2-1/2 in. (44 mm to 64 mm)	3,000 lb (1350 kg)																									
Over 2-1/2 in. to 5 in. (6 mm to 127 mm)	6,000 lb (2700 kg)																									
Over 5 in. (127 mm)	10,000 lb (4500 kg)																									
Diameter	Weight																									
1-3/4 in. (44 mm) and less	1,500 lb (680 kg)																									
Over 1-3/4 in. to 2-1/2 in. (44 mm to 64 mm)	3,000 lb (1350 kg)																									
Over 2-1/2 in. to 5 in. (6 mm to 127 mm)	6,000 lb (2700 kg)																									
Over 5 in. (127 mm)	10,000 lb (4500 kg)																									

WB - BOLTING	WC - BOLTING	COMMENTS
<p><b>WB-2500 EXAMINATION AND REPAIR OF CONTAINMENT MATERIAL</b></p> <p><b>WB-2580 EXAMINATION OF BOLTS, STUDS, AND NUTS</b></p> <p><b>WB-2581 Requirements</b></p> <p>ALL bolting material shall be visually examined in accordance with WB-2582. Normal sizes greater than 1 in. (25 mm) shall be examined by either the magnetic particle or the liquid penetrant method. In addition, nominal sizes greater than 2 in. (50 mm) but not over 4 in. (100 mm) shall be examined by the ultrasonic method in accordance with WB-2585 and nominal sizes greater than 4 in. (100 mm) shall be examined by the ultrasonic method in accordance with both WB-2585 and WB-2586.</p> <p><b>WB-2582 Visual Examination</b></p> <p>The areas of threads, shanks, and heads of final machined parts shall be visually examined. The requirements of WB-5520 do not apply to personnel performing this examination. Harmful discontinuities such as laps, seams, or cracks that would be detrimental to the intended service are unacceptable.</p> <p><b>WB-2583 Magnetic Particle Examination (for Ferritic Steel Bolting Material Only)</b></p> <p><b>WB-2583.1 Examination Procedures.</b> All bolts, studs, and nuts greater than 1 in. (25 mm) nominal bolt size shall be examined by the magnetic particle method in accordance with ASTM A 275. If desired, the supplier may perform liquid penetrant examination in accordance with WB-2584 instead of magnetic particle examination. Such examination shall be performed on the finished component after threading or on the materials stock at approximately the finished diameter before threading and after heading (if involved).</p>	<p><b>WC-2500 EXAMINATION AND REPAIR OF CONTAINMENT MATERIAL</b></p> <p><b>WC-2580 EXAMINATION OF BOLTS, STUDS, AND NUTS</b></p> <p><b>WC-2581 Requirements</b></p> <p>ALL bolting material shall be visually examined in accordance with WC-2582.</p> <p><b>WC-2582 Visual Examination</b></p> <p>Visual examination shall be applied to the areas of threads, shanks, and heads of final machined parts. Harmful discontinuities such as laps, seams, or cracks that would be detrimental to the intended service are unacceptable.</p>	WB and WC are significantly different.

WB - BOLTING	WC - BOLTING	COMMENTS
<p><b>WB-2583.2 Evaluation of Indications</b></p> <p>(a) All indications shall be evaluated in terms of the acceptance standards. Linear indications are those indications in which the length is more than three times the width. Rounded indications are those which are circular or elliptical with the length equal to or less than three times the width.</p> <p>(b) All indications are not necessarily relevant: leakage of magnetic fields and permeability variations may produce indications that are not relevant to the detection of unacceptable discontinuities. Indications with major dimensions of 1/16 in. (1.5 mm) or less are not relevant.</p> <p>(c) Any indication that is believed to be nonrelevant, and that is larger than acceptable, shall be considered to be a defect and shall be reexamined after light surface conditioning.</p> <p>(d) Any indication observed during such reexamination shall be considered relevant and shall be evaluated in terms of the acceptance standards.</p> <p>(e) As an alternative to magnetic particle reexamination, other nondestructive examination means (such as liquid penetrant examination for surface discontinuities) may be used to determine relevancy.</p> <p><b>WB-2583.3 Acceptance Standard.</b> Linear nonaxial indications are unacceptable. Linear axial indications greater than 1 in. (25 mm) in length are unacceptable.</p> <p><b>WB-2584 Liquid Penetrant Examination</b></p> <p><b>WB-2584.1 Examination Procedure.</b> All bolts, studs, and nuts greater than 1 in. (25 mm) nominal bolt size shall be examined by a liquid penetrant method in accordance with the methods of Section V, Article 6. Such examination shall be performed on the finished component after threading or on the materials stock at approximately the finished diameter before threading and after</p>		

WB - BOLTING	WC - BOLTING	COMMENTS
<p>heading (if involved).</p> <p><b>WB-2584.2 Evaluation of Indications.</b> All indications shall be evaluated in terms of the acceptance standards. Linear indications are those indications in which the length is more than three times the width. Rounded indications are those which are circular to elliptical with the length equal to or less than three times the width. All penetrant indications are not necessarily relevant. Surface imperfections such as machining marks and scratches may produce indications that are nonrelevant to the detection of unacceptable discontinuities. Broad areas of pigmentation, which could mask indications of defects, are unacceptable. Indications with major dimensions of 1/16 in. (1.5 mm) or less are not relevant. Any indication that is believed to be nonrelevant, and that is larger than acceptable, shall be considered to be a defect and shall be reexamined after light surface conditioning. Any area of pigmentation also shall be reexamined after recleaning or light surface conditioning, as appropriate. Any indication observed during such reexamination shall be considered relevant and shall be evaluated in terms of the acceptance standards.</p> <p><b>WB-2584.3 Acceptance Standard.</b> Linear nonaxial indications are unacceptable. Linear axial indications greater than 1 in. (25 mm) long are unacceptable.</p> <p><b>WB-2585 Ultrasonic Examination for Sizes Greater Than 2 in. (50 mm)</b></p> <p>All bolts, studs, and nuts greater than 2 in. (50 mm) nominal bolt size shall be ultrasonically examined over the entire cylindrical surface prior to threading in accordance with the following requirements:</p> <p><b>WB-2585.1 Ultrasonic Method.</b> Examination shall be carried out by the straight-beam, radial-scan method in accordance with Section V, Article 23, SA-388.</p>		

WB - BOLTING	WC - BOLTING	COMMENTS
<p><b>WB-2585.2 Examination Procedures.</b> Examination shall be performed at a nominal frequency of 2.25 MHz with a search unit area not to exceed 1 in.<sup>2</sup> (650 mm<sup>2</sup>).</p> <p><b>WB-2585.3 Calibration of Equipment.</b> Calibration sensitivity shall be established by adjustment of the instrument so that the first back reflection is 75% to 90% of full-screen height.</p> <p><b>WB-2585.4 Acceptance Standard.</b> Any discontinuity that causes an indication in excess of 20% of the height of the first back reflection or any discontinuity that prevents the production of a first back reflection of 50% of the calibration amplitude is not acceptable.</p> <p><b>WB-2586 Ultrasonic Examination for Sizes Over 4 in. (100 mm)</b></p> <p>In addition to the requirements of WB-2585, all bolts, studs, and nuts over 4 in. (100 mm) nominal bolt size shall be ultrasonically examined over the entire surface of each end before or after threading in accordance with the following requirements:</p> <p><b>WB-2586.1 Ultrasonic Method.</b> Examination shall be carried out by the straight-beam, longitudinal-scan method.</p> <p><b>WB-2586.2 Examination Procedure.</b> Examination shall be performed at a nominal frequency of 2.25 MHz with a search unit having a circular cross section with a diameter not less than <math>\frac{1}{2}</math> in. (13 mm) nor more than 1-1/8 in/ (29 mm).</p> <p><b>WB-2586.3 Calibration of Equipment.</b> Calibration shall be established on a test bar of the same nominal composition and diameter as the production part and a minimum of one-half of the length. A 3/8 in. (10 mm) diameter by 3 in. (75 mm) deep flat-bottom hole shall be drilled in one end of the bar and plugged to full depth. A distance-amplitude curve shall be established by scanning from both ends of the test bar.</p>		

WB - BOLTING	WC - BOLTING	COMMENTS
<p><b>WB-2586.4 Acceptance Standard.</b> Any discontinuity that causes an indication in excess of that produced by the calibration hole in the reference specimen as corrected by the distance-amplitude curve is not acceptable.</p> <p><b>WB-2587 Time of Examination</b> Acceptance examinations shall be performed after the final heat treatment required by the basic material specification.</p> <p><b>WB-2588 Elimination of Surface Defects</b> Unacceptable surface defects on finished bolts, studs, and nuts are not permitted, and are cause for rejection.</p> <p><b>WB-2589 Repair by Welding</b> Weld repairs of bolts, studs, and nuts are not permitted.</p>		

WB - BOLTING	WC - BOLTING	COMMENTS
ARTICLE WB-3000 DESIGN	ARTICLE WC-3000 DESIGN	
WB-3100 GENERAL DESIGN  WB-3130 GENERAL DESIGN RULES  WB-3134 Leak Tightness  The leak tightness requirements for each containment shall be set forth in the Design Specification.	WC-3100 GENERAL DESIGN  WC-3130 GENERAL DESIGN RULES  N/A	No similar paragraph exists in WC.
WB-3200 DESIGN RULES FOR CONTAINMENTS  WB-3220 STRESS LIMITS FOR OTHER THAN BOLTS  N/A	WC-3200 DESIGN RULES FOR CONTAINMENTS  WC-3220 DESIGN CONSIDERATIONS  WC-3225 Flat Heads and Covers  Discusses both welded and bolted flat heads and covers, but does not address the design of the bolts  WC-3225.1 Nomenclature  Addresses nomenclature applicable to flat heads and closures.	No similar paragraph exists in WB.
N/A	WC-3225.2 Equations for Minimum Thickness  Provides equations for minimum thickness of flat heads and closures.	No similar paragraph exists in WB.
N/A	Fig. WC-3225-2	No similar paragraph exists in WB.

WB - BOLTING	WC - BOLTING	COMMENTS
	Provides illustrations of some acceptable types of unstayed flat heads and covers.	
<p><b>WB-3230 STRESS LIMITS FOR BOLTS</b></p> <p><i>This paragraph discusses general aspects of stress limits for bolts.</i></p> <p>The evaluation of bolting requires a number of analysis considerations, including (a) through (f) below and the criteria specified in this subsubarticle for the loads imposed.</p> <p>(a) When gaskets are used for preservice testing only, the design is satisfactory if WB-3231 requirements are satisfied for <math>m = y = 0</math>, and the requirements of WB-3232 are satisfied when the appropriate <math>m</math> and <math>y</math> factors are used for the test gasket.</p> <p>(b) The membrane and bending stresses in the bolt produced by thermal expansion due to differences in the temperature or thermal expansion coefficients shall be treated as primary stresses in bolting analysis.</p> <p>(c) The bolting analysis shall consider the effects of loading eccentricities due to puncture loads and eccentric impact loads.</p> <p>(d) The bolting analysis shall consider prying effects, which cause amplification of the bolt loads due to rotation of the closure surfaces.</p> <p>(e) Bolting analysis shall consider bolt preload application methodology and resulting bolt forces.</p> <p>(f) Gasket characteristics and leak tightness requirements shall be considered in the bolting analysis.</p>	N/A	No similar paragraph exists in WC.

WB - BOLTING	WC - BOLTING	COMMENTS
<p><b>WB-3231 Design Limits</b></p> <p><i>This paragraph provides instructions to determine the number and cross-sectional area of bolts.</i></p> <p>The number and cross-sectional area of bolts required to resist the Design Pressure shall be determined in accordance with the procedures of Division 1, Appendix E, using the larger of the bolt loads, given by the equations of Division 1, Appendix E, as a Design Mechanical Load.</p> <p>The stress limits shall be the values given in Section II, Part D, Subpart 1, Table 4 for bolting material.</p>	N/A	No similar paragraph exists in WC.
<p><b>WB-3232 Level A Service Limits</b></p> <p><i>This paragraph addresses stresses in bolts for Level A Service Limits.</i></p> <p>Actual stresses in bolts, such as those produced by the combination of preload, pressure, and differential thermal expansion, may be higher than the values given in Section II, Part D, Subpart 1, Table 4.</p>	N/A	No similar paragraph exists in WC.
<p><b>WB-3232.1 Average Stress</b></p> <p>Provides requirements to handle average bolt stresses.</p> <p>The maximum value of stress, averaged across the bolt cross section and neglecting stress concentrations, shall not exceed two times the stress values of Section II, Part D, Subpart 1, Table 4.</p>	N/A	No similar paragraph exists in WC.

WB - BOLTING	WC - BOLTING	COMMENTS
<p><b>WB-3232.2 Shear Stress:</b></p> <p>Provides requirements to handle average bolt shear stresses.</p> <p>The average bolt shear stress expressed in terms of available shear stress area shall not exceed <math>1.2 Sm</math> (at temperature) from Section II, Part D, Subpart 1, Table 4.</p>	N/A	No similar paragraph exists in WC.
<p><b>WB-3232.3 Maximum Stress</b></p> <p>Provides requirements for handling maximum stress in bolts.</p> <p>The maximum value of stress, except as restricted by WB-3232.4(b), at the periphery of the bolt cross section resulting from direct tension plus bending, and neglecting stress concentrations, shall not exceed three times the stress values of Section II, Part D, Subpart 1, Table 4. Stress intensity, rather than maximum stress, shall be limited to this value when the bolts are tightened by methods other than heaters, stretchers, or other means that minimize residual torsion.</p>	N/A	No similar paragraph exists in WC.
<p><b>WB-3232.4 Fatigue Analyses of Bolts</b></p> <p>Provides requirements for handling fatigue analyses in bolts. Contains parts (a) through (e).</p> <p>Unless the components on which they are installed meet all the conditions of WB-3222.9(d) and thus require no fatigue analysis, the suitability of bolts for cyclic service shall be determined in accordance with the procedures of (a) through (e) below.</p> <p>Thermal stress ratchet shall be evaluated in accordance with WB-3222.9(a).</p> <p>(a) <i>Bolting Having Less Than 100.0 ksi (689 MPa) Tensile</i></p>	N/A	No similar paragraph exists in WC.

WB - BOLTING	WC - BOLTING	COMMENTS
<p><i>Strength.</i> Bolts made of material which has specified minimum tensile strength of less than 100.0 ksi (689 MPa) shall be evaluated for cyclic service by the methods of WB-3222.9(e), using the applicable design fatigue curve of Division 1, Appendix I, Figs. 1-9.0 and an appropriate fatigue strength reduction factor [WB-3232.4(c)].</p> <p>(b) <i>High Strength Alloy Steel Bolting.</i> High strength alloy steel bolts and studs may be evaluated for cyclic service by the methods of WB-3222.9(e) using the design fatigue curve of Division 1, Appendix I, Figs. 1-9.4 provided:</p> <ul style="list-style-type: none"> <li>(1) the maximum value of the stress (WB-3232.3) at the periphery of the bolt cross section, resulting from direct tension plus bending and neglecting stress concentration, shall not exceed <math>2.7Sm</math> if the higher of the two fatigue design curves given in Division 1, Appendix I, Figs. 1-9.4 is used. The <math>2Sm</math> limit for direct tension is unchanged.</li> <li>(2) threads shall be of a Vee-type having a minimum thread root radius no smaller than 0.003 in. (0.08 mm).</li> <li>(3) fillet radii at the end of the shank shall be such that the ratio of fillet radius to shank diameter is not less than 0.060.</li> </ul> <p>(c) <i>Fatigue Strength Reduction Factor (WB 3213.17).</i> Unless it can be shown by analysis or tests that a lower value is appropriate, the fatigue strength reduction factor used in the fatigue evaluation of threaded members shall be not less than 4.0. However, when applying the rules of WB-3232.4(b) for high strength alloy steel bolts, the value used shall be not less than 4.0.</p> <p>(d) <i>Effect of Elastic Modulus.</i> Multiply <math>S_{alt}</math> (as determined in WB-3216.1 or WB-3216.2) by the ratio of the modulus of elasticity given on the design fatigue curve to the value of</p>		

WB - BOLTING	WC - BOLTING	COMMENTS
<p>the modulus of elasticity used in the analysis. Enter the applicable design fatigue curve at this value on the ordinate axis and find the corresponding number of cycles on the abscissa. If the cyclic service being considered is the only one which produces significant fluctuating stresses, this is the allowable number of cycles.</p> <p>(e) <i>Cumulative Damage.</i> The bolts shall be acceptable for the specified cyclic application of loads and thermal stresses provided the cumulative usage factor U, as determined in WB-3222.9(e)(5), does not exceed 1.0.</p>		
<p><b>WB-3234 Level D Service Limits</b></p> <p>This paragraph addresses stresses in bolts for Level A Service Limits.</p> <p>(a) The rules contained in Division 1, Appendix F may be used in evaluating loadings for which Level D Service Limits are specified, independently of all other loadings.</p> <p>(b) If leak tightness of the closure is required by the Design Specification, the analysis of the bolting shall demonstrate that no yielding occurs in the bolt or sealing surface materials. This requirement may be satisfied by using the rules of WB-3232.</p>	N/A	No similar paragraph exists in WC.
<p><b>WB-3235 Testing Limits</b></p> <p>Bolts shall not yield for test conditions.</p>	N/A	No similar paragraph exists in WC.
<p><b>WB-3236 Design Stress Intensity Values</b></p> <p>States where Design Stress intensity values may be found.</p>	N/A	No similar paragraph exists in WC.

WB - BOLTING	WC - BOLTING	COMMENTS
The design stress intensity values $Sm$ are given in Section II, Part D, Subpart 1, Table 4 for bolting. Values for intermediate temperature may be found by interpolation.		
ARTICLE WB-4000 FABRICATION	ARTICLE WC-4000 FABRICATION	
<b>WB-4700 MECHANICAL JOINTS</b>	<b>WC-4700 MECHANICAL JOINTS</b>	WB and WC are identical.
<b>WB-4710 BOLTING AND THREADING</b>	<b>WC-4710 BOLTING AND THREADING</b>	
<b>WB-4711 Thread Engagement</b>  The threads of all bolts or studs shall be engaged in accordance with the design.	<b>WC-4711 Thread Engagement:</b>  The threads of all bolts or studs shall be engaged in accordance with the design.	
<b>WB-4712 Thread Lubricants</b>  Any lubricant or compound used in threaded joints shall be suitable for the service conditions and shall not react unfavorably with either the service fluid or any <u>containment</u> material in the system.	<b>WC-4712 Thread Lubricants</b>  Any lubricant or compound used in threaded joints shall be suitable for the service conditions and shall not react unfavorably with either the service fluid or any <u>component</u> material in the system.	WB and WC are identical except that the word <u>containment</u> is used in WB, and the word <u>component</u> is used in WC. This difference is acceptable.
<b>WB-4713 Removal of Thread Lubricants</b>  All threading lubricants or compounds shall be removed from surfaces which are to be seal welded.	<b>WC-4713 Removal of Thread Lubricants</b>  All threading lubricants or compounds shall be removed from surfaces which are to be seal welded.	WB and WC are identical.
<b>WB-4720 Bolting Flanged Joints</b>  This paragraph discusses bolting of gasketed flange joints.	<b>WC-4720 Bolting Flanged Joints</b>  This paragraph discusses bolting of gasketed flange joints.	WB and WC are identical.

WB - BOLTING	WC - BOLTING	COMMENTS
<p>In bolting gasketed flanged joints, the contact faces of the flanges shall bear uniformly on the gasket and the gasket shall be properly compressed in accordance with the design principles applicable to the type of gasket used.</p> <p>All flanged joints shall be made up with relatively uniform bolt stress.</p>	<p>In bolting gasketed flanged joints, the contact faces of the flanges shall bear uniformly on the gasket and the gasket shall be properly compressed in accordance with the design principles applicable to the type of gasket used.</p> <p>All flanged joints shall be made up with relatively uniform bolt stress.</p>	

**Table 2 Comparison of Requirements for Design Based on Stress Analysis of Bolts in ASME Section III, Subsection WB-3000 and Appendix XIII**

	Article WB-3200	Article XIII-1100
Stress Limits & bolt and gasket requirements	<p><b>WB-3230 Stress Limits for Bolts</b></p> <p>The evaluation of bolting requires a number of analysis considerations, including (a) through (f) below and the criteria specified in this subsubarticle for the loads imposed.</p> <p>(a) When gaskets are used for preservice testing only, the design is satisfactory if WB-3231 requirements are satisfied for <math>m = y = 0</math>, and the requirements of WB-3232 are satisfied when the appropriate <math>m</math> and <math>y</math> factors are used for the test gasket.</p> <p><b>WB-3231 Design Limits</b></p> <p>The number and cross-sectional area of bolts required to resist the Design Pressure shall be determined in accordance with the procedures of Division 1, Appendix E, using the larger of the bolt loads, given by the equations of Division 1, Appendix E, as a Design Mechanical Load.</p> <p>The stress limits shall be the values given in Section II, Part D, Subpart 1, Table 4 for bolting material.</p>	<p><b>XIII-1180 BOLTING</b></p> <p><b>XIII-1181 Bolt and Gasket Requirements</b></p> <p>(a) The number and cross-sectional area of bolts required to resist internal pressure shall be determined in accordance with the procedures of Mandatory Appendix XI. The allowable bolt design stresses, as used in the equations of Mandatory Appendix XI, shall be the values given in Section II, part D, Subpart 1, Table 4 for bolting materials. When sealing is affected by a seal weld instead of a gasket, the gasket factor <math>m</math> and the minimum design seating stress <math>y</math> may be taken as zero.</p> <p>(b) When gaskets are used for preservice testing only, the design is satisfactory if the above requirements are satisfied for <math>m=y=0</math> and the requirements of XIII-1182 are satisfied when the appropriate <math>m</math> and <math>y</math> are used for test gasket.</p>
Maximum Service Stress	<p><b>WB-3232.1 Average Stress</b></p> <p>The maximum value of stress, averaged across the bolt cross section and neglecting stress concentrations, shall not exceed two times the stress values of Section II, Part D, Subpart 1, Table 4.</p> <p><b>WB-3232.3 Maximum Stress</b></p>	<p><b>XIII-1182 Allowable Maximum Service Stresses in Bolts</b></p> <p>It is recognized that actual service stresses in bolts, such as those produced by the combination of preload, pressure, and differential thermal expansion, may be higher than the values given in Section II,</p>

	<p>Provides requirements for handling maximum stress in bolts.</p> <p>The maximum value of stress, except as restricted by WB-3232.4(b), at the periphery of the bolt cross section resulting from direct tension plus bending and neglecting stress concentrations shall not exceed three times the stress values of Section II, Part D, Subpart 1, Table 4. Stress intensity, rather than maximum stress, shall be limited to this value when the bolts are tightened by methods other than heaters, stretchers, or other means that minimize residual torsion.</p>	<p>Part D, Subpart 1, Table 4. The maximum of such service stress, averaged across the bolt cross section and neglecting stress concentrations, shall not exceed two times the stress values of Section II, Part 1, Table 4. Except as restricted by XIV-1322(b), the maximum value of such service stress as the periphery of the bolt cross section resulting from direct tension plus bending and neglecting stress concentrations shall not exceed three times the stress values of Section II, Part D, Subpart 1, Table 4. Stress intensity, rather than maximum stress, shall be limited to this value when the bolts are tightened by methods other than heaters, stretchers, or other means that minimize residual torsion.</p>
--	---	---

**Table 3 Comparison of Requirements for Analysis of Cyclic Service of Bolts in ASME Section III, Subsection WB-3000 and Appendix XIV**

	<b>Article WB-3232.4</b>	<b>Article XIV-1300</b>
Bolts with less than 100 ksi tensile strength	WB-3232.4(a) Requires appropriate fatigue strength reduction factor	Requires that fatigue strength reduction factor not be less than 4
High-strength bolting	WB-3232.4(b) does not specify material	Specifies materials: SA-193 Grade B7 or B-16 SA-320 Grade L-43 SA-540 Grades B-23 and B-24
Maximum value of stress intensity at the periphery of bolt cross section	WB-3232.4(b)(1)	XIV-1322(b) The requirements are exactly the same.
Thread type and fillet radii	WB-3232.4(b)(2) and (3)	XIV-1322(c) and (d) The requirements are exactly the same.
Fatigue strength reduction factor	WB-3232.4(c) <sup>1</sup>	XIV-1324 Both articles require that the factor not be less than 4 unless a lower value can be justified.
Effect of elastic modulus	WB-3232.4(d)	Not considered.
Cumulative damage	WB-3232.4(f)	XIV-1323 The requirements are exactly the same.

<sup>1</sup>The last statement in WB-3232.4(c) is confusing. It states, “However, when applying the rules of WB-3232.4(b) above for high strength alloy steel bolts, the value used shall not be less than 4.0.” This statement is not included in the above comparison.

# FCT Quality Assurance Program Document

## Appendix E FCT Document Cover Sheet

Name/Title of Deliverable/Milestone

Used Fuel Disposition (UFD) Year End Letter Report – FY2012

Work Package Title and Number

ST Transportation - ANL

Work Package WBS Number

FT-12AN081301

Responsible Work Package Manager

Yung Liu

(Name/Signature)

Date Submitted 9/11/2012

Quality Rigor Level for Deliverable/Milestone	<input checked="" type="checkbox"/> QRL-3	<input type="checkbox"/> QRL-2	<input type="checkbox"/> QRL-1	<input type="checkbox"/> N/A*
			<input type="checkbox"/> Nuclear Data	

This deliverable was prepared in accordance with

Argonne National Laboratory

*(Participant/National Laboratory Name)*

QA program which meets the requirements of

DOE Order 414.1       NQA-1-2000

### This Deliverable was subjected to:

Technical Review

Peer Review

### Technical Review (TR)

### Peer Review (PR)

### Review Documentation Provided

Signed TR Report or,

Signed PR Report or,

Signed TR Concurrence Sheet or,

Signed PR Concurrence Sheet or,

Signature of TR Reviewer(s) below

Signature of PR Reviewer(s) below

### Name and Signature of Reviewers

Yung Liu

\_\_\_\_\_  
\_\_\_\_\_  
\_\_\_\_\_

\*Note: In some cases there may be a milestone where an item is being fabricated, maintenance is being performed on a facility, or a document is being issued through a formal document control process where it specifically calls out a formal review of the document. In these cases, documentation (e.g., inspection report, maintenance request, work planning package documentation or the documented review of the issued document through the document control process) of the completion of the activity along with the Document Cover Sheet is sufficient to demonstrate achieving the milestone. QRL for such milestones may be also be marked N/A in the work package provided the work package clearly specifies the requirement to use the Document Cover Sheet and provide supporting documentation.

## **APPENDIX B**

### **Cladding Embrittlement Concerns for Storage and Transportation of High-Burnup Fuel**

# **Cladding Embrittlement Concerns for Storage and Transportation of High-Burnup Fuel**

M.C. Billone and Y.Y. Liu  
Argonne National Laboratory  
September 10, 2012

Structural analyses of high-burnup fuel require cladding mechanical properties and failure limits to assess fuel behavior during long-term dry cask storage and transportation. Pre-storage drying-transfer operations and early stage storage subject cladding to higher temperatures and much higher hoop stresses relative to in-reactor operation and pool storage. Under these conditions, radial hydrides may precipitate during slow cooling and provide an additional embrittlement mechanism as the cladding temperature decreases below the ductile-to-brittle transition temperature (DBTT).

In Interim Staff Guidance – 11, Revision 3 (ISG-11 Rev. 3), the NRC recommends a peak cladding temperature limit of 400°C for drying-transfer operations and storage of used fuel in storage and transport casks containing high-burnup fuel [1]. Limits are also placed on the number of drying cycles and the temperature drop per cycle. One concern for high-burnup cladding is the possible precipitation of radial hydrides, which could embrittle cladding in response to tensile hoop stress caused by the internal pressure loading. Limits established in ISG-11 Rev. 3 relied on data available prior to 2003, which were primarily for low-burnup and non-irradiated/pre-hydrided Zircaloy-4. At the time ISG-11 Rev. 3 was issued, NRC recognized that data for all high-burnup cladding alloys were needed to determine the extent of radial-hydride embrittlement under conditions relevant to drying-transfer operations and storage. Data generated since 2003, mostly at Argonne, indicate that limits imposed by ISG-11 Rev. 3 do not protect high-burnup cladding from embrittlement due to radial hydrides. Recent NRC reviews of applications for license renewal of the Prairie Island ISFSI and Amendment 5 of the CoC for Transnuclear MP-197 have raised concerns for long-term storage and transportation of high-burnup fuel. The issues are summarized in “Compatibility of Requirements for Storage and Transportation of Spent Nuclear Fuel (Retrievability, Cladding Integrity, and Safe Handling),” — a summary paper presented at the NRC Public Meeting to obtain stakeholder feedback on enhancements to the licensing and inspection programs for spent fuel storage and transportation under 10 CFR Parts 71 and 72 [2]. A major concern is whether or not the high-burnup fuel will maintain cladding integrity and be readily retrievable after more than 20 years of storage. License approvals for the transport of high-burnup fuel have been delayed because of a lack of data on high-burnup fuel cladding embrittlement after more than 20 years of storage, which corresponds to peak cladding temperatures of  $\approx$ 200°C or less.

## **Status of the Database for High-Burnup Cladding Embrittlement**

Argonne has developed a test protocol for studying high-burnup cladding embrittlement that has been approved by NRC. Experimentally, the protocol involves two steps: (1) radial-hydride treatment (RHT), during which high-burnup cladding is exposed to simulated drying-storage temperature and hoop stress conditions, including slow cooling, and (2) a ring compression test (RCT), for which a sample ring from the RHT high-burnup cladding is compressed to determine strength and ductility as function of test temperature. The RCT is used as a ductility screening test to simulate pinch-type loading on the high-burnup cladding that occurs during normal conditions of cask transport and/or drop accidents. The protocol was used to generate the DBTT data for high-burnup Zircaloy-4 and ZIRLO™ [3] (sponsored by NRC) and high-burnup M5® (sponsored by DOE) [4]. Under DOE-sponsored research, Argonne has also generated baseline properties for the strength and ductility of as-irradiated (i.e., pre-drying) Zry-4,

ZIRLO™, and M5® that are important not only to determine the degrading effects of drying and early stage storage, but also to serve as references for other high-burnup cladding alloys in future studies.

Argonne data were generated for the peak cladding temperature (400°C) recommended in ISG-11 (Rev. 3) for drying-transfer operations and storage. Peak cladding hoop stresses at 400°C were 110 MPa and 140 MPa, which are in the intermediate range of the 80–160 MPa characteristic of high-burnup PWR fuel rods. The upper limit is based on the industry technical specification limit of  $\approx$ 3200 psi (22 MPa) internal pressure for in-reactor operation, which is intended to prevent cladding liftoff from the fuel. The internal gas pressure is due to as-fabricated helium fill gas, fission gas release (increases with burnup), and helium release from certain burnable poisons (e.g., ZrB<sub>2</sub> coating used in Westinghouse's Integral Fuel Burnable Absorber [IFBA] design).

Figure 1 shows the hydride distribution and orientation in high-burnup ZIRLO™ before (Fig. 1a) and after (Fig. 1b) subjecting the cladding to slow cooling (5°C/h) from 400°C and decreasing tensile hoop stress from 140 MPa. Hydrogen contents for both samples were high (530 wppm and 650 wppm). The extent of radial-hydride precipitation (extending through 80% of the wall thickness) following slow cooling is quite dramatic. Figure 2 compares the ductility and strength of as-irradiated (tested at 30°C) and RHT high-burnup cladding (tested at 150°C) in ring compression tests. Even with the elevated test temperature, the ductility decreased from 7% to 0% and the strength (based on the 1<sup>st</sup> load-drop) decreased by 60% as a result of exposure to simulated drying-storage conditions. Furthermore, RHT high-burnup ZIRLO™ failed (>50% wall crack) during elastic loading and exhibited no plastic deformation. The DBTT for high-burnup ZIRLO™ is clearly >150°C for a peak drying-storage stress of 140 MPa. In a second set of tests, the simulated drying-storage peak stress was reduced to 110 MPa. At the lower stress level, the DBTT decreased by about 60°C to 125°C.

Figure 3 shows the hydride distribution and orientation in high-burnup M5® before (Fig. 3a) and after (Fig. 3b) subjecting the cladding to 400°C and 140 MPa and slow cooling (5°C/h). Hydrogen contents for both samples were low (76 wppm and 94 wppm), which is characteristic of high-burnup M5®. The hydrides in Fig. 3a are oriented primarily in the circumferential direction, with some of the hydrides oriented in the radial direction. During cooling from simulated drying-storage conditions, long radial hydrides precipitated (see Fig. 3b). Figure 4 compares the ductility and strength of as-irradiated (tested at 26°C) and RHT (tested at 60°C) high-burnup M5® in ring compression tests. The ductility decreased from >10% to 0%, and the strength (based on the 1<sup>st</sup> load-drop) decreased by about 50% as a result of simulated drying-storage conditions. Furthermore, the RHT high-burnup M5® failed (>50% wall crack) during elastic loading and exhibited no plastic deformation. Figure 5 shows the extensive cracking in RHT M5® for the 60°C RCT temperature. Ductility was retained at 90°C RCT temperature. The DBTT for high-burnup M5® was about 80°C for a peak drying-storage stress of 140 MPa. Lowering the peak drying-storage stress to 110 MPa decreased the DBTT by only 10°C, as illustrated in Figure 6.

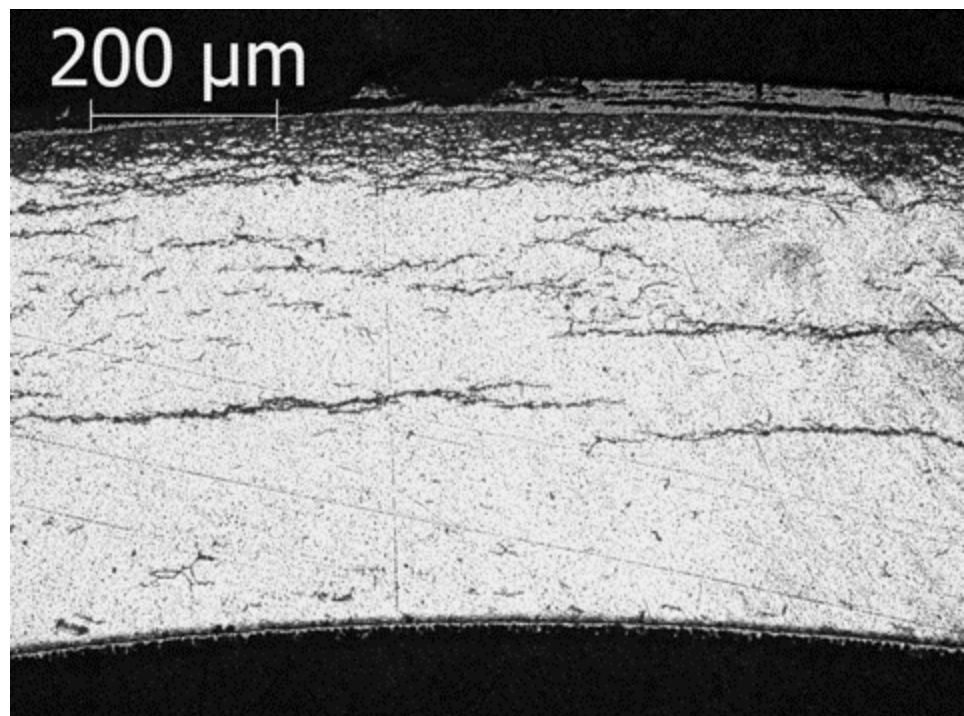
Figures 7 and 8 show DBTT curves for three high-burnup (HB) PWR cladding alloys following RHT at 400°C and peak hoop stresses of 140 MPa and 110 MPa, respectively. "HB Clad C" data are from the DOE-sponsored work using HB M5® [4]. NRC will release identification of and data for "HB Clad A" and "HB Clad B" after Ref. 5 is accepted for publication (the paper was submitted in June 2012). For the 140-MPa case (Fig. 7), the DBTT values are about 55°C, 185°C, and 80°C for HB Clad alloys A, B, and C, respectively. Lowering the peak RHT hoop stress to 110 MPa (Fig. 8) decreased the DBTT values to <25°C, 125°C, and 70°C, respectively. The effect of the peak tensile hoop stress is most pronounced for HB Clad alloy B; the DBTT drops from 185°C to 125°C, which is too high for transport and/or retrieval. The DBTTs for HB Clad alloys A and C are lower than that of HB Clad alloy B, but they are still above ambient.

To complete the DBTT curves for the relevant range of drying-storage peak temperatures, data are needed for PWR high-burnup cladding alloys subjected to 80 and 160 MPa and BWR high-burnup Zry-2 subjected to 60–120 MPa at the ISG-11 (Rev. 3) -recommended limit of 400°C and with limited temperature cycling. As cladding temperatures are likely to be <400°C by using current cask loading and drying practices, RCT tests should be repeated at 350°C for PWR high-burnup cladding (80–160 MPa) and for BWR high-burnup cladding alloys (at 60–120 MPa). Specific test matrices can be found in the appendix of Ref. 4. The goal of the planned Argonne RCT testing and modeling is to define the parameter space, mainly temperature and hoop stress, to minimize radial-hydride embrittlement such that the DBTT could fall below ambient for each HB Clad alloy.

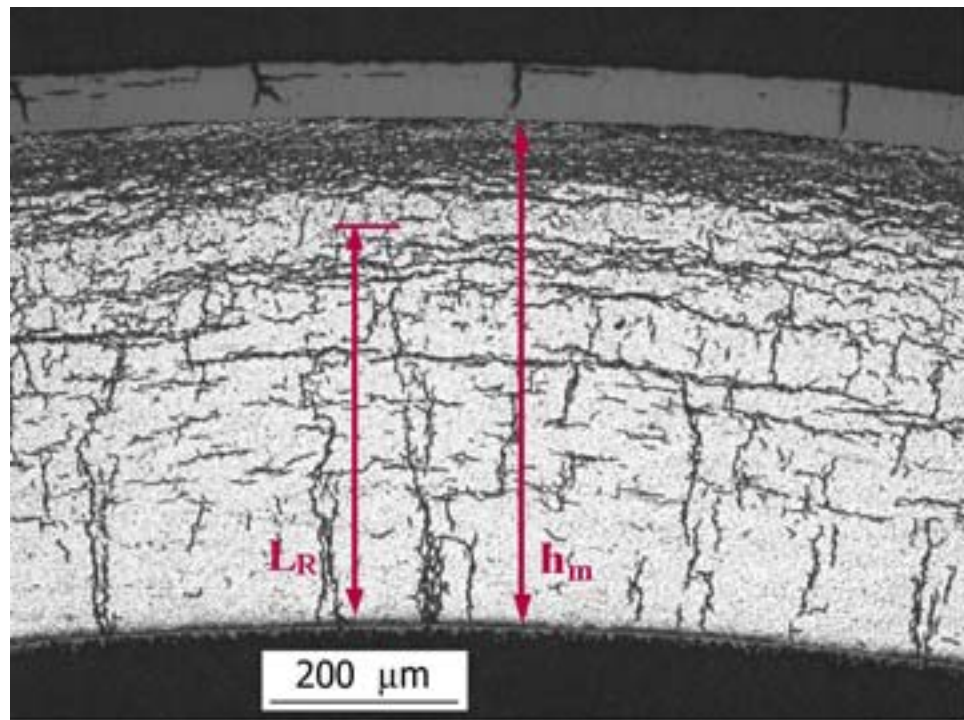
Note that from the load-displacement curves in the ring compression tests, one can obtain stress and strain mechanical properties and failure limits above and below the DBTT for each HB Clad alloy. Such data are directly applicable in the structural analyses to support license applications for long-term storage and transportation of high-burnup fuels.

## References

- 1) Nuclear Regulatory Commission 2003 Interim Staff Guidance (ISG)-11, Revision 3, “Cladding Considerations for the Transportation and Storage of Spent Fuel,” November 2003. [ML033230335 at <http://www.nrc.gov/reading-rm/adams.html>]
- 2) NRC Public Meeting Obtain Stakeholder Feedback on Enhancements to the Licensing and Inspection Programs for Spent Fuel Storage and Transportation under 10 CFR Parts 71 and 72, August 16–17, 2012, Rockville, MD. [<http://www.nrc.gov/public-involve/conference-symposia/2012-sfst-lic-process-conf.html>]
- 3) T.A. Burtseva, Y. Yan, and M.C. Billone, “Radial-Hydride-Induced Embrittlement of High-Burnup ZIRLO Cladding Exposed to Simulated Drying Conditions,” ANL letter report to NRC, June 20, 2010. Available online as ML101620301 at <http://www.nrc.gov/reading-rm/adams/web-based.html>.
- 4) M.C. Billone, T.A. Burtseva, J.P. Dobrzynski, D.P. McGann, K. Byrne, Z. Han, and Y.Y. Liu, “Phase I Ring Compression Testing of High-Burnup Cladding,” FCRD-USED-2012-000039, Dec. 31, 2011.
- 5) M.C. Billone, T.A. Burtseva, and R.E. Einziger, “Ductile-to-Brittle Transition Temperature for High-Burnup Cladding Alloys Exposed to Simulated Drying-Storage Conditions,” submitted to Journal of Nuclear Materials (June 2012).



(a) As-irradiated



(b) After simulated drying-storage

Fig. 1. Hydride distribution and orientation in high-burnup ZIRLO™ cladding: (a) as-irradiated with 530-wppm hydrogen and (b) after simulated drying-storage conditions (at 400°C and 140 MPa) with 650-wppm hydrogen.

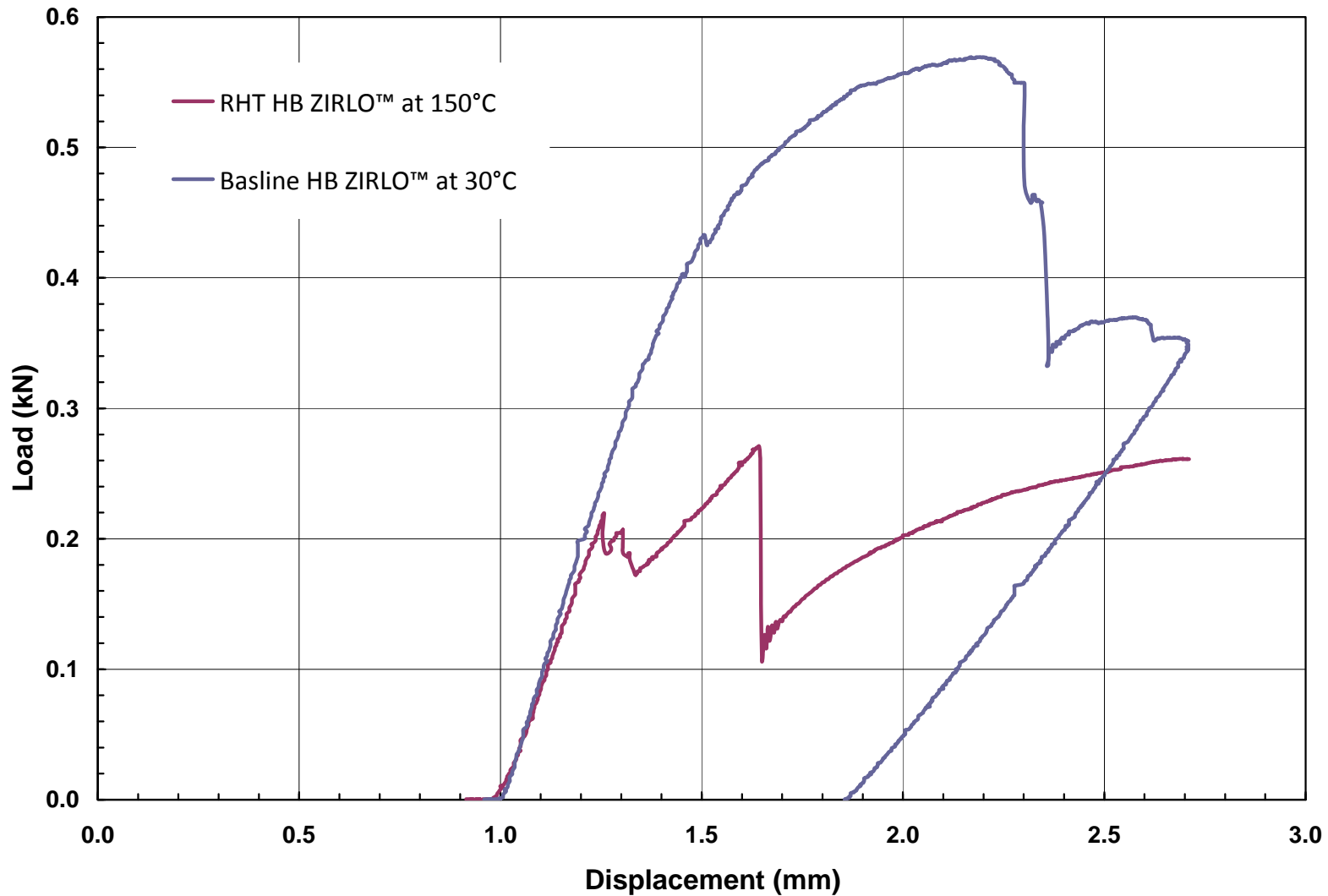


Fig. 2. RCT load-displacement curves for high-burnup ZIRLO™: (a) baseline as-irradiated condition (pre-drying, see Fig. 1a) tested at 30°C and (b) following simulated drying-storage conditions or RHT (see Fig. 1b) tested at 150°C.

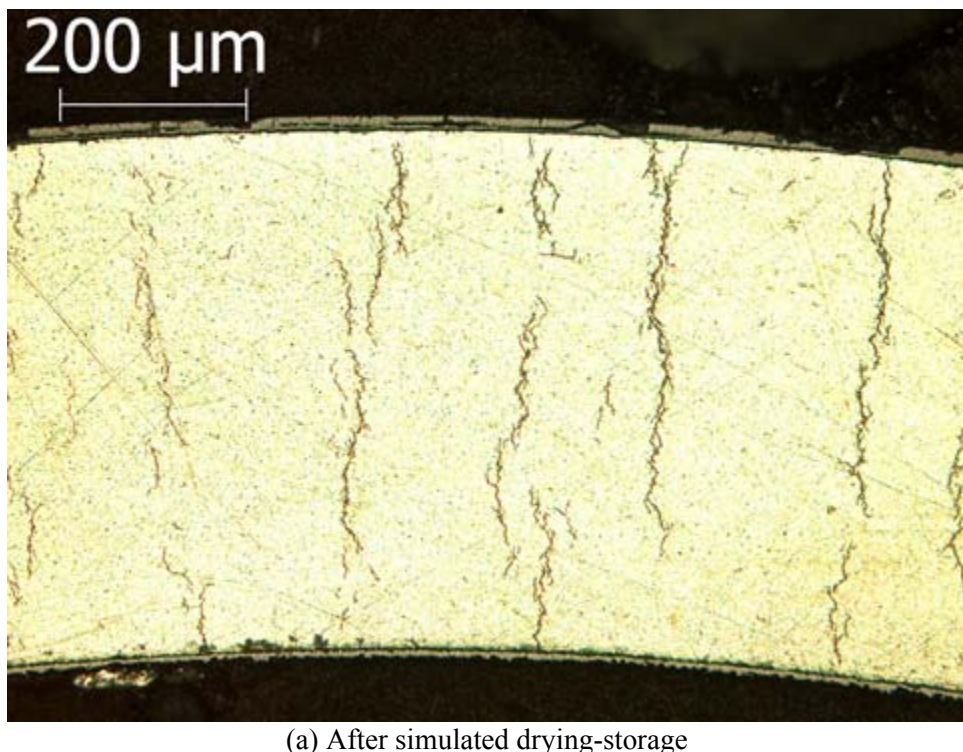
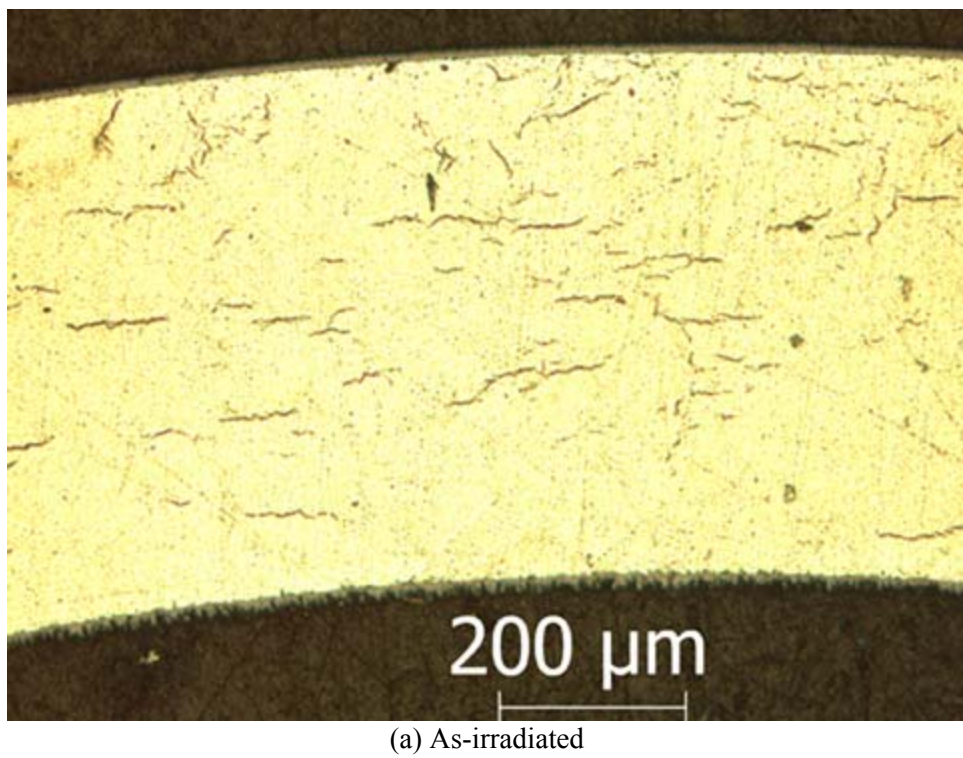


Fig. 3. Hydride distribution and orientation in high-burnup M5® cladding: (a) as-irradiated with 76-wppm hydrogen and (b) after simulated drying-storage conditions (at 400°C and 140 MPa) with 94-wppm hydrogen.

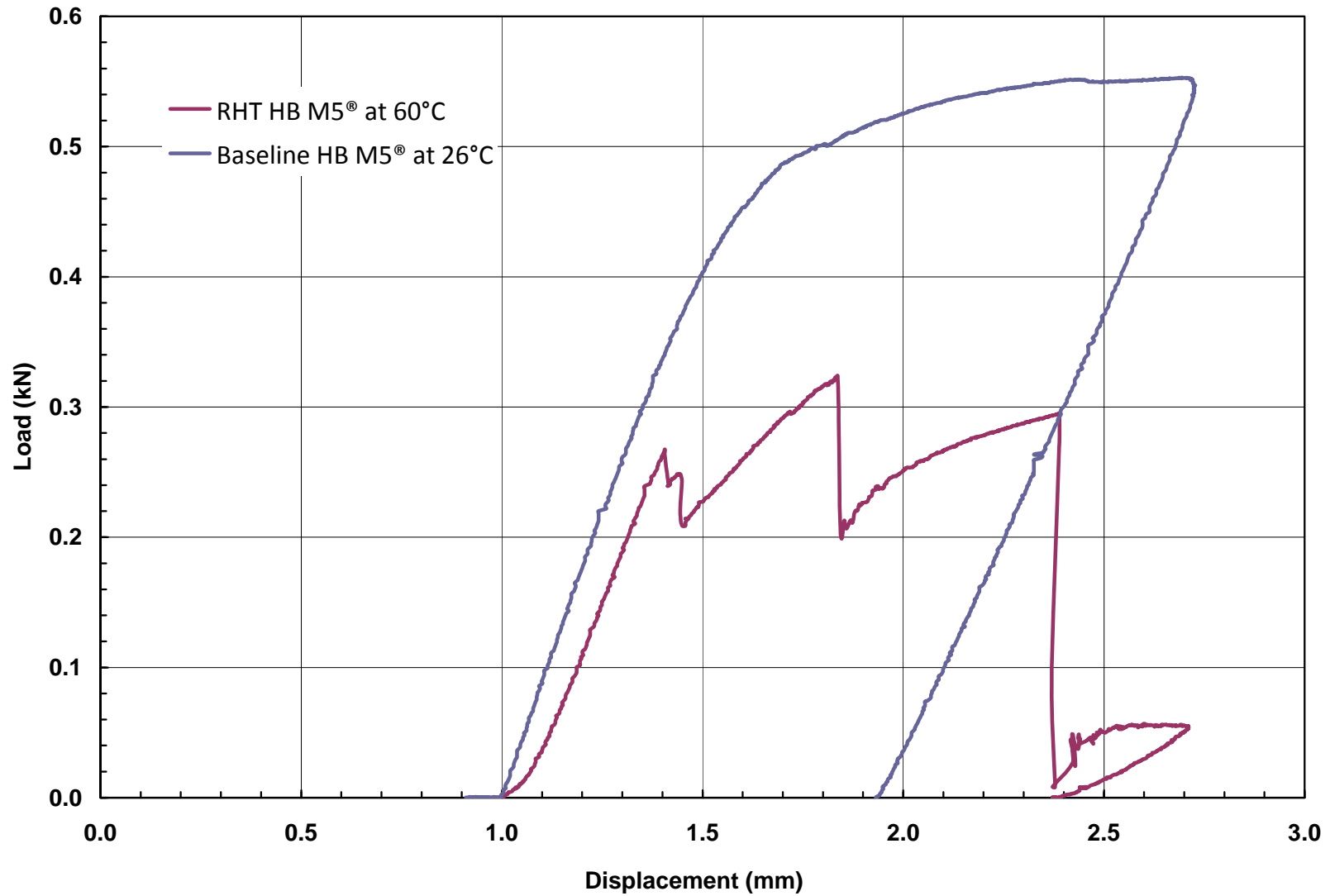
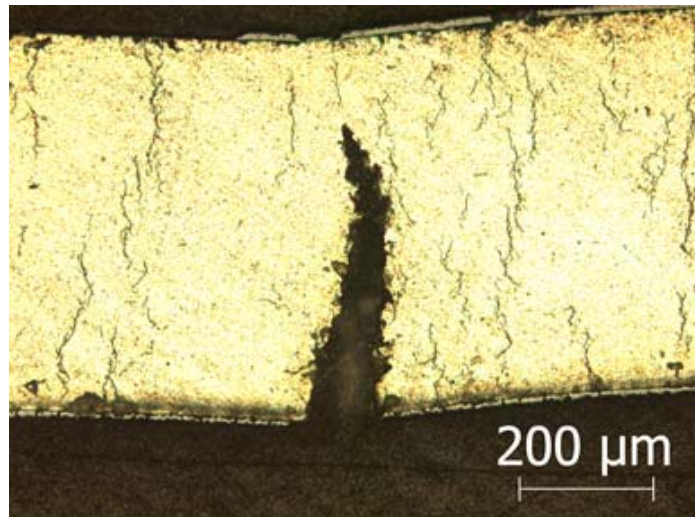
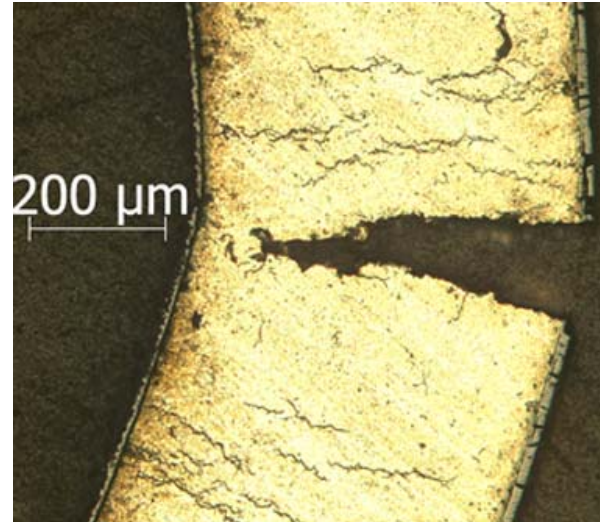


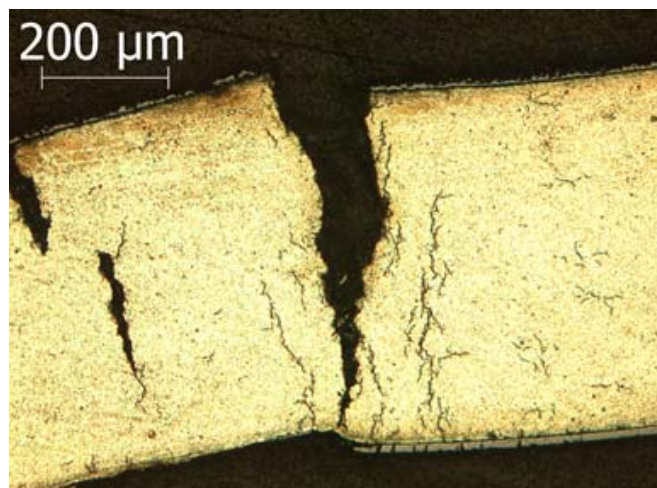
Fig. 4. RCT load-displacement curves for high-burnup M5<sup>®</sup>: (a) as-irradiated condition (pre-drying, see Fig. 3a) tested at 26°C and (b) following simulated drying-storage conditions (see Fig. 3b) tested at 60°C.



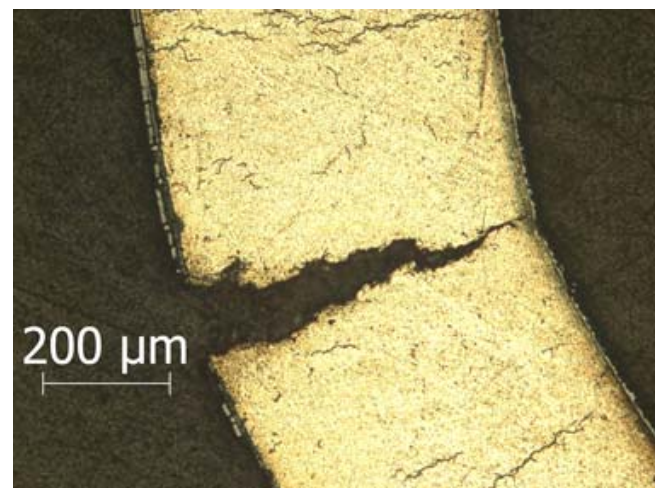
(a) 12 o'clock



(b) 3 o'clock



(c) 6 o'clock



(d) 9 o'clock

Fig. 5. Major cracks that formed during 60°C RCT of high-burnup M5® following simulated drying-storage conditions at 400°C and 140 MPa.

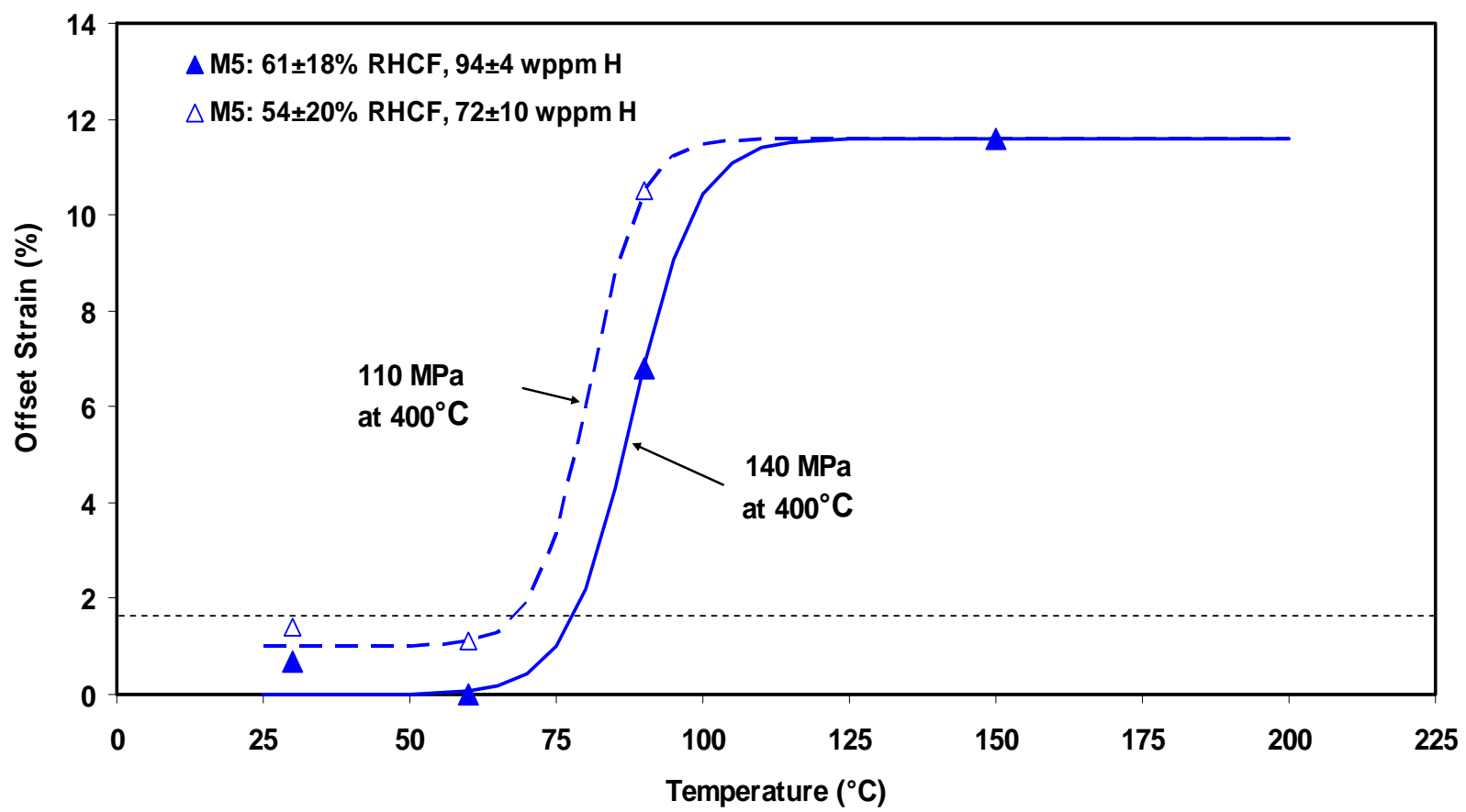


Fig. 6. Ductile-to-brittle transition temperatures (DBTT) of high-burnup M5<sup>®</sup> as determined in RCT following simulated drying-storage conditions at 400°C and 140 and 110 MPa hoop stresses, respectively. RHCF is the radial hydride continuity factor.

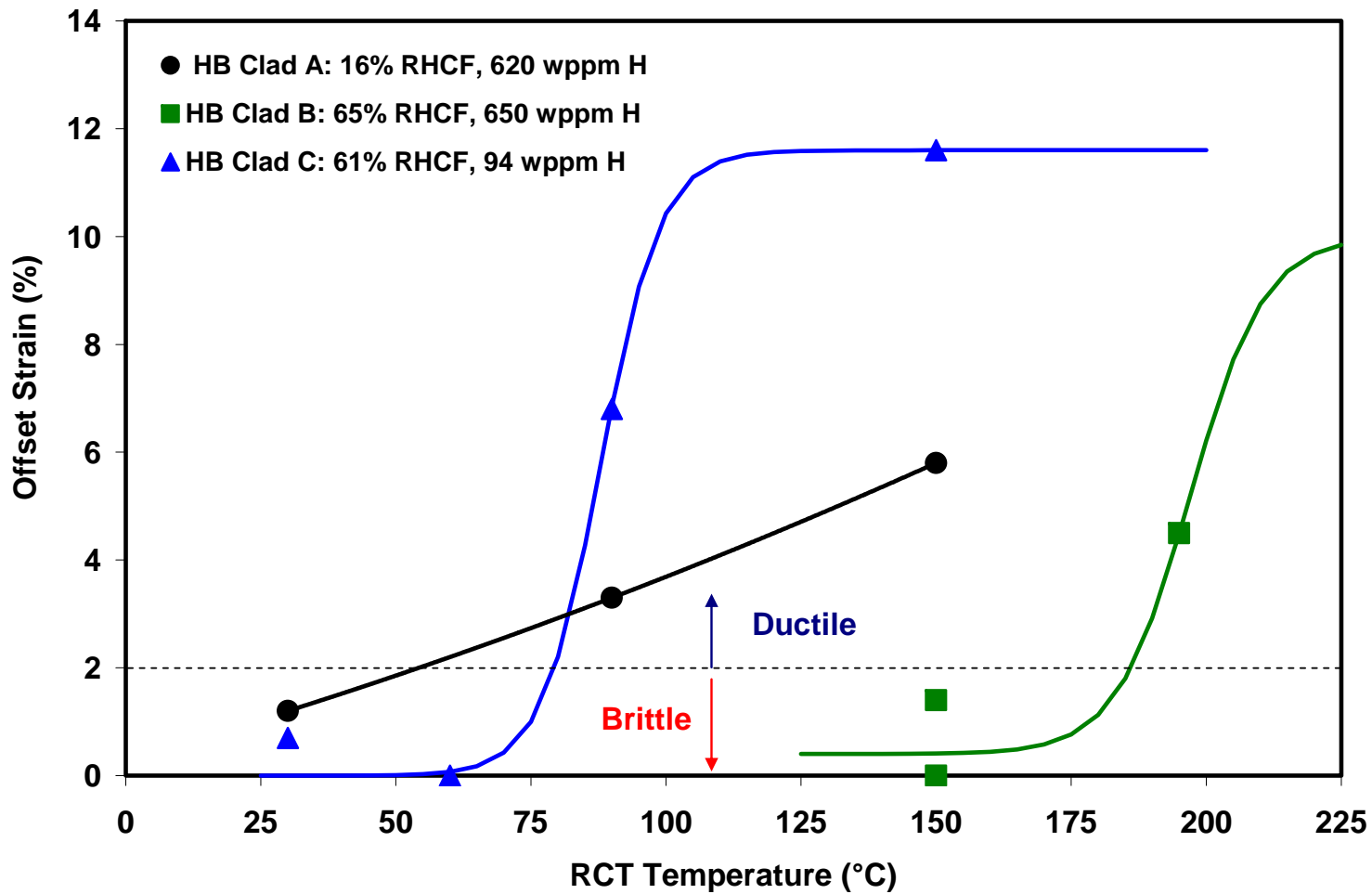


Fig. 7. RCT ductility data vs. test temperature for high-burnup (HB) PWR cladding alloys following slow cooling at 5°C/h from 400°C and 140-MPa hoop stress. RHCF is the radial hydride continuity factor.

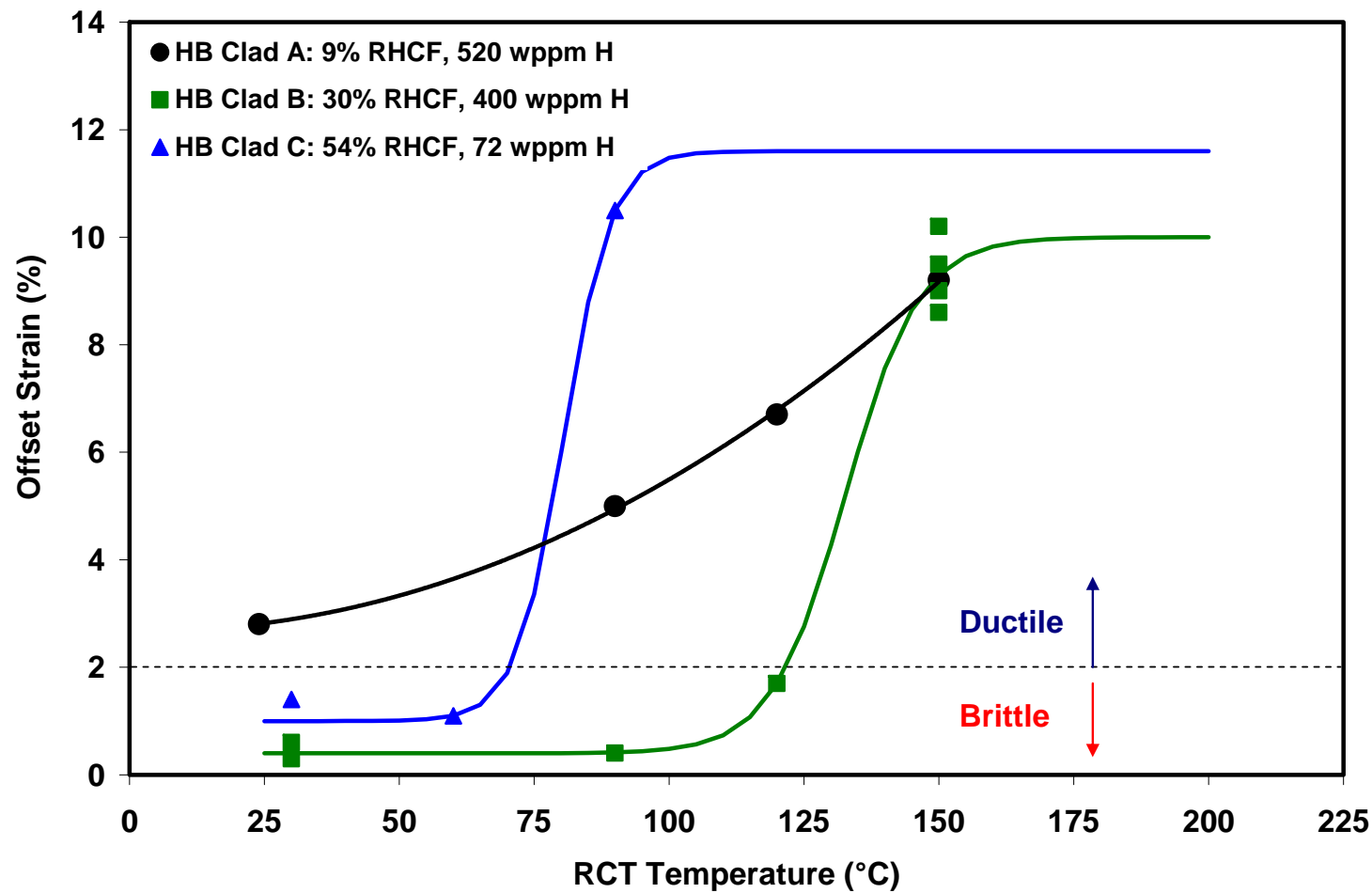


Fig. 8. RCT ductility data vs. test temperature for high-burnup (HB) PWR cladding alloys following slow cooling at 5°C/h from 400°C and 110-MPa hoop stress. RHCF is the radial hydride continuity factor.

# FCT Quality Assurance Program Document

## Appendix E FCT Document Cover Sheet

Name/Title of Deliverable/Milestone

Used Fuel Disposition (UFD) Year End Letter Report – FY2012

Work Package Title and Number

ST Engineering Materials Experimental - ANL

Work Package WBS Number

FT-12AN080508

Responsible Work Package Manager

Yung Liu

(Name/Signature)

Date Submitted 9/10/2012

Quality Rigor Level for Deliverable/Milestone	<input checked="" type="checkbox"/> QRL-3	<input type="checkbox"/> QRL-2	<input type="checkbox"/> QRL-1	<input type="checkbox"/> N/A*
			<input type="checkbox"/> Nuclear Data	

This deliverable was prepared in accordance with

Argonne National Laboratory

(Participant/National Laboratory Name)

QA program which meets the requirements of

DOE Order 414.1       NQA-1-2000

### This Deliverable was subjected to:

Technical Review

Peer Review

### Technical Review (TR)

### Peer Review (PR)

### Review Documentation Provided

- Signed TR Report or,  
 Signed TR Concurrence Sheet or,  
 Signature of TR Reviewer(s) below

- Signed PR Report or,  
 Signed PR Concurrence Sheet or,  
 Signature of PR Reviewer(s) below

### Name and Signature of Reviewers

Yung Liu

\_\_\_\_\_  
\_\_\_\_\_  
\_\_\_\_\_

\*Note: In some cases there may be a milestone where an item is being fabricated, maintenance is being performed on a facility, or a document is being issued through a formal document control process where it specifically calls out a formal review of the document. In these cases, documentation (e.g., inspection report, maintenance request, work planning package documentation or the documented review of the issued document through the document control process) of the completion of the activity along with the Document Cover Sheet is sufficient to demonstrate achieving the milestone. QRL for such milestones may be also be marked N/A in the work package provided the work package clearly specifies the requirement to use the Document Cover Sheet and provide supporting documentation.

## **APPENDIX C**

### **FY 2012 Used Fuel Disposition Campaign Transportation Task Report on INL Efforts Supporting the Moderator Exclusion Concept and Standardized Transportation**

**FY 2012  
USED FUEL DISPOSITION CAMPAIGN  
TRANSPORTATION TASK REPORT  
ON INL EFFORTS SUPPORTING THE  
MODERATOR EXCLUSION CONCEPT  
AND  
STANDARDIZED TRANSPORTATION**

D. K. Morton

August 2012



The INL is a U.S. Department of Energy National Laboratory  
operated by Battelle Energy Alliance

#### **DISCLAIMER**

This information was prepared as an account of work sponsored by an agency of the U.S. Government. Neither the U.S. Government nor any agency thereof, nor any of their employees, makes any warranty, expressed or implied, or assumes any legal liability or responsibility for the accuracy, completeness, or usefulness, of any information, apparatus, product, or process disclosed, or represents that its use would not infringe privately owned rights. References herein to any specific commercial product, process, or service by trade name, trade mark, manufacturer, or otherwise, does not necessarily constitute or imply its endorsement, recommendation, or favoring by the U.S. Government or any agency thereof. The views and opinions of authors expressed herein do not necessarily state or reflect those of the U.S. Government or any agency thereof.

**FY 2012 USED FUEL DISPOSITION CAMPAIGN  
TRANSPORTATION TASK REPORT ON INL EFFORTS  
SUPPORTING THE MODERATOR EXCLUSION  
CONCEPT AND STANDARDIZED TRANSPORTATION**

**D. Keith Morton**

**August 2012**

**Idaho National Laboratory  
Idaho Falls, Idaho 83415**

**<http://www.inl.gov>**

**Prepared for the  
U.S. Department of Energy  
Office of Nuclear Energy  
Under DOE Idaho Operations Office  
Contract DE-AC07-05ID14517**



**Idaho National Laboratory**

**FY 2012 USED FUEL DISPOSITION CAMPAIGN  
TRANSPORTATION TASK REPORT ON INL EFFORTS  
SUPPORTING THE MODERATOR EXCLUSION  
CONCEPT AND STANDARDIZED TRANSPORTATION**

**INL/EXT-12-26798  
FCRD-UFD-2012-000195**

**August 2012**

**Approved by:**

---

D. Keith Morton  
Author

Date

---

Sandra M. Birk  
Nuclear Material Disposition & Engineering Manager

Date



## **ABSTRACT**

Following the defunding of the Yucca Mountain Project, it is reasonable to assume that commercial used fuel will remain in storage for a longer time period than initially assumed. Previous transportation task work in FY 2011, under the Department of Energy's Office of Nuclear Energy, Used Fuel Disposition Campaign, proposed an alternative for safely transporting used fuel regardless of the structural integrity of the used fuel, baskets, poisons, or storage canisters after an extended period of storage. This alternative assures criticality safety during transportation by implementing a concept that achieves moderator exclusion (no in-leakage of moderator into the used fuel cavity). By relying upon a component inside of the transportation cask that provides a watertight function, a strong argument can be made that moderator intrusion is not credible and should not be a required assumption for criticality evaluations during normal or hypothetical accident conditions of transportation.

This Transportation Task report addresses the assigned FY 2012 work that supports the proposed moderator exclusion concept as well as a standardized transportation system. The two tasks assigned were to (1) promote the proposed moderator exclusion concept to both regulatory and nuclear industry audiences and (2) advance specific technical issues in order to improve American Society of Mechanical Engineers Boiler and Pressure Vessel Code, Section III, Division 3 rules for storage and transportation containments. The common point behind both of the assigned tasks is to provide more options that can be used to resolve current issues being debated regarding the future transportation of used fuel after extended storage.



## **ACKNOWLEDGEMENTS**

The author would like to acknowledge the technical support and translation of documentation provided by Dr. Toshiari Saegusa of Japan's Central Research Institute of Electric Power Industry. The author would also like to acknowledge two Idaho National Laboratory personnel: Ms. Sandra Birk for her management support and Mr. Brett Carlsen for his willingness to attend meetings when the author had previous commitments.



## **CONTENTS**

ABSTRACT.....	v
ACKNOWLEDGEMENTS .....	vii
ACRONYMS .....	xi
1. INTRODUCTION .....	1
2. BACKGROUND .....	1
3. TASK 1: PROMOTE PROPOSED CONCEPT .....	3
3.1 NRC SFST Technical Exchange Meeting.....	4
3.2 27 <sup>th</sup> INMM Spent Fuel Management Seminar .....	5
3.3 EPRI Extended Storage Collaboration Program Meeting.....	5
3.4 NEI Used Fuel Management Conference .....	6
3.5 Future FY2012 NRC NMSS Meetings .....	6
3.5.1 NRC Enhancements to the Licensing and Inspection Programs for Spent Fuel Storage and Transportation .....	6
3.5.2 NRC 2012 SFST Regulatory Conference .....	6
3.6 Task 1 Summary .....	7
4. TASK 2: ADVANCING TECHNICAL ISSUES .....	7
4.1 Literature Search.....	7
4.1.1 Purpose.....	7
4.1.2 Approach to Literature Search .....	7
4.1.3 Results of Literature Search.....	8
4.2 ASME BPV, Section III, Division 3 Activities.....	14
5. CONCLUSIONS .....	15
6. REFERENCES .....	15

## **FIGURES**

Figure 1. Proposed Concept for Moderator Exclusion .....	2
Figure 2. Watertight Barrier Determination .....	3

## **TABLES**

Table 1. Summary of Applicable Strain Rate Literature Search Results for 304/304L .....	9
Table 2. Summary of Applicable Strain Rate Literature Search Results for 316/316L .....	10
Table 3. Strain Rate Data Coverage for 304/304L Base Material .....	11
Table 4. Strain Rate Data Coverage for 304/304L Weld Material .....	11
Table 5. Strain Rate Data Coverage for 316/316L Base Material .....	12
Table 6. Strain Rate Data Coverage for 316/316L Weld Material .....	12



## ACRONYMS

AISI	American Iron and Steel Institute
ASME	American Society of Mechanical Engineers
BPV	Boiler and Pressure Vessel
CFR	Code of Federal Regulations
CoCs	Certificates of Compliance
DOE	U.S. Department of Energy
EPRI	Electric Power Research Institute
FY	Fiscal Year
HT	heat treated
IAEA	International Atomic Energy Agency
INL	Idaho National Laboratory
INMM	Institute of Nuclear Materials Management
ISG	interim staff guidance
JSME	Japan Society of Mechanical Engineers
MSHPB	Modified Split Hopkinson Pressure Bar
NE	DOE Office of Nuclear Energy
NEI	Nuclear Energy Institute
NMSS	Office of Nuclear Material Safety and Safeguards
NRC	U.S. Nuclear Regulatory Commission
RT	Room temperature
SFST	Spent Fuel Storage and Transportation (a division under NRC's Office of Nuclear Material Safety and Safeguards)
SRM	Staff Requirements Memoranda
UFDC	Used Fuel Disposition Campaign



# FY 2012 USED FUEL DISPOSITION CAMPAIGN TRANSPORTATION TASK REPORT ON INL EFFORTS SUPPORTING THE MODERATOR EXCLUSION CONCEPT AND STANDARDIZED TRANSPORTATION

## 1. INTRODUCTION

Following the defunding of the Yucca Mountain Project, the Department of Energy (DOE) transitioned the former Office of Civilian Radioactive Waste Management responsibilities to the Office of Nuclear Energy (NE). One of the new offices created under NE was the Office of Used Nuclear Fuel Disposition Research and Development (NE-53). A Used Fuel Disposition Campaign Implementation Plan was approved on March 29, 2010 with the following mission (Reference 1):

*“The mission of the Used Fuel Disposition Campaign is to identify alternatives and conduct scientific research and technology development to enable storage, transportation and disposal of used nuclear fuel and wastes generated by existing and future nuclear fuel cycles.”*

In the absence of a currently identified disposition path for commercial used nuclear fuel,<sup>a</sup> it is reasonable to assume that used fuel will remain in storage for the foreseeable future. In addition to future disposal issues, the Used Fuel Disposition Campaign (UFDC) is addressing the many issues related to the consequences of this longer than anticipated storage period. The UFDC Transportation Team, composed of a number of personnel from various DOE National Laboratories, began their efforts during Fiscal Year (FY) 2011 and are continuing to support those research and development aspects necessary to successfully carry out the transportation of used fuel, considering the potential adverse effects of long-term storage.

This report provides a summary of the assigned UFDC transportation activities completed by the Idaho National Laboratory (INL) during FY 2012. These activities were performed to support the proposed concept of achieving moderator exclusion with a standardized transportation system. This proposed concept was the assigned INL Transportation task for FY 2011.

## 2. BACKGROUND

The INL's assigned task during FY 2011 for UFDC Transportation was to address the issue of moderator exclusion. This concept was pursued in order to provide options for the transportation of used fuel. After extended storage, if the structural integrity of the fuel, cladding, baskets, or poisons cannot be determined or is too costly to assess, the potential for satisfying the criticality safety requirements become problematic. However, if moderator (e.g., water) is prevented from entering the cavity where the commercial used fuel is located, the used fuel cannot achieve criticality regardless of any degradation consequences due to the 5 wt. % U-235 enrichment limit of the fuel. A basic principle of defense-in-depth is the use of multiple barriers. An engineered barrier, placed inside of a transportation cask, can provide

---

a. The term ‘commercial used nuclear fuel’ (hereafter referred to as ‘used fuel’) is used in this report to reflect that the material being transported may still be a resource to be recovered through processing, whereas ‘spent fuel’ may be considered to be more a waste. This ‘used fuel’ terminology (which includes the cladding) is not intended to conflict with the vast magnitude of literature, regulations, codes, and standards that have used the term ‘spent fuel’ or ‘spent nuclear fuel’. ‘Used fuel’ is simply being used herein to indicate that a decision regarding its usefulness has not yet been determined. The term ‘spent fuel’ or ‘spent nuclear fuel’ will continue to be used in this report when used in a direct quotation, title, or the name of a specific item. Although DOE is also responsible for DOE-owned used fuel and high-level radioactive waste, the main focus of this report is commercial used fuel.

the solution to achieve moderator exclusion. If the storage canister can be shown to provide a watertight barrier during normal and hypothetical accident transportation conditions, moderator exclusion is achieved. If the storage canister cannot provide a watertight barrier, then an additional inner containment inside of the transportation cask can provide the necessary watertight function necessary for moderator exclusion during both normal and hypothetical accident conditions.

Current International Atomic Energy Agency (IAEA) transportation regulations for used fuel (Reference 2) do not require the assumption of moderator leakage past multiple barriers (not less than two), when each barrier can be demonstrated to remain watertight under prescribed normal and accident condition tests and each packaging (before each shipment) is tested to demonstrate the closure. A separate and distinct component inside of a transportation cask and capable of performing the watertight function for moderator exclusion is believed to satisfy the “special design features” condition of the applicable U.S. Code of Federal Regulations (CFR) requirements [10 CFR Part 71.55(c)] (Reference 3), ensuring that no single packaging error would permit in-leakage of moderator into the used fuel cavity.

This engineered concept, discussed in INL/EXT-11-22559 (Reference 4, the FY 2011 INL UFDC Transportation task report), also simultaneously supports standardized transportation. New transportation packagings need to be constructed in order to transport the large amount of available used fuel. This new design opportunity can establish a fleet of transportation packagings that can accommodate most if not all of the current used fuel storage systems. A “one size fits all” approach produces a standardized transportation system. But this does create a need to adapt to the many varied storage canister geometries so they properly fit into the one-sized transportation cask cavity (eliminate excessive rattle room). The solution is to use an adaptable insert (one or more designs as needed) that fits into the transportation cask cavity and properly supports the storage canister. This adaptable insert can also become an inner containment when needed, simply by attaching a lid. Hence, a standardized transportation system can be created that allows even degraded used fuel to be safely transported, providing the options needed to safely and efficiently transport used fuel after extended storage. Figure 1 illustrates this proposed concept.

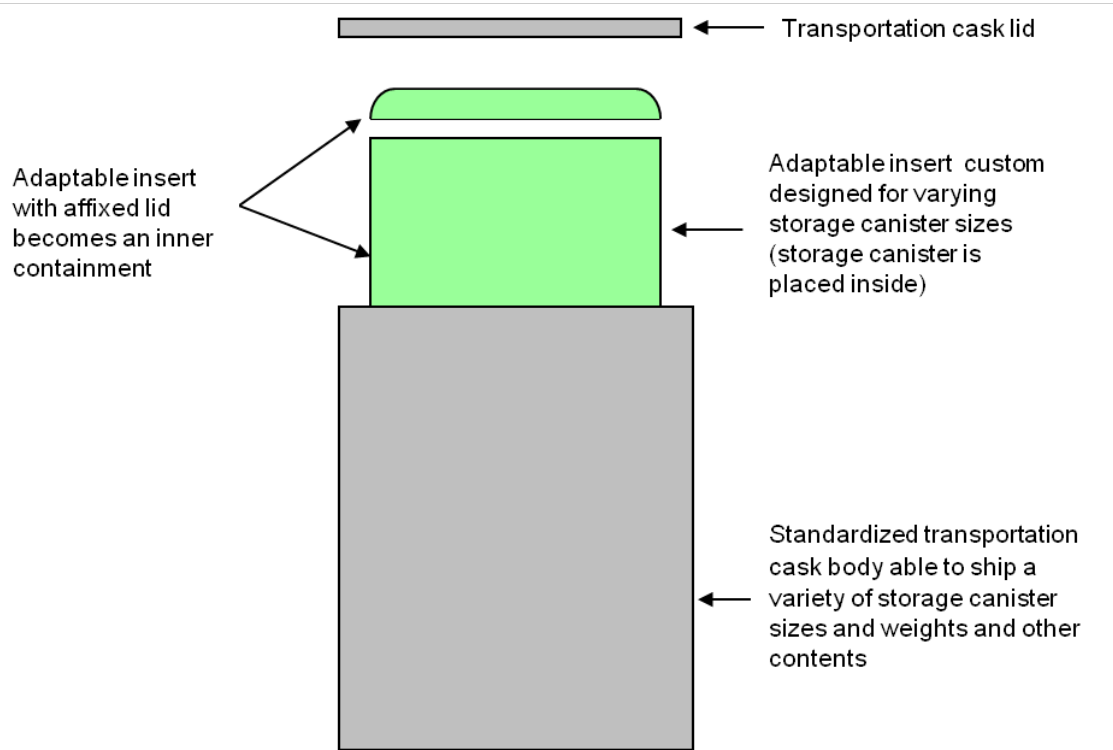


Figure 1. Proposed Concept for Moderator Exclusion

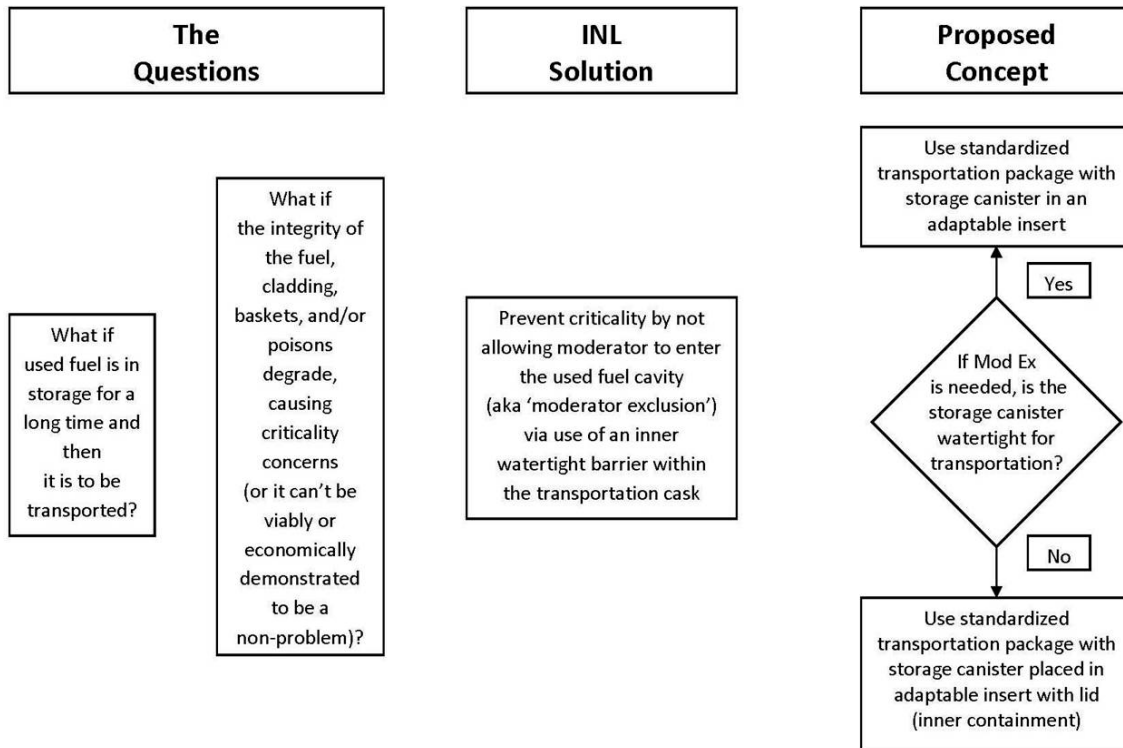


Figure 2. Inner Watertight Barrier Determination

Figure 2 illustrates the logic when evaluating whether the storage canister or the adaptable insert with an affixed lid (inner containment) will provide the watertight barrier function necessary for moderator exclusion.

### 3. TASK 1: PROMOTE PROPOSED CONCEPT

As explained in INL/EXT-11-22559, if the U.S. Nuclear Regulatory Commission (NRC), Office of Nuclear Material Safety and Safeguards (NMSS) would accept the proposed moderator exclusion approach [essentially be willing to invoke 10 CFR Part 71.55(c)] for general approval of designs rather than on a case-by-case basis, it is believed that more parties would be willing to submit designs invoking moderator exclusion for both normal and hypothetical accident conditions. All licensing interactions with the NRC cost money to complete and there is a natural hesitancy to pursue design options that may be rejected by the NRC. As an additional deterrent, a recent NRC Commission ruling on moderator exclusion [Staff Requirements Memoranda (SRM) dated December 18, 2007 (Reference 5) regarding SECY-07-0185 (Reference 6)] indicated that the Commission rejected the NRC staff's recommendation for rulemaking to incorporate regulatory provisions addressing moderator exclusion. The Commission required the NRC staff to continue to gain more experience through processing applicant's requests and to focus its efforts on using burn-up credit. What was believed not to have been specifically considered in those deliberations was the consequences of extended storage and the presence of an inner watertight barrier, separate from and inside of the transportation containment, as required by the INL's proposed moderator exclusion concept. Other requirements such as addressing fuel retrievability add to the current hesitancy of applicants to pursue moderator exclusion approval for both normal and hypothetical accident conditions.

Therefore, the primary intent of Task 1 was to simply promote the proposed moderator exclusion concept that also incorporated a standardized transportation system. If efforts could be made to provide input to the NRC during their on-going review of storage and transportation regulations in light of

extended storage, the potential for the NRC to seriously consider the proposed concept improved greatly. The INL proposed concept is not a new concept, but it is a proven concept, since it was used to transport the damaged Three Mile Island fuel and core across most of the United States to the INL. So the goal of Task 1 was to simply help keep this engineered design option fresh in the NRC's, potential applicants', and the nuclear industry's minds. This promotional effort was considered especially important if proposed extended storage used fuel demonstration tests prove too costly, if the research efforts do not yield the desired outcome, or if it becomes difficult to assure the condition of the fuel, cladding, baskets, or poisons inside any specific storage canister for whatever reason. The INL proposed concept provides alternative transportation options for the future.

### **3.1 NRC SFST Technical Exchange Meeting**

The first opportunity to promote the INL's proposed concept came early in FY 2012. On November 1, 2011, the Division of Spent Fuel Storage and Transportation (SFST) under NMSS sponsored a technical exchange meeting. NRC, DOE, and nuclear industry representatives served on panels and presented their perspectives on a variety of issues in the areas of transportation technical issues and storage technical issues. Two concurrent meetings were held but it was at the "Interfaces Between Storage and Transportation Casks" meeting where pertinent presentations were held regarding moderator exclusion. The morning session was a presentation/discussion on high burnup fuel, including discussions on alternatives for addressing criticality safety requirements for high burnup fuel transportation.

Presentations included:

- NRC's View on Cladding Material Properties – Bob Einziger
- Industry's View on Cladding - Albert Machiels from EPRI
- NRC's View on Moderator Exclusion – John Vera
- Industry's View on Moderator Exclusion – Charlie Pennington from NAC International and D. Keith Morton from the Idaho National Laboratory
- NRC's View on Reconfiguration – David Tang and Zhian Li
- Industry's View on Reconfiguration – Albert Machiels from EPRI

The afternoon session of "Interfaces Between Storage and Transportation Casks" continued the same format, including discussions on retrievability requirements (by fuel assembly or canister), casks/contents integrity after a period of storage, and the use of common criticality safety methods for satisfying both storage and transportation regulations. Presentations included:

- NRC's View on Retrievability – Earl Easton
- Industry's View on Retrievability – Adam Levin from Exelon Corporation
- NRC's View on Acceptance Testing and Aging Management – Bob Einziger
- Industry's View on Acceptance Testing and Aging Management – Jim Connell from Maine Yankee
- NRC's View on Burnup Credit versus Boron Credit – Drew Barto
- Industry's View on Burnup Credit versus Boron Credit – Prakash Narayanan from Transnuclear

Two interesting comments from the NRC staff were made at this meeting. First, Dr. John Vera mentioned in his morning presentation that the concept proposed in INL Report 11-22559 could be a "possible" option for moderator exclusion by implementing double containment. Second, Mr. Earl Easton discussed potential future paradigm shifts in regulations, where for 'retrievability', a shift from the fuel assembly to the canister could occur and that for 'criticality safety', a shift from cladding to canister could be possible. These comments supported the position of the INL presentation and were very well received by the audience. This meeting provided an excellent opportunity for the industry and NRC personnel to

exchange technical ideas and opinions. The proposed moderator exclusion presentation was well received. After the presentations, in direct discussions with Mr. Earl Easton, NRC Senior Level Transportation Advisor, he indicated that there were still differing opinions within the NRC staff on various storage and transportation subjects but he believed that a new paradigm existed with the probability of extended storage intervals and felt that it was necessary for the NRC to adapt with the change. Hence, the goal of keeping moderator exclusion on the discussion forefront as an item for potential regulatory change was achieved.

### **3.2 27<sup>th</sup> INMM Spent Fuel Management Seminar**

Mr. Paul McConnell, from Sandia National Laboratories and UFDC Technical Laboratory Lead for Transportation, gave a presentation on the UFDC Transportation Program on February 1, 2012 at the Institute of Nuclear Materials Management 27<sup>th</sup> Spent Fuel Management Seminar. The presentation included a brief summary of the proposed moderator exclusion concept. Again, more people were exposed or reminded of the potential benefits of moderator exclusion.

One of the more intriguing aspects that occurred at this three day meeting was comments made on the last day (February 2, 2012) by Mr. Doug Weaver, Acting Director for the NRC SFST Division. Some of his more interesting comments regarding possible future licensing strategies due to extended storage included:

- “If the fuel cladding is not relied upon to perform safety functions such as geometry control, degradation of fuel cladding may not pose a significant problem from the perspective of storage and transportation.”
- “An engineering approach that relies on canisters or individual cans rather than cladding integrity may also lessen the burden on cask designers and regulators to do extensive research on fuel cladding properties. It should be noted however that, due to increased reliance on integrity of canisters/casks and overpacks, these safety components may have to perform to higher standards.”
- “In summary, I believe that NRC’s future regulatory framework should be flexible enough to consider both “scientific” and “engineering” solutions – for example, developing licensing solutions that rely both on keeping the cladding intact, as well as those which might base safety more on canisters or cans.”

The good news is that all participants in the nuclear industry appear to be recognizing that past processes, evaluations, assumptions, and regulations may be inadequate in light of extended storage and that new general design approaches (e.g., using an inner containment) should be considered along with revised regulations.

### **3.3 EPRI Extended Storage Collaboration Program Meeting**

After generating a presentation (improved over that presented at the November 1 NRC Technical Exchange Meeting), discussing the presentation and submitting the presentation with meeting organizers, the author attended the Electric Power Research Institute (EPRI) Extended Storage Collaboration Program (ESCP) meeting held Monday, May 7, 2012 in St. Petersburg, Florida. The focus of that meeting was to discuss aging effects and mitigation options for the extended storage and transportation of used fuel. Due to the fact that the meeting went long and certain agenda items were not covered, the presentation on the INL’s proposed moderator exclusion concept was not given. However, after the author made a brief announcement of a willingness to discuss moderator exclusion options after the meeting, two nuclear industry participants briefly explained their future expectations and both believed that moderator exclusion provided the most likely option for future transportation of used fuel.

### **3.4 NEI Used Fuel Management Conference**

Since the Nuclear Energy Institute (NEI) Used Fuel Management Conference began the day after the ESCP meeting at the same location, the author also attended this conference. Although no presentation was planned, attending this conference provided an opportunity to listen to a number of pertinent presentations, mainly from the nuclear industry perspective. This provided a better understanding of the nuclear industry's perspective on what needs to be accomplished in order to continue the safe storage of used fuel and the actions needed to move forward with storage, transportation, and disposal. Moderator exclusion was high on the list of NEI issues needing to be discussed and utilized for future transportation of used fuel.

### **3.5 Future FY2012 NRC NMSS Meetings**

The NRC is organizing two meetings to be held late in FY2012, after the writing and approval of this FY2012 UFDC Transportation Task report.

#### **3.5.1 NRC Enhancements to the Licensing and Inspection Programs for Spent Fuel Storage and Transportation**

This NRC SFST meeting is scheduled to be held August 16-17, 2012 at NRC Headquarters in Rockville Maryland. As the draft agenda indicates, the following issues are to be discussed:

- Administration of Storage Certificates of Compliance (CoCs) and Amendments to CoCs
- Applicability, Compatibility, and Consistency of Spent Fuel Storage Requirements for Specific Licensees, General Licensees, and Certificate of Compliance Holders
- Regulating Stand-Alone Independent Spent Fuel Storage Installations
- Harmonization of Retrievability and Cladding Integrity Requirements for Storage and Transportation of Spent Nuclear Fuel

In particular, the last item could have interesting implications for transportation, especially if any shifts in fuel retrievability regulations are discussed. INL personnel are planning to attend/participate in this meeting but no presentation is planned.

#### **3.5.2 NRC 2012 SFST Regulatory Conference**

This NRC SFST meeting is an annual forum to discuss NRC regulatory and technical issues involving spent fuel storage and the transportation of radioactive material. The goal of the conference is for the regulators to share their perspectives on licensing, inspection, and regulatory challenges as well as for the nuclear industry to share their insights on improving regulatory oversight, all through constructive dialogue. This meeting is scheduled to be held September 12-13, 2012 at NRC Headquarters in Rockville Maryland. Per the draft agenda, the following issues are to be discussed:

- Operating Experience
- Non-Spent Fuel Transportation
- Information on NUREG-2150 and NUREG-2125
- High Burnup Fuel Storage and Transportation
- Technical Issues Related to Storage

Again, various agenda items could have interesting implications for transportation, especially the high burnup fuel discussion. INL personnel are planning to attend/participate in this meeting, although presenters and panels have not yet been finalized.

### **3.6 Task 1 Summary**

A number of opportunities were pursued to promote the proposed moderator exclusion concept for standardized transportation systems. Presentations were made at various meeting types and interaction with meeting attendees succeeded in heightening the awareness of the beneficial aspects of moderator exclusion. Moderator exclusion is attainable and keeping this option “on the table” for future consideration by both nuclear industry and regulatory personnel was achieved.

## **4. TASK 2: ADVANCING TECHNICAL ISSUES**

Task 2 was to perform a literature search for readily available strain rate data that would support implementing proposed strain-based acceptance criteria for the American Society of Mechanical Engineers (ASME) Boiler and Pressure Vessel (BPV) Code, Section III, Division 3 (Reference 7) rules for both storage and transportation containments. Funding was also provided to attend the ASME BPV Code Week Division 3 meetings. Therefore, Section 4.1 below addresses the completed literature search and Section 4.2 addresses the advances made in developing the proposed strain-based acceptance criteria and the progress to date of obtaining ASME approval of the proposal, along with other pertinent Section III, Division 3 rule changes.

### **4.1 Literature Search**

This subsection describes in more detail the literature search performed in order to establish the quantity of strain rate data readily available in the technical literature. This information is expected to be used to determine future needs, such as defining test program needs and validation efforts.

#### **4.1.1 Purpose**

The purpose of this task was to perform a limited literature search in order to determine the quantity of applicable strain rate data readily available. Regulatory requirements mandate the consideration of accidental drops and impacts when designing storage and transportation containments. These energy-limited loads typically govern the structural design of these containments, especially when elastic analyses are used. But this significantly increases the cost of these containments. In recognition of this fact, the ASME BPV Code, Section III, Division 3 committees have pursued the development of strain-based acceptance criteria. These criteria will make the design of containments more efficient but will still maintain appropriate safety margins. These acceptance criteria require inelastic analyses be performed. Strain rate data are required to properly perform inelastic analyses of accidental drop or impact events on storage and transportation containments. So strain rate data support implementation of the proposed strain-based acceptance criteria, which can support the design of a new and efficient standardized transportation system.

#### **4.1.2 Approach to Literature Search**

A significant amount of strain rate research has been performed on multiple materials, at multiple temperatures, and for a variety of reasons. However, this literature search needed to obtain information pertinent to the common materials used for the containment of used fuel during storage and transportation uses. Therefore, the search parameters were narrowed to focus on strain rate data for 304, 304L, 316, or 316L stainless steels, at temperatures ranging from -40°F to 800°F, and at strain rates between 1 and 510 in/in/sec. In years past, before the late 1980’s, it was common to be able to procure just one type (304, 304L, 316, or 316L) of austenitic stainless steel material. However, for new construction, one is likely to obtain material that is marked with two or more material types, such as 304/304L or 316/316L. These materials can satisfy both material types because all of the measured and controlled attributes (e.g., chemistry, mechanical properties, dimensions, and tolerances) of that material fall within the overlapping ranges of both specifications. This dual marking notation (304/304L and 316/316L) will be used herein to

denote either material that satisfies each unique and separate specification (covering older testing efforts) or material that satisfies the dual specifications (covering more recent testing efforts).

Past efforts to acquire strain rate documentation within the data ranges specified above, including requests to ASME Code committee volunteers, yielded relevant documents. These documents were combined with the new FY2012 search efforts made for this task.

Obviously, in order to better understand the material performance conforming to the restricted conditions identified above, the ideal strain rate data would include digitized tensile engineering stress-strain curves. This would provide material data performance, including values for the uniform strain limit and fracture strain limit. True stress-strain curves could also be generated from this data. However, not all documentation would be expected to provide this detailed level of information. Therefore, documents with true stress-strain curves, or reports that provided information on how the strain rate effects changed the material response in relation to the quasi-static engineering or true stress-strain curve were also of importance. Even with these narrowed search parameters, it was still necessary to obtain the potential papers, reports, and other documentation, scan for the minimal data of interest, and then determine if that data would provide any beneficial insights. This determination was necessary because some data may have included pertinent data but if the quasi-static engineering or true stress-strain curve was not provided, a quantification of the material response change could not be made. Other reasons to not include documents was that the data did not go far enough in terms of strain, difficulty in reading the data, data units not specified, or the data were not within the specified parameters. Documents with compression test data were not considered viable since the behavior of these materials is different between tensile and compression loading. Another aspect not considered at this time was the effects of irradiation, due to the limited funding.

#### **4.1.3 Results of Literature Search**

A significant number of hours were invested in this literature search. However, the search results yielded only nine viable references (References 8 – 16). This was not unexpected since past efforts yielded few references. The current fiscal year effort was fruitful and did add to the total number of viable strain rate references. Due to copyright constraints, rather than providing copies of the entire reference, the search results are summarized in tabular form, differentiated by material type (304/304L or 316/316L). Table 1 provides a summary of pertinent strain rate data provided by each reference, separated by test temperature, for 304/304L base and weld material. Table 2 provides the same information for 316/316L base and weld material. Tables 1 and 2 also provide information regarding the dynamic test method used, test specimen geometry insights, and the form of the documented strain rate data.

When evaluating the results of a literature search of this nature, the issue of data completeness needs to be considered. The goal was to get viable strain rate data over a range of 1 to 510 in/in/sec and at a variety of temperatures ranging from -40°F to 800°F. Tables 3, 4, 5, and 6 were generated to provide a visual answer to the question. Tables 3 and 4 address 304/304L material and Tables 5 and 6 address 316/316L. Table 3 and 5 address base material and Tables 4 and 6 address weld material. The first realization is that only a limited number of the boxes are marked (yellow highlight with an ‘X’), indicating at least one set of data is available in the indicated range. Less than 18% of the 316/316L base material ranges have data and only 12% of the 304/304L base material ranges have any data. The data coverage for welds is even lower; approximately 5% of the ranges have any data for either 304/304L or 316/316L. As one would expect, most of the strain rate data that is available is for the temperature range that includes room temperature and for the lowest strain rate range (1 to 50 in/in/sec). These data points are the easiest to obtain. Clearly, the general need is to obtain more data at higher strain rates and at higher temperatures. This insight is very useful for planning future strain rate testing needs.

Of the data that are available, a few cursory observations can be made and are presented below. However, it is necessary to incorporate additional strain rate data before any final conclusions can be stated.

**Table 1. Summary of Applicable Strain Rate Literature Search Results for 304/304L**

Author	Ref.	Material	Dynamic Test Method	Test Temp.	Strain Rates	Specimen	Comments
Albertini & Montagnani	8	AISI 304L	MSHPB	RT	$10^{-4}$ , $10^{-2}$ , 502	Small, 8 mm active length	Engr. stress-strain curves
Albertini & Montagnani	9	AISI 304L	MSHPB	68°F	$3.8 \times 10^{-3}$ , 50, 450	Small	Engr. stress-strain curves
Albertini & Montagnani	9	AISI 304L	MSHPB	752°F	$3.5 \times 10^{-3}$ , 50, 500	Small	Engr. stress-strain curves
JSME	10 (B-46)	304	Amsler type accumulated gas	68°F	$5.05 \times 10^{-4}$ , $6.26 \times 10^{-2}$ , 54.8	1/3-in. dia. 2-in. gauge	Limited true stress-strain curve s& data
JSME	10 (B-46)	304	Amsler type accumulated gas	-87°F	$5.45 \times 10^{-4}$ , $4.99 \times 10^{-2}$ , 48	1/3-in. dia. 2-in. gauge	Limited data
Marschall, Landow, Wilkowski	11	304 and SAW	Hydraulic tensile	550°F	Varying: approx. $10^{-4}$ , 1, 8-14	1/8-in. sheet	Engr. & true stress-strain curves
Talonen, Nenonen, Pape, & Hänninen	14	AISI 304	Hydraulic tensile	RT*	$3 \times 10^{-4}$ , 0.1, 200	0.04 in. thick	True stress-strain curves
Lichtenfeld, Mataya, & Van Tyne	15	304L	Hydraulic tensile	75°F	$1.25 \times 10^{-4}$ , $1.25 \times 10^{-3}$ , $1.25 \times 10^{-2}$ , 0.125, 1.25, 10, 100, 400	0.06 in. thick etched	True stress-strain curves with yield and tensile strengths
Morton & Blandford	16	304/304L base and weld	Drop weight	-20°F	$10^{-4}$ to $10^{-3}$ , 5 - 36	1/4 and 1/2-inch thick plate	Data & factored true stress-strain curves
Morton & Blandford	16	304/304L base and weld	Drop weight	RT	$10^{-4}$ to $10^{-3}$ , 5 - 33	1/4 and 1/2-inch thick plate	Data & factored true stress-strain curves
Morton & Blandford	16	304/304L base and weld	Drop weight	300°F	$10^{-4}$ to $10^{-3}$ , 5 - 35	1/4 and 1/2-inch thick plate	Data & factored true stress-strain curves
Morton & Blandford	16	304/304L base and weld	Drop weight	600°F	$10^{-4}$ to $10^{-3}$ , 5 - 23	1/4 and 1/2-inch thick plate	Data & factored true stress-strain curves

Notes:

AISI – American Iron and Steel Institute

MSHPB – Modified Split Hopkinson Pressure Bar or similar device

RT – room temperature

\* - assumed value based on paper inferences

**Table 2. Summary of Applicable Strain Rate Literature Search Results for 316/316L**

Author	Ref.	Material	Dynamic Test Method	Test Temp.	Strain Rates	Specimen	Comments
Albertini & Montagnani	9	AISI 316L	MSHPB	68°F	$4.0 \times 10^{-3}$ , 15, 44, 420	Small bar	Engr. stress-strain curves
Albertini & Montagnani	9	AISI 316L weld	MSHPB	68°F	$3.5 \times 10^{-3}$ , 5, 440	Small bar	Engr. stress-strain curves
JSME	10 (B-3)	AISI 316L	*	68°F	$3 \times 10^{-3}$ , 12, 36, 360	*	Limited true stress-strain curves & data
JSME	10 (B-27)	316L (HT & annealed)	MSHPB	68°F	$3.9 \times 10^{-3}$ , 15, 43, 410	*	Limited true stress-strain curves & data
JSME	10 (B-27)	316L (HT & annealed)	MSHPB	752°F	$2.9 \times 10^{-3}$ , 44, 69, 460	*	Limited data
O'Toole	12	316L	Drop weight	RT	Approx. $10^{-4}$ , 0.02, 0.2, 75, 100, 130, 165, 200	0.35 in. long 1/8-in. dia.	Raw data
O'Toole	12	316L	Drop weight	175°F	Approx. 90, 170	0.35 in. long 1/8-in. dia.	Raw data
O'Toole	12	316L	Drop weight	350°F	Approx. 110, 145, 170	0.35 in. long 1/8-in. dia.	Raw data
Langdon & Schleyer	13	316L	Hydraulic tensile	RT	0.03, 0.2, 18, 20, 55, 118	0.12 and 0.16 thick	Engr. stress-strain curves
Morton & Blandford	16	316/316L base and weld	Drop weight	-20°F	$10^{-4}$ to $10^{-3}$ , 5 - 39	$\frac{1}{4}$ and $\frac{1}{2}$ -inch thick plate	Data & factored true stress-strain curves
Morton & Blandford	16	316/316L base and weld	Drop weight	RT	$10^{-4}$ to $10^{-3}$ , 5 - 34	$\frac{1}{4}$ and $\frac{1}{2}$ -inch thick plate	Data & factored true stress-strain curves
Morton & Blandford	16	316/316L base and weld	Drop weight	300°F	$10^{-4}$ to $10^{-3}$ , 4 - 26	$\frac{1}{4}$ and $\frac{1}{2}$ -inch thick plate	Data & factored true stress-strain curves
Morton & Blandford	16	316/316L base and weld	Drop weight	600°F	$10^{-4}$ to $10^{-3}$ , 5 - 24	$\frac{1}{4}$ and $\frac{1}{2}$ -inch thick plate	Data & factored true stress-strain curves

Notes:

AISI – American Iron and Steel Institute

MSHPB – Modified Split Hopkinson Pressure Bar or similar

RT – Room Temperature

JSME – Japan Society of Mechanical Engineers

\* - unstated but MSHPB likely with small bar test specimens

HT – heat treated

**Table 3. Strain Rate Data Coverage for 304/304L Base Material**

Temperature \ Strain Rate	-90°F to 32°F	33°F to 100°F	101°F to 200°F	201°F to 300°F	301°F to 400°F	401°F to 500°F	501°F to 600°F	601°F to 700°F	701°F to 800°F
1 - 50 in/in/sec	X	X		X			X		X
51 - 100 in/in/sec		X							
101 - 150 in/in/sec									
151 - 200 in/in/sec		X							
201 - 250 in/in/sec									
251 - 300 in/in/sec									
301 - 350 in/in/sec									
351 - 400 in/in/sec		X							
401 - 450 in/in/sec		X							
451 - 510 in/in/sec		X							X

**Table 4. Strain Rate Data Coverage for 304/304L Weld Material**

Temperature \ Strain Rate	-90°F to 32°F	33°F to 100°F	101°F to 200°F	201°F to 300°F	301°F to 400°F	401°F to 500°F	501°F to 600°F	601°F to 700°F	701°F to 800°F
1 - 50 in/in/sec	X	X		X			X		
51 - 100 in/in/sec									
101 - 150 in/in/sec									
151 - 200 in/in/sec									
201 - 250 in/in/sec									
251 - 300 in/in/sec									
301 - 350 in/in/sec									
351 - 400 in/in/sec									
401 - 450 in/in/sec									
451 - 510 in/in/sec									

**Table 5. Strain Rate Data Coverage for 316/316L Base Material**

Temperature \ Strain Rate	-90°F to 32°F	33°F to 100°F	101°F to 200°F	201°F to 300°F	301°F to 400°F	401°F to 500°F	501°F to 600°F	601°F to 700°F	701°F to 800°F
1 – 50 in/in/sec	X	X		X			X		X
51 – 100 in/in/sec		X	X						X
101 – 150 in/in/sec		X			X				
151 – 200 in/in/sec		X	X		X				
201 – 250 in/in/sec									
251 – 300 in/in/sec									
301 – 350 in/in/sec									
351 – 400 in/in/sec		X							
401 – 450 in/in/sec		X							
451 – 510 in/in/sec									X

**Table 6. Strain Rate Data Coverage for 316/316L Weld Material**

Temperature \ Strain Rate	-90°F to 32°F	33°F to 100°F	101°F to 200°F	201°F to 300°F	301°F to 400°F	401°F to 500°F	501°F to 600°F	601°F to 700°F	701°F to 800°F
1 – 50 in/in/sec	X	X		X			X		
51 – 100 in/in/sec									
101 – 150 in/in/sec									
151 – 200 in/in/sec									
201 – 250 in/in/sec									
251 – 300 in/in/sec									
301 – 350 in/in/sec									
351 – 400 in/in/sec									
401 – 450 in/in/sec		X							
451 – 510 in/in/sec									

#### **4.1.3.1 Sensitivity of Austenitic Stainless Steel to Strain Rate Effects**

A number of personnel have questioned the sensitivity of austenitic stainless steels to strain rate effects. It is surmised that these individuals may have misread strain rate discussions or information in the past. The final nine references selected for this literature search clearly demonstrate that austenitic stainless steels, types 304/304L and 316/316L, are indeed strain rate sensitive.

#### **4.1.3.2 Factoring of True Stress-Strain Curves**

Looking at the available true stress-strain curves from the nine strain rate references that reflect higher strain rates, a number of those curves (References 10, 14, and 15) appear to be a uniform factor higher (in the stress direction) than the corresponding quasi-static true stress-strain curve. This feature also holds true for other references (References 17 and 18) that contained true stress-strain curves at varying strain rates but did not comply with the literature search limitations established. If this feature continues to hold true with additional strain rate data, this would be a very simple way to correlate strain rate effects to readily available 304/304L and 316/316L quasi-static true stress-strain curves, as was done in Reference 16.

#### **4.1.3.3 Variation of Uniform or Fracture Strain Limits Versus Strain Rate**

Some engineers have indicated an expectation that the uniform strain limit (corresponding to the strain just before the onset of necking) and the fracture strain limit (corresponding to the strain at the point of test specimen fracture or separation) will reduce as the strain rate (over the range of 1 to 510 in/in/sec) increases. Briefly reviewing the nine strain rate references, some show engineering curves where these two strain limits do indeed show indications of reduction but at the upper limits of the strain rates of interest (Reference 8) or indications of reduction at lower and higher strain rates (References 9 and 12). On the other hand, other information collected (References 12, 13, 15, and 16) indicate no significant reductions or some increases in these strain limits as the strain rate increases. Reference 14 indicates that the elongation to fracture increases with the strain rate. Interestingly, where information was available, the earlier testing results tended to show strain limits reduced while later testing results showed strain limits increasing or essentially remaining constant. Test methodology may have an influence as well as how the strain rate was defined. Additional strain rate data is necessary before this trend can be clarified.

#### **4.1.3.4 Validation of Data Generated**

One of the difficulties in utilizing research data from many different sources is ascertaining the validity of those data. If the researcher can perform some level of validation, that provides a major boost in data acceptability. Of the nine references that satisfied the search criteria, only two (References 13 and 16) provided any validation insights. For both of these references, the validation effort indicated that when the strain rate data was incorporated into finite element method inelastic analyses, good agreement was attained when compared to actual test results.

#### **4.1.3.5 Test Specimen Size**

Commentary in various literature have expressed concern over extending small or thin test specimen research results to situations where the actual material used involves much larger and much thicker material. Do thinner materials present different material properties than thicker materials? Are failure responses altered? At this point, any commentary will be withheld until more research data become available.

#### **4.1.3.6 Comparison of Strain Rate Data Between References**

Performing a meaningful comparison between the available strain rate data would indicate if there is agreement or significant differences. Different researchers or different test methods could introduce unknown biases. However, at a minimum, the numerous engineering or true stress-strain curves need to be digitized and plotted on the same graph in order to begin any meaningful comparison. But that

preliminary step can be a time-consuming effort, too much to attempt with the limited funding provided for this task.

## 4.2 ASME BPV, Section III, Division 3 Activities

Another aspect of advancing technical issues that affects the proposed moderator exclusion concept and the standardized transportation system is the updating and revision of rules provided in the ASME BPV Code, Section III, Division 3. Division 3 provides the construction rules for both storage and transportation containments. Although not heavily used in the past, Division 3 has been significantly revised in the last decade to make it more useful and applicable to the storage and transportation industry. In addition, the NRC is currently reviewing Division 3 with the eventual goal of endorsement. History has shown that applicants typically use codes and standards endorsed by the NRC, rather than attempting to justify alternative rules on a case-by-case basis.

Supported by UFDC funding, the author was able to attend all four ASME BPV Code Weeks held during FY 2012. The author is a member of the Working Group on Design of Division 3 Containments, is the Secretary for the Subgroup on Containment Systems for Spent Fuel and High-Level Waste Transport Packagings (otherwise known as Subgroup NUPACK), and is a member of the BPV Standards Committee on Construction of Nuclear Facility Components.

Two Section III, Division 3 actions that directly affect the proposed moderator exclusion concept and standardized transportation were balloted through the various ASME BPV committees during FY 2012 and include:

- clarification of helium leak testing requirements for inner containments in Subsection WB-6120, and
- strain-based acceptance criteria applicable to both storage and transportation containments.

The author was the ASME Project Manager for both of these actions. The ASME Project Manager has the responsibility to develop the revision documentation, submit the action for ASME approval, and monitor the balloting process, answering any comments received during the balloting process.

Regarding the first action, the existing WB-6120, *Testing of Containments*, required all transportation containments to be pressure tested and leak tested except for any final closure welds made on inner containments. The main problem was that no requirements were provided for the final closure welds. WB-6120 was revised to include both final closure welds and final mechanical closures made on inner containments and clarified that both of these final closures shall be leak tested only. No pressure test is required on these final closures made on inner containments after being loaded with spent fuel or high-level waste. This revision received full ASME approval on July 11, 2012 and should be published in the next 2013 Edition of the ASME BPV Code.

The second action is still in the ASME balloting process. The strain-based acceptance criteria deliberations started in the Working Group on Design of Division 3 Containments back in 2006. The Working Group on Design Methodology was also involved since this was a new design approach for Section III. After revising many different proposals, a final version of the strain-based acceptance criteria was finally approved in November 2011 by these two Working Groups. The next step was to begin the ASME balloting process through higher committees and providing presentations to various ASME committees explaining the action and answering committee member questions. As of the writing of this report, the strain-based acceptance criteria have been approved by all of the appropriate committees reporting to the BPV Standards Committee on Construction of Nuclear Facility Components, including the Subgroup on Materials, Fabrication, and Examination, the Subgroup on Component Design, and the Subcommittee on Design.

The next step in the ASME balloting process will be to submit the strain-based acceptance criteria to the BPV Standards Committee on Construction of Nuclear Facility Components. This submittal is

expected to be achieved at the 2012 August Code Week meetings. Actual balloting will likely begin in late August and carry into September.

The current strain-based acceptance criteria require the user to perform material testing in order to obtain the necessary true stress-strain curve material properties to implement the criteria. The criteria currently address strain rate effects separately in a conservative fashion. But the criteria can be improved and made more user friendly if ASME could provide these material data. Discussions with the ASME BPV Code, Section II material experts regarding the incorporation of appropriate true stress-strain curves and strain rate data for use with the strain-based acceptance criteria are on-going. If a more fully defined and validated database of temperature dependent true stress-strain curves and strain rate data for the austenitic stainless steels of interest can be established, certain levels of inelastic analysis conservatism are expected to be reduced, improving the accuracy of inelastic analysis predictions of structural responses to energy-limited events. The strain-based acceptance criteria are believed to be a significant step forward in more accurately evaluating the acceptability of energy-limited dynamic loadings on containments. The significance of the strain-based acceptance criteria is that future storage and transportation containments, including the inner containment (adaptable insert and lid), will be able to be designed more efficiently. The NRC has indicated support for incorporating strain-based acceptance criteria into Division 3.

## 5. CONCLUSIONS

Achieving moderator exclusion by utilizing a watertight inner barrier excludes the possibility of criticality of commercial used fuels during transportation. When the storage canister cannot provide that watertight function, a separate inner containment can provide the watertight function. Following this graded approach, the proposed moderator exclusion concept provides a positive path forward for DOE to transport used fuel after extended storage, regardless of the condition of the fuel, baskets, poisons, or the storage canister. This concept also supports standardization of the transportation system. The significance of what the proposed moderator exclusion concept offers is why the INL believes that it is important to be proactive in discussing the proposal and in keeping the concept fresh in the minds of applicants, regulators, and other decision makers. The assigned Task 1 supported this effort and success was achieved.

Advances on various technical issues are also very important, especially when the technical issues also support the proposed moderator exclusion concept and standardized transportation. Task 2 provided the opportunity to make significant advances in the applicable codes and standards area by revising ASME BVP Code, Section III, Division 3 rules and making progress on new design methods and acceptance criteria. Task 2 was also successfully completed.

Although the FY 2012 funding received was limited, the INL was able to successfully complete its assigned tasks and move the issue of used fuel transportation forward. Many technical decisions still have to be made. With future funding, the INL can continue making progress so that used fuel transportation can be accomplish in a safe and efficient manner.

## 6. REFERENCES

1. Department of Energy presentation by Jeffrey Williams, "DOE/NE Used Fuel Disposition Program Overview," 27<sup>th</sup> INMM Spent Fuel Management Seminar, February 1, 2012.
2. International Atomic Energy Agency, "Regulations for the Safe Transport of Radioactive Material," IAEA Safety Standards Series No. TS-R-1, Paragraph 677, 2009 Edition.
3. U.S. Code of Federal Regulations, Title 10, Part 71, "Packaging and Transportation of Radioactive Material," June 17, 2011.

4. Morton, D. K., et al., *Idaho National Laboratory Transportation Task Report on Achieving Moderator Exclusion and Supporting Standardized Transportation*, INL/EXT-11-22559, September 2011.
5. U.S. Nuclear Regulatory Commission, Staff Requirements Memorandum, “Staff Requirements – SECY-07-0185 – Moderator Exclusion in Transportation Packages,” December 18, 2007.
6. U.S. Nuclear Regulatory Commission, Commission Papers, “Moderator Exclusion in Transportation Packages,” SECY-07-0185, October 22, 2007.
7. American Society of Mechanical Engineers, “Boiler and Pressure Vessel Code,” Section III, Division 3, *Containments for Transportation and Storage of Spent Nuclear Fuel and High Level Radioactive Material and Waste*, 2010 Edition with 2011 Addenda.
8. Albertini, C. and M. Montagnani, “Wave Propagation Effects in Dynamic Loading,” *Nuclear Engineering and Design*, Vol. 37, 1976, pp. 115-124.
9. Albertini, C. and M. Montagnani, “Dynamic Uniaxial and Biaxial Stress-Strain Relationships for Austenitic Stainless Steel,” *Nuclear Engineering and Design*, Vol. 57, 1980, pp. 107-123.
10. Japan Society of Mechanical Engineers, *Report on Database for Structural Analysis of Spent Fuel Shipping Cask*, November 1985.
11. Marschall, C. W., M. P. Landow, and G. M. Wilkowski, *Loading Rate Effects on Strength and Fracture Toughness of Pipe Steels Used in Task 1 of the IPIRG Program*, NUREG/CR-6098, October 1993.
12. O’Toole, B., *Identification of Dynamic Properties of Materials for the Nuclear Waste Package*, TR-02-007, Revision 0, prepared for the U.S. DOE/UCCSN Cooperative Agreement Number: DE-FC08-98NV12081, Task 24, September 30, 2003.
13. Langdon, G. S. and G. K. Schleyer, “Unusual Strain Rate Sensitive Behaviour of AISI 316L Austenitic Stainless Steel,” *Journal of Strain Analysis*, Vol. 39, No. 1, 2003, pp. 71-86.
14. Talonen, J. et al., “Effect of Strain Rate on the Strain-Induced  $\gamma \rightarrow \alpha$ -Martensite Transformation and Mechanical Properties of Austenitic Stainless Steels,” *Metallurgical and Materials Transactions A*, Vol. 36A, February 2005, pp. 421-432.
15. Lichtenfeld, J. A., M. C. Mataya, and C. J. Van Tyne, “Effect of Strain Rate on Stress-Strain Behavior of Alloy 309 and 304L Austenitic Stainless Steel,” *Metallurgical and Materials Transactions A*, Vol. 37A, January 2006, pp. 147-161.
16. Morton, D. K., and R. K. Blandford, *Impact Tensile Testing of Stainless Steels at Various Temperatures*, DOE Report EDF-NSNF-082, Revision 0, March 31, 2008.
17. Lee, W-S and Chi-Feng Lin, “Impact Properties and Microstructure Evolution of 304L Stainless Steel”, *Materials Science and Engineering A308*, 2001, pp. 124-135.
18. Nicholas, T., *Dynamic Tensile Testing of Structural Materials Using a Split Hopkinson Bar Apparatus*, AFWAL-TR-80-4053, October 1980.

## **APPENDIX D**

### **Consequences of Fuel Failure on Criticality Safety of Used Nuclear Fuel**

**FCRD Technical Integration Office (TIO)**  
**DOCUMENT NUMBER REQUEST**

**1. Document Information**

Document Title/Description:	Consequences of Fuel Failure on Criticality Safety of Used Nuclear Fuel				Revision:	0
Assigned Document Number:	FCRD-UFD-2012-000262				Effective Start Date:	September 1, 2012
Document Author/Creator:	W.J. Marshall				OR	
Document Owner:	J.C. Wagner				Date Range:	
Originating Organization:	Oak Ridge National Laboratory				From:	To:
Milestone	<input type="checkbox"/> M1	<input checked="" type="checkbox"/> M2	<input type="checkbox"/> M3	<input type="checkbox"/> M4	<input type="checkbox"/> Not a Milestone	
Milestone Number::	M2FT-12OR0813031					
Work Package WBS Number:	FT-12OR081303/ 1.02.08.13					
Controlled Unclassified Information (CUI) Type	<input checked="" type="checkbox"/> None <input type="checkbox"/> OUO <input type="checkbox"/> AT <input type="checkbox"/> Other					

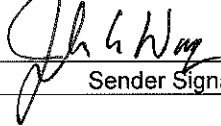
FCRD	<b>SYSTEM:</b>			
	<input type="checkbox"/> FUEL	Advance Fuels		
	<input type="checkbox"/> SWF	Separations and Waste Forms		
	<input type="checkbox"/> MPACT	Materials Protection, Accounting, and Control for Transmutation		
	<input checked="" type="checkbox"/> UFD	Used Fuel Disposition		
	<input type="checkbox"/> FCO	Fuel Cycle Options		
	<input type="checkbox"/> TIO	Technical Integration		
	<input type="checkbox"/>			

**2. Records Management Requirements**

Category:	<input checked="" type="checkbox"/> General Record	<input type="checkbox"/> QA Record	<input type="checkbox"/> Controlled Doc	<input type="checkbox"/> Controlled QA Doc
Keywords:	Used Nuclear Fuel Failure Criticality Safety			
Medium:	<input type="checkbox"/> Hard Copy	<input type="checkbox"/> CD/Disk (each CD/Disk must have an attached index)	<input type="checkbox"/> Electronic:	
Total Number of Pages (including transmittal sheet):				
<u>If QA Record</u>				
QA Classification:	<input type="checkbox"/> Lifetime	<input checked="" type="checkbox"/> Non-Permanent		
Uniform Filing Code:	8406	Disposition Authority:	RD1-A-2	Retention Period:
Level II Cut off after project/program completion, cancellation, or termination. Destroy 25 years after cut off.				

Special Instructions:	None		
-----------------------	------	--	--

**3. Signatures**

SENDER:	John C. Wagner		8/31/12
Print/Type Sender Name		Sender Signature	Date
QA RECORD VALIDATOR:			
Print/Type Authenticator Name	Authenticator Signature		Date
ACCEPTANCE/RECEIPT:			
Print/Type Receiver Name	Receiver Signature		Date

Submit to: **Connie.Bates@inl.gov**

## Appendix E

### FCT Document Cover Sheet

Name/Title of Deliverable/Milestone

Consequences of Fuel Failure on Criticality Safety of Used Nuclear Fuel

Work Package Title and Number

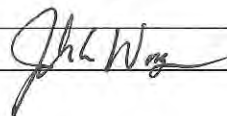
ST Transportation-ORNL / FT-12OR081303

Work Package WBS Number

**1.02.08.13**

Responsible Work Package Manager

John C. Wagner



(Name/Signature)

Date Submitted

Quality Rigor Level for Deliverable/Milestone	<input checked="" type="checkbox"/> QRL-3	<input type="checkbox"/> QRL-2	<input type="checkbox"/> QRL-1 <input type="checkbox"/> Nuclear Data	<input type="checkbox"/> N/A*
---	---	--------------------------------	---	-------------------------------

This deliverable was prepared in accordance with

Oak Ridge National Laboratory

(Participant/National Laboratory Name)

QA program which meets the requirements of

 DOE Order 414.1       NQA-1-2000

This Deliverable was subjected to:

 Technical Review Peer Review**Technical Review (TR)****Peer Review (PR)****Review Documentation Provided** Signed TR Report or,**Review Documentation Provided** Signed TR Concurrence Sheet or, Signed PR Report or, Signature of TR Reviewer(s) below Signed PR Concurrence Sheet or, Signature of PR Reviewer(s) below**Name and Signature of Reviewers**

John Scaglione (Electronic Record Attached)

Donald Mueller (Electronic Record Attached)

\*Note: In some cases there may be a milestone where an item is being fabricated, maintenance is being performed on a facility, or a document is being issued through a formal document control process where it specifically calls out a formal review of the document. In these cases, documentation (e.g., inspection report, maintenance request, work planning package documentation or the documented review of the issued document through the document control process) of the completion of the activity along with the Document Cover Sheet is sufficient to demonstrate achieving the milestone. QRL for such milestones may be also marked N/A in the work package provided the work package clearly specifies the requirement to use the Document Cover Sheet and provide supporting documentation.

 Publication Tracking System

This List: Publication List



Publication Tracking System &gt; Publication List

View Record (Logged in as Weaver, Deborah J.)

<a href="#"> Edit Item</a>   <a href="#"> Change Communication Type</a>   <a href="#"> Delete Item</a>			
<b>Pub ID</b>	38136		
<b>Title</b>	Consequences of Fuel Failure on Criticality Safety of Used Nuclear Fuel		
<b>Status</b>	Awaiting Distribution		
<b>Communication Type</b>	ORNL report		
<b>ORNL Review?</b>	Scientific communication that requires ORNL review		
<b>Information Category</b>	Unlimited		
<b>ORNL Report Classification</b>	Topical		
<b>Contact Person</b>	Marshall, William BJ J		
<b>Responsible Organization</b>	Reactor & Nuclear Systems Division (50159781)		
<b>Prepared at</b>	This scientific communication is being prepared by someone at ORNL.		
<b>Document Access</b>	Available to the public.		
<b>Authors</b>	Marshall, William BJ J.	ORNL (627296)	
	Wagner, John C.	ORNL (37727)	
<b>Workflow</b>	08/16/2012 11:39:02	Draft	Marshall, William BJ J by Weaver, Deborah J
	08/16/2012 14:07:01	Author Certification	Marshall, William BJ J
	08/16/2012 14:07:01	Submitted for review	Marshall, William BJ J
	08/16/2012 13:52:39	Supervisor	Dunn, Michael E
	08/20/2012 08:44:39	Technical Reviewer	Mueller, Don
	08/20/2012 17:47:11	Technical Reviewer	Hu, Jianwei
	08/23/2012 14:01:12	Technical Reviewer	Scaglione, John M
	08/26/2012 16:31:58	Technical Editor	Stevens, Deborah P
	08/27/2012 14:43:55	Administrative Check	Weaver, Deborah J
	08/28/2012 11:18:07	Supervisor	Dunn, Michael E
	08/31/2012 12:33:39	Program Manager	Howard, Rob L
	08/31/2012 16:32:52	Division Approver	Parks, Cecil V by Poarch, Sandra J
	08/31/2012 16:32:52	Awaiting Distribution	Parks, Cecil V by Poarch, Sandra J
			<i>Waiting on contact person to mark as 'Distributed'.</i>
		Distributed	Marshall, William BJ J
<b>Document</b>	<a href="#">edited_UFD_Transportation_Consequences_of_Fuel_Failure_Draft_8_27_2012.pdf</a>		
	<b>Important:</b> Documents containing sensitive information should not be loaded into PTS. For further clarification, please contact ORNL's Technical Information Officer.		
<b>Abstract</b>			
<b>Report Number</b>	ORNL/TM-2012/325		
<b>Secondary ID Number</b>			
<b>Additional Information</b>			
<b>Distribution Month</b>			
<b>Distribution Year</b>			
<b>User Facility</b>	Not related to a user facility		
<b>Account Number(s)</b>	35304813		
<b>B&amp;R Codes</b>	AF5865000		
<b>IANs</b>			
<b>FWP</b> s	NEAF346		
<b>Overhead Categories</b>			
<b>Proposal Numbers</b>			
<b>Keywords</b>			

# ***Consequences of Fuel Failure on Criticality Safety of Used Nuclear Fuel***

---

**Fuel Cycle Research & Development**

*Prepared for*  
**U.S. Department of Energy**  
**Fuel Cycle Technologies Program**  
**W. J. Marshall**  
**J. C. Wagner**  
**Oak Ridge National Laboratory**  
**September 2012**  
ORNL/TM-2012/325  
FCRD-UFD-2012-000262



#### **DISCLAIMER**

This information was prepared as an account of work sponsored by an agency of the U.S. Government. Neither the U.S. Government nor any agency thereof, nor any of their employees, makes any warranty, expressed or implied, or assumes any legal liability or responsibility for the accuracy, completeness, or usefulness, of any information, apparatus, product, or process disclosed, or represents that its use would not infringe privately owned rights. References herein to any specific commercial product, process, or service by trade name, trade mark, manufacturer, or otherwise, does not necessarily constitute or imply its endorsement, recommendation, or favoring by the U.S. Government or any agency thereof. The views and opinions of authors expressed herein do not necessarily state or reflect those of the U.S. Government or any agency thereof.

## EXECUTIVE SUMMARY

This report documents work performed for the Department of Energy's Office of Nuclear Energy (DOE-NE) Fuel Cycle Technologies Used Fuel Disposition Campaign to assess the impact of fuel reconfiguration due to fuel failure on the criticality safety of used nuclear fuel (UNF) in storage and transportation casks. This work was motivated by concerns related to the potential for fuel degradation during extended storage (ES) periods and transportation following ES, but has relevance to other potential causes of fuel reconfiguration.

Commercial UNF in the United States is expected to remain in storage for longer periods than originally intended. Extended storage time and irradiation of nuclear fuel to high-burnup values ( $>45$  GWd/t) may increase the potential for fuel failure during normal and accident conditions involving storage and transportation. Fuel failure, depending on the severity, can result in changes to the geometric configuration of the fuel, which has safety and regulatory implications for virtually all aspects of a UNF storage and transport system's performance. The potential impact of fuel reconfiguration on the safety of UNF in storage and transportation is dependent on the likelihood and extent of the fuel reconfiguration, which is not well understood and is currently an active area of research. The objective of this work is to assess and quantify the impact of postulated failed fuel configurations on the criticality safety of UNF in storage and transportation casks. Although this work is motivated by the potential for fuel degradation during ES periods and transportation following ES, it has relevance to fuel reconfiguration due to the effects of high burnup. Regardless of the ultimate disposition path, UNF will need to be transported at some point in the future.

To investigate and quantify the impact of fuel reconfiguration on criticality safety limits, which are given in terms of the effective neutron multiplication factor,  $k_{\text{eff}}$ , a set of failed fuel configuration categories was developed and specific configurations were evaluated. The various configurations were not developed to represent the results of specific reconfiguration progressions; rather, they were designed to be bounding of any reconfiguration progressions that could occur. The configuration categories considered in this analysis include the following:

- clad thinning/loss – reduced cladding thickness up to the total removal of all cladding material
- rod failures – removal of one or more fuel rods from the assembly lattice
- loss of rod pitch control – rod pitch contraction and expansion within the storage cell
- loss of assembly position control – axial displacement of fuel assemblies
- gross assembly failure – rubblized fuel within the storage cells with varying degrees of moderation
- neutron absorber degradation – gaps of varying location and size; thinning of absorber panels.

Within each category, a number of specific configurations were modeled to calculate the corresponding  $k_{\text{eff}}$  values and the associated consequences of those configurations relative to the reference intact configuration. The consequence of a given configuration is defined as the difference in the calculated  $k_{\text{eff}}$  values for the given configuration and the reference intact configuration, with a positive value indicating an increase in  $k_{\text{eff}}$  as compared to the reference configuration. Several of the specific configurations are not considered credible but are included in the analyses for completeness (e.g., to fully understand trends and worst-case situations). Pending improved understanding of the various material degradation phenomenon, and subsequent determination and justification for what configurations are and are not credible, the assessment of the credibility of configurations provided herein is based on engineering judgment. The credibility of configurations and the impact of the configurations on criticality safety are dependent on many factors, including storage and transportation conditions, the fuel assembly

characteristics, and the storage and/or transportation system characteristics. Therefore, the assessment and analysis of credible configurations for a specific cask system would need to be performed as part of the safety analysis for licensing that system.

Representative pressurized water reactor (PWR) and boiling water reactor (BWR) fuel assembly designs loaded in representative cask systems were considered in this report. The two fuel assembly designs selected for this analysis represent a large portion of the current inventory of discharged UNF and/or a significant portion of the fuel designs currently in use. The cask systems selected for this analysis are high-capacity 32-PWR-assembly general burnup credit cask (GBC-32) and 68-BWR-assembly multipurpose canister (MPC-68) cask designs based on the Holtec International HI-STAR 100 system. The depletion conditions used in this analysis are considered representative of those used in a burnup credit criticality safety evaluation. The analysis focuses on typical discharge fuel conditions (e.g., fuel initial enrichment, discharge burnup, and post-irradiation decay time) that could be loaded into storage and transportation casks. Additional burnup and extended post-irradiation cooling times are considered in this analysis for both PWR and BWR fuel to establish the sensitivity of reconfiguration impacts to these parameters.

For the configurations judged by the authors to be potentially credible, the maximum increase in  $k_{\text{eff}}$  for the PWR cask system (GBC-32) was nearly 4%, corresponding to a nonuniform pitch expansion configuration due to a loss of fuel rod pitch control, and that for the BWR cask system (MPC-68) was 2.4%, corresponding to a configuration with multiple rod failures. It is important to emphasize that these results are contingent on the authors' judgment relative to the potential credibility of configurations, which includes not only whether a configuration category is credible but also whether the resulting configurations within a given category are credible for a specific cask system. For example, for the PWR cask system, axial assembly displacement such that assemblies extended more than 7.5 cm above or below the neutron absorber panel was not considered credible because of the presence of fuel assembly hardware and cask assembly spacers. If it were determined that such a configuration is credible, then that configuration and its specific characteristics may be limiting. Similarly, for the BWR cask system, the fuel assembly channel is assumed to be present and capable of constraining fuel rod pitch expansion. If the channel is not present or unable to constrain rod pitch expansion, then that configuration may be limiting. In addition to representative conditions for fuel burnup and post-irradiation decay time, the effects of higher burnup and longer cooling times were also investigated and found to be smaller than the reduction in  $k_{\text{eff}}$  associated with the higher burnup or cooling time.

Because a wide range of credible and non-credible configurations were analyzed, the calculated consequences also varied widely. For the PWR cask system (GBC-32), the calculated  $k_{\text{eff}}$  increase varied from 0.1% to almost 22.25%  $\Delta k_{\text{eff}}$ . For the BWR cask system (MPC-68), the calculated increase varied from 0.3%  $\Delta k_{\text{eff}}$  to as much as almost 36%  $\Delta k_{\text{eff}}$ . Some configurations in both cask systems result in decreases in  $k_{\text{eff}}$ . As the Nuclear Regulatory Commission (NRC) Standard Review Plans, which provide guidance for demonstrating compliance with the applicable regulations, recommend that  $k_{\text{eff}}$  should not exceed 0.95 under all credible conditions during storage and transportation, such large increases are concerning. However, as noted, a number of the configurations analyzed are not considered credible.

The magnitude of the potential increases in  $k_{\text{eff}}$  and the sensitivity of the potential increases in  $k_{\text{eff}}$  to the determination of the credibility of configurations highlight the importance of being able to determine and justify which configurations are credible under a given set of conditions for a given cask system. It is anticipated, at least in the near term, that these determinations will be done on a case-by-case basis for each cask system and associated licensing conditions.

Given the establishment of a set of credible failed fuel configurations for a given cask system and assuming that one or more of the configurations result in an increase in  $k_{\text{eff}}$  (above the regulatory limit of

0.95), the consequence of this potential increase in  $k_{\text{eff}}$  must be addressed. There are a number of potential options, the viability of which depends on the magnitude of the increase in  $k_{\text{eff}}$ . For example, a cask design and/or fuel assembly loading conditions could be modified to ensure that the current  $k_{\text{eff}}$  limit of 0.95 is satisfied for all credible failed fuel configurations. Separate assembly loading criteria (e.g., loading curves) based on a reduced  $k_{\text{eff}}$  limit could be developed for fuel assemblies that may have questionable integrity. In the context of high-burnup fuel or ES durations, a separate loading curve based on a lower  $k_{\text{eff}}$  limit could be developed and applied to fuel assemblies with burnup greater than 45 GWd/MTU and/or with a post-irradiation storage period beyond some specified value. Alternatively, depending on the probability of fuel reconfiguration, it may be possible that a separate higher limit could be established to allow margin for the increased reactivity effect associated with fuel reconfiguration. This latter approach would be similar to the higher limit (i.e., 0.98) allowed for the unlikely optimum moderation condition in dry storage of fresh fuel under 10 CFR 50.68. In this case, the customary  $k_{\text{eff}}$  limit would still apply to all conditions involving intact fuel. Limits above 0.95 are also allowed in some facilities regulated by the NRC Fuel Cycle Safety and Safeguards Division, and hence precedents for this type of approach exist. For casks that have already been loaded prior to implementation of a generic mitigation strategy, the analysis basis may be extended to include or expand burnup credit, providing mitigation for potential consequences of fuel reconfiguration.

Although the results indicate that the potential impacts on subcriticality can be rather significant for certain configurations, it can be concluded that the consequences of credible fuel failure configurations from ES or transportation following ES are manageable. Some examples for how to address the potential increases in  $k_{\text{eff}}$  in a criticality safety evaluation were provided. Future work to further inform decision-making relative to which configurations are credible, and therefore need to be considered in a safety evaluation, is recommended.



## CONTENTS

	<u>Page</u>
EXECUTIVE SUMMARY .....	iii
FIGURES .....	ix
TABLES .....	xiii
ACRONYMS .....	xvii
1. INTRODUCTION AND BACKGROUND .....	1
2. REVIEW OF LITERATURE .....	2
2.1 NRC Documents .....	2
2.2 EPRI Reports.....	3
2.3 PATRAM Proceedings .....	4
2.3.1 PATRAM 2010.....	4
2.3.2 PATRAM 2007.....	5
2.3.3 PATRAM 2004.....	6
2.3.4 PATRAM 2001 .....	6
2.4 Other Sources.....	7
2.5 Literature Review Summary .....	7
3. FAILED FUEL CONFIGURATIONS .....	7
3.1 Fuel and Cask Reconfiguration Descriptions.....	8
3.1.1 Clad Thinning/Loss.....	8
3.1.2 Rod Failures .....	9
3.1.3 Loss of Rod Pitch Control.....	10
3.1.4 Loss of Assembly Position Control .....	11
3.1.5 Gross Assembly Failure .....	11
3.1.6 Neutron Absorber Degradation.....	13
3.2 Varying Number of Reconfigured Assemblies .....	14
3.3 Multiple Reconfiguration Mechanisms.....	14
3.4 Credibility of Degraded Configurations.....	14
4. MODELS, CODES, AND METHODS USED .....	17
4.1 Fuel Assembly Models.....	17
4.2 Cask Models.....	17
4.2.1 GBC-32 Cask Model.....	17
4.2.2 MPC-68 Cask Model .....	19
4.3 Software Codes .....	20
4.4 Depletion Modeling Parameters.....	20
4.4.1 PWR Depletion Conditions.....	21
4.4.2 BWR Depletion Conditions .....	21

## CONTENTS (continued)

	<u>Page</u>
5. RESULTS.....	22
5.1 GBC-32 Cask Model Results.....	22
5.1.1 Reconfiguration of All Assemblies.....	23
5.1.2 Varying Number of Reconfigured Assemblies.....	38
5.1.3 Combined Configurations.....	44
5.2 MPC-68 Cask Model Results.....	45
5.2.1 Reconfiguration of All Assemblies.....	45
5.2.2 Varying Number of Reconfigured Assemblies.....	61
5.2.3 Combined Configurations.....	69
5.2.4 Part-Length Fuel .....	70
6. SUMMARY AND CONCLUSIONS.....	77
6.1 Summary of Analyses .....	77
6.2 Observations and Conclusions .....	78
7. RECOMMENDATIONS FOR FUTURE WORK .....	80
REFERENCES .....	81
Appendix A Fuel Assembly Modeling Details .....	85
Appendix B MPC-24 Modeling and Results .....	89
Appendix C Sensitivity to Burnup and Cooling Time .....	111
Appendix D Details of Cask Modeling.....	123
Appendix E Development of BWR Depletion Conditions .....	127

## FIGURES

	<u>Page</u>
Figure 1. Sketch showing “birdcaging” as the result of an end drop .....	5
Figure 2. Cross section of GBC-32 half-cask model. ....	18
Figure 3. Representative fuel assembly loading curve for GBC-32. ....	18
Figure 4. Cross section of MPC-68 model.....	19
Figure 5. Increase in $k_{\text{eff}}$ due to reduced cladding thickness .....	24
Figure 6. Configuration with 50% cladding thickness.....	25
Figure 7. Sketch of symmetry, row, and column labels for W 17 × 17 fuel assembly. ....	26
Figure 8. Increase in $k_{\text{eff}}$ in GBC-32 cask as a function of number of rods removed .....	27
Figure 9. Limiting multiple rod removal lattice (44 rods removed). ....	27
Figure 10. Maximum uniform pitch expansion case. ....	29
Figure 11. Increase in $k_{\text{eff}}$ in GBC-32 cask due to increased fuel rod pitch.....	30
Figure 12. Example nonuniform pitch model in GBC-32 storage cell. ....	30
Figure 13. Assembly with axially varying pitch in the GBC-32. ....	31
Figure 14. Misalignment of fuel assembly 20 cm toward lid of GBC-32. ....	32
Figure 15. Increase in $k_{\text{eff}}$ in GBC-32 as a function of assembly axial displacement .....	33
Figure 16. Limiting homogeneous rubble configuration for GBC-32. ....	35
Figure 17. Limiting ordered pellet array configuration for GBC-32. ....	35
Figure 18. Limiting location of 5-cm neutron absorber panel defect in GBC-32. ....	37
Figure 19. Increase in $k_{\text{eff}}$ as a function of remaining neutron absorber panel thickness for fresh 1.92 w/o fuel.....	38
Figure 20. One order of assembly reconfiguration in GBC-32 partial degradation configurations.....	39
Figure 21. Increase in $k_{\text{eff}}$ in GBC-32 as a function of number of reconfigured assemblies, single rod failure (5 w/o initial enrichment, 44.25 GWd/MTU burnup). ....	41
Figure 22. Increase in $k_{\text{eff}}$ in GBC-32 as a function of number of reconfigured assemblies, multiple rod failure (5 w/o initial enrichment, 44.25 GWd/MTU burnup). ....	41
Figure 23. Increase in $k_{\text{eff}}$ in GBC-32 as a function of number of reconfigured assemblies, uniform pitch increase (5 w/o initial enrichment, 44.25 GWd/MTU burnup). ....	42
Figure 24. Increase in $k_{\text{eff}}$ as a function of number of reconfigured assemblies, gross assembly failure. ....	44
Figure 25. Increase in $k_{\text{eff}}$ as a function of fraction of intact cladding, fresh 5 w/o fuel.....	47
Figure 26. Configuration with 25% nominal cladding thickness.....	48
Figure 27. Sketch of symmetry, row, and column labels for GE 10 × 10 fuel assembly. ....	49

## FIGURES (continued)

	<u>Page</u>
Figure 28. Increase in $k_{\text{eff}}$ in MPC-68 as a function of number of rods removed (35 GWd/MTU burnup and 5-year cooling time).....	50
Figure 29. Limiting multiple rod removal lattice (18 rods removed). .....	50
Figure 30. Maximum uniform pitch expansion configuration in MPC-68. ....	52
Figure 31. Example nonuniform pitch model for MPC-68.....	53
Figure 32. Increase in $k_{\text{eff}}$ in MPC-68 as a function of fuel rod pitch, fresh 5 w/o fuel. ....	53
Figure 33. A fresh fuel birdcaging configuration for MPC-68. ....	54
Figure 34. Limited axial misalignment of 20 cm toward cask lid.....	55
Figure 35. Increase in $k_{\text{eff}}$ in MPC-68 as a function of assembly axial displacement (35 GWd/MTU burnup and 5-year cooling time). ....	56
Figure 36. Limiting homogeneous rubble configuration in MPC-68.....	58
Figure 37. Limiting ordered pellet array configuration for MPC-68. ....	58
Figure 38. Limiting neutron absorber defect configuration in MPC-68. ....	60
Figure 39. Increase in $k_{\text{eff}}$ in MPC-68 as a function of remaining neutron absorber panel thickness .....	61
Figure 40. One order of assembly reconfiguration in MPC-68 partial degradation configurations. ....	62
Figure 41. Increase in $k_{\text{eff}}$ in MPC-68 as a function of number of reconfigured assemblies,.....	64
Figure 42. Increase in $k_{\text{eff}}$ in MPC-68 as a function of number of reconfigured assemblies, multiple rod failure (35 GWd/MTU burnup and 5-year cooling time). ....	64
Figure 43. Increase in $k_{\text{eff}}$ in MPC-68 as a function of number of reconfigured assemblies, uniform pitch increase fresh 5 w/o fuel. ....	66
Figure 44. Increase in $k_{\text{eff}}$ as a function of number of reconfigured assemblies, gross assembly failure (35 GWd/MTU burnup and 5-year cooling time). ....	67
Figure 45. Histogram of increases in $k_{\text{eff}}$ for 25 random samples of four reconfigured assemblies. ....	69
Figure 46. Increase in $k_{\text{eff}}$ in MPC-68 as a function of fraction of intact cladding .....	72
Figure 47. Increase in $k_{\text{eff}}$ in MPC-68 as a function of neutron absorber defect axial position,.....	76
Figure 48. Increase in $k_{\text{eff}}$ in MPC-68 as a function of remaining neutron absorber panel thickness, .....	76
Figure A-1. Cross section of $17 \times 17$ OFA assembly.....	86
Figure A-2. Cross section of GE $10 \times 10$ fuel assembly in MPC-68. ....	88
Figure A-3. Location of part-length rods in GE $10 \times 10$ fuel assembly.....	88

## **FIGURES (continued)**

	<u>Page</u>
Figure B-1. Cross section of MPC-24 model.....	89
Figure B-2. Loss of cladding model in MPC-24 storage cell.....	92
Figure B-3. Increase in $k_{\text{eff}}$ in MPC-24 due to reduced cladding thickness.....	92
Figure B-4. Increase in $k_{\text{eff}}$ in MPC-24 versus number of rods removed.....	94
Figure B-5. Limiting multiple rod removal lattice (48 rods removed).....	94
Figure B-6. Increase in $k_{\text{eff}}$ in MPC-24 as a function of fuel rod pitch.....	95
Figure B-7. Maximum pitch expansion case in MPC-24.....	96
Figure B-8. Example axial variation of pitch expansion in MPC-24.....	96
Figure B-9. Increase in $k_{\text{eff}}$ as a function of axial assembly misalignment in MPC-24.....	97
Figure B-10. Assembly in MPC-24 misaligned 20-cm toward cask lid.....	98
Figure B-11. Ordered pellet array configuration for gross assembly failure.....	99
Figure B-12. Homogeneous rubble configuration for gross assembly failure.....	99
Figure B-13. Preferential flooding with only the fuel assemblies flooded.....	100
Figure B-14. 5-cm gap in neutron absorber panels in MPC-24.....	101
Figure B-15. Increase in $k_{\text{eff}}$ in MPC-24 as a function of neutron absorber panel thickness.....	102
Figure B-16. One order of assembly reconfiguration in MPC-24 partial degradation configurations.....	103
Figure B-17. Single rod failure results for a range of number of assemblies experiencing reconfiguration in MPC-24.....	105
Figure B-18. Multiple rod failure results for a range of number of assemblies experiencing reconfiguration in MPC-24.....	105
Figure B-19. Uniform pitch increase results for a range of number of assemblies experiencing reconfiguration in MPC-24.....	106
Figure B-20. Homogeneous rubble results for a range of number of assemblies experiencing reconfiguration.....	108
Figure C-1. Reactivity behavior of fuel with cooling time in a GBC-32 cask.....	111
Figure C-2. Increase in $k_{\text{eff}}$ as a function of cladding thickness remaining.....	113
Figure C-3. Increase in $k_{\text{eff}}$ as a function of cladding thickness remaining.....	118
Figure D-1. Locations of narrow neutron absorber panels in MPC-24 basket.....	124



## TABLES

	<u>Page</u>
Table 1. Credibility and relevance summary.....	16
Table 2. Isotopes included in depleted fuel models.....	21
Table 3. PWR depletion parameters.....	21
Table 4. BWR depletion parameters .....	22
Table 5. Enrichment, burnup, and cooling time for reference cases considered in GBC-32 .....	23
Table 6. Summary of $k_{\text{eff}}$ increases for the GBC-32 cask.....	23
Table 7. Increase in $k_{\text{eff}}$ for cladding removal in GBC-32.....	24
Table 8. Increase in $k_{\text{eff}}$ in GBC-32 cask as a function of cladding fraction remaining .....	24
Table 9. Single rod removal results for $17 \times 17$ OFA in GBC-32.....	26
Table 10. Multiple rod removal results for $17 \times 17$ OFA in GBC-32.....	26
Table 11. Results for loss of rod pitch control in GBC-32.....	29
Table 12. Increase in $k_{\text{eff}}$ for assembly axial displacement in GBC-32 .....	32
Table 13. Increase in $k_{\text{eff}}$ for limited (20 cm displacement relative to the neutron absorber panel).....	32
Table 14. Increase in $k_{\text{eff}}$ in GBC-32 due to gross fuel assembly failure, fissile material outside neutron absorber elevations.....	34
Table 15. Increase in $k_{\text{eff}}$ in GBC-32 due to homogeneous rubble, debris within absorber .....	34
Table 16. Maximum $k_{\text{eff}}$ increase caused by a 5-cm neutron absorber defect in GBC-32.....	36
Table 17. Increase in $k_{\text{eff}}$ caused by a 5-cm neutron absorber defect at various elevations in GBC-32 (5 w/o initial enrichment, 44.25 GWd/MTU burnup).....	36
Table 18. Increase in $k_{\text{eff}}$ caused by uniform neutron absorber panel thinning (fresh 1.92 w/o enrichment).....	37
Table 19. Increase in $k_{\text{eff}}$ in GBC-32, single rod failure .....	40
Table 20. Increase in $k_{\text{eff}}$ in GBC-32, multiple rod failure .....	40
Table 21. Increase in $k_{\text{eff}}$ in GBC-32, uniform pitch increase .....	42
Table 22. Increase in $k_{\text{eff}}$ in GBC-32, homogeneous rubble configuration of gross assembly failure (5 w/o initial enrichment, 44.25 GWd/MTU burnup).....	43
Table 23. Increase in $k_{\text{eff}}$ for combined configurations in GBC-32 .....	45
Table 24. Nominal $k_{\text{eff}}$ results for enrichment, burnup, and cooling time .....	45
Table 25. Summary of $k_{\text{eff}}$ increases for the MPC-68 cask.....	46
Table 26. Increase in $k_{\text{eff}}$ for cladding removal in MPC-68.....	47
Table 27. Increase in $k_{\text{eff}}$ in MPC-68 as a function of fraction of intact cladding, fresh 5 w/o fuel.....	47
Table 28. Single rod removal results for GE $10 \times 10$ fuel in MPC-68.....	49

## TABLES (continued)

	<u>Page</u>
Table 29. Multiple rod removal results for GE 10 × 10 fuel in MPC-68.....	49
Table 30. Results for loss of rod pitch control in MPC-68, no channel restraint.....	52
Table 31. Increase in $k_{\text{eff}}$ caused by loss of assembly position control in MPC-68 .....	55
Table 32. Increase in $k_{\text{eff}}$ for homogeneous rubble configuration of gross fuel assembly failure in MPC-68 .....	57
Table 33. Increase in $k_{\text{eff}}$ for pellet array configuration of gross fuel assembly failure in MPC-68 .....	57
Table 34. Increase in $k_{\text{eff}}$ in MPC-68 due to homogeneous rubble, debris within absorber.....	57
Table 35. Maximum $k_{\text{eff}}$ increase caused by a 5-cm neutron absorber defect in MPC-68.....	59
Table 36. Increase in $k_{\text{eff}}$ caused by a 5-cm neutron absorber defect at various elevations in MPC-68 (35 GWd/MTU burnup and 5-year cooling time) .....	59
Table 37. Increase in $k_{\text{eff}}$ in MPC-68 caused by uniform neutron absorber panel thinning, fresh 5 w/o fuel .....	60
Table 38. Increase in $k_{\text{eff}}$ in MPC-68, single rod failure fresh 5 w/o fuel .....	63
Table 39. Increase in $k_{\text{eff}}$ in MPC-68, multiple rod failure .....	63
Table 40. Increase in $k_{\text{eff}}$ in MPC-68, uniform pitch increase fresh 5 w/o fuel .....	65
Table 41. Increase in $k_{\text{eff}}$ , homogeneous rubble configuration of gross assembly failure.....	67
Table 42. Increase in $k_{\text{eff}}$ for 25 realizations of four randomly selected reconfigured assemblies.....	68
Table 43. Increase in $k_{\text{eff}}$ in combined configurations in MPC-68.....	70
Table 44. Nominal $k_{\text{eff}}$ results for fresh 5 w/o fuel assemblies with part-length rods in MPC-68 .....	71
Table 45. Summary of $k_{\text{eff}}$ impact for fresh 5 w/o fuel with part-length rods in MPC-68 .....	71
Table 46. Increase in $k_{\text{eff}}$ in MPC-68 caused by cladding loss for assemblies with part-length fuel rods, fresh 5 w/o fuel .....	72
Table 47. Increase in $k_{\text{eff}}$ in MPC-68 caused by single rod failure in fresh 5 w/o assemblies with part-length rods.....	73
Table 48. Increase in $k_{\text{eff}}$ in MPC-68 caused by a 5-cm neutron absorber panel defect, fresh 5 w/o fuel with part-length fuel rods .....	75
Table 49. Increase in $k_{\text{eff}}$ in MPC-68 caused by uniform neutron absorber panel thinning, fresh 5 w/o fuel with part-length fuel rods .....	75
Table A-1. Westinghouse 17 × 17 OFA dimensions used in these analyses .....	86
Table A-2. GE 10 × 10 assembly dimensions used in these analyses.....	87
Table B-1. Reference case results for MPC-24 .....	90
Table B-2. Summary of $k_{\text{eff}}$ increases for the MPC-24 cask.....	91

## TABLES (continued)

	<u>Page</u>
Table B-3. Increase in $k_{\text{eff}}$ in MPC-24 due to reduced cladding thickness.....	91
Table B-4. Single rod removal results for $17 \times 17$ OFA in MPC-24.....	93
Table B-5. Increase in $k_{\text{eff}}$ in MPC-24 caused by a 5-cm neutron absorber defect at various elevations.....	101
Table B-6. Increase in $k_{\text{eff}}$ in MPC-24 caused by uniform neutron absorber panel thinning.....	101
Table B-7. Increase in $k_{\text{eff}}$ in MPC-24, single rod failure .....	104
Table B-8. Increase in $k_{\text{eff}}$ in MPC-24, multiple rod failures (48 failed rods) .....	104
Table B-9. Increase in $k_{\text{eff}}$ in MPC-24, uniform pitch increase.....	106
Table B-10. Increase in $k_{\text{eff}}$ in MPC-24, homogeneous rubble configuration of gross assembly failure.....	107
Table B-11. Increase in $k_{\text{eff}}$ in combined configurations for MPC-24.....	109
Table C-1. Nominal $k_{\text{eff}}$ results for enrichment, burnup, and cooling time cases considered in GBC-32.....	112
Table C-2. Single rod removal results for $17 \times 17$ OFA in GBC-32.....	113
Table C-3. Multiple rod removal results for $17 \times 17$ OFA in GBC-32 .....	114
Table C-4. Increase in $k_{\text{eff}}$ caused by uniform fuel pin pitch expansion .....	114
Table C-5. Increase in $k_{\text{eff}}$ for limited assembly axial displacement in GBC-32 .....	115
Table C-6. Increase in $k_{\text{eff}}$ caused by gross fuel assembly failure in GBC-32 .....	115
Table C-7. Increase in $k_{\text{eff}}$ caused by neutron absorber panel defects.....	116
Table C-8. Increase in $k_{\text{eff}}$ caused by uniform neutron absorber panel thinning (44.25 GWd/MTU burnup, 5-year cooling time).....	116
Table C-9. Nominal $k_{\text{eff}}$ results for enrichment, burnup, and cooling time cases considered in MPC-68, channeled and unchanneled fuel .....	117
Table C-10. Single rod removal results for GE $10 \times 10$ fuel in MPC-68, intact channel.....	119
Table C-11. Multiple rod removal results for GE $10 \times 10$ fuel in MPC-68, intact channel .....	119
Table C-12. Results for loss of rod pitch control with cladding intact in MPC-68 .....	120
Table C-13. Increase in $k_{\text{eff}}$ for limited assembly axial displacement in MPC-68, intact channel.....	120
Table C-14. Increase in $k_{\text{eff}}$ caused by gross fuel assembly failure in MPC-68.....	121
Table C-15. Maximum $k_{\text{eff}}$ increase caused by a 5-cm neutron absorber defect in MPC-68, intact channel.....	122
Table C-16. Maximum $k_{\text{eff}}$ increase caused by a 10-cm neutron absorber defect in MPC-68, intact channel.....	122

**TABLES (continued)**

	<u>Page</u>
Table C-17. Increase in $k_{\text{eff}}$ caused by uniform neutron absorber panel thinning (35-GWd/MTU burnup, 5-year cooling time) .....	122
Table D-1. MPC-24 basket dimensions .....	123
Table D-2. MPC-24 Neutron absorber panel dimensions .....	124
Table D-3. MPC-68 basket dimensions .....	125
Table D-4. MPC-68 neutron absorber panel dimensions .....	125
Table E-1. Potentially limiting relative burnup profiles from Quad Cities Unit 2 and LaSalle Unit 1 .....	128
Table E-2. Average moderator density by axial node, based on Assembly C30 from LaSalle Unit 1 .....	129

## ACRONYMS

BWR	boiling water reactor
CRC	commercial reactor critical
DOE-NE	Department of Energy's Office of Nuclear Energy
EIS	environmental impact statement
EPRI	Electric Power Research Institute
ES	extended storage
FIP	fuel integrity project
GBC	generic burnup credit cask
GE	General Electric
GWd/MTU	gigawatt days per metric ton uranium
HAC	hypothesized accident conditions
ICNC	International Conference on Nuclear Criticality Safety
LWR	light water reactor
MPC	multipurpose canister
NRC	United States Nuclear Regulatory Commission
OFA	optimized fuel assembly
PATRAM	International Symposium on the Packaging and Transportation of Radioactive Materials
PRA	probabilistic risk assessment
PWR	pressurized water reactor
SAR	safety analysis report
SFST	Division of Spent Fuel Storage and Transportation, U.S. Nuclear Regulatory Commission
SRP	standard review plan
UNF	used nuclear fuel
WABA	wet annular burnable absorber
w/o	weight percent



# FUEL CYCLE TECHNOLOGIES PROGRAM

## CONSEQUENCES OF FUEL FAILURE ON CRITICALITY SAFETY OF USED NUCLEAR FUEL

### 1. INTRODUCTION AND BACKGROUND

This report documents work performed for the Department of Energy's Office of Nuclear Energy (DOE-NE) Fuel Cycle Technologies Used Fuel Disposition Campaign to assess the impact of fuel reconfiguration due to fuel failure on the criticality safety of used nuclear fuel (UNF) in storage and transportation casks. The consequences of degradation of neutron absorber panels and cask assembly spacers within the casks are also considered. This work is motivated by concerns related to the potential for fuel degradation during extended storage (ES) periods and transportation following ES, but has relevance to other potential causes of fuel reconfiguration.

Fuel reconfiguration could adversely impact virtually all aspects of a UNF storage and transport system's performance, including thermal, radiation dose, criticality safety, containment, structural, and fuel handling and retrievability, and hence is being studied in research and regulatory activities [1–6]. The likelihood and potential extent of fuel reconfiguration during ES and the subsequent impact of reconfiguration on the safety of the UNF are not well understood. Uncertainties related to the mechanical properties of fuel cladding and other structural materials at high burnups ( $>45$  GWd/MTU) and after ES exacerbate these concerns.

A key element of understanding the impacts of ES is related to ensuring that regulatory requirements are met. These requirements address safety-significant aspects of UNF storage and transportation systems, including criticality safety performance and related operational requirements pertaining to UNF handling and retrievability. The results of this study may be used to develop an effective approach to address criticality safety associated with UNF after ES.

This work is an expansion of NUREG/CR-6835, Ref. 7, and includes the same overall strategy. This strategy is to identify relevant potential fuel degradation configurations, quantify the impact of these configurations on  $k_{\text{eff}}$ , and evaluate potential mitigation strategies to meet criticality safety requirements. This work expands on Ref. 7 by including irradiated (or used) boiling water reactor (BWR) fuel as well as used pressurized water reactor (PWR) fuel, considers longer cooling times, and expands the scope of reconfigurations considered.

The criticality safety requirements for dry storage and transportation of UNF are contained in 10 CFR Parts 72 and 71, respectively Refs. 8 and 9. Standard Review Plans (SRPs), Refs. 10–12, provide guidance for meeting the regulatory requirements, such as the  $k_{\text{eff}}$  limit of 0.95 for ensuring the regulatory requirement associated with criticality safety. Estimates of the change in  $k_{\text{eff}}$  ( $\Delta k$ ) due to credible failed fuel configurations are generated in this analysis. A set of failed fuel configuration categories was developed and specific configurations are analyzed to provide a conservative assessment of the impact on  $k_{\text{eff}}$ . The potential credibility of these configurations is also considered, and only those judged to be potentially credible are considered in the development of mitigation strategies. The change in  $k_{\text{eff}}$  due to credible reconfigurations can be used in at least two different ways. A cask design and/or fuel assembly loading conditions could be modified to ensure that the current  $k_{\text{eff}}$  limit of 0.95 is satisfied for all credible failed fuel configurations. The  $\Delta k$  caused by reconfiguration would be accounted for in the determination

of the loading curve to meet the regulatory limit. It is also possible that a separate higher limit could be established to allow margin for the  $\Delta k$  associated with fuel reconfiguration. This latter approach would be similar to the higher limit allowed for the optimum moderation condition applied to dry storage of fresh fuel (i.e.,  $k_{\text{eff}} \leq 0.98$ ), or the unborated condition in a spent fuel pool that credits soluble boron to demonstrate compliance (i.e.,  $k_{\text{eff}} < 1.0$ ) under 10 CFR 50.68, Ref. 13. In this case, the customary  $k_{\text{eff}}$  limit would still apply to all conditions involving intact fuel.

The results of this work may also be used to focus future materials research efforts. The configurations that lead to the highest  $k_{\text{eff}}$  increases may be precluded or determined not to be credible with appropriate material research and testing coupled with mechanical analyses of the UNF.

In addition to criticality safety, the regulatory requirements for UNF storage and transport systems address safety-significant aspects such as structural, thermal, containment and radiation shielding, as well as related operational requirements pertaining to UNF handling and retrievability, such as those contained in the following Sections of 10 CFR 72. 122 (h) *Confinement barriers and systems*:

- (1) “The spent fuel cladding must be protected during storage against degradation that leads to gross ruptures or the fuel must be otherwise confined such that degradation of the fuel during storage will not pose operational safety problems with respect to its removal from storage. This may be accomplished by canning of consolidated fuel rods or unconsolidated assemblies or other means as appropriate.”
- (5) “The high-level radioactive waste and reactor-related GTCC waste must be packaged in a manner that allows handling and retrievability without the release of radioactive materials to the environment or radiation exposures in excess of part 20 limits. The package must be designed to confine the high-level radioactive waste for the duration of the license.”

Because it is possible that, within potential ES time periods, SNF may be transported under 10 CFR 71, and then returned to dry storage (e.g., at another utility or a national interim storage site) under 10 CFR 72, demonstration of compliance with the current handling and retrievability requirements in 10 CFR 72 may pose a significant challenge.

## 2. REVIEW OF LITERATURE

A review of previous work that is potentially relevant to the scope of this report was conducted. The information reviewed provides a historical context for consideration of fuel reconfiguration during transportation, the extent of reconfiguration that may be expected based on material test data, and an indication of the magnitude of reactivity consequences observed involving configurations similar to those considered in this report.

The documents reviewed are grouped by source into four categories: NRC documents, Electric Power Research Institute (EPRI) documents, International Symposium on the Packaging and Transportation of Radioactive Materials (PATRAM) proceedings, and others. NUREG/CR-6835, Ref. 7, is not specifically reviewed as this report is an update and expansion of that work. The primary differences between this analysis and Ref. 7 are discussed in Section 3.

### 2.1 NRC Documents

The first source of documents reviewed from the NRC was the Division of Spent Fuel Storage and Transportation (SFST) technical exchange meeting held on November 1, 2011. The technical exchange

meeting featured presentations from various members of the industry as well as NRC staff members. The NRC gave a presentation, Ref. 14, related to the reactivity impact of fuel reconfiguration. The presentation discussed pin deformation modeling but did not provide estimates of the  $k_{\text{eff}}$  increase associated with this type of fuel damage. In general, the presentation focused on the development and qualification of models to predict the potential deformation that could occur. Some perspectives on the  $k_{\text{eff}}$  changes caused by fuel reconfiguration were presented that referred to NUREG/CR-6835, Ref. 7, and an EPRI study of the reactivity consequence of fuel reconfiguration, Ref. 15. The presentation provided useful information regarding current NRC positions relative to fuel reconfiguration effects in storage/transportation casks.

Other documents reviewed include NUREG/CR-6672, NUREG/CR-4829, and NUREG-0170, Refs. 16–18. These documents provide generic analyses for package response during transportation accidents. NUREG/CR-6672, Ref. 16, includes updated methodologies and data for analyzing truck and rail cask accidents compared to NUREG/CR-4829, Ref. 17, which was an update of the methodologies used in NUREG-0170, Ref. 18. NUREG-0170 is the original environmental impact statement (EIS) for the transportation of radioactive materials. These documents discuss the impact of failed used fuel rods on source terms but do not include reactivity effects.

Overall, based on the NRC documents reviewed, no new information pertinent to modeling fuel reconfiguration conditions for criticality safety evaluations was identified.

## 2.2 EPRI Reports

EPRI has sponsored research culminating in several reports related to shipping UNF. The reports of interest for this effort tend to cover closely related and frequently overlapping areas. Three reports – *Fuel Relocation Effects for Transportation Packages*, Ref. 15, *Transportation of Commercial Spent Nuclear Fuel: Regulatory Issues Resolution*, Ref. 19, and *Criticality Risks during Transportation of Spent Nuclear Fuel: Revision 1*, Ref. 20 – were referenced in the EPRI presentation at the 2011 SFST Technical Exchange meeting, Ref. 21, that are considered relevant to this work.

Reference 15 is largely a critique of NUREG/CR-6835, Ref. 7, and is focused on demonstrating that fuel reconfiguration effects are small and have minimal impacts on the criticality safety of transportation packages. Qualitative arguments were used to eliminate configurations as not practical in many places. The study provides references to additional EPRI reports to support some suppositions about the performance of fuel cladding in the transportation casks. Some lessons learned from radiochemical assay campaigns are also referred to in establishing the impracticality of many of the extreme configurations studied in Ref. 7.

Computational results are also provided for a number of similar configurations that are evaluated in this report. The  $k_{\text{eff}}$  change associated with pitch expansion over the entire length of the fuel array for PWR fuel is reported as 3.1%  $\Delta k_{\text{eff}}$ . The removal of all cladding material is reported as causing a  $k_{\text{eff}}$  increase of 3.3%  $\Delta k_{\text{eff}}$  in a generic 32-PWR-assembly capacity cask. The pellet array configurations considered were significantly different from those evaluated in this report as described in Section 3.1.5.2.

Reference 19 presents several proposed resolutions to various regulatory issues perceived by EPRI to be particularly problematic for licensing transportation packages characterized as high capacity, containing high-burnup UNF, or both. The document discusses several considerations including moderator exclusion, expanded burnup credit, the robust design of used fuel transportation casks, and systematic analyses based on defense-in-depth. The report summarizes other EPRI-sponsored efforts to investigate the performance of fuel cladding during accident conditions, including a summary of the analysis provided in Reference 15. The criticality analysis section includes a discussion of potential benefits from

burnup credit and moderator exclusion, but no new information pertaining to accident configurations or computational results was provided.

Reference 20 contains a probabilistic risk assessment (PRA) quantifying the frequency of criticality accidents during railway shipment of UNF. The results of this research indicate a very low probability for a criticality accident based on several factors, including the low likelihood of severe rail accidents, large safety margins in the determination of the loading curve used in the certificate of compliance, and the difficulty of generating a critical configuration even with severe accident conditions. No new accident configurations or quantitative  $k_{\text{eff}}$  calculations were presented in this report.

The three reports discussed above provide a synopsis of the information contained in several other EPRI documents containing the majority of the information generated by EPRI-sponsored work related to fuel reconfiguration.

## 2.3 PATRAM Proceedings

The PATRAM symposium is the primary international meeting related to packaging and shipping of radioactive materials. The proceedings for the last four PATRAM symposia dating back to 2001 were reviewed, and a summary of the relevant papers to the work in this report is presented in the following subsections.

### 2.3.1 PATRAM 2010

Several papers in the 2010 PATRAM proceedings were identified as providing information related to modeling of fuel reconfiguration and the  $k_{\text{eff}}$  consequences of such events. The papers of interest with regards to this report are “Accelerated Corrosion Testing of Aluminum Carbide Metal Matrix Composite in Simulated PWR Spent Fuel Pool Solution,” Ref. 22, and “Description of Fuel Integrity Project Methodology Principles,” Ref. 23. Papers that did not provide detailed information about fuel deformation or damage and the effects of that damage on  $k_{\text{eff}}$  are not included in this discussion.

Reference 22 provides information related to corrosion testing of  $\text{B}_4\text{C}/\text{Al}$  neutron absorber materials in PWR spent fuel pool environments. This information is not directly relevant to the work performed here but provides some indication that the neutron absorber degradation configurations described in Section 3.1.6 should provide a reasonable upper bound of the potential consequences of neutron absorber degradation during dry storage.

Reference 23 presents progress and a proposed methodology resulting from the Fuel Integrity Project (FIP). The FIP is a joint research program executed between various British and French interests over the last decade. The particular companies and entities involved have evolved somewhat with industry activity over the years, but the project continued during the time period covered by the four PATRAM symposia discussed in this report. The methodology that has been developed as a result of the FIP applies to both fresh and irradiated fuel transported within Europe. Tests were performed on irradiated rod segments to determine the behavior of irradiated cladding specimens under various loadings. The results of various buckling and crushing tests have been used to validate the resulting models. The final results indicate that the three major causes of fissile material relocation with significant potential  $k_{\text{eff}}$  impacts are axial displacement, plastic deformation of fuel rods, and rod ruptures resulting in fuel release. All three of these mechanisms are considered in the configurations documented in this report. Axial displacement is discussed in Section 3.1.4, plastic deformation is bounded by the models discussed in Section 3.1.3, and fuel rod rupture is discussed in Sections 3.1.1, 3.1.2, and 3.1.5. Reference 23 is the most recent and most complete description of fuel reconfiguration modes and modeling approaches identified in the entire literature review.

### 2.3.2 PATRAM 2007

Several papers in the PATRAM 2007 proceedings were identified as providing information on modeling fuel reconfiguration and associated  $k_{\text{eff}}$  consequences. The relevant papers of interest are *Method to Evaluate Limits of Lattice Expansion in Light Water Reactor Fuel from an Axial Impact Accident during Transport*, Ref. 24, and *Influence of the Accident Behaviour of Spent Fuel Elements on Criticality Safety of Transport Packages – Some Basic Considerations*, Ref. 25.

Reference 24 focused on the effect of fuel assembly deformation caused by axial drops on the ends of the fuel assembly. Both PWR and BWR fuel assemblies are considered in the analysis. BWR fuel rods are typically attached to the assembly end fittings, while PWR rods typically are not. This leads to different response in the assembly during the end drop. The pitch in a BWR bundle tends to be compressed near the drop end, while the pitch in a PWR assembly tends to increase in the same transient. This increased fuel pin pitch is considered for both fuel assembly types in this work, as discussed in Section 3.1.3. The axial variation in the pitch change can also lead to regions of expanded pitch and regions of contracted pitch; the effect is referred to as “birdcaging.” A sketch showing this birdcaging effect is provided in Figure 1. Some limited modeling of this phenomenon was also performed as discussed in Section 3.1.3.2. The results presented in Reference 24 ultimately relate to simulation of the distortion of the fuel assembly during the end drop accident. The results presented demonstrate good agreement between the structural computational model and the testing results and more importantly indicate that the modeling approach used in this report is adequate to represent the expected results of such a condition.

Reference 25 investigates the consequences of several accident configurations. The approach described is similar in many respects to the strategy used in the development of configurations for this report in that general accidents are considered in a conservative manner to estimate consequences on  $k_{\text{eff}}$ . Assembly pitch expansion is considered over various lengths, up to the full length of the fuel rods. The reported  $k_{\text{eff}}$  change associated with this full-length expansion is approximately  $3.25\% \Delta k_{\text{eff}}$ , which is similar to the results reported by EPRI in Reference 15. The results reported for the accumulation of fissile material inside the cask body, but outside the poisoned area of the basket, are quite different from those described in this report. The configuration described in Ref. 25 is quite different from that described in Section 3.1.5.1, so direct comparison is not possible. The primary value of this paper relative to the current effort is in providing quantitative  $k_{\text{eff}}$  changes for assembly pitch expansion and axial displacement for comparison with results presented in Section 5.

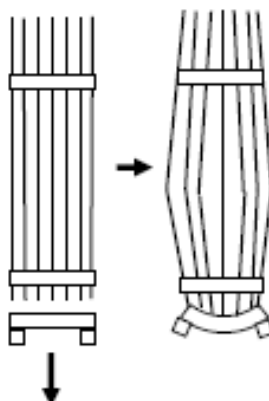


Figure 1. Sketch showing “birdcaging” as the result of an end drop [Source: Ref. 24 (Reprinted from P. Purcell, “Method to Evaluate Limits of Lattice Expansion in Light Water Reactor Fuel from an Axial Impact Accident During Transport” PATRAM 2007. Reprinted with permission.)]

### 2.3.3 PATRAM 2004

The proceedings of PATRAM 2004 contained three papers related to the  $k_{\text{eff}}$  consequences of fuel reconfiguration in storage and/or transportation casks – “Criticality Assessment of Fuel Assemblies with Missing Fuel Rods – An Intractable Problem?,” Ref. 26, “Nuclear Criticality Safety Analysis for the Traveler PWR Fuel Shipping Package,” Ref. 27, and “Harmonisation of Criticality Assessments of Packages for the Transport of Fissile Nuclear Fuel Cycle Materials,” Ref. 28.

Reference 26 examined the practicality of determining an optimum fuel assembly configuration with missing rods. Two techniques were introduced for performing a missing rod analysis. The simple approach proposed in Reference 26 is similar to the approach used in this report, but was performed manually as described in Section 3.1.2.2. No quantitative results were presented that are comparable to configurations included in this report.

Reference 27 presents the criticality safety analysis for a cask for shipping fresh PWR assemblies. Some of the accident configurations considered included uniform pitch expansion restrained by the storage cell wall that is similar to the modeling described in Section 3.1.3. Individual rod axial displacements are considered but shown to have no impact on  $k_{\text{eff}}$ . The axial displacement of the entire assembly was not considered credible. Partial flooding of the cask body was also considered. The results presented are not directly comparable to the results generated in this report because the cask studied in Reference 27 was a single assembly cask; however, the methods used support the basis for some of the configurations used in this report. The trends in the  $k_{\text{eff}}$  consequences of uniform pitch expansion and neutron absorber panel load reduction are similar to the results presented for PWR fuel in Section 5.1.

Reference 28 examines potential accident modeling approaches for  $k_{\text{eff}}$  calculations and discusses elements to consider regarding standardizing scenarios for which analysis is needed. As with Ref. 24, the differences in fuel pin behavior in PWR and BWR assemblies are discussed. Both references contain unreferenced statements supporting the conclusion that PWR pins are likely to be displaced into an increased pitch. Both Refs. 28 and 24 also indicate that BWR pins are likely to decrease in pitch. Ref. 24 cites two instances to support the conclusion for BWR fuel: one was the unrestrained drop of a BWR bundle at a German nuclear power plant and the other was in drop testing being performed as part of package testing. These results were generalized in Ref. 24 to considerations that fuel pins might bend, break, or both. These observations are consistent with the configurations described in Sections 3.1.3, 3.1.4, and 3.1.5. It was also deemed possible that damage to the storage basket or neutron absorber material could result from package-handling accidents. Initial results reported for fuel pin axial displacement indicate that the displacement of some pins within an assembly will not increase  $k_{\text{eff}}$ . This configuration is not considered in this report.

### 2.3.4 PATRAM 2001

Within the proceedings of PATRAM 2001 a few papers were identified that provide information related to fuel reconfiguration and the  $k_{\text{eff}}$  consequences – “Drop Tests with the RA-3D Shipping Container for the Transport of Fresh BWR Fuel Assemblies,” Ref. 29, “Drop Test for the Licensing of the RA-3D Package in the Transport of BWR Fresh Fuel Assemblies,” Ref. 30, and “Effects of Impact Accidents on Transport Criticality Safety Cases for LWR Packages – A New Approach,” Ref. 31.

References 29 and 30 provide the results of drop testing a container intended for shipping fresh BWR bundles. Two containers were each put through a series of drops and evaluated after sequential impacts. The results indicate that some significant assembly distortion is possible, with one assembly suffering a radial rotation (twist) of nearly 45° along its length. Both papers indicate that the general cross section of the bundle was not changed, that is, the pitch was nearly unchanged, but a fairly lengthy section was

twisted by the series of impacts. The drop testing was performed with natural enrichment un-irradiated fuel, and no rod failures were detected.

Reference 31 describes the initial plan for the FIP discussed in Ref. 23. As with other studies discussed before, the initial plan for the FIP includes studying deformation, axial displacement, and rupture as three primary fuel degradation mechanisms. Reference 31 also proposed a PWR pitch expansion configuration in which the outer row of pins is held in place along the storage basket but the inner rows continue to expand towards an optimum pitch. These configurations are considered in Section 3.1.3.1.

## 2.4 Other Sources

Other sources were also reviewed for relevant information related to modeling impact of fuel reconfiguration on criticality safety.

“New Approach to Evaluate Lattice Expansion of Light Water Reactor Fuel Elements on Criticality Safety of Transport Packages under Impact Accidents,” Ref. 32, examined pin pitch deformation in LWR fuel assemblies during transportation accident conditions. The paper proposed a method for generating a regular, nonuniform array of fuel rods with the outer row restrained by the basket walls and the pitch of the inner rows progressively expanded or contracted. This method leads to a larger reactivity increase than uniform pitch expansion and, when combined with similar observations from Ref. 31, motivated the analysis of the nonuniform pitch expansion cases described in Section 3.1.3.1.

## 2.5 Literature Review Summary

A wide range of potentially relevant literature has been reviewed to provide guidance on modeling of fuel reconfiguration after ES and estimate consequences of some configurations. Documents that discuss potentially relevant degraded fuel configurations include Refs. 22–32. A limited number of papers, including Refs. 15 and 25, provide estimates of the consequence of reconfiguration on  $k_{\text{eff}}$ . The PATRAM proceedings contain the largest number of relevant papers, with several directly applicable papers presented at each symposium. The EPRI reports, taken together, may contain the largest quantity of directly applicable information for this analysis. Most of the discussion in the available literature focuses on what reconfigurations could occur with less emphasis made on the direct impacts on  $k_{\text{eff}}$ . Those papers that include calculated  $k_{\text{eff}}$  results tend to take a similar approach to this effort and consider a range of potential configurations to establish a bounding increase in  $k_{\text{eff}}$  without regard for credibility.

## 3. FAILED FUEL CONFIGURATIONS

A set of failed fuel configuration categories was developed, and specific configurations within each category were evaluated. The various configurations represent stylized analyses designed to be bounding of different reconfiguration progressions that could occur, but were not developed to represent the results of any specific reconfiguration progression. The configuration categories considered in this analysis are the following:

- clad thinning/loss – reduced cladding thickness up to the total removal of all cladding material
- rod failures – removal of one or more fuel rods from the assembly lattice
- loss of rod pitch control – rod pitch contraction and expansion within the storage cell
- loss of assembly position control – axial displacement of fuel assemblies

- gross assembly failure – rubblized fuel within the storage cells with varying degrees of moderation
- neutron absorber degradation – gaps of varying location and size; thinning of absorber panels.

Within each category, specific configurations were modeled to calculate the corresponding  $k_{\text{eff}}$  values and the associated consequences of those configurations relative to the reference intact configuration. The consequence of a given configuration is defined as the difference in the calculated  $k_{\text{eff}}$  values for the given configuration and the reference intact configuration, with a positive value indicating an increase in  $k_{\text{eff}}$  as compared to the reference configuration. Several of the specific configurations are not considered credible but are included in the analyses for completeness (e.g., to fully understand trends and worst-case situations and to provide results for configurations that may later be judged to be credible). Pending improved understanding of the various material degradation phenomena, and subsequent determination and justification for what configurations are and are not credible, the assessment of the credibility of configurations provided herein is based on engineering judgment. The credibility of configurations and the impact of the configurations on criticality safety are dependent on many factors, including storage and transportation conditions, the fuel assembly characteristics, and the storage and/or transportation characteristics. The credibility assessment for the specific configurations considered here is presented at the end of this section. The assessment and analysis of credible configurations for a specific cask system would need to be performed as part of the safety analysis for licensing that system.

Each of the configurations is considered with all the assemblies in the cask degraded. As discussed in Section 3.2, a subset of the configurations is also considered for a range of assemblies experiencing degradation. These calculations allow an examination of the impact of reconfiguration as a function of the number of degraded assemblies. Section 3.3 describes the limited number of configurations modeled as a combination of two individual degradations. These models are intended to investigate the potential impact of combined degradation mechanisms occurring within the same cask.

At the end of this section, each of the configurations is reviewed for credibility and applicability. The assessments are based on engineering judgment and are not directly supported by any analysis. Ultimately, the strategies developed to mitigate the consequences of fuel reconfiguration will depend on the classification of each configuration as credible or not credible and the severity of the consequences.

## 3.1 Fuel and Cask Reconfiguration Descriptions

This subsection presents the configurations considered in these analyses. Each of these configurations is considered for each cask design under the assumption that each and every fuel assembly has undergone the reconfiguration discussed. The majority of the cases directly reconfigure fuel, but some consider changes to cladding, neutron absorber material, or fuel assembly axial position. The configurations described in this subsection are used in Section 3.2 to examine the impact of a range of numbers of assemblies experiencing reconfiguration, and in Section 3.3 to investigate the effect of multiple simultaneous degradation mechanisms. Figures demonstrating most of the configurations for each cask are provided in Section 5.

### 3.1.1 Clad Thinning/Loss

The complete loss of all cladding material without subsequent collapse of fuel material is a nonphysical condition but is included in these analyses to provide a bounding estimate of the increase in  $k_{\text{eff}}$  caused by fuel cladding thinning or removal. A series of calculations is also performed to investigate the impact of clad thinning. The reduction of fuel cladding thickness results in an increase in reactivity due to increased moderation within the assembly lattice (cladding material is replaced by water) and the reduced absorption in the cladding. The moderation effect is the larger of the two components. In the models, all

Zircaloy material is replaced with water, including the instrument and guide tubes and water rods. The orientation of the canister, be it horizontal, vertical, or in between, has no impact on the modeling or analysis of this configuration.

### 3.1.2 Rod Failures

Fuel rod failure could result if the fuel rod cladding has failed. After ES periods or as a result of high burnup, or both, fuel rod cladding may become brittle, as discussed in Ref. 1. Cladding failure could be the result of a static or dynamic load. Configurations involving both single and multiple rod failures are included and discussed in more detail below.

#### 3.1.2.1 Single Rod Failure

The single rod failure configuration is predicated on the collapse of an entire fuel rod, potentially due to cladding failure. Regardless of the cause of rod collapse, the fuel and cladding material would be displaced from the assembly lattice, thus leaving an empty rod location. In many internal locations within a fuel assembly lattice, this results in an increase in reactivity in the fully flooded condition due to increased internal moderation. The collapsed rod itself is not modeled as rubble on the bottom of the cask. The fissile material would form a fairly thin, severely undermoderated heap below the fuel assembly if the cask is in a vertical configuration. If the cask is in some other non-vertical configuration, the debris pile will have a larger surface area and thus more neutron leakage. The increase in leakage will increase the margin to criticality in the debris bed. Regardless of configuration, the rubble would have much lower reactivity than the assembly itself.

Separate calculations are performed with each unique rod location replaced with water for both the PWR and BWR fuel assemblies. The assembly and cask symmetries are accounted for in the determination of unique locations, neglecting exceptions for peripheral storage locations.

#### 3.1.2.2 Multiple Rod Failure

Within the multiple rod failure configurations, rods are removed in small groups until an optimum reactivity is achieved. As with the single rod failure cases, the debris at the bottom of the cask is not modeled nor are other cask configuration expected to have a significant impact on the results of the analysis of this configuration. For the larger number of rods removed to achieve optimum reactivity, this assumption is likely conservative as a significant amount of debris material will be accumulating within the assembly storage cell. The homogeneous rubble configuration of gross assembly failure, described in Section 3.1.5.1, provides estimates of the effect of debris collection in the bottom of the fuel storage basket.

For each number of rods removed, a series of potentially limiting configurations is generated to determine the most reactive configuration with the given number of rods removed. These potentially limiting configurations are generated from both the previous limiting configuration and near-limiting configurations. This approach leads to the consideration of several possible configurations to reduce the probability that a more reactive configuration is inadvertently omitted. The increase in  $k_{\text{eff}}$  caused by removing additional rods approaches zero at the optimum number of removed rods, so no attempt is made to identify the exact optimum number of rods. The  $k_{\text{eff}}$  of several configurations would also be statistically equivalent near this point. For the purposes of these analyses, the  $k_{\text{eff}}$  change at this optimum condition has been sufficiently estimated.

### 3.1.3 Loss of Rod Pitch Control

This configuration is based on failure of one or more of the assembly structural grids, resulting in a loss of fuel rod pitch control. For these analyses, this condition is first modeled as a uniform increase in the fuel rod pitch within the assembly lattice. The rod pitch expansion continues until the outer surface of the fuel rod unit cells in the outer row of the assembly has impacted the storage cell walls. A slight gap of half the fuel rod pitch minus the fuel rod radius remains between the fuel rods and the cell walls. The increased moderation within the assembly lattice causes an increase in reactivity. All fuel assemblies are assumed to undergo a uniform rod pitch expansion to completely fill the internal dimension of the storage cell.

These configurations expand the fuel rod center-to-center spacing in several increments to map the impact on  $k_{\text{eff}}$  over the full range of expansion. For the BWR fuel, the expansion is performed both with and without the fuel channel present. Two cases are considered with the channel modeled – one where the channel does not deform and restrains the expansion of the fuel rod pitch and the other is a nonphysical assumption that the channel deforms by expanding with a uniform thickness. In this second case, the channel is still present but expands until the storage cell wall restrains the expansion. To maximize the impact on reactivity, the maximum pitch case is considered both with and without cladding present.

After the limiting combination of enrichment and burnup has been established for each fuel type, an additional model is built with the outer row of rods in contact with the fuel storage cell. The small water gap between the rods and the cell walls has been removed in this model. It is used to establish the  $k_{\text{eff}}$  increase for uniform pitch increase to the limit established by the storage cell walls or assembly channel. The uniform expansion cases with the fuel cladding removed use the same pitch as the cases with cladding intact, so there is no additional pitch expansion caused by cladding removal. The orientation of the cask, vertical or otherwise, is not expected to have any influence on the modeling or analysis of the loss of pitch control configurations.

#### 3.1.3.1 Nonuniform Pitch

Further expansion of the rod pitch for interior rod locations is considered. These models extend further the axially uniform fuel rod pitch expansion discussed above. With the outer row of pins in contact with the storage cell walls, subsequent rows of pins are moved outward until the pins are in contact with the next outermost row. For example, the second row of pins is moved into contact with the first row touching the wall of the storage cell. The process is repeated until additional expansion fails to cause a reactivity increase. Rows containing guide tubes in PWR assemblies are expanded until the guide tubes are in contact with the next row of fuel pins, and the subsequent inner row is moved out until it is in contact with the guide tubes from the inside. These rows have a slightly larger pitch since the outer diameter of the guide tubes is larger than that of the fuel rods.

#### 3.1.3.2 Axial Pitch Variations

One concern associated with the uniform pitch expansion is that it does not account for potential  $k_{\text{eff}}$  increases caused by axial variations in the pitch distortion. This has been referred to in some instances as “birdcaging.” This condition is investigated for the limited uniform expansion case for each cask. The models that are developed are based on the expansion of the assembly until the outer fuel rod unit cell impacts the storage cell wall, not the subsequent case with the rods in contact with the wall. That is, the expanded pitch portion of the assembly maintains a small water gap between the fuel rods and the storage cell walls. The additional pitch in the model that eliminates the water gap is not expected to impact the  $k_{\text{eff}}$  change of birdcaging relative to a uniform pitch expansion. An axial region adjacent to the elevations of highest reactivity is compressed in an attempt to create a more effective reflector and thus increase  $k_{\text{eff}}$ .

The length and position of the compressed pitch segment is varied to determine the maximum impact of this effect. For burned fuel, the compressed zone is selected to match one or more axial zones defined by the axial burnup profile modeling. The high-reactivity region is at the top end of the fuel assembly, so the compressed region is varied in position within the top half of the assembly. For fresh fuel, the central region of the fuel is most reactive, so two compressed zones are modeled. One compressed zone is above the midplane of the assembly, and the other is below it. The two zones are always the same length and in symmetric positions.

### 3.1.4 Loss of Assembly Position Control

The neutron absorber panels in fuel storage and transportation casks are designed to extend beyond the length of the active fuel region within the fuel assembly. In this context, it is important that the active fuel stay in its intended position during and after ES. The cask designs use spacers to ensure that the fuel assemblies are appropriately aligned. If the spacers or assembly end fittings fail, it is possible that the active fuel could shift axially into a region where no neutron absorber separates adjacent assemblies. This would allow for a significant increase in neutronic communication between adjacent assemblies, and a corresponding increase in  $k_{\text{eff}}$ . The cask orientation is not expected to influence the analysis of the loss of assembly position control configuration, but the orientation would certainly influence the actual fuel motion if such an event occurred.

For these models, the maximum axial translation allowed is determined for the active fuel length neglecting the presence of all fuel assembly hardware above or below the pellet stack and the cask assembly spacers. The models of axial displacement translate all the fuel assemblies uniformly up or down into the lower and upper internal regions of the cask. The assemblies are moved in several relatively small intervals in an effort to map out the response as a function of displacement.

### 3.1.5 Gross Assembly Failure

Two configurations for the physical form of the failed fuel are considered in these analyses: the first is a homogeneous mixture of fuel, cladding materials, and water, and the second is a dodecahedral array of fuel pellets suspended in water. The homogeneous mixture is likely more representative of the condition of the assembly after significant degradation and reconfiguration. Modeling an ordered array of pellets provides an upper bound of the reactivity of the fuel rubble since low enriched fuel is more reactive lumped as compared to a homogeneous mixture due to resonance self-shielding effects. Each of the modeling techniques is described in more detail here.

The formation of oxidized forms of UO<sub>2</sub> is not considered in this analysis. The expected formation of higher-order oxidative states would require an ample supply of oxygen which would require a breach of the canister while in storage. Because monitoring is in place to detect and repair breaches, this condition is not being evaluated. Also, as the results presented in Section 5 demonstrate, the UNF casks are undermoderated systems, so representing oxidation of internal components would act to effectively displace the moderator, resulting in a less reactive condition.

#### 3.1.5.1 Homogeneous Rubble

Following a gross assembly failure, a large number of intermediate configurations is possible. To evaluate the effects of varying degrees of rubblization, a series of total debris elevations is considered. This approach considers a range of moderation ratios without specifying the cask orientation. The homogeneous rubble configuration considers the entire fuel assembly to have failed; no calculations are performed for rubblizing a portion of a fuel assembly or for rubble collecting within a partial intact

assembly or skeleton. The parameter that is varied is the height of the debris bed and thus the amount of moderation within the bed.

The homogeneous rubble configuration is modeled as occupying the internal volume of the fuel storage cell to varying elevations. The exact elevations used vary among the cask designs. All the designs are evaluated with the homogeneous rubble replacing the fuel assembly in its original elevation. Other elevations include 40%, 60%, 80%, and 100% of the inside height of the cask from the base plate. The volume occupied by water varies from about 21% to almost 74% of the homogenized mixture. The water volume is determined by subtracting the fuel and cladding volumes from the cask volume modeled as containing debris. A fully compressed case is also considered in which the fuel assembly debris has compacted to just fuel and cladding material, excluding all water, to complete coverage of the parametric space. A range of heights is also considered from nominal assembly height to fully compressed assuming that the debris is maintained within the neutron absorber elevations. These configurations approximate a debris bed that is made up of non-homogeneous pieces, such as fuel rod segments, that are too large to pass through the assembly end hardware and fuel assembly spacer. Some cask models also have configurations for neutron absorber height and/or basket height. Most of these models contain rubble material above and/or below the neutron absorber panels, which are assumed to remain intact. The debris is not necessarily contained by the cask fuel spacers because they are generally designed to allow water to flow through and out of the fuel storage cells. In the full cask height configurations, the fuel rubble is assumed to remain within the radial extent of the fuel storage cell, even above the storage basket. This is assumed mainly as a modeling convenience, and it likely reduces the  $k_{\text{eff}}$  of the configuration slightly. For purposes of these analyses, however, the approximations are sufficient to provide a good estimate of the  $k_{\text{eff}}$  changes associated with gross assembly failure leading to homogeneous rubble within the cask.

All models with homogeneous rubble assume that the cask is maintained in a vertical position. No explicit modeling is performed for horizontal or angled positions which may alter the distribution of rubble within the cask. Given the range of rubble heights considered, it is unlikely that a horizontal or angled configuration would lead to a greater overall  $k_{\text{eff}}$  increase than the maximum calculated in this work, but the intermediate volumes could be impacted in these alternate orientations.

### **3.1.5.2 Dodecahedral Array of Pellets**

The case of gross assembly failure modeled as an ordered array of bare pellets is considered as a bound to the possible  $k_{\text{eff}}$  increase resulting from these configurations. An ordered array of lumped low enriched fuel should lead to a greater  $k_{\text{eff}}$  increase for fuel assembly failure than the homogeneous case described above because of resonance self-shielding of  $^{238}\text{U}$  in low enriched fuel. The complete removal of cladding is nonphysical, as discussed above in Section 3.1.1, but is included to bound possible  $k_{\text{eff}}$  increases.

As with the homogeneous rubble case described above, a range of pellet array heights is considered along with the entire internal area of the storage cell assumed to be filled with the pellet array. The independent parameter for the dodecahedral array is the pitch, so a range of pitches is used in the models to achieve the different heights. Most of the cask models are evaluated with four different pitches/array heights. The minimum pitch in all cases maintains the height of the original fuel assembly, and the maximum pitch fills the inner area of the storage cell for the entire internal height of the cask. Each of the cases is considered with two fuel pellet orientations. The pellets are aligned along the Z axis in one case and along the X axis in the other.

All models with dodecahedral pellet arrays assume that the cask is maintained in a vertical position. No explicit modeling is performed for horizontal or angled positions which may alter the distribution of the pellets within the cask. Given the range of heights considered, it is unlikely that a horizontal or angled

configuration would lead to a greater overall  $k_{\text{eff}}$  increase than the maximum calculated in this work, but the intermediate volumes could be impacted in these alternate orientations.

### 3.1.6 Neutron Absorber Degradation

In addition to the failed fuel configurations, degradation of the neutron absorbers is investigated. Neutron absorber panels in long-term service in spent fuel pools have generally suffered a range of degradation mechanisms, as discussed in Ref. 33 and other sources. Although the environments within the spent fuel pool and the dry storage casks are significantly different, it is reasonable to assume that some degradation and/or damage of the neutron absorber material may occur in ES. A range of configurations is considered in these analyses to provide some estimates for the potential  $k_{\text{eff}}$  changes that could be associated with neutron absorber panel damage or degradation. The orientation of the cask is not expected to effect the  $k_{\text{eff}}$  change caused by neutron absorber degradation, and has no impact on the analysis of the configurations.

#### 3.1.6.1 Limiting Elevation of Neutron Absorber Damage

One aspect that can impact the  $k_{\text{eff}}$  change caused by neutron absorber damage is the axial elevation of the defect. For these analyses the neutron absorber panel damage was assumed to be 5 cm tall and across the full width and thickness of the panel. The gap in the neutron absorber panel is modeled as void, and not water-filled, to maximize the neutron streaming, and associated neutronic communication, through the gap and the corresponding increase in neutron multiplication in neighboring assemblies. Also, all neutron absorber panels in the cask are assumed to contain the same defect at the same elevation. This approach will result in a conservative estimation of the  $k_{\text{eff}}$  increase due to panel damage relative to non-aligned damage modeling. The neutron absorber damage may be highly correlated, in which case modeling the gaps at the same elevation is potentially appropriate.

For fresh fuel, the limiting elevation is most likely in the center of the assembly, so a few widely spaced intervals are used. For used fuel, the limiting elevation should shift to a position near the top end of the assembly. For these conditions, a larger number of cases are investigated with finer resolution in the gap positions between calculations. The minimum spacing is slightly in excess of 5 cm, so a more detailed survey is likely to reveal a slight increase in the  $k_{\text{eff}}$  increase of this neutron absorber degradation. For purposes of these analyses, however, the resolution is sufficient to capture the vast majority of the  $k_{\text{eff}}$  change.

#### 3.1.6.2 Sensitivity to Extent of Damage

To evaluate the sensitivity of the  $k_{\text{eff}}$  change to the extent of panel damage, several additional configurations were evaluated using 7.5 and 10 cm gaps centered at the elevation determined to be limiting with the 5 cm gap cases discussed above in Section 3.1.6.1. As before, the larger gaps extend across the entire width and thickness of the neutron absorber panel, and also occur at the same elevation in all panels. The sizes of the larger gaps have been chosen arbitrarily. It is unlikely that the extent of any potential neutron absorber panel damage can be appropriately bounded without significant material testing. The magnitude of the sensitivity results will provide some indication of the importance of neutron absorber material testing.

#### 3.1.6.3 Neutron Absorber Panel Thinning

While uniform thinning of all neutron absorber panels in the cask may be unlikely, it provides a simple basis for examining the potential impact of general degradation. The neutron absorber material is reduced in thickness in a series of steps so that the magnitude of the effect as a function of neutron absorber loss can be determined.

## 3.2 Varying Number of Reconfigured Assemblies

The  $k_{\text{eff}}$  change caused by fuel reconfiguration is nonlinear with respect to the number of assemblies that experience reconfiguration, and is not well characterized in the available literature. For these reasons, a series of configurations is considered in each cask by varying the number of assemblies that have been degraded for each of four of the configurations described in Section 3.1. The four degraded configurations considered are single rod failure (Section 3.1.2.1), multiple rod failure (Section 3.1.2.2), uniform fuel pin pitch expansion (Section 3.1.3), and the homogeneous rubble configuration of gross assembly failure (Section 3.1.5.1).

The number of assemblies in the cask experiencing reconfiguration is varied from one to all assemblies. A central cell location is selected as the first assembly to experience reconfiguration, and additional assemblies are added in approximately symmetric groups. An example order in which the failed assemblies are added is presented for each cask along with the results of the calculations in Section 5.

## 3.3 Multiple Reconfiguration Mechanisms

Many of the configurations described in Section 3.1 are predicated on the degradation of similar materials. The cladding, guide/instrument tubes, water tubes, and most of the structural grids are all fabricated from the same or very similar zirconium alloys. It is therefore assumed that reconfiguration could occur involving more than one of the degradation mechanisms studied separately for each configuration. For example, if the fuel rod cladding is failing and multiple fuel rods have collapsed, then the cladding on the remaining intact fuel rods may have experienced some thinning. A very large number of combinations of such configurations could be generated, but only a small subset is considered here. The primary purpose of this portion of the analysis is to compare the  $k_{\text{eff}}$  changes of multiple degradation mechanisms with the consequence estimated by simply adding the effects of each separate reconfiguration. To that end, two combinations are considered in both casks: a configuration involving a moderate number of failed fuel rods combined with 50% clad thinning in one study and with a moderate amount of uniform pitch expansion in another. The results for this set of cases are provided in Section 5.

## 3.4 Credibility of Degraded Configurations

Several of the configurations used in this report are not physically possible. These configurations may be disregarded in assessing the mitigation strategies necessary to provide confidence that UNF can be safely transported following ES. The configurations are still useful as they provide indications as to reconfiguration impacts for various changes in fuel, neutron absorber, or structural materials within the casks during or after ES. The consequences that require mitigation are significantly less severe than the most limiting, non-credible configurations reported in Section 5. A summary of the credibility and relevance of each of the configurations discussed in Section 3.1 is presented in Table 1.

The complete removal of all fuel cladding material is not credible as there is no mechanism to remove the cladding from the fuel matrix. There is also no credible place for the cladding material to go within the cask that will not have an impact on the calculated  $k_{\text{eff}}$ . Any event that leads to massive cladding failure will also lead to significant rearrangement of the fissile material. Some amount of clad thinning through corrosion and/or radiation-induced growth of the fuel rods is credible and is included in the results. To observe the impacts of clad thinning effects, the maximum thinning considered is chosen to be up to 50% of the nominal thickness.

Significant neutron absorber panel damage at highly correlated locations is not considered credible in extended dry storage. Many fixed absorber materials have experienced degradation in wet storage, as documented in Ref. 33, and this damage is often caused by the effects of radiation, temperature, and environmental insults. These parameters can be highly correlated based on the proximity of neutron absorber panels to the same high temperatures and high radiation fields in the same region of a spent fuel pool. There are currently no known mechanisms applicable to dry storage systems that could cause the local panel defects or generalized thinning examined in this report.

The cask assembly spacers are unlikely to degrade sufficiently for significant axial misalignment to be possible within the cask. The spacers are designed to withstand loads in excess of 60 g, as documented in Ref. 38. These loads are associated with hypothesized accident conditions (HAC), so the cask assembly spacers can be relied upon to maintain assembly position with the neutron absorber elevations in both storage and transportation. Current practice allows small gaps between the spacers and the fuel, but these gaps are typically on the order of a few inches. It is therefore reasonable to assume that significant misalignments cannot occur and will be limited to less than 20 cm.

Simultaneous gross failure of all fuel assemblies in the cask is also not considered credible in normal conditions of transport. The two configurations used to investigate the consequences of gross failure are also extremely conservative. Both configurations examine a range of debris bed sizes to find the largest increase in  $k_{\text{eff}}$ . Large debris beds, such as those filling the entire inner volume of the fuel cask, are not physically possible. Fuel assembly hardware and fuel spacers would also occupy a significant volume and thus reduce the  $k_{\text{eff}}$  increase. Some smaller debris beds, consistent with partial assembly failure, are potentially credible. These detailed debris models are not considered in this analysis as the primary focus of the configurations analyzed is to establish bounding conditions of the extent of  $k_{\text{eff}}$  increases due to total failure. Gross assembly failure may be plausible in some HACs, but is not considered credible in normal conditions of transport.

**Table 1. Credibility and relevance summary**

<b>Configuration</b>	<b>Credibility and applicability to normal transport analysis</b>
<b>Clad thinning/loss</b>	
Complete cladding loss	Nonphysical condition that is not credible Relevant as potential bound of credible condition
Uniform cladding thinning	Potentially credible as a result of corrosion Relevant to storage and transportation analysis
<b>Rod failures</b>	
Single rod failure	Potentially credible as a result of cladding failure Relevant to storage and transportation analysis
Multiple rod failure	Potentially credible as a result of cladding failure Relevant to storage and transportation analysis
<b>Loss of rod pitch control</b>	
Uniform expansion, constrained by cell or channel	Potentially credible as a result of end load Relevant to storage and transportation analysis
Nonuniform expansion, constrained by cell	Potentially credible as a result of end load Relevant to storage and transportation analysis
Axially variable expansion, constrained by cell	Potentially credible as a result of end load Relevant to storage and transportation analysis
<b>Loss of assembly position control</b>	
Maximum misalignment	Not credible with end fitting and spacers Relevant as potential bound of credible condition
Limited misalignment	Small misalignments credible Relevant to storage and transportation analysis
<b>Gross assembly failure</b>	
Homogeneous rubble of entire assembly with debris beyond neutron absorber elevations	Not credible for normal transport Relevant as potential bound for credible condition
Homogeneous rubble of entire assembly within neutron absorber elevations	Not credible for normal transport Relevant as potential bound for credible condition
Uniform pellet array	Not credible for normal transport Relevant as potential bound for credible condition
<b>Neutron absorber degradation</b>	
5-cm (small) defect in all panels, same elevation	Not credible for intact dry storage system Relevant as potential bound of credible condition
10-cm defect in all panels, same elevation	Not credible for intact dry storage system Relevant as potential bound of credible condition
Uniform thinning of all panels	Not credible for intact dry storage system Relevant as potential bound of credible condition

## 4. MODELS, CODES, AND METHODS USED

The models, codes, and methods used for these analyses are based on similar work completed previously and documented in Ref. 7. The codes used are part of the SCALE code system, Ref. 34.

### 4.1 Fuel Assembly Models

Two fuel assembly designs are used in these analyses: one PWR type and one BWR type. The designs chosen are intended to represent a large portion of the current inventory of discharged UNF and/or a significant portion of the fuel currently in use. The PWR design selected is the Westinghouse  $17 \times 17$  Optimized Fuel Assembly (OFA). The Westinghouse  $17 \times 17$  assembly, as modeled, represents over 14% of the total discharged PWR inventory, as documented in Ref. 35. The BWR design selected is based on a General Electric (GE)  $10 \times 10$  design such as the GE14 fuel product. The GE  $10 \times 10$  represents less than 0.5% of the discharged BWR fuel documented in Ref. 35; however, the  $10 \times 10$  fuel design was just being introduced when the data for Ref. 35 were being collected. The array is the most common fuel design in use in domestic BWRs today. Detailed descriptions of the fuel assembly models used in this analysis are provided in Appendix A.

The use of Westinghouse and GE fuel assemblies is a continuance of the work documented in Ref. 7. The use of these fuel types is not an endorsement of any particular fuel design or vendor relative to any others but is used to provide a basis of comparison with the previous work.

### 4.2 Cask Models

Two cask models were used for the evaluations presented in the main body of this report – the GBC-32 and MPC-68. The MPC-24 cask is also evaluated in Appendix B to complete coverage of the parametric space via the inclusion of fresh 5 weight percent (w/o) PWR fuel. The representative cask models selected are the same as those used in Ref. 7 and are based on the Holtec HI-STAR 100 system, Ref. 36–38. The incorporation of Holtec designs in this work is not an endorsement of any design or vendor relative to any others. The GBC-32 and MPC-68 models are described in more detail in the following subsections.

#### 4.2.1 GBC-32 Cask Model

The GBC-32 model is a generic burnup credit cask benchmark model as defined in Ref. 39. The cask model was designed to be a nonproprietary representation of high-capacity PWR storage and transportation casks used within the nuclear power industry. The dimensions and material specifications of the cask model are described in Section 2.1 of Ref. 39 and are not repeated here. The only notable difference from that description is that the cask lid modeled in these analyses has a thickness of 20 cm instead of 30 cm. This reduced lid thickness has no impact on the analyses presented here because the cavity height is maintained.

The fuel assemblies, cask basket, neutron absorber panels, neutron absorber panel wrappers, cask wall, lid, and base plate are modeled explicitly. The nominal condition for this model is fully flooded with unit density, unborated water. A cross section of the GBC-32 model is shown in Figure 2. The representative assembly design is the Westinghouse  $17 \times 17$  OFA with a range of initial enrichments, burnups, and cooling times considered. For more details about the fuel assembly model, see Appendix A.

A burnup credit loading curve is generated assuming a maximum  $k_{\text{eff}}$  of 0.94, as shown in Figure 3. The maximum fresh enrichment that can be stored is determined to be 1.92 w/o  $^{235}\text{U}$ , and minimum burnups are calculated for 3.5 w/o and 5 w/o initial enrichment fuel with 5 years of post-irradiation cooling time. The minimum burnup for 3.5 w/o fuel is 25.5 GWd/MTU and for 5 w/o is 44.25 GWd/MTU to meet the

$0.94 k_{\text{eff}}$  limit. Explicit degraded configuration calculations are performed for fuel from this loading curve. These two enrichments are used because they encompass the majority of the current UNF inventory as of 2002, and the 5-year cooling time is selected as it is a typical minimum required cooling time for fuel to be placed in dry storage. Sensitivity studies are also performed for fuel of higher burnup (70 GWd/MTU) and for a range of cooling times up to 300 years to establish the sensitivity of the change in  $k_{\text{eff}}$  to these parameters. The results of these sensitivity studies are discussed in Section 5 and in Appendix C.

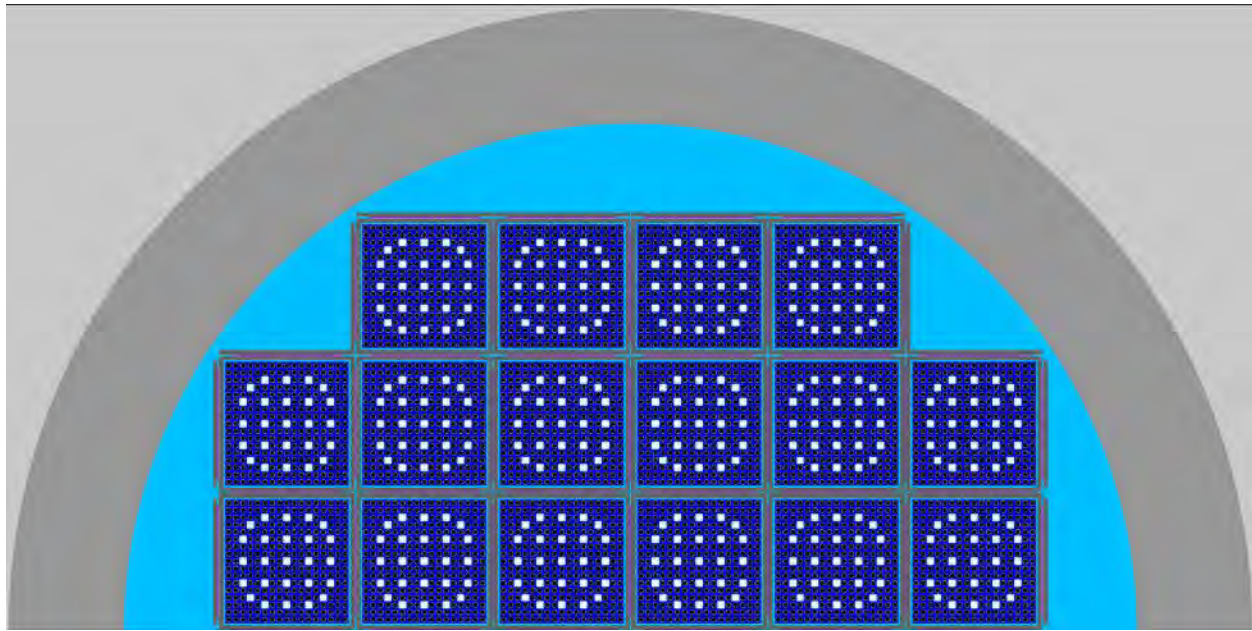


Figure 2. Cross section of GBC-32 half-cask model.

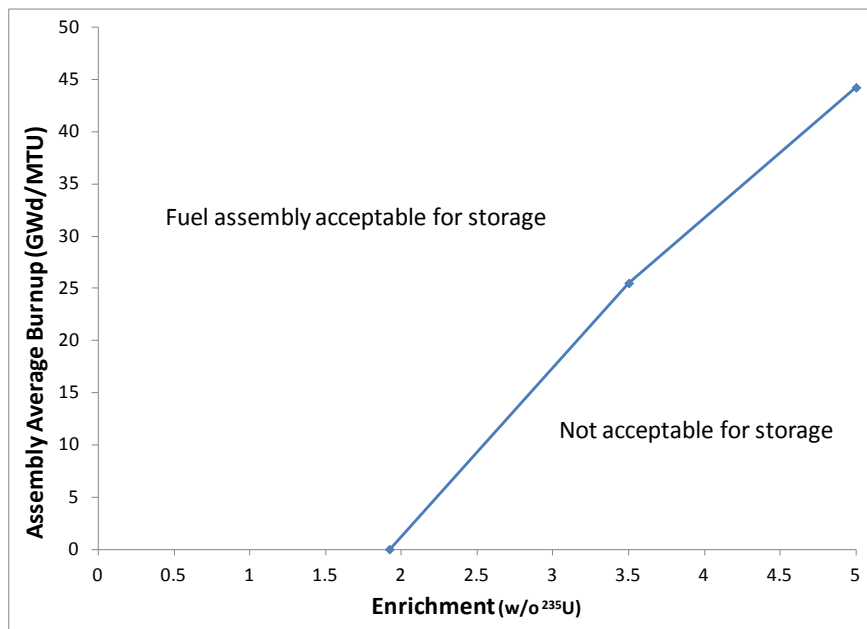


Figure 3. Representative fuel assembly loading curve for GBC-32.

#### 4.2.2 MPC-68 Cask Model

The MPC-68 cask is designed for storage and transportation of up to 68 fresh BWR fuel assemblies but is being used in this analysis for evaluating both fresh and irradiated assemblies. Fresh fuel is considered in these analyses to provide complete coverage of the parametric space; in this case burnup is the parameter of interest. The nominal condition for this model is fully flooded with unit density, unborated water. A cross section of the MPC-68 model is shown in Figure 4. Dimensions and material specifications of the cask model are provided in Appendix D. The fuel assemblies modeled in the MPC-68 are based on a  $10 \times 10$  design similar to the GE14 product. More details about the fuel assembly models are provided in Appendix A.

Fuel assemblies in the MPC-68 models used in these analyses use an initial enrichment of 5 w/o  $^{235}\text{U}$  and consider fresh and irradiated conditions. The nominal model  $k_{\text{eff}}$  value with fresh fuel is in excess of 0.96. A second set of cases considers an assembly average burnup of 35 GWd/MTU and a 5-year cooling time, resulting in a base case  $k_{\text{eff}}$  of approximately 0.83. Sensitivity studies are also performed for fuel of higher burnup (70 GWd/MTU) and for a range of cooling times up to 300 years to establish the sensitivity of the change in  $k_{\text{eff}}$  to these parameters. The results of these sensitivity studies are discussed in Section 5 and in Appendix C.

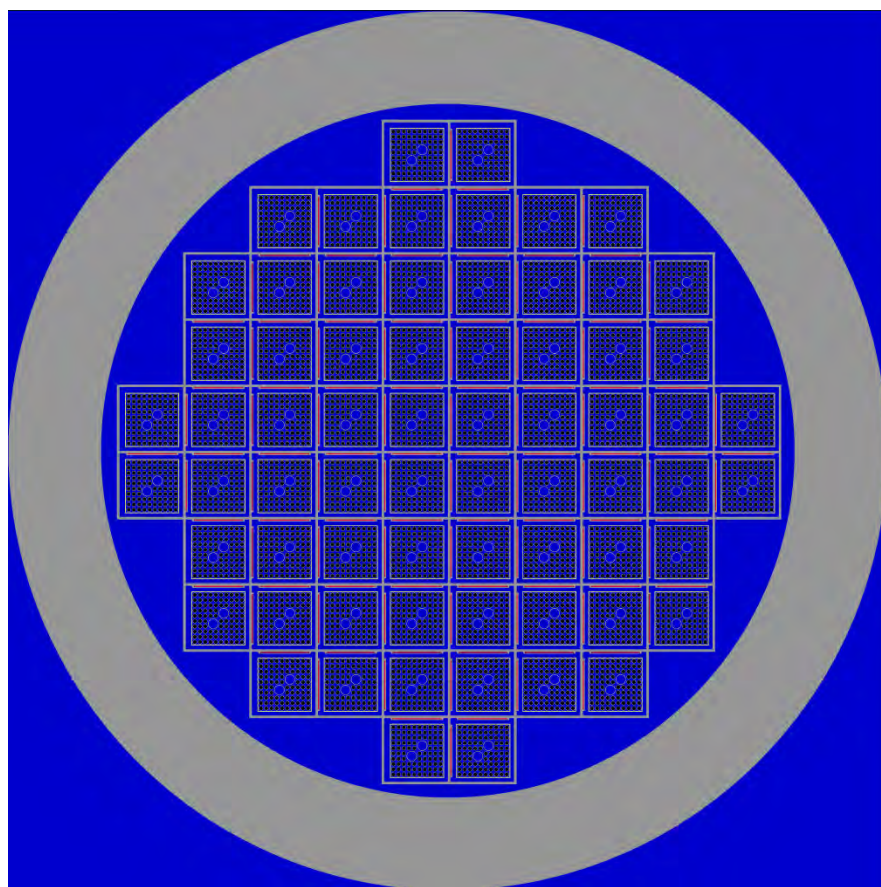


Figure 4. Cross section of MPC-68 model.

### 4.3 Software Codes

The SCALE code system is used to perform the large number of  $k_{\text{eff}}$  and depletion calculations necessary for these analyses. All calculations use the 238-group neutron data library based on ENDF/B-VII.0, distributed with the SCALE system. The same library is used in  $k_{\text{eff}}$  and depletion calculations.

The KENO V.a and KENO-VI Monte Carlo codes are used for  $k_{\text{eff}}$  calculations within the appropriate CSAS5 and CSAS6 sequences. Both codes use Monte Carlo transport to solve the  $k_{\text{eff}}$  eigenvalue problem. KENO-VI uses a generalized geometry process and is used for the fuel pellet array configuration and some increased fuel rod pitch configurations. KENO V.a has a more restrictive geometry package but is significantly faster because of the simpler geometry treatment. KENO V.a is used for the majority of configurations considered in this analysis. The KENO codes and CSAS sequences are further described and documented in Ref. 34. The KENO calculations are run with a large number of particles per generation, typically 10,000, and enough generations to reach an uncertainty less than or equal to 0.00010  $\Delta k_{\text{eff}}$ . The number of generations needed to reach the uncertainty target is determined by KENO during each calculation. In most calculations, the first 100 generations are discarded to ensure proper source convergence.

All depleted fuel isotopic compositions were generated with the STARBUCS sequence. The STARBUCS sequence uses the ORIGEN-ARP methodology to generate depleted fuel compositions and uses the compositions in a KENO model to calculate  $k_{\text{eff}}$ . The TRITON t-depl sequence is used to generate ARP libraries for both PWR and BWR UNF for the depletion conditions described in Section 4.4. The TRITON sequence couples the NEWT discrete-ordinates code with the ORIGEN depletion module. The local fluxes calculated with NEWT are used to perform fuel depletion calculations with ORIGEN. The STARBUCS and TRITON sequences, NEWT and ORIGEN modules, and ORIGEN-ARP methodology are described and documented in Ref. 34.

### 4.4 Depletion Modeling Parameters

For analyses of irradiated fuel, the depletion modeling parameters that the fuel experiences can have a significant impact on the calculated  $k_{\text{eff}}$  values. Several key factors can impact the reactivity of discharged fuel in light water reactor (LWR) burnup credit criticality safety analyses. The key parameters include the nuclides represented in the isotopic compositions, parameters used for the depletion analysis, cooling time, axial burnup profiles, and horizontal burnup profiles, as discussed in Ref. 40.

For the analyses in this report, the depletion parameters used are consistent with burnup credit safety analyses and are not representative of nominal core conditions. It is expected that any operating conditions that are not bounded by the depletion conditions used in this report would result in a higher discharged assembly  $k_{\text{eff}}$ , but the  $k_{\text{eff}}$  increase caused by fuel reconfiguration is expected to be similar to the results determined here. Generic data is used in the PWR depletion conditions as PWR burnup credit has been studied extensively, including in, for example, Refs. 39, 41, 42, 43, 44, and 45. Additional details on the specific PWR conditions used are provided in Section 4.4.1. Because commensurate studies are not available in the literature for BWR burnup credit, the BWR depletion conditions are based on the operating history of a specific assembly as described in Section 4.4.2 and Appendix E.

The  $k_{\text{eff}}$  calculations performed for these analyses involving UNF, for both BWR and PWR fuel, consider the same 12 actinide and 16 fission product isotopes listed in Table 2 (Set 2 Table 1 Ref. 44). Although Ref. 44 specifically addresses PWR burnup credit, the major isotopes affecting reactivity of irradiated uranium oxide fuel will be the same in BWR fuel. The  $k_{\text{eff}}$  impacts caused by the use of this set of

isotopes, as compared to actinide-only burnup credit or a more extensive list of fission products, are discussed in Ref. 39.

Different axial burnup profiles are used for PWR fuel than for BWR fuel, though the same uniform horizontal burnup profile is considered for both fuel types. The PWR axial profiles are taken from Table 4-3 of Ref. 45. Profile 2 is used for fuel discharged at 25.5 GWd/MTU and profile 3 is used for discharged at 44.25 GWd/MTU. The development of the profile used for BWR fuel is described in Appendix E.

**Table 2. Isotopes included in depleted fuel models**

<b>Actinides</b>					
$^{234}\text{U}$	$^{235}\text{U}$	$^{236}\text{U}$	$^{238}\text{U}$	$^{238}\text{Pu}$	$^{239}\text{Pu}$
$^{240}\text{Pu}$	$^{241}\text{Pu}$	$^{242}\text{Pu}$	$^{241}\text{Am}$	$^{243}\text{Am}$	$^{237}\text{Np}$
<b>Fission products</b>					
$^{95}\text{Mo}$	$^{99}\text{Tc}$	$^{101}\text{Ru}$	$^{103}\text{Rh}$	$^{109}\text{Ag}$	$^{133}\text{Cs}$
$^{143}\text{Nd}$	$^{145}\text{Nd}$	$^{147}\text{Sm}$	$^{149}\text{Sm}$	$^{150}\text{Sm}$	$^{151}\text{Sm}$
$^{152}\text{Sm}$	$^{151}\text{Eu}$	$^{153}\text{Eu}$	$^{155}\text{Gd}$		

#### 4.4.1 PWR Depletion Conditions

The depletion parameters that impact discharged fuel reactivity as listed in Ref. 40 are fuel temperature, moderator temperature/density, soluble boron concentration, specific power and operating history, use of fixed burnable poisons, and use of integral burnable poisons. Each of these parameters must be addressed in a burnup credit analysis to demonstrate that conservative depletion parameters have been implemented in the safety basis. These depletion calculations are intended to provide used fuel isotopic compositions that are representative of the compositions generated for a safety analysis and not for nominal core operating conditions. The parameters used in the PWR depletion calculations are listed below in Table 3.

**Table 3. PWR depletion parameters**

Parameter	Value
Fuel temperature	1100 K
Moderator temperature	610 K
Moderator density	0.63 g/cm <sup>3</sup>
Soluble boron concentration	1000 ppm
Specific power and operating history	Constant 60 W/g (MW/MTU)
Fixed burnable absorber	24 Wet Annular Burnable Absorber (WABA)
Integral burnable absorber	None – Bounded by 24 WABA
Control rod insertion	None

#### 4.4.2 BWR Depletion Conditions

The mechanisms whereby depletion conditions influence discharged fuel assembly reactivity are largely similar for BWR and PWR fuel. Data for specific BWR assemblies are gathered and reviewed from the

commercial reactor critical (CRC) state points documented in Refs. 46 and 47. The depletion parameters used in this report are summarized in Table 4. The methods used to generate axial burnup and void profiles and the specific power from the CRC information, Refs. 46 and 47, are presented in Appendix E. The BWR depletion calculations are performed with no control blades present. Although it is more conservative to include the control blades during depletion, their absence is not expected to impact the results of this analysis.

**Table 4. BWR depletion parameters**

Parameter	Value
Fuel temperature	840 K
Moderator temperature	512 K
Moderator density	Varied axially, see Appendix E for details
Specific power and operating history	Constant 30.31 W/g (MW/MTU), see Appendix E for details
Integral burnable absorber	None
Control blade insertion	None

## 5. RESULTS

This section reports the results of the calculations to determine the  $k_{\text{eff}}$  changes associated with each of the configurations described above in Section 3. The results are presented in unique subsections for each cask. The conclusions that can be drawn from these results are presented in Section 6.

The reported consequence is the difference in calculated  $k_{\text{eff}}$  values; the reported changes are not divided by any  $k_{\text{eff}}$  values and therefore do not represent change in reactivity ( $\Delta\rho$ ). The  $\Delta k_{\text{eff}}$  unit indicates that the results presented are the difference in two calculated  $k_{\text{eff}}$  values. The reported  $k_{\text{eff}}$  changes are also best-estimate changes; the difference in  $k_{\text{eff}}$  values is not altered or adjusted to account for the Monte Carlo uncertainties of the calculations. The one standard deviation uncertainty in all calculated  $\Delta k_{\text{eff}}$  values is approximately 0.00014 (0.014%)  $\Delta k_{\text{eff}}$ , unless otherwise noted.

### 5.1 GBC-32 Cask Model Results

The  $k_{\text{eff}}$  change associated with each of the reconfigurations discussed in Section 3 is presented in this section for the GBC-32 cask. The configurations assume a range of loadings of Westinghouse 17 × 17 OFA fuel. The description of the fuel assembly is provided in Appendix A. The enrichments and burnups used are presented in Table 5. The rationale used to select these points is provided in Section 4.2.1. The reference case  $k_{\text{eff}}$  value for intact fuel for each of these cases is also provided in Table 5.

**Table 5. Enrichment, burnup, and cooling time for reference cases considered in GBC-32**

Enrichment (w/o $^{235}\text{U}$ )	Burnups (GWd/MTU)	KENO V.a		KENO-VI	
		$k_{\text{eff}}$	$\sigma$	$k_{\text{eff}}$	$\sigma$
1.92	0	0.94017	0.00010	0.94040	0.00010
3.5	25.5	0.93988	0.00010	0.93976	0.00010
5.0	44.25	0.94000	0.00010	0.93995	0.00010

### 5.1.1 Reconfiguration of All Assemblies

A summary of the  $k_{\text{eff}}$  increase associated with each configuration is provided in Table 6. Additional details for each configuration and the results for non-limiting cases are provided in the subsequent subsections.

**Table 6. Summary of  $k_{\text{eff}}$  increases for the GBC-32 cask**

Configuration	Increase in $k_{\text{eff}}$ (% $\Delta k_{\text{eff}}$ )	Limiting case	
		Enrichment (w/o $^{235}\text{U}$ )	Burnup (GWd/MTU)
<b>Clad thinning/loss</b>			
Cladding removal	3.49	5	44.25
<b>Rod Failures</b>			
Single rod removal	0.09	5	44.25
Multiple rod removal	1.86	5	44.25
<b>Loss of rod pitch control</b>			
Uniform rod pitch expansion, clad	2.65	5	44.25
Uniform rod pitch expansion, unclad	5.34	5	44.25
Nonuniform pitch expansion, clad	3.90	5	44.25
<b>Loss of assembly position control</b>			
Axial displacement (maximum)	16.70	5	44.25
Axial displacement (20 cm)	10.82	5	44.25
<b>Gross assembly failure</b>			
Uniform pellet array	21.37	5	44.25
Homogeneous rubble	14.30	5	44.25
<b>Neutron absorber degradation</b>			
Missing neutron absorber (5-cm segment)	1.05	5	44.25
Missing neutron absorber (10-cm segment)	2.33	5	44.25
50% reduction in neutron absorber panel thickness	1.78	1.92	0

#### 5.1.1.1 Clad Thinning/Loss

The clad thinning and loss configurations are modeled as discussed in Section 3.1.1. As shown in Table 6, the limiting  $k_{\text{eff}}$  increase associated with complete cladding removal is 3.49%  $\Delta k_{\text{eff}}$  and occurs for the 44.25 GWd/MTU burnup case with an initial enrichment of 5 w/o  $^{235}\text{U}$ . The results for all three cases are summarized in Table 7. For the limiting case of 5 w/o and 44.25 GWd/MTU burnup, the  $k_{\text{eff}}$  increase as a function of nominal cladding thickness remaining is shown in Table 8 and Figure 5. The trend of increasing  $k_{\text{eff}}$  with decreasing cladding thickness is similar for the other fuel compositions, and therefore

not shown here. The configuration with 50% of the nominal cladding remaining is shown in Figure 6. The results are in good agreement with those presented in Refs. 7 and 15.

**Table 7. Increase in  $k_{\text{eff}}$  for cladding removal in GBC-32**

Enrichment (w/o $^{235}\text{U}$ )	Burnup (GWd/MTU)	Increase in $k_{\text{eff}}$ (% $\Delta k_{\text{eff}}$ )
1.92	0	2.81
3.5	25.5	3.34
5	44.25	3.49

**Table 8. Increase in  $k_{\text{eff}}$  in GBC-32 cask as a function of cladding fraction remaining  
(5 w/o  $^{235}\text{U}$  initial enrichment, 44.25 GWd/MTU burnup)**

Fraction of cladding thickness remaining	Increase in $k_{\text{eff}}$ (% $\Delta k_{\text{eff}}$ )
0.90	0.38
0.75	0.99
0.50	1.94
0.25	2.76
0.00	3.49

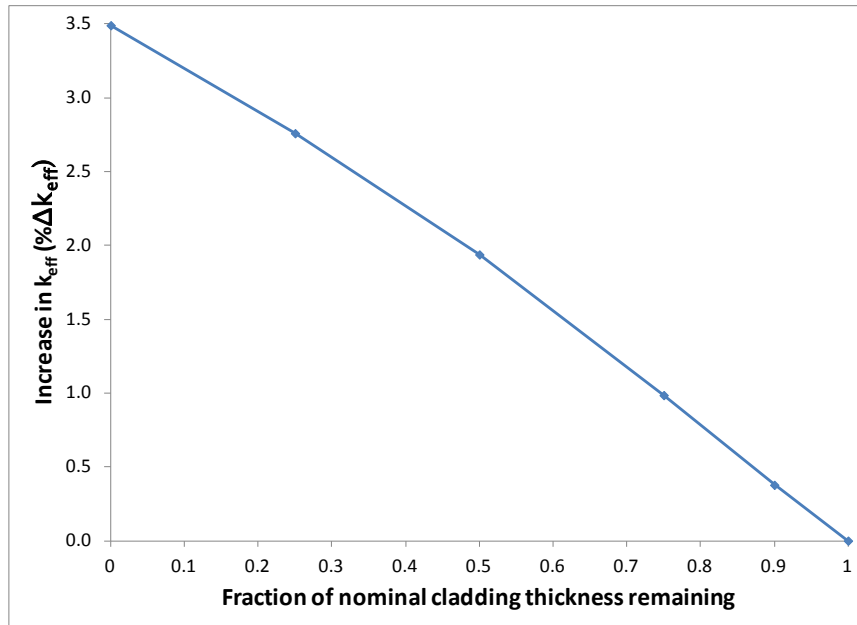
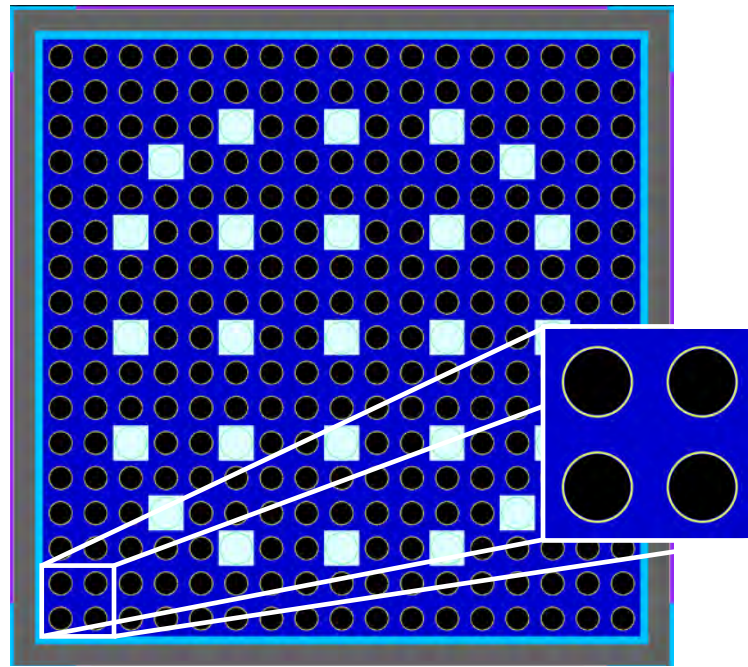


**Figure 5. Increase in  $k_{\text{eff}}$  due to reduced cladding thickness  
(5 w/o  $^{235}\text{U}$  initial enrichment, 44.25 GWd/MTU burnup).**



Notes:

- Fuel shown in black
- Cladding is light grey around fuel material
- Guide/instrument tubes are larger water-filled tubes
- Storage cell is dark grey box
- Neutron absorber panel is purple
- Water is shown in dark blue, light blue, and white

**Figure 6. Configuration with 50% cladding thickness.**

### 5.1.1.2 Rod Failures

Each of the 39 eighth-assembly symmetric rods is removed individually to determine its worth, as discussed in Section 3.1.2.1. Table 9 presents the rod locations and worth of the limiting rod location for each of the three cases. A sketch showing the eighth-assembly symmetry and row and column labels is provided in Figure 7. The maximum  $k_{\text{eff}}$  change is 0.09%  $\Delta k_{\text{eff}}$  and is associated with rod H5 in the 5 w/o, 44.25 GWd/MTU burnup case. The worth of H5 in the GBC-32 cask is. It should be noted that several rods across many of the cases have a reactivity worth that is statistically equivalent to this particular limiting case. The worth is very small relative to the  $k_{\text{eff}}$  increase of other configurations, so further examination is not necessary.

Multiple rods are also removed in groups, as discussed in Section 3.1.2.2. Groups of 2, 4, 8, 16, 24, 28, 32, 36, 40, 44, and 48 rods are considered. The maximum  $k_{\text{eff}}$  increase for each of the enrichment and burnup combinations is shown in Table 10. Figure 8 shows the  $k_{\text{eff}}$  increase as a function of rods removed for the limiting case at 5 w/o and 44.25 GWd/MTU burnup. The limiting lattice is shown in Figure 9. The maximum  $k_{\text{eff}}$  value occurs for 44 rods removed and corresponds to a  $k_{\text{eff}}$  increase of 1.86%  $\Delta k_{\text{eff}}$ .

Multiple rod removal in the fresh fuel 1.92 w/o case resulted in a decrease in the cask reactivity. Hence, the single rod removal case bounds all multiple rod removal configurations considered.

The  $k_{\text{eff}}$  increase for both rod removal configurations in the GBC-32 cask is in generally good agreement with Ref. 7. The multiple rod removal  $k_{\text{eff}}$  increase is somewhat higher, most likely because of the use of a distributed axial burnup profile in this work.

**Table 9. Single rod removal results for  $17 \times 17$  OFA in GBC-32**

Enrichment (w/o $^{235}\text{U}$ )	Burnup (GWd/MTU)	Location	Maximum increase in $k_{\text{eff}}$ (% $\Delta k_{\text{eff}}$ )
1.92	0	H8	0.04
3.5	25.5	H7	0.08
5	44.25	H5	0.09

**Table 10. Multiple rod removal results for  $17 \times 17$  OFA in GBC-32**

Enrichment (w/o $^{235}\text{U}$ )	Burnup (GWd/MTU)	Maximum increase in $k_{\text{eff}}$ (% $\Delta k_{\text{eff}}$ )
1.92	0	N/A*
3.5	25.5	1.07
5	44.25	1.86

\*All multiple removal cases resulted in a decrease in  $k_{\text{eff}}$

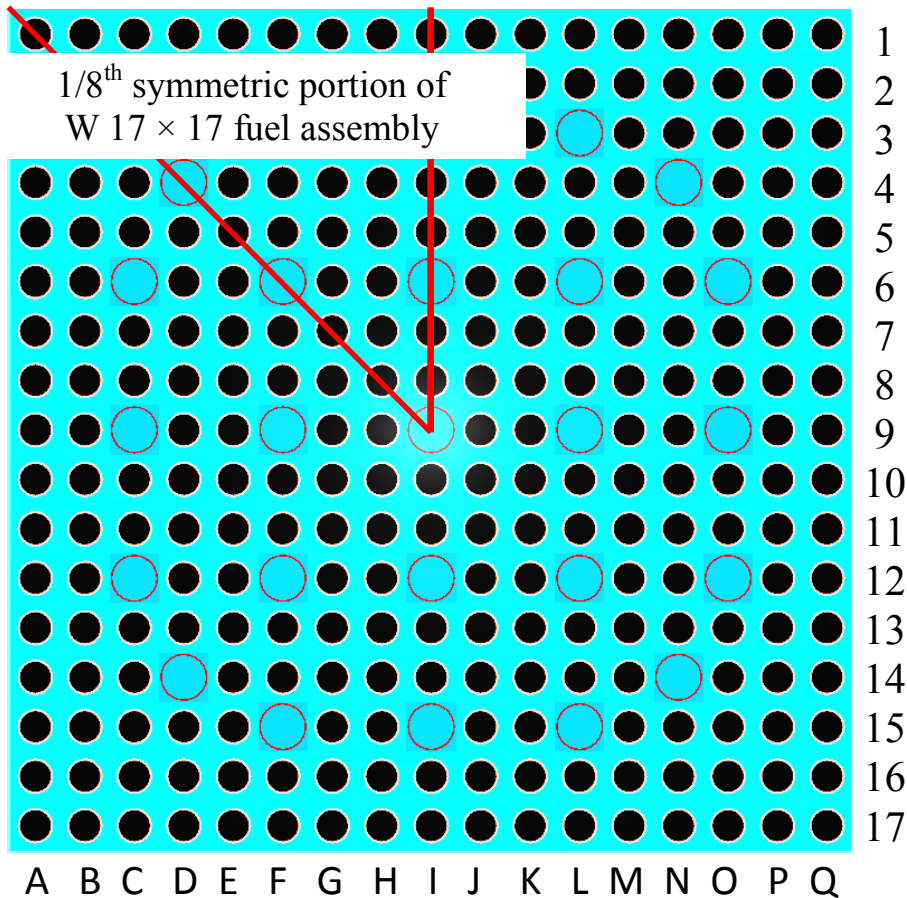


**Figure 7. Sketch of symmetry, row, and column labels for W  $17 \times 17$  fuel assembly.**

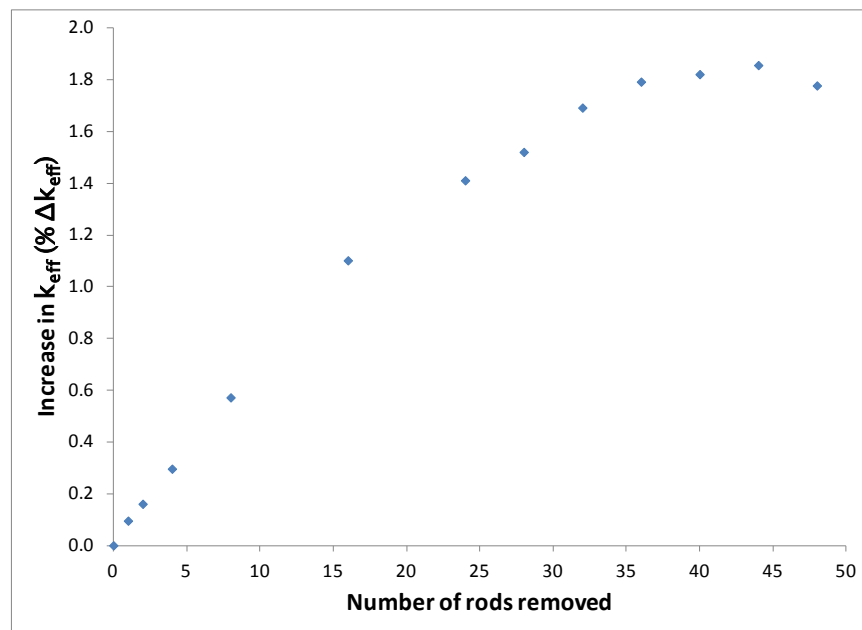
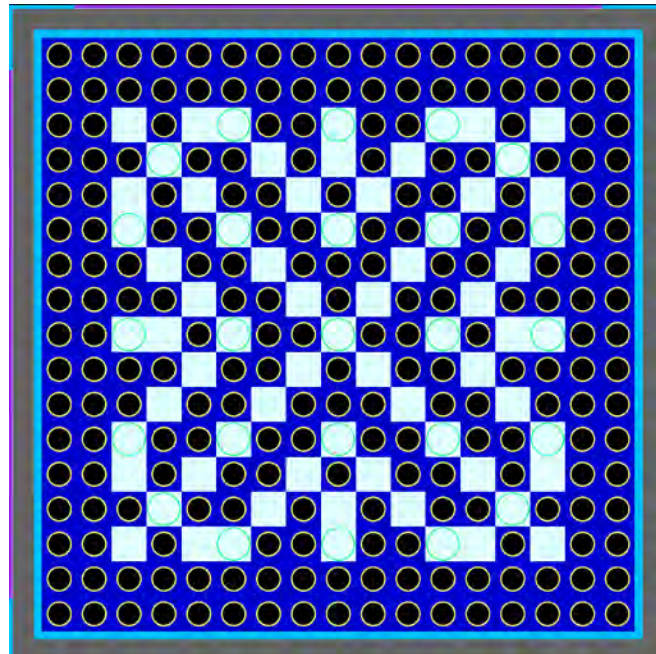


**Figure 8. Increase in  $k_{\text{eff}}$  in GBC-32 cask as a function of number of rods removed  
(5 w/o  $^{235}\text{U}$  initial enrichment, 44.25 GWd/MTU burnup).**



Note: Missing rod locations are shown in white; the same water mixture was used in empty cell locations and guide tube locations

**Figure 9. Limiting multiple rod removal lattice (44 rods removed).**

### 5.1.1.3 Loss of Rod Pitch Control

The loss of rod pitch control is modeled first as a uniform increase in fuel assembly pitch, as discussed in Section 3.1.3. The pitch between rods is expanded uniformly until the rod unit cells of the outer row of fuel rods are coincident with the inner surface of the storage cells. The largest expansion is modeled in two configurations – with the clad fully intact and also completely removed. The limiting condition for both cases is for fuel with an initial enrichment of 5 w/o and 44.25 GWd/MTU burnup. The results with the pitch expanded until the outer unit cell boundary contacts the storage cell, both with and without cladding, for all three combinations of initial enrichment and burnup are shown in Table 11.

The limiting configuration, with 44.25 GWd/MTU burnup, is further expanded until the outermost fuel rods are in contact with the storage cell walls as shown in Figure 10. The increase in  $k_{\text{eff}}$  in this case relative to the nominal configuration is 2.65%  $\Delta k_{\text{eff}}$  with cladding intact and 5.34%  $\Delta k_{\text{eff}}$  with cladding removed. The unclad fuel rods are modeled in the same locations with the cladding removed; the pitch is not increased further to put the fuel material in contact with the storage basket. The first five points in Figure 11 show the increase in  $k_{\text{eff}}$  associated with this uniform pitch expansion. These results indicate a  $k_{\text{eff}}$  increase that is approximately 0.5%  $\Delta k_{\text{eff}}$  lower for loss of rod pitch control compared to Refs. 15 or 25.

Fuel rod pitch is further increased in the GBC-32 model to examine the effect of nonuniform pitch, as discussed in Section 3.1.3.1 and References 31 and 32. The inner portion of the assembly continues to expand until the outer rows are in contact with each other; although the fuel rod pitch is still uniform axially, it is nonuniform in the radial direction. An example model is shown in Figure 12. The pitch in each of the outer rows is constant within the row and is equal to the pitch that caused that row to make contact with the previous row or the basket wall. The increase in pitch in inner rows leads to a nonuniform pitch in the lattice. The results of the calculations with increasing pitch are shown in Figure 11 as a function of the pitch of the inner, uniform portion of the assembly. The maximum  $k_{\text{eff}}$  increase, as shown in Table 6, is 3.90%  $\Delta k_{\text{eff}}$ . The first five points represent the uniform pitch expansion. Nonuniform expansion begins when the fuel rod pitch is in excess of approximately 1.32 cm. The additional  $k_{\text{eff}}$  increase beyond the uniform expansion case reported above is 1.25%  $\Delta k_{\text{eff}}$ , thus indicating that further expansion is a significant effect. This is consistent with the results presented in References 31 and 32.

The limiting pitch expansion case corresponds to 5 w/o fuel with 44.25 GWd/MTU burnup, so the most reactive axial section is near the top end. The fuel rod pitch is varied as function of axial position to investigate the potential effect of birdcaging, as discussed in Section 3.1.3.2. The increased and decreased pitch variations are applied over discrete sections of the fuel rods, and not as continuous changes as a function of elevation. The irradiated fuel is represented with segments 20.32 cm in length to capture the axial burnup gradient, as discussed in Appendix A, and these segments are used as the discrete sections for pitch variation. The size of the compressed pitch region is varied from one and four segments, and the expanded pitch section at the top of the assembly ranges from two to eight segments in length in an effort to identify the maximum change in  $k_{\text{eff}}$  attributable to birdcaging. An example with four segments in the compressed region and four segments in the upper expanded region is shown in Figure 13. Slight reactivity increases are observed in the cases with four or more fuel segments in the expanded pitch zone. The maximum  $k_{\text{eff}}$  change is 0.05%  $\Delta k_{\text{eff}}$  beyond the 2.65%  $\Delta k_{\text{eff}}$  resulting from uniform pitch expansion configuration. This additional increase in  $k_{\text{eff}}$  is negligible.

**Table 11. Results for loss of rod pitch control in GBC-32**

Enrichment (w/o $^{235}\text{U}$ )	Burnup (GWd/MTU)	Increase in $k_{\text{eff}}$ (% $\Delta k_{\text{eff}}$ )
<b>Cladding intact</b>		
1.92	0	0.78
3.5	25.5	1.48
5	44.25	1.69
<b>Cladding removed</b>		
1.92	0	3.30
3.5	25.5	4.49
5	44.25	4.89

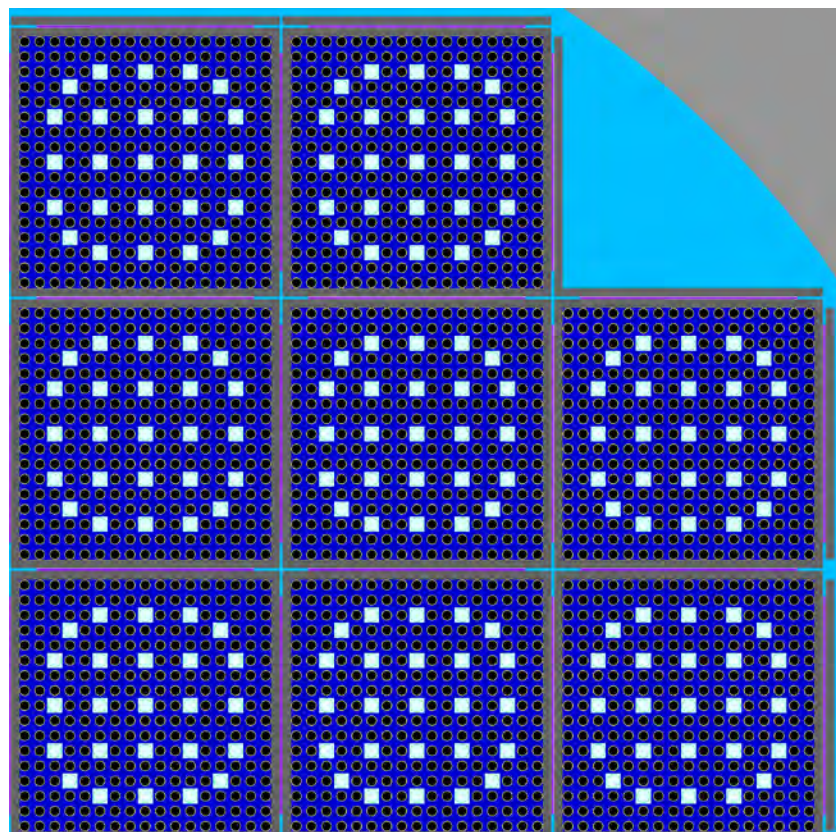


**Figure 10. Maximum uniform pitch expansion case.**

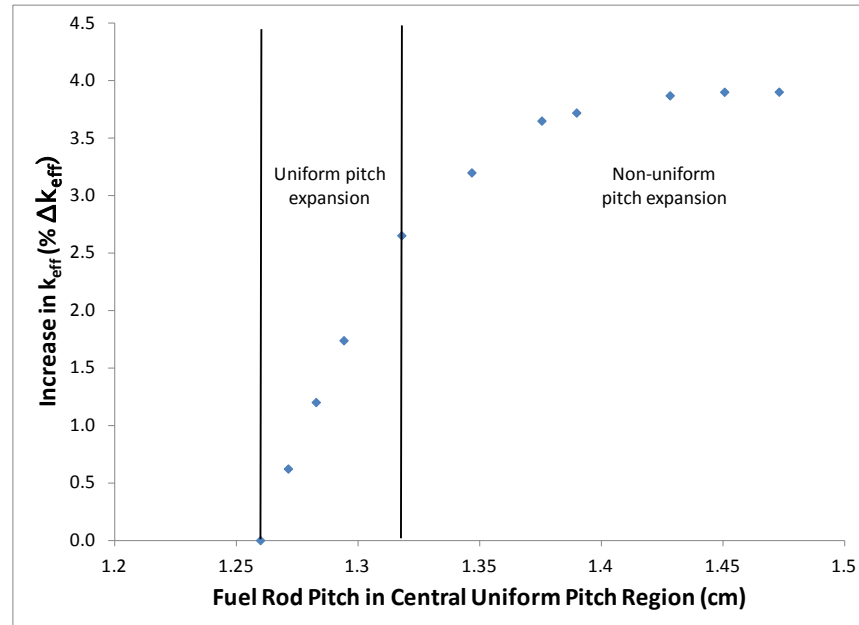
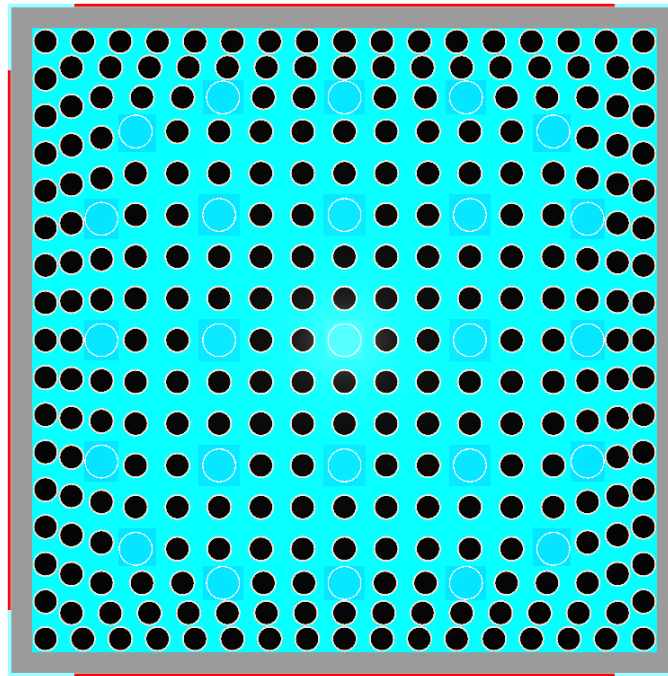
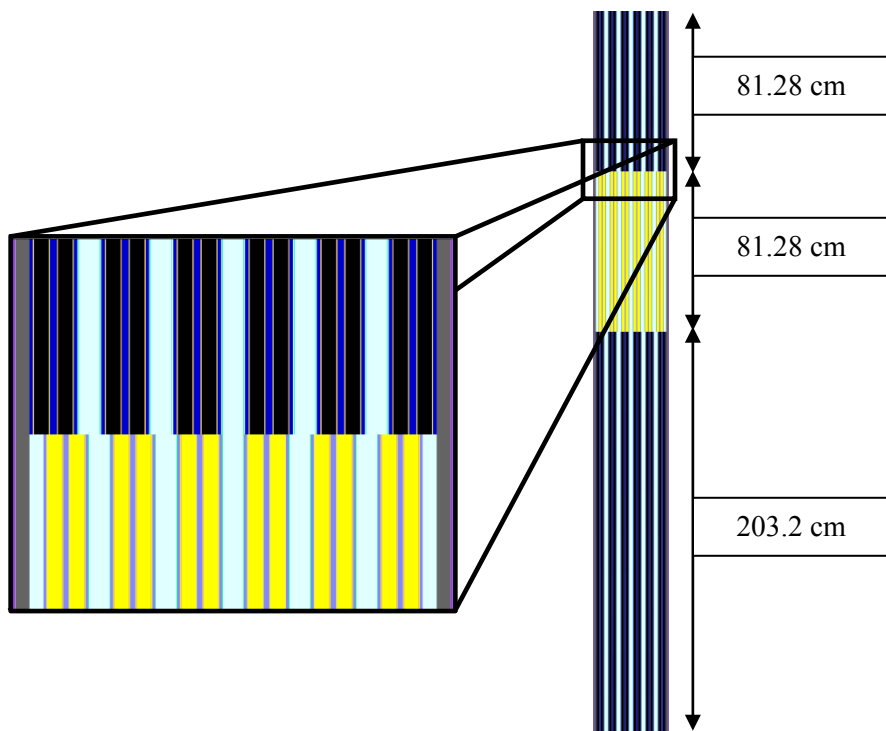


**Figure 11.** Increase in  $k_{\text{eff}}$  in GBC-32 cask due to increased fuel rod pitch (5 w/o initial enrichment, 44.25 GWd/MTU burnup).



Notes: Both shades of light blue are identical water compositions  
Neutron absorber panels are shown in red

**Figure 12.** Example nonuniform pitch model in GBC-32 storage cell.



Notes: Fuel in expanded pitch segments is shown as black, regardless of isotopic composition  
Fuel in compressed pitch segments is shown in yellow, regardless of isotopic composition  
Large gaps between pairs of fuel rods indicate the presence of guide tubes

**Figure 13. Assembly with axially varying pitch in the GBC-32.**

#### 5.1.1.4 Loss of Assembly Position Control

Loss of assembly position control is calculated over a range of displacements. The consequence of the maximum misalignment for all three burnup and enrichment combinations is shown in Table 12 and is over 16%  $\Delta k_{\text{eff}}$  for the limiting condition. A more limited misalignment case (20 cm) is also evaluated as a surrogate for potential degradation of assembly end fittings or the spacers used inside the cask to ensure proper assembly alignment at the time of loading. The consequences of this more limited misalignment, shown in Figure 14 and Table 13, are significantly less, but the increase in  $k_{\text{eff}}$  is still nearly 11%  $\Delta k_{\text{eff}}$ . The limiting condition for misalignment is for fuel with 44.25 GWd/MTU burnup and an initial enrichment of 5 w/o. Misalignment toward the bottom of the cask has significantly less impact because the fuel at the bottom end of the assembly has lower reactivity. The variation of the  $k_{\text{eff}}$  increase as a function of axial position is shown in Figure 15 for fuel with an initial enrichment of 5 w/o  $^{235}\text{U}$  and 44.25 GWd/MTU burnup. The reactivity increase reported here is significantly higher than that reported in Ref. 25. Insufficient detail is available for review in Ref. 25 to propose any likely causes for the differences.

**Table 12. Increase in  $k_{\text{eff}}$  for assembly axial displacement in GBC-32  
(30 cm displacement relative to the neutron absorber panel)**

Enrichment (w/o $^{235}\text{U}$ )	Burnup (GWd/MTU)	Increase in $k_{\text{eff}}$ (% $\Delta k_{\text{eff}}$ )
1.92	0	10.38
3.5	25.5	16.37
5	44.25	16.70

**Table 13. Increase in  $k_{\text{eff}}$  for limited (20 cm displacement relative to the neutron absorber panel)  
assembly axial displacement in GBC-32**

Enrichment (w/o $^{235}\text{U}$ )	Burnup (GWd/MTU)	Increase in $k_{\text{eff}}$ (% $\Delta k_{\text{eff}}$ )
1.92	0	3.85
3.5	25.5	10.22
5	44.25	10.82

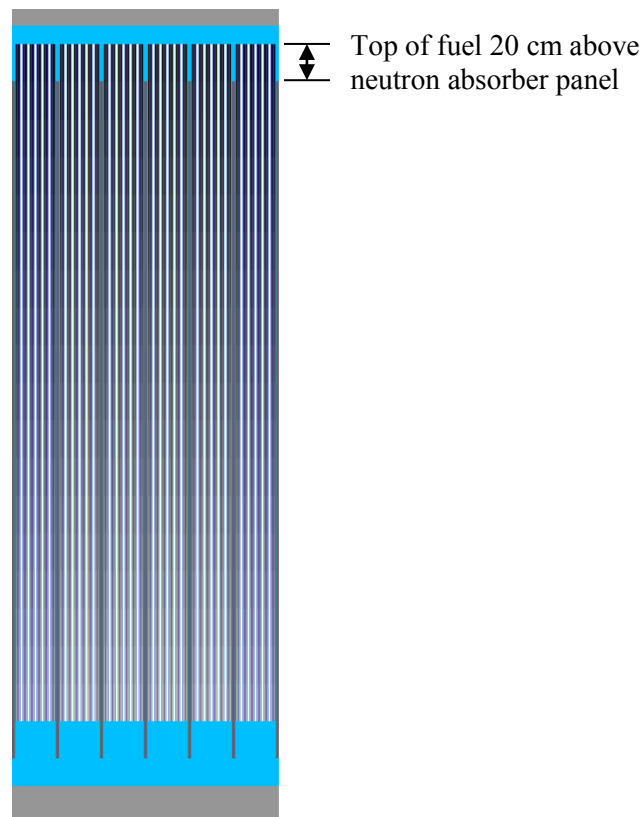


**Figure 14. Misalignment of fuel assembly 20 cm toward lid of GBC-32.**

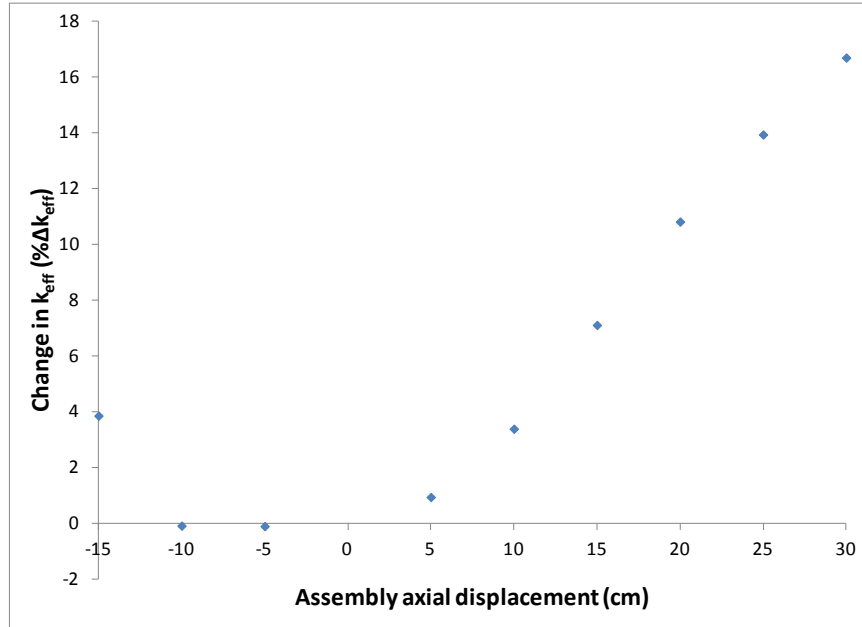


**Figure 15. Increase in  $k_{\text{eff}}$  in GBC-32 as a function of assembly axial displacement (5 w/o initial enrichment and 44.25 GWd/MTU burnup).**

#### 5.1.1.5 Gross Fuel Assembly Failure

The two gross assembly failure configurations described in Section 3.1.5 are investigated in the GBC-32 cask. Axial representations are shown in Figure 16 and 17 for the homogeneous rubble and ordered pellet array cases, respectively. In both cases, the limiting case is the non-physical condition in which the fissile material extends from the base plate to the lid. As expected, these configurations have the highest  $k_{\text{eff}}$  increase, and the ordered pellet array case is more limiting than the homogeneous rubble case. As shown previously in Table 6, the  $k_{\text{eff}}$  associated increase in the homogeneous rubble case is over 14%  $\Delta k_{\text{eff}}$ , and the ordered pellet array case increases  $k_{\text{eff}}$  by over 21%  $\Delta k_{\text{eff}}$ . The limiting case is for the 44.25 GWd/MTU burnup case with 5 w/o initial enrichment for both gross assembly failure configurations. The results for both configurations for all three enrichment and burnup combinations are presented in Table 14 for the maximum increase case. If the fissile material is maintained within the poison panel elevations, the resulting change in  $k_{\text{eff}}$  is reduced to 4.18%  $\Delta k_{\text{eff}}$  for the ordered array of pellets. Results for a range of homogeneous rubble cases within the neutron absorber elevations are provided in Table 15. The results with fissile material restrained in the neutron absorber elevations demonstrate that these cases result in significantly lower  $k_{\text{eff}}$  increases than the unrestrained material cases.

The results for the pellet array case are significantly higher than those reported previously in Ref. 7. There are two main differences between that analysis and this one, both of which contribute to a sizeable  $k_{\text{eff}}$  increase in the work presented here. The pellet array case modeled here includes a distributed burnup profile in the pellet array, and the array is allowed to extend beyond the neutron absorber panel elevations. This latter change is the larger of the two effects, but the former change is also important.

**Table 14. Increase in  $k_{\text{eff}}$  in GBC-32 due to gross fuel assembly failure, fissile material outside neutron absorber elevations**

Enrichment (w/o $^{235}\text{U}$ )	Burnup (GWd/MTU)	Maximum increase in $k_{\text{eff}}$ (% $\Delta k_{\text{eff}}$ )
<b>Limiting pellet array</b>		
1.92	0	11.09
3.5	25.5	20.20
5	44.25	21.37
<b>Homogeneous rubble</b>		
1.92	0	6.66
3.5	25.5	13.95
5	44.25	14.30

**Table 15. Increase in  $k_{\text{eff}}$  in GBC-32 due to homogeneous rubble, debris within absorber elevations (5 w/o initial enrichment, 44.25 GWd/MTU burnup)**

Fraction of nominal assembly height	Increase in $k_{\text{eff}}$ (% $\Delta k_{\text{eff}}$ )
1.0	-4.64
0.9	-7.05
0.8	-10.16
0.7	-14.36
0.6	-20.16
0.5	-28.34
0.4	-39.10
0.36 (Fully compressed rubble)	-45.50



**Figure 16.** Limiting homogeneous rubble configuration for GBC-32.

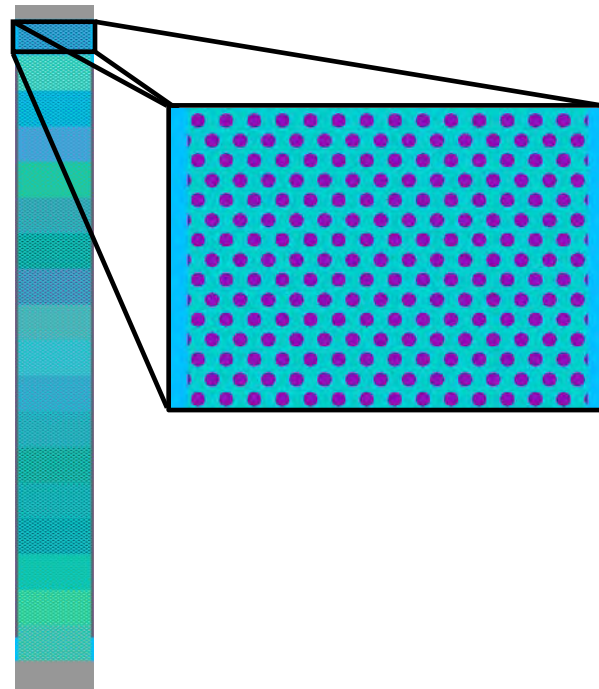


**Figure 17.** Limiting ordered pellet array configuration for GBC-32.

### 5.1.1.6 Neutron Absorber Degradation

The results of the calculations, described in Section 3.1.6.1, considering a 5-cm neutron absorber defect at varying elevations for all three enrichment and burnup combinations are presented in Table 16. The limiting condition is for fuel with an initial enrichment of 5 w/o and 44.25 GWd/MTU burnup. As expected, the limiting elevation is near the top of the active fuel height, as shown in Figure 18. The results for the full range of elevations considered in the limiting fuel condition are presented in Table 17. As expected, the limiting elevation for the fresh 1.92 w/o fuel is located at the centerline. The largest  $k_{\text{eff}}$  increase observed for the 5-cm defect is 1.05%  $\Delta k_{\text{eff}}$  and increases to 2.33%  $\Delta k_{\text{eff}}$  if the defect size is increased to 10 cm. As discussed in Section 3, these defects are assumed to be present at the same elevation in all neutron absorber panels within the cask and the sizes of the defects are chosen arbitrarily.

The consequences of uniform neutron absorber panel thinning as discussed in Section 3.1.6.3 are shown in Table 18 and Figure 19 for fresh 1.92 w/o fuel. The panel thinning results shown in Appendix C confirm that the fresh fuel case is most limiting. As shown in Table 6, a 50% reduction in absorber panel thickness increases  $k_{\text{eff}}$  by 1.78%  $\Delta k_{\text{eff}}$ . Complete removal of the panels causes a  $k_{\text{eff}}$  increase of 9.5%, but the increase is not in excess of 3% until nearly 70% of the neutron absorber panel is removed. The consequence of complete absorber panel removal is less severe than the axial displacement cases discussed in Section 5.1.1.4 because the steel fuel storage basket walls reduce neutronic communication between assemblies.

**Table 16. Maximum  $k_{\text{eff}}$  increase caused by a 5-cm neutron absorber defect in GBC-32**

Enrichment (w/o $^{235}\text{U}$ )	Burnup (GWd/MTU)	Defect center elevation (cm)	Maximum increase in $k_{\text{eff}}$ (% $\Delta k_{\text{eff}}$ )
1.92	0	182.88	0.29
3.5	25.5	342.09	0.94
5	44.25	348.86	1.05

**Table 17. Increase in  $k_{\text{eff}}$  caused by a 5-cm neutron absorber defect at various elevations in GBC-32 (5 w/o initial enrichment, 44.25 GWd/MTU burnup)**

Defect center elevation (cm)	Increase in $k_{\text{eff}}$ (% $\Delta k_{\text{eff}}$ )
321.77	0.44
328.54	0.67
335.31	0.84
342.09	1.00
348.86	1.05
355.64	0.82

**Table 18. Increase in  $k_{\text{eff}}$  caused by uniform neutron absorber panel thinning  
(fresh 1.92 w/o enrichment)**

Fraction of neutron absorber panel thickness remaining	Increase in $k_{\text{eff}}$ (% $\Delta k_{\text{eff}}$ )
0.9	0.29
0.8	0.59
0.7	0.92
0.6	1.32
0.5	1.78
0.4	2.39
0.3	3.15
0.2	4.20
0.1	5.86
0.0	9.51

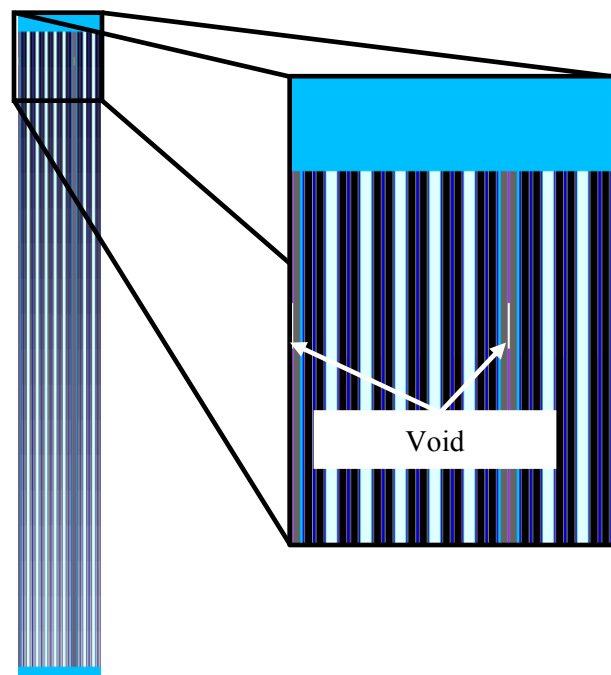


**Figure 18. Limiting location of 5-cm neutron absorber panel defect in GBC-32.**

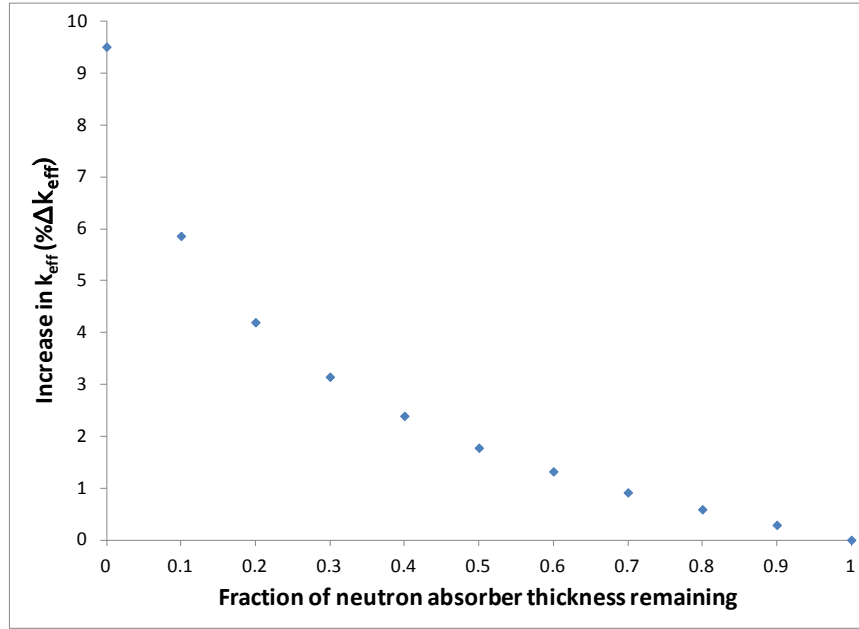


**Figure 19. Increase in  $k_{\text{eff}}$  as a function of remaining neutron absorber panel thickness for fresh 1.92 w/o fuel.**

#### 5.1.1.7 Burnup and Cooling Time Sensitivities

The results of the sensitivity studies relating to additional burnup and cooling time are presented in Appendix C (Section C.1). Each configuration discussed in the previous six subsections is considered explicitly. The results of the calculations for additional burnup and cooling time conditions indicate that the increase in  $k_{\text{eff}}$  reported for each configuration encompasses the changes that may result for additional burnups and cooling times. That is, the differences in the change in  $k_{\text{eff}}$  are smaller than the changes in the base case  $k_{\text{eff}}$  caused by the additional burnup and/or cooling time considered.

#### 5.1.2 Varying Number of Reconfigured Assemblies

The results presented in Section 5.1.1 and Table 6 assume that all 32 fuel assemblies in the GBC-32 cask experience the same fuel or neutron absorber reconfiguration within the respective configuration of interest. As discussed in Section 3.2, a series of calculations is performed to establish the  $k_{\text{eff}}$  increase as a function of the number of reconfigured assemblies within the cask. The four configurations considered are the limiting conditions for single rod failure, multiple rod failure, uniform rod pitch increase, and homogeneous rubble resulting from gross assembly failure.

The first fuel assembly to experience the reconfiguration being examined is selected in an attempt to maximize the  $k_{\text{eff}}$  increase, and is therefore one near the center of the cask. Additional assemblies are added in mostly symmetric groups of equal distance from the first reconfigured assembly. For some low numbers of reconfigured assemblies, multiple combinations of assemblies are considered. Eight combinations of reconfigured assemblies are considered in the GBC-32. One order in which the assemblies experience reconfiguration is shown in Figure 20. Results are presented in the following subsections.

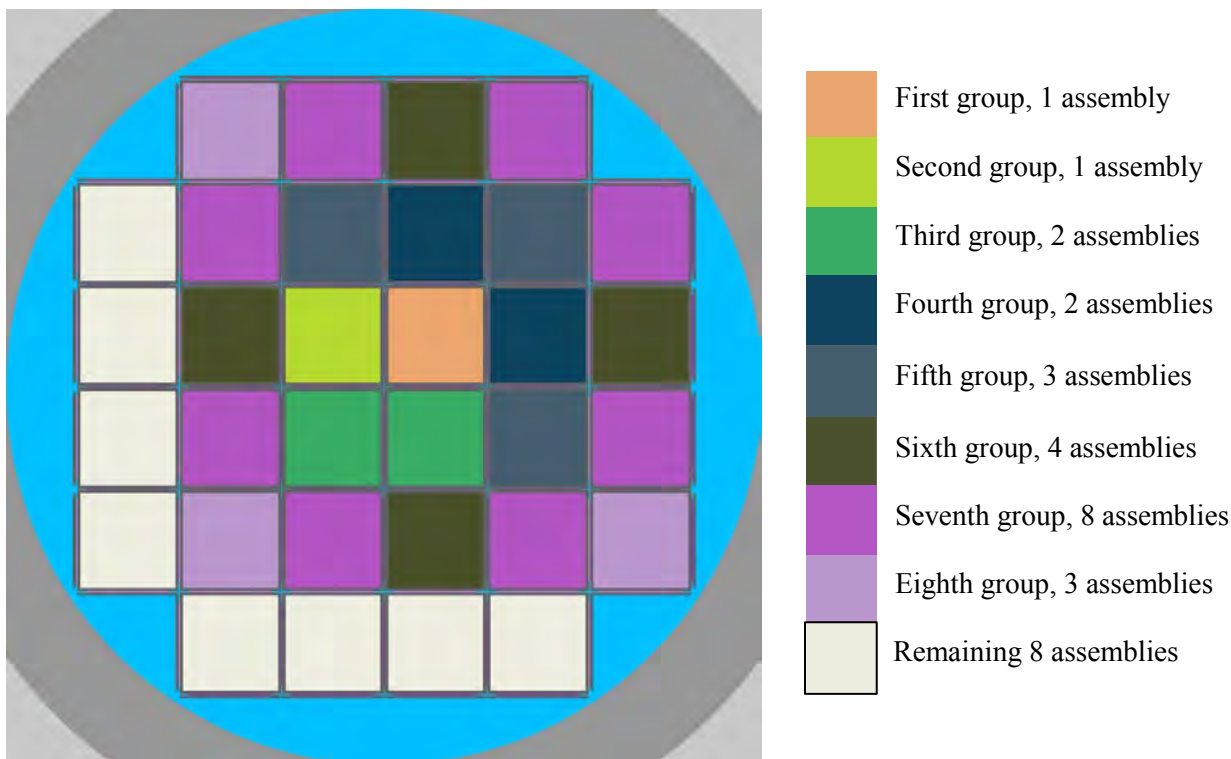


**Figure 20. One order of assembly reconfiguration in GBC-32 partial degradation configurations.**

### 5.1.2.1 Rod Failures

The single and multiple rod failure configurations that result in the largest increase in  $k_{\text{eff}}$ , as discussed in Section 5.1.1.2, are used to study the impact of some assemblies suffering reconfiguration while others in the cask remain intact. All assemblies, reconfigured or intact, use the isotopic number densities representing 5 w/o  $^{235}\text{U}$  fuel depleted to 44.25 GWd/MTU and cooled for 5 years.

The results for single rod failure are shown below in Table 19 and Figure 21. The results for multiple rod failure are shown below in Table 20 and Figure 22. The portion of the  $k_{\text{eff}}$  impact introduced by each group of assemblies for the single rod failure configurations shows more than 50% of the reactivity change coming after only four assemblies experience reconfiguration and more than 75% of the reactivity change caused by the first nine assembly reconfigurations. The Monte Carlo uncertainty is relatively large compared to the  $k_{\text{eff}}$  changes being examined in this series of calculations because of the relative insensitivity of the cask  $k_{\text{eff}}$  to single rod failures. The resulting  $k_{\text{eff}}$  increase is therefore not a smooth function.

The multiple rod failure results are similar, with fewer than nine assemblies causing 50% of the increase in  $k_{\text{eff}}$  and 13 assemblies causing almost 75% of the change. The results indicate that a reduced number of reconfigured assemblies will not significantly reduce the  $k_{\text{eff}}$  increase associated with fuel reconfiguration if the degraded assemblies are in close proximity, and particularly if they are in the center region of the cask.

**Table 19. Increase in  $k_{\text{eff}}$  in GBC-32, single rod failure  
(5 w/o initial enrichment, 44.25 GWd/MTU burnup)**

Number of degraded assemblies	Increase in $k_{\text{eff}}$ (% $\Delta k_{\text{eff}}$ )
1	0.01
2	0.01
2	0.01
4	0.06
5	0.04
5	0.05
9	0.07
13	0.07
21	0.07
24	0.07
32	0.09

**Table 20. Increase in  $k_{\text{eff}}$  in GBC-32, multiple rod failure  
(5 w/o initial enrichment, 44.25 GWd/MTU burnup)**

Number of degraded assemblies	Increase in $k_{\text{eff}}$ (% $\Delta k_{\text{eff}}$ )
1	0.20
2	0.37
2	0.36
4	0.71
5	0.79
5	0.82
9	1.16
13	1.38
21	1.70
24	1.74
32	1.86

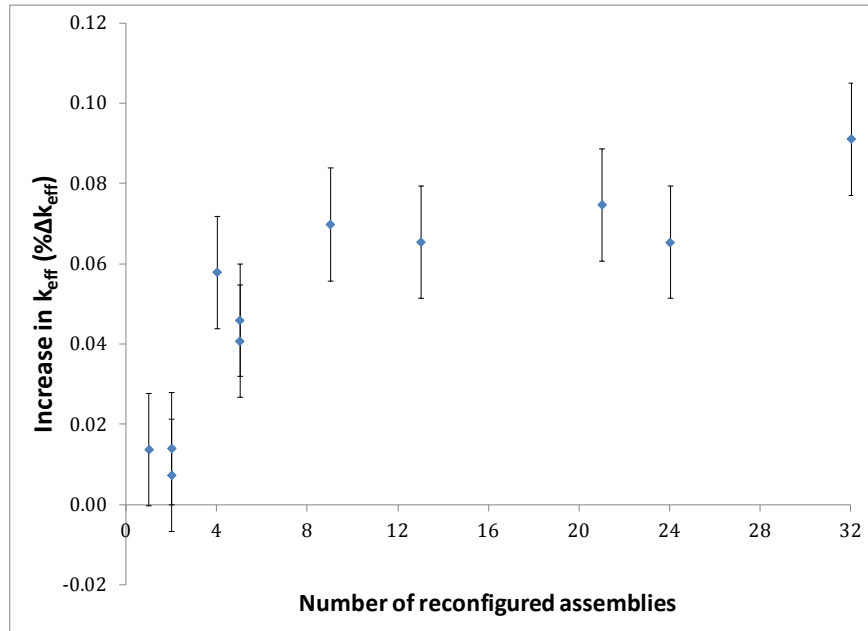


Figure 21. Increase in  $k_{\text{eff}}$  in GBC-32 as a function of number of reconfigured assemblies, single rod failure (5 w/o initial enrichment, 44.25 GWd/MTU burnup).

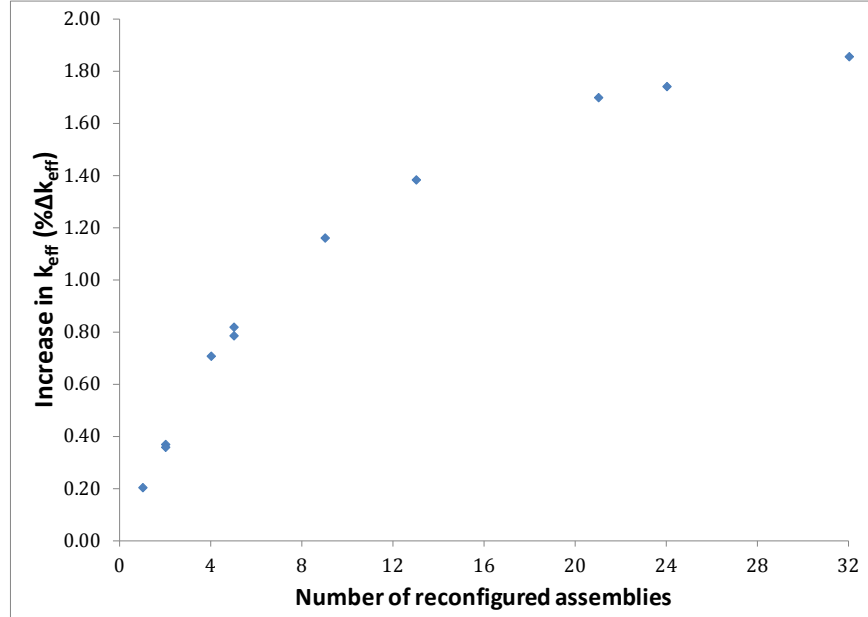


Figure 22. Increase in  $k_{\text{eff}}$  in GBC-32 as a function of number of reconfigured assemblies, multiple rod failure (5 w/o initial enrichment, 44.25 GWd/MTU burnup).

### 5.1.2.2 Loss of Rod Pitch Control, Uniform Pitch Increase

The maximum uniform pitch increase case is used to examine the  $k_{\text{eff}}$  impact of varying the number of assemblies that have experienced reconfiguration. The assembly configuration used for this study models

the outer row of fuel rods in contact with the inner wall of the fuel storage basket in each cell. The fuel composition used for all assemblies corresponds to 5 w/o fuel with 44.25 GWd/MTU burnup and 5 years of cooling time. The increase in  $k_{\text{eff}}$  for each number of reconfigured assemblies is provided in Table 21 as well as Figure 23. The first 50% of the total increase in  $k_{\text{eff}}$  has occurred with about seven reconfigured assemblies. Almost 75% of the increase in  $k_{\text{eff}}$  is caused by the first 13 reconfigured assemblies. The shape of the increase in  $k_{\text{eff}}$  as a function of reconfigured assemblies is similar to that seen for rod failure configurations in Section 5.1.2.1. The results indicate that a reduced number of reconfigured assemblies will not significantly reduce the  $k_{\text{eff}}$  increase associated with fuel reconfiguration if the degraded assemblies are in close proximity, and particularly if they are in the center region of the cask.

**Table 21. Increase in  $k_{\text{eff}}$  in GBC-32, uniform pitch increase  
(5 w/o initial enrichment, 44.25 GWd/MTU burnup)**

Number of degraded assemblies	Increase in $k_{\text{eff}}$ (% $\Delta k_{\text{eff}}$ )
1	0.27
2	0.51
2	0.49
4	1.00
5	1.14
5	1.08
9	1.66
13	1.96
21	2.41
24	2.49
32	2.66

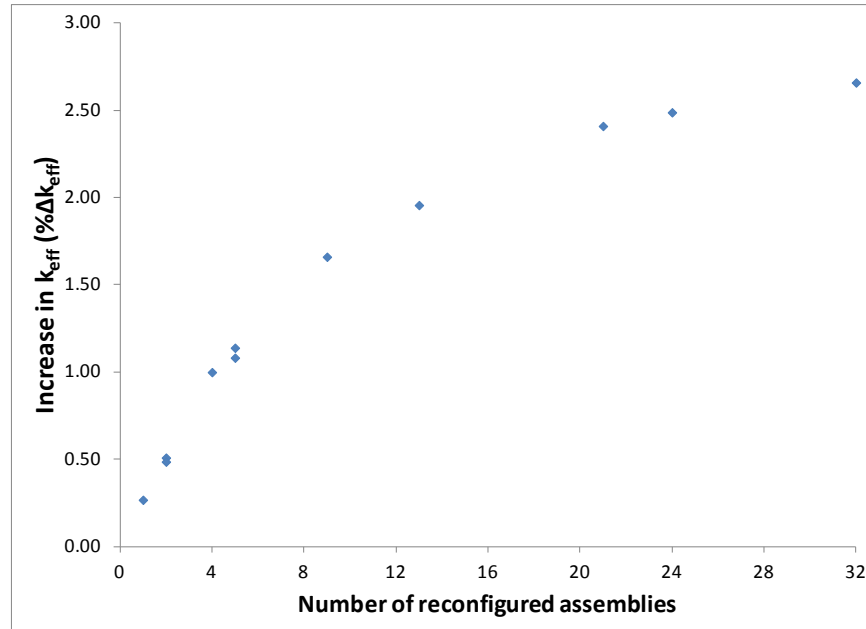


**Figure 23. Increase in  $k_{\text{eff}}$  in GBC-32 as a function of number of reconfigured assemblies, uniform pitch increase (5 w/o initial enrichment, 44.25 GWd/MTU burnup).**

### 5.1.2.3 Gross Assembly Failure, Homogeneous Rubble

The homogeneous rubble modeling of the gross assembly failure configuration is the final configuration used to examine the  $k_{\text{eff}}$  impact of varying the number of assemblies that have experienced reconfiguration. The configuration used for this study fills the entire inside volume of the storage cell with homogeneous rubble, as described in Section 3.1.5.1. Each axial zone of rubble is approximately 23 cm tall; thus, the 18 zones fill the cask from the base plate to the lid and retain the axial burnup profile of the intact assembly. The fuel composition is based on fuel with an initial enrichment of 5 w/o and 44.25 GWd/MTU burnup. This configuration resulted in the largest  $k_{\text{eff}}$  increase of the homogeneous rubble configurations used in Section 5.1.1.5. The increase in  $k_{\text{eff}}$  for each number of reconfigured assemblies is provided in Table 22 as well as Figure 24. The general trend in the  $k_{\text{eff}}$  change for the uniform pitch increase cases is different from that for single and multiple rod failure and uniform pitch expansion configurations presented in Sections 5.1.2.1 and 5.1.2.2. The first two reconfigured assemblies lower the cask  $k_{\text{eff}}$  because of the effects of homogenization and fissile material relocation. An increase in  $k_{\text{eff}}$  is noted for four or more reconfigured assemblies after a sufficient number of assemblies are reconfigured to relocate the most reactive portion of the cask to the top of the homogeneous rubble. More than 60% of the increase in  $k_{\text{eff}}$  is caused by the first nine reconfigured assemblies, and more than 70% of the total  $k_{\text{eff}}$  increase results from the reconfiguration of 13 assemblies.

**Table 22. Increase in  $k_{\text{eff}}$  in GBC-32, homogeneous rubble configuration of gross assembly failure (5 w/o initial enrichment, 44.25 GWd/MTU burnup)**

Number of degraded assemblies	Increase in $k_{\text{eff}}$ (% $\Delta k_{\text{eff}}$ )
1	-0.53
2	-0.87
2	-1.07
4	1.93
5	2.91
5	1.70
9	8.59
13	10.07
21	12.94
24	13.37
32	14.30

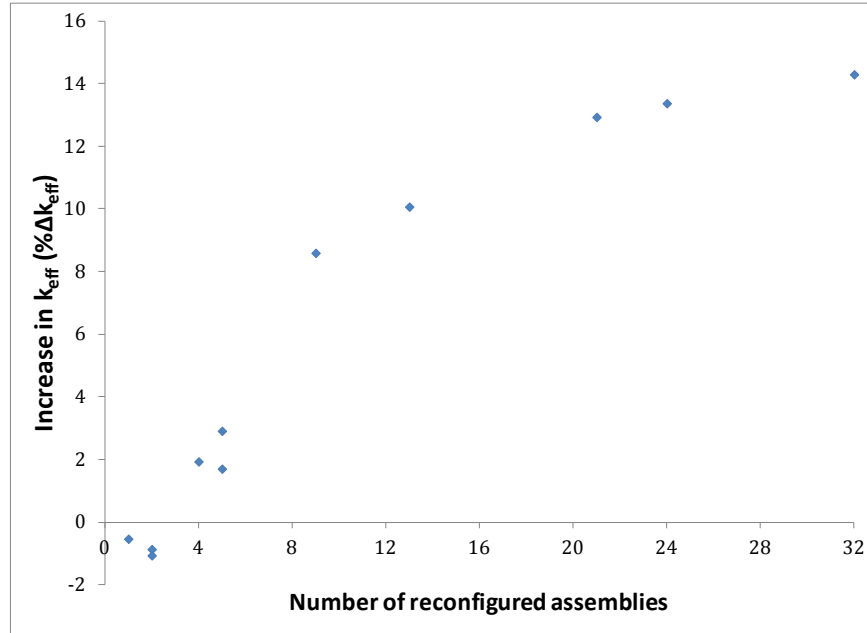


**Figure 24. Increase in  $k_{\text{eff}}$  as a function of number of reconfigured assemblies, gross assembly failure.**

### 5.1.3 Combined Configurations

As discussed in Section 3.3, some of the mechanisms that could result in fuel reconfigurations could result in a combination of configurations. Therefore, selected combined configurations are evaluated, including: 16 failed rods with 50% clad thinning and 16 failed rods with a uniform pitch expansion of 0.011 cm. These combinations of configurations are selected as they both pertain to failure of zirconium alloy components of the fuel assembly. The combined degradation cases consider fuel with an initial enrichment of 5 w/o  $^{235}\text{U}$  depleted to 44.25 GWd/MTU and 5 years of cooling time.

The multiple rod failure results presented in Section 5.1.1.2 indicate that the failure of 16 fuel rods results in an increase in  $k_{\text{eff}}$  of 1.1%  $\Delta k_{\text{eff}}$ . This is approximately half the maximum increase for multiple failed rod configurations and is therefore selected as an intermediate configuration. The cladding thickness on all intact rods in both combined configurations is represented with 50% of the nominal thickness. The pitch increase of 0.011 cm, based on the results presented in Figure 11, is approximately 0.6%  $\Delta k_{\text{eff}}$ . This represents about 15% of the increase in maximum  $k_{\text{eff}}$  associated with the nonuniform pitch expansion.

The results of the two combined configurations considered in the GBC-32 cask are presented in Table 23. For comparison, the  $k_{\text{eff}}$  increase resulting from each degraded configuration separately as well as the sum of the two is provided. The increase in  $k_{\text{eff}}$  associated with explicit modeling of the combined configurations is less than the estimated increase based on summing the individual increases. The conservatism of adding the separate effects is less than 0.4%  $\Delta k_{\text{eff}}$ . It appears that the linear combination of the  $k_{\text{eff}}$  increases is conservative, but more combined configurations would need to be investigated prior to drawing general conclusions. If it is confirmed, the  $k_{\text{eff}}$  increase caused by combinations of degradations could be conservatively bounded by adding the increase associated with individual configurations where applicable.

**Table 23. Increase in  $k_{\text{eff}}$  for combined configurations in GBC-32**

Case	Increase in $k_{\text{eff}}$ (% $\Delta k_{\text{eff}}$ )
<b>Multiple failed rods and clad thinning (44.25 GWd/MTU; 5-y cooling time)</b>	
16 failed rods	1.10
50% clad thinning	1.94
Sum of $k_{\text{eff}}$ increases	3.04
Combined configuration model	2.67
Overestimation of $k_{\text{eff}}$ increase by summing individual effects	0.37
<b>Multiple failed rods and 0.011-cm increase in fuel rod pitch (44.25 GWd/MTU; 5-y cooling time)</b>	
16 failed rods	1.10
Uniform pitch increase	0.62
Sum of $k_{\text{eff}}$ increases	1.72
Combined configuration model	1.63
Overestimation of $k_{\text{eff}}$ increase by summing individual effects	0.09

## 5.2 MPC-68 Cask Model Results

The  $k_{\text{eff}}$  change associated with each of the reconfigurations discussed in Section 3 is presented here for the MPC-68 cask. The configurations assume a range of loadings of  $10 \times 10$  fuel. The description of the fuel assembly modeling is provided in Appendix A. All fuel is modeled with a uniform initial enrichment of 5 w/o. The burnups and cooling times used are presented in Table 24. The basis for selecting these points is provided in Section 4.2.2. All configurations, with the exception of the uniform array of pellets model of gross fuel assembly failure, also consider the fuel both with and without the channel present. The reference case  $k_{\text{eff}}$  results for both fresh and used fuel in both the channeled and unchanneled conditions are provided in Table 24.

**Table 24. Nominal  $k_{\text{eff}}$  results for enrichment, burnup, and cooling time cases considered in MPC-68, channeled and unchanneled fuel**

Channel present	Burnup (GWd/MTU)	Cooling time (years)	KENO V.a		KENO-VI	
			$k_{\text{eff}}$	$\sigma$	$k_{\text{eff}}$	$\sigma$
Yes	0	0	0.96800	0.00010	0.96828	0.00010
	35.0	5	0.83269	0.00010	0.83258	0.00010
No	0	0	0.96768	0.00010	0.96763	0.00010
	35.0	5	0.83434	0.00010	0.83420	0.00010

### 5.2.1 Reconfiguration of All Assemblies

A summary of the increases in  $k_{\text{eff}}$  caused by each configuration is provided in Table 25. Additional details for each configuration and the results for non-limiting cases are provided in the subsequent subsections.

Comparing the results of these analyses to those presented in Ref. 7 is more difficult for the MPC-68 cask than for the GBC-32 cask. The difficulty is primarily a result of the analyses in Ref. 7 using a  $9 \times 9$  fuel assembly.

**Table 25. Summary of  $k_{\text{eff}}$  increases for the MPC-68 cask**

<b>Configuration</b>	<b>Increase in <math>k_{\text{eff}}</math> (% <math>\Delta k_{\text{eff}}</math>)</b>	<b>Limiting case</b>		
		<b>Burnup (GWd/MTU)</b>	<b>Cooling time (years)</b>	<b>Channel present</b>
<b>Clad thinning/loss</b>				
Cladding removal	4.98	0	0	Yes
<b>Rod failures</b>				
Single rod removal	0.29	0	0	Yes
Multiple rod removal	2.40	35	5	Yes
<b>Loss of rod pitch control</b>				
Uniform rod pitch expansion, clad	13.16	0	0	No
Uniform rod pitch expansion, unclad	15.32	0	0	No
Channel constrained uniform expansion, clad	2.09	0	0	Yes
Nonuniform rod pitch expansion, clad	13.31	0	0	No
<b>Loss of assembly position control</b>				
Axial displacement (maximum)	19.40	35	5	Yes
Axial displacement (20 cm)	6.29	35	5	Yes
<b>Gross assembly failure</b>				
Uniform pellet array	34.40	35	5	No
Homogeneous rubble	29.36	35	5	No
<b>Neutron absorber degradation</b>				
Missing neutron absorber (5-cm segment)	2.49	35	5	Yes
Missing neutron absorber (10-cm segment)	5.62	35	5	Yes
50% reduction of neutron absorber panel thickness	3.67	0	0	Yes

### 5.2.1.1 Clad Thinning/Loss

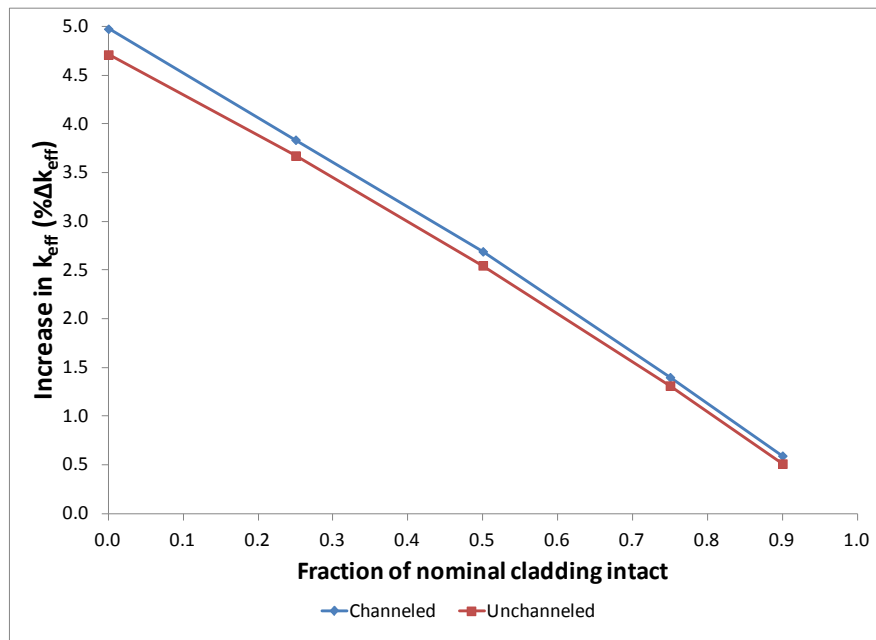
The loss of cladding configuration is modeled as discussed in Section 3.1.1. As shown in Table 25, the limiting  $k_{\text{eff}}$  increase associated with complete cladding removal is 4.98%  $\Delta k_{\text{eff}}$  and occurs with fresh fuel. The results for both fuel burnups, both with and without the fuel channel, are summarized in Table 26. For the limiting case, fresh fuel, the increase in  $k_{\text{eff}}$  as a function of the fraction of nominal cladding thickness remaining is shown in Table 27 and Figure 25. The trend of increasing  $k_{\text{eff}}$  with decreasing cladding thickness is the same for depleted fuel, so these results are not presented here. The configuration with 25% of the nominal cladding remaining is shown in Figure 26. The results are in good agreement with those presented in Ref. 7.

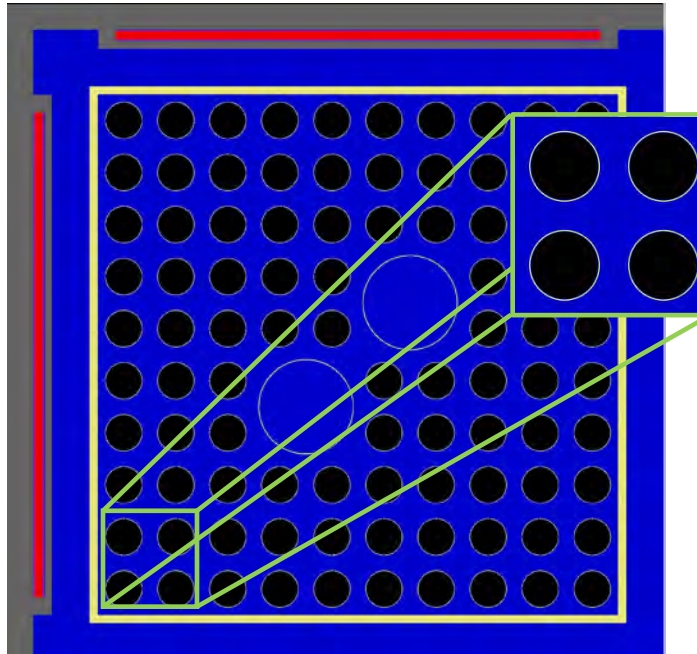
**Table 26. Increase in  $k_{\text{eff}}$  for cladding removal in MPC-68**

Burnup (GWd/MTU)	Cooling time (years)	Channel	Increase in $k_{\text{eff}}$ (% $\Delta k_{\text{eff}}$ )
0	0	Yes	4.98
35	5		4.82
0	0	No	4.71
35	5		4.59

**Table 27. Increase in  $k_{\text{eff}}$  in MPC-68 as a function of fraction of intact cladding, fresh 5 w/o fuel**

Fraction of intact cladding	Increase in $k_{\text{eff}}$ – Channeled (% $\Delta k_{\text{eff}}$ )	Increase in $k_{\text{eff}}$ – Unchanneled (% $\Delta k_{\text{eff}}$ )
0.90	0.59	0.51
0.75	1.40	1.31
0.50	2.69	2.55
0.25	3.84	3.68
0	4.98	4.71

**Figure 25. Increase in  $k_{\text{eff}}$  as a function of fraction of intact cladding, fresh 5 w/o fuel.**



Notes:

- Fuel shown in black
- Cladding is light grey around fuel material
- Water tubes are larger, water-filled tubes
- Storage cell wall and neutron absorber panel wrappers are dark grey
- Neutron absorber panel is red
- Fuel assembly channel yellow box around fuel rods
- Water is shown in dark blue

**Figure 26. Configuration with 25% nominal cladding thickness.**

### 5.2.1.2 Rod Failures

Each of the 51 unique half-assembly symmetric rods is removed individually to determine its worth, as discussed in Section 3.1.2.1. Table 28 presents the rod locations and worth of the limiting rod location for each of the four cases. For both fuel burnups, the  $k_{\text{eff}}$  increase for the channeled fuel assembly is greater than for the unchanneled assembly. This is likely caused by the slightly harder initial spectrum when the channel is present. The increase in moderation caused by the removal of the fuel rods has a greater impact on the harder initial spectrum.

A sketch showing the half-assembly symmetry and row and column labels is provided in Figure 27. The columns in the assembly are designated with a letter, from A to J, and the rows are designated with numbers, from 1 to 10. The maximum worth is 0.29%  $\Delta k_{\text{eff}}$  and is associated with rod H7 with fresh 5 w/o fuel. It should be noted that some rods have a worth that is statistically equivalent to the limiting case presented in Table 28. The worth is very small relative to the  $k_{\text{eff}}$  increases of other configurations, so further examination is not necessary.

The magnitude of the  $k_{\text{eff}}$  change caused by rod failure is somewhat less for these analyses than for the previous work documented in Ref. 7. The primary cause of the reduction is the difference in the size of the fuel rods. The fuel rods in the  $10 \times 10$  fuel assembly have smaller diameters, so the increase in moderation is smaller for a single rod removal.

Multiple rods are removed in groups, as discussed in Section 3.1.2.2. Groups of 2, 4, 8, 12, 16, 18, and 20 rods are considered. The increase in  $k_{\text{eff}}$  is shown for each of the four cases in Table 29. Figure 28 shows the  $k_{\text{eff}}$  change as a function of rods removed for the limiting case at 35 GWd/MTU burnup and 5 years of cooling time with the fuel assembly channel. The limiting lattice is shown in Figure 29. The maximum  $k_{\text{eff}}$  value occurs for 18 rods removed and corresponds to a  $k_{\text{eff}}$  increase of 2.40%  $\Delta k_{\text{eff}}$ . The limiting lattice is determined with the fuel channel intact and then rerun with the fuel channel removed. In each case, the  $k_{\text{eff}}$  increase is higher with the channel intact.

The  $k_{\text{eff}}$  increase for multiple rod removal in the MPC-68 cask is about twice that reported in Ref. 7. This is most likely due to the difference in the fuel assembly modeled in the analysis. The result for fresh fuel shown in Table 29 demonstrates that the effect of depleted fuel instead of fresh fuel is small.

**Table 28. Single rod removal results for GE 10 × 10 fuel in MPC-68**

Burnup (GWd/MTU)	Cooling time (years)	Channel	Location	Maximum increase in $k_{\text{eff}}$ (% $\Delta k_{\text{eff}}$ )
0	0	Yes	H7	0.29
35	5		G7	0.26
0	0	No	H7	0.25
35	5		D3	0.26

**Table 29. Multiple rod removal results for GE 10 × 10 fuel in MPC-68**

Burnup (GWd/MTU)	Cooling time (years)	Channel	Maximum increase in $k_{\text{eff}}$ (% $\Delta k_{\text{eff}}$ )
0	0	Yes	2.24
35	5		2.40
0	0	No	2.11
35	5		2.30

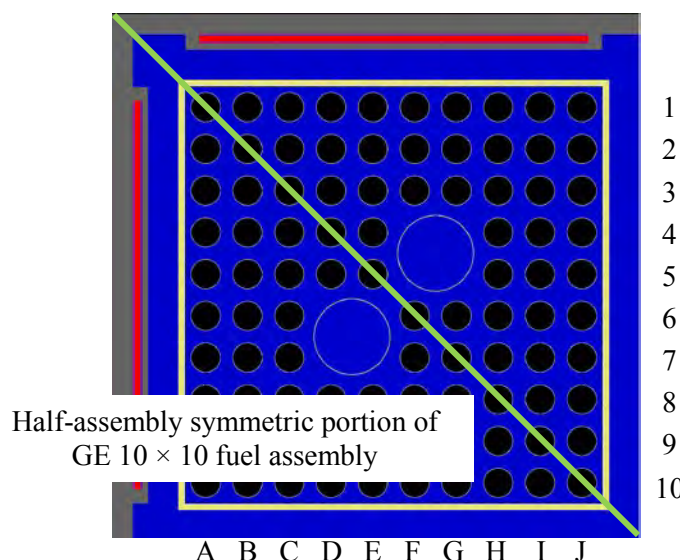


**Figure 27. Sketch of symmetry, row, and column labels for GE 10 × 10 fuel assembly.**

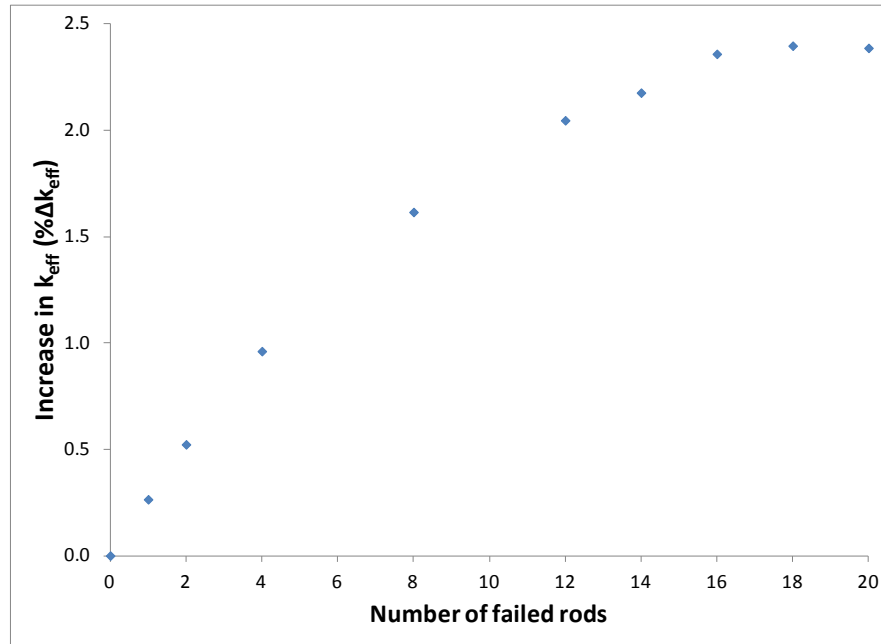


**Figure 28.** Increase in  $k_{\text{eff}}$  in MPC-68 as a function of number of rods removed (35 GWd/MTU burnup and 5-year cooling time).

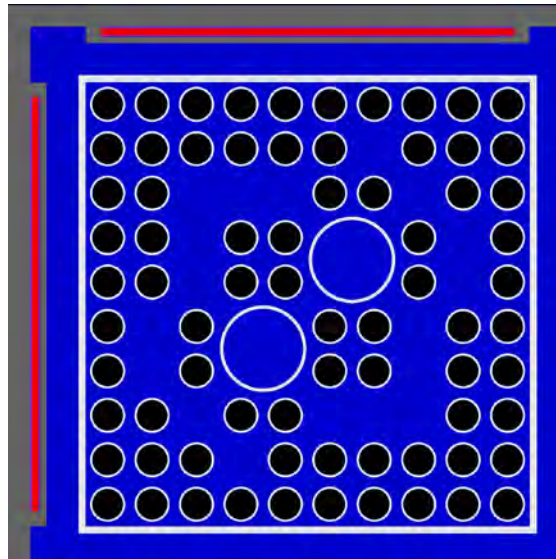


**Figure 29.** Limiting multiple rod removal lattice (18 rods removed).

### 5.2.1.3 Loss of Rod Pitch Control

The loss of rod pitch control is modeled first as a uniform increase in fuel assembly pitch, as discussed in Section 3.1.3. Two different assumptions are made about the condition of an intact fuel assembly channel. In one case, the fuel channel is assumed to expand with uniform thickness along with the fuel bundle. In this nonphysical model, the presence of the channel acts only to limit the uniform pitch increase by the thickness of the channel wall on both sides. The expansion is constrained by the contact of the assembly

channel with the neutron absorber wrappers on one side and the storage cell walls on the other. The second assumption is that the fuel channel does not deform, and thus constrains the expansion of the fuel rod pitch.

The assembly is also considered with no channel present. In this condition, the constraint is provided by fuel rod contact with neutron absorber wrappers. For the unchanneled cases, the modeled expansion ends when the unit cell containing the outermost fuel rods contacts the neutron absorber wrappers and storage cell walls.

The results with and without cladding, with and without the fuel channel, are shown in Table 30. As shown in Table 25, the limiting condition is with fresh fuel. The  $k_{\text{eff}}$  increase for clad fuel restrained by an intact fuel assembly channel is 2.09%  $\Delta k_{\text{eff}}$ .

The limiting condition, with fresh fuel and no assembly channel, is further expanded until the outermost fuel rods are in contact with the neutron absorber wrappers and basket walls, as shown in Figure 30. This pitch is maintained even in cells with fewer than two neutron absorber panels. The resulting increase in  $k_{\text{eff}}$ , is more than 13%  $\Delta k_{\text{eff}}$  with cladding intact and 15.32%  $\Delta k_{\text{eff}}$  with cladding removed.

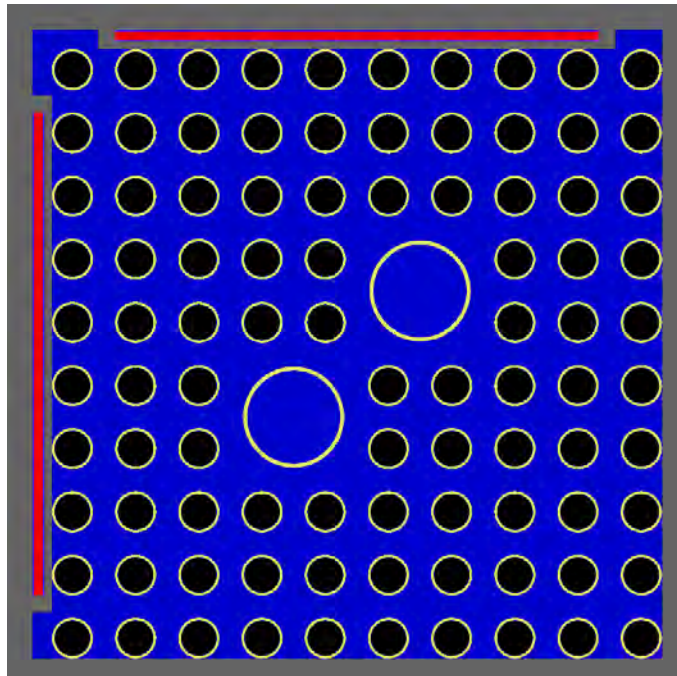
Fuel rod pitch is further increased in the MPC-68 model to examine the effect of nonuniform pitch, as discussed in Section 3.1.3.1 and Refs. 31 and 32. The inner portion of the assembly continues to expand until the outer rows are in contact with each other; although the fuel rod pitch is still uniform axially, it is nonuniform in the radial direction. An example model is shown in Figure 31. In the model with the largest pitch, the outermost fuel is in contact with the walls of the storage cell and the neutron absorber wrappers. The second set of fuel rods is in contact with the outermost rods. The pitch of the outermost fuel is constant within the row and is equal to the pitch that caused the pins to make contact with the basket wall. The increase in pitch in the inner portion of the assembly leads to a nonuniform pitch. The results of the calculations with increasing pitch are shown in Figure 32 as a function of the pitch of the inner, uniform portion of the assembly. The maximum total  $k_{\text{eff}}$  increase is 13.31%  $\Delta k_{\text{eff}}$ . The first six points represent the uniform pitch expansion. Nonuniform expansion begins when the fuel rod pitch is in excess of approximately 1.58 cm. The additional  $k_{\text{eff}}$  increase beyond the uniform expansion case is 0.15%  $\Delta k_{\text{eff}}$ , indicating that further expansion is a minor effect. The additional  $k_{\text{eff}}$  impact caused by nonuniform expansion is consistent with Refs. 31 and 32.

The limiting case for the MPC-68 cask contains fresh fuel, so the most reactive axial portion of the assembly is the center. For that reason, the birdcaging analysis, described in Section 3.1.3.2, includes two compressed pitch sections, each 30.48 cm in length, symmetrically positioned above and below the mid-plane of the assembly. A range of center section lengths is considered, but no  $k_{\text{eff}}$  increase is observed in any case containing the compressed pitch sections. One birdcaging configuration is shown in Figure 33. Birdcaging does not cause any additional  $k_{\text{eff}}$  increase beyond 13.16%  $k_{\text{eff}}$  associated with the uniform pitch expansion configuration for fresh fuel in the MPC-68 cask.

The results presented here show a larger increase in  $k_{\text{eff}}$  than that reported in Ref. 7. This is probably a result of the different fuel assembly lattice. Figure 21 in Ref. 7 indicates that the reactivity consequence of uniform pitch expansion increases with the array size. The effects of the different fuel rod and water rod diameters in the  $10 \times 10$  fuel are not accounted for in Ref. 7, however, so it is possible that these factors also influence the difference between the two analyses.

**Table 30. Results for loss of rod pitch control in MPC-68, no channel restraint**

Burnup (GWd/MTU)	Cooling time (years)	Channel	Maximum increase in $k_{\text{eff}}$ (% $\Delta k_{\text{eff}}$ )
<b>Cladding intact</b>			
0	0	Yes	11.00
35	5	Yes	9.55
0	0	No	12.07
35	5	No	10.56
<b>Cladding removed</b>			
0	0	Yes	14.05
35	5	Yes	12.74
0	0	No	14.70
35	5	No	13.30

**Figure 30. Maximum uniform pitch expansion configuration in MPC-68.**

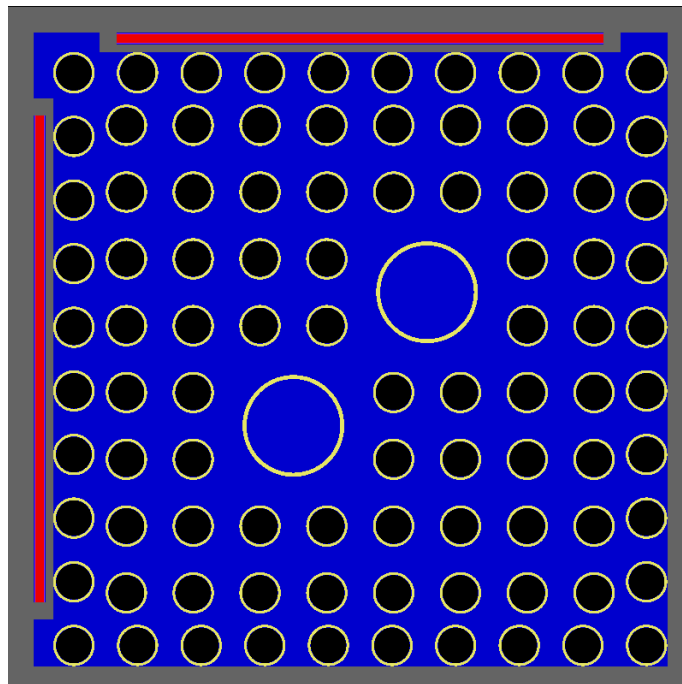


Figure 31. Example nonuniform pitch model for MPC-68.

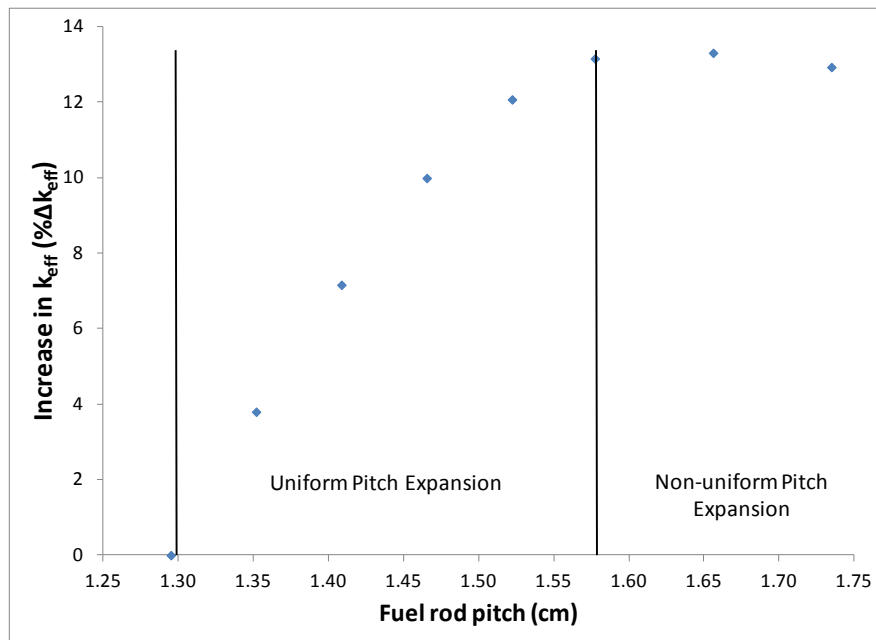
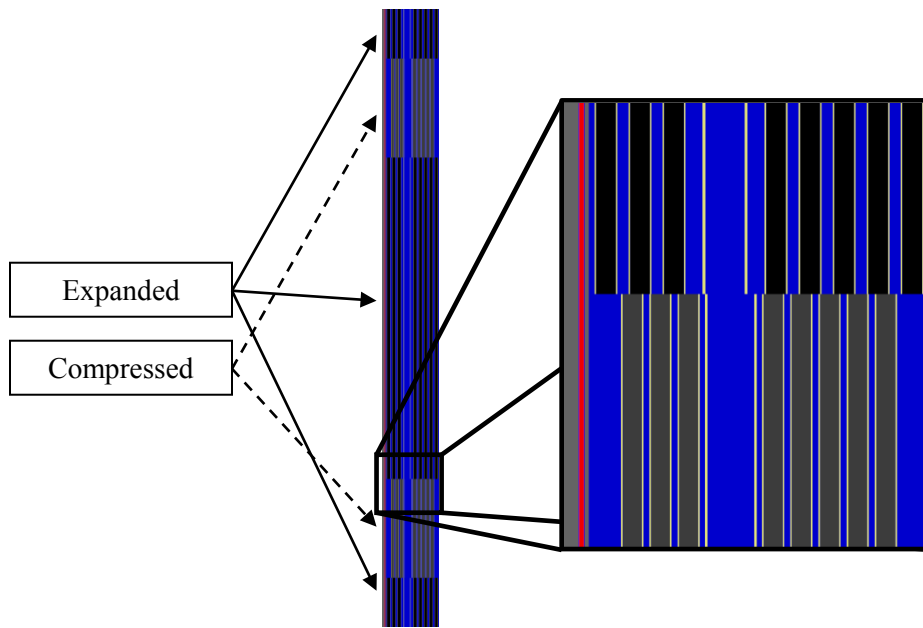


Figure 32. Increase in  $k_{\text{eff}}$  in MPC-68 as a function of fuel rod pitch, fresh 5 w/o fuel.



Notes:

- Expanded section fuel is shown in black
- Compressed section fuel is shown in grey
- All fuel has the same isotopic composition
- The gaps just to the left of the center of the zoomed portion are water tubes

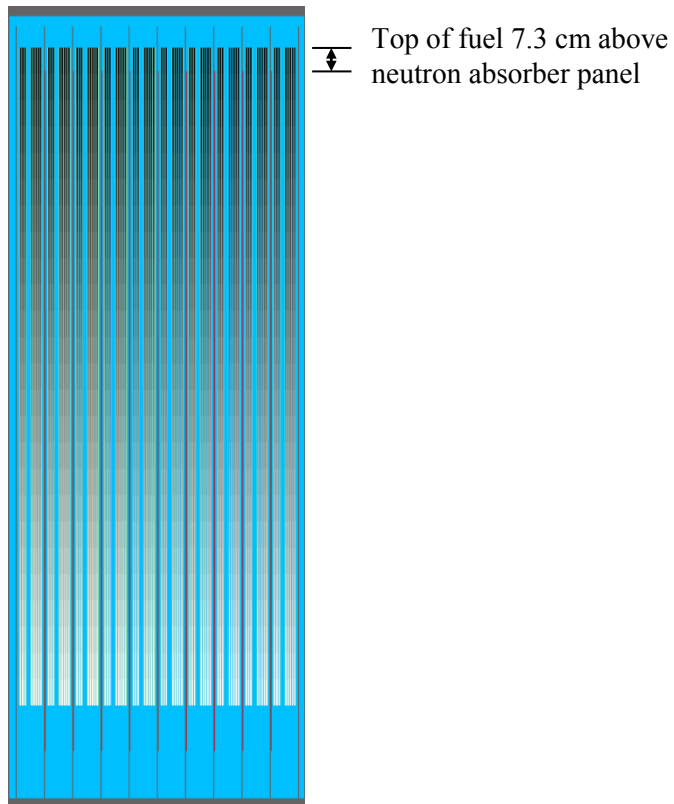
**Figure 33. A fresh fuel birdcaging configuration for MPC-68.**

#### 5.2.1.4 Loss of Assembly Position Control

The loss of assembly position control configuration is calculated over a range of displacements. The consequence of the maximum misalignment for both fresh and irradiated fuel, both with and without the assembly channel, is shown in Table 31 and is almost 20%  $\Delta k_{\text{eff}}$  for the limiting condition. A more limited misalignment case (20 cm) is also evaluated as a surrogate for potential degradation of assembly end fittings or the spacers used inside the cask to ensure proper assembly alignment. The consequences of this more limited misalignment, shown in Figure 34 and Table 31, are significantly less, but the  $k_{\text{eff}}$  increase is still over 6%  $\Delta k_{\text{eff}}$ . The limiting condition for both the maximum and limited misalignment is for fuel with 35 GWd/MTU burnup and 5 years of cooling time. The limited misalignment case is illustrated in Figure 34. Misalignment toward the bottom of the cask causes a significantly smaller  $k_{\text{eff}}$  increase because the fuel at the bottom end of the assembly has lower reactivity. The misalignment toward the cask base plate also differs for the MPC-68 compared to the GBC-32. The MPC-68 model has more distance below the fuel, so larger misalignments are possible. The neutron absorber in the MPC-68 extends below the bottom of the fuel; this difference acts to increase the displacement distance for which no significant change in  $k_{\text{eff}}$  occurs. The variation of the  $k_{\text{eff}}$  changes as a function of axial position is shown in Figure 35 for fuel with 35 GWd/MTU burnup and 5 years of cooling time.

**Table 31. Increase in  $k_{\text{eff}}$  caused by loss of assembly position control in MPC-68**

Burnup (GWd/MTU)	Cooling time (years)	Channel	Increase in $k_{\text{eff}}$ (% $\Delta k_{\text{eff}}$ )
<b>Maximum displacement (33.78 cm displacement relative to basket)</b>			
0	0	Yes	8.18
35	5	Yes	19.40
0	0	No	7.79
35	5	No	18.65
<b>Limited displacement (20 cm displacement relative to basket)</b>			
0	0	Yes	0.33
35	5	Yes	6.29
0	0	No	0.27
35	5	No	6.07

**Figure 34. Limited axial misalignment of 20 cm toward cask lid.**

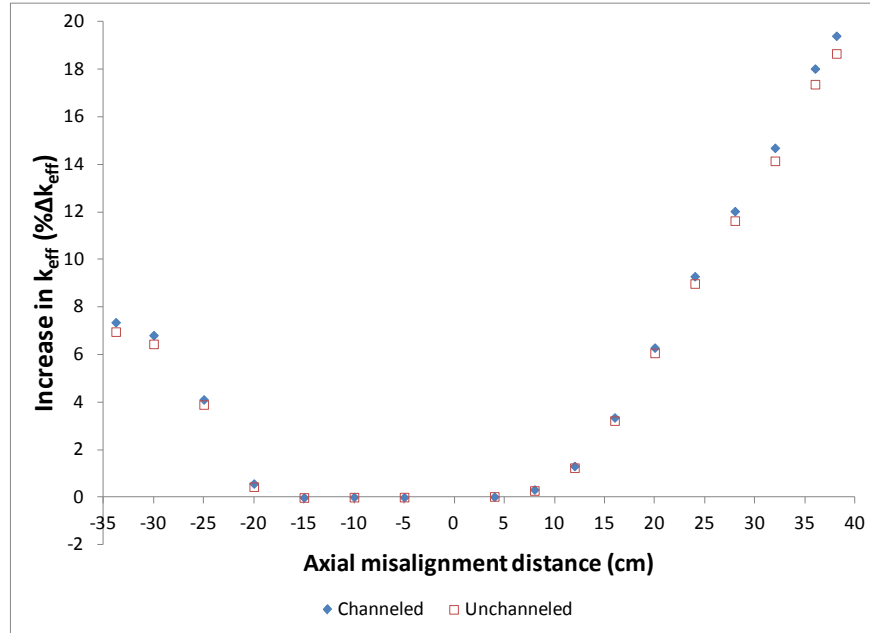


**Figure 35. Increase in  $k_{\text{eff}}$  in MPC-68 as a function of assembly axial displacement (35 GWd/MTU burnup and 5-year cooling time).**

### 5.2.1.5 Gross Assembly Failure

The two gross assembly failure configurations described in Section 3.1.5 are investigated in the MPC-68 cask. Axial representations of the most reactive homogeneous rubble and ordered pellet array configurations are shown in Figure 36 and , respectively. In both cases, the limiting case is the non-physical condition in which the fissile material extends from the base plate to the lid. As expected, this configuration has the highest  $k_{\text{eff}}$  increase, with the ordered pellet array configuration being more limiting than the homogeneous rubble case. As shown previously in Table 25, the  $k_{\text{eff}}$  increase in the homogeneous rubble case is almost 30%  $\Delta k_{\text{eff}}$ , and the pellet array case increases  $k_{\text{eff}}$  by over 34%  $\Delta k_{\text{eff}}$  for the maximum increase case. The limiting case for both configurations is with fuel at 35 GWd/MTU burnup and a 5-year cooling time. The results for the maximum  $k_{\text{eff}}$  increase homogeneous configuration for both fuel burnups with and without the fuel channel are presented in Table 32 and for the pellet array case for both fuel burnups in Table 33. The pellet array case was only considered without the fuel assembly channel. If the fissile material is maintained within the poison panel elevations, the resulting change in  $k_{\text{eff}}$  is reduced to 17.21%  $\Delta k_{\text{eff}}$  for the ordered array of pellets. Results for a range of homogeneous rubble cases within the neutron absorber elevations are provided in Table 34. The largest increase in  $k_{\text{eff}}$  for this configuration corresponds to fresh 5 w/o fuel. The results with fissile material restrained in the neutron absorber elevations demonstrate that these cases result in significantly lower  $k_{\text{eff}}$  increases than the unrestrained material cases.

The results for the pellet array case are significantly higher than those reported previously in Ref. 7. There are two differences between that analysis and this one, both of which contribute to the increased magnitude of the  $k_{\text{eff}}$  increase in the work presented here. The pellet array case modeled here includes a distributed burnup profile in the pellet array, and the array is allowed to extend beyond the neutron absorber panel elevations. This latter change is the larger of the two effects, but the former change is also important. The homogeneous rubble case is not included in Ref. 7.

**Table 32. Increase in  $k_{\text{eff}}$  for homogeneous rubble configuration of gross fuel assembly failure in MPC-68**

Burnup (GWd/MTU)	Cooling time (years)	Channel	Maximum increase in $k_{\text{eff}}$ (% $\Delta k_{\text{eff}}$ )
0	0	Yes	21.68
35	5		28.58
0	0	No	22.90
35	5		29.36

**Table 33. Increase in  $k_{\text{eff}}$  for pellet array configuration of gross fuel assembly failure in MPC-68**

Burnup (GWd/MTU)	Cooling time (years)	Maximum increase in $k_{\text{eff}}$ (% $\Delta k_{\text{eff}}$ )
<b>Channel removed</b>		
0	0	28.12
35	5	34.40

**Table 34. Increase in  $k_{\text{eff}}$  in MPC-68 due to homogeneous rubble, debris within absorber Elevations, fresh 5 w/o fuel**

Fraction of nominal assembly height	Increase in $k_{\text{eff}}$ (% $\Delta k_{\text{eff}}$ )	
	Channeled	Unchanneled
1.0	7.40	9.49
0.9	6.65	9.12
0.8	5.06	8.10
0.7	2.30	6.16
0.6	-2.57	2.66
0.5	-11.07	-3.62
0.4	-25.64	-15.10
Fully compressed rubble*	-34.23	-31.44

\*The fraction of nominal assembly height varies for fully compressed rubble with and without the channel. With the channel it is approximately 0.36 with the channel and 0.32 without it.

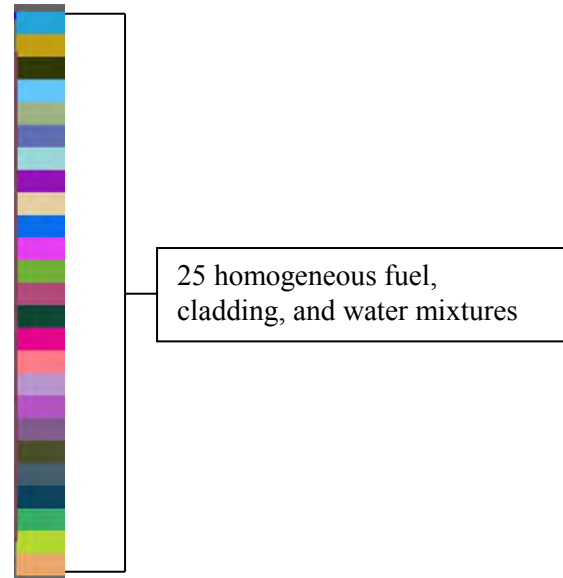


**Figure 36.** Limiting homogeneous rubble configuration in MPC-68.

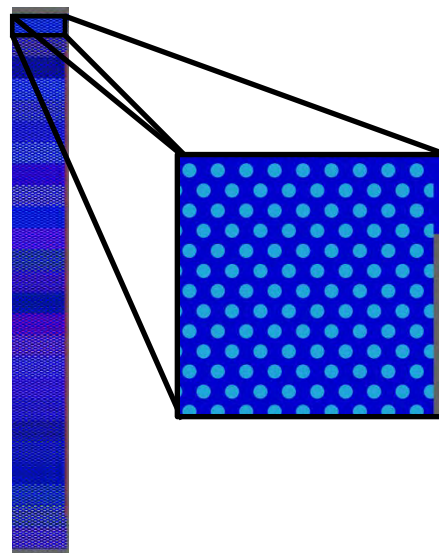


**Figure 37.** Limiting ordered pellet array configuration for MPC-68.

### 5.2.1.6 Neutron Absorber Degradation

The results of the calculations, described in Section 3.1.6.1, considering a 5-cm neutron absorber defect at varying elevations for both fuel burnups, both with and without the fuel channel, are presented in Table 35. The limiting condition is for fuel with 35 GWd/MTU burnup and 5 years of cooling time, with the fuel channel intact. As expected, the limiting elevation is near the top of the active fuel height, as shown in Figure 38. The results for the full range of elevations considered in the limiting fuel condition are presented in Table 36 for cases with the fuel channel intact. As expected, the limiting elevation for the fresh 5 w/o fuel is located at the centerline. The largest  $k_{\text{eff}}$  increase observed for this configuration is 2.49%  $\Delta k_{\text{eff}}$  and increases to 5.62%  $\Delta k_{\text{eff}}$  if the defect size is increased to 10 cm. As discussed in

Section 3, these defects are assumed to be present at the same elevation in all neutron absorber panels within the cask.

The increase in  $k_{\text{eff}}$  associated with uniform neutron absorber panel thinning as discussed in Section 3.1.6.3 is shown in Table 37 and Figure 39 with fresh 5 w/o fuel modeled in the MPC-68 cask. The absorber thinning results shown in Appendix C confirm that the fresh fuel case is most limiting. As shown previously in Table 25, a 50% reduction in thickness results in a 3.67%  $\Delta k_{\text{eff}}$  increase. Complete neutron absorber panel removal increases  $k_{\text{eff}}$  by almost 22%  $\Delta k_{\text{eff}}$ , but more than 40% of the thickness must be removed before an increase of more than 3%  $\Delta k_{\text{eff}}$  is realized.

The complete removal of the neutron absorber panels causes a larger increase in  $k_{\text{eff}}$  than the maximum axial displacement case discussed in Section 5.2.1.4, a result which differs from that observed for the GBC-32 cask presented in Section 5.1. The MPC-68 cask has a smaller distance between the top of the fuel storage basket and the cask lid, allowing for only a shorter portion of the assembly to be above the basket walls. The MPC-68 also has a higher nominal neutron absorber loading, resulting in a larger increase in  $k_{\text{eff}}$  when all the absorber is removed. These two differences in cask design cause the relative consequence of the two configurations to be different for the MPC-68 compared to the GBC-32.

**Table 35. Maximum  $k_{\text{eff}}$  increase caused by a 5-cm neutron absorber defect in MPC-68**

Burnup (GWd/MTU)	Cooling time (years)	Defect center elevation (cm)	Channel	Maximum increase in $k_{\text{eff}}$ (% $\Delta k_{\text{eff}}$ )
0	0	190.50	Yes	0.83
35	5	365.13		2.49
0	0	190.50	No	0.77
35	5	365.13		2.41

**Table 36. Increase in  $k_{\text{eff}}$  caused by a 5-cm neutron absorber defect at various elevations in MPC-68  
(35 GWd/MTU burnup and 5-year cooling time)**

Defect center elevation (cm)	Increase in $k_{\text{eff}}$ (% $\Delta k_{\text{eff}}$ )
0.00	-0.02
95.25	-0.01
190.50	0.00
285.75	0.01
317.50	0.21
333.38	0.52
349.25	1.43
354.54	1.83
359.83	2.29
365.13	2.49
370.42	2.39
375.71	2.00
381.00	0.69

**Table 37. Increase in  $k_{\text{eff}}$  in MPC-68 caused by uniform neutron absorber panel thinning, fresh 5 w/o fuel**

Fraction of neutron absorber panel thickness remaining	Increase in $k_{\text{eff}}$ (% $\Delta k_{\text{eff}}$ )
0.9	0.59
0.8	1.21
0.7	1.91
0.6	2.72
0.5	3.67
0.4	4.87
0.3	6.35
0.2	8.49
0.1	11.93
0.0	21.84

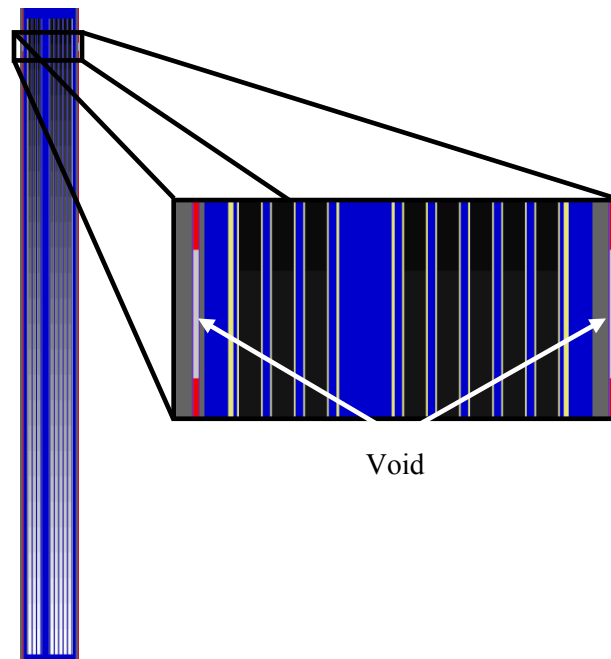


**Figure 38. Limiting neutron absorber defect configuration in MPC-68.**

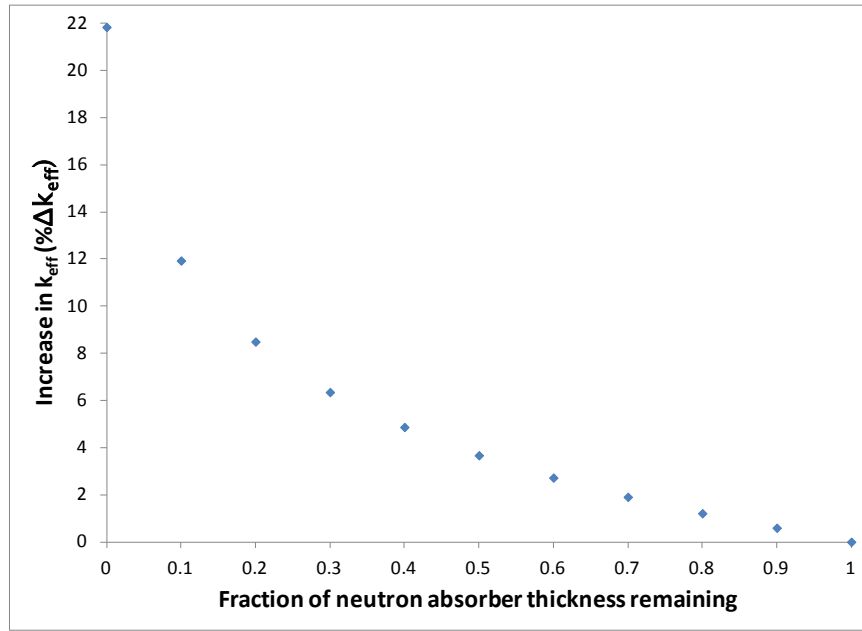


**Figure 39. Increase in  $k_{\text{eff}}$  in MPC-68 as a function of remaining neutron absorber panel thickness for fresh 5 w/o fuel.**

### 5.2.1.7 Burnup and Cooling Time Sensitivities

The results of sensitivity studies relating to addition burnup and cooling time are presented in Appendix C (Section C.2). Each configuration discussed in the previous six subsections is considered explicitly. The results of the calculations for additional burnup and cooling time conditions indicate that the increase in  $k_{\text{eff}}$  reported for each configuration encompass changes that may result for additional burnups and cooling times. That is, the differences in the change in  $k_{\text{eff}}$  are smaller than the changes in the base case  $k_{\text{eff}}$  caused by the additional burnup and/or cooling time considered. For the axial displacement configuration, a high-burnup and cooling time condition causes a larger increase in  $k_{\text{eff}}$ , but that case is significantly subcritical and therefore can be excluded from the results considered here.

### 5.2.2 Varying Number of Reconfigured Assemblies

The results presented in Section 5.2.1 and Table 25 assume that all 68 fuel assemblies in the MPC-68 cask experience the same fuel or neutron absorber reconfiguration within the respective configuration of interest. As discussed in Section 3.2, a series of calculations is performed to establish the  $k_{\text{eff}}$  increase as a function of the number of reconfigured assemblies within the cask. The four configurations considered are the limiting conditions for single rod failure, multiple rod failure, uniform rod pitch increase, and homogeneous rubble resulting from gross assembly failure.

The first fuel assembly to experience the reconfiguration being examined is selected in an attempt to maximize the  $k_{\text{eff}}$  increase, and is therefore one near the center of the cask. Additional assemblies are added in mostly symmetric groups of equal distance from the first reconfigured assembly. For some low numbers of reconfigured assemblies, multiple combinations of assemblies are considered. Sixteen combinations of reconfigured assemblies are considered in the MPC-68. One order in which the assemblies experience reconfiguration is shown in Figure 40. Results are presented in the following subsections.

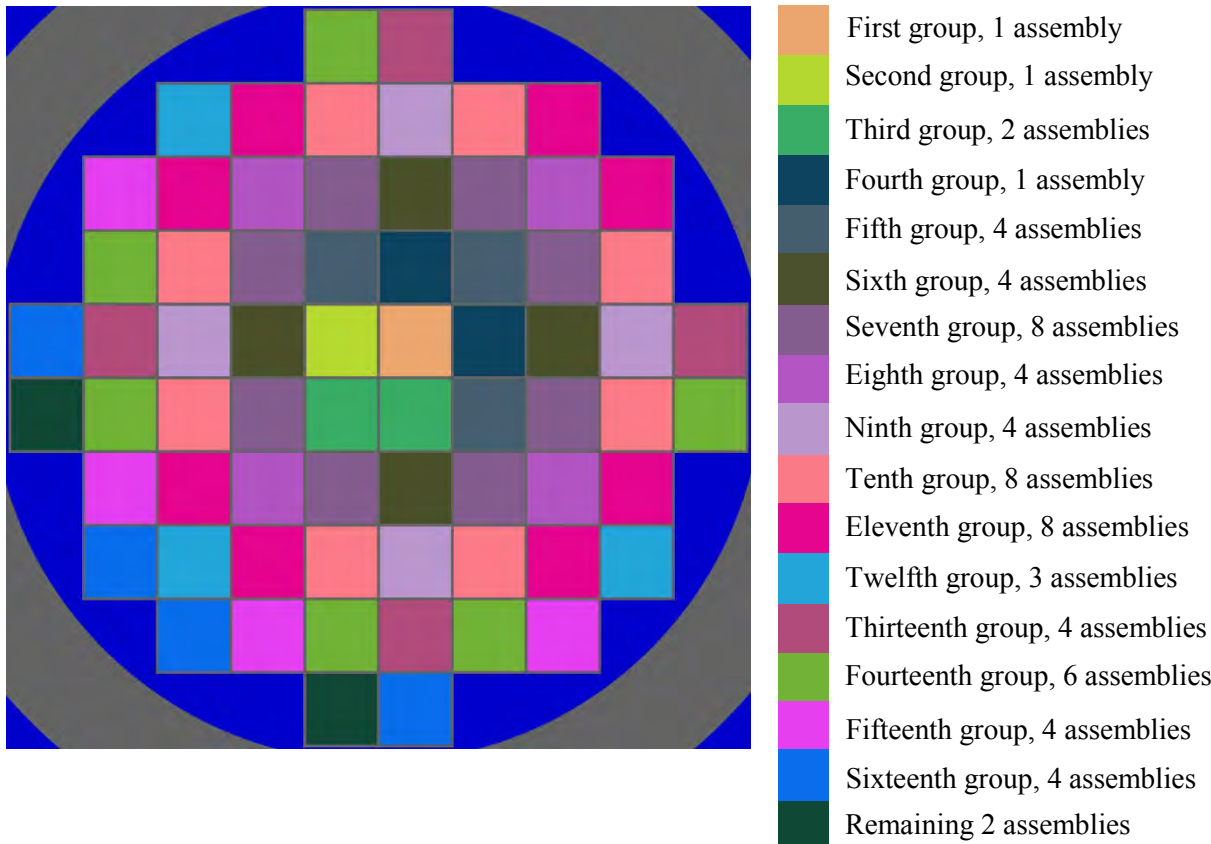


Figure 40. One order of assembly reconfiguration in MPC-68 partial degradation configurations.

### 5.2.2.1 Rod Failures

The single and multiple rod failure configurations that result in the largest increase in  $k_{\text{eff}}$ , as discussed in Section 5.2.1.2, are used to study the impact of some assemblies suffering reconfiguration while others in the cask remain intact. The single rod failure configurations are based on fresh 5 w/o fuel, while the multiple rod failure configurations are based on fuel depleted to 35 GWd/MTU and 5 years of cooling time. The fuel channel is modeled as intact for both rod failure configurations. The results for single rod failure are shown below in Table 38 and Figure 41. The results for multiple rod failure are shown below in Table 39 and Figure 42. The portion of the  $k_{\text{eff}}$  impact introduced by each group of assemblies for both rod failure configurations show nearly 50% or more of the  $k_{\text{eff}}$  change coming after 13 assemblies experience reconfiguration and approximately 75% to 80% of the  $k_{\text{eff}}$  change caused by the first 29 assembly reconfigurations. The Monte Carlo uncertainty is relatively large compared to the  $k_{\text{eff}}$  changes being examined in this series of calculations because of the relative insensitivity of the cask  $k_{\text{eff}}$  to single rod failures. The resulting  $k_{\text{eff}}$  increase is therefore not a smooth function. The single rod failure results are generally similar to the GBC-32 results presented in Section 5.1.2.1. The rate of increase in  $k_{\text{eff}}$  seems to be slightly slower for the MPC-68, but this is a relatively small difference in the trend and may be related to the relatively large uncertainties in the results compared to the  $k_{\text{eff}}$  changes being examined. The multiple rod failure results for the MPC-68 are very similar to the GBC-32 results. The results indicate that a reduced number of reconfigured assemblies will not significantly reduce the  $k_{\text{eff}}$  increase associated with fuel reconfiguration if the degraded assemblies are in close proximity, and particularly if they are in the center region of the cask.

**Table 38. Increase in  $k_{\text{eff}}$  in MPC-68, single rod failure fresh 5 w/o fuel**

Number of degraded assemblies	Increase in $k_{\text{eff}}$ (% $\Delta k_{\text{eff}}$ )
1	0.02
2	0.04
2	0.05
4	0.06
5	0.07
9	0.10
13	0.15
21	0.20
25	0.19
29	0.21
37	0.23
45	0.27
48	0.25
52	0.27
58	0.27
62	0.27
66	0.28
68	0.29

**Table 39. Increase in  $k_{\text{eff}}$  in MPC-68, multiple rod failure  
(5 w/o initial enrichment, 35 GWd/MTU burnup)**

Number of degraded assemblies	Increase in $k_{\text{eff}}$ (% $\Delta k_{\text{eff}}$ )
1	0.11
2	0.21
2	0.23
4	0.45
5	0.56
5	0.55
9	0.93
13	1.19
21	1.62
25	1.79
29	1.89
37	2.10
45	2.22
48	2.26
52	2.28
58	2.33
62	2.36
66	2.37
68	2.40

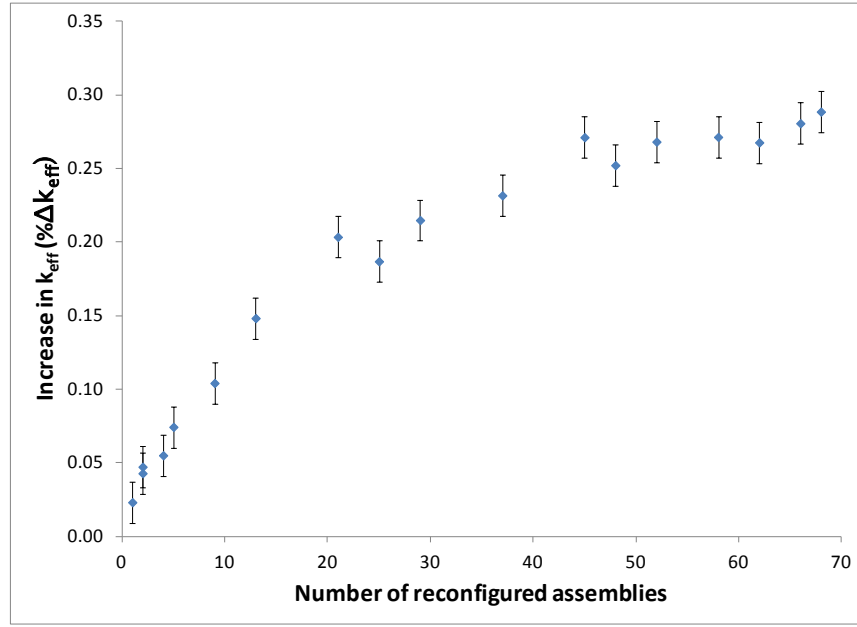


**Figure 41.** Increase in  $k_{\text{eff}}$  in MPC-68 as a function of number of reconfigured assemblies, single rod failure for fresh 5 w/o fuel.

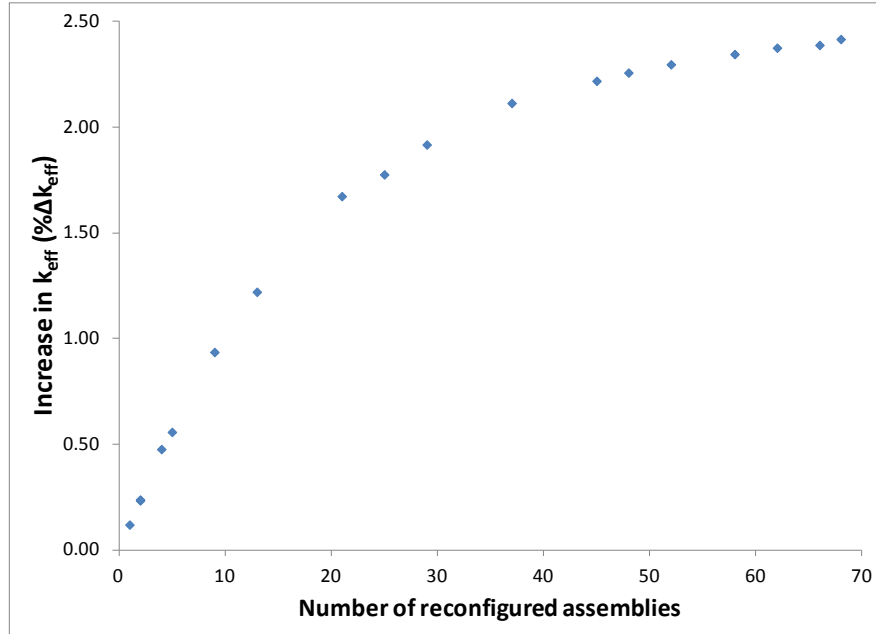


**Figure 42.** Increase in  $k_{\text{eff}}$  in MPC-68 as a function of number of reconfigured assemblies, multiple rod failure (35 GWd/MTU burnup and 5-year cooling time).

### 5.2.2.2 Loss of Rod Pitch Control, Uniform Pitch Increase

The maximum uniform pitch increase case is used to examine the  $k_{\text{eff}}$  impact of varying the number of assemblies that have experienced reconfiguration. The assembly configuration used for this study models

the outer row of fuel rods in contact with the inner wall of the fuel storage basket in each cell. The fresh 5 w/o fuel composition is used for all assemblies. The increase in  $k_{\text{eff}}$  for each number of reconfigured assemblies is provided in Table 40 as well as Figure 43. More than 75% of the increase in  $k_{\text{eff}}$  is caused by the first 21 reconfigured assemblies. The general trend in the  $k_{\text{eff}}$  change for the uniform pitch increase cases is similar to that for single and multiple rod failure configurations presented in Section 5.2.2.1. More than 50% of the total increase in  $k_{\text{eff}}$  has occurred with 13 reconfigured assemblies. The shape of the increase in  $k_{\text{eff}}$  as a function of reconfigured assemblies is similar to that seen for the uniform pitch increase configurations in the GBC-32 cask, as discussed in Section 5.1.2.2. The fraction of the  $k_{\text{eff}}$  increase introduced for a given fraction of reconfigured assemblies is slightly higher for the MPC-68 than for GBC-32 between about 10% and 70% of the assemblies experiencing reconfiguration. The results indicate that a reduced number of reconfigured assemblies will not significantly reduce the  $k_{\text{eff}}$  increase associated with fuel reconfiguration if the degraded assemblies are in close proximity, and particularly if they are in the center region of the cask.

**Table 40. Increase in  $k_{\text{eff}}$  in MPC-68, uniform pitch increase fresh 5 w/o fuel**

Number of degraded assemblies	Increase in $k_{\text{eff}}$ (% $\Delta k_{\text{eff}}$ )
1	0.64
2	1.46
2	1.37
4	3.29
5	3.93
5	3.85
9	6.45
13	7.85
21	10.05
25	10.59
29	11.02
37	11.85
45	12.36
48	12.46
52	12.61
58	12.87
62	13.03
66	13.13
68	13.16

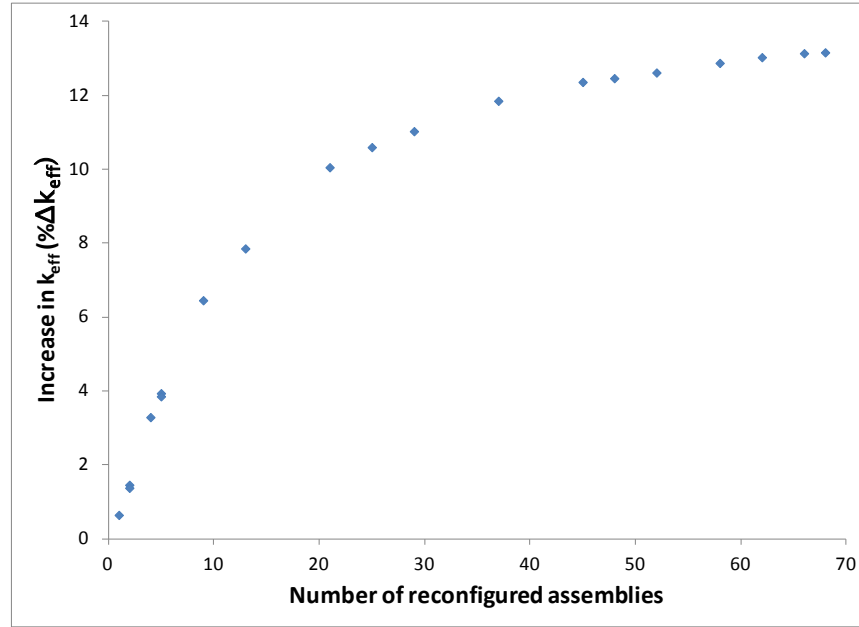


**Figure 43. Increase in  $k_{\text{eff}}$  in MPC-68 as a function of number of reconfigured assemblies, uniform pitch increase fresh 5 w/o fuel.**

### 5.2.2.3 Gross Assembly Failure, Homogeneous Rubble

The homogeneous rubble modeling of the gross assembly failure configuration is the final configuration used to examine the  $k_{\text{eff}}$  impact of varying the number of assemblies that have experienced reconfiguration. The configuration used for this study fills the entire inside volume of the storage cell with homogeneous rubble, as described in Section 3.1.5.1. Each zone is approximately 18 cm tall; thus, the 25 zones fill the cask from the base plate to the lid. The fuel composition corresponds to 5 w/o fuel depleted to 35 GWd/MTU. This configuration resulted in the largest  $k_{\text{eff}}$  increase of the homogeneous rubble configurations used in Section 5.2.1.5. The increase in  $k_{\text{eff}}$  for each number of reconfigured assemblies is provided in Table 41 as well as Figure 44. The first two reconfigured assemblies cause a smaller increase in  $k_{\text{eff}}$  than the other configurations. A more significant increase in  $k_{\text{eff}}$  is noted for four or more reconfigured assemblies. More than 50% of the increase is caused by the first nine reconfigured assemblies, and more than 80% of the total  $k_{\text{eff}}$  increase results from the reconfiguration of 21 assemblies. The results indicate that a reduced number of reconfigured assemblies will not significantly reduce the  $k_{\text{eff}}$  increase associated with fuel reconfiguration if the degraded assemblies are in close proximity, and particularly if they are in the center region of the cask.

**Table 41. Increase in  $k_{\text{eff}}$ , homogeneous rubble configuration of gross assembly failure**

Number of degraded assemblies	Increase in $k_{\text{eff}}$ (% $\Delta k_{\text{eff}}$ )
1	0.03
2	0.10
4	4.48
5	5.04
9	15.67
13	18.60
21	23.73
25	24.78
29	25.42
37	27.05
45	27.97
48	28.14
52	28.35
58	28.82
62	29.10
66	29.26
68	29.36

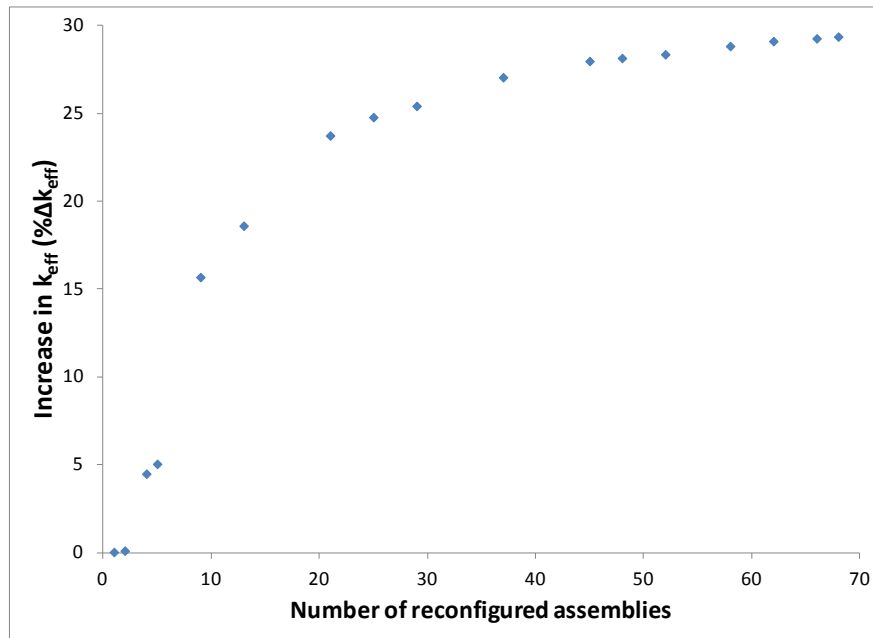


**Figure 44. Increase in  $k_{\text{eff}}$  as a function of number of reconfigured assemblies, gross assembly failure (35 GWd/MTU burnup and 5-year cooling time).**

### Random Assembly Reconfiguration

A series of 25 calculations is performed in which four assemblies are randomly selected to experience reconfiguration into the limiting homogeneous rubble configuration. These calculations use fuel

compositions for fuel with a burnup of 70 GWd/MTU and 300-year cooling time. These compositions are used in the sensitivity studies for higher burnup and cooling times and lead to the largest increase in  $k_{\text{eff}}$  for all burnup and cooling time combinations considered. The increase in  $k_{\text{eff}}$  for four reconfigured assemblies in the center of the cask is 6.95%  $\Delta k_{\text{eff}}$ . The use of four assemblies is somewhat arbitrary but is selected because the increase in  $k_{\text{eff}}$  is significant. The increase in  $k_{\text{eff}}$  for each randomly generated case is provided in Table 42. A histogram of the results with a superimposed normal distribution is shown in Figure 45. While some deviations from the ideal normal distribution are evident, the set of  $k_{\text{eff}}$  increases tests as normal with a 10 bin chi-squared normality test.

The average change in  $k_{\text{eff}}$  is a reduction of about 0.20%  $\Delta k_{\text{eff}}$ , and the standard deviation is approximately 0.25%  $\Delta k_{\text{eff}}$ . The largest increase in  $k_{\text{eff}}$  is 0.14  $\Delta k_{\text{eff}}$ . The one-sided tolerance factor for 95% probability of a 95% confidence interval assuming a normal distribution of 25 samples is 2.292, from Ref. 49. The 95/95 upper bound for the reactivity increase for four random assemblies is 0.37%. This represents a significant reduction in the  $k_{\text{eff}}$  impact compared to the bounding condition of four reconfigured assemblies in the center of the cask. These results are based on only a cursory examination of the effects of random assembly selection, but the results indicate a significant reduction in the  $k_{\text{eff}}$  if the reconfigured assemblies are randomly distributed in the cask.

Random sampling of degraded assemblies will not be valid if assembly degradation is not random. Factors such as environment during ES, assembly burnup and fluence, or other relevant parameters could be highly correlated, invalidating a random sampling approach. The difference between random sampling and deterministic selection of assembly locations will be reduced with a larger number of reconfigured assemblies. More study is needed to examine the validity of random sampling as an alternative to deterministic selection to reduce the impact of fuel reconfiguration on  $k_{\text{eff}}$ .

**Table 42. Increase in  $k_{\text{eff}}$  for 25 realizations of four randomly selected reconfigured assemblies**

Increase in $k_{\text{eff}}$ (% $\Delta k_{\text{eff}}$ )				
-0.02	0.14	-0.04	0.13	-0.33
-0.19	0.09	-0.29	-0.13	-0.19
0.04	-0.75	-0.47	-0.66	-0.38
-0.06	-0.23	-0.19	-0.02	-0.22
-0.01	-0.03	-0.73	-0.13	-0.37

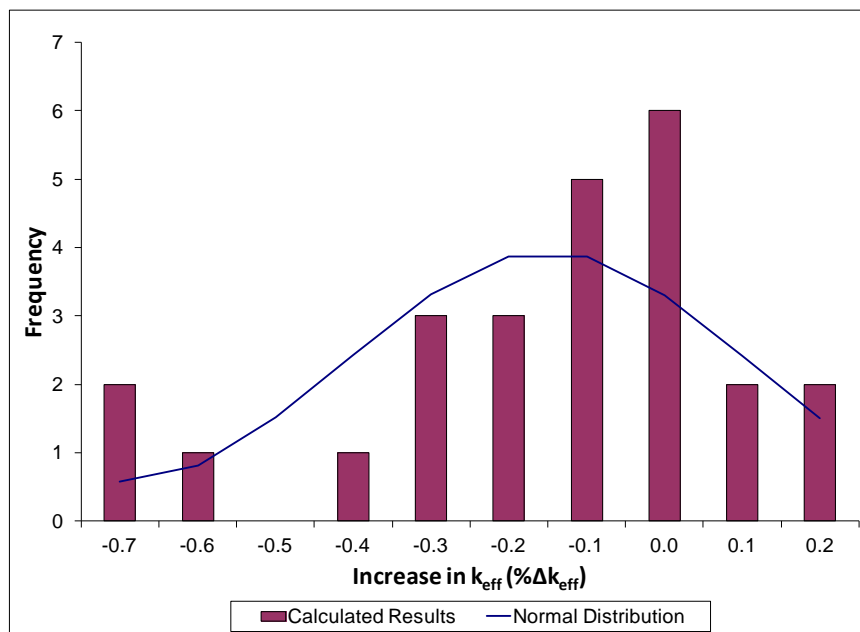


**Figure 45. Histogram of increases in  $k_{\text{eff}}$  for 25 random samples of four reconfigured assemblies.**

### 5.2.3 Combined Configurations

As discussed in Section 3.3, some of the mechanisms that could result in fuel reconfigurations could result in a combination of configurations. Therefore, selected combined configurations are evaluated, including: four failed rods with 50% clad thinning and four failed rods with a uniform pitch increase of 0.062-cm. These combinations of configurations are selected as they both pertain to failure of zirconium alloy components of the fuel assembly. Both combined configurations assume fresh 5 w/o fuel and an intact fuel assembly channel.

The multiple rod failure results presented in Section 5.2.1.2 indicate that the failure of four fuel rods results in an increase in  $k_{\text{eff}}$  of just under 1%  $\Delta k_{\text{eff}}$ . This is approximately 40% of the maximum increase for multiple failed rod configurations and is therefore selected as an intermediate configuration. The cladding thickness on all intact rods in both combined configurations is represented with 50% of the nominal thickness. The pitch increase of 0.062 cm is approximately 4.3%  $\Delta k_{\text{eff}}$ . This represents about one-third of the maximum  $k_{\text{eff}}$  increase associated with the uniform pitch expansion.

The results of the two combined configurations considered in the MPC-68 cask are presented in Table 43. For comparison, the  $k_{\text{eff}}$  increases assuming each degraded configuration separately and the sum of the two is provided. The increase in  $k_{\text{eff}}$  associated with explicit modeling of the combined configuration is less than the estimated increase based on summing the individual increases. The conservatism of adding the separate effects is 0.25%  $\Delta k_{\text{eff}}$  or less. It appears that the linear combination of the  $k_{\text{eff}}$  increases is conservative, but more combined configurations would need to be investigated prior to drawing general conclusions. If it is confirmed, the  $k_{\text{eff}}$  increase caused by combinations of degradations could be conservatively bounded by adding the increase associated with individual configurations where applicable.

**Table 43. Increase in  $k_{\text{eff}}$  in combined configurations in MPC-68**

Case	Increase in $k_{\text{eff}}$ (% $\Delta k_{\text{eff}}$ )
<b>Multiple failed rods and clad thinning</b>	
Four failed rods	0.98
50% clad thinning	2.69
Sum of $k_{\text{eff}}$ increases	3.67
Combined configuration model	3.75
Overestimation of $k_{\text{eff}}$ increase by summing individual effects	0.08
<b>Multiple failed rods and 0.062-cm increase in fuel rod pitch</b>	
Four failed rods	0.98
Uniform pitch increase	4.35
Sum of $k_{\text{eff}}$ increases	5.33
Combined configuration model	5.08
Overestimation of $k_{\text{eff}}$ increase by summing individual effects	0.25

#### 5.2.4 Part-Length Fuel

Part-length rods are common in BWR assembly designs, including the GE14 design, making an investigation of the impact of part-length rods prudent as a part of these analyses. A total of 14 of the 92 rods are modeled as part-length, and more details of the modeling are provided in Appendix A. Only fresh 5 w/o fuel is considered for the part-length rod studies because no axial burnup profiles are available for fuel assemblies with part-length rods. The removal of some of the fuel in the upper portion of the assembly might cause a more bottom-skewed power shape, but the remaining sparser lattice will likely be more reactive. The axial power shape could therefore also be about the same or even more top-skewed than that developed in Appendix E. Given the unknown relative impact of these effects, depleted fuel is not considered in this study.

Most of the degraded fuel and neutron absorber panel configurations are considered for part-length fuel, though not all. The multiple rod failure study is shortened with the results compared to the full-length results presented in Section 5.2.1.2, and the pellet array configuration of gross assembly failure is not considered at all. Other calculations, such as the axial misalignment configuration, are reduced to the conditions shown to be limiting for full-length fuel in Section 5.2.1. The results of the nominal cases without reconfiguration are shown in Table 44. It should be noted that the base case  $k_{\text{eff}}$  values for the fuel with part-length rods are approximately 0.7%  $\Delta k_{\text{eff}}$  higher than the full-length rod base case. The additional moderation introduced in the upper portion of the assembly by the removal of the upper sections of the part-length rods is responsible for this increase in  $k_{\text{eff}}$ , and this in itself is a significant result. Only assemblies with full-length fuel rods were used in the analysis documented in Ref. 7. The use of part-length rods is thus another area of expansion over the previous work.

A summary of the  $k_{\text{eff}}$  impact of the configurations modeled with fresh fuel with part-length rods is shown in Table 45. These results can be compared with those shown in Table 25 to demonstrate the relative impact of reconfiguration for assemblies with part-length rods. In general, it appears that the part-length rods reduce the impact of reconfiguration. This result makes sense as the removal of some fissile material will move the moderator-to-fuel ratio closer to optimum in the base configuration. The neutron absorber defect and limited axial misalignment cases are the only configurations that cause a larger increase in  $k_{\text{eff}}$  than the full-length assembly. Additional details of the modeling of each configuration using assemblies with part-length fuel rods are included in the following subsections. No calculations are performed for a

varying number of reconfigured assemblies, multiple configurations, or combinations of full-length and part-length assemblies.

**Table 44. Nominal  $k_{\text{eff}}$  results for fresh 5 w/o fuel assemblies with part-length rods in MPC-68**

Channel present	Burnup (GWd/MTU)	Cooling time (years)	KENO V.a		KENO-VI	
			$k_{\text{eff}}$	$\sigma$	$k_{\text{eff}}$	$\sigma$
Yes	0	0	0.97497	0.00010	0.97482	0.00019
No	0	0	0.97391	0.00010	0.97396	0.00010

**Table 45. Summary of  $k_{\text{eff}}$  impact for fresh 5 w/o fuel with part-length rods in MPC-68**

Configuration	Reactivity consequence (% $\Delta k_{\text{eff}}$ )	Channel present
<b>Clad thinning/loss</b>		
Cladding removal	4.16	Yes
<b>Rod failures</b>		
Single rod removal	0.18	Yes
Multiple rod removal (2 rods removed)	0.32	Yes
<b>Loss of rod pitch control</b>		
Uniform rod pitch expansion, clad	12.28	No
Uniform rod pitch expansion, unclad	N/C*	N/A
Non-uniform pitch expansion, clad	N/C*	N/A
Channel constrained uniform expansion, clad	N/C*	N/A
<b>Loss of assembly position control</b>		
Axial displacement (30 cm)	6.17	Yes
Axial displacement (20 cm)	0.56	Yes
<b>Gross assembly failure</b>		
Uniform pellet array	N/C*	N/A
Homogeneous rubble	21.96	No
<b>Neutron absorber degradation</b>		
Missing neutron absorber (5-cm segment)	1.01	Yes
Missing neutron absorber (10-cm segment)	2.92	Yes
50% reduction of neutron absorber panel thickness	3.49	Yes

\*Not calculated

#### 5.2.4.1 Clad Thinning/Loss

The loss of cladding configuration is modeled as discussed above in Section 3.1.1. As shown in Table 46, the limiting  $k_{\text{eff}}$  increase associated with complete cladding removal is 4.16%  $\Delta k_{\text{eff}}$  and occurs with channelled fuel. The increase in  $k_{\text{eff}}$  as a function of the fraction of nominal cladding thickness remaining is also shown in Table 46 as well as in Figure 46. The results are consistently smaller increases in  $k_{\text{eff}}$  than those presented in Section 5.2.1.1. The increase in  $k_{\text{eff}}$  caused by the complete loss of cladding for full-length fuel is larger than the difference in the base case  $k_{\text{eff}}$  values presented in Table 24 and Table 44. The actual  $k_{\text{eff}}$  value is therefore larger in the case of full-length fuel with reconfiguration than for part-length fuel.

**Table 46. Increase in  $k_{\text{eff}}$  in MPC-68 caused by cladding loss for assemblies with part-length fuel rods, fresh 5 w/o fuel**

Cladding fraction remaining	Increase in $k_{\text{eff}}$ (% $\Delta k_{\text{eff}}$ )
<b>Channel Intact</b>	
0.9	0.43
0.75	1.09
0.5	2.10
0.25	3.12
0.0	4.16
<b>Channel Removed</b>	
0.9	0.42
0.75	1.03
0.5	2.05
0.25	3.04
0.0	3.98

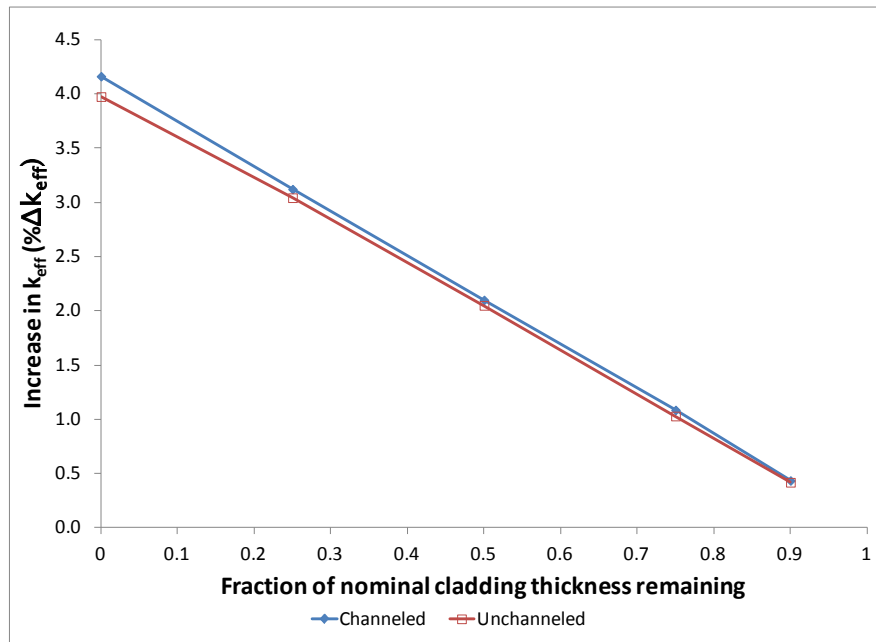


**Figure 46. Increase in  $k_{\text{eff}}$  in MPC-68 as a function of fraction of intact cladding (Fresh 5 w/o fuel with part-length fuel rods).**

#### 5.2.4.2 Rod Failures

Each of the 51 unique half-assembly symmetric rods is removed individually to determine its worth, as discussed in Section 3.1.2.1. Table 47 presents the rod locations and worth of the limiting rod location and the three additional locations that are within approximately two standard deviations of the limiting  $k_{\text{eff}}$  increase. Only channeled fuel is considered since it is shown to be limiting in Section 5.2.1.2. The increase in  $k_{\text{eff}}$  is 0.18%  $\Delta k_{\text{eff}}$ , which is less than the 0.29%  $\Delta k_{\text{eff}}$  increase for fuel with full-length rods. The maximum increase in  $k_{\text{eff}}$  is associated with the removal of rod E3. The location of the limiting rod

appears to have shifted from the location identified in Section 5.2.1.2. More precise calculations could be performed to confirm that the shift is real and not a statistical fluctuation.

The magnitude of the  $k_{\text{eff}}$  change caused by rod failure is somewhat less for fuel with part-length rods than for the full-length fuel used in Section 5.2.1.2. The likely cause of this reduced impact is that the removal of some of the rods in the upper section of the assembly creates a more thermal flux, and reduces the ability of a removed rod to increase thermalization. This is analogous to the reason that the channeled assemblies experience larger  $k_{\text{eff}}$  increases than unchanneled assemblies.

Two rods are removed in several pairs, as discussed in Section 3.1.2.2. The largest  $k_{\text{eff}}$  increase is 0.32%  $\Delta k_{\text{eff}}$ , which is less than the 0.52%  $\Delta k_{\text{eff}}$  increase caused by removing two rods from an assembly with full-length rods. The difference in  $k_{\text{eff}}$  increase is larger for two failed rods than for a single failed rod. This is an expected result since the impact of single rod failure is less for assemblies with part-length fuel than for assemblies with full-length fuel. No calculations are performed for larger numbers of failed rods as the result is likely to be progressively smaller increases in  $k_{\text{eff}}$  when compared with the results for full-length assemblies.

It should be noted that even though the increase in  $k_{\text{eff}}$  is larger for assemblies with full-length fuel, the actual  $k_{\text{eff}}$  for the cask is still higher in the part-length fuel rod case for the single and double rod failure configurations considered for fresh fuel. It is probable that the  $k_{\text{eff}}$  increase is large enough for higher numbers of failed rods that the full-length fuel becomes more limiting.

**Table 47. Increase in  $k_{\text{eff}}$  in MPC-68 caused by single rod failure in fresh 5 w/o assemblies with part-length rods**

Rod location	Increase in $k_{\text{eff}}$ (% $\Delta k_{\text{eff}}$ )
E3	0.18
D4	0.16
D3	0.15
H6	0.14

#### **5.2.4.3 Loss of Rod Pitch Control**

The loss of rod pitch control is modeled largely as described in Section 3.1.3, except that only unchanneled fuel is modeled. That larger pitch expansion resulting from the removal of the channel leads to a larger  $k_{\text{eff}}$  increase, as documented in Section 5.2.1.3. As shown in Table 45, the increase in  $k_{\text{eff}}$  for uniform pitch expansion with part-length rods is 12.28%  $\Delta k_{\text{eff}}$ . This is significantly less than the 13.16% for fuel assemblies with full-length rods. As with the rod failure results discussed in Section 5.2.1.3, the lower impact of loss of array control is most likely due to a more thermal neutron spectrum in the base case and the corresponding reduction in additional thermalization caused by the fuel reconfiguration. In this case, the larger increase in  $k_{\text{eff}}$  is sufficient to result in a larger reconfigured  $k_{\text{eff}}$  for full-length fuel assemblies.

#### **5.2.4.4 Loss of Assembly Position Control**

Assembly axial displacements are calculated for a range of upward displacements up to 30 cm, all with channeled fuel since it is shown to be more reactive than unchanneled fuel in Section 5.2.1.4. As shown in Table 45, the increases in  $k_{\text{eff}}$  caused by 30-cm and 20-cm displacements are 6.17%  $\Delta k_{\text{eff}}$  and 0.56%  $\Delta k_{\text{eff}}$ ,

respectively. The increase in  $k_{\text{eff}}$  associated with the 30-cm misalignment is smaller than that for fresh fuel with full-length fuel rods, but the increase for a 20-cm misalignment is larger for part-length fuel. Both of these increases are significantly non-limiting compared to the cases included in the results shown in Section 5.2.1.4. The impact of axial displacement is strongly influenced by the burnup profile in UNF, so this configuration with part-length rods and an appropriate axial burnup profile should be examined.

#### 5.2.4.5 Gross Assembly Failure

Only the homogeneous rubble configuration of gross assembly failure is modeled for fuel with part-length fuel rods. Only unchanneled fuel is considered because it is shown to be limiting in Section 5.2.1.5. The limiting configuration for gross assembly failure, as with results presented in Sections 5.1.1.5 and 5.2.1.5, is with the entire cask cavity volume filled with rubble. As shown in Table 45, the resulting  $k_{\text{eff}}$  increase is nearly 22%  $\Delta k_{\text{eff}}$ . The overall limiting increase in  $k_{\text{eff}}$  for the homogeneous rubble configuration occurs for UNF and is slightly less than 30%  $\Delta k_{\text{eff}}$ , as shown in Table 25. For fresh fuel, as shown in Table 32, the  $k_{\text{eff}}$  increase associated with the homogeneous rubble configuration is nearly 23%  $\Delta k_{\text{eff}}$ .

A second calculation with the entire cavity filled with rubble is performed to investigate the effect of separate homogenization for the upper portion of the assembly, with reduced fuel loading, and the lower portion of the assembly, with the entire assembly lattice containing fuel rods. The result of this calculation is a slightly smaller increase in  $k_{\text{eff}}$  of approximately 21.2%  $\Delta k_{\text{eff}}$ . The upper portion of the rubble bed, with reduced fuel loading, has a significantly higher volume fraction of water and is likely overmoderated.

#### 5.2.4.6 Neutron Absorber Degradation

The results of the calculations, described in Section 3.1.6.1, considering a 5-cm neutron absorber defect at varying elevations for fuel assemblies with part-length rods and an intact fuel channel are presented in Table 48 and Figure 47. The limiting condition is for the gap centered at an elevation of 270 cm above the bottom of the fuel. The removal of the upper portion of the part-length rods shifts the limiting elevation up relative to the mid-plane location which is limiting for full-length fresh fuel. As mentioned previously, the increased moderation within the assembly lattice results in the upper portion of the assembly being more reactive than the lower portion. This relative reactivity difference is the cause of the shift in the limiting neutron absorber gap location.

The largest  $k_{\text{eff}}$  increase observed for this configuration is 1.01%  $\Delta k_{\text{eff}}$  and increases to 2.92%  $\Delta k_{\text{eff}}$  if the defect size is increased to 10 cm. These results represent a larger increase in  $k_{\text{eff}}$  than for full-length fresh fuel but a smaller increase in  $k_{\text{eff}}$  than the limiting condition involving UNF discussed in Section 5.2.1.6. As discussed in Section 3, these defects are assumed to be present at the same elevation in all neutron absorber panels within the cask.

The increase in  $k_{\text{eff}}$  associated with uniform neutron absorber panel thinning as discussed in Section 3.1.6.3 is shown in Table 49 and Figure 48 with fresh 5 w/o fuel modeled in the MPC-68 cask. As shown in Table 45, a 50% reduction in panel thickness results in a 3.49% increase in  $k_{\text{eff}}$ . Complete neutron absorber panel removal increases  $k_{\text{eff}}$  by more than 21%  $\Delta k_{\text{eff}}$ , but more than 40% of the absorber must be removed before an increase of more than 3% is realized. These results are similar to those presented in Section 5.2.1.6, but the increases in  $k_{\text{eff}}$  are slightly smaller. The full-length fuel does not experience a great enough increase in  $k_{\text{eff}}$  for the resulting cask  $k_{\text{eff}}$  to exceed that for part-length fuel. This configuration is another example of the part-length fuel leading to a higher  $k_{\text{eff}}$  after reconfiguration despite having a smaller  $k_{\text{eff}}$  change because of the higher initial neutron multiplication.

**Table 48. Increase in  $k_{\text{eff}}$  in MPC-68 caused by a 5-cm neutron absorber panel defect, fresh 5 w/o fuel with part-length fuel rods**

Elevation of centerline of defect (cm above bottom of fuel)	Increase in $k_{\text{eff}}$ (% $\Delta k_{\text{eff}}$ )
2.50	-0.01
95.25	0.15
190.50	0.46
222.50	0.77
253.50	0.97
270.00	1.01
285.75	1.00
301.00	0.96
340.00	0.58
378.50	0.00

**Table 49. Increase in  $k_{\text{eff}}$  in MPC-68 caused by uniform neutron absorber panel thinning, fresh 5 w/o fuel with part-length fuel rods**

Fraction of neutron absorber panel thickness remaining	Increase in $k_{\text{eff}}$ (% $\Delta k_{\text{eff}}$ )
0.9	0.53
0.8	1.13
0.7	1.79
0.6	2.57
0.5	3.49
0.4	4.64
0.3	6.08
0.2	8.14
0.1	11.50
0.0	21.33

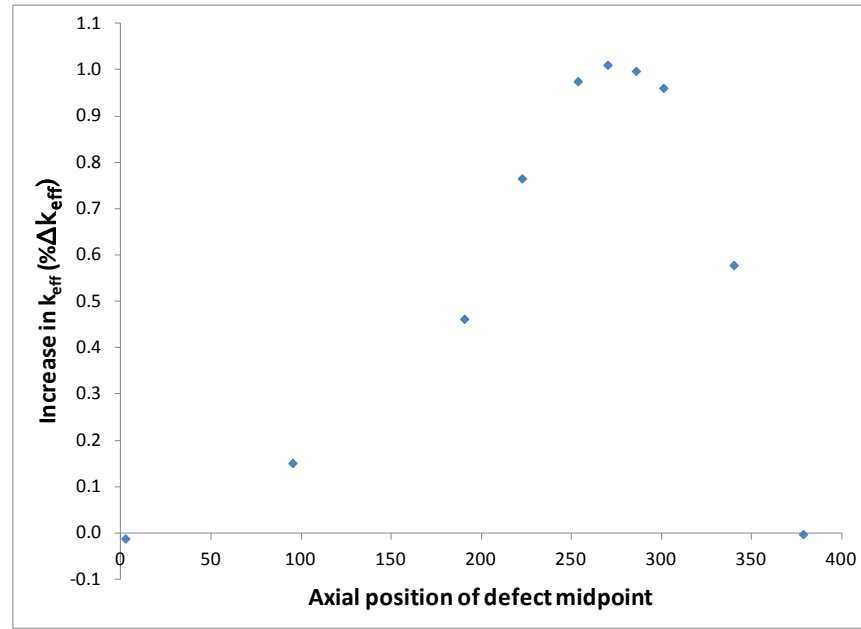


**Figure 47.** Increase in  $k_{\text{eff}}$  in MPC-68 as a function of neutron absorber defect axial position, fresh 5 w/o fuel with part-length fuel rods.

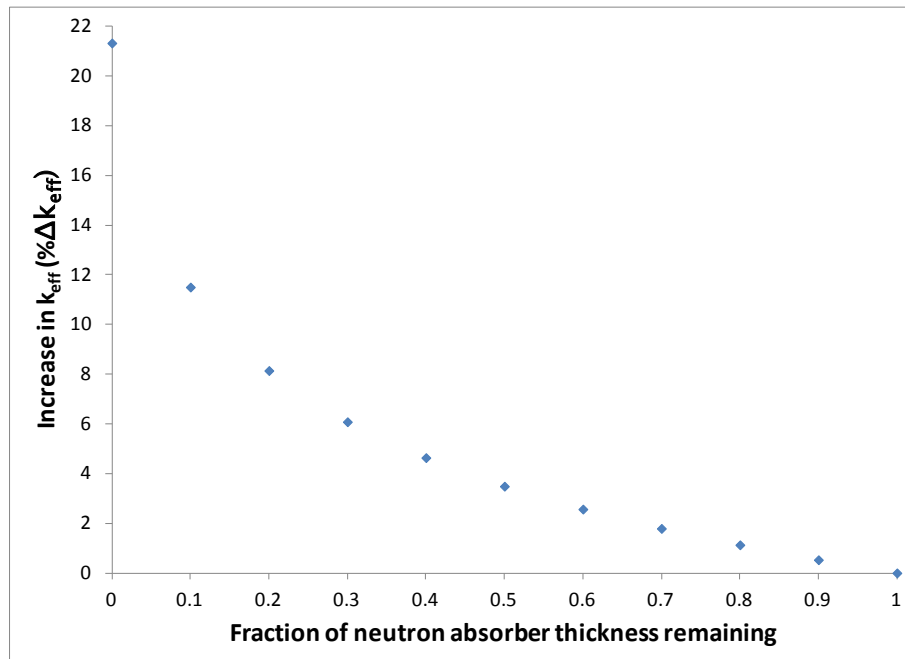


**Figure 48.** Increase in  $k_{\text{eff}}$  in MPC-68 as a function of remaining neutron absorber panel thickness, Fresh 5 w/o fuel with part-length fuel rods.

## 6. SUMMARY AND CONCLUSIONS

This report documents work performed for the DOE-NE Fuel Cycle Technologies Used Fuel Disposition Campaign to assess the consequences of potential fuel failure on the criticality safety of UNF in storage and transportation casks. This work was motivated by concerns related to the potential for fuel degradation during ES periods and transportation following ES, but has relevance to other potential causes of fuel reconfiguration.

Because many of the fuel degradation mechanisms are not well understood, a number of postulated configurations were modeled to calculate the corresponding  $k_{\text{eff}}$  values and the associated consequences of those configurations relative to the reference intact configuration. The consequence of a given configuration was defined as the difference in the calculated  $k_{\text{eff}}$  values for the given configuration and the reference intact configuration, with a positive value indicating an increase in  $k_{\text{eff}}$  as compared to the reference configuration. Because a wide range of configurations was analyzed, the calculated consequences varied widely. Several of the configurations are not considered credible but are included in the analyses for completeness (e.g., to fully understand trends and worst-case situations). Pending improved understanding of the various material degradation phenomena, and subsequent determination and justification for what configurations are and are not credible, the assessment of the credibility of configurations provided herein is based on engineering judgment. The credibility of configurations and the impact of the configurations on criticality safety are dependent on many factors, including storage and transportation conditions, the fuel assembly characteristics, and the storage and/or transportation system characteristics. Therefore, the assessment and analysis of credible configurations for a specific cask system would need to be performed as part of the safety analysis for licensing that system.

### 6.1 Summary of Analyses

The detailed results for each configuration considered in the PWR cask system (GBC-32) are provided in Section 5.1 and summarized in Table 6. For all the credible and non-credible configurations analyzed, the consequence on  $k_{\text{eff}}$  varied from a decrease of several percent (safer condition) to an increase of more than 20%  $\Delta k_{\text{eff}}$ . For configurations judged to be potentially credible, i.e., configurations for which the authors felt additional information was needed to determine credibility, the maximum increase in  $k_{\text{eff}}$  was 3.90%  $\Delta k_{\text{eff}}$ , corresponding to nonuniform fuel rod pitch expansion in all assemblies within the cask. It is important to emphasize that this result is contingent on the authors' judgment relative to the potential credibility of configurations, which includes not only whether a configuration category is credible but also whether the resulting configurations within a given category are credible for a specific cask system. For example, for the GBC-32 cask system, axial assembly displacement such that assemblies extended more than 7.5 cm above or below the neutron absorber panel was not considered credible because of the presence of fuel assembly hardware and cask assembly spacers. If it were determined that such a configuration is credible, then that configuration and its specific characteristics may be limiting.

The detailed results for each configuration considered in the BWR cask system (MPC-68) are provided in Section 5.2 and summarized in Table 25 and Table 45 for fuel assemblies with full- and part-length rods, respectively. For all the credible and non-credible configurations analyzed, the consequence on  $k_{\text{eff}}$  varied from a decrease of several percent (safer condition) to an increase of almost 36%  $\Delta k_{\text{eff}}$ . In most cases, the  $k_{\text{eff}}$  increases for BWR UNF in the MPC-68 were larger than for PWR UNF in the GBC-32. For configurations judged to be potentially credible, the maximum increase in  $k_{\text{eff}}$  was 2.4%  $\Delta k_{\text{eff}}$ , corresponding to a configuration with multiple rod failures for fuel with an initial enrichment of 5 w/o and 35 GWd/MTU of burnup. As emphasized above, it is important to recognize that these results are contingent on the authors' judgment relative to the potential credibility of configurations. For example, for this BWR cask system, the fuel assembly channel is assumed to be present and capable of constraining

fuel rod pitch expansion. If this assumption is not valid for a specific cask loading, then another configuration and its specific characteristics may be limiting.

The maximum increase for a potentially credible configuration in the BWR cask system ( $2.4\% \Delta k_{\text{eff}}$ ) corresponds to a reference case  $k_{\text{eff}}$  of approximately 0.833. The reconfigured  $k_{\text{eff}}$  is therefore only approximately 0.857 and still significantly less than the recommended 0.95  $k_{\text{eff}}$  limit. The large subcritical margin is due to the fact that the MPC-68 was designed and licensed to accommodate unburned fuel, whereas the analyses considered fuel irradiated to 35 GWd/MTU (a relatively low discharge burnup for fuel with initial enrichment of 5 w/o). The largest  $k_{\text{eff}}$  increase associated with fresh fuel is  $2.09\% \Delta k_{\text{eff}}$  and is a result of uniform pitch expansion constrained by the fuel assembly channel. Many of the potential issues associated with crediting the constraint provided by the channel are negated in this case since it is fresh fuel. Results presented for the fuel assemblies with part-length fuel rods in Section 5.2.4 demonstrate the potential importance of this design feature. The reference case  $k_{\text{eff}}$  for fresh assemblies with part-length rods is nearly  $0.7\% \Delta k_{\text{eff}}$  higher than for fresh assemblies with only full-length rods. The  $k_{\text{eff}}$  increase associated with fuel reconfiguration is usually lower for the part-length fuel, but often the difference in the  $k_{\text{eff}}$  change is less than the difference in the reference cases. The absolute  $k_{\text{eff}}$  is therefore higher for many configurations involving fresh assemblies with part-length fuel even though the  $k_{\text{eff}}$  increase is smaller. The effect of varying depletion conditions for assemblies with part-length rods was not considered in this report.

In addition to representative conditions for fuel burnup and post-irradiation decay time, the effects of higher burnup and longer cooling times were also investigated in both PWR and BWR cask systems and found to be smaller than the reduction in  $k_{\text{eff}}$  associated with the higher burnup or cooling time. In addition to the analyses that assume all of the assemblies within the cask have the same degradation condition, analyses were performed to evaluate the consequences of degradation to limited numbers of assemblies. Although the results are configuration dependent, they indicate that the majority of the total potential increase in  $k_{\text{eff}}$  (observed for a cask fully loaded with degraded fuel) is associated with a relatively small fraction of the assemblies having the degraded condition, provided that the reconfigured assemblies are located in close proximity and in the worst-case location in the cask (generally the center region). A limited study performed with the MPC-68 demonstrated that the increase in  $k_{\text{eff}}$  is considerably smaller if the reconfigured assemblies are randomly distributed. A limited set of analyses was also performed to investigate the consequences of combinations of degradation, e.g., a number of failed rods and fuel rod pitch expansion. In the cases analyzed, the sum of the  $k_{\text{eff}}$  increases associated with modeling each configuration separately was determined to be slightly larger than the increase determined from explicitly modeling the combined configurations.

## 6.2 Observations and Conclusions

Similar to previous works, a key conclusion is that the consequences of fuel failure to criticality safety are directly dependent on the configurations that may form as a result of fuel failure. The magnitude of the potential increases in  $k_{\text{eff}}$  and the sensitivity of the potential increases in  $k_{\text{eff}}$  to the determination of the credibility of configurations highlight the importance of being able to determine and justify which configurations are credible under a given set of conditions for a given cask system. It is anticipated, at least in the near term, that these determinations will be done on a case-by-case basis for each cask system and associated licensing conditions.

Analyses of additional large-capacity cask designs and/or additional fuel types are expected to yield  $k_{\text{eff}}$  changes that are similar in magnitude, as compared to those predicted herein, and the limiting configurations are likely to be the same or similar. Large differences in cask design features could cause significant differences in reconfiguration consequences in specific casks, if such large design differences

exist. This conclusion is supported by the similarities in the important effects between PWR and BWR fuel considered in this report. The differences between BWR and PWR fuel designs are more significant than the differences among assembly types within the PWR or BWR fuel classes. The importance of any particular configuration may vary from one cask design to another, but the most limiting configurations will be associated with gross assembly failure and large axial misalignment and are relatively insensitive to assembly design.

The results presented in Section 5 and the cask-specific conclusions presented above indicate larger  $k_{\text{eff}}$  increases for BWR fuel, as compared to PWR fuel. However, current BWR casks, including the MPC-68 considered in this analysis, are designed and licensed to accommodate unburned fuel. Therefore, these casks generally have in excess of 10%  $\Delta k_{\text{eff}}$  margin (as compared to the recommended  $k_{\text{eff}}$  limit of 0.95) when loaded with fuel with typical discharge burnup values.

Specific, realistic configuration development is likely to provide significant margin compared to the bounding configurations considered here. For both casks, the maximum increases in  $k_{\text{eff}}$  are based on analyses that assume all of the assemblies within the cask have the same degradation condition. Analyses that consider limited numbers of reconfigured assemblies, either randomly located within the cask or located together, predict smaller increases in  $k_{\text{eff}}$ . Hence, unless all or most of the assemblies within a cask are expected to have same or a similar degree of reconfiguration, the cited maximum increases in  $k_{\text{eff}}$  are conservative estimates; the extent of the conservatism depends on the number and location of the reconfigured assemblies, as well as the configuration.

Given the establishment of a set of credible failed fuel configurations for a given cask system and assuming that one or more of the configurations result in an increase in  $k_{\text{eff}}$  (above the regulatory limit of 0.95), the consequence of this potential increase in  $k_{\text{eff}}$  must be addressed. There are a number of potential options, the viability of which depends on the magnitude of the increase in  $k_{\text{eff}}$ . For BWR fuel, credit for fuel burnup could be used to offset the potential increase in  $k_{\text{eff}}$  due to fuel failure. Although it is recognized that burnup credit for BWR fuel in storage and transportation casks is not recommended in current regulatory guidance documents, the reactivity reduction associated with burnup is likely sufficient to offset reactivity increases associated with potentially credible BWR failed fuel configurations.

Other potential mitigation options, for either PWR or BWR casks, include 1) separate loading curves for fuel and/or conditions for which fuel integrity cannot be assured, 2) a higher  $k_{\text{eff}}$  limit for such fuel, e.g., 0.98, 3) increased credit for cooling time, 4) credit for the actual, as-loaded conditions in existing casks, and 5) moderator exclusion. For the first option listed above, a cask design and/or fuel assembly loading conditions could be modified to ensure that the current recommended  $k_{\text{eff}}$  limit of 0.95 is satisfied for all credible failed fuel configurations. Separate assembly loading curves based on a reduced  $k_{\text{eff}}$  limit could be developed for fuel assemblies that may have questionable integrity. In the context of high-burnup fuel or ES durations, a separate loading curve based on a lower  $k_{\text{eff}}$  limit could be developed and applied to fuel assemblies with burnup greater than 45 GWd/MTU and/or with a post-irradiation storage period beyond some specified value. Alternatively, depending on the probability of fuel reconfiguration, the second option listed above, i.e., the use of a higher limit, could be established to allow margin for the increased reactivity effect associated with fuel reconfiguration. This option would be similar to the higher limit (i.e., 0.98) allowed for the unlikely optimum moderation condition in dry storage of fresh fuel under 10 CFR 50.68. In this case, the customary  $k_{\text{eff}}$  limit would still apply to all conditions involving intact fuel. The third option above refers to crediting the reduction in reactivity between the minimum time for loading, e.g., 5 years, and some time prior to which fuel reconfiguration is postulated to occur, e.g., 50 years. Because the reactivity of UNF reaches a minimum at approximately 100 years and then begins to increase, the total duration for cask storage and transportation is an important consideration in determining how much reactivity reduction can be credited. For fuel that is already loaded in casks, the fourth option above refers to crediting the specific cask conditions – to the extent needed, the specific

assembly burnup values, cooling times and locations in the cask may be considered to demonstrate sufficient reactivity margin to offset the potential increase in  $k_{\text{eff}}$  due to fuel failure. Finally, moderator exclusion could potentially be used to offset criticality safety concerns related to fuel failure, as is currently allowed for HACs in Ref. 51.

Although the results indicate that the potential impacts on subcriticality can be significant for certain configurations, it can be concluded that the consequences of credible fuel failure configurations from ES or transportation following ES are manageable. Some examples for how to address the potential increases in  $k_{\text{eff}}$  in a criticality safety evaluation were provided. Future work to further inform decision-making relative to which configurations are credible, and therefore need to be considered in a safety evaluation, is recommended.

## 7. RECOMMENDATIONS FOR FUTURE WORK

Future work to extend these analyses could consider additional fuel assembly types, depletion conditions, and cask designs. As noted in Section 6.2, this is not expected to result in significantly different conclusions. It may be beneficial to investigate more accurate modeling of the fuel assemblies to include such features as axial blankets or radial enrichment zoning and different axial burnup and void histories. These details could give more realistic estimates of their impacts on  $k_{\text{eff}}$  but are unlikely to change the salient conclusions regarding the relevance of key configurations.

An expanded study of debris configurations is warranted. The homogeneous debris models used in this analysis do not consider partial assembly failure or any intact assembly structure or hardware. Some of these types of configurations, including debris collecting in structural or flow mixing grids, are potentially more credible than the configurations included in this report. Rubble models including rod segments or fragments may also be relevant. Consideration should be given to a range of final cask orientations if the final debris bed does not fill the entire inner volume of the storage cells. A more complete study of degraded fuel forms is also potentially worth investigating. Many degraded fuel forms would include oxidation to other urania compounds of lower densities, effectively displacing moderator. These changes may not result in any increases in estimated  $k_{\text{eff}}$  but may be worth investigating.

Investigating different enrichments and burnups could be considered. It is unlikely that the relative importance of configurations would be impacted by these changes, but the overall magnitude may be affected. A more complete mapping of the burnup/enrichment space would also allow a quantification of potential conservatisms, especially for BWR fuel, with reduced  $k_{\text{eff}}$  values for reference case conditions.

Future work should investigate the potential impact of loading fuel assemblies with a range of burnups and irradiation histories in storage casks for ES. These configurations are more realistic since each assembly experiences different conditions during irradiation and will have different discharge burnups and cooling times.

It is advisable to consider more combinations of the configurations used here. A very limited number of calculations have been documented in Sections 5.1.3 and 5.2.3, and the results indicate that explicit modeling of combined configurations generates a slightly smaller increase in  $k_{\text{eff}}$  than the sum of the two separate effects. A review of other combined effects could generate additional limiting configurations or provide greater evidence that the effects of combined configurations can be adequately accounted for with separate single configuration models.

Finally, it may be advisable to consider the effect of basket or cask degradation if such events are considered credible. Degradation to these cask components is beyond the scope of these analyses.

## REFERENCES

1. *Gap Analysis to Support Extended Storage of Used Nuclear Fuel*, U.S. Department of Energy, FCRD-USED-2011-000136, REV 0, January 2012.
2. *UFD Storage and Transportation Working Group Report*, U.S. Department of Energy, FCRD-USED-2011-000323, August 2011.
3. *Identification and Prioritization of the Technical Information Needs Affecting Potential Regulation of Extended Storage and Transportation of Spent Nuclear Fuel*, U.S. Nuclear Regulatory Commission, Draft Report for Comment, May 2012, <http://pbadupws.nrc.gov/docs/ML1205/ML120580143.pdf>.
4. *Extended Storage Collaboration Program (ESCP) Progress Report and Review of Gap Analysis*, Electric Power Research Institute, Palo Alto, CA (2011), 1022914.
5. *Evaluation of the Technical Basis for Extended Dry Storage and Transportation of Used Nuclear Fuel – Executive Summary*, U.S. Nuclear Waste Technical Review Board, December 2010, [http://www.nwtrb.gov/reports/eds\\_execsumm.pdf](http://www.nwtrb.gov/reports/eds_execsumm.pdf).
6. *Used Nuclear Fuel Storage and Transportation Research, Development, and Demonstration Plan*, FCRD-FCT-2012-000053, REV 0, April 2012.
7. K. R. Elam, J. C. Wagner, and C. V. Parks, *Effects of Fuel Failure on Criticality Safety and Radiation Dose for Spent Fuel Casks*, NUREG/CR-6835 (ORNL/TM-2002/255), prepared for the U.S. Nuclear Regulatory Commission by Oak Ridge National Laboratory, Oak Ridge, TN, September 2003.
8. Title 10, *Code of Federal Regulations*, Part 72, 73 FR 63572, October 24, 2008.
9. Title 10, *Code of Federal Regulations*, Part 71, 73 FR 63572, October 24, 2008.
10. *Standard Review Plan for Spent Fuel Dry Storage Systems at a General License Facility*, NUREG-1536, Revision 1, Office of Nuclear Material Safety and Safeguards, July 2010.
11. *Standard Review Plan for Spent Fuel Dry Storage Facilities*, NUREG-1567, Office of Nuclear Material Safety and Safeguards, March 2000.
12. *Standard Review Plan for Transportation Packages for Spent Nuclear Fuel*, NUREG-1617, Office of Nuclear Material Safety and Safeguards, March 2000.
13. Title 10, *Code of Federal Regulations*, Part 50.68, 71 FR 66648, November 16, 2006.
14. *Fuel Reconfiguration – Implications to Criticality and Radiation Safety*, 2011 SFST Technical Exchange, November 1, 2011, David Tang and Zhian Li, U.S. Nuclear Regulatory Commission (ADAMS Accession #ML113120530).
15. A. Machiels and A. H. Wells, *Fuel Relocation Effects for Transportation Packages*, EPRI Report 1015050, Palo Alto, CA, 2007.

16. J. L. Sprung et al., *Reexamination of Spent Fuel Shipment Risk Estimates*, NUREG/CR-6672 (SAND2000-0234), prepared for the U.S. Nuclear Regulatory Commission by Sandia National Laboratories, Albuquerque, NM, March 2000.
17. L. E. Fischer et al., *Shipping Container Response to Severe Highway and Railway Accident Conditions*, NUREG/CR-4829 (UCID-20733), prepared for the U.S. Nuclear Regulatory Commission by Lawrence Livermore National Laboratory, Livermore, CA, February 1987.
18. *Final Environmental Impact Statement on the Transportation of Radioactive Material by Air and Other Modes*, NUREG-0170, U.S. Nuclear Regulatory Commission, Rockville, MD, December 1977.
19. A. Machiels et al., *Transportation of Commercial Spent Nuclear Fuel: Regulatory Issues Resolution*, EPRI Report 1016637, Palo Alto, CA, 2010.
20. A. Machiels and A. Dykes, *Criticality Risks during Transportation of Spent Nuclear Fuel: Revision 1*, EPRI Report 1016635, Palo Alto, CA, 2008.
21. *Interfaces Between Storage and Transportation Casks – Panel on High Burnup Fuel – Industry’s View on Spent Fuel Reconfiguration*, 2011 SFST Technical Exchange, November 1, 2011, Albert Machiels, EPRI (ADAMS Accession #ML113120509).
22. D. Nagasawa et al., “Accelerated Corrosion Testing of Aluminum Carbide Metal Matrix Composite in Simulated PWR Spent Fuel Pool Solution,” *Proceedings of 16<sup>th</sup> International Symposium on the Packaging and Transportation of Radioactive Materials* (PATRAM 2010), London, UK, 2010.
23. M. Dallongeville et al., “Description of Fuel Integrity Project Methodology Principles,” *Proceedings of 16<sup>th</sup> International Symposium on the Packaging and Transportation of Radioactive Materials* (PATRAM 2010), London, UK, 2010.
24. P. Purcell, “Method to Evaluate Limits of Lattice Expansion in Light Water Reactor Fuel from an Axial Impact Accident During Transport,” *Proceedings of 15<sup>th</sup> International Symposium on the Packaging and Transportation of Radioactive Materials* (PATRAM 2007), Miami, FL, 2007.
25. I. Reiche, “Influence of the Accident Behaviour of Spent Fuel Elements on Criticality Safety of Transport Packages – Some Basic Considerations,” *Proceedings of 15<sup>th</sup> International Symposium on the Packaging and Transportation of Radioactive Materials* (PATRAM 2007), Miami, FL, 2007.
26. F. Hilbert, “Criticality Assessment of Fuel Assemblies With Missing Fuel Rods – An Intractable Problem?” *Proceedings of 14<sup>th</sup> International Symposium on the Packaging and Transportation of Radioactive Materials* (PATRAM 2004), Berlin, Germany, 2004.
27. P. J. Vescovi and N. A. Kent, “Nuclear Criticality Safety Analysis for the Traveler PWR Fuel Shipping Package,” *Proceedings of 14<sup>th</sup> International Symposium on the Packaging and Transportation of Radioactive Materials* (PATRAM 2004), Berlin, Germany, 2004.
28. L. Farrington, “Harmonisation of Criticality Assessments of Packages for the Transport of Fissile Nuclear Fuel Cycle Materials,” *Proceedings of 14<sup>th</sup> International Symposium on the Packaging and Transportation of Radioactive Materials* (PATRAM 2004), Berlin, Germany, 2004.

29. B. Gogolin et al., "Drop Tests with the RA-3D Shipping Container for the Transport of Fresh BWR Fuel Assemblies," *Proceedings of 13<sup>th</sup> International Symposium on the Packaging and Transportation of Radioactive Materials* (PATRAM 2001), Chicago, IL, 2001.
30. P. Millan et al., "Drop Test for the Licensing of the RA-3D Package in the Transport of BWR Fresh Fuel Assemblies," *Proceedings of 13<sup>th</sup> International Symposium on the Packaging and Transportation of Radioactive Materials* (PATRAM 2001), Chicago, IL, 2001.
31. S. Whittingham et al., "Effects of Impact Accidents on Transport Criticality Safety Cases for LWR Packages – A New Approach," *Proceedings of 13<sup>th</sup> International Symposium on the Packaging and Transportation of Radioactive Materials* (PATRAM 2001), Chicago, IL, 2001.
32. M. Asami and N. Odano, "New Approach to Evaluate Lattice Expansion of Light Water Reactor Fuel Elements on Criticality Safety of Transport Packages under Impact Accidents," *Packaging, Transport, Storage & Security of Radioactive Material* **21**(2), 2010.
33. *Handbook of Neutron Absorber Materials for Spent Nuclear Fuel Transportation and Storage Applications*: 2009 ed., EPRI Technical Report 1019110, Electric Power Research Institute, Palo Alto, CA, November 2009.
34. *SCALE: A Comprehensive Modeling and Simulation Suite for Nuclear Safety Analysis and Design*, ORNL/TM-2005/39, Version 6.1, Oak Ridge National Laboratory, Oak Ridge, TN, June 2011. Available from Radiation Safety Information Computational Center at Oak Ridge National Laboratory as CCC-785.
35. *RW-859 Nuclear Fuel Data*, Energy Information Administration, Washington, D.C., October 2004.
36. *Safety Analysis Report for the Holtec International Storage, Transport, and Repository Cask System (HI-STAR 100 Cask System)*, Table of Contents to Chapter 1, Holtec Report HI-951251, Revision 10, Holtec International, August 2003, ADAMS Accession Number ML071940386.
37. *Safety Analysis Report for the Holtec International Storage, Transport, and Repository Cask System (HI-STAR 100 Cask System)*, Chapter 2 through Chapter 4, Holtec Report HI-951251, Revision 10, Holtec International, August 2003, ADAMS Accession Number ML071940391.
38. *Safety Analysis Report for the Holtec International Storage, Transport, and Repository Cask System (HI-STAR 100 Cask System)*, Chapter 5 to end, Holtec Report HI-951251, Revision 10, Holtec International, August 2003, ADAMS Accession Number ML071940408.
39. J. C. Wagner, *Computation Benchmark for Estimation of Reactivity Margin from Fission Products and Minor Actinides in PWR Burnup Credit*, NUREG/CR-6747 (ORNL/TM-2000/306), prepared for the U.S. Nuclear Regulatory Commission by Oak Ridge National Laboratory, Oak Ridge, TN, October 2001.
40. C. V. Parks, M. D. DeHart, and J. C. Wagner, *Review and Prioritization of Technical Issues Related to Burnup Credit for LWR Fuel*, NUREG/CR-6665 (ORNL/TM-1999/303), prepared for the U.S. Nuclear Regulatory Commission by Oak Ridge National Laboratory, Oak Ridge, TN, February 2000.
41. R. J. Caciapouti and S. Van Volkinburg, *Axial Burnup Profile Database for Pressurized Water Reactors*, YAEC-1937, Yankee Atomic Electric Company, May 1997.

42. J. C. Wagner and C. V. Parks, *Parametric Study for the Effect of Burnable Poison Rods for PWR Burnup Credit*, NUREG/CR-6761 (ORNL/TM-2000/373), prepared for the U.S. Nuclear Regulatory Commission by Oak Ridge National Laboratory, Oak Ridge, TN, March 2002.
43. C. E. Sanders and J. C. Wagner, *Study of the Effect of Integral Burnable Absorbers for PWR Burnup Credit*, NUREG/CR-6760 (ORNL/TM-2000/321), prepared for the U.S. Nuclear Regulatory Commission by Oak Ridge National Laboratory, Oak Ridge, TN, March 2002.
44. J. C. Wagner and C. V. Parks, *Recommendations on the Credit for Cooling Time in PWR Burnup Credit Analysis*, NUREG/CR-6781 (ORNL/TM-2001/272), prepared for the U.S. Nuclear Regulatory Commission by Oak Ridge National Laboratory, Oak Ridge, TN, January 2003.
45. *Topical Report on Actinide-Only Burnup Credit for PWR Spent Nuclear Fuel Packages*, DOE/RW-0472 Rev. 2, U.S. Department of Energy Office of Civilian Radioactive Waste Management, September 1998.
46. D. P. Henderson et al., *Summary Report of Commercial Reactor Criticality Data for Quad Cities Unit 2*, B00000000-01717-5705-00096 Revision 01, Civilian Radioactive Waste Management System Management & Operating Contractor, September 1999.
47. D. P. Henderson et al., *Summary Report of Commercial Reactor Criticality Data for LaSalle Unit 1*, B00000000-01717-5705-00138, Civilian Radioactive Waste Management System Management & Operating Contractor, September 1999.
48. D. E. Mueller et al., *Review and Prioritization of Technical Issues Related to Burnup Credit for BWR Fuel*, NUREG/CR-XXXX (ORNL/TM-2012/261), prepared for the U.S. Nuclear Regulatory Commission by Oak Ridge National Laboratory, Oak Ridge, TN, to be published.
49. M. G. Natrella, *Experimental Statistics*, National Bureau of Standards Handbook 91, August 1963.
50. Fuel Cycle Safety and Safeguard Interim Staff Guidance-10, *Justification for Minimum Margin of Subcriticality for Safety*, Division of Fuel Cycle Safety and Safeguards, Office of Nuclear Material Safety and Safeguards, U.S. Nuclear Regulatory Commission, June 2006.
51. Spent Fuel Storage Transportation Interim Staff Guidance-19, *Moderator Exclusion under Hypothetical Accident Conditions and Demonstrating Subcriticality of Spent Fuel under the Requirements of 10 CFR 71.55(e)*, Division of Spent Fuel Storage and Transportation, Office of Nuclear Material Safety and Safeguard, U.S. Nuclear Regulatory Commission, May 2003.
52. L. E. Fennern, *ABWR Seminar – Reactor, Core & Neutronics*, GE Energy/Nuclear, <http://www.ne.doe.gov/np2010/pdfs/ABWRReactorCoreNeutronics.pdf>, retrieved April 16, 2012.
53. L. B. Wimmer, *BWR Axial Burnup Profile Evaluation*, Framatome ANP Document Number 32-5045751-00, July 16, 2004.

## Appendix A

### Fuel Assembly Modeling Details

#### A.1 WESTINGHOUSE 17 × 17 OFA

Westinghouse 17 × 17 OFA is a fuel design that has been commonly used in the commercial nuclear industry for more than 20 years. This common use makes it a good choice for a representative fuel assembly type for calculations in the PWR storage and transportation casks. For purposes of these analyses, the OFA fuel design encompasses all variations of cladding materials, grids, and assembly hardware which may lead to a different fuel product designation from Westinghouse, such as Vantage5 or Vantage+. The essential features are the fuel rod outer diameter of 0.9144 cm and fuel rod pitch of 1.2598 cm. The dimensions used to model the fuel assembly are provided in Table A-1.

The 17 × 17 OFA model is included in the MPC-24 and GBC-32 casks. The cladding is modeled as Zircaloy-4. The guide tube and instrument tubes are assumed to be identical and are also represented as Zircaloy-4. Unborated, unit density water fills the gap between the pellet and cladding. Water in the pellet/clad gap is conservative for criticality calculations because it causes a slight increase in calculated  $k_{\text{eff}}$  values. In irradiated fuel, pellet swelling closes this gap and causes this assumption to be nonphysical. A cross section of the 17 × 17 OFA model is shown in Figure A-1.

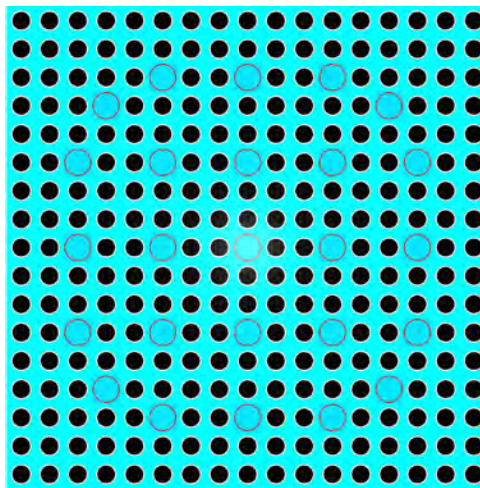
The fuel assemblies are modeled with a uniform initial enrichment in the axial and radial directions. No reduced enrichment and/or annular blanket pellets are included in any of the models. No integral burnable absorbers are modeled in the fuel, though the presence of wet annular burnable absorber (WABA) rods is considered during depletion to provide conservative used fuel isotopic compositions with respect to criticality calculations. The impact of the presence of removable and integral burnable absorbers is discussed in Refs. 42 and 43. The details of the depletion conditions are provided in Section 4.4.1.

Several modeling simplifications have been incorporated that either have a negligible effect or increase assembly calculated  $k_{\text{eff}}$ . Some of these simplifications include omission of fuel assembly hardware beyond the ends of the active fuel as well as the omission of all structural and mixing grids, assembly nozzles, plenums, and end plugs. The hardware beyond the active fuel region has a small effect on  $k_{\text{eff}}$ , and minimal effect on the change in  $k_{\text{eff}}$  associated with fuel reconfiguration. Omitting the grids allows more effective neutron moderation due to less moderator displacement between rods.

For cases involving depleted fuel, the fuel rods are represented with 18 axial regions. Each region is 20.32 cm (8 in.) tall and contains average mixture number densities in each zone. All fuel rods contain the same composition.

**Table A-1. Westinghouse 17 × 17 OFA dimensions used in these analyses [39]**

Parameter	Dimension (cm)	Dimension (in.)
Pellet outer diameter	0.7844	0.3088
Fuel rod outer diameter	0.9144	0.360
Cladding thickness	0.0571	0.0225
Fuel rod pitch	1.2598	0.496
Active fuel height	365.76	144
Guide/instrument tube outer diameter	1.204	0.474
Guide/instrument tube thickness	0.0407	0.016
Fuel density	10.5216 g/cm <sup>3</sup> (96% theoretical density)	
Number of fuel rods	264	
Number of guide/instrument tubes	25	



Note: Fuel shown in black; guide/instrument tubes are larger, water-filled tubes

**Figure A-1. Cross section of 17 × 17 OFA assembly.**

## A.2 GENERAL ELECTRIC 10 × 10

General Electric 10 × 10 fuel assembly designs, such as the GE14 fuel product, are widely used in the commercial nuclear power industry. The 10 × 10 array is representative of existing BWR fuel assembly designs for use in the MPC-68 cask models. The GE 10 × 10 model included in the MPC-68 models uses dimensions shown in Table A-2. Unborated, unit density water fills the gap between the fuel pellet and cladding. The cladding and water tubes are modeled as Zircaloy-4. Each water tube occupies four unit cells in the lattice, displacing a 2 × 2 region of fuel rods. A cross section of the 10 × 10 model is shown in Figure A-2.

The fuel assemblies are considered with a uniform initial enrichment in the axial and radial directions. No reduced enrichment axial blanket pellets are included, and no part-length rods are represented in the fuel assemblies except in the explicit part-length rod sensitivity calculations.

Part-length rods are common in BWR assembly designs, including the GE14 design, making an investigation of the impact of part-length rods prudent as a part of these analyses. The pattern of part-length rods, taken from Ref. 52, is shown in Figure A-3. These shortened rods have fuel only in the bottom 220 cm of the fuel rods. As discussed in Section 5.2.4, only fresh 5 w/o fuel is considered in the part-length rod calculations presented in this report. Only fresh fuel is considered for these studies because no axial burnup profiles are available for fuel assemblies with part-length rods. The removal of some of the fuel in the upper portion of the assembly might cause a more bottom-skewed power shape, but the remaining sparser lattice will also be more reactive. The axial power shape could therefore also be about the same or even more top-skewed than that developed in Appendix E. The lower mass in the upper zone of the assembly also has the effect of increasing burnup since it is measured as energy released per unit mass of uranium. Given the unknown relative impact of these effects, depleted fuel is not considered in this study.

No burnable absorbers are modeled in the fresh fuel assemblies or during depletion. The impact of burnable absorbers is expected to be negligible on the results of this study. The details of the depletion conditions are provided in Section 4.4.2.

Several modeling simplifications that are consistent with industry practice for criticality safety have been incorporated that either have a negligible effect on system reactivity or increase assembly reactivity. Some of these simplifications include omission of fuel assembly hardware beyond the ends of the active fuel as well as the omission of all structural and mixing grids, assembly end fittings, plenums, and end plugs. The hardware beyond the active fuel region has a small effect on  $k_{\text{eff}}$ , and minimal effect on the change in  $k_{\text{eff}}$  associated with fuel reconfiguration. Omitting the grids allows more effective neutron moderation due to less moderator displacement between rods.

For cases involving depleted fuel, the fuel rods are represented with 25 axial regions. Each region is 15.24 cm (6 in.) tall and contains average mixture number densities in each zone. All fuel rods contain the same composition.

**Table A-2. GE 10 × 10 assembly dimensions used in these analyses [34]**

Parameter	Dimension (cm)	Dimension (in.)
Pellet outer diameter	0.876	0.3449
Fuel rod outer diameter	1.026	0.404
Cladding thickness	0.066	0.026
Fuel rod pitch	1.295	0.510
Active fuel height	381	150
Water tube outer diameter	2.522	0.993
Water tube thickness	0.1	0.039
Fuel density	10.5216 g/cm <sup>3</sup> (96% theoretical density)	
Number of fuel rods	92	
Number of water tubes	2 (each displaces four fuel rods)	

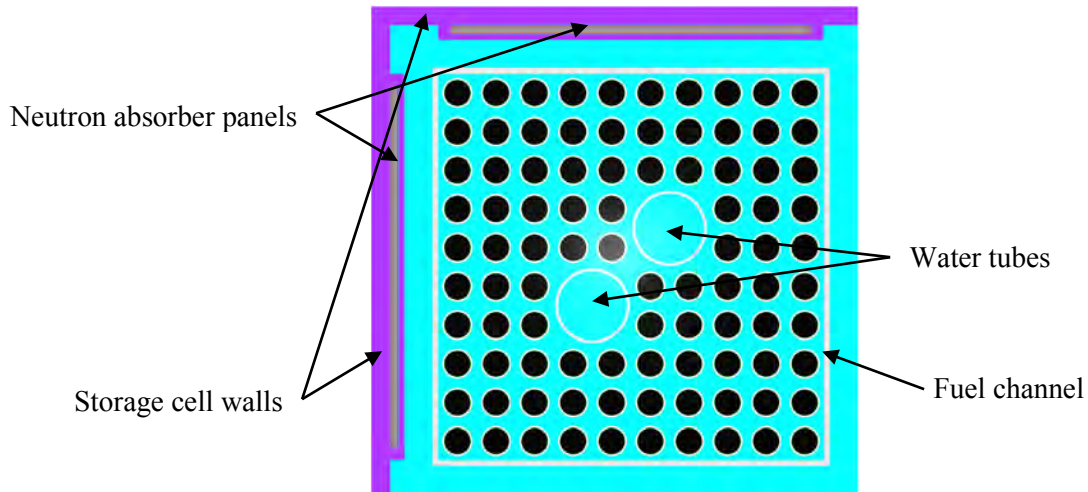


Figure A-2. Cross section of GE  $10 \times 10$  fuel assembly in MPC-68.

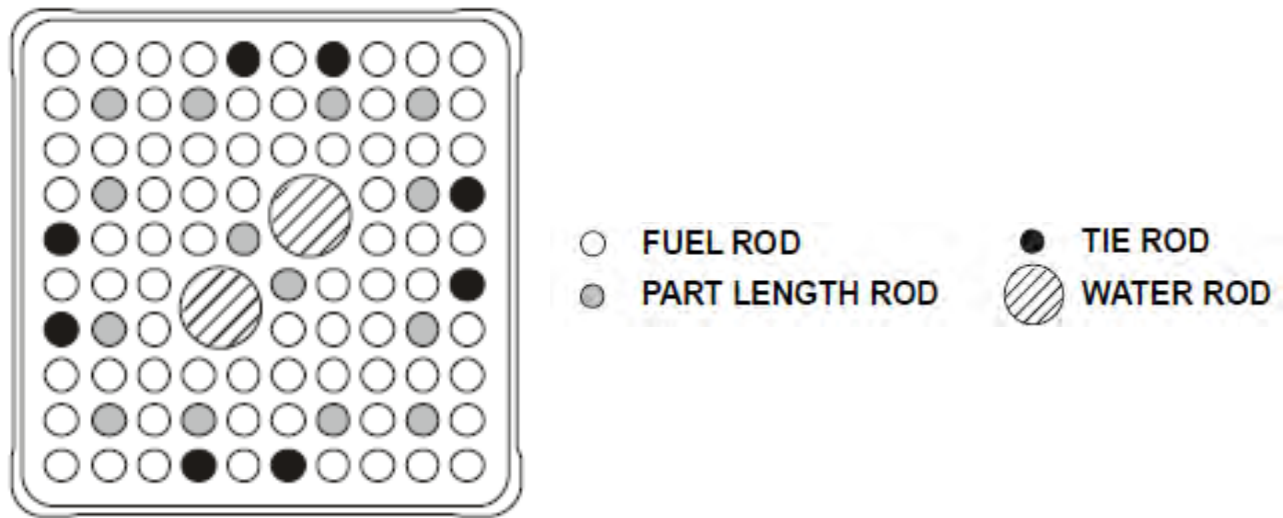


Figure A-3. Location of part-length rods in GE  $10 \times 10$  fuel assembly.

## Appendix B

### MPC-24 Modeling and Results

The MPC-24 cask is designed for the storage and transportation of up to 24 PWR fuel assemblies. The nominal condition for this model is fully flooded with unit density, unborated water. A cross section of the MPC-24 model is shown in Figure B-1. It should be noted that the MPC-24 cask design in Refs. 36–38 has been updated from the design used in Ref. 7. The cask model is consistent with the description and drawings provided in the HI-STAR Safety Analysis Report (SAR), Refs. 36–38. More details of the modeling are provided in Appendix D.

Fresh 5 w/o  $^{235}\text{U}$  enrichment Westinghouse 17 × 17 OFA is modeled in the MPC-24. This fuel represents a limiting case for analysis. It is unlikely that any fresh fuel assemblies would be placed in ES, but this condition is of interest to complete the parameter space to be covered in this study.

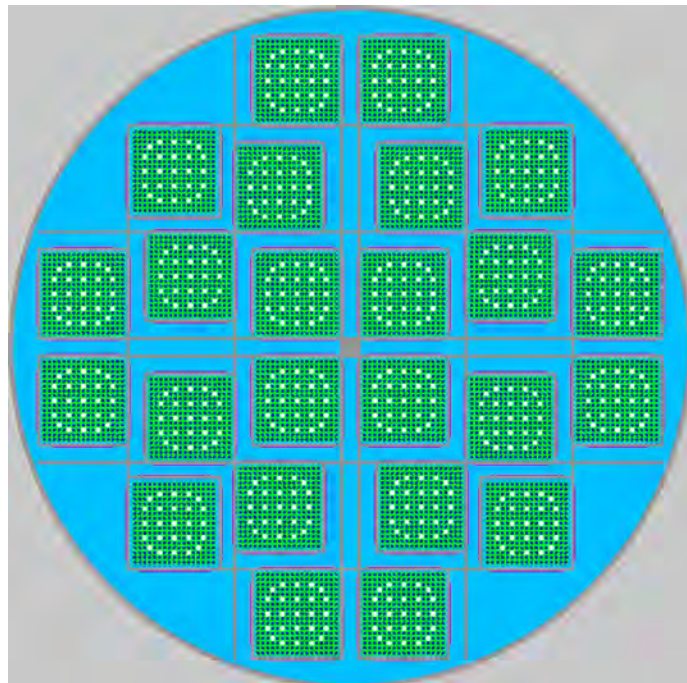


**Figure B-1. Cross section of MPC-24 model.**

#### B.1 ADDITIONAL CONFIGURATION CONSIDERED

The MPC-24 is the only cask design considered that integrates a flux trap into the design of the fuel storage basket. A flux trap is a region of typically water-filled space with neutron absorber panels on both sides of the trap and is positioned between fuel storage cells. The worth of the absorbers is greatly increased by allowing for additional moderation between the panels, thus allowing higher reactivity fuel to be stored safely. Fast neutrons escaping from one cell will be thermalized in the water between cells and are much more likely to be absorbed in the panel on the other side. For this design feature to be

effective, the area within the flux trap must stay flooded in all cases in which the fuel storage cells are flooded. The primary design features that preclude the drainage of only the flux traps are an opening in the bottom of the storage basket walls and a small gap between the top of the storage cell walls and the cask lid. These openings allow water to flow into all regions of the basket. Preferential flooding (i.e., flooding of the fuel storage cells but not the flux traps) is considered here.

The modeling of preferential flooding configurations is straightforward. Two cases are considered: one in which only the flux traps are dry and one in which the area inside the fuel storage cell but outside the fuel assembly is also dry. The latter case is not credible but is included for completeness. No adjustments are needed to the cross section processing because the fuel assembly is always modeled as fully flooded. The orientation of the cask is not considered in the modeling of this configuration. It is not expected to influence the results of the calculations, though it would influence the progression of a flooding event if one occurred.

No preferential flooding cases are considered in Ref. 7.

## B.2 RESULTS

The  $k_{\text{eff}}$  change associated with each of the configurations discussed in Section 3 and Section B.1 is presented in this section for the MPC-24 cask. All configurations assume a full loading of 24 fresh 5 w/o Westinghouse 17 × 17 OFA. The description of the fuel assembly modeling is provided in Appendix A. No used fuel configurations are considered in the MPC-24 model. The reference case  $k_{\text{eff}}$  results from both the KENO V.a and KENO-VI models are provided in Table B-1.

**Table B-1. Reference case results for MPC-24**

<b>Burnup (GWd/MTU)</b>	<b>Cooling time (years)</b>	<b>KENO V.a</b>		<b>KENO-VI</b>	
		$k_{\text{eff}}$	$\sigma$	$k_{\text{eff}}$	$\sigma$
0	0	0.95042	0.00010	0.95065	0.00010

### B.2.1 Reconfiguration of All Assemblies

A summary of the  $k_{\text{eff}}$  consequences associated with each configuration is provided in Table B-2. Additional details for each configuration and the results for non-limiting cases are provided in the subsequent subsections.

**Table B-2. Summary of  $k_{\text{eff}}$  increases for the MPC-24 cask**

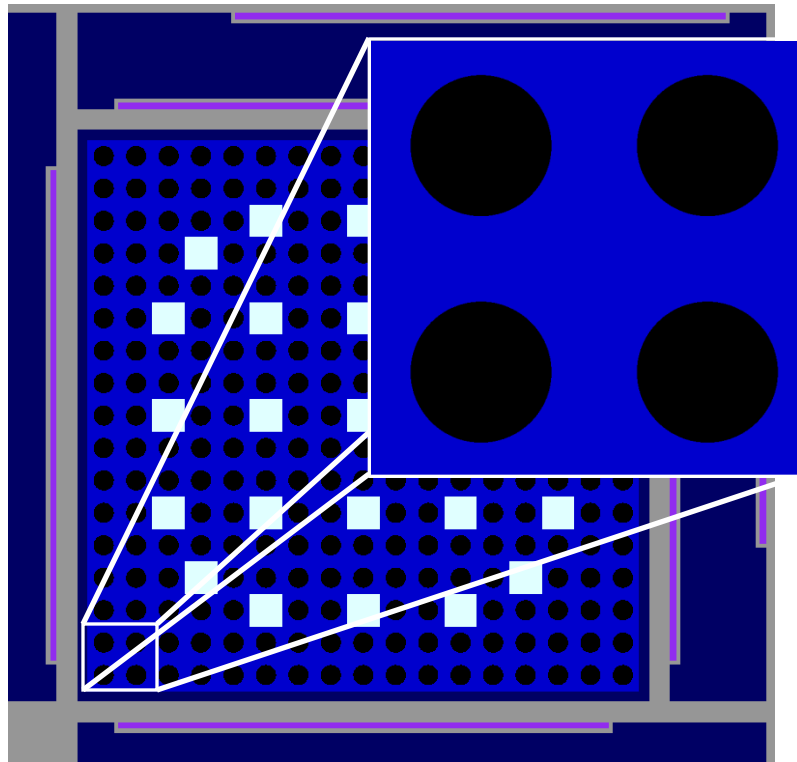
Configuration	Maximum increase in $k_{\text{eff}}$ (% $\Delta k_{\text{eff}}$ )
<b>Clad thinning/loss</b>	
Cladding removal	5.24
<b>Rod failures</b>	
Single rod removal	0.15
Multiple rod removal	2.01
<b>Loss of rod pitch control</b>	
Expanded rod pitch, clad	2.88
Expanded rod pitch, unclad	6.83
<b>Loss of assembly position control</b>	
Axial displacement (maximum)	7.08
Axial displacement (20 cm)	0.03
<b>Gross assembly failure</b>	
Uniform pellet array	13.56
Homogeneous rubble	8.23
<b>Preferential flooding</b>	
Preferential Flooding (dry flux traps)	16.61
<b>Neutron absorber degradation</b>	
Missing neutron absorber (5-cm segment)	0.35
Missing neutron absorber (10-cm segment)	1.07
50% neutron absorber panel thinning	1.11

### B.2.1.1 Clad Thinning/Loss

The loss of cladding configurations are modeled as discussed above in Section 3.1.1; the complete cladding removal configuration is shown in Figure B-2. The results of the calculations are provided in Table B-3, showing that the  $k_{\text{eff}}$  increase associated with complete cladding removal is 5.24%  $\Delta k_{\text{eff}}$ . The results as a function of fractional cladding thickness are shown in Figure B-3. The results presented here are somewhat higher than those presented in Ref. 7. This may be due to an updated cask model that includes the oversized fuel storage cells and the rotation of the standard storage cells relative to each other in the cask basket. These additional details may lead to a slightly more thermal spectrum and a correspondingly higher  $k_{\text{eff}}$  value for this configuration.

**Table B-3. Increase in  $k_{\text{eff}}$  in MPC-24 due to reduced cladding thickness**

Fraction of cladding thickness remaining	Increase in $k_{\text{eff}}$ (% $\Delta k_{\text{eff}}$ )
0.90	0.62
0.75	1.51
0.50	2.87
0.25	4.06
0.00	5.24



Notes:

- Fuel shown in black
- Storage basket structural material is light grey
- Neutron absorber panel is purple
- Water is shown in blue, dark blue, and white
- Guide/instrument tube locations contain water shown in white

**Figure B-2. Loss of cladding model in MPC-24 storage cell.**

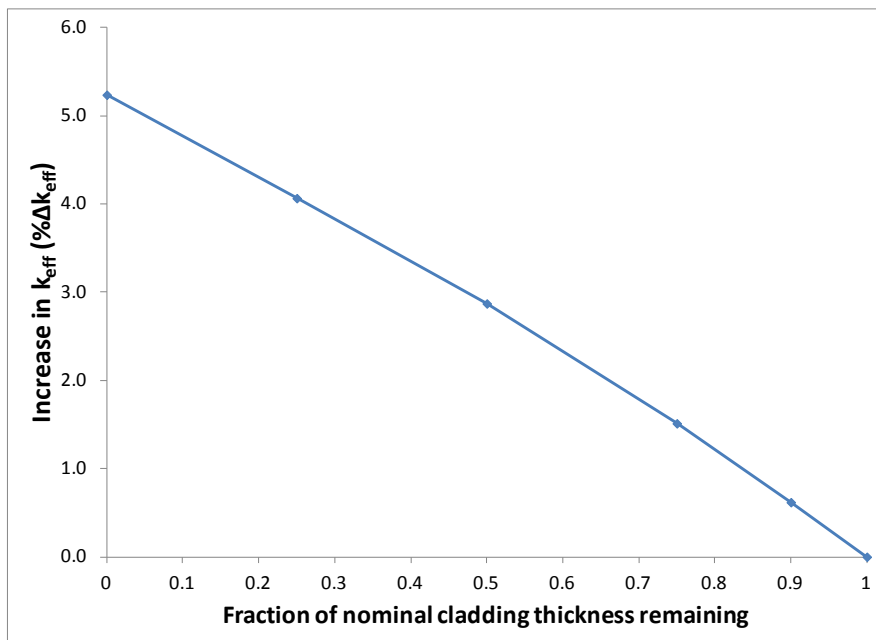


**Figure B-3. Increase in  $k_{\text{eff}}$  in MPC-24 due to reduced cladding thickness.**

### B.2.1.2 Rod Failures

Each of the 39 unique eighth-assembly symmetric rods is removed individually to determine its worth, as discussed in Section 3.1.2.1. A sketch showing the eighth-assembly symmetry and row and column labels is provided in Figure 7. Table B-4 presents the rod locations whose best estimate worth is greater than 0.1%  $\Delta k_{\text{eff}}$ . Both the locations of these rods and the magnitude of the change in  $k_{\text{eff}}$  caused by rod failure are in good agreement with the previous work documented in Ref. 7. The columns in the assembly are designated with a letter, from A to Q, and the rows are designated with numbers, from 1 to 17, as shown in Figure 7. The maximum  $k_{\text{eff}}$  increase is associated with rod H8 and is 0.15%  $\Delta k_{\text{eff}}$ .

Multiple rods are removed in groups, as discussed in Section 3.1.2.2. Groups of 2, 4, 8, 12, 16, 24, 32, 40, 44, 48, and 52 rods are considered. The  $k_{\text{eff}}$  increase is shown as a function of rods removed in Figure B-4. The limiting lattice is shown in Figure B-5. The maximum  $k_{\text{eff}}$  value occurs for 48 rods removed and corresponds to a  $k_{\text{eff}}$  increase of 2.01%  $\Delta k_{\text{eff}}$ .

**Table B-4. Single rod removal results for  
17 × 17 OFA in MPC-24**

Rod location	Increase in $k_{\text{eff}}$ (% $\Delta k_{\text{eff}}$ )
H8	0.15
H5	0.13
H7	0.13
G5	0.12
I7	0.12
I8	0.12
I4	0.11
G7	0.11
G6	0.11

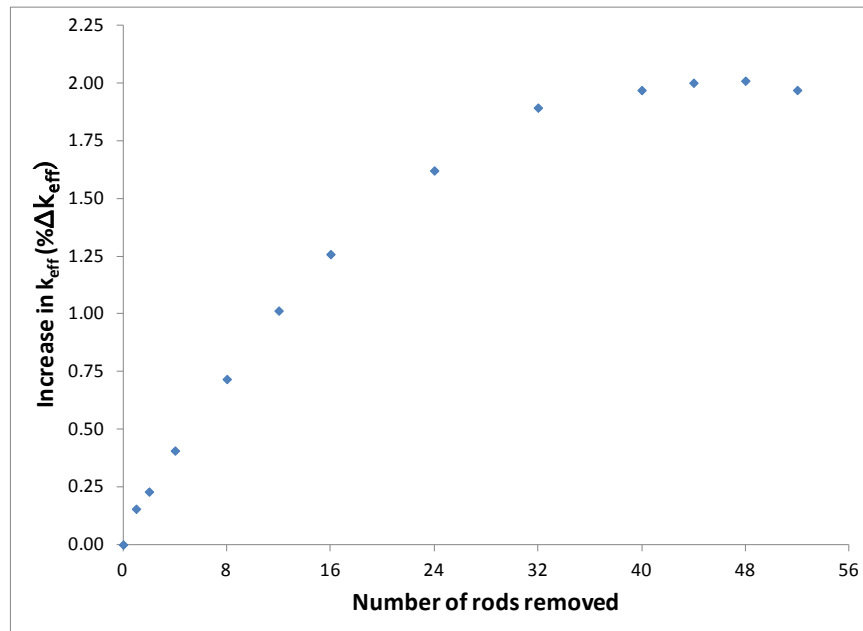
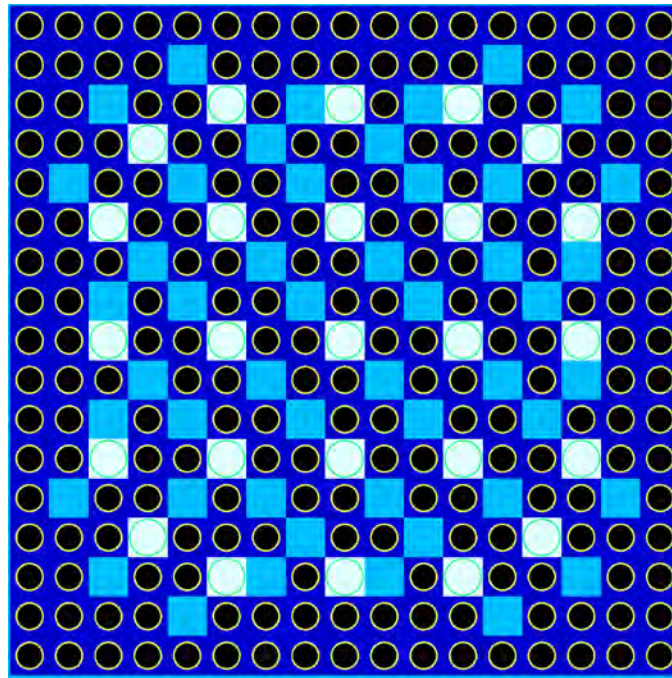


Figure B-4. Increase in  $k_{\text{eff}}$  in MPC-24 versus number of rods removed.



Notes:

- Fuel shown in black
- Water is shown in light blue, dark blue, and white
- Guide/instrument tubes contain water shown in white
- Missing fuel rod locations shown in light blue

Figure B-5. Limiting multiple rod removal lattice (48 rods removed).

### B.2.1.3 Loss of Rod Pitch Control

The loss of rod pitch control is modeled as a uniform increase in fuel assembly pitch, as discussed above in Section 3.1.3. Two different fuel storage cell sizes exist in the MPC-24 basket, as discussed in Appendix D. The four oversized storage cells allow for a larger uniform pitch than the 20 standard storage cells. The fuel assemblies in each type of cell are expanded to account for the larger possible pitch in the oversized storage cells. The maximum increase in  $k_{\text{eff}}$  is 2.88%  $\Delta k_{\text{eff}}$  with cladding intact and 6.83%  $\Delta k_{\text{eff}}$  with cladding removed. The increase in  $k_{\text{eff}}$  as a function of fuel rod pitch is shown in Figure B-6. The pitch used in the standard and oversized storage cells is the same until the pitch reaches approximately 1.31 cm. For the largest pitch, the assemblies in the oversized storage cells have a larger pitch than those in the standard cells so that the fuel rods are in contact with the cell walls in both cell types. A portion of the limiting configuration model with cladding intact is shown in Figure B-7. This result agrees well with the results provided in Ref. 7. Radial nonuniform pitch, as discussed in Section 3.1.3.1, is not considered in the MPC-24 cask.

The MPC-24 cask contains fresh fuel, so the most reactive axial portion of the assembly is the center. For that reason, the birdcage analysis, as discussed in Section 3.1.3.2, includes two compressed pitch sections symmetrically positioned above and below the mid-plane of the assembly. A range of center section and compressed section lengths is considered. A figure showing the axial pitch variation is included as Figure B-8. There is no  $k_{\text{eff}}$  increase associated with an axially variable fuel rod pitch for the MPC-24 model beyond the 2.88%  $\Delta k_{\text{eff}}$  resulting from uniform pitch expansion.

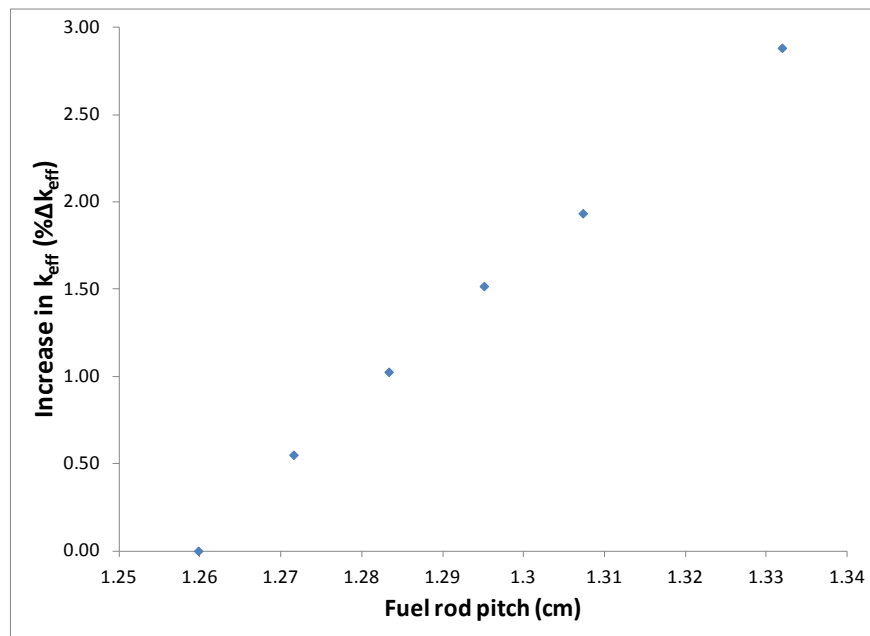


Figure B-6. Increase in  $k_{\text{eff}}$  in MPC-24 as a function of fuel rod pitch.

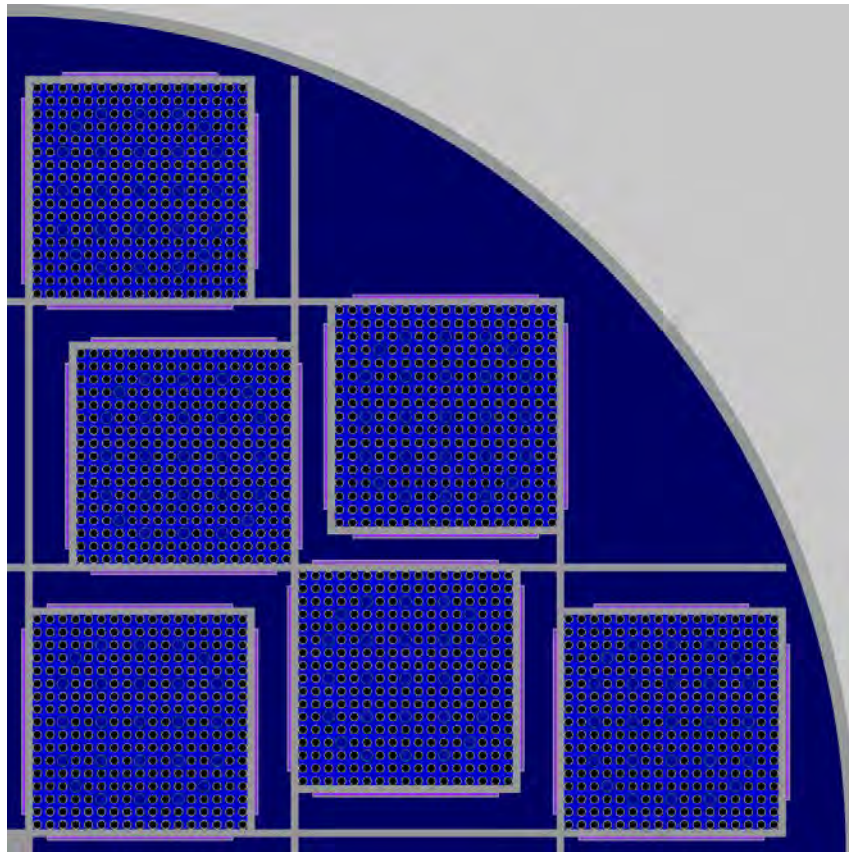


Figure B-7. Maximum pitch expansion case in MPC-24.

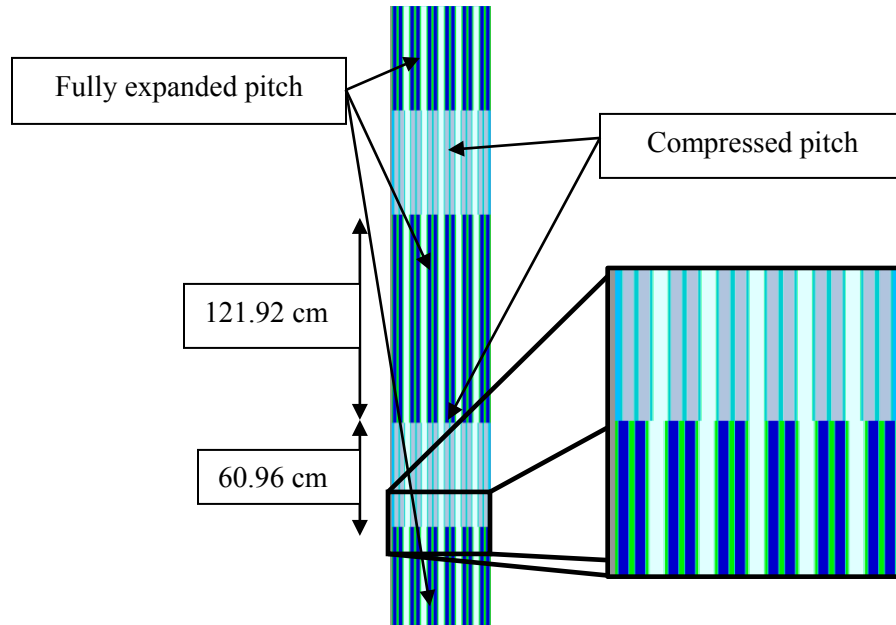


Figure B-8. Example axial variation of pitch expansion in MPC-24.

#### B.2.1.4 Loss of Assembly Position Control

Assembly misalignment is calculated over a range of displacements, as shown in Figure B-9. The consequence of the maximum misalignment is over 7%  $\Delta k_{\text{eff}}$ . A more limited misalignment case (20 cm) is also evaluated as a surrogate for potential degradation of assembly end fittings or the spacers used inside the cask to ensure proper assembly alignment. The consequence of this more limited misalignment case, shown in Figure B-10, is significantly less.

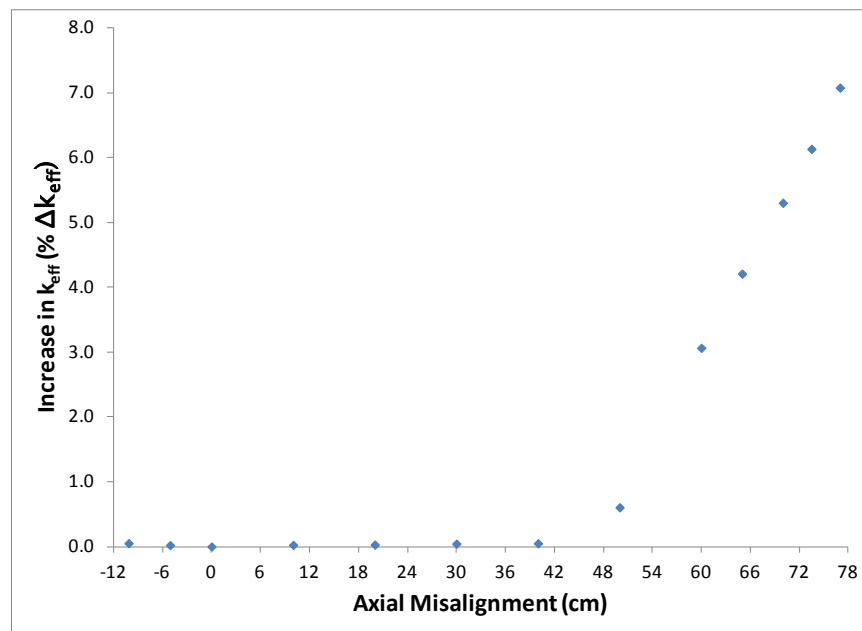


Figure B-9. Increase in  $k_{\text{eff}}$  as a function of axial assembly misalignment in MPC-24.

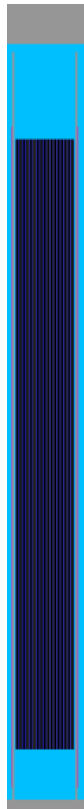
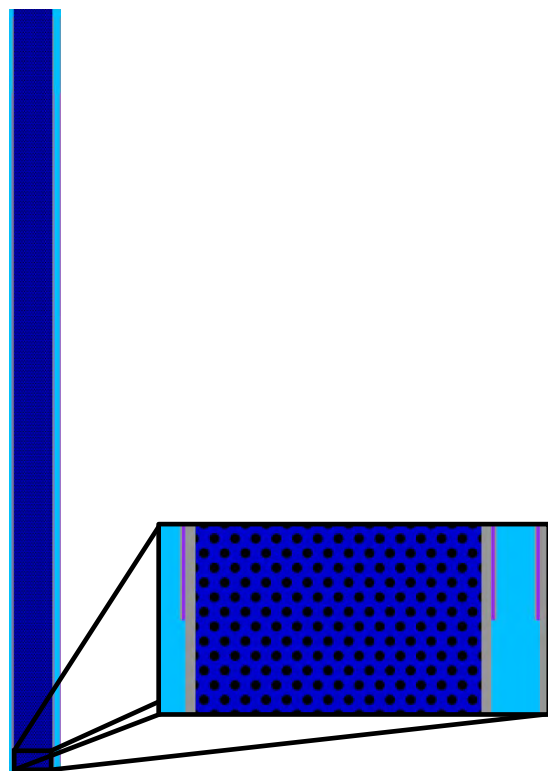


Figure B-10. Assembly in MPC-24 misaligned 20-cm toward cask lid.

#### B.2.1.5 Gross Assembly Failure

The two gross assembly failure configurations described in Section 3.1.5 are investigated in the MPC-24 cask. As expected, this configuration has the highest reactivity increase: the ordered pellet array case has a larger  $k_{\text{eff}}$  increase than the homogeneous rubble case. The  $k_{\text{eff}}$  increase in the homogeneous rubble case is over 8%  $\Delta k_{\text{eff}}$ , and the ordered pellet array case increases  $k_{\text{eff}}$  by over 13.5%  $\Delta k_{\text{eff}}$ . The gross assembly failure configurations are illustrated in Figure B-11 and Figure B-12. The configuration with homogeneous rubble contained only in the neutron absorber elevations is not considered in the MPC-24.

The results for the ordered pellet array case are significantly higher than those reported previously in Ref. 7. This is primarily because the array is also allowed to extend beyond the neutron absorber panel elevations. The homogeneous rubble case was not included in Ref. 7.



**Figure B-11. Ordered pellet array configuration for gross assembly failure.**

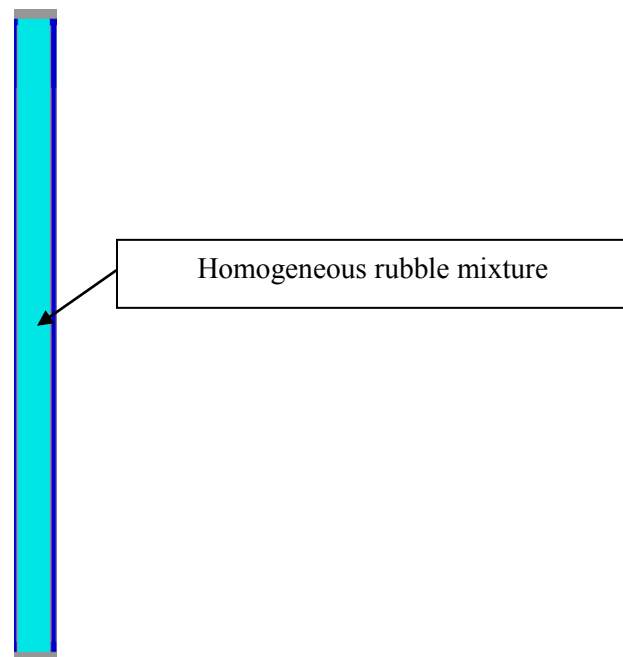
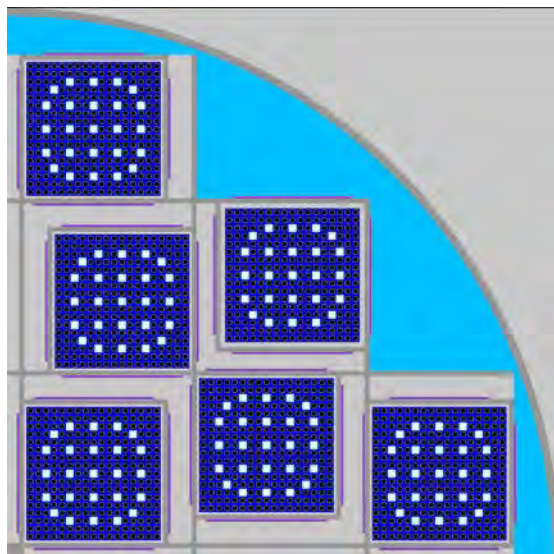


**Figure B-12. Homogeneous rubble configuration for gross assembly failure.**

### B.2.1.6 Preferential Flooding

The preferential flooding configuration that leaves the flux traps dry in the basket is considered only for the MPC-24 cask, as mentioned in Section B.1. The results indicate an increase in  $k_{\text{eff}}$  of more than 16.5%  $\Delta k_{\text{eff}}$ . A preferential flooding configuration is shown in Figure B-13.



Notes: Fuel shown in black  
Water is shown in light blue, dark blue, and white  
Guide/instrument tubes contain water shown in white  
Void in the basket and outside the cask is shown in light grey

**Figure B-13. Preferential flooding with only the fuel assemblies flooded.**

### B.2.1.7 Neutron Absorber Degradation

The results of the calculations, described in Section 3.1.6.1, considering a 5-cm neutron absorber defect at varying elevations are presented in Table B-5. As expected, the limiting elevation is at the centerline of the active fuel height. The model containing the 5-cm gap is shown in Figure B-14. The  $k_{\text{eff}}$  increase for this location is 0.35%  $\Delta k_{\text{eff}}$  and increases to 1.07%  $\Delta k_{\text{eff}}$  if the defect size is increased to 10 cm. As discussed in Section 3, these defects are assumed to be present at the same elevation in all neutron absorber panels within the cask.

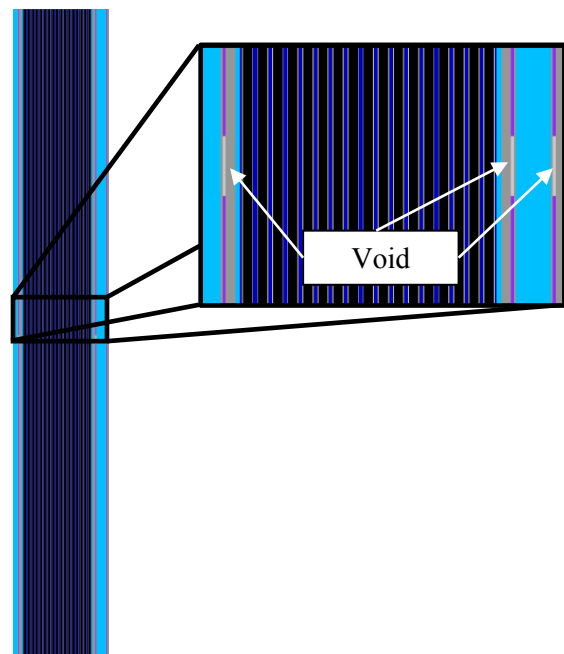
The results of the uniform absorber panel thinning calculations described in Section 3.1.6.3 are provided in Table B-6 and Figure B-15. A 50% decrease in panel thickness creates a 1.11% increase in  $k_{\text{eff}}$ . Complete removal of all neutron absorber material increases  $k_{\text{eff}}$  by over 11%  $\Delta k_{\text{eff}}$ , but the magnitude of the increase does not exceed 3%  $\Delta k_{\text{eff}}$  until more than 80% of the absorber has been eliminated.

**Table B-5. Increase in  $k_{\text{eff}}$  in MPC-24 caused by a 5-cm neutron absorber defect at various elevations**

Defect elevation midpoint (cm above bottom of active fuel)	Increase in $k_{\text{eff}}$ (% $\Delta k_{\text{eff}}$ )
2.50	0.03
91.44	0.28
182.88	0.35
274.32	0.26
363.26	0.03

**Table B-6. Increase in  $k_{\text{eff}}$  in MPC-24 caused by uniform neutron absorber panel thinning**

Fraction of neutron absorber panel thickness remaining	Increase in $k_{\text{eff}}$ (% $\Delta k_{\text{eff}}$ )
0.9	0.16
0.8	0.35
0.7	0.53
0.6	0.81
0.5	1.11
0.4	1.50
0.3	2.08
0.2	2.96
0.1	4.65
0.0	11.42

**Figure B-14. 5-cm gap in neutron absorber panels in MPC-24.**

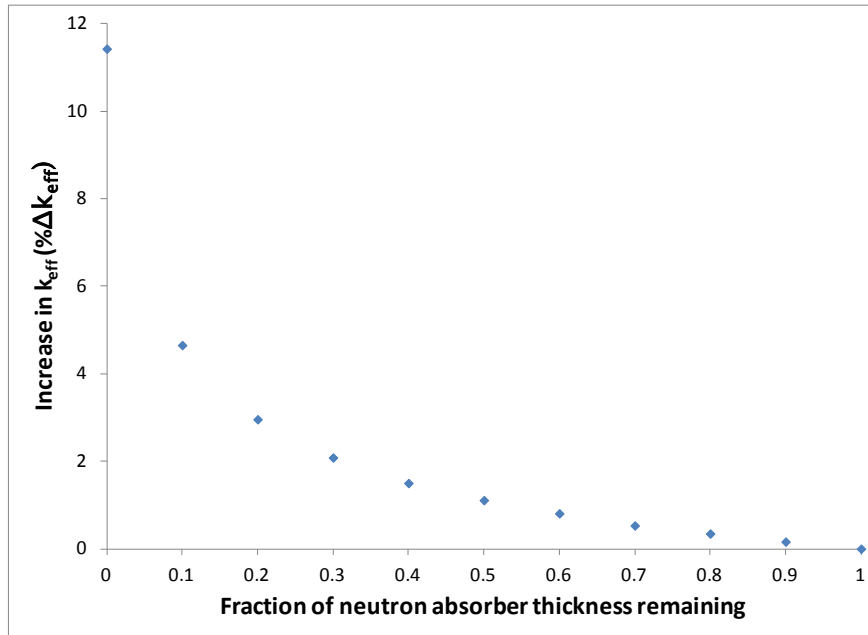
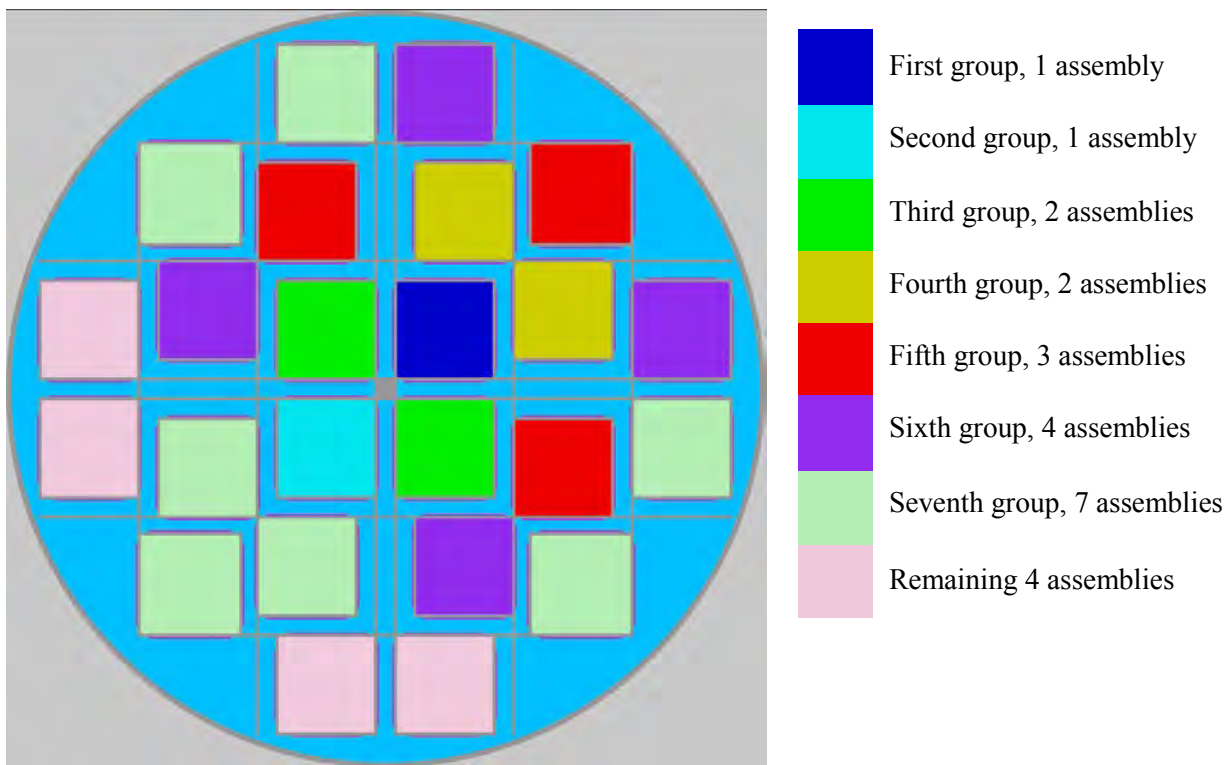


Figure B-15. Increase in  $k_{\text{eff}}$  in MPC-24 as a function of neutron absorber panel thickness.

### B.2.2 Varying Number of Reconfigured Assemblies

The results presented in Section B.2.1 assume that all 24 fuel assemblies in the MPC-24 cask experience the same fuel or neutron absorber reconfiguration within the respective configuration of interest. For each of four of the configurations studied in Section B.2.1, a series of calculations is performed to establish the  $k_{\text{eff}}$  increase as a function of the number of reconfigured assemblies within the cask. The four configurations considered are the limiting conditions for single rod failure, multiple rod failure, uniform rod pitch increase, and homogeneous rubble resulting from gross assembly failure.

The first fuel assembly to experience the reconfiguration being examined is selected in an attempt to maximize the  $k_{\text{eff}}$  increase, and is therefore one near the center of the cask. Additional assemblies are added in mostly symmetric groups of equal distance from the first reconfigured assembly. For some low numbers of reconfigured assemblies, multiple combinations of assemblies are considered. Seven combinations of reconfigured assemblies less are considered in the MPC-24. One order in which the assemblies experience reconfiguration is shown in Figure B-16.



**Figure B-16. One order of assembly reconfiguration in MPC-24 partial degradation configurations.**

#### B.2.2.1 Rod Failures

The single and multiple rod failure configurations that result in the largest increase in  $k_{\text{eff}}$ , as discussed in Section B.2.1.2, are used to study the impact of some assemblies suffering reconfiguration while others in the cask remain intact. The results for single rod failure are shown below in Table B-7 and Figure B-17. The results for multiple rod failure are shown below in Table B-8 and Figure B-18. The portion of the  $k_{\text{eff}}$  impact introduced by each group of assemblies is similar for both configurations, with more than 50% of the reactivity change coming after only four assemblies experience reconfiguration. More than 75% of the  $k_{\text{eff}}$  change is caused by the first 13 assembly reconfigurations, which account for just over half the cask load. This indicates that a reduced number of reconfigured assemblies will not significantly reduce the  $k_{\text{eff}}$  increase associated with fuel reconfiguration if the degraded assemblies are in close proximity, and particularly if they are in the center region of the cask.

**Table B-7. Increase in  $k_{\text{eff}}$  in MPC-24, single rod failure**

Number of degraded assemblies	Increase in $k_{\text{eff}}$ (% $\Delta k_{\text{eff}}$ )
1	0.04
2	0.06
2	0.06
4	0.08
5	0.09
9	0.11
13	0.12
20	0.14
24	0.15

**Table B-8. Increase in  $k_{\text{eff}}$  in MPC-24, multiple rod failures  
(48 failed rods)**

Number of degraded assemblies	Increase in $k_{\text{eff}}$ (% $\Delta k_{\text{eff}}$ )
1	0.34
2	0.56
2	0.60
4	1.11
5	1.10
9	1.53
13	1.69
20	1.98
24	2.01

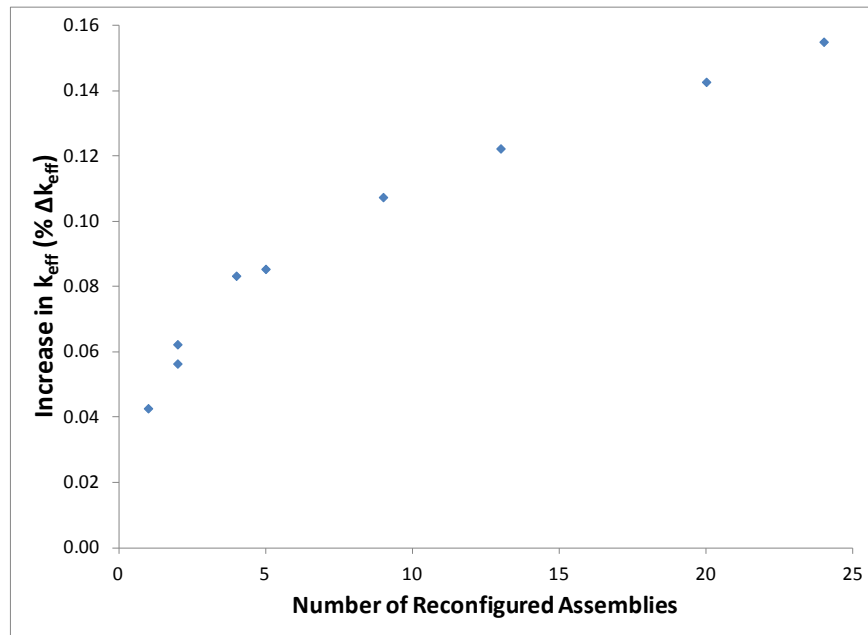


**Figure B-17. Single rod failure results for a range of number of assemblies experiencing reconfiguration in MPC-24.**

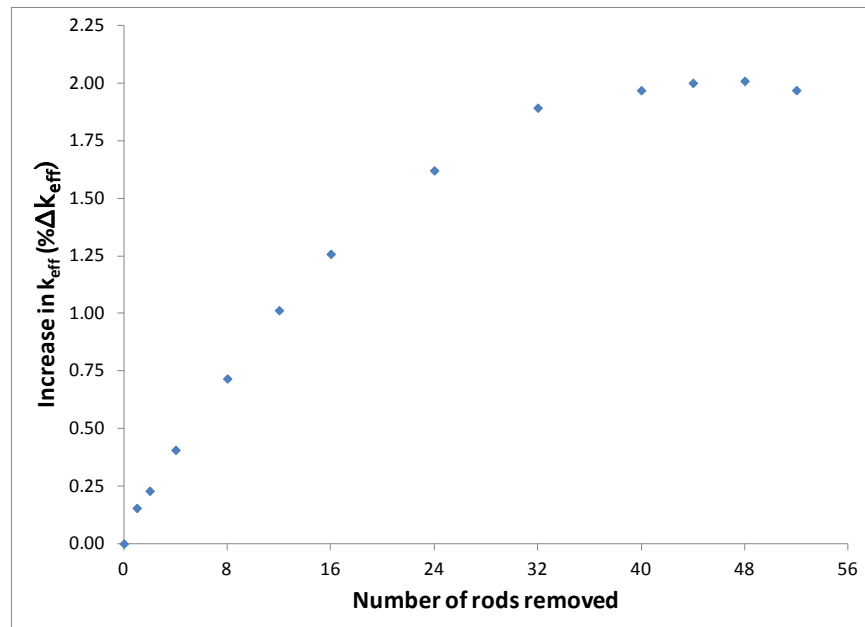


**Figure B-18. Multiple rod failure results for a range of number of assemblies experiencing reconfiguration in MPC-24.**

#### B.2.2.2 Loss of Rod Pitch Control, Uniform Pitch Increase

The maximum uniform pitch increase case is used to examine the  $k_{\text{eff}}$  impact of varying the number of assemblies that have experienced reconfiguration. The assembly configuration used for this study models

the outer row of fuel rods in contact with the inner wall of the fuel storage basket in each cell. The increase in  $k_{\text{eff}}$  for each number of reconfigured assemblies is provided in Table B-9 as well as Figure B-19. The general trend in the  $k_{\text{eff}}$  change for the uniform pitch increase cases is similar to that for single and multiple rod failure configurations presented in Section B.2.2.1. The first two reconfigured assemblies insert about 25% of the total  $k_{\text{eff}}$  increase, and 50% of the change has occurred with about five reconfigured assemblies. Approximately 80% of the increase in  $k_{\text{eff}}$  is caused by the first 13 reconfigured assemblies. This indicates that a reduced number of reconfigured assemblies will not significantly reduce the  $k_{\text{eff}}$  increase associated with fuel reconfiguration if the degraded assemblies are in close proximity, and particularly if they are in the center region of the cask.

**Table B-9. Increase in  $k_{\text{eff}}$  in MPC-24, uniform pitch increase**

Number of degraded assemblies	Increase in $k_{\text{eff}}$ (% $\Delta k_{\text{eff}}$ )
1	0.37
2	0.73
2	0.70
4	1.39
5	1.54
5	1.41
9	2.08
13	2.32
20	2.77
24	2.88

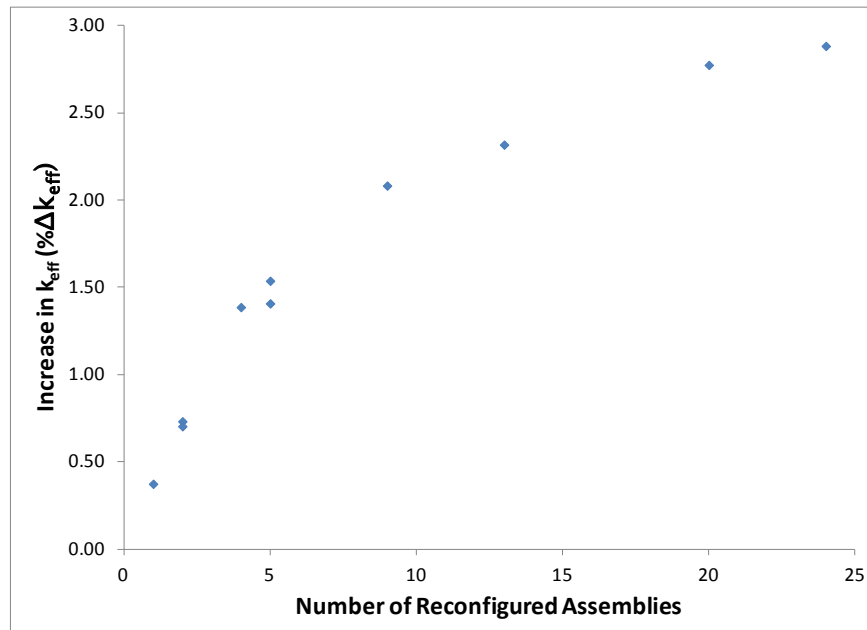


**Figure B-19. Uniform pitch increase results for a range of number of assemblies experiencing reconfiguration in MPC-24.**

### **B.2.2.3 Gross Assembly Failure, Homogeneous Rubble**

The homogeneous rubble modeling of the gross assembly failure configuration is the final configuration used to examine the  $k_{\text{eff}}$  impact of varying the number of assemblies that have experienced reconfiguration. The configuration used for this study models the homogeneous smear of fuel, cladding, and water filling the entire inside volume of the storage cell from the base plate to the lid of the cask. This configuration resulted in the largest  $k_{\text{eff}}$  increase of the homogeneous rubble configurations used in Section B.2.1.5. The increase in  $k_{\text{eff}}$  for each number of reconfigured assemblies is provided in Table B-10 as well as Figure B-20. The general trend in the  $k_{\text{eff}}$  change for the uniform pitch increase cases is different from that for single and multiple rod failure and uniform pitch expansion configurations presented in Sections B.2.2.1 and B.2.2.2. The first two reconfigured assemblies lower the cask  $k_{\text{eff}}$  because of the effects of homogenization and fissile material relocation. An increase in  $k_{\text{eff}}$  is noted for four or more reconfigured assemblies after a sufficient number of assemblies are reconfigured to relocate the most reactive portion of the cask to the top of the homogeneous rubble. Nearly 70% of the increase in  $k_{\text{eff}}$  is caused by the first nine reconfigured assemblies, and more than 80% of the total  $k_{\text{eff}}$  increase results from the reconfiguration of 13 assemblies. This indicates that a reduced number of reconfigured assemblies will not significantly reduce the  $k_{\text{eff}}$  increase associated with fuel reconfiguration if the degraded assemblies are in close proximity, and particularly if they are in the center region of the cask.

**Table B-10. Increase in  $k_{\text{eff}}$  in MPC-24, homogeneous rubble configuration of gross assembly failure**

Number of degraded assemblies	Increase in $k_{\text{eff}}$ (% $\Delta k_{\text{eff}}$ )
1	0.00
2	-0.04
2	-0.03
4	2.39
5	2.21
9	5.68
13	6.68
20	7.92
24	8.23

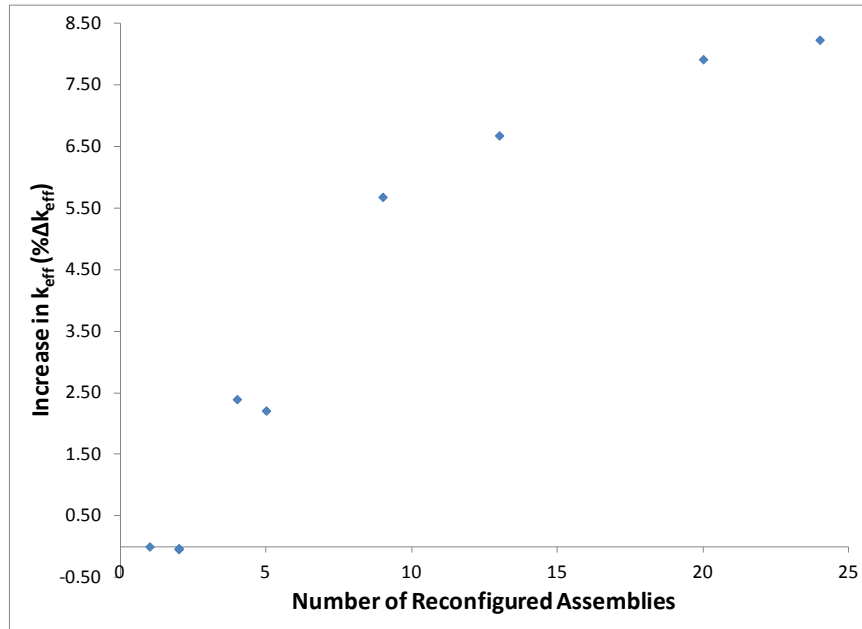


**Figure B-20. Homogeneous rubble results for a range of number of assemblies experiencing reconfiguration.**

### B.2.3 Combined Configurations

As discussed in Section 3.3, some of the mechanisms that could result in fuel reconfigurations could result in a combination of reconfigurations. Combined configurations are evaluated including: 12 failed rods with 50% clad thinning and 12 failed rods with a uniform pitch increase of 0.023-cm.

The multiple rod failure results presented in Section B.2.1.2 indicate that the failure of 12 fuel rods results in an increase in  $k_{\text{eff}}$  of just over 1%  $\Delta k_{\text{eff}}$ . This is approximately half the maximum increase for multiple failed rod configurations and is therefore selected as an intermediate configuration. The pitch increase is approximately half of the maximum pitch increase in the 20 normal storage cells. Based on the results presented in Figure B-6, the  $k_{\text{eff}}$  increase associated with a fuel rod pitch increase of approximately 0.02 cm is around 1%  $\Delta k_{\text{eff}}$ . The cladding thickness on all intact rods in both combined configurations is represented with 50% of the nominal thickness.

The results of the two combined configurations considered in the MPC-24 cask are presented in Table B-11. For comparison, the  $k_{\text{eff}}$  increase assuming each degraded configuration separately and the sum of the two is provided. The increase in  $k_{\text{eff}}$  associated with explicit modeling of the combined configurations is less than the estimated increase based on summing the individual increases. The conservatism of adding the separate effects is less than 0.5%  $\Delta k_{\text{eff}}$ . It appears that the linear combination of the  $k_{\text{eff}}$  increases is conservative, but more combined configurations would need to be investigated prior to drawing general conclusions. If it is confirmed, the  $k_{\text{eff}}$  increase caused by combinations of degradations could be conservatively bounded by adding the increase associated with individual configurations where applicable.

**Table B-11. Increase in  $k_{\text{eff}}$  in combined configurations for MPC-24**

Case	Increase in $k_{\text{eff}}$ (% $\Delta k_{\text{eff}}$ )
<b>Multiple failed rods and clad thinning</b>	
12 failed rods	1.01
50% clad thinning	2.87
Sum of $k_{\text{eff}}$ increases	3.88
Combined configuration model	3.45
Overestimation of $k_{\text{eff}}$ increase by summing individual effects	0.43
<b>Multiple failed rods and 0.02-cm increase in fuel rod pitch</b>	
12 failed rods	1.01
Uniform pitch increase	1.03
Sum of $k_{\text{eff}}$ increases	2.04
Combined configuration model	1.88
Overestimation of $k_{\text{eff}}$ increase by summing individual effects	0.16

### B.3 MPC-24 CASK SUMMARY

The detailed results for each configuration considered in the MPC-24 are provided above in Section B.2 and summarized in Table B-2.

The highest  $k_{\text{eff}}$  impact involves the preferential flooding of the cask basket in such a way as to moderate the fuel but leave the flux traps dry. The flux traps are an essential feature of the cask, and the basket is designed to make this preferential flooding configuration impossible. The preferential flooding configuration is thus viewed as not credible for normal conditions of transport. The configuration is included here to emphasize the importance of maintaining flux trap integrity despite any degradation of fuel, basket, or cask materials that occur during ES.

Other significant  $k_{\text{eff}}$  increases result from the gross assembly failure configurations and large axial misalignments. The gross assembly failure and misalignment configurations are judged not to be credible, so the  $k_{\text{eff}}$  increase associated with these configurations does not require mitigation. Fuel assembly misalignment of as much as 50 cm results in a  $k_{\text{eff}}$  increase of less than 1%  $\Delta k_{\text{eff}}$ , as shown in Figure B-9. Fuel assembly axial position will be sufficiently controlled that the more extreme misalignments need not be considered. The remaining degraded configurations all have  $k_{\text{eff}}$  increases less than 3%  $\Delta k_{\text{eff}}$ . The consequences of potential fuel reconfiguration are therefore judged to be manageable. The  $k_{\text{eff}}$  increase is small enough that the cask will be subcritical considering a safety analysis with intact fuel, which demonstrates that  $k_{\text{eff}}$  will be less than 0.95. This would not, however, be in compliance with current regulations relating to transportation of fissile material.

Analyses of a range of assemblies experiencing reconfiguration are documented in Section B.2.2. Four configurations, listed in Section 3.2, are evaluated, and the relative increase in  $k_{\text{eff}}$  as a function of the number of assemblies experiencing reconfiguration is largely similar among all four configurations. This approach is unlikely to produce a significant reduction in the increase in  $k_{\text{eff}}$  because the majority of the increase is associated with a relatively small fraction of the fuel load suffering reconfiguration if the reconfigured assemblies are selected in a worst-case, deterministic approach.

Two configurations are also investigated in Section B.2.3 that are created by combining two different reconfiguration paths. An intermediate number of failed rods, in this case 12, is combined with clad thinning in one case and with uniform pitch expansion in another. In both cases, the sum of the  $k_{\text{eff}}$

increases of each separate reconfiguration is slightly less than the increase determined from an explicit model of the combined configurations.

## Appendix C

### Sensitivity to Burnup and Cooling Time

A range of post-irradiation cooling times is considered in these analyses for both PWR and BWR fuel. Reference 44 provides details on the reactivity changes experienced by used fuel as a function of time since discharge. For the “Set 2” isotopes considered in these analyses, the reactivity of the depleted fuel decreases fairly steadily between 5 and about 100 years after discharge. The primary decays that drive this change are  $^{241}\text{Pu}$  into  $^{241}\text{Am}$  (14.4-year half-life) and  $^{155}\text{Eu}$  into  $^{155}\text{Gd}$  (4.8-year half-life). Beyond about 100 years after discharge, the reactivity of the fuel increases primarily due to the decay of  $^{241}\text{Am}$  (433-year half-life) and  $^{240}\text{Pu}$  (6561-year half-life). This increase continues until about 20,000 years after discharge. A plot for used PWR fuel considering the “Set 2” isotopes is shown in Figure C-1 and is expected to be similar for BWR fuel as well. Note that the maximum reactivity of used fuel considering “Set 2” isotopes occurs at discharge, and the reactivity after 5 years of cooling time is higher than the subsequent local maximum around 20,000 years later. These analyses considered cooling times ranging from 5 years to 300 years, with explicit reconfiguration calculations at cooling times of 5, 80, and 300 years. The effects of cooling time on the various configurations are considered, and they are discussed in more detail in the following subsections.

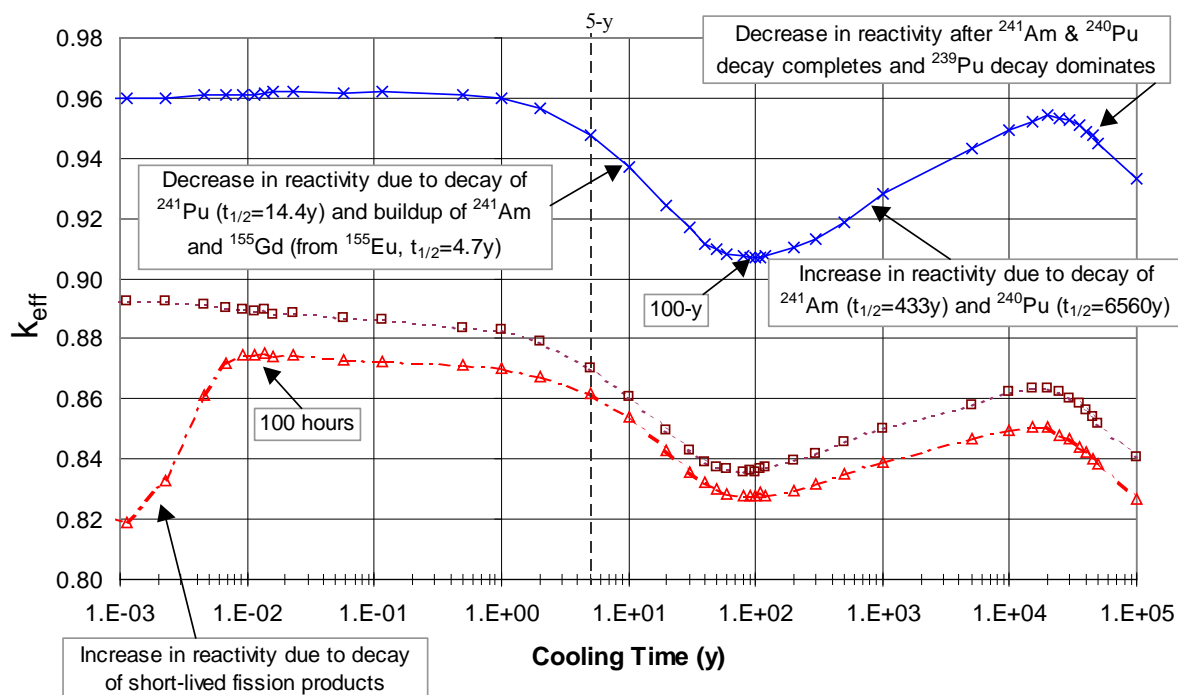


**Figure C-1. Reactivity behavior of fuel with cooling time in a GBC-32 cask (4.0 w/o 40 GWd/MTU burnup) [44].**

## C.1 RESULTS FOR GBC-32 CASK

As discussed in Section 4.2.1, a range of initial fuel enrichments is considered to generate a representative loading curve for fuel to be stored in the GBC-32. The burnup limit for loading fuel with an initial enrichment of 5 w/o  $^{235}\text{U}$  is determined to be approximately 44.25 GWd/MTU with 5 years of post-irradiation cooling time. Fuel with a discharge burnup of 70 GWd/MTU is also considered in the GBC-32 to investigate any potential sensitivity of the consequences of fuel reconfiguration to burnup. For both 5 w/o initial enrichment burnups, cooling times of 5, 80 and 300 years are considered to examine potential impacts of cooling time on the consequences of fuel reconfiguration.

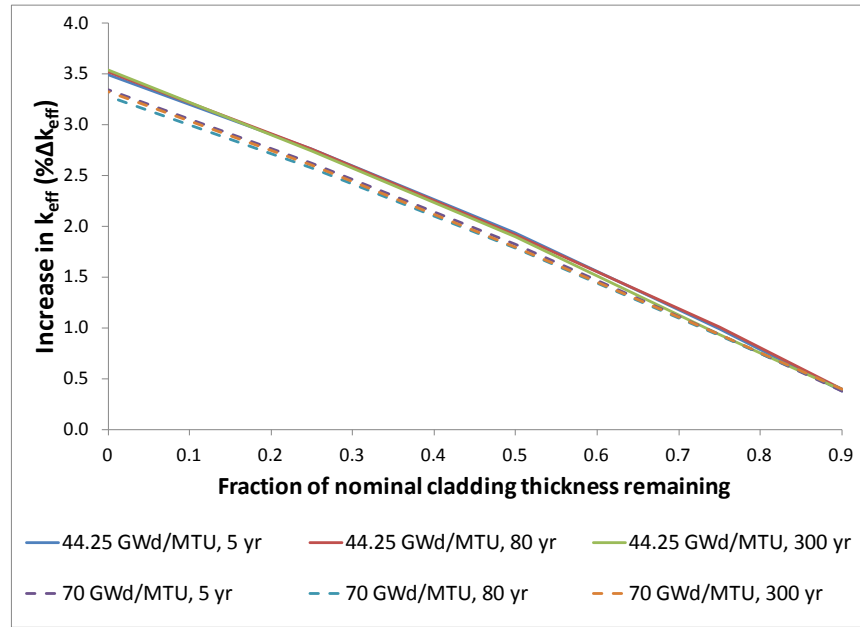
The nominal condition  $k_{\text{eff}}$  values are provided in Table C-1. The reduction in  $k_{\text{eff}}$  caused by cooling time increases with burnup, which is expected given the larger inventory of  $^{241}\text{Am}$  and  $^{155}\text{Gd}$  at higher burnups. The 80-year cooling time also has the smallest  $k_{\text{eff}}$  for intact fuel, which is also expected as discussed above. It should be noted that the nominal  $k_{\text{eff}}$  values after 300 years of cooling time are still significantly lower than those after 5 years of cooling time. This decrease in  $k_{\text{eff}}$  for intact fuel would have to be exceeded by a larger  $k_{\text{eff}}$  increase due to reconfiguration before the longer cooling time case would represent a limiting condition. The results of explicit reconfiguration calculations are presented in subsequent subsections and compared to the differences in nominal  $k_{\text{eff}}$  values.

**Table C-1. Nominal  $k_{\text{eff}}$  results for enrichment, burnup, and cooling time cases considered in GBC-32**

Enrichment (w/o $^{235}\text{U}$ )	Burnup (GWd/MTU)	Cooling time (years)	KENO V.a		KENO-VI	
			$k_{\text{eff}}$	$\sigma$	$k_{\text{eff}}$	$\sigma$
5.0	44.25	5	0.94000	0.00010	0.93995	0.00010
		80	0.90003	0.00010	0.89991	0.00010
		300	0.90477	0.00010	0.90473	0.00010
	70.0	5	0.85040	0.00010	0.85048	0.00010
		80	0.78863	0.00010	0.78865	0.00010
		300	0.79472	0.00010	0.79478	0.00010

### C.1.1 Clad Thinning/Loss

The increase in  $k_{\text{eff}}$  associated with clad thinning and removal is shown as a function of remaining cladding thickness in Figure C-2 for fuel of both burnups and all three cooling times. There is a trend that the increase in  $k_{\text{eff}}$  is smaller at 70 GWd/MTU than it is at 44.25 GWd/MTU. The increase in  $k_{\text{eff}}$  is approximately 0.04%  $\Delta k_{\text{eff}}$  larger after 300 years of cooling time than it is after 5 years, but this difference is very small compared to the change in nominal  $k_{\text{eff}}$ . These results show that the increase in  $k_{\text{eff}}$  shown in Section 5.1.1.1 is sufficiently large.

Figure C-2. Increase in  $k_{\text{eff}}$  as a function of cladding thickness remaining.

### C.1.2 Rod Failures

The results of the single and multiple rod failure configurations of fuel rod failure are provided in Table C-2 and Table C-3, respectively. The variation of the increase in  $k_{\text{eff}}$  for single rod removal is small and shows no significant trends as a function of burnup or cooling time. The multiple rod removal results show a clear trend of reduced consequence at high burnup compared to moderate burnup; thus, the 44.25 GWd/MTU cases manifest a larger  $k_{\text{eff}}$  increase. The effect of cooling time appears to be significantly smaller, with essentially no sensitivity at 44.25 GWd/MTU, and only a reduction in the consequence of reconfiguration at longer cooling times for the high-burnup fuel. These results indicate that the  $k_{\text{eff}}$  increases identified in Section 5.1.1.2 are limiting.

Table C-2. Single rod removal results for 17 × 17 OFA in GBC-32

Burnup (GWd/MTU)	Cooling time (years)	Location	Increase in $k_{\text{eff}}$ (% $\Delta k_{\text{eff}}$ )
44.25	5	H5	0.10
44.25	80	H7	0.09
44.25	300	G7	0.10
70	5	H5	0.09
70	80	G7	0.10
70	300	G5	0.10

**Table C-3. Multiple rod removal results for 17 × 17 OFA in GBC-32**

Burnup (GWd/MTU)	Cooling time (years)	Increase in $k_{\text{eff}}$ (% $\Delta k_{\text{eff}}$ )
44.25	5	1.86
44.25	80	1.86
44.25	300	1.87
70	5	1.69
70	80	1.62
70	300	1.62

**C.1.3 Loss of Rod Pitch Control**

The increase in  $k_{\text{eff}}$  resulting from uniform pin pitch expansion for both burnups and all three cooling times is considered for the configuration in which the unit cell boundary contacts the inside surface of the storage cell wall. The use of this less extreme case provides an acceptable indication of the sensitivity of the consequence of this configuration to burnup and cooling time variations. The results of the fully expanded configuration, with cladding, are presented below in Table C-4. Moderate sensitivities are apparent that lower the impact of reconfiguration both with increasing burnup and with increasing cooling time for a fixed burnup. These results provide confidence that the results presented in Section 5.1.1.3 are limiting.

**Table C-4. Increase in  $k_{\text{eff}}$  caused by uniform fuel pin pitch expansion**

Burnup (GWd/MTU)	Cooling time (years)	Increase in $k_{\text{eff}}$ (% $\Delta k_{\text{eff}}$ )
44.25	5	1.69
44.25	80	1.67
44.25	300	1.66
70	5	1.53
70	80	1.44
70	300	1.42

**C.1.4 Loss of Assembly Position Control**

The increase in  $k_{\text{eff}}$  caused by a 20-cm axial misalignment for both burnups and all three cooling times is presented in Table C-5. The results show that the consequence of fuel displacement increases with both burnup and cooling time. The maximum change relative to the 44.25 GWd/MTU and 5-year cooling is approximately 1.67%  $\Delta k_{\text{eff}}$ . This is a significant increase and occurs for 70 GWd/MTU and 300 years of cooling time. The reduction in base case  $k_{\text{eff}}$  due only to cooling time at this burnup is over 5.5%  $\Delta k_{\text{eff}}$ . The 300-year cooling time condition with only 44.25-GWd/MTU burnup causes an increase that is larger by 0.95%  $\Delta k_{\text{eff}}$ . For this case, the decrease in nominal (i.e., 44.25 GWd/MTU and 300-year cooling time)  $k_{\text{eff}}$  is more than 3.5%  $\Delta k_{\text{eff}}$ , when compared to the  $k_{\text{eff}}$  value for the case with only 5 years of cooling time. These results indicate that the results presented in Section 5.1.1.4 are large enough to account for additional impacts at high burnup and long cooling times.

**Table C-5. Increase in  $k_{\text{eff}}$  for limited assembly axial displacement in GBC-32**

Burnup (GWd/MTU)	Cooling time (years)	Increase in $k_{\text{eff}}$ (% $\Delta k_{\text{eff}}$ )
44.25	5	10.82
44.25	80	11.82
44.25	300	11.77
70	5	11.74
70	80	12.46
70	300	12.49

### C.1.5 Gross Assembly Failure

The results for both configurations of gross assembly failure are provided for both burnups and all three cooling times in Table C-6. Both the uniform pellet array and the homogeneous rubble configuration show little sensitivity to burnup but a larger increase in  $k_{\text{eff}}$  with increasing cooling time. The increases are smaller for the uniform pellet array configuration than for the homogeneous rubble configuration. The maximum difference is for fuel with 44.25-GWd/MTU burnup and 300 years of cooling time and is approximately 1.04%  $\Delta k_{\text{eff}}$ . The decrease in nominal  $k_{\text{eff}}$  for this fuel condition is more than 3.5%  $\Delta k_{\text{eff}}$ , so the results in Section 5.1.1.5 are sufficiently large to account for variations associated with higher burnups and longer cooling times.

**Table C-6. Increase in  $k_{\text{eff}}$  caused by gross fuel assembly failure in GBC-32**

Burnup (GWd/MTU)	Cooling time (years)	Increase in $k_{\text{eff}}$ (% $\Delta k_{\text{eff}}$ )
<b>Ordered pellet array</b>		
44.25	5	21.37
44.25	80	22.21
44.25	300	22.21
70	5	21.43
70	80	21.63
70	300	21.77
<b>Homogeneous rubble</b>		
44.25	5	14.30
44.25	80	15.29
44.25	300	15.34
70	5	14.20
70	80	14.77
70	300	14.90

### C.1.6 Neutron Absorber Degradation

The increase in  $k_{\text{eff}}$  caused by neutron absorber panel defects is shown in Table C-7 for both burnups and all three cooling times for defect sizes of both 5 and 10 cm. The results show an increase in the consequence of panel degradation at higher burnups and higher cooling times. The maximum change in

$k_{\text{eff}}$  increase is approximately 0.3%  $\Delta k_{\text{eff}}$ , which is significantly smaller than the lower nominal  $k_{\text{eff}}$  at the higher burnups and cooling times. The results presented in Section 5.1.1.6 for the neutron absorber panel defect configuration are therefore large enough to account for the effects of higher burnups and cooling times.

The increase in  $k_{\text{eff}}$  increase due to uniform neutron absorber panel thinning at 44.25 GWd/MTU and 5 years of cooling time are shown in Table C-8. The increase in  $k_{\text{eff}}$  is smaller at the higher burnup, thus confirming that the results presented in Section 5.1.1.6 for uniform panel thinning are also conservative.

**Table C-7. Increase in  $k_{\text{eff}}$  caused by neutron absorber panel defects**

Burnup (GWd/MTU)	Cooling time (years)	Defect elevation (cm)	Increase in $k_{\text{eff}}$ (% $\Delta k_{\text{eff}}$ )
5-cm defect			
44.25	5	348.86	1.05
44.25	80	348.86	1.22
44.25	300	348.86	1.21
70	5	348.86	1.17
70	80	348.86	1.24
70	300	348.86	1.24
10-cm defect			
44.25	5	348.86	2.33
44.25	80	348.86	2.59
44.25	300	348.86	2.56
70	5	348.86	2.54
70	80	348.86	2.59
70	300	348.86	2.63

**Table C-8. Increase in  $k_{\text{eff}}$  caused by uniform neutron absorber panel thinning (44.25 GWd/MTU burnup, 5-year cooling time)**

Fraction of neutron absorber panel thickness remaining	Increase in $k_{\text{eff}}$ (% $\Delta k_{\text{eff}}$ )
0.9	0.25
0.8	0.53
0.7	0.87
0.6	1.26
0.5	1.72
0.4	2.30
0.3	2.99
0.2	3.94
0.1	5.36
0.0	8.46

## C.2 RESULTS FOR MPC-68 CASK

As discussed in Section 4.2.2, a range of burnups and cooling times is considered to investigate the sensitivity of the consequence of reconfiguration to these parameters. Fuel with a discharge burnup of 70 GWd/MTU is considered in the MPC-68 in addition to the fresh fuel and 35-GWd/MTU burnup used discussed in Section 5.2. For fuel with 5 w/o initial enrichment and both 35-GWd/MTU and 70-GWd/MTU burnups, cooling times of 5, 80, and 300 years are considered to examine potential impacts of cooling time on the consequences of fuel reconfiguration.

The nominal condition  $k_{\text{eff}}$  values are provided in Table C-9. The reduction in  $k_{\text{eff}}$  caused by cooling time increases with burnup, which is expected given the larger inventory of  $^{241}\text{Am}$  and  $^{155}\text{Gd}$  at higher burnups. The 80-year cooling time also has the smallest  $k_{\text{eff}}$  for intact fuel, which is also expected as discussed above. It should be noted that the nominal  $k_{\text{eff}}$  values after 300 years of cooling time are still lower than after 5 years of cooling time. This decrease in  $k_{\text{eff}}$  for intact fuel would have to be exceeded by a larger  $k_{\text{eff}}$  increase due to reconfiguration before the longer cooling time case would represent a limiting condition. The reductions in nominal  $k_{\text{eff}}$  values for the BWR fuel in the MPC-68 are significantly smaller than those experienced by the PWR fuel in GBC-32, despite similar assembly average burnup values. This effect is the result of the extreme burnup profile, described in Appendix E, which has very low relative burnups in the top few nodes. These lower burnups lead to lower inventories of  $^{241}\text{Am}$  and  $^{155}\text{Eu}$  in the upper regions of the assembly which drive reactivity of the overall cask. These lower inventories lead to smaller changes in  $k_{\text{eff}}$  due to radioactive decay during the period of post-irradiation cooling. The results of explicit reconfiguration calculations are presented in subsequent subsections and compared to the differences in nominal  $k_{\text{eff}}$  values.

**Table C-9. Nominal  $k_{\text{eff}}$  results for enrichment, burnup, and cooling time cases considered in MPC-68, channeled and unchanneled fuel**

Channel present	Burnup (GWd/MTU)	Cooling time (years)	KENO V.a		KENO-VI	
			$k_{\text{eff}}$	$\sigma$	$k_{\text{eff}}$	$\sigma$
Yes	35.0	0	0.96800	0.00010	0.96828	0.00010
		5	0.83269	0.00010	0.83258	0.00010
		80	0.82425	0.00010	0.82416	0.00010
	70.0	300	0.82522	0.00010	0.82528	0.00010
		5	0.76709	0.00010	0.76693	0.00010
		80	0.75256	0.00010	0.75240	0.00010
	0	300	0.75412	0.00010	0.75405	0.00010
		0	0.96768	0.00010	0.96763	0.00010
		5	0.83434	0.00010	0.83420	0.00010
No	35.0	80	0.82615	0.00010	0.82621	0.00010
		300	0.82723	0.00010	0.82714	0.00010
		5	0.76994	0.00010	0.76971	0.00010
	70.0	80	0.75588	0.00010	0.75560	0.00010
		300	0.75731	0.00010	0.75705	0.00010

### C.2.1 Clad Thinning/Loss

The increase in  $k_{\text{eff}}$  associated with clad thinning and removal is shown as a function of remaining cladding thickness in Figure C-3 for fresh fuel and fuel of both burnups and all three cooling times. There

is a trend that the increase in  $k_{\text{eff}}$  is smaller with increasing burnup. There is no clear trend in the increase of  $k_{\text{eff}}$  as a function of cooling time. These results show that the increase in  $k_{\text{eff}}$  reported for fresh fuel in Section 5.2.1.1 bounds the effects of burnup and cooling time.

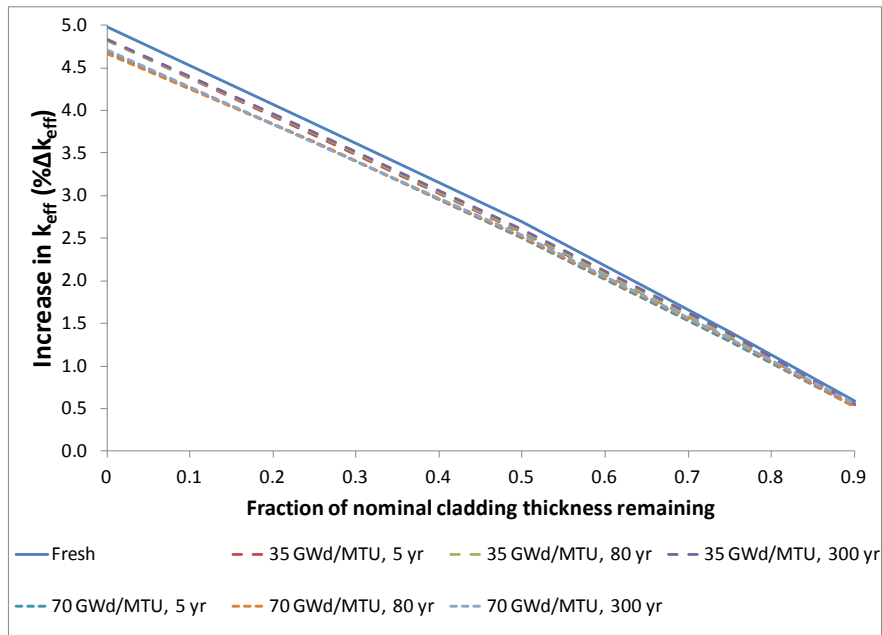


Figure C-3. Increase in  $k_{\text{eff}}$  as a function of cladding thickness remaining.

### C.2.2 Rod Failures

The results of fuel reconfiguration calculations for the single and multiple rod removal configurations are shown below in Table C-10 and Table C-11, respectively. For single rod failure configurations, no sensitivity is apparent as a function of either burnup or cooling time. The fresh fuel single rod removal  $k_{\text{eff}}$  increase is larger than the results for UNF cases. For multiple rod failure configurations, a slight trend appears to cause small increases in  $k_{\text{eff}}$  change with cooling time but a decrease in  $k_{\text{eff}}$  change at high burnup. The largest difference compared to the results presented in Section 5.2.1.2 is approximately 0.02%  $\Delta k_{\text{eff}}$  and occurs for multiple rod failure and UNF with 300 years of cooling time. At this cooling time, the nominal  $k_{\text{eff}}$  is approximately 0.75%  $\Delta k_{\text{eff}}$  lower than the 5-year cooling time base case  $k_{\text{eff}}$  value. These results indicate that the increase in  $k_{\text{eff}}$  reported in Section 5.2.1.2 is sufficiently large to account for potential effects of additional burnup and cooling time for rod failure configurations.

**Table C-10. Single rod removal results for GE  $10 \times 10$  fuel  
in MPC-68, intact channel**

Burnup (GWd/MTU)	Cooling time (years)	Location	Increase in $k_{\text{eff}}$ (% $\Delta k_{\text{eff}}$ )
0	0	H7	0.29
35	5	G7	0.26
35	80	D4	0.27
35	300	G7	0.28
70	5	D3	0.26
70	80	G7	0.25
70	300	G7	0.26

**Table C-11. Multiple rod removal results for  
GE  $10 \times 10$  fuel in MPC-68, intact channel**

Burnup (GWd/MTU)	Cooling time (years)	Increase in $k_{\text{eff}}$ (% $\Delta k_{\text{eff}}$ )
0	0	2.24
35	5	2.40
35	80	2.40
35	300	2.42
70	5	2.30
70	80	2.31
70	300	2.32

### C.2.3 Loss of Rod Pitch Control

The increase in  $k_{\text{eff}}$  resulting from uniform pin pitch expansion for fresh fuel as well as both burnups and all three cooling times is considered for the configuration in which the unit cell boundary contacts the inside surface of the storage cell wall. The use of this less extreme case provides an acceptable indication of the sensitivity of the consequence of this configuration to burnup and cooling time variations. The results of the fully expanded configuration, with cladding, are presented below in Table C-12. The increase in  $k_{\text{eff}}$  drops both as a function of burnup and cooling time, though the effect of burnup appears to be significantly larger. These results provide confidence that the results presented for fresh fuel in Section 5.2.1.3 bound the results for all burnups and cooling times.

**Table C-12. Results for loss of rod pitch control with cladding intact in MPC-68**

Burnup (GWd/MTU)	Cooling time (years)	Increase in $k_{\text{eff}}$ (% $\Delta k_{\text{eff}}$ )
<b>Channel intact</b>		
0	0	11.00
35	5	9.55
35	80	9.46
35	300	9.49
70	5	8.68
70	80	8.51
70	300	8.52
<b>Channel removed</b>		
0	0	12.07
35	5	10.56
35	80	10.45
35	300	10.48
70	5	9.64
70	80	9.40
70	300	9.43

#### C.2.4 Loss of Assembly Position Control

The increase in  $k_{\text{eff}}$  caused by a 20-cm axial misalignment for both burnups and all three cooling times is presented in Table C-13. The results show that the consequence of fuel displacement increases with both burnup and cooling time. The 300-year cooling time condition with 35-GWd/MTU burnup causes an increase that is 0.37%  $\Delta k_{\text{eff}}$  larger than the 5-year cooling time. For this case, the decrease in nominal  $k_{\text{eff}}$  is more than 0.75%  $\Delta k_{\text{eff}}$ ; thus, the cask with displaced fuel has a lower final  $k_{\text{eff}}$  value. The maximum change relative to the 35 GWd/MTU and 5-year cooling time is approximately 2.2%  $\Delta k_{\text{eff}}$  and occurs for 70 GWd/MTU and 300 years of cooling time. The reduction in base case  $k_{\text{eff}}$  due only to cooling time at this burnup is approximately 1.3%  $\Delta k_{\text{eff}}$ . The nominal  $k_{\text{eff}}$  for this high-burnup and high cooling time condition is significantly subcritical, so this fuel condition does not represent a challenge to the criticality safety of the cask.

**Table C-13. Increase in  $k_{\text{eff}}$  for limited assembly axial displacement in MPC-68, intact channel**

Burnup (GWd/MTU)	Cooling time (years)	Increase in $k_{\text{eff}}$ (% $\Delta k_{\text{eff}}$ )
35	5	6.29
35	80	6.70
35	300	6.66
70	5	8.03
70	80	8.52
70	300	8.49

### C.2.5 Gross Assembly Failure

The results for both configurations of gross assembly failure are provided for both burnups and all three cooling times in Table C-14. Both the uniform pellet array and the homogeneous rubble configuration show slightly larger  $k_{\text{eff}}$  increases at higher burnup, and a larger increase in  $k_{\text{eff}}$  with increasing cooling time. The increases are smaller for the homogeneous rubble configuration than for the uniform pellet array configuration. The maximum difference is for fuel with 70-GWd/MTU burnup and 300 years of cooling time and is approximately 1.23%  $\Delta k_{\text{eff}}$ . The decrease in nominal  $k_{\text{eff}}$  for this fuel condition is more than 1.30%  $\Delta k_{\text{eff}}$ , so the results in Section 5.2.1.5 are sufficiently large to account for variations associated with higher burnups and longer cooling times.

**Table C-14. Increase in  $k_{\text{eff}}$  caused by gross fuel assembly failure in MPC-68**

Burnup (GWd/MTU)	Cooling time (years)	Increase in $k_{\text{eff}}$ (% $\Delta k_{\text{eff}}$ )
<b>Homogeneous rubble, channel removed</b>		
35	5	29.36
35	80	29.87
35	300	29.83
70	5	29.93
70	80	30.33
70	300	30.40
<b>Uniform pellet array, channel removed</b>		
35	5	34.40
35	80	34.88
35	300	34.87
70	5	35.22
70	80	35.57
70	300	35.63

### C.2.6 Neutron absorber Degradation

The increase in  $k_{\text{eff}}$  caused by neutron absorber panel defects is shown in Table C-15 for both burnups and all three cooling times for a defect size of 5 cm and in Table C-16 for 10 cm defects. The results show an increase in the consequence of panel degradation at higher burnups and higher cooling times. The maximum change in  $k_{\text{eff}}$  increase is approximately 0.7%  $\Delta k_{\text{eff}}$ , which is smaller than the lower nominal  $k_{\text{eff}}$  at the higher burnups and cooling times. The results presented in Section 5.2.1.6 for the neutron absorber panel defect configuration are therefore large enough to account for the effects of higher burnups and cooling times.

The increase in  $k_{\text{eff}}$  increase due to uniform neutron absorber panel thinning at 35 GWd/MTU and 5 years of cooling time are shown in Table C-17. The increase in  $k_{\text{eff}}$  is smaller at the higher burnup, thus confirming that the results presented in Section 5.2.1.6 for uniform panel thinning are also conservative.

**Table C-15. Maximum  $k_{\text{eff}}$  increase caused by a 5-cm neutron absorber defect in MPC-68, intact channel**

Burnup (GWd/MTU)	Cooling time (years)	Defect elevation (cm)	Increase in $k_{\text{eff}}$ (% $\Delta k_{\text{eff}}$ )
0	0	190.50	0.83
35	5	365.13	2.49
35	80	365.13	2.58
35	300	365.13	2.58
70	5	370.42	2.82
70	80	370.42	2.90
70	300	370.42	2.89

**Table C-16. Maximum  $k_{\text{eff}}$  increase caused by a 10-cm neutron absorber defect in MPC-68, intact channel**

Burnup (GWd/MTU)	Cooling time (years)	Defect elevation (cm)	Increase in $k_{\text{eff}}$ (% $\Delta k_{\text{eff}}$ )
0	0	190.50	2.68
35	5	365.13	5.62
35	80	365.13	5.80
35	300	365.13	5.78
70	5	370.42	6.24
70	80	370.42	6.33
70	300	370.42	6.36

**Table C-17. Increase in  $k_{\text{eff}}$  caused by uniform neutron absorber panel thinning (35-GWd/MTU burnup, 5-year cooling time)**

Fraction of neutron absorber panel thickness remaining	Increase in $k_{\text{eff}}$ (% $\Delta k_{\text{eff}}$ )
0.9	0.47
0.8	1.02
0.7	1.64
0.6	2.33
0.5	3.16
0.4	4.16
0.3	5.45
0.2	7.32
0.1	10.26
0.0	18.80

## Appendix D

### Details of Cask Modeling

This appendix provides additional details of the MPC-24 and MPC-68 cask models used in this analysis. Details of the GBC-32 cask are contained within Section 2.1 of Ref. 39.

#### D.1 MPC-24

The bottom of the active fuel is modeled 10.16 cm (4 in.) above the top surface of the cask base plate. The top of the active fuel is approximately 77 cm (30.3125 in.) from the bottom surface of the cask lid. The volume above and below the active fuel is normally occupied by spacers and fuel assembly hardware, but these are neglected in the model. The material in the spacers is not credited in any configuration, although the axial position control provided by the spacers is considered in assessing credibility of axial misalignment configurations. All fuel assemblies are modeled as nominally centered within the fuel storage cells in the MPC-24 basket.

The basket dimensions are provided in Table D-1. The basket is positioned on the cask base plate, creating a gap of approximately 4.60 cm (1 13/16 in.) between the top of the basket walls and the lower surface of the lid. The basket configuration consists of 20 standard storage cells and four oversized storage cells. The model is created with dimensions taken from the SAR for the HI-STAR 100 system, Refs. 36–38.

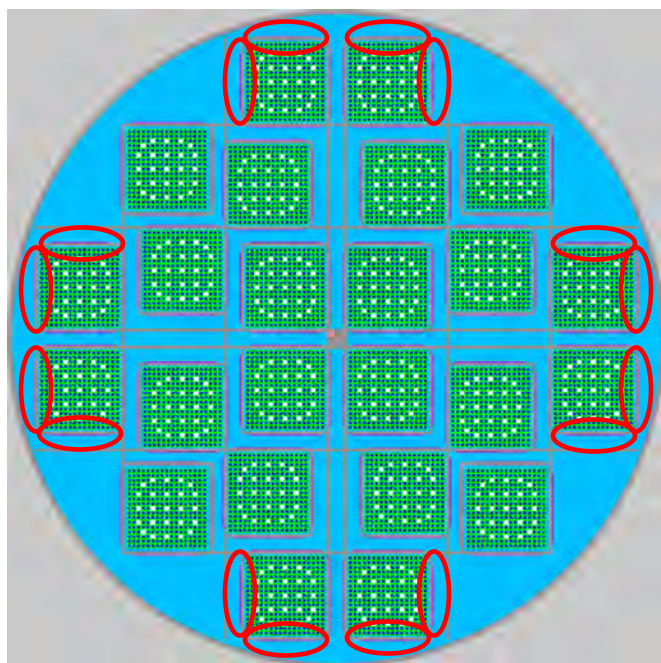
Two widths of neutron absorber panels are used in the MPC-24, and relevant dimensions are provided in Table D-2. The majority of the panels are “wide,” but 16 panels near the periphery of the basket are “narrow” panels. The locations containing narrow neutron absorber panels are indicated in Figure D-1. It is assumed that the entire panel thickness is neutron absorber; in other words, no face cladding is included in the panel models. The panels overlap the bottom of the active fuel by approximately 2.86 cm (1 1/8 in.) and overlap the top of the active fuel by approximately 27.6 cm (10 7/8 in.). The panel dimensions are taken from the SAR for the HI-STAR 100 system Refs. 36–38.

**Table D-1. MPC-24 basket dimensions**

Parameter	Dimension (cm)	Dimension (in.)
Wall thickness	0.79	0.3125
Basket height	448.31	176.5
Standard cell inner dimension	22.225	8.75
Oversized cell inner dimension	22.987	9.05

**Table D-2. MPC-24 Neutron absorber panel dimensions**

Parameter	Dimension (cm)	Dimension (in.)
Wide panel width	19.05	7.5
Narrow panel width	15.875	6.25
Panel thickness	0.26	0.101
Panel length	396.24	156
Panel axial position (from base plate)	7.30	2.875
Wrapper thickness	0.15	0.06
Neutron absorber areal density	0.0372 g $^{10}\text{B}/\text{cm}^2$	

**Figure D-1. Locations of narrow neutron absorber panels in MPC-24 basket.**

## D.2 MPC-68

The bottom of the active fuel is modeled 33.78 cm (~13.3 in.) above the top surface of the cask base plate. The top of the active fuel is approximately 38.13 cm (~15 in.) from the bottom surface of the cask lid. The volume above and below the active fuel is normally occupied by spacers and fuel assembly hardware, but these are neglected in the model. The material in the spacers is not credited in any configuration, although the axial position control provided by the spacers is considered in assessing credibility of axial misalignment configurations. All fuel assemblies are modeled as nominally centered within the fuel storage cells in the MPC-68 basket.

The basket dimensions are provided in Table D-3. The basket is positioned on the cask base plate. A gap of 5.87 cm (~2.31 in.) exists between the top of the basket walls and the lower surface of the cask lid.

The boron-based neutron absorber panels used in the MPC-68 are modeled with dimensions shown in Table D-4. The face clad is modeled as pure aluminum. The neutron absorber panel is modeled as centered in a channel with a thickness of 0.2844 cm (0.112 in.). The gaps between the neutron absorber panel faces and the wrapper walls are filled with water. The panels overlap the top and bottom of the active fuel by 6.35 cm (2.5 in.). The dimensions for the MPC-68 models are taken from Ref. 7.

**Table D-3. MPC-68 basket dimensions**

<b>Parameter</b>	<b>Dimension (cm)</b>	<b>Dimension (in.)</b>
Wall thickness	0.635	0.25
Basket height	447.04	176.0
Cell inner dimension	15.69	6.18

**Table D-4. MPC-68 neutron absorber panel dimensions**

<b>Parameter</b>	<b>Dimension (cm)</b>	<b>Dimension (in.)</b>
Panel width	12.065	4.750
Neutron absorber core thickness	0.2054	0.081
Face cladding thickness	0.0256	0.010
Panel length	393.7	155
Panel axial position (from base plate)	27.43	10.799
Wrapper thickness	0.1905	0.075
Neutron absorber areal density	0.0276 g $^{10}\text{B}/\text{cm}^2$	



## Appendix E

### Development of BWR Depletion Conditions

This appendix provides details about the selection of the axial burnup profile, the development of the axial moderator profile, and the calculation of the specific power used in the BWR depletion calculations. The data is selected from the CRC data available in Refs. 46 and 47.

The axial burnup profile modeled impacts the calculated  $k_{\text{eff}}$  of UNF. As discussed in Ref. 40, the gradient at the top end of the fuel assembly is the most important feature in driving reactivity in one profile relative to another. It is expected that BWR profiles are more severe than PWR profiles because the top of the assemblies experience high void fractions. This high void fraction and corresponding lack of moderation lead to lower relative burnups in the top section of a BWR assembly than a PWR assembly. The low-burnup region will also have a relative increase in plutonium generation at the same burnup. For these reasons, the axial burnup profiles in the PWR database [41] should not be used for BWR fuel. No analogous database of BWR axial burnup profiles exists, so axial burnup profiles from the CRC data for Quad Cities Unit 2 [46] and LaSalle Unit 1 [47] are surveyed for profile selection.

The relative burnup profiles for all assemblies presented in Refs. 46 and 47 are generated and compared to determine a potentially limiting burnup profile for use in these analyses. The two plants have different active fuel heights, so candidates are first selected from each plant, and then the potentially limiting profiles are compared to select the profile for use in these calculations. The relative burnup profiles are compared based on the integral relative burnup over two different axial extents from the top of the assembly. The relative burnups of the top three and top six nodes are summed, with lower sums indicating lower relative burnup leading to higher reactivity. The top three nodes include the top 45.72 cm (18 in.) and the top six nodes include the top 91.44 cm (36 in.) for each assembly. For Quad Cities Unit 2, assembly E7 has the lowest relative burnup in the top three nodes, but assembly F8 has the lowest relative burnup over the top six nodes. For LaSalle Unit 1, assembly C30 has the lowest relative burnup over both three and six nodes for all the assemblies considered. The relative burnup profile for assembly C30 is more severe over both the top three nodes and top six nodes than either E7 or F8 from Quad Cities Unit 2. The three potential profiles, including the integrated relative burnup over the top three and top six nodes, are provided in Table E-1. The LaSalle fuel has an active length of 150 in., compared to the 144-in. active length of fuel used at Quad Cities. This difference in length is not expected to cause a significant difference in calculated  $k_{\text{eff}}$ , so the use of LaSalle Unit 1 fuel data is acceptable for these calculations. A comprehensive study would be required to identify a limiting axial burnup profile for BWR fuel, though the profile used here is similar to a potentially limiting profile identified in Ref. 53.

The water density, which includes both the actual water density and the density reduction due to the presence of steam voids, is provided for each axial node at each case for each assembly in Refs. 46 and 47. This information is used to generate the axial moderator profile for the assembly with the limiting axial burnup profile: Assembly C30 from LaSalle Unit 1. The moderator profile that is used is the average of the water densities in each of the eight cases which include Assembly C30. This profile is presented in Table E-2. The simple average used varies by less than 0.3% at all elevations from a burnup-weighted average. The axial moderator density profile is also lower at nearly all elevations than the limiting distribution from the Quad Cities Unit 2 data in Ref. 46. The lower moderator density will lead to a harder neutron spectrum and more plutonium generation. The profile selected is therefore judged to be sufficiently conservative for use in these calculations.

Discharged assembly reactivity is not highly sensitive to operating history or specific power. The depletion calculations for these analyses model a specific assembly, C30, from a specific commercial BWR plant, LaSalle Unit 1. The specific power can be estimated from data provided in Ref. 47. The core power, number of assemblies, and MTU loading per assembly can be used to determine the average specific power in MW/MTU (W/g). The average burnup of the assembly compared to the cycle burnup can be determined for each case, and thus a relative power can be calculated. The burnup-weighted average specific power for assembly C30 is slightly greater than 30 MW/MTU. This specific power is used in the TRITON depletion calculations to generate the ARP libraries for the STARBUCS calculations. Both TRITON and STARBUCS depletion calculations assume a constant, full-power operating history. These assumptions provide realistic estimates of the UNF reactivity.

**Table E-1. Potentially limiting relative burnup profiles from Quad Cities Unit 2 and LaSalle Unit 1**

Axial zone midpoint elevation (cm)	Assembly C30 (LS U1)	Assembly E7 (QC U2)	Assembly F8 (QC U2)
7.62	0.2461	0.2141	0.2228
22.86	0.7879	0.7470	0.7500
38.10	1.0175	0.9788	0.9813
53.34	1.1026	1.0980	1.0996
68.58	1.1751	1.1518	1.1568
83.82	1.1942	1.1781	1.1877
99.06	1.2052	1.1967	1.2087
114.30	1.2168	1.2125	1.2270
129.54	1.2481	1.2522	1.2668
144.78	1.2535	1.2602	1.2743
160.02	1.2526	1.2589	1.2734
175.26	1.2485	1.2523	1.2657
190.50	1.2419	1.2458	1.2531
205.74	1.2320	1.2391	1.2361
220.98	1.2170	1.2306	1.2139
236.22	1.1955	1.2084	1.1843
251.46	1.1655	1.1651	1.1412
266.70	1.1260	1.1165	1.0940
281.94	1.0759	1.0555	1.0358
297.18	1.0118	0.9569	0.9425
312.42	0.9112	0.8369	0.8270
327.66	0.7873	0.6815	0.6773
342.90	0.6336	0.2968	0.3065
358.14	0.2886	0.1662	0.1742
373.38	0.1656	Not Applicable	
Top Three Nodes	1.0878	1.1446	1.1580
Top Six Nodes	3.7980	3.9939	3.9633

**Table E-2. Average moderator density by axial node, based on Assembly C30 from LaSalle Unit 1**

Axial zone midpoint elevation (cm)	Average moderator density (g/cm <sup>3</sup> )	Axial zone midpoint elevation (cm)	Average moderator density (g/cm <sup>3</sup> )
7.62	0.7396	205.74	0.3126
22.86	0.7396	220.98	0.2953
38.10	0.7288	236.22	0.2802
53.34	0.6875	251.46	0.2668
68.58	0.6349	266.70	0.2549
83.82	0.5798	281.94	0.2445
99.06	0.5284	297.18	0.2354
114.30	0.4831	312.42	0.2276
129.54	0.4434	327.66	0.2213
144.78	0.4089	342.90	0.2163
160.02	0.3794	358.14	0.2128
175.26	0.3539	373.38	0.2115
190.50	0.3317		



## **APPENDIX E**

### **A Preliminary Evaluation of Using Fill Materials to Stabilize Used Nuclear Fuel During Storage and Transportation**

# *A Preliminary Evaluation of Using Fill Materials to Stabilize Used Nuclear Fuel During Storage and Transportation*

**Fuel Cycle Research & Development**

*Prepared for  
U.S. Department of Energy  
Used Fuel Disposition Campaign*

*Steven J. Maheras*

*Ralph E. Best*

*Steven B. Ross*

*Erik A. Lahti*

*David J. Richmond*

*Pacific Northwest National Laboratory*

*August 28, 2012*

*FCRD-UFD-2012-000243*

*PNNL-21664*



#### **DISCLAIMER**

This information was prepared as an account of work sponsored by an agency of the U.S. Government. Neither the U.S. Government nor any agency thereof, nor any of their employees, makes any warranty, expressed or implied, or assumes any legal liability or responsibility for the accuracy, completeness, or usefulness, of any information, apparatus, product, or process disclosed, or represents that its use would not infringe privately owned rights. References herein to any specific commercial product, process, or service by trade name, trade mark, manufacturer, or otherwise, does not necessarily constitute or imply its endorsement, recommendation, or favoring by the U.S. Government or any agency thereof. The views and opinions of authors expressed herein do not necessarily state or reflect those of the U.S. Government or any agency thereof.

**Used Fuel Disposition Campaign Storage and Transportation**

**A Preliminary Evaluation of Using Fill Materials to Stabilize Used Nuclear During Storage and**

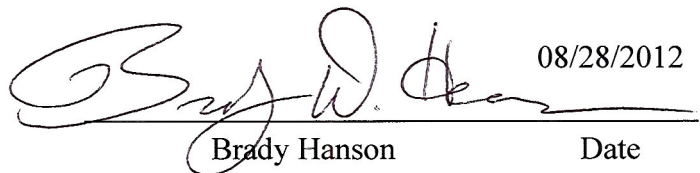
**Transportation**

August 31, 2012

iii

**Reviewed by:**

PNNL Project Manager

  
Brady Hanson

08/28/2012

Date

**Used Fuel Disposition Campaign Storage and Transportation**  
**A Preliminary Evaluation of Using Fill Materials to Stabilize Used Nuclear During Storage and**  
**Transportation**

iv

August 31, 2012

## SUMMARY

The objective of the research described in this report was to conduct a preliminary evaluation of potential fill materials that could be used to fill void spaces in and around used nuclear fuel contained in dry storage canisters in order to stabilize the geometry and mechanical structure of the used nuclear fuel during extended storage and subsequent transportation. The use of fill material to stabilize used nuclear fuel is not considered to be a primary option for safely transporting used nuclear fuel after extended storage. However, the evaluation of potential fill materials, such as those described in this report, might provide the U.S. Department of Energy Used Fuel Disposition Campaign with an option that would allow continued safe storage and transportation if other options such as showing that the fuel remains intact or canning of used nuclear fuel do not prove to be feasible.

As a first step in evaluating fill materials, previous work done in this area was summarized. This involved studies done by the Spent Fuel Stabilizer Materials Program, Allied-General Nuclear Services, the Canadian Nuclear Fuel Waste Management Program, the U.S. Department of Energy, Spain, Sweden, and the Department of Energy's Yucca Mountain Project. A wide variety of potential fill materials were evaluated in these studies, ranging from molten metal to particulates and beads to liquids and gases. The common element in the studies was that they were focused on the use of fill materials in waste packages for disposal, not in storage canisters or transportation casks. In addition, very few studies involved actual experiments that measured some physical property of the fill material to be used as a stabilizing material, and no studies were found that analyzed the performance of transportation casks containing fill material during the normal conditions of transport specified in 10 CFR 71.71 or under hypothetical accident conditions specified in 10 CFR 71.73. In addition, most studies did not address issues that would be associated with production-scale emplacement of fill material in canisters, as opposed to laboratory- or experimental-scale use of fill material. It is noteworthy that Sweden abandoned its plan to use fill materials to stabilize waste packages due to the complexity of emplacing the fill material.

A part of the evaluation of fill materials, conceptual descriptions of how canisters might be filled were developed with different concepts for liquids, particles, and foams. The requirements for fill materials were also developed. Elements of the requirements included criticality avoidance, heat transfer or thermodynamic properties, homogeneity and rheological properties, retrievability, material availability and cost, weight and radiation shielding, and operational considerations.

Potential fill materials were grouped into 5 categories and their properties, advantages, disadvantages, and requirements for future testing were discussed. The categories were molten materials, which included molten metals and paraffin; particulates and beads; resins; foams; and grout. Based on this analysis, further development of fill materials to stabilize used nuclear fuel during storage and transportation is not recommended unless options such as showing that the fuel remains intact or canning of used nuclear fuel do not prove to be feasible.

## CONTENTS

SUMMARY .....	v
ACRONYMS .....	viii
DEFINITIONS .....	ix
1. INTRODUCTION .....	1
2. SUMMARY OF PREVIOUS WORK .....	4
2.1 Spent Fuel Stabilizer Materials Program .....	4
2.2 Allied-General Nuclear Services .....	5
2.3 Canadian Nuclear Fuel Waste Management Program .....	7
2.4 U.S. Department of Energy .....	10
2.5 Belgium .....	11
2.6 Spain .....	11
2.7 Sweden .....	12
2.8 Yucca Mountain Project .....	15
3. FILLING OF CANISTERS .....	17
4. REQUIREMENTS FOR FILL MATERIALS .....	24
4.1 Criticality Avoidance .....	25
4.2 Heat Transfer and Thermodynamic Properties .....	25
4.3 Homogeneity and Rheological Properties .....	26
4.4 Retrievability .....	26
4.5 Material Availability and Cost .....	26
4.6 Weight and Radiation Shielding .....	26
4.7 Operational Considerations .....	26
5. POTENTIAL FILL MATERIALS .....	27
5.1 Molten Materials .....	27
5.1.1 Molten Metals .....	27
5.1.2 Paraffin .....	29
5.2 Particulates and Beads .....	30
5.3 Resins .....	35
5.4 Foams .....	36
5.5 Grout .....	38
6. CONCLUSIONS AND RECOMMENDATIONS .....	40

7. REFERENCES.....	43
--------------------	----

## **TABLES**

Table 1. Recommended Candidate Stabilizer Materials.....	5
Table 2. Physical Properties of Recommended Reference Stabilizer Materials.....	5
Table 3. Selected Physical Properties of Granular Solid Fill Materials .....	6
Table 4. Selected Physical Properties of Liquid Fill Materials .....	6
Table 5. Selected Physical Properties of Gaseous Fill Materials.....	7
Table 6. Necessary and Desirable Criteria for Fill Material.....	8
Table 7. Selected Material Properties for Lead and Zinc .....	10
Table 8. Requirements for Fill Materials (Spain) .....	12
Table 9. Requirements for Fill Materials (Sweden).....	14
Table 10. Summary of Experiments Involving Steel Shot .....	16
Table 11. Conceptual Approaches for Introducing Fill Material into Dry Storage Canisters Containing Used Nuclear Fuel.....	21
Table 12. Potential Requirements for Fill Materials.....	24
Table 13. Representative Properties of Candidate Molten Metals .....	28
Table 14. Particulates and Beads Evaluated in Previous Studies .....	33
Table 15. Material Properties of Resins.....	36
Table 16. Material Properties of Foams.....	38

## **FIGURES**

Figure 1. Used Nuclear Fuel Canister Loading Sequence .....	20
---	----

## ACRONYMS

GWd/MTU	Gigawatt-day per metric ton uranium
HAC	Hypothetical accident conditions
$k_{\text{eff}}$	Effective neutron multiplication factor
NCT	Normal conditions of transport
UFDC	Used Fuel Disposition Campaign

## DEFINITIONS

Alumina	$\text{Al}_2\text{O}_3$
Bauxite	An aluminum ore composed of primarily aluminum hydroxide minerals as well as mixtures of silica, iron oxide, and other impurities.
Bentonite	Bentonite is a natural clay that swells with the absorption of water and has good ion exchange properties.
Bondate	Bondate is an organic-based chemical bonding agent for aggregates and fibers.
Boron carbide	$\text{B}_4\text{C}$
Dowtherm	Dowtherm is a heat transfer fluid.
Hematite	$\alpha\text{-Fe}_2\text{O}_3$
Interprop	Interprop is a ceramic proppant composed of 35-65% mullite (aluminum silicate) and 35-65% corundum (aluminum oxide).
Magnetite	$\text{Fe}_3\text{O}_4$
Mullite	$\text{Al}_6\text{Si}_2\text{O}_{13}$
Olivine	$(\text{Mg},\text{Fe})_2\text{SiO}_4$
Phosphates	$\text{Ca}_5(\text{PO}_4)_3(\text{OH},\text{F},\text{Cl})$
Proppant	A proppant is a material that will keep an induced hydraulic fracture open.
Quartz	$\text{SiO}_2$
Rutile	$\text{TiO}_2$
Silica	$\text{SiO}_2$
Spinel	$\text{MgAl}_2\text{O}_4$
Wood's metal	A low melting fusible alloy that is a mixture of 50% bismuth, 25% lead, 12.5% tin, and 12.5% cadmium.
Zeolite	Hydrated aluminosilicates of the alkaline and alkaline-earth metals.
Zircon	$\text{ZrSiO}_4$
Zirconia	$\text{ZrO}_2$



# **USED FUEL DISPOSITION CAMPAIGN**

## **A PRELIMINARY EVALUATION OF USING FILL MATERIALS TO STABILIZE USED NUCLEAR FUEL DURING STORAGE AND TRANSPORTATION**

### **1. INTRODUCTION**

With the U.S. Department of Energy's Yucca Mountain repository project no longer a workable option, there is no longer a national program for the disposal of used nuclear fuel from commercial nuclear power plants in the United States. As a consequence, used nuclear fuel may continue to be stored for an extended period of time, potentially much longer than originally intended. The U.S. Department of Energy Used Fuel Disposition Campaign (UFDC) is tasked with developing the technical bases to support the continued safe and secure storage and subsequent transportation of used nuclear fuel while maintaining options for its final disposition.

However, most storage pools for used nuclear fuel at reactor sites are now filled to capacity. To provide space for continuing discharges of used nuclear fuel, plant operators began transferring the used nuclear fuel into dry storage systems. These systems are located on the reactor plant's site external to the original nuclear plant facilities. In the dry storage systems, used nuclear fuel is stored in a dry, inert environment in bolted direct-load metal storage casks or in sealed metal canisters. The metal canisters containing used nuclear fuel are stored within steel-reinforced concrete overpacks or storage modules.

The majority of the used nuclear fuel that is in storage is classified as "intact fuel". Intact fuel is the U.S. Nuclear Regulatory Commission classification of used nuclear fuel where the defects in cladding that could expose nuclear fuel material to an oxidizing environment or could allow release of fuel particles and radionuclides from inside the cladding are limited to hairline cracks and pinhole leaks. Fuel assemblies that are classified as "intact" can be stored and transported without having to be additionally enclosed within a "failed-fuel" can within a transportation cask or transportable dry storage canister. In some cases, plant operators have placed used nuclear fuel into failed fuel cans then into storage canisters because it was not feasible to verify that the fuel met the requirements for "intact" fuel.

During extended storage, structures, systems, and components that are important to safety (including fuel cladding and fuel assembly structures) may degrade. The stressors, degradation mechanisms, and data gaps associated with extended storage and subsequent transportation are discussed by UFDC (2012). UFDC (2012) also discuss the stressors, degradation mechanisms, and data gaps associated with extended storage and subsequent transportation of high burnup fuel (exceeding 45 gigawatt-days per metric tonne of uranium [GWd/MTU]). Much of the fuel currently being discharged from reactors exceeds the high-burnup threshold and there is limited information available on the properties of this used nuclear fuel (UFDC 2012).

The focus of the gap analysis by UFDC (2012) is on evaluating the likelihood that the used nuclear fuel remains undamaged (i.e., intact, retrievable, and transportable) after extended storage. The ability of the used nuclear fuel to remain intact is especially important for assuring that a nuclear criticality cannot occur in a storage system or a transportation cask. If fuel cladding degrades during long-term storage, the geometric configuration of a fuel assembly and its fuel component could not be assured under normal conditions of transport (NCT) or hypothetical accident conditions (HAC). A change in the geometric configuration of the fuel inside a transportation cask would change the nuclear reactivity of the cask's contents and could compromise the ability to ensure that a nuclear criticality could not occur in the fuel during transportation.

The UFDC is conducting research and development aimed at developing objective technical evidence that can be used to project and assess the condition of used nuclear fuel during and following extended storage and subsequent transportation. This evidence is expected to show that used nuclear fuel can sustain extended dry storage in an inert atmosphere without substantial change in its properties. However, it is possible that the research will identify unexpected degradation mechanisms or will determine the condition of cladding for high-burnup used nuclear fuel such that the integrity of fuel cladding cannot be sufficiently verified for NCT and HAC.

Thus, the UFDC could consider other options to ensure that used nuclear fuel can be transported following extended storage. The range of these options includes: requiring that all used nuclear fuel assemblies be placed into failed-fuel cans before being placed into a dry storage cask or canister system and use of a fill material to stabilize the contents of a metal canister prior to transportation. Ideally, the use of a fill material would render the question of whether used nuclear fuel was intact or damaged immaterial because the fill material would preserve the geometric configuration of the used nuclear fuel and/or provide for moderator exclusion and thereby prevent a nuclear criticality. The objective of this report is to evaluate potential fill materials that could be used for this purpose.

There are several reasons why the use of a fill material might be preferable to options such as demonstrating that the used nuclear fuel remains intact or canning of all used nuclear fuel. For example, it may not be possible to provide objective evidence with the requisite reasonable assurance, at a reasonable cost, that used nuclear fuel will remain intact after extended storage. Under this circumstance, the use of fill material or canning of individual fuel assemblies might be the only options available that would allow transportation of large amounts of used nuclear fuel to a geologic repository, a consolidated storage facility, or a reprocessing facility. However, canning of used nuclear fuel would require repackaging of fuel already in storage and could also substantially increase the number of shipments. If feasible, the use of fill materials could be desirable when compared to canning and repackaging of used nuclear fuel.

There are also disadvantages to the use of fill materials. For example, placing a fill material in a metal canister subsequently loaded into a transportation cask could increase the weight of the transportation cask to the point where it could not be handled or transported. In addition,

**Used Fuel Disposition Campaign Storage and Transportation**  
**A Preliminary Evaluation of Using Fill Materials to Stabilize Used Nuclear During Storage and Transportation**

August 31, 2012

3

verifying that the fill material was fully and uniformly distributed within the metal canister may not be feasible. A closely related issue is that it may be difficult to load the fill material into metal canisters that were not designed with this capability, and it could be difficult to subsequently retrieve the used nuclear fuel without having to resort to time consuming or costly measures. The fill material would also have to be chosen so that it did not have undesirable properties during the normal conditions of transport specified in 10 CFR 71.71 or hypothetical accident conditions specified in 10 CFR 71.73, and the transportation casks would have to be re-licensed by the U.S. Nuclear Regulatory Commission based on the presence of the fill material, or more likely, entirely new transportation casks would have to be licensed.

For the reasons stated above, the use of fill material to stabilize used nuclear fuel is not considered to be a primary option for safely transporting used nuclear fuel after extended storage. However, evaluation of potential fill materials could provide the UFDC with an option that would allow continued safe storage and transportation if other options such as showing that the fuel remains intact or canning do not prove to be feasible.

## **2. SUMMARY OF PREVIOUS WORK**

This section summarizes previous work done to investigate the use of fill materials to stabilize used nuclear fuel in waste packages, storage containers, or transportation casks. The studies that are summarized were identified by literature searches and searches of project records from available U.S. and international sources. Other work involving fill materials that is not available in the literature or project records is not included in the descriptions that follow.

The majority of the studies have been literature studies that did not involve experimental work. The only studies that involved experimental work were studies conducted by the Spent Fuel Stabilizer Materials Program, the Canadian Nuclear Fuel Waste Management Program, and the Yucca Mountain Project. In addition, the majority of studies were focused on the use of fill materials in waste packages for disposal of used nuclear fuel. No experimental work was found that analyzed the performance of transportation casks containing fill material during the normal conditions of transport specified in 10 CFR 71.71 or during hypothetical accident conditions specified in 10 CFR 71.73.

### **2.1 Spent Fuel Stabilizer Materials Program**

The Spent Fuel Stabilizer Materials Program was conducted for the National Waste Terminal Storage Program, a predecessor to the Office of Civilian Radioactive Waste Management in the U.S. Department of Energy, and had the objective of identifying, testing, and selecting stabilizer materials for use in used nuclear fuel waste packages for disposal. Stabilizers were materials that would fill the space in a waste package that was not filled with used nuclear fuel (Fish et al. 1982).

Wynhoff et al. (1982) identified 34 candidate stabilizer materials based on analysis of thermal gradients within the waste package, thermal stress analysis (thermal gradient stress analysis and differential thermal expansion stress analysis), nuclear criticality, radiation attenuation, and cost and material availability. Table 1 lists these candidate materials. Fish et al. (1982) conducted a series of experimental tests and evaluated the 34 materials against the following functions:

- Help resist lithostatic and hydrostatic pressures on the waste package after emplacement
- Maintain the used nuclear fuel geometry, prevent motion and mechanical abrasion or rod failure due to handling and accidents
- Promote heat transfer from the fuel assembly to minimize fuel temperature
- Chemical compatibility with the waste package
- Long-term chemical and radiation stability
- Use of an organic material was strongly discouraged because organic materials tend to decompose at elevated temperatures and in radiation environments creating a potential for harmful interaction with fill material after a waste package is breached.

Additional screening criteria used by Fish et al. (1982) included criteria for emplacement temperature limits, shrinkage and voids, material interactions, moisture release, and gas

generation. The tests conducted by Fish et al. (1982) included temperature limit tests, fill process tests, prebreach disposal condition tests (including loss-on-ignition tests and tests to evaluate fuel cladding-stabilizer material interactions), and electrochemical tests. As a result of these tests and evaluations, 1% antimonial lead and zirconia were recommended to be used as the reference materials used in waste package designs calling for the use of stabilizers. Table 2 summarizes selected physical properties of these materials.

Table 1. Recommended Candidate Stabilizer Materials

Material	Material
Silica – amorphous	Sand
Silica – quartz	Graphite
Silica – quartz/bondate	Graphite/bondate
85% silica – quartz/15% bentonite	Air
Mullite	Helium
Mullite/bondate	Nitrogen
85% mullite/15% bentonite	1% antimonial lead
Zircon	Calcium lead
Zirconia	Commercial lead
Zirconia/bondate	Zinc alloy AG40A
85% zirconia/15% bentonite	Zinc alloy AC41A
Basalt	Zinc-copper-titanium alloy
Basalt/bondate	Commercial zinc
85% basalt/15% bentonite	Copper casting alloy 3A (high-lead tin bronze)
Granite	Copper casting alloy 8A (manganese bronze)
Shale	Copper casting alloy 13B (silicon brass)
Tuff	Commercial copper

Source: Wynhoff et al. (1982)  
Bondate is an organic-based chemical bonding agent for aggregates and fibers.

Table 2. Physical Properties of Recommended Reference Stabilizer Materials

Material	Density (g/cm <sup>3</sup> )	Thermal Conductivity (W/m-K)
1% antimonial lead	11.27	33.47
Zirconia	5.68	1.45

Source: Wynhoff et al. (1982)

## 2.2 Allied-General Nuclear Services

Anderson (1981) investigated the use of fill materials to be used to encapsulate used nuclear fuel within a canister during the dry storage. The purpose of the study was to determine if encapsulation of used nuclear fuel with a fill material was desirable, compare physical and economic characteristics of alternative fill materials, and to review appropriate means to seal the

**Used Fuel Disposition Campaign Storage and Transportation**  
**A Preliminary Evaluation of Using Fill Materials to Stabilize Used Nuclear During Storage and Transportation**

6

August 31, 2012

storage canisters if fill materials were used. Tables 3, 4, and 5 summarize the materials evaluated and selected physical properties.

Table 3. Selected Physical Properties of Granular Solid Fill Materials

Material		Solid Density (g/cm <sup>3</sup> )	Solid-Gas Mixture Thermal Conductivity (W/m-K)	Solid Melting Temperature (°C)
Solid	Gas <sup>a</sup>			
Copper spheres	Air	8.97	0.68	1083
Aluminum spheres	Air	2.70	--	660
Graphite	Air	1.50	1.2	3700
Zinc spheres	Air	7.14	0.46	283
Steel spheres	Air	7.85	0.25	1426
Lead spheres	Air	11.3	--	327
Boron carbide	Air	2.52	--	2450
Uranium oxide powder	Helium	10.8	1.5	2750
Alumina	Air	4.00	0.67	2050
Sand	Air	1.52	0.26	--
Glass	Air	2.22	0.18	1200
Mortar	--	2.20	0.92	--
Rock or glass wool	Air	0.16	0.050	--

Source: Anderson (1981)

a. The gases listed fill the interstices of the solid fill material.

Table 4. Selected Physical Properties of Liquid Fill Materials

Material	Density (g/cm <sup>3</sup> )	Boiling Temperature (°C)	Pressure at Boiling (psia)	Thermal Conductivity (W/m-K)
Water	0.956 0.786	100 260	14.7 680.8	0.67 0.61
Ethylene glycol and water	1.013 0.963	100 177	13.8 103.0	0.40 0.36
Dowtherm	0.860 0.739	258 380	14.7 119.0	0.10 0.084
Silicone	0.900 0.744	100 300	0.077 20.9	0.12 0.071

Source: Anderson (1981)

Dowtherm is a heat transfer fluid.

Table 5. Selected Physical Properties of Gaseous Fill Materials

Material	Density (g/cm <sup>3</sup> )	Thermal Conductivity (W/m-K)
Helium	0.000164	0.18
Air	0.00120	0.034
Nitrogen	0.00120	0.033
Carbon dioxide	0.00184	0.025
Argon	0.00166	0.022

Source: Anderson (1981)

Anderson (1981) noted several advantages of fill materials. For example, by selecting the proper fill material one might reduce corrosion of the fuel cladding, increase the thermal conductivity of the contained fuel assembly, and reduce criticality considerations by lowering the effective neutron multiplication factor ( $k_{eff}$ ) value of the used nuclear fuel container. The main disadvantage to the use of fill materials that was noted was economic. A second disadvantage that was noted was feasibility. Another potential disadvantage of using fill materials noted by Anderson (1981) involves the increased difficulty of retrieving the used nuclear fuel if retrieval is necessary at a later date. If the used nuclear fuel has been stabilized in a solid matrix (for example, by melting a metal, pouring it in a canister containing used nuclear fuel, and allowing the package to solidify), the removal of the used nuclear fuel could be quite difficult (Anderson 1981). In addition, the fill material could be slightly contaminated resulting in the generation of radioactive waste or additional process steps to decontaminate the fill material (Anderson 1981).

For the dry storage of spent fuel, Anderson (1981) found that air would be the best fill material. The use of fill materials other than air for dry storage of used nuclear fuel could be justified only if a specific end result, e.g., containment or criticality control, was deemed very important.

### **2.3 Canadian Nuclear Fuel Waste Management Program**

The Canadian Nuclear Fuel Waste Management Program investigated alternative fill materials to be placed inside two types of waste containers: a thin-walled particulate-packed container and a structurally supported particulate-packed container. The purpose of the fill material was to provide structural support for the container against the hydrostatic pressure that could exist in a flooded, 1000-m deep disposal vault.

Shelson (1983) established a set of initial criteria for selecting particulates for future study and experiments. These criteria included necessary properties and desirable properties. Necessary properties were further grouped into criteria related to mechanical strength and criteria related to stability. Table 6 lists these criteria.

Table 6. Necessary and Desirable Criteria for Fill Material

Necessary Criteria	Desirable Criteria
Mechanical Strength High strength to breakdown (>20 MPa) High bulk modulus (>200 MPa) High Young's modulus (>200 MPa)	High heat transfer coefficient Low thermal expansion coefficient Low dust content Impede radionuclide migration Attenuate radiation from fuel bundles Low specific gravity
Stability Radiation stability Chemical stability Not Reactive with titanium or heavy metals No interference with welding of shells Thermal stability (>1500 °C) Low water absorptivity (low swelling) No change over container life (300-500 years)	

Source: Shelson (1983)

From initial studies (Shelson 1983), twelve candidate particulate materials were selected for study (Teper 1987). These materials were:

- Sand
- Fine glass beads (0.002-0.3 mm)
- Coarse glass beads (0.8-1.2 mm)
- Steel shot (0.6-1.0 mm)
- Aluminum oxide powder
- Crushed bauxite grains
- Sintered bauxite
- Interprop<sup>a</sup>
- Ceramic zirconia
- Rutile-Zircon-Garnet mixture
- Zircon
- Rutile

---

<sup>a</sup> Interprop is a ceramic proppant composed of 35-65% mullite (aluminum silicate) and 35-65% corundum (aluminum oxide). A proppant is a material that will keep an induced hydraulic fracture open.

The criteria used by Teper (1987) to select the fill material to be used in the container included:

- Fill all voids without clogging
- Be small enough to flow between the fuel bundle elements (less than 1.2 mm diameter) but the grains should be heavy enough to avoid becoming airborne during vibratory compaction
- Have sufficient strength to withstand a pressure of 20 MPa
- Have adequate stiffness to prevent large plastic deformations of the container shell
- Have low dust content to minimize airborne particles
- Should not adhere to the container wall, to simplify welding of top lid
- Have small creep deformations over the 500-year container life
- Have sufficiently high bulk modulus under external pressure

The particulates underwent vibratory compaction tests, compression tests, and creep tests. The details of the tests and their results are discussed in Teper (1987). Based on the results of the tests, three fill materials were considered viable: glass beads, interprop, and sintered bauxite. Coarse glass beads generated the least amount of dust during compaction and produced the highest bulk modulus of elasticity in the compacted state, and were therefore selected as the fill material for the packed particulate and structurally supported containers (Johnson et al. 1994). The use of glass beads as a fill material was abandoned because glass beads could not provide assurance that the container would not collapse due to anticipated hydraulic pressures in the vault and was replaced with a carbon steel inner vessel to provide mechanical strength to the used nuclear fuel container (NWMO 2005).

The Canadian Nuclear Fuel Waste Management Program also investigated a metal matrix container, where cast metal surrounded the fuel bundles and forms a layer between the outer bundles and the shell of the container. Johnson et al. (1994) lists the following requirements for a candidate casting metal or alloy:

- The cast matrix should be free of major defects such as shrinkage voids
- During casting, the molten metal should neither chemically react with the corrosion-resistant shell nor otherwise reduce the thickness of the corrosion barrier.
- Interactions with the used nuclear fuel cladding should be minimal to ensure that the fuel elements are not damaged.
- Following solidification of the cast matrix, chemical stability between the matrix and the container shell should persist.
- The casting process should be conducted at as low a temperature as possible in order to reduce the preheating requirements of the container and its contents, decreasing the possibility of promoting thermal stress defects in the used nuclear fuel cladding material, and shorten the solidification period, during which chemical interactions between the matrix and the used nuclear fuel cladding material and/or the container shell are more likely.

Lead, zinc, and aluminum, and lead-antimony, aluminum-silicon, and aluminum-copper alloys were studied as candidate casting materials, and lead or zinc were recommended as the preferred casting materials. Table 7 summarizes some selected physical properties of lead and zinc. Subsequent research and development activities focused on lead. Four half-scale models, denoted MM1, MM2, MM3, and MM4, were cast and structural performance tests conducted. Testing and analysis showed that a metal matrix container was a viable option.

Table 7. Selected Material Properties for Lead and Zinc

Material	Density (g/cm <sup>3</sup> )	Thermal Conductivity (W/m-K)	Melting Point (°C)
Lead	11.35	33.0	327.5
Zinc	7.10	112.2	419.58

## 2.4 U.S. Department of Energy

The U.S. Department of Energy has studied the use of depleted uranium oxide particulates as a fill material in used nuclear fuel waste packages (Forsberg 2000), and the use of depleted uranium silicate glass beads as a fill material in used nuclear fuel waste packages, storage containers, and transportation casks (Forsberg et al. 1995, 1996; Pope et al. 1996a, 1996b). In terms of the long-term performance of a geologic repository, the use of either depleted uranium oxide particulates or depleted uranium silicate glass beads has two advantages. First, it will retard the release of radionuclides from the waste package by creating a chemically reducing environment that slows the degradation of the uranium oxide contained in the used nuclear fuel, and by reducing ground water flow through the waste package (Forsberg 2000). In addition, the use of depleted uranium as a fill material minimizes the potential for a long-term criticality by isotopic dilution of U-233 and U-235 (Forsberg 2000).

In terms of storage and transportation, the use of depleted uranium silicate glass beads could have several benefits (Forsberg et al. 1995):

- The amount of gamma shielding material in the walls of the storage casks and transportation casks may be reduced.
- The neutron shielding materials in the walls of the storage casks and transportation casks may be reduced.
- The need to include burnup credit for criticality control may be eliminated.

Pope et al. (1996a, 1996b) acknowledges that there significant uncertainties associated with using depleted uranium silicate glass beads as a fill material, and that additional studies are necessary. The studies recommended by Pope et al. (1996a, 1996b) included:

- Developing and demonstrating the ability to produce depleted uranium silicate glass.
- Performing leaching tests on the depleted uranium silicate glass.
- Defining a preferred method for loading the depleted uranium silicate glass into a storage or transportation cask after they have been loaded with used nuclear fuel assemblies.

- Performing design alternative studies and defining costs and benefits of the various alternatives, including assessments of storage canister, transportation cask, storage cask, and waste package alternatives.
- Assessing trade-offs for and defining systems and interfaces for applying the concept of using depleted uranium silicate glass as a fill material to the waste management system.

## **2.5 Belgium**

Belgium incorporated sand as a fill material in their used nuclear fuel canister design (Bennett and Gens 2008, ONDRAF/NIRAS 2001). The sand is a dry, halide-free rolled sand which fills the voids in the canister after being vibrated (ONDRAF/NIRAS 2001). As noted in ONDRAF/NIRAS (2001), the sand has a number of functions:

- The walls of the canister can be made thinner as the sand provides resistance to crushing
- The sand stabilizes the used nuclear fuel assembly in a centered position and so reduces criticality risks by mechanical convergence
- The sand limits the moderator density should water penetrate the canister
- The sand limits the void space which is a general requirement for waste intended for deep disposal.

After the canister has been filled with sand it is purged with a dry inert gas to minimize the risks of corrosive agents such as nitric acid being produced by radiologically induced reaction with humid air (ONDRAF/NIRAS 2001). The use of glass frit to fill the annulus between high level radioactive waste canisters and their overpacks is also being evaluated (ONDRAF/NIRAS 2001).

## **2.6 Spain**

Puig et al. (2008a, 2008b, 2009) evaluated alternative fill materials that could be placed inside a used nuclear fuel canister that would be disposed of in a geological repository. The primary purpose of the fill material was to avoid the possibility of a criticality event once the canister was breached by corrosion and was flooded by ground water. Five groups of requirements for these fill materials were developed. These included requirements for criticality, general requirements to fulfill, general requirements to avoid, performance improvement requirements, and other interesting requirements. These requirements are listed in Table 8. Eight materials were evaluated:

- Cast iron or steel
- Borosilicate glass
- Spinel
- Depleted uranium
- Dehydrated zeolites
- Hematite
- Phosphates
- Olivine

Based on the evaluations of the materials against the requirements, four materials were found to be promising for use as a fill material: cast iron or steel, borosilicate glass, spinel, and depleted uranium.

Table 8. Requirements for Fill Materials (Spain)

<b>Criticality Requirements</b> Fill 60% of the canister inner free volume Significant neutron absorption capability Minimize neutron moderation Radiation resistance Thermal stability Chemical stability
<b>General Requirements to Fulfill</b> Thermodynamic equilibrium with conditions and materials in repository Homogeneous batches Good rheological properties to ensure proper filling Ability to be placed in canister without damaging fuel assemblies Does not affect fabrication, encapsulation, or other processes (i.e., welding of canister lid) Possible to disassemble canister Allow retrievability if needed
<b>General Requirements to Avoid</b> Limited availability of material Potential to increase corrosion of the canister, fuel cladding, or fuel itself. Increase the potential for radionuclide transport through bentonite barrier or chemically alter the barrier's properties Retain significant amounts of air that could lead to formation of nitric acid through radiolysis and contribute to stress corrosion cracking
<b>Performance Improvement Requirements</b> High mechanical strength to contribute to canister structural integrity Sorption capability for key radionuclides
<b>Other Interesting Properties</b> Well-documented long-term durability Low material density to reduce additional weight of canister Low overall cost of material (raw materials, processing, and fabrication) Good intrinsic radiation shielding properties Material that allows a relatively simple process, including the necessary facilities and equipment
Source: Puig et al. (2008a)

## 2.7 Sweden

Oversby and Werme (1995) evaluated alternative fill materials that could be placed inside a copper and steel used nuclear fuel canister that would be placed inside a geological repository.

As with the fill materials analyzed by Puig et al. (2008a, 2008b, 2009), the primary purpose of the fill material was to avoid the possibility of a criticality event once the canister was breached by corrosion and was flooded by ground water. Design requirements were developed for the canister fill material and divided into three classes: essential requirements, desirable features, and undesirable features. These requirements are listed in Table 9. Eleven materials were evaluated:

- Glass beads
- Lead shot
- Copper spheres
- Sand
- Olivine
- Hematite
- Magnetite
- Crushed rock
- Bentonite
- Other clays
- Concrete

Based on the evaluations of the materials against the design requirements, three materials were found to be candidates for further evaluation as fill materials: glass beads, copper spheres, and magnetite. Because of the complexity of the filling process, canister designs without fill material were evaluated (Werme and Eriksson 1995) and current canister designs do not include a fill material (SKB 2010).

Sweden has also investigated a steel canister with lead fill, a copper canister with lead fill, and a titanium canister with concrete fill (SKB 1992). The titanium canister with concrete fill was used for very deep hole disposal, not for disposal in a geologic repository. Emplacing the lead in a steel or copper canister involved pre-heating the canister in an induction furnace to 380 °C for 6 hours, adding molten lead which was then allowed to solidify slowly from the bottom up to avoid voids, and cooling the canister for 12 hours to 60 °C. The entire time to pre-heat, fill, and cool a canister was estimated to be 24 hours (SKB 1992).

Table 9. Requirements for Fill Materials (Sweden)

<b>Essential Requirements</b> The filling material must be capable of being placed into the canister in a manner that does not damage the fuel and that results in a residual void volume of less than 40% of the void volume in the absence of the filling material. The filling material must have a solubility of less than 100 milligrams per liter at 50 °C in pure water and in waters of the expected repository environment. The filling material shall not compact by more than 10% of its original volume under its own weight or as the result of shipping, handling, or emplacing the canister in storage or disposal sites.
<b>Desirable Requirements</b> Material is in thermodynamic equilibrium with the disposal system, thus ensuring chemical compatibility. Material has homogeneous properties within a batch and between batches, which makes quality control and performance modeling more secure. Material possesses well documented long-term durability, which ensures that predictions concerning the condition of the material through time will be reliable. Material has good rheological properties for emplacement into the canister, which ensures that the operations in the encapsulation facility will not be unduly difficult. Material contains a burnable poison to absorb neutrons, which will enhance the criticality control of the filling material even if the void volume exceeds 40%. Material has the potential to sorb radionuclides from aqueous solutions, thus lowering the release of radioactive materials from the waste package. Material has the potential to suppress generation of hydrogen, which helps protect the bentonite buffer material from disruption due to passage of gas bubbles through the bentonite. Material has low cost. Material has low density, so performs its space-filling function with minimal addition of weight to the canister system.
<b>Undesirable Requirements</b> Limited availability of the material. Potential for the material to enhance corrosion of the canister, the fuel cladding, or the fuel. Material generates gas when it alters. Material contains water, which diminishes the effectiveness of the material to prevent moderation of the neutron energies. Material has a high affinity for absorbing air on its surface, which is undesirable because the nitrogen in air can be converted to nitric acid in the presence of water and radiation.

Source: Oversby and Werme (1995)

## 2.8 Yucca Mountain Project

Wallin et al. (1994) evaluated alternative fill materials that could be placed inside a waste package which in turn would be emplaced inside a geologic repository located at Yucca Mountain, Nevada. The objectives of adding the fill materials included (Wallin et al. 1994):

- Criticality control: moderator displacement by means of minimization of waste package internal void space, to minimize the amount of water which could enter the waste package in the event of repository flooding and a breach of the waste package containment barriers
- Chemical buffering for radionuclides in the event of water intrusion into the waste package upon breach of the containment barriers
- Cathodic protection by virtue of having highest electrochemical activity, in the event of water intrusion into the waste package upon breach of the containment barriers
- Function as mechanical packing to inhibit movement (collapse) of other materials internal to the waste package (fuel rods, fuel pellets, and/or basket materials)
- Improve thermal conductance, which would improve heat transfer and decrease fuel rod temperatures

Seven materials were evaluated:

- Tin (emplaced molten)
- Lead (emplaced molten)
- Zinc (emplaced molten)
- Zinc alloy (emplaced molten)
- Magnetite
- Iron shot
- Borosilicate glass beads

Iron shot was chosen as the first fill material to be experimentally investigated. Characteristics of iron shot that led to this choice included: 1) relative ease of placement (near-spherical shot “flows” readily), 2) commercial availability in a variety of graded sizes, 3) cost (inexpensive), 4) iron is a plentiful natural resource, 5) iron is a reactive anodic material providing protection to the fuel cladding and to Stainless Steel 316 components, and 6) iron would inhibit radionuclide release (Wallin et al. 1994).

Cogar (1996a and 1996b) contain the plans and technical guidelines used to conduct experiments conducted on steel shot, which was chosen over iron shot for the experiments because it was more readily available. These experiments involved:

- Fabricating two dummy fuel assemblies, a 15×15 B&W Mark-B pressurized water reactor assembly and a 17×17 B&W Mark-BW pressurized water reactor assembly.

- Fabricating a simulated spent nuclear fuel basket test fixture from Lexan. The dimensions of the test fixture were  $8.81 \times 8.81 \times 180$  inches. The test fixture had two vibrators attached.
- Using two grades of shot: SAE Shot Size S230 and SAE Shot Size S330. The S230 shot had a nominal diameter of 0.7 mm and the S330 shot had a nominal diameter of 1.0 mm.
- As-poured versus vibrated fill tests.

Cogar (1996c) conducted bulk density tests, fill placement tests, eight fill tests, angle of repose tests, and thermal conductivity tests. The eight fill tests conducted involved combinations of shot size (S230 and S330), assembly ( $15 \times 15$  and  $17 \times 17$ ), and as poured versus vibrated conditions. Cogar (1996c) contains the detailed results of experiments. Table 10 summarizes these results.

Table 10. Summary of Experiments Involving Steel Shot

Material	Density (g/cm <sup>3</sup> )	Thermal Conductivity (W/m-K)
SAE Shot Size S230	4.490-4.538 (as-poured)	0.379-0.658
	4.568-4.653 (vibrated)	
SAE Shot Size S330	4.353-4.397 (as-poured)	0.325-0.591
	4.441-4.483 (vibrated)	

Source: Cogar (1996c)

Arthur (2000), Montierth (2000), and Radulescu (2000) also evaluated the use of aluminum shot containing gadolinium phosphate as a fill material in waste packages containing Shippingport light water breeder reactor thorium-uranium oxide seed assemblies. The results show that the Shippingport used nuclear fuel would not form critical configurations for any credible degradation scenarios when 1 weight percent gadolinium is added to the aluminum shot-gadolinium phosphate fill material. Similar analyses were performed for Enrico Fermi fast reactor used nuclear fuel using iron shot containing gadolinium phosphate as a fill material (Mobasheran 1999, Moscalu et al. 2000).

### **3. FILLING OF CANISTERS**

The introduction of a fill material into a dry storage canister containing used nuclear fuel assemblies would be a significant departure from established industry practice for dry storage and planned subsequent transportation of used nuclear fuel. Consequently, any initiative to use such an approach would have to surmount a high hurdle of justification including consideration of alternatives such as repackaging the used nuclear fuel into another canister. Such justification could include:

- Use of a fill material was determined to be the best alternative for remediating a known defect in a canister or canister contents in order to provide reasonable assurance of continued protection of public safety and to ensure continued compliance with regulatory requirements.
- Use of a fill material was determined to be the best alternative for eliminating uncertainties regarding the integrity of fuel cladding, fuel structures, or canister internal structures or safety-related components to provide reasonable confidence in storage or transportation safety performance and assurance of compliance with regulatory requirements.

It is unlikely that fill materials could be introduced into dry storage canisters in an operating nuclear power plant's used nuclear fuel storage pool. The reasons include issues regarding the compatibility of fill materials with the chemistry of the fuel pool water and the added operational complexity of adding fill materials. As a consequence, any activity to introduce fill materials to dry storage canisters would need to be conducted in a facility that would have the necessary health protection systems for workers and the public and systems to prevent releases of radioactive materials to the environment. It is beyond the scope of this report to provide a concept for such a facility. However, Carlsen and Brady Raap (2012) discusses various dry transfer systems for used nuclear fuel that could be applicable for use in introducing fill materials into dry storage canisters.

The objectives for introducing fill material into a canister could be several including:

1. To structurally stabilize (hold in place) the canister's contents and geometry by filling in all of the available free space in and around the nuclear fuel assemblies and in and around the structures of the fuel assembly basket. This would protect the used nuclear fuel cladding from damage and preserve the geometric orientation of nuclear fuel and other materials and structures in order to provide assurance that a nuclear criticality could not occur.
2. To provide a medium that would exclude the potential for a significant amount of water moderator to intrude in and around the fuel assemblies thereby assuring a nuclear criticality could not occur.
3. To provide a medium that contains neutron absorber materials to enhance assurance that a nuclear criticality could not occur

4. To provide a barrier that impedes the release of radioactive material from used nuclear fuel assemblies to the environment.
5. To provide radiation shielding to reduce the radiation dose rate external to the canister.

Possible approaches for introducing a fill material that fills the free space in a dry storage canister containing used nuclear fuel include:

- Adding fill material to a canister containing used nuclear fuel before the closure lid is first installed.
- Using canisters that have access ports that are designed to be removed at a future date to provide openings for adding fill material.
- Unsealing and re-opening the ports that were originally used to drain, vent, dry, and backfill the canister with inert gas to provide openings through which fill material could be added.
- Unsealing and removing the canister lid to add fill material.
- Cutting access ports through the canister lid to provide openings for adding fill material.
- Cutting access ports through the side of a canister to provide openings for adding fill material.

The time when fill material might be added to a canister could be as early as when the canister is first loaded with used nuclear fuel or it could be 100 to 300 years in the future when the canister is being prepared for shipment following extended storage. Fill material might also be added to a canister at any time available information indicates that the integrity of fuel cladding, fuel structures, or canister internal structures or safety-related components has (or may have) degraded in a manner that compromises storage or transportation safety performance. This would include canisters with detected defects or when research results or other information suggest there are likely safety related defects in a particular canister design or design feature or a category of used nuclear fuel contained in a canister.

Fill material might also be added to a canister immediately prior to transportation whenever the integrity of fuel cladding, fuel structures, or canister internal structures or safety-related components cannot be verified sufficiently to provide reasonable assurance of transportation safety and compliance with regulatory requirements for transportation. This would include canisters containing used nuclear fuel following extended storage and canisters containing high burnup used nuclear fuel.

Possible fill materials can be grouped into 3 categories:

1. Liquids, including molten metals, waxes, resins, and grout, that would flow into and fill a canister before undergoing physical change to become a solid.
2. Particulates, including sand, borosilicate glass beads, and metal shot, that would be introduced to canisters to fill available spaces through cascading gravity flow (Wallin 1996).

3. Foams that would be introduced into selected locations in a canister and then would expand and infuse through available internal openings and gaps to fill open spaces.

These categories determine the process that would need to be used to introduce fill materials into a canister.

Processes for filling canisters would be determined by the type of fill material that was used and the approach taken to transfer the material into the canister. Table 11 summarizes the conceptual filling processes that could be employed for each of the different kinds of fill materials and for the different approaches to filling a canister that are described above. Figure 1 provides a conceptual illustration of the process for filling a canister that has its lid removed. The processes described assume that the canister is filled in a facility designed and dedicated for that purpose. The concepts described are unproven. It would be necessary to design and conduct a program that would include tests that demonstrated the feasibility of a fill material concept before any decision was made to use a fill material to stabilize the used nuclear fuel contents of a storage canister.

**Used Fuel Disposition Campaign Storage and Transportation**  
**A Preliminary Evaluation of Using Fill Materials to Stabilize Used Nuclear During Storage and Transportation**

20

August 31, 2012

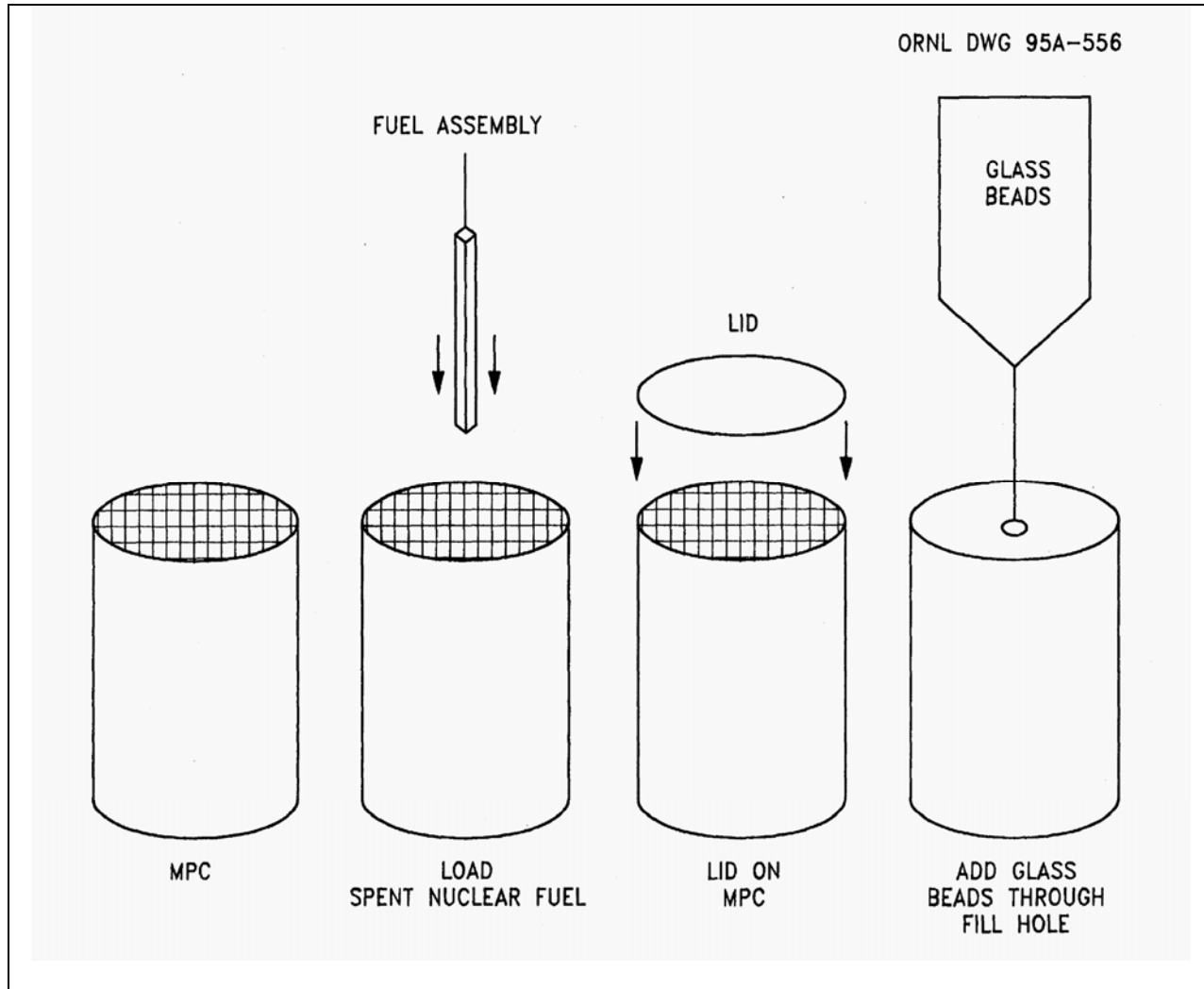


Figure 1. Used Nuclear Fuel Canister Loading Sequence

(Source: Forsberg et al. 1995)

Table 11. Conceptual Approaches for Introducing Fill Material into Dry Storage Canisters Containing Used Nuclear Fuel

Fill Material Type	Approach for Introducing Fill Materials				
	Unseal and remove lid from loaded canister	Unseal and reopen canister drain and vent ports	Canister with ports for adding fill material	Cut openings into canister lid	Cut openings into canister side wall
Liquid	The canister lid's seal weld is cut and lid is removed. Liquid fill is introduced into the canister via a down-tube (vent tube) into the bottom of the open canister and is allowed to flow up to fill the canister before solidifying. The canister's lid is reinstalled and re-welded. An additional external canister may be used if the canister is defective.	The canister's drain and vent ports are unsealed and opened. Liquid fill is introduced into the canister via the vent tube into the bottom of the open canister and is allowed to flow up to fill the canister before solidifying. The canister's drain and vent ports are closed and resealed. An additional external canister may be used if the canister is defective.	Liquid fill is introduced via the inlet port into the canister and is allowed to flow up to fill the canister before solidifying. The canister's ports are re-sealed. An additional external canister may be used if the canister is defective.	Liquid fill is introduced via the cut opening into the canister and is allowed to flow up to fill the canister before solidifying. The openings are re-sealed. An additional external canister may be used if the canister is defective.	Liquid fill is introduced via the cut opening into the canister and is allowed to flow up to fill the canister before solidifying. The openings are re-sealed. An additional external canister may be used if the canister is defective.

Table 11. (contd)

Fill Material Type	Approach for Introducing Fill Materials				
	Unseal and remove lid from loaded canister	Unseal and reopen canister drain and vent ports	Canister with ports for adding fill material	Cut openings into canister lid	Cut openings into canister side wall
Particles	The canister lid's seal weld is cut and lid is removed. Particulate fill is introduced into the top of the canister and is allowed to fill the canister by cascading gravity flow. Vibration may be used to speed up the flow of particulates and to enhance compaction of the particle bed. The canister's lid is reinstalled and re-welded. An additional external canister may be used if the canister is defective.	This approach will not work with particles. There are only two relatively small diameter ports in a canister lid and, even with vibration, the particles will not flow to fill the remaining sections of the canister once a section directly under the ports is filled in.	The canister fill ports are removed. Particulate fill is introduced into the top of the canister through the ports and is allowed to fill the canister by cascading gravity flow. Vibration may be used to speed up the flow of particulates and to enhance compaction of the particle bed. The canister's lid is reinstalled and re-welded. An additional external canister may be used if the canister is defective.	Particulate fill is introduced into the top of the canister through the cut openings and is allowed to fill the canister by cascading gravity flow. Vibration may be used to speed up the flow of particulates and to enhance compaction of the particle bed. The openings are closed and sealed. An additional external canister may be used if the canister is defective.	This approach will not work with particles. Particles will not flow up channels and openings to fill spaces and therefore will not move from the sides of a canister toward the center.

Table 11. (contd)

Fill Material Type	Approach for Introducing Fill Materials				
	Unseal and remove lid from loaded canister	Unseal and reopen canister drain and vent ports	Canister with ports for adding fill material	Cut openings into canister lid	Cut openings into canister side wall
Foam	The canister lid's seal weld is cut and lid is removed. Liquid that will expand to become foam is introduced via a down-tube into the bottom of the canister and is allowed to fill the canister and all available spaces by expanding upward as a medium-viscosity high-density foam. The canister's lid is reinstalled and re-welded. An additional external canister may be used if the canister is defective.	The canister drain and vent ports are unsealed and opened. Liquid that will expand to become foam is introduced via the vent tube into the bottom of the canister and is allowed to fill the canister and all available spaces by expanding upward as a medium-viscosity high-density foam. The canister's drain and vent ports are closed and sealed. An additional external canister may be used if the canister is defective.	The canister fill ports are unsealed and opened. Liquid that will expand to become foam is introduced via a down-tube into the bottom of the canister and is allowed to fill the canister and all available spaces by expanding upward as a medium-viscosity high-density foam. The canister's fill ports are closed and sealed. An additional external canister may be used if the canister is defective.	Liquid that will expand to become foam is introduced via a down-tube extending from the cut opening in the canister lid into the bottom of the canister. The foam is allowed to fill the canister and all available spaces by expanding upward as a medium-viscosity high-density foam. The openings in the canister lid are closed and sealed. An additional external canister may be used if the canister is defective.	Liquid that will expand to become foam is introduced through a side hole that is cut into the canister wall and flows down into the inside wall into the bottom of the canister. The foam then fills the canister and all available spaces by expanding upward as a medium-viscosity high-density foam. The openings in the canister lid are closed and sealed. An additional external canister may be used if the canister is defective.

## **4. REQUIREMENTS FOR FILL MATERIALS**

The previous work discussed in Chapter 2 used various criteria for choosing a fill material. Many of these criteria were specific to used nuclear fuel in waste packages for disposal and thus were related to post-closure performance of a geologic repository. Although many of the criteria could be applicable, they were not selected with consideration of storage or transportation of used nuclear fuel.

This section discusses potential criteria that could be considered when selecting a fill material for a used fuel canister. In contrast to many of the criteria presented in Section 2, these criteria are based on storage and transportation and do not consider post-closure performance. Each requirement is presented in Table 12 along with a summary of the critical elements of that requirement.

Table 12. Potential Requirements for Fill Materials

Evaluation Criteria for Candidate Canister Fill Material	Elements
Criticality Avoidance	Provide moderator exclusion Neutron absorption capability Minimize neutron moderation Provide dilution of fissile radionuclides Capacity to fill over 60% of the inner free volume of the canister Fill material does not compact by more than 10% of its original volume under its own weight or as the result of shipping or handling
Heat Transfer or Thermodynamic Properties	Promote heat transfer from the fuel Thermal stability Chemical stability Radiation stability Chemically compatible with fuel cladding, fuel, neutron poisons, fuel baskets, and other structural materials within canister
Homogeneity and Rheological Properties	Homogeneous batches Good rheological properties to ensure proper filling Ability to be placed in the canister without damaging fuel assemblies
Retrievability	Allows for safe retrieval of used nuclear fuel from a canister without need to resort to time consuming or costly measures and without further compromise of the integrity of used nuclear fuel assemblies
Material Availability and Cost	Low cost Material available in required purity
Weight and Radiation Shielding	Fill material doesn't add significantly to the weight of the container/cask system Good radiation shielding properties
Operational Considerations	Easy to emplace Fill material does not adversely react to normal conditions of transport or hypothetical accident conditions

## **4.1 Criticality Avoidance**

One of the most important criterion for fill material to meet is criticality avoidance, and one potential outcome of the use of certain fill materials could be the ability to eliminate the need to consider burnup credit in the design of the storage container or transportation cask. The standard for criticality is maintaining the effective neutron multiplication factor ( $k_{\text{eff}}$ ) at 0.95 or below. There are several ways to ensure a  $k_{\text{eff}}$  of 0.95, such as use of a fill material with significant neutron adsorption capability, by moderator exclusion, or by dilution of fissile radionuclides. The material should also be chosen so that it does not provide neutron moderation to ensure that a subcritical  $k_{\text{eff}}$  is maintained. In addition, based on analyses cited in Oversby and Werme (1995), the candidate fill material should occupy at least 60% of the original void space in the canister and the material should not compact under its own weight or as the result of shipping or handling by more than 10%.

The need for criticality avoidance as a criterion for fill material may be reduced based on the draft burnup credit guidance contained in NRC (2012), which extends the current major actinide burnup credit (NRC 2002) to include minor actinides and fission products. As discussed in Marshall and Wagner (2012), identification of credible fuel configurations may also reduce the need for a criticality avoidance criterion for fill material.

## **4.2 Heat Transfer and Thermodynamic Properties**

The fill material should also not have a detrimental impact on heat transfer. The temperature of the cladding should be demonstrated to not exceed 400 °C which is regarded as protective of used nuclear fuel cladding. Depending on the fill material and how compacted it is, the radiative and convective heat transfer mechanisms may be virtually eliminated. It is possible that this could be offset by the increase in the thermal conductivity of the fill material. However, each material would need to be evaluated for thermal properties and their effect on the thermal performance of the used nuclear fuel in the canister.

The fill material should also be chemically compatible with the fuel cladding, fuel, neutron poisons, fuel baskets, and other structural materials within canister. Also, the fill material should not undergo adverse interactions with the residual moisture within the canister such as rusting of steel shot, catalysis or radiolytic decomposition of water, or galvanic interactions with cladding or neutron shielding materials. Also, the fill material should be stable within the canister and not degrade due to heat, radiation, or by chemical reaction. The fill material should also not degrade and produce hydrogen or other gases.

Because the duration of long-term storage is also uncertain, the fill material should be relatively unaffected by age or the importance of the fill material properties demonstrated to be less important as the fuel ages. Aging of the fill material would not be important if the fill material was emplaced a short time before transportation and removed soon thereafter.

### **4.3 Homogeneity and Rheological Properties**

Good rheological properties would allow easier flow or flow readily into the canister without agitation and would allow greater assurance of meeting the fill criteria. Another consideration is that the fill material should have homogeneous properties throughout the canister fill. The fill material should also have the ability of being placed in the canister without damaging the fuel assemblies.

### **4.4 Retrievability**

The fill material should allow for the safe retrieval of used nuclear fuel from a canister without the need to resort to timely or costly measures and without further compromise of the integrity of the used nuclear fuel assemblies.

### **4.5 Material Availability and Cost**

The cost and availability of the fill material should be considered when choosing a fill material. This would include the costs of the raw materials with the required purity, processing the materials, and the cost of emplacing the materials in the canister. The ease at which the fill material could be provided to multiple locations such as nuclear power plant sites should also be considered.

### **4.6 Weight and Radiation Shielding**

First, the additional mass that the fill material provides should not result in the canister and cask weight exceeding or approaching weight restrictions for handling or transportation. However, it is possible that certain fill materials would result in a reduction in the need for shielding and as a result a reduction in the overall mass attributed to shielding. This would need to be verified with modeling. Second, the project fill material mass would need to be evaluated against the overall mass of the cask/canister system and its mass limits and any potential modifications to the canister design (wall thickness) to accommodate the additional mass. Third, the fill material may require a reduction in the number of assemblies that a canister would hold to accommodate the mass and volume occupied by the fill material and its desired properties.

### **4.7 Operational Considerations**

The fill material should be easy to emplace in the canister and the fill material should also not interfere with the sealing of the canister, such as welding of the canister lid. The fill material should not adversely react to normal conditions of transport or hypothetical accident conditions.

## **5. POTENTIAL FILL MATERIALS**

This section discusses potential fill materials. Potential fill materials were grouped into several categories such as molten materials, particulates and beads, resins, foams, and grout.

### **5.1 Molten Materials**

Two types of molten materials were evaluated, molten metals and paraffin. As discussed in Chapter 2, molten metals have been evaluated as potential fill materials for waste packages in several studies but no studies were found that had evaluated paraffin as a fill material.

#### **5.1.1 Molten Metals**

The first instance identified of a molten material being proposed for use to stabilize used nuclear fuel during transportation was a patent granted in 1974 to Wurm and Heylen (1974). In this patent, fuel rods would be placed inside a can and the filling alloy would fill the space between the fuel rods and the can. These cans containing the alloy-encased fuel rods would then be placed inside a transportation cask and shipped to their destination, typically a reprocessing plant. The filling alloy performs several functions: 1) the filling alloy stiffens the structure of the fuel element so that the fuel rods cannot break during transportation, 2) if the rods were to break, no radioactive gas would escape, and 3) the filling alloy would conduct heat from the rods to the can. It is not known if used nuclear fuel has ever been transported using the filling alloy method outlined in Wurm and Heylen (1974).

The use of molten metals as a fill material has also been investigated by the Spent Fuel Stabilizer Materials Program and the Canadian Nuclear Fuel Waste Management Program. The Spent Fuel Stabilizer Materials Program recommended 1% antimonial lead as a reference material, while the Canadian Nuclear Fuel Waste Management Program focused research and development activities on lead.

The Yucca Mountain Project also evaluated the use of a tin, lead, zinc, and zinc alloy as fill materials inside a waste package as an alternative to an inert gas (Wallin et al. 1994). Tin was rejected by Wallin et al. (1994) as not being sufficiently plentiful. Lead was rejected because it is toxic, very heavy, and can cause embrittlement of other metal components. Unalloyed zinc was rejected because it was determined that the zinc will interact with the Zircaloy fuel cladding material. Zinc alloys such as AG40B could possibly be acceptable from that standpoint, as they would have a lower tendency to interact with the cladding.

In this evaluation, 5 representative molten metals were considered:

- Tin
- Lead
- Zinc
- Zinc alloy (AG40A and AG40B)
- Wood's metal

These materials are representative of materials with relatively low melting points, less than approximately 420 °C. This temperature was chosen because it would limit the potential for gross rupture of the cladding and preserve the geometric configuration of the used nuclear fuel (NRC 2003). In addition, this temperature is well below the melting point of aluminum (660.37 °C), which is often contained in structural components of metal canisters and in neutron poisons. Table 13 lists representative properties of these materials.

Table 13. Representative Properties of Candidate Molten Metals

Material	Melting Point (°C)	Density (g/cm <sup>3</sup> )	Thermal Conductivity (W/m-K)
Tin	232	7.29	63.2
Lead	327.5	11.35	33.0
Zinc	419.58	7.10	112.2
Zinc alloy (AG40A or AG40B)	381-387	6.60	113
Wood's metal	70.0	9.58	18.0

Source: MatWeb (2012)

One of the primary requirements for a fill material is weight. Based on current designs for used nuclear fuel storage systems, the free volume in a storage canister is in the range of about 4000 to 7000 liters. Assuming that a storage canister was completely filled with molten metal, the weight of a canister would be increased by 58,200 to 102,000 lbs. for zinc alloy, the lowest density material, and by 100,000 to 175,000 lbs. for lead, the highest density material. Current canisters weigh in the range of about 80,000 to 100,000 lbs., so adding a molten metal fill material would approximately double the weight of an existing canister. The addition of a molten metal fill material to a canister would result in the canister not meeting the current requirements of the canister's 10 CFR 72 storage certificate of compliance and the 10 CFR 71 transportation certificate of compliance under which it would be shipped. The additional weight and changed contents would make it necessary to reanalyze the performance of the canister, and recertify the modified canister for continued storage. The changes would also be significant in regard to the design of the transportation cask and would require reanalysis, a probable redesign, and recertification. Therefore, for current canister designs, adding a molten metal fill material appears not to be feasible based on weight and other considerations. Future canisters and their associated transportation casks would need to be designed, possibly with lower capacities and thicker walls, to allow for the increase in weight due to the fill material. Unless the weight of the transportation cask could be reduced as a result of longer cooling times for the used nuclear fuel and possibly because of increased self-shielding by the canister, the decrease in the capacity of the canisters would be as much as 50 percent, which would double the number of canisters that would eventually have to be shipped.

### **5.1.2 Paraffin**

No studies were found where paraffin wax had been investigated as a fill material for used nuclear fuel canisters. Paraffin wax is a mixture of pure alkanes with a chemical formula of  $C_nH_{2n+2}$ . It has a melting point between about 46 and 68 °C, has a density of about 0.9 g/cm<sup>3</sup>, and burns readily if a fire retardant is not incorporated. Paraffin also has a relatively low thermal conductivity, 0.25 W/m-K. Because of its low melting point, paraffin wax could be melted for easy pouring and then hardened to insure complete covering of the used nuclear fuel in a canister. However, there are issues with the use of paraffin as a fill material. For example, paraffin is a hydrocarbon and, if neutron absorber materials are not incorporated, it is an effective neutron moderator. Thus, to make this material a viable fill material, a neutron absorber such as boron would need to be added to the paraffin before pouring. In addition, because of its flammability, a flame retardant would need to be added to the paraffin so that the paraffin material would not burn if released during a transportation accident. Also, because paraffin is a hydrocarbon, it would be subject to radiolytic decomposition that would progress over time. Consequently, except for used nuclear fuel that had been stored for long periods of time such that the source of ionizing radiation was significantly diminished, paraffin could not be used if it was to remain in a canister for a prolonged period of time. Future tests would need to be conducted to determine if paraffin would generate hydrogen or other gases during transportation, especially for used nuclear fuel that had relatively short cooling times. Interactions of paraffin with used nuclear fuel cladding and canister material would also need to be evaluated.

Another issue that would need to be resolved regarding the use of paraffin is its relatively low melting point and at what time in the future the decay heat from used nuclear fuel would be low enough such that the material would remain a solid during transportation. Alternatively, it would be necessary to determine whether a paraffin-containing transportation cask could be shipped when the paraffin was in a liquid state.

A key benefit of using paraffin would be its weight. The density of most paraffin waxes is slightly less than that of water: approximately 0.9 g/cm<sup>3</sup>. Based on current designs for used nuclear fuel storage systems, the free volume in a storage canister is in the range of about 4000 to 7000 liters. Assuming that a storage canister was completely filled with paraffin, the weight of a canister would be increased by 7,900 to 13,900 lb. This is much less than other candidate fill materials. Nonetheless, this increase in the weight of the canister would result in the canister not meeting the requirements of its current 10 CFR 71 transportation certificate of compliance. It is assumed that because paraffin would undergo radiolytic decomposition, it could not be used to stabilize the contents of a canister that would continue to be used for storing used nuclear fuel. The additional weight and changed contents would make it necessary to reanalyze the performance of, and recertify, the modified canister and transportation cask. Therefore, for current canister designs, it is uncertain whether adding paraffin would be feasible based on weight considerations. Assuming that the weight of the transportation cask would be reduced as a result of longer cooling times for the used nuclear fuel that is stabilized by paraffin fill material, it is likely that future canisters and their associated transportation casks would have capacities comparable to present day systems. This would be the case even though the canister would weigh more because of a paraffin fill material. Thus, unlike canisters that would be filled

with molten metal, there would not be an increase in the number of canisters that would need to be shipped.

## **5.2 Particulates and Beads**

As discussed in Section 2, the use of particulates and beads has been extensively studied as a fill material for waste packages. It has also been studied on an extremely limited basis as a fill material for storage containers, and transportation casks. Table 14 lists particulates and beads that have been previously studied.

In experiments conducted to determine potential interactions between particulates and Zircaloy-4, Fish et al. (1982) found that mullite, graphite, basalt, zircon, zirconia, amorphous silica, and quartz formed a brittle interaction layer at the cladding-particulate interface. Fish et al. (1982) postulated that the interaction layers consisted of zirconium oxide. The interaction layers were thought to form due to the extraction of oxygen from the silicon oxide contained in these materials and the formation of zirconium oxide. Graphite also formed an interaction layer with Zircaloy-4 cladding which was likely zirconium carbide. The formation of these interaction layers has the potential to weaken the cladding. Other materials such as interprop and sand/bondate also contain silica and would also likely form the interaction layers observed by Fish et al. (1982).

Fish et al. (1982) also conducted loss-on-ignition tests of candidate particulates. Basalt and bentonite were found to have greater than 1 percent moisture release, which could contribute to corrosion and internal pressurization of a canister.

The density of solid lead is 11.35 g/cm<sup>3</sup>. Assuming a packing fraction of 65% for lead spheres, the effective density of lead spheres would be about 7.4 g/cm<sup>3</sup>. As with the molten metals discussed in Section 5.1.1, this would substantially increase the weight of the canister by 65,300 to 114,000 lb. and would result in an extremely heavy canister. Lead spheres could also potentially compact under their own weight and form voids within the canister.

Depending on how the canisters containing the used nuclear fuel were filled, generation of dust is likely to be an issue because this dust could contaminate the welds used to seal the canister. During packing experiments conducted for the Canadian Nuclear Fuel Waste Management Program, Teper (1987) found that aluminum oxide powder, sand, zircon, rutile, ceramic zirconia, and rutile-zircon-garnet generated excessive dust. In addition, ceramic zirconia had a tendency to form voids.

Depleted uranium oxide particulates or depleted uranium silicate beads have been evaluated by Puig et al. (2008a), Forsberg (2000), Forsberg et al. (1995, 1996), and Pope et al. (1996a, 1996b). Depleted uranium particulates as a fill material for waste packages could have several desirable qualities such as criticality control, radiation shielding, and slowing the release of radionuclides from the waste package. The density of depleted uranium oxide is 10.96 g/cm<sup>3</sup>. Assuming a packing fraction of 65% for depleted uranium oxide particulates, the effective density of depleted uranium oxide particulates would be about 7.1 g/cm<sup>3</sup>. As with the molten

metals discussed in Section 5.1.1 and lead spheres, this would substantially increase the weight of the canister by 62,600 to 110,000 lb. and would result in an extremely heavy canister.

Depleted uranium silicate beads have a density of about  $4.1 \text{ g/cm}^3$ . Assuming a packing fraction of 65% for depleted uranium silicate glass beads, the effective density of depleted uranium silicate beads would be about  $2.7 \text{ g/cm}^3$ , which would increase the weight of a canister by 23,800 to 41,700 lb. This increase in weight would mean that filling existing canisters might not be feasible. However, if used nuclear fuel were cooled long enough, the added weight of the fill material might be offset by a reduction in the weight of the transportation cask. Nonetheless, because of the changed contents and added weight, it would be necessary to provide a new analysis of the performance of the canister for storage and transportation. Based only on weight, it is possible that filling future smaller (less capacity) canisters with the depleted-uranium silicate beads would be feasible, with a corresponding increase in the number of used nuclear fuel canisters. Filling canisters with depleted uranium silicate beads might also eliminate the need for burnup credit for these new canister-transportation cask systems. However, the same benefit could be realized by using boron-containing glass beads, i.e., borosilicate glass beads, which would have a poured density of about  $1.9 \text{ g/cm}^3$  and consequently would not have as much of a weight penalty as would the depleted uranium silicate beads and would also not have the radiation protection issues associated with the use of depleted uranium.

Particulate materials such as magnetite, hematite, olivine, phosphates, and zeolites have been studied as waste package fill materials by Puig et al. (2008a, 2008b, 2009) and Oversby and Werme (1995). The properties of interest were oriented towards post-closure performance of a geological repository, such as the ability to sorb radionuclides and the ability to maintain reducing conditions in the near field around a waste package. In addition, based on the results of packing experiments involving aluminum oxide powder, sand, zircon, rutile, ceramic zirconia, and rutile-zircon-garnet, there is the potential that these materials could generate excessive dust.

Metal shot, such as aluminum, steel, and copper shot, and borosilicate glass beads have been suggested as a potential fill material in several of the studies discussed in Chapter 2. The density of emplaced shot would range from about  $1.8 \text{ g/cm}^3$  for aluminum shot to about  $5.8 \text{ g/cm}^3$  for copper shot, and would be about  $1.9 \text{ g/cm}^3$  for glass beads. As with other materials of relatively high densities, this would increase the weight of existing canisters containing the used nuclear fuel and would result in the canisters not meeting the requirements of their 10 CFR 72 storage certificate of compliance and their 10 CFR 71 transportation certificate of compliance. Therefore, for current canister designs and certifications, adding metal shot or borosilicate glass beads would not be feasible solely based on weight considerations. Future canisters and their associated transportation casks would need to be designed, possibly with lower capacities, to allow for the increase in weight due to the metal shot or borosilicate glass beads. If the capacities of these canisters were less than that of current canisters the increase in the number of canisters would not be as large as for other fill materials with higher densities.

An additional issue associated with materials such as particulates and beads is the potential to compact during the normal conditions of transport. For example, during transportation of a prototype container from Toronto, Ontario, Canada to the Whiteshell Laboratories located in

**Used Fuel Disposition Campaign Storage and Transportation**  
**A Preliminary Evaluation of Using Fill Materials to Stabilize Used Nuclear During Storage and Transportation**

32

August 31, 2012

Pinawa, Manitoba, Canada, the glass-bead particulate within the container appeared to have settled, causing a 14 mm gap between the top head of the container and the top of the particulate (Crosthwaite 1994).

Table 14. Particulates and Beads Evaluated in Previous Studies

Country	Purpose	Materials Studied	References
U.S.	Waste package fill material, used nuclear fuel storage container fill material, transportation cask fill material	Sand Copper spheres Aluminum shot and spheres Zinc spheres Lead spheres Steel shot and spheres Iron shot Magnetite Rutile Amorphous silica Quartz Mullite Zircon Zirconia Basalt Graphite Sand/bondate Bentonite Glass beads and spheres Boron carbide powder Uranium oxide powder Alumina and alumina powder Depleted uranium oxide Depleted uranium silicate glass	Anderson (1981) Pope et al. (1996a, 1996b) Forsberg et al. (1995, 1996) Forsberg (2000) Wallin et al. (1994) Cogar (1996) Montierth (2000) Arthur (2000) Fish et al. (1982)
Spain	Waste package fill material	Steel shot Glass beads Spinel Depleted uranium oxide spheres Zeolites Hematite Phosphates Olivine	Puig et al. (2008a, 2008b, 2009)

Table 14. (contd)

Country	Purpose	Materials Studied	References
Canada	Waste package fill material	Sand Fine glass beads (0.002-0.3 mm) Coarse glass beads (0.8-1.2 mm) Steel shot (0.6-1.0 mm) Aluminum oxide powder Crushed bauxite grains Sintered bauxite Interprop Ceramic zirconia Rutile-Zircon-Garnet mixture Zircon Rutile	Teper (1987) Forsberg (1997)
Belgium	Waste package fill material	Sand	Bennett and Gens (2008) ONDRAF/NIRAS (2001)
Sweden	Waste package fill material	Glass beads Lead shot Copper spheres Sand Olivine Hematite Magnetite Crushed rock	Oversby and Werme (1995)

Interprop is a ceramic proppant composed of 35-65% mullite (aluminum silicate) and 35-65% corundum (aluminum oxide). A proppant is a material that will keep an induced hydraulic fracture open.  
 Bondate is an organic-based chemical bonding agent for aggregates and fibers.

### **5.3 Resins**

No studies were found where liquid resins had been investigated as a fill material for used nuclear fuel canisters. Resins are potentially good candidates for a fill material due to their ability to be poured into a canister as a liquid and then solidify to provide for total coverage of the used nuclear fuel. The fact that resins are organic and are thus moderators of neutrons could be compensated for by adding neutron absorbing materials to the resin. There are other concerns, however, that must be addressed to allow resins to be a viable fill material. These include thermal conductivity, softening point, radiation stability, density, viscosity, and ignition point.

There are many types of resins, each with varying properties, so several are researched in the present paper. These resins include FF grade wood rosin, polyurethane resin, polystyrene resin, epoxy resin, unsaturated polystyrene resin, acrylic resin and silicone resin. The material properties for several resin types are summarized in Table 15.

The densities of these resins are all relatively the same, ranging from 1.00 to 2.00 g/cm<sup>3</sup>. This equates to the addition of 8,800 to 30,800 lb. to the weight of the canister, depending on the void volume within the canister. These values are adjustable based on what curing agent is used. These curing agents can also greatly affect the other properties of the resin. Due to the high degree of fill expected when using these resins, existing canisters could not be filled with resin and shipped unless an analysis to demonstrate performance was done and approval was given by the U.S. Nuclear Regulatory Commission, and future canisters and their associated transportation casks would need to be designed with somewhat lower capacities unless the designs assumed longer cooling times before transportation and the resulting reduced weight of transportation casks offset the increased weight of the canisters.

The thermal conductivities of the resins are also all expected to be relatively the same, ranging from 0.10 to 1.00 W/m-K. This is relatively low, but with longer-cooled or low-heat used nuclear fuel it is not likely to be a concern. If necessary, it may be possible to add a material to the resin to help conduct the heat to the canister structure, such as a metal. There is very little data on thermal conductivities for resins, and so future tests would need to be conducted to establish this physical property.

Another similar characteristic shared by most resins are their resistance to radiation damage. The major damage to resins (and most polymers) from radiation is induced cross-linking or chain scission. Since the resins are cured, this damage would be reduced significantly. As stated in ATL (2001), most resins can withstand a radiation dose of 10<sup>6</sup> Gy. However, a radiation dose 10<sup>7</sup> to 10<sup>8</sup> Gy can produce damage. If the resin were poured inside the canister just before shipment of used nuclear fuel that had been in extended storage for 100 to 300 years, this potentially would probably not be an issue. Future tests would need to be conducted to verify this.

Pour viscosity is another property where most resins share a similar value. Most resins have a viscosity on the order of 1 Pa-s, about 1000 times more viscous than water and on the same order of viscosity as honey. Although this is relatively viscous, it should pose no real impedance to filling a canister other than allowing for an appropriate amount of time to fill the canister before

the curing process can take place. However, future tests would have to be conducted to verify that resins could be poured into a canister without creating significant void spaces.

The major issues with resins lie in their chemical stability, both in terms of softening and ignition points. Although cured resins soften at higher temperatures than the uncured resins that are poured into the canister to begin with, these softening points can still be well below the 400 °C temperature that is regarded as protective of used nuclear fuel cladding. In this capacity, polyurethane, epoxy and silicone resins perform best with softening points of approximately 150 °C. Further research is needed to find curing agents that would be able to increase the softening point if 150 °C is not sufficiently high.

Although resins melt at low temperatures, their ignition points can exceed 400 °C. For example, if the right curing agents are used, polystyrene, polyester and silicone resins will not ignite until temperatures of 430, 500 and 760 °C, respectively. If the resin could be exposed to the atmosphere following a fire accident, it might be necessary to include ignition retardants in the resin formulation or to conduct tests to verify that the ignition point of the resin used as a fill material is not reached, especially during the hypothetical accident conditions specified in 10 CFR 71.73. Future tests would also be needed to determine if resins could generate hydrogen or other gases when they decompose.

Table 15. Material Properties of Resins

Resin	Density (g/cm <sup>3</sup> )	Softening Point (°C)	Thermal Conductivity (W/m-K)	Viscosity (mPa-s)	Ignition Temperature (°C)
FF Wood Rosin	1.089	100–120	--	4000	--
Polyurethane	1.490	144	0.65	6000	N/A
Polystyrene	1.040	105	--	--	430
Epoxy	1.335	80–162	0.2	5000	390
Unsaturated Polyester	1.900	70–100	--	2000	500
Acrylic	1.160	108	--	1500	340
Silicone	1.000	7–138 <sup>a</sup>	--	200	760

a. Flashpoint.

Note: The material properties are representative of the type of resin and the properties of specific resins may vary.

## 5.4 Foams

No studies were found where foams were investigated as a fill material for used nuclear fuel canisters. As with resins, there are many types of foams. Table 16 summarizes the material properties of several foams.

Foams could potentially insure an easy filling process with complete coverage and support of the used nuclear fuel as well as having a low density which would not increase the weight of the canister significantly. However, the ability to inject foam inside a used nuclear fuel canister without significant void spaces would need to be verified with future experiments.

Foams have several downfalls, but like paraffin, these downfalls may be compensated for by the addition of other materials or further research. Most foams are organic in nature, and so are excellent neutron moderators. This can be compensated for by adding a neutron absorbing material to the foam before injection, or by using inorganic foams instead. Foams may also provide moderator exclusion.

Organic foams can also burn readily at relatively low temperatures (approximately 400 °C). However, foams have been used in the design of Type B radioactive materials containers. For example, the TRUPACT-II container (Docket Number 71-9218) and TRUPACT-III container (Docket Number 71-9305) both contain polyurethane foam. Nonetheless, tests would be needed to determine if foams could ignite or decompose inside a canister, especially during hypothetical accident conditions. Future tests would also be needed to determine if foams could generate hydrogen or other gases when they decompose. In addition to chemical and radiation stability, foams must have desirable properties in the thermal stability, rheology, density, and strength criteria. Based on the ignition temperatures in Table 16, organic foams my not be the best choice for a fill material due to low ignition temperatures, and metal or ceramic foams may have desirable properties in the areas of structural integrity, increased thermal conductivity, lack of neutron moderation, and their high temperature performance.

The density of foams can vary widely based on what material they are, as well as whether they have open- or closed-cell structures. An open-cell foam is one where the gas is not trapped within the foam structure, much like that of a common sponge, while a closed-cell foam is a solid material with gas bubbles are trapped inside. Thus, the open-cell foams are less dense, but the closed-cell foams have a higher strength.

Although the addition of neutron absorbers to the foam before pouring would prevent criticality, the radiation from the used nuclear fuel may also cause material degradation. In Huang et al. (2007), the radiation dose at which degradation begins is  $10^6$  Gy. This is similar to the degradation threshold for resins. If foam were injected into the canister just before shipment of the used nuclear fuel that had been in extended storage for 100 to 300 years, this potentially would not be an issue. Future tests would be needed to verify this.

Table 16. Material Properties of Foams

Foam	Density (g/cm <sup>3</sup> )	Thermal Conductivity (W/m-K)	Ignition Temperature (°C)
Polyurethane	0.013–0.160	0.03	400
Polystyrene	0.032–0.050	0.03	350
Aluminum	0.216–0.675	5.80	660 <sup>a</sup>
Steel	0.040–0.950	0.80	1535 <sup>a</sup>
Silicon Carbide	0.257–0.803	5.28	2700 <sup>b</sup>

a. Melting point  
b. Sublimation point

Note: The material properties are representative of the type of foam and the properties of specific foams may vary.

## 5.5 Grout

Two studies (Anderson 1981 and Oversby and Werme 1995) discussed in Chapter 2 evaluated the use of cement grout (i.e., concrete or mortar) as a fill material for used nuclear fuel canisters. Sweden also evaluated concrete as a fill material in a titanium canister used for very deep hole disposal (SKB 1992). Grout is commonly used to solidify liquid low-level radioactive and to stabilize low-level radioactive waste prior to disposal. Grout has also been used to solidify liquid high-level radioactive waste in Italy (Alonzo et al. 2001) and to stabilize empty high-level radioactive waste tanks at the Savannah River Site. Grout has also been used to stabilize used nuclear fuel sludge at the Hanford Site.

A primary issue associated with using grout as a fill material would be its weight. Grout has a density of about 2.0 g/cm<sup>3</sup> which would increase the weight of a canister with used nuclear fuel contents by 17,600 to 30,900 lb. A significant consequence of the combined increased weight and addition of grout to the canister's contents would be that existing canisters would not comply with the requirements of their current 10 CFR 72 storage certificate of compliance and their 10 CFR 71 transportation certificate of compliance. Therefore, for current canister designs, adding grout would not be possible unless the safety analyses for storage and transportation were revised to demonstrate that the canisters with grout fill material would satisfy the requirements of U.S. Nuclear Regulatory Commission regulations and U.S. Nuclear Regulatory Commission approval was obtained. It might be feasible to ship the heavier canisters if the used nuclear fuel had cooled sufficiently to allow an offsetting reduction in the shielding needed and a new design for the transportation cask with reduced weight was developed and certified. Future canisters and their associated transportation casks would need to be designed with somewhat lower capacities unless the designs assumed longer cooling times before transportation and the resulting reduced weight of transportation casks offset the increased weight of the canisters.

Another issue associated with using grout as a fill material would be its ability to flow between the fuel rods and around other structural materials in the canister. Future tests would be needed to verify that this was feasible. In addition, cement grout contains water, which is a neutron

**Used Fuel Disposition Campaign Storage and Transportation**  
**A Preliminary Evaluation of Using Fill Materials to Stabilize Used Nuclear During Storage and Transportation**

August 31, 2012

39

moderator, so a neutron absorbing material might have to be added to the grout to ensure subcriticality. Also because grout contains water, future tests would also be necessary to evaluate radiolysis and interactions of grout with fuel cladding, fuel, neutron poisons, fuel baskets, other structural materials within canister, the canister itself.

## **6. CONCLUSIONS AND RECOMMENDATIONS**

Based on the weight of the potential fill materials discussed in Chapter 5, adding fill materials to existing canisters would result in the canisters not meeting the current requirements of their 10 CFR 72 storage certificate of compliance and their 10 CFR 71 transportation certificate of compliance. Depending on the cooling time assumed for the used nuclear fuel, future canisters and their associated transportation casks might need to be designed with lower capacities and thicker walls to allow for the increase in weight due to the addition of the fill material. Foam fill materials might be an exception to this.

Most studies that have evaluated fill materials and their properties have been literature reviews; few have been studies that conducted experiments. Also, from the perspective of the Used Fuel Disposition Campaign, a significant gap in the existing studies is that none have evaluated the performance of the fill materials during the normal conditions of transport or during hypothetical transportation accident conditions. Studies that addressed this gap would need to include ones that assessed the ability of the fill material to maintain its own geometric configuration (e.g., not slump) and maintain the geometric configuration of the used nuclear fuel under normal conditions of transport and under hypothetical accident conditions. Such studies would provide the information that would be needed to determine whether credit could be taken for the fill material being able to exclude water moderator or provide neutron absorbers such that the fissile material package requirements in 10 CFR 71.55 could be shown to be satisfied.

Consequently, the use of fill materials to stabilize used nuclear fuel in canisters would require a comprehensive experimental program. Especially important would be:

- Experiments that would evaluate the interactions among the fill material, fuel cladding, fuel, fuel baskets, neutron poisons, and other structural materials including the canister itself.
- Experiments that would determine if a fill material could be efficiently, effectively, and reliably emplaced inside a canister containing used nuclear fuel, filling the free volume without leaving an excessive number of, or large voids
- Experiments that would evaluate the efficacy of heat conduction from fuel rods in fuel assemblies through the fill material to the heat removal features of the canister and determine the resulting temperatures of fuel cladding.

Molten materials, particulates, and beads have been extensively studied as fill materials for waste packages and their ability to function in this capacity is reasonably well known. Nonetheless, the scope of the research and development effort would be greatest if molten metal fill was used, for which canisters that contain used nuclear fuel would have to be preheated and cooled under carefully controlled conditions. The research and development would necessarily determine the process and procedure, and alternatives, for retrieving used nuclear fuel from canisters where molten metal fill had been used. Other issues such as the compatibility of the molten metal fill material and fuel cladding and safety related components of a canister would need to be determined. Techniques would also need to be developed and demonstrated for filling a canister

with molten metal, for determining that the fill was successful and that voids did not remain within the cast metal matrix, and for recovering from an unsuccessful fill.

Paraffin is an alternative molten material that might be used to fill canisters if the decay heat of the used nuclear fuel was not too great. Although paraffin is a neutron moderator and is flammable, a neutron absorber material might be dissolved in it as might a fire retardant material. As with molten metal fill materials, it would likely be necessary to heat canisters to ensure that the molten paraffin infiltrated into all of the available spaces in the canister. Unlike molten metal, high temperatures would probably not be necessary. It would be necessary to demonstrate that the paraffin would not be molten during normal transportation, could maintain the geometric configuration of the used nuclear fuel during normal and hypothetical accident conditions of transportation, and that it would not leak out following a transportation accident if temperatures were great enough to re-melt the material. Paraffin would be subject to radiolysis and therefore could not be used for extended storage during periods when the radiation source of the used nuclear fuel remained high.

If the fill material was a particulate or bead, it is likely that the canister and its used nuclear fuel contents would have to be vibrated during the filling process to ensure that the particles filled the available void spaces and with the desired packing density. It would be necessary to conduct research to develop techniques and tests to demonstrate, with high confidence, that particulate fill material would successfully infiltrate into all of the available open spaces within a canister and in and around the fuel assemblies leaving few if any voids. Because the condition of the fuel cladding would be suspect or unverified (otherwise, it would not be necessary to introduce fill material into a canister), tests would be necessary to determine if vibrating the canister could further damage the fuel cladding.

Because resins contain organic compounds, it may not be possible to formulate one that does not decompose or produce hydrogen or other gases when subjected to the heat and radiation environment in a dry used nuclear fuel canister, or when subjected to temperatures that might occur during hypothetical accident conditions.

Foams, especially inorganic foams, show some promise for use as fill materials. Nonetheless, it would be necessary to conduct extensive tests and demonstrations to show that a foam would reliably flow into and fill, at the required density, all of the void spaces and in and around the fuel rods in a canister that contained used nuclear fuel. Also, as with resins it would also be necessary to demonstrate that the foam did not decompose or produce hydrogen or other gases as a consequence of being exposed to heat and radiation or to temperatures that would exist following hypothetical transportation accident conditions.

Grout has also been extensively studied for stabilizing low-level radioactive waste and other waste and its ability to function in this capacity is also reasonably well known.

In addition to the research and development that would be required for the fill material that would be used, the process for emplacing the fill material into canisters containing used nuclear fuel would have to be demonstrated for its reliability, safety, and efficiency. The process would

need to be located in a dedicated facility, possibly a facility that can be disassembled and moved for use at multiple sites, or a dedicated area within an existing facility. Whether the process was to be installed in a new facility or an existing facility, it would be necessary to design, license, and construct/install the facility at every site where canisters were to be filled with a fill material, or develop a mobile facility. Conceptual designs for a facility that could be moved among sites have been proposed in the past. Such a design might be adopted, with modifications for use at a single site where fill material was to be placed into canisters containing used nuclear fuel. The design of such a facility could require substantial research and development.

Before fill materials could be used to stabilize used nuclear fuel contained in storage and transportation canisters a substantial development, design, and licensing effort would need to be undertaken. In addition, the results of previous work show that use of fill materials to stabilize used nuclear fuel inside storage and transportation canisters would present significant technical challenges. Therefore, further research on the use of fill materials to stabilize used nuclear fuel during storage and transportation is not recommended unless options such as showing that the fuel remains intact or canning of used nuclear fuel do not prove to be feasible.

## 7. REFERENCES

- 10 CFR 71            10 CFR 71. "Packaging and Transportation of Radioactive Material." Code of Federal Regulations, U.S. Nuclear Regulatory Commission.
- 10 CFR 72            10 CFR 72. "Licensing Requirements for the Independent Storage of Spent Nuclear Fuel, High-Level Radioactive Waste, and Reactor-Related Greater Than Class C Waste." Code of Federal Regulations, U.S. Nuclear Regulatory Commission.
- ATL 2001            Advanced Technologies and Laboratories International, Inc. 2001. "Technical Assistance on the Evaluation of Resin Polymers Used in Storage and Transportation Cask Shield Designs." Accession Number ML011860442. Germantown, Maryland.
- Alonzo et al. 2001    Alonzo G, M Casarci, C Pastore, E Petagna, P Tortorelli, S Bolgherini, G Jacovazzi, F Pietrini, S Campa. 2001. "Conditioning of HLW by Immobilizing in Concrete at SIRTE-MOWA Plant." In WM'01 Conference, February 25-March 1, 2001, Tucson, Arizona.
- Anderson 1981        Anderson KJ. 1981. "The Use of Filler Materials to Aid Spent Nuclear Fuel Dry Storage." AGNS-35900-1.3-143. Allied-General Nuclear Services, Barnwell, South Carolina.
- Arthur 2000           Arthur S. 2000. "EQ6 Calculation for Chemical Degradation of Shippingport LWBR (Th/U Oxide) Spent Nuclear Fuel Waste Packages." CAL-EDC-MD-000008 REV 00. Accession Number MOL.20000926.0295. CRWMS M&O, Las Vegas, Nevada.
- Bennett and Gens 2008    Bennett DG and R Gens. 2008. "Overview of European Concepts for High-Level Waste and Spent Fuel Disposal with Special Reference Waste Container Corrosion." Journal of Nuclear Materials 379:1-8.
- Carlsen and Brady Raap 2012    Carlsen BW and M Brady Raap. 2012. "Dry Transfer Systems for Used Nuclear Fuel." FCRD-UFD-2012-000115. Used Fuel Disposition Campaign, U.S. Department of Energy, Washington, DC.
- Cogar 1996a           Cogar JA. 1996. "Technical Document Preparation Plan for Waste Package Filler Material Testing Report." BBA000000-01717-2500-00007 REV 00. Accession Number MOL.19961007.0209. CRWMS M&O, Las Vegas, Nevada.

**Used Fuel Disposition Campaign Storage and Transportation  
A Preliminary Evaluation of Using Fill Materials to Stabilize Used Nuclear During Storage and  
Transportation**

44

August 31, 2012

- Cogar 1996b Cogar JA. 1996. "Spent Nuclear Fuel Waste Package Filler Testing Technical Guidelines Document." BBA000000-01717-2500-00003 REV 03. Accession Number MOL.19970421.0214. CRWMS M&O, Las Vegas, Nevada.
- Cogar 1996c Cogar JA. 1996. "Waste Package Filler Material Testing Report." BBA000000-01717-2500-00008 REV 02. Accession Number MOL.19970121.0004. CRWMS M&O, Las Vegas, Nevada.
- Crosthwaite 1994 Crosthwaite JL. 1994. "The Performance, Assessment and Ranking of Container Design Options for the Canadian Nuclear Fuel Waste Management Program." TR-500, COG-93-410. Whiteshell Laboratories, Pinawa, Manitoba, Canada.
- Fish et al. 1982 Fish RL, N Wynhoff, and VJ Ferrell. 1982. "Spent LWR-Fuel Waste-Package-Stabilizer Recommendations." HEDL-7204. Hanford Engineering Development Laboratory, Richland, Washington.
- Forsberg 1997 Forsberg CW. 1997. "Description of the Canadian Particulate-Fill Waste-Package (WP) System for Spent-Nuclear-Fuel (SNF) and its Applicability to Light-Water Reactor SNF WPs with Depleted Uranium-Dioxide Fill." ORNL/TM-13502. Oak Ridge National Laboratory, Oak Ridge, Tennessee.
- Forsberg 2000 Forsberg CW. 2000. "Effect of Depleted-Uranium Dioxide Particulate Fill on Spent-Nuclear-Fuel Waste Packages." Nuclear Technology 131:337-353.
- Forsberg et al. 1995 Forsberg CW, RB Pope, RC Ashline, MD DeHart, KW Childs, and JS Tang. 1995. DUSCOBS – A Depleted-Uranium Silicate Backfill for Transport, Storage, and Disposal of Spent Nuclear Fuel. ORNL/TM-13045. Oak Ridge National Laboratory, Oak Ridge, Tennessee.
- Forsberg et al. 1996 Forsberg CW, RB Pope, RC Ashline, MD DeHart, KW Childs, and JS Tang. 1996. "Depleted-Uranium-Silicate Backfill of Spent-Fuel Waste Packages for Repository Containment and Criticality Control." In High Level Radioactive Waste Management, Proceedings of the Seventh Annual International Conference. pp. 366-368. April 29-May 3, 1996, Las Vegas, Nevada.
- Huang et al. 2007 Huang W, YS Xu, XJ Chen, XL Gao, and YB Fu. 2007. "Study on the Radiation Effect of Polyether-Urethane in the Gamma-Radiation Field." Journal of Radioanalytical and Nuclear Chemistry 273(1):91-98.

**Used Fuel Disposition Campaign Storage and Transportation**  
**A Preliminary Evaluation of Using Fill Materials to Stabilize Used Nuclear During Storage and Transportation**

August 31, 2012

45

- Johnson et al. 1994 Johnson LH, JC Tait, DW Shoesmith, JL Crosthwaite, and MN Gray. 1994. "The Disposal of Canada's Nuclear Fuel Waste: Engineered Barriers Alternatives." AECL-10718, COG-93-8. Whiteshell Laboratories, Pinawa, Manitoba, Canada.
- Marshall and Wagner (2012) Marshall W and J Wagner. 2012. "Impact of Fuel Failure on Criticality Safety of Used Nuclear Fuel." Presented at 11th International Probabilistic Safety Assessment and Management Conference and the Annual European Safety and Reliability Conference. June 25-29, 2012. Helsinki, Finland.
- MatWeb (2012) MatWeb. 2012. "MatWeb Material Property Data." [www.matweb.com](http://www.matweb.com).
- Mobasheran 1999 Mobasheran AS. 1999. "Enrico Fermi Fast Reactor Spent Nuclear Fuel Criticality Calculations: Intact Mode." BBA000000-01717-0210-00037 REV 00. Accession Number MOL.19990125.0079. CRWMS M&O, Las Vegas, Nevada.
- Montierth 2000 Montierth LM. 2000. "Intact and Degraded Criticality Calculations for the Codisposal of Shippingport LWBR Spent Nuclear Fuel in a Waste Package." CAL-EDC-NU-000004 REV 00. Accession Number MOL.20000922.0093. CRWMS M&O, Las Vegas, Nevada.
- Moscalu et al. 2000 Moscalu DR, L Angers, J Monroe-Rammsy, and HR Radulescu. 2000. "Enrico Fermi Fast Reactor Spent Nuclear Fuel Criticality Calculations: Degraded Mode." CAL-EDC-NU-000001 REV 00. Accession Number MOL.20000802. 0002. CRWMS M&O, Las Vegas, Nevada.
- NRC 2002 U.S. Nuclear Regulatory Commission. 2002. "Burnup Credit in the Criticality Safety Analyses of PWR Spent Fuel in Transport and Storage Casks." Spent Fuel Project Office, Interim Staff Guidance-8, Revision 2. Washington, DC.
- NRC 2003 U.S. Nuclear Regulatory Commission. 2003. "Cladding Considerations for the Transportation and Storage of Spent Fuel." Spent Fuel Project Office, Interim Staff Guidance-11, Revision 3. Washington, DC.
- NRC 2012 U.S. Nuclear Regulatory Commission. 2012. "Burnup Credit in the Criticality Safety Analyses of PWR Spent Fuel in Transport and Storage Casks." Spent Fuel Project Office, Interim Staff Guidance-8, Revision 3 (Draft), Accession Number ML12115A303. Washington, DC.
- NWMO 2005 Nuclear Waste Management Organization. 2005. "Incorporation of Seaborn Panel Recommendations and Insights in Work of the NWMO." NWMO Background Paper 2-8. Toronto, Ontario, Canada.

**Used Fuel Disposition Campaign Storage and Transportation**  
**A Preliminary Evaluation of Using Fill Materials to Stabilize Used Nuclear During Storage and Transportation**

46

August 31, 2012

- ONDRAF/NIRAS 2001 ONDRAF/NIRAS. 2001. “SAFIR 2: Safety Assessment and Feasibility Interim Report 2.” Report No. NIROND 2001-06 E. Belgian Agency for Radioactive Waste and Enriched Fissile Materials.
- Oversby and Werme 1995 Oversby VM and LO Werme. 1995. “Canister Filling Materials – Design Requirements and Evaluation of Candidate Materials.” In Scientific Basis for Nuclear Waste Management XVIII. Materials Research Society Symposium Proceedings 353:743-750. October 23-27, 1994, Kyoto, Japan.
- Pope et al. 1996a Pope RB, CW Forsberg, MD DeHart, KW Childs, and JS Tang. 1996. “Potential Benefits and Impacts on the CRWMS Transportation System of Filling Spent Nuclear Fuel Shipping Casks with Depleted Uranium Silicate Glass.” In SPECTRUM ’96: Proceedings of the International Topical Meeting on Nuclear and Hazardous Waste Management. August 18-23, 1996, Seattle, Washington.
- Pope et al. 1996b Pope RB, CW Forsberg, RC Ashline, MD DeHart, KW Childs, and JS Tang. 1996. “Benefits/Impacts of Utilizing Depleted Uranium Silicate Glass as Backfill for Spent Fuel Waste Packages.” In High Level Radioactive Waste Management, Proceedings of the Seventh Annual International Conference. pp. 369-371. April 29-May 3, 1996, Las Vegas, Nevada.
- Puig et al. 2008a Puig F, J Dies, J de Pablo, and A Martinez-Esparza. 2008. “Spent Fuel Canister for Geological Repository: Inner Material Requirements and Candidates Evaluation.” Journal of Nuclear Materials 376:181-191.
- Puig et al. 2008b Puig F, J Dies, M Sevilla, J de Pablo, JJ Pueyo, L Miralles, and A Martinez-Esparza. 2008. “Inner Material Requirements and Candidates Screening for Spent Fuel Disposal Canister.” In Scientific Basis for Nuclear Waste Management XXXI. Materials Research Society Symposium Proceedings 1107:67-74. September 16-21, 2007, Sheffield, England.
- Puig et al. 2009 Puig F, J Dies, M Sevilla, J de Pablo, JJ Pueyo, L Miralles, and A Martinez-Esparza. 2009. “Selection and Evaluation of Inner Material Candidates for Spanish High Level Radioactive Waste Containers.” In ICEM2007: Proceedings of the 11th International Conference on Environmental Remediation and Radioactive Waste Management. pp. 285-292. September 2-6, 2007, Bruges, Belgium.
- Radulescu 2000 Radulescu HR. 2000. “Evaluation of Codisposal Viability for Th/U Oxide (Shippingport LWBR) DOE-Owned Fuel.” TDR-EDC-NU-000005 REV 00. CRWMS M&O, Las Vegas, Nevada.

**Used Fuel Disposition Campaign Storage and Transportation**  
**A Preliminary Evaluation of Using Fill Materials to Stabilize Used Nuclear During Storage and Transportation**

August 31, 2012

47

- Shelson 1983 Shelson KN. 1983. "Particulate Packings for Irradiated Fuel Disposal Containers." Report No. 83085. Ontario Hydro Design and Development Division, Ontario Hydro Technologies, Toronto, Canada.
- SKB 1992 Svensk Kärnbränslehantering AB. 1992. "Project on Alternative Systems Study (PASS) Final Report." Technical Report 93-04. Stockholm, Sweden.
- SKB 2010 Svensk Kärnbränslehantering AB. 2010. "Design, Production and Initial State of the Canister." Technical Report TR-10-14. Stockholm, Sweden.
- Teper 1987 Teper B. 1987. "Test Program of Granular Materials for the Thin-Walled Particulate-Packed Container." Report No. 87-154-K. Ontario Hydro Research Division.
- UFDC 2012 Used Fuel Disposition Campaign. 2012. "Gap Analysis to Support Extended Storage of Used Nuclear Fuel." FCRD-USED-2011-000136 Rev. 0, PNNL-20509. Used Fuel Disposition Campaign, U.S. Department of Energy, Washington, DC.
- Wallin et al. 1994 Wallin WE, RH Bahney, and DA Thomas. 1994. "Initial Review/Analysis of Thermal and Neutronic Characteristics of Potential MPC/WP Filler Materials." BBA000000-01717-5705-00001 REV 00. Accession Number NNA.940602.0019. CRWMS M&O, Las Vegas, Nevada.
- Wallin 1996 Wallin WE. 1996. "Analysis of MPC Access Requirements for Addition of Filler Materials." BB0000000-01717-0200-00010 REV 00. Accession Number MOL.19960917.0030. CRWMS M&O, Las Vegas, Nevada.
- Werme and Eriksson 1995 Werme L and J Eriksson. 1995. "Copper Canister with Cast Inner Component, Amendment to Project on Alternative Systems Study (PASS), SKB TR 93-04." Technical Report 95-02. Svensk Kärnbränslehantering AB, Stockholm, Sweden.
- Wurm and Heylen 1974 Wurm JG and PR Heylen. July 23, 1974. "Method of Transporting and Processing Irradiated Fuel Elements." US Patent 3,824,673.
- Wynhoff et al. 1982 Wynhoff N, SE Girault, and RL Fish. 1982. "Spent Fuel Stabilizer Material Characterization and Screening." HEDL-7210. Hanford Engineering Development Laboratory, Richland, Washington.

## **APPENDIX F**

### **Summary of PNNL Transportation Activities for FY12 to Support the UFD Program**

## Summary of PNNL Transportation Activities for FY12 to Support the UFD Program

### 1. Integration of Transportation Gap Analysis with the Storage Gap Analysis

For this task the Features, Events, and Processes (FEPs) for Transportation that were identified and documented in the FY11 mid-year and year-end reports were further evaluated to understand the differences between the transportation gaps and the storage gaps. The transportation gaps report was modified to facilitate consolidate of the transportation FEPs with the storage FEPs. The list of SSCs and the associated degradation mechanisms [known as features, events, and processes (FEPs)] were based on the list of used nuclear fuel (UNF) storage system SSCs and degradation mechanisms developed by the UFD Storage Task (Hanson et al. 2011). Other sources of information surveyed to develop the list of SSCs and their degradation mechanisms included references such as Evaluation of the Technical Basis for Extended Dry Storage and Transportation of Used Nuclear Fuel (NWTRB 2010), Transportation, Aging and Disposal Canister System Performance Specification, Revision 1 (OCRW 2008), Data Needs for Long-Term Storage of LWR Fuel (EPRI 1998), Technical Bases for Extended Dry Storage of Spent Nuclear Fuel (EPRI 2002), Used Fuel and High-Level Radioactive Waste Extended Storage Collaboration Program (EPRI 2010a), *Industry Spent Fuel Storage Handbook* (EPRI 2010b), and *Transportation of Commercial Spent Nuclear Fuel, Issues Resolution* (EPRI 2010c). SSCs include items such as the fuel, cladding, fuel baskets, neutron poisons, metal canisters, etc. Potential degradation mechanisms (FEPs) included mechanical, thermal, radiation and chemical stressors, such as fuel fragmentation, embrittlement of cladding by hydrogen, oxidation of cladding, metal fatigue, corrosion, etc. The degradation mechanisms were evaluated for influence by high burnup, additional data needs, importance of research and development (R&D), and the importance to transportation. These categories were used to identify the most significant transportation degradation mechanisms. In general, the Transportation Importance assigned in above mirrored the importance assigned by the UFD Storage Task. However, there were a few differences as noted in Table 1 below.

Table 1 – Summary of Storage and Transportation Importance Differences

Stressor	Degradation Mechanism	Importance		Comments
		Storage	Trans	
<b>Neutron Poisons</b>				
Thermal	Thermal aging affects	Med	HIGH	Aging effects on poisons could affect structural properties to the extent that they would not survive the loads of transportation hypothetical accident conditions and compromise the ability to prevent a nuclear criticality. For storage moderator control is the primary mechanism for criticality

Stressor	Degradation Mechanism	Importance		Comments
		Storage	Trans	
				control.
<b>Bolted Direct-Load Casks</b>				
Thermal and Mechanical	Thermo mechanical fatigue of seals and bolts	Med	Low	Failure of seals and bolts due to thermomechanical fatigue is important for storage relicensing. It is expected that bolts and seals would be inspected prior to transportation to assure their integrity. However, if issues are found with seals that could mean having to replace the seals in a pool.

In addition to the comparison of storage and transportation gaps the following discussions were prepared as contributions to the storage and transportation gap analysis report.

- Transportation Regulation History including a summary of historical shipment
- Used Nuclear Fuel Transportation Casks including key functional and performance requirements of UNF transportation casks. It also described modern UNF shipping casks for both legal weight truck and rail transportation.
- Regulations and Regulatory Guidance Governing Transportation of UNF
- Application of NRC Regulations in the Design and use of Used Nuclear Fuel Transportation Casks
- Current Issues Surrounding the Application of NRC Regulations in the Design and use of UNF Transportation Casks

## 2. Orphan Site Task

A report is in progress that will be completed in October 2012 that analyzes in detail each of the orphan sites. Specifically, the report will present the following discussions:

- Current State
- Desired End State
- Assumptions
- Actions Necessary to Achieve Desired End State
- Conclusions

The discussion on the current state of each of the 9 orphan sites will describe the UNF and GTCC inventory at the 9 orphan sites, and will include items such as the number of canisters/casks of UNF and GTCC, the storage system used at the site, the associated transportation cask, whether a transfer cask would be necessary, and whether impact limiters and transportation casks have been fabricated. Information on the UNF will be collected to the extent available from sources such as the RW-859 database and utility site managers. Specific items to be discussed with site managers will include the type of used nuclear fuel (BWR or PWR); the design, configuration, and composition (including type of cladding) of the used nuclear fuel assemblies; the number of assemblies and canisters in storage; the types of canister and storage system; the number of assemblies per canister; the identification numbers for the fuel assemblies contained in each canister; the condition of each fuel assembly (undamaged, intact, failed); the reported range of burnups, enrichments, and discharge dates (and the associated decay heats, isotopic compositions, and radiation source terms); and whether the canisters, as loaded, are transportable; and, if transportable, the name of the transportation cask and associated current NRC 10 CFR 71 Certificate of Compliance. It is acknowledged that all this information may not be available from all sites. The section will also describe any unique considerations associated with the storage and transportation system used at the site.

In addition, this section will also describe the equipment that is present at the site, the infrastructure at the sites (e.g., secure cask handling and loading equipment, facilities, and support structures; secure equipment, cask, and railcar staging and parking areas; radiological health support facilities and services or areas for installation of temporary facilities; electric power, water, and fire-protection services or access to same; site operations and personnel sheltering and safety facilities or areas for installation of temporary facilities), and the nearest transportation interfaces for rail, barge, and heavy haul truck (including limitations such as railcar weight limits for local transportation route segments; known or expected restrictions on use of the local routes; permitting requirements; and additional resources (including equipment such as cranes and public safety services such as physical security).

As part of this task each of the orphan sites will be visited. During the week of 8/27/12 Maine Yankee, Connecticut Yankee, and Yankee Rowe were visited. Other sites will be visited in FY2013. For sites not visited, information from Facility Interface Data Sheets, Services Planning Documents, Near-Site Transportation Infrastructure Reports, and Facility Interface Capability Assessment Cask-Handling Assessments will be used to establish a baseline, augmented by information from site managers and web resources.

The section on the Desired End State will describe the desired end state of the sites, i.e., UNF and GTCC removed.

The assumptions section will list and describe the assumptions used in the preparation of the report. Examples of these assumptions include:

- The location of the Consolidated Storage Facility (CSF), site selection, waste acceptance criteria, and licensing are outside of the scope of this report. Note—there may be multiple CSFs.
- UNF and GTCC in canisters or casks will meet the waste acceptance criteria and documented safety analysis requirements of the CSFs.
- No repackaging of UNF or GTCC will be necessary at the origin sites.
- UNF and GTCC will be shipped using rail, barge, or heavy-haul truck. Legal weight truck and overweight trucks (< 115,000-125,000 lbs) will not be used to ship UNF or GTCC. However, they may be used to ship campaign kits.
- UNF and GTCC will be shipped using AAR specification railcar.
- An MOU between DOE and each utility defining roles and responsibilities at each site would be established. Would vary at each site; could vary by utility.
  - The utility is responsible for all operations inside ISFSI boundary and all operations necessary to put UNF and GTCC into 10 CFR 71 shippable configuration.
  - DOE is shipper of record; utilities must provide detailed content information.
  - DOE procures railcars, DOE procures escort cars.
  - DOE hires heavy haul truck contractor. DOE hires railroads.
  - DOE provides security; tracking; security at ISFSI site is utility responsibility. During loading, utility provides security. After loading and outside ISFSI boundary, DOE provides security.
- Open Items:
  - Who (DOE or utility) provides transportation cask?
  - Who pays for restablishing transportation infrastructure?

The section describing the Actions Necessary to Achieve Desired End State will describe the actions (i.e., task list) necessary to achieve the desired end state. The section will describe actions such as (not all inclusive):

- What equipment (casks, transfer casks [if needed], handling equipment [leak test equipment, rotating equipment, cask fixtures, cranes, lift equipment], is needed for each of 9 sites.
- Cask fabrication schedules.
- Regulatory licensing—which casks are licensed, not built; licensed, built, no impact limiters; not licensed, not built, etc.
- Content reviews to meet CoC requirements.
- How many transportation casks, impact limiters, rail cars, buffer cars, escort cars, heavy haul truck movements, etc. per site.
- Training of site personnel and transportation personnel and security personnel (Every site will have different equipment, organize by cask system?)

This section will also contain a generic schedule and task list to perform these actions.

Cases to be examined include:

1. Direct rail (CSF has rail capability)
2. Heavy haul truck -> rail (CSF has rail capability)
3. Heavy haul truck -> barge -> rail (CSF has rail capability)
4. Heavy haul truck -> barge -> Heavy haul truck (CSF has barge capability, e.g., SRS)

The conclusions section will discuss the overall conclusions for the orphan sites study including items such as shipping considerations and hurdles for each site

### 3. Evaluation of Issues Associated with Canister Stabilization

The following report was issued on August 28<sup>th</sup>, 2012 -

*A Preliminary Evaluation of Using Fill Materials to Stabilize Used Nuclear Fuel During Storage and Transportation – FCRD-UFD-2012-000243* (PNNL-21664).

The objective of the research described in this report was to conduct a preliminary evaluation of potential fill materials that could be used to fill void spaces in and around used nuclear fuel contained in dry storage canisters in order to stabilize the geometry and mechanical structure of the used nuclear fuel during extended storage and subsequent transportation. The use of fill material to stabilize used nuclear fuel is not considered to be a primary option for safely transporting used nuclear fuel after extended storage. However, the evaluation of potential fill materials, such as those described in this report, might provide the U.S. Department of Energy Used Fuel Disposition Campaign with an option that would allow continued safe storage and transportation if other options such as showing that the fuel remains intact or canning of used nuclear fuel do not prove to be feasible.

As a first step in evaluating fill materials, previous work done in this area was summarized. This involved studies done by the Spent Fuel Stabilizer Materials Program, Allied-General Nuclear Services, the Canadian Nuclear Fuel Waste Management Program, the U.S. Department of Energy, Spain, Sweden, and the Department of Energy's Yucca Mountain Project. A wide variety of potential fill materials were evaluated in these studies, ranging from molten metal to particulates and beads to liquids and gases. The common element in the studies was that they were focused on the use of fill materials in waste packages for disposal, not in storage canisters or transportation casks. In addition, very few studies involved actual experiments that measured some physical property of the fill material to be used as a stabilizing material, and no studies were found that analyzed the performance of transportation casks containing fill material during the normal conditions of transport specified in 10 CFR 71.71 or under hypothetical accident conditions specified in 10 CFR 71.73. In addition, most studies did not address issues that would be associated with production-scale emplacement of fill material in canisters, as opposed to laboratory- or experimental-scale use of fill material. It is noteworthy that Sweden abandoned its plan to use fill materials to stabilize waste packages due to the complexity of emplacing the fill material.

A part of the evaluation of fill materials, conceptual descriptions of how canisters might be filled were developed with different concepts for liquids, particles, and foams. The requirements for fill materials were also developed. Elements of the requirements included criticality avoidance, heat transfer or thermodynamic properties, homogeneity and rheological properties, retrievability, material availability and cost, weight and radiation shielding, and operational considerations.

Potential fill materials were grouped into 5 categories and their properties, advantages, disadvantages, and requirements for future testing were discussed. The categories were molten materials, which included molten metals and paraffin; particulates and beads; resins; foams; and grout. Based on this analysis, further development of fill materials to stabilize used nuclear fuel during storage and transportation is not recommended unless options such as showing that the fuel remains intact or canning of used nuclear fuel do not prove to be feasible.

## **APPENDIX G**

### **Dry Storage of Used Fuel Transition to Transport**

# **Dry Storage of Used Fuel Transition to Transport**

## **Fuel Cycle Research & Development**

Prepared for  
U.S. Department of Energy  
Transportation UFD

D.R. Leduc

Savannah River National Laboratory

August 2012

FCRD-UFD-2012-000253



**DISCLAIMER**

This information was prepared as an account of work sponsored by an agency of the U.S. Government. Neither the U.S. Government nor any agency thereof, nor any of their employees, makes any warranty, expressed or implied, or assumes any legal liability or responsibility for the accuracy, completeness, or usefulness, of any information, apparatus, product, or process disclosed, or represents that its use would not infringe privately owned rights. References herein to any specific commercial product, process, or service by trade name, trade mark, manufacturer, or otherwise, does not necessarily constitute or imply its endorsement, recommendation, or favoring by the U.S. Government or any agency thereof. The views and opinions of authors expressed herein do not necessarily state or reflect those of the U.S. Government or any agency thereof.

Prepared by:

SRNL Transportation Lead

---

Dan Leduc

Date

Concurred by:

UFD Transportation Lead

---

Paul McConnel

Date

## SUMMARY

This report provides details of dry storage cask systems and contents in U.S. for commercial light water reactor fuel. Section 2 contains details on the canisters used to store approximately 86% of assemblies in dry storage in the U.S. Transport cask details for bare fuels, dual purpose casks and canister transport casks are included in Section 3. Section 4 details the inventory of those shutdown sites without any operating reactors. Information includes the cask type deployed, transport license and status as well as fuel types allowed in the specified cask system and allowable parameters. Section 5 contains details on the transfer casks used with each cask system including the current number of transfer casks of each type fabricated.

## TABLE OF CONTENTS

1.	INTRODUCTION .....	1
2.	Status of Fuel in Dry Storage .....	1
2.1	Dry Storage Canisters .....	4
3.	Cask Systems for Dry Fuel Storage.....	5
3.1	Bare Fuel Casks .....	5
3.1.1	Transnuclear TN-32, TN-40 and TN-68 Casks.....	6
3.1.2	CASTOR V/21 and X/33 .....	7
3.1.3	NAC-I28 .....	9
3.1.4	Westinghouse MC-10 .....	9
3.2	Canister Transport Casks .....	10
3.2.1	NUHOMS MP187.....	11
3.2.2	NUHOMS MP197 (MP-197HB) .....	13
3.2.3	HOLTECH HISTAR 100.....	15
3.2.4	NAC-STC .....	16
3.2.5	NAC UMS .....	17
3.2.6	FuelSolutions™ TS125 Cask .....	19
3.2.7	4.2.7 TN-FSV.....	21
4.	Orphan Site Storage and Transport .....	21
5.	Transfer Cask Designs.....	24
5.1	NAC Transfer Casks .....	24
5.2	HOLTEC Transfer Casks .....	27
5.2.1	HI-TRAC Standard Design.....	27
5.2.2	HI-TRAC 100D and 125D Transfer Casks .....	28
5.2.3	TN/NUHOMS Transfer Casks .....	29
5.2.4	Fuel Solutions Transfer Casks .....	30
6.	References .....	32
	Appendix A.....	34

## LIST OF FIGURES

Figure 3-1 MP187 Transportation Cask.....	13
Figure 3-2 NUHOMS MP197 Cask Components <sup>10</sup> .....	14
Figure 3-3 61BT DSC Canister Configuration <sup>10</sup> .....	15
Figure 3-4 HISTAR 100 Transport Cask .....	16
Figure 3-5 NAC-STC Basic Cask Dimensions <sup>13</sup> .....	18
Figure 3-6 NAC-UMS Basic Cask Dimensions <sup>14</sup> .....	18
Figure 3-7 NAC-UMS on heavy haul rolling stock .....	19
Figure 3-8 Expanded Cutaway View of FuelSolutions TS125 Transportation Package <sup>15</sup> .....	20

Figure 3-9 TN-FSV Cask.....	21
Figure 5-1 NAC Transfer Cask Fabrication.....	25
Figure 5-2 NAC Transfer Cask Body (NAC SNFDS Seminar) .....	26
Figure 5-3 NAC Adaptor Plate Door Operation (NAC SNFDS Seminar) .....	26
Figure 5-4 HI-TRAC 125 Pool Lid (Left) Transfer lid (Right) <sup>25</sup> .....	28
Figure 5-5 HI-TRAC 125D Lower Assembly Detail <sup>25,26</sup> .....	29
Figure 5-6 OS187H On-Site Transfer Cask <sup>27</sup> .....	30

## LIST OF TABLES

Table 2-1 UNF Dry Storage Cask/Vault Systems.....	2
Table 2-2 Key Dimensions of Dry Storage Canisters.....	4
Table 3-1 Bare Fuel Casks.....	6
Table 3-2 Transnuclear Metal Cask Parameters (NEI 2010).....	7
Table 3-3 Castor, NAC and Westinghouse Metal Cask Parameters .....	8
Table 3-4 Canister Transport Cask Basic Dimensions .....	11
Table 3-5 Key Dimensions of the NUHOMS transportation cask.....	12
Table 4-1 Shutdown Reactor Site Inventory.....	23
Table 5-1 NAC Transfer Cask Models (NEI 2010) <sup>24</sup> .....	24
Table 5-2 HOLTEC Transfer Cask Models <sup>25</sup> .....	27
Table 5-3 TN Transfer Cask Designs <sup>2,27</sup> .....	30
Table A-1Transportation Matrix for Commercial Reactor Fuel (Dry Storage, and Away from Reactor Wet Storage).....	37
Table A-2 Storage Summary – U.S. Wet Storage at Shutdown Reactor Sites .....	39

## ACRONYMS

10CFR50	Title 10, U.S. Code of Federal Regulations, Part 50
10CFR71	Title 10, U.S. Code of Federal Regulations, Part 71
10CFR72	Title 10, U.S. Code of Federal Regulations, Part 72
ANSI	American National Standards Institute
ASME	American Society of Mechanical Engineers
BFS/ES	BNFL Fuel Solutions/Energy Solutions
BNFL	British Nuclear Fuels Limited
BWR	Boiling Water Reactor
DPC	Dual-Purpose Cask or Dual Purpose Canister
DSC	Dry Shielded Canister (used with NUHOMS systems)
ISFSI	Independent Spent Fuel Storage Installation
MPC	Multi-Purpose Canister (used with HOLTEC and some NAC systems)
ANSI	American National Standards Institute
NRC	Nuclear Regulatory Commission
NUHOMS	NUclear HOrizontal MOdular Storage
PWR	Pressurized Water Reactor
TC	Transfer Cask
TSC	Transportable Storage Canister (used with certain NAC and BFS/ES systems)
UMS	Universal MPC System (used with certain NAC systems)
VCC	Ventilated Concrete Cask

## 1. INTRODUCTION

Used U.S. light water power reactor fuel has been placed in Dry Storage Canisters (DSC) and casks since the mid-1980s and during that time the canister/cask systems have continuously evolved. Currently, there are more than 1,600 dry storage canisters containing roughly 64,000 assemblies or approximately 20,000 MTHM at Independent Spent Fuel Installations (ISFSI) in the U.S.<sup>1</sup> Updated information on the details of dry stored commercial light water reactor fuel is available from recently published documents including the EPRI Industry Spent Fuel Storage Handbook<sup>2</sup> and the Gap Analysis to Support Extended Storage of Used Nuclear<sup>3</sup>.

## 2. Status of Fuel in Dry Storage

Most assemblies in dry storage in the U.S. are in welded metal canisters inside vented concrete vertical overpacks or horizontal storage module. For this configuration, the canister with its internal basket, fuel and fuel component contents is the only portion of the storage cask system which is transported. These systems all require a separate transportation cask with a type B containment vessel to overpack the fuel canister (see reference 13 for an example of this type of cask). The transfer usually requires the use of a transfer cask except for the NUHOMS transportation casks which can interface directly with the horizontal storage module (see Section 3.2). Some welded metal canisters cannot currently be transported for various design reasons. The number and types of these canisters are detailed in Appendix A.

There are four categorical descriptions of dry cask storage:

1. Metal canisters in vertical concrete overpacks or horizontal concrete modules,
2. Metal canisters in metal overpack/storage/shipping casks,
3. Metal canisters in concrete vaults and
4. Bare fuel casks that provide both primary containment and shielding for storage and transportation. (A number of these casks have never been certified for transport as detailed in section 3.1.)

The Consolidated Storage Facility concepts must be capable of receiving any of these dry storage canister and transportation over-pack configurations. Since the mid 1980's 8 cask vendors have provided 11 cask systems comprised of 30 different canister types. Table 2-1 summarizes these canister and casks, provides the quantity of each cask type, as of May 2012 as well as the storage configuration and transition required in order to ship and receive the casks at the consolidated storage facility. For those bare fuel casks which do not have a transport license, the transition to transport requires a wet transfer of the fuel to a licensed transport cask or to a canister that is capable of transport. Some bare fuel Casks may still be licensable for direct transport of their contents as identified in the footnotes.

A number of the canisters listed in Table 2-1 are designated as "storage only" canisters by the associated cask vendor. These are identified in footnotes e and f of Table 2-1. For these canisters, repackaging in a canister capable of transport may be necessary if a direct shipment transport license cannot be obtained. This will depend on whether compensatory measures such as burnup credit or moderator exclusion can be utilized in the transport license.

Table 2-1 UNF Dry Storage Cask/Vault Systems

<b>Vendor</b>	<b>Cask System</b>	<b>Canister Type</b>	<b>Storage Configuration</b>	<b>May 2012</b>	<b>Transition to Transport Required Operation</b>
<b>Welded Metal Canister in Vented Concrete Overpack (84.1%)<sup>a</sup></b>					
BFS/ES	Fuel Solutions	W150	Vertical Cylinder	8	Canister Transfer to Transport Cask
		VSC-24	Vertical Cylinder	58	Canister Transfer to Transport Cask <sup>f</sup>
NAC	NAC-MPC	MPC-26	Vertical Cylinder	43	Canister Transfer to Transport Cask
		MPC-36	Vertical Cylinder	16	Canister Transfer to Transport Cask
	NAC-UMS	UMS-24	Vertical Cylinder	210	Canister Transfer to Transport Cask
TransNuclear	NUHOMS	7P	Horizontal Rectangular	8	Canister Transfer to Transport Cask <sup>e</sup>
		24P	Horizontal Rectangular	135	Canister Transfer to Transport Cask <sup>e</sup>
		32P	Horizontal Rectangular	21	Canister Transfer to Transport Cask <sup>e</sup>
		24PT	Horizontal Rectangular	22	Canister Transfer to Transport Cask <sup>e</sup>
		24PT1	Horizontal Rectangular	18	Canister Transfer to Transport Cask <sup>e</sup>
		24PT4	Horizontal Rectangular	28	Canister Transfer to Transport Cask <sup>e</sup>
		32PT	Horizontal Rectangular	63	Canister Transfer to Transport Cask <sup>e</sup>
		12T	Horizontal Rectangular	29	Canister Transfer to Transport Cask <sup>e</sup>
		24PTH	Horizontal Rectangular	27	Canister Transfer to Transport Cask <sup>e</sup>
		32PTH	Horizontal Rectangular	66	Canister Transfer to Transport Cask <sup>e</sup>
		24PHB	Horizontal Rectangular	38	Canister Transfer to Transport Cask <sup>e</sup>
		61BT	Horizontal Rectangular	117	Canister Transfer to Transport Cask <sup>e</sup>
		61BTH	Horizontal Rectangular	8	Canister Transfer to Transport Cask <sup>e</sup>
		52B	Horizontal Rectangular	27	Canister Transfer to Transport Cask <sup>e</sup>

Table 2-1 (Continued)

<b>Vendor</b>	<b>Cask System</b>	<b>Canister Type</b>	<b>Storage Configuration</b>	<b>May 2012</b>	<b>Transition to Transport Required Operation</b>
HOLTEC	HI-STORM	MPC-24	Vertical Cylinder	22	Canister Transfer to Transport Cask
		MPC-32	Vertical Cylinder	145	Canister Transfer to Transport Cask
		MPC-68	Vertical Cylinder	258	Canister Transfer to Transport Cask
HOLTEC	TransStor	MPC-24E/EF	Vertical Cylinder	34	Canister Transfer to Transport Cask
<b>Welded Metal Canister in Metal Sealed Overpack (1.4%)</b>					
HOLTEC	HISTAR 100	MPC-68	Vertical Cylinder	7	Direct Ship Possible
		MPC-80	Vertical Cylinder	5	Direct Ship Possible
<b>Welded Metal Canister in Vault Storage (2.4%)</b>					
Foster Wheeler	MVDS	6 assembly canisters	Vault	244	Canister Transfer to Transport Cask
<b>Bare Fuel Casks with Bolted Closure (12.1%)</b>					
NAC	NAC I28	I28	Vertical Cylinder	2	Fuel Transfer to Transport. Cask <sup>b</sup>
TransNuclear	TN Metal Casks	TN-32	Vertical Cylinder	63	Fuel Transfer to Transport. Cask <sup>c</sup>
		TN-40	Vertical Cylinder	29	Direct Ship Possible
		TN-68	Vertical Cylinder	57	Direct Ship Possible
GNB	CASTOR	V/21,X-33	Vertical Cylinder	26	Fuel Transfer to Transport Cask <sup>d</sup>
Westinghouse	MC-10	MC-10	Vertical Cylinder	1	Fuel Transfer to Transport. Cask <sup>d</sup>

<sup>a</sup>% of assemblies in dry storage<sup>b</sup> Direct shipment of the NAC I28 may be possible see 3.1.3.<sup>c</sup> Direct shipment of the TN-32 may be possible see 3.1.1.<sup>d</sup>. Cannot currently be transported for various design reasons see 3.1.2. and 3.1.4.<sup>e</sup> NUHOMS 7P, 12T, 24P, 24PHB, 32P, and 52B cannot currently be transported for various design reasons; however, NUHOMS 24PT, 24PT1, 24PT4, 24PTH, 32PT, 32PTH, 61BT, and 61BTH are transportable by canister transfer to transport cask<sup>f</sup> Fuel Solutions VSC-24 canisters are classified by the cask vendor as storage only canisters

## 2.1 Dry Storage Canisters

Table 2-2 Key Dimensions of Dry Storage Canisters

Vendor	Cask System	Canister Type	Inside Diameter	Outside Diameter	Length	Gross Weight (lbs)	Reactor Type
<b>Welded Metal Canister in Vented Concrete Overpack</b>							
Fuel Solutions		W74	64.74	66.0	192.25	85,000	BWR
		VSC-24	60.5	62.5	192.5 (max)	69,000	PWR
NAC	NAC-MPC	MPC-26	69.39	70.64	151.75	67,195	PWR
		MPC-36	69.39	70.64	122.5	55,590	PWR
	NAC-UMS	UMS-24	65.81	67.06	191.75 (max)	73,000	PWR
	NAC-MAGNAS.	TSC-37	71	72	191.8/184.8	104,500	PWR
TransNuclear	NUHOMS	7P	a	a	a	a	PWR
		24P	66.0	67.25	186.0	80,000	PWR
		32P	a	a	a	a	PWR
		24PT	a	a	a	a	PWR
		24PT1	65.9	67.19	186.5(max)	82,000	PWR
		24PT4	65.9	67.19	196.5	a	PWR
		32PT	65.9	67.19	193(max)		PWR
		12T	a	a	a	a	PWR
		24PTH	65.9	67.19	192.2		PWR
		32PTH	68.75	69.75	185.75 (max)	82,000	PWR
		24PHB	65.9	a	186.17	a	PWR
		61BT	66.25	67.25	195.92	89,390	BWR
		61BTH	67	67	196 (max)	a	BWR
		52B	65.9	67.19	195.9	a	BWR
HOLTEC	HI-STORM	MPC-24	67.375	68.5 (max)	190.3125 (max)	82,494	PWR
		MPC-32	67.375	68.5 (max)	190.3125 (max)	89,765	PWR
		MPC-68	67.375	68.5 (max)	190.3125 (max)	87,171	BWR
HOLTEC	TransStor	MPC-24E/EF	67.375	68.5 (max)	190.3125 (max)	80,963	PWR
<b>Welded Metal Canister in Metal Sealed Overpack</b>							
HOLTEC	HISTAR 100	MPC-68	67.375	68.5 (max)	190.3125 (max)	240,881	BWR
		MPC-80	67.375	68.5 (max)	a	a	BWR

<sup>a</sup>Detail redacted from publically available licensing documents in accordance with 10 CFR 2.390. Data requested directly from cask vendor and table will be revised if and when data is received.

### **3. Cask Systems for Dry Fuel Storage**

Dry storage in the U.S can be divided into two broad categories, those in which the fuel is stored bare in a fuel basket inside a metal cask and those in which the fuel is in a welded canister inside a vented concrete overpack or inside a metal dual purpose cask. Details on both categories are provided below.

#### **3.1 Bare Fuel Casks**

Light water power reactor transportation casks capable of meeting the 10CFR71 requirements for Normal Conditions of Transport (NCT) and Hypothetical Accident Conditions (HAC) are generally metal casks with bolted closures and containment vessels which meet leak tight requirements of ANSI N14.5<sup>4</sup>. For the case where fuel is placed directly into such a cask and used for long term storage in that cask, the cask is often referred to as a “bare fuel” cask since no welded canister is used. If the cask also has a licensed transport configuration it is also sometimes referred to as a dual purpose cask.

Bare fuel casks employ bolted closures with the fuel is placed directly in a basket inside the cask cavity. Each of the bare fuel casks listed below was designed for transportation cask licensing although as shown in Table 3-1, few of these casks have an existing transportation license nor are in application for a 10CFR71 license for transport. Dry storing fuel in a bare fuel cask is most beneficial if the storage times are short and a receipt facility exists that can directly handle and unload fuel from the cask. They also eliminate the need for a transfer cask and/or canister transfer operation inherent in canister storage.

Only two reactor sites in the U.S. continue to load fuel into bare fuel metal casks, Peach Bottom which uses the Transnuclear TN-68 cask and Prairie Island which continues to load TN-40 casks. Both these casks have current transport licenses as shown in Table 3-1. The remaining bare fuel casks are described as legacy casks since no new casks of these types are being loaded and reactor sites which once employed them are now loading out fuel in canister cask systems. Of the legacy casks, licensing of the TN-32 cask for transport has been discussed by Transnuclear in the past and direct shipment of these casks remains a possibility. Likewise the, NAC I28 cask is an earlier evolution of the currently licensed NAC-STC cask and direct shipment of the NAC I28 also remains a possibility although no transport license is currently being pursued.

Obtaining a transport license for the CASTOR V21 and X33 casks is more problematic since these casks are composed of monolithic cast iron which has not been licensed as a cask configuration in the U.S. as described in 3.1.2 below. Shipment of the single Westinghouse MC-10 in dry storage at Surry is also problematic since Westinghouse, although still active in radioactive material packaging, is not an active vendor supplying dry cask storage systems in the U.S. It is unclear whether the work necessary to ship this cask would be more beneficial than repackaging of its contents into a cask system with a licensed transport configuration,

Table 3-1 Bare Fuel Casks

	<b>VENDOR</b>	<b>CASK</b>	<b>NUMBER OF CASKS (7/2012)</b>	<b>TRANSPORT LICENSE</b>	<b>LOCATION</b>
<b>ACTIVE CASKS (STILL LOADED)</b>	TN	TN-68	57	71-9239	Peach Bottom
		TN-40	29	71-9313	Prairie Island
<b>LEGACY CASKS (NO LONGER LOADED)</b>	TN	TN-32	63	NO	Surry, McGuire, North-Anna
	GNB	CASTOR V21&X33	26	NO	Surry
	NAC	I-28	2	NO	Surry
	Westinghouse	MC-10	1	NO	Surry

Descriptions of the direct loaded bare fuel casks in storage are included below. For direct loaded bare fuel casks, the portion of the cask designated as the “containment” vessel when discussed for transportation purposes below is often referred to as a “confinement” vessel in its storage configuration.

### **3.1.1 Transnuclear TN-32, TN-40 and TN-68 Casks**

The TN series of metal casks is currently used to store the largest amount of un-canisterized fuel in dry storage cask systems in the U.S. These are also the only bare fuel casks which continue to be loaded into dry storage in the U.S.<sup>1</sup> The number following the TN designator is the number of assembly positions in the internal cask basket for the various casks. The TN-32 casks hold PWR assemblies from Surry, McGuire, and North Anna. The TN-40 casks hold PWR assemblies from Prairie Island only and the TN-68 holds GE BWR fuel from Peach Bottom only. Only Prairie Island and Peach Bottom continue to load TN-40 and TN-68 casks respectively, with Prairie Island loading 3 casks and Peach Bottom adding 5 casks in 2010. Surry and North Anna are now utilizing the NUHOMS canister system while McGuire uses the NAC-UMS canister system for new fuel loads.

The TN-68 and the TN-40 are the only casks in the TN metal cask family that have a current transportation license. The TN-40 received its license in June 2011 after a five year review period by the NRC. This transportation license is only for intact fuel from Prairie Island Unit 1 cycles 1 through 16 and Unit 2 cycles 1 through 15. The maximum initial enrichment for fuel under this license is no more than 3.85 weight percent U<sup>235</sup>, and the assembly average burnup is required to be no more than 45,000MWd/MTU.

Now that the TN-40 transportation license has been obtained, TN plans to submit an application for a TN-40 variant designated as the TN-40HT. Contents under the transportation application will include fuel with a maximum initial enrichment of 5 weight percent U<sup>235</sup> and a maximum bundle average burnup limited to 60 GWd/MTU. Fuel transported under this license must have a minimum cooling time of 12 years with a maximum heat load of 0.8Kw/assembly. Indications are that the initial transportation application will include intact fuel only.

There are no current transportation license applications for the TN-32 Cask design. TN has discussed applying for a transport certificate during the time period that this cask model was being produced for domestic dry fuel storage. Since the reactor sites using this cask design have switched to canister based systems, no transport license has been pursued for the TN-32 cask in the U.S. However, given the design similarity between the TN-32 and other TN casks licensed for transport and TNs continued presence in both the storage and transport cask market, it is reasonable to assume that licensing the TN-32 for transport and direct shipment remains a possibility.

Basic information for the TN family of metal casks is shown in Table 3-2 (EPRI 2010 updated for Transportation).<sup>5,6</sup>

Table 3-2 Transnuclear Metal Cask Parameters (NEI 2010)

TN Cask Type	TN-32	TN-40	TN-40HT	TN-68
Fuel Type	PWR	PWR	PWR	BWR
# of Assemblies	32	40	40	68
Maximum Heat Load (kilowatts)	32.7	27	32	30
Minimum Cooling Time (Years)	7	10	18	7
Maximum Fuel Burnup (GWd/MTU)	40	45	60	60
Storage Cask				
Length [m] (in)	4.9(184)	4.4(175)	4.6(181.75)	5.5(215)
Length with protective cover [m](in)	5.13(201.88)	5.13(202.0)	5.07(199.6)	
Outer Diameter [m](in)	2.48(97.75)	2.53(99.52)	2.57(101)	2.49(98)
Loaded Weight lbs.	231,000	226,000	242,000	230,000
NRC Part 71 License	None	71-9313	Planned	71-9293

### 3.1.2 CASTOR V/21 and X/33

The CASTOR V/21 and X/33 casks are metal cask currently used for storage at the Surry power generating station. CASTOR casks are also used in dry storage at INL which is not licensed by the NRC.

Both casks designs consist of a cask body made of thick-walled nodular cast iron with two stainless steel lids sealed with both elastomer and metal seals to provide leak tightness. Polyethylene rods are incorporated into the walls of both cask designs that enhance the neutron shielding of each cask. Otherwise, no special shielding materials are incorporated into the cask with shielding provided by the cast iron and stainless steel cask composition. In both cask designs, the external surface is covered with heat transfer fins that run circumferentially around the cask with an epoxy resin coating protecting the outside cask surface. For the V/21, the internal structure of the cask consists of a welded stainless steel basket with 21 square tube positions with borated stainless steel plates for criticality control while the X/33 has a similar internal structure with 33 square tube positions. Both these CASTOR cask systems use a pressure-sensing device to monitor the pressure in the interspace between the primary and secondary lids verifying seal integrity in storage.

Basic information for the Castor family of metal casks is shown in Table 3-3. All Castor casks used to dry store fuel under NRC license are located at Surry. Early fracture toughness concerns at the NRC prevented the licensing for transport of monolithic nodular cast iron casks like the CASTOR casks in the U.S. However, in the last 20 years, European experience with testing, analysis, use and licensing of nodular cast iron casks has garnered international acceptance of this cask type by the International Atomic Energy Agency<sup>7</sup>. Since then the NRC has indicated that they would accept license applications for nodular cast iron shielded casks like the CASTORs. Any such submittal would be a first time licensing cycle for this cask type and no vendor has yet approached the NRC with a submittal of transport license for this cask type.

Table 3-3 Castor, NAC and Westinghouse Metal Cask Parameters

TN Cask Description	V/21	X/33	NAC I28	Westinghouse MC-10
Fuel Type	PWR	PWR	PWR	PWR
# of Assemblies	21	33	28	24
Maximum Heat Load (kilowatts)	21	33	32.7 <sup>a</sup>	32.7 <sup>a</sup>
Minimum Cooling Time (Years)	7 <sup>a</sup>	10 <sup>c</sup>	10 <sup>c</sup>	10 <sup>c</sup>
Maximum Fuel Burnup (GWd/MTU)	35	35	22 <sup>c</sup>	35 <sup>c</sup>
<b>Storage Cask</b>				
Length [m] (in)	4.9(193)	4.8(189)	4.6(181.2)	4.79(188.4)
Outer Diameter [m](in)	2.8(110.25)	2.8(110.25)	2.4(94.8)	2.71(106.8)
Loaded Weight lbs <sup>b</sup>	233,800	236,000	250,000 <sup>d</sup>	250,000 <sup>d</sup>
<b>NRC Part 71 License</b>	None	None	None	None

<sup>a</sup>TN-32 cask bounding value

<sup>b</sup> Storage configuration gross weight

<sup>c</sup> Surry ISFSI SAR

<sup>d</sup> Surry ISFSI SAR weight limit

### 3.1.3 NAC-I28

The NAC-I28 is a variant of the NAC-STC cask which is licensed for transport as described in section 3.2.4. Two NAC-I28 casks are used to dry store PWR fuel assemblies at the Surry power generating station which is the only NRC licensed ISFSI location utilizing this cask design. One NAC-I28 cask is also used in dry storage at INL which is not licensed by the NRC.

The NAC-I28 S/T cask is a smooth right circular cylinder of multiwall construction with a 1.5 inch thick inner shell and a 2.63 inch thick outer shell of austenitic stainless steel separated by 3.2 inches of lead gamma shielding. The inner and outer shells are connected to each other at the ends by an austenitic stainless steel ring and plate. The upper end of the cask is sealed by an austenitic stainless steel bolted closure lid which is 6.5 inches thick in the edge flange region and has a 1-inch inner closure plate and a 5.5-inch outer closure plate. The closure plates are separated by two inches of lead gamma shielding. The closure lid utilizes a double barrier seal system with two metallic o-rings forming the seals. The lower end of the cask is 6 inch thick austenitic stainless steel with a 1 inch outer closure plate. The bottom end closure plates are separated by 1.80 inches of lead gamma shielding. The cask body is approximately 181 inches long and 94 inches in diameter. Neutron emissions from the stored fuel are attenuated by an integral neutron shield located outside the outer shell which contains a 7-inch thickness of borated solid neutron shield material. Neutron emissions from the top of the cask are attenuated during storage by a 3-inch thick solid neutron shield cap encased in stainless steel.<sup>8</sup>

There is no active transportation license for the NAC-I28 package.

For long term storage, the cask cavity is backfilled with helium to one atmosphere. The inner lid interseal volume between the two inner lid metallic gaskets and the interseal volume between the O-rings in the vent and drain port covers are backfilled with 15 psig of helium. The space between the inner and outer lid is pressurized with helium to 100psig and that pressure is monitored during storage for pressure loss by a transducer installed in the cask upper forging. The storage configuration of the NAC I28 Cask includes a tip over impact limiter.<sup>8</sup>

### 3.1.4 Westinghouse MC-10

The Westinghouse MC-10 cask is a metal cask designed to vertically store 24 PWR SNF assemblies. There is only one MC-10 stored at a NRC licensed ISFSI which is the model at the Surry Power station.

The cask body is a right circular cylinder composed low alloy steel with forged steel walls and a bottom. The basic parameters of the MC-10 design are shown in Table 3-3.

The inside surface of the MC-10 cask is thermally sprayed with aluminum for corrosion protection. The twenty-four carbon steel heat transfer fins are welded axially along the outside of the cask wall. Carbon steel plates are welded between the fins to provide an outer protective skin. Neutron shielding is provided by a layer of BISCO NS-3 cured in the cavity between the cask wall and outer protective skin.<sup>2,8</sup>

This thick walled structure provides the gamma shielding for the cask. A low alloy steel shield cover with a metallic O-ring provides the initial seal and shielding following fuel loading. A carbon steel primary cover lid, with a metallic O-ring seal, provides the primary containment seal

and envelopes the shield cover. An additional seal cover, containing BISCO NS-3 neutron-absorbing material is welded over the first two seals.<sup>2,8</sup>

### **3.2 Canister Transport Casks**

As detailed in Table 2-1 and Appendix A, approximately 84% of commercial fuel in the U.S. is stored in single welded canisters inside individual concrete or steel-encapsulated concrete cylindrical storage overpacks or rectangular horizontal storage modules. All of the storage systems whether cylindrical vertical overpacks or horizontal storage modules in the U.S. contain upper and lower vents that allow passive cooling of the internal canister. The canisters for these systems consist of a basket inside a steel shell with an outer diameter ranging from five to six feet in diameter as shown in Table 2-2. Cask vendors use different designators on their particular canister system. These include Multi-Purpose Canister (MPC), Dry Shielded Canisters (DSC), and Transportable Storage Canister (TSC). See the Client Canister descriptions in sections 3.2.1 through 3.2.6 for specific canister designs by cask vendor.

As noted in Table 2-1, there are 12 HISTAR 100 transportation casks which are also storing canisters at three reactor sites in the U.S. including the Humboldt Bay shutdown reactor site. These 12 casks are the only case in the U.S. where seal welded canisters of commercial fuel are stored directly in the transportation package intended for transport. Since the HISTAR 100 transportation cask provides the containment for the future transportation phase, it does not incorporate vents for passive cooling and requires more restrictive limits for heat load and cooling time than concrete overpacks (or storage modules), such as the HISTORM system.

Documents discussing canister transport casks often refer to the transportation containment vessel as an “overpack”, or “transportation over-pack” since it over-packs the canister during transport. Except in the case of the 12 direct stored HISTAR canisters, all other canisters in the U.S. require transfer of the canister from the storage over-pack into the transportation over-pack prior to shipment. This operation must be reversed at the consolidated storage facility in order to place the canister in a low cost vented concrete overpack for long term storage. The receiving facility must be configured to accommodate any of the existing transportation over-packs described below. Table 3-4 gives basic dimension of transport casks designed to ship canisters of dry stored used fuel. In no case is a transport cask of one vendor licensed to ship a canister design of another vendor listed in table 3-4.

Table 3-4 Canister Transport Cask Basic Dimensions

CASK VENDOR	TRANSPORT CASK	GROSS WEIGHT (LBS) <sup>a</sup>	LENGTH (in) <sup>b</sup>	DIAMETER (in)	CAVITY LENGTH (in)	CAVITY DIAMETER (in)
FUEL SOLUTIONS	TS-125	285,000	210.4/324.4	94.2/143.5	193.0	67
TN (NUHOMS)	MP-187	282,000	201.5/308	92.5/ <sup>c</sup>	187	68
	MP-197	265,100	208/281.25	91.5/122	197	68
	MP-197HB	304,000	210.25/ 271.25	84.5/126	199.25	70.5
NAC	NAC-STC	47,000	/247	31/78	199	18
	NAC-UMS	260,000	193/257	99 <sup>d</sup> /128	165	71
	NAC-MAGNATRAN	255,022	209.3/ 275	92.9/124	192.5	67.6
HOLTEC	HISTAR 100	312,000	213.9/	109.8/	192.5	72.25
		282,000	203.25/ 305.875	96/128	191.25	68.56

<sup>a</sup> Gross Weight of Heaviest Configuration (may be bounding analytical weight)

<sup>b</sup> Without Impact Limiters/With Impact Limiters

<sup>c</sup> MP-187 Impact Limiter Not Round

<sup>d</sup> Across Corners

### 3.2.1 NUHOMS MP187

The first transportation cask licensed to ship dual purpose canisters in the U.S. is the MP187<sup>a</sup> Cask. The NUHOMS storage system consists of Dry Shielded Canisters (DSC) stored in concrete Horizontal Storage Modules. The MP187 is designed to accept a single DSC within its containment cavity as described below. The cask is a composite structure of steel and lead surrounded by neutron shielding material. The cask, including the DSC is protected at each end by energy absorbing impact limiters which consist of stainless steel skins filled with poly urethane foam and aluminum honeycomb. These impact limiters also provide thermal insulation

<sup>a</sup> The MP187 designator is derived from the cavity interior height of 187 inches. The cavity height of the MP197 is 197 inches.

which protects the cask top and bottom seal areas during the hypothetical fire transient event. The cask is fabricated primarily of stainless steel. Non-stainless steel members include the cast lead shielding between the containment boundary inner shell and the structural outer shell, the o-ring seals, the cementitious neutron shield material and the carbon steel closure bolts. Key features and dimension of the MP-187 cask are shown in Table 3-5 and Figure 3-1.<sup>9,10</sup> The maximum heat load of the MP-187 cask is 13.5kW.

Table 3-5 Key Dimensions of the NUHOMS transportation cask

Cask	Cavity Length (in)	ID (in)	Height (in)*	OD (in)*	Base Thick(in)	Structural Lid Thick. (in)	Radial Neutron Shield Thick. (in)	Inner Shell Thick. (in)	Gamma Shield Thick. (in)	Total Wall Thick (in)	Max Gross Weight (lbs.)**
MP187	187	68	201.5	92.5	8	6.5	4.3	1.25	4	12.3	282,000
MP197	197	68	208	91.5	6.5	4.5	4.5	1.25	3.25	11.75	265,100
MP197HB	199.25	70.5	210.25	97.75	6.5	4.5	6.25	1.25	3		304,000

\*Does not include impact limiter

\*\*Depends on DSC configuration reported

**MP 187 Client Canisters<sup>9</sup>:** The DSC is a high integrity stainless steel, welded pressure vessel that provides confinement of the radioactive materials, encapsulates the fuel in an inert atmosphere, and provides axial biological shielding during DSC closure, transfer operations, storage and transport. The DSC internal basket assembly contains a storage position for each fuel assembly. It is composed of circular spacer discs machined from thick carbon steel plates or austenitic stainless steel. Axial support for the DSC basket is provided by four high strength stainless steel support rods and four carbon steel or austenitic stainless steel support plates which extend over the full length of the DSC cavity and bear on the canister top and bottom end assemblies. Carbon steel components of each DSC basket assembly are coated with a thin corrosion resistant layer of nickel to provide corrosion resistance for the short time that the DSC is in the spent fuel pool for fuel loading. All DSC types licensed in the MP187 have an approximate outside diameter of 67 inches and a maximum external length of 186.5 inches.

Per the certificate USA/9255/B(U)F-85, the cask is currently licensed to transport four types of DSCs designated as the FO-DSC (Fuel Only), FC-DSC(Fuel/Control Components), FF-DSC(Failed Fuel) and the 24PT1 DSC. The license allows the transport of failed fuel in limited quantities. Although the MP187 is capable of handling other canisters that have a maximum length of 186.5 inches and maximum diameter of 67.2 inches, no submittals for the transport of other canisters in this cask have been pursued. Application for transport of other NUHOMS canisters have been pursued in the MP 197HB, the newest NUHOM transport cask design.

Only one production unit MP187 Cask has been fabricated as of the issue of this report.

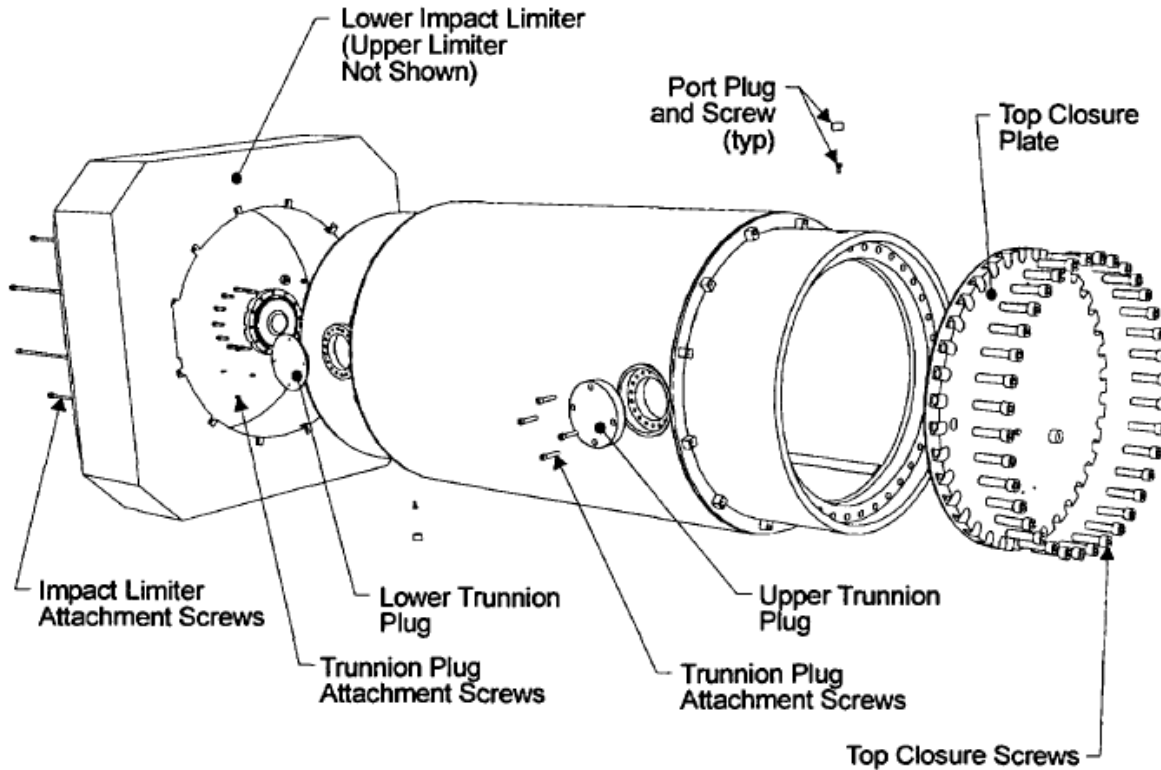


Figure 3-1 MP187 Transportation Cask

### 3.2.2 NUHOMS MP197 (MP-197HB)

The MP197 and the MP197HB are cask configurations for shipping a single NUHOMS canister which uses the same horizontal loading configuration as the MP187. The basic parameters of the MP197 and MP197HB are provided in Table 3-5. The MP197 and MP197HB are different cask designs with different overall dimensions as well as some difference in materials of construction even though they share the same certificate number. The MP197HB has an internal cavity that is 70.5 inches in diameter and 199.25 inches long.<sup>b</sup> To accommodate smaller DSC designs, an aluminum sleeve and aluminum or stainless steel spacers are provided to limit radial and axial movement of the payload. 61BT DSCs. Both the MP197 and MP197HB casks consist of a containment boundary, structural outer shell, gamma shielding material and solid neutron shield. The containment vessel of both cask designs contains an integrally-welded bottom closure and a bolted and flanged top closure lid. The maximum heat load for the MP197 and MP197 HB casks are 15.86 kW and 24 kW respectively.<sup>10,11</sup>

As of the date of this report, no NUHOMS MP197 or MP197HB casks have been fabricated.

<sup>b</sup> Thus the 197 designator is not strictly accurate with regard to the MP197HB

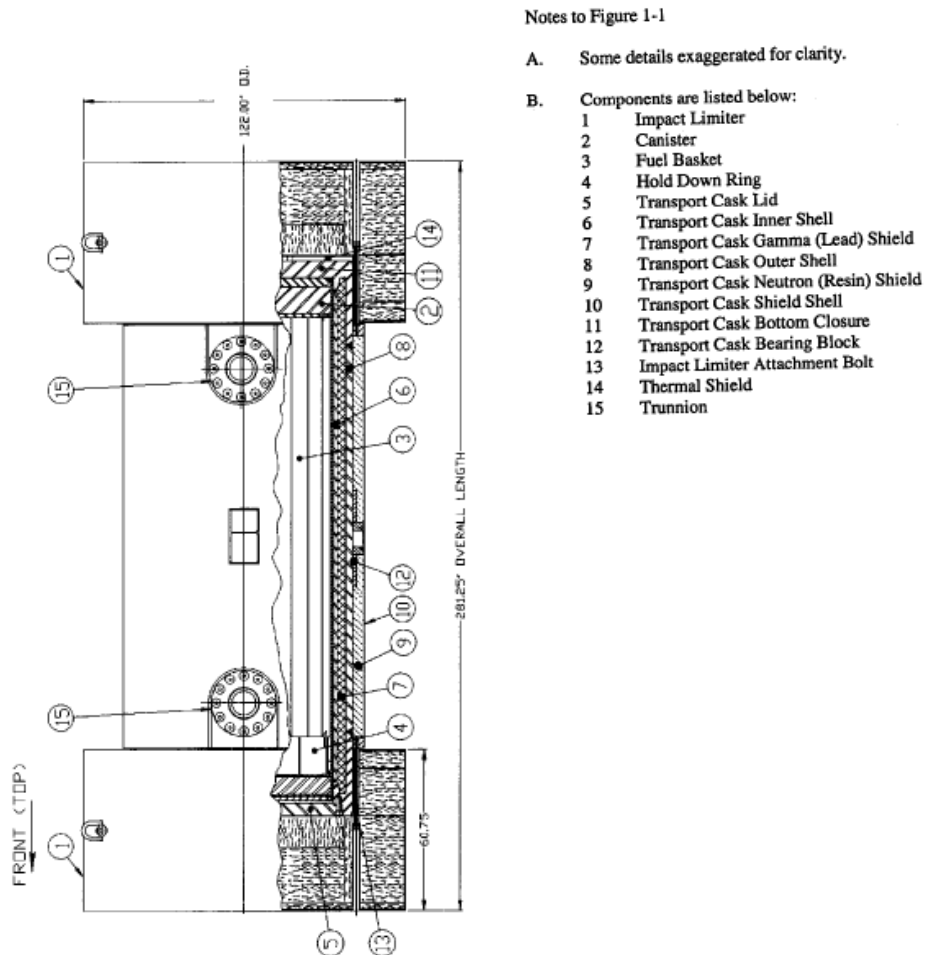


Figure 3-2 NUHOMS MP197 Cask Components<sup>10</sup>

MP197 Client Canisters<sup>10,11</sup>: The MP197 transportation cask is currently only licensed to carry the 61BT DSC. This DSC consists of a cylindrical shell, top and bottom shield plugs, inner and outer bottom closure plates, and inner and outer top cover plates. The shell assembly is a high integrity stainless steel welded pressure vessel that provides containment of radioactive material, encapsulates the fuel in an inert atmosphere (the canister is back-filled with Helium before being seal welded closed) and provides biological shielding in the axial direction. The bottom end assembly welds are made during fabrication of the DSC. The top end closure welds are made after fuel loading. Both top plug penetrations (siphon and vent ports) are redundantly sealed after the DSC drying operations are complete.

MP197HB Client Canisters<sup>11</sup> The MP197HB is currently licensed for transport of four DSC designs as well as radioactive waste containers. These are the 69BTH, 24PT4, 61BT and 61BTH DSC designs. The 69BTH DSC has the largest over all outside diameter at 69.8 inches. To accommodate the smaller 67.3 inch diameter of the other DSCs (24PT4, 61BT, and 61BTH) an aluminum sleeve is used in transport. Since canisters with the same designator vary in length, stainless steel or aluminum spacers are used to limit the axial gap between the DSC and the cask body to 0.5 inches or less. A crosssection of the 61BT Canister is shown in figure 3-3 below. Unlike canister types from other cask vendors, shield plugs are provided at both the top and the bottom of the NUHOMS canister. The top shield plug provides shielding

for personnel during final welding and drying operations while the bottom shield plug, which is put in place before fuel loading, provides shielding at the face of the horizontal storage module. TN continues to pursue licensing for transport of other NUHOMS canisters in the MP197HB.

As detailed in Appendix A, a certain subset of NUHOMS canisters are designated by TN as “storage only” canisters. These canisters have certain design features which make for a more difficult licensing process for the transport cask configuration in the transport accident sequence required to be evaluated in 10CFR71. Per the cask vendor, licensing of these canisters in transport may still be possible, especially if certain burn-up credit is allowed or moderator exclusion under 71.55 was obtained. Currently, the NUHOMS canisters are not credited with serving any containment function during transport.

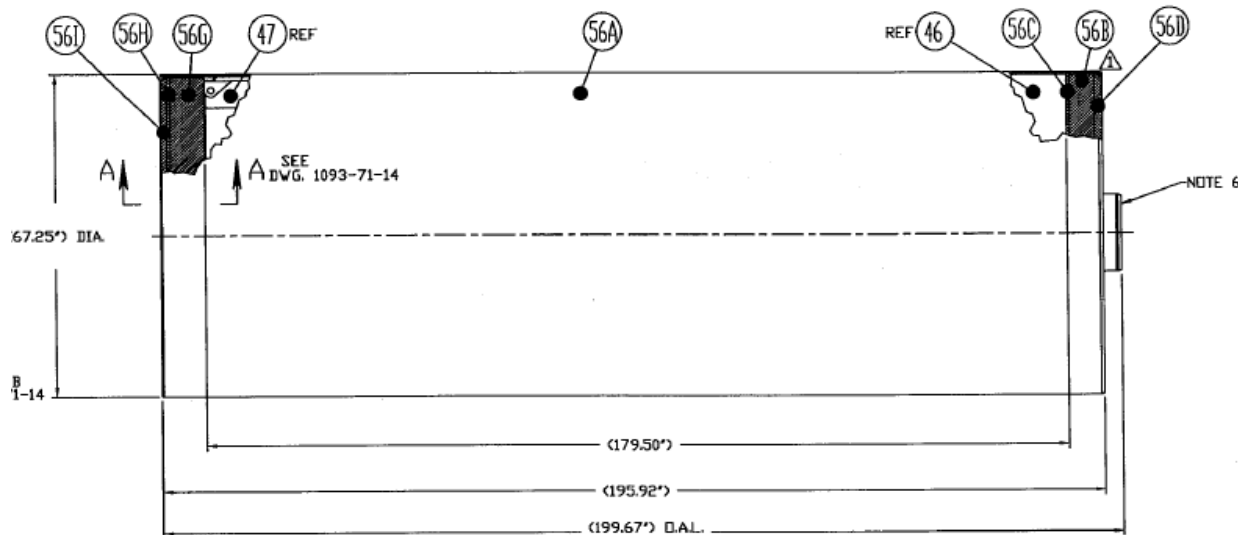


Figure 3-3 61BT DSC Canister Configuration<sup>10</sup>

### 3.2.3 HOLTECH HISTAR 100

The HISTAR 100 transportation cask consists of a single, sealed metal multi-purpose canister (MPC) contained within a multilayered overpack with impact limiters. The inner diameter of the overpack is approximately 68-3/4 inches and the height of the cavity is approximately 191-1/8 inches. The overpack inner cavity is sized to accommodate the MPCs. The outer diameter of the overpack is approximately 96 inches and the height is approximately 203-1/4 inches (Humboldt Bay overpacks have the same inner and outer diameter but have an inner height of 115 inches and an outer height of 128 inches). Fitted with impact limiters on each end which are composed of aluminum honeycomb, the cask has a maximum outside diameter of 128 inches and a total overall length of 305.9 inches. The gross weight of the HISTAR 100 system depends on which of the MPCs is loaded into the overpack for shipment but can weigh as much as 277,299 for the heaviest licensed configuration. The maximum total heat load of the HISTAR transport cask is 20kW for PWR fuel contents and 18.5kW for BWR fuel contents.<sup>12</sup>

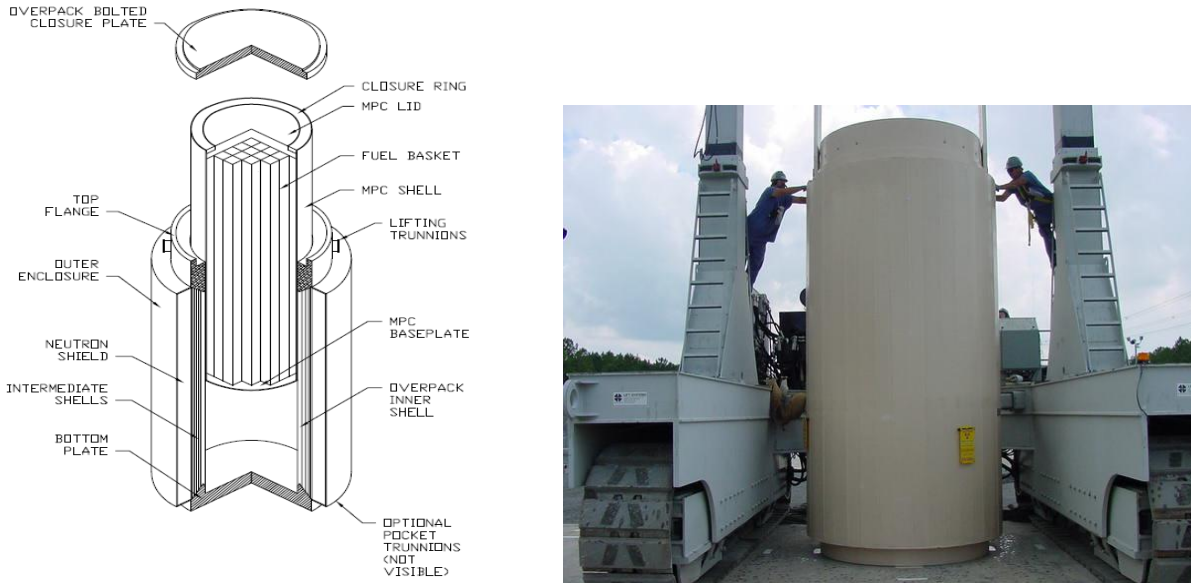


Figure 3-4 HISTAR 100 Transport Cask

**Client Canisters:** The HI-STAR 100 System is designed to accommodate a wide variety of spent fuel assemblies in a single overpack design by utilizing different MPC basket designs. The exterior dimensions of all Holtec MPCs (except the custom-designed Trojan and Humboldt Bay MPCs) are identical to allow the use of a single overpack design. The generic Holtec MPC design has maximum exterior dimension of approximately 68.5 inches in diameter by 190.3125 inches long. The Trojan plant MPCs are approximately nine inches shorter than the generic Holtec MPC design and have the same outer diameter. The Humboldt Bay MPCs are approximately 6.3 feet shorter than the generic Holtec MPC design and have the same outer diameter. Each of the MPCs has different design features (e.g., fuel baskets) to accommodate distinct fuel characteristics. Each MPC is identified by the maximum quantity of fuel assemblies it is capable of receiving. The MPC-24, -24E, and -24EF each can contain a maximum of 24 PWR assemblies; the MPC-32 can contain up to 32 PWR assemblies; the MPC-68 and -68F each can contain a maximum of 68BWR fuel assemblies; and the MPC-HB for Humboldt Bay can contain up to 80 fuel assemblies.<sup>12</sup>

The overpack containment boundary is formed by a steel inner shell welded at the bottom to an end plate and at the top to a heavy flange with a bolted closure plate.

### 3.2.4 NAC-STC

The NAC-STC (Storage Transport Cask)<sup>c</sup> is a metal cask design that is licensed for the transport of NAC Multi-Purpose Canisters (MPC) of fuel from Connecticut Yankee and Yankee Rowe “ISFSI Only” sites as well as bare fuel in an internal basket configuration. The NAC-STC is a smooth right-circular cylinder of multiwall construction, consisting of stainless steel inner and outer shells separated by lead gamma radiation shielding. The inner and outer shells are welded to the 304 stainless steel top forging, which is a ring that is machined to mate with the inner and outer lids. The inner and outer shells are also welded to the Type 304 stainless steel bottom inner and outer forgings respectively. The cask bottom consists of two forgings and a plate with neutron shield material sandwiched between the bottom inner forging and the bottom plate. Neutron shield material is also placed in an annulus that surrounds the cask outer shell along the length of the cask cavity. Twenty-four explosively bonded copper and Type 304 stainless steel

<sup>c</sup> Even though the “S” in the STC designator stands for storage, there are no NAC-STC casks used for storing fuel at U.S. dry storage sites although the NAC-I28 is a similar design.

fins are located in the radial neutron shield to enhance the heat rejection capability of the NAC-STC and to support the neutron shield shell and end plates.<sup>13</sup>

**NAC STC Client Canisters:** The basic NAC-STC cask body dimensions are shown in Figure 3-5. The 71.1 inch diameter cavity accommodates 24 or 26 assembly MPCs from Connecticut Yankee, 36 assembly MPCs from Yankee Rowe or 26 PWR Assemblies stored in a bare fuel basket. Since the fuel canisters include all the fuel from the shutdown reactor, both canister designs allow storage of damaged fuel assemblies. With a cavity length of 165 inches, the STC cavity is shorter than most transport casks for used commercial fuel but the diameter is slightly larger. The cask body outside diameter is approximately 87.7 inches with the outside length of 190.5 inches without impact limiters. In the transport configuration two impact limiters are fitted to either end of the cask body in a typical dumbbell configuration. These are composed of either balsa wood or a combination of redwood and balsa wood encased in stainless steel. The all balsa wood impact limiters have a lower weight and improved crush characteristics compared to the combination redwood and balsawood impact limiters and accommodate a higher cask content weight and higher cask total weight. With impact limiters, the NAC-STC has a maximum outer diameter of 124 inches and an overall length of 257 inches.<sup>13</sup>

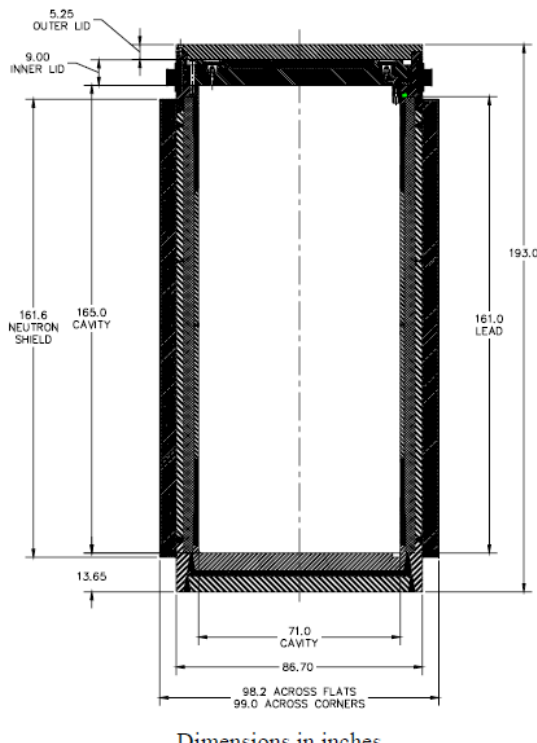
The NAC STC has a bare fuel configuration included in its current transport license.<sup>13</sup>

The NAC-STC, when loaded, has a maximum design weight of 260,000 pounds. The maximum heat load of the NAC-STC cask is 22.1 kW for direct loaded PWR fuel in the 26 position internal basket configuration with each assembly 0.85 kW or less. For Yankee Rowe fuel, the maximum canistered fuel assembly decay heat load is 0.347 kW per assembly for 36 assemblies and 0.259 kW per assembly for a canister of 24 stainless steel-clad assemblies. For Connecticut Yankee fuel, the maximum decay heat load is 0.654 kW per assembly for a canister of 26 assemblies.<sup>13</sup>

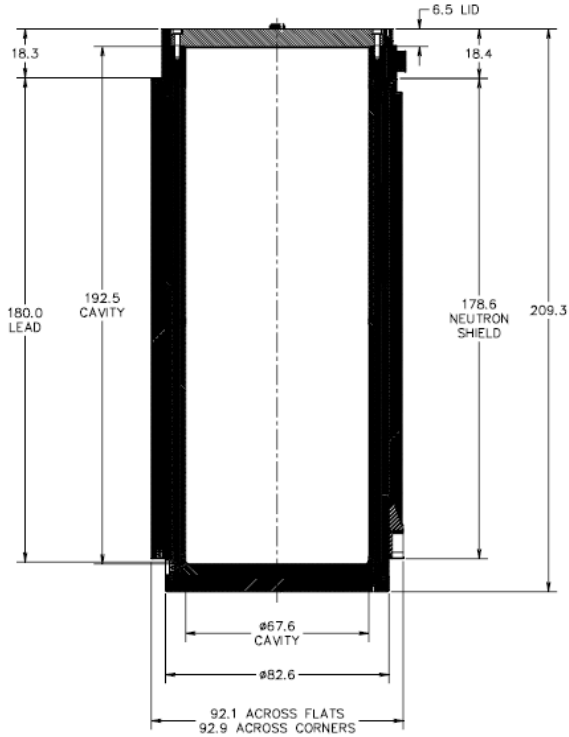
As of the date of this report, no NAC-STC casks have been fabricated for use in the U.S. This cask design is likely to be replaced by the NAC MAGNATRAN design for future fuel shipments upon certification of this cask design.

### **3.2.5 NAC UMS**

The Universal Transport Cask is designed to safely transport a Transportable Storage Canisters TSCs containing 24 intact PWR spent fuel assemblies, 56 intact BWR spent fuel Assemblies or Greater Than Class C (GTCC) waste. NAC-UMS canisters are utilized to store fuel from the Maine Yankee “ISFSI Only” site. The design layout of the NAC-UMS is similar to the NAC-STC as can be seen in Figure 3-6. Some of the differences include a single lid vs. the double lid STC design and the fact that it has a cavity which is smaller in diameter but is considerably longer than the NAC-STC design. The maximum gross weight of the NAC-UMS when loaded with the heaviest TSC configuration is 254,004lbs.<sup>14</sup>



Dimensions in inches

Figure 3-5 NAC-STC Basic Cask Dimensions<sup>13</sup>Figure 3-6 NAC-UMS Basic Cask Dimensions<sup>14</sup>

Like the NAC-STC, the NAC-UMS cask contains a neutron shield placed in an annulus that surrounds the cask outer shell along the length of the cask cavity. It also has twenty-four bonded copper and Type 304 stainless steel fins located in the radial neutron shield to enhance the heat rejection capability of the cask. The NAC-UMS maximum decay heat load is 20kW for PWR fuel and 16kW for BWR fuel. In the transport configuration two impact limiters are fitted to either end of the cask body in a typical dumbbell configuration (Figure 3-7). Unlike the NAC-STC design, only one impact limiter design is licensed which is composed of a combination of redwood and balsa wood enclosed in stainless steel shell. With impact limiters attached, the NAC-UMS has a maximum outer diameter of 124 inches and an overall length of approaching 275 inches.<sup>14</sup>

As of the date of this report, no NAC-UMS casks have been fabricated either domestically or for use overseas. This cask design is likely to be replaced by NAC's new MAGNATRAN design for future fuel shipments when this cask design is certified.

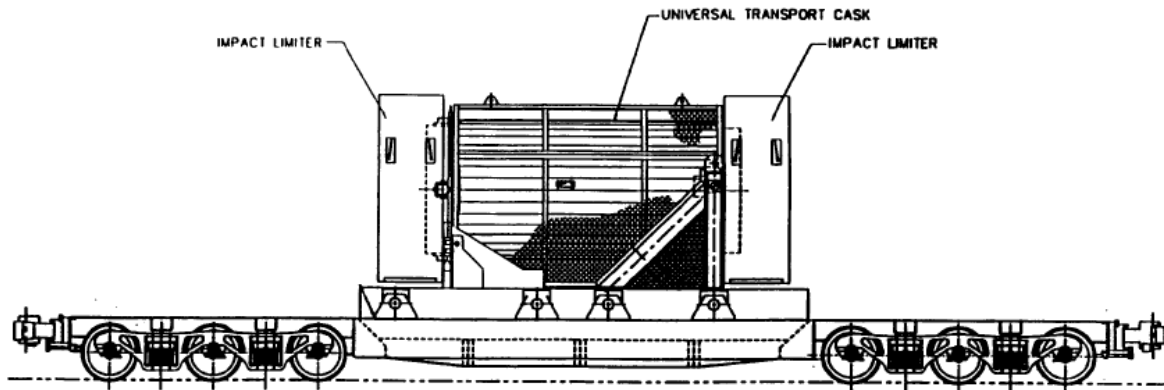


Figure 3-7 NAC-UMS on heavy haul rolling stock

### 3.2.6 FuelSolutions™ TS125 Cask

The FuelSolutions™ Transportation Package consists of a FuelSolutions™ TS125 Transportation Cask and impact limiters, together with a FuelSolutions™ canister and its UNF payload. This cask is designed to transport a single W21 canister containing 21 PWR assemblies or W74 canister containing up to 64 Big Rock Point<sup>d</sup> fuel assemblies in two stackable basket assemblies. An exploded view of the TS-125 cask is shown in Figure 3-7. The TS125 Transportation Cask body is an assembly composed of stainless steel components of an inner shell, an outer shell, a top ring forging, a closure lid with a seal test port and a cavity vent port, a bottom plate forging, and a cavity drain port. The inner and outer shells are welded to the bottom plate forging and the top ring forging. The cask body also includes an annular lead gamma shield; an annular neutron shield with cask tie-down rings, support angles, and jacket; a bottom end neutron shield with a support ring and jacket; a longitudinal shear block; and lifting trunnion mounting bosses. The inner and outer shells form the annular cavity for the lead gamma shield. The outer shell and the neutron shield jacket form the annular cavity for the solid neutron shield. The neutron shield support angles facilitate heat rejection through the solid neutron shielding material to the outer surface of the cask body.<sup>15</sup>

<sup>d</sup> Big Rock Point is an "ISFSI Only" Site

As of the date of this report, no TS125 casks have been fabricated either domestically or for use overseas. No intentions for a replacement cask have been announced.

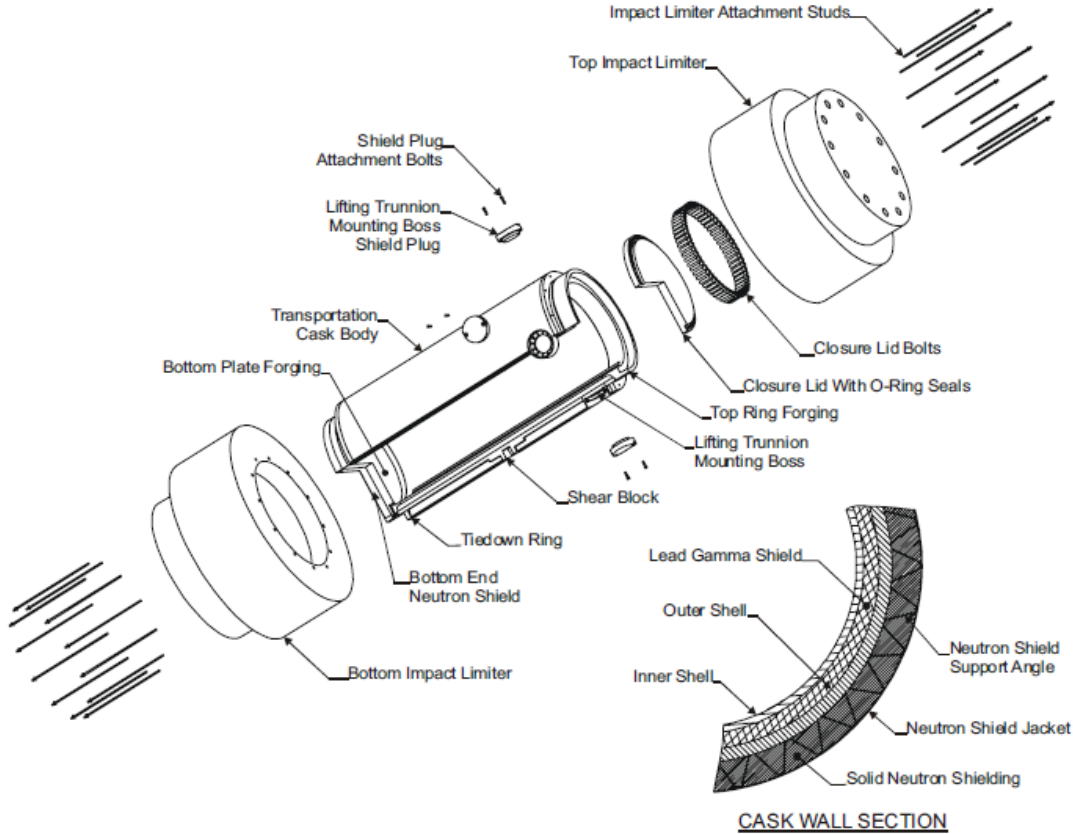


Figure 3-8 Expanded Cutaway View of FuelSolutions TS125 Transportation Package<sup>15</sup>

The TS125 cask cavity is 67 inches in diameter and 193 inches in length. The external dimensions of the cask body include an overall length of 324.4 inches and overall diameter of 143.5 inches diameter with impact limiters (210.4 inches long by 94.2 inches without the impact limiters). The maximum gross weight of the transport cask with the maximum payload is 285,000 pounds. The design basis decay heat load for the TS-125 transportation cask is 22kW.<sup>15</sup>

**Client Canisters:** The W21 and W274 FuelSolutions canisters consist of a steel shell assembly and an internal basket assembly. The canister shell assembly consists of a steel cylindrical shell, bottom end closure, bottom shield plug, bottom shell extension, bottom outer plate, top shield plug, top inner closure plate and top outer closure plate. All structural components of the canister shell assembly are constructed of austenitic stainless steel, with the exception of the shield plugs. The shield plug materials may be composed of lead, depleted uranium or carbon steel, depending on the specific canister variant.

The W21 TSC basket consists of 21 guide tubes that are positioned and supported by a series of circular spacer plates, which in turn are positioned and supported by support rod assemblies. The W21 guide tubes include neutron absorber sheets on all four sides. The W 74 canister includes two stackable basket assemblies with a capacity to accommodate up to 64 Big Rock Point Assemblies. Details on these canister designs are contained in References 29 and 30.

### **3.2.7 4.2.7 TN-FSV**

The TN-FSV is the smallest cask described in this report and is the only commercial used cask described that is designed primarily for road rather than rail transport. The cask body consists of two concentric shells of Type 304 Stainless Steel, welded to a bottom plate and a top closure flange. The inner shell has an inner diameter of approximately 18 inches, a typical wall thickness of 1.12 inches and an overall interior length of 199 inches. The inner cavity is capable of containing one fuel storage canister (FSC) which has exterior dimension of approximately 17.6 inches in diameter and 195 inches in overall length. The outer shell of the cask body has an outside diameter of 31 inches, a wall thickness of 1.5 inches and an overall exterior length of 247 inches. The annular space between the inner and outer shells is filled with lead. The maximum gross weight of the TN-FSV when transporting a FSC is 47,000 pounds.<sup>16</sup>

The TN-FSV does not include a variant for long-term storage of fuel and is sealed with butyl O-ring elastomer seals. The maximum heat load for the TN FSV with six HTGR fuel assemblies is 360 watts with an individual assembly heat load limit of 60 watts<sup>16</sup>.



Figure 3-9 TN-FSV Cask

## **4. Orphan Site Storage and Transport**

There are seven former commercial reactor sites in the U.S. which are considered by the NRC to be “ISFSI Only” sites where the plant license has been reduced to include only the spent fuel storage facility.<sup>e</sup> One of these sites stores fuel from a gas cooled reactor, Fort Saint Vrain, while the remaining

<sup>e</sup> Some of these sites are also storing Greater than Class C and Low Level Waste.

ISFSI sites contain the fuel of light water reactors. In addition to these sites, Humboldt Bay is a reactor site still being decommissioned and dismantled where all fuel has been placed into a below grade ISFSI. The Humboldt Bay spent fuel pool removal is scheduled for 2012. There are two more shutdown reactor sites, LaCrosse and Zion, where plans call for all spent fuel to be transferred to dry storage followed by decommissioning of all wet storage and transfer capabilities. As of the date of this report, three casks at LaCrosse have been loaded with two more planned. Collectively, these sites are often referred to as “orphan” sites, although sometimes this term is applied to only the first seven reactor sites listed in Table 4-1.

All fuel assemblies at “ISFSI Only” sites as well as those planned to become “ISFSI Only” sites in the near future, are stored in canisters that are dry, seal welded and purged with an inert gas. None of these sites use casks where the fuel is stored directly in a storage cask with a bolted closure and mechanical seal (“bare fuel” or “dual purpose” type cask).

Table 4-1 contains a listing of all the “ISFSI Only” sites as well as those planned to become “ISFSI Only” sites in the near future (Ft St Vrain is omitted from this list since it is a HTGR site). Although Table 4-1 is titled “Shutdown Reactor Site Inventory” it only refers to reactor sites where all reactors have been permanently shut down. It does not include reactor sites where one or more reactors have been permanently shutdown while others continue to operate<sup>f</sup>.

Table 4-1 lists the shutdown date of the last reactor shutdown at each site as well as the type of reactor. The third column lists the start and end dates of the loading of all fuel assemblies into dry storage or the planned load dates. The fourth column lists the cask system used at each site, the canister types used at that site, the transport cask model number and certificate number associated with the casks/canister system. If the storage technical specifications are publically available to check for consistency with the transport certificate, this is listed in column 4. Other comments or details associated with the site inventory are also listed in column 4. The fifth column gives the expiration date of the certificate listed in column 4.

The sixth column contains the number of fuel cask canisters as well as canisters with GTCC waste in storage at the ISFSI while column seven lists the number of assemblies in dry storage.<sup>1</sup> the eighth column lists the Metric Tons Initial Heavy Metal included in the dry stored fuel at each reactor. The ninth column contains information on the number of damaged fuel assemblies or cans at the ISFSI or the number damaged fuel assemblies or cans allowed per cask. The remaining columns list the specific fuel types and classifications as well as the associated limits for maximum burnup initial enrichment and heat load. The information in columns nine through 13 are generally taken from the cask or ISFSI technical specification listed except for the case of the Trojan and Zion ISFSI sites. The Trojan fuel details come from a report by the State of Oregon referenced in the table while the Zion information is mostly TBD.

<sup>f</sup> See Appendix A, such sites include Dresden, Indian Point, Millstone, Peach Bottom, and the San Onofre Nuclear Generating Station (SONGS)

Table 4-1 Shutdown Reactor Site Inventory

Reactor Site (Shutdown Date) (1)	Type (2)	ISFSI Load Dates (3)	Cask System/Canister(s)/ Transport Cask (4)	Transport Cask Status (5)	Total Casks Fuel/GTCC (6)	Total Assemblies (7)	MTHM (8)	Damaged Fuel Assemblies or Cans (9)	Fuel Types(Cladding) (10)	Max Burnup GWD/MTU(12)	Maximum Enrichment wt.% <sup>235</sup> U (13)	Heat Load Limit Assembly/Cask (14)
Big Rock Point 8/97	BWR	12/02-03/03	Fuel Solutions W150 Storage Overpack/W74 Canister/TS-125 71-9276. BRG Tech Spec. contents match transport CoC contents including MOX fuel. -96 upgrade needed.	TS-125 Certificate Expires 10/31/2012 Timely Renewal Expected. Cask Never Fabricated	8/1	441	58	8 Maximum per Cask <sup>18</sup>	GE 9x9,(Zircaloy) <sup>18</sup> ANF 9x9 (Zircaloy) ANF 11x11 (Zircaloy) J2(9X9) MOX (Zircaloy) DA (11x11) MOX (Zircaloy) G-Pu (11x11) MOX (Zircaloy)	40 40 40 22.82 21.85 34.22	4.10 4.10 4.10 4.50/3.65 PuO <sub>2</sub> 2.40/2.45 PuO <sub>2</sub> 4.60/5.45 PuO <sub>2</sub>	338W/26.4kW 338W/26.4kW 338W/26.4kW 338W/26.4kW 338W/26.4kW 338W/26.4kW
Connecticut Yankee 12/96	PWR	05/04-03/05	NAC MPC/MPC-26 & MPC-24/ NAC-STC Cask 71-9235. CY Tech. Spec. contents match transport CoC contents including Reconfigured Fuel and Damaged Fuel cans.	NAC-STC Certificate Expires 05/31/2014. Foreign use versions of Cask have been fabricated. No domestic units fabricated.	40/3	1019	412	4 Maximum per Cask <sup>19</sup>	West. 15x15 (SS) <sup>19</sup> NUMEC 15x15(SS) B&W(GUNF) 15x15(SS) B&W 15x15 (SS) G A 15x15(Zircaloy) NUMEC 15x 15 (Zircaloy) B&W 15x15, (Zircaloy) B&W 15x15 (Zircaloy) Vantage 15x15(Zircaloy)	38 30 38 38 30 30 40 43 30	4.03 4.03 4.03 4.03 3.42 3.42 3.42 3.93 4.61	264W/17.5kW 264W/17.5kW 264W/17.5kW 264W/17.5kW 347W/17.5kW 347W/17.5kW 347W/17.5kW 347W/17.5kW 347W/17.5kW
Maine Yankee 8/97	PWR	08/02-03/04	NAC UMS/UMS-24/NAC-UMS Cask 71-9270. MY Tech. Spec. contents match transport CoC including High Burnup and Damaged Fuel. One Assembly cannot be transported until 2015	NAC-UMS Certificate Expires 10/31/2012 Timely Renewal Expected Cask Never Fabricated	60/4	1434	483	14 initial, Some of the 90 High Burnup Assemblies are Likely in MYFCs <sup>20</sup>	CE 14x14 (Zircaloy) <sup>20</sup> CE 14x14 High Burnup (Zircaloy) CE 14x14 w/SS Repl. Rods (Zr&SS)	45 50 50	4.2 4.2 4.2	830W/20kW 830W/20kW 830W/20kW
Yankee Rowe 9/91	PWR	06/02-06/03	NAC MPC/MPC-36/ NAC-STC Cask 71-9235. YR fuels called out in transport CoC including Reconfigured Fuel and Damaged Fuel cans.	NAC-STC Certificate Expires 05/31/2014. (See CY above)	15/1	533	127	4 max per canister <sup>19</sup>	CE Types A&B (Zircaloy), <sup>19</sup> ExxonTypes A&B (Zircaloy), Westinghouse Types A&B (SS) UN Types A&B (Zircaloy) Reconfigured Fuel (Zr or SS)	36 36 32 32	3.93 4.03 4.97 4.03	320W/12.5kW 320W/12.5kW 264W/12.5kW 320W/12.5kW 102W/12.5kW
Ranco Seco 6/89	PWR	04/01-08/02	TN/FO,FC,FF-DSCs/MP187 71-9255 RS fuels included in Transport CoC. Canister and fuel in RS TS match CoC	NUHOMS MP-187 Certificate Expires 11/30/2013 Timely Renewal Expected. One Cask has been Fabricated. No impact limiters Fabricated	21/1	493	228	13 in single FF DSC, 6 in FC DSC <sup>21</sup>	B&W 15x15 (Zircaloy-4) <sup>21</sup>	38.268	3.43	N.L./13.5kW
Trojan 11/92	PWR	12/02-9/03	HOLTEC MPC /MPC-24E/24EF /HISTAR 100 71-9261.	HISTAR 100 Certificate Expires 03/31/2014. Units Fabricated but not impact limiters	34/?	780	359	22 failed fuel cans <sup>22</sup>	17x17B (Zircaloy) <sup>22</sup>	42	3.7	725W/20kW
Humboldt Bay 7/76	BWR	08/08-12/08	HOLTEC HISTAR HB/ MPC-HB (MPC-80)/HISTAR HB 71-9261 HB Contents in TS match transport certificate	HISTAR HB Certificate Expires 03/31/2014. Fuel in Fabricated Casks. Impact Limiters not Fabricated	5/1	390	29	28 max per canister <sup>23</sup>	GE TYPE II 7x7 (Zircaloy) <sup>23</sup> GE TYPE III, 6x6 (Zircaloy) Exxon Types III 6x6 (Zircaloy) Exxon Type IV 6x6 (Zircaloy)	23 23 23 23	2.60 2.60 2.60 2.60	50W/2kW 50W/2kW 50W/2kW 50W/2kW
LaCrosse 4/87	BWR	07/12-Ongoing	NAC MPC-LACBWR/MPC-LACBWR 68 positions/ NAC-STC 71-9235 Contents described to right are included in current transport cert.	NAC-STC Certificate Expires 05/31/2014. (See CY above)	5(estimated)	333	38	155 (preliminary) <sup>19</sup>	Allis Chalmers (SS) <sup>19</sup> Allis Chalmers (SS) Exxon (SS)	22 22 21	3.64 3.94 3.71	63W/4.5kW 63W/4.5kW 62W/4.5kW
Zion 1 and 2 7/98	PWR	Planned 2013	NAC MAGNATRAN/TSC-37/MAGNATRAN 71-9356 UNDER REVIEW.	NAC MAGNATRAN License under review. Never Fabricated	61(estimated)	2,226	1018	10 damaged or reconsolidated fuel cans (preliminary) <sup>1</sup>	LOPAR (Zircaloy) OFA (Zircaloy-4) VANTAGE 5(Zircaloy-4) VANTAGE 5 w/ IFMs (Zircaloy-4)	TBD TBD TBD TBD	TBD TBD TBD TBD	TBD TBD TBD TBD

## 5. Transfer Cask Designs

Transfer casks are lead and steel casks used for handling of fuel canisters during loading, drying, welding and transfer operations. Transfer casks provide biological (gamma and neutron) shielding during canister closure, drying, welding and transfer but do not provide containment or criticality control features. Unlike the Canister Transport Casks described in Section 3.2, the transfer casks described in this section do not meet 10CFR 71 requirements for shipment of used fuel in commerce. In general, transfer casks are not pressure vessels and do not consist of a pressure boundary. Some transfer casks are designed to ASME Section III Subsection NF or NC, and other aspects of the ASME Boiler & Pressure Vessel code such as welding and weld inspections may apply to their fabrication and inspection. Each transfer cask in use at U.S. ISFSIs is designed to transfer and handle a single canister at a time. Transfer casks are a heavy lift device designed, fabricated and proof load tested to the requirements of NUREG-0612 and ANSI N14.6 (withdrawn ANSI standard still cited by the industry). Transfer casks are fabricated predominantly of carbon steel meeting ASTM specification.

Neutron shielding is provided by either water jacket or solid neutron absorber material. Water jackets often contain ethylene glycol or another agent to prevent freezing.

### 5.1 NAC Transfer Casks

There are four NAC transfer cask designs, three of which have been used for canister loading and transfer operations and the fourth planned for use at Zion. There are two different cask designs originally designed for interface with the MPC canister systems used at Connecticut Yankee and Yankee Rowe respectively. The transfer cask for Connecticut Yankee has a slightly thicker gamma shield and neutron shield. The inner and outer shells of both these cask designs consisted of ASTM A588 Low alloy steel. The transfer cask from Yankee Rowe has been purchased by Dairyland power for transfer of fuel into dry storage at Lacrosse.

Table 5-1 NAC Transfer Cask Models (NEI 2010)<sup>24</sup>

Transfer Cask	NAC MPC YR	NAC MPC CY	NAC UMS	MAGNASTOR
<b>Number of Fabricated Casks</b>	1	2	4	2
<b>Transfer Cask Dimensions</b>				
Length [m] (in)	3.39(133.4)	4.8(189)	4.6(181.2)	4.79(188.4)
Outer Diameter [m](in)	2.20(86.5)	2.26(89)	2.4(94.8)	2.71(106.8)
Loaded Weight with water [t.] (lbs.)	61.45 135,473	78.34 172,708	90.6-97.2 199,800- 214,300	104.1 229,500

NAC prefers to use machined bricks which are curved at interface surfaces to reduce shine paths rather than pouring monolithic shield assemblies (Figure 5-1). Between the lead brick and the transfer cask outer shell is an annulus filled with a solid synthetic polymer neutron shield material. The solid neutron shield material placement stabilizes the lead brick structure although neither is a credited structural component. Shielding at the bottom of the transfer cask is provided by thick (~9 inch) sliding shield

doors. The top of the transfer cask is essentially open except for a retaining ring which bolts to the cask body preventing a loaded canister from being inadvertently removed through the top of the transfer cask. Shielding at the top of the transfer cask is provided by the canister shield lid while loaded.<sup>24</sup>



Figure 5-1 NAC Transfer Cask Fabrication

The transfer cask has retractable bottom shield doors which slide in rails incorporated in the transfer cask bottom. During loading operations, the doors are closed and secured by lock bolts/lock pins, so they cannot inadvertently open. During unloading, the doors are retracted using hydraulic cylinders to allow the canister to be lowered into the storage or transport cask. During transfer of the cask with a loaded canister, only the doors held in place by two door rails and the lock bolts/lock pins. The hydraulic actuators are integrated into an adaptor plate that attaches to a storage overpack or to a transport cask. With NAC systems, the transfer of the loaded canister to the storage overpack usually occurs inside the 10CFR50 facility. The storage overpack is then moved from the 10CFR50 facility to the ISFSI pad using either a heavy haul trailer or cask transporter. The transfer cask and adaptor plate are designed to also be capable of directly loading the storage overpack at the ISFSI pad.

To minimize potential contamination of the canister and transfer cask during loading operations in the spent fuel pool, clean water is circulated in the gap between the transfer cask interior surface and the canister exterior surface using fill and drain lines in the wall of the transfer cask. Clean water is injected into the annular space during the entire time the transfer cask is submerged. No seals are used on the bottom door interface or at the top of the canister. This design and process has been adequate in ensuring acceptable contamination levels on the canister exterior. Each of the fill and drain ports are offset to minimize shine paths from the unshielded fuel canister sidewall.<sup>24</sup>

Figure 5-2 shows a picture of the basic transfer cask body without the bottom doors in place. Figure 5-3 shows the adaptor plate mechanism with the doors in the open position



Figure 5-2 NAC Transfer Cask Body (NAC SNFDS Seminar)



Figure 5-3 NAC Adaptor Plate Door Operation (NAC SNFDS Seminar)

## 5.2 HOLTEC Transfer Casks

HI-TRAC is an acronym for Holtec International Transfer Cask. There are four basic HI-TRAC cask designs, the 125-ton standard design (HI-TRAC-125), the 125-ton dual-purpose lid design (HI-TRAC-125D), the 100 ton standard design (HI-TRAC -100) and the 100-ton dual purpose lid design (HI-TRAC-100D). The 100 ton HI-TRAC is used at sites with a maximum crane capacity less than 125 tons. All the HI-TRAC design variations use lead for gamma shielding and a water jacket for neutron shielding, the configuration of layers from interior to exterior being steel, lead, steel, water space, steel. Each of the transfer casks listed in Table 5-2 is designed and constructed in accordance with ASME Section III, Subsection NF, with certain NRC approved alternatives. Since all HOLTEC canisters have the same exterior dimensions, the basic internal diameter of all HI-TRAC transfer casks is the same.

Table 5-2 HOLTEC Transfer Cask Models<sup>25</sup>

<b>Transfer Cask</b>	HI-TRAC 100	HI-TRAC 100D	HI-TRAC 125	HI-TRAC 125D
<b>Number of Fabricated Casks</b>	2	4	5	11
<b>Transfer Cask Dimensions</b>				
Length (in)	191.25	191.25	201.5	201.5
Outer Diameter (in)	89	91.25	Water J. 93.75	Water J. 93.75
Inner Diameter (in)	68.75	68.75	Base Plate 104	Base Plate 104
Loaded Weight with water(lbs.)	192,000- 199,999	192,000- 199,000	228,500- 236,000	228,500- 236,000

### 5.2.1 HI-TRAC Standard Design

The standard design HI-TRAC transfer casks are heavy-walled cylindrical vessel composed of carbon steel and lead with an exterior water jacket. The top lid of the HI-TRAC 125 has additional neutron shielding to provide neutron attenuation of neutrons from the top of the MPC. The MPC access hole through the HI-TRAC top lid allows the lowering and raising of the MPC between the HI-TRAC transfer cask and the HI-STORM or HI-STAR overpacks. The standard design HI-TRAC (comprised of HI-TRAC 100 and HI-TRAC 125) is provided with two bottom lids, each used separately. The pool lid is bolted to the bottom flange of the HI-TRAC and is utilized during MPC fuel loading and sealing operations. In addition to providing shielding in the axial direction, the pool lid incorporates a seal that is designed to hold clean water in the HI-TRAC inner cavity preventing contamination of the MPC exterior from fuel pool water. After the MPC has been drained, dried and sealed, the pool lid is removed and the HI-TRAC transfer lid is attached (standard design only). The transfer lid incorporates two sliding doors that allow the opening of the HI-TRAC bottom for the MPC to be raised and lowered. Figure 5-4 shows the cross section of a HI-TRAC 125 standard cask with both a pool lid and a transfer lid attached. Both

lid types are attached to the cask body bottom flange with 36 1" diameter bolts in the case of the HI-TRAC 100. Both lid types are blind drilled and tapped to accept the 36 attachment bolts.<sup>25</sup>

There are two standard designs HI-TRAC transfer casks classified by total gross weight of the loaded cask. The HI-TRAC-125 weight does not exceed 125 tons during any loading or transfer operation while the HI-TRAC-100 weight does not exceed 100 tons during any loading or transfer operation. The internal cylindrical cavities of the two standard design HI-TRACs are identical while the exterior dimensions vary. The HI-TRAC 100 has a reduced thickness of lead and water shielding leading to reduction of the outside diameter at several locations, the thickness of the structural steel of the two standard HI-TRAC is identical such that most structural analyses of the HI-TRAC 125 bound the HI-TRAC 100 design.<sup>25</sup>

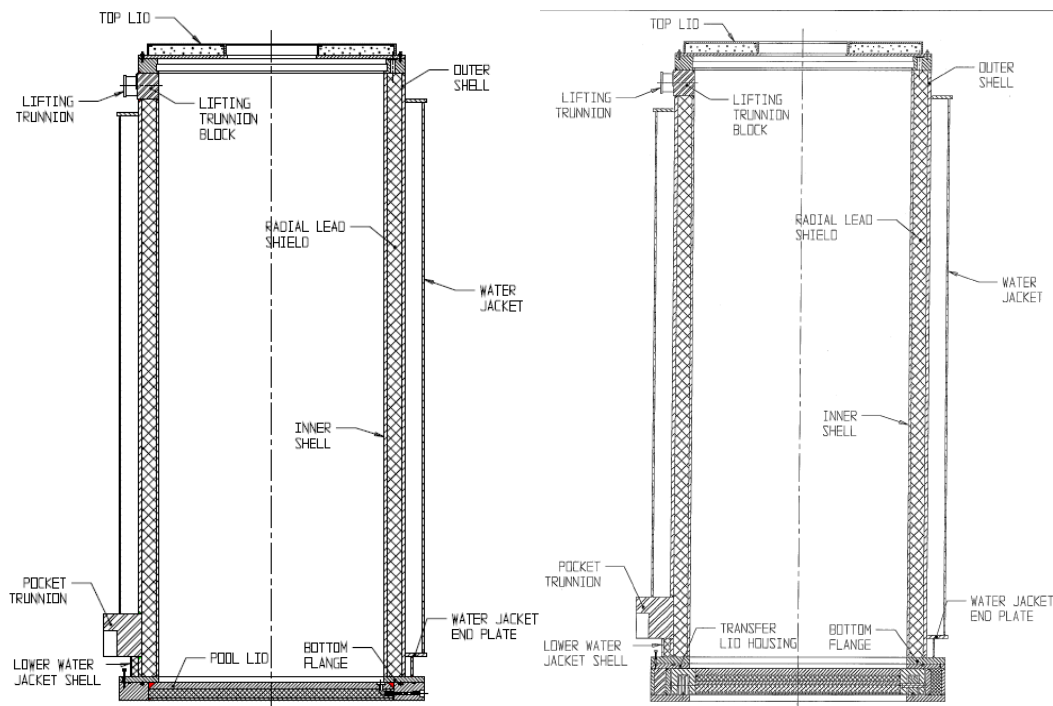


Figure 5-4 HI-TRAC 125 Pool Lid (Left) Transfer lid (Right)<sup>25</sup>

### 5.2.2 HI-TRAC 100D and 125D Transfer Casks

The HI-TRAC 100D and 125D designs are functionally equivalent to the standard design variants but have the following primary differences.

- No pocket trunnions
- No transfer lid (not required)
- HI-STORM mating device is required during MPC transfer operations
- A wider baseplate with attachment points for the mating device is included
- The baseplate incorporates gussets for added structural strength

Unlike the standard transfer cask variants, the 100D and 125D HI-TRAC transfer casks do not require swapping the pool lid for a transfer lid to facilitate transfer of the MPC. The HI-STORM mating device is located between the HI-TRAC and HI-STORM and secured with bolting to both. Figure 5-5 shows the lower assembly detail of a 125 D HI-TRAC. This patented<sup>26</sup> design allows for removal of the pool lid by loosening the inner bolts on the bottom flange lowering it into the cask mating device assembly shown in Figure 5-6.

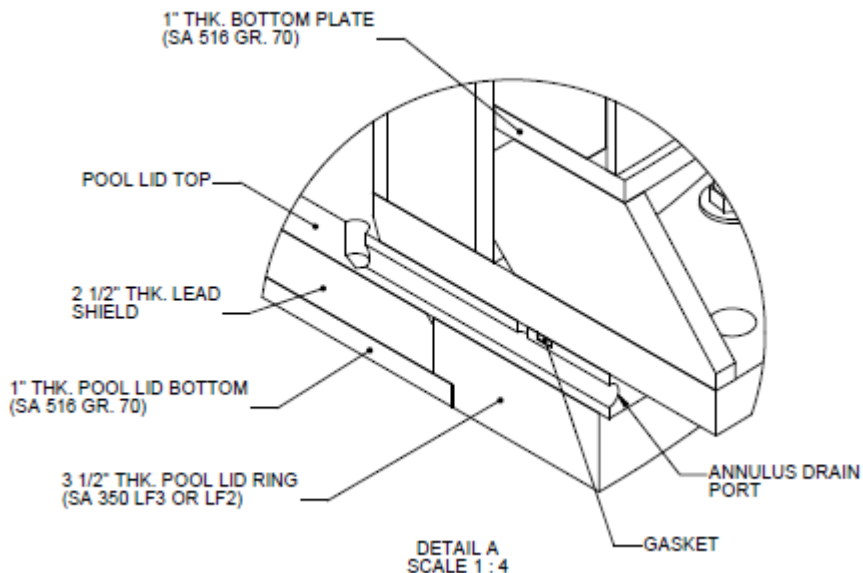


Figure 5-5 HI-TRAC 125D Lower Assembly Detail<sup>25,26</sup>

The patented design incorporates two gasket seals, one between the pool lid top and the bottom flange (Figure 5-5) and the other between the canister outer wall and the transfer cask inner wall close to the top lid of the transfer cask. These seals provide a barrier from pool water contamination while the transfer cask is submerged in the pool.

### 5.2.3 TN/NUHOMS Transfer Casks

TN/NUHOMS systems are unique in that the canister transfer from the transfer cask to the storage module is performed while the transfer cask is in the horizontal position. This transfer to the horizontal storage usually occurs at the ISFSI site such that the transfer cask carries the fuel canister between the 10CFR50 facility and the ISFSI pad vs. the storage overpack being heavy hauled to the storage sites in other systems. The TN systems are also unique in that the TN canister transport casks described in sections 3.2.1 and 3.2.2. above can also be used as transfer casks if desired. They can also be used to directly remove and transport canisters from the Horizontal Storage Modules without the need to an intermediary cask required by other systems. The TN transfer casks listed in Table 5-3 are fabricated and designed to ASME Section III, Division I, Subsection NC, Class 2 (non-pressure retaining components).

Table 5-3 TN Transfer Cask Designs<sup>2,27</sup>

Transfer Cask	OS187H <sup>c</sup>	OS197	OS197L	OS200
<b>Number of Fabricated Casks</b>	2	4	1	1
<b>Transfer Cask Dimensions</b>				
Length (in)	207.22 <sup>c</sup>	207.22	<sup>a</sup>	206.72
Outer Diameter (in)	85.5 <sup>c</sup>	85.5	<sup>a</sup>	92.11
Inner Diameter (in)	68	68	<sup>a</sup>	68
Payload limit(dry) (lbs.) <sup>b</sup>	80,000	97,250	<sup>a</sup>	116,000
Loaded Weight with water (lbs.)	<200,000 <sup>c</sup>	<200,000	<150,000	<250,000

<sup>a</sup>Proprietary Information withheld in accordance with 10 CFR 2.390

<sup>b</sup> Payload limit for analysis. Actual payload depends on as built cask weight and configuration

<sup>c</sup> Values from Reference 2. Reference 27 reports OS187H length of 197.1 in, outer diameter of 92.2in and a gross weight of 114.5 tons or 229,000 pounds.

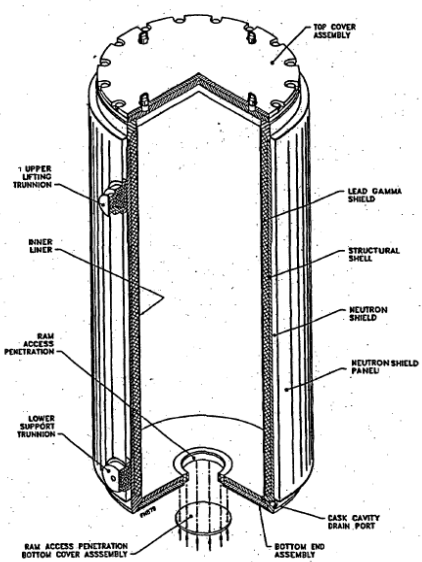


Figure 5-6 OS187H On-Site Transfer Cask<sup>27</sup>

#### 5.2.4 Fuel Solutions Transfer Casks

Fuel Solutions have two transfer cask designs for use with Fuel Solutions systems. The W100 transfer cask used with the W21 and W74 Dual Purpose Canisters<sup>13</sup> and the MTC (Multi-assembly Sealed Basket Transfer Cask) used with the VSC 24 canister system<sup>12</sup>. Details of these cask designs have been redacted

under 10 CFR 2.390. From the canister specifications, the W100 transfer cask must have a cavity capable of accepting a canister 66 inches in outer diameter, 192.25inches in length with a gross weight of 85,000 pounds. Likewise, the MTC must have a cavity capable of accepting a canister 62.5 inches in outer diameter, 192.5 inches long with a gross weight of 69,000pounds. Per available information both casks are capable of horizontal transfer to the TS-125 transport Cask. Actual number of each cask type fabricated are not reported in licensing documents but current storage conditions indicate that at least one W100 and MTC have been fabricated with possibly more than one MTC given two utility use of the VSC 24..

## 6. References

1. StoreFUEL Newsletter, August 07 2012 Vol. 13, No. 168
2. EPRI Industry Spent Fuel Storage Handbook, John Kessler, 1021048, Final Report July 2010
3. Hanson, Stockman, Alsaed, Enos, Gap Analysis to Support Extended Storage of Used Nuclear Fuel, FCRD-USED-2011-000XXX
4. American National Standard for Radioactive Materials- *Leakage Tests on Packages for Shipments*. ANSI N14.5, American National Standards Institute, INC. , New York, NY,(1997)
5. TN 68 Transport Packaging Safety Analysis Report, Revision 0, April 1999
6. TN-40 Transportation Packaging, Safety Analysis Report, E-23861, Revision 0, August 2006
7. Extended Drop Tests of DCI Casks with Artificial Flaws Demonstrating the Existing Safety Margins, B. Droste et. al., RAMTRANS, Volume 6, Nos 2/3 pp 177-182, 1995
8. Surry Independent Spent Fuel Storage Installation, Final Safety Analysis Report, Revision 18, SNM-2501, June 2008
9. Safety Analysis Report, NUHOMS-MP187 Multi-Purpose Cask Transportation Package Document No. NUH-05-151
10. NUHOMS-MP197 Transport Packaging Safety Analysis Report, Revision 4.
11. Certificate of Compliance Model Nos NUHOMS-MP197-MP197HB, USA/9302/B(U)F-96, Revision 4.
12. Safety Analysis Report on The HI-STAR 100 Cask System, Revision 15, HI-951251, October 2010
13. Safety Analysis Report, NAC Storage Transport Cask, Revision 16, September 2006, 71-9235
14. Safety Analysis Report for the Universal Transport Cask, Revision UMST-01D, November 2001, 71-9270
15. FuelSolutions TS125 Transportation Cask Safety Analysis Report, Revision 6, September 2006, WSNF-120
16. Certificate of Compliance Model No TN-FSV, USA/9253/B(U)F-96, Revision 12.
17. Halim Reference Document for MTIHM for Orphans
18. Technical Specification for the FuelSolutions<sup>TM</sup> W74 Canister NRC ML011210170
19. Technical Specifications for the NAC-MPC System Amendment 3 COC No. 1025 ML031340571
20. Technical Specifications for the NAC-UMS System Amendment 2 COC No. 1015 ML020250599
21. Technical Specifications for Rancho Seco Independent Fuel Storage Installation 72-11 ML003689836

22. Staff Evaluation of Holtec Design for Portland General Electric's Independent Spent Nuclear Fuel Storage Installation (ISFSI), Oregon Office of Energy, September 10,2002
23. Technical Specifications for Humboldt Bay Independent Fuel Storage Installation 72-27 ML053140032
24. NAC-MPC, Final Safety Analysis Report, Docket No. 72-1025, April 2012
25. Holtec International Final Safety Analysis Report for the HI-STORM 100 Cask System, 72-1014, HI-2002444, Revision 9, February 2010.
26. Unites States Patent, Singh, US 6,625,246 B1, September 23, 2003
27. Transnuclear Safety Analysis Report (Non-Proprietary), NUHOMS HD, Horizontal Modular Storage System for Irradiated Nuclear Fuel
28. VSC-24 Multi-Assembly Sealed Basket Transportation Safety Analysis Report, 0000-0632, Revision 0, September 2006
29. FuelSolutions W74 Canister Transportation Safety Analysis Report, WSNF-123, Revision 10, September 2006
30. FuelSolutions W21 Canister Transportation Safety Analysis Report, WSNF-121, Revision 6, September 2006

## **Appendix A**

Transportation Matrix for Commercial Power Reactor Fuel (Dry Storage, and  
Away from Reactor Wet Storage)

The accompanying chart details each cask or canister system in dry storage in the U.S. and cross-references these to a transportation pathway. Each row in the chart represents a cask system type at a certain reactor site listed by name of generating station (e.g. if the reactor ISFSI or ISFSIs contains three cask types in total, the chart contains three rows, one for each canister or cask type).

The first entry contains the utility name followed by the reactor name, reactor type (PWR or BWR), ISFSI license type (general or site specific), and year of first load. Next comes the Cask vendor followed by the Cask/Canister System and the specific canister/cask type employed. Generally the canister cask type includes a number that represents the number of assembly storage positions in that cask or canister type. The next column contains the total canisters or casks loaded followed by the assemblies stored in these canisters or casks. After the number of assemblies at each site, a rough estimate of the Metric Tons Initial Heavy metal of the fuel stored in each cask type is provided. (**NOTE: These numbers are based on an average value for PWR and BWR fuel. Actual MTIHM at each site can vary greatly from the number reported here depending on fuel type**)

Column 12 describes the storage configuration (fuel is stored directly in a bare fuel cask, in a canister in a concrete overpack (this includes NUHOMS storage modules and HISTORM concrete overpacks which have a metal skin), in a canister in a metal overpack (HISTAR 100) or in a canister inside a vault (Ft. St.Vrain is the only instance). If the storage configuration is a canister in a metal or concrete storage overpack, column 13 lists the primary transport cask currently licensed to transport the canister (if any) as well as any license applications for transportation casks which include the canister as a licensed content. Column 14 lists whether working units of the primary cask have been fabricated. For canister casks, only models of the NUHOMS MP187, HISTAR 100 and the TN-FSV have been fabricated. There are versions of the NAC-STC that have been fabricated for use overseas which are not available or licensable in the U.S. The NUHOMS MP197 cask has yet to be built as of the date of this report and will likely be replaced by the MP 197HB variant by the time working units are needed. The only domestic HISTAR 100 working transport casks are the 12 used for storage at Humboldt Bay, Dresden and Hatch. No production or full scale prototype units of the Fuel Solutions TS-125 cask have been fabricated as of the date of this report.

Column 15 lists any alternate transport casks which may be licensed for the same canister type or under application or even being considered for licensing of the canister type. If a certificate number is listed along with the cask name in columns 13 or 15, this signifies that that canister is included in the transport certificate. If the cask name is listed but no number is listed, this signifies that either the canister is under application for transport in the cask type named or is considered licensable for transport in the named cask by the cask vendor. Column 16 lists whether working units of the alternate cask in column 15 have been fabricated.

Column 17 applies to bare fuel casks and lists whether a transport license exists for the bare fuel cask with footnotes providing details.

For those systems which employ a fuel canister, Column 18 delineates whether the canister has been classified by the cask vendor as “storage only” canister. Storage only canisters may lack neutron absorbing material or may have simply not been evaluated in the 10 CFR71 accident sequence in a transportation overpack. By definition, each of the canisters listed in this column are not included in any transportation cask license. These canisters may still ultimately be shipped without repackaging of the fuel depending on the reasons for classification as “storage only”.

The final column of the chart contains the minimum lead time for shipment for canisters and casks at each reactor location. The lead time listed in this column only includes the time to prepare existing casks for shipment, time to fabricate casks and the time to obtain transportation licenses. It does not include factors such as approval of routing, security requirements, requirements for special rolling stock or the

implementation of “smart train” technology, or most importantly the time to make available a repository or interim storage site.

The wet storage table on the following page contains most of the same columns as the dry storage stable except that there are no references to bare fuel casks or “storage only” canisters. There are only two shutdown site currently transitioning into “ISFSI Only” status; LaCrosse and Zion. Both these sites have selected cask systems and in the case of LaCrosse, three casks have already been loaded as of August 2012 and the remaining two are expected to be completed in the coming weeks.

GE Morris is an away from reactor used fuel storage facility. There are no announced plans to transition fuel at GE Morris into dry cask storage as of the date of this report.

The final table in Appendix A is a storage summary table that gives a breakdown of the % of assemblies in each category of cask/vault storage listed.

Table A-1 Transportation Matrix for Commercial Reactor Fuel (Dry Storage, and Away from Reactor Wet Storage)

**U.S. Dry Storage Details (08/01/2012)**

Utility	Reactor	Type	License Type	Year of First Load <sup>14</sup>	Vendor	Cask System	Canister or Cask Type	Total Canisters or Casks Loaded	Assemblies Stored	MTIHM (Based on Average Assembly)	Storage Configuration	Primary Canister Transportation Cask (License Num.)	Primary Transport Cask Fabricated?	Alternative Canister Transportation Cask	Alternate Transport Cask Fabricated?	Bare Fuel Cask Transportation License (License Number)	"Storage Only" Canisters or Casks	Minimum Lead Time for Shipment
AEP	D.C.Cook	PWR	GL	2012	Holtec	HI-STORM	MPC-32	1	32	13.9	Canister in Vertical Concrete Overpack	HI-STAR100 (71-9261)	Yes <sup>1</sup>	No	No		14 Months <sup>8</sup>	
APS	Palo Verde	PWR	GL	2003	NAC	NAC-UMS	UMS-24	94	2256	982.5	Canister in Vertical Concrete Overpack	NAC-UMS (71-9270)	No	NAC-MAGNASTOR	No		24 Months <sup>8</sup>	
Constellation	Calvert Cliffs	PWR	SS	1992	TN	NUHOMS	24P	48	1152	501.7	Canister in Horizontal Concrete Overpack		No	No	No	24P	36 Months <sup>10</sup>	
Constellation	Calvert Cliffs	PWR	SS	1992	TN	NUHOMS	32P	21	672	292.7	Canister in Horizontal Concrete Overpack		No	No	No	32P	36 Months <sup>10</sup>	
Constellation	Ginna	PWR	GL	2010		NUHOMS	32PT	6	192	83.6	Canister in Horizontal Concrete Overpack		No	No	No		24 Months <sup>8</sup>	
Consumers	Big Rock Point <sup>12</sup>	BWR	GL	2002	BFS/ES	FuelSolutions	W150	8	441	78.8	Canister in Vertical Concrete Overpack	TS-125 (71-9276)	No	No	No		24 Months <sup>8</sup>	
Ct.Yankee	Conn Yankee <sup>12</sup>	PWR	GL	2004	NAC	NAC-MPC	MPC-26	43	1019	443.8	Canister in Vertical Concrete Overpack	NAC-STC (71-9235)	No	NAC-MAGNASTOR	No		24 Months <sup>8</sup>	
Dairyland Power	Lacrosse	BWR	GL	2012	NAC	NAC	LACBWR	3	204	36.4	Canister in Horizontal Concrete Overpack	NAC-STC (71-9235)	No	NAC-MAGNASTOR	No		24 Months <sup>8</sup>	
DOE	INEEL	PWR	SS	TN	NUHOMS	12T	29	177	77.1	Canister in Horizontal Concrete Overpack		No	No	No	12T	36 Months <sup>10</sup>		
Dominion	Keweenaw	PWR	GL	2009	TN	NUHOMS	32PT	8	256	111.5	Canister in Horizontal Concrete Overpack		No	MP197HB	No		24 Months <sup>8</sup>	
Dominion	Millstone	PWR	GL	2005	TN	NUHOMS	32PT	18	576	250.8	Canister in Horizontal Concrete Overpack		No	MP197HB	No		24 Months <sup>8</sup>	
Dominion	North Anna	PWR	SS	1998	TN	TN Metal Casks	TN-32	27	864	376.3	Bare Fuel	-	-	-	No <sup>3</sup>		24 Months <sup>8</sup>	
Dominion	North Anna	PWR	GL	2008	TN	NUHOMS	32PTH	13	416	181.2	Canister in Horizontal Concrete Overpack		No	MP197HB	No		24 Months <sup>8</sup>	
Dominion	Surry	PWR	SS	1986	GNB	Castor	V/21 and X33	26	558	243.0	Bare Fuel		-	-	-	No <sup>4</sup>	36 Months <sup>10</sup>	
Dominion	Surry	PWR	SS	1986	NAC	NAC-128	NAC-128	2	56	24.4	Bare Fuel		-	-	-	No <sup>5</sup>	24 Months <sup>8</sup>	
Dominion	Surry	PWR	GL	2007	TN	NUHOMS	32PTH	18	576	250.8	Canister in Horizontal Concrete Overpack		No	MP197HB	No		24 Months <sup>8</sup>	
Dominion	Surry	PWR	SS	1986	TN	TN Metal Casks	TN-32	26	832	362.3	Bare Fuel		-	-	-	No <sup>3</sup>	24 Months <sup>7</sup>	
Dominion	Surry	PWR	SS	1986	W	MC-10	MC-10	1	24	10.5	Bare Fuel		-	-	-	No <sup>6</sup>	24 Months <sup>7</sup>	
Duke	Catawba	PWR	GL	2007	NAC	NAC-UMS	UMS-24	24	576	250.8	Canister in Vertical Concrete Overpack		No	NAC-MAGNASTOR	No		24 Months <sup>8</sup>	
Duke	McGuire	PWR	GL	2001	NAC	NAC-UMS	UMS-24	28	672	292.7	Canister in Vertical Concrete Overpack	NAC-UMS (71-9270)	No	NAC-MAGNASTOR	No		24 Months <sup>8</sup>	
Duke	McGuire	PWR	GL	2001	TN	TN Metal Casks	TN-32	10	320	139.4	Bare Fuel		-	-	-	No <sup>3</sup>	24 Months <sup>7</sup>	
Duke	Oconee	PWR	GL/SS	1990	TN	NUHOMS	24P	84	2016	878.0	Canister in Horizontal Concrete Overpack		No	No	No	24P	36 Months <sup>10</sup>	
Duke	Oconee	PWR	GL	2000	TN	NUHOMS	24PHB	38	912	397.2	Canister in Horizontal Concrete Overpack		No	No	No	24PHB	36 Months <sup>10</sup>	
Energy Northwest	Columbia	BWR	GL	2002	Holtec	HI-STORM	MPC-68	27	1836	327.9	Canister in Vertical Concrete Overpack	HI-STAR100 (71-9261)	Yes <sup>1</sup>	No	No	VSC-24	36 Months <sup>10</sup>	
Entergy	ANO	PWR	GL	1996	BFS/ES	FuelSolutions	VSC-24	24	576	250.8	Canister in Vertical Concrete Overpack		No	No	No		14 Months <sup>8</sup>	
Entergy	ANO	PWR	GL	1996	Holtec	HI-STORM	MPC-24	22	528	229.9	Canister in Vertical Concrete Overpack	HI-STAR100 (71-9261)	Yes <sup>1</sup>	No	No		14 Months <sup>8</sup>	
Entergy	ANO	PWR	GL	1996	Holtec	HI-STORM	MPC-32	16	512	223.0	Canister in Vertical Concrete Overpack	HI-STAR100 (71-9261)	Yes <sup>1</sup>	No	No		14 Months <sup>8</sup>	
Entergy	Fitzpatrick	BWR	GL	2002	Holtec	HI-STORM	MPC-68	15	1020	182.2	Canister in Vertical Concrete Overpack	HI-STAR100 (71-9261)	Yes <sup>1</sup>	No	No		14 Months <sup>8</sup>	
Entergy	Grand Gulf	BWR	GL	2006	Holtec	HI-STORM	MPC-68	17	1156	206.5	Canister in Vertical Concrete Overpack	HI-STAR100 (71-9261)	Yes <sup>1</sup>	No	No		14 Months <sup>8</sup>	
Entergy	Indian Point 1	PWR	GL	2008	Holtec	HI-STORM	MPC-32	5	160	69.7	Canister in Vertical Concrete Overpack	HI-STAR100 (71-9261)	Yes <sup>1</sup>	No	No		14 Months <sup>8</sup>	
Entergy	Indian Point 2	PWR	GL	2008	Holtec	HI-STORM	MPC-32	14	448	195.1	Canister in Vertical Concrete Overpack	HI-STAR100 (71-9261)	Yes <sup>1</sup>	No	No		14 Months <sup>8</sup>	
Entergy	Palisades	PWR	GL	1993	BFS/ES	FuelSolutions	VSC-24	18	432	188.1	Canister in Vertical Concrete Overpack		No	No	No	VSC-24	36 Months <sup>10</sup>	
Entergy	Palisades	PWR	GL	1993	TN	NUHOMS	24PTH	13	312	135.9	Canister in Horizontal Concrete Overpack		No	MP197HB	No		24 Months <sup>8</sup>	
Entergy	Palisades	PWR	GL	1993	TN	NUHOMS	32PT	11	352	153.3	Canister in Horizontal Concrete Overpack		No	MP197HB	No		24 Months <sup>8</sup>	
Entergy	River Bend	BWR	GL	2005	Holtec	HI-STORM	MPC-68	15	1020	182.2	Canister in Vertical Concrete Overpack	HI-STAR100 (71-9261)	Yes <sup>1</sup>	No	No		14 Months <sup>8</sup>	
Entergy	Vermont Yankee	BWR	GL	2008	Holtec	HI-STORM	MPC-68	14	952	170.0	Canister in Vertical Concrete Overpack	HI-STAR100 (71-9261)	Yes <sup>1</sup>	No	No		14 Months <sup>8</sup>	
Exelon	Waterford	PWR	GL	2011	Holtec	HI-STORM	MPC-32	9	288	125.4	Canister in Vertical Concrete Overpack	HI-STAR100 (71-9261)	Yes <sup>1</sup>	No	No		14 Months <sup>8</sup>	
Exelon	Braidwood	PWR	GL	2011	Holtec	HI-STORM	MPC-32	3	96	41.8	Canister in Vertical Concrete Overpack	HI-STAR100 (71-9261)	Yes <sup>1</sup>	No	No		14 Months <sup>8</sup>	
Exelon	Byron	PWR	GL	2010	Holtec	HI-STORM	MPC-32	14	448	195.1	Canister in Vertical Concrete Overpack	HI-STAR100 (71-9261)	Yes <sup>1</sup>	No	No		14 Months <sup>8</sup>	
Exelon	Dresden	BWR	GL	2000	Holtec	HI-STORM	MPC-68	49	3332	595.1	Canister in Vertical Concrete Overpack	HI-STAR100 (71-9261)	Yes <sup>1</sup>	No	No		14 Months <sup>8</sup>	
Exelon	Dresden	BWR	GL	2000	Holtec	HI-STAR	MPC-68	4	272	48.6	Canister in Metal Cask	HI-STAR100 (71-9261)	Yes <sup>1</sup>	No	No		12 Months <sup>11</sup>	
Exelon	LaSalle	BWR	GL	2010	Holtec	HI-STORM	MPC-68	6	408	72.9	Canister in Vertical Concrete Overpack	HI-STAR100 (71-9261)	Yes <sup>1</sup>	No	No		14 Months <sup>8</sup>	
Exelon	Limerick	BWR	GL	2008	TN	NUHOMS	61BT	19	1159	207.0	Canister in Horizontal Concrete Overpack	MP197 (71-9302)	No	MP197HB (71-9302)	No		24 Months <sup>8</sup>	
Exelon	Oyster Creek	BWR	GL	2002	TN	NUHOMS	61BT	23	1403	250.6	Canister in Horizontal Concrete Overpack	MP197 (71-9302)	No	MP197HB (71-9302)	No		24 Months <sup>8</sup>	
Exelon	Peach Bottom	BWR	GL	2000	TN	TN Metal Casks	TN-68	59	4012	716.5	Bare Fuel		-	-	-	Yes (71-9293)	12 Months <sup>11</sup>	
Exelon	Quad Cities	BWR	GL	2005	Holtec	HI-STORM	MPC-68	35	2380	425.1	Canister in Vertical Concrete Overpack	HI-STAR100 (71-9261)	Yes <sup>1</sup>	No	No		14 Months <sup>8</sup>	
FirstEnergy	Davis-Besse	PWR	GL	1995</														

Table Appendix A-1 (Continued) Transportation Matrix for Commercial Power Reactor Fuel (Dry Storage, and Away from Reactor Wet Storage)

Portland	GE Trojan	PWR	GL	2002	Holtec	TranStor Cask	MPC-24E/EF	34	780	339.7	Canister in Vertical Concrete Overpack	HISTAR 100 (71-9261)	Yes <sup>1</sup>	No	14 Months <sup>v</sup>	
PPL	Susquehanna	BWR	GL	1999	TN	NUHOMS	52B	27	1404	250.8	Canister in Horizontal Concrete Overpack		No	No	52B	36 Months <sup>10</sup>
PPL	Susquehanna	BWR	GL	1999	TN	NUHOMS	61BT	40	2440	435.8	Canister in Horizontal Concrete Overpack	MP197 (71-9302)	No	MP197HB(71-9302)	No	24 Months <sup>8</sup>
Progress	Brunswick	BWR		2010	TN	NUHOMS	61BTH	8	488	87.2	Canister in Horizontal Concrete Overpack	MP197HB (71-9302)	No	MP197HB(71-9302)	No	24 Months <sup>8</sup>
Progress	Robinson	PWR	SS	1989	TN	NUHOMS	7P	8	56	24.4	Canister in Horizontal Concrete Overpack		No	No	7P	36 Months <sup>10</sup>
Progress	Robinson	PWR	GL	2007	TN	NUHOMS	24PTH	14	336	146.3	Canister in Horizontal Concrete Overpack		No	MP197HB	No	24 Months <sup>9</sup>
PS Colorado	Ft. St. Vrain <sup>11</sup>	HTGR	SS	1991	DOE	Foster Wheeler	MVDS		1464	1,023.3	Canister in Vault	TN-FSV (71-9253)	Yes <sup>2</sup>	No		12 Months <sup>v</sup>
PSE&G	Hope Creek	BWR	GL	2006	Holtec	HI-STORM	MPC-68	16	1088	194.3	Canister in Vertical Concrete Overpack	HI-STAR100 (71-9261)	Yes <sup>1</sup>	No		14 Months <sup>8</sup>
PSE&G	Salem	PWR	GL	2010	Holtec	HI-STORM	MPC-32	14	448	195.1	Canister in Vertical Concrete Overpack	HI-STAR100 (71-9261)	Yes <sup>1</sup>	No		14 Months <sup>8</sup>
PG&E	Diablo Canyon	PWR	SS	2009	Holtec	HI-STORM	MPC-32	23	736	320.5	Canister in Vertical Concrete Overpack	HI-STAR100 (71-9261)	Yes <sup>1</sup>	No		14 Months <sup>9</sup>
PG&E	Humboldt Bay <sup>12</sup>	BWR	SS	2008	Holtec	HI-STAR	MPC-80	5	390	69.7	Canister in Metal Cask	HI-STAR100 (71-9261)	Yes <sup>1</sup>	No		12 Months <sup>11</sup>
SMUD	Rancho Seco <sup>12</sup>	PWR	SS	2001	TN	NUHOMS	24PT	22	493	214.7	Canister in Horizontal Concrete Overpack	MP187 (71-9255)	Yes <sup>2</sup>	MP197HB	No	12 Months <sup>v</sup>
Southern Cal Edison	SONGS 1 <sup>13</sup>	PWR	GL	2003	TN	NUHOMS	24PT1	18	395	172.0	Canister in Horizontal Concrete Overpack	MP187 (71-9255)	Yes	MP197HB	No	24 Months <sup>v</sup>
Southern Cal Edison	SONGS 2	PWR	GL	2003	TN	NUHOMS	24PT4	29	696	303.1	Canister in Horizontal Concrete Overpack		No	MP197HB (71-9302)	No	24 Months <sup>9</sup>
Southern Nuclear	Farley	PWR	GL	2005	Holtec	HI-STORM	MPC-32	15	480	209.0	Canister in Vertical Concrete Overpack	HI-STAR100 (71-9261)	Yes <sup>1</sup>	No		24 Months <sup>8</sup>
Southern Nuclear	Hatch	BWR	GL	2000	Holtec	HI-STORM	MPC-68	47	3196	570.8	Canister in Vertical Concrete Overpack	HI-STAR100 (71-9261)	Yes <sup>1</sup>	No		24 Months <sup>8</sup>
Southern Nuclear	Hatch	BWR	GL	2000	Holtec	HI-STAR	MPC-68	3	204	36.4	Canister in Metal Cask	HI-STAR100 (71-9261)	Yes <sup>1</sup>	No		12 Months <sup>11</sup>
TVA	Browns Ferry	BWR	GL	2005	Holtec	HI-STORM	MPC-68	37	2516	449.4	Canister in Vertical Concrete Overpack	HI-STAR100 (71-9261)	Yes <sup>1</sup>	No		14 Months <sup>8</sup>
TVA	Sequoyah	PWR	GL	2004	Holtec	HI-STORM	MPC-32	32	1024	446.0	Canister in Vertical Concrete Overpack	HI-STAR100 (71-9261)	Yes <sup>1</sup>	No		14 Months <sup>8</sup>
Xcel Energy	Prairie Island	PWR	SS	1993	TN	TN Metal Casks	TN-40	29	1160	505.2	Bare Fuel	-	-	-	Yes (71-9313)	12 Months <sup>9</sup>
Xcel Energy	Monticello	BWR	GL	2008	TN	NUHOMS	61BT	10	610	108.9	Canister in Horizontal Concrete Overpack	MP197 (MP197HB)	No	No		24 Months <sup>9</sup>
YAEC	Yankee Rowe <sup>13</sup>	PWR	GL	2002	NAC	NAC-MPC	MPC-36	16	533	232.1	Canister in Vertical Concrete Overpack	NAC-STC (71-9235)	No			24 Months <sup>v</sup>
Totals:								1640	64804	19,966.0						

Table A-2 Storage Summary – U.S. Wet Storage at Shutdown Reactor Sites

**U.S. Wet Storage at Shutdown Reactor Sites**

Utility	Reactor / Storage Facility	Reactor Type	ISFSI License Type	Planned Load Date	Vendor	Cask System	Canister or Cask Type	Estimated Canisters or Casks to be Loaded	Assemblies in Wet Storage	Future Dry Storage Configuration	Primary Canister Transportation Cask	Primary Transport Cask Fabricated?	Alternative Canister Transportation Cask	Alternate Transport Cask Fabricated?
Dairyland Power	Lacrosse	BWR	SS	2012	NAC	MPC-LACBWR	MPC-LACBWR	2	129	Canister in Vertical Concrete Overpack	NAC-STC (71-9235)	No	NAC-MAGNATRAN	No
Zion Solutions	Zion	PWR	SS	2013	NAC	MAGNASTOR	TSC-37	61	2,226	Canister in Vertical Concrete Overpack	NAC-MAGNATRAN	No	-	-
General Electric	GE Morris	NA	SS	NA	NA	NA	NA		3,217	Storage System not Selected	NA	NA	NA	NA
							<b>Totals:</b>		<b>63 5572</b>					

**Storage Summary**

	Number of Casks	Number of Assemblies	% of Dry Stored Assemblies
Bare Fuel Casks	180	7826	12.1 %
Canisters in Concrete Overpacks	1447	54648	84.3 %
Canisters in Transport Casks	12	866.0	1.3 %
Vault Storage	NA	1464	2.3 %
			100 %



Red Border indicates "ISFSI Only Site"

Orange border indicates a Site with a Shutdown Reactor but One or More Operating Reactors Remaining

<sup>1</sup>12 units actively storing fuel are the only HISTAR 100 Casks available in U.S. 7 of these can accommodate standard size MPCs

<sup>2</sup>One MP187 staged empty at Rancho Seco Site; one TN-FSV staged empty at INL.(Only one canister per shipment possible)

<sup>3</sup>No TN-32 Transportation License under review

<sup>4</sup>Castor Casks not licensed for shipment in the U.S.

<sup>5</sup>No NAC-128 Transportation License under review

<sup>6</sup>No MC-10 Transportation License under review

<sup>7</sup>Lead time mostly cask license application and review

<sup>8</sup>Lead time due to primary cask not yet fabricated

<sup>9</sup>TN-40 Certificate issued June 2011, TN-40HT Submittal which includes High Burnup Fuel as Content to follow in 2011

<sup>10</sup>Lead time addresses "Storage Only" canister issue, and cast iron bare-fuel

casks. Repackaging might be required.

<sup>11</sup>Designates Shortest Lead Time for Shipment of Fuel in Dry Storage. Fuel is Already in Cask

Licensed for Transportation. 6 Months Includes Cask Preparation Time, Leak Tests, Impact Limiter Mounting, etc.

<sup>12</sup>includes GTCC waste

<sup>13</sup>All the spent fuel from the shuttered Unit 1

<sup>14</sup>For multiple cask ISFSI sites the earliest load date applies to all casks

<sup>15</sup>Ft St Vrain Initial Heavy Metal does not include Thorium

Green shading indicates shortest lead time of 12 months -- fuel is already in casks licensed (Impact Limiter Fabrication Required) for transportation.

Red shading indicates indefinite lead time to first shipment -- canisters are "storage only" and casks are not licensed, or fuel is in cast iron bare-fuel casks that are not licensable.

Unshaded indicates intermediate lead time -- cask is licensed but not fabricated (or available), or cask license is in progress but not fabricated, or fuel is in (bare-fuel) cask but cask not licensed.

Filename: Dry Storage of Used Fuel\_Transition to Transport\_20120913FINAL.doc  
Directory: C:\Documents and Settings\l4184\Desktop  
Template: C:\Documents and Settings\l4184\Application Data\Microsoft\Templates\Normal.dotm  
Title: DOE/ID-Number  
Subject:  
Author: Bates  
Keywords:  
Comments:  
Creation Date: 9/13/2012 3:46:00 PM  
Change Number: 18  
Last Saved On: 9/25/2012 10:56:00 AM  
Last Saved By: SMITH, PATRICIA ANN  
Total Editing Time: 316 Minutes  
Last Printed On: 9/25/2012 10:57:00 AM  
As of Last Complete Printing  
Number of Pages: 46  
Number of Words: 12,385 (approx.)  
Number of Characters: 70,596 (approx.)

## **APPENDIX H**

### **Fuel-Assembly Shaker Test Plan Tests for Determining Loads on Used Nuclear Fuel under Normal Conditions of Transport**

# FUEL-ASSEMBLY SHAKER TEST PLAN

Tests for Determining Loads on Used Nuclear  
Fuel under Normal Conditions of Transport

**Fuel Cycle Research & Development**

*Prepared for  
US Department of Energy  
UFD Campaign  
Paul McConnell  
Sandia National Laboratories  
September 30, 2012  
FCRD-UFD-2012-000341*



**DISCLAIMER**

This information was prepared as an account of work sponsored by an agency of the U.S. Government. Neither the U.S. Government nor any agency thereof, nor any of their employees, makes any warranty, expressed or implied, or assumes any legal liability or responsibility for the accuracy, completeness, or usefulness, of any information, apparatus, product, or process disclosed, or represents that its use would not infringe privately owned rights. References herein to any specific commercial product, process, or service by trade name, trade mark, manufacturer, or otherwise, does not necessarily constitute or imply its endorsement, recommendation, or favoring by the U.S. Government or any agency thereof. The views and opinions of authors expressed herein do not necessarily state or reflect those of the U.S. Government or any agency thereof.



**Sandia National Laboratories**

Sandia National Laboratories is a multi-program laboratory managed and operated by Sandia Corporation, a wholly owned subsidiary of Lockheed Martin Corporation, for the U.S. Department of Energy's National Nuclear Security Administration under contract DE-AC04-94AL85000.

## FCT Quality Assurance Program Document

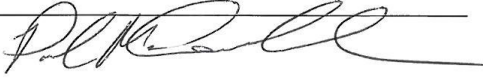
### Appendix E FCT Document Cover Sheet

Fuel-Assembly Shaker Test. Tests for Determining Loads on  
Used Nuclear Fuel under Normal Conditions of Transport

ST Transportation – SNL / FT-12SN081305 (Rev. 1)

**1.02.08.13**

Paul McConnell

(Name/Signature) 

Date Submitted

Quality Rigor Level for Deliverable/Milestone	<input checked="" type="checkbox"/> QRL-3	<input type="checkbox"/> QRL-2	<input type="checkbox"/> QRL-1	<input type="checkbox"/> N/A*
			<input type="checkbox"/> Nuclear Data	

This deliverable was prepared in accordance with

Sandia National Laboratories  
(Participant/National Laboratory Name)

QA program which meets the requirements of

DOE Order 414.1       NQA-1-2000

**This Deliverable was subjected to:**

Technical Review

**Technical Review (TR)**

**Review Documentation Provided**

Signed TR Report or,

Signed TR Concurrence Sheet or,

Signature of TR Reviewer(s) below

Peer Review

**Peer Review (PR)**

**Review Documentation Provided**

Signed PR Report or,

Signed PR Concurrence Sheet or,

Signature of PR Reviewer(s) below

**Name and Signature of Reviewers**

Gregg Flores



\*Note: In some cases there may be a milestone where an item is being fabricated, maintenance is being performed on a facility, or a document is being issued through a formal document control process where it specifically calls out a formal review of the document. In these cases, documentation (e.g., inspection report, maintenance request, work planning package documentation or the documented review of the issued document through the document control process) of the completion of the activity along with the Document Cover Sheet is sufficient to demonstrate achieving the milestone. QRL for such milestones may be also be marked N/A in the work package provided the work package clearly specifies the requirement to use the Document Cover Sheet and provide supporting documentation.

## SUMMARY

This report is the Sandia National Laboratories milestone (M3FT-12SN0813055) “Normal transport test report” for the Used Fuel Disposition Campaign Storage and Transportation (ST) Work Package.

This test plan defines a test designed to capture the response of a representative fuel assembly in its representative transportation configuration (i.e., *in-an-assembly-within-a-basket-within-a-cask-tied-to-a-transport-conveyance*) to actual loadings imposed during normal conditions of transport.

The representative assembly planned for the test is a 17x17 pressurized water reactor (PWR) assembly.

The assembly rods to be used for the tests will not be actual irradiated zirconium alloy/UO<sub>2</sub>-pellet rods. Surrogate rods shall be selected that have similar mass and stiffness as the actual irradiated rods. Due to the cost and availability, copper B280 alloy tubes filled with lead rods approximately meet the criteria for simulating Zircaloy-4/UO<sub>2</sub>-pellet rods. They shall be used for most of the positions within the assembly; Zircaloy-4/Pb rods shall be used for those assembly positions which will be instrumented for the test.

Finite-element modeling before the test shall provide information on which rod locations within the assembly should be instrumented and on which locations on those rods the instrumentation for measuring strains and accelerations should be placed. Finite-element modeling after the simulated normal transport tests will allow an estimate of the response all the rods may experience during normal transport based upon the test data from the surrogate rods. The test data will also allow the finite element model to be benchmarked.

The test results will allow for an analytic assessment of the ability of aged, high burnup cladding to withstand normal transport loads by assessing the strength of the aged, high burnup cladding relative to the stresses imposed on the cladding during normal transport.

## CONTENTS

SUMMARY .....	iv
CONTENTS.....	v
FIGURES .....	vii
TABLES .....	viii
ACRONYMS .....	ix
1 INTRODUCTION .....	1
2 BACKGROUND .....	3
2.1 Regulations.....	3
2.2 Shock and Vibration.....	4
3 NORMAL CONDITIONS OF TRANSPORT TEST PLAN .....	6
3.1 Introduction .....	6
3.1.1 Basis of test .....	6
3.1.2 General description of test .....	7
3.2 Purpose of Test Plan .....	7
3.3 Test Description .....	8
3.3.1 Acquisition of an unirradiated fuel assembly.....	8
3.3.2 Instrumentation .....	9
3.3.3 The 0.3-meter drop test .....	10
4 SCOPE.....	11
4.1 Test Parameters .....	11
4.1.1 Vibration facility .....	19
4.2 Instrumentation Installation Tables.....	23
4.3 Vibration Test Procedure .....	28
4.3.1 Test preparation.....	28
4.3.2 Test set-up .....	28
4.3.3 Post-test activities .....	28
5 TEST INPUT SPECIFICATIONS: RECOMMENDED VIBRATION AND SHOCK TRANSPORTATION TEST SPECIFICATIONS FOR THE REACTOR FUEL ASSEMBLY <sup>10</sup> .....	29
5.1 Introduction.....	29
5.2 Instrumentation .....	29
5.3 Random Vibration Test Specifications .....	31
5.4 Shock – Decayed Sine Specifications and Time Histories .....	33
5.5 Derivation of Test Specifications.....	44
5.5.1 Derivation of random vibration test specification.....	44

5.5.2	Derivation of shock test specification .....	45
6	PREVIOUS OVER-THE-ROAD TEST PROGRAMS.....	55
6.1	“Over-the-road testing of radioactive materials packagings” .....	55
6.1.1	Instrumentation .....	56
6.1.2	Test results .....	56
6.2	“Test specification for TRUPACT-I vibration assessment” .....	56
6.2.1	Instrumentation .....	57
7	KEY BACKGROUND INFORMATION.....	59
7.1	Souce of Vibration and Shock Data for Test.....	59
7.2	Related Documents .....	62
7.2.1	“Approach for the Use of Acceleration Values for Packages of Radioactive Material under Routine Conditions of Transport,” Andreas Apel, Viktor Ballheimer, Christian Kuschke, Sven Schubert, Frank Wille, Proceedings of the 9th International Conference on the Radioactive Materials Transport and Storage, May 2012, London.....	62
7.2.2	“Transportation Activities for BWR Fuels at NFI,” S. Uchikawa, H. Kishita, H. Ide, M. Owaki, K. Ohira, Nuclear Fuel Industries, LTD., Proceedings of Global 2009, Paris, September 2009.....	62
7.2.3	“High Burn-up Used Nuclear Fuel Vibration Integrity Study - Out-of-Cell Fatigue Testing Development,” , Jy-An John Wang, Hong Wang, Yong Yan, Rob Howard, Bruce Bevard, January 2011, Oak Ridge National Laboratory.....	62
7.2.4	Other documents related to this work include.....	65
8	REFERENCES .....	66

## **FIGURES**

Figure 1. Used nuclear fuel transportation modes, transportation vibration spectra (which result in loads applied to cladding), and material property data. ....	2
Figure 2. Bounding acceleration shock response spectrum for a truck cask at 3% damping . .....	5
Figure 3. Bounding truck vibration data for all three axes . .....	5
Figure 4. Fuel assembly. ....	8
Figure 5. Placement of assembly with rods, basket, and support beams on shaker.....	12
Figure 6. Differences between an actual test in a truck cask and the shaker test.....	12
Figure 7. Technical data used to select copper tubes as surrogate rods.....	13
Figure 8. Location of Zircaloy rods within the assembly which will be instrumented.....	14
Figure 9. Shock data from the 1978 truck cask transportation report. ....	17
Figure 10. Data derived from the truck cask transportation report to be used as input to the shaker. ....	18
Figure 11. Vibration facility. ....	19
Figure 12. Shaker to be used for test.....	20
Figure 13. Copper tube containing a lead rod to be used as a surrogate Zircaloy/UO <sub>2</sub> rod. ....	21
Figure 14. Dimensions of basket to be used to contain the assembly on the shaker (Safety Analysis Report for the NAC-LWT, Revision 27, June 1999, Docket No. 9925 T-88004). ....	22
Figure 15. Fuel reactor assembly on shaker table. ....	30
Figure 16. Cross-section of fuel reactor assembly. ....	31
Figure 17. Recommended random vibration test specification.....	32
Figure 18. Recommended shock test specification. ....	33
Figure 19. Recommended test specification & underlying ASDs. ....	45
Figure 20. Recommended test specification & underlying shock spectra. ....	46
Figure 21. Range of frequencies. ....	46
Figure 22. Decayed sine initial realization. ....	47
Figure 23. Decayed sine second realization. ....	47

---

Figure 24. Decayed sine third realization.....	48
Figure 25. Decayed sine fourth realization.....	48
Figure 26. Decayed sine fifth realization.....	49
Figure 27. Representative normal transport load data.....	58

## TABLES

Table 1. Instrumentation Installation Data.....	23
Table 3: Response Accelerometers & Strain Gages.....	30
Table 4: Vibration Breakpoints.....	32
Table 5: Reference Shock Breakpoints.....	33
Table 6: Initial Realization of Decayed Sine Parameters.....	34
Table 7: Second Realization of Decayed Sine Parameters.....	36
Table 8: Third Realization of Decayed Sine Parameters.....	38
Table 9: Fourth Realization of Decayed Sine Parameters.....	40
Table 10: Fifth Realization of Decayed Sine Parameters.....	42
Table 11: Input to Cargo (g) – Vertical Axis.....	44

## **ACRONYMS**

BWR	Boiling Water Reactor
CFR	Code of Federal Regulations
FAST	Facility for Accelerated Service Testing
IAEA	International Atomic Energy Agency
NEPA	National Environmental Policy Act
NRC	Nuclear Regulatory Commission
PNNL	Pacific Northwest National Laboratory
PWR	Pressurized Water Reactor
QA	Quality Assurance
SNL	Sandia National Laboratories
ST	Storage and Transportation
TRUPACT	Transuranic Package Transporter
TTC	Transportation Technology Center
US	United States



# FUEL-ASSEMBLY SHAKER TEST PLAN

## Tests for Determining Loads on Used Nuclear Fuel under Normal Conditions of Transport

### 1 INTRODUCTION

There is an international issue concerning storage and subsequent transportation of used nuclear fuel that requires quantitative knowledge of used nuclear fuel material properties and response to mechanical loadings during transport.

Many countries are in the position of having to store their used nuclear fuel longer than originally expected. For example, the closing of Yucca Mountain in the United States (US) and the German response to Fukushima will result in the need for extended storage times in these countries. Other countries are still in the planning stages for disposition of their used nuclear fuel, but they will also require extended storage times to accommodate deliberations on fuel disposition.

There are legitimate concerns for long-term storage associated with the degradation of material properties over time for the entire storage system: fuel, canister, overpack, and pad. An understanding of how degraded materials affect their safety functions over time is important to licensing these systems past their original design life. In addition, degradation of used nuclear fuel may adversely affect cladding integrity during transport after storage. Of the storage system components mentioned above, fuel clad integrity is the first line of defense for containment of the used nuclear fuel and so there is a high priority for better understanding of how its material properties may degrade over time, and if these degraded properties are sufficient to maintain fuel integrity during transportation.

This test program is designed to better understand fuel response to *normal* conditions of transport loadings and to estimate the ability of used nuclear fuel with degraded properties to withstand these loadings. This will be done with a combination of experimental data collection and numerical analyses. The experimental work will focus on using full-scale test articles that are subjected to realistic normal conditions of transport loadings. The test unit will be appropriately instrumented to capture the data needed to conduct numerical analyses. The numerical analyses will be used to augment the experimental data set to a more comprehensive set of conditions that will enable a better understanding of used nuclear fuel behavior under normal conditions of transport. The numerical analyses shall also provide the means to extend the test results from a specific package and assembly to other package/assembly configurations.

The data from the tests described herein shall also be compared to data to be generated in other Department of Energy Used Nuclear Fuel Disposition Campaign activities that will measure mechanical properties of both high burnup and aged used nuclear fuel. By comparing the loads applied to fuel cladding during normal transportation to the strength of used nuclear fuel, an assessment can be made of the ability of the cladding to withstand post-storage transportation environments (Figure 1).

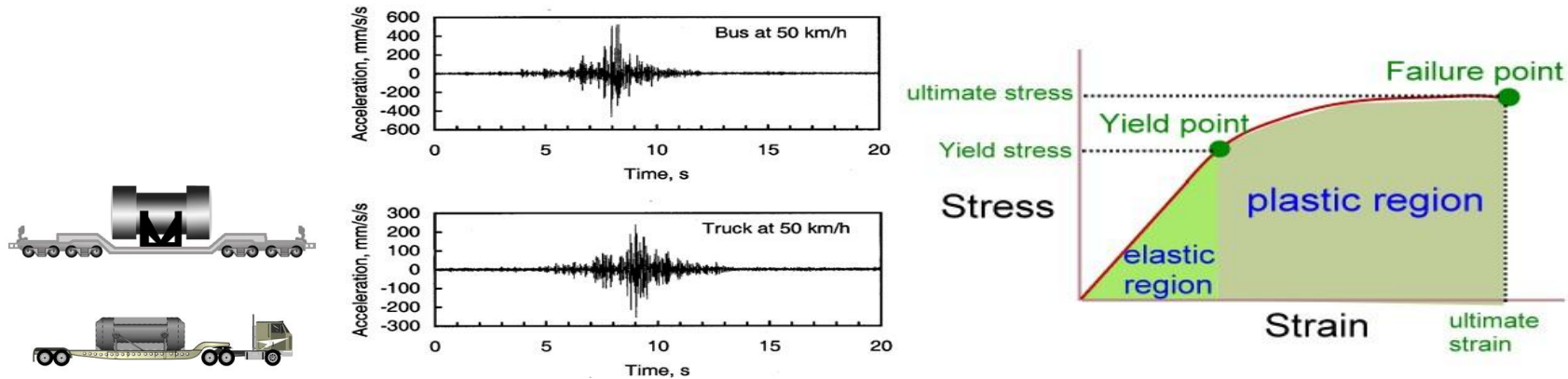


Figure 1. Used nuclear fuel transportation modes, transportation vibration spectra (which result in loads applied to cladding), and material property data.

## 2 BACKGROUND

### 2.1 Regulations

US regulations are harmonized with the International Atomic Energy Agency (IAEA) regulations. In the US, the design of casks and performance of the fuel within the casks is governed by 10 CFR Part 71 in the US Code of Federal Regulations. The regulations cover two loading conditions that are important to assure the integrity of used nuclear fuel and are, therefore, important to this test proposal.

- Incident-free transportation: Nuclear fuel must have sufficient strength to sustain its integrity during normal operations. For truck transport, this basically means that the fuel must be strong enough to withstand loadings imposed from driving on roads with various road conditions. For rail, the fuel must be strong enough to withstand loading from over the rail transport as well as longitudinal coupling loads that are imposed. Loading forces and vibrations are the primary loads that need to be obtained for both truck and rail.
- 0.3 meter drop tests: The 0.3 meter drop represents an in-plant accident that may occur while transferring the payload from its storage to its transport configuration. This drop test must be performed (or analyzed) with the package in an orientation that would cause maximum damage.<sup>1</sup> Numerical methods are more easily applied to the analysis of the effects on transport packages and their contents due to a 0.3-meter drop than they are for analysis of the vibrational loading inherent to normal transport conditions.<sup>2</sup>

The loads, to which the used nuclear fuel cladding is subjected during normal conditions of transport, either by truck or by rail, are the result of the induced vibrations and intermittent shock loads. There are virtually no known data for the loads to which used nuclear fuel – the individual pins, the assemblies, the baskets – is subjected during normal transport conditions.

Without mechanical property data for high burnup fuel cladding and knowledge of the loads to which that cladding would experience in a transport environment, predictions of the integrity of the used nuclear fuel during normal transport are speculative and possibly inexact. Mechanical property data for high burnup used nuclear fuel cladding alone is not sufficient for accurate predictions of the behavior of the cladding during normal transport – the applied loads to the cladding during normal transport are also required. Hence this test

---

<sup>1</sup> The regulations are silent regarding the presence of impact limiters on the cask for the 0.3-meter drop. The definition of a transport package in 10 CFR 71.4 “means the packaging together with its radioactive contents *as presented for transport*” and “Packaging means the assembly of components necessary to ensure compliance with the packaging requirements of this part [and]...*may consist of...devices for...absorbing mechanical shocks*.” Furthermore, 10 CFR 71.71(a) Normal Conditions of Transport states that this section is an “[e]valuation of [the] package design.”

<sup>2</sup> A detailed discussion of the US Nuclear Regulatory Commission (NRC) intent regarding the analysis necessary for the drop test may be gleaned from NUREG-1536, Revision 1A, “Standard Review Plan for Used Nuclear Fuel Dry Storage Systems at a General License Facility.” But, note that this document addresses used nuclear fuel casks used for dry storage, not transport.

proposal for obtaining load data applied to used nuclear fuel cladding residing within a transport package during normal transport.<sup>3</sup>

## 2.2 Shock and Vibration

Normal transport loads can be divided into two categories:

- Shock and vibration loading caused by normal over-the-road operations. (A fuel assembly is subjected to cyclic loading conditions as a result of random shock and vibration loading during normal transport conditions.<sup>4</sup>)
- The 0.3-m normal regulatory drop event, which is intended to be an initial condition before entering the accident environments.

A large quantity of experimental data has been derived from various sources to quantify the shock and vibration environment of cargo during truck and rail transport. The data usually were collected from instrumentation located at the interface between the packaging or cargo and the transporter, and generally consist of acceleration-response spectra as a function of frequency. The total acceleration response measured for a cargo includes response to superimposed shock and vibration. The vibration component is usually identified as a continuous excitation comprising all responses lower than or equal to 99% of the peaks in the acceleration response records. The remaining higher intensity, infrequently occurring acceleration peaks, correspond to sporadic shock events.

The bounding acceleration shock response spectrum for used nuclear fuel in truck casks for this test program is based on the union of triaxial data (longitudinal, transverse, and vertical axis accelerations) for 20- and 25-tonne cargoes reported in [2-4]. These data are shown in Figure 2. The suggested bilinear curve (in the log-log plane) that bounds these data from above consists of a linearly increasing portion up to a frequency of approximately 3.5 Hz, followed by a constant segment at 4.4-g acceleration, up to a maximum frequency of 300 Hz. For even greater simplicity, the dashed line indicated on the figure could be used at low frequencies, but this may be overly conservative because low-frequency response may be of dominant importance for the fuel assembly system. The data from [2] have been analyzed in a more detailed manner for this test as described in Section 5.

---

<sup>3</sup> Sandia National Laboratories conducted many tests in the late 1980s – early 1990s to establish the loading on transport packages during normal transport (summarized in a later section). This test campaign measured loading on the external surface of the transport package, not on the contents, which experience a somewhat different loading profile. The methodology for measuring the loads in the previous Sandia National Laboratories program has some analogies to the current test proposal, so pertinent aspects of the previous work can be applied to the current test proposal.

<sup>4</sup> The sensitivity of fuel rod failure due to fatigue was investigated in [1]. Analyses indicate that the magnitudes of the cyclic loads are such that the stresses induced in the cladding are below the endurance limit of the Zircaloy cladding. Even an infinite number of cyclic loads apparently would not propagate existing cracks into fuel rod failures. But, the fatigue strength of high burnup cladding – currently unknown – may require reanalysis of the fatigue issue.

The bounding rail shock spectrum is based on the union of measured triaxial data for a 45-tonne cargo reported by Magnuson [4-5]. The measured data include responses to typical shock generating events, e.g., crossing of bridges and switches, and coupling event shocks.

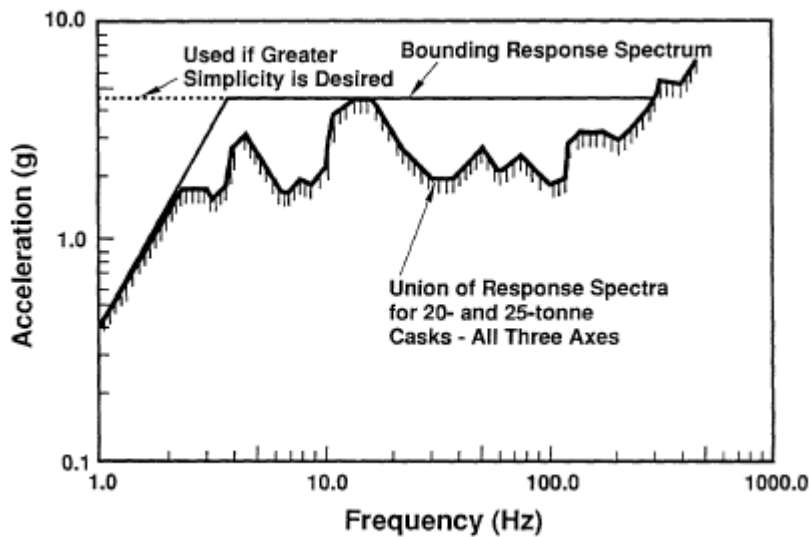


**Figure 2. Bounding acceleration shock response spectrum for a truck cask at 3% damping [1].**

The bounding truck vibration data for all three response directions are shown in Figure 3.

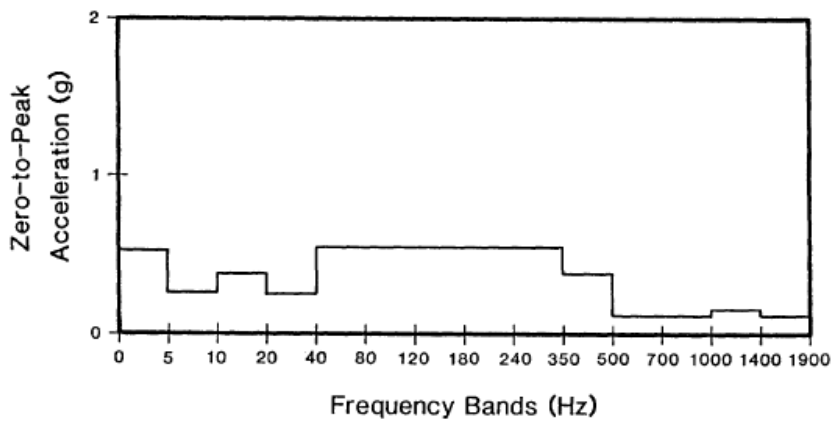


**Figure 3. Bounding truck vibration data for all three axes [1].**

The analyses in [1] showed that an unirradiated assembly will remain elastic under normal transportation shock and vibration loading conditions. The maximum tensile stress is 155 MPa and occurs at the bottom of the rod adjacent to the end plate. The corresponding maximum spacer grid pinch force is 80.1 N.

### 3 NORMAL CONDITIONS OF TRANSPORT TEST PLAN

#### 3.1 Introduction

The test is designed to capture the response of used nuclear fuel in its representative configuration to actual loadings imposed during normal conditions of transport. The normal conditions of transport are those defined within the US NRC regulations in 10 Code of Federal Regulations Part 71 [6].

Fuel rods are required to meet conditions defined in 10 CFR Part 71, Subpart F, ¶71.71 during normal transport. In particular, the rods must withstand vibrations and shocks associated with normal transport (while in a transport cask which is tied down to the transport conveyance). NRC guidance is also found in §2.5.6.5 *Vibration* in the “Standard Review Plan for Transportation Packages for Radioactive Material” (US Nuclear Regulatory Commission NUREG-1609 which cites NUREG/CR-2146 and NUREG/CR-0128). [2, 7-8]

To date, licensees have made the technical argument that unirradiated fuel rods and rods irradiated to relatively low burnup levels can withstand the loads imposed upon them by normal transport.

However, fuel is being irradiated to higher burnup levels – which further degrades the cladding – and shall be stored (aged) for longer periods of time. Both of these conditions – high burnup levels and aging during storage – may lead to a situation where the cladding is degraded to such an extent that it may not withstand normal transport loads. There are no data to justify the technical basis for asserting that aged, high burnup fuel can withstand normal transport conditions. The NRC has expressed concerns about approving transport of aged, high burnup fuel without such information.

The data needed to fill this technical gap falls in two categories: 1) the loads imposed directly on rods during normal transport; and 2) the material properties of aged, high burnup cladding. (See Figure 1.)

The goals of this test program are to expand understanding of used nuclear fuel loading environments and subsequent response to these environments. Given a quantitative understanding of fuel rod response, material properties of high burnup, degraded fuel can be coupled with realistic loadings to analytically estimate degraded fuel response to these transport conditions.

The objectives of this test program are to

- Simulate over-the-road tests on a full-scale fuel assembly by applying loadings that used nuclear fuel cladding would experience during normal conditions of transport.
- Instrument the cladding to capture mechanical load, strain, vibration, and shock inputs imposed by the mechanical loadings resulting from the normal condition of transport loading.

##### 3.1.1 Basis of test

The ideal test would be to place an *irradiated* fuel assembly in an actual cask and do over-the-road/rail tests to measure the vibrational loads on the rods. But, doing such a test with an irradiated assembly would be extremely difficult and expensive.

So, an alternative solution is to use an *unirradiated* assembly with surrogate rods (no UO<sub>2</sub> pellets) in an actual cask. However, the only casks available are truck casks and all of those are contaminated on the inside - the

casks have all been in pools - a major detriment for performing the tests due to Environmental, Safety, & Health considerations. In addition, the lease price for such a truck cask is significant.

The practical alternative is to place a representative, surrogate fuel assembly on a shaker and subject the assembly to vibrations and shocks simulating normal transport via a truck (or rail) cask. That is the basis of this test plan.

### 3.1.2 General description of test

This test proposal is designed to capture the response of cladding in its representative configuration (i.e., in-an-assembly-within-a-basket-within-a-cask-tied-to-a-transport-conveyance) to actual loadings imposed during normal conditions of transport. Finite-element modeling after the normal transport tests, coupled with degraded material property data from other UFD experimental work, will allow an estimate of the response irradiated rods would have experienced during the road tests based upon the test data from the surrogate rods.

The assembly planned for the test will represent a 17x17 PWR assembly.

The rods to be used for the tests will not be actual irradiated zirconium-alloy/UO<sub>2</sub>-pellet rods. Surrogate rods shall be selected that have similar mass and stiffness as the actual irradiated rods. Copper B280 alloy tubes filled with lead rods approximately meet the criteria for simulating Zircaloy-4/UO<sub>2</sub>-pellet rods. They shall be used for most of the positions with the assembly; Zircaloy-4/Pb rods shall be used for those assembly positions which will be instrumented for the test.

Finite-element modeling before the test shall provide information on which rod locations within the assembly should be instrumented and on which locations on those rods the instrumentation for measuring strains and accelerations should be placed. Finite-element modeling after the normal transport tests are conducted will allow an estimate of the response all the rods would have experienced during the road tests based upon the test data from the surrogate rods. The test data will also allow the finite element model to be benchmarked.

The test results will allow for an analytic assessment of the ability of aged, high burnup cladding to withstand normal transport loads by comparing the strength of the aged, high burnup cladding to the stresses imposed on the cladding during normal transport.

This test proposal provides data for the mechanical loads to which fuel rods are subjected during normal transport conditions. The integrity of the cladding is a function of its 1) material properties – yield and tensile strength, elastic modulus, fatigue strength, fracture toughness – all of which may degrade with high burnup and long aging times - and 2) the mechanical loads to which the cladding may be subjected. This test proposal addresses only the latter – the mechanical loads applied to the cladding during normal transport conditions.

## 3.2 Purpose of Test Plan

This document defines the testing of a 17x17 pressurized water reactor (PWR) assembly (Figure 4) containing surrogate fuel rods placed upon a shaker to simulate vibrational and shock loading associated with a normal

transport of an assembly within a truck (or rail) cask on a trailer. This test series will be performed by implementing plans and procedures identified in this document.

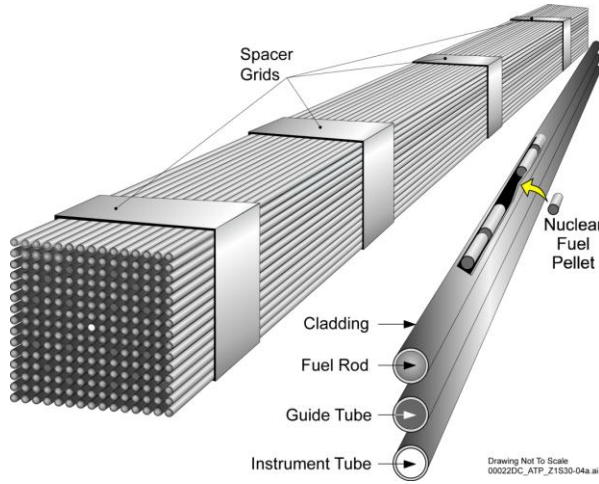


**Figure 4. Fuel assembly.**

### 3.3 Test Description

#### 3.3.1 Acquisition of an unirradiated fuel assembly

The most important requirement for the tests is to have available an actual fuel assembly. The assembly could be either PWR or boiling water reactor (BWR).

Both PWR and BWR fuel components have recently been procured by Sandia National Laboratories for an unrelated test program. It is proposed that a PWR assembly be used for the tests described in this plan. PWR fuel is more common than BWR fuel.

Ideally, irradiated, high burnup, aged fuel rods would be used for the tests. Actual fuel, let alone irradiated cladding and fuel, is not an option for the tests, so a surrogate material for the fuel pellets is required.<sup>5</sup> The vibration tests will be conducted with new hollow clad pins (Zircaloy-4 and copper tubing). For the over-the-road test simulation, these pins will be filled with a lead surrogate to represent the mass of the fuel.

The ideal surrogate rod for testing would have the same mass and flexibility as an irradiated rod. Unirradiated fuel has a gap between the fuel pellets and the cladding; irradiated fuel swells closing that gap. Thus, unirradiated fuel rods are not an exact surrogate for irradiated rods. A solid rod of some metal may be appropriate, but a survey indicated that the cost is prohibitive in the lengths necessary to match that of the PWR rods (e.g., thirteen-foot molybdenum rods). It is necessary to attempt to match the properties of surrogate rods with those of irradiated rods, although differences in the rod response can be accounted for by numerical analysis post-test. Using estimated properties of irradiated rods allowed selection of a surrogate rod of appropriate stiffness and mass.

<sup>5</sup> The cost is significant – approximately \$100k for a 17X17-PWR assembly with Zircaloy rods (sans fuel).

### 3.3.2 Instrumentation

#### 3.3.2.1 Placement of the instruments on the test unit

Strain gages must be placed on the assembly and cladding to obtain the maximum peak loads to which those components are subjected during normal transport.<sup>6</sup> Triaxial accelerometers will be placed at strategic locations on the assembly and rods. A total of thirty-two to forty-eight channels of data (strain gages plus accelerometers) are reasonable based on experience from previous test programs (the number of gages is to be determined based upon finite element analyses).

Modeling of an assembly will be employed to identify the optimum locations for the instrumentation. But, it is intuitive that placing strain gages on the cladding at the mid-point between spacer grid supports and adjacent to the grids would provide a representative profile of the loading on the rods. The strain gages should be placed on rods at both the top and the bottom of the assembly. Gauges will be placed in such locations along one-half of the length of the assembly.

#### 3.3.2.2 Data reduction and analysis

The protocol for processing the data shall be established using the example of previous test programs at Sandia National Laboratories. The results shall be collated in such a manner as to facilitate future modeling that could estimate loading on other assembly configurations not directly subjected to the transport tests.

The results shall be assessed relative to known or estimated properties of cladding to judge the effect of the normal transport conditions on the integrity of the cladding. Cladding properties of interest, likely available for unirradiated or low burnup conditions, are the yield strength and elastic modulus. The fracture toughness and fatigue strength of cladding, although relevant, are not available.

A LS-DYNA structural model of a detailed 17x17 assembly will be refined and modified at Pacific Northwest National Laboratory (PNNL) to include specific details for the test assembly and basket that will be utilized to impose the loading time history during the actual shaker testing.

Scoping pre-test evaluations will be performed to identify appropriate data collection sites within and about the test assembly. This information will help finalize the test design and provide baseline analyses for future benchmarking and validation of modeling techniques involving LS-DYNA.

A script will be written that converts LS-DYNA fuel assembly specific geometric data and shall port it to Sandia's PRESTO Structural Dynamics code. This tool will help provide baseline analyses for future benchmarking and validation of modeling techniques involving PRESTO as well as cross-comparison between LS-DYNA and PRESTO.

---

<sup>6</sup> Piezo-electric strain gauges are recommended. Piezo-electric sensors are able to achieve a better resolution than piezo-resistors, while piezo-resistors can be built in much smaller areas. Both types of the strain sensors are capable of high sensitivity measurements, however, and could be used for the tests.

### 3.3.2.3 Rail Tests

The simulated rail cask tests may be performed at Sandia National Laboratories using vibration and shock inputs from [5].<sup>7</sup>

### 3.3.3 The 0.3-meter drop test

It is proposed that the 0.3-meter drop test be conducted in a subsequent phase of the test program. The same assembly could be used for the drop tests after the vibrational tests, but not vice versa due to possible damage to the assembly resulting from the drop. It is also proposed that only one cask type, truck or rail, be used for the 0.3-meter drop test.

The 0.3-meter drop represents an accident that may occur while transferring the loaded cask *in its transport configuration* from one position to another, such as, the transfer of the cask from a trailer to a pad. This drop test must be performed (or analyzed) with the package in an orientation that would cause maximum damage.<sup>8,9</sup>

The US regulations are silent regarding the presence of impact limiters on the cask for the 0.3-meter drop. The definition of a transport package in 10 CFR 71.4 is “...the *packaging* together with its radioactive contents as presented for transport” and “*Packaging* means the assembly of components necessary to ensure compliance with the packaging requirements of this part [and]...may consist of...devices for...absorbing mechanical shocks.” Furthermore, 10 CFR 71.71(a) Normal Conditions of Transport states that this section is an “[e]valuation of [the] package design.” Thus, this test proposal interprets the regulations to allow for the use of “absorbing mechanical shocks” on the cask for the 0.3-meter drop test.

Regardless of whether impact limiters are used for the 0.3-meter drop test, the larger issue is procuring a cask for the test. Owners of existing casks would be reluctant to allow the cask to be dropped, with or without impact limiters. An option is to construct a surrogate cask – a cylinder – into which the fuel assembly can be placed for the drop test.

---

<sup>7</sup> Access to the rail car and transport system (although not a rail cask) may be possible through the US Federal Railroad Administration which has test tracks and has expressed a willingness to participate in such tests. Per the FRA website:

“There are 48 miles of railroad track available for testing locomotives, vehicles, track components, and signaling devices at the Transportation Technology Center’s (TTC) Facility for Accelerated Service Testing (FAST), Pueblo, Colorado. Specialized tracks are used to evaluate vehicle stability, safety, endurance, reliability, and ride comfort. The TTC’s tracks eliminate the interferences, delays, and safety issues encountered on an operating rail system (<http://www.aar.com/tracks.php>).”

<sup>8</sup> Numerical methods are more easily applied to the analysis of the effects on transport packages and their contents due to a 0.3-meter drop than they are for analysis of the vibrational loading inherent to normal transport conditions and they may be an option to an actual drop test.

<sup>9</sup> A detailed discussion of the US NRC intent regarding the analysis necessary for the drop test may be gleaned from NUREG-1536, Revision 1A, “Standard Review Plan for Used nuclear fuel Dry Storage Systems at a General License Facility.” But, note that this document addresses used nuclear fuel casks used for dry storage, not transport.

## 4 SCOPE

This test procedure

- Defines instrumentation requirements
- Defines pre-test and post-test inspection and construction tasks
- Describes steps required to perform the shaker tests
- Identifies applicable supporting and controlling documents
- Defines information, documentation, and data required to document the tests

This procedure, in conjunction with the Sandia National Laboratories (SNL) Job Safety Analysis, Work Control – Level of Rigor, National Environmental Policy Act (NEPA) Review Information, Accept Work, and the Quality Assurance (QA) Program Plan documents, are the planning package for the test program.

Any changes to this procedure will be documented in accordance with the instructions in the SNL Quality Assurance Program Plan.

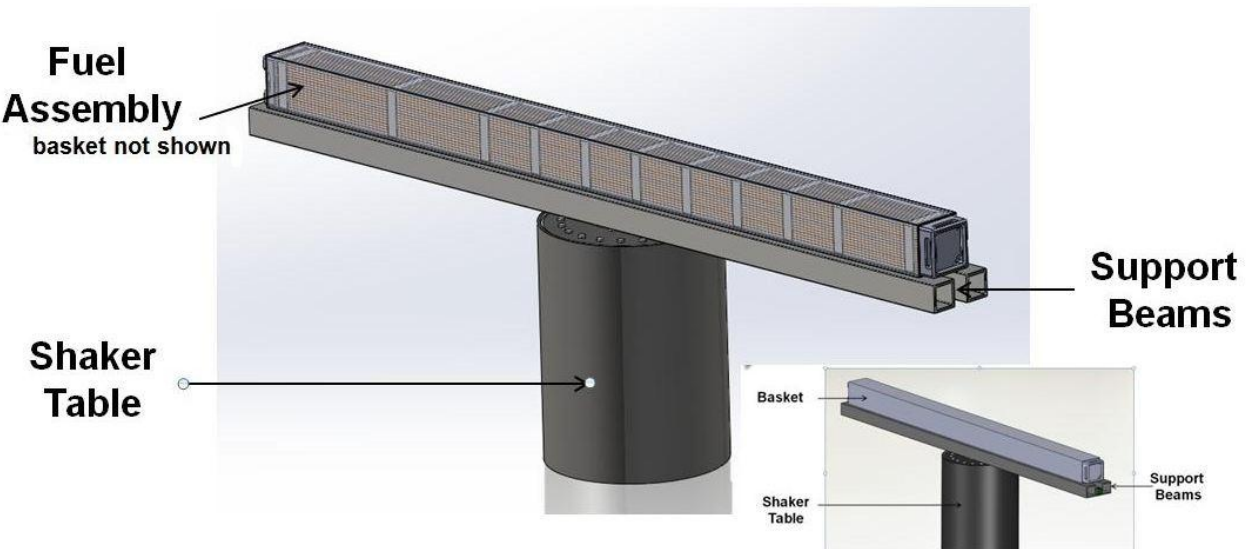
All supplementary information and test data (calibrations, inspections, change reports, etc.) for this test will be logged and attached to the test results report.

### 4.1 Test Parameters

The instrumented fuel assembly within its surrogate basket shall be securely affixed upon the shaker. Using the inputs from the analyses of the vibration and shock data from Section 5 the shaker shall impart loads to the assembly and the shaker data acquisition system shall record the responses from the accelerometers on the strain gages attached to the selected fuel rods.

The vibration facility in Excitation Equipment Building 6610 Area III at Sandia National Laboratories supports a wide spectrum of activities for the US Department of Energy Nuclear Weapons Complex. These capabilities provide the versatile and controllable simulation of vibration, acceleration, and shock environments, as well as tailored excitations for the development and validation of analytical models. The facility is used extensively for system level tests of full-scale assemblies or items requiring high vibration levels.

The following Figures 5 – 8 describe the test in more detail.



**Note:** Shaker table not long enough to support entire assembly. Beams used to simulate rigidity of an assembly-within-a-basket-within-a-cask-affixed-to-a-trailer under normal transport conditions.

Figure 5. Placement of assembly with rods, basket, and support beams on shaker.

Experimental Problem	Solution
Actual truck casks too costly (NAC-LWT)	Perform test without a cask
Available truck casks are contaminated	Simulate truck transport with shaker table*
Using UO <sub>2</sub> pellets not feasible	Use Pb rods as surrogate
Availability of Zircaloy tubes limited	Use Cu tubes as surrogate
Surrogates possess material properties dissimilar to Zircaloy	Adjust wall thickness of Cu tubes so that $EI_{Cu} = EI_{Zirc}$ Adjust amount of Pb in tubes to that total assembly weight is that of actual assembly
Assembly is in a basket in a truck cask	Construct basket to NAC-LWT specifications. Place assembly on "stiffeners" to ensure unrealistic bending does not occur about assembly midpoint

\*U.S. Nuclear Regulatory Commission, "Shock and Vibration Environments for a Large Shipping Container During Truck Transport (Part II)," NUREG/CR-0128 (SAND Report 78-0337), August 1978.  
(Referenced in Section 2.5.6.5 Vibration in NUREG-1609, "Standard Review Plan for Transportation Packages for Radioactive Material")

Figure 6. Differences between an actual test in a truck cask and the shaker test.

Zirc and Surrogate Material Properties (Based on equivalent thickness and variable EI)									
Zirc		Aluminum		Brass		Carbon Steel		Copper	
$E_{\text{Zirc}}$ (GPa)	99	$E_{\text{Al}}$ (GPa)	70	$E_{\text{Brass}}$ (GPa)	110	$E_{\text{SS}}$ (GPa)	205	$E_{\text{Cu}}$ (GPa)	115
$E_{\text{Zirc}}$ (ksi)	14359	$E_{\text{Al}}$ (ksi)	10153	$E_{\text{Brass}}$ (ksi)	15954	$E_{\text{SS}}$ (ksi)	29733	$E_{\text{Cu}}$ (ksi)	16679
$\rho_{\text{Zirc}}$ (g/cm <sup>3</sup> )	6.55	$\rho_{\text{Al}}$ (g/cm <sup>3</sup> )	2.7	$\rho_{\text{Brass}}$ (g/cm <sup>3</sup> )	8.5	$\rho_{\text{SS}}$ (g/cm <sup>3</sup> )	7.85	$\rho_{\text{Cu}}$ (g/cm <sup>3</sup> )	8.94
$\rho_{\text{Zirc}}$ (g/in <sup>3</sup> )	107	$\rho_{\text{Al}}$ (g/in <sup>3</sup> )	44	$\rho_{\text{Brass}}$ (g/in <sup>3</sup> )	139	$\rho_{\text{SS}}$ (g/in <sup>3</sup> )	129	$\rho_{\text{Cu}}$ (g/in <sup>3</sup> )	147
$h$ (in)	151.79	$h$ (in)	144	$h$ (in)	151.79	$h$ (in)	151.79	$h$ (in)	151.79
$\text{Vol}_{\text{Zirc}}$ (in <sup>3</sup> )	3.77	$\text{Vol}_{\text{Al}}$ (in <sup>3</sup> )	5.38	$\text{Vol}_{\text{Brass}}$ (in <sup>3</sup> )	5.67	$\text{Vol}_{\text{SS}}$ (in <sup>3</sup> )	5.67	$\text{Vol}_{\text{Cu}}$ (in <sup>3</sup> )	5.67
Mass (g)	404.80	Mass (g)	238.19	Mass (g)	790.42	Mass (g)	729.98	Mass (g)	831.34
$t$ (in)	0.0225	$t$ (in)	0.03500	$t$ (in)	0.03500	$t$ (in)	0.03500	$t$ (in)	0.03500
$D_{\text{Zirc}}$ (in)	0.374	$D_{\text{Al}}$ (in)	0.375	$D_{\text{Brass}}$ (in)	0.375	$D_{\text{SS}}$ (in)	0.375	$D_{\text{Cu}}$ (in)	0.375
$d_{\text{Zirc}}$ (in)	0.329	$d_{\text{Al}}$ (in)	0.305	$d_{\text{Brass}}$ (in)	0.305	$d_{\text{SS}}$ (in)	0.305	$d_{\text{Cu}}$ (in)	0.305
$EI$ (k <sup>4</sup> in <sup>2</sup> )	5.532	$EI$ (k <sup>4</sup> in <sup>2</sup> )	5.543	$EI$ (k <sup>4</sup> in <sup>2</sup> )	8.710	$EI$ (k <sup>4</sup> in <sup>2</sup> )	16.232	$EI$ (k <sup>4</sup> in <sup>2</sup> )	9.106
Zirc Rod (lbs)	0.891	Al Rod (lbs)	0.525	Brass Rod (lbs)	1.739	CS Rod (lbs)	1.606	Cu Rod (lbs)	1.829

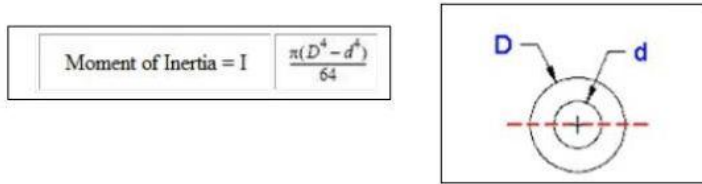


Figure 7. Technical data used to select copper tubes as surrogate rods.

The most important parameter for the test assembly is that its mass be close to the mass of a real assembly. Stiffness of the rods is a secondary but important parameter. This is a non-sequiturA SOLIDWORKSTM simulation predicts a bending response difference of less than 5% between the Cu-Pb rod and Zircaloy-Pb rods.

The combined Modulus / Moment of Inertia properties were checked in order to get an idea on the combined stiffness of each rod:

- $EI_{\text{Cu}} = 9.106 \text{ K-in}^2$
- $EI_{\text{Zirc}} = 5.53 \text{ K-in}^2$

The conclusion is that Cu tubing is slightly stiffer than Zircaloy.

Although the material surrogates do not mimic the true material properties exactly, they are the best as far as availability, constructability, and cost. UO<sub>2</sub> and lead share very similar densities but UO<sub>2</sub> is considerably stiffer than Pb. Zircaloy is 30% less dense than copper but Zircaloy shares a similar stiffness with Cu. An actual assembly weighs approximately 1404 lbs. The experimental assembly weighs approximately 1446 lbs. The difference in weight between the actual and experimental assemblies is 42 lbs (3% difference). Although the stiffness of the actual and experimental rods are not the same (mostly due to properties of the UO<sub>2</sub> v. Pb), the weights are nearly exact and weight is considered the most important parameter to simulate. Thus, dynamic response of the surrogate test assembly is expected to represent that of a real fuel assembly.

Figure 8 shows the locations of the Zircaloy rods within the assembly (locations are tentative pending finite element analyses).

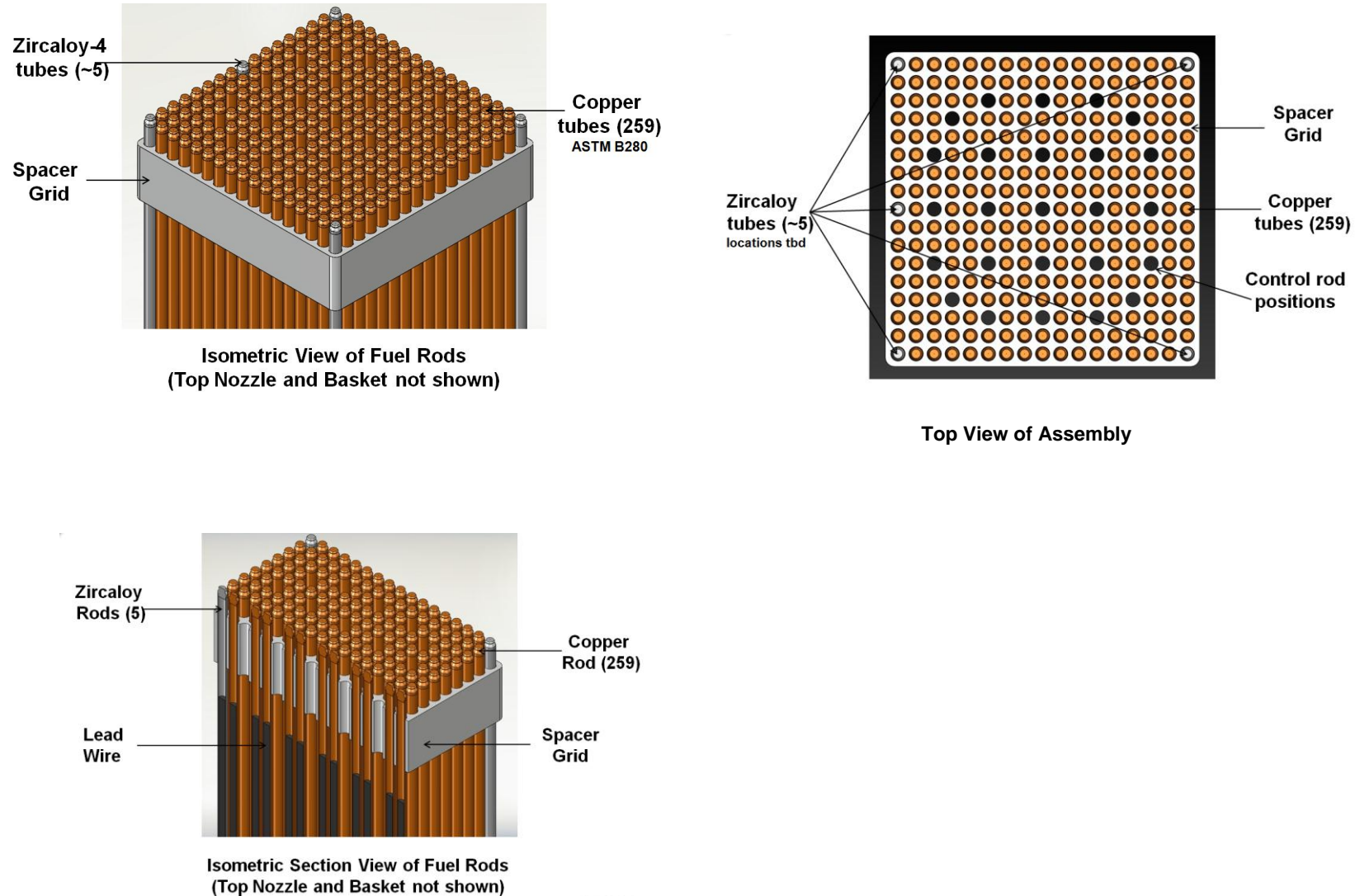


Figure 8. Location of Zircaloy rods within the assembly which will be instrumented.



Input for the shaker table was taken from US Nuclear Regulatory Commission, “Shock and Vibration Environments for a Large Shipping Container During Truck Transport (Part II),” NUREG/CR-0128, August 1978 [2] (referenced in *Section 2.5.6.5 Vibration* in NUREG-1609, “Standard Review Plan for Transportation Packages for Radioactive Material”). Key details from this report are

- Vibration and shock data were measured by accelerometers over a 700 mile journey
- 56,000 lb load for test 1 and 44000 lb for test 2
- Speeds ranged from 0 to 55 mph

Figure 9 shows data from this report.

Using the most conservative data from the 1978 report, the shaker table will simulate the vibration and shock experienced by the cask during transport.

Accelerometers will be placed along the length of the Zircaloy rods in order to measure shock and vertical vibration. Strain gauges will be placed along the length of the rods in order to measure strain. The stress state of the fuel rods will be calculated based on the strain gauge readings.

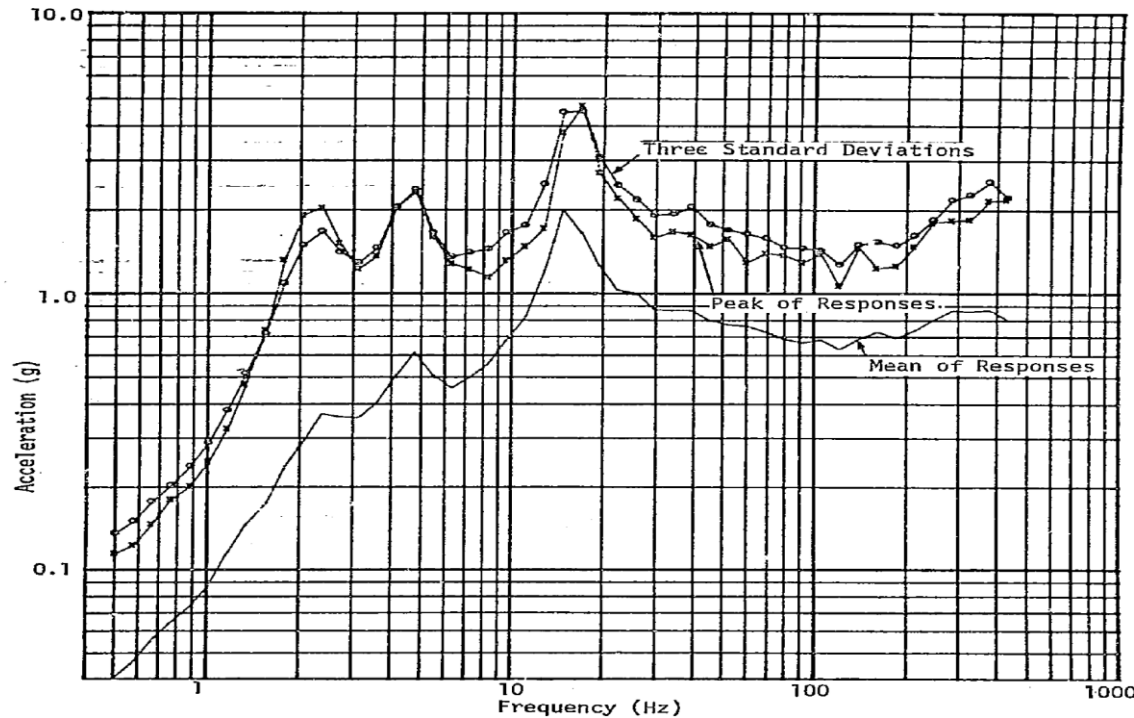


Figure 5. Superimposed Shock Response Spectra,  
3% Damping, Vertical Axis

20

Figure 9. Shock data from the 1978 truck cask transportation report [2].

The following Figure 10 shows data derived from the vibration and shock measured on the truck cask and are the inputs to the shaker as described in Section 5.

Figure 3.0-1: Recommended Random Vibration Test Specification

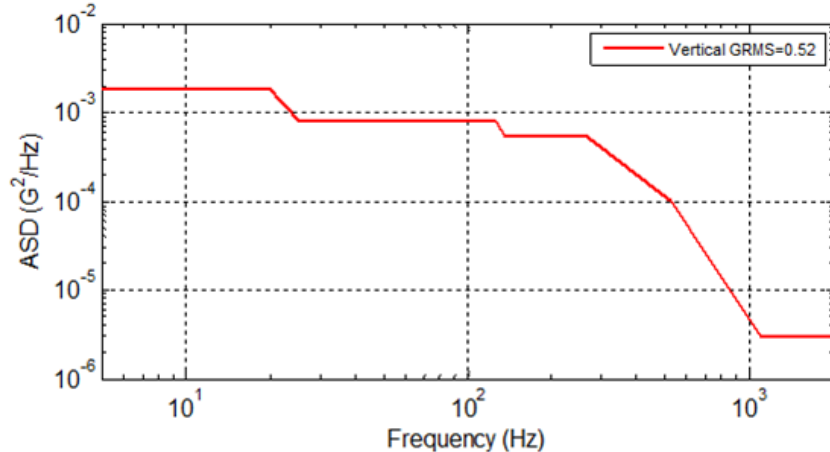


Table 3.0-1: Vibration Breakpoints

Frequency (HZ)	ASD (G^2/Hz)
5	1.8e-3
20	1.8e-3
25	8.0e-4
125	8.0e-4
135	5.5e-4
265	5.5e-4
530	1.0e-4
1100	3.0e-6
2000	3.0e-6

Figure 4.0-1: Recommended Shock Test Specification

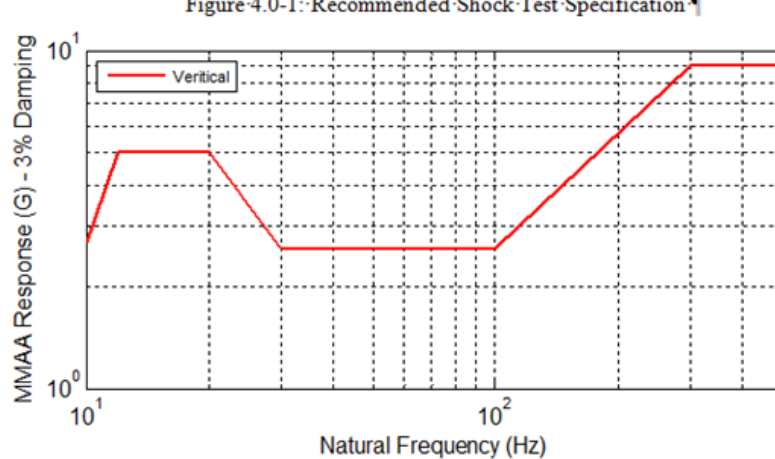


Table 4.0-1: Reference Shock Breakpoints

Frequency (HZ)	MMAA 3% (G)
10	2.7
12	5.0
20	5.0
30	2.6
100	2.6
300	9.0
600	9.0

Figure 10. Data derived from the truck cask transportation report to be used as input to the shaker.

The following Figures 11 and 12 show the vibration facility and the capabilities of the facility.

#### 4.1.1 Vibration facility



**Figure 11.** Vibration facility.

##### 4.1.1.1 Vibration facility capabilities

A vertical UD T4000 electrodynamic shaker shall be used for the testing. The system includes

- Control and data acquisition state-of-the-art digital vibration controller
  - 38 input channels available for control, limiting, or real-time monitoring
  - average, maximum, or minimum spectrum control options
- Computer controlled signal conditioning system
  - over 200 channels
  - conditions various types of sensors (e.g., strain gage, force, displacement)
- Data acquisition and analysis system
  - 208 channels
  - 102.4 kilo-samples/s, 24bit resolution
  - data streaming to disk array for long duration recording

Shakers at Sandia used for system level tests of full-scale assemblies or items requiring high vibration levels.

Shown is the Unholtz-Dickie Corporation T4000 electrodynamic shaker for vertical testing

[<http://www.udco.com/largetseries.shtml>](http://www.udco.com/largetseries.shtml)



Figure 12. Shaker to be used for test.

The following photograph shows a lead rod inserted in to a copper tube which shall be used as a surrogate Zircaloy/UO<sub>2</sub> rod.



Initial Dimensions for Simulated Copper Fuel Rod Mock-up

OD (in.)	0.3750
ID (in.)	0.3120
Thickness (in.)	0.0315
Sample Length (in.)	24.0000
Clearance Between Cu & Pb	0.0300

**Figure 13. Copper tube containing a lead rod to be used as a surrogate Zircaloy/UO<sub>2</sub> rod.**

The following figure shows the dimensions of the simulated basket that will support the assembly on the shaker table (as a basket supports an assembly in a truck cask).

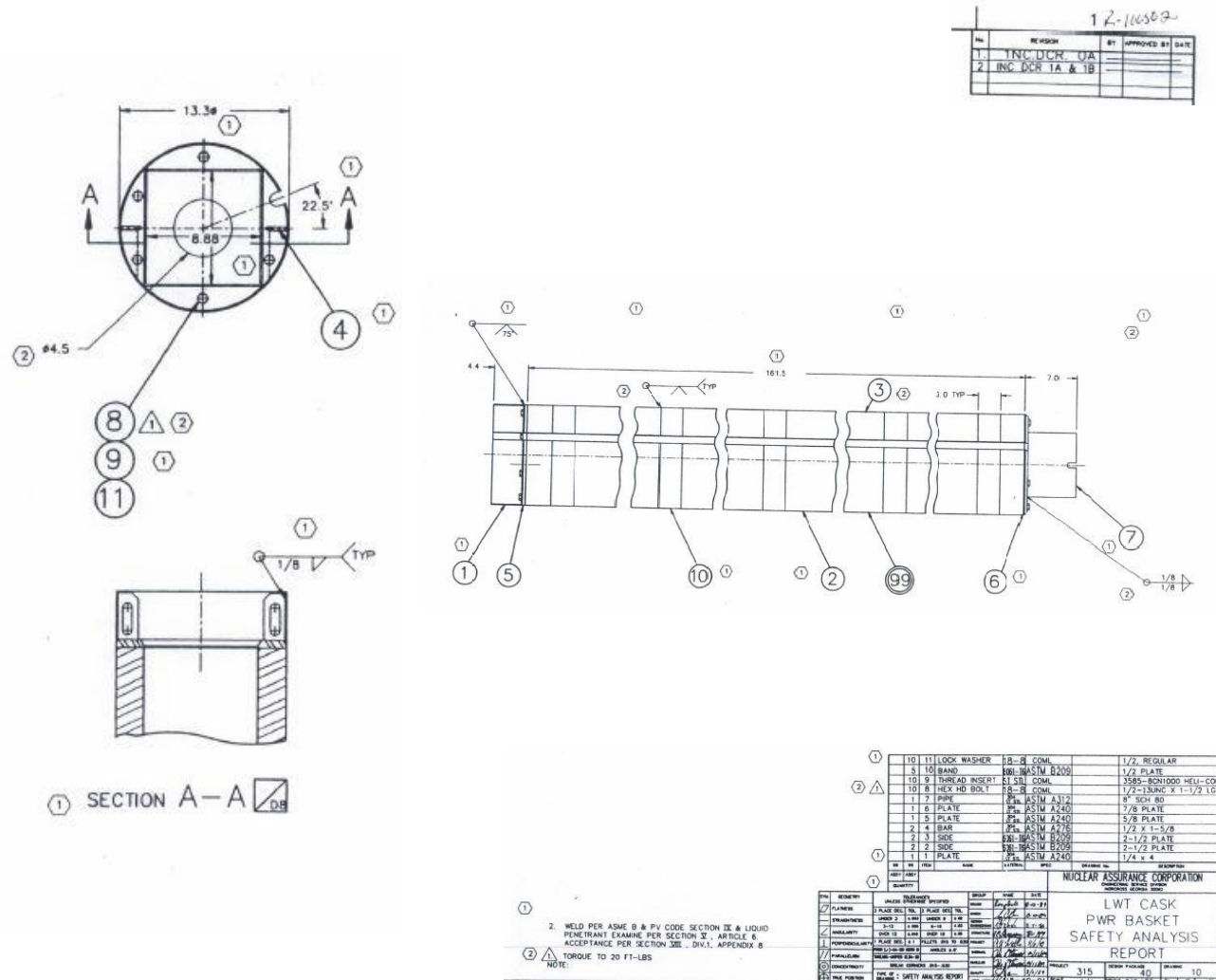


**Figure 14. Dimensions of basket to be used to contain the assembly on the shaker (Safety Analysis Report for the NAC-LWT, Revision 27, June 1999, Docket No. 9925 T-88004).**

## 4.2 Instrumentation Installation Tables

Each rod to be instrumented shall have the gauges recorded per the following tables. The strain gages and accelerometers are identified in the figures following the table.

**Table 1. Instrumentation Installation Data.  
Accelerometers and Strain Gages**

Gage ID	Range	Serial Number	Input Resistance (ohms)	Output Resistance (ohms)	Insulation Resistance (ohms)	Field Wire No.	Interface Panel No.	Check OK	Rod Location
A1-1X	20K								
SG1-1X	20K								
A1-2X	20K								
SG1-2X	20K								
A1-3X	20K								
SG1-3X	20K								
A1-4X	20K								
SG1-4X	20K								

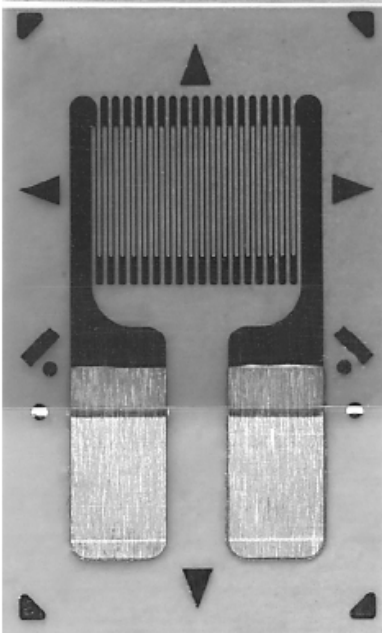
ROD #1 (SAME TABLE FOR EACH ROD TO BE INSTRUMENTED)

Accelerometer model #: Model 25 Isotron

Strain gage model #: Vishay Micro-Measurements CEA-03-062UW-350

Installed by \_\_\_\_\_

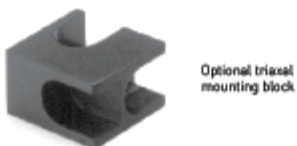
Witnessed by \_\_\_\_\_

GAGE PATTERN DATA					
 <div style="text-align: center;">           actual size       </div>			GAGE DESIGNATION	RESISTANCE (OHMS)	OPTIONS AVAILABLE
			See Note 1		See Note 2
			CEA-XX-062UW-120 CEA-XX-062UW-350	120 ± 0.3% 350 ± 0.3%	P2 P2
DESCRIPTION					
General-purpose gage. Exposed solder tab area is 0.07 x 0.04 in [1.8 x 1.0 mm].					
GAGE DIMENSIONS		Legend:	ES = Each Section S = Section (S1 = Sec 1)	CP = Complete Pattern M = Matrix	inch millimeter
Gage Length	Overall Length	Grid Width	Overall Width	Matrix Length	Matrix Width
0.062	0.220	0.120	0.120	0.31	0.19
1.57	5.59	3.05	3.05	7.9	4.8
GAGE SERIES DATA					
See Gage Series data sheet for complete specifications.					
Series	Description			Strain Range	Temperature Range
CEA	Universal general-purpose strain gages.			±3%	-100° to +350°F [-75° to +175°C]

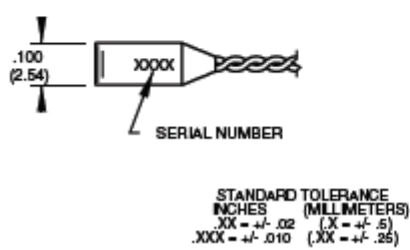
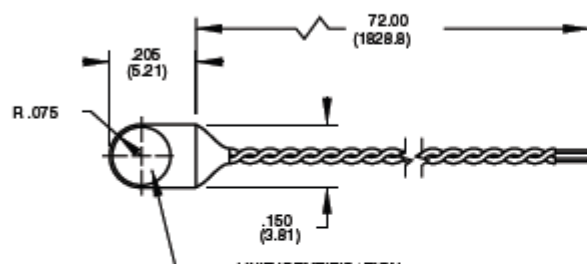
## Model 25A Isotron® accelerometer

### Features

- World's smallest Isotron®
- Light weight (0.2 gm)
- Flexible cable
- Low impedance output
- Excellent for printed circuit board and disk drive testing



Optional triaxial  
mounting block

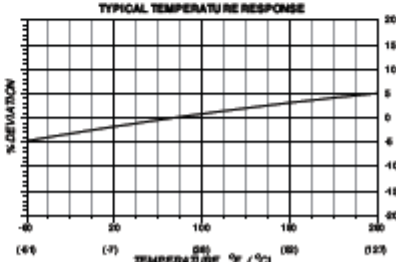
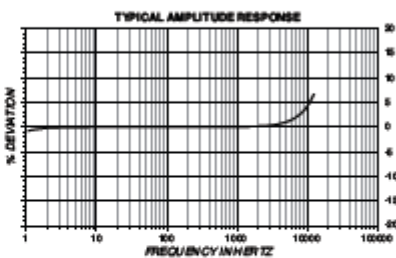


### Description

The Endevco® model 25A Isomin™ is an extremely small, adhesive mounted piezoelectric accelerometer with integral electronics, designed specifically for measuring vibration on very small objects. The unit weighs only 0.2 gm, reducing unwanted mass loading effects. The unit comes with two pre-installed fine gage (34 AWG) wires as output leads. These leads can be easily repaired in the field, or a new lead assembly may be reinstalled at the factory. A heavier gage (28 AWG) cable is also provided for extension purpose. The model 25A is ideal for measuring vibration in scaled models, small electronic components, and biomedical research. An optional triaxial mounting block (model 2950M16) is available for setting up three-axis measurement. If a detachable coaxial cable, which can be replaced by the user in the field, is desired, model 25B is available.

The model 25A features Endevco's Piezite® Type sensing element operating in shear mode. The internal electronics inside the accelerometer converts high impedance input into low impedance voltage output through the same cable that supplies the required 4 mA constant current power. Signal ground is isolated from the mounting surface of the unit by a hard anodized surface. A removal tool is included for proper removal in the field.

Endevco signal conditioner models 133, 4416B, 2793, 2776B, 4999, 6634C or Oaxis 2000 (4998A-X with cards 428 and/or 433) computer controlled system are recommended for use with this accelerometer.



## Model 25A Isotron® accelerometer



### Specifications

The following performance specifications conform to ISA-RP-37.2 (1964) and are typical values, referenced at +75°F (+24°C), 4 mA and 100 Hz, unless otherwise noted. Calibration data, traceable to National Institute of Standards and Technology (NIST), is supplied.

#### Dynamic characteristics

	Units	
Range	g	±740
Voltage sensitivity		
Typical	mV/g	5
Minimum	mV/g	4
Frequency response		See typical amplitude response
Resonance frequency		
Typical	kHz	50
Minimum	kHz	45
Amplitude response		
±5%	Hz	2 to 8000
±1 dB	Hz	1 to 12 000
Temperature response		See typical curve
Transverse sensitivity	%	≤ 5
Amplitude linearity	%	≤ 2 to full scale

#### Output characteristics

Output polarity		Acceleration directed into base of unit produces positive output
DC output bias voltage		+8.5 to +11.5
-67°F to +257°F (-55°C to +125°C)	%	±5 typical
Output impedance	Ω	≤ 600
Full scale output voltage	V	±3.7
Residual noise		≤ 0.007
Grounding		Signal ground isolated from mounting surface
Load		See load diagram

#### Power requirement

Supply current [1]	mA	+3.5 to +4.5
Voltage	Vdc	+18 to +24
Warm-up time	sec	≤ 3

#### Environmental characteristics

Temperature range		-67°F to +257°F (-55°C to +125°C)
Humidity		Epoxy sealed, non-hermetic
Sinusoidal vibration limit (survival)	g pk	1000
Shock limit (survival) [2]	g pk	2000
Base strain sensitivity		0.002
Electromagnetic sensitivity		0.09
Acoustic sensitivity at 140 dB SPL	equiv. g	0.008

#### Physical characteristics

Dimensions		See outline drawing
Weight without cable	oz (gm)	0.01 [0.2]
Case material		Aluminum alloy, hard anodized
Mounting [3]		Adhesive

#### Calibration

Supplied:		
Sensitivity	mV/g	
Transverse sensitivity	%	
Frequency response	%	20 Hz to 12 kHz

#### Included accessories

3024-120 [10 ft]	cable assembly, twisted pair [4]
31275	removal tool
32279	mounting wax

#### Optional accessories

2950M16	triaxial mounting block
133	Signal conditioner
2775B	Signal conditioner
2793	Isotron signal conditioner
4416B	Signal conditioner
4999	Signal conditioner
6634C	Signal conditioner
4990A-X	Oasis 2000 computer-controlled system with cards 428 and/or 433

#### Notes:

1. Excessive current supply may cause permanent damage to accelerometer.
2. Short duration shock pulses, such as those generated by metal-to-metal impacts, may excite transducer resonance and cause linearity errors. See Tech Paper 290 for more details.
3. Depending on the dynamic and environmental requirements, adhesives such as petro-wax, hot-melt glue, and cyanoacrylate epoxy (super glue) may be used to mount the accelerometer temporarily to the test structure. When removing an epoxy mounted accelerometer, first soften the epoxy with an appropriate solvent, then twist the unit off with the supplied removal tool. Failure to heed this caution may cause permanent damage to the transducer, which is not covered under warranty.
4. Small gage wires are soldered to the terminals at the factory. They are to be spliced together with the supplied cable assembly in the field for extension purpose.
5. Maintain high levels of precision and accuracy using Meggitt's factory calibration services. Call Meggitt's inside sales force at 800-982-6732 for recommended intervals, pricing and turnaround time for these services as well as for quotations on our standard products.

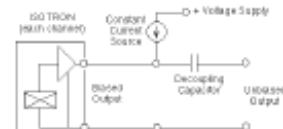


**Table 1. Instrumentation Installation Data. (Continued)**  
**Ambient Air Thermocouples**

TC ID	TC Type	Serial No.	Loop Resistance (ohms)	Sheath Resistance (ohms)	Location
TC-1 ID TC-1					

Installed by \_\_\_\_\_

Witnessed by \_\_\_\_\_

Multimeter:

Manufacturer/Model \_\_\_\_\_

Serial Number \_\_\_\_\_

Calibration Expiration Date \_\_\_\_\_

## 4.3 Vibration Test Procedure

### 4.3.1 Test preparation

Construct basket by welding four plates of steel per dimensions indicated in Figure 14. Provide cutouts of instrumentation wires.

Insert lead rods into the surrogate copper tubes and the Zircaloy tubes.

Insert all rods into the assembly.

Construct support beams from two square tubes by welding cross-bars along the length of the tubes.

Attach strain gages and accelerometers onto the rods selected for instrumentation.

Complete instrumentation installation forms.

### 4.3.2 Test set-up

Place support tubes onto shaker. Bolt to shaker.

Place basket/assembly onto support tubes. Bolt to support tubes.

Attach instrumentation from rods, assembly, and shaker surface to the vibration facility recording equipment. Calibrate instrumentation.

Apply vibration input to the shaker.

Apply shock input to the shaker.

Photograph shaker and test unit.

### 4.3.3 Post-test activities

Disassemble test unit.

Collect test data for post-test analyses.

## 5 TEST INPUT SPECIFICATIONS: RECOMMENDED VIBRATION AND SHOCK TRANSPORTATION TEST SPECIFICATIONS FOR THE REACTOR FUEL ASSEMBLY<sup>10</sup>

### 5.1 Introduction

The Environments Engineering Group at SNL was asked to derive a set of random vibration and shock test specifications for a laboratory test of a reactor fuel assembly. These specifications were derived from the vibration and shocks presented in references [2,8]. The purpose of the laboratory test is to measure loads during normal highway transportation. This memo presents test specifications for the vertical axis only since it is believed that is the direction which will affect the loading.

At this time the instrumentation has not been optimized and is subject to change. Section 5.2 presents the instrumentation.

Section 5.3 presents the random vibration specification. Section 4 presents the decayed sine specifications.

### 5.2 Instrumentation

The placement of instrumentation is designed to obtain the peak strain and has not been optimized. Therefore it is subject to change after further discussion with the model group. The accelerometers are used to get insight into what the structure is doing.

Table 2 presents the input accelerometers and their locations. Table 3 presents the response accelerometer and strain gage locations. The first few node shapes will determine where on the tube sections the strain gages are placed. Figure 15 shows the fuel reactor assembly on the shaker table and the input and response locations. Figure 16 shows a cross section of the fuel reactor assembly and the location of Tubes 1 thru 5.

---

<sup>10</sup> Letter report from Melissa C de Baca to Paul McConnell, April 30, 2012.

**Table 2: Response Accelerometers & Strain Gages.**

Location	Tube 1	Tube 2	Tube 3	Tube 4	Tube 5
End Spacer	A		A	A	
End Tube Section	A, S				
Mid Span Spacer	A		A	A	
Mid Span Tube Section	A, S				

Note: A – denotes accelerometer; S – denotes strain gage

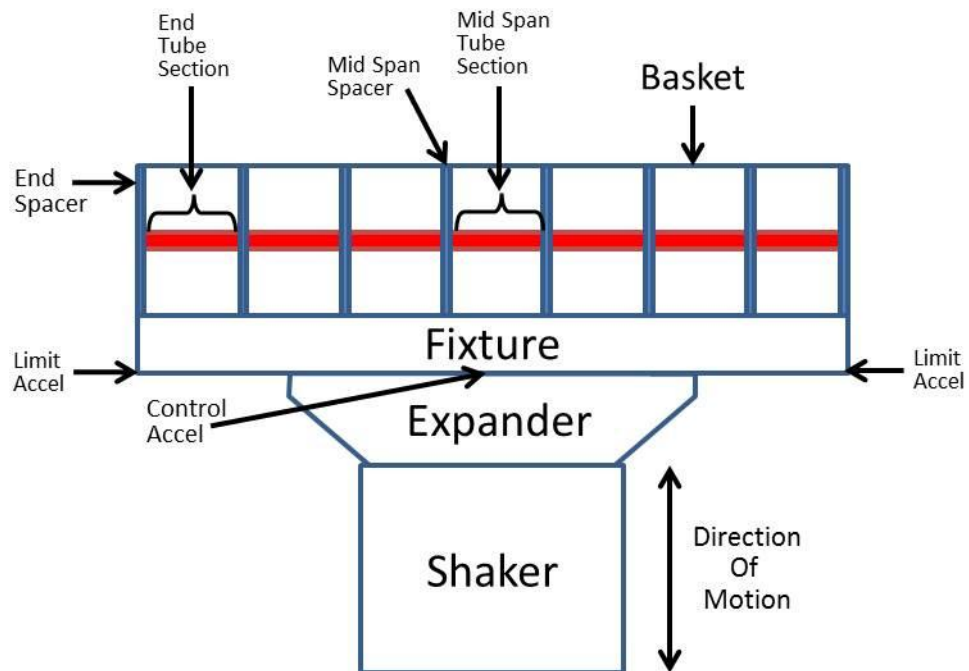


**Figure 15. Fuel reactor assembly on shaker table.**

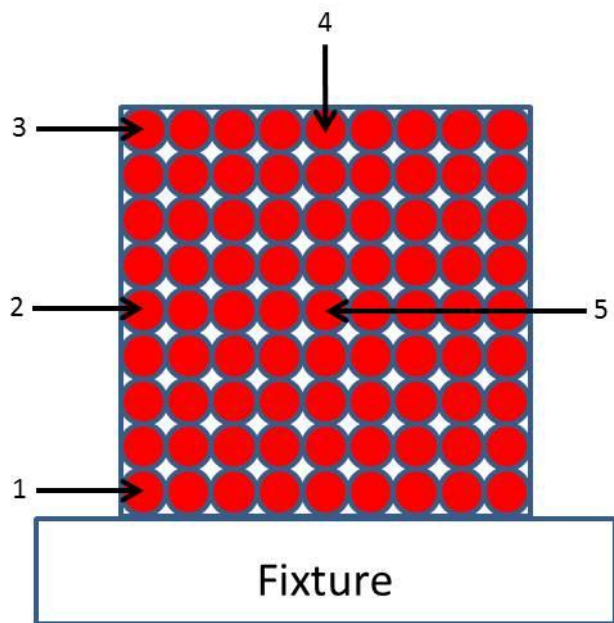
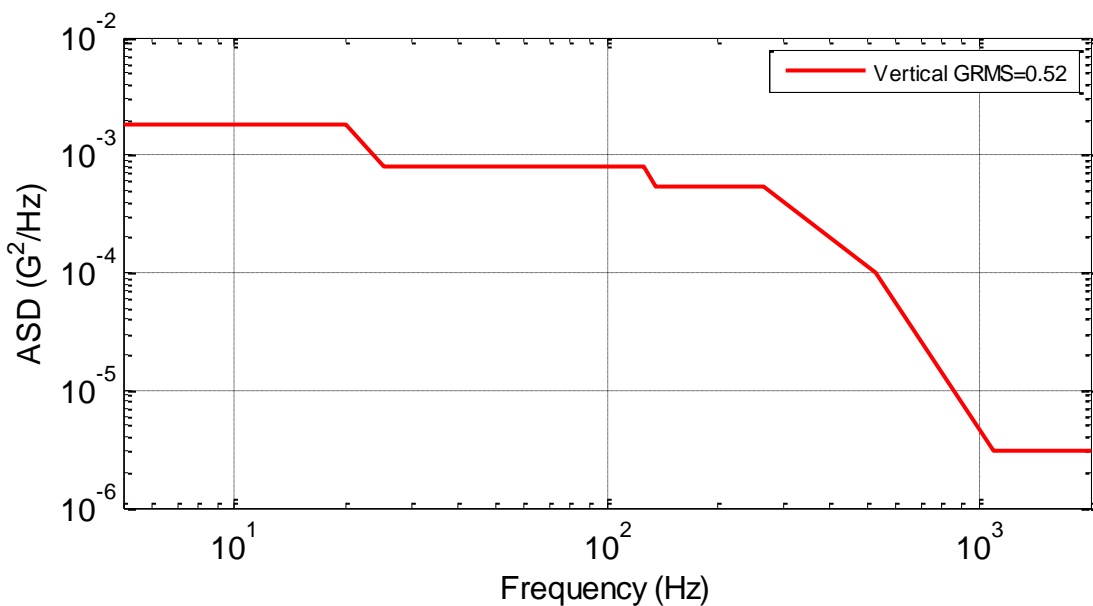


Figure 16. Cross-section of fuel reactor assembly.

### 5.3 Random Vibration Test Specifications

Figure 17 shows the recommended random vibration test specification to be applied at the midpoint of the fixture. Table 4 presents the corresponding breakpoints. The test should be run for a duration of one minute or long enough to obtain good data. Section 5.5 shows the derivation of this test specification.

We do not know what shape the limit channels should have; therefore they will be a scaled version of the control channel applied at the left and right ends of the fixture. The scaling will be determined at the time of the test.



**Figure 17. Recommended random vibration test specification.**

**Table 3: Vibration Breakpoints.**

Frequency (HZ)	ASD ( $\text{G}^2/\text{Hz}$ )
5	$1.8 \times 10^{-3}$
20	$1.8 \times 10^{-3}$
25	$8.0 \times 10^{-4}$
125	$8.0 \times 10^{-4}$
135	$5.5 \times 10^{-4}$
265	$5.5 \times 10^{-4}$
530	$1.0 \times 10^{-4}$
1100	$3.0 \times 10^{-6}$
2000	$3.0 \times 10^{-6}$

## 5.4 Shock – Decayed Sine Specifications and Time Histories

Figure 18 shows the recommended shock test specification. Table 5 lists the corresponding breakpoints. Appendix A shows the derivation of the test specification.

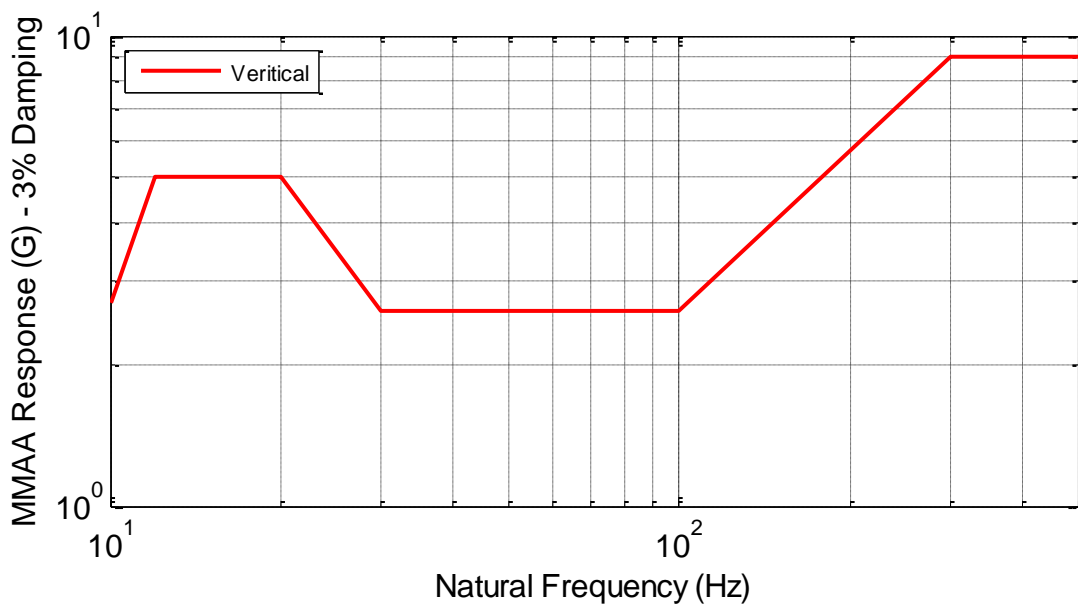


**Figure 18. Recommended shock test specification.**

**Table 4: Reference Shock Breakpoints.**

Frequency (HZ)	MMAA 3% (G)
10	2.7
12	5.0
20	5.0
30	2.6
100	2.6
300	9.0
600	9.0

Tables 6 thru 10 list the parameters for the five decayed sine realizations. Shown in these tables are the SRS parameters, the acceleration parameters, and the decayed sine parameters.

**Table 5: Initial Realization of Decayed Sine Parameters.**

SRS Parameters				
fmin	fmax	pts/oct	Damp	SRS Type
10.00	600.00	8.00	0.03	MMAA
Acceleration History Parameters				
Sample Rate	Frame Size	Gravity Constant	Ptype	
5120	8192	386.00	1	
Value	Acceleration (G)	Velocity (in/sec)	Displacement (in)	
Min	-2.28	-4.51	-0.0530	
Max	2.41	4.65	0.0592	
Res	-0.18	-0.06	0.0063	
Decayed Sine Parameters				
Frequency (Hz)	Accel (G)	Decay Rate	Delay	Frequency (Hz)
10.4	-0.359	0.0286	0.0000	82.6
11.4	0.487	0.0262	0.0000	90.1
12.4	-0.440	0.0241	0.0000	98.2
13.5	0.353	0.0221	0.0000	107.0
14.7	-0.300	0.0202	0.0000	116.7
16.1	0.265	0.0186	0.0000	127.2

17.5	-0.252	0.0170	0.0000	138.6	-0.149	0.0022	0.0000
19.1	0.237	0.0156	0.0000	151.1	0.144	0.0020	0.0000
20.8	-0.218	0.0143	0.0000	164.7	-0.165	0.0018	0.0000
22.7	0.201	0.0132	0.0000	179.5	0.183	0.0017	0.0000
24.7	-0.186	0.0121	0.0000	195.7	-0.193	0.0015	0.0000
26.9	0.120	0.0111	0.0000	213.3	0.219	0.0014	0.0000
29.4	-0.063	0.0102	0.0000	232.5	-0.221	0.0013	0.0000
32.0	0.082	0.0093	0.0000	253.4	0.271	0.0012	0.0000
34.9	-0.122	0.0086	0.0000	276.2	-0.270	0.0011	0.0000
38.0	0.087	0.0078	0.0000	301.1	0.324	0.0010	0.0000
41.5	-0.092	0.0072	0.0000	328.2	-0.294	0.0009	0.0000
45.2	0.114	0.0066	0.0000	357.7	0.283	0.0008	0.0000
49.3	-0.105	0.0061	0.0000	389.9	-0.295	0.0008	0.0000
53.7	0.101	0.0056	0.0000	425.0	0.225	0.0007	0.0000
58.5	-0.067	0.0051	0.0000	463.3	-0.350	0.0006	0.0000
63.8	0.083	0.0047	0.0000	505.0	0.243	0.0006	0.0000
69.5	-0.100	0.0043	0.0000	550.4	-0.259	0.0005	0.0000
75.8	0.093	0.0039	0.0000	600.0	0.393	0.0005	0.0000
				3.5	0.087	0.9500	-0.0457

**Table 6: Second Realization of Decayed Sine Parameters.**

SRS Parameters				
fmin	fmax	pts/oct	Damp	SRS Type
10.00	600.00	8.00	0.03	MMAA
Acceleration History Parameters				
Sample Rate	Frame Size	Gravity Constant	Ptype	
5120	8192	386.00	1	
Value	Acceleration (G)	Velocity (in/sec)	Displacement (in)	
Min	-2.40	-4.47	-0.0544	
Max	2.04	4.25	0.0530	
Res	0.01	-0.04	0.0057	
Decayed Sine Parameters				
Frequency (Hz)	Accel (G)	Decay Rate	Delay	Frequency (Hz)
10.4	-0.360	0.0286	0.0000	81.5
11.4	0.483	0.0263	0.0000	88.6
12.4	-0.496	0.0241	0.0000	96.9
13.4	0.354	0.0223	0.0000	106.8
14.8	-0.300	0.0202	0.0000	115.6
16.1	0.300	0.0185	0.0000	130.1
17.8	-0.210	0.0168	0.0000	138.2
19.4	0.242	0.0154	0.0000	148.8

21.0	-0.242	0.0142	0.0000	168.3	-0.135	0.0018	0.0000
22.6	0.210	0.0132	0.0000	184.1	0.184	0.0016	0.0000
25.1	-0.122	0.0119	0.0000	195.2	-0.206	0.0015	0.0000
27.0	0.147	0.0110	0.0000	209.2	0.207	0.0014	0.0000
29.2	-0.122	0.0102	0.0000	229.8	-0.295	0.0013	0.0000
32.8	0.074	0.0091	0.0000	252.4	0.223	0.0012	0.0000
35.6	-0.119	0.0084	0.0000	277.8	-0.277	0.0011	0.0000
38.2	0.104	0.0078	0.0000	297.6	0.423	0.0010	0.0000
41.8	-0.075	0.0071	0.0000	330.2	-0.244	0.0009	0.0000
45.4	0.061	0.0066	0.0000	362.0	0.243	0.0008	0.0000
48.6	-0.119	0.0061	0.0000	384.7	-0.315	0.0008	0.0000
53.2	0.081	0.0056	0.0000	417.0	0.244	0.0007	0.0000
58.5	-0.100	0.0051	0.0000	458.8	-0.280	0.0007	0.0000
63.0	0.108	0.0047	0.0000	500.7	0.254	0.0006	0.0000
70.9	-0.116	0.0042	0.0000	548.8	-0.320	0.0005	0.0000
74.7	0.096	0.0040	0.0000	574.7	0.358	0.0005	0.0000
				3.5	0.084	0.9500	-0.0457

**Table 7: Third Realization of Decayed Sine Parameters.**

SRS Parameters				
fmin	fmax	pts/oct	Damp	SRS Type
10.00	600.00	8.00	0.03	MMAA
Acceleration History Parameters				
Sample Rate		Frame Size	Gravity Constant	Ptype
5120		8192	386.00	1
Value		Accel (G)	Velocity (in/sec)	Disp (in)
Min		-2.13	-5.18	-0.0644
Max		2.36	5.06	0.0561
Res		0.03	0.15	-0.0017
Decayed Sine Parameters				
Frequency (Hz)	Accel (G)	Decay Rate	Delay	Frequency (Hz)
10.2	-0.311	0.0292	0.0000	81.0
11.3	0.399	0.0265	0.0000	89.0
12.6	-0.675	0.0237	0.0000	97.4
13.2	0.600	0.0226	0.0000	108.1
15.1	-0.267	0.0198	0.0000	114.6
16.3	0.300	0.0183	0.0000	128.7
17.5	-0.225	0.0170	0.0000	135.9
19.2	0.212	0.0156	0.0000	152.4

20.5	-0.246	0.0145	0.0000	164.8	-0.108	0.0018	0.0000
22.7	0.228	0.0132	0.0000	182.3	0.257	0.0016	0.0000
25.3	-0.191	0.0118	0.0000	198.0	-0.167	0.0015	0.0000
27.0	0.136	0.0110	0.0000	217.9	0.191	0.0014	0.0000
29.4	-0.069	0.0101	0.0000	237.4	-0.283	0.0013	0.0000
31.6	0.093	0.0094	0.0000	251.5	0.256	0.0012	0.0000
34.9	-0.107	0.0085	0.0000	279.3	-0.154	0.0011	0.0000
38.3	0.094	0.0078	0.0000	296.6	0.298	0.0010	0.0000
41.9	-0.061	0.0071	0.0000	320.5	-0.393	0.0009	0.0000
45.0	0.114	0.0066	0.0000	362.6	0.323	0.0008	0.0000
49.0	-0.134	0.0061	0.0000	390.3	-0.359	0.0008	0.0000
55.1	0.116	0.0054	0.0000	425.0	0.347	0.0007	0.0000
57.2	-0.070	0.0052	0.0000	473.4	-0.189	0.0006	0.0000
65.1	0.130	0.0046	0.0000	508.3	0.318	0.0006	0.0000
71.1	-0.086	0.0042	0.0000	554.3	-0.262	0.0005	0.0000
77.0	0.082	0.0039	0.0000	574.7	0.281	0.0005	0.0000
				3.4	0.040	0.9500	-0.0466

**Table 8: Fourth Realization of Decayed Sine Parameters.**

SRS Parameters				
fmin	fmax	pts/oct	Damp	SRS Type
10.00	600.00	8.00	0.03	MMAA
Acceleration History Parameters				
Sample Rate	Frame Size	Gravity Constant	Ptype	
5120	8192	386.00	1	
Value	Accel (G)	Velocity (in/sec)	Disp (in)	
Min	-2.26	-4.52	-0.0492	
Max	2.28	4.23	0.0572	
Res	-0.03	-0.01	0.0041	
Decayed Sine Parameters				
Frequency (Hz)	Accel (G)	Decay Rate	Delay	Frequency (Hz)
10.6	-0.364	0.0281	0.0000	84.7
11.4	0.522	0.0261	0.0000	90.8
12.2	-0.535	0.0244	0.0000	99.8
13.4	0.353	0.0223	0.0000	106.9
15.0	-0.412	0.0198	0.0000	116.4
15.7	0.405	0.0190	0.0000	129.4
17.5	-0.236	0.0170	0.0000	135.7
18.8	0.375	0.0159	0.0000	148.3
				0.171
				0.0020
				0.0000

21.3	-0.239	0.0140	0.0000	162.0	-0.160	0.0018	0.0000
22.9	0.232	0.0130	0.0000	178.7	0.203	0.0017	0.0000
24.7	-0.157	0.0121	0.0000	199.2	-0.208	0.0015	0.0000
26.9	0.153	0.0111	0.0000	216.8	0.237	0.0014	0.0000
28.7	-0.050	0.0104	0.0000	227.4	-0.199	0.0013	0.0000
32.3	0.078	0.0092	0.0000	252.3	0.238	0.0012	0.0000
34.1	-0.103	0.0088	0.0000	276.8	-0.295	0.0011	0.0000
37.2	0.114	0.0080	0.0000	300.1	0.342	0.0010	0.0000
41.5	-0.126	0.0072	0.0000	331.1	-0.308	0.0009	0.0000
44.3	0.074	0.0067	0.0000	360.4	0.281	0.0008	0.0000
50.1	-0.114	0.0060	0.0000	386.1	-0.195	0.0008	0.0000
54.6	0.100	0.0055	0.0000	423.9	0.260	0.0007	0.0000
59.3	-0.114	0.0050	0.0000	452.1	-0.418	0.0007	0.0000
62.7	0.086	0.0048	0.0000	518.1	0.265	0.0006	0.0000
70.2	-0.096	0.0043	0.0000	541.5	-0.170	0.0006	0.0000
76.0	0.081	0.0039	0.0000	574.7	0.350	0.0005	0.0000
				3.5	0.030	0.9500	-0.0449

**Table 9: Fifth Realization of Decayed Sine Parameters.**

SRS Parameters				
fmin	fmax	pts/oct	Damp	SRS Type
10.00	600.00	8.00	0.03	MMAA
Acceleration History Parameters				
Sample Rate	Frame Size	Gravity Constant	Ptype	
5120	8192	386.00	1	
Value	Acceleration (G)	Velocity (in/sec)	Displacement (in)	
Min	-1.99	-4.91	-0.0592	
Max	2.11	5.18	0.0631	
Res	-0.04	-0.01	0.0035	
Decayed Sine Parameters				
Frequency (Hz)	Accel (G)	Decay Rate	Delay	Frequency (Hz)
10.4	-0.360	0.0287	0.0000	80.7
11.2	0.438	0.0266	0.0000	90.4
12.4	-0.508	0.0240	0.0000	100.2
13.4	0.344	0.0222	0.0000	108.1
15.1	-0.296	0.0198	0.0000	114.9
16.4	0.464	0.0182	0.0000	126.4
17.1	-0.494	0.0174	0.0000	138.4
19.3	0.224	0.0154	0.0000	155.0
				0.131
				0.0019
				0.0000

20.6	-0.197	0.0145	0.0000	161.9	-0.148	0.0018	0.0000
22.6	0.218	0.0132	0.0000	183.0	0.194	0.0016	0.0000
24.8	-0.193	0.0120	0.0000	197.3	-0.185	0.0015	0.0000
27.6	0.127	0.0108	0.0000	212.1	0.167	0.0014	0.0000
29.3	-0.125	0.0102	0.0000	229.0	-0.293	0.0013	0.0000
32.8	0.093	0.0091	0.0000	252.7	0.166	0.0012	0.0000
34.6	-0.059	0.0086	0.0000	276.2	-0.372	0.0011	0.0000
38.5	0.080	0.0078	0.0000	295.4	0.327	0.0010	0.0000
41.9	-0.124	0.0071	0.0000	330.0	-0.307	0.0009	0.0000
45.3	0.111	0.0066	0.0000	353.0	0.297	0.0008	0.0000
49.8	-0.088	0.0060	0.0000	388.0	-0.241	0.0008	0.0000
54.2	0.075	0.0055	0.0000	427.2	0.326	0.0007	0.0000
57.6	-0.086	0.0052	0.0000	457.8	-0.306	0.0007	0.0000
62.6	0.110	0.0048	0.0000	500.0	0.182	0.0006	0.0000
71.4	-0.128	0.0042	0.0000	554.3	-0.266	0.0005	0.0000
74.6	0.077	0.0040	0.0000	574.7	0.329	0.0005	0.0000
				3.5	0.171	0.9500	-0.0459

## 5.5 Derivation of Test Specifications

The initial plan of the customer was to have a reactor fuel assembly in a large truck cast with the fuel rods instrumented within the cast to measure loads during normal highway transport. The cask was to be placed upon a trailer in a horizontal position for the test. However, procuring a cask was not realistic and plans were made to use the shaker.

The only data available to derive the laboratory test specifications are from two shock and vibration tests for large shipping containers during truck transport performed in the late 70's [8,9]. Section 5.6.1 describes the derivation of the random vibration test specification. Section A.2 describes the derivation of the shock test specification.

### 5.5.1 Derivation of random vibration test specification

The two documents presented the random vibration data as VIBRAN data which was the 99% level of 0 to peak amplitudes over a frequency band. Table 11 shows the VIBRAN data for the vertical axis.

**Table 10: Input to Cargo (g) – Vertical Axis.**  
99% Level of 0 to Peak Amplitude

Frequency Range	44,000 lb. [1]	56,000 lb. [2]
0 – 5	0.27	0.52
5 – 10	0.19	0.27
10 – 20	0.27	0.37
20 – 40	0.27	0.19
40 – 80	0.52	0.37
80 – 120	0.52	0.37
120 – 180	0.52	0.52
180 – 240	0.52	0.52
240 – 350	0.52	0.52
350 – 500	0.14	0.37
500 – 700	0.07	0.10
700 – 1000	0.07	0.10
1000 – 1400	0.05	0.10
1400 – 1900	0.05	0.10

The first step was to convert the data into an ASD. This is shown in {Eq. A.1-1} where ZPA is the zero to peak amplitude and FR is the frequency band.

$$ASD = (ZPA \div 3)^2 \div (FR(2) - FR(1)) \quad \{Eq. A.1-1\}$$

Once the ASDs were generated the straight line test specification was created. The actual weight of the fuel reactor assembly falls between 44,000 lbs. and 56,000 lbs. therefore it was decided that enveloping the two ASDs would be conservative. Figure 19 shows the recommended test specification and the underlying ASDs.

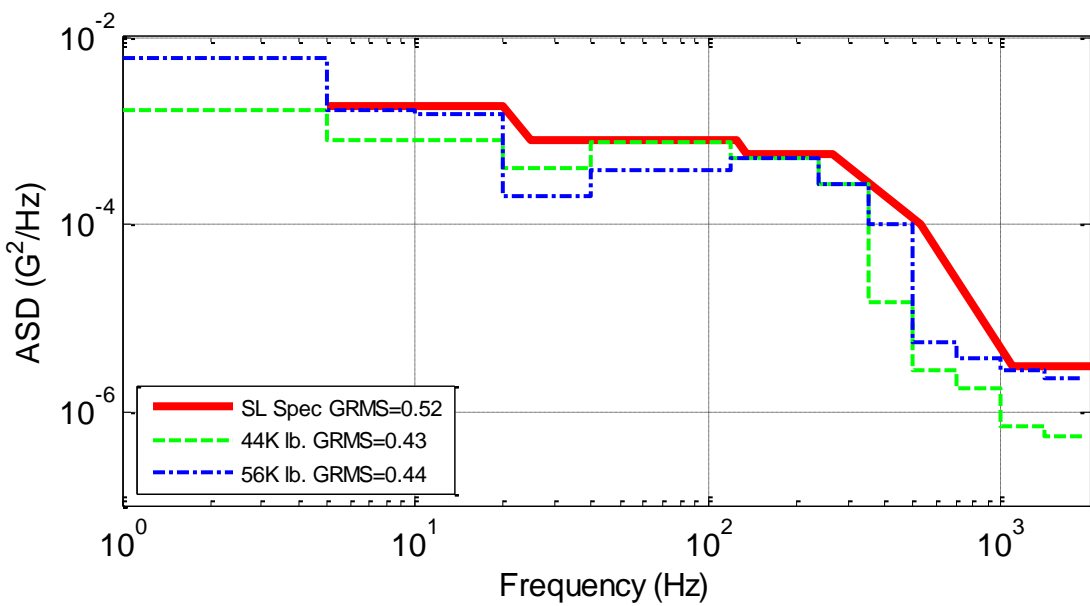


**Figure 19. Recommended test specification & underlying ASDs.**

### 5.5.2 Derivation of shock test specification

The shock response spectra were displayed as plots in References 8 and 9. Therefore before being able to use them the data had to be digitized to obtain electronic data. There were three shock responses displayed; the  $3\sigma$ , the peak of responses, and the mean of responses. Due to the quality of the plot it was decided to envelope the three shock responses when digitizing. Shock response spectra for the 44,000 lb. cargo and the 56,000 lb. cargo were obtained.

The straight line shock test specification was created to envelope the 44,000 lb. shock spectra and the 56,000 lb. shock spectra. Figure 20 shows the recommended test specification and the underlying shock response spectra.

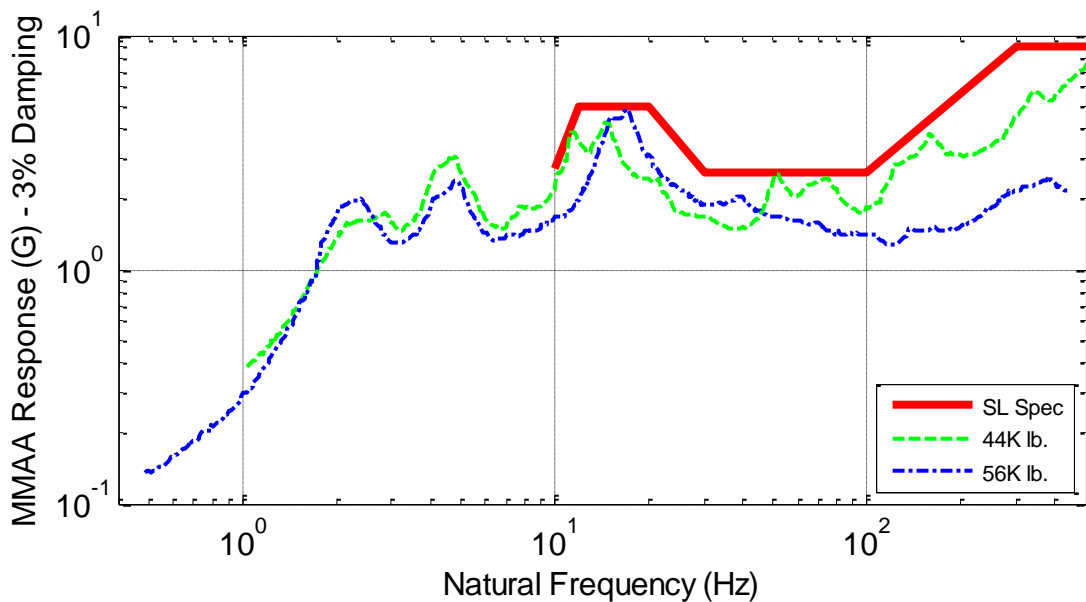


**Figure 20. Recommended test specification & underlying shock spectra.**

The next step was to obtain the five decayed sine realizations. The transients synthesized are composed of sum of decaying sinusoids which match the specified shock response spectrum. The pulse is compensated for velocity and displacement by adding a delayed decayed sinusoid.

In order to obtain five unique transients, “jitter” was added to the frequencies of the specified shock response spectrums. Figure 21 shows the range a given frequency was allowed to vary. The frequencies were allowed to vary a maximum of 80% from the midpoint (i.e.,  $F_1$ ) in the positive and negative direction (i.e.,  $F_{1\text{low}}$  and  $F_{1\text{high}}$ ). A uniform random distribution was used to determine the amount each frequency varied within its specified range.

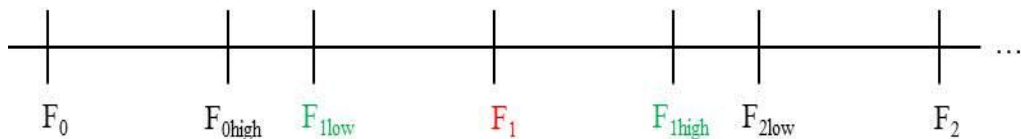


**Figure 21. Range of frequencies.**

Figures 22 through 26 show the acceleration history, velocity, displacement, and the decayed sine shock spectra versus the reference shock spectra for the five realizations.

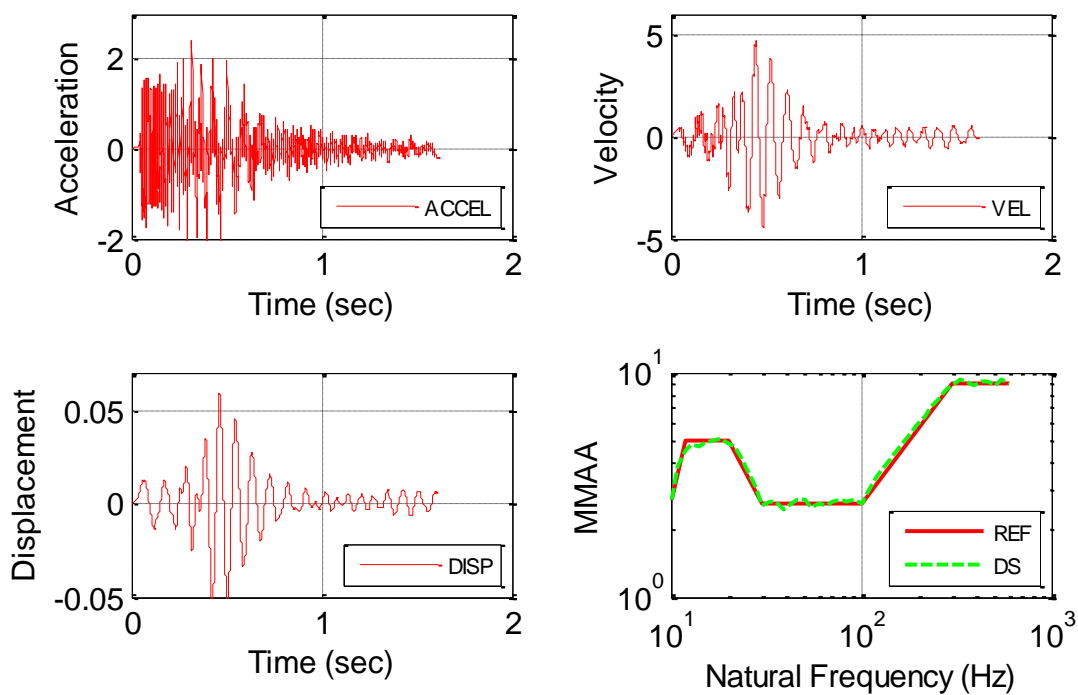


**Figure 22. Decayed sine initial realization.**

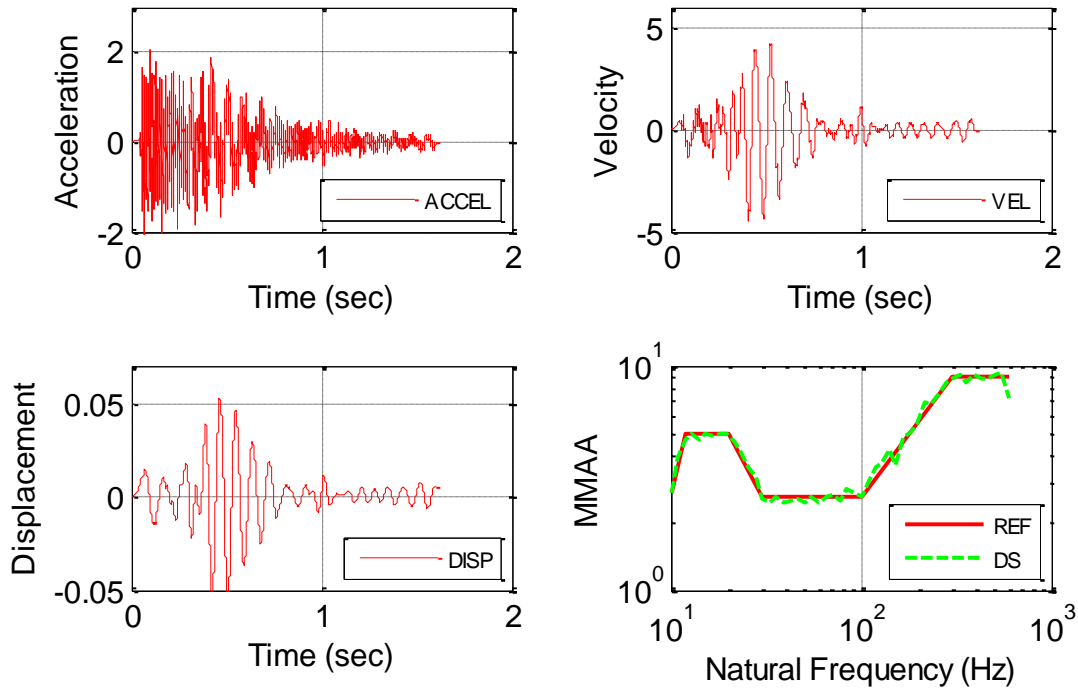


**Figure 23. Decayed sine second realization.**

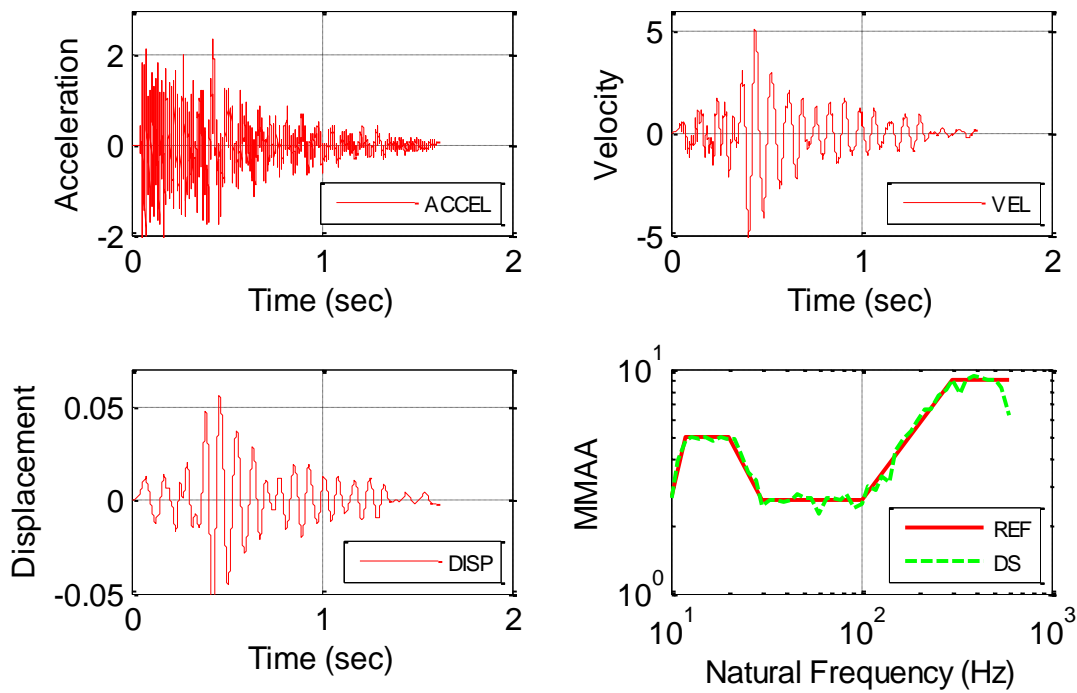


**Figure 24. Decayed sine third realization.**

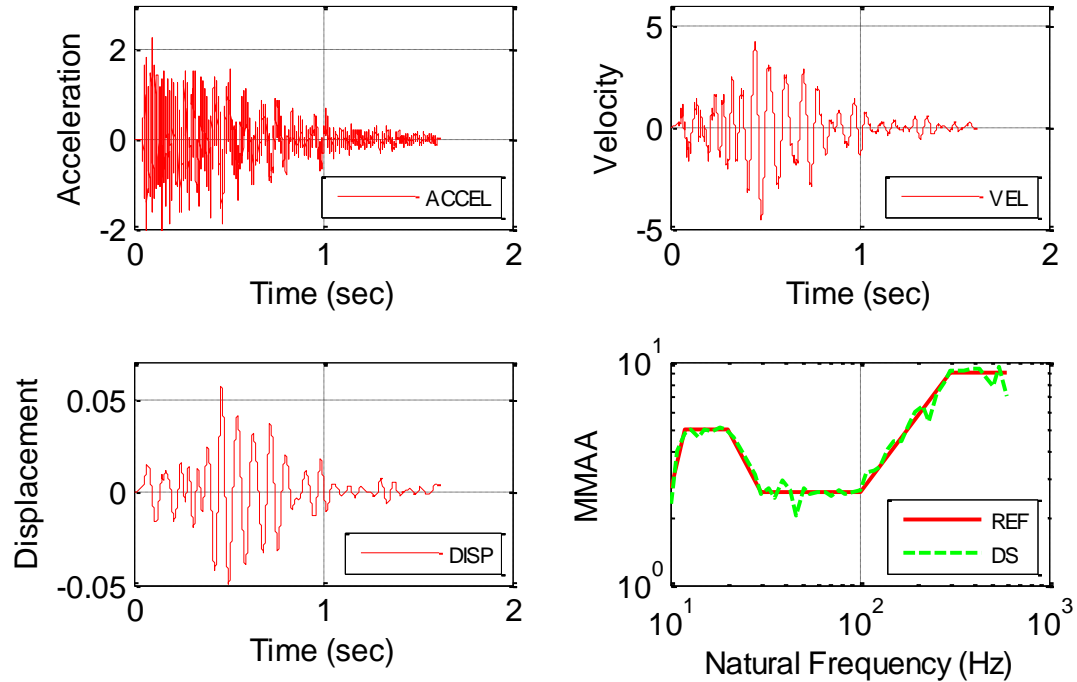


**Figure 25. Decayed sine fourth realization.**

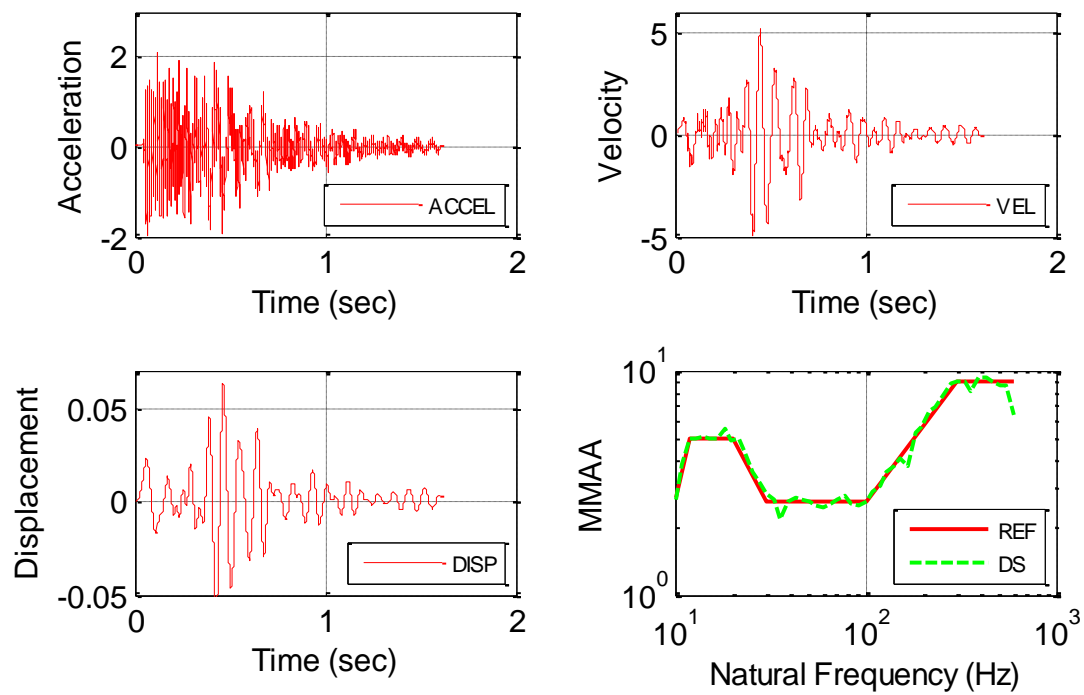


Figure 26. Decayed sine fifth realization.



## 6 PREVIOUS OVER-THE-ROAD TEST PROGRAMS

Note: The following describes testing where the instrumentation for measuring loads was on the transport package, not on the contents. For the current test proposal, some instruments may be placed on the external package, but the primary objective is to place instruments on the package internals – the basket, fuel assembly and fuel cladding.

### 6.1 “Over-the-road testing of radioactive materials packagings”<sup>11</sup>

Sandia National Laboratories had a program to characterize the normal environments encountered during the transport of radioactive materials. This effort consisted of obtaining experimental data from the external surface of the transport package and the transport bed during both road simulator and over-the-road tests and of analyzing the data to obtain numerical models to simulate those environments.

Test activities included 1) over-the-road testing, 2) hard braking, and 3) hard turning. Package response during any given test is specific to that package and trailer. The trailer and packaging were subjected to nine separate events to determine both the acceleration and tiedown loads experienced during normal transport. Five types of roads were used: 1) smooth asphalt primary; 2) rough asphalt primary; 3) rough concrete primary; 4) rough asphalt secondary; and 5) spalled asphalt secondary. The roads provided a vibrational environment for the packaging. To subject the packaging to a shock environment, a railroad crossing and bridge approach were selected. Finally, to determine the package’s response to maneuvering, a hard turn and a stop were executed. The speed driven for each event was the lesser of either the posted legal speed limit or the fastest speed consistent with safe operation of the tractor.

For each event, approximately 15 seconds of data were recorded. This provides 15,000 samples per data channel. This was adequate time to capture shock events, such as the rail crossing plus damping back to the random vibration state. For the random vibration events, such as smooth asphalt roads, it provided a representative sampling.

---

<sup>11</sup> R.E. Glass & K.W. Gwinn, “Over-the-Road Tests of Nuclear Materials Package Response to Normal Environments,” SAND91-0079, Sandia National Laboratories, December 1991.

### 6.1.1 Instrumentation

The primary role of the instrumentation was to obtain the acceleration at various points on the trailer and package. A total of nine instruments were used in each test. A *triaxial accelerometer* was placed on the package's center top to measure the package response along each axis. The stiffness of the package made this measurement representative of the entire package. At the same longitudinal location, an accelerometer measured the trailer's vertical acceleration. The maximum accelerations on a trailer were obtained at its front and rear. Longitudinal and vertical accelerometers were placed on the trailer bed over the rear axle, and a vertical accelerometer placed on the trailer over the kingpin. The combination of vertical accelerometer sat these three trailer locations allowed the bounce, pitch, and bending modes to be detected. The longitudinal and transverse accelerometers were useful in detecting the effects of braking and turning.

The response of the tiedown systems was determined from *load cells* in the links between attachment points and with *strain gages* mounted on the cradle straps.

### 6.1.2 Test results

A large volume of information is acquired from tests of this type, the actual time histories and resultant power spectral densities for each transducer. The time histories provide the mean-to-peak response at the different locations. From these time histories, the power spectral densities are generated. The power spectral densities transform the time history data into the frequency domain to relate how the response energy varies as a function of frequency. From this data, it is determined which modes of vibration are contributing to the overall response, and the root-mean square response can also be calculated. The mean squared response is the area under the power spectral densities response curve. The root mean square is the square root of this value. The root mean square relates the probability of a certain level of response occurring, and is equal to the standard deviation since the mean is zero. Three times the root mean square will envelope 99.9 percent of all expected responses. The transform magnitude plots are discrete Fourier transforms of the measured response and provide the frequency content of the transient record.

## 6.2 “Test specification for TRUPACT-I vibration assessment”<sup>12</sup>

This specification establishes the requirements for the vibration testing of a production unit Transuranic Package Transporter (TRUPACT-I). The in-service tests determined the normal transport shock and vibration environment. The purpose of the in-service tests was to determine the vibration and shock

---

<sup>12</sup> K.W. Gwinn, R.E. Glass, and L.E. Romesberg, “Test Specification for TRUPACT-I Vibration Assessment,” SAND85-1369, Sandia National Laboratories, February 1986

environments encountered by the TRUPACT-I during normal service conditions. The tests will consist of monitoring vibration and shock levels of an instrumented TRUPACT-I under normal operating conditions. The monitoring was accomplished using accelerometers located at the attachment points of the trailer.

A digital recorder was mounted on the trailer during the tests. Specific shock events of interest included railroad grade crossings, bridge approaches, potholes, raised bumps, and diagonal bumps. Vibration test events included normal primary asphaltic and concrete pavements, rough primary asphaltic and concrete surfaces, and rough secondary surfaces at a range of operating speeds. These shock and vibration events include most of the normal operating environments that would be experienced by a transport package.

### 6.2.1 Instrumentation

Six uniaxial piezoresistive accelerometers were attached. An accelerometer was used at each corner to measure the vertical accelerations, and the remaining two were used at the forward castings to measure longitudinal accelerations. The wiring was constrained to prevent straining during the tests. The recorder was mounted on shock isolating material to prevent recording errors and damage. All accelerometers were calibrated for a range of  $\pm 20$  g.

All road simulator and over-the-road tests were instrumented to determine the loads acting on the packages. Accelerometers were used to obtain vertical, longitudinal, and transverse accelerations. Load cells were used to directly monitor tie-down loads. Strain gages were used so that tie-down loads could be calculated.

A sample of the Normal transport transducer data is given in the table below.

Peak Response for Road Surface Events

Transducer <u>Location</u>	Event				
	Smooth <u>Asphalt</u>	Rough <u>Asphalt</u>	Rough <u>Concrete</u>	Secondary <u>Asphalt</u>	Spalled <u>Asphalt</u>
Cask top					
Transverse (g)	0.17	0.21	0.12	0.13	0.22
Vertical (g)	0.23	0.32	0.20	0.35	0.58
Longitudinal (g)	0.17	0.38	0.22	0.65	0.88
Trailer, mid					
Vertical (g)	0.21	0.37	0.07	0.07	0.08
Trailer, rear					
Vertical (g)	0.46	1.4	0.95	1.68	3.1
Longitudinal (g)	0.14	0.37	0.22	0.43	0.85
Trailer, front					
Vertical (g)	0.73	1.7	1.3	2.7	4.5
Front tiedown (lb) (N)	430 1900	580 2600	220 980	350 1600	460 2000
Rear tiedown (lb) (N)	220 980	360 1600	150 670	280 1200	650 2900

Both peak and root mean square values that the cask response was less than 1 g.

The representative time history is shown in Figure 27 (Figure 9a) - the measured vertical acceleration of the rear trailer bed in response to the spalled asphalt event. This figure shows a fairly severe vibrational environment, with two large transient events occurring 3 and 9 seconds into the run. Figure 27 (Figure 9b) shows the same response in the frequency domain in power spectral density form. The response is shown as  $\text{g}^2/\text{Hz}$  on a log-log plot. The larger response at 1.5 Hz is due to the first bounce mode of the tractor/trailer combination. This bounce mode of the vehicle is caused by the structure bouncing in unison on the suspension system of the trailer. The next feature seen is the response at 4 Hz. This is the frequency of the vehicle's first pitching mode. This is caused by the kingpin/rear tractor suspension deflecting down while the trailer rear suspension and tractor front suspension deflect up. The high-frequency modes, from 10 to 20 Hz, are combinations of the trailer bending with the tractor pitching and bending. The first bending mode occurs at approximately 11 Hz.

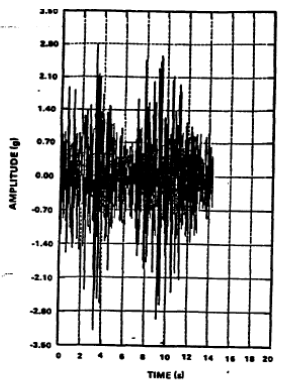


Figure 9a. Representative Time History

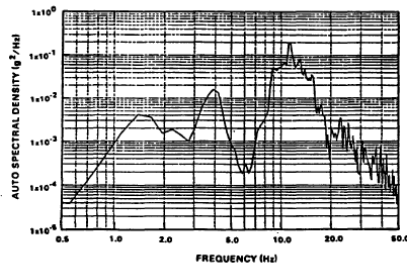


Figure 9b. Representative PSD

**Figure 27. Representative normal transport load data.**

## 7 KEY BACKGROUND INFORMATION

### 7.1 Source of Vibration and Shock Data for Test

EDB #A2164  
EXTRACTED FROM

SAND77-1110  
Unlimited Release  
Printed September 1977

NRC-12

#### SHOCK AND VIBRATION ENVIRONMENTS FOR LARGE SHIPPING CONTAINER DURING TRUCK TRANSPORT (PART I)

Cliff F. Magnuson  
Applied Mechanics Division K 1282  
Sandia Laboratories, Albuquerque, NM 87115

[3]

#### ABSTRACT

The purpose of this study was to obtain vibration and shock data during truck shipment of heavy cargo. Currently available data were taken on trucks bearing lighter loads than the loads of current interest. In addition, the new data are expected to be useful in the determination of any trends of vibration and shock environments with increased cargo weight. These new data were obtained on a "piggyback" basis during truck transport of 195 700 N (44,000 lb) cargo which consisted of a spent fuel container and its supporting structure from Mercury, Nevada, to Albuquerque, New Mexico. The routes traveled were US 95 from Mercury, Nevada, to Las Vegas, Nevada; US 93 from Las Vegas to Kingman, Arizona; and I-40/US 66 from Kingman to Albuquerque, New Mexico. Speeds varied from very slow during hill climbs to 101 km/hr (63 mph). A comparison of these data with a collectively reduced set of data for cargo weights varying from no-load to 133 400 N (30,000 lb) showed that the zero to peak amplitude levels of vibration were significantly lower for frequencies less than 40 Hz in the vertical axis and that there was a reduction in the vibration amplitude levels in all axes for frequencies greater than 500 Hz. The shock response amplitude was less severe for the entire frequency spectrum in the vertical axis, but it was not significantly different in the other axes. Data measurements were made on a truck shipment of a 249 100 N (56,000 lb) container over the same routes as were used for the shipment discussed in this report. These data will be presented in a subsequent report along with any additional data trends that result from studies of trucks carrying increased cargo weight.

EDB #A2165  
EXTRACTED FROM

NUREG/CR-0128  
SAND78-0337  
RT

SHOCK AND VIBRATION ENVIRONMENTS  
FOR A LARGE SHIPPING CONTAINER  
DURING TRUCK TRANSPORT (PART II)

Clifford F. Magnuson

Manuscript Submitted: February 13, 1978  
Date Published: May 1978

[2]

Manuscript Submitted: February 13, 1978  
Date Published: May 1978

Sandia Laboratories  
Albuquerque, New Mexico 87185  
operated by  
Sandia Corporation  
for the  
U.S. Department of Energy

Prepared for  
Division of Safeguards, Fuel Cycle and Environmental Research  
Office of Nuclear Regulatory Research  
U.S. Nuclear Regulatory Commission  
Washington, DC 20555  
Under Interagency Agreement DOE 40-550-75  
NRC FIN No. A-1049-6

#### ABSTRACT

The purpose of this study was to obtain vibration and shock data during truck shipment of heavy cargo. These data were for use in determining any trends of vibration and shock environments with increased cargo weight. The new data were obtained on a "piggyback" basis during truck transport of 249 100N (56,000-pound) cargo which consisted of a spent fuel container and its supporting structure. The truck was driven from Mercury, Nevada, to Albuquerque, New Mexico. The routes traveled were US 95 from Mercury, Nevada, to Las Vegas, Nevada; US 93 from Las Vegas to Kingman, Arizona; and I-40/US 66 from Kingman to Albuquerque, New Mexico. Speeds varied from very slow to 88 km/hr (55 mph). A comparison of data from similar experiments with cargo weights varying from no-load to this load shows that the zero-to-peak acceleration amplitude levels of vibration are highest when trucks carry relatively light loads. This is true for the longitudinal and vertical axes of the vehicles in most frequency bands and for the transverse axis above 700 Hz. The shock response acceleration amplitudes for heavier cargo weights were less severe above 3 Hz in the vertical axis and higher between 8 and 20 Hz in the transverse axis. The highest acceleration amplitude of shock response in the longitudinal axis below about 20 Hz was produced in a trailer having a spring suspension system and carrying the 249 100N (56,000 pounds) load.

## 7.2 Related Documents

- 7.2.1 “Approach for the Use of Acceleration Values for Packages of Radioactive Material under Routine Conditions of Transport,” Andreas Apel, Viktor Ballheimer, Christian Kuschke, Sven Schubert, Frank Wille, Proceedings of the 9th International Conference on the Radioactive Materials Transport and Storage, May 2012, London.**
- 7.2.2 “Transportation Activities for BWR Fuels at NFI,” S. Uchikawa, H. Kishita, H. Ide, M. Owaki, K. Ohira, Nuclear Fuel Industries, LTD., Proceedings of Global 2009, Paris, September 2009.**

Nuclear Fuel Industries, LTD. (NFI) supplies fuel assemblies for both PWR and BWR nuclear power plants in Japan. We also are involved in the field of nuclear fuel recycling and we manage transportation of the fuel assemblies from our fabrication facilities to the Japanese nuclear power plants. The NT-XII transportation container was developed by NFI for fresh BWR fuel assemblies. The foremost design priorities for this NT-XII container were transportation efficiency and ensuring fuel integrity during transportation. In addition to the design of new containers, we also develop improved packaging methods. Recently, NFI performed tests intended to determine the need for packing separators to mitigate vibration induced wear during fuel transportation. The transportation test was performed using dummy fuel assemblies and included wear data analysis and post-disassembly inspections. The fretting wear on the surface of fuel rods and spacer spring force degradation were measured. Results from these evaluations indicated that there was no significant difference in the vibration induced wear on the fuel between the packaging methods with and without packing separators. As a result, NFI developed a new packaging method which improves the packing and unpacking efficiency for fuel rods transported from the fuel fabrication facility to another facility. This method also enables the fuel assembly container to be used without the need for modifications to the design of container.

- 7.2.3 “High Burn-up Used Nuclear Fuel Vibration Integrity Study - Out-of-Cell Fatigue Testing Development,”, Jy-An John Wang, Hong Wang, Yong Yan, Rob Howard, Bruce Bevard, January 2011, Oak Ridge National Laboratory.**

For high burn-up spent nuclear fuel (SNF), it is expected that the used nuclear fuel cladding will have a high population of microcracks and hydrides, including macro-hydrides and micro-hydrides. This will reduce the stress intensity required to advance the crack growth. The linking of these microcracks during vibration loading may also reduce the fatigue threshold/incubation period, accelerating fatigue failure. In addition to the cladding damage, the microstructure of comprising fuel pellets and the interfaces of fuel rod have changed dramatically after high burn-up in the reactor. These changes may have a direct impact on the structural integrity and vibration response of SNF rods in transportation.

As a result, vibration has been included as a mandatory test condition for the structural evaluation of package that is used in transporting spent nuclear fuel by US NRC (Nuclear Regulatory Commission) in 10 CFR §71.71. Currently, no testing system is available to test the spent nuclear fuel and evaluate the

performance of fuel rods during transportation. It is the aim of this research project to develop a system that can appropriately test the response of high burn-up SNF rods under simulated loading conditions.

The SNF rods lie horizontally in a transportation cask and are supported by the spacers within fuel rod assembly. These rods are subjected to oscillatory bending due to inertia effects. This oscillatory bending is the major vibrational load of SNF rods as mentioned in 10 CFR §71.71 and its effect on integrity of the SNF rods needs to be captured by the designed testing system. The SNF rods include various burn-induced damage (pores and micro cracks), oxide and hydride layers, residual stresses, altered interfaces, and trapped fission products. They are highly radioactive. These factors complicate conventional cyclic bending testing and need to be considered in the development of the test apparatus.

An extensive literature survey revealed that a variety of bending fatigue testing methods have been developed including cantilever beam bending, three-point/ four-point bending, and pure bending, as well as their variants considering environmental factors, particularly temperature. Bending fatigue testing approaches also account for rotation based on if the rotation is introduced to carry out the reverse bending. However, the vibration of SNF rods during transportation usually involves deflection instead of rotation, and at the same time, the dominant frequencies involved with these dynamical events are generally less than 100 Hz. Therefore, the non-rotating reverse bending that can be accomplished by a universal material testing machine or its equivalent is the focus of this report.

Currently, bending cyclic fatigue test methods are used in testing and characterizing various engineering materials and their components including concrete, composites, ceramics, metal alloys, metallic glasses, and so forth. Available approaches include unipolar mode without reversal, and bipolar mode with full reversal. Mechanical support/ contact techniques to enable the designed beam bending boundary condition have been advanced significantly. But most of the bending fatigue tests are application-based. The following conclusions can be drawn from the literature survey:

- Among the bending fatigue testing methods reviewed, four-point bending fatigue testing is a mature experimental technology in testing materials and components that have a limited deformation before failure. Demonstration of this technology includes asphalt beam and the development of a self-aligning test rig.
- The above-mentioned techniques are mainly used in fatigue tests without bending reversal.
- A variety of supports were developed in bending fatigue testing including rotary joints, slide connection, and flexures. They either deviate from a true fixed boundary condition or involve contact damage.
- Four-point/ three-point bending and cantilever bending all suffer from an inherent drawback related to shear in the beam that has a non-uniform bending moment. This has a significant impact on testing materials that are sensitive to the shear.
- Pure bending fatigue has been used for high strain fatigue testing of metal alloys and composites. The implementation of the pure bending concept is application-based and has been partially successful.
- Environmental chambers and/or high temperature furnaces are currently incorporated into some critical bending fatigue tests. Specimen setup is usually manual and therefore insufficient for testing materials that are radioactive.

A bending fatigue testing system has been proposed and developed in this report to test high burn-up SNF rods. Pure bending is adopted as the bending mode of testing system. The use of a pure bending method in which a uniform bending moment is exerted on the gage length of the specimen should eliminate the effect of shear. The shear can eventually lead to a failure mode that is not relevant to the fatigue failure of concern. Two implementation concepts are presented with emphasis on bending fatigue testing on rod specimens in reversal bending.

The first implementation relates to an approach in which the specimen is setup horizontally. Some important features are

- It is based on the principle of four-point bending, but the gage length of the specimen is arranged in the part of beam that has a uniform bending moment. The driving mechanisms in conventional four-point testing can be applied to the horizontal setup.
- Rigid sleeves are introduced to reinforce the extensional parts of specimen and to convert external force couples into the bending moments.
- It accommodates various connections to loading contacts and supports. These connection options enable the free rotation and horizontal translation of beam boundary condition as required by reversal bending and can best fit into the different applications.

The second implementation concerns the design with the specimen setup vertically. The main features are

- Bending moments are applied through two horizontal rigid arms of a U-frame structure. The arms are equipped with two co-axial holes that accommodate the test specimen.
- Roller bearings or equivalent bearing sets in the arms of the U-frame allow the release of any axial load related to the loading of specimen and, at the same time, transfer the bending moments from the rigid arms to the specimen.
- The initial setup of a test specimen can be accomplished by a simple insertion of the specimen into the holes. This is advantageous for a hot-cell environment because most of the operations can be adapted for this testing environment.
- The U-frame has fewer components, which would result in a test system with enhanced reliability and controllability.
- Versatile designs in the vertical member and joints or corners of the U-frame provide options for different experimental studies.

Overall, the proposed test system has the following unique characteristics in comparison with the conventional bending fatigue testing methods:

- Bending fatigue testing is carried out under pure bending, eliminating the effect of the shearing force encountered in three-point bend and four-point bend testing.
- The bending fatigue is conducted in a reversal mode and the system approaches the loading condition of used nuclear fuel in transportation more closely than repeated three-point or four-point bending testing.
- Compliant layers are incorporated into the rigid sleeve to control the effect of contact on the fatigue failure in the specimen retaining areas.

- The system can test and examine specimens in very hostile or radioactive environments.

#### **7.2.4 Other documents related to this work include**

- 7.2.4.1 “Mechanical Behaviour of High Burn-Up SNF under Normal and Accident Transport Conditions – Present Approaches and Perspectives,” Fanke Wille, Viktor Ballheimer, Annette Rolle, Berhard Droste, Bundesanstalt für Materialforschung und –prüfung (BAM).**
- 7.2.4.2 “CANDU Irradiated Fuel Transportation: The Shock and Vibration Program,” B.P. Dalziel, M.A. Elbestawi, J.W. Forest, Ontario Hydro, Research Agreement Report No. 2715/R1/CF.**
- 7.2.4.3 “Transportation Shock and Vibration Descriptions for Package Designers,” J.T. Foley, Sandia National Laboratories Report SC-M-72 0076, July 1972.**
- 7.2.4.4 “Design Basis for Resistance to Shock and Vibration,” SAND89-0937C, R.E. Glass, K.W. Gwinn, Sandia National Laboratories.**
- 7.2.4.5 “Over-the-Road Testing of Radioactive Materials Packaging” SAND91-2709C, R.E. Glass and K.W. Gwinn, Sandia National Laboratories.**

## 8 REFERENCES

- [1] "A Method for Determining the Spent-Fuel Contribution to Transport Cask Containment Requirements," Thomas L. Sanders, Kevin D. Seager, Sandia National Laboratories; Yusef R. Rashid, Peter R. Barrett, ANATECH Research Corporation; Anthony P. Malinauskas, Oak Ridge National Laboratory; Robert E. Einziger, Pacific Northwest Laboratory; Hans Jordan, EG&G Rocky Flats Inc.; Thomas A. Duffey, Stephen H. Sutherland, APTEK Incorporated; Philip C. Reardon, GRAM Incorporated, SAND90-2406, November 1992.
- [2] "Shock and Vibration Environments for a Large Shipping Container during Truck Transport (Part II)," Clifford F. Magnuson, Extracted from NUREG/CR-0128, SAND78-0337, Sandia National Laboratories, May 1978.
- [3] "Shock and Vibration Environments for a Large Shipping Container during Truck Transport (Part I), Clifford F. Magnuson, SAND77-1110, Sandia National Laboratories, September 1977.
- [4] "Shock and Vibration Environments Encountered During Normal Rail Transportation of Highway Cargo," Magnuson, C.F., Sandia National Laboratories, Albuquerque, NM, SAND82-0819, August 1982.
- [5] "Shock Environments for Large Transport Containers during Rail-Coupling Operations," Magnuson, C.F., Sandia National Laboratories, Albuquerque, NM, SAND79-2168, NUREG/CR-1277, June 1980.
- [6] US Code of Federal Regulations, Title 10-Energy, Part 71 (10 CFR 71), "Packaging and Transportation of Radioactive Material."
- [7] "Standard Review Plan for Transportation Packages for Radioactive Material," NUREG-1609, US Nuclear Regulatory Commission, March 1999.
- [8] "Dynamic Analysis to Establish Normal Shock and Vibration of Radioactive Material Shipping Packages, Volumes 1-3," S.R. Fields, NUREG/CR-2146, US Nuclear Regulatory Commission, 1983.

## **APPENDIX A**

### **Development of Closure Bolt Analysis Rules on Design of ASME Section III, Division 3 Containments**

# **Development of Closure Bolt Analysis Rules on Design of ASME Section III, Division 3 Containments**

Z.H. Han, V.N. Shah and Y.Y. Liu

Argonne National Laboratory

September 11, 2012

The ASME BPV Code Subcommittee responsible for Section III Division 3 is currently revising Subsections WB and WC and developing Subsection WD. Subsections WB and WC contain rules for the material, design, fabrication, examination, testing, marking, stamping, and preparation of reports by the Certificate Holder for Class TC transportation containments and Class SC storage containments, respectively, for spent nuclear fuel and high-level radioactive waste and materials. Subsection WD, which is under development, contains rules similar to those in Subsections WB and WC, but for internal supports inside the transportation and storage containments. The Working Group on the Design of Section III Division 3 Containments is addressing design issues, i.e., rules and/or guidance, for the bolted joints beyond the current Subsections WB and WC (and WD) limits. Further development of closure bolt analysis rules has been identified as a priority. As a member of the ASME BVP Code Subcommittee and the Working Group, Argonne National Laboratory has been tasked to assist in the further development of the closure bolt analysis rules.

Three tables have been created to compare the bolting rules between Subsections WB and WC, and between the rules in the mandatory Appendices XIII and XIV and Article WB-3000. The bolting rules in Subsections WB and WC are compared in Table 1 and the results were presented at the Working Group meeting in May 2012. The mandatory Appendices XIII and XIV to Section III Division 1 of the ASME BPV Code also contain bolting design analysis rules in Article XIII-1000, "Design Based on Stress Analysis," and Article XIV-1000, "Design Based on Fatigue Analysis." Although the rules in these two appendices are only applicable to the design of Class 2 vessels, they could be considered for use for containments meeting the requirements of WC-3200. The design rules and guidance in these two appendices are compared in Tables 2 and 3, respectively, against those in Subsection WB, for potential incorporation into Article WC-3000.

Subsection WB addresses the design stress limit for bolted closures under Level A and Level D service limits to ensure integrity of the bolted flange. Properly applied bolt preloads introduce clamping force in the bolted joint, ensuring leak-tightness of the transportation and storage casks. Work has begun in reviewing the bolting analysis rules in NUREG/CR-6007 "Stress Analysis of Closure Bolts for Shipping Casks" and the current practices for installing bolt preloads in the closure joints of transportation casks for hazardous and radioactive materials in ASME PCC-1, "Guidelines for Pressure Boundary Bolted Flange Joint Assembly."

## **Future Work**

Evaluation of the bolting analysis rules will continue, along with literature review of bolting analyses and practices for used fuel storage and transportation casks with bolted closures. Current practices for installing bolt preloads will be examined and finite-element analyses may need to be performed to determine preload uncertainties and scatters resulting from the different bolting-up methods.

The closure integrity of the storage and transportation casks in service is also affected by other factors such as aging and/or vibration during storage and transport, as well as the performance of seals. Aging effects on the bolted closure of storage and transportation casks could lead to a loss of preload due to

stress relaxation and self-loosening, or loss of bolting material due to corrosion and fatigue. Therefore, the impact of aging effects on the closure bolts and seals, and aging management programs and practices for bolted closures in storage and transportation casks should be evaluated.

Managing aging effects on the closure bolts of storage and transportation casks requires an aging management program (AMP) to prevent, mitigate, and detect aging effects, by condition and/or performance monitoring. One AMP titled “Bolted Canister Seal and Leakage Monitoring Program” has been developed for inclusion in Chapter IV of the report by O.K. Chopra, et al. [1]. The effectiveness of this AMP will be assessed against the operating experience from the storage and transportation casks with bolted closures in the future.

## **Reference**

- 1) O.K. Chopra, et al., *Managing Aging Effects on Dry Cask Storage Systems for Extended Long-Term Storage and Transportation of Used Fuel*, FCRD-USED-2012-000119 (ANL-12/29), June 30, 2012.

**Table 1 Comparison Matrix of Bolting Rules in Subsections WB and WC**

WB - BOLTING	WC - BOLTING	COMMENTS
ARTICLE WB-2000 MATERIAL	ARTICLE WC-2120 MATERIAL	
<b>WB-2100 GENERAL REQUIREMENTS FOR MATERIAL</b>	<b>WC-2100 GENERAL REQUIREMENTS FOR MATERIAL</b>	WB and WC are identical.
<b>WB-2120 CONTAINMENT MATERIAL</b>	<b>WC-2120 CONTAINMENT MATERIAL</b>	
<b>WB-2125 Bolting Material</b>  (a) Material for bolts and studs shall conform to the requirements of one of the specifications listed in Section II, Part D, Subpart 1, Table 4. Material for nuts shall conform to SA-194 or to the requirements of one of the specifications for nuts or bolting listed in Section II, Part D, Subpart 1, Table 4.  (b) The use of washers is optional. When used, they shall be made of wrought material with mechanical properties compatible with the nuts with which they are to be employed.	<b>WC-2128 Bolting Material</b>  (a) Material for bolts and studs shall conform to the requirements of one of the specifications listed in Table 4, Section II, Part D, Subpart 1. Material for nuts shall conform to SA-194 or to the requirements of one of the specifications for nuts or bolting listed in Table 4, Section II, Part D, Subpart 1.  (b) The use of washers is optional. When used, they shall be made of wrought material with mechanical properties compatible with the nuts with which they are to be employed.	
<b>WB-2200 MATERIAL TEST COUPONS AND SPECIMENS FOR FERRITIC STEEL MATERIAL AND DUCTILE CAST IRON</b>	<b>WC-2200 MATERIAL TEST COUPONS AND SPECIMENS FOR FERRITIC STEEL MATERIAL AND DUCTILE CAST IRON</b>	WB and WC have different requirements for test coupons and tests.
<b>WB-2220 PROCEDURE FOR OBTAINING TEST COUPONS AND SPECIMENS FOR QUENCHED AND TEMPERED MATERIAL AND FOR DUCTILE CAST IRON</b>	<b>WC-2220 PROCEDURE FOR OBTAINING TEST COUPONS AND SPECIMENS FOR QUENCHED AND TEMPERED MATERIAL AND FOR DUCTILE CAST IRON</b>	
<b>WB-2224 Location of Coupons</b>  (b) For bolting materials, test shall be made of either full-size bolts or test coupons are required by the base specification. The gauge length of the tension specimens and the area under the notch of Charpy specimens shall be at least one diameter or	<b>WC-2224 Bars and Bolting Material</b>  <b>WC-2224.3 Bolting Material</b>  For bolting material, the coupons shall be taken in conformance with the applicable material specification and with the	

WB - BOLTING	WC - BOLTING	COMMENTS
thickness from the heat treated end.	applicable material specification and with the midlength of the specimen at least one diameter or thickness from a heat treated end. When the studs, nuts, or bolts are not of sufficient length, the midlength of the specimen shall be at the midlength of the studs, nuts, or bolts. The studs, nuts, or bolts selected to provide test coupon material shall be identical with respect to the quenched contour and size except for length, which shall equal or exceed the length of the represented studs, nuts, or bolts.	
<p><b>WB-2300 FRACTURE TOUGHNESS REQUIREMENTS FOR MATERIAL</b></p> <p><b>WB-2310 MATERIAL TO BE TOUGHNESS TESTED</b></p> <p><b>WB-2311 Material for Which Toughness Testing Is Required</b></p> <p>(2) bolting, including studs, nuts, and bolts, with a nominal size of 1 in. (25 mm) and less;</p> <p><b>WB-2320 IMPACT TEST PROCEDURES</b></p> <p><b>WB-2322 Test Specimens</b></p> <p><b>WB-2322.1 Location of Test Specimens</b></p> <p>(a) ...When the studs, nuts, or bolts are not of sufficient length, the midlength of the specimen shall be at the midlength of the studs, nuts, or bolts. The studs, nuts, or bolts selected to provide test coupon material shall be identical with respect to the quenched contour and size except for length, which shall equal or exceed the length of the represented studs, nuts, or bolts.</p>	<p><b>WC-2300 FRACTURE TOUGHNESS REQUIREMENTS FOR MATERIAL</b></p> <p><b>WC-2310 MATERIAL TO BE IMPACT TESTED</b></p> <p><b>WC-2311 Material for Which Impact Testing Is Required</b></p> <p>(2) bolting, including studs, nuts, and bolts, with a nominal size of 1 in. (25 mm) and less;</p> <p><b>WC-2320 IMPACT TEST PROCEDURES</b></p> <p><b>WC-2322 Test Specimens</b></p> <p><b>WC-2322.1 Location of Test Specimens</b></p> <p>(a) ...When the studs, nuts, or bolts are not of sufficient length, the midlength of the specimen shall be at the midlength of the studs, nuts, or bolts. The studs, nuts, or bolts selected to provide test coupon material shall be identical with respect to the quenched contour and size except for length, which shall equal or exceed the length of the represented studs, nuts, or bolts.</p>	WB and WC are identical.
<b>WB-2330 TEST REQUIREMENTS AND ACCEPTANCE STANDARDS</b>	<b>WC-2330 TEST REQUIREMENTS AND ACCEPTANCE STANDARDS</b>	WB and WC are similar except for the test temperature.

WB - BOLTING	WC - BOLTING	COMMENTS																								
<b>WB-2333 Bolting Material</b>  For bolting material, including studs, nuts, and bolts, test three $C_v$ specimens at a temperature no higher than the preload temperature or the lowest service temperature, whichever is less. All three specimens shall meet the requirements of Table WB-2333-1.  Table WB-2333-1 Required $C_v$ Values for Bolting Material	<b>WC-2332.3 Bolting Material</b>  For bolting material, including nuts, studs, and bolts, a Charpy V-notch test shall be performed. The tests shall be performed at or below the Lowest Service Metal Temperature, and all three specimens shall meet the requirements of Table WC-2332.3-1.  Table WC-2332.3-1 Required $C_v$ Values for Bolting Material Tested in Accordance with WC-2332.3																									
<table border="1"> <thead> <tr> <th>Nominal Diameter, in. (mm)</th> <th>Lateral Expansion, mils (mm)</th> <th>Absorbed Energy, ft-lb (J)</th> </tr> </thead> <tbody> <tr> <td>1 (25) or less</td> <td>No test required</td> <td>No test required</td> </tr> <tr> <td>Over 1 to 4 (25 to 100), incl.</td> <td>25 (0.64)</td> <td>No requirements</td> </tr> <tr> <td>Over 4 (100)</td> <td>25 (0.64)</td> <td>45 (61)</td> </tr> </tbody> </table>	Nominal Diameter, in. (mm)	Lateral Expansion, mils (mm)	Absorbed Energy, ft-lb (J)	1 (25) or less	No test required	No test required	Over 1 to 4 (25 to 100), incl.	25 (0.64)	No requirements	Over 4 (100)	25 (0.64)	45 (61)	<table border="1"> <thead> <tr> <th>Nominal Diameter, in. (mm)</th> <th>Lateral Expansion, mils (mm)</th> <th>Absorbed Energy, ft-lb (J)</th> </tr> </thead> <tbody> <tr> <td>1 (25) or less</td> <td>No test required</td> <td>No test required</td> </tr> <tr> <td>Over 1 through 4 (25 through 100)</td> <td>25 (0.64)</td> <td>No requirements</td> </tr> <tr> <td>Over 4 (100)</td> <td>25 (0.64)</td> <td>45 (61)</td> </tr> </tbody> </table>	Nominal Diameter, in. (mm)	Lateral Expansion, mils (mm)	Absorbed Energy, ft-lb (J)	1 (25) or less	No test required	No test required	Over 1 through 4 (25 through 100)	25 (0.64)	No requirements	Over 4 (100)	25 (0.64)	45 (61)	
Nominal Diameter, in. (mm)	Lateral Expansion, mils (mm)	Absorbed Energy, ft-lb (J)																								
1 (25) or less	No test required	No test required																								
Over 1 to 4 (25 to 100), incl.	25 (0.64)	No requirements																								
Over 4 (100)	25 (0.64)	45 (61)																								
Nominal Diameter, in. (mm)	Lateral Expansion, mils (mm)	Absorbed Energy, ft-lb (J)																								
1 (25) or less	No test required	No test required																								
Over 1 through 4 (25 through 100)	25 (0.64)	No requirements																								
Over 4 (100)	25 (0.64)	45 (61)																								
<b>WB-2340 NUMBER OF TOUGHNESS TESTS REQUIRED</b>  <b>WB-2345 Bolting Material</b>  One test shall be made for each lot of material where a lot is defined as one heat of material heat treated in one charge or as one continuous operation, not to exceed the following:	<b>WC-2340 NUMBER OF IMPACT TESTS REQUIRED</b>  <b>WC-2345 Bolting Material</b>  One test shall be made for each lot of material where a lot is defined as one heat of material heat treated in one charge or as one continuous operation, not to exceed the following:	WB and WC are identical.																								
<table> <thead> <tr> <th>Diameter</th> <th>Weight</th> </tr> </thead> <tbody> <tr> <td>1-3/4 in. (44 mm) and less</td> <td>1,500 lb (680 kg)</td> </tr> <tr> <td>Over 1-3/4 in. to 2-1/2 in. (44 mm to 64 mm)</td> <td>3,000 lb (1350 kg)</td> </tr> <tr> <td>Over 2-1/2 in. to 5 in. (6 mm to 127 mm)</td> <td>6,000 lb (2700 kg)</td> </tr> <tr> <td>Over 5 in. (127 mm)</td> <td>10,000 lb (4500 kg)</td> </tr> </tbody> </table>	Diameter	Weight	1-3/4 in. (44 mm) and less	1,500 lb (680 kg)	Over 1-3/4 in. to 2-1/2 in. (44 mm to 64 mm)	3,000 lb (1350 kg)	Over 2-1/2 in. to 5 in. (6 mm to 127 mm)	6,000 lb (2700 kg)	Over 5 in. (127 mm)	10,000 lb (4500 kg)	<table> <thead> <tr> <th>Diameter</th> <th>Weight</th> </tr> </thead> <tbody> <tr> <td>1-3/4 in. (44 mm) and less</td> <td>1,500 lb (680 kg)</td> </tr> <tr> <td>Over 1-3/4 in. to 2-1/2 in. (44 mm to 64 mm)</td> <td>3,000 lb (1350 kg)</td> </tr> <tr> <td>Over 2-1/2 in. to 5 in. (6 mm to 127 mm)</td> <td>6,000 lb (2700 kg)</td> </tr> <tr> <td>Over 5 in. (127 mm)</td> <td>10,000 lb (4500 kg)</td> </tr> </tbody> </table>	Diameter	Weight	1-3/4 in. (44 mm) and less	1,500 lb (680 kg)	Over 1-3/4 in. to 2-1/2 in. (44 mm to 64 mm)	3,000 lb (1350 kg)	Over 2-1/2 in. to 5 in. (6 mm to 127 mm)	6,000 lb (2700 kg)	Over 5 in. (127 mm)	10,000 lb (4500 kg)					
Diameter	Weight																									
1-3/4 in. (44 mm) and less	1,500 lb (680 kg)																									
Over 1-3/4 in. to 2-1/2 in. (44 mm to 64 mm)	3,000 lb (1350 kg)																									
Over 2-1/2 in. to 5 in. (6 mm to 127 mm)	6,000 lb (2700 kg)																									
Over 5 in. (127 mm)	10,000 lb (4500 kg)																									
Diameter	Weight																									
1-3/4 in. (44 mm) and less	1,500 lb (680 kg)																									
Over 1-3/4 in. to 2-1/2 in. (44 mm to 64 mm)	3,000 lb (1350 kg)																									
Over 2-1/2 in. to 5 in. (6 mm to 127 mm)	6,000 lb (2700 kg)																									
Over 5 in. (127 mm)	10,000 lb (4500 kg)																									

WB - BOLTING	WC - BOLTING	COMMENTS
<p><b>WB-2500 EXAMINATION AND REPAIR OF CONTAINMENT MATERIAL</b></p> <p><b>WB-2580 EXAMINATION OF BOLTS, STUDS, AND NUTS</b></p> <p><b>WB-2581 Requirements</b></p> <p>ALL bolting material shall be visually examined in accordance with WB-2582. Normal sizes greater than 1 in. (25 mm) shall be examined by either the magnetic particle or the liquid penetrant method. In addition, nominal sizes greater than 2 in. (50 mm) but not over 4 in. (100 mm) shall be examined by the ultrasonic method in accordance with WB-2585 and nominal sizes greater than 4 in. (100 mm) shall be examined by the ultrasonic method in accordance with both WB-2585 and WB-2586.</p> <p><b>WB-2582 Visual Examination</b></p> <p>The areas of threads, shanks, and heads of final machined parts shall be visually examined. The requirements of WB-5520 do not apply to personnel performing this examination. Harmful discontinuities such as laps, seams, or cracks that would be detrimental to the intended service are unacceptable.</p> <p><b>WB-2583 Magnetic Particle Examination (for Ferritic Steel Bolting Material Only)</b></p> <p><b>WB-2583.1 Examination Procedures.</b> All bolts, studs, and nuts greater than 1 in. (25 mm) nominal bolt size shall be examined by the magnetic particle method in accordance with ASTM A 275. If desired, the supplier may perform liquid penetrant examination in accordance with WB-2584 instead of magnetic particle examination. Such examination shall be performed on the finished component after threading or on the materials stock at approximately the finished diameter before threading and after heading (if involved).</p>	<p><b>WC-2500 EXAMINATION AND REPAIR OF CONTAINMENT MATERIAL</b></p> <p><b>WC-2580 EXAMINATION OF BOLTS, STUDS, AND NUTS</b></p> <p><b>WC-2581 Requirements</b></p> <p>ALL bolting material shall be visually examined in accordance with WC-2582.</p> <p><b>WC-2582 Visual Examination</b></p> <p>Visual examination shall be applied to the areas of threads, shanks, and heads of final machined parts. Harmful discontinuities such as laps, seams, or cracks that would be detrimental to the intended service are unacceptable.</p>	WB and WC are significantly different.

WB - BOLTING	WC - BOLTING	COMMENTS
<p><b>WB-2583.2 Evaluation of Indications</b></p> <p>(a) All indications shall be evaluated in terms of the acceptance standards. Linear indications are those indications in which the length is more than three times the width. Rounded indications are those which are circular or elliptical with the length equal to or less than three times the width.</p> <p>(b) All indications are not necessarily relevant: leakage of magnetic fields and permeability variations may produce indications that are not relevant to the detection of unacceptable discontinuities. Indications with major dimensions of 1/16 in. (1.5 mm) or less are not relevant.</p> <p>(c) Any indication that is believed to be nonrelevant, and that is larger than acceptable, shall be considered to be a defect and shall be reexamined after light surface conditioning.</p> <p>(d) Any indication observed during such reexamination shall be considered relevant and shall be evaluated in terms of the acceptance standards.</p> <p>(e) As an alternative to magnetic particle reexamination, other nondestructive examination means (such as liquid penetrant examination for surface discontinuities) may be used to determine relevancy.</p> <p><b>WB-2583.3 Acceptance Standard.</b> Linear nonaxial indications are unacceptable. Linear axial indications greater than 1 in. (25 mm) in length are unacceptable.</p> <p><b>WB-2584 Liquid Penetrant Examination</b></p> <p><b>WB-2584.1 Examination Procedure.</b> All bolts, studs, and nuts greater than 1 in. (25 mm) nominal bolt size shall be examined by a liquid penetrant method in accordance with the methods of Section V, Article 6. Such examination shall be performed on the finished component after threading or on the materials stock at approximately the finished diameter before threading and after</p>		

WB - BOLTING	WC - BOLTING	COMMENTS
<p>heading (if involved).</p> <p><b>WB-2584.2 Evaluation of Indications.</b> All indications shall be evaluated in terms of the acceptance standards. Linear indications are those indications in which the length is more than three times the width. Rounded indications are those which are circular to elliptical with the length equal to or less than three times the width. All penetrant indications are not necessarily relevant. Surface imperfections such as machining marks and scratches may produce indications that are nonrelevant to the detection of unacceptable discontinuities. Broad areas of pigmentation, which could mask indications of defects, are unacceptable. Indications with major dimensions of 1/16 in. (1.5 mm) or less are not relevant. Any indication that is believed to be nonrelevant, and that is larger than acceptable, shall be considered to be a defect and shall be reexamined after light surface conditioning. Any area of pigmentation also shall be reexamined after recleaning or light surface conditioning, as appropriate. Any indication observed during such reexamination shall be considered relevant and shall be evaluated in terms of the acceptance standards.</p> <p><b>WB-2584.3 Acceptance Standard.</b> Linear nonaxial indications are unacceptable. Linear axial indications greater than 1 in. (25 mm) long are unacceptable.</p> <p><b>WB-2585 Ultrasonic Examination for Sizes Greater Than 2 in. (50 mm)</b></p> <p>All bolts, studs, and nuts greater than 2 in. (50 mm) nominal bolt size shall be ultrasonically examined over the entire cylindrical surface prior to threading in accordance with the following requirements:</p> <p><b>WB-2585.1 Ultrasonic Method.</b> Examination shall be carried out by the straight-beam, radial-scan method in accordance with Section V, Article 23, SA-388.</p>		

WB - BOLTING	WC - BOLTING	COMMENTS
<p><b>WB-2585.2 Examination Procedures.</b> Examination shall be performed at a nominal frequency of 2.25 MHz with a search unit area not to exceed 1 in.<sup>2</sup> (650 mm<sup>2</sup>).</p> <p><b>WB-2585.3 Calibration of Equipment.</b> Calibration sensitivity shall be established by adjustment of the instrument so that the first back reflection is 75% to 90% of full-screen height.</p> <p><b>WB-2585.4 Acceptance Standard.</b> Any discontinuity that causes an indication in excess of 20% of the height of the first back reflection or any discontinuity that prevents the production of a first back reflection of 50% of the calibration amplitude is not acceptable.</p> <p><b>WB-2586 Ultrasonic Examination for Sizes Over 4 in. (100 mm)</b></p> <p>In addition to the requirements of WB-2585, all bolts, studs, and nuts over 4 in. (100 mm) nominal bolt size shall be ultrasonically examined over the entire surface of each end before or after threading in accordance with the following requirements:</p> <p><b>WB-2586.1 Ultrasonic Method.</b> Examination shall be carried out by the straight-beam, longitudinal-scan method.</p> <p><b>WB-2586.2 Examination Procedure.</b> Examination shall be performed at a nominal frequency of 2.25 MHz with a search unit having a circular cross section with a diameter not less than <math>\frac{1}{2}</math> in. (13 mm) nor more than 1-1/8 in/ (29 mm).</p> <p><b>WB-2586.3 Calibration of Equipment.</b> Calibration shall be established on a test bar of the same nominal composition and diameter as the production part and a minimum of one-half of the length. A 3/8 in. (10 mm) diameter by 3 in. (75 mm) deep flat-bottom hole shall be drilled in one end of the bar and plugged to full depth. A distance-amplitude curve shall be established by scanning from both ends of the test bar.</p>		

WB - BOLTING	WC - BOLTING	COMMENTS
<p><b>WB-2586.4 Acceptance Standard.</b> Any discontinuity that causes an indication in excess of that produced by the calibration hole in the reference specimen as corrected by the distance-amplitude curve is not acceptable.</p> <p><b>WB-2587 Time of Examination</b> Acceptance examinations shall be performed after the final heat treatment required by the basic material specification.</p> <p><b>WB-2588 Elimination of Surface Defects</b> Unacceptable surface defects on finished bolts, studs, and nuts are not permitted, and are cause for rejection.</p> <p><b>WB-2589 Repair by Welding</b> Weld repairs of bolts, studs, and nuts are not permitted.</p>		

WB - BOLTING	WC - BOLTING	COMMENTS
ARTICLE WB-3000 DESIGN	ARTICLE WC-3000 DESIGN	
WB-3100 GENERAL DESIGN  WB-3130 GENERAL DESIGN RULES  WB-3134 Leak Tightness  The leak tightness requirements for each containment shall be set forth in the Design Specification.	WC-3100 GENERAL DESIGN  WC-3130 GENERAL DESIGN RULES  N/A	No similar paragraph exists in WC.
WB-3200 DESIGN RULES FOR CONTAINMENTS  WB-3220 STRESS LIMITS FOR OTHER THAN BOLTS  N/A	WC-3200 DESIGN RULES FOR CONTAINMENTS  WC-3220 DESIGN CONSIDERATIONS  WC-3225 Flat Heads and Covers  Discusses both welded and bolted flat heads and covers, but does not address the design of the bolts  WC-3225.1 Nomenclature  Addresses nomenclature applicable to flat heads and closures.	No similar paragraph exists in WB.
N/A	WC-3225.2 Equations for Minimum Thickness  Provides equations for minimum thickness of flat heads and closures.	No similar paragraph exists in WB.
N/A	Fig. WC-3225-2	No similar paragraph exists in WB.

WB - BOLTING	WC - BOLTING	COMMENTS
	Provides illustrations of some acceptable types of unstayed flat heads and covers.	
<p><b>WB-3230 STRESS LIMITS FOR BOLTS</b></p> <p><i>This paragraph discusses general aspects of stress limits for bolts.</i></p> <p>The evaluation of bolting requires a number of analysis considerations, including (a) through (f) below and the criteria specified in this subsubarticle for the loads imposed.</p> <p>(a) When gaskets are used for preservice testing only, the design is satisfactory if WB-3231 requirements are satisfied for <math>m = y = 0</math>, and the requirements of WB-3232 are satisfied when the appropriate <math>m</math> and <math>y</math> factors are used for the test gasket.</p> <p>(b) The membrane and bending stresses in the bolt produced by thermal expansion due to differences in the temperature or thermal expansion coefficients shall be treated as primary stresses in bolting analysis.</p> <p>(c) The bolting analysis shall consider the effects of loading eccentricities due to puncture loads and eccentric impact loads.</p> <p>(d) The bolting analysis shall consider prying effects, which cause amplification of the bolt loads due to rotation of the closure surfaces.</p> <p>(e) Bolting analysis shall consider bolt preload application methodology and resulting bolt forces.</p> <p>(f) Gasket characteristics and leak tightness requirements shall be considered in the bolting analysis.</p>	N/A	No similar paragraph exists in WC.

WB - BOLTING	WC - BOLTING	COMMENTS
<p><b>WB-3231 Design Limits</b></p> <p><i>This paragraph provides instructions to determine the number and cross-sectional area of bolts.</i></p> <p>The number and cross-sectional area of bolts required to resist the Design Pressure shall be determined in accordance with the procedures of Division 1, Appendix E, using the larger of the bolt loads, given by the equations of Division 1, Appendix E, as a Design Mechanical Load.</p> <p>The stress limits shall be the values given in Section II, Part D, Subpart 1, Table 4 for bolting material.</p>	N/A	No similar paragraph exists in WC.
<p><b>WB-3232 Level A Service Limits</b></p> <p><i>This paragraph addresses stresses in bolts for Level A Service Limits.</i></p> <p>Actual stresses in bolts, such as those produced by the combination of preload, pressure, and differential thermal expansion, may be higher than the values given in Section II, Part D, Subpart 1, Table 4.</p>	N/A	No similar paragraph exists in WC.
<p><b>WB-3232.1 Average Stress</b></p> <p>Provides requirements to handle average bolt stresses.</p> <p>The maximum value of stress, averaged across the bolt cross section and neglecting stress concentrations, shall not exceed two times the stress values of Section II, Part D, Subpart 1, Table 4.</p>	N/A	No similar paragraph exists in WC.

WB - BOLTING	WC - BOLTING	COMMENTS
<p><b>WB-3232.2 Shear Stress:</b></p> <p>Provides requirements to handle average bolt shear stresses.</p> <p>The average bolt shear stress expressed in terms of available shear stress area shall not exceed 1.2 <math>S_m</math> (at temperature) from Section II, Part D, Subpart 1, Table 4.</p>	N/A	No similar paragraph exists in WC.
<p><b>WB-3232.3 Maximum Stress</b></p> <p>Provides requirements for handling maximum stress in bolts.</p> <p>The maximum value of stress, except as restricted by WB-3232.4(b), at the periphery of the bolt cross section resulting from direct tension plus bending, and neglecting stress concentrations, shall not exceed three times the stress values of Section II, Part D, Subpart 1, Table 4. Stress intensity, rather than maximum stress, shall be limited to this value when the bolts are tightened by methods other than heaters, stretchers, or other means that minimize residual torsion.</p>	N/A	No similar paragraph exists in WC.
<p><b>WB-3232.4 Fatigue Analyses of Bolts</b></p> <p>Provides requirements for handling fatigue analyses in bolts. Contains parts (a) through (e).</p> <p>Unless the components on which they are installed meet all the conditions of WB-3222.9(d) and thus require no fatigue analysis, the suitability of bolts for cyclic service shall be determined in accordance with the procedures of (a) through (e) below.</p> <p>Thermal stress ratchet shall be evaluated in accordance with WB-3222.9(a).</p> <p>(a) <i>Bolting Having Less Than 100.0 ksi (689 MPa) Tensile</i></p>	N/A	No similar paragraph exists in WC.

WB - BOLTING	WC - BOLTING	COMMENTS
<p><i>Strength.</i> Bolts made of material which has specified minimum tensile strength of less than 100.0 ksi (689 MPa) shall be evaluated for cyclic service by the methods of WB-3222.9(e), using the applicable design fatigue curve of Division 1, Appendix I, Figs. 1-9.0 and an appropriate fatigue strength reduction factor [WB-3232.4(c)].</p> <p>(b) <i>High Strength Alloy Steel Bolting.</i> High strength alloy steel bolts and studs may be evaluated for cyclic service by the methods of WB-3222.9(e) using the design fatigue curve of Division 1, Appendix I, Figs. 1-9.4 provided:</p> <ul style="list-style-type: none"> <li>(1) the maximum value of the stress (WB-3232.3) at the periphery of the bolt cross section, resulting from direct tension plus bending and neglecting stress concentration, shall not exceed <math>2.7Sm</math> if the higher of the two fatigue design curves given in Division 1, Appendix I, Figs. 1-9.4 is used. The <math>2Sm</math> limit for direct tension is unchanged.</li> <li>(2) threads shall be of a Vee-type having a minimum thread root radius no smaller than 0.003 in. (0.08 mm).</li> <li>(3) fillet radii at the end of the shank shall be such that the ratio of fillet radius to shank diameter is not less than 0.060.</li> </ul> <p>(c) <i>Fatigue Strength Reduction Factor (WB 3213.17).</i> Unless it can be shown by analysis or tests that a lower value is appropriate, the fatigue strength reduction factor used in the fatigue evaluation of threaded members shall be not less than 4.0. However, when applying the rules of WB-3232.4(b) for high strength alloy steel bolts, the value used shall be not less than 4.0.</p> <p>(d) <i>Effect of Elastic Modulus.</i> Multiply <math>S_{alt}</math> (as determined in WB-3216.1 or WB-3216.2) by the ratio of the modulus of elasticity given on the design fatigue curve to the value of</p>		

WB - BOLTING	WC - BOLTING	COMMENTS
<p>the modulus of elasticity used in the analysis. Enter the applicable design fatigue curve at this value on the ordinate axis and find the corresponding number of cycles on the abscissa. If the cyclic service being considered is the only one which produces significant fluctuating stresses, this is the allowable number of cycles.</p> <p>(e) <i>Cumulative Damage.</i> The bolts shall be acceptable for the specified cyclic application of loads and thermal stresses provided the cumulative usage factor U, as determined in WB-3222.9(e)(5), does not exceed 1.0.</p>		
<p><b>WB-3234 Level D Service Limits</b></p> <p>This paragraph addresses stresses in bolts for Level A Service Limits.</p> <p>(a) The rules contained in Division 1, Appendix F may be used in evaluating loadings for which Level D Service Limits are specified, independently of all other loadings.</p> <p>(b) If leak tightness of the closure is required by the Design Specification, the analysis of the bolting shall demonstrate that no yielding occurs in the bolt or sealing surface materials. This requirement may be satisfied by using the rules of WB-3232.</p>	N/A	No similar paragraph exists in WC.
<p><b>WB-3235 Testing Limits</b></p> <p>Bolts shall not yield for test conditions.</p>	N/A	No similar paragraph exists in WC.
<p><b>WB-3236 Design Stress Intensity Values</b></p> <p>States where Design Stress intensity values may be found.</p>	N/A	No similar paragraph exists in WC.

WB - BOLTING	WC - BOLTING	COMMENTS
The design stress intensity values $Sm$ are given in Section II, Part D, Subpart 1, Table 4 for bolting. Values for intermediate temperature may be found by interpolation.		
ARTICLE WB-4000 FABRICATION	ARTICLE WC-4000 FABRICATION	
<b>WB-4700 MECHANICAL JOINTS</b>	<b>WC-4700 MECHANICAL JOINTS</b>	WB and WC are identical.
<b>WB-4710 BOLTING AND THREADING</b>	<b>WC-4710 BOLTING AND THREADING</b>	
<b>WB-4711 Thread Engagement</b>  The threads of all bolts or studs shall be engaged in accordance with the design.	<b>WC-4711 Thread Engagement:</b>  The threads of all bolts or studs shall be engaged in accordance with the design.	
<b>WB-4712 Thread Lubricants</b>  Any lubricant or compound used in threaded joints shall be suitable for the service conditions and shall not react unfavorably with either the service fluid or any <u>containment</u> material in the system.	<b>WC-4712 Thread Lubricants</b>  Any lubricant or compound used in threaded joints shall be suitable for the service conditions and shall not react unfavorably with either the service fluid or any <u>component</u> material in the system.	WB and WC are identical except that the word <u>containment</u> is used in WB, and the word <u>component</u> is used in WC. This difference is acceptable.
<b>WB-4713 Removal of Thread Lubricants</b>  All threading lubricants or compounds shall be removed from surfaces which are to be seal welded.	<b>WC-4713 Removal of Thread Lubricants</b>  All threading lubricants or compounds shall be removed from surfaces which are to be seal welded.	WB and WC are identical.
<b>WB-4720 Bolting Flanged Joints</b>  This paragraph discusses bolting of gasketed flange joints.	<b>WC-4720 Bolting Flanged Joints</b>  This paragraph discusses bolting of gasketed flange joints.	WB and WC are identical.

WB - BOLTING	WC - BOLTING	COMMENTS
<p>In bolting gasketed flanged joints, the contact faces of the flanges shall bear uniformly on the gasket and the gasket shall be properly compressed in accordance with the design principles applicable to the type of gasket used.</p> <p>All flanged joints shall be made up with relatively uniform bolt stress.</p>	<p>In bolting gasketed flanged joints, the contact faces of the flanges shall bear uniformly on the gasket and the gasket shall be properly compressed in accordance with the design principles applicable to the type of gasket used.</p> <p>All flanged joints shall be made up with relatively uniform bolt stress.</p>	

**Table 2 Comparison of Requirements for Design Based on Stress Analysis of Bolts in ASME Section III, Subsection WB-3000 and Appendix XIII**

	<b>Article WB-3200</b>	<b>Article XIII-1100</b>
Stress Limits & bolt and gasket requirements	<p><b>WB-3230 Stress Limits for Bolts</b></p> <p>The evaluation of bolting requires a number of analysis considerations, including (a) through (f) below and the criteria specified in this subsubarticle for the loads imposed.</p> <p>(a) When gaskets are used for preservice testing only, the design is satisfactory if WB-3231 requirements are satisfied for <math>m = y = 0</math>, and the requirements of WB-3232 are satisfied when the appropriate <math>m</math> and <math>y</math> factors are used for the test gasket.</p> <p><b>WB-3231 Design Limits</b></p> <p>The number and cross-sectional area of bolts required to resist the Design Pressure shall be determined in accordance with the procedures of Division 1, Appendix E, using the larger of the bolt loads, given by the equations of Division 1, Appendix E, as a Design Mechanical Load.</p> <p>The stress limits shall be the values given in Section II, Part D, Subpart 1, Table 4 for bolting material.</p>	<p><b>XIII-1180 BOLTING</b></p> <p><b>XIII-1181 Bolt and Gasket Requirements</b></p> <p>(a) The number and cross-sectional area of bolts required to resist internal pressure shall be determined in accordance with the procedures of Mandatory Appendix XI. The allowable bolt design stresses, as used in the equations of Mandatory Appendix XI, shall be the values given in Section II, part D, Subpart 1, Table 4 for bolting materials. When sealing is affected by a seal weld instead of a gasket, the gasket factor <math>m</math> and the minimum design seating stress <math>y</math> may be taken as zero.</p> <p>(b) When gaskets are used for preservice testing only, the design is satisfactory if the above requirements are satisfied for <math>m=y=0</math> and the requirements of XIII-1182 are satisfied when the appropriate <math>m</math> and <math>y</math> are used for test gasket.</p>
Maximum Service Stress	<p><b>WB-3232.1 Average Stress</b></p> <p>The maximum value of stress, averaged across the bolt cross section and neglecting stress concentrations, shall not exceed two times the stress values of Section II, Part D, Subpart 1, Table 4.</p> <p><b>WB-3232.3 Maximum Stress</b></p>	<p><b>XIII-1182 Allowable Maximum Service Stresses in Bolts</b></p> <p>It is recognized that actual service stresses in bolts, such as those produced by the combination of preload, pressure, and differential thermal expansion, may be higher than the values given in Section II,</p>

	<p>Provides requirements for handling maximum stress in bolts.</p> <p>The maximum value of stress, except as restricted by WB-3232.4(b), at the periphery of the bolt cross section resulting from direct tension plus bending and neglecting stress concentrations shall not exceed three times the stress values of Section II, Part D, Subpart 1, Table 4. Stress intensity, rather than maximum stress, shall be limited to this value when the bolts are tightened by methods other than heaters, stretchers, or other means that minimize residual torsion.</p>	<p>Part D, Subpart 1, Table 4. The maximum of such service stress, averaged across the bolt cross section and neglecting stress concentrations, shall not exceed two times the stress values of Section II, Part 1, Table 4. Except as restricted by XIV-1322(b), the maximum value of such service stress as the periphery of the bolt cross section resulting from direct tension plus bending and neglecting stress concentrations shall not exceed three times the stress values of Section II, Part D, Subpart 1, Table 4. Stress intensity, rather than maximum stress, shall be limited to this value when the bolts are tightened by methods other than heaters, stretchers, or other means that minimize residual torsion.</p>
--	---	---

**Table 3 Comparison of Requirements for Analysis of Cyclic Service of Bolts in ASME Section III, Subsection WB-3000 and Appendix XIV**

	<b>Article WB-3232.4</b>	<b>Article XIV-1300</b>
Bolts with less than 100 ksi tensile strength	WB-3232.4(a) Requires appropriate fatigue strength reduction factor	Requires that fatigue strength reduction factor not be less than 4
High-strength bolting	WB-3232.4(b) does not specify material	Specifies materials: SA-193 Grade B7 or B-16 SA-320 Grade L-43 SA-540 Grades B-23 and B-24
Maximum value of stress intensity at the periphery of bolt cross section	WB-3232.4(b)(1)	XIV-1322(b) The requirements are exactly the same.
Thread type and fillet radii	WB-3232.4(b)(2) and (3)	XIV-1322(c) and (d) The requirements are exactly the same.
Fatigue strength reduction factor	WB-3232.4(c) <sup>1</sup>	XIV-1324 Both articles require that the factor not be less than 4 unless a lower value can be justified.
Effect of elastic modulus	WB-3232.4(d)	Not considered.
Cumulative damage	WB-3232.4(f)	XIV-1323 The requirements are exactly the same.

<sup>1</sup>The last statement in WB-3232.4(c) is confusing. It states, “However, when applying the rules of WB-3232.4(b) above for high strength alloy steel bolts, the value used shall not be less than 4.0.” This statement is not included in the above comparison.

# FCT Quality Assurance Program Document

## Appendix E FCT Document Cover Sheet

Name/Title of Deliverable/Milestone

Used Fuel Disposition (UFD) Year End Letter Report – FY2012

Work Package Title and Number

ST Transportation - ANL

Work Package WBS Number

FT-12AN081301

Responsible Work Package Manager

Yung Liu

(Name/Signature)

Date Submitted 9/11/2012

Quality Rigor Level for Deliverable/Milestone	<input checked="" type="checkbox"/> QRL-3	<input type="checkbox"/> QRL-2	<input type="checkbox"/> QRL-1	<input type="checkbox"/> N/A*
			<input type="checkbox"/> Nuclear Data	

This deliverable was prepared in accordance with

Argonne National Laboratory

*(Participant/National Laboratory Name)*

QA program which meets the requirements of

DOE Order 414.1       NQA-1-2000

### This Deliverable was subjected to:

Technical Review

Peer Review

### Technical Review (TR)

### Peer Review (PR)

### Review Documentation Provided

Signed TR Report or,

Signed PR Report or,

Signed TR Concurrence Sheet or,

Signed PR Concurrence Sheet or,

Signature of TR Reviewer(s) below

Signature of PR Reviewer(s) below

### Name and Signature of Reviewers

Yung Liu

\_\_\_\_\_  
\_\_\_\_\_  
\_\_\_\_\_

\*Note: In some cases there may be a milestone where an item is being fabricated, maintenance is being performed on a facility, or a document is being issued through a formal document control process where it specifically calls out a formal review of the document. In these cases, documentation (e.g., inspection report, maintenance request, work planning package documentation or the documented review of the issued document through the document control process) of the completion of the activity along with the Document Cover Sheet is sufficient to demonstrate achieving the milestone. QRL for such milestones may be also be marked N/A in the work package provided the work package clearly specifies the requirement to use the Document Cover Sheet and provide supporting documentation.

## **APPENDIX B**

### **Cladding Embrittlement Concerns for Storage and Transportation of High-Burnup Fuel**

# **Cladding Embrittlement Concerns for Storage and Transportation of High-Burnup Fuel**

M.C. Billone and Y.Y. Liu  
Argonne National Laboratory  
September 10, 2012

Structural analyses of high-burnup fuel require cladding mechanical properties and failure limits to assess fuel behavior during long-term dry cask storage and transportation. Pre-storage drying-transfer operations and early stage storage subject cladding to higher temperatures and much higher hoop stresses relative to in-reactor operation and pool storage. Under these conditions, radial hydrides may precipitate during slow cooling and provide an additional embrittlement mechanism as the cladding temperature decreases below the ductile-to-brittle transition temperature (DBTT).

In Interim Staff Guidance – 11, Revision 3 (ISG-11 Rev. 3), the NRC recommends a peak cladding temperature limit of 400°C for drying-transfer operations and storage of used fuel in storage and transport casks containing high-burnup fuel [1]. Limits are also placed on the number of drying cycles and the temperature drop per cycle. One concern for high-burnup cladding is the possible precipitation of radial hydrides, which could embrittle cladding in response to tensile hoop stress caused by the internal pressure loading. Limits established in ISG-11 Rev. 3 relied on data available prior to 2003, which were primarily for low-burnup and non-irradiated/pre-hydrided Zircaloy-4. At the time ISG-11 Rev. 3 was issued, NRC recognized that data for all high-burnup cladding alloys were needed to determine the extent of radial-hydride embrittlement under conditions relevant to drying-transfer operations and storage. Data generated since 2003, mostly at Argonne, indicate that limits imposed by ISG-11 Rev. 3 do not protect high-burnup cladding from embrittlement due to radial hydrides. Recent NRC reviews of applications for license renewal of the Prairie Island ISFSI and Amendment 5 of the CoC for Transnuclear MP-197 have raised concerns for long-term storage and transportation of high-burnup fuel. The issues are summarized in “Compatibility of Requirements for Storage and Transportation of Spent Nuclear Fuel (Retrievability, Cladding Integrity, and Safe Handling),” — a summary paper presented at the NRC Public Meeting to obtain stakeholder feedback on enhancements to the licensing and inspection programs for spent fuel storage and transportation under 10 CFR Parts 71 and 72 [2]. A major concern is whether or not the high-burnup fuel will maintain cladding integrity and be readily retrievable after more than 20 years of storage. License approvals for the transport of high-burnup fuel have been delayed because of a lack of data on high-burnup fuel cladding embrittlement after more than 20 years of storage, which corresponds to peak cladding temperatures of  $\approx$ 200°C or less.

## **Status of the Database for High-Burnup Cladding Embrittlement**

Argonne has developed a test protocol for studying high-burnup cladding embrittlement that has been approved by NRC. Experimentally, the protocol involves two steps: (1) radial-hydride treatment (RHT), during which high-burnup cladding is exposed to simulated drying-storage temperature and hoop stress conditions, including slow cooling, and (2) a ring compression test (RCT), for which a sample ring from the RHT high-burnup cladding is compressed to determine strength and ductility as function of test temperature. The RCT is used as a ductility screening test to simulate pinch-type loading on the high-burnup cladding that occurs during normal conditions of cask transport and/or drop accidents. The protocol was used to generate the DBTT data for high-burnup Zircaloy-4 and ZIRLO™ [3] (sponsored by NRC) and high-burnup M5® (sponsored by DOE) [4]. Under DOE-sponsored research, Argonne has also generated baseline properties for the strength and ductility of as-irradiated (i.e., pre-drying) Zry-4,

ZIRLO™, and M5® that are important not only to determine the degrading effects of drying and early stage storage, but also to serve as references for other high-burnup cladding alloys in future studies.

Argonne data were generated for the peak cladding temperature (400°C) recommended in ISG-11 (Rev. 3) for drying-transfer operations and storage. Peak cladding hoop stresses at 400°C were 110 MPa and 140 MPa, which are in the intermediate range of the 80–160 MPa characteristic of high-burnup PWR fuel rods. The upper limit is based on the industry technical specification limit of  $\approx$ 3200 psi (22 MPa) internal pressure for in-reactor operation, which is intended to prevent cladding liftoff from the fuel. The internal gas pressure is due to as-fabricated helium fill gas, fission gas release (increases with burnup), and helium release from certain burnable poisons (e.g., ZrB<sub>2</sub> coating used in Westinghouse's Integral Fuel Burnable Absorber [IFBA] design).

Figure 1 shows the hydride distribution and orientation in high-burnup ZIRLO™ before (Fig. 1a) and after (Fig. 1b) subjecting the cladding to slow cooling (5°C/h) from 400°C and decreasing tensile hoop stress from 140 MPa. Hydrogen contents for both samples were high (530 wppm and 650 wppm). The extent of radial-hydride precipitation (extending through 80% of the wall thickness) following slow cooling is quite dramatic. Figure 2 compares the ductility and strength of as-irradiated (tested at 30°C) and RHT high-burnup cladding (tested at 150°C) in ring compression tests. Even with the elevated test temperature, the ductility decreased from 7% to 0% and the strength (based on the 1<sup>st</sup> load-drop) decreased by 60% as a result of exposure to simulated drying-storage conditions. Furthermore, RHT high-burnup ZIRLO™ failed (>50% wall crack) during elastic loading and exhibited no plastic deformation. The DBTT for high-burnup ZIRLO™ is clearly >150°C for a peak drying-storage stress of 140 MPa. In a second set of tests, the simulated drying-storage peak stress was reduced to 110 MPa. At the lower stress level, the DBTT decreased by about 60°C to 125°C.

Figure 3 shows the hydride distribution and orientation in high-burnup M5® before (Fig. 3a) and after (Fig. 3b) subjecting the cladding to 400°C and 140 MPa and slow cooling (5°C/h). Hydrogen contents for both samples were low (76 wppm and 94 wppm), which is characteristic of high-burnup M5®. The hydrides in Fig. 3a are oriented primarily in the circumferential direction, with some of the hydrides oriented in the radial direction. During cooling from simulated drying-storage conditions, long radial hydrides precipitated (see Fig. 3b). Figure 4 compares the ductility and strength of as-irradiated (tested at 26°C) and RHT (tested at 60°C) high-burnup M5® in ring compression tests. The ductility decreased from >10% to 0%, and the strength (based on the 1<sup>st</sup> load-drop) decreased by about 50% as a result of simulated drying-storage conditions. Furthermore, the RHT high-burnup M5® failed (>50% wall crack) during elastic loading and exhibited no plastic deformation. Figure 5 shows the extensive cracking in RHT M5® for the 60°C RCT temperature. Ductility was retained at 90°C RCT temperature. The DBTT for high-burnup M5® was about 80°C for a peak drying-storage stress of 140 MPa. Lowering the peak drying-storage stress to 110 MPa decreased the DBTT by only 10°C, as illustrated in Figure 6.

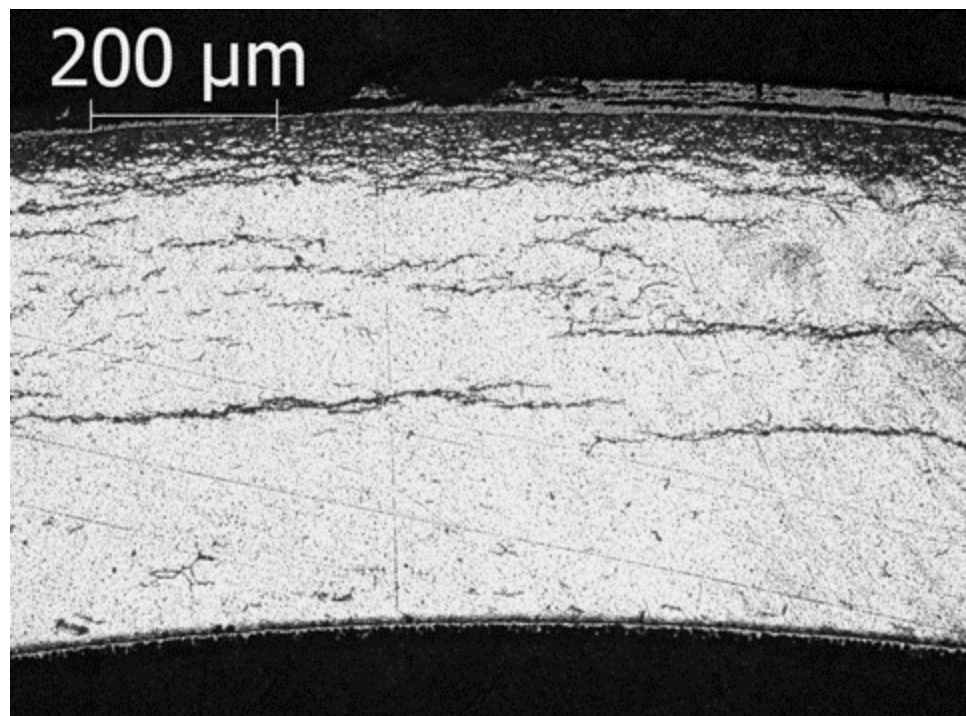
Figures 7 and 8 show DBTT curves for three high-burnup (HB) PWR cladding alloys following RHT at 400°C and peak hoop stresses of 140 MPa and 110 MPa, respectively. "HB Clad C" data are from the DOE-sponsored work using HB M5® [4]. NRC will release identification of and data for "HB Clad A" and "HB Clad B" after Ref. 5 is accepted for publication (the paper was submitted in June 2012). For the 140-MPa case (Fig. 7), the DBTT values are about 55°C, 185°C, and 80°C for HB Clad alloys A, B, and C, respectively. Lowering the peak RHT hoop stress to 110 MPa (Fig. 8) decreased the DBTT values to <25°C, 125°C, and 70°C, respectively. The effect of the peak tensile hoop stress is most pronounced for HB Clad alloy B; the DBTT drops from 185°C to 125°C, which is too high for transport and/or retrieval. The DBTTs for HB Clad alloys A and C are lower than that of HB Clad alloy B, but they are still above ambient.

To complete the DBTT curves for the relevant range of drying-storage peak temperatures, data are needed for PWR high-burnup cladding alloys subjected to 80 and 160 MPa and BWR high-burnup Zry-2 subjected to 60–120 MPa at the ISG-11 (Rev. 3) -recommended limit of 400°C and with limited temperature cycling. As cladding temperatures are likely to be <400°C by using current cask loading and drying practices, RCT tests should be repeated at 350°C for PWR high-burnup cladding (80–160 MPa) and for BWR high-burnup cladding alloys (at 60–120 MPa). Specific test matrices can be found in the appendix of Ref. 4. The goal of the planned Argonne RCT testing and modeling is to define the parameter space, mainly temperature and hoop stress, to minimize radial-hydride embrittlement such that the DBTT could fall below ambient for each HB Clad alloy.

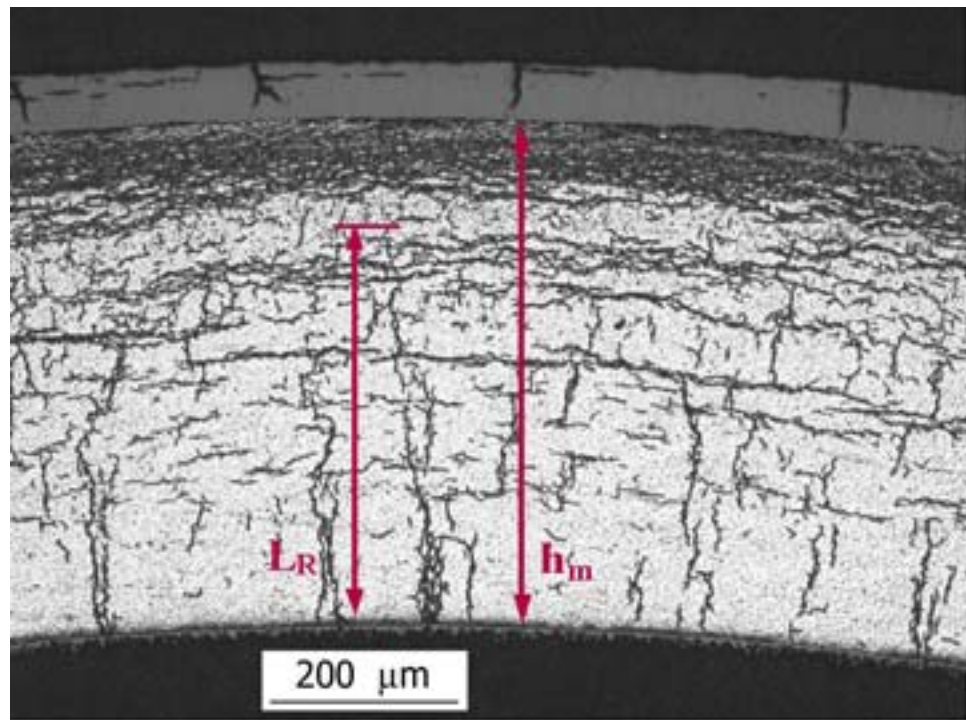
Note that from the load-displacement curves in the ring compression tests, one can obtain stress and strain mechanical properties and failure limits above and below the DBTT for each HB Clad alloy. Such data are directly applicable in the structural analyses to support license applications for long-term storage and transportation of high-burnup fuels.

## References

- 1) Nuclear Regulatory Commission 2003 Interim Staff Guidance (ISG)-11, Revision 3, “Cladding Considerations for the Transportation and Storage of Spent Fuel,” November 2003. [ML033230335 at <http://www.nrc.gov/reading-rm/adams.html>]
- 2) NRC Public Meeting Obtain Stakeholder Feedback on Enhancements to the Licensing and Inspection Programs for Spent Fuel Storage and Transportation under 10 CFR Parts 71 and 72, August 16–17, 2012, Rockville, MD. [<http://www.nrc.gov/public-involve/conference-symposia/2012-sfst-lic-process-conf.html>]
- 3) T.A. Burtseva, Y. Yan, and M.C. Billone, “Radial-Hydride-Induced Embrittlement of High-Burnup ZIRLO Cladding Exposed to Simulated Drying Conditions,” ANL letter report to NRC, June 20, 2010. Available online as ML101620301 at <http://www.nrc.gov/reading-rm/adams/web-based.html>.
- 4) M.C. Billone, T.A. Burtseva, J.P. Dobrzynski, D.P. McGann, K. Byrne, Z. Han, and Y.Y. Liu, “Phase I Ring Compression Testing of High-Burnup Cladding,” FCRD-USED-2012-000039, Dec. 31, 2011.
- 5) M.C. Billone, T.A. Burtseva, and R.E. Einziger, “Ductile-to-Brittle Transition Temperature for High-Burnup Cladding Alloys Exposed to Simulated Drying-Storage Conditions,” submitted to Journal of Nuclear Materials (June 2012).



(a) As-irradiated



(b) After simulated drying-storage

Fig. 1. Hydride distribution and orientation in high-burnup ZIRLO™ cladding: (a) as-irradiated with 530-wppm hydrogen and (b) after simulated drying-storage conditions (at 400°C and 140 MPa) with 650-wppm hydrogen.

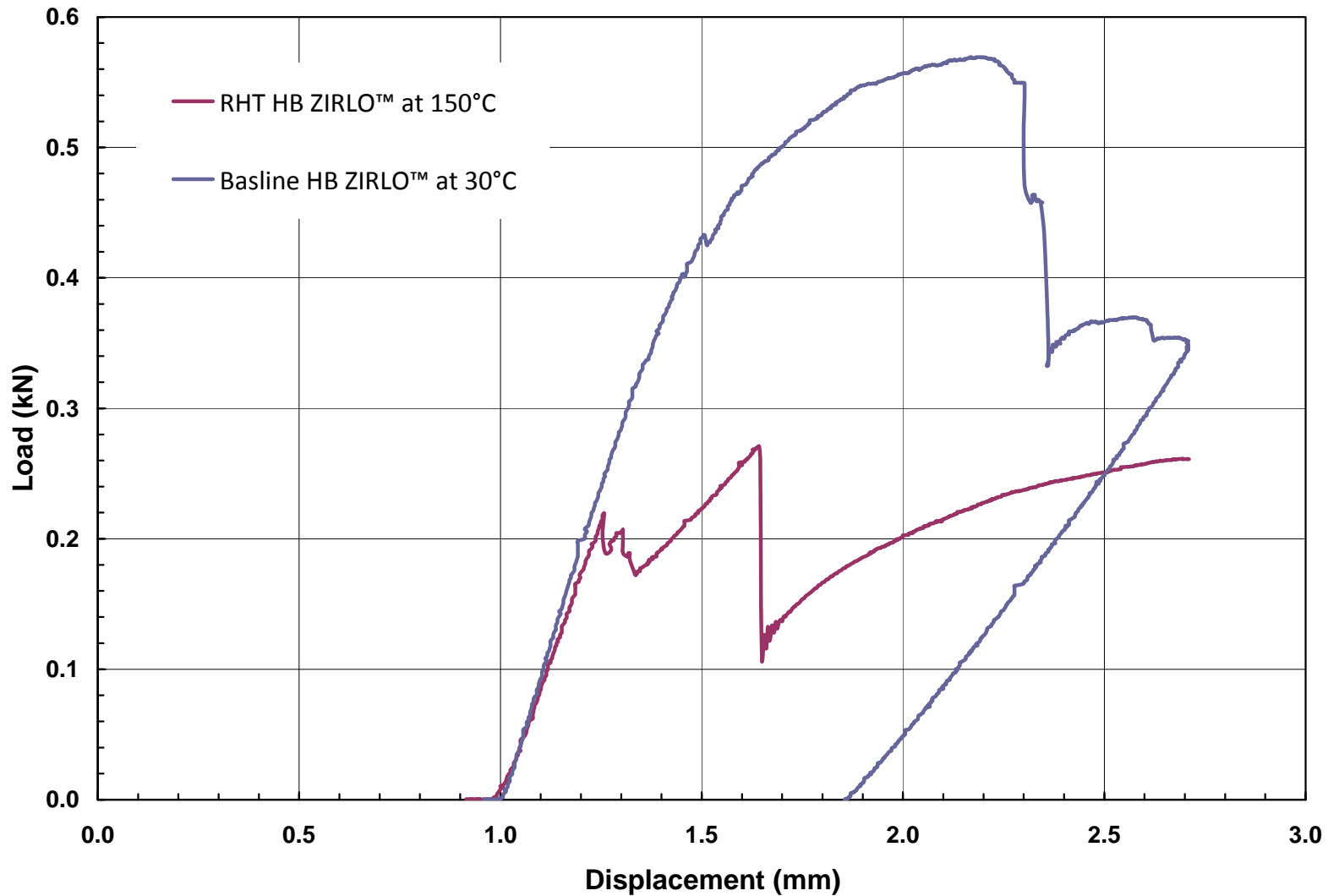


Fig. 2. RCT load-displacement curves for high-burnup ZIRLO™: (a) baseline as-irradiated condition (pre-drying, see Fig. 1a) tested at 30°C and (b) following simulated drying-storage conditions or RHT (see Fig. 1b) tested at 150°C.

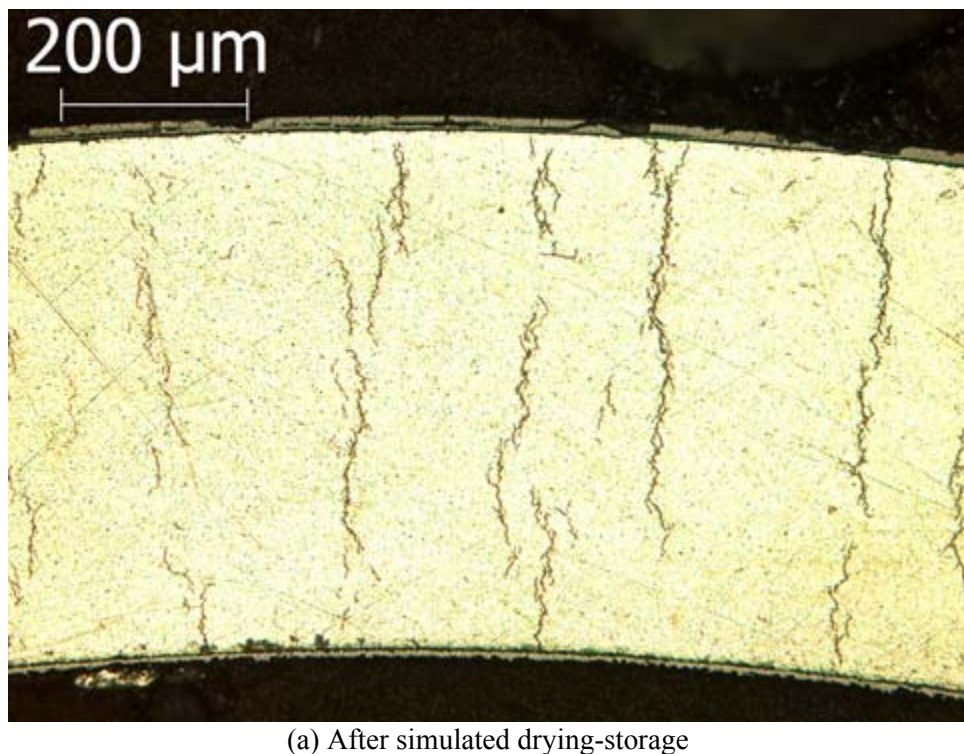
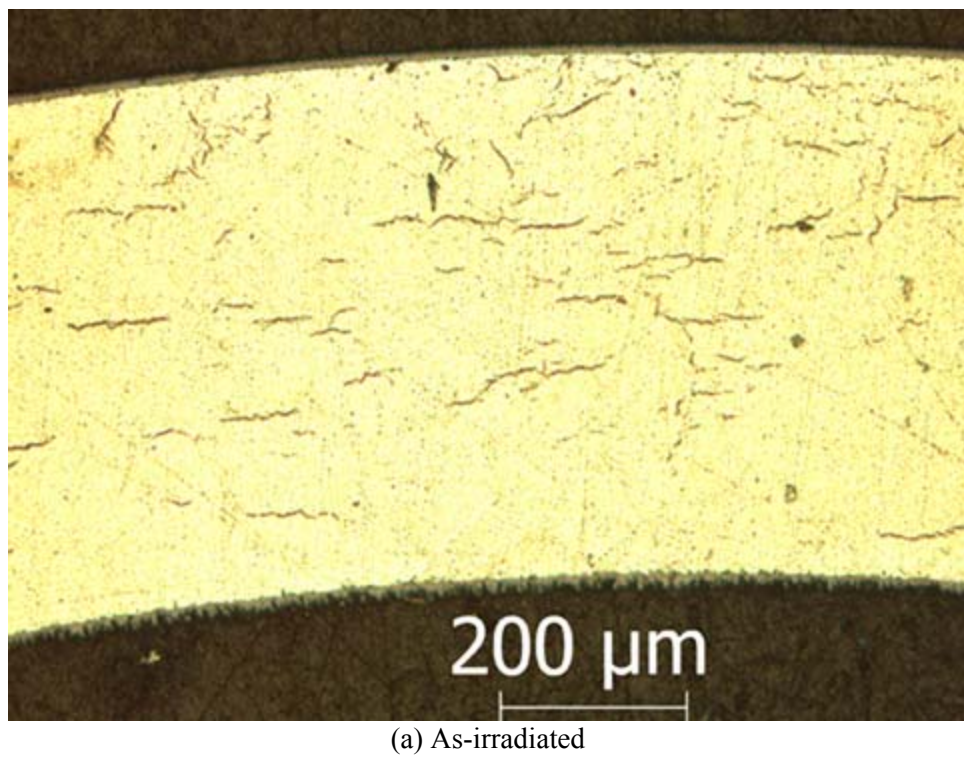


Fig. 3. Hydride distribution and orientation in high-burnup M5® cladding: (a) as-irradiated with 76-wppm hydrogen and (b) after simulated drying-storage conditions (at 400°C and 140 MPa) with 94-wppm hydrogen.

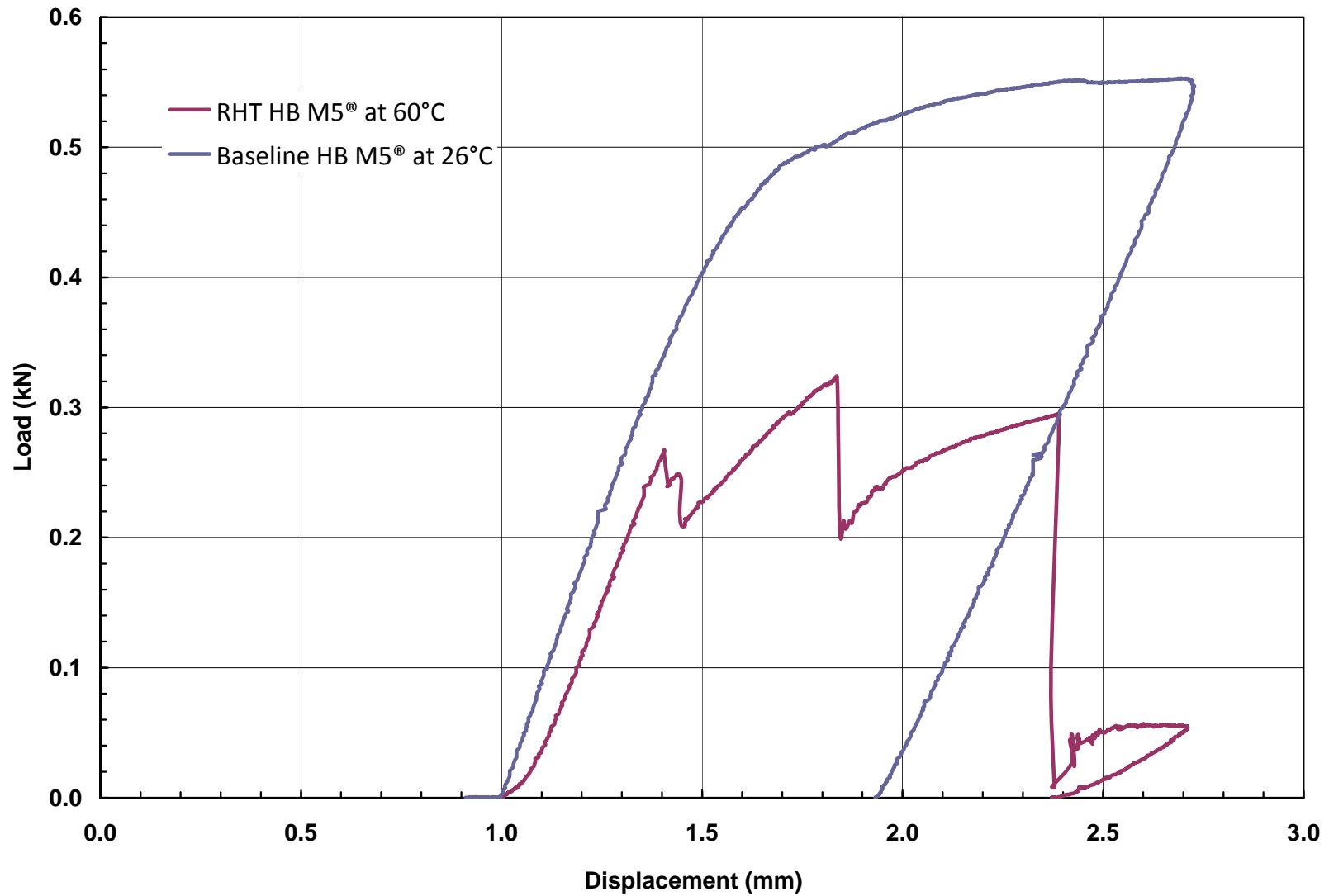
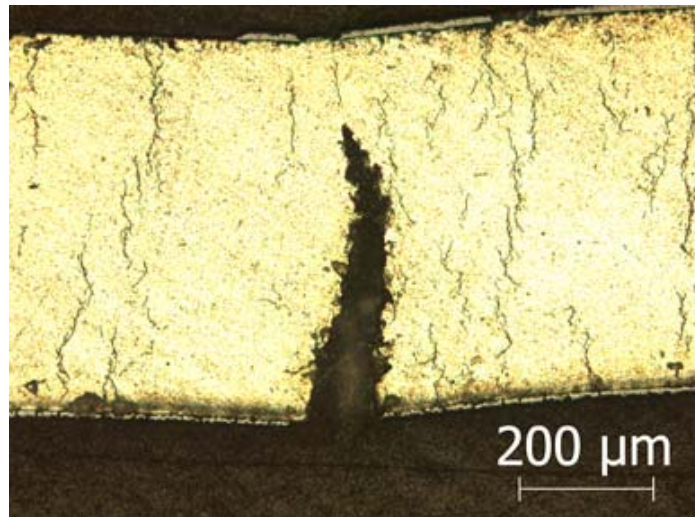
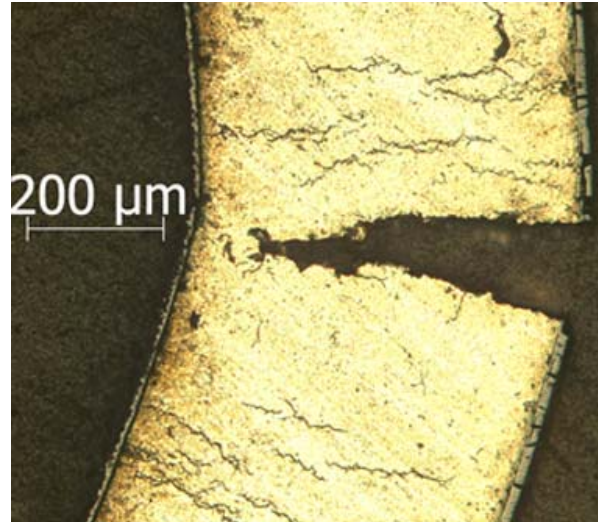


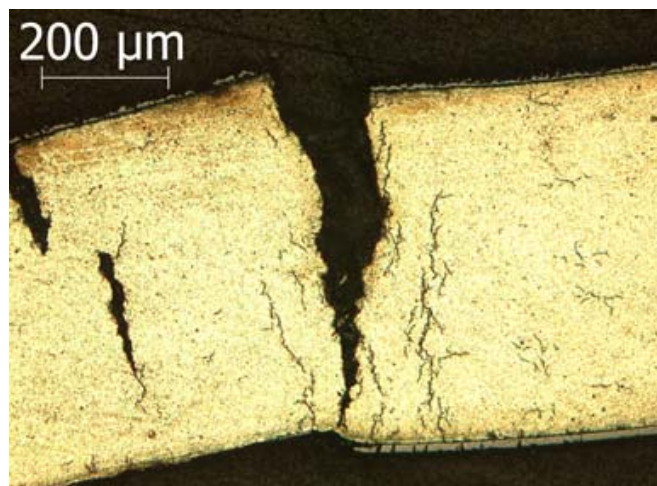
Fig. 4. RCT load-displacement curves for high-burnup M5<sup>®</sup>: (a) as-irradiated condition (pre-drying, see Fig. 3a) tested at 26°C and (b) following simulated drying-storage conditions (see Fig. 3b) tested at 60°C.



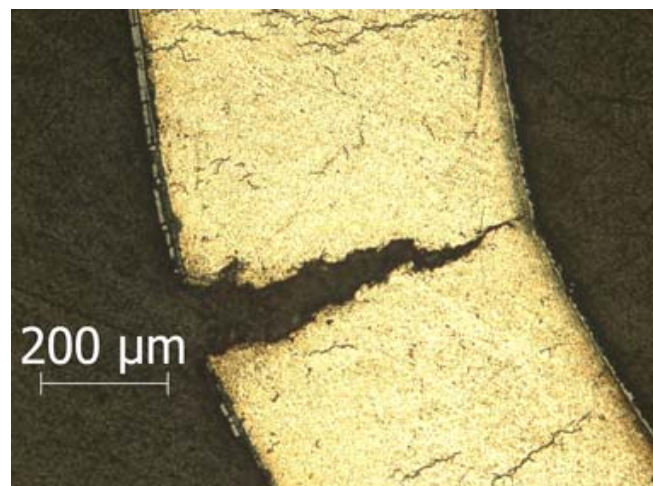
(a) 12 o'clock



(b) 3 o'clock



(c) 6 o'clock



(d) 9 o'clock

Fig. 5. Major cracks that formed during 60°C RCT of high-burnup M5® following simulated drying-storage conditions at 400°C and 140 MPa.

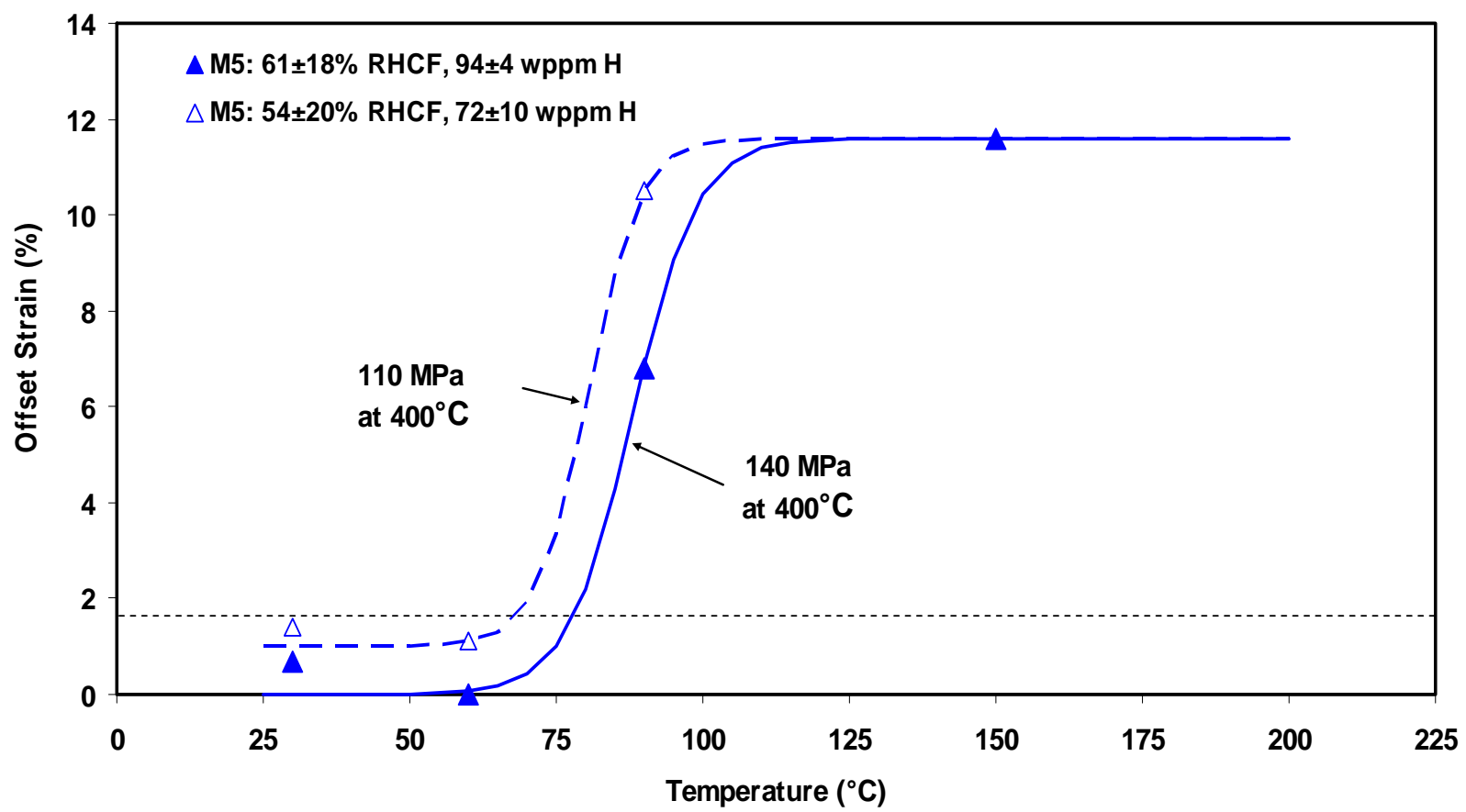


Fig. 6. Ductile-to-brittle transition temperatures (DBTT) of high-burnup M5<sup>®</sup> as determined in RCT following simulated drying-storage conditions at 400°C and 140 and 110 MPa hoop stresses, respectively. RHCF is the radial hydride continuity factor.

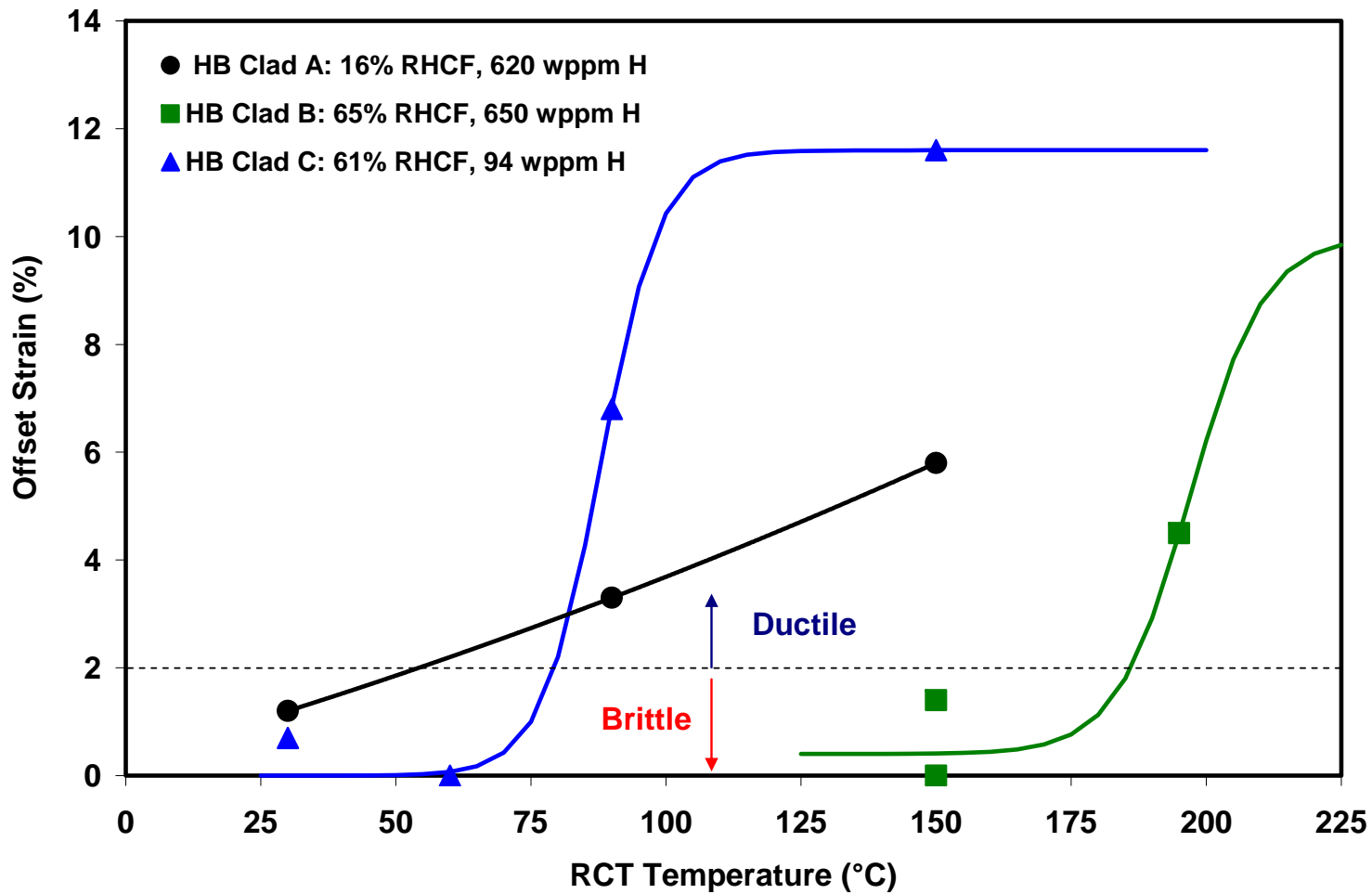


Fig. 7. RCT ductility data vs. test temperature for high-burnup (HB) PWR cladding alloys following slow cooling at 5°C/h from 400°C and 140-MPa hoop stress. RHCF is the radial hydride continuity factor.

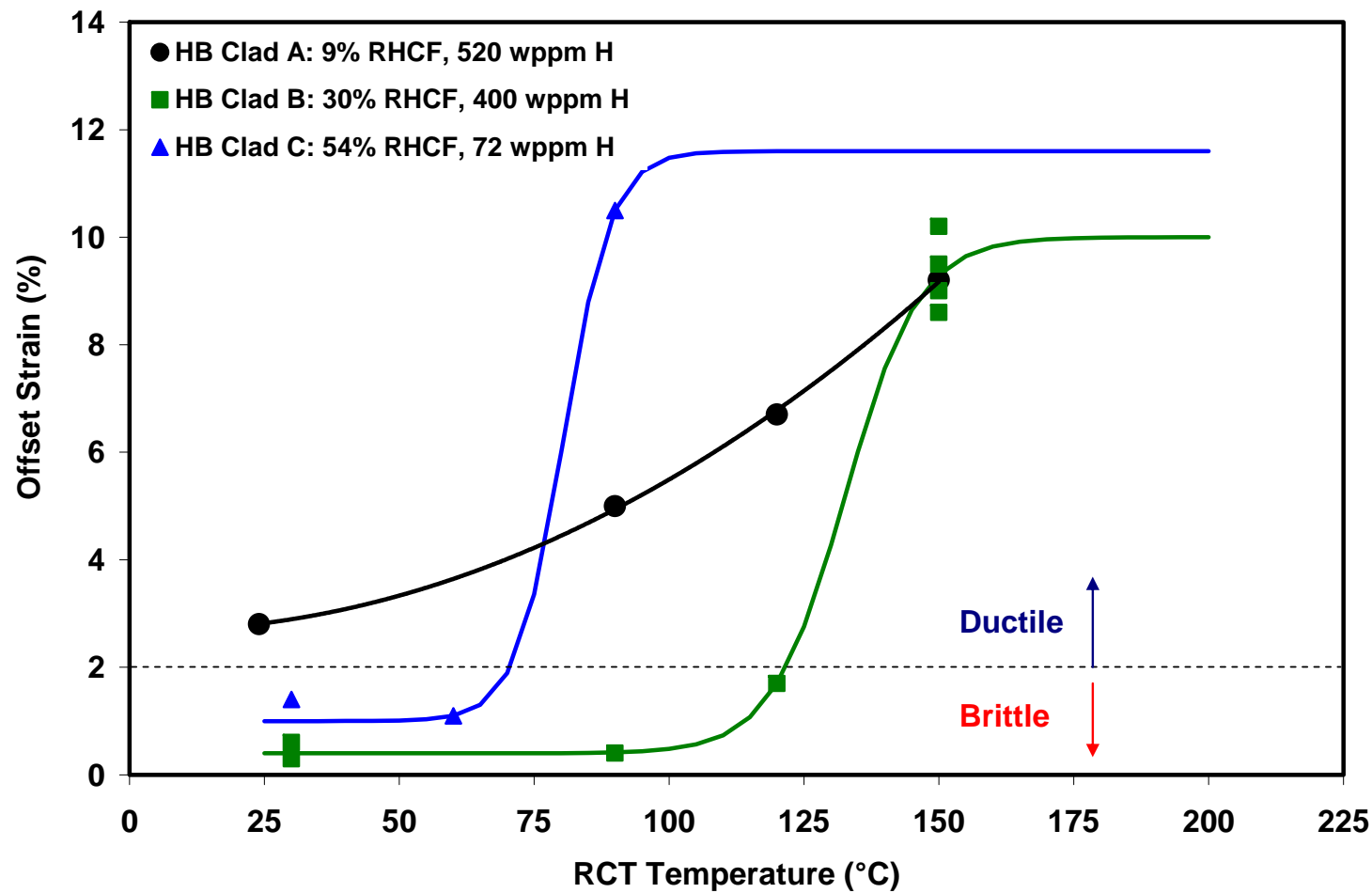


Fig. 8. RCT ductility data vs. test temperature for high-burnup (HB) PWR cladding alloys following slow cooling at 5°C/h from 400°C and 110-MPa hoop stress. RHCF is the radial hydride continuity factor.

# FCT Quality Assurance Program Document

## Appendix E FCT Document Cover Sheet

Name/Title of Deliverable/Milestone

Used Fuel Disposition (UFD) Year End Letter Report – FY2012

Work Package Title and Number

ST Engineering Materials Experimental - ANL

Work Package WBS Number

FT-12AN080508

Responsible Work Package Manager

Yung Liu

(Name/Signature)

Date Submitted 9/10/2012

Quality Rigor Level for Deliverable/Milestone	<input checked="" type="checkbox"/> QRL-3	<input type="checkbox"/> QRL-2	<input type="checkbox"/> QRL-1	<input type="checkbox"/> N/A*
			<input type="checkbox"/> Nuclear Data	

This deliverable was prepared in accordance with

Argonne National Laboratory

*(Participant/National Laboratory Name)*

QA program which meets the requirements of

DOE Order 414.1       NQA-1-2000

### This Deliverable was subjected to:

Technical Review

Peer Review

### Technical Review (TR)

### Peer Review (PR)

### Review Documentation Provided

Signed TR Report or,

Signed PR Report or,

Signed TR Concurrence Sheet or,

Signed PR Concurrence Sheet or,

Signature of TR Reviewer(s) below

Signature of PR Reviewer(s) below

### Name and Signature of Reviewers

Yung Liu

\_\_\_\_\_  
\_\_\_\_\_  
\_\_\_\_\_

\*Note: In some cases there may be a milestone where an item is being fabricated, maintenance is being performed on a facility, or a document is being issued through a formal document control process where it specifically calls out a formal review of the document. In these cases, documentation (e.g., inspection report, maintenance request, work planning package documentation or the documented review of the issued document through the document control process) of the completion of the activity along with the Document Cover Sheet is sufficient to demonstrate achieving the milestone. QRL for such milestones may be also be marked N/A in the work package provided the work package clearly specifies the requirement to use the Document Cover Sheet and provide supporting documentation.

## **APPENDIX C**

### **FY 2012 Used Fuel Disposition Campaign Transportation Task Report on INL Efforts Supporting the Moderator Exclusion Concept and Standardized Transportation**

**FY 2012  
USED FUEL DISPOSITION CAMPAIGN  
TRANSPORTATION TASK REPORT  
ON INL EFFORTS SUPPORTING THE  
MODERATOR EXCLUSION CONCEPT  
AND  
STANDARDIZED TRANSPORTATION**

D. K. Morton

August 2012



The INL is a U.S. Department of Energy National Laboratory  
operated by Battelle Energy Alliance

#### **DISCLAIMER**

This information was prepared as an account of work sponsored by an agency of the U.S. Government. Neither the U.S. Government nor any agency thereof, nor any of their employees, makes any warranty, expressed or implied, or assumes any legal liability or responsibility for the accuracy, completeness, or usefulness, of any information, apparatus, product, or process disclosed, or represents that its use would not infringe privately owned rights. References herein to any specific commercial product, process, or service by trade name, trade mark, manufacturer, or otherwise, does not necessarily constitute or imply its endorsement, recommendation, or favoring by the U.S. Government or any agency thereof. The views and opinions of authors expressed herein do not necessarily state or reflect those of the U.S. Government or any agency thereof.

**FY 2012 USED FUEL DISPOSITION CAMPAIGN  
TRANSPORTATION TASK REPORT ON INL EFFORTS  
SUPPORTING THE MODERATOR EXCLUSION  
CONCEPT AND STANDARDIZED TRANSPORTATION**

**D. Keith Morton**

**August 2012**

**Idaho National Laboratory  
Idaho Falls, Idaho 83415**

**<http://www.inl.gov>**

**Prepared for the  
U.S. Department of Energy  
Office of Nuclear Energy  
Under DOE Idaho Operations Office  
Contract DE-AC07-05ID14517**



**Idaho National Laboratory**

**FY 2012 USED FUEL DISPOSITION CAMPAIGN  
TRANSPORTATION TASK REPORT ON INL EFFORTS  
SUPPORTING THE MODERATOR EXCLUSION  
CONCEPT AND STANDARDIZED TRANSPORTATION**

**INL/EXT-12-26798  
FCRD-UFD-2012-000195**

**August 2012**

**Approved by:**

---

D. Keith Morton  
Author

Date

---

Sandra M. Birk  
Nuclear Material Disposition & Engineering Manager

Date



## **ABSTRACT**

Following the defunding of the Yucca Mountain Project, it is reasonable to assume that commercial used fuel will remain in storage for a longer time period than initially assumed. Previous transportation task work in FY 2011, under the Department of Energy's Office of Nuclear Energy, Used Fuel Disposition Campaign, proposed an alternative for safely transporting used fuel regardless of the structural integrity of the used fuel, baskets, poisons, or storage canisters after an extended period of storage. This alternative assures criticality safety during transportation by implementing a concept that achieves moderator exclusion (no in-leakage of moderator into the used fuel cavity). By relying upon a component inside of the transportation cask that provides a watertight function, a strong argument can be made that moderator intrusion is not credible and should not be a required assumption for criticality evaluations during normal or hypothetical accident conditions of transportation.

This Transportation Task report addresses the assigned FY 2012 work that supports the proposed moderator exclusion concept as well as a standardized transportation system. The two tasks assigned were to (1) promote the proposed moderator exclusion concept to both regulatory and nuclear industry audiences and (2) advance specific technical issues in order to improve American Society of Mechanical Engineers Boiler and Pressure Vessel Code, Section III, Division 3 rules for storage and transportation containments. The common point behind both of the assigned tasks is to provide more options that can be used to resolve current issues being debated regarding the future transportation of used fuel after extended storage.



## **ACKNOWLEDGEMENTS**

The author would like to acknowledge the technical support and translation of documentation provided by Dr. Toshiari Saegusa of Japan's Central Research Institute of Electric Power Industry. The author would also like to acknowledge two Idaho National Laboratory personnel: Ms. Sandra Birk for her management support and Mr. Brett Carlsen for his willingness to attend meetings when the author had previous commitments.



## **CONTENTS**

ABSTRACT.....	v
ACKNOWLEDGEMENTS .....	vii
ACRONYMS .....	xi
1. INTRODUCTION .....	1
2. BACKGROUND .....	1
3. TASK 1: PROMOTE PROPOSED CONCEPT .....	3
3.1 NRC SFST Technical Exchange Meeting.....	4
3.2 27 <sup>th</sup> INMM Spent Fuel Management Seminar .....	5
3.3 EPRI Extended Storage Collaboration Program Meeting.....	5
3.4 NEI Used Fuel Management Conference .....	6
3.5 Future FY2012 NRC NMSS Meetings .....	6
3.5.1 NRC Enhancements to the Licensing and Inspection Programs for Spent Fuel Storage and Transportation .....	6
3.5.2 NRC 2012 SFST Regulatory Conference .....	6
3.6 Task 1 Summary .....	7
4. TASK 2: ADVANCING TECHNICAL ISSUES .....	7
4.1 Literature Search.....	7
4.1.1 Purpose.....	7
4.1.2 Approach to Literature Search .....	7
4.1.3 Results of Literature Search.....	8
4.2 ASME BPV, Section III, Division 3 Activities.....	14
5. CONCLUSIONS .....	15
6. REFERENCES .....	15

## **FIGURES**

Figure 1. Proposed Concept for Moderator Exclusion .....	2
Figure 2. Watertight Barrier Determination .....	3

## **TABLES**

Table 1. Summary of Applicable Strain Rate Literature Search Results for 304/304L .....	9
Table 2. Summary of Applicable Strain Rate Literature Search Results for 316/316L .....	10
Table 3. Strain Rate Data Coverage for 304/304L Base Material .....	11
Table 4. Strain Rate Data Coverage for 304/304L Weld Material .....	11
Table 5. Strain Rate Data Coverage for 316/316L Base Material .....	12
Table 6. Strain Rate Data Coverage for 316/316L Weld Material .....	12



## ACRONYMS

AISI	American Iron and Steel Institute
ASME	American Society of Mechanical Engineers
BPV	Boiler and Pressure Vessel
CFR	Code of Federal Regulations
CoCs	Certificates of Compliance
DOE	U.S. Department of Energy
EPRI	Electric Power Research Institute
FY	Fiscal Year
HT	heat treated
IAEA	International Atomic Energy Agency
INL	Idaho National Laboratory
INMM	Institute of Nuclear Materials Management
ISG	interim staff guidance
JSME	Japan Society of Mechanical Engineers
MSHPB	Modified Split Hopkinson Pressure Bar
NE	DOE Office of Nuclear Energy
NEI	Nuclear Energy Institute
NMSS	Office of Nuclear Material Safety and Safeguards
NRC	U.S. Nuclear Regulatory Commission
RT	Room temperature
SFST	Spent Fuel Storage and Transportation (a division under NRC's Office of Nuclear Material Safety and Safeguards)
SRM	Staff Requirements Memoranda
UFDC	Used Fuel Disposition Campaign



# FY 2012 USED FUEL DISPOSITION CAMPAIGN TRANSPORTATION TASK REPORT ON INL EFFORTS SUPPORTING THE MODERATOR EXCLUSION CONCEPT AND STANDARDIZED TRANSPORTATION

## 1. INTRODUCTION

Following the defunding of the Yucca Mountain Project, the Department of Energy (DOE) transitioned the former Office of Civilian Radioactive Waste Management responsibilities to the Office of Nuclear Energy (NE). One of the new offices created under NE was the Office of Used Nuclear Fuel Disposition Research and Development (NE-53). A Used Fuel Disposition Campaign Implementation Plan was approved on March 29, 2010 with the following mission (Reference 1):

*“The mission of the Used Fuel Disposition Campaign is to identify alternatives and conduct scientific research and technology development to enable storage, transportation and disposal of used nuclear fuel and wastes generated by existing and future nuclear fuel cycles.”*

In the absence of a currently identified disposition path for commercial used nuclear fuel,<sup>a</sup> it is reasonable to assume that used fuel will remain in storage for the foreseeable future. In addition to future disposal issues, the Used Fuel Disposition Campaign (UFDC) is addressing the many issues related to the consequences of this longer than anticipated storage period. The UFDC Transportation Team, composed of a number of personnel from various DOE National Laboratories, began their efforts during Fiscal Year (FY) 2011 and are continuing to support those research and development aspects necessary to successfully carry out the transportation of used fuel, considering the potential adverse effects of long-term storage.

This report provides a summary of the assigned UFDC transportation activities completed by the Idaho National Laboratory (INL) during FY 2012. These activities were performed to support the proposed concept of achieving moderator exclusion with a standardized transportation system. This proposed concept was the assigned INL Transportation task for FY 2011.

## 2. BACKGROUND

The INL's assigned task during FY 2011 for UFDC Transportation was to address the issue of moderator exclusion. This concept was pursued in order to provide options for the transportation of used fuel. After extended storage, if the structural integrity of the fuel, cladding, baskets, or poisons cannot be determined or is too costly to assess, the potential for satisfying the criticality safety requirements become problematic. However, if moderator (e.g., water) is prevented from entering the cavity where the commercial used fuel is located, the used fuel cannot achieve criticality regardless of any degradation consequences due to the 5 wt. % U-235 enrichment limit of the fuel. A basic principle of defense-in-depth is the use of multiple barriers. An engineered barrier, placed inside of a transportation cask, can provide

---

a. The term ‘commercial used nuclear fuel’ (hereafter referred to as ‘used fuel’) is used in this report to reflect that the material being transported may still be a resource to be recovered through processing, whereas ‘spent fuel’ may be considered to be more a waste. This ‘used fuel’ terminology (which includes the cladding) is not intended to conflict with the vast magnitude of literature, regulations, codes, and standards that have used the term ‘spent fuel’ or ‘spent nuclear fuel’. ‘Used fuel’ is simply being used herein to indicate that a decision regarding its usefulness has not yet been determined. The term ‘spent fuel’ or ‘spent nuclear fuel’ will continue to be used in this report when used in a direct quotation, title, or the name of a specific item. Although DOE is also responsible for DOE-owned used fuel and high-level radioactive waste, the main focus of this report is commercial used fuel.

the solution to achieve moderator exclusion. If the storage canister can be shown to provide a watertight barrier during normal and hypothetical accident transportation conditions, moderator exclusion is achieved. If the storage canister cannot provide a watertight barrier, then an additional inner containment inside of the transportation cask can provide the necessary watertight function necessary for moderator exclusion during both normal and hypothetical accident conditions.

Current International Atomic Energy Agency (IAEA) transportation regulations for used fuel (Reference 2) do not require the assumption of moderator leakage past multiple barriers (not less than two), when each barrier can be demonstrated to remain watertight under prescribed normal and accident condition tests and each packaging (before each shipment) is tested to demonstrate the closure. A separate and distinct component inside of a transportation cask and capable of performing the watertight function for moderator exclusion is believed to satisfy the “special design features” condition of the applicable U.S. Code of Federal Regulations (CFR) requirements [10 CFR Part 71.55(c)] (Reference 3), ensuring that no single packaging error would permit in-leakage of moderator into the used fuel cavity.

This engineered concept, discussed in INL/EXT-11-22559 (Reference 4, the FY 2011 INL UFDC Transportation task report), also simultaneously supports standardized transportation. New transportation packagings need to be constructed in order to transport the large amount of available used fuel. This new design opportunity can establish a fleet of transportation packagings that can accommodate most if not all of the current used fuel storage systems. A “one size fits all” approach produces a standardized transportation system. But this does create a need to adapt to the many varied storage canister geometries so they properly fit into the one-sized transportation cask cavity (eliminate excessive rattle room). The solution is to use an adaptable insert (one or more designs as needed) that fits into the transportation cask cavity and properly supports the storage canister. This adaptable insert can also become an inner containment when needed, simply by attaching a lid. Hence, a standardized transportation system can be created that allows even degraded used fuel to be safely transported, providing the options needed to safely and efficiently transport used fuel after extended storage. Figure 1 illustrates this proposed concept.

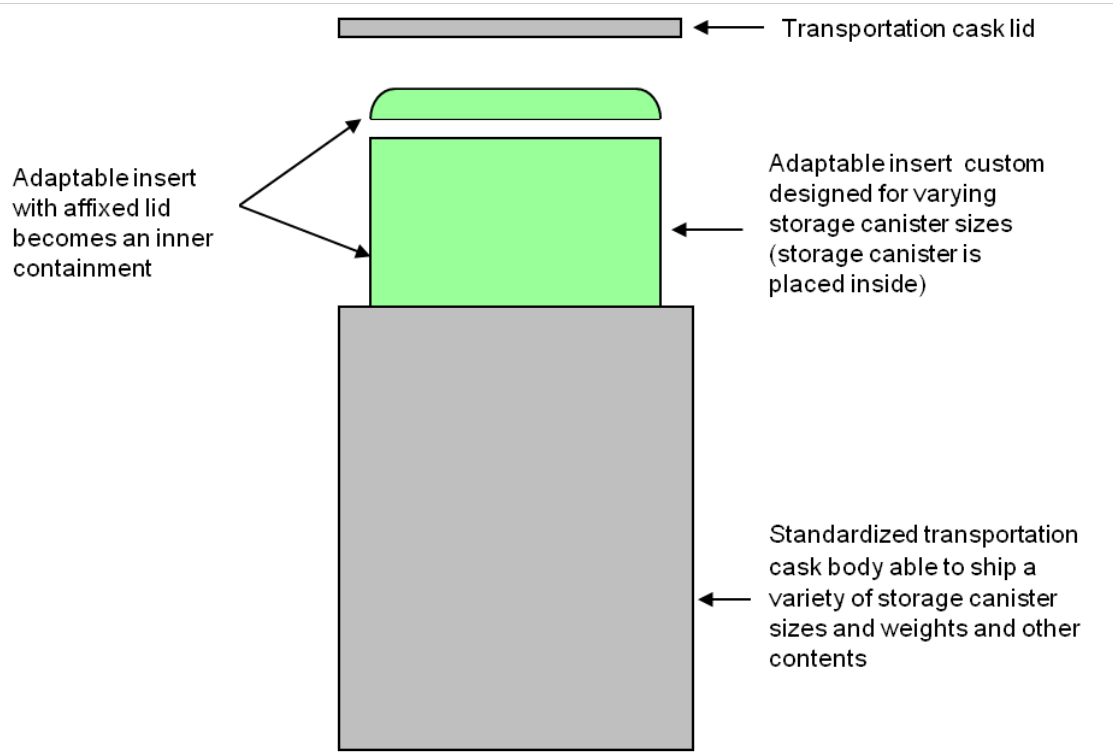


Figure 1. Proposed Concept for Moderator Exclusion

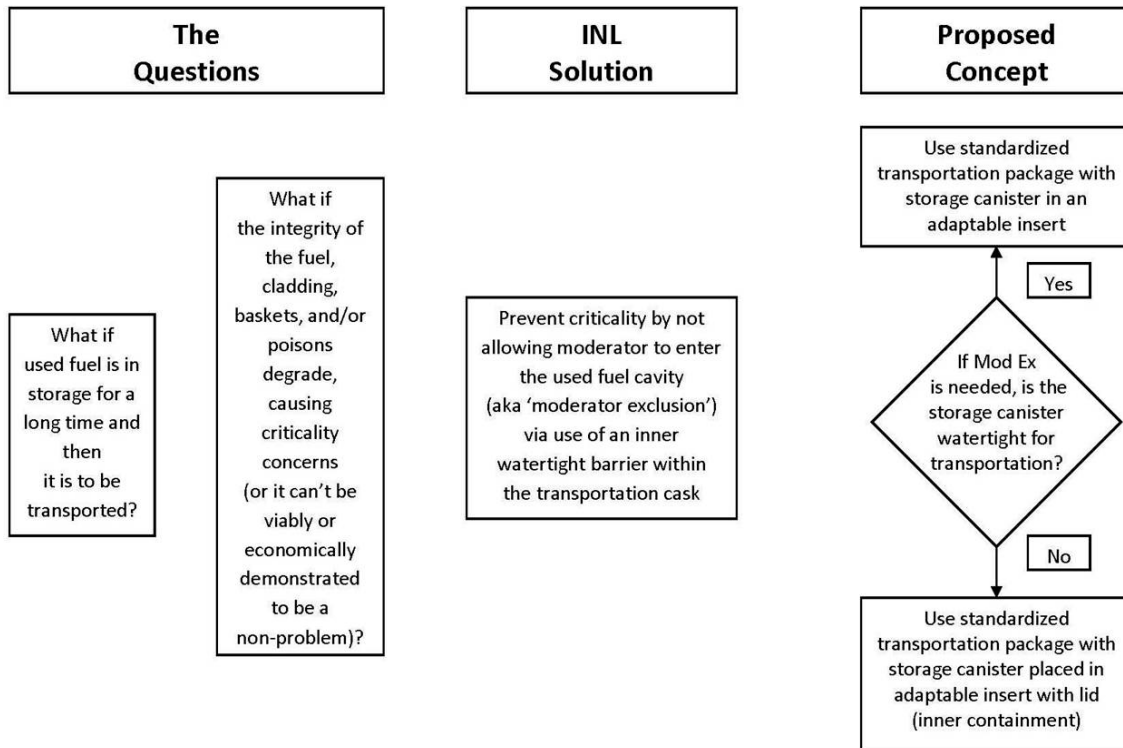


Figure 2. Inner Watertight Barrier Determination

Figure 2 illustrates the logic when evaluating whether the storage canister or the adaptable insert with an affixed lid (inner containment) will provide the watertight barrier function necessary for moderator exclusion.

### 3. TASK 1: PROMOTE PROPOSED CONCEPT

As explained in INL/EXT-11-22559, if the U.S. Nuclear Regulatory Commission (NRC), Office of Nuclear Material Safety and Safeguards (NMSS) would accept the proposed moderator exclusion approach [essentially be willing to invoke 10 CFR Part 71.55(c)] for general approval of designs rather than on a case-by-case basis, it is believed that more parties would be willing to submit designs invoking moderator exclusion for both normal and hypothetical accident conditions. All licensing interactions with the NRC cost money to complete and there is a natural hesitancy to pursue design options that may be rejected by the NRC. As an additional deterrent, a recent NRC Commission ruling on moderator exclusion [Staff Requirements Memoranda (SRM) dated December 18, 2007 (Reference 5) regarding SECY-07-0185 (Reference 6)] indicated that the Commission rejected the NRC staff's recommendation for rulemaking to incorporate regulatory provisions addressing moderator exclusion. The Commission required the NRC staff to continue to gain more experience through processing applicant's requests and to focus its efforts on using burn-up credit. What was believed not to have been specifically considered in those deliberations was the consequences of extended storage and the presence of an inner watertight barrier, separate from and inside of the transportation containment, as required by the INL's proposed moderator exclusion concept. Other requirements such as addressing fuel retrievability add to the current hesitancy of applicants to pursue moderator exclusion approval for both normal and hypothetical accident conditions.

Therefore, the primary intent of Task 1 was to simply promote the proposed moderator exclusion concept that also incorporated a standardized transportation system. If efforts could be made to provide input to the NRC during their on-going review of storage and transportation regulations in light of

extended storage, the potential for the NRC to seriously consider the proposed concept improved greatly. The INL proposed concept is not a new concept, but it is a proven concept, since it was used to transport the damaged Three Mile Island fuel and core across most of the United States to the INL. So the goal of Task 1 was to simply help keep this engineered design option fresh in the NRC's, potential applicants', and the nuclear industry's minds. This promotional effort was considered especially important if proposed extended storage used fuel demonstration tests prove too costly, if the research efforts do not yield the desired outcome, or if it becomes difficult to assure the condition of the fuel, cladding, baskets, or poisons inside any specific storage canister for whatever reason. The INL proposed concept provides alternative transportation options for the future.

### **3.1 NRC SFST Technical Exchange Meeting**

The first opportunity to promote the INL's proposed concept came early in FY 2012. On November 1, 2011, the Division of Spent Fuel Storage and Transportation (SFST) under NMSS sponsored a technical exchange meeting. NRC, DOE, and nuclear industry representatives served on panels and presented their perspectives on a variety of issues in the areas of transportation technical issues and storage technical issues. Two concurrent meetings were held but it was at the "Interfaces Between Storage and Transportation Casks" meeting where pertinent presentations were held regarding moderator exclusion. The morning session was a presentation/discussion on high burnup fuel, including discussions on alternatives for addressing criticality safety requirements for high burnup fuel transportation. Presentations included:

- NRC's View on Cladding Material Properties – Bob Einziger
- Industry's View on Cladding - Albert Machiels from EPRI
- NRC's View on Moderator Exclusion – John Vera
- Industry's View on Moderator Exclusion – Charlie Pennington from NAC International and D. Keith Morton from the Idaho National Laboratory
- NRC's View on Reconfiguration – David Tang and Zhian Li
- Industry's View on Reconfiguration – Albert Machiels from EPRI

The afternoon session of "Interfaces Between Storage and Transportation Casks" continued the same format, including discussions on retrievability requirements (by fuel assembly or canister), casks/contents integrity after a period of storage, and the use of common criticality safety methods for satisfying both storage and transportation regulations. Presentations included:

- NRC's View on Retrievability – Earl Easton
- Industry's View on Retrievability – Adam Levin from Exelon Corporation
- NRC's View on Acceptance Testing and Aging Management – Bob Einziger
- Industry's View on Acceptance Testing and Aging Management – Jim Connell from Maine Yankee
- NRC's View on Burnup Credit versus Boron Credit – Drew Barto
- Industry's View on Burnup Credit versus Boron Credit – Prakash Narayanan from Transnuclear

Two interesting comments from the NRC staff were made at this meeting. First, Dr. John Vera mentioned in his morning presentation that the concept proposed in INL Report 11-22559 could be a "possible" option for moderator exclusion by implementing double containment. Second, Mr. Earl Easton discussed potential future paradigm shifts in regulations, where for 'retrievability', a shift from the fuel assembly to the canister could occur and that for 'criticality safety', a shift from cladding to canister could be possible. These comments supported the position of the INL presentation and were very well received by the audience. This meeting provided an excellent opportunity for the industry and NRC personnel to

exchange technical ideas and opinions. The proposed moderator exclusion presentation was well received. After the presentations, in direct discussions with Mr. Earl Easton, NRC Senior Level Transportation Advisor, he indicated that there were still differing opinions within the NRC staff on various storage and transportation subjects but he believed that a new paradigm existed with the probability of extended storage intervals and felt that it was necessary for the NRC to adapt with the change. Hence, the goal of keeping moderator exclusion on the discussion forefront as an item for potential regulatory change was achieved.

### **3.2 27<sup>th</sup> INMM Spent Fuel Management Seminar**

Mr. Paul McConnell, from Sandia National Laboratories and UFDC Technical Laboratory Lead for Transportation, gave a presentation on the UFDC Transportation Program on February 1, 2012 at the Institute of Nuclear Materials Management 27<sup>th</sup> Spent Fuel Management Seminar. The presentation included a brief summary of the proposed moderator exclusion concept. Again, more people were exposed or reminded of the potential benefits of moderator exclusion.

One of the more intriguing aspects that occurred at this three day meeting was comments made on the last day (February 2, 2012) by Mr. Doug Weaver, Acting Director for the NRC SFST Division. Some of his more interesting comments regarding possible future licensing strategies due to extended storage included:

- “If the fuel cladding is not relied upon to perform safety functions such as geometry control, degradation of fuel cladding may not pose a significant problem from the perspective of storage and transportation.”
- “An engineering approach that relies on canisters or individual cans rather than cladding integrity may also lessen the burden on cask designers and regulators to do extensive research on fuel cladding properties. It should be noted however that, due to increased reliance on integrity of canisters/casks and overpacks, these safety components may have to perform to higher standards.”
- “In summary, I believe that NRC’s future regulatory framework should be flexible enough to consider both “scientific” and “engineering” solutions – for example, developing licensing solutions that rely both on keeping the cladding intact, as well as those which might base safety more on canisters or cans.”

The good news is that all participants in the nuclear industry appear to be recognizing that past processes, evaluations, assumptions, and regulations may be inadequate in light of extended storage and that new general design approaches (e.g., using an inner containment) should be considered along with revised regulations.

### **3.3 EPRI Extended Storage Collaboration Program Meeting**

After generating a presentation (improved over that presented at the November 1 NRC Technical Exchange Meeting), discussing the presentation and submitting the presentation with meeting organizers, the author attended the Electric Power Research Institute (EPRI) Extended Storage Collaboration Program (ESCP) meeting held Monday, May 7, 2012 in St. Petersburg, Florida. The focus of that meeting was to discuss aging effects and mitigation options for the extended storage and transportation of used fuel. Due to the fact that the meeting went long and certain agenda items were not covered, the presentation on the INL’s proposed moderator exclusion concept was not given. However, after the author made a brief announcement of a willingness to discuss moderator exclusion options after the meeting, two nuclear industry participants briefly explained their future expectations and both believed that moderator exclusion provided the most likely option for future transportation of used fuel.

### **3.4 NEI Used Fuel Management Conference**

Since the Nuclear Energy Institute (NEI) Used Fuel Management Conference began the day after the ESCP meeting at the same location, the author also attended this conference. Although no presentation was planned, attending this conference provided an opportunity to listen to a number of pertinent presentations, mainly from the nuclear industry perspective. This provided a better understanding of the nuclear industry's perspective on what needs to be accomplished in order to continue the safe storage of used fuel and the actions needed to move forward with storage, transportation, and disposal. Moderator exclusion was high on the list of NEI issues needing to be discussed and utilized for future transportation of used fuel.

### **3.5 Future FY2012 NRC NMSS Meetings**

The NRC is organizing two meetings to be held late in FY2012, after the writing and approval of this FY2012 UFDC Transportation Task report.

#### **3.5.1 NRC Enhancements to the Licensing and Inspection Programs for Spent Fuel Storage and Transportation**

This NRC SFST meeting is scheduled to be held August 16-17, 2012 at NRC Headquarters in Rockville Maryland. As the draft agenda indicates, the following issues are to be discussed:

- Administration of Storage Certificates of Compliance (CoCs) and Amendments to CoCs
- Applicability, Compatibility, and Consistency of Spent Fuel Storage Requirements for Specific Licensees, General Licensees, and Certificate of Compliance Holders
- Regulating Stand-Alone Independent Spent Fuel Storage Installations
- Harmonization of Retrievability and Cladding Integrity Requirements for Storage and Transportation of Spent Nuclear Fuel

In particular, the last item could have interesting implications for transportation, especially if any shifts in fuel retrievability regulations are discussed. INL personnel are planning to attend/participate in this meeting but no presentation is planned.

#### **3.5.2 NRC 2012 SFST Regulatory Conference**

This NRC SFST meeting is an annual forum to discuss NRC regulatory and technical issues involving spent fuel storage and the transportation of radioactive material. The goal of the conference is for the regulators to share their perspectives on licensing, inspection, and regulatory challenges as well as for the nuclear industry to share their insights on improving regulatory oversight, all through constructive dialogue. This meeting is scheduled to be held September 12-13, 2012 at NRC Headquarters in Rockville Maryland. Per the draft agenda, the following issues are to be discussed:

- Operating Experience
- Non-Spent Fuel Transportation
- Information on NUREG-2150 and NUREG-2125
- High Burnup Fuel Storage and Transportation
- Technical Issues Related to Storage

Again, various agenda items could have interesting implications for transportation, especially the high burnup fuel discussion. INL personnel are planning to attend/participate in this meeting, although presenters and panels have not yet been finalized.

### **3.6 Task 1 Summary**

A number of opportunities were pursued to promote the proposed moderator exclusion concept for standardized transportation systems. Presentations were made at various meeting types and interaction with meeting attendees succeeded in heightening the awareness of the beneficial aspects of moderator exclusion. Moderator exclusion is attainable and keeping this option “on the table” for future consideration by both nuclear industry and regulatory personnel was achieved.

## **4. TASK 2: ADVANCING TECHNICAL ISSUES**

Task 2 was to perform a literature search for readily available strain rate data that would support implementing proposed strain-based acceptance criteria for the American Society of Mechanical Engineers (ASME) Boiler and Pressure Vessel (BPV) Code, Section III, Division 3 (Reference 7) rules for both storage and transportation containments. Funding was also provided to attend the ASME BPV Code Week Division 3 meetings. Therefore, Section 4.1 below addresses the completed literature search and Section 4.2 addresses the advances made in developing the proposed strain-based acceptance criteria and the progress to date of obtaining ASME approval of the proposal, along with other pertinent Section III, Division 3 rule changes.

### **4.1 Literature Search**

This subsection describes in more detail the literature search performed in order to establish the quantity of strain rate data readily available in the technical literature. This information is expected to be used to determine future needs, such as defining test program needs and validation efforts.

#### **4.1.1 Purpose**

The purpose of this task was to perform a limited literature search in order to determine the quantity of applicable strain rate data readily available. Regulatory requirements mandate the consideration of accidental drops and impacts when designing storage and transportation containments. These energy-limited loads typically govern the structural design of these containments, especially when elastic analyses are used. But this significantly increases the cost of these containments. In recognition of this fact, the ASME BPV Code, Section III, Division 3 committees have pursued the development of strain-based acceptance criteria. These criteria will make the design of containments more efficient but will still maintain appropriate safety margins. These acceptance criteria require inelastic analyses be performed. Strain rate data are required to properly perform inelastic analyses of accidental drop or impact events on storage and transportation containments. So strain rate data support implementation of the proposed strain-based acceptance criteria, which can support the design of a new and efficient standardized transportation system.

#### **4.1.2 Approach to Literature Search**

A significant amount of strain rate research has been performed on multiple materials, at multiple temperatures, and for a variety of reasons. However, this literature search needed to obtain information pertinent to the common materials used for the containment of used fuel during storage and transportation uses. Therefore, the search parameters were narrowed to focus on strain rate data for 304, 304L, 316, or 316L stainless steels, at temperatures ranging from -40°F to 800°F, and at strain rates between 1 and 510 in/in/sec. In years past, before the late 1980’s, it was common to be able to procure just one type (304, 304L, 316, or 316L) of austenitic stainless steel material. However, for new construction, one is likely to obtain material that is marked with two or more material types, such as 304/304L or 316/316L. These materials can satisfy both material types because all of the measured and controlled attributes (e.g., chemistry, mechanical properties, dimensions, and tolerances) of that material fall within the overlapping ranges of both specifications. This dual marking notation (304/304L and 316/316L) will be used herein to

denote either material that satisfies each unique and separate specification (covering older testing efforts) or material that satisfies the dual specifications (covering more recent testing efforts).

Past efforts to acquire strain rate documentation within the data ranges specified above, including requests to ASME Code committee volunteers, yielded relevant documents. These documents were combined with the new FY2012 search efforts made for this task.

Obviously, in order to better understand the material performance conforming to the restricted conditions identified above, the ideal strain rate data would include digitized tensile engineering stress-strain curves. This would provide material data performance, including values for the uniform strain limit and fracture strain limit. True stress-strain curves could also be generated from this data. However, not all documentation would be expected to provide this detailed level of information. Therefore, documents with true stress-strain curves, or reports that provided information on how the strain rate effects changed the material response in relation to the quasi-static engineering or true stress-strain curve were also of importance. Even with these narrowed search parameters, it was still necessary to obtain the potential papers, reports, and other documentation, scan for the minimal data of interest, and then determine if that data would provide any beneficial insights. This determination was necessary because some data may have included pertinent data but if the quasi-static engineering or true stress-strain curve was not provided, a quantification of the material response change could not be made. Other reasons to not include documents was that the data did not go far enough in terms of strain, difficulty in reading the data, data units not specified, or the data were not within the specified parameters. Documents with compression test data were not considered viable since the behavior of these materials is different between tensile and compression loading. Another aspect not considered at this time was the effects of irradiation, due to the limited funding.

#### **4.1.3 Results of Literature Search**

A significant number of hours were invested in this literature search. However, the search results yielded only nine viable references (References 8 – 16). This was not unexpected since past efforts yielded few references. The current fiscal year effort was fruitful and did add to the total number of viable strain rate references. Due to copyright constraints, rather than providing copies of the entire reference, the search results are summarized in tabular form, differentiated by material type (304/304L or 316/316L). Table 1 provides a summary of pertinent strain rate data provided by each reference, separated by test temperature, for 304/304L base and weld material. Table 2 provides the same information for 316/316L base and weld material. Tables 1 and 2 also provide information regarding the dynamic test method used, test specimen geometry insights, and the form of the documented strain rate data.

When evaluating the results of a literature search of this nature, the issue of data completeness needs to be considered. The goal was to get viable strain rate data over a range of 1 to 510 in/in/sec and at a variety of temperatures ranging from -40°F to 800°F. Tables 3, 4, 5, and 6 were generated to provide a visual answer to the question. Tables 3 and 4 address 304/304L material and Tables 5 and 6 address 316/316L. Table 3 and 5 address base material and Tables 4 and 6 address weld material. The first realization is that only a limited number of the boxes are marked (yellow highlight with an ‘X’), indicating at least one set of data is available in the indicated range. Less than 18% of the 316/316L base material ranges have data and only 12% of the 304/304L base material ranges have any data. The data coverage for welds is even lower; approximately 5% of the ranges have any data for either 304/304L or 316/316L. As one would expect, most of the strain rate data that is available is for the temperature range that includes room temperature and for the lowest strain rate range (1 to 50 in/in/sec). These data points are the easiest to obtain. Clearly, the general need is to obtain more data at higher strain rates and at higher temperatures. This insight is very useful for planning future strain rate testing needs.

Of the data that are available, a few cursory observations can be made and are presented below. However, it is necessary to incorporate additional strain rate data before any final conclusions can be stated.

**Table 1. Summary of Applicable Strain Rate Literature Search Results for 304/304L**

Author	Ref.	Material	Dynamic Test Method	Test Temp.	Strain Rates	Specimen	Comments
Albertini & Montagnani	8	AISI 304L	MSHPB	RT	$10^{-4}$ , $10^{-2}$ , 502	Small, 8 mm active length	Engr. stress-strain curves
Albertini & Montagnani	9	AISI 304L	MSHPB	68°F	$3.8 \times 10^{-3}$ , 50, 450	Small	Engr. stress-strain curves
Albertini & Montagnani	9	AISI 304L	MSHPB	752°F	$3.5 \times 10^{-3}$ , 50, 500	Small	Engr. stress-strain curves
JSME	10 (B-46)	304	Amsler type accumulated gas	68°F	$5.05 \times 10^{-4}$ , $6.26 \times 10^{-2}$ , 54.8	1/3-in. dia. 2-in. gauge	Limited true stress-strain curve s& data
JSME	10 (B-46)	304	Amsler type accumulated gas	-87°F	$5.45 \times 10^{-4}$ , $4.99 \times 10^{-2}$ , 48	1/3-in. dia. 2-in. gauge	Limited data
Marschall, Landow, Wilkowski	11	304 and SAW	Hydraulic tensile	550°F	Varying: approx. $10^{-4}$ , 1, 8-14	1/8-in. sheet	Engr. & true stress-strain curves
Talonen, Nenonen, Pape, & Hänninen	14	AISI 304	Hydraulic tensile	RT*	$3 \times 10^{-4}$ , 0.1, 200	0.04 in. thick	True stress-strain curves
Lichtenfeld, Mataya, & Van Tyne	15	304L	Hydraulic tensile	75°F	$1.25 \times 10^{-4}$ , $1.25 \times 10^{-3}$ , $1.25 \times 10^{-2}$ , 0.125, 1.25, 10, 100, 400	0.06 in. thick etched	True stress-strain curves with yield and tensile strengths
Morton & Blandford	16	304/304L base and weld	Drop weight	-20°F	$10^{-4}$ to $10^{-3}$ , 5 - 36	1/4 and 1/2-inch thick plate	Data & factored true stress-strain curves
Morton & Blandford	16	304/304L base and weld	Drop weight	RT	$10^{-4}$ to $10^{-3}$ , 5 - 33	1/4 and 1/2-inch thick plate	Data & factored true stress-strain curves
Morton & Blandford	16	304/304L base and weld	Drop weight	300°F	$10^{-4}$ to $10^{-3}$ , 5 - 35	1/4 and 1/2-inch thick plate	Data & factored true stress-strain curves
Morton & Blandford	16	304/304L base and weld	Drop weight	600°F	$10^{-4}$ to $10^{-3}$ , 5 - 23	1/4 and 1/2-inch thick plate	Data & factored true stress-strain curves

Notes:

AISI – American Iron and Steel Institute

MSHPB – Modified Split Hopkinson Pressure Bar or similar device

RT – room temperature

\* - assumed value based on paper inferences

**Table 2. Summary of Applicable Strain Rate Literature Search Results for 316/316L**

Author	Ref.	Material	Dynamic Test Method	Test Temp.	Strain Rates	Specimen	Comments
Albertini & Montagnani	9	AISI 316L	MSHPB	68°F	$4.0 \times 10^{-3}$ , 15, 44, 420	Small bar	Engr. stress-strain curves
Albertini & Montagnani	9	AISI 316L weld	MSHPB	68°F	$3.5 \times 10^{-3}$ , 5, 440	Small bar	Engr. stress-strain curves
JSME	10 (B-3)	AISI 316L	*	68°F	$3 \times 10^{-3}$ , 12, 36, 360	*	Limited true stress-strain curves & data
JSME	10 (B-27)	316L (HT & annealed)	MSHPB	68°F	$3.9 \times 10^{-3}$ , 15, 43, 410	*	Limited true stress-strain curves & data
JSME	10 (B-27)	316L (HT & annealed)	MSHPB	752°F	$2.9 \times 10^{-3}$ , 44, 69, 460	*	Limited data
O'Toole	12	316L	Drop weight	RT	Approx. $10^{-4}$ , 0.02, 0.2, 75, 100, 130, 165, 200	0.35 in. long 1/8-in. dia.	Raw data
O'Toole	12	316L	Drop weight	175°F	Approx. 90, 170	0.35 in. long 1/8-in. dia.	Raw data
O'Toole	12	316L	Drop weight	350°F	Approx. 110, 145, 170	0.35 in. long 1/8-in. dia.	Raw data
Langdon & Schleyer	13	316L	Hydraulic tensile	RT	0.03, 0.2, 18, 20, 55, 118	0.12 and 0.16 thick	Engr. stress-strain curves
Morton & Blandford	16	316/316L base and weld	Drop weight	-20°F	$10^{-4}$ to $10^{-3}$ , 5 - 39	$\frac{1}{4}$ and $\frac{1}{2}$ -inch thick plate	Data & factored true stress-strain curves
Morton & Blandford	16	316/316L base and weld	Drop weight	RT	$10^{-4}$ to $10^{-3}$ , 5 - 34	$\frac{1}{4}$ and $\frac{1}{2}$ -inch thick plate	Data & factored true stress-strain curves
Morton & Blandford	16	316/316L base and weld	Drop weight	300°F	$10^{-4}$ to $10^{-3}$ , 4 - 26	$\frac{1}{4}$ and $\frac{1}{2}$ -inch thick plate	Data & factored true stress-strain curves
Morton & Blandford	16	316/316L base and weld	Drop weight	600°F	$10^{-4}$ to $10^{-3}$ , 5 - 24	$\frac{1}{4}$ and $\frac{1}{2}$ -inch thick plate	Data & factored true stress-strain curves

Notes:

AISI – American Iron and Steel Institute

MSHPB – Modified Split Hopkinson Pressure Bar or similar

RT – Room Temperature

JSME – Japan Society of Mechanical Engineers

\* - unstated but MSHPB likely with small bar test specimens

HT – heat treated

**Table 3. Strain Rate Data Coverage for 304/304L Base Material**

Temperature \ Strain Rate	-90°F to 32°F	33°F to 100°F	101°F to 200°F	201°F to 300°F	301°F to 400°F	401°F to 500°F	501°F to 600°F	601°F to 700°F	701°F to 800°F
1 - 50 in/in/sec	X	X		X			X		X
51 - 100 in/in/sec		X							
101 - 150 in/in/sec									
151 - 200 in/in/sec		X							
201 - 250 in/in/sec									
251 - 300 in/in/sec									
301 - 350 in/in/sec									
351 - 400 in/in/sec		X							
401 - 450 in/in/sec		X							
451 - 510 in/in/sec		X							X

**Table 4. Strain Rate Data Coverage for 304/304L Weld Material**

Temperature \ Strain Rate	-90°F to 32°F	33°F to 100°F	101°F to 200°F	201°F to 300°F	301°F to 400°F	401°F to 500°F	501°F to 600°F	601°F to 700°F	701°F to 800°F
1 - 50 in/in/sec	X	X		X			X		
51 - 100 in/in/sec									
101 - 150 in/in/sec									
151 - 200 in/in/sec									
201 - 250 in/in/sec									
251 - 300 in/in/sec									
301 - 350 in/in/sec									
351 - 400 in/in/sec									
401 - 450 in/in/sec									
451 - 510 in/in/sec									

**Table 5. Strain Rate Data Coverage for 316/316L Base Material**

Temperature \ Strain Rate	-90°F to 32°F	33°F to 100°F	101°F to 200°F	201°F to 300°F	301°F to 400°F	401°F to 500°F	501°F to 600°F	601°F to 700°F	701°F to 800°F
1 – 50 in/in/sec	X	X		X			X		X
51 – 100 in/in/sec		X	X						X
101 – 150 in/in/sec		X			X				
151 – 200 in/in/sec		X	X		X				
201 – 250 in/in/sec									
251 – 300 in/in/sec									
301 – 350 in/in/sec									
351 – 400 in/in/sec		X							
401 – 450 in/in/sec		X							
451 – 510 in/in/sec									X

**Table 6. Strain Rate Data Coverage for 316/316L Weld Material**

Temperature \ Strain Rate	-90°F to 32°F	33°F to 100°F	101°F to 200°F	201°F to 300°F	301°F to 400°F	401°F to 500°F	501°F to 600°F	601°F to 700°F	701°F to 800°F
1 – 50 in/in/sec	X	X		X			X		
51 – 100 in/in/sec									
101 – 150 in/in/sec									
151 – 200 in/in/sec									
201 – 250 in/in/sec									
251 – 300 in/in/sec									
301 – 350 in/in/sec									
351 – 400 in/in/sec									
401 – 450 in/in/sec		X							
451 – 510 in/in/sec									

#### **4.1.3.1 Sensitivity of Austenitic Stainless Steel to Strain Rate Effects**

A number of personnel have questioned the sensitivity of austenitic stainless steels to strain rate effects. It is surmised that these individuals may have misread strain rate discussions or information in the past. The final nine references selected for this literature search clearly demonstrate that austenitic stainless steels, types 304/304L and 316/316L, are indeed strain rate sensitive.

#### **4.1.3.2 Factoring of True Stress-Strain Curves**

Looking at the available true stress-strain curves from the nine strain rate references that reflect higher strain rates, a number of those curves (References 10, 14, and 15) appear to be a uniform factor higher (in the stress direction) than the corresponding quasi-static true stress-strain curve. This feature also holds true for other references (References 17 and 18) that contained true stress-strain curves at varying strain rates but did not comply with the literature search limitations established. If this feature continues to hold true with additional strain rate data, this would be a very simple way to correlate strain rate effects to readily available 304/304L and 316/316L quasi-static true stress-strain curves, as was done in Reference 16.

#### **4.1.3.3 Variation of Uniform or Fracture Strain Limits Versus Strain Rate**

Some engineers have indicated an expectation that the uniform strain limit (corresponding to the strain just before the onset of necking) and the fracture strain limit (corresponding to the strain at the point of test specimen fracture or separation) will reduce as the strain rate (over the range of 1 to 510 in/in/sec) increases. Briefly reviewing the nine strain rate references, some show engineering curves where these two strain limits do indeed show indications of reduction but at the upper limits of the strain rates of interest (Reference 8) or indications of reduction at lower and higher strain rates (References 9 and 12). On the other hand, other information collected (References 12, 13, 15, and 16) indicate no significant reductions or some increases in these strain limits as the strain rate increases. Reference 14 indicates that the elongation to fracture increases with the strain rate. Interestingly, where information was available, the earlier testing results tended to show strain limits reduced while later testing results showed strain limits increasing or essentially remaining constant. Test methodology may have an influence as well as how the strain rate was defined. Additional strain rate data is necessary before this trend can be clarified.

#### **4.1.3.4 Validation of Data Generated**

One of the difficulties in utilizing research data from many different sources is ascertaining the validity of those data. If the researcher can perform some level of validation, that provides a major boost in data acceptability. Of the nine references that satisfied the search criteria, only two (References 13 and 16) provided any validation insights. For both of these references, the validation effort indicated that when the strain rate data was incorporated into finite element method inelastic analyses, good agreement was attained when compared to actual test results.

#### **4.1.3.5 Test Specimen Size**

Commentary in various literature have expressed concern over extending small or thin test specimen research results to situations where the actual material used involves much larger and much thicker material. Do thinner materials present different material properties than thicker materials? Are failure responses altered? At this point, any commentary will be withheld until more research data become available.

#### **4.1.3.6 Comparison of Strain Rate Data Between References**

Performing a meaningful comparison between the available strain rate data would indicate if there is agreement or significant differences. Different researchers or different test methods could introduce unknown biases. However, at a minimum, the numerous engineering or true stress-strain curves need to be digitized and plotted on the same graph in order to begin any meaningful comparison. But that

preliminary step can be a time-consuming effort, too much to attempt with the limited funding provided for this task.

## 4.2 ASME BPV, Section III, Division 3 Activities

Another aspect of advancing technical issues that affects the proposed moderator exclusion concept and the standardized transportation system is the updating and revision of rules provided in the ASME BPV Code, Section III, Division 3. Division 3 provides the construction rules for both storage and transportation containments. Although not heavily used in the past, Division 3 has been significantly revised in the last decade to make it more useful and applicable to the storage and transportation industry. In addition, the NRC is currently reviewing Division 3 with the eventual goal of endorsement. History has shown that applicants typically use codes and standards endorsed by the NRC, rather than attempting to justify alternative rules on a case-by-case basis.

Supported by UFDC funding, the author was able to attend all four ASME BPV Code Weeks held during FY 2012. The author is a member of the Working Group on Design of Division 3 Containments, is the Secretary for the Subgroup on Containment Systems for Spent Fuel and High-Level Waste Transport Packagings (otherwise known as Subgroup NUPACK), and is a member of the BPV Standards Committee on Construction of Nuclear Facility Components.

Two Section III, Division 3 actions that directly affect the proposed moderator exclusion concept and standardized transportation were balloted through the various ASME BPV committees during FY 2012 and include:

- clarification of helium leak testing requirements for inner containments in Subsection WB-6120, and
- strain-based acceptance criteria applicable to both storage and transportation containments.

The author was the ASME Project Manager for both of these actions. The ASME Project Manager has the responsibility to develop the revision documentation, submit the action for ASME approval, and monitor the balloting process, answering any comments received during the balloting process.

Regarding the first action, the existing WB-6120, *Testing of Containments*, required all transportation containments to be pressure tested and leak tested except for any final closure welds made on inner containments. The main problem was that no requirements were provided for the final closure welds. WB-6120 was revised to include both final closure welds and final mechanical closures made on inner containments and clarified that both of these final closures shall be leak tested only. No pressure test is required on these final closures made on inner containments after being loaded with spent fuel or high-level waste. This revision received full ASME approval on July 11, 2012 and should be published in the next 2013 Edition of the ASME BPV Code.

The second action is still in the ASME balloting process. The strain-based acceptance criteria deliberations started in the Working Group on Design of Division 3 Containments back in 2006. The Working Group on Design Methodology was also involved since this was a new design approach for Section III. After revising many different proposals, a final version of the strain-based acceptance criteria was finally approved in November 2011 by these two Working Groups. The next step was to begin the ASME balloting process through higher committees and providing presentations to various ASME committees explaining the action and answering committee member questions. As of the writing of this report, the strain-based acceptance criteria have been approved by all of the appropriate committees reporting to the BPV Standards Committee on Construction of Nuclear Facility Components, including the Subgroup on Materials, Fabrication, and Examination, the Subgroup on Component Design, and the Subcommittee on Design.

The next step in the ASME balloting process will be to submit the strain-based acceptance criteria to the BPV Standards Committee on Construction of Nuclear Facility Components. This submittal is

expected to be achieved at the 2012 August Code Week meetings. Actual balloting will likely begin in late August and carry into September.

The current strain-based acceptance criteria require the user to perform material testing in order to obtain the necessary true stress-strain curve material properties to implement the criteria. The criteria currently address strain rate effects separately in a conservative fashion. But the criteria can be improved and made more user friendly if ASME could provide these material data. Discussions with the ASME BPV Code, Section II material experts regarding the incorporation of appropriate true stress-strain curves and strain rate data for use with the strain-based acceptance criteria are on-going. If a more fully defined and validated database of temperature dependent true stress-strain curves and strain rate data for the austenitic stainless steels of interest can be established, certain levels of inelastic analysis conservatism are expected to be reduced, improving the accuracy of inelastic analysis predictions of structural responses to energy-limited events. The strain-based acceptance criteria are believed to be a significant step forward in more accurately evaluating the acceptability of energy-limited dynamic loadings on containments. The significance of the strain-based acceptance criteria is that future storage and transportation containments, including the inner containment (adaptable insert and lid), will be able to be designed more efficiently. The NRC has indicated support for incorporating strain-based acceptance criteria into Division 3.

## 5. CONCLUSIONS

Achieving moderator exclusion by utilizing a watertight inner barrier excludes the possibility of criticality of commercial used fuels during transportation. When the storage canister cannot provide that watertight function, a separate inner containment can provide the watertight function. Following this graded approach, the proposed moderator exclusion concept provides a positive path forward for DOE to transport used fuel after extended storage, regardless of the condition of the fuel, baskets, poisons, or the storage canister. This concept also supports standardization of the transportation system. The significance of what the proposed moderator exclusion concept offers is why the INL believes that it is important to be proactive in discussing the proposal and in keeping the concept fresh in the minds of applicants, regulators, and other decision makers. The assigned Task 1 supported this effort and success was achieved.

Advances on various technical issues are also very important, especially when the technical issues also support the proposed moderator exclusion concept and standardized transportation. Task 2 provided the opportunity to make significant advances in the applicable codes and standards area by revising ASME BVP Code, Section III, Division 3 rules and making progress on new design methods and acceptance criteria. Task 2 was also successfully completed.

Although the FY 2012 funding received was limited, the INL was able to successfully complete its assigned tasks and move the issue of used fuel transportation forward. Many technical decisions still have to be made. With future funding, the INL can continue making progress so that used fuel transportation can be accomplish in a safe and efficient manner.

## 6. REFERENCES

1. Department of Energy presentation by Jeffrey Williams, "DOE/NE Used Fuel Disposition Program Overview," 27<sup>th</sup> INMM Spent Fuel Management Seminar, February 1, 2012.
2. International Atomic Energy Agency, "Regulations for the Safe Transport of Radioactive Material," IAEA Safety Standards Series No. TS-R-1, Paragraph 677, 2009 Edition.
3. U.S. Code of Federal Regulations, Title 10, Part 71, "Packaging and Transportation of Radioactive Material," June 17, 2011.

4. Morton, D. K., et al., *Idaho National Laboratory Transportation Task Report on Achieving Moderator Exclusion and Supporting Standardized Transportation*, INL/EXT-11-22559, September 2011.
5. U.S. Nuclear Regulatory Commission, Staff Requirements Memorandum, “Staff Requirements – SECY-07-0185 – Moderator Exclusion in Transportation Packages,” December 18, 2007.
6. U.S. Nuclear Regulatory Commission, Commission Papers, “Moderator Exclusion in Transportation Packages,” SECY-07-0185, October 22, 2007.
7. American Society of Mechanical Engineers, “Boiler and Pressure Vessel Code,” Section III, Division 3, *Containments for Transportation and Storage of Spent Nuclear Fuel and High Level Radioactive Material and Waste*, 2010 Edition with 2011 Addenda.
8. Albertini, C. and M. Montagnani, “Wave Propagation Effects in Dynamic Loading,” *Nuclear Engineering and Design*, Vol. 37, 1976, pp. 115-124.
9. Albertini, C. and M. Montagnani, “Dynamic Uniaxial and Biaxial Stress-Strain Relationships for Austenitic Stainless Steel,” *Nuclear Engineering and Design*, Vol. 57, 1980, pp. 107-123.
10. Japan Society of Mechanical Engineers, *Report on Database for Structural Analysis of Spent Fuel Shipping Cask*, November 1985.
11. Marschall, C. W., M. P. Landow, and G. M. Wilkowski, *Loading Rate Effects on Strength and Fracture Toughness of Pipe Steels Used in Task 1 of the IPIRG Program*, NUREG/CR-6098, October 1993.
12. O’Toole, B., *Identification of Dynamic Properties of Materials for the Nuclear Waste Package*, TR-02-007, Revision 0, prepared for the U.S. DOE/UCCSN Cooperative Agreement Number: DE-FC08-98NV12081, Task 24, September 30, 2003.
13. Langdon, G. S. and G. K. Schleyer, “Unusual Strain Rate Sensitive Behaviour of AISI 316L Austenitic Stainless Steel,” *Journal of Strain Analysis*, Vol. 39, No. 1, 2003, pp. 71-86.
14. Talonen, J. et al., “Effect of Strain Rate on the Strain-Induced  $\gamma \rightarrow \alpha$ -Martensite Transformation and Mechanical Properties of Austenitic Stainless Steels,” *Metallurgical and Materials Transactions A*, Vol. 36A, February 2005, pp. 421-432.
15. Lichtenfeld, J. A., M. C. Mataya, and C. J. Van Tyne, “Effect of Strain Rate on Stress-Strain Behavior of Alloy 309 and 304L Austenitic Stainless Steel,” *Metallurgical and Materials Transactions A*, Vol. 37A, January 2006, pp. 147-161.
16. Morton, D. K., and R. K. Blandford, *Impact Tensile Testing of Stainless Steels at Various Temperatures*, DOE Report EDF-NSNF-082, Revision 0, March 31, 2008.
17. Lee, W-S and Chi-Feng Lin, “Impact Properties and Microstructure Evolution of 304L Stainless Steel”, *Materials Science and Engineering A308*, 2001, pp. 124-135.
18. Nicholas, T., *Dynamic Tensile Testing of Structural Materials Using a Split Hopkinson Bar Apparatus*, AFWAL-TR-80-4053, October 1980.

## **APPENDIX D**

### **Consequences of Fuel Failure on Criticality Safety of Used Nuclear Fuel**

**FCRD Technical Integration Office (TIO)**  
**DOCUMENT NUMBER REQUEST**

**1. Document Information**

Document Title/Description:	Consequences of Fuel Failure on Criticality Safety of Used Nuclear Fuel				Revision:	0
Assigned Document Number:	FCRD-UFD-2012-000262				Effective Start Date:	September 1, 2012
Document Author/Creator:	W.J. Marshall				OR	
Document Owner:	J.C. Wagner				Date Range:	
Originating Organization:	Oak Ridge National Laboratory				From:	To:
Milestone	<input type="checkbox"/> M1	<input checked="" type="checkbox"/> M2	<input type="checkbox"/> M3	<input type="checkbox"/> M4	<input type="checkbox"/> Not a Milestone	
Milestone Number::	M2FT-12OR0813031					
Work Package WBS Number:	FT-12OR081303/ 1.02.08.13					
Controlled Unclassified Information (CUI) Type	<input checked="" type="checkbox"/> None <input type="checkbox"/> OUO <input type="checkbox"/> AT <input type="checkbox"/> Other					

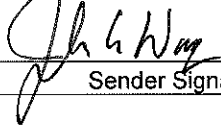
FCRD	<b>SYSTEM:</b>			
	<input type="checkbox"/> FUEL	Advance Fuels		
	<input type="checkbox"/> SWF	Separations and Waste Forms		
	<input type="checkbox"/> MPACT	Materials Protection, Accounting, and Control for Transmutation		
	<input checked="" type="checkbox"/> UFD	Used Fuel Disposition		
	<input type="checkbox"/> FCO	Fuel Cycle Options		
	<input type="checkbox"/> TIO	Technical Integration		
	<input type="checkbox"/>			

**2. Records Management Requirements**

Category:	<input checked="" type="checkbox"/> General Record	<input type="checkbox"/> QA Record	<input type="checkbox"/> Controlled Doc	<input type="checkbox"/> Controlled QA Doc
Keywords:	Used Nuclear Fuel Failure Criticality Safety			
Medium:	<input type="checkbox"/> Hard Copy	<input type="checkbox"/> CD/Disk (each CD/Disk must have an attached index)	<input type="checkbox"/> Electronic:	
Total Number of Pages (including transmittal sheet):				
<u>If QA Record</u>				
QA Classification:	<input type="checkbox"/> Lifetime	<input checked="" type="checkbox"/> Non-Permanent		
Uniform Filing Code:	8406	Disposition Authority:	RD1-A-2	Retention Period:
Level II Cut off after project/program completion, cancellation, or termination. Destroy 25 years after cut off.				

Special Instructions:	None		
-----------------------	------	--	--

**3. Signatures**

SENDER:	John C. Wagner		8/31/12
Print/Type Sender Name		Sender Signature	Date
QA RECORD VALIDATOR:			
Print/Type Authenticator Name	Authenticator Signature		Date
ACCEPTANCE/RECEIPT:			
Print/Type Receiver Name	Receiver Signature		Date

Submit to: **Connie.Bates@inl.gov**

## Appendix E

### FCT Document Cover Sheet

Name/Title of Deliverable/Milestone

Consequences of Fuel Failure on Criticality Safety of Used Nuclear Fuel

Work Package Title and Number

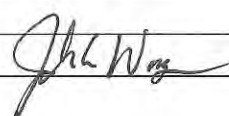
ST Transportation-ORNL / FT-12OR081303

Work Package WBS Number

**1.02.08.13**

Responsible Work Package Manager

John C. Wagner



(Name/Signature)

Date Submitted

Quality Rigor Level for Deliverable/Milestone	<input checked="" type="checkbox"/> QRL-3	<input type="checkbox"/> QRL-2	<input type="checkbox"/> QRL-1 <input type="checkbox"/> Nuclear Data	<input type="checkbox"/> N/A*
---	---	--------------------------------	---	-------------------------------

This deliverable was prepared in accordance with

Oak Ridge National Laboratory

(Participant/National Laboratory Name)

QA program which meets the requirements of

 DOE Order 414.1       NQA-1-2000

This Deliverable was subjected to:

 Technical Review Peer Review**Technical Review (TR)****Peer Review (PR)****Review Documentation Provided** Signed TR Report or,**Review Documentation Provided** Signed TR Concurrence Sheet or, Signed PR Report or, Signature of TR Reviewer(s) below Signed PR Concurrence Sheet or, Signature of PR Reviewer(s) below**Name and Signature of Reviewers**

John Scaglione (Electronic Record Attached)

Donald Mueller (Electronic Record Attached)

\*Note: In some cases there may be a milestone where an item is being fabricated, maintenance is being performed on a facility, or a document is being issued through a formal document control process where it specifically calls out a formal review of the document. In these cases, documentation (e.g., inspection report, maintenance request, work planning package documentation or the documented review of the issued document through the document control process) of the completion of the activity along with the Document Cover Sheet is sufficient to demonstrate achieving the milestone. QRL for such milestones may be also marked N/A in the work package provided the work package clearly specifies the requirement to use the Document Cover Sheet and provide supporting documentation.

 Publication Tracking System

This List: Publication List



Publication Tracking System &gt; Publication List

View Record (Logged in as Weaver, Deborah J)

<a href="#"> Edit Item</a>   <a href="#"> Change Communication Type</a>   <a href="#"> Delete Item</a>			
<b>Pub ID</b>	38136		
<b>Title</b>	Consequences of Fuel Failure on Criticality Safety of Used Nuclear Fuel		
<b>Status</b>	Awaiting Distribution		
<b>Communication Type</b>	ORNL report		
<b>ORNL Review?</b>	Scientific communication that requires ORNL review		
<b>Information Category</b>	Unlimited		
<b>ORNL Report Classification</b>	Topical		
<b>Contact Person</b>	Marshall, William BJ J		
<b>Responsible Organization</b>	Reactor & Nuclear Systems Division (50159781)		
<b>Prepared at</b>	This scientific communication is being prepared by someone at ORNL.		
<b>Document Access</b>	Available to the public.		
<b>Authors</b>	Marshall, William BJ J.	ORNL (627296)	
	Wagner, John C.	ORNL (37727)	
<b>Workflow</b>	08/16/2012 11:39:02	Draft	Marshall, William BJ J by Weaver, Deborah J
	08/16/2012 14:07:01	Author Certification	Marshall, William BJ J
	08/16/2012 14:07:01	Submitted for review	Marshall, William BJ J
	08/16/2012 13:52:39	Supervisor	Dunn, Michael E
	08/20/2012 08:44:39	Technical Reviewer	Mueller, Don
	08/20/2012 17:47:11	Technical Reviewer	Hu, Jianwei
	08/23/2012 14:01:12	Technical Reviewer	Scaglione, John M
	08/26/2012 16:31:58	Technical Editor	Stevens, Deborah P
	08/27/2012 14:43:55	Administrative Check	Weaver, Deborah J
	08/28/2012 11:18:07	Supervisor	Dunn, Michael E
	08/31/2012 12:33:39	Program Manager	Howard, Rob L
	08/31/2012 16:32:52	Division Approver	Parks, Cecil V by Poarch, Sandra J
	08/31/2012 16:32:52	Awaiting Distribution	Parks, Cecil V by Poarch, Sandra J
			<i>Waiting on contact person to mark as 'Distributed'.</i>
		Distributed	Marshall, William BJ J
<b>Document</b>	<a href="#">edited_UFD_Transportation_Consequences_of_Fuel_Failure_Draft_8_27_2012.pdf</a>		
	<b>Important:</b> Documents containing sensitive information should not be loaded into PTS. For further clarification, please contact ORNL's Technical Information Officer.		
<b>Abstract</b>			
<b>Report Number</b>	ORNL/TM-2012/325		
<b>Secondary ID Number</b>			
<b>Additional Information</b>			
<b>Distribution Month</b>			
<b>Distribution Year</b>			
<b>User Facility</b>	Not related to a user facility		
<b>Account Number(s)</b>	35304813		
<b>B&amp;R Codes</b>	AF5865000		
<b>IANs</b>			
<b>FWP</b> s	NEAF346		
<b>Overhead Categories</b>			
<b>Proposal Numbers</b>			
<b>Keywords</b>			

# ***Consequences of Fuel Failure on Criticality Safety of Used Nuclear Fuel***

---

**Fuel Cycle Research & Development**

*Prepared for*  
**U.S. Department of Energy**  
**Fuel Cycle Technologies Program**  
**W. J. Marshall**  
**J. C. Wagner**  
**Oak Ridge National Laboratory**  
**September 2012**  
ORNL/TM-2012/325  
FCRD-UFD-2012-000262



#### **DISCLAIMER**

This information was prepared as an account of work sponsored by an agency of the U.S. Government. Neither the U.S. Government nor any agency thereof, nor any of their employees, makes any warranty, expressed or implied, or assumes any legal liability or responsibility for the accuracy, completeness, or usefulness, of any information, apparatus, product, or process disclosed, or represents that its use would not infringe privately owned rights. References herein to any specific commercial product, process, or service by trade name, trade mark, manufacturer, or otherwise, does not necessarily constitute or imply its endorsement, recommendation, or favoring by the U.S. Government or any agency thereof. The views and opinions of authors expressed herein do not necessarily state or reflect those of the U.S. Government or any agency thereof.

## EXECUTIVE SUMMARY

This report documents work performed for the Department of Energy's Office of Nuclear Energy (DOE-NE) Fuel Cycle Technologies Used Fuel Disposition Campaign to assess the impact of fuel reconfiguration due to fuel failure on the criticality safety of used nuclear fuel (UNF) in storage and transportation casks. This work was motivated by concerns related to the potential for fuel degradation during extended storage (ES) periods and transportation following ES, but has relevance to other potential causes of fuel reconfiguration.

Commercial UNF in the United States is expected to remain in storage for longer periods than originally intended. Extended storage time and irradiation of nuclear fuel to high-burnup values ( $>45$  GWd/t) may increase the potential for fuel failure during normal and accident conditions involving storage and transportation. Fuel failure, depending on the severity, can result in changes to the geometric configuration of the fuel, which has safety and regulatory implications for virtually all aspects of a UNF storage and transport system's performance. The potential impact of fuel reconfiguration on the safety of UNF in storage and transportation is dependent on the likelihood and extent of the fuel reconfiguration, which is not well understood and is currently an active area of research. The objective of this work is to assess and quantify the impact of postulated failed fuel configurations on the criticality safety of UNF in storage and transportation casks. Although this work is motivated by the potential for fuel degradation during ES periods and transportation following ES, it has relevance to fuel reconfiguration due to the effects of high burnup. Regardless of the ultimate disposition path, UNF will need to be transported at some point in the future.

To investigate and quantify the impact of fuel reconfiguration on criticality safety limits, which are given in terms of the effective neutron multiplication factor,  $k_{\text{eff}}$ , a set of failed fuel configuration categories was developed and specific configurations were evaluated. The various configurations were not developed to represent the results of specific reconfiguration progressions; rather, they were designed to be bounding of any reconfiguration progressions that could occur. The configuration categories considered in this analysis include the following:

- clad thinning/loss – reduced cladding thickness up to the total removal of all cladding material
- rod failures – removal of one or more fuel rods from the assembly lattice
- loss of rod pitch control – rod pitch contraction and expansion within the storage cell
- loss of assembly position control – axial displacement of fuel assemblies
- gross assembly failure – rubblized fuel within the storage cells with varying degrees of moderation
- neutron absorber degradation – gaps of varying location and size; thinning of absorber panels.

Within each category, a number of specific configurations were modeled to calculate the corresponding  $k_{\text{eff}}$  values and the associated consequences of those configurations relative to the reference intact configuration. The consequence of a given configuration is defined as the difference in the calculated  $k_{\text{eff}}$  values for the given configuration and the reference intact configuration, with a positive value indicating an increase in  $k_{\text{eff}}$  as compared to the reference configuration. Several of the specific configurations are not considered credible but are included in the analyses for completeness (e.g., to fully understand trends and worst-case situations). Pending improved understanding of the various material degradation phenomenon, and subsequent determination and justification for what configurations are and are not credible, the assessment of the credibility of configurations provided herein is based on engineering judgment. The credibility of configurations and the impact of the configurations on criticality safety are dependent on many factors, including storage and transportation conditions, the fuel assembly

characteristics, and the storage and/or transportation system characteristics. Therefore, the assessment and analysis of credible configurations for a specific cask system would need to be performed as part of the safety analysis for licensing that system.

Representative pressurized water reactor (PWR) and boiling water reactor (BWR) fuel assembly designs loaded in representative cask systems were considered in this report. The two fuel assembly designs selected for this analysis represent a large portion of the current inventory of discharged UNF and/or a significant portion of the fuel designs currently in use. The cask systems selected for this analysis are high-capacity 32-PWR-assembly general burnup credit cask (GBC-32) and 68-BWR-assembly multipurpose canister (MPC-68) cask designs based on the Holtec International HI-STAR 100 system. The depletion conditions used in this analysis are considered representative of those used in a burnup credit criticality safety evaluation. The analysis focuses on typical discharge fuel conditions (e.g., fuel initial enrichment, discharge burnup, and post-irradiation decay time) that could be loaded into storage and transportation casks. Additional burnup and extended post-irradiation cooling times are considered in this analysis for both PWR and BWR fuel to establish the sensitivity of reconfiguration impacts to these parameters.

For the configurations judged by the authors to be potentially credible, the maximum increase in  $k_{\text{eff}}$  for the PWR cask system (GBC-32) was nearly 4%, corresponding to a nonuniform pitch expansion configuration due to a loss of fuel rod pitch control, and that for the BWR cask system (MPC-68) was 2.4%, corresponding to a configuration with multiple rod failures. It is important to emphasize that these results are contingent on the authors' judgment relative to the potential credibility of configurations, which includes not only whether a configuration category is credible but also whether the resulting configurations within a given category are credible for a specific cask system. For example, for the PWR cask system, axial assembly displacement such that assemblies extended more than 7.5 cm above or below the neutron absorber panel was not considered credible because of the presence of fuel assembly hardware and cask assembly spacers. If it were determined that such a configuration is credible, then that configuration and its specific characteristics may be limiting. Similarly, for the BWR cask system, the fuel assembly channel is assumed to be present and capable of constraining fuel rod pitch expansion. If the channel is not present or unable to constrain rod pitch expansion, then that configuration may be limiting. In addition to representative conditions for fuel burnup and post-irradiation decay time, the effects of higher burnup and longer cooling times were also investigated and found to be smaller than the reduction in  $k_{\text{eff}}$  associated with the higher burnup or cooling time.

Because a wide range of credible and non-credible configurations were analyzed, the calculated consequences also varied widely. For the PWR cask system (GBC-32), the calculated  $k_{\text{eff}}$  increase varied from 0.1% to almost 22.25%  $\Delta k_{\text{eff}}$ . For the BWR cask system (MPC-68), the calculated increase varied from 0.3%  $\Delta k_{\text{eff}}$  to as much as almost 36%  $\Delta k_{\text{eff}}$ . Some configurations in both cask systems result in decreases in  $k_{\text{eff}}$ . As the Nuclear Regulatory Commission (NRC) Standard Review Plans, which provide guidance for demonstrating compliance with the applicable regulations, recommend that  $k_{\text{eff}}$  should not exceed 0.95 under all credible conditions during storage and transportation, such large increases are concerning. However, as noted, a number of the configurations analyzed are not considered credible.

The magnitude of the potential increases in  $k_{\text{eff}}$  and the sensitivity of the potential increases in  $k_{\text{eff}}$  to the determination of the credibility of configurations highlight the importance of being able to determine and justify which configurations are credible under a given set of conditions for a given cask system. It is anticipated, at least in the near term, that these determinations will be done on a case-by-case basis for each cask system and associated licensing conditions.

Given the establishment of a set of credible failed fuel configurations for a given cask system and assuming that one or more of the configurations result in an increase in  $k_{\text{eff}}$  (above the regulatory limit of

0.95), the consequence of this potential increase in  $k_{\text{eff}}$  must be addressed. There are a number of potential options, the viability of which depends on the magnitude of the increase in  $k_{\text{eff}}$ . For example, a cask design and/or fuel assembly loading conditions could be modified to ensure that the current  $k_{\text{eff}}$  limit of 0.95 is satisfied for all credible failed fuel configurations. Separate assembly loading criteria (e.g., loading curves) based on a reduced  $k_{\text{eff}}$  limit could be developed for fuel assemblies that may have questionable integrity. In the context of high-burnup fuel or ES durations, a separate loading curve based on a lower  $k_{\text{eff}}$  limit could be developed and applied to fuel assemblies with burnup greater than 45 GWd/MTU and/or with a post-irradiation storage period beyond some specified value. Alternatively, depending on the probability of fuel reconfiguration, it may be possible that a separate higher limit could be established to allow margin for the increased reactivity effect associated with fuel reconfiguration. This latter approach would be similar to the higher limit (i.e., 0.98) allowed for the unlikely optimum moderation condition in dry storage of fresh fuel under 10 CFR 50.68. In this case, the customary  $k_{\text{eff}}$  limit would still apply to all conditions involving intact fuel. Limits above 0.95 are also allowed in some facilities regulated by the NRC Fuel Cycle Safety and Safeguards Division, and hence precedents for this type of approach exist. For casks that have already been loaded prior to implementation of a generic mitigation strategy, the analysis basis may be extended to include or expand burnup credit, providing mitigation for potential consequences of fuel reconfiguration.

Although the results indicate that the potential impacts on subcriticality can be rather significant for certain configurations, it can be concluded that the consequences of credible fuel failure configurations from ES or transportation following ES are manageable. Some examples for how to address the potential increases in  $k_{\text{eff}}$  in a criticality safety evaluation were provided. Future work to further inform decision-making relative to which configurations are credible, and therefore need to be considered in a safety evaluation, is recommended.



## CONTENTS

	<u>Page</u>
EXECUTIVE SUMMARY .....	iii
FIGURES .....	ix
TABLES .....	xiii
ACRONYMS .....	xvii
1. INTRODUCTION AND BACKGROUND .....	1
2. REVIEW OF LITERATURE .....	2
2.1 NRC Documents .....	2
2.2 EPRI Reports.....	3
2.3 PATRAM Proceedings .....	4
2.3.1 PATRAM 2010.....	4
2.3.2 PATRAM 2007.....	5
2.3.3 PATRAM 2004.....	6
2.3.4 PATRAM 2001 .....	6
2.4 Other Sources.....	7
2.5 Literature Review Summary .....	7
3. FAILED FUEL CONFIGURATIONS .....	7
3.1 Fuel and Cask Reconfiguration Descriptions.....	8
3.1.1 Clad Thinning/Loss.....	8
3.1.2 Rod Failures .....	9
3.1.3 Loss of Rod Pitch Control.....	10
3.1.4 Loss of Assembly Position Control .....	11
3.1.5 Gross Assembly Failure .....	11
3.1.6 Neutron Absorber Degradation.....	13
3.2 Varying Number of Reconfigured Assemblies .....	14
3.3 Multiple Reconfiguration Mechanisms.....	14
3.4 Credibility of Degraded Configurations.....	14
4. MODELS, CODES, AND METHODS USED .....	17
4.1 Fuel Assembly Models.....	17
4.2 Cask Models.....	17
4.2.1 GBC-32 Cask Model.....	17
4.2.2 MPC-68 Cask Model .....	19
4.3 Software Codes .....	20
4.4 Depletion Modeling Parameters.....	20
4.4.1 PWR Depletion Conditions.....	21
4.4.2 BWR Depletion Conditions .....	21

## CONTENTS (continued)

	<u>Page</u>
5. RESULTS.....	22
5.1 GBC-32 Cask Model Results.....	22
5.1.1 Reconfiguration of All Assemblies.....	23
5.1.2 Varying Number of Reconfigured Assemblies.....	38
5.1.3 Combined Configurations.....	44
5.2 MPC-68 Cask Model Results.....	45
5.2.1 Reconfiguration of All Assemblies.....	45
5.2.2 Varying Number of Reconfigured Assemblies.....	61
5.2.3 Combined Configurations.....	69
5.2.4 Part-Length Fuel .....	70
6. SUMMARY AND CONCLUSIONS.....	77
6.1 Summary of Analyses .....	77
6.2 Observations and Conclusions .....	78
7. RECOMMENDATIONS FOR FUTURE WORK .....	80
REFERENCES .....	81
Appendix A Fuel Assembly Modeling Details .....	85
Appendix B MPC-24 Modeling and Results .....	89
Appendix C Sensitivity to Burnup and Cooling Time .....	111
Appendix D Details of Cask Modeling.....	123
Appendix E Development of BWR Depletion Conditions .....	127

## FIGURES

	<u>Page</u>
Figure 1. Sketch showing “birdcaging” as the result of an end drop .....	5
Figure 2. Cross section of GBC-32 half-cask model. ....	18
Figure 3. Representative fuel assembly loading curve for GBC-32. ....	18
Figure 4. Cross section of MPC-68 model.....	19
Figure 5. Increase in $k_{\text{eff}}$ due to reduced cladding thickness .....	24
Figure 6. Configuration with 50% cladding thickness.....	25
Figure 7. Sketch of symmetry, row, and column labels for W 17 × 17 fuel assembly. ....	26
Figure 8. Increase in $k_{\text{eff}}$ in GBC-32 cask as a function of number of rods removed .....	27
Figure 9. Limiting multiple rod removal lattice (44 rods removed). ....	27
Figure 10. Maximum uniform pitch expansion case. ....	29
Figure 11. Increase in $k_{\text{eff}}$ in GBC-32 cask due to increased fuel rod pitch.....	30
Figure 12. Example nonuniform pitch model in GBC-32 storage cell. ....	30
Figure 13. Assembly with axially varying pitch in the GBC-32. ....	31
Figure 14. Misalignment of fuel assembly 20 cm toward lid of GBC-32. ....	32
Figure 15. Increase in $k_{\text{eff}}$ in GBC-32 as a function of assembly axial displacement .....	33
Figure 16. Limiting homogeneous rubble configuration for GBC-32. ....	35
Figure 17. Limiting ordered pellet array configuration for GBC-32. ....	35
Figure 18. Limiting location of 5-cm neutron absorber panel defect in GBC-32. ....	37
Figure 19. Increase in $k_{\text{eff}}$ as a function of remaining neutron absorber panel thickness for fresh 1.92 w/o fuel.....	38
Figure 20. One order of assembly reconfiguration in GBC-32 partial degradation configurations.....	39
Figure 21. Increase in $k_{\text{eff}}$ in GBC-32 as a function of number of reconfigured assemblies, single rod failure (5 w/o initial enrichment, 44.25 GWd/MTU burnup). ....	41
Figure 22. Increase in $k_{\text{eff}}$ in GBC-32 as a function of number of reconfigured assemblies, multiple rod failure (5 w/o initial enrichment, 44.25 GWd/MTU burnup). ....	41
Figure 23. Increase in $k_{\text{eff}}$ in GBC-32 as a function of number of reconfigured assemblies, uniform pitch increase (5 w/o initial enrichment, 44.25 GWd/MTU burnup). ....	42
Figure 24. Increase in $k_{\text{eff}}$ as a function of number of reconfigured assemblies, gross assembly failure. ....	44
Figure 25. Increase in $k_{\text{eff}}$ as a function of fraction of intact cladding, fresh 5 w/o fuel.....	47
Figure 26. Configuration with 25% nominal cladding thickness.....	48
Figure 27. Sketch of symmetry, row, and column labels for GE 10 × 10 fuel assembly. ....	49

## FIGURES (continued)

	<u>Page</u>
Figure 28. Increase in $k_{\text{eff}}$ in MPC-68 as a function of number of rods removed (35 GWd/MTU burnup and 5-year cooling time).....	50
Figure 29. Limiting multiple rod removal lattice (18 rods removed). .....	50
Figure 30. Maximum uniform pitch expansion configuration in MPC-68. ....	52
Figure 31. Example nonuniform pitch model for MPC-68.....	53
Figure 32. Increase in $k_{\text{eff}}$ in MPC-68 as a function of fuel rod pitch, fresh 5 w/o fuel. ....	53
Figure 33. A fresh fuel birdcaging configuration for MPC-68. ....	54
Figure 34. Limited axial misalignment of 20 cm toward cask lid.....	55
Figure 35. Increase in $k_{\text{eff}}$ in MPC-68 as a function of assembly axial displacement (35 GWd/MTU burnup and 5-year cooling time). ....	56
Figure 36. Limiting homogeneous rubble configuration in MPC-68.....	58
Figure 37. Limiting ordered pellet array configuration for MPC-68. ....	58
Figure 38. Limiting neutron absorber defect configuration in MPC-68. ....	60
Figure 39. Increase in $k_{\text{eff}}$ in MPC-68 as a function of remaining neutron absorber panel thickness .....	61
Figure 40. One order of assembly reconfiguration in MPC-68 partial degradation configurations. ....	62
Figure 41. Increase in $k_{\text{eff}}$ in MPC-68 as a function of number of reconfigured assemblies,.....	64
Figure 42. Increase in $k_{\text{eff}}$ in MPC-68 as a function of number of reconfigured assemblies, multiple rod failure (35 GWd/MTU burnup and 5-year cooling time). ....	64
Figure 43. Increase in $k_{\text{eff}}$ in MPC-68 as a function of number of reconfigured assemblies, uniform pitch increase fresh 5 w/o fuel. ....	66
Figure 44. Increase in $k_{\text{eff}}$ as a function of number of reconfigured assemblies, gross assembly failure (35 GWd/MTU burnup and 5-year cooling time). ....	67
Figure 45. Histogram of increases in $k_{\text{eff}}$ for 25 random samples of four reconfigured assemblies. ....	69
Figure 46. Increase in $k_{\text{eff}}$ in MPC-68 as a function of fraction of intact cladding .....	72
Figure 47. Increase in $k_{\text{eff}}$ in MPC-68 as a function of neutron absorber defect axial position,.....	76
Figure 48. Increase in $k_{\text{eff}}$ in MPC-68 as a function of remaining neutron absorber panel thickness, .....	76
Figure A-1. Cross section of $17 \times 17$ OFA assembly.....	86
Figure A-2. Cross section of GE $10 \times 10$ fuel assembly in MPC-68. ....	88
Figure A-3. Location of part-length rods in GE $10 \times 10$ fuel assembly.....	88

## **FIGURES (continued)**

	<u>Page</u>
Figure B-1. Cross section of MPC-24 model.....	89
Figure B-2. Loss of cladding model in MPC-24 storage cell.....	92
Figure B-3. Increase in $k_{\text{eff}}$ in MPC-24 due to reduced cladding thickness.....	92
Figure B-4. Increase in $k_{\text{eff}}$ in MPC-24 versus number of rods removed.....	94
Figure B-5. Limiting multiple rod removal lattice (48 rods removed).....	94
Figure B-6. Increase in $k_{\text{eff}}$ in MPC-24 as a function of fuel rod pitch.....	95
Figure B-7. Maximum pitch expansion case in MPC-24.....	96
Figure B-8. Example axial variation of pitch expansion in MPC-24.....	96
Figure B-9. Increase in $k_{\text{eff}}$ as a function of axial assembly misalignment in MPC-24.....	97
Figure B-10. Assembly in MPC-24 misaligned 20-cm toward cask lid.....	98
Figure B-11. Ordered pellet array configuration for gross assembly failure.....	99
Figure B-12. Homogeneous rubble configuration for gross assembly failure.....	99
Figure B-13. Preferential flooding with only the fuel assemblies flooded.....	100
Figure B-14. 5-cm gap in neutron absorber panels in MPC-24.....	101
Figure B-15. Increase in $k_{\text{eff}}$ in MPC-24 as a function of neutron absorber panel thickness.....	102
Figure B-16. One order of assembly reconfiguration in MPC-24 partial degradation configurations.....	103
Figure B-17. Single rod failure results for a range of number of assemblies experiencing reconfiguration in MPC-24.....	105
Figure B-18. Multiple rod failure results for a range of number of assemblies experiencing reconfiguration in MPC-24.....	105
Figure B-19. Uniform pitch increase results for a range of number of assemblies experiencing reconfiguration in MPC-24.....	106
Figure B-20. Homogeneous rubble results for a range of number of assemblies experiencing reconfiguration.....	108
Figure C-1. Reactivity behavior of fuel with cooling time in a GBC-32 cask.....	111
Figure C-2. Increase in $k_{\text{eff}}$ as a function of cladding thickness remaining.....	113
Figure C-3. Increase in $k_{\text{eff}}$ as a function of cladding thickness remaining.....	118
Figure D-1. Locations of narrow neutron absorber panels in MPC-24 basket.....	124



## TABLES

	<u>Page</u>
Table 1. Credibility and relevance summary.....	16
Table 2. Isotopes included in depleted fuel models.....	21
Table 3. PWR depletion parameters.....	21
Table 4. BWR depletion parameters .....	22
Table 5. Enrichment, burnup, and cooling time for reference cases considered in GBC-32 .....	23
Table 6. Summary of $k_{\text{eff}}$ increases for the GBC-32 cask.....	23
Table 7. Increase in $k_{\text{eff}}$ for cladding removal in GBC-32.....	24
Table 8. Increase in $k_{\text{eff}}$ in GBC-32 cask as a function of cladding fraction remaining .....	24
Table 9. Single rod removal results for $17 \times 17$ OFA in GBC-32.....	26
Table 10. Multiple rod removal results for $17 \times 17$ OFA in GBC-32.....	26
Table 11. Results for loss of rod pitch control in GBC-32.....	29
Table 12. Increase in $k_{\text{eff}}$ for assembly axial displacement in GBC-32 .....	32
Table 13. Increase in $k_{\text{eff}}$ for limited (20 cm displacement relative to the neutron absorber panel).....	32
Table 14. Increase in $k_{\text{eff}}$ in GBC-32 due to gross fuel assembly failure, fissile material outside neutron absorber elevations.....	34
Table 15. Increase in $k_{\text{eff}}$ in GBC-32 due to homogeneous rubble, debris within absorber .....	34
Table 16. Maximum $k_{\text{eff}}$ increase caused by a 5-cm neutron absorber defect in GBC-32.....	36
Table 17. Increase in $k_{\text{eff}}$ caused by a 5-cm neutron absorber defect at various elevations in GBC-32 (5 w/o initial enrichment, 44.25 GWd/MTU burnup).....	36
Table 18. Increase in $k_{\text{eff}}$ caused by uniform neutron absorber panel thinning (fresh 1.92 w/o enrichment).....	37
Table 19. Increase in $k_{\text{eff}}$ in GBC-32, single rod failure .....	40
Table 20. Increase in $k_{\text{eff}}$ in GBC-32, multiple rod failure .....	40
Table 21. Increase in $k_{\text{eff}}$ in GBC-32, uniform pitch increase .....	42
Table 22. Increase in $k_{\text{eff}}$ in GBC-32, homogeneous rubble configuration of gross assembly failure (5 w/o initial enrichment, 44.25 GWd/MTU burnup).....	43
Table 23. Increase in $k_{\text{eff}}$ for combined configurations in GBC-32 .....	45
Table 24. Nominal $k_{\text{eff}}$ results for enrichment, burnup, and cooling time .....	45
Table 25. Summary of $k_{\text{eff}}$ increases for the MPC-68 cask.....	46
Table 26. Increase in $k_{\text{eff}}$ for cladding removal in MPC-68.....	47
Table 27. Increase in $k_{\text{eff}}$ in MPC-68 as a function of fraction of intact cladding, fresh 5 w/o fuel.....	47
Table 28. Single rod removal results for GE $10 \times 10$ fuel in MPC-68.....	49

## TABLES (continued)

	<u>Page</u>
Table 29. Multiple rod removal results for GE 10 × 10 fuel in MPC-68.....	49
Table 30. Results for loss of rod pitch control in MPC-68, no channel restraint.....	52
Table 31. Increase in $k_{\text{eff}}$ caused by loss of assembly position control in MPC-68 .....	55
Table 32. Increase in $k_{\text{eff}}$ for homogeneous rubble configuration of gross fuel assembly failure in MPC-68 .....	57
Table 33. Increase in $k_{\text{eff}}$ for pellet array configuration of gross fuel assembly failure in MPC-68 .....	57
Table 34. Increase in $k_{\text{eff}}$ in MPC-68 due to homogeneous rubble, debris within absorber.....	57
Table 35. Maximum $k_{\text{eff}}$ increase caused by a 5-cm neutron absorber defect in MPC-68.....	59
Table 36. Increase in $k_{\text{eff}}$ caused by a 5-cm neutron absorber defect at various elevations in MPC-68 (35 GWd/MTU burnup and 5-year cooling time) .....	59
Table 37. Increase in $k_{\text{eff}}$ in MPC-68 caused by uniform neutron absorber panel thinning, fresh 5 w/o fuel .....	60
Table 38. Increase in $k_{\text{eff}}$ in MPC-68, single rod failure fresh 5 w/o fuel .....	63
Table 39. Increase in $k_{\text{eff}}$ in MPC-68, multiple rod failure .....	63
Table 40. Increase in $k_{\text{eff}}$ in MPC-68, uniform pitch increase fresh 5 w/o fuel .....	65
Table 41. Increase in $k_{\text{eff}}$ , homogeneous rubble configuration of gross assembly failure.....	67
Table 42. Increase in $k_{\text{eff}}$ for 25 realizations of four randomly selected reconfigured assemblies.....	68
Table 43. Increase in $k_{\text{eff}}$ in combined configurations in MPC-68.....	70
Table 44. Nominal $k_{\text{eff}}$ results for fresh 5 w/o fuel assemblies with part-length rods in MPC-68 .....	71
Table 45. Summary of $k_{\text{eff}}$ impact for fresh 5 w/o fuel with part-length rods in MPC-68 .....	71
Table 46. Increase in $k_{\text{eff}}$ in MPC-68 caused by cladding loss for assemblies with part-length fuel rods, fresh 5 w/o fuel .....	72
Table 47. Increase in $k_{\text{eff}}$ in MPC-68 caused by single rod failure in fresh 5 w/o assemblies with part-length rods.....	73
Table 48. Increase in $k_{\text{eff}}$ in MPC-68 caused by a 5-cm neutron absorber panel defect, fresh 5 w/o fuel with part-length fuel rods .....	75
Table 49. Increase in $k_{\text{eff}}$ in MPC-68 caused by uniform neutron absorber panel thinning, fresh 5 w/o fuel with part-length fuel rods .....	75
Table A-1. Westinghouse 17 × 17 OFA dimensions used in these analyses .....	86
Table A-2. GE 10 × 10 assembly dimensions used in these analyses.....	87
Table B-1. Reference case results for MPC-24 .....	90
Table B-2. Summary of $k_{\text{eff}}$ increases for the MPC-24 cask.....	91

## TABLES (continued)

	<u>Page</u>
Table B-3. Increase in $k_{\text{eff}}$ in MPC-24 due to reduced cladding thickness.....	91
Table B-4. Single rod removal results for $17 \times 17$ OFA in MPC-24.....	93
Table B-5. Increase in $k_{\text{eff}}$ in MPC-24 caused by a 5-cm neutron absorber defect at various elevations.....	101
Table B-6. Increase in $k_{\text{eff}}$ in MPC-24 caused by uniform neutron absorber panel thinning.....	101
Table B-7. Increase in $k_{\text{eff}}$ in MPC-24, single rod failure .....	104
Table B-8. Increase in $k_{\text{eff}}$ in MPC-24, multiple rod failures (48 failed rods) .....	104
Table B-9. Increase in $k_{\text{eff}}$ in MPC-24, uniform pitch increase.....	106
Table B-10. Increase in $k_{\text{eff}}$ in MPC-24, homogeneous rubble configuration of gross assembly failure.....	107
Table B-11. Increase in $k_{\text{eff}}$ in combined configurations for MPC-24.....	109
Table C-1. Nominal $k_{\text{eff}}$ results for enrichment, burnup, and cooling time cases considered in GBC-32.....	112
Table C-2. Single rod removal results for $17 \times 17$ OFA in GBC-32.....	113
Table C-3. Multiple rod removal results for $17 \times 17$ OFA in GBC-32 .....	114
Table C-4. Increase in $k_{\text{eff}}$ caused by uniform fuel pin pitch expansion .....	114
Table C-5. Increase in $k_{\text{eff}}$ for limited assembly axial displacement in GBC-32 .....	115
Table C-6. Increase in $k_{\text{eff}}$ caused by gross fuel assembly failure in GBC-32 .....	115
Table C-7. Increase in $k_{\text{eff}}$ caused by neutron absorber panel defects.....	116
Table C-8. Increase in $k_{\text{eff}}$ caused by uniform neutron absorber panel thinning (44.25 GWd/MTU burnup, 5-year cooling time).....	116
Table C-9. Nominal $k_{\text{eff}}$ results for enrichment, burnup, and cooling time cases considered in MPC-68, channeled and unchanneled fuel .....	117
Table C-10. Single rod removal results for GE $10 \times 10$ fuel in MPC-68, intact channel.....	119
Table C-11. Multiple rod removal results for GE $10 \times 10$ fuel in MPC-68, intact channel .....	119
Table C-12. Results for loss of rod pitch control with cladding intact in MPC-68 .....	120
Table C-13. Increase in $k_{\text{eff}}$ for limited assembly axial displacement in MPC-68, intact channel.....	120
Table C-14. Increase in $k_{\text{eff}}$ caused by gross fuel assembly failure in MPC-68.....	121
Table C-15. Maximum $k_{\text{eff}}$ increase caused by a 5-cm neutron absorber defect in MPC-68, intact channel.....	122
Table C-16. Maximum $k_{\text{eff}}$ increase caused by a 10-cm neutron absorber defect in MPC-68, intact channel.....	122

**TABLES (continued)**

	<u>Page</u>
Table C-17. Increase in $k_{\text{eff}}$ caused by uniform neutron absorber panel thinning (35-GWd/MTU burnup, 5-year cooling time) .....	122
Table D-1. MPC-24 basket dimensions .....	123
Table D-2. MPC-24 Neutron absorber panel dimensions .....	124
Table D-3. MPC-68 basket dimensions .....	125
Table D-4. MPC-68 neutron absorber panel dimensions .....	125
Table E-1. Potentially limiting relative burnup profiles from Quad Cities Unit 2 and LaSalle Unit 1 .....	128
Table E-2. Average moderator density by axial node, based on Assembly C30 from LaSalle Unit 1 .....	129

## ACRONYMS

BWR	boiling water reactor
CRC	commercial reactor critical
DOE-NE	Department of Energy's Office of Nuclear Energy
EIS	environmental impact statement
EPRI	Electric Power Research Institute
ES	extended storage
FIP	fuel integrity project
GBC	generic burnup credit cask
GE	General Electric
GWd/MTU	gigawatt days per metric ton uranium
HAC	hypothesized accident conditions
ICNC	International Conference on Nuclear Criticality Safety
LWR	light water reactor
MPC	multipurpose canister
NRC	United States Nuclear Regulatory Commission
OFA	optimized fuel assembly
PATRAM	International Symposium on the Packaging and Transportation of Radioactive Materials
PRA	probabilistic risk assessment
PWR	pressurized water reactor
SAR	safety analysis report
SFST	Division of Spent Fuel Storage and Transportation, U.S. Nuclear Regulatory Commission
SRP	standard review plan
UNF	used nuclear fuel
WABA	wet annular burnable absorber
w/o	weight percent



# FUEL CYCLE TECHNOLOGIES PROGRAM

## CONSEQUENCES OF FUEL FAILURE ON CRITICALITY SAFETY OF USED NUCLEAR FUEL

### 1. INTRODUCTION AND BACKGROUND

This report documents work performed for the Department of Energy's Office of Nuclear Energy (DOE-NE) Fuel Cycle Technologies Used Fuel Disposition Campaign to assess the impact of fuel reconfiguration due to fuel failure on the criticality safety of used nuclear fuel (UNF) in storage and transportation casks. The consequences of degradation of neutron absorber panels and cask assembly spacers within the casks are also considered. This work is motivated by concerns related to the potential for fuel degradation during extended storage (ES) periods and transportation following ES, but has relevance to other potential causes of fuel reconfiguration.

Fuel reconfiguration could adversely impact virtually all aspects of a UNF storage and transport system's performance, including thermal, radiation dose, criticality safety, containment, structural, and fuel handling and retrievability, and hence is being studied in research and regulatory activities [1–6]. The likelihood and potential extent of fuel reconfiguration during ES and the subsequent impact of reconfiguration on the safety of the UNF are not well understood. Uncertainties related to the mechanical properties of fuel cladding and other structural materials at high burnups ( $>45$  GWd/MTU) and after ES exacerbate these concerns.

A key element of understanding the impacts of ES is related to ensuring that regulatory requirements are met. These requirements address safety-significant aspects of UNF storage and transportation systems, including criticality safety performance and related operational requirements pertaining to UNF handling and retrievability. The results of this study may be used to develop an effective approach to address criticality safety associated with UNF after ES.

This work is an expansion of NUREG/CR-6835, Ref. 7, and includes the same overall strategy. This strategy is to identify relevant potential fuel degradation configurations, quantify the impact of these configurations on  $k_{\text{eff}}$ , and evaluate potential mitigation strategies to meet criticality safety requirements. This work expands on Ref. 7 by including irradiated (or used) boiling water reactor (BWR) fuel as well as used pressurized water reactor (PWR) fuel, considers longer cooling times, and expands the scope of reconfigurations considered.

The criticality safety requirements for dry storage and transportation of UNF are contained in 10 CFR Parts 72 and 71, respectively Refs. 8 and 9. Standard Review Plans (SRPs), Refs. 10–12, provide guidance for meeting the regulatory requirements, such as the  $k_{\text{eff}}$  limit of 0.95 for ensuring the regulatory requirement associated with criticality safety. Estimates of the change in  $k_{\text{eff}}$  ( $\Delta k$ ) due to credible failed fuel configurations are generated in this analysis. A set of failed fuel configuration categories was developed and specific configurations are analyzed to provide a conservative assessment of the impact on  $k_{\text{eff}}$ . The potential credibility of these configurations is also considered, and only those judged to be potentially credible are considered in the development of mitigation strategies. The change in  $k_{\text{eff}}$  due to credible reconfigurations can be used in at least two different ways. A cask design and/or fuel assembly loading conditions could be modified to ensure that the current  $k_{\text{eff}}$  limit of 0.95 is satisfied for all credible failed fuel configurations. The  $\Delta k$  caused by reconfiguration would be accounted for in the determination

of the loading curve to meet the regulatory limit. It is also possible that a separate higher limit could be established to allow margin for the  $\Delta k$  associated with fuel reconfiguration. This latter approach would be similar to the higher limit allowed for the optimum moderation condition applied to dry storage of fresh fuel (i.e.,  $k_{\text{eff}} \leq 0.98$ ), or the unborated condition in a spent fuel pool that credits soluble boron to demonstrate compliance (i.e.,  $k_{\text{eff}} < 1.0$ ) under 10 CFR 50.68, Ref. 13. In this case, the customary  $k_{\text{eff}}$  limit would still apply to all conditions involving intact fuel.

The results of this work may also be used to focus future materials research efforts. The configurations that lead to the highest  $k_{\text{eff}}$  increases may be precluded or determined not to be credible with appropriate material research and testing coupled with mechanical analyses of the UNF.

In addition to criticality safety, the regulatory requirements for UNF storage and transport systems address safety-significant aspects such as structural, thermal, containment and radiation shielding, as well as related operational requirements pertaining to UNF handling and retrievability, such as those contained in the following Sections of 10 CFR 72. 122 (h) *Confinement barriers and systems*:

- (1) “The spent fuel cladding must be protected during storage against degradation that leads to gross ruptures or the fuel must be otherwise confined such that degradation of the fuel during storage will not pose operational safety problems with respect to its removal from storage. This may be accomplished by canning of consolidated fuel rods or unconsolidated assemblies or other means as appropriate.”
- (5) “The high-level radioactive waste and reactor-related GTCC waste must be packaged in a manner that allows handling and retrievability without the release of radioactive materials to the environment or radiation exposures in excess of part 20 limits. The package must be designed to confine the high-level radioactive waste for the duration of the license.”

Because it is possible that, within potential ES time periods, SNF may be transported under 10 CFR 71, and then returned to dry storage (e.g., at another utility or a national interim storage site) under 10 CFR 72, demonstration of compliance with the current handling and retrievability requirements in 10 CFR 72 may pose a significant challenge.

## 2. REVIEW OF LITERATURE

A review of previous work that is potentially relevant to the scope of this report was conducted. The information reviewed provides a historical context for consideration of fuel reconfiguration during transportation, the extent of reconfiguration that may be expected based on material test data, and an indication of the magnitude of reactivity consequences observed involving configurations similar to those considered in this report.

The documents reviewed are grouped by source into four categories: NRC documents, Electric Power Research Institute (EPRI) documents, International Symposium on the Packaging and Transportation of Radioactive Materials (PATRAM) proceedings, and others. NUREG/CR-6835, Ref. 7, is not specifically reviewed as this report is an update and expansion of that work. The primary differences between this analysis and Ref. 7 are discussed in Section 3.

### 2.1 NRC Documents

The first source of documents reviewed from the NRC was the Division of Spent Fuel Storage and Transportation (SFST) technical exchange meeting held on November 1, 2011. The technical exchange

meeting featured presentations from various members of the industry as well as NRC staff members. The NRC gave a presentation, Ref. 14, related to the reactivity impact of fuel reconfiguration. The presentation discussed pin deformation modeling but did not provide estimates of the  $k_{\text{eff}}$  increase associated with this type of fuel damage. In general, the presentation focused on the development and qualification of models to predict the potential deformation that could occur. Some perspectives on the  $k_{\text{eff}}$  changes caused by fuel reconfiguration were presented that referred to NUREG/CR-6835, Ref. 7, and an EPRI study of the reactivity consequence of fuel reconfiguration, Ref. 15. The presentation provided useful information regarding current NRC positions relative to fuel reconfiguration effects in storage/transportation casks.

Other documents reviewed include NUREG/CR-6672, NUREG/CR-4829, and NUREG-0170, Refs. 16–18. These documents provide generic analyses for package response during transportation accidents. NUREG/CR-6672, Ref. 16, includes updated methodologies and data for analyzing truck and rail cask accidents compared to NUREG/CR-4829, Ref. 17, which was an update of the methodologies used in NUREG-0170, Ref. 18. NUREG-0170 is the original environmental impact statement (EIS) for the transportation of radioactive materials. These documents discuss the impact of failed used fuel rods on source terms but do not include reactivity effects.

Overall, based on the NRC documents reviewed, no new information pertinent to modeling fuel reconfiguration conditions for criticality safety evaluations was identified.

## 2.2 EPRI Reports

EPRI has sponsored research culminating in several reports related to shipping UNF. The reports of interest for this effort tend to cover closely related and frequently overlapping areas. Three reports – *Fuel Relocation Effects for Transportation Packages*, Ref. 15, *Transportation of Commercial Spent Nuclear Fuel: Regulatory Issues Resolution*, Ref. 19, and *Criticality Risks during Transportation of Spent Nuclear Fuel: Revision 1*, Ref. 20 – were referenced in the EPRI presentation at the 2011 SFST Technical Exchange meeting, Ref. 21, that are considered relevant to this work.

Reference 15 is largely a critique of NUREG/CR-6835, Ref. 7, and is focused on demonstrating that fuel reconfiguration effects are small and have minimal impacts on the criticality safety of transportation packages. Qualitative arguments were used to eliminate configurations as not practical in many places. The study provides references to additional EPRI reports to support some suppositions about the performance of fuel cladding in the transportation casks. Some lessons learned from radiochemical assay campaigns are also referred to in establishing the impracticality of many of the extreme configurations studied in Ref. 7.

Computational results are also provided for a number of similar configurations that are evaluated in this report. The  $k_{\text{eff}}$  change associated with pitch expansion over the entire length of the fuel array for PWR fuel is reported as 3.1%  $\Delta k_{\text{eff}}$ . The removal of all cladding material is reported as causing a  $k_{\text{eff}}$  increase of 3.3%  $\Delta k_{\text{eff}}$  in a generic 32-PWR-assembly capacity cask. The pellet array configurations considered were significantly different from those evaluated in this report as described in Section 3.1.5.2.

Reference 19 presents several proposed resolutions to various regulatory issues perceived by EPRI to be particularly problematic for licensing transportation packages characterized as high capacity, containing high-burnup UNF, or both. The document discusses several considerations including moderator exclusion, expanded burnup credit, the robust design of used fuel transportation casks, and systematic analyses based on defense-in-depth. The report summarizes other EPRI-sponsored efforts to investigate the performance of fuel cladding during accident conditions, including a summary of the analysis provided in Reference 15. The criticality analysis section includes a discussion of potential benefits from

burnup credit and moderator exclusion, but no new information pertaining to accident configurations or computational results was provided.

Reference 20 contains a probabilistic risk assessment (PRA) quantifying the frequency of criticality accidents during railway shipment of UNF. The results of this research indicate a very low probability for a criticality accident based on several factors, including the low likelihood of severe rail accidents, large safety margins in the determination of the loading curve used in the certificate of compliance, and the difficulty of generating a critical configuration even with severe accident conditions. No new accident configurations or quantitative  $k_{\text{eff}}$  calculations were presented in this report.

The three reports discussed above provide a synopsis of the information contained in several other EPRI documents containing the majority of the information generated by EPRI-sponsored work related to fuel reconfiguration.

## 2.3 PATRAM Proceedings

The PATRAM symposium is the primary international meeting related to packaging and shipping of radioactive materials. The proceedings for the last four PATRAM symposia dating back to 2001 were reviewed, and a summary of the relevant papers to the work in this report is presented in the following subsections.

### 2.3.1 PATRAM 2010

Several papers in the 2010 PATRAM proceedings were identified as providing information related to modeling of fuel reconfiguration and the  $k_{\text{eff}}$  consequences of such events. The papers of interest with regards to this report are “Accelerated Corrosion Testing of Aluminum Carbide Metal Matrix Composite in Simulated PWR Spent Fuel Pool Solution,” Ref. 22, and “Description of Fuel Integrity Project Methodology Principles,” Ref. 23. Papers that did not provide detailed information about fuel deformation or damage and the effects of that damage on  $k_{\text{eff}}$  are not included in this discussion.

Reference 22 provides information related to corrosion testing of  $\text{B}_4\text{C}/\text{Al}$  neutron absorber materials in PWR spent fuel pool environments. This information is not directly relevant to the work performed here but provides some indication that the neutron absorber degradation configurations described in Section 3.1.6 should provide a reasonable upper bound of the potential consequences of neutron absorber degradation during dry storage.

Reference 23 presents progress and a proposed methodology resulting from the Fuel Integrity Project (FIP). The FIP is a joint research program executed between various British and French interests over the last decade. The particular companies and entities involved have evolved somewhat with industry activity over the years, but the project continued during the time period covered by the four PATRAM symposia discussed in this report. The methodology that has been developed as a result of the FIP applies to both fresh and irradiated fuel transported within Europe. Tests were performed on irradiated rod segments to determine the behavior of irradiated cladding specimens under various loadings. The results of various buckling and crushing tests have been used to validate the resulting models. The final results indicate that the three major causes of fissile material relocation with significant potential  $k_{\text{eff}}$  impacts are axial displacement, plastic deformation of fuel rods, and rod ruptures resulting in fuel release. All three of these mechanisms are considered in the configurations documented in this report. Axial displacement is discussed in Section 3.1.4, plastic deformation is bounded by the models discussed in Section 3.1.3, and fuel rod rupture is discussed in Sections 3.1.1, 3.1.2, and 3.1.5. Reference 23 is the most recent and most complete description of fuel reconfiguration modes and modeling approaches identified in the entire literature review.

### 2.3.2 PATRAM 2007

Several papers in the PATRAM 2007 proceedings were identified as providing information on modeling fuel reconfiguration and associated  $k_{\text{eff}}$  consequences. The relevant papers of interest are *Method to Evaluate Limits of Lattice Expansion in Light Water Reactor Fuel from an Axial Impact Accident during Transport*, Ref. 24, and *Influence of the Accident Behaviour of Spent Fuel Elements on Criticality Safety of Transport Packages – Some Basic Considerations*, Ref. 25.

Reference 24 focused on the effect of fuel assembly deformation caused by axial drops on the ends of the fuel assembly. Both PWR and BWR fuel assemblies are considered in the analysis. BWR fuel rods are typically attached to the assembly end fittings, while PWR rods typically are not. This leads to different response in the assembly during the end drop. The pitch in a BWR bundle tends to be compressed near the drop end, while the pitch in a PWR assembly tends to increase in the same transient. This increased fuel pin pitch is considered for both fuel assembly types in this work, as discussed in Section 3.1.3. The axial variation in the pitch change can also lead to regions of expanded pitch and regions of contracted pitch; the effect is referred to as “birdcaging.” A sketch showing this birdcaging effect is provided in Figure 1. Some limited modeling of this phenomenon was also performed as discussed in Section 3.1.3.2. The results presented in Reference 24 ultimately relate to simulation of the distortion of the fuel assembly during the end drop accident. The results presented demonstrate good agreement between the structural computational model and the testing results and more importantly indicate that the modeling approach used in this report is adequate to represent the expected results of such a condition.

Reference 25 investigates the consequences of several accident configurations. The approach described is similar in many respects to the strategy used in the development of configurations for this report in that general accidents are considered in a conservative manner to estimate consequences on  $k_{\text{eff}}$ . Assembly pitch expansion is considered over various lengths, up to the full length of the fuel rods. The reported  $k_{\text{eff}}$  change associated with this full-length expansion is approximately  $3.25\% \Delta k_{\text{eff}}$ , which is similar to the results reported by EPRI in Reference 15. The results reported for the accumulation of fissile material inside the cask body, but outside the poisoned area of the basket, are quite different from those described in this report. The configuration described in Ref. 25 is quite different from that described in Section 3.1.5.1, so direct comparison is not possible. The primary value of this paper relative to the current effort is in providing quantitative  $k_{\text{eff}}$  changes for assembly pitch expansion and axial displacement for comparison with results presented in Section 5.

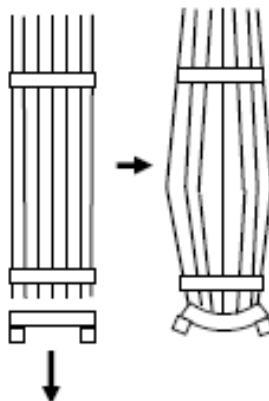


Figure 1. Sketch showing “birdcaging” as the result of an end drop [Source: Ref. 24 (Reprinted from P. Purcell, “Method to Evaluate Limits of Lattice Expansion in Light Water Reactor Fuel from an Axial Impact Accident During Transport” PATRAM 2007. Reprinted with permission.)]

### 2.3.3 PATRAM 2004

The proceedings of PATRAM 2004 contained three papers related to the  $k_{\text{eff}}$  consequences of fuel reconfiguration in storage and/or transportation casks – “Criticality Assessment of Fuel Assemblies with Missing Fuel Rods – An Intractable Problem?,” Ref. 26, “Nuclear Criticality Safety Analysis for the Traveler PWR Fuel Shipping Package,” Ref. 27, and “Harmonisation of Criticality Assessments of Packages for the Transport of Fissile Nuclear Fuel Cycle Materials,” Ref. 28.

Reference 26 examined the practicality of determining an optimum fuel assembly configuration with missing rods. Two techniques were introduced for performing a missing rod analysis. The simple approach proposed in Reference 26 is similar to the approach used in this report, but was performed manually as described in Section 3.1.2.2. No quantitative results were presented that are comparable to configurations included in this report.

Reference 27 presents the criticality safety analysis for a cask for shipping fresh PWR assemblies. Some of the accident configurations considered included uniform pitch expansion restrained by the storage cell wall that is similar to the modeling described in Section 3.1.3. Individual rod axial displacements are considered but shown to have no impact on  $k_{\text{eff}}$ . The axial displacement of the entire assembly was not considered credible. Partial flooding of the cask body was also considered. The results presented are not directly comparable to the results generated in this report because the cask studied in Reference 27 was a single assembly cask; however, the methods used support the basis for some of the configurations used in this report. The trends in the  $k_{\text{eff}}$  consequences of uniform pitch expansion and neutron absorber panel load reduction are similar to the results presented for PWR fuel in Section 5.1.

Reference 28 examines potential accident modeling approaches for  $k_{\text{eff}}$  calculations and discusses elements to consider regarding standardizing scenarios for which analysis is needed. As with Ref. 24, the differences in fuel pin behavior in PWR and BWR assemblies are discussed. Both references contain unreferenced statements supporting the conclusion that PWR pins are likely to be displaced into an increased pitch. Both Refs. 28 and 24 also indicate that BWR pins are likely to decrease in pitch. Ref. 24 cites two instances to support the conclusion for BWR fuel: one was the unrestrained drop of a BWR bundle at a German nuclear power plant and the other was in drop testing being performed as part of package testing. These results were generalized in Ref. 24 to considerations that fuel pins might bend, break, or both. These observations are consistent with the configurations described in Sections 3.1.3, 3.1.4, and 3.1.5. It was also deemed possible that damage to the storage basket or neutron absorber material could result from package-handling accidents. Initial results reported for fuel pin axial displacement indicate that the displacement of some pins within an assembly will not increase  $k_{\text{eff}}$ . This configuration is not considered in this report.

### 2.3.4 PATRAM 2001

Within the proceedings of PATRAM 2001 a few papers were identified that provide information related to fuel reconfiguration and the  $k_{\text{eff}}$  consequences – “Drop Tests with the RA-3D Shipping Container for the Transport of Fresh BWR Fuel Assemblies,” Ref. 29, “Drop Test for the Licensing of the RA-3D Package in the Transport of BWR Fresh Fuel Assemblies,” Ref. 30, and “Effects of Impact Accidents on Transport Criticality Safety Cases for LWR Packages – A New Approach,” Ref. 31.

References 29 and 30 provide the results of drop testing a container intended for shipping fresh BWR bundles. Two containers were each put through a series of drops and evaluated after sequential impacts. The results indicate that some significant assembly distortion is possible, with one assembly suffering a radial rotation (twist) of nearly 45° along its length. Both papers indicate that the general cross section of the bundle was not changed, that is, the pitch was nearly unchanged, but a fairly lengthy section was

twisted by the series of impacts. The drop testing was performed with natural enrichment un-irradiated fuel, and no rod failures were detected.

Reference 31 describes the initial plan for the FIP discussed in Ref. 23. As with other studies discussed before, the initial plan for the FIP includes studying deformation, axial displacement, and rupture as three primary fuel degradation mechanisms. Reference 31 also proposed a PWR pitch expansion configuration in which the outer row of pins is held in place along the storage basket but the inner rows continue to expand towards an optimum pitch. These configurations are considered in Section 3.1.3.1.

## 2.4 Other Sources

Other sources were also reviewed for relevant information related to modeling impact of fuel reconfiguration on criticality safety.

“New Approach to Evaluate Lattice Expansion of Light Water Reactor Fuel Elements on Criticality Safety of Transport Packages under Impact Accidents,” Ref. 32, examined pin pitch deformation in LWR fuel assemblies during transportation accident conditions. The paper proposed a method for generating a regular, nonuniform array of fuel rods with the outer row restrained by the basket walls and the pitch of the inner rows progressively expanded or contracted. This method leads to a larger reactivity increase than uniform pitch expansion and, when combined with similar observations from Ref. 31, motivated the analysis of the nonuniform pitch expansion cases described in Section 3.1.3.1.

## 2.5 Literature Review Summary

A wide range of potentially relevant literature has been reviewed to provide guidance on modeling of fuel reconfiguration after ES and estimate consequences of some configurations. Documents that discuss potentially relevant degraded fuel configurations include Refs. 22–32. A limited number of papers, including Refs. 15 and 25, provide estimates of the consequence of reconfiguration on  $k_{\text{eff}}$ . The PATRAM proceedings contain the largest number of relevant papers, with several directly applicable papers presented at each symposium. The EPRI reports, taken together, may contain the largest quantity of directly applicable information for this analysis. Most of the discussion in the available literature focuses on what reconfigurations could occur with less emphasis made on the direct impacts on  $k_{\text{eff}}$ . Those papers that include calculated  $k_{\text{eff}}$  results tend to take a similar approach to this effort and consider a range of potential configurations to establish a bounding increase in  $k_{\text{eff}}$  without regard for credibility.

# 3. FAILED FUEL CONFIGURATIONS

A set of failed fuel configuration categories was developed, and specific configurations within each category were evaluated. The various configurations represent stylized analyses designed to be bounding of different reconfiguration progressions that could occur, but were not developed to represent the results of any specific reconfiguration progression. The configuration categories considered in this analysis are the following:

- clad thinning/loss – reduced cladding thickness up to the total removal of all cladding material
- rod failures – removal of one or more fuel rods from the assembly lattice
- loss of rod pitch control – rod pitch contraction and expansion within the storage cell
- loss of assembly position control – axial displacement of fuel assemblies

- gross assembly failure – rubblized fuel within the storage cells with varying degrees of moderation
- neutron absorber degradation – gaps of varying location and size; thinning of absorber panels.

Within each category, specific configurations were modeled to calculate the corresponding  $k_{\text{eff}}$  values and the associated consequences of those configurations relative to the reference intact configuration. The consequence of a given configuration is defined as the difference in the calculated  $k_{\text{eff}}$  values for the given configuration and the reference intact configuration, with a positive value indicating an increase in  $k_{\text{eff}}$  as compared to the reference configuration. Several of the specific configurations are not considered credible but are included in the analyses for completeness (e.g., to fully understand trends and worst-case situations and to provide results for configurations that may later be judged to be credible). Pending improved understanding of the various material degradation phenomena, and subsequent determination and justification for what configurations are and are not credible, the assessment of the credibility of configurations provided herein is based on engineering judgment. The credibility of configurations and the impact of the configurations on criticality safety are dependent on many factors, including storage and transportation conditions, the fuel assembly characteristics, and the storage and/or transportation characteristics. The credibility assessment for the specific configurations considered here is presented at the end of this section. The assessment and analysis of credible configurations for a specific cask system would need to be performed as part of the safety analysis for licensing that system.

Each of the configurations is considered with all the assemblies in the cask degraded. As discussed in Section 3.2, a subset of the configurations is also considered for a range of assemblies experiencing degradation. These calculations allow an examination of the impact of reconfiguration as a function of the number of degraded assemblies. Section 3.3 describes the limited number of configurations modeled as a combination of two individual degradations. These models are intended to investigate the potential impact of combined degradation mechanisms occurring within the same cask.

At the end of this section, each of the configurations is reviewed for credibility and applicability. The assessments are based on engineering judgment and are not directly supported by any analysis. Ultimately, the strategies developed to mitigate the consequences of fuel reconfiguration will depend on the classification of each configuration as credible or not credible and the severity of the consequences.

## 3.1 Fuel and Cask Reconfiguration Descriptions

This subsection presents the configurations considered in these analyses. Each of these configurations is considered for each cask design under the assumption that each and every fuel assembly has undergone the reconfiguration discussed. The majority of the cases directly reconfigure fuel, but some consider changes to cladding, neutron absorber material, or fuel assembly axial position. The configurations described in this subsection are used in Section 3.2 to examine the impact of a range of numbers of assemblies experiencing reconfiguration, and in Section 3.3 to investigate the effect of multiple simultaneous degradation mechanisms. Figures demonstrating most of the configurations for each cask are provided in Section 5.

### 3.1.1 Clad Thinning/Loss

The complete loss of all cladding material without subsequent collapse of fuel material is a nonphysical condition but is included in these analyses to provide a bounding estimate of the increase in  $k_{\text{eff}}$  caused by fuel cladding thinning or removal. A series of calculations is also performed to investigate the impact of clad thinning. The reduction of fuel cladding thickness results in an increase in reactivity due to increased moderation within the assembly lattice (cladding material is replaced by water) and the reduced absorption in the cladding. The moderation effect is the larger of the two components. In the models, all

Zircaloy material is replaced with water, including the instrument and guide tubes and water rods. The orientation of the canister, be it horizontal, vertical, or in between, has no impact on the modeling or analysis of this configuration.

### **3.1.2 Rod Failures**

Fuel rod failure could result if the fuel rod cladding has failed. After ES periods or as a result of high burnup, or both, fuel rod cladding may become brittle, as discussed in Ref. 1. Cladding failure could be the result of a static or dynamic load. Configurations involving both single and multiple rod failures are included and discussed in more detail below.

#### **3.1.2.1 Single Rod Failure**

The single rod failure configuration is predicated on the collapse of an entire fuel rod, potentially due to cladding failure. Regardless of the cause of rod collapse, the fuel and cladding material would be displaced from the assembly lattice, thus leaving an empty rod location. In many internal locations within a fuel assembly lattice, this results in an increase in reactivity in the fully flooded condition due to increased internal moderation. The collapsed rod itself is not modeled as rubble on the bottom of the cask. The fissile material would form a fairly thin, severely undermoderated heap below the fuel assembly if the cask is in a vertical configuration. If the cask is in some other non-vertical configuration, the debris pile will have a larger surface area and thus more neutron leakage. The increase in leakage will increase the margin to criticality in the debris bed. Regardless of configuration, the rubble would have much lower reactivity than the assembly itself.

Separate calculations are performed with each unique rod location replaced with water for both the PWR and BWR fuel assemblies. The assembly and cask symmetries are accounted for in the determination of unique locations, neglecting exceptions for peripheral storage locations.

#### **3.1.2.2 Multiple Rod Failure**

Within the multiple rod failure configurations, rods are removed in small groups until an optimum reactivity is achieved. As with the single rod failure cases, the debris at the bottom of the cask is not modeled nor are other cask configuration expected to have a significant impact on the results of the analysis of this configuration. For the larger number of rods removed to achieve optimum reactivity, this assumption is likely conservative as a significant amount of debris material will be accumulating within the assembly storage cell. The homogeneous rubble configuration of gross assembly failure, described in Section 3.1.5.1, provides estimates of the effect of debris collection in the bottom of the fuel storage basket.

For each number of rods removed, a series of potentially limiting configurations is generated to determine the most reactive configuration with the given number of rods removed. These potentially limiting configurations are generated from both the previous limiting configuration and near-limiting configurations. This approach leads to the consideration of several possible configurations to reduce the probability that a more reactive configuration is inadvertently omitted. The increase in  $k_{\text{eff}}$  caused by removing additional rods approaches zero at the optimum number of removed rods, so no attempt is made to identify the exact optimum number of rods. The  $k_{\text{eff}}$  of several configurations would also be statistically equivalent near this point. For the purposes of these analyses, the  $k_{\text{eff}}$  change at this optimum condition has been sufficiently estimated.

### 3.1.3 Loss of Rod Pitch Control

This configuration is based on failure of one or more of the assembly structural grids, resulting in a loss of fuel rod pitch control. For these analyses, this condition is first modeled as a uniform increase in the fuel rod pitch within the assembly lattice. The rod pitch expansion continues until the outer surface of the fuel rod unit cells in the outer row of the assembly has impacted the storage cell walls. A slight gap of half the fuel rod pitch minus the fuel rod radius remains between the fuel rods and the cell walls. The increased moderation within the assembly lattice causes an increase in reactivity. All fuel assemblies are assumed to undergo a uniform rod pitch expansion to completely fill the internal dimension of the storage cell.

These configurations expand the fuel rod center-to-center spacing in several increments to map the impact on  $k_{\text{eff}}$  over the full range of expansion. For the BWR fuel, the expansion is performed both with and without the fuel channel present. Two cases are considered with the channel modeled – one where the channel does not deform and restrains the expansion of the fuel rod pitch and the other is a nonphysical assumption that the channel deforms by expanding with a uniform thickness. In this second case, the channel is still present but expands until the storage cell wall restrains the expansion. To maximize the impact on reactivity, the maximum pitch case is considered both with and without cladding present.

After the limiting combination of enrichment and burnup has been established for each fuel type, an additional model is built with the outer row of rods in contact with the fuel storage cell. The small water gap between the rods and the cell walls has been removed in this model. It is used to establish the  $k_{\text{eff}}$  increase for uniform pitch increase to the limit established by the storage cell walls or assembly channel. The uniform expansion cases with the fuel cladding removed use the same pitch as the cases with cladding intact, so there is no additional pitch expansion caused by cladding removal. The orientation of the cask, vertical or otherwise, is not expected to have any influence on the modeling or analysis of the loss of pitch control configurations.

#### 3.1.3.1 Nonuniform Pitch

Further expansion of the rod pitch for interior rod locations is considered. These models extend further the axially uniform fuel rod pitch expansion discussed above. With the outer row of pins in contact with the storage cell walls, subsequent rows of pins are moved outward until the pins are in contact with the next outermost row. For example, the second row of pins is moved into contact with the first row touching the wall of the storage cell. The process is repeated until additional expansion fails to cause a reactivity increase. Rows containing guide tubes in PWR assemblies are expanded until the guide tubes are in contact with the next row of fuel pins, and the subsequent inner row is moved out until it is in contact with the guide tubes from the inside. These rows have a slightly larger pitch since the outer diameter of the guide tubes is larger than that of the fuel rods.

#### 3.1.3.2 Axial Pitch Variations

One concern associated with the uniform pitch expansion is that it does not account for potential  $k_{\text{eff}}$  increases caused by axial variations in the pitch distortion. This has been referred to in some instances as “birdcaging.” This condition is investigated for the limited uniform expansion case for each cask. The models that are developed are based on the expansion of the assembly until the outer fuel rod unit cell impacts the storage cell wall, not the subsequent case with the rods in contact with the wall. That is, the expanded pitch portion of the assembly maintains a small water gap between the fuel rods and the storage cell walls. The additional pitch in the model that eliminates the water gap is not expected to impact the  $k_{\text{eff}}$  change of birdcaging relative to a uniform pitch expansion. An axial region adjacent to the elevations of highest reactivity is compressed in an attempt to create a more effective reflector and thus increase  $k_{\text{eff}}$ .

The length and position of the compressed pitch segment is varied to determine the maximum impact of this effect. For burned fuel, the compressed zone is selected to match one or more axial zones defined by the axial burnup profile modeling. The high-reactivity region is at the top end of the fuel assembly, so the compressed region is varied in position within the top half of the assembly. For fresh fuel, the central region of the fuel is most reactive, so two compressed zones are modeled. One compressed zone is above the midplane of the assembly, and the other is below it. The two zones are always the same length and in symmetric positions.

### 3.1.4 Loss of Assembly Position Control

The neutron absorber panels in fuel storage and transportation casks are designed to extend beyond the length of the active fuel region within the fuel assembly. In this context, it is important that the active fuel stay in its intended position during and after ES. The cask designs use spacers to ensure that the fuel assemblies are appropriately aligned. If the spacers or assembly end fittings fail, it is possible that the active fuel could shift axially into a region where no neutron absorber separates adjacent assemblies. This would allow for a significant increase in neutronic communication between adjacent assemblies, and a corresponding increase in  $k_{\text{eff}}$ . The cask orientation is not expected to influence the analysis of the loss of assembly position control configuration, but the orientation would certainly influence the actual fuel motion if such an event occurred.

For these models, the maximum axial translation allowed is determined for the active fuel length neglecting the presence of all fuel assembly hardware above or below the pellet stack and the cask assembly spacers. The models of axial displacement translate all the fuel assemblies uniformly up or down into the lower and upper internal regions of the cask. The assemblies are moved in several relatively small intervals in an effort to map out the response as a function of displacement.

### 3.1.5 Gross Assembly Failure

Two configurations for the physical form of the failed fuel are considered in these analyses: the first is a homogeneous mixture of fuel, cladding materials, and water, and the second is a dodecahedral array of fuel pellets suspended in water. The homogeneous mixture is likely more representative of the condition of the assembly after significant degradation and reconfiguration. Modeling an ordered array of pellets provides an upper bound of the reactivity of the fuel rubble since low enriched fuel is more reactive lumped as compared to a homogeneous mixture due to resonance self-shielding effects. Each of the modeling techniques is described in more detail here.

The formation of oxidized forms of UO<sub>2</sub> is not considered in this analysis. The expected formation of higher-order oxidative states would require an ample supply of oxygen which would require a breach of the canister while in storage. Because monitoring is in place to detect and repair breaches, this condition is not being evaluated. Also, as the results presented in Section 5 demonstrate, the UNF casks are undermoderated systems, so representing oxidation of internal components would act to effectively displace the moderator, resulting in a less reactive condition.

#### 3.1.5.1 Homogeneous Rubble

Following a gross assembly failure, a large number of intermediate configurations is possible. To evaluate the effects of varying degrees of rubblization, a series of total debris elevations is considered. This approach considers a range of moderation ratios without specifying the cask orientation. The homogeneous rubble configuration considers the entire fuel assembly to have failed; no calculations are performed for rubblizing a portion of a fuel assembly or for rubble collecting within a partial intact

assembly or skeleton. The parameter that is varied is the height of the debris bed and thus the amount of moderation within the bed.

The homogeneous rubble configuration is modeled as occupying the internal volume of the fuel storage cell to varying elevations. The exact elevations used vary among the cask designs. All the designs are evaluated with the homogeneous rubble replacing the fuel assembly in its original elevation. Other elevations include 40%, 60%, 80%, and 100% of the inside height of the cask from the base plate. The volume occupied by water varies from about 21% to almost 74% of the homogenized mixture. The water volume is determined by subtracting the fuel and cladding volumes from the cask volume modeled as containing debris. A fully compressed case is also considered in which the fuel assembly debris has compacted to just fuel and cladding material, excluding all water, to complete coverage of the parametric space. A range of heights is also considered from nominal assembly height to fully compressed assuming that the debris is maintained within the neutron absorber elevations. These configurations approximate a debris bed that is made up of non-homogeneous pieces, such as fuel rod segments, that are too large to pass through the assembly end hardware and fuel assembly spacer. Some cask models also have configurations for neutron absorber height and/or basket height. Most of these models contain rubble material above and/or below the neutron absorber panels, which are assumed to remain intact. The debris is not necessarily contained by the cask fuel spacers because they are generally designed to allow water to flow through and out of the fuel storage cells. In the full cask height configurations, the fuel rubble is assumed to remain within the radial extent of the fuel storage cell, even above the storage basket. This is assumed mainly as a modeling convenience, and it likely reduces the  $k_{\text{eff}}$  of the configuration slightly. For purposes of these analyses, however, the approximations are sufficient to provide a good estimate of the  $k_{\text{eff}}$  changes associated with gross assembly failure leading to homogeneous rubble within the cask.

All models with homogeneous rubble assume that the cask is maintained in a vertical position. No explicit modeling is performed for horizontal or angled positions which may alter the distribution of rubble within the cask. Given the range of rubble heights considered, it is unlikely that a horizontal or angled configuration would lead to a greater overall  $k_{\text{eff}}$  increase than the maximum calculated in this work, but the intermediate volumes could be impacted in these alternate orientations.

### **3.1.5.2 Dodecahedral Array of Pellets**

The case of gross assembly failure modeled as an ordered array of bare pellets is considered as a bound to the possible  $k_{\text{eff}}$  increase resulting from these configurations. An ordered array of lumped low enriched fuel should lead to a greater  $k_{\text{eff}}$  increase for fuel assembly failure than the homogeneous case described above because of resonance self-shielding of  $^{238}\text{U}$  in low enriched fuel. The complete removal of cladding is nonphysical, as discussed above in Section 3.1.1, but is included to bound possible  $k_{\text{eff}}$  increases.

As with the homogeneous rubble case described above, a range of pellet array heights is considered along with the entire internal area of the storage cell assumed to be filled with the pellet array. The independent parameter for the dodecahedral array is the pitch, so a range of pitches is used in the models to achieve the different heights. Most of the cask models are evaluated with four different pitches/array heights. The minimum pitch in all cases maintains the height of the original fuel assembly, and the maximum pitch fills the inner area of the storage cell for the entire internal height of the cask. Each of the cases is considered with two fuel pellet orientations. The pellets are aligned along the Z axis in one case and along the X axis in the other.

All models with dodecahedral pellet arrays assume that the cask is maintained in a vertical position. No explicit modeling is performed for horizontal or angled positions which may alter the distribution of the pellets within the cask. Given the range of heights considered, it is unlikely that a horizontal or angled

configuration would lead to a greater overall  $k_{\text{eff}}$  increase than the maximum calculated in this work, but the intermediate volumes could be impacted in these alternate orientations.

### 3.1.6 Neutron Absorber Degradation

In addition to the failed fuel configurations, degradation of the neutron absorbers is investigated. Neutron absorber panels in long-term service in spent fuel pools have generally suffered a range of degradation mechanisms, as discussed in Ref. 33 and other sources. Although the environments within the spent fuel pool and the dry storage casks are significantly different, it is reasonable to assume that some degradation and/or damage of the neutron absorber material may occur in ES. A range of configurations is considered in these analyses to provide some estimates for the potential  $k_{\text{eff}}$  changes that could be associated with neutron absorber panel damage or degradation. The orientation of the cask is not expected to effect the  $k_{\text{eff}}$  change caused by neutron absorber degradation, and has no impact on the analysis of the configurations.

#### 3.1.6.1 Limiting Elevation of Neutron Absorber Damage

One aspect that can impact the  $k_{\text{eff}}$  change caused by neutron absorber damage is the axial elevation of the defect. For these analyses the neutron absorber panel damage was assumed to be 5 cm tall and across the full width and thickness of the panel. The gap in the neutron absorber panel is modeled as void, and not water-filled, to maximize the neutron streaming, and associated neutronic communication, through the gap and the corresponding increase in neutron multiplication in neighboring assemblies. Also, all neutron absorber panels in the cask are assumed to contain the same defect at the same elevation. This approach will result in a conservative estimation of the  $k_{\text{eff}}$  increase due to panel damage relative to non-aligned damage modeling. The neutron absorber damage may be highly correlated, in which case modeling the gaps at the same elevation is potentially appropriate.

For fresh fuel, the limiting elevation is most likely in the center of the assembly, so a few widely spaced intervals are used. For used fuel, the limiting elevation should shift to a position near the top end of the assembly. For these conditions, a larger number of cases are investigated with finer resolution in the gap positions between calculations. The minimum spacing is slightly in excess of 5 cm, so a more detailed survey is likely to reveal a slight increase in the  $k_{\text{eff}}$  increase of this neutron absorber degradation. For purposes of these analyses, however, the resolution is sufficient to capture the vast majority of the  $k_{\text{eff}}$  change.

#### 3.1.6.2 Sensitivity to Extent of Damage

To evaluate the sensitivity of the  $k_{\text{eff}}$  change to the extent of panel damage, several additional configurations were evaluated using 7.5 and 10 cm gaps centered at the elevation determined to be limiting with the 5 cm gap cases discussed above in Section 3.1.6.1. As before, the larger gaps extend across the entire width and thickness of the neutron absorber panel, and also occur at the same elevation in all panels. The sizes of the larger gaps have been chosen arbitrarily. It is unlikely that the extent of any potential neutron absorber panel damage can be appropriately bounded without significant material testing. The magnitude of the sensitivity results will provide some indication of the importance of neutron absorber material testing.

#### 3.1.6.3 Neutron Absorber Panel Thinning

While uniform thinning of all neutron absorber panels in the cask may be unlikely, it provides a simple basis for examining the potential impact of general degradation. The neutron absorber material is reduced in thickness in a series of steps so that the magnitude of the effect as a function of neutron absorber loss can be determined.

## 3.2 Varying Number of Reconfigured Assemblies

The  $k_{\text{eff}}$  change caused by fuel reconfiguration is nonlinear with respect to the number of assemblies that experience reconfiguration, and is not well characterized in the available literature. For these reasons, a series of configurations is considered in each cask by varying the number of assemblies that have been degraded for each of four of the configurations described in Section 3.1. The four degraded configurations considered are single rod failure (Section 3.1.2.1), multiple rod failure (Section 3.1.2.2), uniform fuel pin pitch expansion (Section 3.1.3), and the homogeneous rubble configuration of gross assembly failure (Section 3.1.5.1).

The number of assemblies in the cask experiencing reconfiguration is varied from one to all assemblies. A central cell location is selected as the first assembly to experience reconfiguration, and additional assemblies are added in approximately symmetric groups. An example order in which the failed assemblies are added is presented for each cask along with the results of the calculations in Section 5.

## 3.3 Multiple Reconfiguration Mechanisms

Many of the configurations described in Section 3.1 are predicated on the degradation of similar materials. The cladding, guide/instrument tubes, water tubes, and most of the structural grids are all fabricated from the same or very similar zirconium alloys. It is therefore assumed that reconfiguration could occur involving more than one of the degradation mechanisms studied separately for each configuration. For example, if the fuel rod cladding is failing and multiple fuel rods have collapsed, then the cladding on the remaining intact fuel rods may have experienced some thinning. A very large number of combinations of such configurations could be generated, but only a small subset is considered here. The primary purpose of this portion of the analysis is to compare the  $k_{\text{eff}}$  changes of multiple degradation mechanisms with the consequence estimated by simply adding the effects of each separate reconfiguration. To that end, two combinations are considered in both casks: a configuration involving a moderate number of failed fuel rods combined with 50% clad thinning in one study and with a moderate amount of uniform pitch expansion in another. The results for this set of cases are provided in Section 5.

## 3.4 Credibility of Degraded Configurations

Several of the configurations used in this report are not physically possible. These configurations may be disregarded in assessing the mitigation strategies necessary to provide confidence that UNF can be safely transported following ES. The configurations are still useful as they provide indications as to reconfiguration impacts for various changes in fuel, neutron absorber, or structural materials within the casks during or after ES. The consequences that require mitigation are significantly less severe than the most limiting, non-credible configurations reported in Section 5. A summary of the credibility and relevance of each of the configurations discussed in Section 3.1 is presented in Table 1.

The complete removal of all fuel cladding material is not credible as there is no mechanism to remove the cladding from the fuel matrix. There is also no credible place for the cladding material to go within the cask that will not have an impact on the calculated  $k_{\text{eff}}$ . Any event that leads to massive cladding failure will also lead to significant rearrangement of the fissile material. Some amount of clad thinning through corrosion and/or radiation-induced growth of the fuel rods is credible and is included in the results. To observe the impacts of clad thinning effects, the maximum thinning considered is chosen to be up to 50% of the nominal thickness.

Significant neutron absorber panel damage at highly correlated locations is not considered credible in extended dry storage. Many fixed absorber materials have experienced degradation in wet storage, as documented in Ref. 33, and this damage is often caused by the effects of radiation, temperature, and environmental insults. These parameters can be highly correlated based on the proximity of neutron absorber panels to the same high temperatures and high radiation fields in the same region of a spent fuel pool. There are currently no known mechanisms applicable to dry storage systems that could cause the local panel defects or generalized thinning examined in this report.

The cask assembly spacers are unlikely to degrade sufficiently for significant axial misalignment to be possible within the cask. The spacers are designed to withstand loads in excess of 60 g, as documented in Ref. 38. These loads are associated with hypothesized accident conditions (HAC), so the cask assembly spacers can be relied upon to maintain assembly position with the neutron absorber elevations in both storage and transportation. Current practice allows small gaps between the spacers and the fuel, but these gaps are typically on the order of a few inches. It is therefore reasonable to assume that significant misalignments cannot occur and will be limited to less than 20 cm.

Simultaneous gross failure of all fuel assemblies in the cask is also not considered credible in normal conditions of transport. The two configurations used to investigate the consequences of gross failure are also extremely conservative. Both configurations examine a range of debris bed sizes to find the largest increase in  $k_{\text{eff}}$ . Large debris beds, such as those filling the entire inner volume of the fuel cask, are not physically possible. Fuel assembly hardware and fuel spacers would also occupy a significant volume and thus reduce the  $k_{\text{eff}}$  increase. Some smaller debris beds, consistent with partial assembly failure, are potentially credible. These detailed debris models are not considered in this analysis as the primary focus of the configurations analyzed is to establish bounding conditions of the extent of  $k_{\text{eff}}$  increases due to total failure. Gross assembly failure may be plausible in some HACs, but is not considered credible in normal conditions of transport.

**Table 1. Credibility and relevance summary**

<b>Configuration</b>	<b>Credibility and applicability to normal transport analysis</b>
<b>Clad thinning/loss</b>	
Complete cladding loss	Nonphysical condition that is not credible Relevant as potential bound of credible condition
Uniform cladding thinning	Potentially credible as a result of corrosion Relevant to storage and transportation analysis
<b>Rod failures</b>	
Single rod failure	Potentially credible as a result of cladding failure Relevant to storage and transportation analysis
Multiple rod failure	Potentially credible as a result of cladding failure Relevant to storage and transportation analysis
<b>Loss of rod pitch control</b>	
Uniform expansion, constrained by cell or channel	Potentially credible as a result of end load Relevant to storage and transportation analysis
Nonuniform expansion, constrained by cell	Potentially credible as a result of end load Relevant to storage and transportation analysis
Axially variable expansion, constrained by cell	Potentially credible as a result of end load Relevant to storage and transportation analysis
<b>Loss of assembly position control</b>	
Maximum misalignment	Not credible with end fitting and spacers Relevant as potential bound of credible condition
Limited misalignment	Small misalignments credible Relevant to storage and transportation analysis
<b>Gross assembly failure</b>	
Homogeneous rubble of entire assembly with debris beyond neutron absorber elevations	Not credible for normal transport Relevant as potential bound for credible condition
Homogeneous rubble of entire assembly within neutron absorber elevations	Not credible for normal transport Relevant as potential bound for credible condition
Uniform pellet array	Not credible for normal transport Relevant as potential bound for credible condition
<b>Neutron absorber degradation</b>	
5-cm (small) defect in all panels, same elevation	Not credible for intact dry storage system Relevant as potential bound of credible condition
10-cm defect in all panels, same elevation	Not credible for intact dry storage system Relevant as potential bound of credible condition
Uniform thinning of all panels	Not credible for intact dry storage system Relevant as potential bound of credible condition

## 4. MODELS, CODES, AND METHODS USED

The models, codes, and methods used for these analyses are based on similar work completed previously and documented in Ref. 7. The codes used are part of the SCALE code system, Ref. 34.

### 4.1 Fuel Assembly Models

Two fuel assembly designs are used in these analyses: one PWR type and one BWR type. The designs chosen are intended to represent a large portion of the current inventory of discharged UNF and/or a significant portion of the fuel currently in use. The PWR design selected is the Westinghouse  $17 \times 17$  Optimized Fuel Assembly (OFA). The Westinghouse  $17 \times 17$  assembly, as modeled, represents over 14% of the total discharged PWR inventory, as documented in Ref. 35. The BWR design selected is based on a General Electric (GE)  $10 \times 10$  design such as the GE14 fuel product. The GE  $10 \times 10$  represents less than 0.5% of the discharged BWR fuel documented in Ref. 35; however, the  $10 \times 10$  fuel design was just being introduced when the data for Ref. 35 were being collected. The array is the most common fuel design in use in domestic BWRs today. Detailed descriptions of the fuel assembly models used in this analysis are provided in Appendix A.

The use of Westinghouse and GE fuel assemblies is a continuance of the work documented in Ref. 7. The use of these fuel types is not an endorsement of any particular fuel design or vendor relative to any others but is used to provide a basis of comparison with the previous work.

### 4.2 Cask Models

Two cask models were used for the evaluations presented in the main body of this report – the GBC-32 and MPC-68. The MPC-24 cask is also evaluated in Appendix B to complete coverage of the parametric space via the inclusion of fresh 5 weight percent (w/o) PWR fuel. The representative cask models selected are the same as those used in Ref. 7 and are based on the Holtec HI-STAR 100 system, Ref. 36–38. The incorporation of Holtec designs in this work is not an endorsement of any design or vendor relative to any others. The GBC-32 and MPC-68 models are described in more detail in the following subsections.

#### 4.2.1 GBC-32 Cask Model

The GBC-32 model is a generic burnup credit cask benchmark model as defined in Ref. 39. The cask model was designed to be a nonproprietary representation of high-capacity PWR storage and transportation casks used within the nuclear power industry. The dimensions and material specifications of the cask model are described in Section 2.1 of Ref. 39 and are not repeated here. The only notable difference from that description is that the cask lid modeled in these analyses has a thickness of 20 cm instead of 30 cm. This reduced lid thickness has no impact on the analyses presented here because the cavity height is maintained.

The fuel assemblies, cask basket, neutron absorber panels, neutron absorber panel wrappers, cask wall, lid, and base plate are modeled explicitly. The nominal condition for this model is fully flooded with unit density, unborated water. A cross section of the GBC-32 model is shown in Figure 2. The representative assembly design is the Westinghouse  $17 \times 17$  OFA with a range of initial enrichments, burnups, and cooling times considered. For more details about the fuel assembly model, see Appendix A.

A burnup credit loading curve is generated assuming a maximum  $k_{\text{eff}}$  of 0.94, as shown in Figure 3. The maximum fresh enrichment that can be stored is determined to be 1.92 w/o  $^{235}\text{U}$ , and minimum burnups are calculated for 3.5 w/o and 5 w/o initial enrichment fuel with 5 years of post-irradiation cooling time. The minimum burnup for 3.5 w/o fuel is 25.5 GWd/MTU and for 5 w/o is 44.25 GWd/MTU to meet the

$0.94 k_{\text{eff}}$  limit. Explicit degraded configuration calculations are performed for fuel from this loading curve. These two enrichments are used because they encompass the majority of the current UNF inventory as of 2002, and the 5-year cooling time is selected as it is a typical minimum required cooling time for fuel to be placed in dry storage. Sensitivity studies are also performed for fuel of higher burnup (70 GWd/MTU) and for a range of cooling times up to 300 years to establish the sensitivity of the change in  $k_{\text{eff}}$  to these parameters. The results of these sensitivity studies are discussed in Section 5 and in Appendix C.

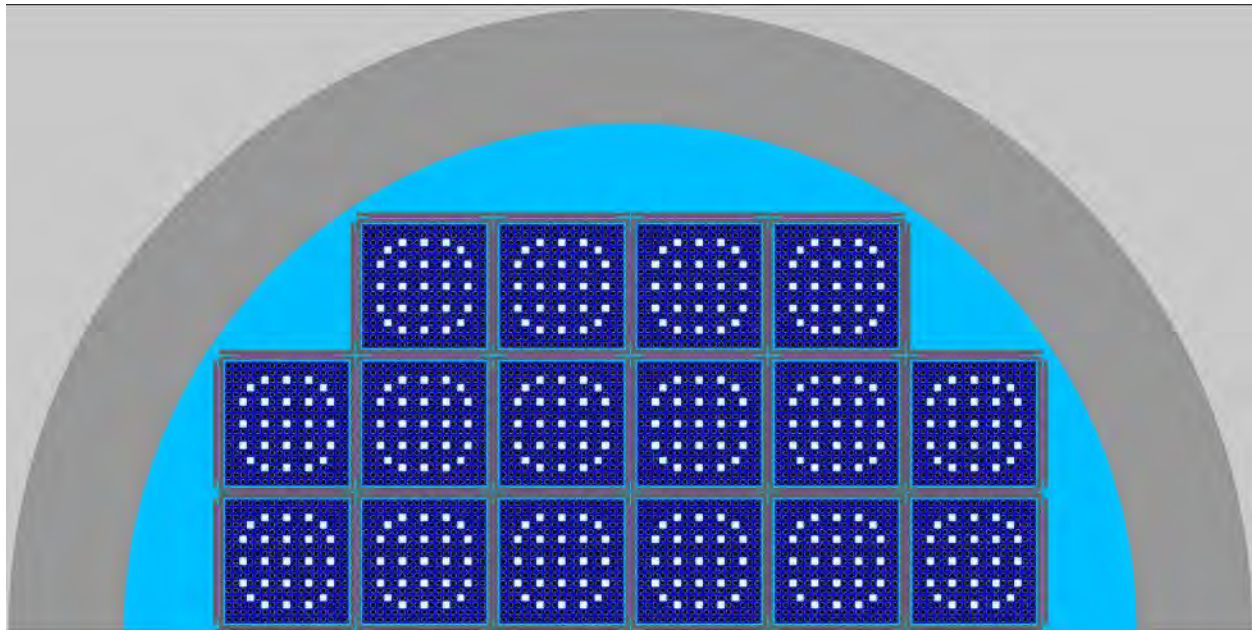


Figure 2. Cross section of GBC-32 half-cask model.

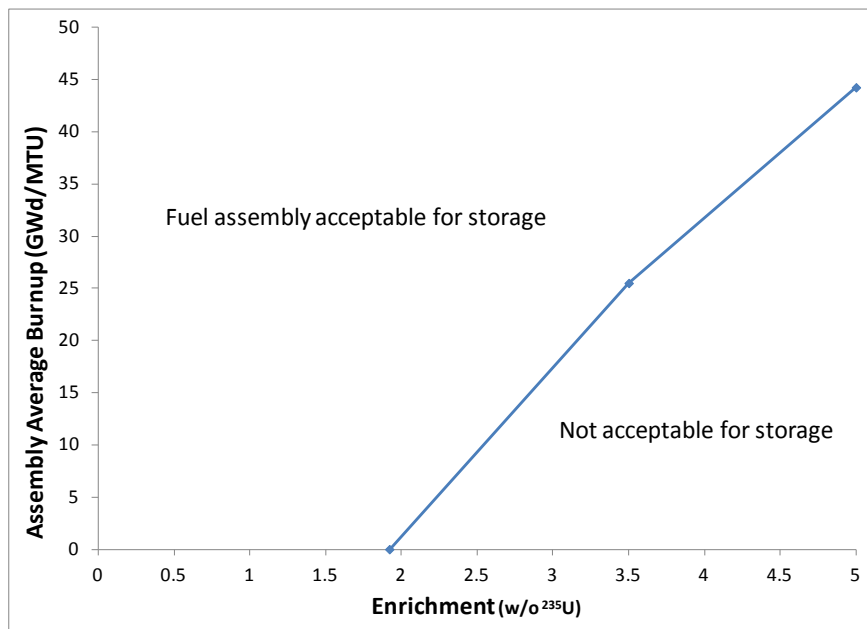


Figure 3. Representative fuel assembly loading curve for GBC-32.

#### 4.2.2 MPC-68 Cask Model

The MPC-68 cask is designed for storage and transportation of up to 68 fresh BWR fuel assemblies but is being used in this analysis for evaluating both fresh and irradiated assemblies. Fresh fuel is considered in these analyses to provide complete coverage of the parametric space; in this case burnup is the parameter of interest. The nominal condition for this model is fully flooded with unit density, unborated water. A cross section of the MPC-68 model is shown in Figure 4. Dimensions and material specifications of the cask model are provided in Appendix D. The fuel assemblies modeled in the MPC-68 are based on a  $10 \times 10$  design similar to the GE14 product. More details about the fuel assembly models are provided in Appendix A.

Fuel assemblies in the MPC-68 models used in these analyses use an initial enrichment of 5 w/o  $^{235}\text{U}$  and consider fresh and irradiated conditions. The nominal model  $k_{\text{eff}}$  value with fresh fuel is in excess of 0.96. A second set of cases considers an assembly average burnup of 35 GWd/MTU and a 5-year cooling time, resulting in a base case  $k_{\text{eff}}$  of approximately 0.83. Sensitivity studies are also performed for fuel of higher burnup (70 GWd/MTU) and for a range of cooling times up to 300 years to establish the sensitivity of the change in  $k_{\text{eff}}$  to these parameters. The results of these sensitivity studies are discussed in Section 5 and in Appendix C.

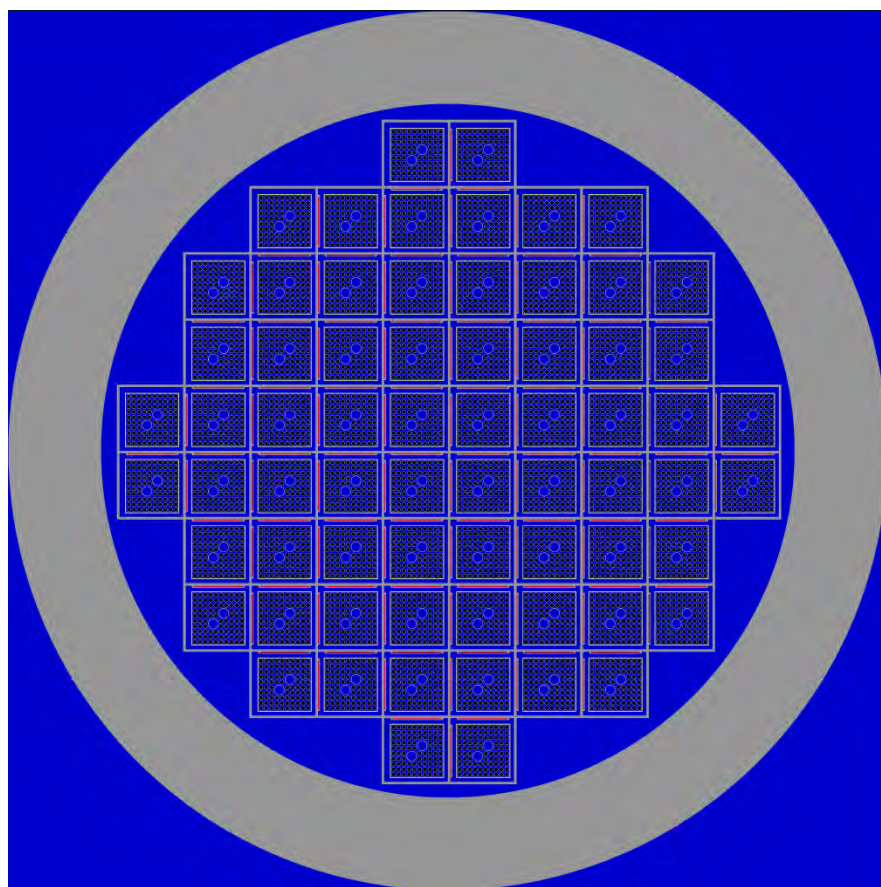


Figure 4. Cross section of MPC-68 model.

### 4.3 Software Codes

The SCALE code system is used to perform the large number of  $k_{\text{eff}}$  and depletion calculations necessary for these analyses. All calculations use the 238-group neutron data library based on ENDF/B-VII.0, distributed with the SCALE system. The same library is used in  $k_{\text{eff}}$  and depletion calculations.

The KENO V.a and KENO-VI Monte Carlo codes are used for  $k_{\text{eff}}$  calculations within the appropriate CSAS5 and CSAS6 sequences. Both codes use Monte Carlo transport to solve the  $k_{\text{eff}}$  eigenvalue problem. KENO-VI uses a generalized geometry process and is used for the fuel pellet array configuration and some increased fuel rod pitch configurations. KENO V.a has a more restrictive geometry package but is significantly faster because of the simpler geometry treatment. KENO V.a is used for the majority of configurations considered in this analysis. The KENO codes and CSAS sequences are further described and documented in Ref. 34. The KENO calculations are run with a large number of particles per generation, typically 10,000, and enough generations to reach an uncertainty less than or equal to 0.00010  $\Delta k_{\text{eff}}$ . The number of generations needed to reach the uncertainty target is determined by KENO during each calculation. In most calculations, the first 100 generations are discarded to ensure proper source convergence.

All depleted fuel isotopic compositions were generated with the STARBUCS sequence. The STARBUCS sequence uses the ORIGEN-ARP methodology to generate depleted fuel compositions and uses the compositions in a KENO model to calculate  $k_{\text{eff}}$ . The TRITON t-depl sequence is used to generate ARP libraries for both PWR and BWR UNF for the depletion conditions described in Section 4.4. The TRITON sequence couples the NEWT discrete-ordinates code with the ORIGEN depletion module. The local fluxes calculated with NEWT are used to perform fuel depletion calculations with ORIGEN. The STARBUCS and TRITON sequences, NEWT and ORIGEN modules, and ORIGEN-ARP methodology are described and documented in Ref. 34.

### 4.4 Depletion Modeling Parameters

For analyses of irradiated fuel, the depletion modeling parameters that the fuel experiences can have a significant impact on the calculated  $k_{\text{eff}}$  values. Several key factors can impact the reactivity of discharged fuel in light water reactor (LWR) burnup credit criticality safety analyses. The key parameters include the nuclides represented in the isotopic compositions, parameters used for the depletion analysis, cooling time, axial burnup profiles, and horizontal burnup profiles, as discussed in Ref. 40.

For the analyses in this report, the depletion parameters used are consistent with burnup credit safety analyses and are not representative of nominal core conditions. It is expected that any operating conditions that are not bounded by the depletion conditions used in this report would result in a higher discharged assembly  $k_{\text{eff}}$ , but the  $k_{\text{eff}}$  increase caused by fuel reconfiguration is expected to be similar to the results determined here. Generic data is used in the PWR depletion conditions as PWR burnup credit has been studied extensively, including in, for example, Refs. 39, 41, 42, 43, 44, and 45. Additional details on the specific PWR conditions used are provided in Section 4.4.1. Because commensurate studies are not available in the literature for BWR burnup credit, the BWR depletion conditions are based on the operating history of a specific assembly as described in Section 4.4.2 and Appendix E.

The  $k_{\text{eff}}$  calculations performed for these analyses involving UNF, for both BWR and PWR fuel, consider the same 12 actinide and 16 fission product isotopes listed in Table 2 (Set 2 Table 1 Ref. 44). Although Ref. 44 specifically addresses PWR burnup credit, the major isotopes affecting reactivity of irradiated uranium oxide fuel will be the same in BWR fuel. The  $k_{\text{eff}}$  impacts caused by the use of this set of

isotopes, as compared to actinide-only burnup credit or a more extensive list of fission products, are discussed in Ref. 39.

Different axial burnup profiles are used for PWR fuel than for BWR fuel, though the same uniform horizontal burnup profile is considered for both fuel types. The PWR axial profiles are taken from Table 4-3 of Ref. 45. Profile 2 is used for fuel discharged at 25.5 GWd/MTU and profile 3 is used for discharged at 44.25 GWd/MTU. The development of the profile used for BWR fuel is described in Appendix E.

**Table 2. Isotopes included in depleted fuel models**

<b>Actinides</b>					
$^{234}\text{U}$	$^{235}\text{U}$	$^{236}\text{U}$	$^{238}\text{U}$	$^{238}\text{Pu}$	$^{239}\text{Pu}$
$^{240}\text{Pu}$	$^{241}\text{Pu}$	$^{242}\text{Pu}$	$^{241}\text{Am}$	$^{243}\text{Am}$	$^{237}\text{Np}$
<b>Fission products</b>					
$^{95}\text{Mo}$	$^{99}\text{Tc}$	$^{101}\text{Ru}$	$^{103}\text{Rh}$	$^{109}\text{Ag}$	$^{133}\text{Cs}$
$^{143}\text{Nd}$	$^{145}\text{Nd}$	$^{147}\text{Sm}$	$^{149}\text{Sm}$	$^{150}\text{Sm}$	$^{151}\text{Sm}$
$^{152}\text{Sm}$	$^{151}\text{Eu}$	$^{153}\text{Eu}$	$^{155}\text{Gd}$		

#### 4.4.1 PWR Depletion Conditions

The depletion parameters that impact discharged fuel reactivity as listed in Ref. 40 are fuel temperature, moderator temperature/density, soluble boron concentration, specific power and operating history, use of fixed burnable poisons, and use of integral burnable poisons. Each of these parameters must be addressed in a burnup credit analysis to demonstrate that conservative depletion parameters have been implemented in the safety basis. These depletion calculations are intended to provide used fuel isotopic compositions that are representative of the compositions generated for a safety analysis and not for nominal core operating conditions. The parameters used in the PWR depletion calculations are listed below in Table 3.

**Table 3. PWR depletion parameters**

Parameter	Value
Fuel temperature	1100 K
Moderator temperature	610 K
Moderator density	0.63 g/cm <sup>3</sup>
Soluble boron concentration	1000 ppm
Specific power and operating history	Constant 60 W/g (MW/MTU)
Fixed burnable absorber	24 Wet Annular Burnable Absorber (WABA)
Integral burnable absorber	None – Bounded by 24 WABA
Control rod insertion	None

#### 4.4.2 BWR Depletion Conditions

The mechanisms whereby depletion conditions influence discharged fuel assembly reactivity are largely similar for BWR and PWR fuel. Data for specific BWR assemblies are gathered and reviewed from the

commercial reactor critical (CRC) state points documented in Refs. 46 and 47. The depletion parameters used in this report are summarized in Table 4. The methods used to generate axial burnup and void profiles and the specific power from the CRC information, Refs. 46 and 47, are presented in Appendix E. The BWR depletion calculations are performed with no control blades present. Although it is more conservative to include the control blades during depletion, their absence is not expected to impact the results of this analysis.

**Table 4. BWR depletion parameters**

Parameter	Value
Fuel temperature	840 K
Moderator temperature	512 K
Moderator density	Varied axially, see Appendix E for details
Specific power and operating history	Constant 30.31 W/g (MW/MTU), see Appendix E for details
Integral burnable absorber	None
Control blade insertion	None

## 5. RESULTS

This section reports the results of the calculations to determine the  $k_{\text{eff}}$  changes associated with each of the configurations described above in Section 3. The results are presented in unique subsections for each cask. The conclusions that can be drawn from these results are presented in Section 6.

The reported consequence is the difference in calculated  $k_{\text{eff}}$  values; the reported changes are not divided by any  $k_{\text{eff}}$  values and therefore do not represent change in reactivity ( $\Delta\rho$ ). The  $\Delta k_{\text{eff}}$  unit indicates that the results presented are the difference in two calculated  $k_{\text{eff}}$  values. The reported  $k_{\text{eff}}$  changes are also best-estimate changes; the difference in  $k_{\text{eff}}$  values is not altered or adjusted to account for the Monte Carlo uncertainties of the calculations. The one standard deviation uncertainty in all calculated  $\Delta k_{\text{eff}}$  values is approximately 0.00014 (0.014%)  $\Delta k_{\text{eff}}$ , unless otherwise noted.

### 5.1 GBC-32 Cask Model Results

The  $k_{\text{eff}}$  change associated with each of the reconfigurations discussed in Section 3 is presented in this section for the GBC-32 cask. The configurations assume a range of loadings of Westinghouse 17 × 17 OFA fuel. The description of the fuel assembly is provided in Appendix A. The enrichments and burnups used are presented in Table 5. The rationale used to select these points is provided in Section 4.2.1. The reference case  $k_{\text{eff}}$  value for intact fuel for each of these cases is also provided in Table 5.

**Table 5. Enrichment, burnup, and cooling time for reference cases considered in GBC-32**

Enrichment (w/o $^{235}\text{U}$ )	Burnups (GWd/MTU)	KENO V.a		KENO-VI	
		$k_{\text{eff}}$	$\sigma$	$k_{\text{eff}}$	$\sigma$
1.92	0	0.94017	0.00010	0.94040	0.00010
3.5	25.5	0.93988	0.00010	0.93976	0.00010
5.0	44.25	0.94000	0.00010	0.93995	0.00010

### 5.1.1 Reconfiguration of All Assemblies

A summary of the  $k_{\text{eff}}$  increase associated with each configuration is provided in Table 6. Additional details for each configuration and the results for non-limiting cases are provided in the subsequent subsections.

**Table 6. Summary of  $k_{\text{eff}}$  increases for the GBC-32 cask**

Configuration	Increase in $k_{\text{eff}}$ (% $\Delta k_{\text{eff}}$ )	Limiting case	
		Enrichment (w/o $^{235}\text{U}$ )	Burnup (GWd/MTU)
<b>Clad thinning/loss</b>			
Cladding removal	3.49	5	44.25
<b>Rod Failures</b>			
Single rod removal	0.09	5	44.25
Multiple rod removal	1.86	5	44.25
<b>Loss of rod pitch control</b>			
Uniform rod pitch expansion, clad	2.65	5	44.25
Uniform rod pitch expansion, unclad	5.34	5	44.25
Nonuniform pitch expansion, clad	3.90	5	44.25
<b>Loss of assembly position control</b>			
Axial displacement (maximum)	16.70	5	44.25
Axial displacement (20 cm)	10.82	5	44.25
<b>Gross assembly failure</b>			
Uniform pellet array	21.37	5	44.25
Homogeneous rubble	14.30	5	44.25
<b>Neutron absorber degradation</b>			
Missing neutron absorber (5-cm segment)	1.05	5	44.25
Missing neutron absorber (10-cm segment)	2.33	5	44.25
50% reduction in neutron absorber panel thickness	1.78	1.92	0

#### 5.1.1.1 Clad Thinning/Loss

The clad thinning and loss configurations are modeled as discussed in Section 3.1.1. As shown in Table 6, the limiting  $k_{\text{eff}}$  increase associated with complete cladding removal is 3.49%  $\Delta k_{\text{eff}}$  and occurs for the 44.25 GWd/MTU burnup case with an initial enrichment of 5 w/o  $^{235}\text{U}$ . The results for all three cases are summarized in Table 7. For the limiting case of 5 w/o and 44.25 GWd/MTU burnup, the  $k_{\text{eff}}$  increase as a function of nominal cladding thickness remaining is shown in Table 8 and Figure 5. The trend of increasing  $k_{\text{eff}}$  with decreasing cladding thickness is similar for the other fuel compositions, and therefore

not shown here. The configuration with 50% of the nominal cladding remaining is shown in Figure 6. The results are in good agreement with those presented in Refs. 7 and 15.

**Table 7. Increase in  $k_{\text{eff}}$  for cladding removal in GBC-32**

Enrichment (w/o $^{235}\text{U}$ )	Burnup (GWd/MTU)	Increase in $k_{\text{eff}}$ (% $\Delta k_{\text{eff}}$ )
1.92	0	2.81
3.5	25.5	3.34
5	44.25	3.49

**Table 8. Increase in  $k_{\text{eff}}$  in GBC-32 cask as a function of cladding fraction remaining  
(5 w/o  $^{235}\text{U}$  initial enrichment, 44.25 GWd/MTU burnup)**

Fraction of cladding thickness remaining	Increase in $k_{\text{eff}}$ (% $\Delta k_{\text{eff}}$ )
0.90	0.38
0.75	0.99
0.50	1.94
0.25	2.76
0.00	3.49

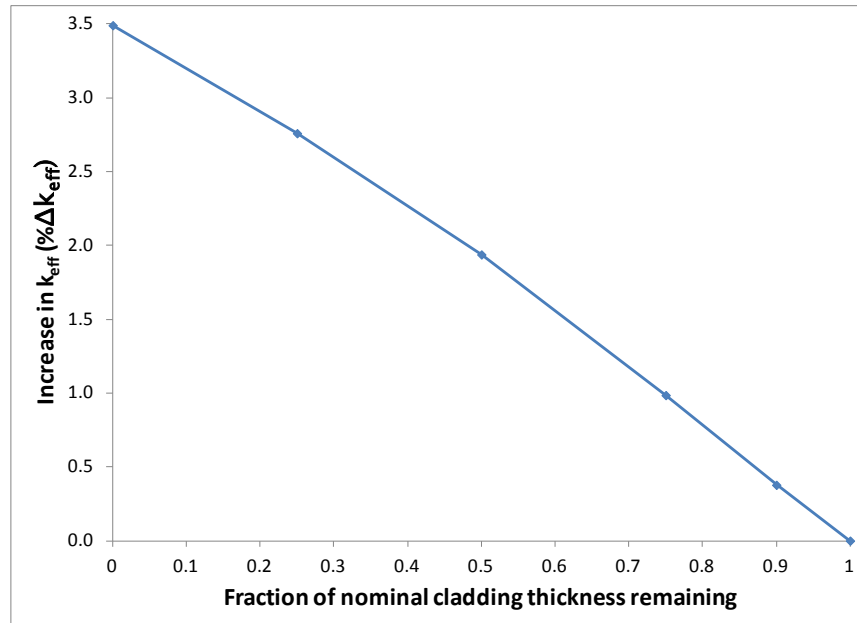
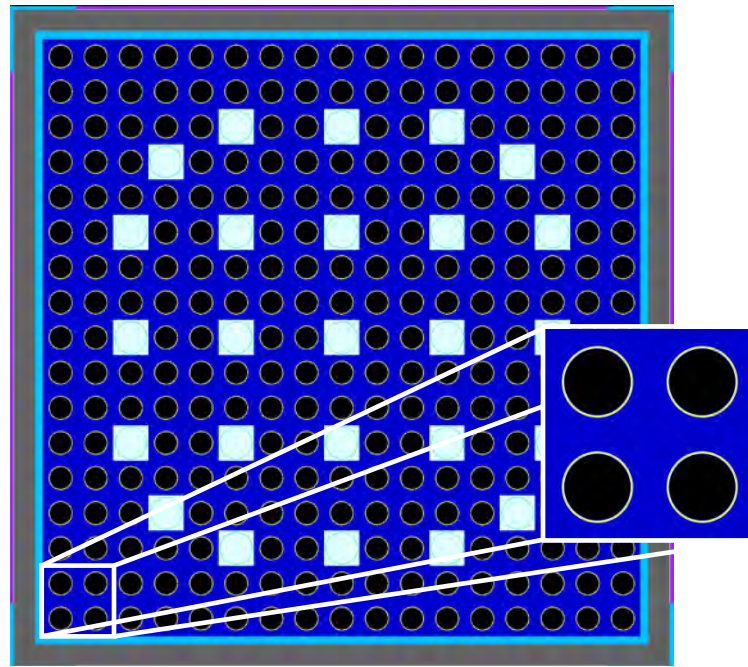


**Figure 5. Increase in  $k_{\text{eff}}$  due to reduced cladding thickness  
(5 w/o  $^{235}\text{U}$  initial enrichment, 44.25 GWd/MTU burnup).**



Notes:

- Fuel shown in black
- Cladding is light grey around fuel material
- Guide/instrument tubes are larger water-filled tubes
- Storage cell is dark grey box
- Neutron absorber panel is purple
- Water is shown in dark blue, light blue, and white

**Figure 6. Configuration with 50% cladding thickness.**

### 5.1.1.2 Rod Failures

Each of the 39 eighth-assembly symmetric rods is removed individually to determine its worth, as discussed in Section 3.1.2.1. Table 9 presents the rod locations and worth of the limiting rod location for each of the three cases. A sketch showing the eighth-assembly symmetry and row and column labels is provided in Figure 7. The maximum  $k_{\text{eff}}$  change is 0.09%  $\Delta k_{\text{eff}}$  and is associated with rod H5 in the 5 w/o, 44.25 GWd/MTU burnup case. The worth of H5 in the GBC-32 cask is. It should be noted that several rods across many of the cases have a reactivity worth that is statistically equivalent to this particular limiting case. The worth is very small relative to the  $k_{\text{eff}}$  increase of other configurations, so further examination is not necessary.

Multiple rods are also removed in groups, as discussed in Section 3.1.2.2. Groups of 2, 4, 8, 16, 24, 28, 32, 36, 40, 44, and 48 rods are considered. The maximum  $k_{\text{eff}}$  increase for each of the enrichment and burnup combinations is shown in Table 10. Figure 8 shows the  $k_{\text{eff}}$  increase as a function of rods removed for the limiting case at 5 w/o and 44.25 GWd/MTU burnup. The limiting lattice is shown in Figure 9. The maximum  $k_{\text{eff}}$  value occurs for 44 rods removed and corresponds to a  $k_{\text{eff}}$  increase of 1.86%  $\Delta k_{\text{eff}}$ .

Multiple rod removal in the fresh fuel 1.92 w/o case resulted in a decrease in the cask reactivity. Hence, the single rod removal case bounds all multiple rod removal configurations considered.

The  $k_{\text{eff}}$  increase for both rod removal configurations in the GBC-32 cask is in generally good agreement with Ref. 7. The multiple rod removal  $k_{\text{eff}}$  increase is somewhat higher, most likely because of the use of a distributed axial burnup profile in this work.

**Table 9. Single rod removal results for  $17 \times 17$  OFA in GBC-32**

Enrichment (w/o $^{235}\text{U}$ )	Burnup (GWd/MTU)	Location	Maximum increase in $k_{\text{eff}}$ (% $\Delta k_{\text{eff}}$ )
1.92	0	H8	0.04
3.5	25.5	H7	0.08
5	44.25	H5	0.09

**Table 10. Multiple rod removal results for  $17 \times 17$  OFA in GBC-32**

Enrichment (w/o $^{235}\text{U}$ )	Burnup (GWd/MTU)	Maximum increase in $k_{\text{eff}}$ (% $\Delta k_{\text{eff}}$ )
1.92	0	N/A*
3.5	25.5	1.07
5	44.25	1.86

\*All multiple removal cases resulted in a decrease in  $k_{\text{eff}}$

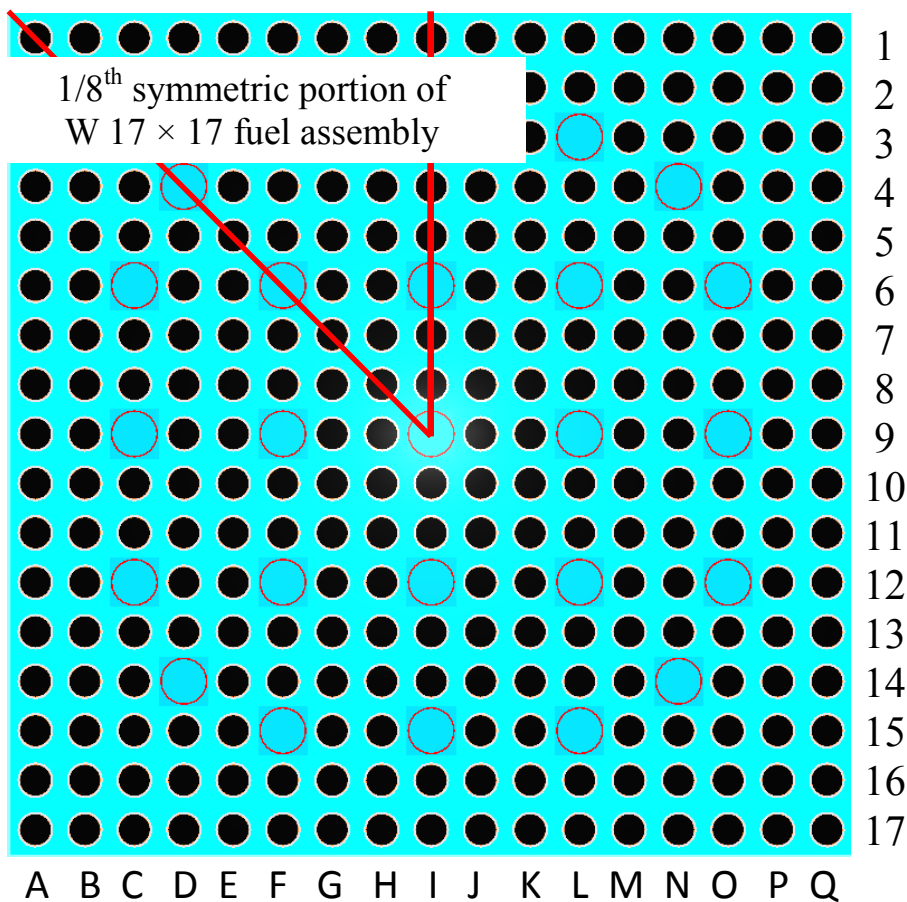


**Figure 7. Sketch of symmetry, row, and column labels for W  $17 \times 17$  fuel assembly.**

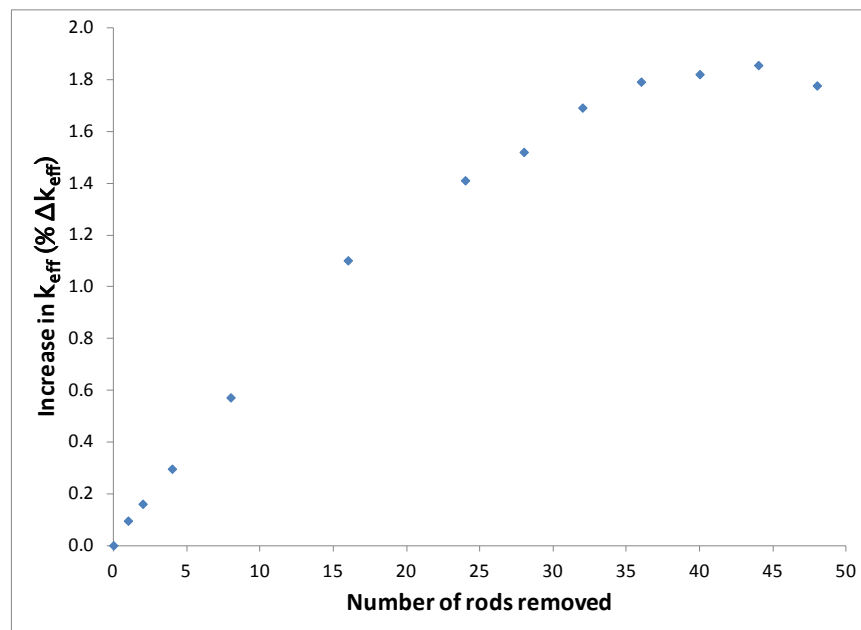
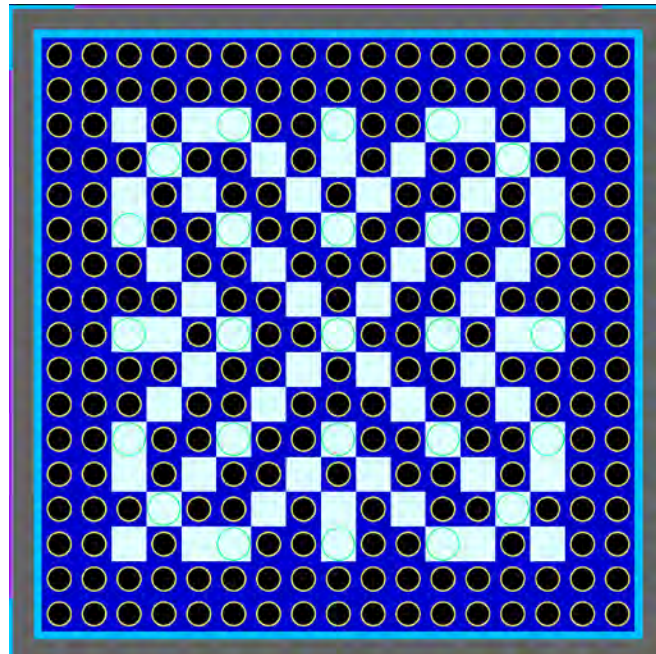


**Figure 8. Increase in  $k_{\text{eff}}$  in GBC-32 cask as a function of number of rods removed  
(5 w/o  $^{235}\text{U}$  initial enrichment, 44.25 GWd/MTU burnup).**



Note: Missing rod locations are shown in white; the same water mixture was used in empty cell locations and guide tube locations

**Figure 9. Limiting multiple rod removal lattice (44 rods removed).**

### 5.1.1.3 Loss of Rod Pitch Control

The loss of rod pitch control is modeled first as a uniform increase in fuel assembly pitch, as discussed in Section 3.1.3. The pitch between rods is expanded uniformly until the rod unit cells of the outer row of fuel rods are coincident with the inner surface of the storage cells. The largest expansion is modeled in two configurations – with the clad fully intact and also completely removed. The limiting condition for both cases is for fuel with an initial enrichment of 5 w/o and 44.25 GWd/MTU burnup. The results with the pitch expanded until the outer unit cell boundary contacts the storage cell, both with and without cladding, for all three combinations of initial enrichment and burnup are shown in Table 11.

The limiting configuration, with 44.25 GWd/MTU burnup, is further expanded until the outermost fuel rods are in contact with the storage cell walls as shown in Figure 10. The increase in  $k_{\text{eff}}$  in this case relative to the nominal configuration is 2.65%  $\Delta k_{\text{eff}}$  with cladding intact and 5.34%  $\Delta k_{\text{eff}}$  with cladding removed. The unclad fuel rods are modeled in the same locations with the cladding removed; the pitch is not increased further to put the fuel material in contact with the storage basket. The first five points in Figure 11 show the increase in  $k_{\text{eff}}$  associated with this uniform pitch expansion. These results indicate a  $k_{\text{eff}}$  increase that is approximately 0.5%  $\Delta k_{\text{eff}}$  lower for loss of rod pitch control compared to Refs. 15 or 25.

Fuel rod pitch is further increased in the GBC-32 model to examine the effect of nonuniform pitch, as discussed in Section 3.1.3.1 and References 31 and 32. The inner portion of the assembly continues to expand until the outer rows are in contact with each other; although the fuel rod pitch is still uniform axially, it is nonuniform in the radial direction. An example model is shown in Figure 12. The pitch in each of the outer rows is constant within the row and is equal to the pitch that caused that row to make contact with the previous row or the basket wall. The increase in pitch in inner rows leads to a nonuniform pitch in the lattice. The results of the calculations with increasing pitch are shown in Figure 11 as a function of the pitch of the inner, uniform portion of the assembly. The maximum  $k_{\text{eff}}$  increase, as shown in Table 6, is 3.90%  $\Delta k_{\text{eff}}$ . The first five points represent the uniform pitch expansion. Nonuniform expansion begins when the fuel rod pitch is in excess of approximately 1.32 cm. The additional  $k_{\text{eff}}$  increase beyond the uniform expansion case reported above is 1.25%  $\Delta k_{\text{eff}}$ , thus indicating that further expansion is a significant effect. This is consistent with the results presented in References 31 and 32.

The limiting pitch expansion case corresponds to 5 w/o fuel with 44.25 GWd/MTU burnup, so the most reactive axial section is near the top end. The fuel rod pitch is varied as function of axial position to investigate the potential effect of birdcaging, as discussed in Section 3.1.3.2. The increased and decreased pitch variations are applied over discrete sections of the fuel rods, and not as continuous changes as a function of elevation. The irradiated fuel is represented with segments 20.32 cm in length to capture the axial burnup gradient, as discussed in Appendix A, and these segments are used as the discrete sections for pitch variation. The size of the compressed pitch region is varied from one and four segments, and the expanded pitch section at the top of the assembly ranges from two to eight segments in length in an effort to identify the maximum change in  $k_{\text{eff}}$  attributable to birdcaging. An example with four segments in the compressed region and four segments in the upper expanded region is shown in Figure 13. Slight reactivity increases are observed in the cases with four or more fuel segments in the expanded pitch zone. The maximum  $k_{\text{eff}}$  change is 0.05%  $\Delta k_{\text{eff}}$  beyond the 2.65%  $\Delta k_{\text{eff}}$  resulting from uniform pitch expansion configuration. This additional increase in  $k_{\text{eff}}$  is negligible.

**Table 11. Results for loss of rod pitch control in GBC-32**

Enrichment (w/o $^{235}\text{U}$ )	Burnup (GWd/MTU)	Increase in $k_{\text{eff}}$ (% $\Delta k_{\text{eff}}$ )
<b>Cladding intact</b>		
1.92	0	0.78
3.5	25.5	1.48
5	44.25	1.69
<b>Cladding removed</b>		
1.92	0	3.30
3.5	25.5	4.49
5	44.25	4.89

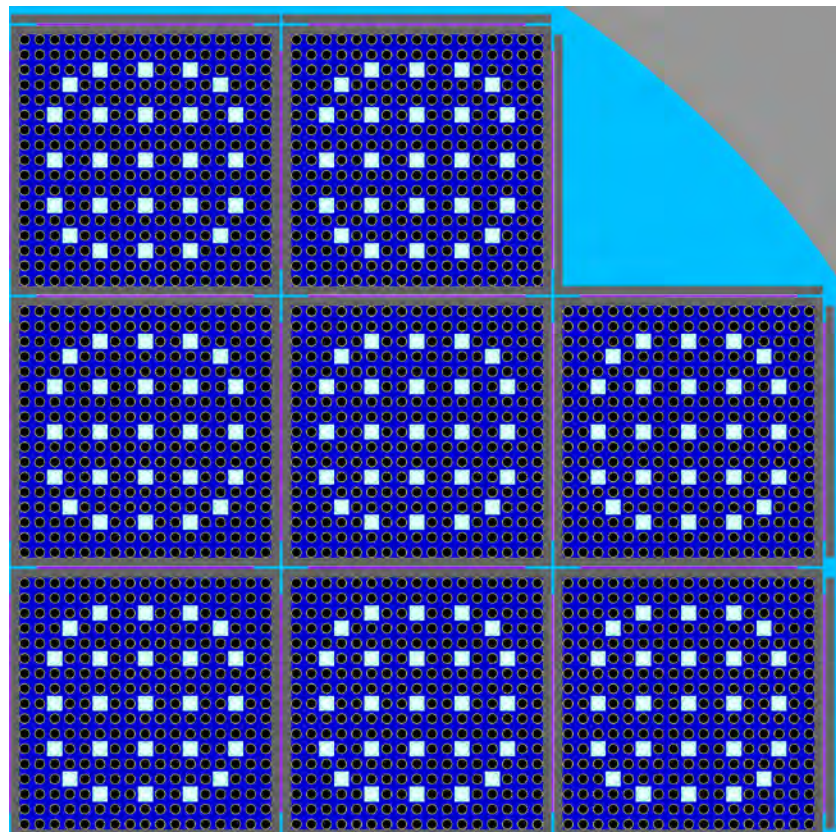


**Figure 10. Maximum uniform pitch expansion case.**

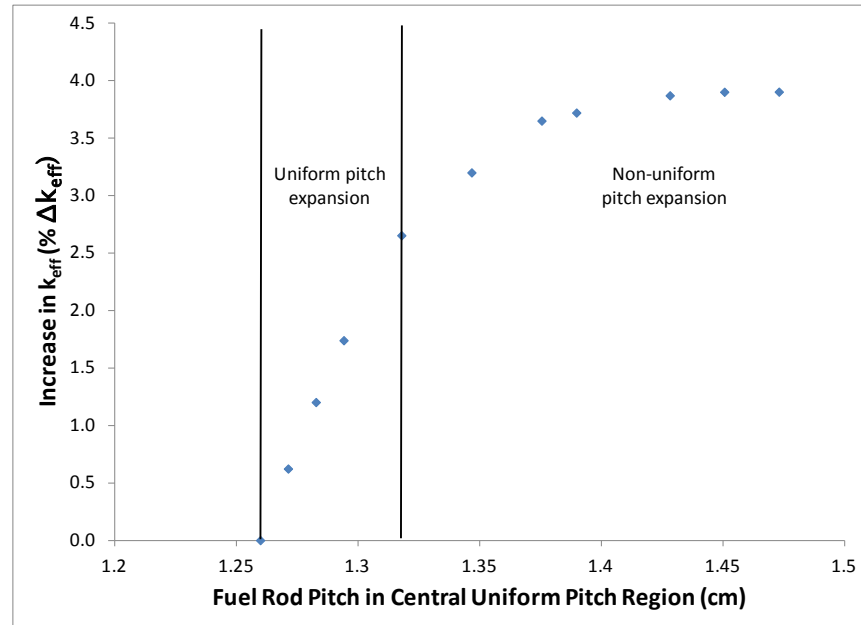
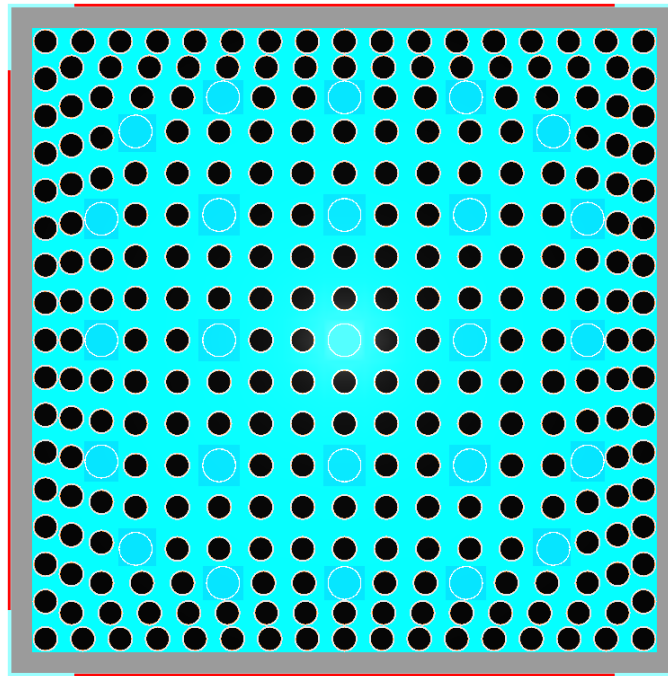
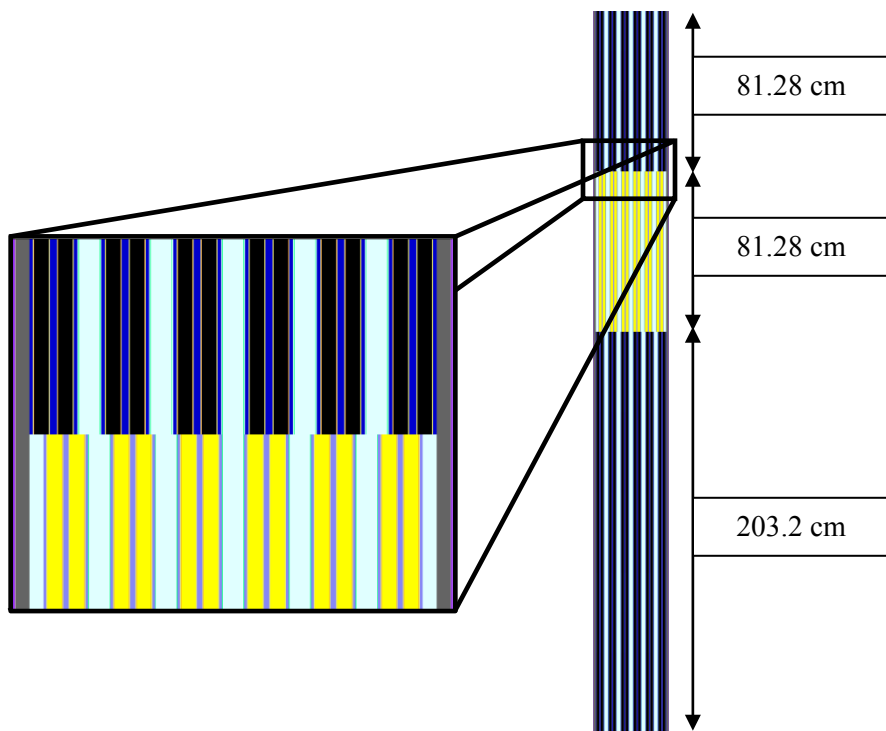


**Figure 11.** Increase in  $k_{\text{eff}}$  in GBC-32 cask due to increased fuel rod pitch (5 w/o initial enrichment, 44.25 GWd/MTU burnup).



Notes: Both shades of light blue are identical water compositions  
Neutron absorber panels are shown in red

**Figure 12.** Example nonuniform pitch model in GBC-32 storage cell.



Notes: Fuel in expanded pitch segments is shown as black, regardless of isotopic composition  
Fuel in compressed pitch segments is shown in yellow, regardless of isotopic composition  
Large gaps between pairs of fuel rods indicate the presence of guide tubes

**Figure 13. Assembly with axially varying pitch in the GBC-32.**

#### 5.1.1.4 Loss of Assembly Position Control

Loss of assembly position control is calculated over a range of displacements. The consequence of the maximum misalignment for all three burnup and enrichment combinations is shown in Table 12 and is over 16%  $\Delta k_{\text{eff}}$  for the limiting condition. A more limited misalignment case (20 cm) is also evaluated as a surrogate for potential degradation of assembly end fittings or the spacers used inside the cask to ensure proper assembly alignment at the time of loading. The consequences of this more limited misalignment, shown in Figure 14 and Table 13, are significantly less, but the increase in  $k_{\text{eff}}$  is still nearly 11%  $\Delta k_{\text{eff}}$ . The limiting condition for misalignment is for fuel with 44.25 GWd/MTU burnup and an initial enrichment of 5 w/o. Misalignment toward the bottom of the cask has significantly less impact because the fuel at the bottom end of the assembly has lower reactivity. The variation of the  $k_{\text{eff}}$  increase as a function of axial position is shown in Figure 15 for fuel with an initial enrichment of 5 w/o  $^{235}\text{U}$  and 44.25 GWd/MTU burnup. The reactivity increase reported here is significantly higher than that reported in Ref. 25. Insufficient detail is available for review in Ref. 25 to propose any likely causes for the differences.

**Table 12. Increase in  $k_{\text{eff}}$  for assembly axial displacement in GBC-32  
(30 cm displacement relative to the neutron absorber panel)**

Enrichment (w/o $^{235}\text{U}$ )	Burnup (GWd/MTU)	Increase in $k_{\text{eff}}$ (% $\Delta k_{\text{eff}}$ )
1.92	0	10.38
3.5	25.5	16.37
5	44.25	16.70

**Table 13. Increase in  $k_{\text{eff}}$  for limited (20 cm displacement relative to the neutron absorber panel)  
assembly axial displacement in GBC-32**

Enrichment (w/o $^{235}\text{U}$ )	Burnup (GWd/MTU)	Increase in $k_{\text{eff}}$ (% $\Delta k_{\text{eff}}$ )
1.92	0	3.85
3.5	25.5	10.22
5	44.25	10.82

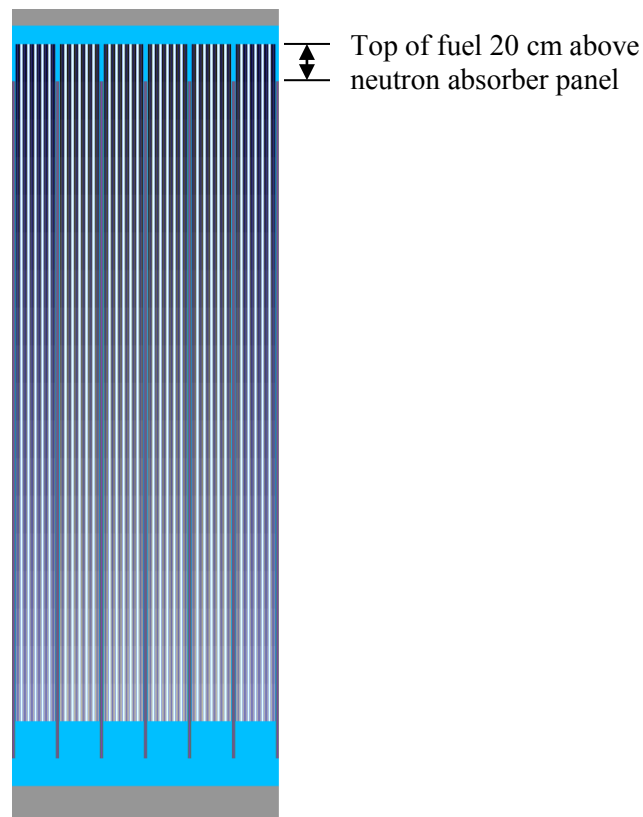


**Figure 14. Misalignment of fuel assembly 20 cm toward lid of GBC-32.**

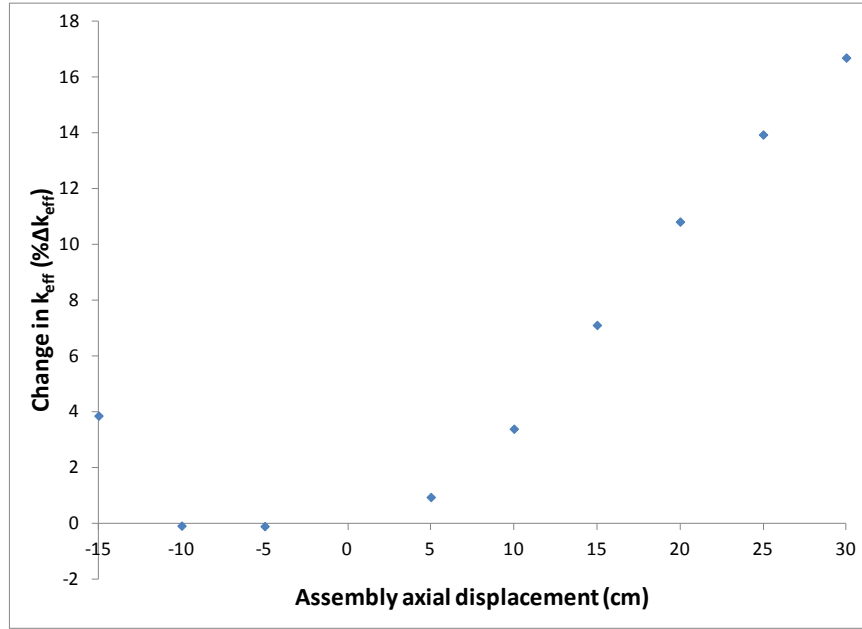


**Figure 15. Increase in  $k_{\text{eff}}$  in GBC-32 as a function of assembly axial displacement (5 w/o initial enrichment and 44.25 GWd/MTU burnup).**

#### 5.1.1.5 Gross Fuel Assembly Failure

The two gross assembly failure configurations described in Section 3.1.5 are investigated in the GBC-32 cask. Axial representations are shown in Figure 16 and 17 for the homogeneous rubble and ordered pellet array cases, respectively. In both cases, the limiting case is the non-physical condition in which the fissile material extends from the base plate to the lid. As expected, these configurations have the highest  $k_{\text{eff}}$  increase, and the ordered pellet array case is more limiting than the homogeneous rubble case. As shown previously in Table 6, the  $k_{\text{eff}}$  associated increase in the homogeneous rubble case is over 14%  $\Delta k_{\text{eff}}$ , and the ordered pellet array case increases  $k_{\text{eff}}$  by over 21%  $\Delta k_{\text{eff}}$ . The limiting case is for the 44.25 GWd/MTU burnup case with 5 w/o initial enrichment for both gross assembly failure configurations. The results for both configurations for all three enrichment and burnup combinations are presented in Table 14 for the maximum increase case. If the fissile material is maintained within the poison panel elevations, the resulting change in  $k_{\text{eff}}$  is reduced to 4.18%  $\Delta k_{\text{eff}}$  for the ordered array of pellets. Results for a range of homogeneous rubble cases within the neutron absorber elevations are provided in Table 15. The results with fissile material restrained in the neutron absorber elevations demonstrate that these cases result in significantly lower  $k_{\text{eff}}$  increases than the unrestrained material cases.

The results for the pellet array case are significantly higher than those reported previously in Ref. 7. There are two main differences between that analysis and this one, both of which contribute to a sizeable  $k_{\text{eff}}$  increase in the work presented here. The pellet array case modeled here includes a distributed burnup profile in the pellet array, and the array is allowed to extend beyond the neutron absorber panel elevations. This latter change is the larger of the two effects, but the former change is also important.

**Table 14. Increase in  $k_{\text{eff}}$  in GBC-32 due to gross fuel assembly failure, fissile material outside neutron absorber elevations**

Enrichment (w/o $^{235}\text{U}$ )	Burnup (GWd/MTU)	Maximum increase in $k_{\text{eff}}$ (% $\Delta k_{\text{eff}}$ )
<b>Limiting pellet array</b>		
1.92	0	11.09
3.5	25.5	20.20
5	44.25	21.37
<b>Homogeneous rubble</b>		
1.92	0	6.66
3.5	25.5	13.95
5	44.25	14.30

**Table 15. Increase in  $k_{\text{eff}}$  in GBC-32 due to homogeneous rubble, debris within absorber elevations (5 w/o initial enrichment, 44.25 GWd/MTU burnup)**

Fraction of nominal assembly height	Increase in $k_{\text{eff}}$ (% $\Delta k_{\text{eff}}$ )
1.0	-4.64
0.9	-7.05
0.8	-10.16
0.7	-14.36
0.6	-20.16
0.5	-28.34
0.4	-39.10
0.36 (Fully compressed rubble)	-45.50



**Figure 16.** Limiting homogeneous rubble configuration for GBC-32.

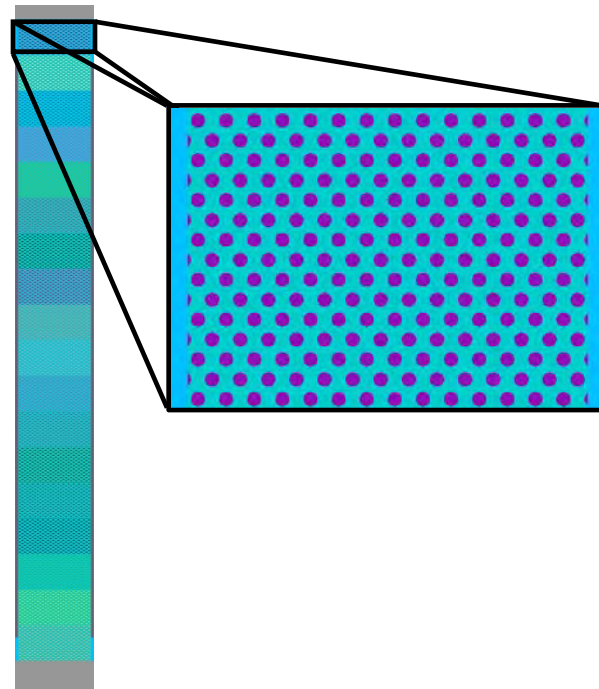


**Figure 17.** Limiting ordered pellet array configuration for GBC-32.

### 5.1.1.6 Neutron Absorber Degradation

The results of the calculations, described in Section 3.1.6.1, considering a 5-cm neutron absorber defect at varying elevations for all three enrichment and burnup combinations are presented in Table 16. The limiting condition is for fuel with an initial enrichment of 5 w/o and 44.25 GWd/MTU burnup. As expected, the limiting elevation is near the top of the active fuel height, as shown in Figure 18. The results for the full range of elevations considered in the limiting fuel condition are presented in Table 17. As expected, the limiting elevation for the fresh 1.92 w/o fuel is located at the centerline. The largest  $k_{\text{eff}}$  increase observed for the 5-cm defect is 1.05%  $\Delta k_{\text{eff}}$  and increases to 2.33%  $\Delta k_{\text{eff}}$  if the defect size is increased to 10 cm. As discussed in Section 3, these defects are assumed to be present at the same elevation in all neutron absorber panels within the cask and the sizes of the defects are chosen arbitrarily.

The consequences of uniform neutron absorber panel thinning as discussed in Section 3.1.6.3 are shown in Table 18 and Figure 19 for fresh 1.92 w/o fuel. The panel thinning results shown in Appendix C confirm that the fresh fuel case is most limiting. As shown in Table 6, a 50% reduction in absorber panel thickness increases  $k_{\text{eff}}$  by 1.78%  $\Delta k_{\text{eff}}$ . Complete removal of the panels causes a  $k_{\text{eff}}$  increase of 9.5%, but the increase is not in excess of 3% until nearly 70% of the neutron absorber panel is removed. The consequence of complete absorber panel removal is less severe than the axial displacement cases discussed in Section 5.1.1.4 because the steel fuel storage basket walls reduce neutronic communication between assemblies.

**Table 16. Maximum  $k_{\text{eff}}$  increase caused by a 5-cm neutron absorber defect in GBC-32**

Enrichment (w/o $^{235}\text{U}$ )	Burnup (GWd/MTU)	Defect center elevation (cm)	Maximum increase in $k_{\text{eff}}$ (% $\Delta k_{\text{eff}}$ )
1.92	0	182.88	0.29
3.5	25.5	342.09	0.94
5	44.25	348.86	1.05

**Table 17. Increase in  $k_{\text{eff}}$  caused by a 5-cm neutron absorber defect at various elevations in GBC-32 (5 w/o initial enrichment, 44.25 GWd/MTU burnup)**

Defect center elevation (cm)	Increase in $k_{\text{eff}}$ (% $\Delta k_{\text{eff}}$ )
321.77	0.44
328.54	0.67
335.31	0.84
342.09	1.00
348.86	1.05
355.64	0.82

**Table 18. Increase in  $k_{\text{eff}}$  caused by uniform neutron absorber panel thinning  
(fresh 1.92 w/o enrichment)**

Fraction of neutron absorber panel thickness remaining	Increase in $k_{\text{eff}}$ (% $\Delta k_{\text{eff}}$ )
0.9	0.29
0.8	0.59
0.7	0.92
0.6	1.32
0.5	1.78
0.4	2.39
0.3	3.15
0.2	4.20
0.1	5.86
0.0	9.51

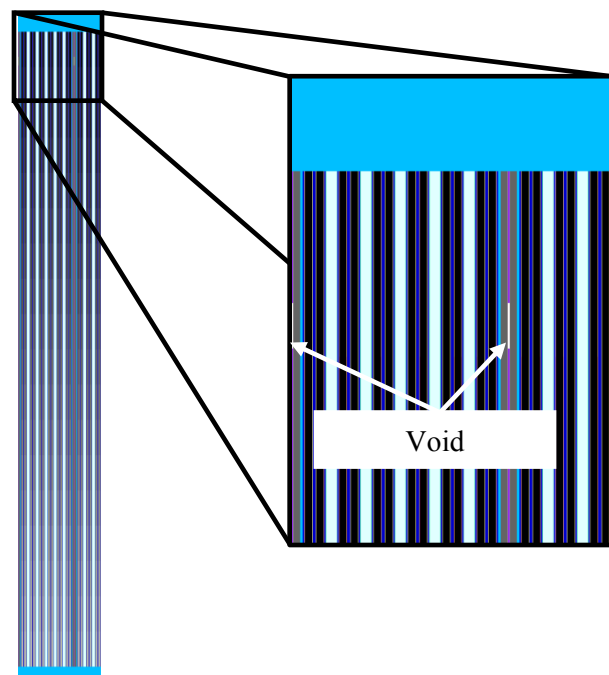


**Figure 18. Limiting location of 5-cm neutron absorber panel defect in GBC-32.**

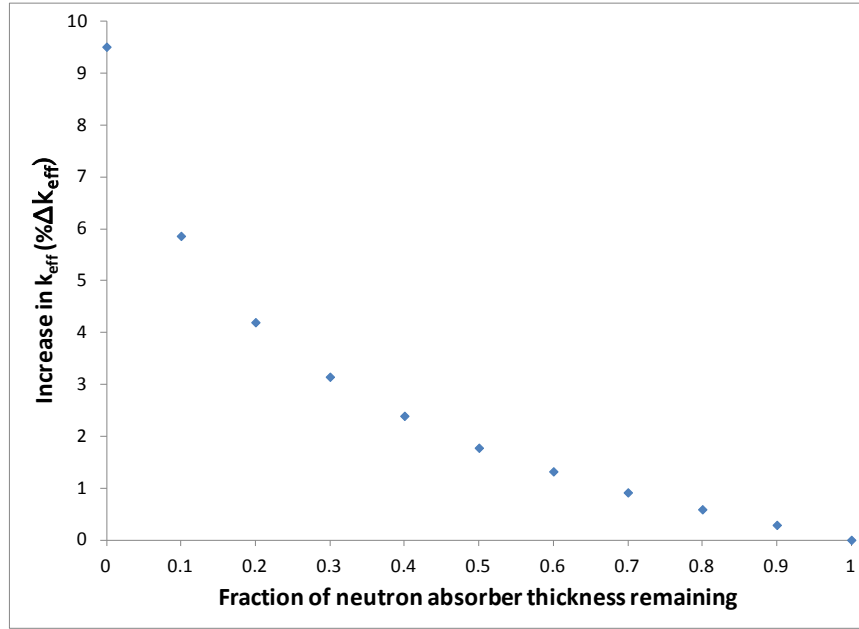


**Figure 19. Increase in  $k_{\text{eff}}$  as a function of remaining neutron absorber panel thickness for fresh 1.92 w/o fuel.**

#### 5.1.1.7 Burnup and Cooling Time Sensitivities

The results of the sensitivity studies relating to additional burnup and cooling time are presented in Appendix C (Section C.1). Each configuration discussed in the previous six subsections is considered explicitly. The results of the calculations for additional burnup and cooling time conditions indicate that the increase in  $k_{\text{eff}}$  reported for each configuration encompasses the changes that may result for additional burnups and cooling times. That is, the differences in the change in  $k_{\text{eff}}$  are smaller than the changes in the base case  $k_{\text{eff}}$  caused by the additional burnup and/or cooling time considered.

#### 5.1.2 Varying Number of Reconfigured Assemblies

The results presented in Section 5.1.1 and Table 6 assume that all 32 fuel assemblies in the GBC-32 cask experience the same fuel or neutron absorber reconfiguration within the respective configuration of interest. As discussed in Section 3.2, a series of calculations is performed to establish the  $k_{\text{eff}}$  increase as a function of the number of reconfigured assemblies within the cask. The four configurations considered are the limiting conditions for single rod failure, multiple rod failure, uniform rod pitch increase, and homogeneous rubble resulting from gross assembly failure.

The first fuel assembly to experience the reconfiguration being examined is selected in an attempt to maximize the  $k_{\text{eff}}$  increase, and is therefore one near the center of the cask. Additional assemblies are added in mostly symmetric groups of equal distance from the first reconfigured assembly. For some low numbers of reconfigured assemblies, multiple combinations of assemblies are considered. Eight combinations of reconfigured assemblies are considered in the GBC-32. One order in which the assemblies experience reconfiguration is shown in Figure 20. Results are presented in the following subsections.

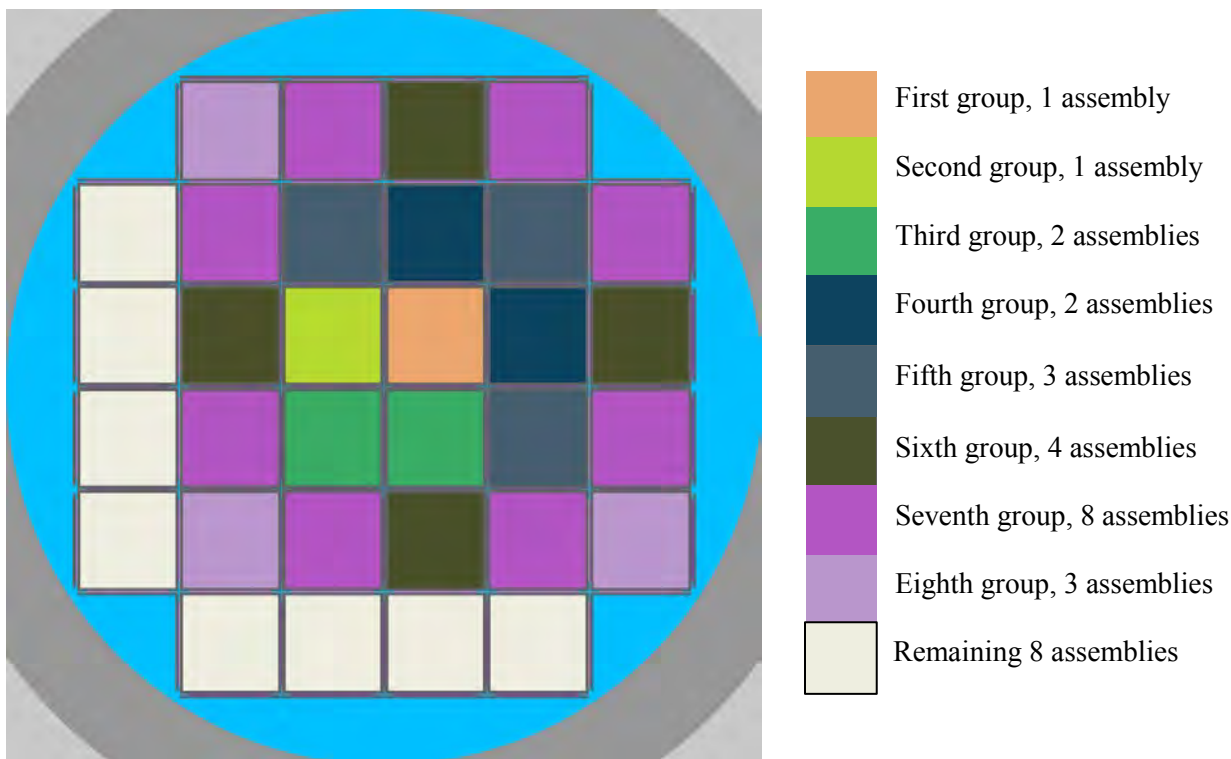


**Figure 20. One order of assembly reconfiguration in GBC-32 partial degradation configurations.**

### 5.1.2.1 Rod Failures

The single and multiple rod failure configurations that result in the largest increase in  $k_{\text{eff}}$ , as discussed in Section 5.1.1.2, are used to study the impact of some assemblies suffering reconfiguration while others in the cask remain intact. All assemblies, reconfigured or intact, use the isotopic number densities representing 5 w/o  $^{235}\text{U}$  fuel depleted to 44.25 GWd/MTU and cooled for 5 years.

The results for single rod failure are shown below in Table 19 and Figure 21. The results for multiple rod failure are shown below in Table 20 and Figure 22. The portion of the  $k_{\text{eff}}$  impact introduced by each group of assemblies for the single rod failure configurations shows more than 50% of the reactivity change coming after only four assemblies experience reconfiguration and more than 75% of the reactivity change caused by the first nine assembly reconfigurations. The Monte Carlo uncertainty is relatively large compared to the  $k_{\text{eff}}$  changes being examined in this series of calculations because of the relative insensitivity of the cask  $k_{\text{eff}}$  to single rod failures. The resulting  $k_{\text{eff}}$  increase is therefore not a smooth function.

The multiple rod failure results are similar, with fewer than nine assemblies causing 50% of the increase in  $k_{\text{eff}}$  and 13 assemblies causing almost 75% of the change. The results indicate that a reduced number of reconfigured assemblies will not significantly reduce the  $k_{\text{eff}}$  increase associated with fuel reconfiguration if the degraded assemblies are in close proximity, and particularly if they are in the center region of the cask.

**Table 19. Increase in  $k_{\text{eff}}$  in GBC-32, single rod failure  
(5 w/o initial enrichment, 44.25 GWd/MTU burnup)**

Number of degraded assemblies	Increase in $k_{\text{eff}}$ (% $\Delta k_{\text{eff}}$ )
1	0.01
2	0.01
2	0.01
4	0.06
5	0.04
5	0.05
9	0.07
13	0.07
21	0.07
24	0.07
32	0.09

**Table 20. Increase in  $k_{\text{eff}}$  in GBC-32, multiple rod failure  
(5 w/o initial enrichment, 44.25 GWd/MTU burnup)**

Number of degraded assemblies	Increase in $k_{\text{eff}}$ (% $\Delta k_{\text{eff}}$ )
1	0.20
2	0.37
2	0.36
4	0.71
5	0.79
5	0.82
9	1.16
13	1.38
21	1.70
24	1.74
32	1.86

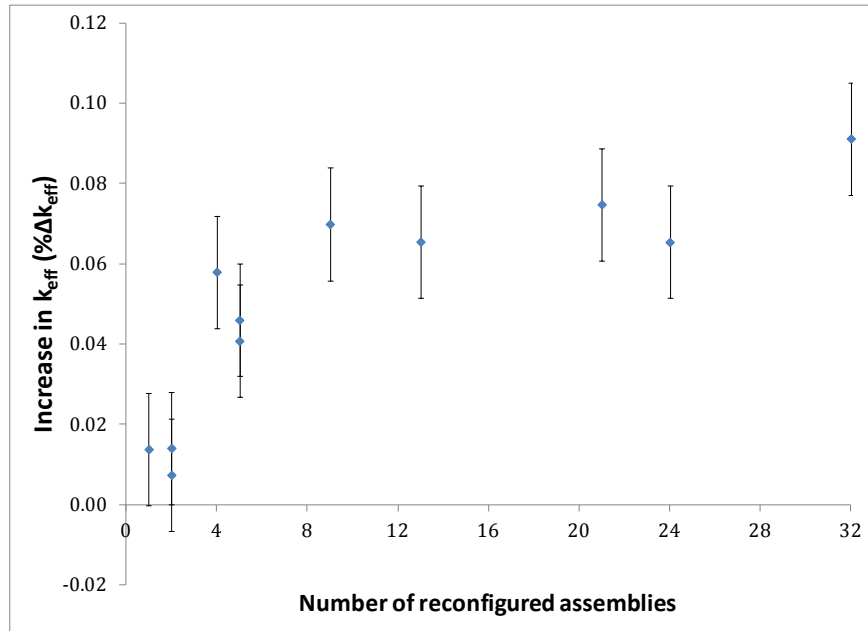


Figure 21. Increase in  $k_{\text{eff}}$  in GBC-32 as a function of number of reconfigured assemblies, single rod failure (5 w/o initial enrichment, 44.25 GWd/MTU burnup).

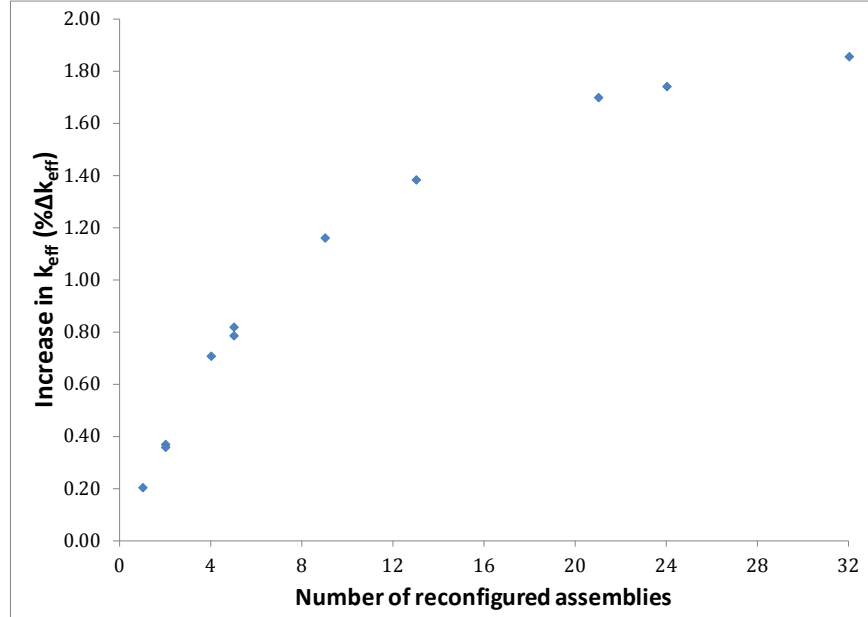


Figure 22. Increase in  $k_{\text{eff}}$  in GBC-32 as a function of number of reconfigured assemblies, multiple rod failure (5 w/o initial enrichment, 44.25 GWd/MTU burnup).

### 5.1.2.2 Loss of Rod Pitch Control, Uniform Pitch Increase

The maximum uniform pitch increase case is used to examine the  $k_{\text{eff}}$  impact of varying the number of assemblies that have experienced reconfiguration. The assembly configuration used for this study models

the outer row of fuel rods in contact with the inner wall of the fuel storage basket in each cell. The fuel composition used for all assemblies corresponds to 5 w/o fuel with 44.25 GWd/MTU burnup and 5 years of cooling time. The increase in  $k_{\text{eff}}$  for each number of reconfigured assemblies is provided in Table 21 as well as Figure 23. The first 50% of the total increase in  $k_{\text{eff}}$  has occurred with about seven reconfigured assemblies. Almost 75% of the increase in  $k_{\text{eff}}$  is caused by the first 13 reconfigured assemblies. The shape of the increase in  $k_{\text{eff}}$  as a function of reconfigured assemblies is similar to that seen for rod failure configurations in Section 5.1.2.1. The results indicate that a reduced number of reconfigured assemblies will not significantly reduce the  $k_{\text{eff}}$  increase associated with fuel reconfiguration if the degraded assemblies are in close proximity, and particularly if they are in the center region of the cask.

**Table 21. Increase in  $k_{\text{eff}}$  in GBC-32, uniform pitch increase  
(5 w/o initial enrichment, 44.25 GWd/MTU burnup)**

Number of degraded assemblies	Increase in $k_{\text{eff}}$ (% $\Delta k_{\text{eff}}$ )
1	0.27
2	0.51
2	0.49
4	1.00
5	1.14
5	1.08
9	1.66
13	1.96
21	2.41
24	2.49
32	2.66

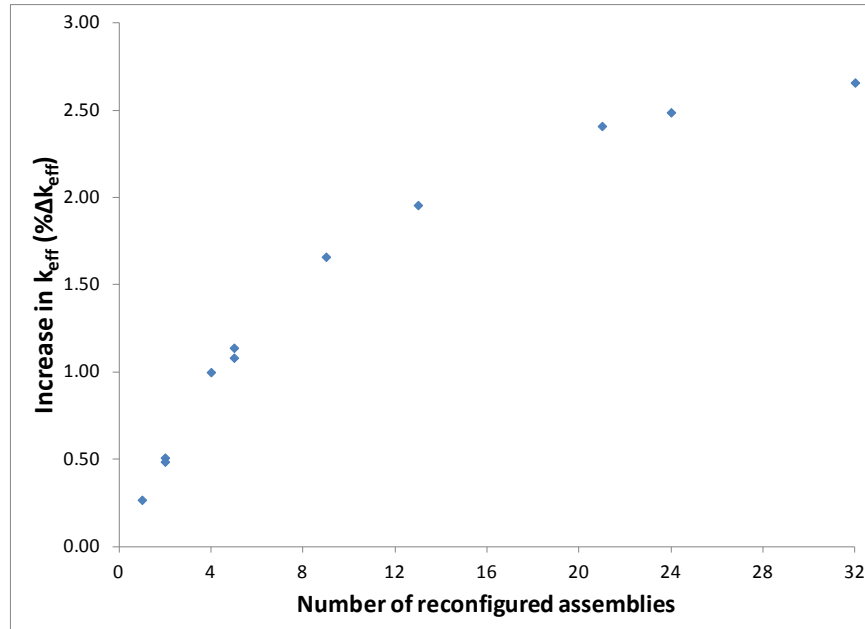


**Figure 23. Increase in  $k_{\text{eff}}$  in GBC-32 as a function of number of reconfigured assemblies, uniform pitch increase (5 w/o initial enrichment, 44.25 GWd/MTU burnup).**

### 5.1.2.3 Gross Assembly Failure, Homogeneous Rubble

The homogeneous rubble modeling of the gross assembly failure configuration is the final configuration used to examine the  $k_{\text{eff}}$  impact of varying the number of assemblies that have experienced reconfiguration. The configuration used for this study fills the entire inside volume of the storage cell with homogeneous rubble, as described in Section 3.1.5.1. Each axial zone of rubble is approximately 23 cm tall; thus, the 18 zones fill the cask from the base plate to the lid and retain the axial burnup profile of the intact assembly. The fuel composition is based on fuel with an initial enrichment of 5 w/o and 44.25 GWd/MTU burnup. This configuration resulted in the largest  $k_{\text{eff}}$  increase of the homogeneous rubble configurations used in Section 5.1.1.5. The increase in  $k_{\text{eff}}$  for each number of reconfigured assemblies is provided in Table 22 as well as Figure 24. The general trend in the  $k_{\text{eff}}$  change for the uniform pitch increase cases is different from that for single and multiple rod failure and uniform pitch expansion configurations presented in Sections 5.1.2.1 and 5.1.2.2. The first two reconfigured assemblies lower the cask  $k_{\text{eff}}$  because of the effects of homogenization and fissile material relocation. An increase in  $k_{\text{eff}}$  is noted for four or more reconfigured assemblies after a sufficient number of assemblies are reconfigured to relocate the most reactive portion of the cask to the top of the homogeneous rubble. More than 60% of the increase in  $k_{\text{eff}}$  is caused by the first nine reconfigured assemblies, and more than 70% of the total  $k_{\text{eff}}$  increase results from the reconfiguration of 13 assemblies.

**Table 22. Increase in  $k_{\text{eff}}$  in GBC-32, homogeneous rubble configuration of gross assembly failure (5 w/o initial enrichment, 44.25 GWd/MTU burnup)**

Number of degraded assemblies	Increase in $k_{\text{eff}}$ (% $\Delta k_{\text{eff}}$ )
1	-0.53
2	-0.87
2	-1.07
4	1.93
5	2.91
5	1.70
9	8.59
13	10.07
21	12.94
24	13.37
32	14.30

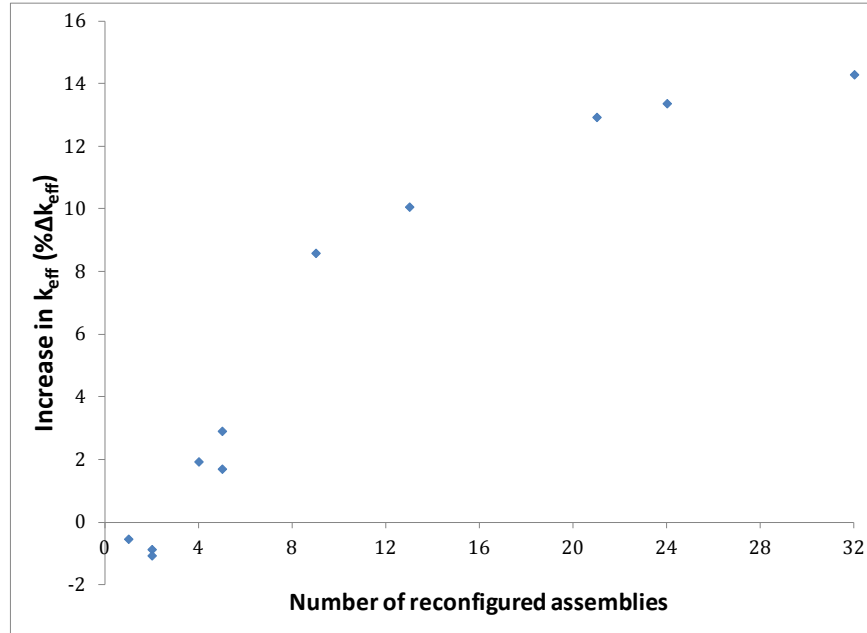


**Figure 24. Increase in  $k_{\text{eff}}$  as a function of number of reconfigured assemblies, gross assembly failure.**

### 5.1.3 Combined Configurations

As discussed in Section 3.3, some of the mechanisms that could result in fuel reconfigurations could result in a combination of configurations. Therefore, selected combined configurations are evaluated, including: 16 failed rods with 50% clad thinning and 16 failed rods with a uniform pitch expansion of 0.011 cm. These combinations of configurations are selected as they both pertain to failure of zirconium alloy components of the fuel assembly. The combined degradation cases consider fuel with an initial enrichment of 5 w/o  $^{235}\text{U}$  depleted to 44.25 GWd/MTU and 5 years of cooling time.

The multiple rod failure results presented in Section 5.1.1.2 indicate that the failure of 16 fuel rods results in an increase in  $k_{\text{eff}}$  of 1.1%  $\Delta k_{\text{eff}}$ . This is approximately half the maximum increase for multiple failed rod configurations and is therefore selected as an intermediate configuration. The cladding thickness on all intact rods in both combined configurations is represented with 50% of the nominal thickness. The pitch increase of 0.011 cm, based on the results presented in Figure 11, is approximately 0.6%  $\Delta k_{\text{eff}}$ . This represents about 15% of the increase in maximum  $k_{\text{eff}}$  associated with the nonuniform pitch expansion.

The results of the two combined configurations considered in the GBC-32 cask are presented in Table 23. For comparison, the  $k_{\text{eff}}$  increase resulting from each degraded configuration separately as well as the sum of the two is provided. The increase in  $k_{\text{eff}}$  associated with explicit modeling of the combined configurations is less than the estimated increase based on summing the individual increases. The conservatism of adding the separate effects is less than 0.4%  $\Delta k_{\text{eff}}$ . It appears that the linear combination of the  $k_{\text{eff}}$  increases is conservative, but more combined configurations would need to be investigated prior to drawing general conclusions. If it is confirmed, the  $k_{\text{eff}}$  increase caused by combinations of degradations could be conservatively bounded by adding the increase associated with individual configurations where applicable.

**Table 23. Increase in  $k_{\text{eff}}$  for combined configurations in GBC-32**

Case	Increase in $k_{\text{eff}}$ (% $\Delta k_{\text{eff}}$ )
<b>Multiple failed rods and clad thinning (44.25 GWd/MTU; 5-y cooling time)</b>	
16 failed rods	1.10
50% clad thinning	1.94
Sum of $k_{\text{eff}}$ increases	3.04
Combined configuration model	2.67
Overestimation of $k_{\text{eff}}$ increase by summing individual effects	0.37
<b>Multiple failed rods and 0.011-cm increase in fuel rod pitch (44.25 GWd/MTU; 5-y cooling time)</b>	
16 failed rods	1.10
Uniform pitch increase	0.62
Sum of $k_{\text{eff}}$ increases	1.72
Combined configuration model	1.63
Overestimation of $k_{\text{eff}}$ increase by summing individual effects	0.09

## 5.2 MPC-68 Cask Model Results

The  $k_{\text{eff}}$  change associated with each of the reconfigurations discussed in Section 3 is presented here for the MPC-68 cask. The configurations assume a range of loadings of  $10 \times 10$  fuel. The description of the fuel assembly modeling is provided in Appendix A. All fuel is modeled with a uniform initial enrichment of 5 w/o. The burnups and cooling times used are presented in Table 24. The basis for selecting these points is provided in Section 4.2.2. All configurations, with the exception of the uniform array of pellets model of gross fuel assembly failure, also consider the fuel both with and without the channel present. The reference case  $k_{\text{eff}}$  results for both fresh and used fuel in both the channeled and unchanneled conditions are provided in Table 24.

**Table 24. Nominal  $k_{\text{eff}}$  results for enrichment, burnup, and cooling time cases considered in MPC-68, channeled and unchanneled fuel**

Channel present	Burnup (GWd/MTU)	Cooling time (years)	KENO V.a		KENO-VI	
			$k_{\text{eff}}$	$\sigma$	$k_{\text{eff}}$	$\sigma$
Yes	0	0	0.96800	0.00010	0.96828	0.00010
	35.0	5	0.83269	0.00010	0.83258	0.00010
No	0	0	0.96768	0.00010	0.96763	0.00010
	35.0	5	0.83434	0.00010	0.83420	0.00010

### 5.2.1 Reconfiguration of All Assemblies

A summary of the increases in  $k_{\text{eff}}$  caused by each configuration is provided in Table 25. Additional details for each configuration and the results for non-limiting cases are provided in the subsequent subsections.

Comparing the results of these analyses to those presented in Ref. 7 is more difficult for the MPC-68 cask than for the GBC-32 cask. The difficulty is primarily a result of the analyses in Ref. 7 using a  $9 \times 9$  fuel assembly.

**Table 25. Summary of  $k_{\text{eff}}$  increases for the MPC-68 cask**

<b>Configuration</b>	<b>Increase in <math>k_{\text{eff}}</math> (% <math>\Delta k_{\text{eff}}</math>)</b>	<b>Limiting case</b>		
		<b>Burnup (GWd/MTU)</b>	<b>Cooling time (years)</b>	<b>Channel present</b>
<b>Clad thinning/loss</b>				
Cladding removal	4.98	0	0	Yes
<b>Rod failures</b>				
Single rod removal	0.29	0	0	Yes
Multiple rod removal	2.40	35	5	Yes
<b>Loss of rod pitch control</b>				
Uniform rod pitch expansion, clad	13.16	0	0	No
Uniform rod pitch expansion, unclad	15.32	0	0	No
Channel constrained uniform expansion, clad	2.09	0	0	Yes
Nonuniform rod pitch expansion, clad	13.31	0	0	No
<b>Loss of assembly position control</b>				
Axial displacement (maximum)	19.40	35	5	Yes
Axial displacement (20 cm)	6.29	35	5	Yes
<b>Gross assembly failure</b>				
Uniform pellet array	34.40	35	5	No
Homogeneous rubble	29.36	35	5	No
<b>Neutron absorber degradation</b>				
Missing neutron absorber (5-cm segment)	2.49	35	5	Yes
Missing neutron absorber (10-cm segment)	5.62	35	5	Yes
50% reduction of neutron absorber panel thickness	3.67	0	0	Yes

### 5.2.1.1 Clad Thinning/Loss

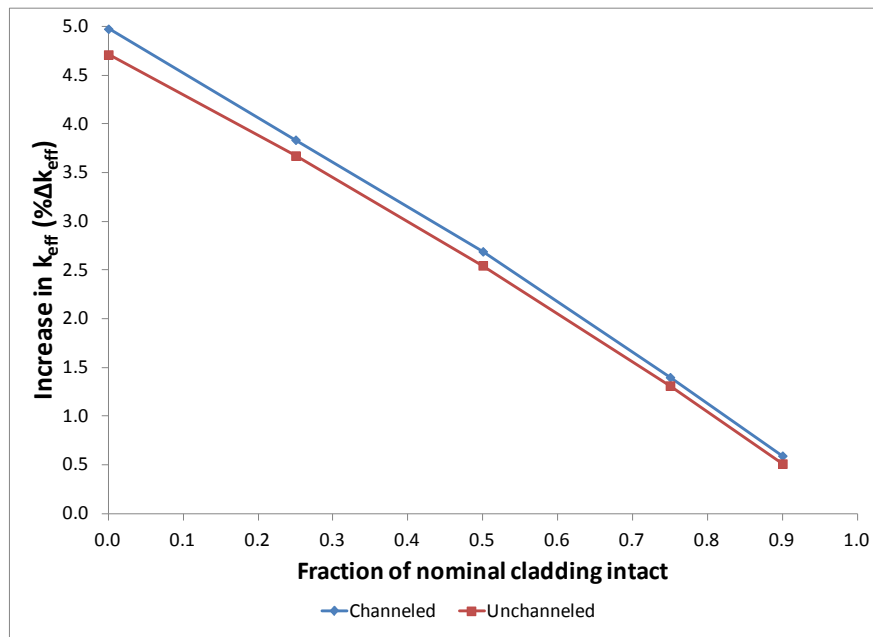
The loss of cladding configuration is modeled as discussed in Section 3.1.1. As shown in Table 25, the limiting  $k_{\text{eff}}$  increase associated with complete cladding removal is 4.98%  $\Delta k_{\text{eff}}$  and occurs with fresh fuel. The results for both fuel burnups, both with and without the fuel channel, are summarized in Table 26. For the limiting case, fresh fuel, the increase in  $k_{\text{eff}}$  as a function of the fraction of nominal cladding thickness remaining is shown in Table 27 and Figure 25. The trend of increasing  $k_{\text{eff}}$  with decreasing cladding thickness is the same for depleted fuel, so these results are not presented here. The configuration with 25% of the nominal cladding remaining is shown in Figure 26. The results are in good agreement with those presented in Ref. 7.

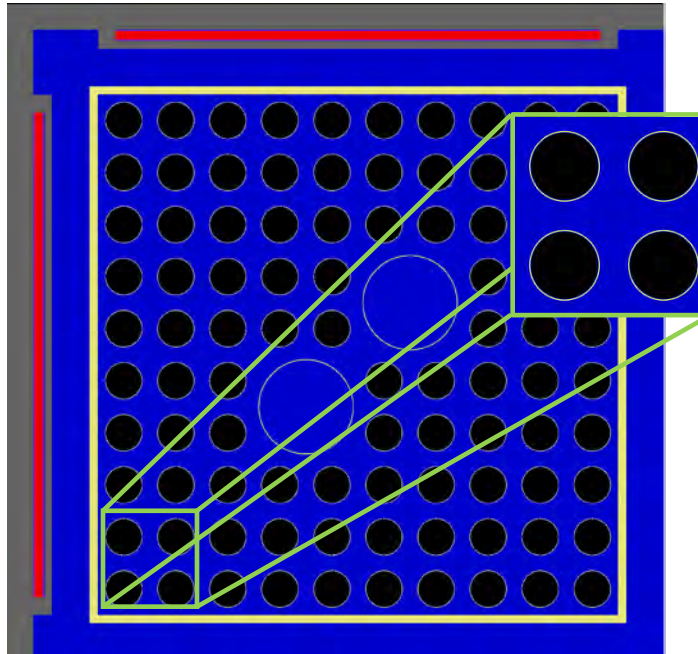
**Table 26. Increase in  $k_{\text{eff}}$  for cladding removal in MPC-68**

Burnup (GWd/MTU)	Cooling time (years)	Channel	Increase in $k_{\text{eff}}$ (% $\Delta k_{\text{eff}}$ )
0	0	Yes	4.98
35	5		4.82
0	0	No	4.71
35	5		4.59

**Table 27. Increase in  $k_{\text{eff}}$  in MPC-68 as a function of fraction of intact cladding, fresh 5 w/o fuel**

Fraction of intact cladding	Increase in $k_{\text{eff}}$ – Channeled (% $\Delta k_{\text{eff}}$ )	Increase in $k_{\text{eff}}$ – Unchanneled (% $\Delta k_{\text{eff}}$ )
0.90	0.59	0.51
0.75	1.40	1.31
0.50	2.69	2.55
0.25	3.84	3.68
0	4.98	4.71

**Figure 25. Increase in  $k_{\text{eff}}$  as a function of fraction of intact cladding, fresh 5 w/o fuel.**



Notes:

- Fuel shown in black
- Cladding is light grey around fuel material
- Water tubes are larger, water-filled tubes
- Storage cell wall and neutron absorber panel wrappers are dark grey
- Neutron absorber panel is red
- Fuel assembly channel yellow box around fuel rods
- Water is shown in dark blue

**Figure 26. Configuration with 25% nominal cladding thickness.**

### 5.2.1.2 Rod Failures

Each of the 51 unique half-assembly symmetric rods is removed individually to determine its worth, as discussed in Section 3.1.2.1. Table 28 presents the rod locations and worth of the limiting rod location for each of the four cases. For both fuel burnups, the  $k_{\text{eff}}$  increase for the channeled fuel assembly is greater than for the unchanneled assembly. This is likely caused by the slightly harder initial spectrum when the channel is present. The increase in moderation caused by the removal of the fuel rods has a greater impact on the harder initial spectrum.

A sketch showing the half-assembly symmetry and row and column labels is provided in Figure 27. The columns in the assembly are designated with a letter, from A to J, and the rows are designated with numbers, from 1 to 10. The maximum worth is 0.29%  $\Delta k_{\text{eff}}$  and is associated with rod H7 with fresh 5 w/o fuel. It should be noted that some rods have a worth that is statistically equivalent to the limiting case presented in Table 28. The worth is very small relative to the  $k_{\text{eff}}$  increases of other configurations, so further examination is not necessary.

The magnitude of the  $k_{\text{eff}}$  change caused by rod failure is somewhat less for these analyses than for the previous work documented in Ref. 7. The primary cause of the reduction is the difference in the size of the fuel rods. The fuel rods in the  $10 \times 10$  fuel assembly have smaller diameters, so the increase in moderation is smaller for a single rod removal.

Multiple rods are removed in groups, as discussed in Section 3.1.2.2. Groups of 2, 4, 8, 12, 16, 18, and 20 rods are considered. The increase in  $k_{\text{eff}}$  is shown for each of the four cases in Table 29. Figure 28 shows the  $k_{\text{eff}}$  change as a function of rods removed for the limiting case at 35 GWd/MTU burnup and 5 years of cooling time with the fuel assembly channel. The limiting lattice is shown in Figure 29. The maximum  $k_{\text{eff}}$  value occurs for 18 rods removed and corresponds to a  $k_{\text{eff}}$  increase of 2.40%  $\Delta k_{\text{eff}}$ . The limiting lattice is determined with the fuel channel intact and then rerun with the fuel channel removed. In each case, the  $k_{\text{eff}}$  increase is higher with the channel intact.

The  $k_{\text{eff}}$  increase for multiple rod removal in the MPC-68 cask is about twice that reported in Ref. 7. This is most likely due to the difference in the fuel assembly modeled in the analysis. The result for fresh fuel shown in Table 29 demonstrates that the effect of depleted fuel instead of fresh fuel is small.

**Table 28. Single rod removal results for GE 10 × 10 fuel in MPC-68**

Burnup (GWd/MTU)	Cooling time (years)	Channel	Location	Maximum increase in $k_{\text{eff}}$ (% $\Delta k_{\text{eff}}$ )
0	0	Yes	H7	0.29
35	5		G7	0.26
0	0	No	H7	0.25
35	5		D3	0.26

**Table 29. Multiple rod removal results for GE 10 × 10 fuel in MPC-68**

Burnup (GWd/MTU)	Cooling time (years)	Channel	Maximum increase in $k_{\text{eff}}$ (% $\Delta k_{\text{eff}}$ )
0	0	Yes	2.24
35	5		2.40
0	0	No	2.11
35	5		2.30

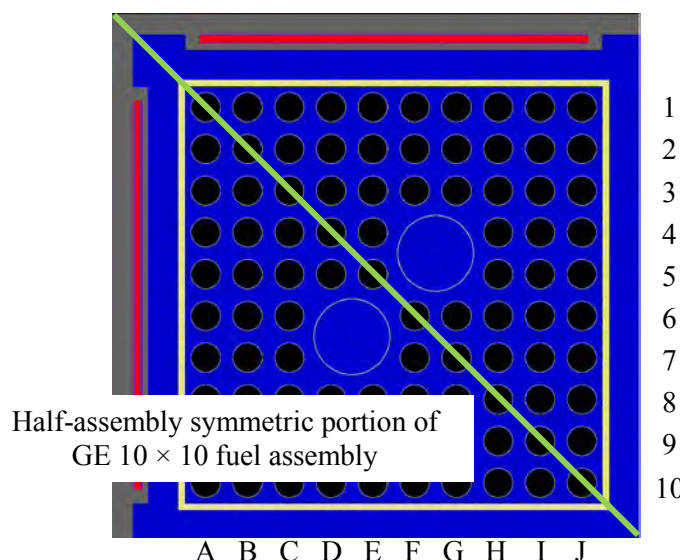


**Figure 27. Sketch of symmetry, row, and column labels for GE 10 × 10 fuel assembly.**

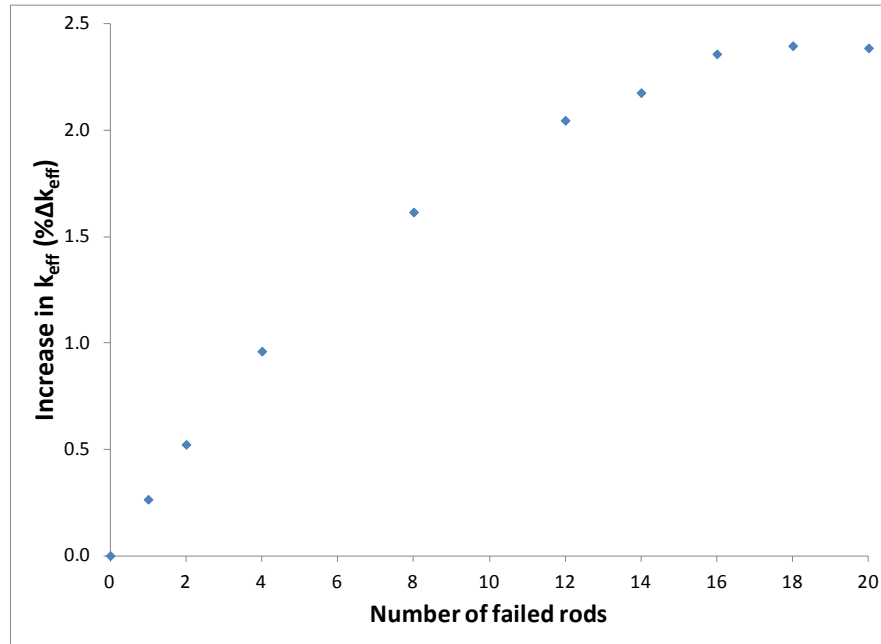


**Figure 28.** Increase in  $k_{\text{eff}}$  in MPC-68 as a function of number of rods removed (35 GWd/MTU burnup and 5-year cooling time).

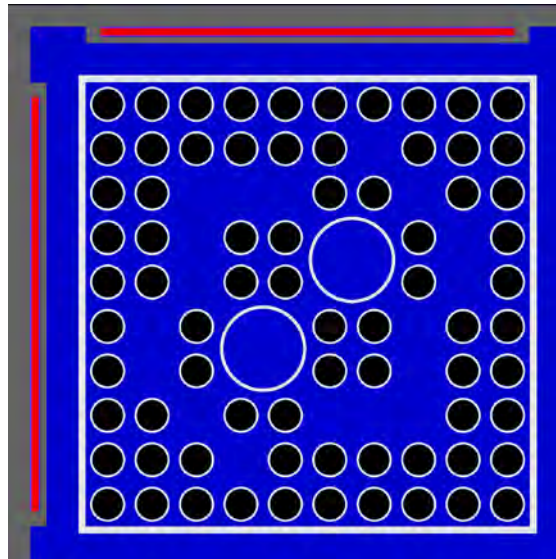


**Figure 29.** Limiting multiple rod removal lattice (18 rods removed).

### 5.2.1.3 Loss of Rod Pitch Control

The loss of rod pitch control is modeled first as a uniform increase in fuel assembly pitch, as discussed in Section 3.1.3. Two different assumptions are made about the condition of an intact fuel assembly channel. In one case, the fuel channel is assumed to expand with uniform thickness along with the fuel bundle. In this nonphysical model, the presence of the channel acts only to limit the uniform pitch increase by the thickness of the channel wall on both sides. The expansion is constrained by the contact of the assembly

channel with the neutron absorber wrappers on one side and the storage cell walls on the other. The second assumption is that the fuel channel does not deform, and thus constrains the expansion of the fuel rod pitch.

The assembly is also considered with no channel present. In this condition, the constraint is provided by fuel rod contact with neutron absorber wrappers. For the unchanneled cases, the modeled expansion ends when the unit cell containing the outermost fuel rods contacts the neutron absorber wrappers and storage cell walls.

The results with and without cladding, with and without the fuel channel, are shown in Table 30. As shown in Table 25, the limiting condition is with fresh fuel. The  $k_{\text{eff}}$  increase for clad fuel restrained by an intact fuel assembly channel is 2.09%  $\Delta k_{\text{eff}}$ .

The limiting condition, with fresh fuel and no assembly channel, is further expanded until the outermost fuel rods are in contact with the neutron absorber wrappers and basket walls, as shown in Figure 30. This pitch is maintained even in cells with fewer than two neutron absorber panels. The resulting increase in  $k_{\text{eff}}$ , is more than 13%  $\Delta k_{\text{eff}}$  with cladding intact and 15.32%  $\Delta k_{\text{eff}}$  with cladding removed.

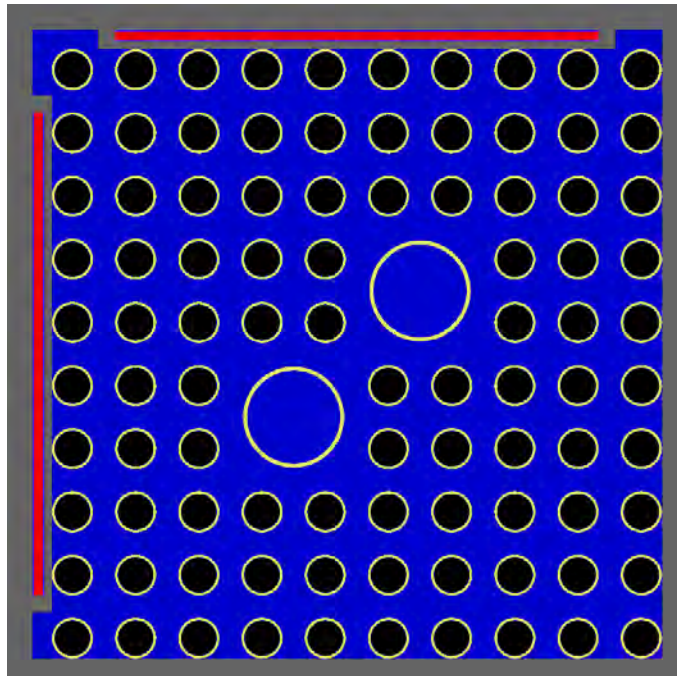
Fuel rod pitch is further increased in the MPC-68 model to examine the effect of nonuniform pitch, as discussed in Section 3.1.3.1 and Refs. 31 and 32. The inner portion of the assembly continues to expand until the outer rows are in contact with each other; although the fuel rod pitch is still uniform axially, it is nonuniform in the radial direction. An example model is shown in Figure 31. In the model with the largest pitch, the outermost fuel is in contact with the walls of the storage cell and the neutron absorber wrappers. The second set of fuel rods is in contact with the outermost rods. The pitch of the outermost fuel is constant within the row and is equal to the pitch that caused the pins to make contact with the basket wall. The increase in pitch in the inner portion of the assembly leads to a nonuniform pitch. The results of the calculations with increasing pitch are shown in Figure 32 as a function of the pitch of the inner, uniform portion of the assembly. The maximum total  $k_{\text{eff}}$  increase is 13.31%  $\Delta k_{\text{eff}}$ . The first six points represent the uniform pitch expansion. Nonuniform expansion begins when the fuel rod pitch is in excess of approximately 1.58 cm. The additional  $k_{\text{eff}}$  increase beyond the uniform expansion case is 0.15%  $\Delta k_{\text{eff}}$ , indicating that further expansion is a minor effect. The additional  $k_{\text{eff}}$  impact caused by nonuniform expansion is consistent with Refs. 31 and 32.

The limiting case for the MPC-68 cask contains fresh fuel, so the most reactive axial portion of the assembly is the center. For that reason, the birdcaging analysis, described in Section 3.1.3.2, includes two compressed pitch sections, each 30.48 cm in length, symmetrically positioned above and below the mid-plane of the assembly. A range of center section lengths is considered, but no  $k_{\text{eff}}$  increase is observed in any case containing the compressed pitch sections. One birdcaging configuration is shown in Figure 33. Birdcaging does not cause any additional  $k_{\text{eff}}$  increase beyond 13.16%  $k_{\text{eff}}$  associated with the uniform pitch expansion configuration for fresh fuel in the MPC-68 cask.

The results presented here show a larger increase in  $k_{\text{eff}}$  than that reported in Ref. 7. This is probably a result of the different fuel assembly lattice. Figure 21 in Ref. 7 indicates that the reactivity consequence of uniform pitch expansion increases with the array size. The effects of the different fuel rod and water rod diameters in the  $10 \times 10$  fuel are not accounted for in Ref. 7, however, so it is possible that these factors also influence the difference between the two analyses.

**Table 30. Results for loss of rod pitch control in MPC-68, no channel restraint**

Burnup (GWd/MTU)	Cooling time (years)	Channel	Maximum increase in $k_{\text{eff}}$ (% $\Delta k_{\text{eff}}$ )
<b>Cladding intact</b>			
0	0	Yes	11.00
35	5	Yes	9.55
0	0	No	12.07
35	5	No	10.56
<b>Cladding removed</b>			
0	0	Yes	14.05
35	5	Yes	12.74
0	0	No	14.70
35	5	No	13.30

**Figure 30. Maximum uniform pitch expansion configuration in MPC-68.**

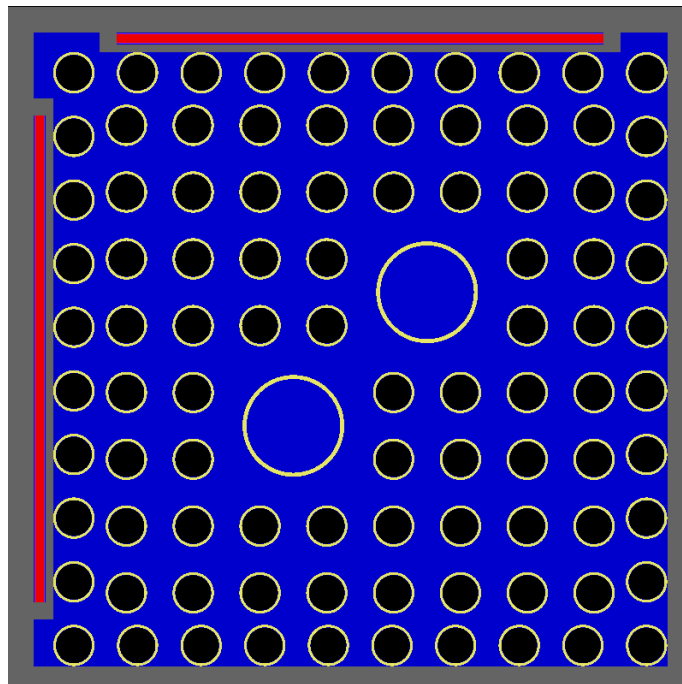


Figure 31. Example nonuniform pitch model for MPC-68.

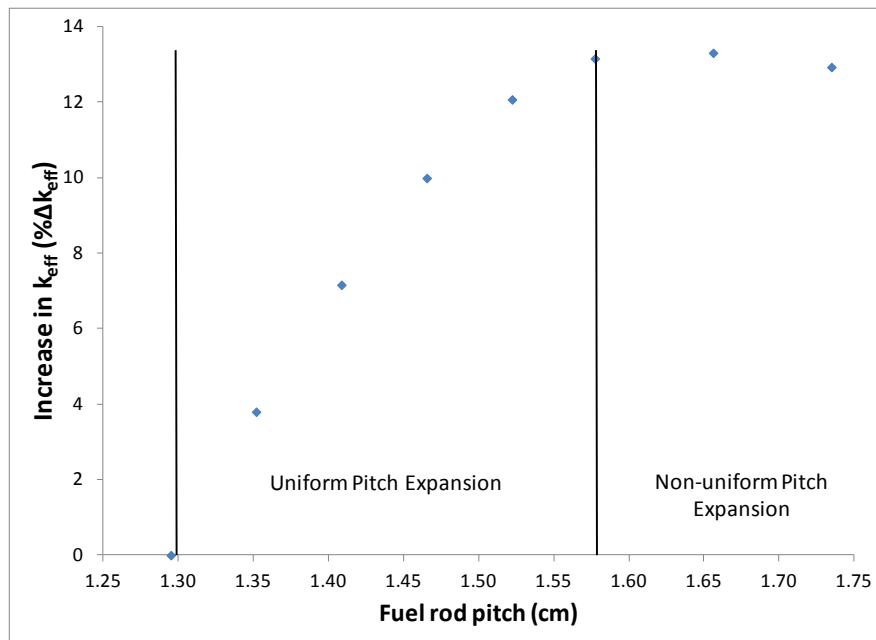
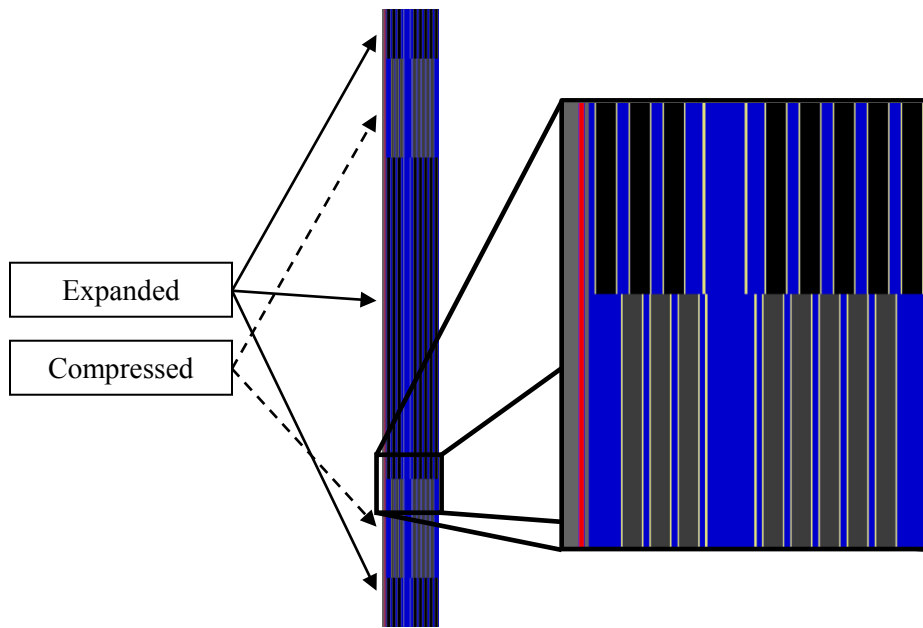


Figure 32. Increase in  $k_{\text{eff}}$  in MPC-68 as a function of fuel rod pitch, fresh 5 w/o fuel.



Notes:

- Expanded section fuel is shown in black
- Compressed section fuel is shown in grey
- All fuel has the same isotopic composition
- The gaps just to the left of the center of the zoomed portion are water tubes

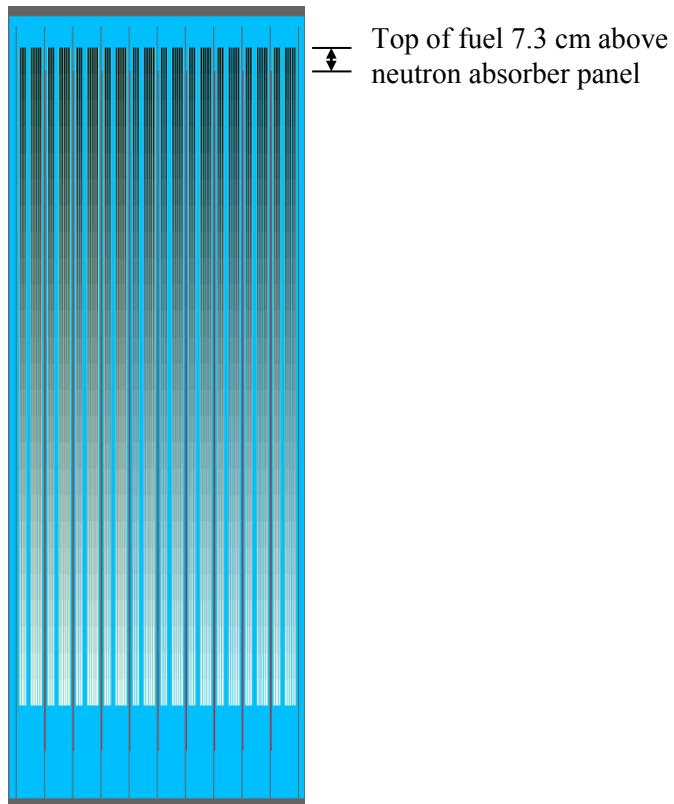
**Figure 33. A fresh fuel birdcaging configuration for MPC-68.**

#### 5.2.1.4 Loss of Assembly Position Control

The loss of assembly position control configuration is calculated over a range of displacements. The consequence of the maximum misalignment for both fresh and irradiated fuel, both with and without the assembly channel, is shown in Table 31 and is almost 20%  $\Delta k_{\text{eff}}$  for the limiting condition. A more limited misalignment case (20 cm) is also evaluated as a surrogate for potential degradation of assembly end fittings or the spacers used inside the cask to ensure proper assembly alignment. The consequences of this more limited misalignment, shown in Figure 34 and Table 31, are significantly less, but the  $k_{\text{eff}}$  increase is still over 6%  $\Delta k_{\text{eff}}$ . The limiting condition for both the maximum and limited misalignment is for fuel with 35 GWd/MTU burnup and 5 years of cooling time. The limited misalignment case is illustrated in Figure 34. Misalignment toward the bottom of the cask causes a significantly smaller  $k_{\text{eff}}$  increase because the fuel at the bottom end of the assembly has lower reactivity. The misalignment toward the cask base plate also differs for the MPC-68 compared to the GBC-32. The MPC-68 model has more distance below the fuel, so larger misalignments are possible. The neutron absorber in the MPC-68 extends below the bottom of the fuel; this difference acts to increase the displacement distance for which no significant change in  $k_{\text{eff}}$  occurs. The variation of the  $k_{\text{eff}}$  changes as a function of axial position is shown in Figure 35 for fuel with 35 GWd/MTU burnup and 5 years of cooling time.

**Table 31. Increase in  $k_{\text{eff}}$  caused by loss of assembly position control in MPC-68**

Burnup (GWd/MTU)	Cooling time (years)	Channel	Increase in $k_{\text{eff}}$ (% $\Delta k_{\text{eff}}$ )
<b>Maximum displacement (33.78 cm displacement relative to basket)</b>			
0	0	Yes	8.18
35	5	Yes	19.40
0	0	No	7.79
35	5	No	18.65
<b>Limited displacement (20 cm displacement relative to basket)</b>			
0	0	Yes	0.33
35	5	Yes	6.29
0	0	No	0.27
35	5	No	6.07

**Figure 34. Limited axial misalignment of 20 cm toward cask lid.**

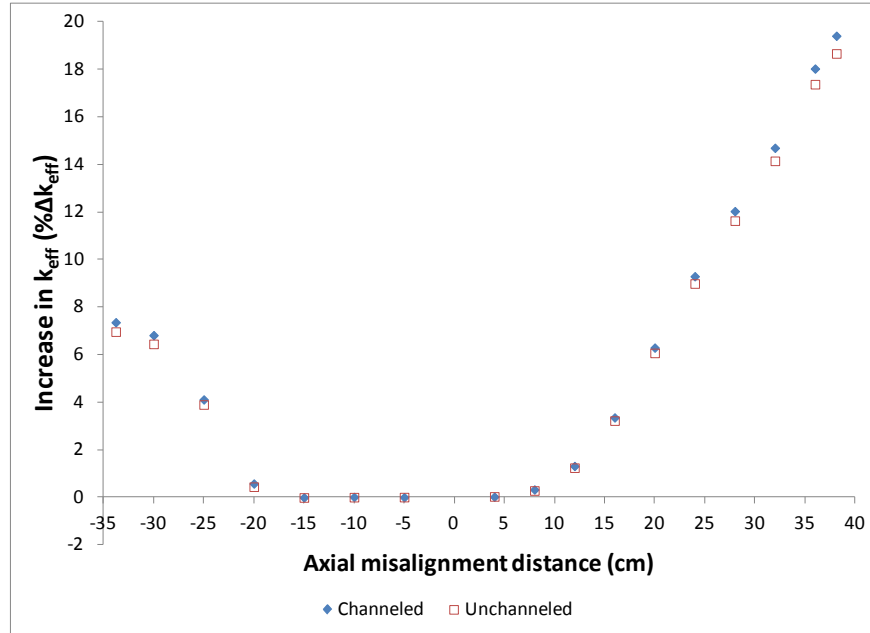


**Figure 35. Increase in  $k_{\text{eff}}$  in MPC-68 as a function of assembly axial displacement (35 GWd/MTU burnup and 5-year cooling time).**

### 5.2.1.5 Gross Assembly Failure

The two gross assembly failure configurations described in Section 3.1.5 are investigated in the MPC-68 cask. Axial representations of the most reactive homogeneous rubble and ordered pellet array configurations are shown in Figure 36 and , respectively. In both cases, the limiting case is the non-physical condition in which the fissile material extends from the base plate to the lid. As expected, this configuration has the highest  $k_{\text{eff}}$  increase, with the ordered pellet array configuration being more limiting than the homogeneous rubble case. As shown previously in Table 25, the  $k_{\text{eff}}$  increase in the homogeneous rubble case is almost 30%  $\Delta k_{\text{eff}}$ , and the pellet array case increases  $k_{\text{eff}}$  by over 34%  $\Delta k_{\text{eff}}$  for the maximum increase case. The limiting case for both configurations is with fuel at 35 GWd/MTU burnup and a 5-year cooling time. The results for the maximum  $k_{\text{eff}}$  increase homogeneous configuration for both fuel burnups with and without the fuel channel are presented in Table 32 and for the pellet array case for both fuel burnups in Table 33. The pellet array case was only considered without the fuel assembly channel. If the fissile material is maintained within the poison panel elevations, the resulting change in  $k_{\text{eff}}$  is reduced to 17.21%  $\Delta k_{\text{eff}}$  for the ordered array of pellets. Results for a range of homogeneous rubble cases within the neutron absorber elevations are provided in Table 34. The largest increase in  $k_{\text{eff}}$  for this configuration corresponds to fresh 5 w/o fuel. The results with fissile material restrained in the neutron absorber elevations demonstrate that these cases result in significantly lower  $k_{\text{eff}}$  increases than the unrestrained material cases.

The results for the pellet array case are significantly higher than those reported previously in Ref. 7. There are two differences between that analysis and this one, both of which contribute to the increased magnitude of the  $k_{\text{eff}}$  increase in the work presented here. The pellet array case modeled here includes a distributed burnup profile in the pellet array, and the array is allowed to extend beyond the neutron absorber panel elevations. This latter change is the larger of the two effects, but the former change is also important. The homogeneous rubble case is not included in Ref. 7.

**Table 32. Increase in  $k_{\text{eff}}$  for homogeneous rubble configuration of gross fuel assembly failure in MPC-68**

Burnup (GWd/MTU)	Cooling time (years)	Channel	Maximum increase in $k_{\text{eff}}$ (% $\Delta k_{\text{eff}}$ )
0	0	Yes	21.68
35	5		28.58
0	0	No	22.90
35	5		29.36

**Table 33. Increase in  $k_{\text{eff}}$  for pellet array configuration of gross fuel assembly failure in MPC-68**

Burnup (GWd/MTU)	Cooling time (years)	Maximum increase in $k_{\text{eff}}$ (% $\Delta k_{\text{eff}}$ )
<b>Channel removed</b>		
0	0	28.12
35	5	34.40

**Table 34. Increase in  $k_{\text{eff}}$  in MPC-68 due to homogeneous rubble, debris within absorber Elevations, fresh 5 w/o fuel**

Fraction of nominal assembly height	Increase in $k_{\text{eff}}$ (% $\Delta k_{\text{eff}}$ )	
	Channeled	Unchanneled
1.0	7.40	9.49
0.9	6.65	9.12
0.8	5.06	8.10
0.7	2.30	6.16
0.6	-2.57	2.66
0.5	-11.07	-3.62
0.4	-25.64	-15.10
Fully compressed rubble*	-34.23	-31.44

\*The fraction of nominal assembly height varies for fully compressed rubble with and without the channel. With the channel it is approximately 0.36 with the channel and 0.32 without it.

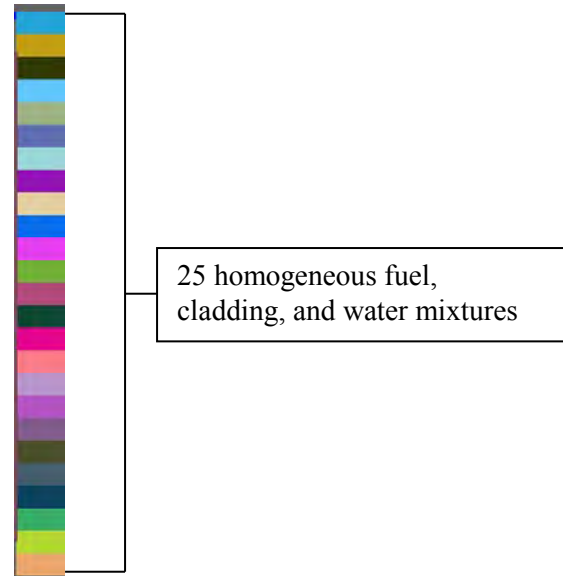


**Figure 36.** Limiting homogeneous rubble configuration in MPC-68.

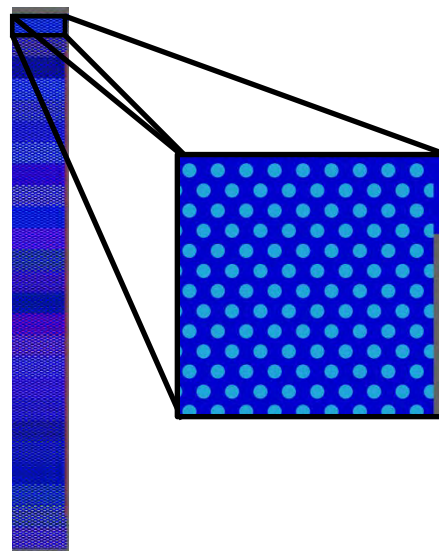


**Figure 37.** Limiting ordered pellet array configuration for MPC-68.

### 5.2.1.6 Neutron Absorber Degradation

The results of the calculations, described in Section 3.1.6.1, considering a 5-cm neutron absorber defect at varying elevations for both fuel burnups, both with and without the fuel channel, are presented in Table 35. The limiting condition is for fuel with 35 GWd/MTU burnup and 5 years of cooling time, with the fuel channel intact. As expected, the limiting elevation is near the top of the active fuel height, as shown in Figure 38. The results for the full range of elevations considered in the limiting fuel condition are presented in Table 36 for cases with the fuel channel intact. As expected, the limiting elevation for the fresh 5 w/o fuel is located at the centerline. The largest  $k_{\text{eff}}$  increase observed for this configuration is 2.49%  $\Delta k_{\text{eff}}$  and increases to 5.62%  $\Delta k_{\text{eff}}$  if the defect size is increased to 10 cm. As discussed in

Section 3, these defects are assumed to be present at the same elevation in all neutron absorber panels within the cask.

The increase in  $k_{\text{eff}}$  associated with uniform neutron absorber panel thinning as discussed in Section 3.1.6.3 is shown in Table 37 and Figure 39 with fresh 5 w/o fuel modeled in the MPC-68 cask. The absorber thinning results shown in Appendix C confirm that the fresh fuel case is most limiting. As shown previously in Table 25, a 50% reduction in thickness results in a 3.67%  $\Delta k_{\text{eff}}$  increase. Complete neutron absorber panel removal increases  $k_{\text{eff}}$  by almost 22%  $\Delta k_{\text{eff}}$ , but more than 40% of the thickness must be removed before an increase of more than 3%  $\Delta k_{\text{eff}}$  is realized.

The complete removal of the neutron absorber panels causes a larger increase in  $k_{\text{eff}}$  than the maximum axial displacement case discussed in Section 5.2.1.4, a result which differs from that observed for the GBC-32 cask presented in Section 5.1. The MPC-68 cask has a smaller distance between the top of the fuel storage basket and the cask lid, allowing for only a shorter portion of the assembly to be above the basket walls. The MPC-68 also has a higher nominal neutron absorber loading, resulting in a larger increase in  $k_{\text{eff}}$  when all the absorber is removed. These two differences in cask design cause the relative consequence of the two configurations to be different for the MPC-68 compared to the GBC-32.

**Table 35. Maximum  $k_{\text{eff}}$  increase caused by a 5-cm neutron absorber defect in MPC-68**

Burnup (GWd/MTU)	Cooling time (years)	Defect center elevation (cm)	Channel	Maximum increase in $k_{\text{eff}}$ (% $\Delta k_{\text{eff}}$ )
0	0	190.50	Yes	0.83
35	5	365.13		2.49
0	0	190.50	No	0.77
35	5	365.13		2.41

**Table 36. Increase in  $k_{\text{eff}}$  caused by a 5-cm neutron absorber defect at various elevations in MPC-68  
(35 GWd/MTU burnup and 5-year cooling time)**

Defect center elevation (cm)	Increase in $k_{\text{eff}}$ (% $\Delta k_{\text{eff}}$ )
0.00	-0.02
95.25	-0.01
190.50	0.00
285.75	0.01
317.50	0.21
333.38	0.52
349.25	1.43
354.54	1.83
359.83	2.29
365.13	2.49
370.42	2.39
375.71	2.00
381.00	0.69

**Table 37. Increase in  $k_{\text{eff}}$  in MPC-68 caused by uniform neutron absorber panel thinning, fresh 5 w/o fuel**

Fraction of neutron absorber panel thickness remaining	Increase in $k_{\text{eff}}$ (% $\Delta k_{\text{eff}}$ )
0.9	0.59
0.8	1.21
0.7	1.91
0.6	2.72
0.5	3.67
0.4	4.87
0.3	6.35
0.2	8.49
0.1	11.93
0.0	21.84

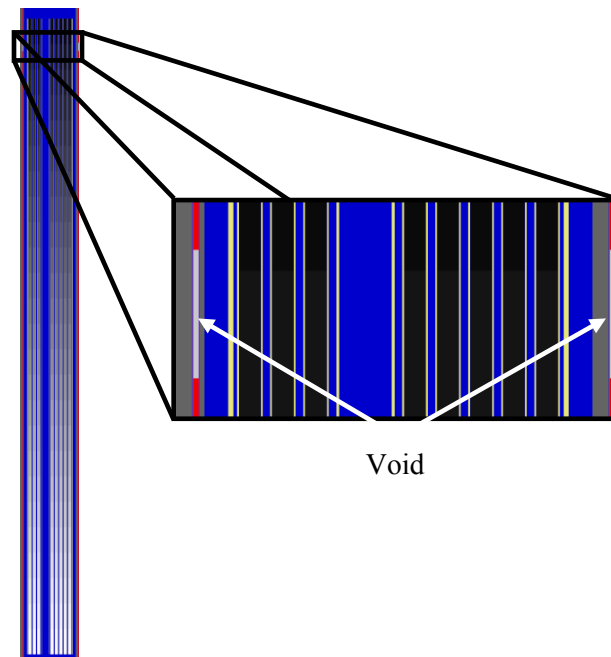


**Figure 38. Limiting neutron absorber defect configuration in MPC-68.**

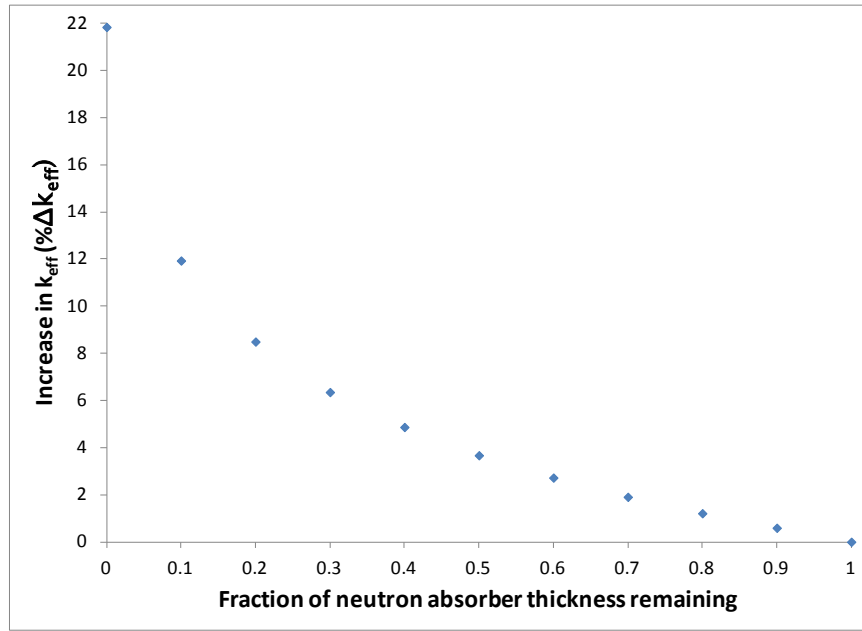


**Figure 39. Increase in  $k_{\text{eff}}$  in MPC-68 as a function of remaining neutron absorber panel thickness for fresh 5 w/o fuel.**

### 5.2.1.7 Burnup and Cooling Time Sensitivities

The results of sensitivity studies relating to addition burnup and cooling time are presented in Appendix C (Section C.2). Each configuration discussed in the previous six subsections is considered explicitly. The results of the calculations for additional burnup and cooling time conditions indicate that the increase in  $k_{\text{eff}}$  reported for each configuration encompass changes that may result for additional burnups and cooling times. That is, the differences in the change in  $k_{\text{eff}}$  are smaller than the changes in the base case  $k_{\text{eff}}$  caused by the additional burnup and/or cooling time considered. For the axial displacement configuration, a high-burnup and cooling time condition causes a larger increase in  $k_{\text{eff}}$ , but that case is significantly subcritical and therefore can be excluded from the results considered here.

### 5.2.2 Varying Number of Reconfigured Assemblies

The results presented in Section 5.2.1 and Table 25 assume that all 68 fuel assemblies in the MPC-68 cask experience the same fuel or neutron absorber reconfiguration within the respective configuration of interest. As discussed in Section 3.2, a series of calculations is performed to establish the  $k_{\text{eff}}$  increase as a function of the number of reconfigured assemblies within the cask. The four configurations considered are the limiting conditions for single rod failure, multiple rod failure, uniform rod pitch increase, and homogeneous rubble resulting from gross assembly failure.

The first fuel assembly to experience the reconfiguration being examined is selected in an attempt to maximize the  $k_{\text{eff}}$  increase, and is therefore one near the center of the cask. Additional assemblies are added in mostly symmetric groups of equal distance from the first reconfigured assembly. For some low numbers of reconfigured assemblies, multiple combinations of assemblies are considered. Sixteen combinations of reconfigured assemblies are considered in the MPC-68. One order in which the assemblies experience reconfiguration is shown in Figure 40. Results are presented in the following subsections.

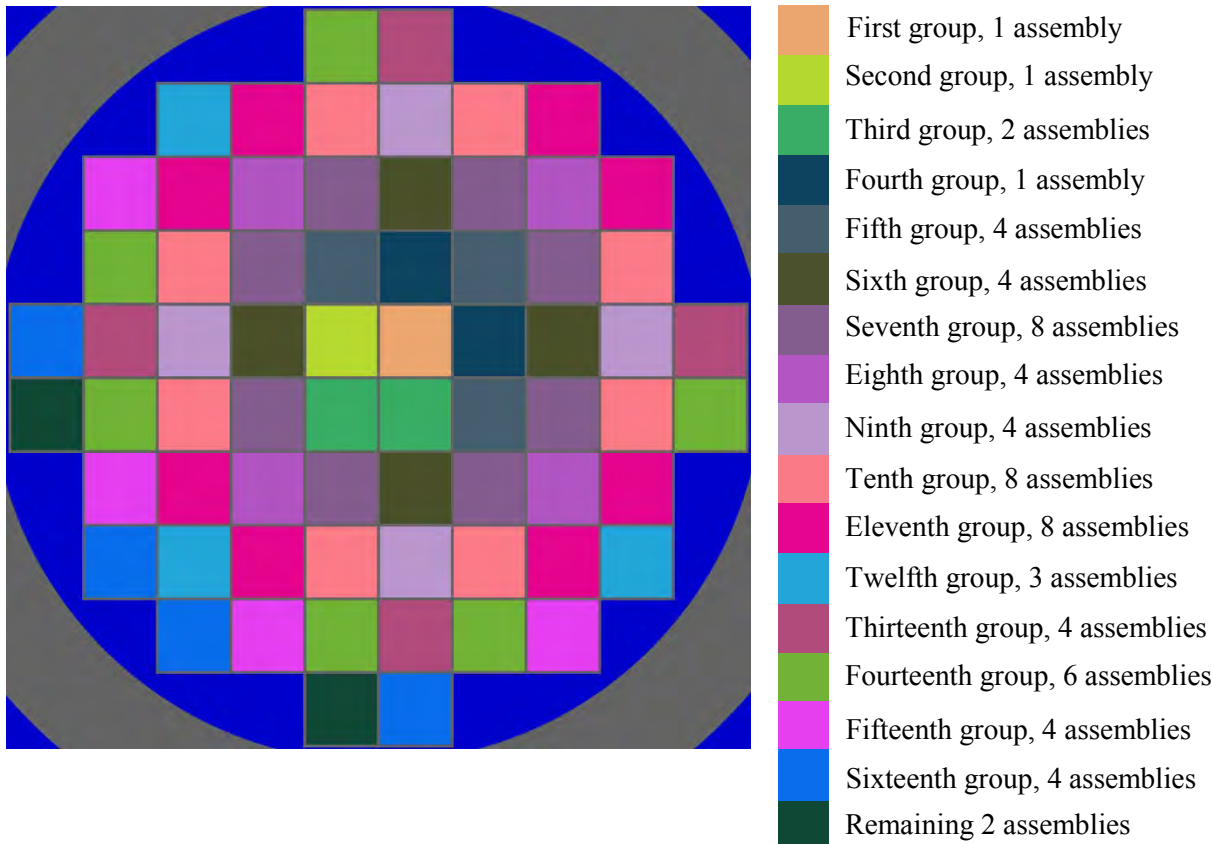


Figure 40. One order of assembly reconfiguration in MPC-68 partial degradation configurations.

### 5.2.2.1 Rod Failures

The single and multiple rod failure configurations that result in the largest increase in  $k_{\text{eff}}$ , as discussed in Section 5.2.1.2, are used to study the impact of some assemblies suffering reconfiguration while others in the cask remain intact. The single rod failure configurations are based on fresh 5 w/o fuel, while the multiple rod failure configurations are based on fuel depleted to 35 GWd/MTU and 5 years of cooling time. The fuel channel is modeled as intact for both rod failure configurations. The results for single rod failure are shown below in Table 38 and Figure 41. The results for multiple rod failure are shown below in Table 39 and Figure 42. The portion of the  $k_{\text{eff}}$  impact introduced by each group of assemblies for both rod failure configurations show nearly 50% or more of the  $k_{\text{eff}}$  change coming after 13 assemblies experience reconfiguration and approximately 75% to 80% of the  $k_{\text{eff}}$  change caused by the first 29 assembly reconfigurations. The Monte Carlo uncertainty is relatively large compared to the  $k_{\text{eff}}$  changes being examined in this series of calculations because of the relative insensitivity of the cask  $k_{\text{eff}}$  to single rod failures. The resulting  $k_{\text{eff}}$  increase is therefore not a smooth function. The single rod failure results are generally similar to the GBC-32 results presented in Section 5.1.2.1. The rate of increase in  $k_{\text{eff}}$  seems to be slightly slower for the MPC-68, but this is a relatively small difference in the trend and may be related to the relatively large uncertainties in the results compared to the  $k_{\text{eff}}$  changes being examined. The multiple rod failure results for the MPC-68 are very similar to the GBC-32 results. The results indicate that a reduced number of reconfigured assemblies will not significantly reduce the  $k_{\text{eff}}$  increase associated with fuel reconfiguration if the degraded assemblies are in close proximity, and particularly if they are in the center region of the cask.

**Table 38. Increase in  $k_{\text{eff}}$  in MPC-68, single rod failure fresh 5 w/o fuel**

Number of degraded assemblies	Increase in $k_{\text{eff}}$ (% $\Delta k_{\text{eff}}$ )
1	0.02
2	0.04
2	0.05
4	0.06
5	0.07
9	0.10
13	0.15
21	0.20
25	0.19
29	0.21
37	0.23
45	0.27
48	0.25
52	0.27
58	0.27
62	0.27
66	0.28
68	0.29

**Table 39. Increase in  $k_{\text{eff}}$  in MPC-68, multiple rod failure  
(5 w/o initial enrichment, 35 GWd/MTU burnup)**

Number of degraded assemblies	Increase in $k_{\text{eff}}$ (% $\Delta k_{\text{eff}}$ )
1	0.11
2	0.21
2	0.23
4	0.45
5	0.56
5	0.55
9	0.93
13	1.19
21	1.62
25	1.79
29	1.89
37	2.10
45	2.22
48	2.26
52	2.28
58	2.33
62	2.36
66	2.37
68	2.40

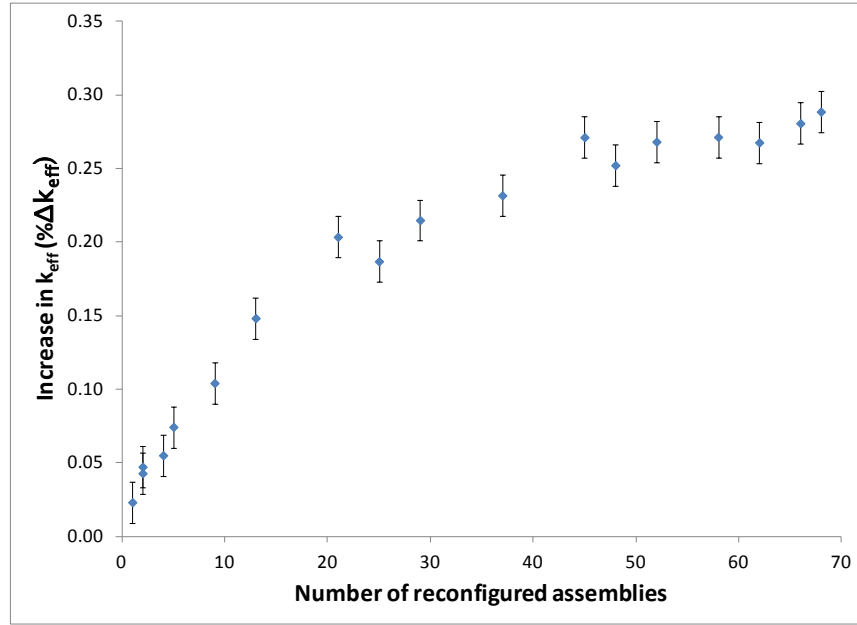


**Figure 41.** Increase in  $k_{\text{eff}}$  in MPC-68 as a function of number of reconfigured assemblies, single rod failure for fresh 5 w/o fuel.

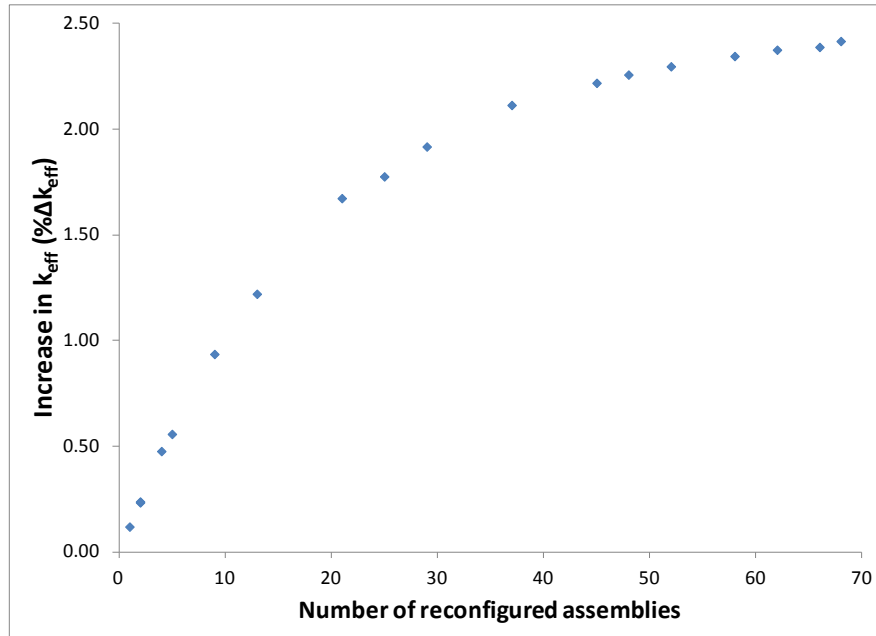


**Figure 42.** Increase in  $k_{\text{eff}}$  in MPC-68 as a function of number of reconfigured assemblies, multiple rod failure (35 GWd/MTU burnup and 5-year cooling time).

### 5.2.2.2 Loss of Rod Pitch Control, Uniform Pitch Increase

The maximum uniform pitch increase case is used to examine the  $k_{\text{eff}}$  impact of varying the number of assemblies that have experienced reconfiguration. The assembly configuration used for this study models

the outer row of fuel rods in contact with the inner wall of the fuel storage basket in each cell. The fresh 5 w/o fuel composition is used for all assemblies. The increase in  $k_{\text{eff}}$  for each number of reconfigured assemblies is provided in Table 40 as well as Figure 43. More than 75% of the increase in  $k_{\text{eff}}$  is caused by the first 21 reconfigured assemblies. The general trend in the  $k_{\text{eff}}$  change for the uniform pitch increase cases is similar to that for single and multiple rod failure configurations presented in Section 5.2.2.1. More than 50% of the total increase in  $k_{\text{eff}}$  has occurred with 13 reconfigured assemblies. The shape of the increase in  $k_{\text{eff}}$  as a function of reconfigured assemblies is similar to that seen for the uniform pitch increase configurations in the GBC-32 cask, as discussed in Section 5.1.2.2. The fraction of the  $k_{\text{eff}}$  increase introduced for a given fraction of reconfigured assemblies is slightly higher for the MPC-68 than for GBC-32 between about 10% and 70% of the assemblies experiencing reconfiguration. The results indicate that a reduced number of reconfigured assemblies will not significantly reduce the  $k_{\text{eff}}$  increase associated with fuel reconfiguration if the degraded assemblies are in close proximity, and particularly if they are in the center region of the cask.

**Table 40. Increase in  $k_{\text{eff}}$  in MPC-68, uniform pitch increase fresh 5 w/o fuel**

Number of degraded assemblies	Increase in $k_{\text{eff}}$ (% $\Delta k_{\text{eff}}$ )
1	0.64
2	1.46
2	1.37
4	3.29
5	3.93
5	3.85
9	6.45
13	7.85
21	10.05
25	10.59
29	11.02
37	11.85
45	12.36
48	12.46
52	12.61
58	12.87
62	13.03
66	13.13
68	13.16

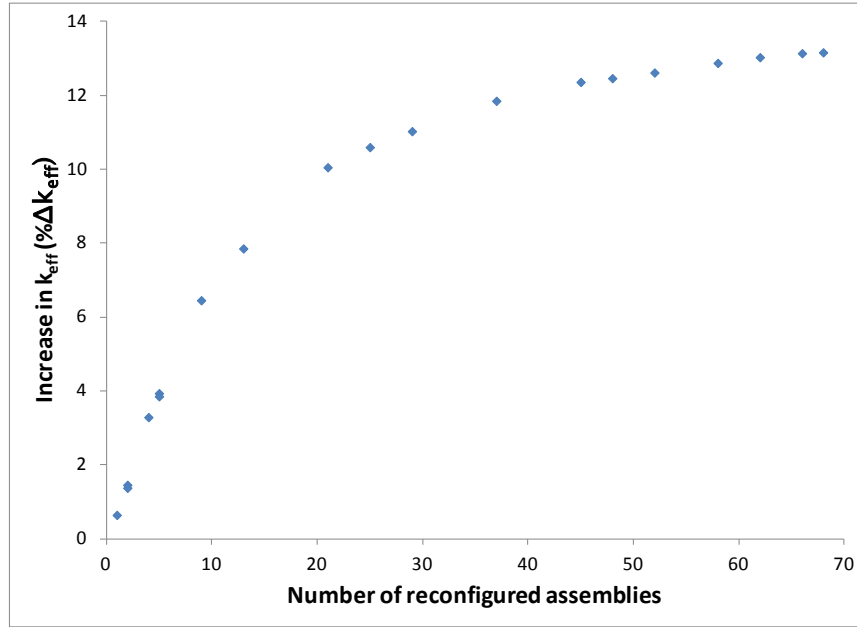


**Figure 43. Increase in  $k_{\text{eff}}$  in MPC-68 as a function of number of reconfigured assemblies, uniform pitch increase fresh 5 w/o fuel.**

### 5.2.2.3 Gross Assembly Failure, Homogeneous Rubble

The homogeneous rubble modeling of the gross assembly failure configuration is the final configuration used to examine the  $k_{\text{eff}}$  impact of varying the number of assemblies that have experienced reconfiguration. The configuration used for this study fills the entire inside volume of the storage cell with homogeneous rubble, as described in Section 3.1.5.1. Each zone is approximately 18 cm tall; thus, the 25 zones fill the cask from the base plate to the lid. The fuel composition corresponds to 5 w/o fuel depleted to 35 GWd/MTU. This configuration resulted in the largest  $k_{\text{eff}}$  increase of the homogeneous rubble configurations used in Section 5.2.1.5. The increase in  $k_{\text{eff}}$  for each number of reconfigured assemblies is provided in Table 41 as well as Figure 44. The first two reconfigured assemblies cause a smaller increase in  $k_{\text{eff}}$  than the other configurations. A more significant increase in  $k_{\text{eff}}$  is noted for four or more reconfigured assemblies. More than 50% of the increase is caused by the first nine reconfigured assemblies, and more than 80% of the total  $k_{\text{eff}}$  increase results from the reconfiguration of 21 assemblies. The results indicate that a reduced number of reconfigured assemblies will not significantly reduce the  $k_{\text{eff}}$  increase associated with fuel reconfiguration if the degraded assemblies are in close proximity, and particularly if they are in the center region of the cask.

**Table 41. Increase in  $k_{\text{eff}}$ , homogeneous rubble configuration of gross assembly failure**

Number of degraded assemblies	Increase in $k_{\text{eff}}$ (% $\Delta k_{\text{eff}}$ )
1	0.03
2	0.10
4	4.48
5	5.04
9	15.67
13	18.60
21	23.73
25	24.78
29	25.42
37	27.05
45	27.97
48	28.14
52	28.35
58	28.82
62	29.10
66	29.26
68	29.36

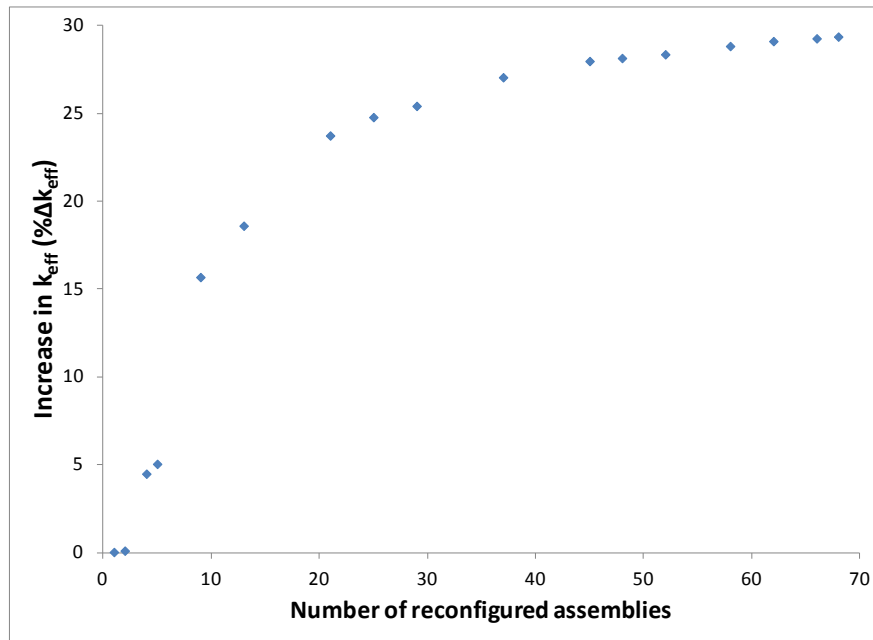


**Figure 44. Increase in  $k_{\text{eff}}$  as a function of number of reconfigured assemblies, gross assembly failure (35 GWd/MTU burnup and 5-year cooling time).**

### Random Assembly Reconfiguration

A series of 25 calculations is performed in which four assemblies are randomly selected to experience reconfiguration into the limiting homogeneous rubble configuration. These calculations use fuel

compositions for fuel with a burnup of 70 GWd/MTU and 300-year cooling time. These compositions are used in the sensitivity studies for higher burnup and cooling times and lead to the largest increase in  $k_{\text{eff}}$  for all burnup and cooling time combinations considered. The increase in  $k_{\text{eff}}$  for four reconfigured assemblies in the center of the cask is 6.95%  $\Delta k_{\text{eff}}$ . The use of four assemblies is somewhat arbitrary but is selected because the increase in  $k_{\text{eff}}$  is significant. The increase in  $k_{\text{eff}}$  for each randomly generated case is provided in Table 42. A histogram of the results with a superimposed normal distribution is shown in Figure 45. While some deviations from the ideal normal distribution are evident, the set of  $k_{\text{eff}}$  increases tests as normal with a 10 bin chi-squared normality test.

The average change in  $k_{\text{eff}}$  is a reduction of about 0.20%  $\Delta k_{\text{eff}}$ , and the standard deviation is approximately 0.25%  $\Delta k_{\text{eff}}$ . The largest increase in  $k_{\text{eff}}$  is 0.14  $\Delta k_{\text{eff}}$ . The one-sided tolerance factor for 95% probability of a 95% confidence interval assuming a normal distribution of 25 samples is 2.292, from Ref. 49. The 95/95 upper bound for the reactivity increase for four random assemblies is 0.37%. This represents a significant reduction in the  $k_{\text{eff}}$  impact compared to the bounding condition of four reconfigured assemblies in the center of the cask. These results are based on only a cursory examination of the effects of random assembly selection, but the results indicate a significant reduction in the  $k_{\text{eff}}$  if the reconfigured assemblies are randomly distributed in the cask.

Random sampling of degraded assemblies will not be valid if assembly degradation is not random. Factors such as environment during ES, assembly burnup and fluence, or other relevant parameters could be highly correlated, invalidating a random sampling approach. The difference between random sampling and deterministic selection of assembly locations will be reduced with a larger number of reconfigured assemblies. More study is needed to examine the validity of random sampling as an alternative to deterministic selection to reduce the impact of fuel reconfiguration on  $k_{\text{eff}}$ .

**Table 42. Increase in  $k_{\text{eff}}$  for 25 realizations of four randomly selected reconfigured assemblies**

Increase in $k_{\text{eff}}$ (% $\Delta k_{\text{eff}}$ )				
-0.02	0.14	-0.04	0.13	-0.33
-0.19	0.09	-0.29	-0.13	-0.19
0.04	-0.75	-0.47	-0.66	-0.38
-0.06	-0.23	-0.19	-0.02	-0.22
-0.01	-0.03	-0.73	-0.13	-0.37

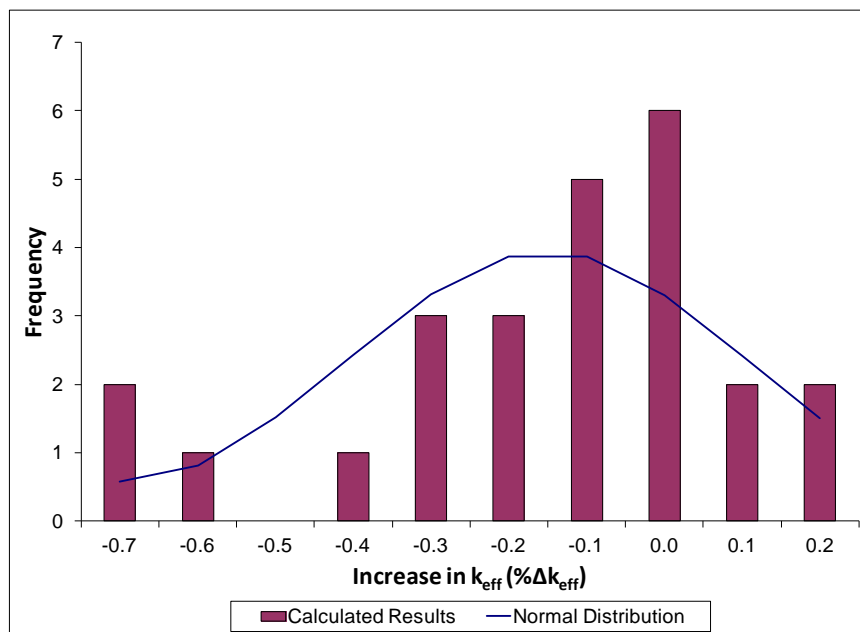


**Figure 45. Histogram of increases in  $k_{\text{eff}}$  for 25 random samples of four reconfigured assemblies.**

### 5.2.3 Combined Configurations

As discussed in Section 3.3, some of the mechanisms that could result in fuel reconfigurations could result in a combination of configurations. Therefore, selected combined configurations are evaluated, including: four failed rods with 50% clad thinning and four failed rods with a uniform pitch increase of 0.062-cm. These combinations of configurations are selected as they both pertain to failure of zirconium alloy components of the fuel assembly. Both combined configurations assume fresh 5 w/o fuel and an intact fuel assembly channel.

The multiple rod failure results presented in Section 5.2.1.2 indicate that the failure of four fuel rods results in an increase in  $k_{\text{eff}}$  of just under 1%  $\Delta k_{\text{eff}}$ . This is approximately 40% of the maximum increase for multiple failed rod configurations and is therefore selected as an intermediate configuration. The cladding thickness on all intact rods in both combined configurations is represented with 50% of the nominal thickness. The pitch increase of 0.062 cm is approximately 4.3%  $\Delta k_{\text{eff}}$ . This represents about one-third of the maximum  $k_{\text{eff}}$  increase associated with the uniform pitch expansion.

The results of the two combined configurations considered in the MPC-68 cask are presented in Table 43. For comparison, the  $k_{\text{eff}}$  increases assuming each degraded configuration separately and the sum of the two is provided. The increase in  $k_{\text{eff}}$  associated with explicit modeling of the combined configuration is less than the estimated increase based on summing the individual increases. The conservatism of adding the separate effects is 0.25%  $\Delta k_{\text{eff}}$  or less. It appears that the linear combination of the  $k_{\text{eff}}$  increases is conservative, but more combined configurations would need to be investigated prior to drawing general conclusions. If it is confirmed, the  $k_{\text{eff}}$  increase caused by combinations of degradations could be conservatively bounded by adding the increase associated with individual configurations where applicable.

**Table 43. Increase in  $k_{\text{eff}}$  in combined configurations in MPC-68**

Case	Increase in $k_{\text{eff}}$ (% $\Delta k_{\text{eff}}$ )
<b>Multiple failed rods and clad thinning</b>	
Four failed rods	0.98
50% clad thinning	2.69
Sum of $k_{\text{eff}}$ increases	3.67
Combined configuration model	3.75
Overestimation of $k_{\text{eff}}$ increase by summing individual effects	0.08
<b>Multiple failed rods and 0.062-cm increase in fuel rod pitch</b>	
Four failed rods	0.98
Uniform pitch increase	4.35
Sum of $k_{\text{eff}}$ increases	5.33
Combined configuration model	5.08
Overestimation of $k_{\text{eff}}$ increase by summing individual effects	0.25

#### 5.2.4 Part-Length Fuel

Part-length rods are common in BWR assembly designs, including the GE14 design, making an investigation of the impact of part-length rods prudent as a part of these analyses. A total of 14 of the 92 rods are modeled as part-length, and more details of the modeling are provided in Appendix A. Only fresh 5 w/o fuel is considered for the part-length rod studies because no axial burnup profiles are available for fuel assemblies with part-length rods. The removal of some of the fuel in the upper portion of the assembly might cause a more bottom-skewed power shape, but the remaining sparser lattice will likely be more reactive. The axial power shape could therefore also be about the same or even more top-skewed than that developed in Appendix E. Given the unknown relative impact of these effects, depleted fuel is not considered in this study.

Most of the degraded fuel and neutron absorber panel configurations are considered for part-length fuel, though not all. The multiple rod failure study is shortened with the results compared to the full-length results presented in Section 5.2.1.2, and the pellet array configuration of gross assembly failure is not considered at all. Other calculations, such as the axial misalignment configuration, are reduced to the conditions shown to be limiting for full-length fuel in Section 5.2.1. The results of the nominal cases without reconfiguration are shown in Table 44. It should be noted that the base case  $k_{\text{eff}}$  values for the fuel with part-length rods are approximately 0.7%  $\Delta k_{\text{eff}}$  higher than the full-length rod base case. The additional moderation introduced in the upper portion of the assembly by the removal of the upper sections of the part-length rods is responsible for this increase in  $k_{\text{eff}}$ , and this in itself is a significant result. Only assemblies with full-length fuel rods were used in the analysis documented in Ref. 7. The use of part-length rods is thus another area of expansion over the previous work.

A summary of the  $k_{\text{eff}}$  impact of the configurations modeled with fresh fuel with part-length rods is shown in Table 45. These results can be compared with those shown in Table 25 to demonstrate the relative impact of reconfiguration for assemblies with part-length rods. In general, it appears that the part-length rods reduce the impact of reconfiguration. This result makes sense as the removal of some fissile material will move the moderator-to-fuel ratio closer to optimum in the base configuration. The neutron absorber defect and limited axial misalignment cases are the only configurations that cause a larger increase in  $k_{\text{eff}}$  than the full-length assembly. Additional details of the modeling of each configuration using assemblies with part-length fuel rods are included in the following subsections. No calculations are performed for a

varying number of reconfigured assemblies, multiple configurations, or combinations of full-length and part-length assemblies.

**Table 44. Nominal  $k_{\text{eff}}$  results for fresh 5 w/o fuel assemblies with part-length rods in MPC-68**

Channel present	Burnup (GWd/MTU)	Cooling time (years)	KENO V.a		KENO-VI	
			$k_{\text{eff}}$	$\sigma$	$k_{\text{eff}}$	$\sigma$
Yes	0	0	0.97497	0.00010	0.97482	0.00019
No	0	0	0.97391	0.00010	0.97396	0.00010

**Table 45. Summary of  $k_{\text{eff}}$  impact for fresh 5 w/o fuel with part-length rods in MPC-68**

Configuration	Reactivity consequence (% $\Delta k_{\text{eff}}$ )	Channel present
<b>Clad thinning/loss</b>		
Cladding removal	4.16	Yes
<b>Rod failures</b>		
Single rod removal	0.18	Yes
Multiple rod removal (2 rods removed)	0.32	Yes
<b>Loss of rod pitch control</b>		
Uniform rod pitch expansion, clad	12.28	No
Uniform rod pitch expansion, unclad	N/C*	N/A
Non-uniform pitch expansion, clad	N/C*	N/A
Channel constrained uniform expansion, clad	N/C*	N/A
<b>Loss of assembly position control</b>		
Axial displacement (30 cm)	6.17	Yes
Axial displacement (20 cm)	0.56	Yes
<b>Gross assembly failure</b>		
Uniform pellet array	N/C*	N/A
Homogeneous rubble	21.96	No
<b>Neutron absorber degradation</b>		
Missing neutron absorber (5-cm segment)	1.01	Yes
Missing neutron absorber (10-cm segment)	2.92	Yes
50% reduction of neutron absorber panel thickness	3.49	Yes

\*Not calculated

#### 5.2.4.1 Clad Thinning/Loss

The loss of cladding configuration is modeled as discussed above in Section 3.1.1. As shown in Table 46, the limiting  $k_{\text{eff}}$  increase associated with complete cladding removal is 4.16%  $\Delta k_{\text{eff}}$  and occurs with channelled fuel. The increase in  $k_{\text{eff}}$  as a function of the fraction of nominal cladding thickness remaining is also shown in Table 46 as well as in Figure 46. The results are consistently smaller increases in  $k_{\text{eff}}$  than those presented in Section 5.2.1.1. The increase in  $k_{\text{eff}}$  caused by the complete loss of cladding for full-length fuel is larger than the difference in the base case  $k_{\text{eff}}$  values presented in Table 24 and Table 44. The actual  $k_{\text{eff}}$  value is therefore larger in the case of full-length fuel with reconfiguration than for part-length fuel.

**Table 46. Increase in  $k_{\text{eff}}$  in MPC-68 caused by cladding loss for assemblies with part-length fuel rods, fresh 5 w/o fuel**

Cladding fraction remaining	Increase in $k_{\text{eff}}$ (% $\Delta k_{\text{eff}}$ )
<b>Channel Intact</b>	
0.9	0.43
0.75	1.09
0.5	2.10
0.25	3.12
0.0	4.16
<b>Channel Removed</b>	
0.9	0.42
0.75	1.03
0.5	2.05
0.25	3.04
0.0	3.98

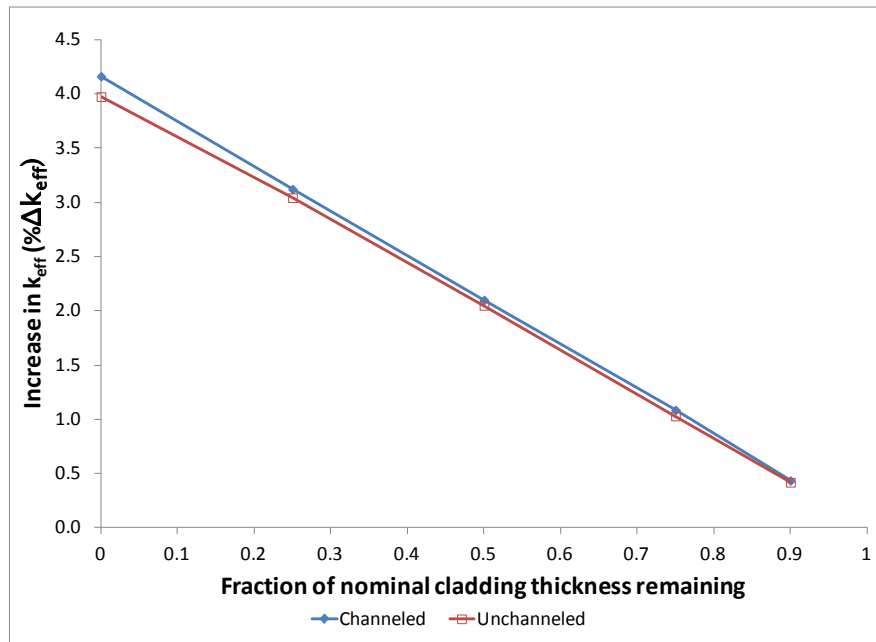


**Figure 46. Increase in  $k_{\text{eff}}$  in MPC-68 as a function of fraction of intact cladding (Fresh 5 w/o fuel with part-length fuel rods).**

#### 5.2.4.2 Rod Failures

Each of the 51 unique half-assembly symmetric rods is removed individually to determine its worth, as discussed in Section 3.1.2.1. Table 47 presents the rod locations and worth of the limiting rod location and the three additional locations that are within approximately two standard deviations of the limiting  $k_{\text{eff}}$  increase. Only channeled fuel is considered since it is shown to be limiting in Section 5.2.1.2. The increase in  $k_{\text{eff}}$  is 0.18%  $\Delta k_{\text{eff}}$ , which is less than the 0.29%  $\Delta k_{\text{eff}}$  increase for fuel with full-length rods. The maximum increase in  $k_{\text{eff}}$  is associated with the removal of rod E3. The location of the limiting rod

appears to have shifted from the location identified in Section 5.2.1.2. More precise calculations could be performed to confirm that the shift is real and not a statistical fluctuation.

The magnitude of the  $k_{\text{eff}}$  change caused by rod failure is somewhat less for fuel with part-length rods than for the full-length fuel used in Section 5.2.1.2. The likely cause of this reduced impact is that the removal of some of the rods in the upper section of the assembly creates a more thermal flux, and reduces the ability of a removed rod to increase thermalization. This is analogous to the reason that the channeled assemblies experience larger  $k_{\text{eff}}$  increases than unchanneled assemblies.

Two rods are removed in several pairs, as discussed in Section 3.1.2.2. The largest  $k_{\text{eff}}$  increase is 0.32%  $\Delta k_{\text{eff}}$ , which is less than the 0.52%  $\Delta k_{\text{eff}}$  increase caused by removing two rods from an assembly with full-length rods. The difference in  $k_{\text{eff}}$  increase is larger for two failed rods than for a single failed rod. This is an expected result since the impact of single rod failure is less for assemblies with part-length fuel than for assemblies with full-length fuel. No calculations are performed for larger numbers of failed rods as the result is likely to be progressively smaller increases in  $k_{\text{eff}}$  when compared with the results for full-length assemblies.

It should be noted that even though the increase in  $k_{\text{eff}}$  is larger for assemblies with full-length fuel, the actual  $k_{\text{eff}}$  for the cask is still higher in the part-length fuel rod case for the single and double rod failure configurations considered for fresh fuel. It is probable that the  $k_{\text{eff}}$  increase is large enough for higher numbers of failed rods that the full-length fuel becomes more limiting.

**Table 47. Increase in  $k_{\text{eff}}$  in MPC-68 caused by single rod failure in fresh 5 w/o assemblies with part-length rods**

Rod location	Increase in $k_{\text{eff}}$ (% $\Delta k_{\text{eff}}$ )
E3	0.18
D4	0.16
D3	0.15
H6	0.14

#### **5.2.4.3 Loss of Rod Pitch Control**

The loss of rod pitch control is modeled largely as described in Section 3.1.3, except that only unchanneled fuel is modeled. That larger pitch expansion resulting from the removal of the channel leads to a larger  $k_{\text{eff}}$  increase, as documented in Section 5.2.1.3. As shown in Table 45, the increase in  $k_{\text{eff}}$  for uniform pitch expansion with part-length rods is 12.28%  $\Delta k_{\text{eff}}$ . This is significantly less than the 13.16% for fuel assemblies with full-length rods. As with the rod failure results discussed in Section 5.2.1.3, the lower impact of loss of array control is most likely due to a more thermal neutron spectrum in the base case and the corresponding reduction in additional thermalization caused by the fuel reconfiguration. In this case, the larger increase in  $k_{\text{eff}}$  is sufficient to result in a larger reconfigured  $k_{\text{eff}}$  for full-length fuel assemblies.

#### **5.2.4.4 Loss of Assembly Position Control**

Assembly axial displacements are calculated for a range of upward displacements up to 30 cm, all with channeled fuel since it is shown to be more reactive than unchanneled fuel in Section 5.2.1.4. As shown in Table 45, the increases in  $k_{\text{eff}}$  caused by 30-cm and 20-cm displacements are 6.17%  $\Delta k_{\text{eff}}$  and 0.56%  $\Delta k_{\text{eff}}$ ,

respectively. The increase in  $k_{\text{eff}}$  associated with the 30-cm misalignment is smaller than that for fresh fuel with full-length fuel rods, but the increase for a 20-cm misalignment is larger for part-length fuel. Both of these increases are significantly non-limiting compared to the cases included in the results shown in Section 5.2.1.4. The impact of axial displacement is strongly influenced by the burnup profile in UNF, so this configuration with part-length rods and an appropriate axial burnup profile should be examined.

#### 5.2.4.5 Gross Assembly Failure

Only the homogeneous rubble configuration of gross assembly failure is modeled for fuel with part-length fuel rods. Only unchanneled fuel is considered because it is shown to be limiting in Section 5.2.1.5. The limiting configuration for gross assembly failure, as with results presented in Sections 5.1.1.5 and 5.2.1.5, is with the entire cask cavity volume filled with rubble. As shown in Table 45, the resulting  $k_{\text{eff}}$  increase is nearly 22%  $\Delta k_{\text{eff}}$ . The overall limiting increase in  $k_{\text{eff}}$  for the homogeneous rubble configuration occurs for UNF and is slightly less than 30%  $\Delta k_{\text{eff}}$ , as shown in Table 25. For fresh fuel, as shown in Table 32, the  $k_{\text{eff}}$  increase associated with the homogeneous rubble configuration is nearly 23%  $\Delta k_{\text{eff}}$ .

A second calculation with the entire cavity filled with rubble is performed to investigate the effect of separate homogenization for the upper portion of the assembly, with reduced fuel loading, and the lower portion of the assembly, with the entire assembly lattice containing fuel rods. The result of this calculation is a slightly smaller increase in  $k_{\text{eff}}$  of approximately 21.2%  $\Delta k_{\text{eff}}$ . The upper portion of the rubble bed, with reduced fuel loading, has a significantly higher volume fraction of water and is likely overmoderated.

#### 5.2.4.6 Neutron Absorber Degradation

The results of the calculations, described in Section 3.1.6.1, considering a 5-cm neutron absorber defect at varying elevations for fuel assemblies with part-length rods and an intact fuel channel are presented in Table 48 and Figure 47. The limiting condition is for the gap centered at an elevation of 270 cm above the bottom of the fuel. The removal of the upper portion of the part-length rods shifts the limiting elevation up relative to the mid-plane location which is limiting for full-length fresh fuel. As mentioned previously, the increased moderation within the assembly lattice results in the upper portion of the assembly being more reactive than the lower portion. This relative reactivity difference is the cause of the shift in the limiting neutron absorber gap location.

The largest  $k_{\text{eff}}$  increase observed for this configuration is 1.01%  $\Delta k_{\text{eff}}$  and increases to 2.92%  $\Delta k_{\text{eff}}$  if the defect size is increased to 10 cm. These results represent a larger increase in  $k_{\text{eff}}$  than for full-length fresh fuel but a smaller increase in  $k_{\text{eff}}$  than the limiting condition involving UNF discussed in Section 5.2.1.6. As discussed in Section 3, these defects are assumed to be present at the same elevation in all neutron absorber panels within the cask.

The increase in  $k_{\text{eff}}$  associated with uniform neutron absorber panel thinning as discussed in Section 3.1.6.3 is shown in Table 49 and Figure 48 with fresh 5 w/o fuel modeled in the MPC-68 cask. As shown in Table 45, a 50% reduction in panel thickness results in a 3.49% increase in  $k_{\text{eff}}$ . Complete neutron absorber panel removal increases  $k_{\text{eff}}$  by more than 21%  $\Delta k_{\text{eff}}$ , but more than 40% of the absorber must be removed before an increase of more than 3% is realized. These results are similar to those presented in Section 5.2.1.6, but the increases in  $k_{\text{eff}}$  are slightly smaller. The full-length fuel does not experience a great enough increase in  $k_{\text{eff}}$  for the resulting cask  $k_{\text{eff}}$  to exceed that for part-length fuel. This configuration is another example of the part-length fuel leading to a higher  $k_{\text{eff}}$  after reconfiguration despite having a smaller  $k_{\text{eff}}$  change because of the higher initial neutron multiplication.

**Table 48. Increase in  $k_{\text{eff}}$  in MPC-68 caused by a 5-cm neutron absorber panel defect, fresh 5 w/o fuel with part-length fuel rods**

Elevation of centerline of defect (cm above bottom of fuel)	Increase in $k_{\text{eff}}$ (% $\Delta k_{\text{eff}}$ )
2.50	-0.01
95.25	0.15
190.50	0.46
222.50	0.77
253.50	0.97
270.00	1.01
285.75	1.00
301.00	0.96
340.00	0.58
378.50	0.00

**Table 49. Increase in  $k_{\text{eff}}$  in MPC-68 caused by uniform neutron absorber panel thinning, fresh 5 w/o fuel with part-length fuel rods**

Fraction of neutron absorber panel thickness remaining	Increase in $k_{\text{eff}}$ (% $\Delta k_{\text{eff}}$ )
0.9	0.53
0.8	1.13
0.7	1.79
0.6	2.57
0.5	3.49
0.4	4.64
0.3	6.08
0.2	8.14
0.1	11.50
0.0	21.33

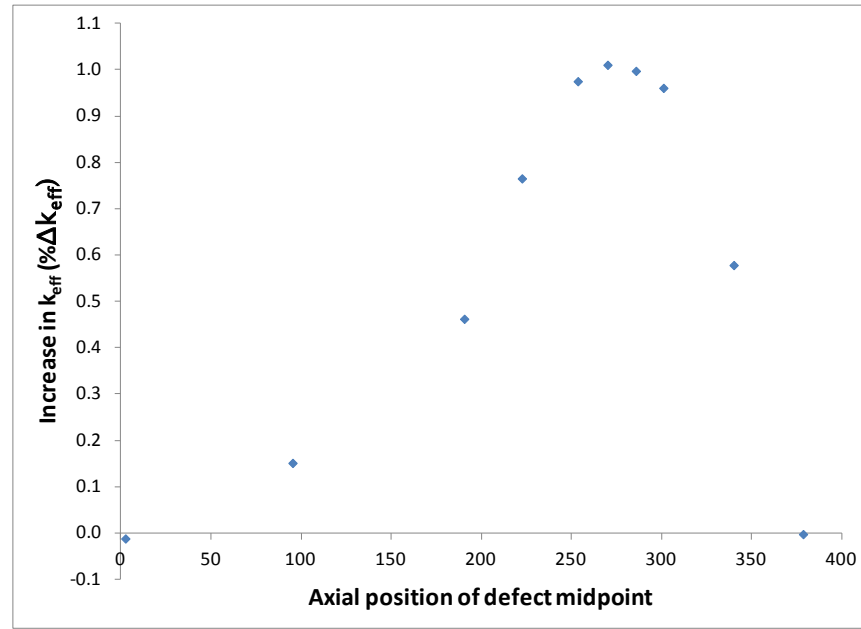


**Figure 47.** Increase in  $k_{\text{eff}}$  in MPC-68 as a function of neutron absorber defect axial position, fresh 5 w/o fuel with part-length fuel rods.

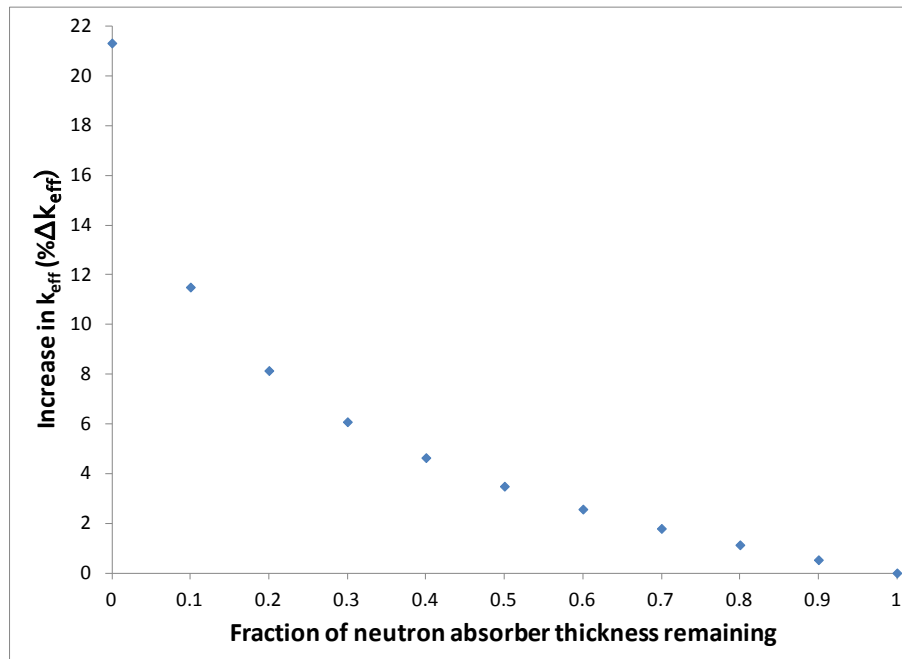


**Figure 48.** Increase in  $k_{\text{eff}}$  in MPC-68 as a function of remaining neutron absorber panel thickness, Fresh 5 w/o fuel with part-length fuel rods.

## 6. SUMMARY AND CONCLUSIONS

This report documents work performed for the DOE-NE Fuel Cycle Technologies Used Fuel Disposition Campaign to assess the consequences of potential fuel failure on the criticality safety of UNF in storage and transportation casks. This work was motivated by concerns related to the potential for fuel degradation during ES periods and transportation following ES, but has relevance to other potential causes of fuel reconfiguration.

Because many of the fuel degradation mechanisms are not well understood, a number of postulated configurations were modeled to calculate the corresponding  $k_{\text{eff}}$  values and the associated consequences of those configurations relative to the reference intact configuration. The consequence of a given configuration was defined as the difference in the calculated  $k_{\text{eff}}$  values for the given configuration and the reference intact configuration, with a positive value indicating an increase in  $k_{\text{eff}}$  as compared to the reference configuration. Because a wide range of configurations was analyzed, the calculated consequences varied widely. Several of the configurations are not considered credible but are included in the analyses for completeness (e.g., to fully understand trends and worst-case situations). Pending improved understanding of the various material degradation phenomena, and subsequent determination and justification for what configurations are and are not credible, the assessment of the credibility of configurations provided herein is based on engineering judgment. The credibility of configurations and the impact of the configurations on criticality safety are dependent on many factors, including storage and transportation conditions, the fuel assembly characteristics, and the storage and/or transportation system characteristics. Therefore, the assessment and analysis of credible configurations for a specific cask system would need to be performed as part of the safety analysis for licensing that system.

### 6.1 Summary of Analyses

The detailed results for each configuration considered in the PWR cask system (GBC-32) are provided in Section 5.1 and summarized in Table 6. For all the credible and non-credible configurations analyzed, the consequence on  $k_{\text{eff}}$  varied from a decrease of several percent (safer condition) to an increase of more than 20%  $\Delta k_{\text{eff}}$ . For configurations judged to be potentially credible, i.e., configurations for which the authors felt additional information was needed to determine credibility, the maximum increase in  $k_{\text{eff}}$  was 3.90%  $\Delta k_{\text{eff}}$ , corresponding to nonuniform fuel rod pitch expansion in all assemblies within the cask. It is important to emphasize that this result is contingent on the authors' judgment relative to the potential credibility of configurations, which includes not only whether a configuration category is credible but also whether the resulting configurations within a given category are credible for a specific cask system. For example, for the GBC-32 cask system, axial assembly displacement such that assemblies extended more than 7.5 cm above or below the neutron absorber panel was not considered credible because of the presence of fuel assembly hardware and cask assembly spacers. If it were determined that such a configuration is credible, then that configuration and its specific characteristics may be limiting.

The detailed results for each configuration considered in the BWR cask system (MPC-68) are provided in Section 5.2 and summarized in Table 25 and Table 45 for fuel assemblies with full- and part-length rods, respectively. For all the credible and non-credible configurations analyzed, the consequence on  $k_{\text{eff}}$  varied from a decrease of several percent (safer condition) to an increase of almost 36%  $\Delta k_{\text{eff}}$ . In most cases, the  $k_{\text{eff}}$  increases for BWR UNF in the MPC-68 were larger than for PWR UNF in the GBC-32. For configurations judged to be potentially credible, the maximum increase in  $k_{\text{eff}}$  was 2.4%  $\Delta k_{\text{eff}}$ , corresponding to a configuration with multiple rod failures for fuel with an initial enrichment of 5 w/o and 35 GWd/MTU of burnup. As emphasized above, it is important to recognize that these results are contingent on the authors' judgment relative to the potential credibility of configurations. For example, for this BWR cask system, the fuel assembly channel is assumed to be present and capable of constraining

fuel rod pitch expansion. If this assumption is not valid for a specific cask loading, then another configuration and its specific characteristics may be limiting.

The maximum increase for a potentially credible configuration in the BWR cask system ( $2.4\% \Delta k_{\text{eff}}$ ) corresponds to a reference case  $k_{\text{eff}}$  of approximately 0.833. The reconfigured  $k_{\text{eff}}$  is therefore only approximately 0.857 and still significantly less than the recommended 0.95  $k_{\text{eff}}$  limit. The large subcritical margin is due to the fact that the MPC-68 was designed and licensed to accommodate unburned fuel, whereas the analyses considered fuel irradiated to 35 GWd/MTU (a relatively low discharge burnup for fuel with initial enrichment of 5 w/o). The largest  $k_{\text{eff}}$  increase associated with fresh fuel is  $2.09\% \Delta k_{\text{eff}}$  and is a result of uniform pitch expansion constrained by the fuel assembly channel. Many of the potential issues associated with crediting the constraint provided by the channel are negated in this case since it is fresh fuel. Results presented for the fuel assemblies with part-length fuel rods in Section 5.2.4 demonstrate the potential importance of this design feature. The reference case  $k_{\text{eff}}$  for fresh assemblies with part-length rods is nearly  $0.7\% \Delta k_{\text{eff}}$  higher than for fresh assemblies with only full-length rods. The  $k_{\text{eff}}$  increase associated with fuel reconfiguration is usually lower for the part-length fuel, but often the difference in the  $k_{\text{eff}}$  change is less than the difference in the reference cases. The absolute  $k_{\text{eff}}$  is therefore higher for many configurations involving fresh assemblies with part-length fuel even though the  $k_{\text{eff}}$  increase is smaller. The effect of varying depletion conditions for assemblies with part-length rods was not considered in this report.

In addition to representative conditions for fuel burnup and post-irradiation decay time, the effects of higher burnup and longer cooling times were also investigated in both PWR and BWR cask systems and found to be smaller than the reduction in  $k_{\text{eff}}$  associated with the higher burnup or cooling time. In addition to the analyses that assume all of the assemblies within the cask have the same degradation condition, analyses were performed to evaluate the consequences of degradation to limited numbers of assemblies. Although the results are configuration dependent, they indicate that the majority of the total potential increase in  $k_{\text{eff}}$  (observed for a cask fully loaded with degraded fuel) is associated with a relatively small fraction of the assemblies having the degraded condition, provided that the reconfigured assemblies are located in close proximity and in the worst-case location in the cask (generally the center region). A limited study performed with the MPC-68 demonstrated that the increase in  $k_{\text{eff}}$  is considerably smaller if the reconfigured assemblies are randomly distributed. A limited set of analyses was also performed to investigate the consequences of combinations of degradation, e.g., a number of failed rods and fuel rod pitch expansion. In the cases analyzed, the sum of the  $k_{\text{eff}}$  increases associated with modeling each configuration separately was determined to be slightly larger than the increase determined from explicitly modeling the combined configurations.

## 6.2 Observations and Conclusions

Similar to previous works, a key conclusion is that the consequences of fuel failure to criticality safety are directly dependent on the configurations that may form as a result of fuel failure. The magnitude of the potential increases in  $k_{\text{eff}}$  and the sensitivity of the potential increases in  $k_{\text{eff}}$  to the determination of the credibility of configurations highlight the importance of being able to determine and justify which configurations are credible under a given set of conditions for a given cask system. It is anticipated, at least in the near term, that these determinations will be done on a case-by-case basis for each cask system and associated licensing conditions.

Analyses of additional large-capacity cask designs and/or additional fuel types are expected to yield  $k_{\text{eff}}$  changes that are similar in magnitude, as compared to those predicted herein, and the limiting configurations are likely to be the same or similar. Large differences in cask design features could cause significant differences in reconfiguration consequences in specific casks, if such large design differences

exist. This conclusion is supported by the similarities in the important effects between PWR and BWR fuel considered in this report. The differences between BWR and PWR fuel designs are more significant than the differences among assembly types within the PWR or BWR fuel classes. The importance of any particular configuration may vary from one cask design to another, but the most limiting configurations will be associated with gross assembly failure and large axial misalignment and are relatively insensitive to assembly design.

The results presented in Section 5 and the cask-specific conclusions presented above indicate larger  $k_{\text{eff}}$  increases for BWR fuel, as compared to PWR fuel. However, current BWR casks, including the MPC-68 considered in this analysis, are designed and licensed to accommodate unburned fuel. Therefore, these casks generally have in excess of 10%  $\Delta k_{\text{eff}}$  margin (as compared to the recommended  $k_{\text{eff}}$  limit of 0.95) when loaded with fuel with typical discharge burnup values.

Specific, realistic configuration development is likely to provide significant margin compared to the bounding configurations considered here. For both casks, the maximum increases in  $k_{\text{eff}}$  are based on analyses that assume all of the assemblies within the cask have the same degradation condition. Analyses that consider limited numbers of reconfigured assemblies, either randomly located within the cask or located together, predict smaller increases in  $k_{\text{eff}}$ . Hence, unless all or most of the assemblies within a cask are expected to have same or a similar degree of reconfiguration, the cited maximum increases in  $k_{\text{eff}}$  are conservative estimates; the extent of the conservatism depends on the number and location of the reconfigured assemblies, as well as the configuration.

Given the establishment of a set of credible failed fuel configurations for a given cask system and assuming that one or more of the configurations result in an increase in  $k_{\text{eff}}$  (above the regulatory limit of 0.95), the consequence of this potential increase in  $k_{\text{eff}}$  must be addressed. There are a number of potential options, the viability of which depends on the magnitude of the increase in  $k_{\text{eff}}$ . For BWR fuel, credit for fuel burnup could be used to offset the potential increase in  $k_{\text{eff}}$  due to fuel failure. Although it is recognized that burnup credit for BWR fuel in storage and transportation casks is not recommended in current regulatory guidance documents, the reactivity reduction associated with burnup is likely sufficient to offset reactivity increases associated with potentially credible BWR failed fuel configurations.

Other potential mitigation options, for either PWR or BWR casks, include 1) separate loading curves for fuel and/or conditions for which fuel integrity cannot be assured, 2) a higher  $k_{\text{eff}}$  limit for such fuel, e.g., 0.98, 3) increased credit for cooling time, 4) credit for the actual, as-loaded conditions in existing casks, and 5) moderator exclusion. For the first option listed above, a cask design and/or fuel assembly loading conditions could be modified to ensure that the current recommended  $k_{\text{eff}}$  limit of 0.95 is satisfied for all credible failed fuel configurations. Separate assembly loading curves based on a reduced  $k_{\text{eff}}$  limit could be developed for fuel assemblies that may have questionable integrity. In the context of high-burnup fuel or ES durations, a separate loading curve based on a lower  $k_{\text{eff}}$  limit could be developed and applied to fuel assemblies with burnup greater than 45 GWd/MTU and/or with a post-irradiation storage period beyond some specified value. Alternatively, depending on the probability of fuel reconfiguration, the second option listed above, i.e., the use of a higher limit, could be established to allow margin for the increased reactivity effect associated with fuel reconfiguration. This option would be similar to the higher limit (i.e., 0.98) allowed for the unlikely optimum moderation condition in dry storage of fresh fuel under 10 CFR 50.68. In this case, the customary  $k_{\text{eff}}$  limit would still apply to all conditions involving intact fuel. The third option above refers to crediting the reduction in reactivity between the minimum time for loading, e.g., 5 years, and some time prior to which fuel reconfiguration is postulated to occur, e.g., 50 years. Because the reactivity of UNF reaches a minimum at approximately 100 years and then begins to increase, the total duration for cask storage and transportation is an important consideration in determining how much reactivity reduction can be credited. For fuel that is already loaded in casks, the fourth option above refers to crediting the specific cask conditions – to the extent needed, the specific

assembly burnup values, cooling times and locations in the cask may be considered to demonstrate sufficient reactivity margin to offset the potential increase in  $k_{\text{eff}}$  due to fuel failure. Finally, moderator exclusion could potentially be used to offset criticality safety concerns related to fuel failure, as is currently allowed for HACs in Ref. 51.

Although the results indicate that the potential impacts on subcriticality can be significant for certain configurations, it can be concluded that the consequences of credible fuel failure configurations from ES or transportation following ES are manageable. Some examples for how to address the potential increases in  $k_{\text{eff}}$  in a criticality safety evaluation were provided. Future work to further inform decision-making relative to which configurations are credible, and therefore need to be considered in a safety evaluation, is recommended.

## 7. RECOMMENDATIONS FOR FUTURE WORK

Future work to extend these analyses could consider additional fuel assembly types, depletion conditions, and cask designs. As noted in Section 6.2, this is not expected to result in significantly different conclusions. It may be beneficial to investigate more accurate modeling of the fuel assemblies to include such features as axial blankets or radial enrichment zoning and different axial burnup and void histories. These details could give more realistic estimates of their impacts on  $k_{\text{eff}}$  but are unlikely to change the salient conclusions regarding the relevance of key configurations.

An expanded study of debris configurations is warranted. The homogeneous debris models used in this analysis do not consider partial assembly failure or any intact assembly structure or hardware. Some of these types of configurations, including debris collecting in structural or flow mixing grids, are potentially more credible than the configurations included in this report. Rubble models including rod segments or fragments may also be relevant. Consideration should be given to a range of final cask orientations if the final debris bed does not fill the entire inner volume of the storage cells. A more complete study of degraded fuel forms is also potentially worth investigating. Many degraded fuel forms would include oxidation to other urania compounds of lower densities, effectively displacing moderator. These changes may not result in any increases in estimated  $k_{\text{eff}}$  but may be worth investigating.

Investigating different enrichments and burnups could be considered. It is unlikely that the relative importance of configurations would be impacted by these changes, but the overall magnitude may be affected. A more complete mapping of the burnup/enrichment space would also allow a quantification of potential conservatisms, especially for BWR fuel, with reduced  $k_{\text{eff}}$  values for reference case conditions.

Future work should investigate the potential impact of loading fuel assemblies with a range of burnups and irradiation histories in storage casks for ES. These configurations are more realistic since each assembly experiences different conditions during irradiation and will have different discharge burnups and cooling times.

It is advisable to consider more combinations of the configurations used here. A very limited number of calculations have been documented in Sections 5.1.3 and 5.2.3, and the results indicate that explicit modeling of combined configurations generates a slightly smaller increase in  $k_{\text{eff}}$  than the sum of the two separate effects. A review of other combined effects could generate additional limiting configurations or provide greater evidence that the effects of combined configurations can be adequately accounted for with separate single configuration models.

Finally, it may be advisable to consider the effect of basket or cask degradation if such events are considered credible. Degradation to these cask components is beyond the scope of these analyses.

## REFERENCES

1. *Gap Analysis to Support Extended Storage of Used Nuclear Fuel*, U.S. Department of Energy, FCRD-USED-2011-000136, REV 0, January 2012.
2. *UFD Storage and Transportation Working Group Report*, U.S. Department of Energy, FCRD-USED-2011-000323, August 2011.
3. *Identification and Prioritization of the Technical Information Needs Affecting Potential Regulation of Extended Storage and Transportation of Spent Nuclear Fuel*, U.S. Nuclear Regulatory Commission, Draft Report for Comment, May 2012, <http://pbadupws.nrc.gov/docs/ML1205/ML120580143.pdf>.
4. *Extended Storage Collaboration Program (ESCP) Progress Report and Review of Gap Analysis*, Electric Power Research Institute, Palo Alto, CA (2011), 1022914.
5. *Evaluation of the Technical Basis for Extended Dry Storage and Transportation of Used Nuclear Fuel – Executive Summary*, U.S. Nuclear Waste Technical Review Board, December 2010, [http://www.nwtrb.gov/reports/eds\\_execsumm.pdf](http://www.nwtrb.gov/reports/eds_execsumm.pdf).
6. *Used Nuclear Fuel Storage and Transportation Research, Development, and Demonstration Plan*, FCRD-FCT-2012-000053, REV 0, April 2012.
7. K. R. Elam, J. C. Wagner, and C. V. Parks, *Effects of Fuel Failure on Criticality Safety and Radiation Dose for Spent Fuel Casks*, NUREG/CR-6835 (ORNL/TM-2002/255), prepared for the U.S. Nuclear Regulatory Commission by Oak Ridge National Laboratory, Oak Ridge, TN, September 2003.
8. Title 10, *Code of Federal Regulations*, Part 72, 73 FR 63572, October 24, 2008.
9. Title 10, *Code of Federal Regulations*, Part 71, 73 FR 63572, October 24, 2008.
10. *Standard Review Plan for Spent Fuel Dry Storage Systems at a General License Facility*, NUREG-1536, Revision 1, Office of Nuclear Material Safety and Safeguards, July 2010.
11. *Standard Review Plan for Spent Fuel Dry Storage Facilities*, NUREG-1567, Office of Nuclear Material Safety and Safeguards, March 2000.
12. *Standard Review Plan for Transportation Packages for Spent Nuclear Fuel*, NUREG-1617, Office of Nuclear Material Safety and Safeguards, March 2000.
13. Title 10, *Code of Federal Regulations*, Part 50.68, 71 FR 66648, November 16, 2006.
14. *Fuel Reconfiguration – Implications to Criticality and Radiation Safety*, 2011 SFST Technical Exchange, November 1, 2011, David Tang and Zhian Li, U.S. Nuclear Regulatory Commission (ADAMS Accession #ML113120530).
15. A. Machiels and A. H. Wells, *Fuel Relocation Effects for Transportation Packages*, EPRI Report 1015050, Palo Alto, CA, 2007.

16. J. L. Sprung et al., *Reexamination of Spent Fuel Shipment Risk Estimates*, NUREG/CR-6672 (SAND2000-0234), prepared for the U.S. Nuclear Regulatory Commission by Sandia National Laboratories, Albuquerque, NM, March 2000.
17. L. E. Fischer et al., *Shipping Container Response to Severe Highway and Railway Accident Conditions*, NUREG/CR-4829 (UCID-20733), prepared for the U.S. Nuclear Regulatory Commission by Lawrence Livermore National Laboratory, Livermore, CA, February 1987.
18. *Final Environmental Impact Statement on the Transportation of Radioactive Material by Air and Other Modes*, NUREG-0170, U.S. Nuclear Regulatory Commission, Rockville, MD, December 1977.
19. A. Machiels et al., *Transportation of Commercial Spent Nuclear Fuel: Regulatory Issues Resolution*, EPRI Report 1016637, Palo Alto, CA, 2010.
20. A. Machiels and A. Dykes, *Criticality Risks during Transportation of Spent Nuclear Fuel: Revision 1*, EPRI Report 1016635, Palo Alto, CA, 2008.
21. *Interfaces Between Storage and Transportation Casks – Panel on High Burnup Fuel – Industry’s View on Spent Fuel Reconfiguration*, 2011 SFST Technical Exchange, November 1, 2011, Albert Machiels, EPRI (ADAMS Accession #ML113120509).
22. D. Nagasawa et al., “Accelerated Corrosion Testing of Aluminum Carbide Metal Matrix Composite in Simulated PWR Spent Fuel Pool Solution,” *Proceedings of 16<sup>th</sup> International Symposium on the Packaging and Transportation of Radioactive Materials* (PATRAM 2010), London, UK, 2010.
23. M. Dallongeville et al., “Description of Fuel Integrity Project Methodology Principles,” *Proceedings of 16<sup>th</sup> International Symposium on the Packaging and Transportation of Radioactive Materials* (PATRAM 2010), London, UK, 2010.
24. P. Purcell, “Method to Evaluate Limits of Lattice Expansion in Light Water Reactor Fuel from an Axial Impact Accident During Transport,” *Proceedings of 15<sup>th</sup> International Symposium on the Packaging and Transportation of Radioactive Materials* (PATRAM 2007), Miami, FL, 2007.
25. I. Reiche, “Influence of the Accident Behaviour of Spent Fuel Elements on Criticality Safety of Transport Packages – Some Basic Considerations,” *Proceedings of 15<sup>th</sup> International Symposium on the Packaging and Transportation of Radioactive Materials* (PATRAM 2007), Miami, FL, 2007.
26. F. Hilbert, “Criticality Assessment of Fuel Assemblies With Missing Fuel Rods – An Intractable Problem?” *Proceedings of 14<sup>th</sup> International Symposium on the Packaging and Transportation of Radioactive Materials* (PATRAM 2004), Berlin, Germany, 2004.
27. P. J. Vescovi and N. A. Kent, “Nuclear Criticality Safety Analysis for the Traveler PWR Fuel Shipping Package,” *Proceedings of 14<sup>th</sup> International Symposium on the Packaging and Transportation of Radioactive Materials* (PATRAM 2004), Berlin, Germany, 2004.
28. L. Farrington, “Harmonisation of Criticality Assessments of Packages for the Transport of Fissile Nuclear Fuel Cycle Materials,” *Proceedings of 14<sup>th</sup> International Symposium on the Packaging and Transportation of Radioactive Materials* (PATRAM 2004), Berlin, Germany, 2004.

29. B. Gogolin et al., "Drop Tests with the RA-3D Shipping Container for the Transport of Fresh BWR Fuel Assemblies," *Proceedings of 13<sup>th</sup> International Symposium on the Packaging and Transportation of Radioactive Materials* (PATRAM 2001), Chicago, IL, 2001.
30. P. Millan et al., "Drop Test for the Licensing of the RA-3D Package in the Transport of BWR Fresh Fuel Assemblies," *Proceedings of 13<sup>th</sup> International Symposium on the Packaging and Transportation of Radioactive Materials* (PATRAM 2001), Chicago, IL, 2001.
31. S. Whittingham et al., "Effects of Impact Accidents on Transport Criticality Safety Cases for LWR Packages – A New Approach," *Proceedings of 13<sup>th</sup> International Symposium on the Packaging and Transportation of Radioactive Materials* (PATRAM 2001), Chicago, IL, 2001.
32. M. Asami and N. Odano, "New Approach to Evaluate Lattice Expansion of Light Water Reactor Fuel Elements on Criticality Safety of Transport Packages under Impact Accidents," *Packaging, Transport, Storage & Security of Radioactive Material* **21**(2), 2010.
33. *Handbook of Neutron Absorber Materials for Spent Nuclear Fuel Transportation and Storage Applications*: 2009 ed., EPRI Technical Report 1019110, Electric Power Research Institute, Palo Alto, CA, November 2009.
34. *SCALE: A Comprehensive Modeling and Simulation Suite for Nuclear Safety Analysis and Design*, ORNL/TM-2005/39, Version 6.1, Oak Ridge National Laboratory, Oak Ridge, TN, June 2011. Available from Radiation Safety Information Computational Center at Oak Ridge National Laboratory as CCC-785.
35. *RW-859 Nuclear Fuel Data*, Energy Information Administration, Washington, D.C., October 2004.
36. *Safety Analysis Report for the Holtec International Storage, Transport, and Repository Cask System (HI-STAR 100 Cask System)*, Table of Contents to Chapter 1, Holtec Report HI-951251, Revision 10, Holtec International, August 2003, ADAMS Accession Number ML071940386.
37. *Safety Analysis Report for the Holtec International Storage, Transport, and Repository Cask System (HI-STAR 100 Cask System)*, Chapter 2 through Chapter 4, Holtec Report HI-951251, Revision 10, Holtec International, August 2003, ADAMS Accession Number ML071940391.
38. *Safety Analysis Report for the Holtec International Storage, Transport, and Repository Cask System (HI-STAR 100 Cask System)*, Chapter 5 to end, Holtec Report HI-951251, Revision 10, Holtec International, August 2003, ADAMS Accession Number ML071940408.
39. J. C. Wagner, *Computation Benchmark for Estimation of Reactivity Margin from Fission Products and Minor Actinides in PWR Burnup Credit*, NUREG/CR-6747 (ORNL/TM-2000/306), prepared for the U.S. Nuclear Regulatory Commission by Oak Ridge National Laboratory, Oak Ridge, TN, October 2001.
40. C. V. Parks, M. D. DeHart, and J. C. Wagner, *Review and Prioritization of Technical Issues Related to Burnup Credit for LWR Fuel*, NUREG/CR-6665 (ORNL/TM-1999/303), prepared for the U.S. Nuclear Regulatory Commission by Oak Ridge National Laboratory, Oak Ridge, TN, February 2000.
41. R. J. Caciapouti and S. Van Volkinburg, *Axial Burnup Profile Database for Pressurized Water Reactors*, YAEC-1937, Yankee Atomic Electric Company, May 1997.

42. J. C. Wagner and C. V. Parks, *Parametric Study for the Effect of Burnable Poison Rods for PWR Burnup Credit*, NUREG/CR-6761 (ORNL/TM-2000/373), prepared for the U.S. Nuclear Regulatory Commission by Oak Ridge National Laboratory, Oak Ridge, TN, March 2002.
43. C. E. Sanders and J. C. Wagner, *Study of the Effect of Integral Burnable Absorbers for PWR Burnup Credit*, NUREG/CR-6760 (ORNL/TM-2000/321), prepared for the U.S. Nuclear Regulatory Commission by Oak Ridge National Laboratory, Oak Ridge, TN, March 2002.
44. J. C. Wagner and C. V. Parks, *Recommendations on the Credit for Cooling Time in PWR Burnup Credit Analysis*, NUREG/CR-6781 (ORNL/TM-2001/272), prepared for the U.S. Nuclear Regulatory Commission by Oak Ridge National Laboratory, Oak Ridge, TN, January 2003.
45. *Topical Report on Actinide-Only Burnup Credit for PWR Spent Nuclear Fuel Packages*, DOE/RW-0472 Rev. 2, U.S. Department of Energy Office of Civilian Radioactive Waste Management, September 1998.
46. D. P. Henderson et al., *Summary Report of Commercial Reactor Criticality Data for Quad Cities Unit 2*, B00000000-01717-5705-00096 Revision 01, Civilian Radioactive Waste Management System Management & Operating Contractor, September 1999.
47. D. P. Henderson et al., *Summary Report of Commercial Reactor Criticality Data for LaSalle Unit 1*, B00000000-01717-5705-00138, Civilian Radioactive Waste Management System Management & Operating Contractor, September 1999.
48. D. E. Mueller et al., *Review and Prioritization of Technical Issues Related to Burnup Credit for BWR Fuel*, NUREG/CR-XXXX (ORNL/TM-2012/261), prepared for the U.S. Nuclear Regulatory Commission by Oak Ridge National Laboratory, Oak Ridge, TN, to be published.
49. M. G. Natrella, *Experimental Statistics*, National Bureau of Standards Handbook 91, August 1963.
50. Fuel Cycle Safety and Safeguard Interim Staff Guidance-10, *Justification for Minimum Margin of Subcriticality for Safety*, Division of Fuel Cycle Safety and Safeguards, Office of Nuclear Material Safety and Safeguards, U.S. Nuclear Regulatory Commission, June 2006.
51. Spent Fuel Storage Transportation Interim Staff Guidance-19, *Moderator Exclusion under Hypothetical Accident Conditions and Demonstrating Subcriticality of Spent Fuel under the Requirements of 10 CFR 71.55(e)*, Division of Spent Fuel Storage and Transportation, Office of Nuclear Material Safety and Safeguard, U.S. Nuclear Regulatory Commission, May 2003.
52. L. E. Fennern, *ABWR Seminar – Reactor, Core & Neutronics*, GE Energy/Nuclear, <http://www.ne.doe.gov/np2010/pdfs/ABWRReactorCoreNeutronics.pdf>, retrieved April 16, 2012.
53. L. B. Wimmer, *BWR Axial Burnup Profile Evaluation*, Framatome ANP Document Number 32-5045751-00, July 16, 2004.

## Appendix A

### Fuel Assembly Modeling Details

#### A.1 WESTINGHOUSE 17 × 17 OFA

Westinghouse 17 × 17 OFA is a fuel design that has been commonly used in the commercial nuclear industry for more than 20 years. This common use makes it a good choice for a representative fuel assembly type for calculations in the PWR storage and transportation casks. For purposes of these analyses, the OFA fuel design encompasses all variations of cladding materials, grids, and assembly hardware which may lead to a different fuel product designation from Westinghouse, such as Vantage5 or Vantage+. The essential features are the fuel rod outer diameter of 0.9144 cm and fuel rod pitch of 1.2598 cm. The dimensions used to model the fuel assembly are provided in Table A-1.

The 17 × 17 OFA model is included in the MPC-24 and GBC-32 casks. The cladding is modeled as Zircaloy-4. The guide tube and instrument tubes are assumed to be identical and are also represented as Zircaloy-4. Unborated, unit density water fills the gap between the pellet and cladding. Water in the pellet/clad gap is conservative for criticality calculations because it causes a slight increase in calculated  $k_{\text{eff}}$  values. In irradiated fuel, pellet swelling closes this gap and causes this assumption to be nonphysical. A cross section of the 17 × 17 OFA model is shown in Figure A-1.

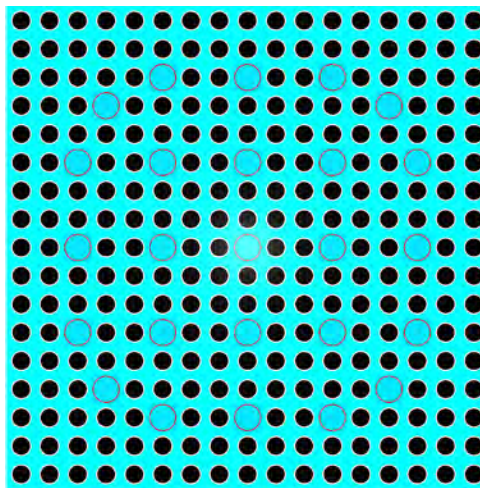
The fuel assemblies are modeled with a uniform initial enrichment in the axial and radial directions. No reduced enrichment and/or annular blanket pellets are included in any of the models. No integral burnable absorbers are modeled in the fuel, though the presence of wet annular burnable absorber (WABA) rods is considered during depletion to provide conservative used fuel isotopic compositions with respect to criticality calculations. The impact of the presence of removable and integral burnable absorbers is discussed in Refs. 42 and 43. The details of the depletion conditions are provided in Section 4.4.1.

Several modeling simplifications have been incorporated that either have a negligible effect or increase assembly calculated  $k_{\text{eff}}$ . Some of these simplifications include omission of fuel assembly hardware beyond the ends of the active fuel as well as the omission of all structural and mixing grids, assembly nozzles, plenums, and end plugs. The hardware beyond the active fuel region has a small effect on  $k_{\text{eff}}$ , and minimal effect on the change in  $k_{\text{eff}}$  associated with fuel reconfiguration. Omitting the grids allows more effective neutron moderation due to less moderator displacement between rods.

For cases involving depleted fuel, the fuel rods are represented with 18 axial regions. Each region is 20.32 cm (8 in.) tall and contains average mixture number densities in each zone. All fuel rods contain the same composition.

**Table A-1. Westinghouse 17 × 17 OFA dimensions used in these analyses [39]**

Parameter	Dimension (cm)	Dimension (in.)
Pellet outer diameter	0.7844	0.3088
Fuel rod outer diameter	0.9144	0.360
Cladding thickness	0.0571	0.0225
Fuel rod pitch	1.2598	0.496
Active fuel height	365.76	144
Guide/instrument tube outer diameter	1.204	0.474
Guide/instrument tube thickness	0.0407	0.016
Fuel density	10.5216 g/cm <sup>3</sup> (96% theoretical density)	
Number of fuel rods	264	
Number of guide/instrument tubes	25	



Note: Fuel shown in black; guide/instrument tubes are larger, water-filled tubes

**Figure A-1. Cross section of 17 × 17 OFA assembly.**

## A.2 GENERAL ELECTRIC 10 × 10

General Electric 10 × 10 fuel assembly designs, such as the GE14 fuel product, are widely used in the commercial nuclear power industry. The 10 × 10 array is representative of existing BWR fuel assembly designs for use in the MPC-68 cask models. The GE 10 × 10 model included in the MPC-68 models uses dimensions shown in Table A-2. Unborated, unit density water fills the gap between the fuel pellet and cladding. The cladding and water tubes are modeled as Zircaloy-4. Each water tube occupies four unit cells in the lattice, displacing a 2 × 2 region of fuel rods. A cross section of the 10 × 10 model is shown in Figure A-2.

The fuel assemblies are considered with a uniform initial enrichment in the axial and radial directions. No reduced enrichment axial blanket pellets are included, and no part-length rods are represented in the fuel assemblies except in the explicit part-length rod sensitivity calculations.

Part-length rods are common in BWR assembly designs, including the GE14 design, making an investigation of the impact of part-length rods prudent as a part of these analyses. The pattern of part-length rods, taken from Ref. 52, is shown in Figure A-3. These shortened rods have fuel only in the bottom 220 cm of the fuel rods. As discussed in Section 5.2.4, only fresh 5 w/o fuel is considered in the part-length rod calculations presented in this report. Only fresh fuel is considered for these studies because no axial burnup profiles are available for fuel assemblies with part-length rods. The removal of some of the fuel in the upper portion of the assembly might cause a more bottom-skewed power shape, but the remaining sparser lattice will also be more reactive. The axial power shape could therefore also be about the same or even more top-skewed than that developed in Appendix E. The lower mass in the upper zone of the assembly also has the effect of increasing burnup since it is measured as energy released per unit mass of uranium. Given the unknown relative impact of these effects, depleted fuel is not considered in this study.

No burnable absorbers are modeled in the fresh fuel assemblies or during depletion. The impact of burnable absorbers is expected to be negligible on the results of this study. The details of the depletion conditions are provided in Section 4.4.2.

Several modeling simplifications that are consistent with industry practice for criticality safety have been incorporated that either have a negligible effect on system reactivity or increase assembly reactivity. Some of these simplifications include omission of fuel assembly hardware beyond the ends of the active fuel as well as the omission of all structural and mixing grids, assembly end fittings, plenums, and end plugs. The hardware beyond the active fuel region has a small effect on  $k_{\text{eff}}$ , and minimal effect on the change in  $k_{\text{eff}}$  associated with fuel reconfiguration. Omitting the grids allows more effective neutron moderation due to less moderator displacement between rods.

For cases involving depleted fuel, the fuel rods are represented with 25 axial regions. Each region is 15.24 cm (6 in.) tall and contains average mixture number densities in each zone. All fuel rods contain the same composition.

**Table A-2. GE 10 × 10 assembly dimensions used in these analyses [34]**

Parameter	Dimension (cm)	Dimension (in.)
Pellet outer diameter	0.876	0.3449
Fuel rod outer diameter	1.026	0.404
Cladding thickness	0.066	0.026
Fuel rod pitch	1.295	0.510
Active fuel height	381	150
Water tube outer diameter	2.522	0.993
Water tube thickness	0.1	0.039
Fuel density	10.5216 g/cm <sup>3</sup> (96% theoretical density)	
Number of fuel rods	92	
Number of water tubes	2 (each displaces four fuel rods)	

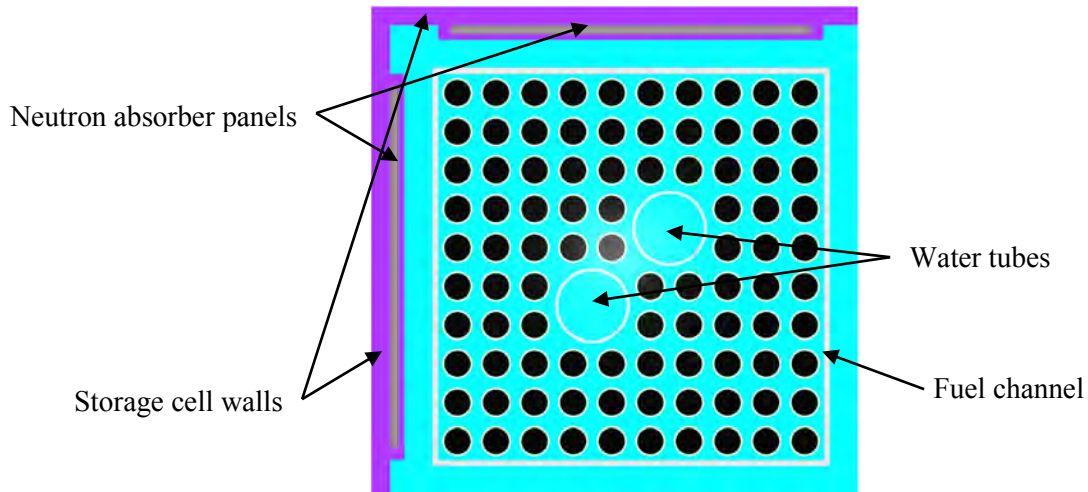


Figure A-2. Cross section of GE  $10 \times 10$  fuel assembly in MPC-68.

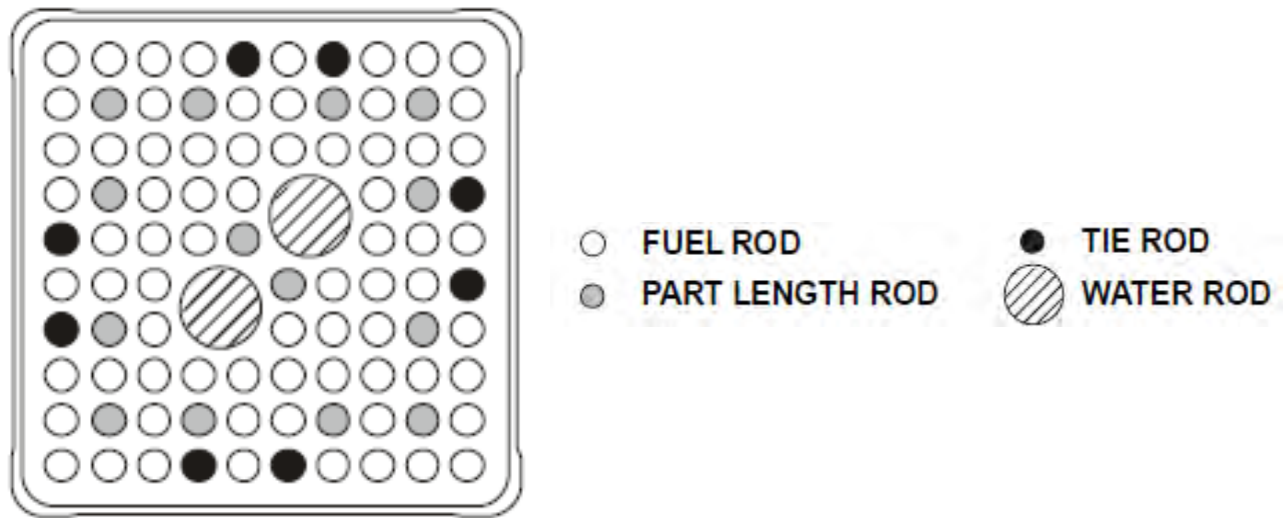


Figure A-3. Location of part-length rods in GE  $10 \times 10$  fuel assembly.

## Appendix B

### MPC-24 Modeling and Results

The MPC-24 cask is designed for the storage and transportation of up to 24 PWR fuel assemblies. The nominal condition for this model is fully flooded with unit density, unborated water. A cross section of the MPC-24 model is shown in Figure B-1. It should be noted that the MPC-24 cask design in Refs. 36–38 has been updated from the design used in Ref. 7. The cask model is consistent with the description and drawings provided in the HI-STAR Safety Analysis Report (SAR), Refs. 36–38. More details of the modeling are provided in Appendix D.

Fresh 5 w/o  $^{235}\text{U}$  enrichment Westinghouse 17 × 17 OFA is modeled in the MPC-24. This fuel represents a limiting case for analysis. It is unlikely that any fresh fuel assemblies would be placed in ES, but this condition is of interest to complete the parameter space to be covered in this study.

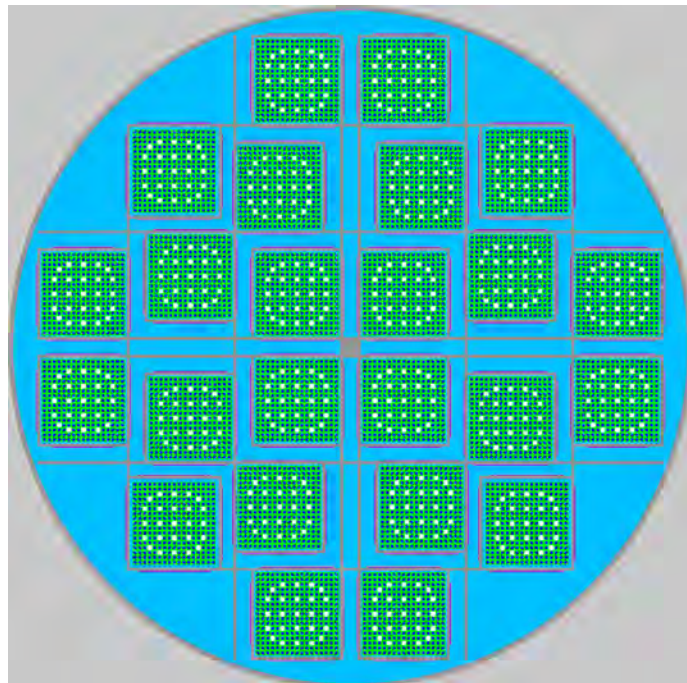


**Figure B-1. Cross section of MPC-24 model.**

#### B.1 ADDITIONAL CONFIGURATION CONSIDERED

The MPC-24 is the only cask design considered that integrates a flux trap into the design of the fuel storage basket. A flux trap is a region of typically water-filled space with neutron absorber panels on both sides of the trap and is positioned between fuel storage cells. The worth of the absorbers is greatly increased by allowing for additional moderation between the panels, thus allowing higher reactivity fuel to be stored safely. Fast neutrons escaping from one cell will be thermalized in the water between cells and are much more likely to be absorbed in the panel on the other side. For this design feature to be

effective, the area within the flux trap must stay flooded in all cases in which the fuel storage cells are flooded. The primary design features that preclude the drainage of only the flux traps are an opening in the bottom of the storage basket walls and a small gap between the top of the storage cell walls and the cask lid. These openings allow water to flow into all regions of the basket. Preferential flooding (i.e., flooding of the fuel storage cells but not the flux traps) is considered here.

The modeling of preferential flooding configurations is straightforward. Two cases are considered: one in which only the flux traps are dry and one in which the area inside the fuel storage cell but outside the fuel assembly is also dry. The latter case is not credible but is included for completeness. No adjustments are needed to the cross section processing because the fuel assembly is always modeled as fully flooded. The orientation of the cask is not considered in the modeling of this configuration. It is not expected to influence the results of the calculations, though it would influence the progression of a flooding event if one occurred.

No preferential flooding cases are considered in Ref. 7.

## B.2 RESULTS

The  $k_{\text{eff}}$  change associated with each of the configurations discussed in Section 3 and Section B.1 is presented in this section for the MPC-24 cask. All configurations assume a full loading of 24 fresh 5 w/o Westinghouse 17 × 17 OFA. The description of the fuel assembly modeling is provided in Appendix A. No used fuel configurations are considered in the MPC-24 model. The reference case  $k_{\text{eff}}$  results from both the KENO V.a and KENO-VI models are provided in Table B-1.

**Table B-1. Reference case results for MPC-24**

<b>Burnup (GWd/MTU)</b>	<b>Cooling time (years)</b>	<b>KENO V.a</b>		<b>KENO-VI</b>	
		$k_{\text{eff}}$	$\sigma$	$k_{\text{eff}}$	$\sigma$
0	0	0.95042	0.00010	0.95065	0.00010

### B.2.1 Reconfiguration of All Assemblies

A summary of the  $k_{\text{eff}}$  consequences associated with each configuration is provided in Table B-2. Additional details for each configuration and the results for non-limiting cases are provided in the subsequent subsections.

**Table B-2. Summary of  $k_{\text{eff}}$  increases for the MPC-24 cask**

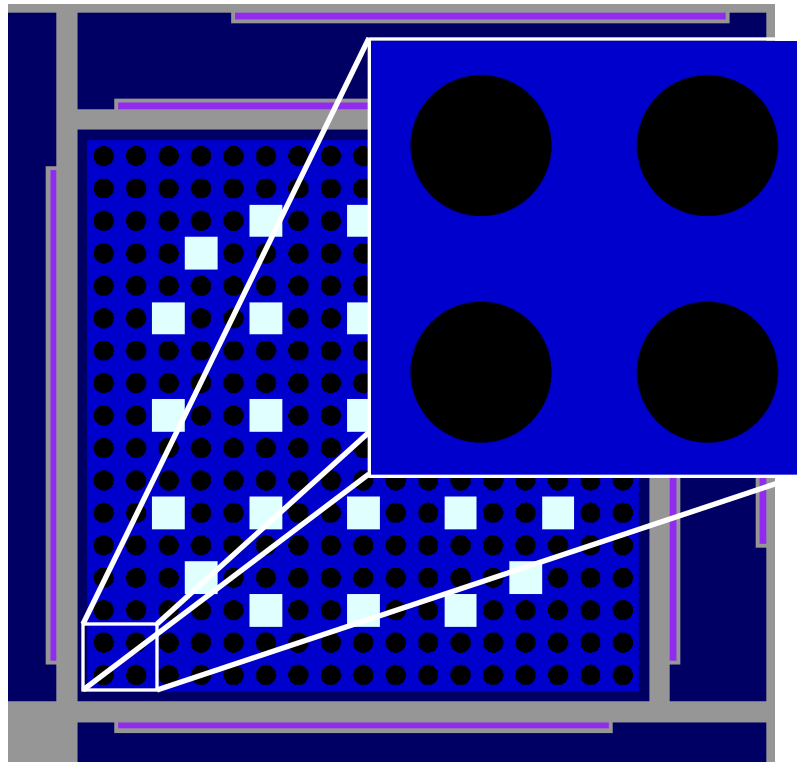
<b>Configuration</b>	<b>Maximum increase in <math>k_{\text{eff}}</math> (% <math>\Delta k_{\text{eff}}</math>)</b>
<b>Clad thinning/loss</b>	
Cladding removal	5.24
<b>Rod failures</b>	
Single rod removal	0.15
Multiple rod removal	2.01
<b>Loss of rod pitch control</b>	
Expanded rod pitch, clad	2.88
Expanded rod pitch, unclad	6.83
<b>Loss of assembly position control</b>	
Axial displacement (maximum)	7.08
Axial displacement (20 cm)	0.03
<b>Gross assembly failure</b>	
Uniform pellet array	13.56
Homogeneous rubble	8.23
<b>Preferential flooding</b>	
Preferential Flooding (dry flux traps)	16.61
<b>Neutron absorber degradation</b>	
Missing neutron absorber (5-cm segment)	0.35
Missing neutron absorber (10-cm segment)	1.07
50% neutron absorber panel thinning	1.11

### B.2.1.1 Clad Thinning/Loss

The loss of cladding configurations are modeled as discussed above in Section 3.1.1; the complete cladding removal configuration is shown in Figure B-2. The results of the calculations are provided in Table B-3, showing that the  $k_{\text{eff}}$  increase associated with complete cladding removal is 5.24%  $\Delta k_{\text{eff}}$ . The results as a function of fractional cladding thickness are shown in Figure B-3. The results presented here are somewhat higher than those presented in Ref. 7. This may be due to an updated cask model that includes the oversized fuel storage cells and the rotation of the standard storage cells relative to each other in the cask basket. These additional details may lead to a slightly more thermal spectrum and a correspondingly higher  $k_{\text{eff}}$  value for this configuration.

**Table B-3. Increase in  $k_{\text{eff}}$  in MPC-24 due to reduced cladding thickness**

<b>Fraction of cladding thickness remaining</b>	<b>Increase in <math>k_{\text{eff}}</math> (% <math>\Delta k_{\text{eff}}</math>)</b>
0.90	0.62
0.75	1.51
0.50	2.87
0.25	4.06
0.00	5.24



Notes:

- Fuel shown in black
- Storage basket structural material is light grey
- Neutron absorber panel is purple
- Water is shown in blue, dark blue, and white
- Guide/instrument tube locations contain water shown in white

**Figure B-2. Loss of cladding model in MPC-24 storage cell.**

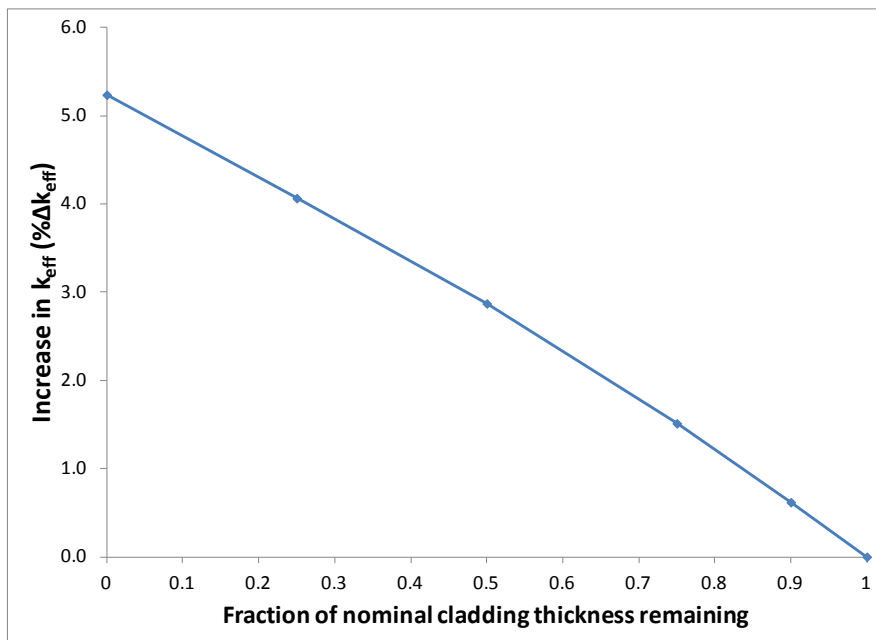


**Figure B-3. Increase in  $k_{\text{eff}}$  in MPC-24 due to reduced cladding thickness.**

### B.2.1.2 Rod Failures

Each of the 39 unique eighth-assembly symmetric rods is removed individually to determine its worth, as discussed in Section 3.1.2.1. A sketch showing the eighth-assembly symmetry and row and column labels is provided in Figure 7. Table B-4 presents the rod locations whose best estimate worth is greater than 0.1%  $\Delta k_{\text{eff}}$ . Both the locations of these rods and the magnitude of the change in  $k_{\text{eff}}$  caused by rod failure are in good agreement with the previous work documented in Ref. 7. The columns in the assembly are designated with a letter, from A to Q, and the rows are designated with numbers, from 1 to 17, as shown in Figure 7. The maximum  $k_{\text{eff}}$  increase is associated with rod H8 and is 0.15%  $\Delta k_{\text{eff}}$ .

Multiple rods are removed in groups, as discussed in Section 3.1.2.2. Groups of 2, 4, 8, 12, 16, 24, 32, 40, 44, 48, and 52 rods are considered. The  $k_{\text{eff}}$  increase is shown as a function of rods removed in Figure B-4. The limiting lattice is shown in Figure B-5. The maximum  $k_{\text{eff}}$  value occurs for 48 rods removed and corresponds to a  $k_{\text{eff}}$  increase of 2.01%  $\Delta k_{\text{eff}}$ .

**Table B-4. Single rod removal results for  
17 × 17 OFA in MPC-24**

Rod location	Increase in $k_{\text{eff}}$ (% $\Delta k_{\text{eff}}$ )
H8	0.15
H5	0.13
H7	0.13
G5	0.12
I7	0.12
I8	0.12
I4	0.11
G7	0.11
G6	0.11

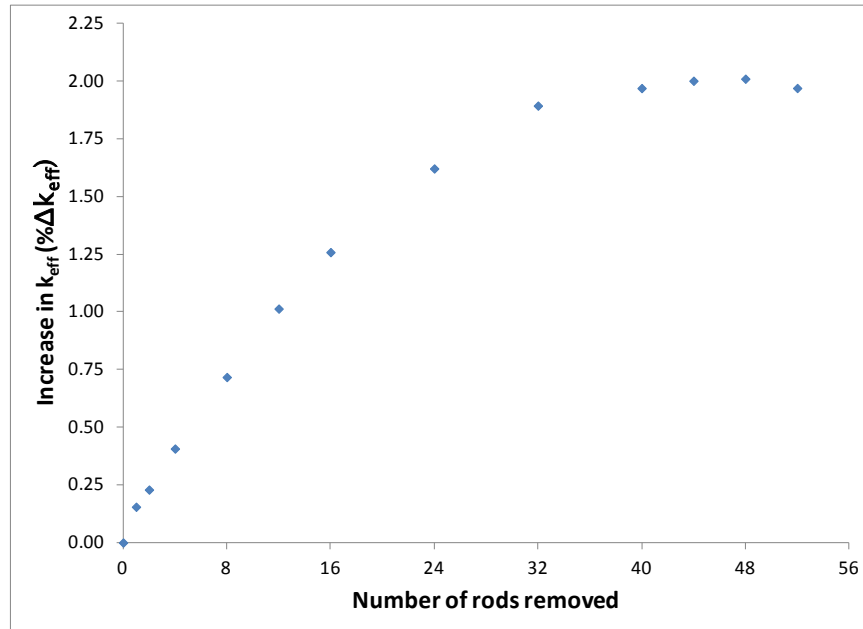
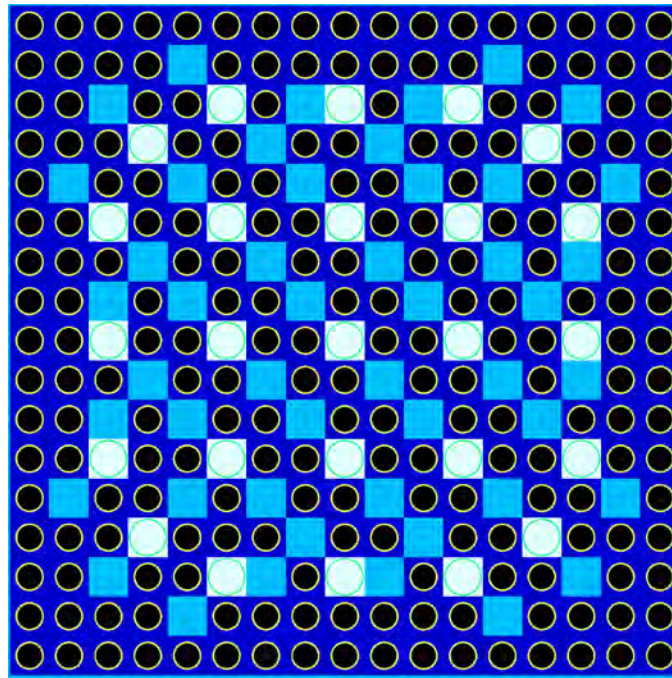


Figure B-4. Increase in  $k_{\text{eff}}$  in MPC-24 versus number of rods removed.



Notes:

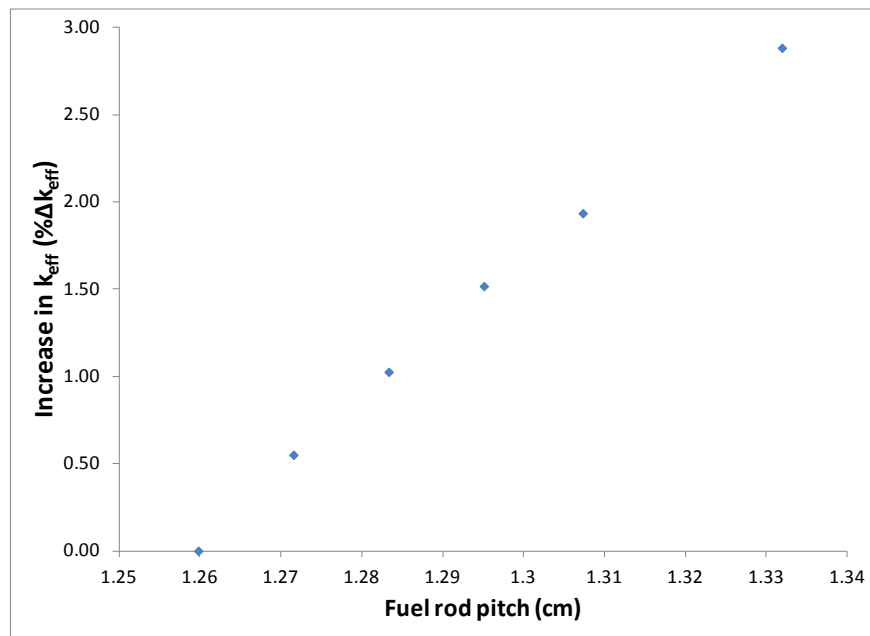
- Fuel shown in black
- Water is shown in light blue, dark blue, and white
- Guide/instrument tubes contain water shown in white
- Missing fuel rod locations shown in light blue

Figure B-5. Limiting multiple rod removal lattice (48 rods removed).

### B.2.1.3 Loss of Rod Pitch Control

The loss of rod pitch control is modeled as a uniform increase in fuel assembly pitch, as discussed above in Section 3.1.3. Two different fuel storage cell sizes exist in the MPC-24 basket, as discussed in Appendix D. The four oversized storage cells allow for a larger uniform pitch than the 20 standard storage cells. The fuel assemblies in each type of cell are expanded to account for the larger possible pitch in the oversized storage cells. The maximum increase in  $k_{\text{eff}}$  is 2.88%  $\Delta k_{\text{eff}}$  with cladding intact and 6.83%  $\Delta k_{\text{eff}}$  with cladding removed. The increase in  $k_{\text{eff}}$  as a function of fuel rod pitch is shown in Figure B-6. The pitch used in the standard and oversized storage cells is the same until the pitch reaches approximately 1.31 cm. For the largest pitch, the assemblies in the oversized storage cells have a larger pitch than those in the standard cells so that the fuel rods are in contact with the cell walls in both cell types. A portion of the limiting configuration model with cladding intact is shown in Figure B-7. This result agrees well with the results provided in Ref. 7. Radial nonuniform pitch, as discussed in Section 3.1.3.1, is not considered in the MPC-24 cask.

The MPC-24 cask contains fresh fuel, so the most reactive axial portion of the assembly is the center. For that reason, the birdcage analysis, as discussed in Section 3.1.3.2, includes two compressed pitch sections symmetrically positioned above and below the mid-plane of the assembly. A range of center section and compressed section lengths is considered. A figure showing the axial pitch variation is included as Figure B-8. There is no  $k_{\text{eff}}$  increase associated with an axially variable fuel rod pitch for the MPC-24 model beyond the 2.88%  $\Delta k_{\text{eff}}$  resulting from uniform pitch expansion.



**Figure B-6. Increase in  $k_{\text{eff}}$  in MPC-24 as a function of fuel rod pitch.**

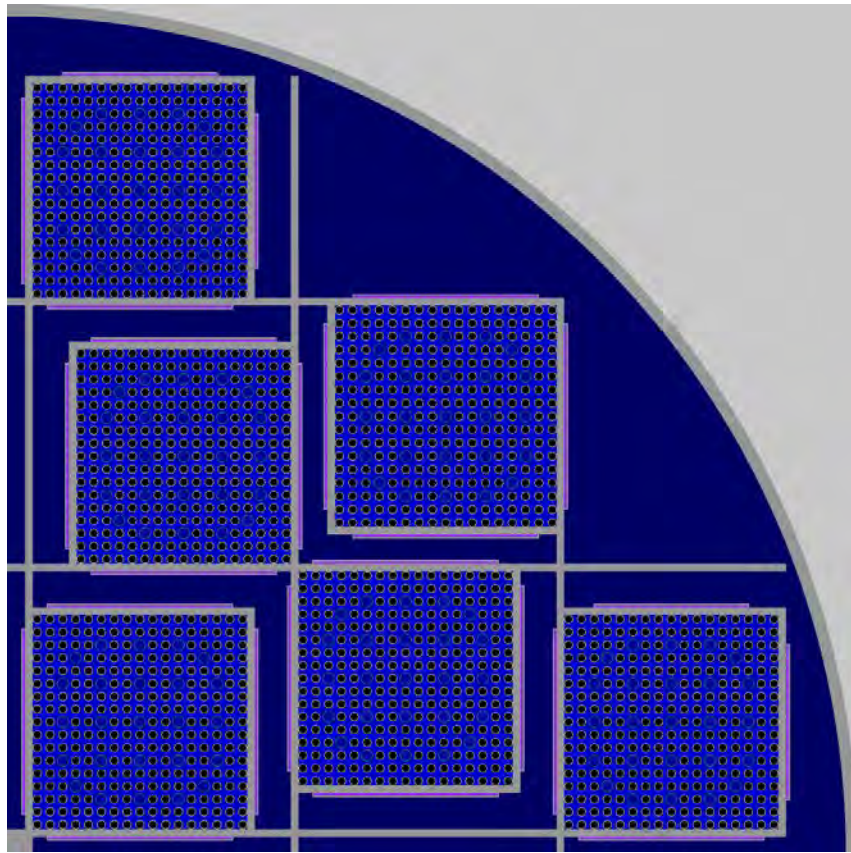


Figure B-7. Maximum pitch expansion case in MPC-24.

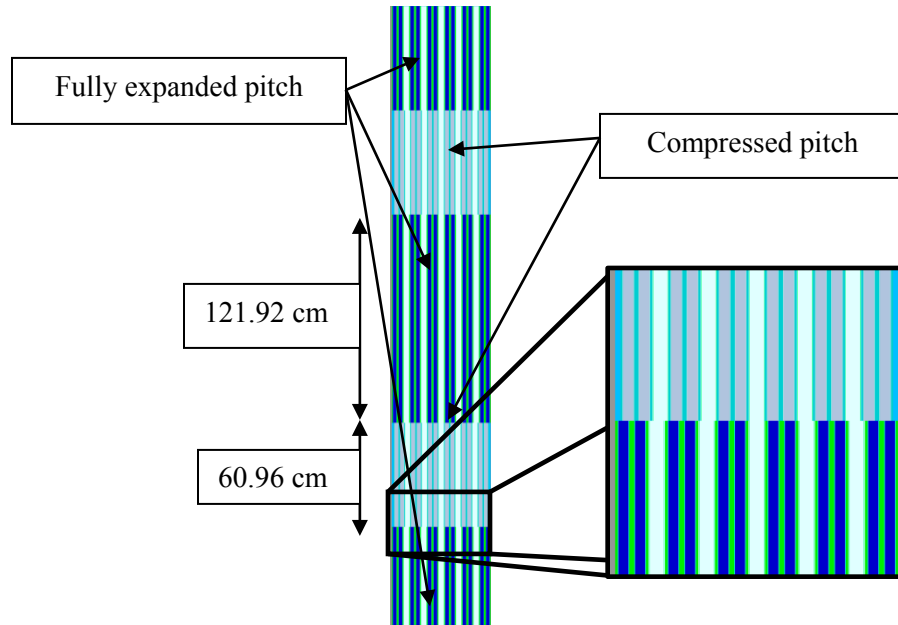


Figure B-8. Example axial variation of pitch expansion in MPC-24.

#### B.2.1.4 Loss of Assembly Position Control

Assembly misalignment is calculated over a range of displacements, as shown in Figure B-9. The consequence of the maximum misalignment is over 7%  $\Delta k_{\text{eff}}$ . A more limited misalignment case (20 cm) is also evaluated as a surrogate for potential degradation of assembly end fittings or the spacers used inside the cask to ensure proper assembly alignment. The consequence of this more limited misalignment case, shown in Figure B-10, is significantly less.

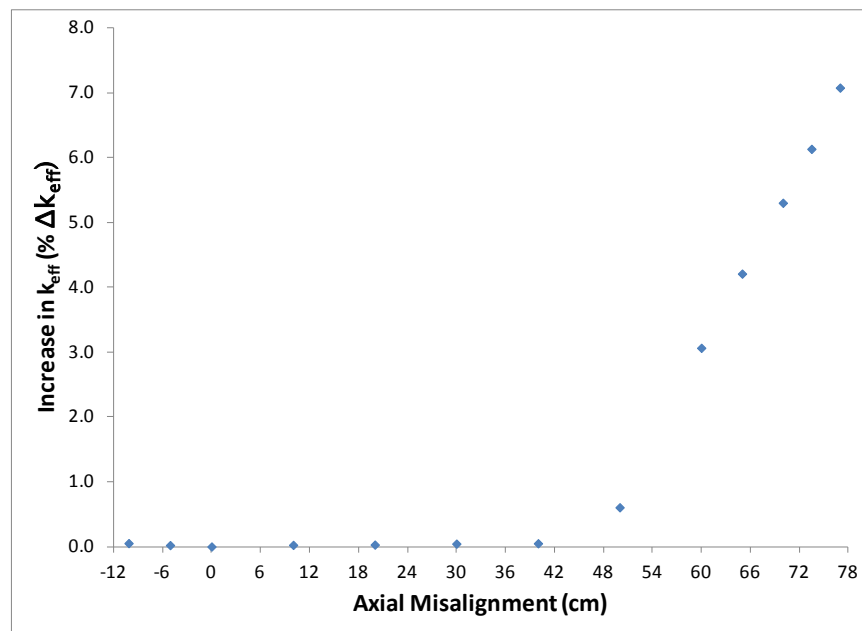


Figure B-9. Increase in  $k_{\text{eff}}$  as a function of axial assembly misalignment in MPC-24.

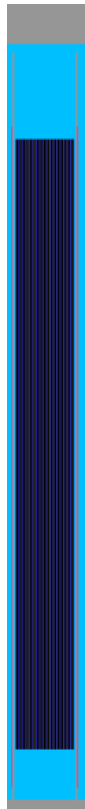
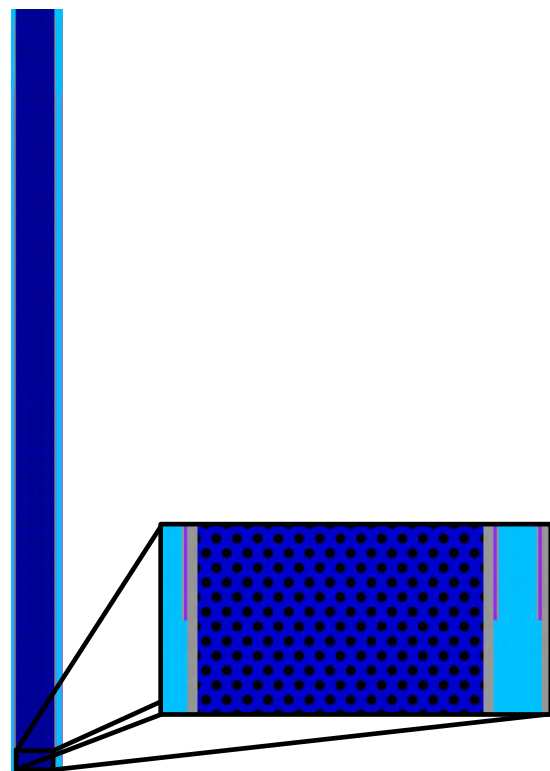


Figure B-10. Assembly in MPC-24 misaligned 20-cm toward cask lid.

#### B.2.1.5 Gross Assembly Failure

The two gross assembly failure configurations described in Section 3.1.5 are investigated in the MPC-24 cask. As expected, this configuration has the highest reactivity increase: the ordered pellet array case has a larger  $k_{\text{eff}}$  increase than the homogeneous rubble case. The  $k_{\text{eff}}$  increase in the homogeneous rubble case is over 8%  $\Delta k_{\text{eff}}$ , and the ordered pellet array case increases  $k_{\text{eff}}$  by over 13.5%  $\Delta k_{\text{eff}}$ . The gross assembly failure configurations are illustrated in Figure B-11 and Figure B-12. The configuration with homogeneous rubble contained only in the neutron absorber elevations is not considered in the MPC-24.

The results for the ordered pellet array case are significantly higher than those reported previously in Ref. 7. This is primarily because the array is also allowed to extend beyond the neutron absorber panel elevations. The homogeneous rubble case was not included in Ref. 7.



**Figure B-11. Ordered pellet array configuration for gross assembly failure.**

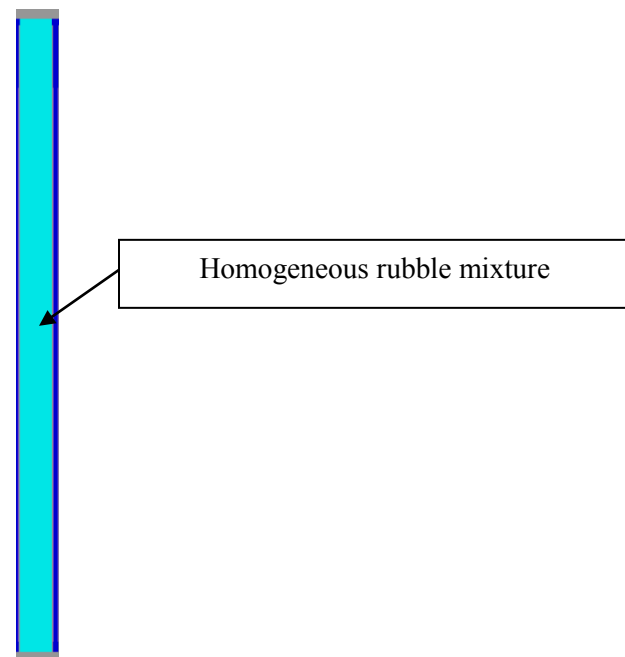
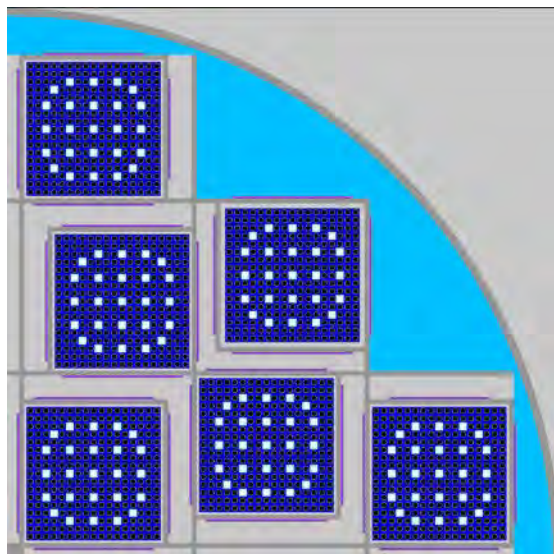


**Figure B-12. Homogeneous rubble configuration for gross assembly failure.**

### B.2.1.6 Preferential Flooding

The preferential flooding configuration that leaves the flux traps dry in the basket is considered only for the MPC-24 cask, as mentioned in Section B.1. The results indicate an increase in  $k_{\text{eff}}$  of more than 16.5%  $\Delta k_{\text{eff}}$ . A preferential flooding configuration is shown in Figure B-13.



Notes: Fuel shown in black  
Water is shown in light blue, dark blue, and white  
Guide/instrument tubes contain water shown in white  
Void in the basket and outside the cask is shown in light grey

**Figure B-13. Preferential flooding with only the fuel assemblies flooded.**

### B.2.1.7 Neutron Absorber Degradation

The results of the calculations, described in Section 3.1.6.1, considering a 5-cm neutron absorber defect at varying elevations are presented in Table B-5. As expected, the limiting elevation is at the centerline of the active fuel height. The model containing the 5-cm gap is shown in Figure B-14. The  $k_{\text{eff}}$  increase for this location is 0.35%  $\Delta k_{\text{eff}}$  and increases to 1.07%  $\Delta k_{\text{eff}}$  if the defect size is increased to 10 cm. As discussed in Section 3, these defects are assumed to be present at the same elevation in all neutron absorber panels within the cask.

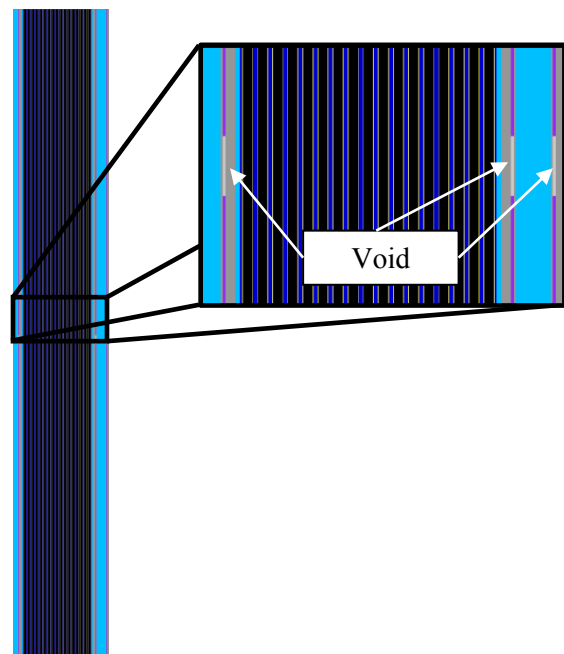
The results of the uniform absorber panel thinning calculations described in Section 3.1.6.3 are provided in Table B-6 and Figure B-15. A 50% decrease in panel thickness creates a 1.11% increase in  $k_{\text{eff}}$ . Complete removal of all neutron absorber material increases  $k_{\text{eff}}$  by over 11%  $\Delta k_{\text{eff}}$ , but the magnitude of the increase does not exceed 3%  $\Delta k_{\text{eff}}$  until more than 80% of the absorber has been eliminated.

**Table B-5. Increase in  $k_{\text{eff}}$  in MPC-24 caused by a 5-cm neutron absorber defect at various elevations**

Defect elevation midpoint (cm above bottom of active fuel)	Increase in $k_{\text{eff}}$ (% $\Delta k_{\text{eff}}$ )
2.50	0.03
91.44	0.28
182.88	0.35
274.32	0.26
363.26	0.03

**Table B-6. Increase in  $k_{\text{eff}}$  in MPC-24 caused by uniform neutron absorber panel thinning**

Fraction of neutron absorber panel thickness remaining	Increase in $k_{\text{eff}}$ (% $\Delta k_{\text{eff}}$ )
0.9	0.16
0.8	0.35
0.7	0.53
0.6	0.81
0.5	1.11
0.4	1.50
0.3	2.08
0.2	2.96
0.1	4.65
0.0	11.42

**Figure B-14. 5-cm gap in neutron absorber panels in MPC-24.**

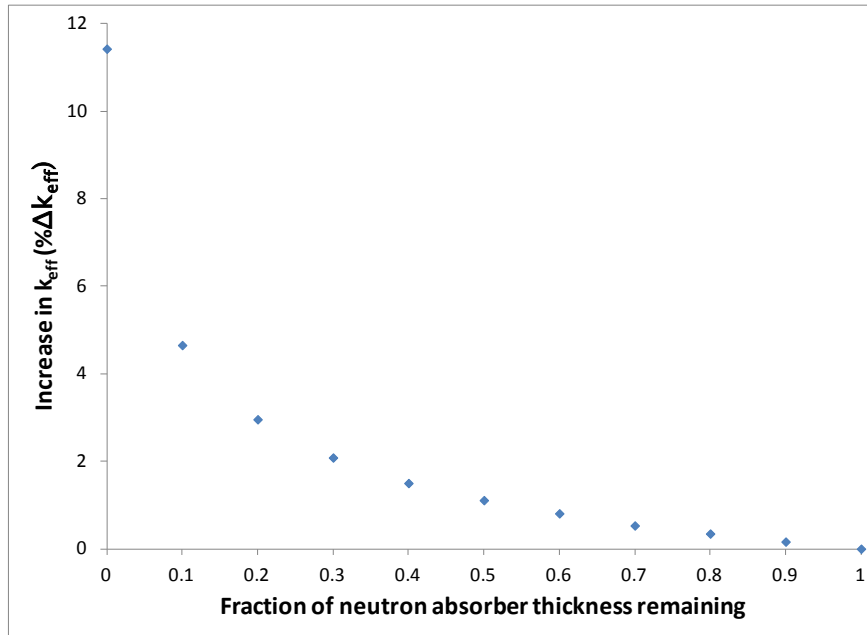
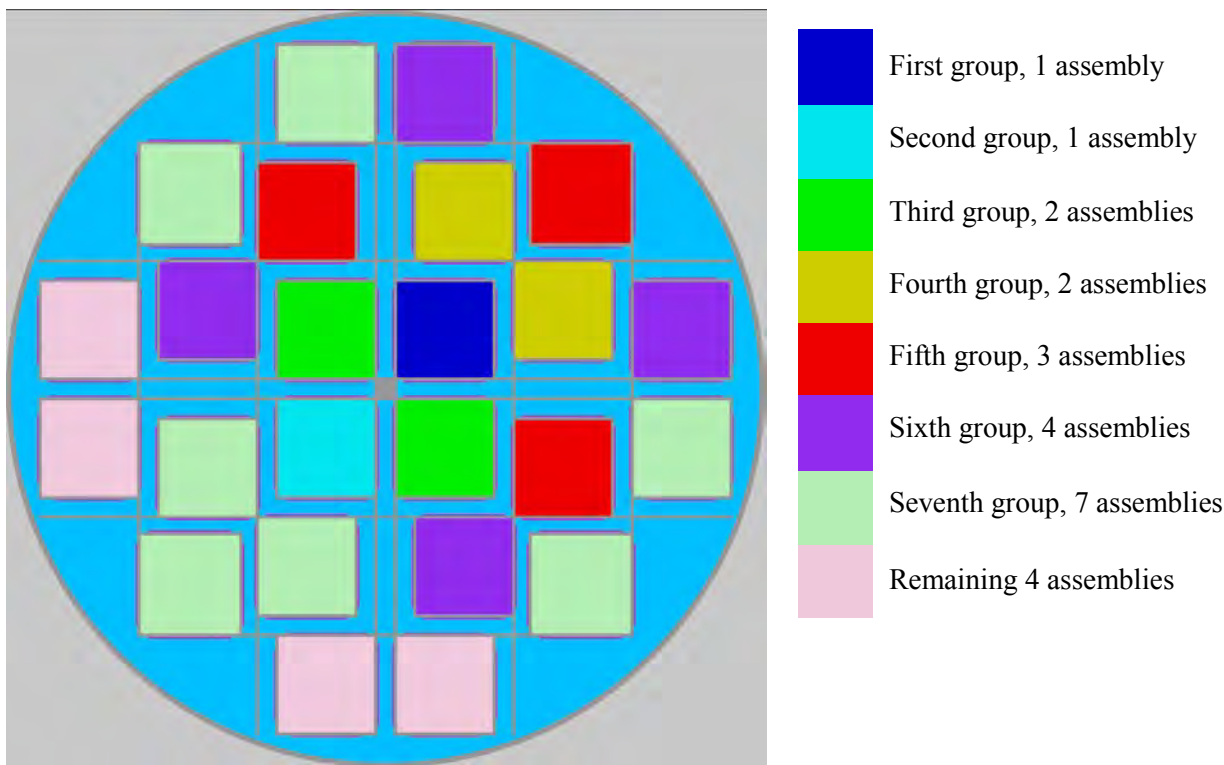


Figure B-15. Increase in  $k_{\text{eff}}$  in MPC-24 as a function of neutron absorber panel thickness.

### B.2.2 Varying Number of Reconfigured Assemblies

The results presented in Section B.2.1 assume that all 24 fuel assemblies in the MPC-24 cask experience the same fuel or neutron absorber reconfiguration within the respective configuration of interest. For each of four of the configurations studied in Section B.2.1, a series of calculations is performed to establish the  $k_{\text{eff}}$  increase as a function of the number of reconfigured assemblies within the cask. The four configurations considered are the limiting conditions for single rod failure, multiple rod failure, uniform rod pitch increase, and homogeneous rubble resulting from gross assembly failure.

The first fuel assembly to experience the reconfiguration being examined is selected in an attempt to maximize the  $k_{\text{eff}}$  increase, and is therefore one near the center of the cask. Additional assemblies are added in mostly symmetric groups of equal distance from the first reconfigured assembly. For some low numbers of reconfigured assemblies, multiple combinations of assemblies are considered. Seven combinations of reconfigured assemblies less are considered in the MPC-24. One order in which the assemblies experience reconfiguration is shown in Figure B-16.



**Figure B-16. One order of assembly reconfiguration in MPC-24 partial degradation configurations.**

### B.2.2.1 Rod Failures

The single and multiple rod failure configurations that result in the largest increase in  $k_{\text{eff}}$ , as discussed in Section B.2.1.2, are used to study the impact of some assemblies suffering reconfiguration while others in the cask remain intact. The results for single rod failure are shown below in Table B-7 and Figure B-17. The results for multiple rod failure are shown below in Table B-8 and Figure B-18. The portion of the  $k_{\text{eff}}$  impact introduced by each group of assemblies is similar for both configurations, with more than 50% of the reactivity change coming after only four assemblies experience reconfiguration. More than 75% of the  $k_{\text{eff}}$  change is caused by the first 13 assembly reconfigurations, which account for just over half the cask load. This indicates that a reduced number of reconfigured assemblies will not significantly reduce the  $k_{\text{eff}}$  increase associated with fuel reconfiguration if the degraded assemblies are in close proximity, and particularly if they are in the center region of the cask.

**Table B-7. Increase in  $k_{\text{eff}}$  in MPC-24, single rod failure**

Number of degraded assemblies	Increase in $k_{\text{eff}}$ (% $\Delta k_{\text{eff}}$ )
1	0.04
2	0.06
2	0.06
4	0.08
5	0.09
9	0.11
13	0.12
20	0.14
24	0.15

**Table B-8. Increase in  $k_{\text{eff}}$  in MPC-24, multiple rod failures  
(48 failed rods)**

Number of degraded assemblies	Increase in $k_{\text{eff}}$ (% $\Delta k_{\text{eff}}$ )
1	0.34
2	0.56
2	0.60
4	1.11
5	1.10
9	1.53
13	1.69
20	1.98
24	2.01

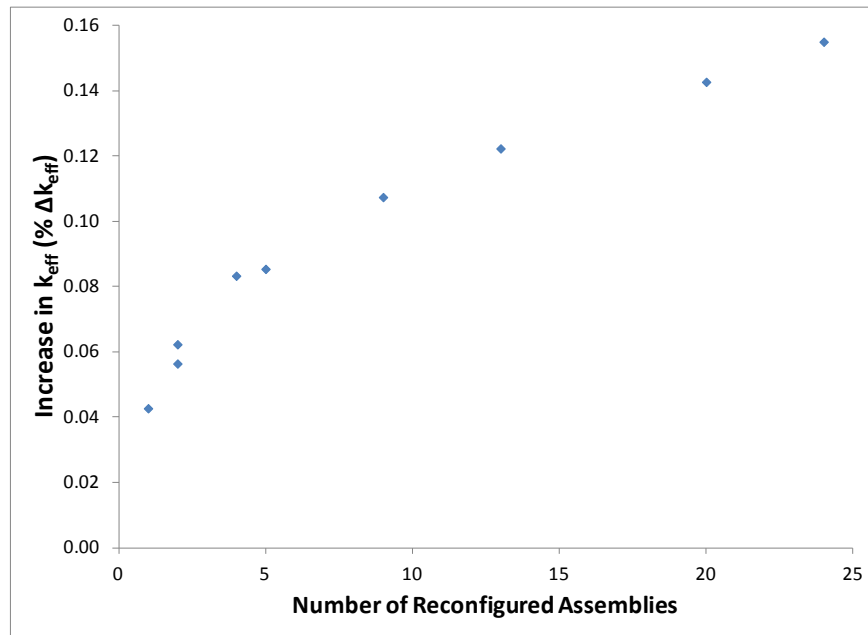


**Figure B-17.** Single rod failure results for a range of number of assemblies experiencing reconfiguration in MPC-24.

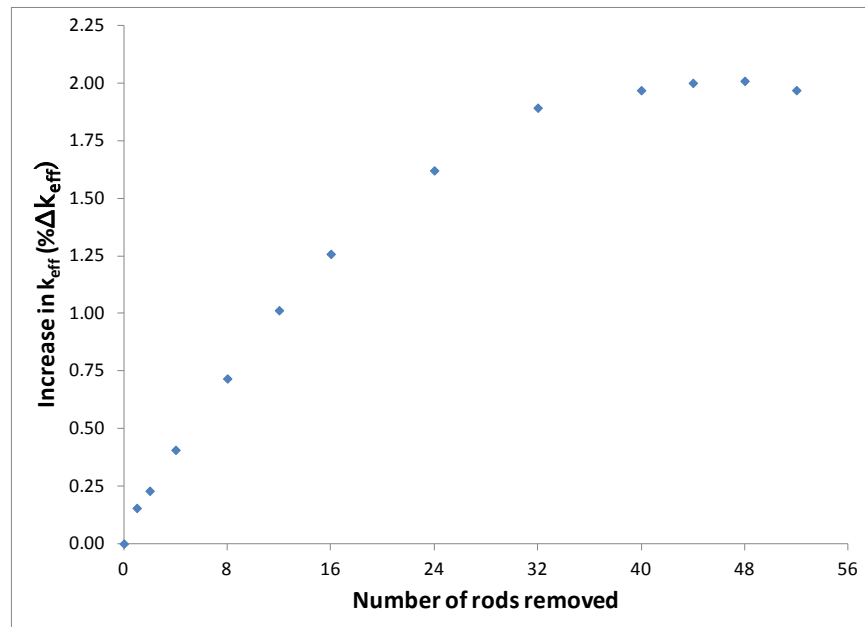


**Figure B-18.** Multiple rod failure results for a range of number of assemblies experiencing reconfiguration in MPC-24.

#### B.2.2.2 Loss of Rod Pitch Control, Uniform Pitch Increase

The maximum uniform pitch increase case is used to examine the  $k_{\text{eff}}$  impact of varying the number of assemblies that have experienced reconfiguration. The assembly configuration used for this study models

the outer row of fuel rods in contact with the inner wall of the fuel storage basket in each cell. The increase in  $k_{\text{eff}}$  for each number of reconfigured assemblies is provided in Table B-9 as well as Figure B-19. The general trend in the  $k_{\text{eff}}$  change for the uniform pitch increase cases is similar to that for single and multiple rod failure configurations presented in Section B.2.2.1. The first two reconfigured assemblies insert about 25% of the total  $k_{\text{eff}}$  increase, and 50% of the change has occurred with about five reconfigured assemblies. Approximately 80% of the increase in  $k_{\text{eff}}$  is caused by the first 13 reconfigured assemblies. This indicates that a reduced number of reconfigured assemblies will not significantly reduce the  $k_{\text{eff}}$  increase associated with fuel reconfiguration if the degraded assemblies are in close proximity, and particularly if they are in the center region of the cask.

**Table B-9. Increase in  $k_{\text{eff}}$  in MPC-24, uniform pitch increase**

Number of degraded assemblies	Increase in $k_{\text{eff}}$ (% $\Delta k_{\text{eff}}$ )
1	0.37
2	0.73
2	0.70
4	1.39
5	1.54
5	1.41
9	2.08
13	2.32
20	2.77
24	2.88

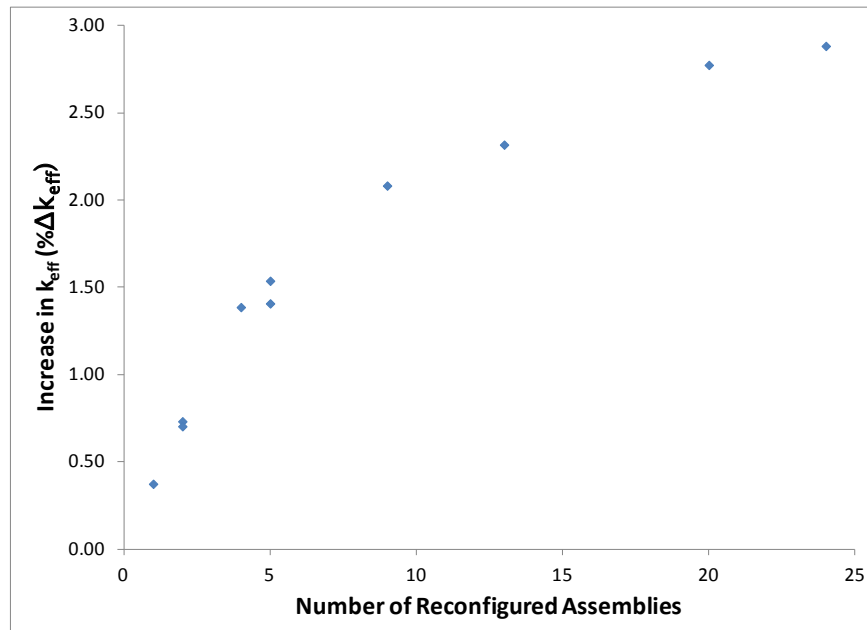


**Figure B-19. Uniform pitch increase results for a range of number of assemblies experiencing reconfiguration in MPC-24.**

### **B.2.2.3 Gross Assembly Failure, Homogeneous Rubble**

The homogeneous rubble modeling of the gross assembly failure configuration is the final configuration used to examine the  $k_{\text{eff}}$  impact of varying the number of assemblies that have experienced reconfiguration. The configuration used for this study models the homogeneous smear of fuel, cladding, and water filling the entire inside volume of the storage cell from the base plate to the lid of the cask. This configuration resulted in the largest  $k_{\text{eff}}$  increase of the homogeneous rubble configurations used in Section B.2.1.5. The increase in  $k_{\text{eff}}$  for each number of reconfigured assemblies is provided in Table B-10 as well as Figure B-20. The general trend in the  $k_{\text{eff}}$  change for the uniform pitch increase cases is different from that for single and multiple rod failure and uniform pitch expansion configurations presented in Sections B.2.2.1 and B.2.2.2. The first two reconfigured assemblies lower the cask  $k_{\text{eff}}$  because of the effects of homogenization and fissile material relocation. An increase in  $k_{\text{eff}}$  is noted for four or more reconfigured assemblies after a sufficient number of assemblies are reconfigured to relocate the most reactive portion of the cask to the top of the homogeneous rubble. Nearly 70% of the increase in  $k_{\text{eff}}$  is caused by the first nine reconfigured assemblies, and more than 80% of the total  $k_{\text{eff}}$  increase results from the reconfiguration of 13 assemblies. This indicates that a reduced number of reconfigured assemblies will not significantly reduce the  $k_{\text{eff}}$  increase associated with fuel reconfiguration if the degraded assemblies are in close proximity, and particularly if they are in the center region of the cask.

**Table B-10. Increase in  $k_{\text{eff}}$  in MPC-24, homogeneous rubble configuration of gross assembly failure**

Number of degraded assemblies	Increase in $k_{\text{eff}}$ (% $\Delta k_{\text{eff}}$ )
1	0.00
2	-0.04
2	-0.03
4	2.39
5	2.21
9	5.68
13	6.68
20	7.92
24	8.23

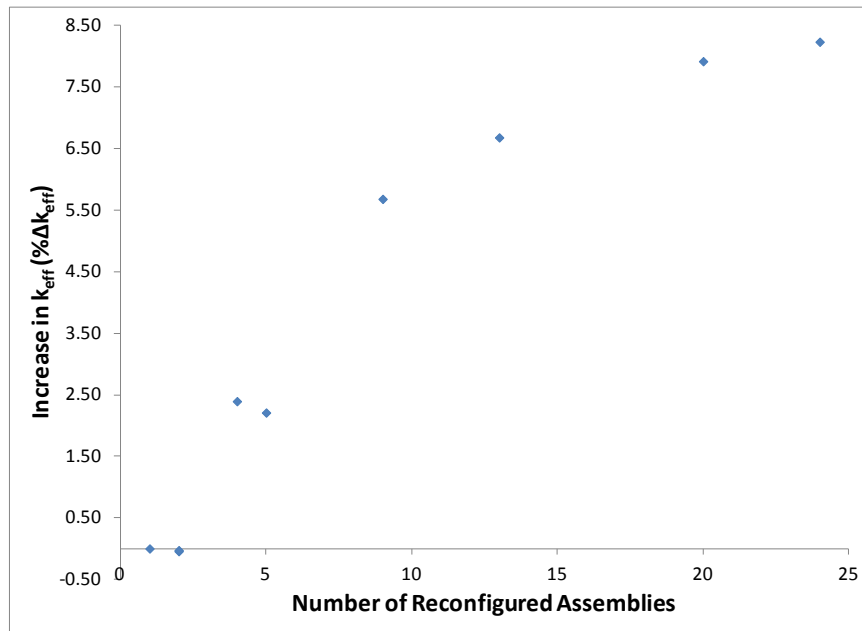


**Figure B-20. Homogeneous rubble results for a range of number of assemblies experiencing reconfiguration.**

### B.2.3 Combined Configurations

As discussed in Section 3.3, some of the mechanisms that could result in fuel reconfigurations could result in a combination of reconfigurations. Combined configurations are evaluated including: 12 failed rods with 50% clad thinning and 12 failed rods with a uniform pitch increase of 0.023-cm.

The multiple rod failure results presented in Section B.2.1.2 indicate that the failure of 12 fuel rods results in an increase in  $k_{\text{eff}}$  of just over 1%  $\Delta k_{\text{eff}}$ . This is approximately half the maximum increase for multiple failed rod configurations and is therefore selected as an intermediate configuration. The pitch increase is approximately half of the maximum pitch increase in the 20 normal storage cells. Based on the results presented in Figure B-6, the  $k_{\text{eff}}$  increase associated with a fuel rod pitch increase of approximately 0.02 cm is around 1%  $\Delta k_{\text{eff}}$ . The cladding thickness on all intact rods in both combined configurations is represented with 50% of the nominal thickness.

The results of the two combined configurations considered in the MPC-24 cask are presented in Table B-11. For comparison, the  $k_{\text{eff}}$  increase assuming each degraded configuration separately and the sum of the two is provided. The increase in  $k_{\text{eff}}$  associated with explicit modeling of the combined configurations is less than the estimated increase based on summing the individual increases. The conservatism of adding the separate effects is less than 0.5%  $\Delta k_{\text{eff}}$ . It appears that the linear combination of the  $k_{\text{eff}}$  increases is conservative, but more combined configurations would need to be investigated prior to drawing general conclusions. If it is confirmed, the  $k_{\text{eff}}$  increase caused by combinations of degradations could be conservatively bounded by adding the increase associated with individual configurations where applicable.

**Table B-11. Increase in  $k_{\text{eff}}$  in combined configurations for MPC-24**

Case	Increase in $k_{\text{eff}}$ (% $\Delta k_{\text{eff}}$ )
<b>Multiple failed rods and clad thinning</b>	
12 failed rods	1.01
50% clad thinning	2.87
Sum of $k_{\text{eff}}$ increases	3.88
Combined configuration model	3.45
Overestimation of $k_{\text{eff}}$ increase by summing individual effects	0.43
<b>Multiple failed rods and 0.02-cm increase in fuel rod pitch</b>	
12 failed rods	1.01
Uniform pitch increase	1.03
Sum of $k_{\text{eff}}$ increases	2.04
Combined configuration model	1.88
Overestimation of $k_{\text{eff}}$ increase by summing individual effects	0.16

### B.3 MPC-24 CASK SUMMARY

The detailed results for each configuration considered in the MPC-24 are provided above in Section B.2 and summarized in Table B-2.

The highest  $k_{\text{eff}}$  impact involves the preferential flooding of the cask basket in such a way as to moderate the fuel but leave the flux traps dry. The flux traps are an essential feature of the cask, and the basket is designed to make this preferential flooding configuration impossible. The preferential flooding configuration is thus viewed as not credible for normal conditions of transport. The configuration is included here to emphasize the importance of maintaining flux trap integrity despite any degradation of fuel, basket, or cask materials that occur during ES.

Other significant  $k_{\text{eff}}$  increases result from the gross assembly failure configurations and large axial misalignments. The gross assembly failure and misalignment configurations are judged not to be credible, so the  $k_{\text{eff}}$  increase associated with these configurations does not require mitigation. Fuel assembly misalignment of as much as 50 cm results in a  $k_{\text{eff}}$  increase of less than 1%  $\Delta k_{\text{eff}}$ , as shown in Figure B-9. Fuel assembly axial position will be sufficiently controlled that the more extreme misalignments need not be considered. The remaining degraded configurations all have  $k_{\text{eff}}$  increases less than 3%  $\Delta k_{\text{eff}}$ . The consequences of potential fuel reconfiguration are therefore judged to be manageable. The  $k_{\text{eff}}$  increase is small enough that the cask will be subcritical considering a safety analysis with intact fuel, which demonstrates that  $k_{\text{eff}}$  will be less than 0.95. This would not, however, be in compliance with current regulations relating to transportation of fissile material.

Analyses of a range of assemblies experiencing reconfiguration are documented in Section B.2.2. Four configurations, listed in Section 3.2, are evaluated, and the relative increase in  $k_{\text{eff}}$  as a function of the number of assemblies experiencing reconfiguration is largely similar among all four configurations. This approach is unlikely to produce a significant reduction in the increase in  $k_{\text{eff}}$  because the majority of the increase is associated with a relatively small fraction of the fuel load suffering reconfiguration if the reconfigured assemblies are selected in a worst-case, deterministic approach.

Two configurations are also investigated in Section B.2.3 that are created by combining two different reconfiguration paths. An intermediate number of failed rods, in this case 12, is combined with clad thinning in one case and with uniform pitch expansion in another. In both cases, the sum of the  $k_{\text{eff}}$

increases of each separate reconfiguration is slightly less than the increase determined from an explicit model of the combined configurations.

## Appendix C

### Sensitivity to Burnup and Cooling Time

A range of post-irradiation cooling times is considered in these analyses for both PWR and BWR fuel. Reference 44 provides details on the reactivity changes experienced by used fuel as a function of time since discharge. For the “Set 2” isotopes considered in these analyses, the reactivity of the depleted fuel decreases fairly steadily between 5 and about 100 years after discharge. The primary decays that drive this change are  $^{241}\text{Pu}$  into  $^{241}\text{Am}$  (14.4-year half-life) and  $^{155}\text{Eu}$  into  $^{155}\text{Gd}$  (4.8-year half-life). Beyond about 100 years after discharge, the reactivity of the fuel increases primarily due to the decay of  $^{241}\text{Am}$  (433-year half-life) and  $^{240}\text{Pu}$  (6561-year half-life). This increase continues until about 20,000 years after discharge. A plot for used PWR fuel considering the “Set 2” isotopes is shown in Figure C-1 and is expected to be similar for BWR fuel as well. Note that the maximum reactivity of used fuel considering “Set 2” isotopes occurs at discharge, and the reactivity after 5 years of cooling time is higher than the subsequent local maximum around 20,000 years later. These analyses considered cooling times ranging from 5 years to 300 years, with explicit reconfiguration calculations at cooling times of 5, 80, and 300 years. The effects of cooling time on the various configurations are considered, and they are discussed in more detail in the following subsections.

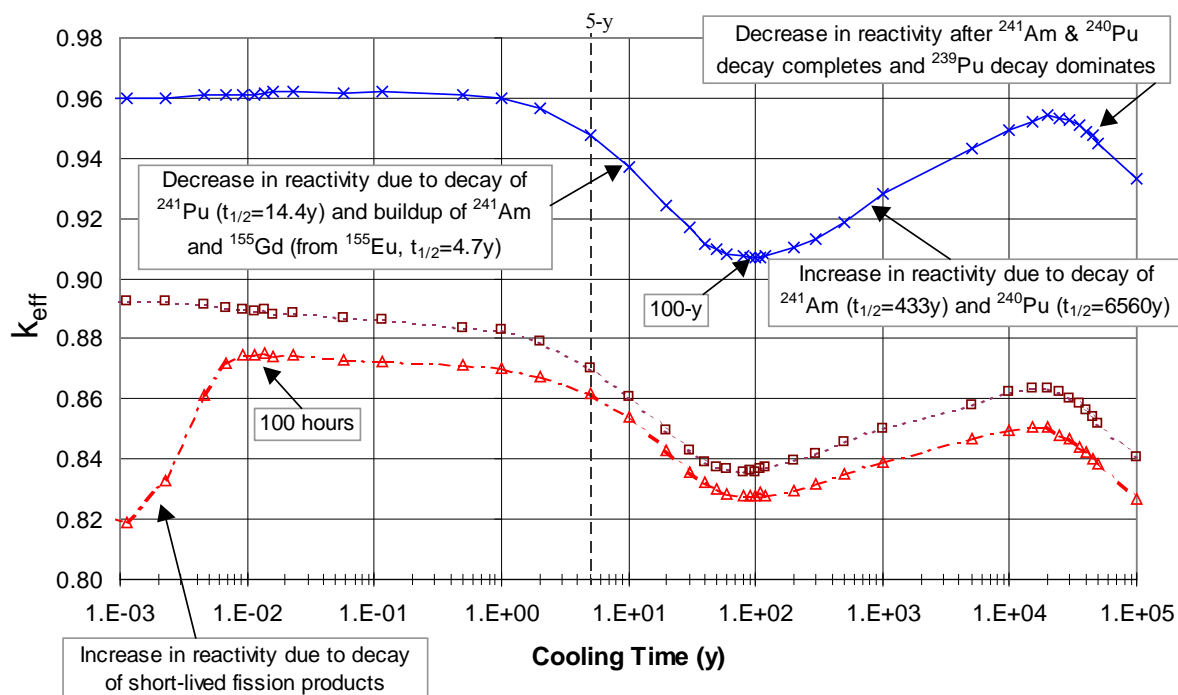


**Figure C-1. Reactivity behavior of fuel with cooling time in a GBC-32 cask (4.0 w/o 40 GWd/MTU burnup) [44].**

## C.1 RESULTS FOR GBC-32 CASK

As discussed in Section 4.2.1, a range of initial fuel enrichments is considered to generate a representative loading curve for fuel to be stored in the GBC-32. The burnup limit for loading fuel with an initial enrichment of 5 w/o  $^{235}\text{U}$  is determined to be approximately 44.25 GWd/MTU with 5 years of post-irradiation cooling time. Fuel with a discharge burnup of 70 GWd/MTU is also considered in the GBC-32 to investigate any potential sensitivity of the consequences of fuel reconfiguration to burnup. For both 5 w/o initial enrichment burnups, cooling times of 5, 80 and 300 years are considered to examine potential impacts of cooling time on the consequences of fuel reconfiguration.

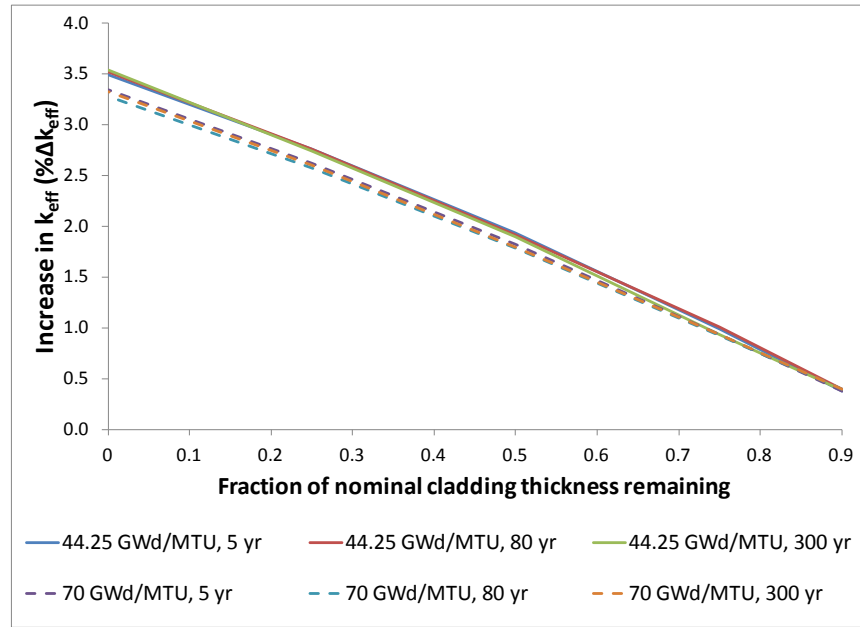
The nominal condition  $k_{\text{eff}}$  values are provided in Table C-1. The reduction in  $k_{\text{eff}}$  caused by cooling time increases with burnup, which is expected given the larger inventory of  $^{241}\text{Am}$  and  $^{155}\text{Gd}$  at higher burnups. The 80-year cooling time also has the smallest  $k_{\text{eff}}$  for intact fuel, which is also expected as discussed above. It should be noted that the nominal  $k_{\text{eff}}$  values after 300 years of cooling time are still significantly lower than those after 5 years of cooling time. This decrease in  $k_{\text{eff}}$  for intact fuel would have to be exceeded by a larger  $k_{\text{eff}}$  increase due to reconfiguration before the longer cooling time case would represent a limiting condition. The results of explicit reconfiguration calculations are presented in subsequent subsections and compared to the differences in nominal  $k_{\text{eff}}$  values.

**Table C-1. Nominal  $k_{\text{eff}}$  results for enrichment, burnup, and cooling time cases considered in GBC-32**

Enrichment (w/o $^{235}\text{U}$ )	Burnup (GWd/MTU)	Cooling time (years)	KENO V.a		KENO-VI	
			$k_{\text{eff}}$	$\sigma$	$k_{\text{eff}}$	$\sigma$
5.0	44.25	5	0.94000	0.00010	0.93995	0.00010
		80	0.90003	0.00010	0.89991	0.00010
		300	0.90477	0.00010	0.90473	0.00010
	70.0	5	0.85040	0.00010	0.85048	0.00010
		80	0.78863	0.00010	0.78865	0.00010
		300	0.79472	0.00010	0.79478	0.00010

### C.1.1 Clad Thinning/Loss

The increase in  $k_{\text{eff}}$  associated with clad thinning and removal is shown as a function of remaining cladding thickness in Figure C-2 for fuel of both burnups and all three cooling times. There is a trend that the increase in  $k_{\text{eff}}$  is smaller at 70 GWd/MTU than it is at 44.25 GWd/MTU. The increase in  $k_{\text{eff}}$  is approximately 0.04%  $\Delta k_{\text{eff}}$  larger after 300 years of cooling time than it is after 5 years, but this difference is very small compared to the change in nominal  $k_{\text{eff}}$ . These results show that the increase in  $k_{\text{eff}}$  shown in Section 5.1.1.1 is sufficiently large.

Figure C-2. Increase in  $k_{\text{eff}}$  as a function of cladding thickness remaining.

### C.1.2 Rod Failures

The results of the single and multiple rod failure configurations of fuel rod failure are provided in Table C-2 and Table C-3, respectively. The variation of the increase in  $k_{\text{eff}}$  for single rod removal is small and shows no significant trends as a function of burnup or cooling time. The multiple rod removal results show a clear trend of reduced consequence at high burnup compared to moderate burnup; thus, the 44.25 GWd/MTU cases manifest a larger  $k_{\text{eff}}$  increase. The effect of cooling time appears to be significantly smaller, with essentially no sensitivity at 44.25 GWd/MTU, and only a reduction in the consequence of reconfiguration at longer cooling times for the high-burnup fuel. These results indicate that the  $k_{\text{eff}}$  increases identified in Section 5.1.1.2 are limiting.

Table C-2. Single rod removal results for 17 × 17 OFA in GBC-32

Burnup (GWd/MTU)	Cooling time (years)	Location	Increase in $k_{\text{eff}}$ (% $\Delta k_{\text{eff}}$ )
44.25	5	H5	0.10
44.25	80	H7	0.09
44.25	300	G7	0.10
70	5	H5	0.09
70	80	G7	0.10
70	300	G5	0.10

**Table C-3. Multiple rod removal results for 17 × 17 OFA in GBC-32**

Burnup (GWd/MTU)	Cooling time (years)	Increase in $k_{\text{eff}}$ (% $\Delta k_{\text{eff}}$ )
44.25	5	1.86
44.25	80	1.86
44.25	300	1.87
70	5	1.69
70	80	1.62
70	300	1.62

**C.1.3 Loss of Rod Pitch Control**

The increase in  $k_{\text{eff}}$  resulting from uniform pin pitch expansion for both burnups and all three cooling times is considered for the configuration in which the unit cell boundary contacts the inside surface of the storage cell wall. The use of this less extreme case provides an acceptable indication of the sensitivity of the consequence of this configuration to burnup and cooling time variations. The results of the fully expanded configuration, with cladding, are presented below in Table C-4. Moderate sensitivities are apparent that lower the impact of reconfiguration both with increasing burnup and with increasing cooling time for a fixed burnup. These results provide confidence that the results presented in Section 5.1.1.3 are limiting.

**Table C-4. Increase in  $k_{\text{eff}}$  caused by uniform fuel pin pitch expansion**

Burnup (GWd/MTU)	Cooling time (years)	Increase in $k_{\text{eff}}$ (% $\Delta k_{\text{eff}}$ )
44.25	5	1.69
44.25	80	1.67
44.25	300	1.66
70	5	1.53
70	80	1.44
70	300	1.42

**C.1.4 Loss of Assembly Position Control**

The increase in  $k_{\text{eff}}$  caused by a 20-cm axial misalignment for both burnups and all three cooling times is presented in Table C-5. The results show that the consequence of fuel displacement increases with both burnup and cooling time. The maximum change relative to the 44.25 GWd/MTU and 5-year cooling is approximately 1.67%  $\Delta k_{\text{eff}}$ . This is a significant increase and occurs for 70 GWd/MTU and 300 years of cooling time. The reduction in base case  $k_{\text{eff}}$  due only to cooling time at this burnup is over 5.5%  $\Delta k_{\text{eff}}$ . The 300-year cooling time condition with only 44.25-GWd/MTU burnup causes an increase that is larger by 0.95%  $\Delta k_{\text{eff}}$ . For this case, the decrease in nominal (i.e., 44.25 GWd/MTU and 300-year cooling time)  $k_{\text{eff}}$  is more than 3.5%  $\Delta k_{\text{eff}}$ , when compared to the  $k_{\text{eff}}$  value for the case with only 5 years of cooling time. These results indicate that the results presented in Section 5.1.1.4 are large enough to account for additional impacts at high burnup and long cooling times.

**Table C-5. Increase in  $k_{\text{eff}}$  for limited assembly axial displacement in GBC-32**

Burnup (GWd/MTU)	Cooling time (years)	Increase in $k_{\text{eff}}$ (% $\Delta k_{\text{eff}}$ )
44.25	5	10.82
44.25	80	11.82
44.25	300	11.77
70	5	11.74
70	80	12.46
70	300	12.49

### C.1.5 Gross Assembly Failure

The results for both configurations of gross assembly failure are provided for both burnups and all three cooling times in Table C-6. Both the uniform pellet array and the homogeneous rubble configuration show little sensitivity to burnup but a larger increase in  $k_{\text{eff}}$  with increasing cooling time. The increases are smaller for the uniform pellet array configuration than for the homogeneous rubble configuration. The maximum difference is for fuel with 44.25-GWd/MTU burnup and 300 years of cooling time and is approximately 1.04%  $\Delta k_{\text{eff}}$ . The decrease in nominal  $k_{\text{eff}}$  for this fuel condition is more than 3.5%  $\Delta k_{\text{eff}}$ , so the results in Section 5.1.1.5 are sufficiently large to account for variations associated with higher burnups and longer cooling times.

**Table C-6. Increase in  $k_{\text{eff}}$  caused by gross fuel assembly failure in GBC-32**

Burnup (GWd/MTU)	Cooling time (years)	Increase in $k_{\text{eff}}$ (% $\Delta k_{\text{eff}}$ )
<b>Ordered pellet array</b>		
44.25	5	21.37
44.25	80	22.21
44.25	300	22.21
70	5	21.43
70	80	21.63
70	300	21.77
<b>Homogeneous rubble</b>		
44.25	5	14.30
44.25	80	15.29
44.25	300	15.34
70	5	14.20
70	80	14.77
70	300	14.90

### C.1.6 Neutron Absorber Degradation

The increase in  $k_{\text{eff}}$  caused by neutron absorber panel defects is shown in Table C-7 for both burnups and all three cooling times for defect sizes of both 5 and 10 cm. The results show an increase in the consequence of panel degradation at higher burnups and higher cooling times. The maximum change in

$k_{\text{eff}}$  increase is approximately 0.3%  $\Delta k_{\text{eff}}$ , which is significantly smaller than the lower nominal  $k_{\text{eff}}$  at the higher burnups and cooling times. The results presented in Section 5.1.1.6 for the neutron absorber panel defect configuration are therefore large enough to account for the effects of higher burnups and cooling times.

The increase in  $k_{\text{eff}}$  increase due to uniform neutron absorber panel thinning at 44.25 GWd/MTU and 5 years of cooling time are shown in Table C-8. The increase in  $k_{\text{eff}}$  is smaller at the higher burnup, thus confirming that the results presented in Section 5.1.1.6 for uniform panel thinning are also conservative.

**Table C-7. Increase in  $k_{\text{eff}}$  caused by neutron absorber panel defects**

Burnup (GWd/MTU)	Cooling time (years)	Defect elevation (cm)	Increase in $k_{\text{eff}}$ (% $\Delta k_{\text{eff}}$ )
5-cm defect			
44.25	5	348.86	1.05
44.25	80	348.86	1.22
44.25	300	348.86	1.21
70	5	348.86	1.17
70	80	348.86	1.24
70	300	348.86	1.24
10-cm defect			
44.25	5	348.86	2.33
44.25	80	348.86	2.59
44.25	300	348.86	2.56
70	5	348.86	2.54
70	80	348.86	2.59
70	300	348.86	2.63

**Table C-8. Increase in  $k_{\text{eff}}$  caused by uniform neutron absorber panel thinning (44.25 GWd/MTU burnup, 5-year cooling time)**

Fraction of neutron absorber panel thickness remaining	Increase in $k_{\text{eff}}$ (% $\Delta k_{\text{eff}}$ )
0.9	0.25
0.8	0.53
0.7	0.87
0.6	1.26
0.5	1.72
0.4	2.30
0.3	2.99
0.2	3.94
0.1	5.36
0.0	8.46

## C.2 RESULTS FOR MPC-68 CASK

As discussed in Section 4.2.2, a range of burnups and cooling times is considered to investigate the sensitivity of the consequence of reconfiguration to these parameters. Fuel with a discharge burnup of 70 GWd/MTU is considered in the MPC-68 in addition to the fresh fuel and 35-GWd/MTU burnup used discussed in Section 5.2. For fuel with 5 w/o initial enrichment and both 35-GWd/MTU and 70-GWd/MTU burnups, cooling times of 5, 80, and 300 years are considered to examine potential impacts of cooling time on the consequences of fuel reconfiguration.

The nominal condition  $k_{\text{eff}}$  values are provided in Table C-9. The reduction in  $k_{\text{eff}}$  caused by cooling time increases with burnup, which is expected given the larger inventory of  $^{241}\text{Am}$  and  $^{155}\text{Gd}$  at higher burnups. The 80-year cooling time also has the smallest  $k_{\text{eff}}$  for intact fuel, which is also expected as discussed above. It should be noted that the nominal  $k_{\text{eff}}$  values after 300 years of cooling time are still lower than after 5 years of cooling time. This decrease in  $k_{\text{eff}}$  for intact fuel would have to be exceeded by a larger  $k_{\text{eff}}$  increase due to reconfiguration before the longer cooling time case would represent a limiting condition. The reductions in nominal  $k_{\text{eff}}$  values for the BWR fuel in the MPC-68 are significantly smaller than those experienced by the PWR fuel in GBC-32, despite similar assembly average burnup values. This effect is the result of the extreme burnup profile, described in Appendix E, which has very low relative burnups in the top few nodes. These lower burnups lead to lower inventories of  $^{241}\text{Am}$  and  $^{155}\text{Eu}$  in the upper regions of the assembly which drive reactivity of the overall cask. These lower inventories lead to smaller changes in  $k_{\text{eff}}$  due to radioactive decay during the period of post-irradiation cooling. The results of explicit reconfiguration calculations are presented in subsequent subsections and compared to the differences in nominal  $k_{\text{eff}}$  values.

**Table C-9. Nominal  $k_{\text{eff}}$  results for enrichment, burnup, and cooling time cases considered in MPC-68, channeled and unchanneled fuel**

Channel present	Burnup (GWd/MTU)	Cooling time (years)	KENO V.a		KENO-VI	
			$k_{\text{eff}}$	$\sigma$	$k_{\text{eff}}$	$\sigma$
Yes	35.0	0	0.96800	0.00010	0.96828	0.00010
		5	0.83269	0.00010	0.83258	0.00010
		80	0.82425	0.00010	0.82416	0.00010
	70.0	300	0.82522	0.00010	0.82528	0.00010
		5	0.76709	0.00010	0.76693	0.00010
		80	0.75256	0.00010	0.75240	0.00010
	0	300	0.75412	0.00010	0.75405	0.00010
		0	0.96768	0.00010	0.96763	0.00010
		5	0.83434	0.00010	0.83420	0.00010
No	35.0	80	0.82615	0.00010	0.82621	0.00010
		300	0.82723	0.00010	0.82714	0.00010
		5	0.76994	0.00010	0.76971	0.00010
	70.0	80	0.75588	0.00010	0.75560	0.00010
		300	0.75731	0.00010	0.75705	0.00010

### C.2.1 Clad Thinning/Loss

The increase in  $k_{\text{eff}}$  associated with clad thinning and removal is shown as a function of remaining cladding thickness in Figure C-3 for fresh fuel and fuel of both burnups and all three cooling times. There

is a trend that the increase in  $k_{\text{eff}}$  is smaller with increasing burnup. There is no clear trend in the increase of  $k_{\text{eff}}$  as a function of cooling time. These results show that the increase in  $k_{\text{eff}}$  reported for fresh fuel in Section 5.2.1.1 bounds the effects of burnup and cooling time.

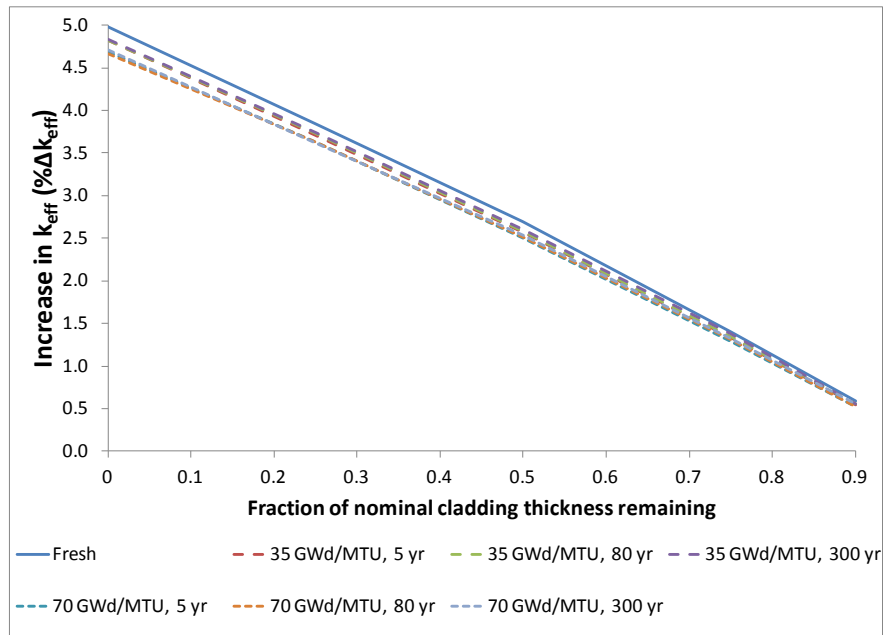


Figure C-3. Increase in  $k_{\text{eff}}$  as a function of cladding thickness remaining.

### C.2.2 Rod Failures

The results of fuel reconfiguration calculations for the single and multiple rod removal configurations are shown below in Table C-10 and Table C-11, respectively. For single rod failure configurations, no sensitivity is apparent as a function of either burnup or cooling time. The fresh fuel single rod removal  $k_{\text{eff}}$  increase is larger than the results for UNF cases. For multiple rod failure configurations, a slight trend appears to cause small increases in  $k_{\text{eff}}$  change with cooling time but a decrease in  $k_{\text{eff}}$  change at high burnup. The largest difference compared to the results presented in Section 5.2.1.2 is approximately 0.02%  $\Delta k_{\text{eff}}$  and occurs for multiple rod failure and UNF with 300 years of cooling time. At this cooling time, the nominal  $k_{\text{eff}}$  is approximately 0.75%  $\Delta k_{\text{eff}}$  lower than the 5-year cooling time base case  $k_{\text{eff}}$  value. These results indicate that the increase in  $k_{\text{eff}}$  reported in Section 5.2.1.2 is sufficiently large to account for potential effects of additional burnup and cooling time for rod failure configurations.

**Table C-10. Single rod removal results for GE  $10 \times 10$  fuel  
in MPC-68, intact channel**

Burnup (GWd/MTU)	Cooling time (years)	Location	Increase in $k_{\text{eff}}$ (% $\Delta k_{\text{eff}}$ )
0	0	H7	0.29
35	5	G7	0.26
35	80	D4	0.27
35	300	G7	0.28
70	5	D3	0.26
70	80	G7	0.25
70	300	G7	0.26

**Table C-11. Multiple rod removal results for  
GE  $10 \times 10$  fuel in MPC-68, intact channel**

Burnup (GWd/MTU)	Cooling time (years)	Increase in $k_{\text{eff}}$ (% $\Delta k_{\text{eff}}$ )
0	0	2.24
35	5	2.40
35	80	2.40
35	300	2.42
70	5	2.30
70	80	2.31
70	300	2.32

### C.2.3 Loss of Rod Pitch Control

The increase in  $k_{\text{eff}}$  resulting from uniform pin pitch expansion for fresh fuel as well as both burnups and all three cooling times is considered for the configuration in which the unit cell boundary contacts the inside surface of the storage cell wall. The use of this less extreme case provides an acceptable indication of the sensitivity of the consequence of this configuration to burnup and cooling time variations. The results of the fully expanded configuration, with cladding, are presented below in Table C-12. The increase in  $k_{\text{eff}}$  drops both as a function of burnup and cooling time, though the effect of burnup appears to be significantly larger. These results provide confidence that the results presented for fresh fuel in Section 5.2.1.3 bound the results for all burnups and cooling times.

**Table C-12. Results for loss of rod pitch control with cladding intact in MPC-68**

Burnup (GWd/MTU)	Cooling time (years)	Increase in $k_{\text{eff}}$ (% $\Delta k_{\text{eff}}$ )
<b>Channel intact</b>		
0	0	11.00
35	5	9.55
35	80	9.46
35	300	9.49
70	5	8.68
70	80	8.51
70	300	8.52
<b>Channel removed</b>		
0	0	12.07
35	5	10.56
35	80	10.45
35	300	10.48
70	5	9.64
70	80	9.40
70	300	9.43

#### C.2.4 Loss of Assembly Position Control

The increase in  $k_{\text{eff}}$  caused by a 20-cm axial misalignment for both burnups and all three cooling times is presented in Table C-13. The results show that the consequence of fuel displacement increases with both burnup and cooling time. The 300-year cooling time condition with 35-GWd/MTU burnup causes an increase that is 0.37%  $\Delta k_{\text{eff}}$  larger than the 5-year cooling time. For this case, the decrease in nominal  $k_{\text{eff}}$  is more than 0.75%  $\Delta k_{\text{eff}}$ ; thus, the cask with displaced fuel has a lower final  $k_{\text{eff}}$  value. The maximum change relative to the 35 GWd/MTU and 5-year cooling time is approximately 2.2%  $\Delta k_{\text{eff}}$  and occurs for 70 GWd/MTU and 300 years of cooling time. The reduction in base case  $k_{\text{eff}}$  due only to cooling time at this burnup is approximately 1.3%  $\Delta k_{\text{eff}}$ . The nominal  $k_{\text{eff}}$  for this high-burnup and high cooling time condition is significantly subcritical, so this fuel condition does not represent a challenge to the criticality safety of the cask.

**Table C-13. Increase in  $k_{\text{eff}}$  for limited assembly axial displacement in MPC-68, intact channel**

Burnup (GWd/MTU)	Cooling time (years)	Increase in $k_{\text{eff}}$ (% $\Delta k_{\text{eff}}$ )
35	5	6.29
35	80	6.70
35	300	6.66
70	5	8.03
70	80	8.52
70	300	8.49

### C.2.5 Gross Assembly Failure

The results for both configurations of gross assembly failure are provided for both burnups and all three cooling times in Table C-14. Both the uniform pellet array and the homogeneous rubble configuration show slightly larger  $k_{\text{eff}}$  increases at higher burnup, and a larger increase in  $k_{\text{eff}}$  with increasing cooling time. The increases are smaller for the homogeneous rubble configuration than for the uniform pellet array configuration. The maximum difference is for fuel with 70-GWd/MTU burnup and 300 years of cooling time and is approximately 1.23%  $\Delta k_{\text{eff}}$ . The decrease in nominal  $k_{\text{eff}}$  for this fuel condition is more than 1.30%  $\Delta k_{\text{eff}}$ , so the results in Section 5.2.1.5 are sufficiently large to account for variations associated with higher burnups and longer cooling times.

**Table C-14. Increase in  $k_{\text{eff}}$  caused by gross fuel assembly failure in MPC-68**

Burnup (GWd/MTU)	Cooling time (years)	Increase in $k_{\text{eff}}$ (% $\Delta k_{\text{eff}}$ )
<b>Homogeneous rubble, channel removed</b>		
35	5	29.36
35	80	29.87
35	300	29.83
70	5	29.93
70	80	30.33
70	300	30.40
<b>Uniform pellet array, channel removed</b>		
35	5	34.40
35	80	34.88
35	300	34.87
70	5	35.22
70	80	35.57
70	300	35.63

### C.2.6 Neutron absorber Degradation

The increase in  $k_{\text{eff}}$  caused by neutron absorber panel defects is shown in Table C-15 for both burnups and all three cooling times for a defect size of 5 cm and in Table C-16 for 10 cm defects. The results show an increase in the consequence of panel degradation at higher burnups and higher cooling times. The maximum change in  $k_{\text{eff}}$  increase is approximately 0.7%  $\Delta k_{\text{eff}}$ , which is smaller than the lower nominal  $k_{\text{eff}}$  at the higher burnups and cooling times. The results presented in Section 5.2.1.6 for the neutron absorber panel defect configuration are therefore large enough to account for the effects of higher burnups and cooling times.

The increase in  $k_{\text{eff}}$  increase due to uniform neutron absorber panel thinning at 35 GWd/MTU and 5 years of cooling time are shown in Table C-17. The increase in  $k_{\text{eff}}$  is smaller at the higher burnup, thus confirming that the results presented in Section 5.2.1.6 for uniform panel thinning are also conservative.

**Table C-15. Maximum  $k_{\text{eff}}$  increase caused by a 5-cm neutron absorber defect in MPC-68, intact channel**

Burnup (GWd/MTU)	Cooling time (years)	Defect elevation (cm)	Increase in $k_{\text{eff}}$ (% $\Delta k_{\text{eff}}$ )
0	0	190.50	0.83
35	5	365.13	2.49
35	80	365.13	2.58
35	300	365.13	2.58
70	5	370.42	2.82
70	80	370.42	2.90
70	300	370.42	2.89

**Table C-16. Maximum  $k_{\text{eff}}$  increase caused by a 10-cm neutron absorber defect in MPC-68, intact channel**

Burnup (GWd/MTU)	Cooling time (years)	Defect elevation (cm)	Increase in $k_{\text{eff}}$ (% $\Delta k_{\text{eff}}$ )
0	0	190.50	2.68
35	5	365.13	5.62
35	80	365.13	5.80
35	300	365.13	5.78
70	5	370.42	6.24
70	80	370.42	6.33
70	300	370.42	6.36

**Table C-17. Increase in  $k_{\text{eff}}$  caused by uniform neutron absorber panel thinning (35-GWd/MTU burnup, 5-year cooling time)**

Fraction of neutron absorber panel thickness remaining	Increase in $k_{\text{eff}}$ (% $\Delta k_{\text{eff}}$ )
0.9	0.47
0.8	1.02
0.7	1.64
0.6	2.33
0.5	3.16
0.4	4.16
0.3	5.45
0.2	7.32
0.1	10.26
0.0	18.80

## Appendix D

### Details of Cask Modeling

This appendix provides additional details of the MPC-24 and MPC-68 cask models used in this analysis. Details of the GBC-32 cask are contained within Section 2.1 of Ref. 39.

#### D.1 MPC-24

The bottom of the active fuel is modeled 10.16 cm (4 in.) above the top surface of the cask base plate. The top of the active fuel is approximately 77 cm (30.3125 in.) from the bottom surface of the cask lid. The volume above and below the active fuel is normally occupied by spacers and fuel assembly hardware, but these are neglected in the model. The material in the spacers is not credited in any configuration, although the axial position control provided by the spacers is considered in assessing credibility of axial misalignment configurations. All fuel assemblies are modeled as nominally centered within the fuel storage cells in the MPC-24 basket.

The basket dimensions are provided in Table D-1. The basket is positioned on the cask base plate, creating a gap of approximately 4.60 cm (1 13/16 in.) between the top of the basket walls and the lower surface of the lid. The basket configuration consists of 20 standard storage cells and four oversized storage cells. The model is created with dimensions taken from the SAR for the HI-STAR 100 system, Refs. 36–38.

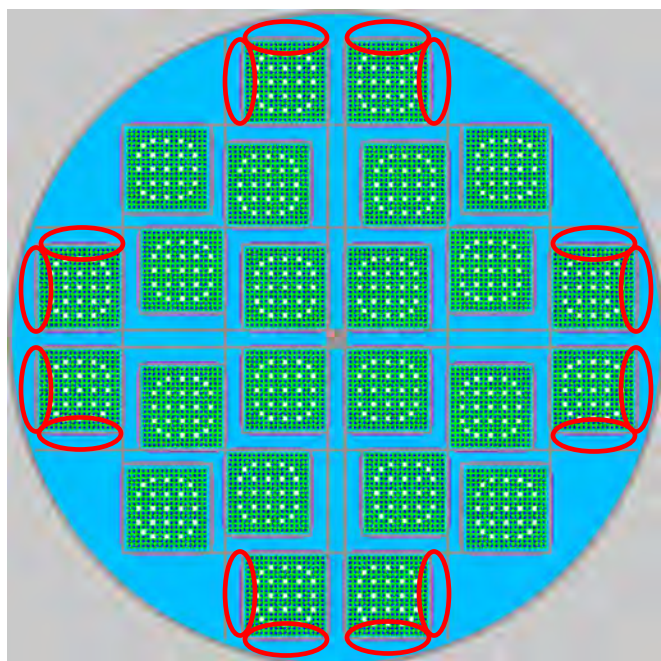
Two widths of neutron absorber panels are used in the MPC-24, and relevant dimensions are provided in Table D-2. The majority of the panels are “wide,” but 16 panels near the periphery of the basket are “narrow” panels. The locations containing narrow neutron absorber panels are indicated in Figure D-1. It is assumed that the entire panel thickness is neutron absorber; in other words, no face cladding is included in the panel models. The panels overlap the bottom of the active fuel by approximately 2.86 cm (1 1/8 in.) and overlap the top of the active fuel by approximately 27.6 cm (10 7/8 in.). The panel dimensions are taken from the SAR for the HI-STAR 100 system Refs. 36–38.

**Table D-1. MPC-24 basket dimensions**

Parameter	Dimension (cm)	Dimension (in.)
Wall thickness	0.79	0.3125
Basket height	448.31	176.5
Standard cell inner dimension	22.225	8.75
Oversized cell inner dimension	22.987	9.05

**Table D-2. MPC-24 Neutron absorber panel dimensions**

Parameter	Dimension (cm)	Dimension (in.)
Wide panel width	19.05	7.5
Narrow panel width	15.875	6.25
Panel thickness	0.26	0.101
Panel length	396.24	156
Panel axial position (from base plate)	7.30	2.875
Wrapper thickness	0.15	0.06
Neutron absorber areal density	0.0372 g $^{10}\text{B}/\text{cm}^2$	

**Figure D-1. Locations of narrow neutron absorber panels in MPC-24 basket.**

## D.2 MPC-68

The bottom of the active fuel is modeled 33.78 cm (~13.3 in.) above the top surface of the cask base plate. The top of the active fuel is approximately 38.13 cm (~15 in.) from the bottom surface of the cask lid. The volume above and below the active fuel is normally occupied by spacers and fuel assembly hardware, but these are neglected in the model. The material in the spacers is not credited in any configuration, although the axial position control provided by the spacers is considered in assessing credibility of axial misalignment configurations. All fuel assemblies are modeled as nominally centered within the fuel storage cells in the MPC-68 basket.

The basket dimensions are provided in Table D-3. The basket is positioned on the cask base plate. A gap of 5.87 cm (~2.31 in.) exists between the top of the basket walls and the lower surface of the cask lid.

The boron-based neutron absorber panels used in the MPC-68 are modeled with dimensions shown in Table D-4. The face clad is modeled as pure aluminum. The neutron absorber panel is modeled as centered in a channel with a thickness of 0.2844 cm (0.112 in.). The gaps between the neutron absorber panel faces and the wrapper walls are filled with water. The panels overlap the top and bottom of the active fuel by 6.35 cm (2.5 in.). The dimensions for the MPC-68 models are taken from Ref. 7.

**Table D-3. MPC-68 basket dimensions**

<b>Parameter</b>	<b>Dimension (cm)</b>	<b>Dimension (in.)</b>
Wall thickness	0.635	0.25
Basket height	447.04	176.0
Cell inner dimension	15.69	6.18

**Table D-4. MPC-68 neutron absorber panel dimensions**

<b>Parameter</b>	<b>Dimension (cm)</b>	<b>Dimension (in.)</b>
Panel width	12.065	4.750
Neutron absorber core thickness	0.2054	0.081
Face cladding thickness	0.0256	0.010
Panel length	393.7	155
Panel axial position (from base plate)	27.43	10.799
Wrapper thickness	0.1905	0.075
Neutron absorber areal density	0.0276 g $^{10}\text{B}/\text{cm}^2$	



## Appendix E

### Development of BWR Depletion Conditions

This appendix provides details about the selection of the axial burnup profile, the development of the axial moderator profile, and the calculation of the specific power used in the BWR depletion calculations. The data is selected from the CRC data available in Refs. 46 and 47.

The axial burnup profile modeled impacts the calculated  $k_{\text{eff}}$  of UNF. As discussed in Ref. 40, the gradient at the top end of the fuel assembly is the most important feature in driving reactivity in one profile relative to another. It is expected that BWR profiles are more severe than PWR profiles because the top of the assemblies experience high void fractions. This high void fraction and corresponding lack of moderation lead to lower relative burnups in the top section of a BWR assembly than a PWR assembly. The low-burnup region will also have a relative increase in plutonium generation at the same burnup. For these reasons, the axial burnup profiles in the PWR database [41] should not be used for BWR fuel. No analogous database of BWR axial burnup profiles exists, so axial burnup profiles from the CRC data for Quad Cities Unit 2 [46] and LaSalle Unit 1 [47] are surveyed for profile selection.

The relative burnup profiles for all assemblies presented in Refs. 46 and 47 are generated and compared to determine a potentially limiting burnup profile for use in these analyses. The two plants have different active fuel heights, so candidates are first selected from each plant, and then the potentially limiting profiles are compared to select the profile for use in these calculations. The relative burnup profiles are compared based on the integral relative burnup over two different axial extents from the top of the assembly. The relative burnups of the top three and top six nodes are summed, with lower sums indicating lower relative burnup leading to higher reactivity. The top three nodes include the top 45.72 cm (18 in.) and the top six nodes include the top 91.44 cm (36 in.) for each assembly. For Quad Cities Unit 2, assembly E7 has the lowest relative burnup in the top three nodes, but assembly F8 has the lowest relative burnup over the top six nodes. For LaSalle Unit 1, assembly C30 has the lowest relative burnup over both three and six nodes for all the assemblies considered. The relative burnup profile for assembly C30 is more severe over both the top three nodes and top six nodes than either E7 or F8 from Quad Cities Unit 2. The three potential profiles, including the integrated relative burnup over the top three and top six nodes, are provided in Table E-1. The LaSalle fuel has an active length of 150 in., compared to the 144-in. active length of fuel used at Quad Cities. This difference in length is not expected to cause a significant difference in calculated  $k_{\text{eff}}$ , so the use of LaSalle Unit 1 fuel data is acceptable for these calculations. A comprehensive study would be required to identify a limiting axial burnup profile for BWR fuel, though the profile used here is similar to a potentially limiting profile identified in Ref. 53.

The water density, which includes both the actual water density and the density reduction due to the presence of steam voids, is provided for each axial node at each case for each assembly in Refs. 46 and 47. This information is used to generate the axial moderator profile for the assembly with the limiting axial burnup profile: Assembly C30 from LaSalle Unit 1. The moderator profile that is used is the average of the water densities in each of the eight cases which include Assembly C30. This profile is presented in Table E-2. The simple average used varies by less than 0.3% at all elevations from a burnup-weighted average. The axial moderator density profile is also lower at nearly all elevations than the limiting distribution from the Quad Cities Unit 2 data in Ref. 46. The lower moderator density will lead to a harder neutron spectrum and more plutonium generation. The profile selected is therefore judged to be sufficiently conservative for use in these calculations.

Discharged assembly reactivity is not highly sensitive to operating history or specific power. The depletion calculations for these analyses model a specific assembly, C30, from a specific commercial BWR plant, LaSalle Unit 1. The specific power can be estimated from data provided in Ref. 47. The core power, number of assemblies, and MTU loading per assembly can be used to determine the average specific power in MW/MTU (W/g). The average burnup of the assembly compared to the cycle burnup can be determined for each case, and thus a relative power can be calculated. The burnup-weighted average specific power for assembly C30 is slightly greater than 30 MW/MTU. This specific power is used in the TRITON depletion calculations to generate the ARP libraries for the STARBUCS calculations. Both TRITON and STARBUCS depletion calculations assume a constant, full-power operating history. These assumptions provide realistic estimates of the UNF reactivity.

**Table E-1. Potentially limiting relative burnup profiles from Quad Cities Unit 2 and LaSalle Unit 1**

Axial zone midpoint elevation (cm)	Assembly C30 (LS U1)	Assembly E7 (QC U2)	Assembly F8 (QC U2)
7.62	0.2461	0.2141	0.2228
22.86	0.7879	0.7470	0.7500
38.10	1.0175	0.9788	0.9813
53.34	1.1026	1.0980	1.0996
68.58	1.1751	1.1518	1.1568
83.82	1.1942	1.1781	1.1877
99.06	1.2052	1.1967	1.2087
114.30	1.2168	1.2125	1.2270
129.54	1.2481	1.2522	1.2668
144.78	1.2535	1.2602	1.2743
160.02	1.2526	1.2589	1.2734
175.26	1.2485	1.2523	1.2657
190.50	1.2419	1.2458	1.2531
205.74	1.2320	1.2391	1.2361
220.98	1.2170	1.2306	1.2139
236.22	1.1955	1.2084	1.1843
251.46	1.1655	1.1651	1.1412
266.70	1.1260	1.1165	1.0940
281.94	1.0759	1.0555	1.0358
297.18	1.0118	0.9569	0.9425
312.42	0.9112	0.8369	0.8270
327.66	0.7873	0.6815	0.6773
342.90	0.6336	0.2968	0.3065
358.14	0.2886	0.1662	0.1742
373.38	0.1656	Not Applicable	
Top Three Nodes	1.0878	1.1446	1.1580
Top Six Nodes	3.7980	3.9939	3.9633

**Table E-2. Average moderator density by axial node, based on Assembly C30 from LaSalle Unit 1**

Axial zone midpoint elevation (cm)	Average moderator density (g/cm <sup>3</sup> )	Axial zone midpoint elevation (cm)	Average moderator density (g/cm <sup>3</sup> )
7.62	0.7396	205.74	0.3126
22.86	0.7396	220.98	0.2953
38.10	0.7288	236.22	0.2802
53.34	0.6875	251.46	0.2668
68.58	0.6349	266.70	0.2549
83.82	0.5798	281.94	0.2445
99.06	0.5284	297.18	0.2354
114.30	0.4831	312.42	0.2276
129.54	0.4434	327.66	0.2213
144.78	0.4089	342.90	0.2163
160.02	0.3794	358.14	0.2128
175.26	0.3539	373.38	0.2115
190.50	0.3317		



## **APPENDIX E**

### **A Preliminary Evaluation of Using Fill Materials to Stabilize Used Nuclear Fuel During Storage and Transportation**

# *A Preliminary Evaluation of Using Fill Materials to Stabilize Used Nuclear Fuel During Storage and Transportation*

**Fuel Cycle Research & Development**

*Prepared for  
U.S. Department of Energy  
Used Fuel Disposition Campaign*

*Steven J. Maheras*

*Ralph E. Best*

*Steven B. Ross*

*Erik A. Lahti*

*David J. Richmond*

*Pacific Northwest National Laboratory*

*August 28, 2012*

*FCRD-UFD-2012-000243*

*PNNL-21664*



#### **DISCLAIMER**

This information was prepared as an account of work sponsored by an agency of the U.S. Government. Neither the U.S. Government nor any agency thereof, nor any of their employees, makes any warranty, expressed or implied, or assumes any legal liability or responsibility for the accuracy, completeness, or usefulness, of any information, apparatus, product, or process disclosed, or represents that its use would not infringe privately owned rights. References herein to any specific commercial product, process, or service by trade name, trade mark, manufacturer, or otherwise, does not necessarily constitute or imply its endorsement, recommendation, or favoring by the U.S. Government or any agency thereof. The views and opinions of authors expressed herein do not necessarily state or reflect those of the U.S. Government or any agency thereof.

**Used Fuel Disposition Campaign Storage and Transportation**

**A Preliminary Evaluation of Using Fill Materials to Stabilize Used Nuclear During Storage and**

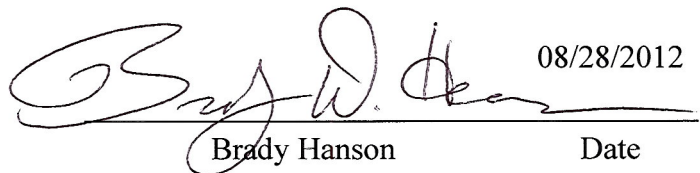
**Transportation**

August 31, 2012

iii

**Reviewed by:**

PNNL Project Manager



08/28/2012

Brady Hanson

Date

**Used Fuel Disposition Campaign Storage and Transportation**  
**A Preliminary Evaluation of Using Fill Materials to Stabilize Used Nuclear During Storage and**  
**Transportation**

iv

August 31, 2012

## SUMMARY

The objective of the research described in this report was to conduct a preliminary evaluation of potential fill materials that could be used to fill void spaces in and around used nuclear fuel contained in dry storage canisters in order to stabilize the geometry and mechanical structure of the used nuclear fuel during extended storage and subsequent transportation. The use of fill material to stabilize used nuclear fuel is not considered to be a primary option for safely transporting used nuclear fuel after extended storage. However, the evaluation of potential fill materials, such as those described in this report, might provide the U.S. Department of Energy Used Fuel Disposition Campaign with an option that would allow continued safe storage and transportation if other options such as showing that the fuel remains intact or canning of used nuclear fuel do not prove to be feasible.

As a first step in evaluating fill materials, previous work done in this area was summarized. This involved studies done by the Spent Fuel Stabilizer Materials Program, Allied-General Nuclear Services, the Canadian Nuclear Fuel Waste Management Program, the U.S. Department of Energy, Spain, Sweden, and the Department of Energy's Yucca Mountain Project. A wide variety of potential fill materials were evaluated in these studies, ranging from molten metal to particulates and beads to liquids and gases. The common element in the studies was that they were focused on the use of fill materials in waste packages for disposal, not in storage canisters or transportation casks. In addition, very few studies involved actual experiments that measured some physical property of the fill material to be used as a stabilizing material, and no studies were found that analyzed the performance of transportation casks containing fill material during the normal conditions of transport specified in 10 CFR 71.71 or under hypothetical accident conditions specified in 10 CFR 71.73. In addition, most studies did not address issues that would be associated with production-scale emplacement of fill material in canisters, as opposed to laboratory- or experimental-scale use of fill material. It is noteworthy that Sweden abandoned its plan to use fill materials to stabilize waste packages due to the complexity of emplacing the fill material.

A part of the evaluation of fill materials, conceptual descriptions of how canisters might be filled were developed with different concepts for liquids, particles, and foams. The requirements for fill materials were also developed. Elements of the requirements included criticality avoidance, heat transfer or thermodynamic properties, homogeneity and rheological properties, retrievability, material availability and cost, weight and radiation shielding, and operational considerations.

Potential fill materials were grouped into 5 categories and their properties, advantages, disadvantages, and requirements for future testing were discussed. The categories were molten materials, which included molten metals and paraffin; particulates and beads; resins; foams; and grout. Based on this analysis, further development of fill materials to stabilize used nuclear fuel during storage and transportation is not recommended unless options such as showing that the fuel remains intact or canning of used nuclear fuel do not prove to be feasible.

## **CONTENTS**

SUMMARY .....	v
ACRONYMS .....	viii
DEFINITIONS .....	ix
1. INTRODUCTION .....	1
2. SUMMARY OF PREVIOUS WORK .....	4
2.1 Spent Fuel Stabilizer Materials Program .....	4
2.2 Allied-General Nuclear Services .....	5
2.3 Canadian Nuclear Fuel Waste Management Program .....	7
2.4 U.S. Department of Energy .....	10
2.5 Belgium .....	11
2.6 Spain .....	11
2.7 Sweden .....	12
2.8 Yucca Mountain Project .....	15
3. FILLING OF CANISTERS .....	17
4. REQUIREMENTS FOR FILL MATERIALS .....	24
4.1 Criticality Avoidance .....	25
4.2 Heat Transfer and Thermodynamic Properties .....	25
4.3 Homogeneity and Rheological Properties .....	26
4.4 Retrievability .....	26
4.5 Material Availability and Cost .....	26
4.6 Weight and Radiation Shielding .....	26
4.7 Operational Considerations .....	26
5. POTENTIAL FILL MATERIALS .....	27
5.1 Molten Materials .....	27
5.1.1 Molten Metals .....	27
5.1.2 Paraffin .....	29
5.2 Particulates and Beads .....	30
5.3 Resins .....	35
5.4 Foams .....	36
5.5 Grout .....	38
6. CONCLUSIONS AND RECOMMENDATIONS .....	40

7. REFERENCES.....	43
--------------------	----

## **TABLES**

Table 1. Recommended Candidate Stabilizer Materials.....	5
Table 2. Physical Properties of Recommended Reference Stabilizer Materials.....	5
Table 3. Selected Physical Properties of Granular Solid Fill Materials .....	6
Table 4. Selected Physical Properties of Liquid Fill Materials .....	6
Table 5. Selected Physical Properties of Gaseous Fill Materials.....	7
Table 6. Necessary and Desirable Criteria for Fill Material.....	8
Table 7. Selected Material Properties for Lead and Zinc .....	10
Table 8. Requirements for Fill Materials (Spain) .....	12
Table 9. Requirements for Fill Materials (Sweden).....	14
Table 10. Summary of Experiments Involving Steel Shot .....	16
Table 11. Conceptual Approaches for Introducing Fill Material into Dry Storage Canisters Containing Used Nuclear Fuel.....	21
Table 12. Potential Requirements for Fill Materials.....	24
Table 13. Representative Properties of Candidate Molten Metals .....	28
Table 14. Particulates and Beads Evaluated in Previous Studies .....	33
Table 15. Material Properties of Resins.....	36
Table 16. Material Properties of Foams.....	38

## **FIGURES**

Figure 1. Used Nuclear Fuel Canister Loading Sequence .....	20
---	----

## ACRONYMS

GWd/MTU	Gigawatt-day per metric ton uranium
HAC	Hypothetical accident conditions
$k_{\text{eff}}$	Effective neutron multiplication factor
NCT	Normal conditions of transport
UFDC	Used Fuel Disposition Campaign

## DEFINITIONS

Alumina	$\text{Al}_2\text{O}_3$
Bauxite	An aluminum ore composed of primarily aluminum hydroxide minerals as well as mixtures of silica, iron oxide, and other impurities.
Bentonite	Bentonite is a natural clay that swells with the absorption of water and has good ion exchange properties.
Bondate	Bondate is an organic-based chemical bonding agent for aggregates and fibers.
Boron carbide	$\text{B}_4\text{C}$
Dowtherm	Dowtherm is a heat transfer fluid.
Hematite	$\alpha\text{-Fe}_2\text{O}_3$
Interprop	Interprop is a ceramic proppant composed of 35-65% mullite (aluminum silicate) and 35-65% corundum (aluminum oxide).
Magnetite	$\text{Fe}_3\text{O}_4$
Mullite	$\text{Al}_6\text{Si}_2\text{O}_{13}$
Olivine	$(\text{Mg},\text{Fe})_2\text{SiO}_4$
Phosphates	$\text{Ca}_5(\text{PO}_4)_3(\text{OH},\text{F},\text{Cl})$
Proppant	A proppant is a material that will keep an induced hydraulic fracture open.
Quartz	$\text{SiO}_2$
Rutile	$\text{TiO}_2$
Silica	$\text{SiO}_2$
Spinel	$\text{MgAl}_2\text{O}_4$
Wood's metal	A low melting fusible alloy that is a mixture of 50% bismuth, 25% lead, 12.5% tin, and 12.5% cadmium.
Zeolite	Hydrated aluminosilicates of the alkaline and alkaline-earth metals.
Zircon	$\text{ZrSiO}_4$
Zirconia	$\text{ZrO}_2$



# **USED FUEL DISPOSITION CAMPAIGN**

## **A PRELIMINARY EVALUATION OF USING FILL MATERIALS TO STABILIZE USED NUCLEAR FUEL DURING STORAGE AND TRANSPORTATION**

### **1. INTRODUCTION**

With the U.S. Department of Energy's Yucca Mountain repository project no longer a workable option, there is no longer a national program for the disposal of used nuclear fuel from commercial nuclear power plants in the United States. As a consequence, used nuclear fuel may continue to be stored for an extended period of time, potentially much longer than originally intended. The U.S. Department of Energy Used Fuel Disposition Campaign (UFDC) is tasked with developing the technical bases to support the continued safe and secure storage and subsequent transportation of used nuclear fuel while maintaining options for its final disposition.

However, most storage pools for used nuclear fuel at reactor sites are now filled to capacity. To provide space for continuing discharges of used nuclear fuel, plant operators began transferring the used nuclear fuel into dry storage systems. These systems are located on the reactor plant's site external to the original nuclear plant facilities. In the dry storage systems, used nuclear fuel is stored in a dry, inert environment in bolted direct-load metal storage casks or in sealed metal canisters. The metal canisters containing used nuclear fuel are stored within steel-reinforced concrete overpacks or storage modules.

The majority of the used nuclear fuel that is in storage is classified as "intact fuel". Intact fuel is the U.S. Nuclear Regulatory Commission classification of used nuclear fuel where the defects in cladding that could expose nuclear fuel material to an oxidizing environment or could allow release of fuel particles and radionuclides from inside the cladding are limited to hairline cracks and pinhole leaks. Fuel assemblies that are classified as "intact" can be stored and transported without having to be additionally enclosed within a "failed-fuel" can within a transportation cask or transportable dry storage canister. In some cases, plant operators have placed used nuclear fuel into failed fuel cans then into storage canisters because it was not feasible to verify that the fuel met the requirements for "intact" fuel.

During extended storage, structures, systems, and components that are important to safety (including fuel cladding and fuel assembly structures) may degrade. The stressors, degradation mechanisms, and data gaps associated with extended storage and subsequent transportation are discussed by UFDC (2012). UFDC (2012) also discuss the stressors, degradation mechanisms, and data gaps associated with extended storage and subsequent transportation of high burnup fuel (exceeding 45 gigawatt-days per metric tonne of uranium [GWd/MTU]). Much of the fuel currently being discharged from reactors exceeds the high-burnup threshold and there is limited information available on the properties of this used nuclear fuel (UFDC 2012).

The focus of the gap analysis by UFDC (2012) is on evaluating the likelihood that the used nuclear fuel remains undamaged (i.e., intact, retrievable, and transportable) after extended storage. The ability of the used nuclear fuel to remain intact is especially important for assuring that a nuclear criticality cannot occur in a storage system or a transportation cask. If fuel cladding degrades during long-term storage, the geometric configuration of a fuel assembly and its fuel component could not be assured under normal conditions of transport (NCT) or hypothetical accident conditions (HAC). A change in the geometric configuration of the fuel inside a transportation cask would change the nuclear reactivity of the cask's contents and could compromise the ability to ensure that a nuclear criticality could not occur in the fuel during transportation.

The UFDC is conducting research and development aimed at developing objective technical evidence that can be used to project and assess the condition of used nuclear fuel during and following extended storage and subsequent transportation. This evidence is expected to show that used nuclear fuel can sustain extended dry storage in an inert atmosphere without substantial change in its properties. However, it is possible that the research will identify unexpected degradation mechanisms or will determine the condition of cladding for high-burnup used nuclear fuel such that the integrity of fuel cladding cannot be sufficiently verified for NCT and HAC.

Thus, the UFDC could consider other options to ensure that used nuclear fuel can be transported following extended storage. The range of these options includes: requiring that all used nuclear fuel assemblies be placed into failed-fuel cans before being placed into a dry storage cask or canister system and use of a fill material to stabilize the contents of a metal canister prior to transportation. Ideally, the use of a fill material would render the question of whether used nuclear fuel was intact or damaged immaterial because the fill material would preserve the geometric configuration of the used nuclear fuel and/or provide for moderator exclusion and thereby prevent a nuclear criticality. The objective of this report is to evaluate potential fill materials that could be used for this purpose.

There are several reasons why the use of a fill material might be preferable to options such as demonstrating that the used nuclear fuel remains intact or canning of all used nuclear fuel. For example, it may not be possible to provide objective evidence with the requisite reasonable assurance, at a reasonable cost, that used nuclear fuel will remain intact after extended storage. Under this circumstance, the use of fill material or canning of individual fuel assemblies might be the only options available that would allow transportation of large amounts of used nuclear fuel to a geologic repository, a consolidated storage facility, or a reprocessing facility. However, canning of used nuclear fuel would require repackaging of fuel already in storage and could also substantially increase the number of shipments. If feasible, the use of fill materials could be desirable when compared to canning and repackaging of used nuclear fuel.

There are also disadvantages to the use of fill materials. For example, placing a fill material in a metal canister subsequently loaded into a transportation cask could increase the weight of the transportation cask to the point where it could not be handled or transported. In addition,

**Used Fuel Disposition Campaign Storage and Transportation**  
**A Preliminary Evaluation of Using Fill Materials to Stabilize Used Nuclear During Storage and Transportation**

August 31, 2012

3

verifying that the fill material was fully and uniformly distributed within the metal canister may not be feasible. A closely related issue is that it may be difficult to load the fill material into metal canisters that were not designed with this capability, and it could be difficult to subsequently retrieve the used nuclear fuel without having to resort to time consuming or costly measures. The fill material would also have to be chosen so that it did not have undesirable properties during the normal conditions of transport specified in 10 CFR 71.71 or hypothetical accident conditions specified in 10 CFR 71.73, and the transportation casks would have to be re-licensed by the U.S. Nuclear Regulatory Commission based on the presence of the fill material, or more likely, entirely new transportation casks would have to be licensed.

For the reasons stated above, the use of fill material to stabilize used nuclear fuel is not considered to be a primary option for safely transporting used nuclear fuel after extended storage. However, evaluation of potential fill materials could provide the UFDC with an option that would allow continued safe storage and transportation if other options such as showing that the fuel remains intact or canning do not prove to be feasible.

## **2. SUMMARY OF PREVIOUS WORK**

This section summarizes previous work done to investigate the use of fill materials to stabilize used nuclear fuel in waste packages, storage containers, or transportation casks. The studies that are summarized were identified by literature searches and searches of project records from available U.S. and international sources. Other work involving fill materials that is not available in the literature or project records is not included in the descriptions that follow.

The majority of the studies have been literature studies that did not involve experimental work. The only studies that involved experimental work were studies conducted by the Spent Fuel Stabilizer Materials Program, the Canadian Nuclear Fuel Waste Management Program, and the Yucca Mountain Project. In addition, the majority of studies were focused on the use of fill materials in waste packages for disposal of used nuclear fuel. No experimental work was found that analyzed the performance of transportation casks containing fill material during the normal conditions of transport specified in 10 CFR 71.71 or during hypothetical accident conditions specified in 10 CFR 71.73.

### **2.1 Spent Fuel Stabilizer Materials Program**

The Spent Fuel Stabilizer Materials Program was conducted for the National Waste Terminal Storage Program, a predecessor to the Office of Civilian Radioactive Waste Management in the U.S. Department of Energy, and had the objective of identifying, testing, and selecting stabilizer materials for use in used nuclear fuel waste packages for disposal. Stabilizers were materials that would fill the space in a waste package that was not filled with used nuclear fuel (Fish et al. 1982).

Wynhoff et al. (1982) identified 34 candidate stabilizer materials based on analysis of thermal gradients within the waste package, thermal stress analysis (thermal gradient stress analysis and differential thermal expansion stress analysis), nuclear criticality, radiation attenuation, and cost and material availability. Table 1 lists these candidate materials. Fish et al. (1982) conducted a series of experimental tests and evaluated the 34 materials against the following functions:

- Help resist lithostatic and hydrostatic pressures on the waste package after emplacement
- Maintain the used nuclear fuel geometry, prevent motion and mechanical abrasion or rod failure due to handling and accidents
- Promote heat transfer from the fuel assembly to minimize fuel temperature
- Chemical compatibility with the waste package
- Long-term chemical and radiation stability
- Use of an organic material was strongly discouraged because organic materials tend to decompose at elevated temperatures and in radiation environments creating a potential for harmful interaction with fill material after a waste package is breached.

Additional screening criteria used by Fish et al. (1982) included criteria for emplacement temperature limits, shrinkage and voids, material interactions, moisture release, and gas

generation. The tests conducted by Fish et al. (1982) included temperature limit tests, fill process tests, prebreach disposal condition tests (including loss-on-ignition tests and tests to evaluate fuel cladding-stabilizer material interactions), and electrochemical tests. As a result of these tests and evaluations, 1% antimonial lead and zirconia were recommended to be used as the reference materials used in waste package designs calling for the use of stabilizers. Table 2 summarizes selected physical properties of these materials.

Table 1. Recommended Candidate Stabilizer Materials

Material	Material
Silica – amorphous	Sand
Silica – quartz	Graphite
Silica – quartz/bondate	Graphite/bondate
85% silica – quartz/15% bentonite	Air
Mullite	Helium
Mullite/bondate	Nitrogen
85% mullite/15% bentonite	1% antimonial lead
Zircon	Calcium lead
Zirconia	Commercial lead
Zirconia/bondate	Zinc alloy AG40A
85% zirconia/15% bentonite	Zinc alloy AC41A
Basalt	Zinc-copper-titanium alloy
Basalt/bondate	Commercial zinc
85% basalt/15% bentonite	Copper casting alloy 3A (high-lead tin bronze)
Granite	Copper casting alloy 8A (manganese bronze)
Shale	Copper casting alloy 13B (silicon brass)
Tuff	Commercial copper

Source: Wynhoff et al. (1982)  
 Bondate is an organic-based chemical bonding agent for aggregates and fibers.

Table 2. Physical Properties of Recommended Reference Stabilizer Materials

Material	Density (g/cm <sup>3</sup> )	Thermal Conductivity (W/m-K)
1% antimonial lead	11.27	33.47
Zirconia	5.68	1.45

Source: Wynhoff et al. (1982)

## 2.2 Allied-General Nuclear Services

Anderson (1981) investigated the use of fill materials to be used to encapsulate used nuclear fuel within a canister during the dry storage. The purpose of the study was to determine if encapsulation of used nuclear fuel with a fill material was desirable, compare physical and economic characteristics of alternative fill materials, and to review appropriate means to seal the

**Used Fuel Disposition Campaign Storage and Transportation**  
**A Preliminary Evaluation of Using Fill Materials to Stabilize Used Nuclear During Storage and Transportation**

6

August 31, 2012

storage canisters if fill materials were used. Tables 3, 4, and 5 summarize the materials evaluated and selected physical properties.

Table 3. Selected Physical Properties of Granular Solid Fill Materials

Material		Solid Density (g/cm <sup>3</sup> )	Solid-Gas Mixture Thermal Conductivity (W/m-K)	Solid Melting Temperature (°C)
Solid	Gas <sup>a</sup>			
Copper spheres	Air	8.97	0.68	1083
Aluminum spheres	Air	2.70	--	660
Graphite	Air	1.50	1.2	3700
Zinc spheres	Air	7.14	0.46	283
Steel spheres	Air	7.85	0.25	1426
Lead spheres	Air	11.3	--	327
Boron carbide	Air	2.52	--	2450
Uranium oxide powder	Helium	10.8	1.5	2750
Alumina	Air	4.00	0.67	2050
Sand	Air	1.52	0.26	--
Glass	Air	2.22	0.18	1200
Mortar	--	2.20	0.92	--
Rock or glass wool	Air	0.16	0.050	--

Source: Anderson (1981)

a. The gases listed fill the interstices of the solid fill material.

Table 4. Selected Physical Properties of Liquid Fill Materials

Material	Density (g/cm <sup>3</sup> )	Boiling Temperature (°C)	Pressure at Boiling (psia)	Thermal Conductivity (W/m-K)
Water	0.956 0.786	100 260	14.7 680.8	0.67 0.61
Ethylene glycol and water	1.013 0.963	100 177	13.8 103.0	0.40 0.36
Dowtherm	0.860 0.739	258 380	14.7 119.0	0.10 0.084
Silicone	0.900 0.744	100 300	0.077 20.9	0.12 0.071

Source: Anderson (1981)

Dowtherm is a heat transfer fluid.

Table 5. Selected Physical Properties of Gaseous Fill Materials

Material	Density (g/cm <sup>3</sup> )	Thermal Conductivity (W/m-K)
Helium	0.000164	0.18
Air	0.00120	0.034
Nitrogen	0.00120	0.033
Carbon dioxide	0.00184	0.025
Argon	0.00166	0.022

Source: Anderson (1981)

Anderson (1981) noted several advantages of fill materials. For example, by selecting the proper fill material one might reduce corrosion of the fuel cladding, increase the thermal conductivity of the contained fuel assembly, and reduce criticality considerations by lowering the effective neutron multiplication factor ( $k_{eff}$ ) value of the used nuclear fuel container. The main disadvantage to the use of fill materials that was noted was economic. A second disadvantage that was noted was feasibility. Another potential disadvantage of using fill materials noted by Anderson (1981) involves the increased difficulty of retrieving the used nuclear fuel if retrieval is necessary at a later date. If the used nuclear fuel has been stabilized in a solid matrix (for example, by melting a metal, pouring it in a canister containing used nuclear fuel, and allowing the package to solidify), the removal of the used nuclear fuel could be quite difficult (Anderson 1981). In addition, the fill material could be slightly contaminated resulting in the generation of radioactive waste or additional process steps to decontaminate the fill material (Anderson 1981).

For the dry storage of spent fuel, Anderson (1981) found that air would be the best fill material. The use of fill materials other than air for dry storage of used nuclear fuel could be justified only if a specific end result, e.g., containment or criticality control, was deemed very important.

### **2.3 Canadian Nuclear Fuel Waste Management Program**

The Canadian Nuclear Fuel Waste Management Program investigated alternative fill materials to be placed inside two types of waste containers: a thin-walled particulate-packed container and a structurally supported particulate-packed container. The purpose of the fill material was to provide structural support for the container against the hydrostatic pressure that could exist in a flooded, 1000-m deep disposal vault.

Shelson (1983) established a set of initial criteria for selecting particulates for future study and experiments. These criteria included necessary properties and desirable properties. Necessary properties were further grouped into criteria related to mechanical strength and criteria related to stability. Table 6 lists these criteria.

Table 6. Necessary and Desirable Criteria for Fill Material

Necessary Criteria	Desirable Criteria
Mechanical Strength High strength to breakdown (>20 MPa) High bulk modulus (>200 MPa) High Young's modulus (>200 MPa)	High heat transfer coefficient Low thermal expansion coefficient Low dust content Impede radionuclide migration Attenuate radiation from fuel bundles Low specific gravity
Stability Radiation stability Chemical stability Not Reactive with titanium or heavy metals No interference with welding of shells Thermal stability (>1500 °C) Low water absorptivity (low swelling) No change over container life (300-500 years)	

Source: Shelson (1983)

From initial studies (Shelson 1983), twelve candidate particulate materials were selected for study (Teper 1987). These materials were:

- Sand
- Fine glass beads (0.002-0.3 mm)
- Coarse glass beads (0.8-1.2 mm)
- Steel shot (0.6-1.0 mm)
- Aluminum oxide powder
- Crushed bauxite grains
- Sintered bauxite
- Interprop<sup>a</sup>
- Ceramic zirconia
- Rutile-Zircon-Garnet mixture
- Zircon
- Rutile

---

<sup>a</sup> Interprop is a ceramic proppant composed of 35-65% mullite (aluminum silicate) and 35-65% corundum (aluminum oxide). A proppant is a material that will keep an induced hydraulic fracture open.

The criteria used by Teper (1987) to select the fill material to be used in the container included:

- Fill all voids without clogging
- Be small enough to flow between the fuel bundle elements (less than 1.2 mm diameter) but the grains should be heavy enough to avoid becoming airborne during vibratory compaction
- Have sufficient strength to withstand a pressure of 20 MPa
- Have adequate stiffness to prevent large plastic deformations of the container shell
- Have low dust content to minimize airborne particles
- Should not adhere to the container wall, to simplify welding of top lid
- Have small creep deformations over the 500-year container life
- Have sufficiently high bulk modulus under external pressure

The particulates underwent vibratory compaction tests, compression tests, and creep tests. The details of the tests and their results are discussed in Teper (1987). Based on the results of the tests, three fill materials were considered viable: glass beads, interprop, and sintered bauxite. Coarse glass beads generated the least amount of dust during compaction and produced the highest bulk modulus of elasticity in the compacted state, and were therefore selected as the fill material for the packed particulate and structurally supported containers (Johnson et al. 1994). The use of glass beads as a fill material was abandoned because glass beads could not provide assurance that the container would not collapse due to anticipated hydraulic pressures in the vault and was replaced with a carbon steel inner vessel to provide mechanical strength to the used nuclear fuel container (NWMO 2005).

The Canadian Nuclear Fuel Waste Management Program also investigated a metal matrix container, where cast metal surrounded the fuel bundles and forms a layer between the outer bundles and the shell of the container. Johnson et al. (1994) lists the following requirements for a candidate casting metal or alloy:

- The cast matrix should be free of major defects such as shrinkage voids
- During casting, the molten metal should neither chemically react with the corrosion-resistant shell nor otherwise reduce the thickness of the corrosion barrier.
- Interactions with the used nuclear fuel cladding should be minimal to ensure that the fuel elements are not damaged.
- Following solidification of the cast matrix, chemical stability between the matrix and the container shell should persist.
- The casting process should be conducted at as low a temperature as possible in order to reduce the preheating requirements of the container and its contents, decreasing the possibility of promoting thermal stress defects in the used nuclear fuel cladding material, and shorten the solidification period, during which chemical interactions between the matrix and the used nuclear fuel cladding material and/or the container shell are more likely.

Lead, zinc, and aluminum, and lead-antimony, aluminum-silicon, and aluminum-copper alloys were studied as candidate casting materials, and lead or zinc were recommended as the preferred casting materials. Table 7 summarizes some selected physical properties of lead and zinc. Subsequent research and development activities focused on lead. Four half-scale models, denoted MM1, MM2, MM3, and MM4, were cast and structural performance tests conducted. Testing and analysis showed that a metal matrix container was a viable option.

Table 7. Selected Material Properties for Lead and Zinc

Material	Density (g/cm <sup>3</sup> )	Thermal Conductivity (W/m-K)	Melting Point (°C)
Lead	11.35	33.0	327.5
Zinc	7.10	112.2	419.58

## 2.4 U.S. Department of Energy

The U.S. Department of Energy has studied the use of depleted uranium oxide particulates as a fill material in used nuclear fuel waste packages (Forsberg 2000), and the use of depleted uranium silicate glass beads as a fill material in used nuclear fuel waste packages, storage containers, and transportation casks (Forsberg et al. 1995, 1996; Pope et al. 1996a, 1996b). In terms of the long-term performance of a geologic repository, the use of either depleted uranium oxide particulates or depleted uranium silicate glass beads has two advantages. First, it will retard the release of radionuclides from the waste package by creating a chemically reducing environment that slows the degradation of the uranium oxide contained in the used nuclear fuel, and by reducing ground water flow through the waste package (Forsberg 2000). In addition, the use of depleted uranium as a fill material minimizes the potential for a long-term criticality by isotopic dilution of U-233 and U-235 (Forsberg 2000).

In terms of storage and transportation, the use of depleted uranium silicate glass beads could have several benefits (Forsberg et al. 1995):

- The amount of gamma shielding material in the walls of the storage casks and transportation casks may be reduced.
- The neutron shielding materials in the walls of the storage casks and transportation casks may be reduced.
- The need to include burnup credit for criticality control may be eliminated.

Pope et al. (1996a, 1996b) acknowledges that there significant uncertainties associated with using depleted uranium silicate glass beads as a fill material, and that additional studies are necessary. The studies recommended by Pope et al. (1996a, 1996b) included:

- Developing and demonstrating the ability to produce depleted uranium silicate glass.
- Performing leaching tests on the depleted uranium silicate glass.
- Defining a preferred method for loading the depleted uranium silicate glass into a storage or transportation cask after they have been loaded with used nuclear fuel assemblies.

- Performing design alternative studies and defining costs and benefits of the various alternatives, including assessments of storage canister, transportation cask, storage cask, and waste package alternatives.
- Assessing trade-offs for and defining systems and interfaces for applying the concept of using depleted uranium silicate glass as a fill material to the waste management system.

## **2.5 Belgium**

Belgium incorporated sand as a fill material in their used nuclear fuel canister design (Bennett and Gens 2008, ONDRAF/NIRAS 2001). The sand is a dry, halide-free rolled sand which fills the voids in the canister after being vibrated (ONDRAF/NIRAS 2001). As noted in ONDRAF/NIRAS (2001), the sand has a number of functions:

- The walls of the canister can be made thinner as the sand provides resistance to crushing
- The sand stabilizes the used nuclear fuel assembly in a centered position and so reduces criticality risks by mechanical convergence
- The sand limits the moderator density should water penetrate the canister
- The sand limits the void space which is a general requirement for waste intended for deep disposal.

After the canister has been filled with sand it is purged with a dry inert gas to minimize the risks of corrosive agents such as nitric acid being produced by radiologically induced reaction with humid air (ONDRAF/NIRAS 2001). The use of glass frit to fill the annulus between high level radioactive waste canisters and their overpacks is also being evaluated (ONDRAF/NIRAS 2001).

## **2.6 Spain**

Puig et al. (2008a, 2008b, 2009) evaluated alternative fill materials that could be placed inside a used nuclear fuel canister that would be disposed of in a geological repository. The primary purpose of the fill material was to avoid the possibility of a criticality event once the canister was breached by corrosion and was flooded by ground water. Five groups of requirements for these fill materials were developed. These included requirements for criticality, general requirements to fulfill, general requirements to avoid, performance improvement requirements, and other interesting requirements. These requirements are listed in Table 8. Eight materials were evaluated:

- Cast iron or steel
- Borosilicate glass
- Spinel
- Depleted uranium
- Dehydrated zeolites
- Hematite
- Phosphates
- Olivine

Based on the evaluations of the materials against the requirements, four materials were found to be promising for use as a fill material: cast iron or steel, borosilicate glass, spinel, and depleted uranium.

Table 8. Requirements for Fill Materials (Spain)

<b>Criticality Requirements</b> Fill 60% of the canister inner free volume Significant neutron absorption capability Minimize neutron moderation Radiation resistance Thermal stability Chemical stability
<b>General Requirements to Fulfill</b> Thermodynamic equilibrium with conditions and materials in repository Homogeneous batches Good rheological properties to ensure proper filling Ability to be placed in canister without damaging fuel assemblies Does not affect fabrication, encapsulation, or other processes (i.e., welding of canister lid) Possible to disassemble canister Allow retrievability if needed
<b>General Requirements to Avoid</b> Limited availability of material Potential to increase corrosion of the canister, fuel cladding, or fuel itself. Increase the potential for radionuclide transport through bentonite barrier or chemically alter the barrier's properties Retain significant amounts of air that could lead to formation of nitric acid through radiolysis and contribute to stress corrosion cracking
<b>Performance Improvement Requirements</b> High mechanical strength to contribute to canister structural integrity Sorption capability for key radionuclides
<b>Other Interesting Properties</b> Well-documented long-term durability Low material density to reduce additional weight of canister Low overall cost of material (raw materials, processing, and fabrication) Good intrinsic radiation shielding properties Material that allows a relatively simple process, including the necessary facilities and equipment
Source: Puig et al. (2008a)

## 2.7 Sweden

Oversby and Werme (1995) evaluated alternative fill materials that could be placed inside a copper and steel used nuclear fuel canister that would be placed inside a geological repository.

As with the fill materials analyzed by Puig et al. (2008a, 2008b, 2009), the primary purpose of the fill material was to avoid the possibility of a criticality event once the canister was breached by corrosion and was flooded by ground water. Design requirements were developed for the canister fill material and divided into three classes: essential requirements, desirable features, and undesirable features. These requirements are listed in Table 9. Eleven materials were evaluated:

- Glass beads
- Lead shot
- Copper spheres
- Sand
- Olivine
- Hematite
- Magnetite
- Crushed rock
- Bentonite
- Other clays
- Concrete

Based on the evaluations of the materials against the design requirements, three materials were found to be candidates for further evaluation as fill materials: glass beads, copper spheres, and magnetite. Because of the complexity of the filling process, canister designs without fill material were evaluated (Werme and Eriksson 1995) and current canister designs do not include a fill material (SKB 2010).

Sweden has also investigated a steel canister with lead fill, a copper canister with lead fill, and a titanium canister with concrete fill (SKB 1992). The titanium canister with concrete fill was used for very deep hole disposal, not for disposal in a geologic repository. Emplacing the lead in a steel or copper canister involved pre-heating the canister in an induction furnace to 380 °C for 6 hours, adding molten lead which was then allowed to solidify slowly from the bottom up to avoid voids, and cooling the canister for 12 hours to 60 °C. The entire time to pre-heat, fill, and cool a canister was estimated to be 24 hours (SKB 1992).

Table 9. Requirements for Fill Materials (Sweden)

<b>Essential Requirements</b> The filling material must be capable of being placed into the canister in a manner that does not damage the fuel and that results in a residual void volume of less than 40% of the void volume in the absence of the filling material. The filling material must have a solubility of less than 100 milligrams per liter at 50 °C in pure water and in waters of the expected repository environment. The filling material shall not compact by more than 10% of its original volume under its own weight or as the result of shipping, handling, or emplacing the canister in storage or disposal sites.
<b>Desirable Requirements</b> Material is in thermodynamic equilibrium with the disposal system, thus ensuring chemical compatibility. Material has homogeneous properties within a batch and between batches, which makes quality control and performance modeling more secure. Material possesses well documented long-term durability, which ensures that predictions concerning the condition of the material through time will be reliable. Material has good rheological properties for emplacement into the canister, which ensures that the operations in the encapsulation facility will not be unduly difficult. Material contains a burnable poison to absorb neutrons, which will enhance the criticality control of the filling material even if the void volume exceeds 40%. Material has the potential to sorb radionuclides from aqueous solutions, thus lowering the release of radioactive materials from the waste package. Material has the potential to suppress generation of hydrogen, which helps protect the bentonite buffer material from disruption due to passage of gas bubbles through the bentonite. Material has low cost. Material has low density, so performs its space-filling function with minimal addition of weight to the canister system.
<b>Undesirable Requirements</b> Limited availability of the material. Potential for the material to enhance corrosion of the canister, the fuel cladding, or the fuel. Material generates gas when it alters. Material contains water, which diminishes the effectiveness of the material to prevent moderation of the neutron energies. Material has a high affinity for absorbing air on its surface, which is undesirable because the nitrogen in air can be converted to nitric acid in the presence of water and radiation.

Source: Oversby and Werme (1995)

## 2.8 Yucca Mountain Project

Wallin et al. (1994) evaluated alternative fill materials that could be placed inside a waste package which in turn would be emplaced inside a geologic repository located at Yucca Mountain, Nevada. The objectives of adding the fill materials included (Wallin et al. 1994):

- Criticality control: moderator displacement by means of minimization of waste package internal void space, to minimize the amount of water which could enter the waste package in the event of repository flooding and a breach of the waste package containment barriers
- Chemical buffering for radionuclides in the event of water intrusion into the waste package upon breach of the containment barriers
- Cathodic protection by virtue of having highest electrochemical activity, in the event of water intrusion into the waste package upon breach of the containment barriers
- Function as mechanical packing to inhibit movement (collapse) of other materials internal to the waste package (fuel rods, fuel pellets, and/or basket materials)
- Improve thermal conductance, which would improve heat transfer and decrease fuel rod temperatures

Seven materials were evaluated:

- Tin (emplaced molten)
- Lead (emplaced molten)
- Zinc (emplaced molten)
- Zinc alloy (emplaced molten)
- Magnetite
- Iron shot
- Borosilicate glass beads

Iron shot was chosen as the first fill material to be experimentally investigated. Characteristics of iron shot that led to this choice included: 1) relative ease of placement (near-spherical shot “flows” readily), 2) commercial availability in a variety of graded sizes, 3) cost (inexpensive), 4) iron is a plentiful natural resource, 5) iron is a reactive anodic material providing protection to the fuel cladding and to Stainless Steel 316 components, and 6) iron would inhibit radionuclide release (Wallin et al. 1994).

Cogar (1996a and 1996b) contain the plans and technical guidelines used to conduct experiments conducted on steel shot, which was chosen over iron shot for the experiments because it was more readily available. These experiments involved:

- Fabricating two dummy fuel assemblies, a 15×15 B&W Mark-B pressurized water reactor assembly and a 17×17 B&W Mark-BW pressurized water reactor assembly.

- Fabricating a simulated spent nuclear fuel basket test fixture from Lexan. The dimensions of the test fixture were  $8.81 \times 8.81 \times 180$  inches. The test fixture had two vibrators attached.
- Using two grades of shot: SAE Shot Size S230 and SAE Shot Size S330. The S230 shot had a nominal diameter of 0.7 mm and the S330 shot had a nominal diameter of 1.0 mm.
- As-poured versus vibrated fill tests.

Cogar (1996c) conducted bulk density tests, fill placement tests, eight fill tests, angle of repose tests, and thermal conductivity tests. The eight fill tests conducted involved combinations of shot size (S230 and S330), assembly ( $15 \times 15$  and  $17 \times 17$ ), and as poured versus vibrated conditions. Cogar (1996c) contains the detailed results of experiments. Table 10 summarizes these results.

Table 10. Summary of Experiments Involving Steel Shot

Material	Density (g/cm <sup>3</sup> )	Thermal Conductivity (W/m-K)
SAE Shot Size S230	4.490-4.538 (as-poured)	0.379-0.658
	4.568-4.653 (vibrated)	
SAE Shot Size S330	4.353-4.397 (as-poured)	0.325-0.591
	4.441-4.483 (vibrated)	

Source: Cogar (1996c)

Arthur (2000), Montierth (2000), and Radulescu (2000) also evaluated the use of aluminum shot containing gadolinium phosphate as a fill material in waste packages containing Shippingport light water breeder reactor thorium-uranium oxide seed assemblies. The results show that the Shippingport used nuclear fuel would not form critical configurations for any credible degradation scenarios when 1 weight percent gadolinium is added to the aluminum shot-gadolinium phosphate fill material. Similar analyses were performed for Enrico Fermi fast reactor used nuclear fuel using iron shot containing gadolinium phosphate as a fill material (Mobasheran 1999, Moscalu et al. 2000).

### **3. FILLING OF CANISTERS**

The introduction of a fill material into a dry storage canister containing used nuclear fuel assemblies would be a significant departure from established industry practice for dry storage and planned subsequent transportation of used nuclear fuel. Consequently, any initiative to use such an approach would have to surmount a high hurdle of justification including consideration of alternatives such as repackaging the used nuclear fuel into another canister. Such justification could include:

- Use of a fill material was determined to be the best alternative for remediating a known defect in a canister or canister contents in order to provide reasonable assurance of continued protection of public safety and to ensure continued compliance with regulatory requirements.
- Use of a fill material was determined to be the best alternative for eliminating uncertainties regarding the integrity of fuel cladding, fuel structures, or canister internal structures or safety-related components to provide reasonable confidence in storage or transportation safety performance and assurance of compliance with regulatory requirements.

It is unlikely that fill materials could be introduced into dry storage canisters in an operating nuclear power plant's used nuclear fuel storage pool. The reasons include issues regarding the compatibility of fill materials with the chemistry of the fuel pool water and the added operational complexity of adding fill materials. As a consequence, any activity to introduce fill materials to dry storage canisters would need to be conducted in a facility that would have the necessary health protection systems for workers and the public and systems to prevent releases of radioactive materials to the environment. It is beyond the scope of this report to provide a concept for such a facility. However, Carlsen and Brady Raap (2012) discusses various dry transfer systems for used nuclear fuel that could be applicable for use in introducing fill materials into dry storage canisters.

The objectives for introducing fill material into a canister could be several including:

1. To structurally stabilize (hold in place) the canister's contents and geometry by filling in all of the available free space in and around the nuclear fuel assemblies and in and around the structures of the fuel assembly basket. This would protect the used nuclear fuel cladding from damage and preserve the geometric orientation of nuclear fuel and other materials and structures in order to provide assurance that a nuclear criticality could not occur.
2. To provide a medium that would exclude the potential for a significant amount of water moderator to intrude in and around the fuel assemblies thereby assuring a nuclear criticality could not occur.
3. To provide a medium that contains neutron absorber materials to enhance assurance that a nuclear criticality could not occur

4. To provide a barrier that impedes the release of radioactive material from used nuclear fuel assemblies to the environment.
5. To provide radiation shielding to reduce the radiation dose rate external to the canister.

Possible approaches for introducing a fill material that fills the free space in a dry storage canister containing used nuclear fuel include:

- Adding fill material to a canister containing used nuclear fuel before the closure lid is first installed.
- Using canisters that have access ports that are designed to be removed at a future date to provide openings for adding fill material.
- Unsealing and re-opening the ports that were originally used to drain, vent, dry, and backfill the canister with inert gas to provide openings through which fill material could be added.
- Unsealing and removing the canister lid to add fill material.
- Cutting access ports through the canister lid to provide openings for adding fill material.
- Cutting access ports through the side of a canister to provide openings for adding fill material.

The time when fill material might be added to a canister could be as early as when the canister is first loaded with used nuclear fuel or it could be 100 to 300 years in the future when the canister is being prepared for shipment following extended storage. Fill material might also be added to a canister at any time available information indicates that the integrity of fuel cladding, fuel structures, or canister internal structures or safety-related components has (or may have) degraded in a manner that compromises storage or transportation safety performance. This would include canisters with detected defects or when research results or other information suggest there are likely safety related defects in a particular canister design or design feature or a category of used nuclear fuel contained in a canister.

Fill material might also be added to a canister immediately prior to transportation whenever the integrity of fuel cladding, fuel structures, or canister internal structures or safety-related components cannot be verified sufficiently to provide reasonable assurance of transportation safety and compliance with regulatory requirements for transportation. This would include canisters containing used nuclear fuel following extended storage and canisters containing high burnup used nuclear fuel.

Possible fill materials can be grouped into 3 categories:

1. Liquids, including molten metals, waxes, resins, and grout, that would flow into and fill a canister before undergoing physical change to become a solid.
2. Particulates, including sand, borosilicate glass beads, and metal shot, that would be introduced to canisters to fill available spaces through cascading gravity flow (Wallin 1996).

3. Foams that would be introduced into selected locations in a canister and then would expand and infuse through available internal openings and gaps to fill open spaces.

These categories determine the process that would need to be used to introduce fill materials into a canister.

Processes for filling canisters would be determined by the type of fill material that was used and the approach taken to transfer the material into the canister. Table 11 summarizes the conceptual filling processes that could be employed for each of the different kinds of fill materials and for the different approaches to filling a canister that are described above. Figure 1 provides a conceptual illustration of the process for filling a canister that has its lid removed. The processes described assume that the canister is filled in a facility designed and dedicated for that purpose. The concepts described are unproven. It would be necessary to design and conduct a program that would include tests that demonstrated the feasibility of a fill material concept before any decision was made to use a fill material to stabilize the used nuclear fuel contents of a storage canister.

**Used Fuel Disposition Campaign Storage and Transportation**  
**A Preliminary Evaluation of Using Fill Materials to Stabilize Used Nuclear During Storage and Transportation**

20

August 31, 2012

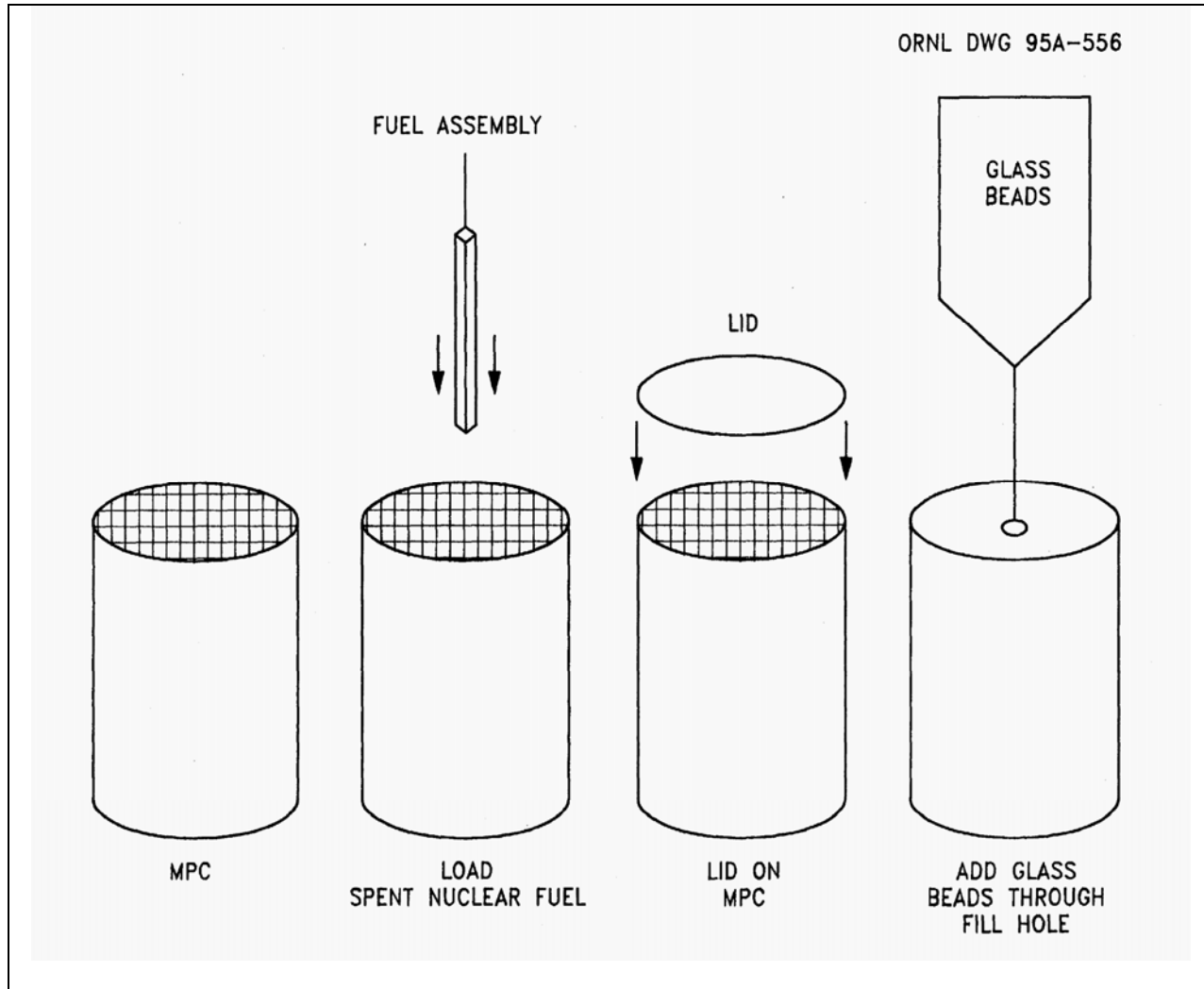


Figure 1. Used Nuclear Fuel Canister Loading Sequence

(Source: Forsberg et al. 1995)

Table 11. Conceptual Approaches for Introducing Fill Material into Dry Storage Canisters Containing Used Nuclear Fuel

Fill Material Type	Approach for Introducing Fill Materials				
	Unseal and remove lid from loaded canister	Unseal and reopen canister drain and vent ports	Canister with ports for adding fill material	Cut openings into canister lid	Cut openings into canister side wall
Liquid	The canister lid's seal weld is cut and lid is removed. Liquid fill is introduced into the canister via a down-tube (vent tube) into the bottom of the open canister and is allowed to flow up to fill the canister before solidifying. The canister's lid is reinstalled and re-welded. An additional external canister may be used if the canister is defective.	The canister's drain and vent ports are unsealed and opened. Liquid fill is introduced into the canister via the vent tube into the bottom of the open canister and is allowed to flow up to fill the canister before solidifying. The canister's drain and vent ports are closed and resealed. An additional external canister may be used if the canister is defective.	Liquid fill is introduced via the inlet port into the canister and is allowed to flow up to fill the canister before solidifying. The canister's ports are re-sealed. An additional external canister may be used if the canister is defective.	Liquid fill is introduced via the cut opening into the canister and is allowed to flow up to fill the canister before solidifying. The openings are re-sealed. An additional external canister may be used if the canister is defective.	Liquid fill is introduced via the cut opening into the canister and is allowed to flow up to fill the canister before solidifying. The openings are re-sealed. An additional external canister may be used if the canister is defective.

Table 11. (contd)

Fill Material Type	Approach for Introducing Fill Materials				
	Unseal and remove lid from loaded canister	Unseal and reopen canister drain and vent ports	Canister with ports for adding fill material	Cut openings into canister lid	Cut openings into canister side wall
Particles	The canister lid's seal weld is cut and lid is removed. Particulate fill is introduced into the top of the canister and is allowed to fill the canister by cascading gravity flow. Vibration may be used to speed up the flow of particulates and to enhance compaction of the particle bed. The canister's lid is reinstalled and re-welded. An additional external canister may be used if the canister is defective.	This approach will not work with particles. There are only two relatively small diameter ports in a canister lid and, even with vibration, the particles will not flow to fill the remaining sections of the canister once a section directly under the ports is filled in.	The canister fill ports are removed. Particulate fill is introduced into the top of the canister through the ports and is allowed to fill the canister by cascading gravity flow. Vibration may be used to speed up the flow of particulates and to enhance compaction of the particle bed. The canister's lid is reinstalled and re-welded. An additional external canister may be used if the canister is defective.	Particulate fill is introduced into the top of the canister through the cut openings and is allowed to fill the canister by cascading gravity flow. Vibration may be used to speed up the flow of particulates and to enhance compaction of the particle bed. The openings are closed and sealed. An additional external canister may be used if the canister is defective.	This approach will not work with particles. Particles will not flow up channels and openings to fill spaces and therefore will not move from the sides of a canister toward the center.

Table 11. (contd)

Fill Material Type	Approach for Introducing Fill Materials				
	Unseal and remove lid from loaded canister	Unseal and reopen canister drain and vent ports	Canister with ports for adding fill material	Cut openings into canister lid	Cut openings into canister side wall
Foam	The canister lid's seal weld is cut and lid is removed. Liquid that will expand to become foam is introduced via a down-tube into the bottom of the canister and is allowed to fill the canister and all available spaces by expanding upward as a medium-viscosity high-density foam. The canister's lid is reinstalled and re-welded. An additional external canister may be used if the canister is defective.	The canister drain and vent ports are unsealed and opened. Liquid that will expand to become foam is introduced via the vent tube into the bottom of the canister and is allowed to fill the canister and all available spaces by expanding upward as a medium-viscosity high-density foam. The canister's drain and vent ports are closed and sealed. An additional external canister may be used if the canister is defective.	The canister fill ports are unsealed and opened. Liquid that will expand to become foam is introduced via a down-tube into the bottom of the canister and is allowed to fill the canister and all available spaces by expanding upward as a medium-viscosity high-density foam. The canister's fill ports are closed and sealed. An additional external canister may be used if the canister is defective.	Liquid that will expand to become foam is introduced via a down-tube extending from the cut opening in the canister lid into the bottom of the canister. The foam is allowed to fill the canister and all available spaces by expanding upward as a medium-viscosity high-density foam. The openings in the canister lid are closed and sealed. An additional external canister may be used if the canister is defective.	Liquid that will expand to become foam is introduced through a side hole that is cut into the canister wall and flows down into the inside wall into the bottom of the canister. The foam then fills the canister and all available spaces by expanding upward as a medium-viscosity high-density foam. The openings in the canister lid are closed and sealed. An additional external canister may be used if the canister is defective.

## **4. REQUIREMENTS FOR FILL MATERIALS**

The previous work discussed in Chapter 2 used various criteria for choosing a fill material. Many of these criteria were specific to used nuclear fuel in waste packages for disposal and thus were related to post-closure performance of a geologic repository. Although many of the criteria could be applicable, they were not selected with consideration of storage or transportation of used nuclear fuel.

This section discusses potential criteria that could be considered when selecting a fill material for a used fuel canister. In contrast to many of the criteria presented in Section 2, these criteria are based on storage and transportation and do not consider post-closure performance. Each requirement is presented in Table 12 along with a summary of the critical elements of that requirement.

Table 12. Potential Requirements for Fill Materials

Evaluation Criteria for Candidate Canister Fill Material	Elements
Criticality Avoidance	Provide moderator exclusion Neutron absorption capability Minimize neutron moderation Provide dilution of fissile radionuclides Capacity to fill over 60% of the inner free volume of the canister Fill material does not compact by more than 10% of its original volume under its own weight or as the result of shipping or handling
Heat Transfer or Thermodynamic Properties	Promote heat transfer from the fuel Thermal stability Chemical stability Radiation stability Chemically compatible with fuel cladding, fuel, neutron poisons, fuel baskets, and other structural materials within canister
Homogeneity and Rheological Properties	Homogeneous batches Good rheological properties to ensure proper filling Ability to be placed in the canister without damaging fuel assemblies
Retrievability	Allows for safe retrieval of used nuclear fuel from a canister without need to resort to time consuming or costly measures and without further compromise of the integrity of used nuclear fuel assemblies
Material Availability and Cost	Low cost Material available in required purity
Weight and Radiation Shielding	Fill material doesn't add significantly to the weight of the container/cask system Good radiation shielding properties
Operational Considerations	Easy to emplace Fill material does not adversely react to normal conditions of transport or hypothetical accident conditions

## **4.1 Criticality Avoidance**

One of the most important criterion for fill material to meet is criticality avoidance, and one potential outcome of the use of certain fill materials could be the ability to eliminate the need to consider burnup credit in the design of the storage container or transportation cask. The standard for criticality is maintaining the effective neutron multiplication factor ( $k_{\text{eff}}$ ) at 0.95 or below. There are several ways to ensure a  $k_{\text{eff}}$  of 0.95, such as use of a fill material with significant neutron adsorption capability, by moderator exclusion, or by dilution of fissile radionuclides. The material should also be chosen so that it does not provide neutron moderation to ensure that a subcritical  $k_{\text{eff}}$  is maintained. In addition, based on analyses cited in Oversby and Werme (1995), the candidate fill material should occupy at least 60% of the original void space in the canister and the material should not compact under its own weight or as the result of shipping or handling by more than 10%.

The need for criticality avoidance as a criterion for fill material may be reduced based on the draft burnup credit guidance contained in NRC (2012), which extends the current major actinide burnup credit (NRC 2002) to include minor actinides and fission products. As discussed in Marshall and Wagner (2012), identification of credible fuel configurations may also reduce the need for a criticality avoidance criterion for fill material.

## **4.2 Heat Transfer and Thermodynamic Properties**

The fill material should also not have a detrimental impact on heat transfer. The temperature of the cladding should be demonstrated to not exceed 400 °C which is regarded as protective of used nuclear fuel cladding. Depending on the fill material and how compacted it is, the radiative and convective heat transfer mechanisms may be virtually eliminated. It is possible that this could be offset by the increase in the thermal conductivity of the fill material. However, each material would need to be evaluated for thermal properties and their effect on the thermal performance of the used nuclear fuel in the canister.

The fill material should also be chemically compatible with the fuel cladding, fuel, neutron poisons, fuel baskets, and other structural materials within canister. Also, the fill material should not undergo adverse interactions with the residual moisture within the canister such as rusting of steel shot, catalysis or radiolytic decomposition of water, or galvanic interactions with cladding or neutron shielding materials. Also, the fill material should be stable within the canister and not degrade due to heat, radiation, or by chemical reaction. The fill material should also not degrade and produce hydrogen or other gases.

Because the duration of long-term storage is also uncertain, the fill material should be relatively unaffected by age or the importance of the fill material properties demonstrated to be less important as the fuel ages. Aging of the fill material would not be important if the fill material was emplaced a short time before transportation and removed soon thereafter.

### **4.3 Homogeneity and Rheological Properties**

Good rheological properties would allow easier flow or flow readily into the canister without agitation and would allow greater assurance of meeting the fill criteria. Another consideration is that the fill material should have homogeneous properties throughout the canister fill. The fill material should also have the ability of being placed in the canister without damaging the fuel assemblies.

### **4.4 Retrievability**

The fill material should allow for the safe retrieval of used nuclear fuel from a canister without the need to resort to timely or costly measures and without further compromise of the integrity of the used nuclear fuel assemblies.

### **4.5 Material Availability and Cost**

The cost and availability of the fill material should be considered when choosing a fill material. This would include the costs of the raw materials with the required purity, processing the materials, and the cost of emplacing the materials in the canister. The ease at which the fill material could be provided to multiple locations such as nuclear power plant sites should also be considered.

### **4.6 Weight and Radiation Shielding**

First, the additional mass that the fill material provides should not result in the canister and cask weight exceeding or approaching weight restrictions for handling or transportation. However, it is possible that certain fill materials would result in a reduction in the need for shielding and as a result a reduction in the overall mass attributed to shielding. This would need to be verified with modeling. Second, the project fill material mass would need to be evaluated against the overall mass of the cask/canister system and its mass limits and any potential modifications to the canister design (wall thickness) to accommodate the additional mass. Third, the fill material may require a reduction in the number of assemblies that a canister would hold to accommodate the mass and volume occupied by the fill material and its desired properties.

### **4.7 Operational Considerations**

The fill material should be easy to emplace in the canister and the fill material should also not interfere with the sealing of the canister, such as welding of the canister lid. The fill material should not adversely react to normal conditions of transport or hypothetical accident conditions.

## **5. POTENTIAL FILL MATERIALS**

This section discusses potential fill materials. Potential fill materials were grouped into several categories such as molten materials, particulates and beads, resins, foams, and grout.

### **5.1 Molten Materials**

Two types of molten materials were evaluated, molten metals and paraffin. As discussed in Chapter 2, molten metals have been evaluated as potential fill materials for waste packages in several studies but no studies were found that had evaluated paraffin as a fill material.

#### **5.1.1 Molten Metals**

The first instance identified of a molten material being proposed for use to stabilize used nuclear fuel during transportation was a patent granted in 1974 to Wurm and Heylen (1974). In this patent, fuel rods would be placed inside a can and the filling alloy would fill the space between the fuel rods and the can. These cans containing the alloy-encased fuel rods would then be placed inside a transportation cask and shipped to their destination, typically a reprocessing plant. The filling alloy performs several functions: 1) the filling alloy stiffens the structure of the fuel element so that the fuel rods cannot break during transportation, 2) if the rods were to break, no radioactive gas would escape, and 3) the filling alloy would conduct heat from the rods to the can. It is not known if used nuclear fuel has ever been transported using the filling alloy method outlined in Wurm and Heylen (1974).

The use of molten metals as a fill material has also been investigated by the Spent Fuel Stabilizer Materials Program and the Canadian Nuclear Fuel Waste Management Program. The Spent Fuel Stabilizer Materials Program recommended 1% antimonial lead as a reference material, while the Canadian Nuclear Fuel Waste Management Program focused research and development activities on lead.

The Yucca Mountain Project also evaluated the use of a tin, lead, zinc, and zinc alloy as fill materials inside a waste package as an alternative to an inert gas (Wallin et al. 1994). Tin was rejected by Wallin et al. (1994) as not being sufficiently plentiful. Lead was rejected because it is toxic, very heavy, and can cause embrittlement of other metal components. Unalloyed zinc was rejected because it was determined that the zinc will interact with the Zircaloy fuel cladding material. Zinc alloys such as AG40B could possibly be acceptable from that standpoint, as they would have a lower tendency to interact with the cladding.

In this evaluation, 5 representative molten metals were considered:

- Tin
- Lead
- Zinc
- Zinc alloy (AG40A and AG40B)
- Wood's metal

These materials are representative of materials with relatively low melting points, less than approximately 420 °C. This temperature was chosen because it would limit the potential for gross rupture of the cladding and preserve the geometric configuration of the used nuclear fuel (NRC 2003). In addition, this temperature is well below the melting point of aluminum (660.37 °C), which is often contained in structural components of metal canisters and in neutron poisons. Table 13 lists representative properties of these materials.

Table 13. Representative Properties of Candidate Molten Metals

Material	Melting Point (°C)	Density (g/cm <sup>3</sup> )	Thermal Conductivity (W/m-K)
Tin	232	7.29	63.2
Lead	327.5	11.35	33.0
Zinc	419.58	7.10	112.2
Zinc alloy (AG40A or AG40B)	381-387	6.60	113
Wood's metal	70.0	9.58	18.0

Source: MatWeb (2012)

One of the primary requirements for a fill material is weight. Based on current designs for used nuclear fuel storage systems, the free volume in a storage canister is in the range of about 4000 to 7000 liters. Assuming that a storage canister was completely filled with molten metal, the weight of a canister would be increased by 58,200 to 102,000 lbs. for zinc alloy, the lowest density material, and by 100,000 to 175,000 lbs. for lead, the highest density material. Current canisters weigh in the range of about 80,000 to 100,000 lbs., so adding a molten metal fill material would approximately double the weight of an existing canister. The addition of a molten metal fill material to a canister would result in the canister not meeting the current requirements of the canister's 10 CFR 72 storage certificate of compliance and the 10 CFR 71 transportation certificate of compliance under which it would be shipped. The additional weight and changed contents would make it necessary to reanalyze the performance of the canister, and recertify the modified canister for continued storage. The changes would also be significant in regard to the design of the transportation cask and would require reanalysis, a probable redesign, and recertification. Therefore, for current canister designs, adding a molten metal fill material appears not to be feasible based on weight and other considerations. Future canisters and their associated transportation casks would need to be designed, possibly with lower capacities and thicker walls, to allow for the increase in weight due to the fill material. Unless the weight of the transportation cask could be reduced as a result of longer cooling times for the used nuclear fuel and possibly because of increased self-shielding by the canister, the decrease in the capacity of the canisters would be as much as 50 percent, which would double the number of canisters that would eventually have to be shipped.

### **5.1.2 Paraffin**

No studies were found where paraffin wax had been investigated as a fill material for used nuclear fuel canisters. Paraffin wax is a mixture of pure alkanes with a chemical formula of  $C_nH_{2n+2}$ . It has a melting point between about 46 and 68 °C, has a density of about 0.9 g/cm<sup>3</sup>, and burns readily if a fire retardant is not incorporated. Paraffin also has a relatively low thermal conductivity, 0.25 W/m-K. Because of its low melting point, paraffin wax could be melted for easy pouring and then hardened to insure complete covering of the used nuclear fuel in a canister. However, there are issues with the use of paraffin as a fill material. For example, paraffin is a hydrocarbon and, if neutron absorber materials are not incorporated, it is an effective neutron moderator. Thus, to make this material a viable fill material, a neutron absorber such as boron would need to be added to the paraffin before pouring. In addition, because of its flammability, a flame retardant would need to be added to the paraffin so that the paraffin material would not burn if released during a transportation accident. Also, because paraffin is a hydrocarbon, it would be subject to radiolytic decomposition that would progress over time. Consequently, except for used nuclear fuel that had been stored for long periods of time such that the source of ionizing radiation was significantly diminished, paraffin could not be used if it was to remain in a canister for a prolonged period of time. Future tests would need to be conducted to determine if paraffin would generate hydrogen or other gases during transportation, especially for used nuclear fuel that had relatively short cooling times. Interactions of paraffin with used nuclear fuel cladding and canister material would also need to be evaluated.

Another issue that would need to be resolved regarding the use of paraffin is its relatively low melting point and at what time in the future the decay heat from used nuclear fuel would be low enough such that the material would remain a solid during transportation. Alternatively, it would be necessary to determine whether a paraffin-containing transportation cask could be shipped when the paraffin was in a liquid state.

A key benefit of using paraffin would be its weight. The density of most paraffin waxes is slightly less than that of water: approximately 0.9 g/cm<sup>3</sup>. Based on current designs for used nuclear fuel storage systems, the free volume in a storage canister is in the range of about 4000 to 7000 liters. Assuming that a storage canister was completely filled with paraffin, the weight of a canister would be increased by 7,900 to 13,900 lb. This is much less than other candidate fill materials. Nonetheless, this increase in the weight of the canister would result in the canister not meeting the requirements of its current 10 CFR 71 transportation certificate of compliance. It is assumed that because paraffin would undergo radiolytic decomposition, it could not be used to stabilize the contents of a canister that would continue to be used for storing used nuclear fuel. The additional weight and changed contents would make it necessary to reanalyze the performance of, and recertify, the modified canister and transportation cask. Therefore, for current canister designs, it is uncertain whether adding paraffin would be feasible based on weight considerations. Assuming that the weight of the transportation cask would be reduced as a result of longer cooling times for the used nuclear fuel that is stabilized by paraffin fill material, it is likely that future canisters and their associated transportation casks would have capacities comparable to present day systems. This would be the case even though the canister would weigh more because of a paraffin fill material. Thus, unlike canisters that would be filled

with molten metal, there would not be an increase in the number of canisters that would need to be shipped.

## **5.2 Particulates and Beads**

As discussed in Section 2, the use of particulates and beads has been extensively studied as a fill material for waste packages. It has also been studied on an extremely limited basis as a fill material for storage containers, and transportation casks. Table 14 lists particulates and beads that have been previously studied.

In experiments conducted to determine potential interactions between particulates and Zircaloy-4, Fish et al. (1982) found that mullite, graphite, basalt, zircon, zirconia, amorphous silica, and quartz formed a brittle interaction layer at the cladding-particulate interface. Fish et al. (1982) postulated that the interaction layers consisted of zirconium oxide. The interaction layers were thought to form due to the extraction of oxygen from the silicon oxide contained in these materials and the formation of zirconium oxide. Graphite also formed an interaction layer with Zircaloy-4 cladding which was likely zirconium carbide. The formation of these interaction layers has the potential to weaken the cladding. Other materials such as interprop and sand/bondate also contain silica and would also likely form the interaction layers observed by Fish et al. (1982).

Fish et al. (1982) also conducted loss-on-ignition tests of candidate particulates. Basalt and bentonite were found to have greater than 1 percent moisture release, which could contribute to corrosion and internal pressurization of a canister.

The density of solid lead is 11.35 g/cm<sup>3</sup>. Assuming a packing fraction of 65% for lead spheres, the effective density of lead spheres would be about 7.4 g/cm<sup>3</sup>. As with the molten metals discussed in Section 5.1.1, this would substantially increase the weight of the canister by 65,300 to 114,000 lb. and would result in an extremely heavy canister. Lead spheres could also potentially compact under their own weight and form voids within the canister.

Depending on how the canisters containing the used nuclear fuel were filled, generation of dust is likely to be an issue because this dust could contaminate the welds used to seal the canister. During packing experiments conducted for the Canadian Nuclear Fuel Waste Management Program, Teper (1987) found that aluminum oxide powder, sand, zircon, rutile, ceramic zirconia, and rutile-zircon-garnet generated excessive dust. In addition, ceramic zirconia had a tendency to form voids.

Depleted uranium oxide particulates or depleted uranium silicate beads have been evaluated by Puig et al. (2008a), Forsberg (2000), Forsberg et al. (1995, 1996), and Pope et al. (1996a, 1996b). Depleted uranium particulates as a fill material for waste packages could have several desirable qualities such as criticality control, radiation shielding, and slowing the release of radionuclides from the waste package. The density of depleted uranium oxide is 10.96 g/cm<sup>3</sup>. Assuming a packing fraction of 65% for depleted uranium oxide particulates, the effective density of depleted uranium oxide particulates would be about 7.1 g/cm<sup>3</sup>. As with the molten

metals discussed in Section 5.1.1 and lead spheres, this would substantially increase the weight of the canister by 62,600 to 110,000 lb. and would result in an extremely heavy canister.

Depleted uranium silicate beads have a density of about  $4.1 \text{ g/cm}^3$ . Assuming a packing fraction of 65% for depleted uranium silicate glass beads, the effective density of depleted uranium silicate beads would be about  $2.7 \text{ g/cm}^3$ , which would increase the weight of a canister by 23,800 to 41,700 lb. This increase in weight would mean that filling existing canisters might not be feasible. However, if used nuclear fuel were cooled long enough, the added weight of the fill material might be offset by a reduction in the weight of the transportation cask. Nonetheless, because of the changed contents and added weight, it would be necessary to provide a new analysis of the performance of the canister for storage and transportation. Based only on weight, it is possible that filling future smaller (less capacity) canisters with the depleted-uranium silicate beads would be feasible, with a corresponding increase in the number of used nuclear fuel canisters. Filling canisters with depleted uranium silicate beads might also eliminate the need for burnup credit for these new canister-transportation cask systems. However, the same benefit could be realized by using boron-containing glass beads, i.e., borosilicate glass beads, which would have a poured density of about  $1.9 \text{ g/cm}^3$  and consequently would not have as much of a weight penalty as would the depleted uranium silicate beads and would also not have the radiation protection issues associated with the use of depleted uranium.

Particulate materials such as magnetite, hematite, olivine, phosphates, and zeolites have been studied as waste package fill materials by Puig et al. (2008a, 2008b, 2009) and Oversby and Werme (1995). The properties of interest were oriented towards post-closure performance of a geological repository, such as the ability to sorb radionuclides and the ability to maintain reducing conditions in the near field around a waste package. In addition, based on the results of packing experiments involving aluminum oxide powder, sand, zircon, rutile, ceramic zirconia, and rutile-zircon-garnet, there is the potential that these materials could generate excessive dust.

Metal shot, such as aluminum, steel, and copper shot, and borosilicate glass beads have been suggested as a potential fill material in several of the studies discussed in Chapter 2. The density of emplaced shot would range from about  $1.8 \text{ g/cm}^3$  for aluminum shot to about  $5.8 \text{ g/cm}^3$  for copper shot, and would be about  $1.9 \text{ g/cm}^3$  for glass beads. As with other materials of relatively high densities, this would increase the weight of existing canisters containing the used nuclear fuel and would result in the canisters not meeting the requirements of their 10 CFR 72 storage certificate of compliance and their 10 CFR 71 transportation certificate of compliance. Therefore, for current canister designs and certifications, adding metal shot or borosilicate glass beads would not be feasible solely based on weight considerations. Future canisters and their associated transportation casks would need to be designed, possibly with lower capacities, to allow for the increase in weight due to the metal shot or borosilicate glass beads. If the capacities of these canisters were less than that of current canisters the increase in the number of canisters would not be as large as for other fill materials with higher densities.

An additional issue associated with materials such as particulates and beads is the potential to compact during the normal conditions of transport. For example, during transportation of a prototype container from Toronto, Ontario, Canada to the Whiteshell Laboratories located in

**Used Fuel Disposition Campaign Storage and Transportation**  
**A Preliminary Evaluation of Using Fill Materials to Stabilize Used Nuclear During Storage and Transportation**

32

August 31, 2012

Pinawa, Manitoba, Canada, the glass-bead particulate within the container appeared to have settled, causing a 14 mm gap between the top head of the container and the top of the particulate (Crosthwaite 1994).

Table 14. Particulates and Beads Evaluated in Previous Studies

Country	Purpose	Materials Studied	References
U.S.	Waste package fill material, used nuclear fuel storage container fill material, transportation cask fill material	Sand Copper spheres Aluminum shot and spheres Zinc spheres Lead spheres Steel shot and spheres Iron shot Magnetite Rutile Amorphous silica Quartz Mullite Zircon Zirconia Basalt Graphite Sand/bondate Bentonite Glass beads and spheres Boron carbide powder Uranium oxide powder Alumina and alumina powder Depleted uranium oxide Depleted uranium silicate glass	Anderson (1981) Pope et al. (1996a, 1996b) Forsberg et al. (1995, 1996) Forsberg (2000) Wallin et al. (1994) Cogar (1996) Montierth (2000) Arthur (2000) Fish et al. (1982)
Spain	Waste package fill material	Steel shot Glass beads Spinel Depleted uranium oxide spheres Zeolites Hematite Phosphates Olivine	Puig et al. (2008a, 2008b, 2009)

Table 14. (contd)

Country	Purpose	Materials Studied	References
Canada	Waste package fill material	Sand Fine glass beads (0.002-0.3 mm) Coarse glass beads (0.8-1.2 mm) Steel shot (0.6-1.0 mm) Aluminum oxide powder Crushed bauxite grains Sintered bauxite Interprop Ceramic zirconia Rutile-Zircon-Garnet mixture Zircon Rutile	Teper (1987) Forsberg (1997)
Belgium	Waste package fill material	Sand	Bennett and Gens (2008) ONDRAF/NIRAS (2001)
Sweden	Waste package fill material	Glass beads Lead shot Copper spheres Sand Olivine Hematite Magnetite Crushed rock	Oversby and Werme (1995)

Interprop is a ceramic proppant composed of 35-65% mullite (aluminum silicate) and 35-65% corundum (aluminum oxide). A proppant is a material that will keep an induced hydraulic fracture open.  
 Bondate is an organic-based chemical bonding agent for aggregates and fibers.

### **5.3 Resins**

No studies were found where liquid resins had been investigated as a fill material for used nuclear fuel canisters. Resins are potentially good candidates for a fill material due to their ability to be poured into a canister as a liquid and then solidify to provide for total coverage of the used nuclear fuel. The fact that resins are organic and are thus moderators of neutrons could be compensated for by adding neutron absorbing materials to the resin. There are other concerns, however, that must be addressed to allow resins to be a viable fill material. These include thermal conductivity, softening point, radiation stability, density, viscosity, and ignition point.

There are many types of resins, each with varying properties, so several are researched in the present paper. These resins include FF grade wood rosin, polyurethane resin, polystyrene resin, epoxy resin, unsaturated polystyrene resin, acrylic resin and silicone resin. The material properties for several resin types are summarized in Table 15.

The densities of these resins are all relatively the same, ranging from 1.00 to 2.00 g/cm<sup>3</sup>. This equates to the addition of 8,800 to 30,800 lb. to the weight of the canister, depending on the void volume within the canister. These values are adjustable based on what curing agent is used. These curing agents can also greatly affect the other properties of the resin. Due to the high degree of fill expected when using these resins, existing canisters could not be filled with resin and shipped unless an analysis to demonstrate performance was done and approval was given by the U.S. Nuclear Regulatory Commission, and future canisters and their associated transportation casks would need to be designed with somewhat lower capacities unless the designs assumed longer cooling times before transportation and the resulting reduced weight of transportation casks offset the increased weight of the canisters.

The thermal conductivities of the resins are also all expected to be relatively the same, ranging from 0.10 to 1.00 W/m-K. This is relatively low, but with longer-cooled or low-heat used nuclear fuel it is not likely to be a concern. If necessary, it may be possible to add a material to the resin to help conduct the heat to the canister structure, such as a metal. There is very little data on thermal conductivities for resins, and so future tests would need to be conducted to establish this physical property.

Another similar characteristic shared by most resins are their resistance to radiation damage. The major damage to resins (and most polymers) from radiation is induced cross-linking or chain scission. Since the resins are cured, this damage would be reduced significantly. As stated in ATL (2001), most resins can withstand a radiation dose of 10<sup>6</sup> Gy. However, a radiation dose 10<sup>7</sup> to 10<sup>8</sup> Gy can produce damage. If the resin were poured inside the canister just before shipment of used nuclear fuel that had been in extended storage for 100 to 300 years, this potentially would probably not be an issue. Future tests would need to be conducted to verify this.

Pour viscosity is another property where most resins share a similar value. Most resins have a viscosity on the order of 1 Pa-s, about 1000 times more viscous than water and on the same order of viscosity as honey. Although this is relatively viscous, it should pose no real impedance to filling a canister other than allowing for an appropriate amount of time to fill the canister before

the curing process can take place. However, future tests would have to be conducted to verify that resins could be poured into a canister without creating significant void spaces.

The major issues with resins lie in their chemical stability, both in terms of softening and ignition points. Although cured resins soften at higher temperatures than the uncured resins that are poured into the canister to begin with, these softening points can still be well below the 400 °C temperature that is regarded as protective of used nuclear fuel cladding. In this capacity, polyurethane, epoxy and silicone resins perform best with softening points of approximately 150 °C. Further research is needed to find curing agents that would be able to increase the softening point if 150 °C is not sufficiently high.

Although resins melt at low temperatures, their ignition points can exceed 400 °C. For example, if the right curing agents are used, polystyrene, polyester and silicone resins will not ignite until temperatures of 430, 500 and 760 °C, respectively. If the resin could be exposed to the atmosphere following a fire accident, it might be necessary to include ignition retardants in the resin formulation or to conduct tests to verify that the ignition point of the resin used as a fill material is not reached, especially during the hypothetical accident conditions specified in 10 CFR 71.73. Future tests would also be needed to determine if resins could generate hydrogen or other gases when they decompose.

Table 15. Material Properties of Resins

Resin	Density (g/cm <sup>3</sup> )	Softening Point (°C)	Thermal Conductivity (W/m-K)	Viscosity (mPa-s)	Ignition Temperature (°C)
FF Wood Rosin	1.089	100–120	--	4000	--
Polyurethane	1.490	144	0.65	6000	N/A
Polystyrene	1.040	105	--	--	430
Epoxy	1.335	80–162	0.2	5000	390
Unsaturated Polyester	1.900	70–100	--	2000	500
Acrylic	1.160	108	--	1500	340
Silicone	1.000	7–138 <sup>a</sup>	--	200	760

a. Flashpoint.

Note: The material properties are representative of the type of resin and the properties of specific resins may vary.

## 5.4 Foams

No studies were found where foams were investigated as a fill material for used nuclear fuel canisters. As with resins, there are many types of foams. Table 16 summarizes the material properties of several foams.

Foams could potentially insure an easy filling process with complete coverage and support of the used nuclear fuel as well as having a low density which would not increase the weight of the canister significantly. However, the ability to inject foam inside a used nuclear fuel canister without significant void spaces would need to be verified with future experiments.

Foams have several downfalls, but like paraffin, these downfalls may be compensated for by the addition of other materials or further research. Most foams are organic in nature, and so are excellent neutron moderators. This can be compensated for by adding a neutron absorbing material to the foam before injection, or by using inorganic foams instead. Foams may also provide moderator exclusion.

Organic foams can also burn readily at relatively low temperatures (approximately 400 °C). However, foams have been used in the design of Type B radioactive materials containers. For example, the TRUPACT-II container (Docket Number 71-9218) and TRUPACT-III container (Docket Number 71-9305) both contain polyurethane foam. Nonetheless, tests would be needed to determine if foams could ignite or decompose inside a canister, especially during hypothetical accident conditions. Future tests would also be needed to determine if foams could generate hydrogen or other gases when they decompose. In addition to chemical and radiation stability, foams must have desirable properties in the thermal stability, rheology, density, and strength criteria. Based on the ignition temperatures in Table 16, organic foams may not be the best choice for a fill material due to low ignition temperatures, and metal or ceramic foams may have desirable properties in the areas of structural integrity, increased thermal conductivity, lack of neutron moderation, and their high temperature performance.

The density of foams can vary widely based on what material they are, as well as whether they have open- or closed-cell structures. An open-cell foam is one where the gas is not trapped within the foam structure, much like that of a common sponge, while a closed-cell foam is a solid material with gas bubbles are trapped inside. Thus, the open-cell foams are less dense, but the closed-cell foams have a higher strength.

Although the addition of neutron absorbers to the foam before pouring would prevent criticality, the radiation from the used nuclear fuel may also cause material degradation. In Huang et al. (2007), the radiation dose at which degradation begins is  $10^6$  Gy. This is similar to the degradation threshold for resins. If foam were injected into the canister just before shipment of the used nuclear fuel that had been in extended storage for 100 to 300 years, this potentially would not be an issue. Future tests would be needed to verify this.

Table 16. Material Properties of Foams

Foam	Density (g/cm <sup>3</sup> )	Thermal Conductivity (W/m-K)	Ignition Temperature (°C)
Polyurethane	0.013–0.160	0.03	400
Polystyrene	0.032–0.050	0.03	350
Aluminum	0.216–0.675	5.80	660 <sup>a</sup>
Steel	0.040–0.950	0.80	1535 <sup>a</sup>
Silicon Carbide	0.257–0.803	5.28	2700 <sup>b</sup>

a. Melting point  
b. Sublimation point

Note: The material properties are representative of the type of foam and the properties of specific foams may vary.

## 5.5 Grout

Two studies (Anderson 1981 and Oversby and Werme 1995) discussed in Chapter 2 evaluated the use of cement grout (i.e., concrete or mortar) as a fill material for used nuclear fuel canisters. Sweden also evaluated concrete as a fill material in a titanium canister used for very deep hole disposal (SKB 1992). Grout is commonly used to solidify liquid low-level radioactive and to stabilize low-level radioactive waste prior to disposal. Grout has also been used to solidify liquid high-level radioactive waste in Italy (Alonzo et al. 2001) and to stabilize empty high-level radioactive waste tanks at the Savannah River Site. Grout has also been used to stabilize used nuclear fuel sludge at the Hanford Site.

A primary issue associated with using grout as a fill material would be its weight. Grout has a density of about 2.0 g/cm<sup>3</sup> which would increase the weight of a canister with used nuclear fuel contents by 17,600 to 30,900 lb. A significant consequence of the combined increased weight and addition of grout to the canister's contents would be that existing canisters would not comply with the requirements of their current 10 CFR 72 storage certificate of compliance and their 10 CFR 71 transportation certificate of compliance. Therefore, for current canister designs, adding grout would not be possible unless the safety analyses for storage and transportation were revised to demonstrate that the canisters with grout fill material would satisfy the requirements of U.S. Nuclear Regulatory Commission regulations and U.S. Nuclear Regulatory Commission approval was obtained. It might be feasible to ship the heavier canisters if the used nuclear fuel had cooled sufficiently to allow an offsetting reduction in the shielding needed and a new design for the transportation cask with reduced weight was developed and certified. Future canisters and their associated transportation casks would need to be designed with somewhat lower capacities unless the designs assumed longer cooling times before transportation and the resulting reduced weight of transportation casks offset the increased weight of the canisters.

Another issue associated with using grout as a fill material would be its ability to flow between the fuel rods and around other structural materials in the canister. Future tests would be needed to verify that this was feasible. In addition, cement grout contains water, which is a neutron

**Used Fuel Disposition Campaign Storage and Transportation**  
**A Preliminary Evaluation of Using Fill Materials to Stabilize Used Nuclear During Storage and Transportation**

August 31, 2012

39

moderator, so a neutron absorbing material might have to be added to the grout to ensure subcriticality. Also because grout contains water, future tests would also be necessary to evaluate radiolysis and interactions of grout with fuel cladding, fuel, neutron poisons, fuel baskets, other structural materials within canister, the canister itself.

## **6. CONCLUSIONS AND RECOMMENDATIONS**

Based on the weight of the potential fill materials discussed in Chapter 5, adding fill materials to existing canisters would result in the canisters not meeting the current requirements of their 10 CFR 72 storage certificate of compliance and their 10 CFR 71 transportation certificate of compliance. Depending on the cooling time assumed for the used nuclear fuel, future canisters and their associated transportation casks might need to be designed with lower capacities and thicker walls to allow for the increase in weight due to the addition of the fill material. Foam fill materials might be an exception to this.

Most studies that have evaluated fill materials and their properties have been literature reviews; few have been studies that conducted experiments. Also, from the perspective of the Used Fuel Disposition Campaign, a significant gap in the existing studies is that none have evaluated the performance of the fill materials during the normal conditions of transport or during hypothetical transportation accident conditions. Studies that addressed this gap would need to include ones that assessed the ability of the fill material to maintain its own geometric configuration (e.g., not slump) and maintain the geometric configuration of the used nuclear fuel under normal conditions of transport and under hypothetical accident conditions. Such studies would provide the information that would be needed to determine whether credit could be taken for the fill material being able to exclude water moderator or provide neutron absorbers such that the fissile material package requirements in 10 CFR 71.55 could be shown to be satisfied.

Consequently, the use of fill materials to stabilize used nuclear fuel in canisters would require a comprehensive experimental program. Especially important would be:

- Experiments that would evaluate the interactions among the fill material, fuel cladding, fuel, fuel baskets, neutron poisons, and other structural materials including the canister itself.
- Experiments that would determine if a fill material could be efficiently, effectively, and reliably emplaced inside a canister containing used nuclear fuel, filling the free volume without leaving an excessive number of, or large voids
- Experiments that would evaluate the efficacy of heat conduction from fuel rods in fuel assemblies through the fill material to the heat removal features of the canister and determine the resulting temperatures of fuel cladding.

Molten materials, particulates, and beads have been extensively studied as fill materials for waste packages and their ability to function in this capacity is reasonably well known. Nonetheless, the scope of the research and development effort would be greatest if molten metal fill was used, for which canisters that contain used nuclear fuel would have to be preheated and cooled under carefully controlled conditions. The research and development would necessarily determine the process and procedure, and alternatives, for retrieving used nuclear fuel from canisters where molten metal fill had been used. Other issues such as the compatibility of the molten metal fill material and fuel cladding and safety related components of a canister would need to be determined. Techniques would also need to be developed and demonstrated for filling a canister

with molten metal, for determining that the fill was successful and that voids did not remain within the cast metal matrix, and for recovering from an unsuccessful fill.

Paraffin is an alternative molten material that might be used to fill canisters if the decay heat of the used nuclear fuel was not too great. Although paraffin is a neutron moderator and is flammable, a neutron absorber material might be dissolved in it as might a fire retardant material. As with molten metal fill materials, it would likely be necessary to heat canisters to ensure that the molten paraffin infiltrated into all of the available spaces in the canister. Unlike molten metal, high temperatures would probably not be necessary. It would be necessary to demonstrate that the paraffin would not be molten during normal transportation, could maintain the geometric configuration of the used nuclear fuel during normal and hypothetical accident conditions of transportation, and that it would not leak out following a transportation accident if temperatures were great enough to re-melt the material. Paraffin would be subject to radiolysis and therefore could not be used for extended storage during periods when the radiation source of the used nuclear fuel remained high.

If the fill material was a particulate or bead, it is likely that the canister and its used nuclear fuel contents would have to be vibrated during the filling process to ensure that the particles filled the available void spaces and with the desired packing density. It would be necessary to conduct research to develop techniques and tests to demonstrate, with high confidence, that particulate fill material would successfully infiltrate into all of the available open spaces within a canister and in and around the fuel assemblies leaving few if any voids. Because the condition of the fuel cladding would be suspect or unverified (otherwise, it would not be necessary to introduce fill material into a canister), tests would be necessary to determine if vibrating the canister could further damage the fuel cladding.

Because resins contain organic compounds, it may not be possible to formulate one that does not decompose or produce hydrogen or other gases when subjected to the heat and radiation environment in a dry used nuclear fuel canister, or when subjected to temperatures that might occur during hypothetical accident conditions.

Foams, especially inorganic foams, show some promise for use as fill materials. Nonetheless, it would be necessary to conduct extensive tests and demonstrations to show that a foam would reliably flow into and fill, at the required density, all of the void spaces and in and around the fuel rods in a canister that contained used nuclear fuel. Also, as with resins it would also be necessary to demonstrate that the foam did not decompose or produce hydrogen or other gases as a consequence of being exposed to heat and radiation or to temperatures that would exist following hypothetical transportation accident conditions.

Grout has also been extensively studied for stabilizing low-level radioactive waste and other waste and its ability to function in this capacity is also reasonably well known.

In addition to the research and development that would be required for the fill material that would be used, the process for emplacing the fill material into canisters containing used nuclear fuel would have to be demonstrated for its reliability, safety, and efficiency. The process would

**Used Fuel Disposition Campaign Storage and Transportation  
A Preliminary Evaluation of Using Fill Materials to Stabilize Used Nuclear During Storage and  
Transportation**

42

August 31, 2012

need to be located in a dedicated facility, possibly a facility that can be disassembled and moved for use at multiple sites, or a dedicated area within an existing facility. Whether the process was to be installed in a new facility or an existing facility, it would be necessary to design, license, and construct/install the facility at every site where canisters were to be filled with a fill material, or develop a mobile facility. Conceptual designs for a facility that could be moved among sites have been proposed in the past. Such a design might be adopted, with modifications for use at a single site where fill material was to be placed into canisters containing used nuclear fuel. The design of such a facility could require substantial research and development.

Before fill materials could be used to stabilize used nuclear fuel contained in storage and transportation canisters a substantial development, design, and licensing effort would need to be undertaken. In addition, the results of previous work show that use of fill materials to stabilize used nuclear fuel inside storage and transportation canisters would present significant technical challenges. Therefore, further research on the use of fill materials to stabilize used nuclear fuel during storage and transportation is not recommended unless options such as showing that the fuel remains intact or canning of used nuclear fuel do not prove to be feasible.

## 7. REFERENCES

- 10 CFR 71            10 CFR 71. "Packaging and Transportation of Radioactive Material." Code of Federal Regulations, U.S. Nuclear Regulatory Commission.
- 10 CFR 72            10 CFR 72. "Licensing Requirements for the Independent Storage of Spent Nuclear Fuel, High-Level Radioactive Waste, and Reactor-Related Greater Than Class C Waste." Code of Federal Regulations, U.S. Nuclear Regulatory Commission.
- ATL 2001            Advanced Technologies and Laboratories International, Inc. 2001. "Technical Assistance on the Evaluation of Resin Polymers Used in Storage and Transportation Cask Shield Designs." Accession Number ML011860442. Germantown, Maryland.
- Alonzo et al. 2001    Alonzo G, M Casarci, C Pastore, E Petagna, P Tortorelli, S Bolgherini, G Jacovazzi, F Pietrini, S Campa. 2001. "Conditioning of HLW by Immobilizing in Concrete at SIRTE-MOWA Plant." In WM'01 Conference, February 25-March 1, 2001, Tucson, Arizona.
- Anderson 1981        Anderson KJ. 1981. "The Use of Filler Materials to Aid Spent Nuclear Fuel Dry Storage." AGNS-35900-1.3-143. Allied-General Nuclear Services, Barnwell, South Carolina.
- Arthur 2000           Arthur S. 2000. "EQ6 Calculation for Chemical Degradation of Shippingport LWBR (Th/U Oxide) Spent Nuclear Fuel Waste Packages." CAL-EDC-MD-000008 REV 00. Accession Number MOL.20000926.0295. CRWMS M&O, Las Vegas, Nevada.
- Bennett and Gens 2008    Bennett DG and R Gens. 2008. "Overview of European Concepts for High-Level Waste and Spent Fuel Disposal with Special Reference Waste Container Corrosion." Journal of Nuclear Materials 379:1-8.
- Carlsen and Brady Raap 2012    Carlsen BW and M Brady Raap. 2012. "Dry Transfer Systems for Used Nuclear Fuel." FCRD-UFD-2012-000115. Used Fuel Disposition Campaign, U.S. Department of Energy, Washington, DC.
- Cogar 1996a           Cogar JA. 1996. "Technical Document Preparation Plan for Waste Package Filler Material Testing Report." BBA000000-01717-2500-00007 REV 00. Accession Number MOL.19961007.0209. CRWMS M&O, Las Vegas, Nevada.

**Used Fuel Disposition Campaign Storage and Transportation  
A Preliminary Evaluation of Using Fill Materials to Stabilize Used Nuclear During Storage and  
Transportation**

44

August 31, 2012

- Cogar 1996b Cogar JA. 1996. "Spent Nuclear Fuel Waste Package Filler Testing Technical Guidelines Document." BBA000000-01717-2500-00003 REV 03. Accession Number MOL.19970421.0214. CRWMS M&O, Las Vegas, Nevada.
- Cogar 1996c Cogar JA. 1996. "Waste Package Filler Material Testing Report." BBA000000-01717-2500-00008 REV 02. Accession Number MOL.19970121.0004. CRWMS M&O, Las Vegas, Nevada.
- Crosthwaite 1994 Crosthwaite JL. 1994. "The Performance, Assessment and Ranking of Container Design Options for the Canadian Nuclear Fuel Waste Management Program." TR-500, COG-93-410. Whiteshell Laboratories, Pinawa, Manitoba, Canada.
- Fish et al. 1982 Fish RL, N Wynhoff, and VJ Ferrell. 1982. "Spent LWR-Fuel Waste-Package-Stabilizer Recommendations." HEDL-7204. Hanford Engineering Development Laboratory, Richland, Washington.
- Forsberg 1997 Forsberg CW. 1997. "Description of the Canadian Particulate-Fill Waste-Package (WP) System for Spent-Nuclear-Fuel (SNF) and its Applicability to Light-Water Reactor SNF WPs with Depleted Uranium-Dioxide Fill." ORNL/TM-13502. Oak Ridge National Laboratory, Oak Ridge, Tennessee.
- Forsberg 2000 Forsberg CW. 2000. "Effect of Depleted-Uranium Dioxide Particulate Fill on Spent-Nuclear-Fuel Waste Packages." Nuclear Technology 131:337-353.
- Forsberg et al. 1995 Forsberg CW, RB Pope, RC Ashline, MD DeHart, KW Childs, and JS Tang. 1995. DUSCOBS – A Depleted-Uranium Silicate Backfill for Transport, Storage, and Disposal of Spent Nuclear Fuel. ORNL/TM-13045. Oak Ridge National Laboratory, Oak Ridge, Tennessee.
- Forsberg et al. 1996 Forsberg CW, RB Pope, RC Ashline, MD DeHart, KW Childs, and JS Tang. 1996. "Depleted-Uranium-Silicate Backfill of Spent-Fuel Waste Packages for Repository Containment and Criticality Control." In High Level Radioactive Waste Management, Proceedings of the Seventh Annual International Conference. pp. 366-368. April 29-May 3, 1996, Las Vegas, Nevada.
- Huang et al. 2007 Huang W, YS Xu, XJ Chen, XL Gao, and YB Fu. 2007. "Study on the Radiation Effect of Polyether-Urethane in the Gamma-Radiation Field." Journal of Radioanalytical and Nuclear Chemistry 273(1):91-98.

**Used Fuel Disposition Campaign Storage and Transportation**  
**A Preliminary Evaluation of Using Fill Materials to Stabilize Used Nuclear During Storage and Transportation**

August 31, 2012

45

- Johnson et al. 1994 Johnson LH, JC Tait, DW Shoesmith, JL Crosthwaite, and MN Gray. 1994. "The Disposal of Canada's Nuclear Fuel Waste: Engineered Barriers Alternatives." AECL-10718, COG-93-8. Whiteshell Laboratories, Pinawa, Manitoba, Canada.
- Marshall and Wagner (2012) Marshall W and J Wagner. 2012. "Impact of Fuel Failure on Criticality Safety of Used Nuclear Fuel." Presented at 11th International Probabilistic Safety Assessment and Management Conference and the Annual European Safety and Reliability Conference. June 25-29, 2012. Helsinki, Finland.
- MatWeb (2012) MatWeb. 2012. "MatWeb Material Property Data." [www.matweb.com](http://www.matweb.com).
- Mobasheran 1999 Mobasheran AS. 1999. "Enrico Fermi Fast Reactor Spent Nuclear Fuel Criticality Calculations: Intact Mode." BBA000000-01717-0210-00037 REV 00. Accession Number MOL.19990125.0079. CRWMS M&O, Las Vegas, Nevada.
- Montierth 2000 Montierth LM. 2000. "Intact and Degraded Criticality Calculations for the Codisposal of Shippingport LWBR Spent Nuclear Fuel in a Waste Package." CAL-EDC-NU-000004 REV 00. Accession Number MOL.20000922.0093. CRWMS M&O, Las Vegas, Nevada.
- Moscalu et al. 2000 Moscalu DR, L Angers, J Monroe-Rammsy, and HR Radulescu. 2000. "Enrico Fermi Fast Reactor Spent Nuclear Fuel Criticality Calculations: Degraded Mode." CAL-EDC-NU-000001 REV 00. Accession Number MOL.20000802. 0002. CRWMS M&O, Las Vegas, Nevada.
- NRC 2002 U.S. Nuclear Regulatory Commission. 2002. "Burnup Credit in the Criticality Safety Analyses of PWR Spent Fuel in Transport and Storage Casks." Spent Fuel Project Office, Interim Staff Guidance-8, Revision 2. Washington, DC.
- NRC 2003 U.S. Nuclear Regulatory Commission. 2003. "Cladding Considerations for the Transportation and Storage of Spent Fuel." Spent Fuel Project Office, Interim Staff Guidance-11, Revision 3. Washington, DC.
- NRC 2012 U.S. Nuclear Regulatory Commission. 2012. "Burnup Credit in the Criticality Safety Analyses of PWR Spent Fuel in Transport and Storage Casks." Spent Fuel Project Office, Interim Staff Guidance-8, Revision 3 (Draft), Accession Number ML12115A303. Washington, DC.
- NWMO 2005 Nuclear Waste Management Organization. 2005. "Incorporation of Seaborn Panel Recommendations and Insights in Work of the NWMO." NWMO Background Paper 2-8. Toronto, Ontario, Canada.

**Used Fuel Disposition Campaign Storage and Transportation**  
**A Preliminary Evaluation of Using Fill Materials to Stabilize Used Nuclear During Storage and Transportation**

46

August 31, 2012

- ONDRAF/NIRAS 2001 ONDRAF/NIRAS. 2001. “SAFIR 2: Safety Assessment and Feasibility Interim Report 2.” Report No. NIROND 2001-06 E. Belgian Agency for Radioactive Waste and Enriched Fissile Materials.
- Oversby and Werme 1995 Oversby VM and LO Werme. 1995. “Canister Filling Materials – Design Requirements and Evaluation of Candidate Materials.” In Scientific Basis for Nuclear Waste Management XVIII. Materials Research Society Symposium Proceedings 353:743-750. October 23-27, 1994, Kyoto, Japan.
- Pope et al. 1996a Pope RB, CW Forsberg, MD DeHart, KW Childs, and JS Tang. 1996. “Potential Benefits and Impacts on the CRWMS Transportation System of Filling Spent Nuclear Fuel Shipping Casks with Depleted Uranium Silicate Glass.” In SPECTRUM ’96: Proceedings of the International Topical Meeting on Nuclear and Hazardous Waste Management. August 18-23, 1996, Seattle, Washington.
- Pope et al. 1996b Pope RB, CW Forsberg, RC Ashline, MD DeHart, KW Childs, and JS Tang. 1996. “Benefits/Impacts of Utilizing Depleted Uranium Silicate Glass as Backfill for Spent Fuel Waste Packages.” In High Level Radioactive Waste Management, Proceedings of the Seventh Annual International Conference. pp. 369-371. April 29-May 3, 1996, Las Vegas, Nevada.
- Puig et al. 2008a Puig F, J Dies, J de Pablo, and A Martinez-Esparza. 2008. “Spent Fuel Canister for Geological Repository: Inner Material Requirements and Candidates Evaluation.” Journal of Nuclear Materials 376:181-191.
- Puig et al. 2008b Puig F, J Dies, M Sevilla, J de Pablo, JJ Pueyo, L Miralles, and A Martinez-Esparza. 2008. “Inner Material Requirements and Candidates Screening for Spent Fuel Disposal Canister.” In Scientific Basis for Nuclear Waste Management XXXI. Materials Research Society Symposium Proceedings 1107:67-74. September 16-21, 2007, Sheffield, England.
- Puig et al. 2009 Puig F, J Dies, M Sevilla, J de Pablo, JJ Pueyo, L Miralles, and A Martinez-Esparza. 2009. “Selection and Evaluation of Inner Material Candidates for Spanish High Level Radioactive Waste Containers.” In ICEM2007: Proceedings of the 11th International Conference on Environmental Remediation and Radioactive Waste Management. pp. 285-292. September 2-6, 2007, Bruges, Belgium.
- Radulescu 2000 Radulescu HR. 2000. “Evaluation of Codisposal Viability for Th/U Oxide (Shippingport LWBR) DOE-Owned Fuel.” TDR-EDC-NU-000005 REV 00. CRWMS M&O, Las Vegas, Nevada.

**Used Fuel Disposition Campaign Storage and Transportation**  
**A Preliminary Evaluation of Using Fill Materials to Stabilize Used Nuclear During Storage and Transportation**

August 31, 2012

47

- Shelson 1983 Shelson KN. 1983. "Particulate Packings for Irradiated Fuel Disposal Containers." Report No. 83085. Ontario Hydro Design and Development Division, Ontario Hydro Technologies, Toronto, Canada.
- SKB 1992 Svensk Kärnbränslehantering AB. 1992. "Project on Alternative Systems Study (PASS) Final Report." Technical Report 93-04. Stockholm, Sweden.
- SKB 2010 Svensk Kärnbränslehantering AB. 2010. "Design, Production and Initial State of the Canister." Technical Report TR-10-14. Stockholm, Sweden.
- Teper 1987 Teper B. 1987. "Test Program of Granular Materials for the Thin-Walled Particulate-Packed Container." Report No. 87-154-K. Ontario Hydro Research Division.
- UFDC 2012 Used Fuel Disposition Campaign. 2012. "Gap Analysis to Support Extended Storage of Used Nuclear Fuel." FCRD-USED-2011-000136 Rev. 0, PNNL-20509. Used Fuel Disposition Campaign, U.S. Department of Energy, Washington, DC.
- Wallin et al. 1994 Wallin WE, RH Bahney, and DA Thomas. 1994. "Initial Review/Analysis of Thermal and Neutronic Characteristics of Potential MPC/WP Filler Materials." BBA000000-01717-5705-00001 REV 00. Accession Number NNA.940602.0019. CRWMS M&O, Las Vegas, Nevada.
- Wallin 1996 Wallin WE. 1996. "Analysis of MPC Access Requirements for Addition of Filler Materials." BB0000000-01717-0200-00010 REV 00. Accession Number MOL.19960917.0030. CRWMS M&O, Las Vegas, Nevada.
- Werme and Eriksson 1995 Werme L and J Eriksson. 1995. "Copper Canister with Cast Inner Component, Amendment to Project on Alternative Systems Study (PASS), SKB TR 93-04." Technical Report 95-02. Svensk Kärnbränslehantering AB, Stockholm, Sweden.
- Wurm and Heylen 1974 Wurm JG and PR Heylen. July 23, 1974. "Method of Transporting and Processing Irradiated Fuel Elements." US Patent 3,824,673.
- Wynhoff et al. 1982 Wynhoff N, SE Girault, and RL Fish. 1982. "Spent Fuel Stabilizer Material Characterization and Screening." HEDL-7210. Hanford Engineering Development Laboratory, Richland, Washington.

## **APPENDIX F**

### **Summary of PNNL Transportation Activities for FY12 to Support the UFD Program**

## Summary of PNNL Transportation Activities for FY12 to Support the UFD Program

### 1. Integration of Transportation Gap Analysis with the Storage Gap Analysis

For this task the Features, Events, and Processes (FEPs) for Transportation that were identified and documented in the FY11 mid-year and year-end reports were further evaluated to understand the differences between the transportation gaps and the storage gaps. The transportation gaps report was modified to facilitate consolidate of the transportation FEPs with the storage FEPs. The list of SSCs and the associated degradation mechanisms [known as features, events, and processes (FEPs)] were based on the list of used nuclear fuel (UNF) storage system SSCs and degradation mechanisms developed by the UFD Storage Task (Hanson et al. 2011). Other sources of information surveyed to develop the list of SSCs and their degradation mechanisms included references such as Evaluation of the Technical Basis for Extended Dry Storage and Transportation of Used Nuclear Fuel (NWTRB 2010), Transportation, Aging and Disposal Canister System Performance Specification, Revision 1 (OCRW 2008), Data Needs for Long-Term Storage of LWR Fuel (EPRI 1998), Technical Bases for Extended Dry Storage of Spent Nuclear Fuel (EPRI 2002), Used Fuel and High-Level Radioactive Waste Extended Storage Collaboration Program (EPRI 2010a), *Industry Spent Fuel Storage Handbook* (EPRI 2010b), and *Transportation of Commercial Spent Nuclear Fuel, Issues Resolution* (EPRI 2010c). SSCs include items such as the fuel, cladding, fuel baskets, neutron poisons, metal canisters, etc. Potential degradation mechanisms (FEPs) included mechanical, thermal, radiation and chemical stressors, such as fuel fragmentation, embrittlement of cladding by hydrogen, oxidation of cladding, metal fatigue, corrosion, etc. The degradation mechanisms were evaluated for influence by high burnup, additional data needs, importance of research and development (R&D), and the importance to transportation. These categories were used to identify the most significant transportation degradation mechanisms. In general, the Transportation Importance assigned in above mirrored the importance assigned by the UFD Storage Task. However, there were a few differences as noted in Table 1 below.

Table 1 – Summary of Storage and Transportation Importance Differences

Stressor	Degradation Mechanism	Importance		Comments
		Storage	Trans	
<b>Neutron Poisons</b>				
Thermal	Thermal aging affects	Med	HIGH	Aging effects on poisons could affect structural properties to the extent that they would not survive the loads of transportation hypothetical accident conditions and compromise the ability to prevent a nuclear criticality. For storage moderator control is the primary mechanism for criticality

Stressor	Degradation Mechanism	Importance		Comments
		Storage	Trans	
				control.
<b>Bolted Direct-Load Casks</b>				
Thermal and Mechanical	Thermo mechanical fatigue of seals and bolts	Med	Low	Failure of seals and bolts due to thermomechanical fatigue is important for storage relicensing. It is expected that bolts and seals would be inspected prior to transportation to assure their integrity. However, if issues are found with seals that could mean having to replace the seals in a pool.

In addition to the comparison of storage and transportation gaps the following discussions were prepared as contributions to the storage and transportation gap analysis report.

- Transportation Regulation History including a summary of historical shipment
- Used Nuclear Fuel Transportation Casks including key functional and performance requirements of UNF transportation casks. It also described modern UNF shipping casks for both legal weight truck and rail transportation.
- Regulations and Regulatory Guidance Governing Transportation of UNF
- Application of NRC Regulations in the Design and use of Used Nuclear Fuel Transportation Casks
- Current Issues Surrounding the Application of NRC Regulations in the Design and use of UNF Transportation Casks

## 2. Orphan Site Task

A report is in progress that will be completed in October 2012 that analyzes in detail each of the orphan sites. Specifically, the report will present the following discussions:

- Current State
- Desired End State
- Assumptions
- Actions Necessary to Achieve Desired End State
- Conclusions

The discussion on the current state of each of the 9 orphan sites will describe the UNF and GTCC inventory at the 9 orphan sites, and will include items such as the number of canisters/casks of UNF and GTCC, the storage system used at the site, the associated transportation cask, whether a transfer cask would be necessary, and whether impact limiters and transportation casks have been fabricated. Information on the UNF will be collected to the extent available from sources such as the RW-859 database and utility site managers. Specific items to be discussed with site managers will include the type of used nuclear fuel (BWR or PWR); the design, configuration, and composition (including type of cladding) of the used nuclear fuel assemblies; the number of assemblies and canisters in storage; the types of canister and storage system; the number of assemblies per canister; the identification numbers for the fuel assemblies contained in each canister; the condition of each fuel assembly (undamaged, intact, failed); the reported range of burnups, enrichments, and discharge dates (and the associated decay heats, isotopic compositions, and radiation source terms); and whether the canisters, as loaded, are transportable; and, if transportable, the name of the transportation cask and associated current NRC 10 CFR 71 Certificate of Compliance. It is acknowledged that all this information may not be available from all sites. The section will also describe any unique considerations associated with the storage and transportation system used at the site.

In addition, this section will also describe the equipment that is present at the site, the infrastructure at the sites (e.g., secure cask handling and loading equipment, facilities, and support structures; secure equipment, cask, and railcar staging and parking areas; radiological health support facilities and services or areas for installation of temporary facilities; electric power, water, and fire-protection services or access to same; site operations and personnel sheltering and safety facilities or areas for installation of temporary facilities), and the nearest transportation interfaces for rail, barge, and heavy haul truck (including limitations such as railcar weight limits for local transportation route segments; known or expected restrictions on use of the local routes; permitting requirements; and additional resources (including equipment such as cranes and public safety services such as physical security).

As part of this task each of the orphan sites will be visited. During the week of 8/27/12 Maine Yankee, Connecticut Yankee, and Yankee Rowe were visited. Other sites will be visited in FY2013. For sites not visited, information from Facility Interface Data Sheets, Services Planning Documents, Near-Site Transportation Infrastructure Reports, and Facility Interface Capability Assessment Cask-Handling Assessments will be used to establish a baseline, augmented by information from site managers and web resources.

The section on the Desired End State will describe the desired end state of the sites, i.e., UNF and GTCC removed.

The assumptions section will list and describe the assumptions used in the preparation of the report. Examples of these assumptions include:

- The location of the Consolidated Storage Facility (CSF), site selection, waste acceptance criteria, and licensing are outside of the scope of this report. Note—there may be multiple CSFs.
- UNF and GTCC in canisters or casks will meet the waste acceptance criteria and documented safety analysis requirements of the CSFs.
- No repackaging of UNF or GTCC will be necessary at the origin sites.
- UNF and GTCC will be shipped using rail, barge, or heavy-haul truck. Legal weight truck and overweight trucks (< 115,000-125,000 lbs) will not be used to ship UNF or GTCC. However, they may be used to ship campaign kits.
- UNF and GTCC will be shipped using AAR specification railcar.
- An MOU between DOE and each utility defining roles and responsibilities at each site would be established. Would vary at each site; could vary by utility.
  - The utility is responsible for all operations inside ISFSI boundary and all operations necessary to put UNF and GTCC into 10 CFR 71 shippable configuration.
  - DOE is shipper of record; utilities must provide detailed content information.
  - DOE procures railcars, DOE procures escort cars.
  - DOE hires heavy haul truck contractor. DOE hires railroads.
  - DOE provides security; tracking; security at ISFSI site is utility responsibility. During loading, utility provides security. After loading and outside ISFSI boundary, DOE provides security.
- Open Items:
  - Who (DOE or utility) provides transportation cask?
  - Who pays for restablishing transportation infrastructure?

The section describing the Actions Necessary to Achieve Desired End State will describe the actions (i.e., task list) necessary to achieve the desired end state. The section will describe actions such as (not all inclusive):

- What equipment (casks, transfer casks [if needed], handling equipment [leak test equipment, rotating equipment, cask fixtures, cranes, lift equipment], is needed for each of 9 sites.
- Cask fabrication schedules.
- Regulatory licensing—which casks are licensed, not built; licensed, built, no impact limiters; not licensed, not built, etc.
- Content reviews to meet CoC requirements.
- How many transportation casks, impact limiters, rail cars, buffer cars, escort cars, heavy haul truck movements, etc. per site.
- Training of site personnel and transportation personnel and security personnel (Every site will have different equipment, organize by cask system?)

This section will also contain a generic schedule and task list to perform these actions.

Cases to be examined include:

1. Direct rail (CSF has rail capability)
2. Heavy haul truck -> rail (CSF has rail capability)
3. Heavy haul truck -> barge -> rail (CSF has rail capability)
4. Heavy haul truck -> barge -> Heavy haul truck (CSF has barge capability, e.g., SRS)

The conclusions section will discuss the overall conclusions for the orphan sites study including items such as shipping considerations and hurdles for each site

### 3. Evaluation of Issues Associated with Canister Stabilization

The following report was issued on August 28<sup>th</sup>, 2012 -

*A Preliminary Evaluation of Using Fill Materials to Stabilize Used Nuclear Fuel During Storage and Transportation – FCRD-UFD-2012-000243* (PNNL-21664).

The objective of the research described in this report was to conduct a preliminary evaluation of potential fill materials that could be used to fill void spaces in and around used nuclear fuel contained in dry storage canisters in order to stabilize the geometry and mechanical structure of the used nuclear fuel during extended storage and subsequent transportation. The use of fill material to stabilize used nuclear fuel is not considered to be a primary option for safely transporting used nuclear fuel after extended storage. However, the evaluation of potential fill materials, such as those described in this report, might provide the U.S. Department of Energy Used Fuel Disposition Campaign with an option that would allow continued safe storage and transportation if other options such as showing that the fuel remains intact or canning of used nuclear fuel do not prove to be feasible.

As a first step in evaluating fill materials, previous work done in this area was summarized. This involved studies done by the Spent Fuel Stabilizer Materials Program, Allied-General Nuclear Services, the Canadian Nuclear Fuel Waste Management Program, the U.S. Department of Energy, Spain, Sweden, and the Department of Energy's Yucca Mountain Project. A wide variety of potential fill materials were evaluated in these studies, ranging from molten metal to particulates and beads to liquids and gases. The common element in the studies was that they were focused on the use of fill materials in waste packages for disposal, not in storage canisters or transportation casks. In addition, very few studies involved actual experiments that measured some physical property of the fill material to be used as a stabilizing material, and no studies were found that analyzed the performance of transportation casks containing fill material during the normal conditions of transport specified in 10 CFR 71.71 or under hypothetical accident conditions specified in 10 CFR 71.73. In addition, most studies did not address issues that would be associated with production-scale emplacement of fill material in canisters, as opposed to laboratory- or experimental-scale use of fill material. It is noteworthy that Sweden abandoned its plan to use fill materials to stabilize waste packages due to the complexity of emplacing the fill material.

A part of the evaluation of fill materials, conceptual descriptions of how canisters might be filled were developed with different concepts for liquids, particles, and foams. The requirements for fill materials were also developed. Elements of the requirements included criticality avoidance, heat transfer or thermodynamic properties, homogeneity and rheological properties, retrievability, material availability and cost, weight and radiation shielding, and operational considerations.

Potential fill materials were grouped into 5 categories and their properties, advantages, disadvantages, and requirements for future testing were discussed. The categories were molten materials, which included molten metals and paraffin; particulates and beads; resins; foams; and grout. Based on this analysis, further development of fill materials to stabilize used nuclear fuel during storage and transportation is not recommended unless options such as showing that the fuel remains intact or canning of used nuclear fuel do not prove to be feasible.

## **APPENDIX G**

### **Dry Storage of Used Fuel Transition to Transport**

# **Dry Storage of Used Fuel Transition to Transport**

## **Fuel Cycle Research & Development**

Prepared for  
U.S. Department of Energy  
Transportation UFD

D.R. Leduc

Savannah River National Laboratory

August 2012

FCRD-UFD-2012-000253



**DISCLAIMER**

This information was prepared as an account of work sponsored by an agency of the U.S. Government. Neither the U.S. Government nor any agency thereof, nor any of their employees, makes any warranty, expressed or implied, or assumes any legal liability or responsibility for the accuracy, completeness, or usefulness, of any information, apparatus, product, or process disclosed, or represents that its use would not infringe privately owned rights. References herein to any specific commercial product, process, or service by trade name, trade mark, manufacturer, or otherwise, does not necessarily constitute or imply its endorsement, recommendation, or favoring by the U.S. Government or any agency thereof. The views and opinions of authors expressed herein do not necessarily state or reflect those of the U.S. Government or any agency thereof.

Prepared by:

SRNL Transportation Lead

---

Dan Leduc

Date

Concurred by:

UFD Transportation Lead

---

Paul McConnel

Date

## SUMMARY

This report provides details of dry storage cask systems and contents in U.S. for commercial light water reactor fuel. Section 2 contains details on the canisters used to store approximately 86% of assemblies in dry storage in the U.S. Transport cask details for bare fuels, dual purpose casks and canister transport casks are included in Section 3. Section 4 details the inventory of those shutdown sites without any operating reactors. Information includes the cask type deployed, transport license and status as well as fuel types allowed in the specified cask system and allowable parameters. Section 5 contains details on the transfer casks used with each cask system including the current number of transfer casks of each type fabricated.

## TABLE OF CONTENTS

1.	INTRODUCTION .....	1
2.	Status of Fuel in Dry Storage .....	1
2.1	Dry Storage Canisters .....	4
3.	Cask Systems for Dry Fuel Storage.....	5
3.1	Bare Fuel Casks .....	5
3.1.1	Transnuclear TN-32, TN-40 and TN-68 Casks.....	6
3.1.2	CASTOR V/21 and X/33 .....	7
3.1.3	NAC-I28 .....	9
3.1.4	Westinghouse MC-10 .....	9
3.2	Canister Transport Casks .....	10
3.2.1	NUHOMS MP187.....	11
3.2.2	NUHOMS MP197 (MP-197HB) .....	13
3.2.3	HOLTECH HISTAR 100.....	15
3.2.4	NAC-STC .....	16
3.2.5	NAC UMS .....	17
3.2.6	FuelSolutions™ TS125 Cask .....	19
3.2.7	4.2.7 TN-FSV.....	21
4.	Orphan Site Storage and Transport .....	21
5.	Transfer Cask Designs.....	24
5.1	NAC Transfer Casks .....	24
5.2	HOLTEC Transfer Casks .....	27
5.2.1	HI-TRAC Standard Design.....	27
5.2.2	HI-TRAC 100D and 125D Transfer Casks .....	28
5.2.3	TN/NUHOMS Transfer Casks .....	29
5.2.4	Fuel Solutions Transfer Casks .....	30
6.	References .....	32
	Appendix A.....	34

## LIST OF FIGURES

Figure 3-1 MP187 Transportation Cask.....	13
Figure 3-2 NUHOMS MP197 Cask Components <sup>10</sup> .....	14
Figure 3-3 61BT DSC Canister Configuration <sup>10</sup> .....	15
Figure 3-4 HISTAR 100 Transport Cask .....	16
Figure 3-5 NAC-STC Basic Cask Dimensions <sup>13</sup> .....	18
Figure 3-6 NAC-UMS Basic Cask Dimensions <sup>14</sup> .....	18
Figure 3-7 NAC-UMS on heavy haul rolling stock .....	19
Figure 3-8 Expanded Cutaway View of FuelSolutions TS125 Transportation Package <sup>15</sup> .....	20

Figure 3-9 TN-FSV Cask.....	21
Figure 5-1 NAC Transfer Cask Fabrication.....	25
Figure 5-2 NAC Transfer Cask Body (NAC SNFDS Seminar) .....	26
Figure 5-3 NAC Adaptor Plate Door Operation (NAC SNFDS Seminar) .....	26
Figure 5-4 HI-TRAC 125 Pool Lid (Left) Transfer lid (Right) <sup>25</sup> .....	28
Figure 5-5 HI-TRAC 125D Lower Assembly Detail <sup>25,26</sup> .....	29
Figure 5-6 OS187H On-Site Transfer Cask <sup>27</sup> .....	30

## LIST OF TABLES

Table 2-1 UNF Dry Storage Cask/Vault Systems.....	2
Table 2-2 Key Dimensions of Dry Storage Canisters.....	4
Table 3-1 Bare Fuel Casks.....	6
Table 3-2 Transnuclear Metal Cask Parameters (NEI 2010).....	7
Table 3-3 Castor, NAC and Westinghouse Metal Cask Parameters .....	8
Table 3-4 Canister Transport Cask Basic Dimensions .....	11
Table 3-5 Key Dimensions of the NUHOMS transportation cask.....	12
Table 4-1 Shutdown Reactor Site Inventory.....	23
Table 5-1 NAC Transfer Cask Models (NEI 2010) <sup>24</sup> .....	24
Table 5-2 HOLTEC Transfer Cask Models <sup>25</sup> .....	27
Table 5-3 TN Transfer Cask Designs <sup>2,27</sup> .....	30
Table A-1Transportation Matrix for Commercial Reactor Fuel (Dry Storage, and Away from Reactor Wet Storage).....	37
Table A-2 Storage Summary – U.S. Wet Storage at Shutdown Reactor Sites .....	39

## ACRONYMS

10CFR50	Title 10, U.S. Code of Federal Regulations, Part 50
10CFR71	Title 10, U.S. Code of Federal Regulations, Part 71
10CFR72	Title 10, U.S. Code of Federal Regulations, Part 72
ANSI	American National Standards Institute
ASME	American Society of Mechanical Engineers
BFS/ES	BNFL Fuel Solutions/Energy Solutions
BNFL	British Nuclear Fuels Limited
BWR	Boiling Water Reactor
DPC	Dual-Purpose Cask or Dual Purpose Canister
DSC	Dry Shielded Canister (used with NUHOMS systems)
ISFSI	Independent Spent Fuel Storage Installation
MPC	Multi-Purpose Canister (used with HOLTEC and some NAC systems)
ANSI	American National Standards Institute
NRC	Nuclear Regulatory Commission
NUHOMS	NUclear HOrizontal MOdular Storage
PWR	Pressurized Water Reactor
TC	Transfer Cask
TSC	Transportable Storage Canister (used with certain NAC and BFS/ES systems)
UMS	Universal MPC System (used with certain NAC systems)
VCC	Ventilated Concrete Cask

## 1. INTRODUCTION

Used U.S. light water power reactor fuel has been placed in Dry Storage Canisters (DSC) and casks since the mid-1980s and during that time the canister/cask systems have continuously evolved. Currently, there are more than 1,600 dry storage canisters containing roughly 64,000 assemblies or approximately 20,000 MTHM at Independent Spent Fuel Installations (ISFSI) in the U.S.<sup>1</sup> Updated information on the details of dry stored commercial light water reactor fuel is available from recently published documents including the EPRI Industry Spent Fuel Storage Handbook<sup>2</sup> and the Gap Analysis to Support Extended Storage of Used Nuclear<sup>3</sup>.

## 2. Status of Fuel in Dry Storage

Most assemblies in dry storage in the U.S. are in welded metal canisters inside vented concrete vertical overpacks or horizontal storage module. For this configuration, the canister with its internal basket, fuel and fuel component contents is the only portion of the storage cask system which is transported. These systems all require a separate transportation cask with a type B containment vessel to overpack the fuel canister (see reference 13 for an example of this type of cask). The transfer usually requires the use of a transfer cask except for the NUHOMS transportation casks which can interface directly with the horizontal storage module (see Section 3.2). Some welded metal canisters cannot currently be transported for various design reasons. The number and types of these canisters are detailed in Appendix A.

There are four categorical descriptions of dry cask storage:

1. Metal canisters in vertical concrete overpacks or horizontal concrete modules,
2. Metal canisters in metal overpack/storage/shipping casks,
3. Metal canisters in concrete vaults and
4. Bare fuel casks that provide both primary containment and shielding for storage and transportation. (A number of these casks have never been certified for transport as detailed in section 3.1.)

The Consolidated Storage Facility concepts must be capable of receiving any of these dry storage canister and transportation over-pack configurations. Since the mid 1980's 8 cask vendors have provided 11 cask systems comprised of 30 different canister types. Table 2-1 summarizes these canister and casks, provides the quantity of each cask type, as of May 2012 as well as the storage configuration and transition required in order to ship and receive the casks at the consolidated storage facility. For those bare fuel casks which do not have a transport license, the transition to transport requires a wet transfer of the fuel to a licensed transport cask or to a canister that is capable of transport. Some bare fuel Casks may still be licensable for direct transport of their contents as identified in the footnotes.

A number of the canisters listed in Table 2-1 are designated as "storage only" canisters by the associated cask vendor. These are identified in footnotes e and f of Table 2-1. For these canisters, repackaging in a canister capable of transport may be necessary if a direct shipment transport license cannot be obtained. This will depend on whether compensatory measures such as burnup credit or moderator exclusion can be utilized in the transport license.

Table 2-1 UNF Dry Storage Cask/Vault Systems

<b>Vendor</b>	<b>Cask System</b>	<b>Canister Type</b>	<b>Storage Configuration</b>	<b>May 2012</b>	<b>Transition to Transport Required Operation</b>
<b>Welded Metal Canister in Vented Concrete Overpack (84.1%)<sup>a</sup></b>					
BFS/ES	Fuel Solutions	W150	Vertical Cylinder	8	Canister Transfer to Transport Cask
		VSC-24	Vertical Cylinder	58	Canister Transfer to Transport Cask <sup>f</sup>
NAC	NAC-MPC	MPC-26	Vertical Cylinder	43	Canister Transfer to Transport Cask
		MPC-36	Vertical Cylinder	16	Canister Transfer to Transport Cask
	NAC-UMS	UMS-24	Vertical Cylinder	210	Canister Transfer to Transport Cask
TransNuclear	NUHOMS	7P	Horizontal Rectangular	8	Canister Transfer to Transport Cask <sup>e</sup>
		24P	Horizontal Rectangular	135	Canister Transfer to Transport Cask <sup>e</sup>
		32P	Horizontal Rectangular	21	Canister Transfer to Transport Cask <sup>e</sup>
		24PT	Horizontal Rectangular	22	Canister Transfer to Transport Cask <sup>e</sup>
		24PT1	Horizontal Rectangular	18	Canister Transfer to Transport Cask <sup>e</sup>
		24PT4	Horizontal Rectangular	28	Canister Transfer to Transport Cask <sup>e</sup>
		32PT	Horizontal Rectangular	63	Canister Transfer to Transport Cask <sup>e</sup>
		12T	Horizontal Rectangular	29	Canister Transfer to Transport Cask <sup>e</sup>
		24PTH	Horizontal Rectangular	27	Canister Transfer to Transport Cask <sup>e</sup>
		32PTH	Horizontal Rectangular	66	Canister Transfer to Transport Cask <sup>e</sup>
		24PHB	Horizontal Rectangular	38	Canister Transfer to Transport Cask <sup>e</sup>
		61BT	Horizontal Rectangular	117	Canister Transfer to Transport Cask <sup>e</sup>
		61BTH	Horizontal Rectangular	8	Canister Transfer to Transport Cask <sup>e</sup>
		52B	Horizontal Rectangular	27	Canister Transfer to Transport Cask <sup>e</sup>

Table 2-1 (Continued)

<b>Vendor</b>	<b>Cask System</b>	<b>Canister Type</b>	<b>Storage Configuration</b>	<b>May 2012</b>	<b>Transition to Transport Required Operation</b>
HOLTEC	HI-STORM	MPC-24	Vertical Cylinder	22	Canister Transfer to Transport Cask
		MPC-32	Vertical Cylinder	145	Canister Transfer to Transport Cask
		MPC-68	Vertical Cylinder	258	Canister Transfer to Transport Cask
HOLTEC	TransStor	MPC-24E/EF	Vertical Cylinder	34	Canister Transfer to Transport Cask
<b>Welded Metal Canister in Metal Sealed Overpack (1.4%)</b>					
HOLTEC	HISTAR 100	MPC-68	Vertical Cylinder	7	Direct Ship Possible
		MPC-80	Vertical Cylinder	5	Direct Ship Possible
<b>Welded Metal Canister in Vault Storage (2.4%)</b>					
Foster Wheeler	MVDS	6 assembly canisters	Vault	244	Canister Transfer to Transport Cask
<b>Bare Fuel Casks with Bolted Closure (12.1%)</b>					
NAC	NAC I28	I28	Vertical Cylinder	2	Fuel Transfer to Transport. Cask <sup>b</sup>
TransNuclear	TN Metal Casks	TN-32	Vertical Cylinder	63	Fuel Transfer to Transport. Cask <sup>c</sup>
		TN-40	Vertical Cylinder	29	Direct Ship Possible
		TN-68	Vertical Cylinder	57	Direct Ship Possible
GNB	CASTOR	V/21,X-33	Vertical Cylinder	26	Fuel Transfer to Transport Cask <sup>d</sup>
Westinghouse	MC-10	MC-10	Vertical Cylinder	1	Fuel Transfer to Transport. Cask <sup>d</sup>

<sup>a</sup>% of assemblies in dry storage<sup>b</sup> Direct shipment of the NAC I28 may be possible see 3.1.3.<sup>c</sup> Direct shipment of the TN-32 may be possible see 3.1.1.<sup>d</sup>. Cannot currently be transported for various design reasons see 3.1.2. and 3.1.4.<sup>e</sup> NUHOMS 7P, 12T, 24P, 24PHB, 32P, and 52B cannot currently be transported for various design reasons; however, NUHOMS 24PT, 24PT1, 24PT4, 24PTH, 32PT, 32PTH, 61BT, and 61BTH are transportable by canister transfer to transport cask<sup>f</sup> Fuel Solutions VSC-24 canisters are classified by the cask vendor as storage only canisters

## 2.1 Dry Storage Canisters

Table 2-2 Key Dimensions of Dry Storage Canisters

Vendor	Cask System	Canister Type	Inside Diameter	Outside Diameter	Length	Gross Weight (lbs)	Reactor Type
<b>Welded Metal Canister in Vented Concrete Overpack</b>							
Fuel Solutions		W74	64.74	66.0	192.25	85,000	BWR
		VSC-24	60.5	62.5	192.5 (max)	69,000	PWR
NAC	NAC-MPC	MPC-26	69.39	70.64	151.75	67,195	PWR
		MPC-36	69.39	70.64	122.5	55,590	PWR
	NAC-UMS	UMS-24	65.81	67.06	191.75 (max)	73,000	PWR
	NAC-MAGNAS.	TSC-37	71	72	191.8/184.8	104,500	PWR
TransNuclear	NUHOMS	7P	a	a	a	a	PWR
		24P	66.0	67.25	186.0	80,000	PWR
		32P	a	a	a	a	PWR
		24PT	a	a	a	a	PWR
		24PT1	65.9	67.19	186.5(max)	82,000	PWR
		24PT4	65.9	67.19	196.5	a	PWR
		32PT	65.9	67.19	193(max)		PWR
		12T	a	a	a	a	PWR
		24PTH	65.9	67.19	192.2		PWR
		32PTH	68.75	69.75	185.75 (max)	82,000	PWR
		24PHB	65.9	a	186.17	a	PWR
		61BT	66.25	67.25	195.92	89,390	BWR
		61BTH	67	67	196 (max)	a	BWR
		52B	65.9	67.19	195.9	a	BWR
HOLTEC	HI-STORM	MPC-24	67.375	68.5 (max)	190.3125 (max)	82,494	PWR
		MPC-32	67.375	68.5 (max)	190.3125 (max)	89,765	PWR
		MPC-68	67.375	68.5 (max)	190.3125 (max)	87,171	BWR
HOLTEC	TransStor	MPC-24E/EF	67.375	68.5 (max)	190.3125 (max)	80,963	PWR
<b>Welded Metal Canister in Metal Sealed Overpack</b>							
HOLTEC	HISTAR 100	MPC-68	67.375	68.5 (max)	190.3125 (max)	240,881	BWR
		MPC-80	67.375	68.5 (max)	a	a	BWR

<sup>a</sup>Detail redacted from publically available licensing documents in accordance with 10 CFR 2.390. Data requested directly from cask vendor and table will be revised if and when data is received.

### **3. Cask Systems for Dry Fuel Storage**

Dry storage in the U.S can be divided into two broad categories, those in which the fuel is stored bare in a fuel basket inside a metal cask and those in which the fuel is in a welded canister inside a vented concrete overpack or inside a metal dual purpose cask. Details on both categories are provided below.

#### **3.1 Bare Fuel Casks**

Light water power reactor transportation casks capable of meeting the 10CFR71 requirements for Normal Conditions of Transport (NCT) and Hypothetical Accident Conditions (HAC) are generally metal casks with bolted closures and containment vessels which meet leak tight requirements of ANSI N14.5<sup>4</sup>. For the case where fuel is placed directly into such a cask and used for long term storage in that cask, the cask is often referred to as a “bare fuel” cask since no welded canister is used. If the cask also has a licensed transport configuration it is also sometimes referred to as a dual purpose cask.

Bare fuel casks employ bolted closures with the fuel is placed directly in a basket inside the cask cavity. Each of the bare fuel casks listed below was designed for transportation cask licensing although as shown in Table 3-1, few of these casks have an existing transportation license nor are in application for a 10CFR71 license for transport. Dry storing fuel in a bare fuel cask is most beneficial if the storage times are short and a receipt facility exists that can directly handle and unload fuel from the cask. They also eliminate the need for a transfer cask and/or canister transfer operation inherent in canister storage.

Only two reactor sites in the U.S. continue to load fuel into bare fuel metal casks, Peach Bottom which uses the Transnuclear TN-68 cask and Prairie Island which continues to load TN-40 casks. Both these casks have current transport licenses as shown in Table 3-1. The remaining bare fuel casks are described as legacy casks since no new casks of these types are being loaded and reactor sites which once employed them are now loading out fuel in canister cask systems. Of the legacy casks, licensing of the TN-32 cask for transport has been discussed by Transnuclear in the past and direct shipment of these casks remains a possibility. Likewise the, NAC I28 cask is an earlier evolution of the currently licensed NAC-STC cask and direct shipment of the NAC I28 also remains a possibility although no transport license is currently being pursued.

Obtaining a transport license for the CASTOR V21 and X33 casks is more problematic since these casks are composed of monolithic cast iron which has not been licensed as a cask configuration in the U.S. as described in 3.1.2 below. Shipment of the single Westinghouse MC-10 in dry storage at Surry is also problematic since Westinghouse, although still active in radioactive material packaging, is not an active vendor supplying dry cask storage systems in the U.S. It is unclear whether the work necessary to ship this cask would be more beneficial than repackaging of its contents into a cask system with a licensed transport configuration,

Table 3-1 Bare Fuel Casks

	<b>VENDOR</b>	<b>CASK</b>	<b>NUMBER OF CASKS (7/2012)</b>	<b>TRANSPORT LICENSE</b>	<b>LOCATION</b>
<b>ACTIVE CASKS (STILL LOADED)</b>	TN	TN-68	57	71-9239	Peach Bottom
		TN-40	29	71-9313	Prairie Island
<b>LEGACY CASKS (NO LONGER LOADED)</b>	TN	TN-32	63	NO	Surry, McGuire, North-Anna
	GNB	CASTOR V21&X33	26	NO	Surry
	NAC	I-28	2	NO	Surry
	Westinghouse	MC-10	1	NO	Surry

Descriptions of the direct loaded bare fuel casks in storage are included below. For direct loaded bare fuel casks, the portion of the cask designated as the “containment” vessel when discussed for transportation purposes below is often referred to as a “confinement” vessel in its storage configuration.

### **3.1.1 Transnuclear TN-32, TN-40 and TN-68 Casks**

The TN series of metal casks is currently used to store the largest amount of un-canisterized fuel in dry storage cask systems in the U.S. These are also the only bare fuel casks which continue to be loaded into dry storage in the U.S.<sup>1</sup> The number following the TN designator is the number of assembly positions in the internal cask basket for the various casks. The TN-32 casks hold PWR assemblies from Surry, McGuire, and North Anna. The TN-40 casks hold PWR assemblies from Prairie Island only and the TN-68 holds GE BWR fuel from Peach Bottom only. Only Prairie Island and Peach Bottom continue to load TN-40 and TN-68 casks respectively, with Prairie Island loading 3 casks and Peach Bottom adding 5 casks in 2010. Surry and North Anna are now utilizing the NUHOMS canister system while McGuire uses the NAC-UMS canister system for new fuel loads.

The TN-68 and the TN-40 are the only casks in the TN metal cask family that have a current transportation license. The TN-40 received its license in June 2011 after a five year review period by the NRC. This transportation license is only for intact fuel from Prairie Island Unit 1 cycles 1 through 16 and Unit 2 cycles 1 through 15. The maximum initial enrichment for fuel under this license is no more than 3.85 weight percent U<sup>235</sup>, and the assembly average burnup is required to be no more than 45,000MWd/MTU.

Now that the TN-40 transportation license has been obtained, TN plans to submit an application for a TN-40 variant designated as the TN-40HT. Contents under the transportation application will include fuel with a maximum initial enrichment of 5 weight percent U<sup>235</sup> and a maximum bundle average burnup limited to 60 GWd/MTU. Fuel transported under this license must have a minimum cooling time of 12 years with a maximum heat load of 0.8Kw/assembly. Indications are that the initial transportation application will include intact fuel only.

There are no current transportation license applications for the TN-32 Cask design. TN has discussed applying for a transport certificate during the time period that this cask model was being produced for domestic dry fuel storage. Since the reactor sites using this cask design have switched to canister based systems, no transport license has been pursued for the TN-32 cask in the U.S. However, given the design similarity between the TN-32 and other TN casks licensed for transport and TNs continued presence in both the storage and transport cask market, it is reasonable to assume that licensing the TN-32 for transport and direct shipment remains a possibility.

Basic information for the TN family of metal casks is shown in Table 3-2 (EPRI 2010 updated for Transportation).<sup>5,6</sup>

Table 3-2 Transnuclear Metal Cask Parameters (NEI 2010)

TN Cask Type	TN-32	TN-40	TN-40HT	TN-68
Fuel Type	PWR	PWR	PWR	BWR
# of Assemblies	32	40	40	68
Maximum Heat Load (kilowatts)	32.7	27	32	30
Minimum Cooling Time (Years)	7	10	18	7
Maximum Fuel Burnup (GWd/MTU)	40	45	60	60
Storage Cask				
Length [m] (in)	4.9(184)	4.4(175)	4.6(181.75)	5.5(215)
Length with protective cover [m](in)	5.13(201.88)	5.13(202.0)	5.07(199.6)	
Outer Diameter [m](in)	2.48(97.75)	2.53(99.52)	2.57(101)	2.49(98)
Loaded Weight lbs.	231,000	226,000	242,000	230,000
NRC Part 71 License	None	71-9313	Planned	71-9293

### 3.1.2 CASTOR V/21 and X/33

The CASTOR V/21 and X/33 casks are metal cask currently used for storage at the Surry power generating station. CASTOR casks are also used in dry storage at INL which is not licensed by the NRC.

Both casks designs consist of a cask body made of thick-walled nodular cast iron with two stainless steel lids sealed with both elastomer and metal seals to provide leak tightness. Polyethylene rods are incorporated into the walls of both cask designs that enhance the neutron shielding of each cask. Otherwise, no special shielding materials are incorporated into the cask with shielding provided by the cast iron and stainless steel cask composition. In both cask designs, the external surface is covered with heat transfer fins that run circumferentially around the cask with an epoxy resin coating protecting the outside cask surface. For the V/21, the internal structure of the cask consists of a welded stainless steel basket with 21 square tube positions with borated stainless steel plates for criticality control while the X/33 has a similar internal structure with 33 square tube positions. Both these CASTOR cask systems use a pressure-sensing device to monitor the pressure in the interspace between the primary and secondary lids verifying seal integrity in storage.

Basic information for the Castor family of metal casks is shown in Table 3-3. All Castor casks used to dry store fuel under NRC license are located at Surry. Early fracture toughness concerns at the NRC prevented the licensing for transport of monolithic nodular cast iron casks like the CASTOR casks in the U.S. However, in the last 20 years, European experience with testing, analysis, use and licensing of nodular cast iron casks has garnered international acceptance of this cask type by the International Atomic Energy Agency<sup>7</sup>. Since then the NRC has indicated that they would accept license applications for nodular cast iron shielded casks like the CASTORs. Any such submittal would be a first time licensing cycle for this cask type and no vendor has yet approached the NRC with a submittal of transport license for this cask type.

Table 3-3 Castor, NAC and Westinghouse Metal Cask Parameters

TN Cask Description	V/21	X/33	NAC I28	Westinghouse MC-10
Fuel Type	PWR	PWR	PWR	PWR
# of Assemblies	21	33	28	24
Maximum Heat Load (kilowatts)	21	33	32.7 <sup>a</sup>	32.7 <sup>a</sup>
Minimum Cooling Time (Years)	7 <sup>a</sup>	10 <sup>c</sup>	10 <sup>c</sup>	10 <sup>c</sup>
Maximum Fuel Burnup (GWd/MTU)	35	35	22 <sup>c</sup>	35 <sup>c</sup>
<b>Storage Cask</b>				
Length [m] (in)	4.9(193)	4.8(189)	4.6(181.2)	4.79(188.4)
Outer Diameter [m](in)	2.8(110.25)	2.8(110.25)	2.4(94.8)	2.71(106.8)
Loaded Weight lbs <sup>b</sup>	233,800	236,000	250,000 <sup>d</sup>	250,000 <sup>d</sup>
<b>NRC Part 71 License</b>	None	None	None	None

<sup>a</sup>TN-32 cask bounding value

<sup>b</sup> Storage configuration gross weight

<sup>c</sup> Surry ISFSI SAR

<sup>d</sup> Surry ISFSI SAR weight limit

### 3.1.3 NAC-I28

The NAC-I28 is a variant of the NAC-STC cask which is licensed for transport as described in section 3.2.4. Two NAC-I28 casks are used to dry store PWR fuel assemblies at the Surry power generating station which is the only NRC licensed ISFSI location utilizing this cask design. One NAC-I28 cask is also used in dry storage at INL which is not licensed by the NRC.

The NAC-I28 S/T cask is a smooth right circular cylinder of multiwall construction with a 1.5 inch thick inner shell and a 2.63 inch thick outer shell of austenitic stainless steel separated by 3.2 inches of lead gamma shielding. The inner and outer shells are connected to each other at the ends by an austenitic stainless steel ring and plate. The upper end of the cask is sealed by an austenitic stainless steel bolted closure lid which is 6.5 inches thick in the edge flange region and has a 1-inch inner closure plate and a 5.5-inch outer closure plate. The closure plates are separated by two inches of lead gamma shielding. The closure lid utilizes a double barrier seal system with two metallic o-rings forming the seals. The lower end of the cask is 6 inch thick austenitic stainless steel with a 1 inch outer closure plate. The bottom end closure plates are separated by 1.80 inches of lead gamma shielding. The cask body is approximately 181 inches long and 94 inches in diameter. Neutron emissions from the stored fuel are attenuated by an integral neutron shield located outside the outer shell which contains a 7-inch thickness of borated solid neutron shield material. Neutron emissions from the top of the cask are attenuated during storage by a 3-inch thick solid neutron shield cap encased in stainless steel.<sup>8</sup>

There is no active transportation license for the NAC-I28 package.

For long term storage, the cask cavity is backfilled with helium to one atmosphere. The inner lid interseal volume between the two inner lid metallic gaskets and the interseal volume between the O-rings in the vent and drain port covers are backfilled with 15 psig of helium. The space between the inner and outer lid is pressurized with helium to 100psig and that pressure is monitored during storage for pressure loss by a transducer installed in the cask upper forging. The storage configuration of the NAC I28 Cask includes a tip over impact limiter.<sup>8</sup>

### 3.1.4 Westinghouse MC-10

The Westinghouse MC-10 cask is a metal cask designed to vertically store 24 PWR SNF assemblies. There is only one MC-10 stored at a NRC licensed ISFSI which is the model at the Surry Power station.

The cask body is a right circular cylinder composed low alloy steel with forged steel walls and a bottom. The basic parameters of the MC-10 design are shown in Table 3-3.

The inside surface of the MC-10 cask is thermally sprayed with aluminum for corrosion protection. The twenty-four carbon steel heat transfer fins are welded axially along the outside of the cask wall. Carbon steel plates are welded between the fins to provide an outer protective skin. Neutron shielding is provided by a layer of BISCO NS-3 cured in the cavity between the cask wall and outer protective skin.<sup>2,8</sup>

This thick walled structure provides the gamma shielding for the cask. A low alloy steel shield cover with a metallic O-ring provides the initial seal and shielding following fuel loading. A carbon steel primary cover lid, with a metallic O-ring seal, provides the primary containment seal

and envelopes the shield cover. An additional seal cover, containing BISCO NS-3 neutron-absorbing material is welded over the first two seals.<sup>2,8</sup>

### **3.2 Canister Transport Casks**

As detailed in Table 2-1 and Appendix A, approximately 84% of commercial fuel in the U.S. is stored in single welded canisters inside individual concrete or steel-encapsulated concrete cylindrical storage overpacks or rectangular horizontal storage modules. All of the storage systems whether cylindrical vertical overpacks or horizontal storage modules in the U.S. contain upper and lower vents that allow passive cooling of the internal canister. The canisters for these systems consist of a basket inside a steel shell with an outer diameter ranging from five to six feet in diameter as shown in Table 2-2. Cask vendors use different designators on their particular canister system. These include Multi-Purpose Canister (MPC), Dry Shielded Canisters (DSC), and Transportable Storage Canister (TSC). See the Client Canister descriptions in sections 3.2.1 through 3.2.6 for specific canister designs by cask vendor.

As noted in Table 2-1, there are 12 HISTAR 100 transportation casks which are also storing canisters at three reactor sites in the U.S. including the Humboldt Bay shutdown reactor site. These 12 casks are the only case in the U.S. where seal welded canisters of commercial fuel are stored directly in the transportation package intended for transport. Since the HISTAR 100 transportation cask provides the containment for the future transportation phase, it does not incorporate vents for passive cooling and requires more restrictive limits for heat load and cooling time than concrete overpacks (or storage modules), such as the HISTORM system.

Documents discussing canister transport casks often refer to the transportation containment vessel as an “overpack”, or “transportation over-pack” since it over-packs the canister during transport. Except in the case of the 12 direct stored HISTAR canisters, all other canisters in the U.S. require transfer of the canister from the storage over-pack into the transportation over-pack prior to shipment. This operation must be reversed at the consolidated storage facility in order to place the canister in a low cost vented concrete overpack for long term storage. The receiving facility must be configured to accommodate any of the existing transportation over-packs described below. Table 3-4 gives basic dimension of transport casks designed to ship canisters of dry stored used fuel. In no case is a transport cask of one vendor licensed to ship a canister design of another vendor listed in table 3-4.

Table 3-4 Canister Transport Cask Basic Dimensions

CASK VENDOR	TRANSPORT CASK	GROSS WEIGHT (LBS) <sup>a</sup>	LENGTH (in) <sup>b</sup>	DIAMETER (in)	CAVITY LENGTH (in)	CAVITY DIAMETER (in)
FUEL SOLUTIONS	TS-125	285,000	210.4/324.4	94.2/143.5	193.0	67
TN (NUHOMS)	MP-187	282,000	201.5/308	92.5/ <sup>c</sup>	187	68
	MP-197	265,100	208/281.25	91.5/122	197	68
	MP-197HB	304,000	210.25/ 271.25	84.5/126	199.25	70.5
NAC	NAC-STC	47,000	/247	31/78	199	18
	NAC-UMS	260,000	193/257	99 <sup>d</sup> /128	165	71
	NAC-MAGNATRAN	255,022	209.3/ 275	92.9/124	192.5	67.6
HOLTEC	HISTAR 100	312,000	213.9/	109.8/	192.5	72.25
		282,000	203.25/ 305.875	96/128	191.25	68.56

<sup>a</sup> Gross Weight of Heaviest Configuration (may be bounding analytical weight)

<sup>b</sup> Without Impact Limiters/With Impact Limiters

<sup>c</sup> MP-187 Impact Limiter Not Round

<sup>d</sup> Across Corners

### 3.2.1 NUHOMS MP187

The first transportation cask licensed to ship dual purpose canisters in the U.S. is the MP187<sup>a</sup> Cask. The NUHOMS storage system consists of Dry Shielded Canisters (DSC) stored in concrete Horizontal Storage Modules. The MP187 is designed to accept a single DSC within its containment cavity as described below. The cask is a composite structure of steel and lead surrounded by neutron shielding material. The cask, including the DSC is protected at each end by energy absorbing impact limiters which consist of stainless steel skins filled with poly urethane foam and aluminum honeycomb. These impact limiters also provide thermal insulation

<sup>a</sup> The MP187 designator is derived from the cavity interior height of 187 inches. The cavity height of the MP197 is 197 inches.

which protects the cask top and bottom seal areas during the hypothetical fire transient event. The cask is fabricated primarily of stainless steel. Non-stainless steel members include the cast lead shielding between the containment boundary inner shell and the structural outer shell, the o-ring seals, the cementitious neutron shield material and the carbon steel closure bolts. Key features and dimension of the MP-187 cask are shown in Table 3-5 and Figure 3-1.<sup>9,10</sup> The maximum heat load of the MP-187 cask is 13.5kW.

Table 3-5 Key Dimensions of the NUHOMS transportation cask

Cask	Cavity Length (in)	ID (in)	Height (in)*	OD (in)*	Base Thick(in)	Structural Lid Thick. (in)	Radial Neutron Shield Thick. (in)	Inner Shell Thick. (in)	Gamma Shield Thick. (in)	Total Wall Thick (in)	Max Gross Weight (lbs.)**
MP187	187	68	201.5	92.5	8	6.5	4.3	1.25	4	12.3	282,000
MP197	197	68	208	91.5	6.5	4.5	4.5	1.25	3.25	11.75	265,100
MP197HB	199.25	70.5	210.25	97.75	6.5	4.5	6.25	1.25	3		304,000

\*Does not include impact limiter

\*\*Depends on DSC configuration reported

**MP 187 Client Canisters<sup>9</sup>:** The DSC is a high integrity stainless steel, welded pressure vessel that provides confinement of the radioactive materials, encapsulates the fuel in an inert atmosphere, and provides axial biological shielding during DSC closure, transfer operations, storage and transport. The DSC internal basket assembly contains a storage position for each fuel assembly. It is composed of circular spacer discs machined from thick carbon steel plates or austenitic stainless steel. Axial support for the DSC basket is provided by four high strength stainless steel support rods and four carbon steel or austenitic stainless steel support plates which extend over the full length of the DSC cavity and bear on the canister top and bottom end assemblies. Carbon steel components of each DSC basket assembly are coated with a thin corrosion resistant layer of nickel to provide corrosion resistance for the short time that the DSC is in the spent fuel pool for fuel loading. All DSC types licensed in the MP187 have an approximate outside diameter of 67 inches and a maximum external length of 186.5 inches.

Per the certificate USA/9255/B(U)F-85, the cask is currently licensed to transport four types of DSCs designated as the FO-DSC (Fuel Only), FC-DSC(Fuel/Control Components), FF-DSC(Failed Fuel) and the 24PT1 DSC. The license allows the transport of failed fuel in limited quantities. Although the MP187 is capable of handling other canisters that have a maximum length of 186.5 inches and maximum diameter of 67.2 inches, no submittals for the transport of other canisters in this cask have been pursued. Application for transport of other NUHOMS canisters have been pursued in the MP 197HB, the newest NUHOM transport cask design.

Only one production unit MP187 Cask has been fabricated as of the issue of this report.

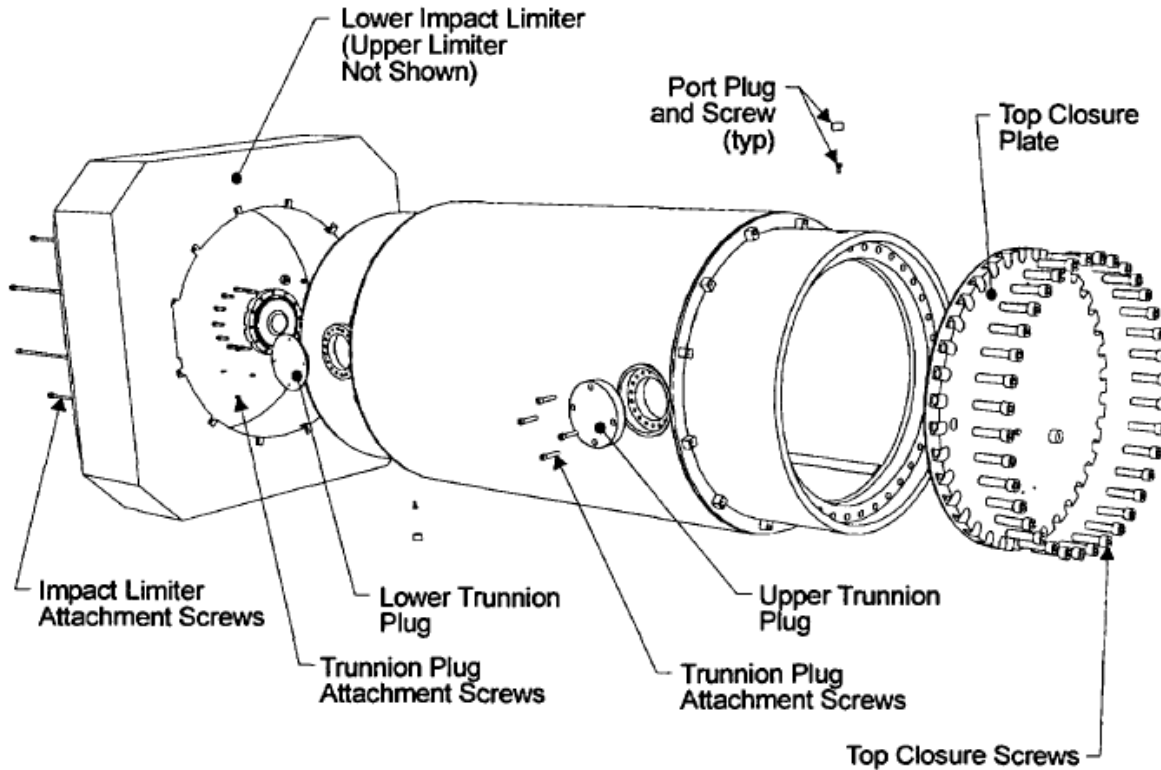


Figure 3-1 MP187 Transportation Cask

### 3.2.2 NUHOMS MP197 (MP-197HB)

The MP197 and the MP197HB are cask configurations for shipping a single NUHOMS canister which uses the same horizontal loading configuration as the MP187. The basic parameters of the MP197 and MP197HB are provided in Table 3-5. The MP197 and MP197HB are different cask designs with different overall dimensions as well as some difference in materials of construction even though they share the same certificate number. The MP197HB has an internal cavity that is 70.5 inches in diameter and 199.25 inches long.<sup>b</sup> To accommodate smaller DSC designs, an aluminum sleeve and aluminum or stainless steel spacers are provided to limit radial and axial movement of the payload. 61BT DSCs. Both the MP197 and MP197HB casks consist of a containment boundary, structural outer shell, gamma shielding material and solid neutron shield. The containment vessel of both cask designs contains an integrally-welded bottom closure and a bolted and flanged top closure lid. The maximum heat load for the MP197 and MP197 HB casks are 15.86 kW and 24 kW respectively.<sup>10,11</sup>

As of the date of this report, no NUHOMS MP197 or MP197HB casks have been fabricated.

<sup>b</sup> Thus the 197 designator is not strictly accurate with regard to the MP197HB

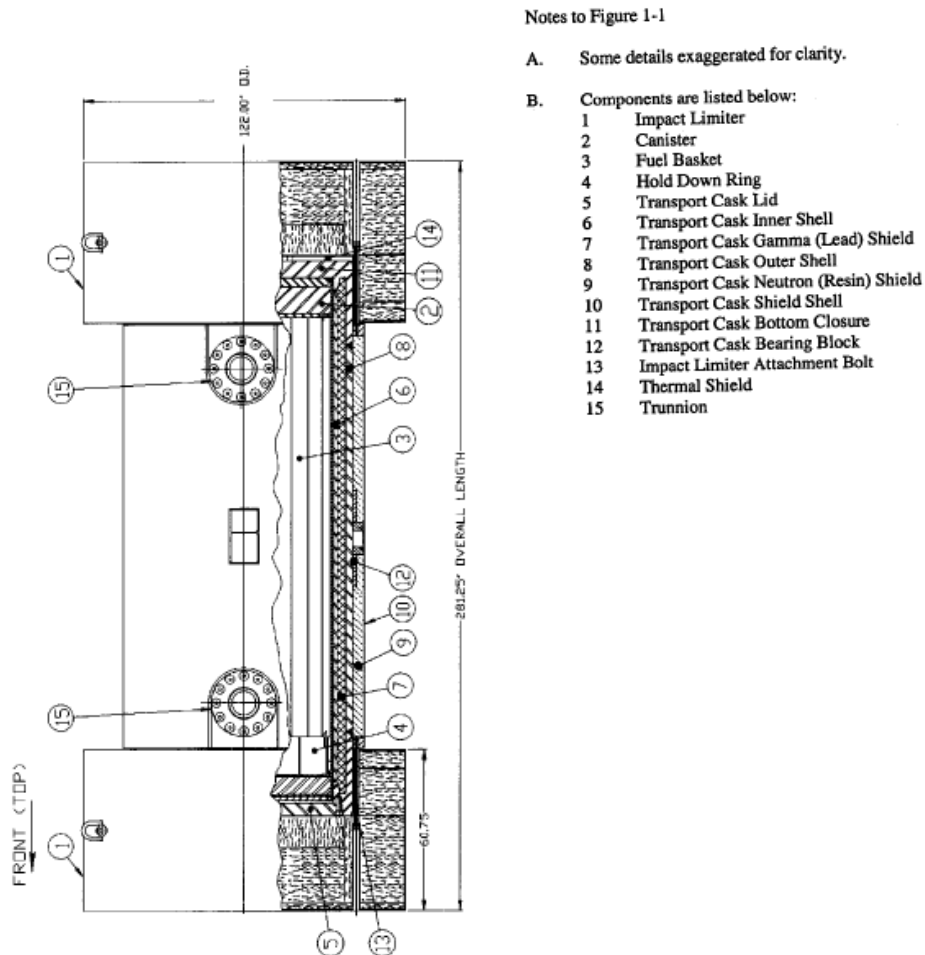


Figure 3-2 NUHOMS MP197 Cask Components<sup>10</sup>

MP197 Client Canisters<sup>10,11</sup>: The MP197 transportation cask is currently only licensed to carry the 61BT DSC. This DSC consists of a cylindrical shell, top and bottom shield plugs, inner and outer bottom closure plates, and inner and outer top cover plates. The shell assembly is a high integrity stainless steel welded pressure vessel that provides containment of radioactive material, encapsulates the fuel in an inert atmosphere (the canister is back-filled with Helium before being seal welded closed) and provides biological shielding in the axial direction. The bottom end assembly welds are made during fabrication of the DSC. The top end closure welds are made after fuel loading. Both top plug penetrations (siphon and vent ports) are redundantly sealed after the DSC drying operations are complete.

MP197HB Client Canisters<sup>11</sup> The MP197HB is currently licensed for transport of four DSC designs as well as radioactive waste containers. These are the 69BTH, 24PT4, 61BT and 61BTH DSC designs. The 69BTH DSC has the largest over all outside diameter at 69.8 inches. To accommodate the smaller 67.3 inch diameter of the other DSCs (24PT4, 61BT, and 61BTH) an aluminum sleeve is used in transport. Since canisters with the same designator vary in length, stainless steel or aluminum spacers are used to limit the axial gap between the DSC and the cask body to 0.5 inches or less. A crosssection of the 61BT Canister is shown in figure 3-3 below. Unlike canister types from other cask vendors, shield plugs are provided at both the top and the bottom of the NUHOMS canister. The top shield plug provides shielding

for personnel during final welding and drying operations while the bottom shield plug, which is put in place before fuel loading, provides shielding at the face of the horizontal storage module. TN continues to pursue licensing for transport of other NUHOMS canisters in the MP197HB.

As detailed in Appendix A, a certain subset of NUHOMS canisters are designated by TN as “storage only” canisters. These canisters have certain design features which make for a more difficult licensing process for the transport cask configuration in the transport accident sequence required to be evaluated in 10CFR71. Per the cask vendor, licensing of these canisters in transport may still be possible, especially if certain burn-up credit is allowed or moderator exclusion under 71.55 was obtained. Currently, the NUHOMS canisters are not credited with serving any containment function during transport.

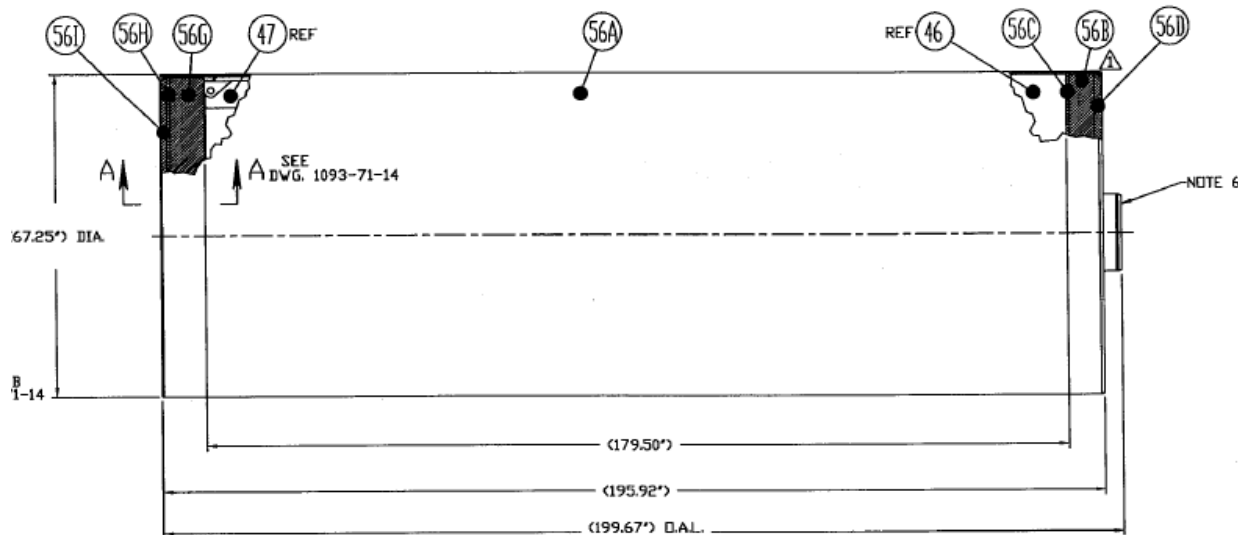


Figure 3-3 61BT DSC Canister Configuration<sup>10</sup>

### 3.2.3 HOLTECH HISTAR 100

The HISTAR 100 transportation cask consists of a single, sealed metal multi-purpose canister (MPC) contained within a multilayered overpack with impact limiters. The inner diameter of the overpack is approximately 68-3/4 inches and the height of the cavity is approximately 191-1/8 inches. The overpack inner cavity is sized to accommodate the MPCs. The outer diameter of the overpack is approximately 96 inches and the height is approximately 203-1/4 inches (Humboldt Bay overpacks have the same inner and outer diameter but have an inner height of 115 inches and an outer height of 128 inches). Fitted with impact limiters on each end which are composed of aluminum honeycomb, the cask has a maximum outside diameter of 128 inches and a total overall length of 305.9 inches. The gross weight of the HISTAR 100 system depends on which of the MPCs is loaded into the overpack for shipment but can weigh as much as 277,299 for the heaviest licensed configuration. The maximum total heat load of the HISTAR transport cask is 20kW for PWR fuel contents and 18.5kW for BWR fuel contents.<sup>12</sup>

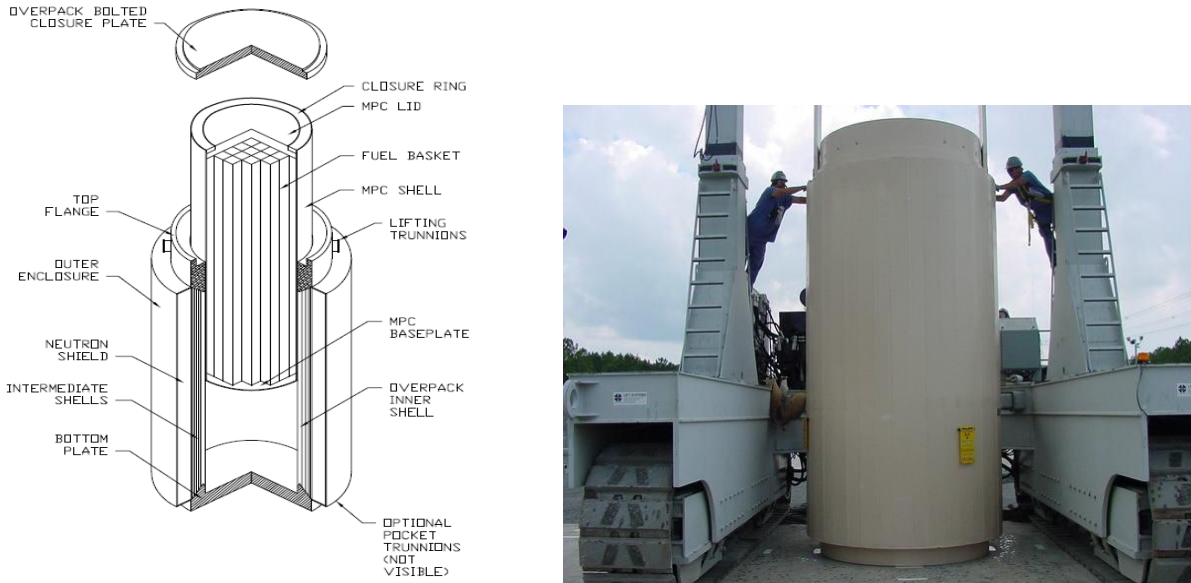


Figure 3-4 HISTAR 100 Transport Cask

**Client Canisters:** The HI-STAR 100 System is designed to accommodate a wide variety of spent fuel assemblies in a single overpack design by utilizing different MPC basket designs. The exterior dimensions of all Holtec MPCs (except the custom-designed Trojan and Humboldt Bay MPCs) are identical to allow the use of a single overpack design. The generic Holtec MPC design has maximum exterior dimension of approximately 68.5 inches in diameter by 190.3125 inches long. The Trojan plant MPCs are approximately nine inches shorter than the generic Holtec MPC design and have the same outer diameter. The Humboldt Bay MPCs are approximately 6.3 feet shorter than the generic Holtec MPC design and have the same outer diameter. Each of the MPCs has different design features (e.g., fuel baskets) to accommodate distinct fuel characteristics. Each MPC is identified by the maximum quantity of fuel assemblies it is capable of receiving. The MPC-24, -24E, and -24EF each can contain a maximum of 24 PWR assemblies; the MPC-32 can contain up to 32 PWR assemblies; the MPC-68 and -68F each can contain a maximum of 68BWR fuel assemblies; and the MPC-HB for Humboldt Bay can contain up to 80 fuel assemblies.<sup>12</sup>

The overpack containment boundary is formed by a steel inner shell welded at the bottom to an end plate and at the top to a heavy flange with a bolted closure plate.

### 3.2.4 NAC-STC

The NAC-STC (Storage Transport Cask)<sup>c</sup> is a metal cask design that is licensed for the transport of NAC Multi-Purpose Canisters (MPC) of fuel from Connecticut Yankee and Yankee Rowe “ISFSI Only” sites as well as bare fuel in an internal basket configuration. The NAC-STC is a smooth right-circular cylinder of multiwall construction, consisting of stainless steel inner and outer shells separated by lead gamma radiation shielding. The inner and outer shells are welded to the 304 stainless steel top forging, which is a ring that is machined to mate with the inner and outer lids. The inner and outer shells are also welded to the Type 304 stainless steel bottom inner and outer forgings respectively. The cask bottom consists of two forgings and a plate with neutron shield material sandwiched between the bottom inner forging and the bottom plate. Neutron shield material is also placed in an annulus that surrounds the cask outer shell along the length of the cask cavity. Twenty-four explosively bonded copper and Type 304 stainless steel

<sup>c</sup> Even though the “S” in the STC designator stands for storage, there are no NAC-STC casks used for storing fuel at U.S. dry storage sites although the NAC-I28 is a similar design.

fins are located in the radial neutron shield to enhance the heat rejection capability of the NAC-STC and to support the neutron shield shell and end plates.<sup>13</sup>

**NAC STC Client Canisters:** The basic NAC-STC cask body dimensions are shown in Figure 3-5. The 71.1 inch diameter cavity accommodates 24 or 26 assembly MPCs from Connecticut Yankee, 36 assembly MPCs from Yankee Rowe or 26 PWR Assemblies stored in a bare fuel basket. Since the fuel canisters include all the fuel from the shutdown reactor, both canister designs allow storage of damaged fuel assemblies. With a cavity length of 165 inches, the STC cavity is shorter than most transport casks for used commercial fuel but the diameter is slightly larger. The cask body outside diameter is approximately 87.7 inches with the outside length of 190.5 inches without impact limiters. In the transport configuration two impact limiters are fitted to either end of the cask body in a typical dumbbell configuration. These are composed of either balsa wood or a combination of redwood and balsa wood encased in stainless steel. The all balsa wood impact limiters have a lower weight and improved crush characteristics compared to the combination redwood and balsawood impact limiters and accommodate a higher cask content weight and higher cask total weight. With impact limiters, the NAC-STC has a maximum outer diameter of 124 inches and an overall length of 257 inches.<sup>13</sup>

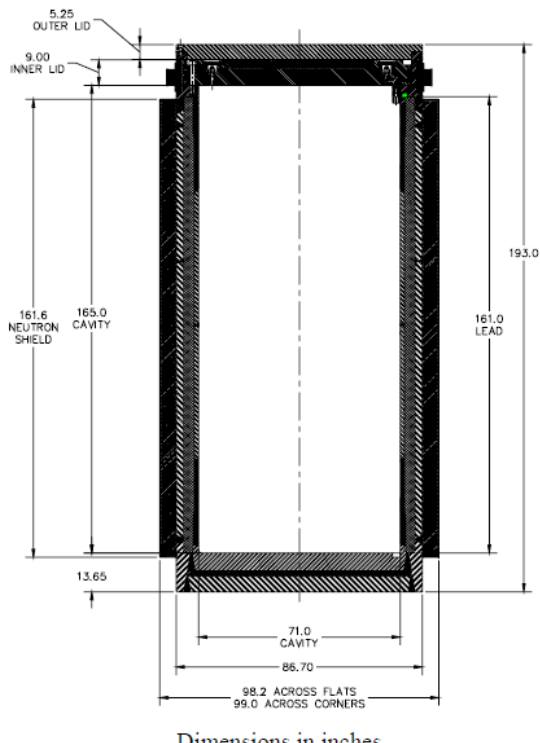
The NAC STC has a bare fuel configuration included in its current transport license.<sup>13</sup>

The NAC-STC, when loaded, has a maximum design weight of 260,000 pounds. The maximum heat load of the NAC-STC cask is 22.1 kW for direct loaded PWR fuel in the 26 position internal basket configuration with each assembly 0.85 kW or less. For Yankee Rowe fuel, the maximum canistered fuel assembly decay heat load is 0.347 kW per assembly for 36 assemblies and 0.259 kW per assembly for a canister of 24 stainless steel-clad assemblies. For Connecticut Yankee fuel, the maximum decay heat load is 0.654 kW per assembly for a canister of 26 assemblies.<sup>13</sup>

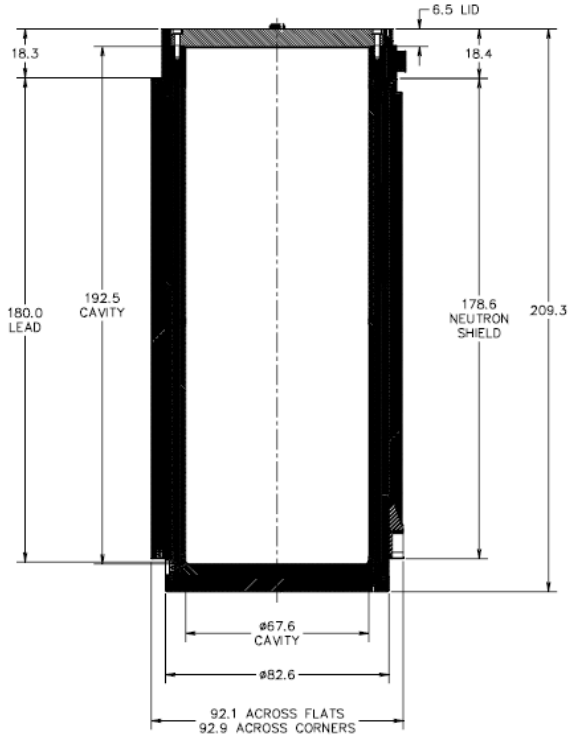
As of the date of this report, no NAC-STC casks have been fabricated for use in the U.S. This cask design is likely to be replaced by the NAC MAGNATRAN design for future fuel shipments upon certification of this cask design.

### **3.2.5 NAC UMS**

The Universal Transport Cask is designed to safely transport a Transportable Storage Canisters TSCs containing 24 intact PWR spent fuel assemblies, 56 intact BWR spent fuel Assemblies or Greater Than Class C (GTCC) waste. NAC-UMS canisters are utilized to store fuel from the Maine Yankee “ISFSI Only” site. The design layout of the NAC-UMS is similar to the NAC-STC as can be seen in Figure 3-6. Some of the differences include a single lid vs. the double lid STC design and the fact that it has a cavity which is smaller in diameter but is considerably longer than the NAC-STC design. The maximum gross weight of the NAC-UMS when loaded with the heaviest TSC configuration is 254,004lbs.<sup>14</sup>



Dimensions in inches

Figure 3-5 NAC-STC Basic Cask Dimensions<sup>13</sup>Figure 3-6 NAC-UMS Basic Cask Dimensions<sup>14</sup>

Like the NAC-STC, the NAC-UMS cask contains a neutron shield placed in an annulus that surrounds the cask outer shell along the length of the cask cavity. It also has twenty-four bonded copper and Type 304 stainless steel fins located in the radial neutron shield to enhance the heat rejection capability of the cask. The NAC-UMS maximum decay heat load is 20kW for PWR fuel and 16kW for BWR fuel. In the transport configuration two impact limiters are fitted to either end of the cask body in a typical dumbbell configuration (Figure 3-7). Unlike the NAC-STC design, only one impact limiter design is licensed which is composed of a combination of redwood and balsa wood enclosed in stainless steel shell. With impact limiters attached, the NAC-UMS has a maximum outer diameter of 124 inches and an overall length of approaching 275 inches.<sup>14</sup>

As of the date of this report, no NAC-UMS casks have been fabricated either domestically or for use overseas. This cask design is likely to be replaced by NAC's new MAGNATRAN design for future fuel shipments when this cask design is certified.

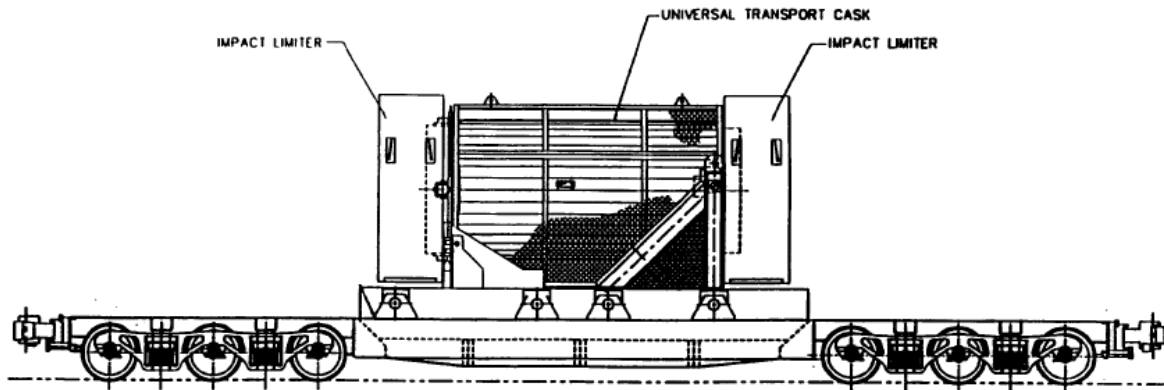


Figure 3-7 NAC-UMS on heavy haul rolling stock

### 3.2.6 FuelSolutions™ TS125 Cask

The FuelSolutions™ Transportation Package consists of a FuelSolutions™ TS125 Transportation Cask and impact limiters, together with a FuelSolutions™ canister and its UNF payload. This cask is designed to transport a single W21 canister containing 21 PWR assemblies or W74 canister containing up to 64 Big Rock Point<sup>d</sup> fuel assemblies in two stackable basket assemblies. An exploded view of the TS-125 cask is shown in Figure 3-7. The TS125 Transportation Cask body is an assembly composed of stainless steel components of an inner shell, an outer shell, a top ring forging, a closure lid with a seal test port and a cavity vent port, a bottom plate forging, and a cavity drain port. The inner and outer shells are welded to the bottom plate forging and the top ring forging. The cask body also includes an annular lead gamma shield; an annular neutron shield with cask tie-down rings, support angles, and jacket; a bottom end neutron shield with a support ring and jacket; a longitudinal shear block; and lifting trunnion mounting bosses. The inner and outer shells form the annular cavity for the lead gamma shield. The outer shell and the neutron shield jacket form the annular cavity for the solid neutron shield. The neutron shield support angles facilitate heat rejection through the solid neutron shielding material to the outer surface of the cask body.<sup>15</sup>

<sup>d</sup> Big Rock Point is an “ISFSI Only” Site

As of the date of this report, no TS125 casks have been fabricated either domestically or for use overseas. No intentions for a replacement cask have been announced.

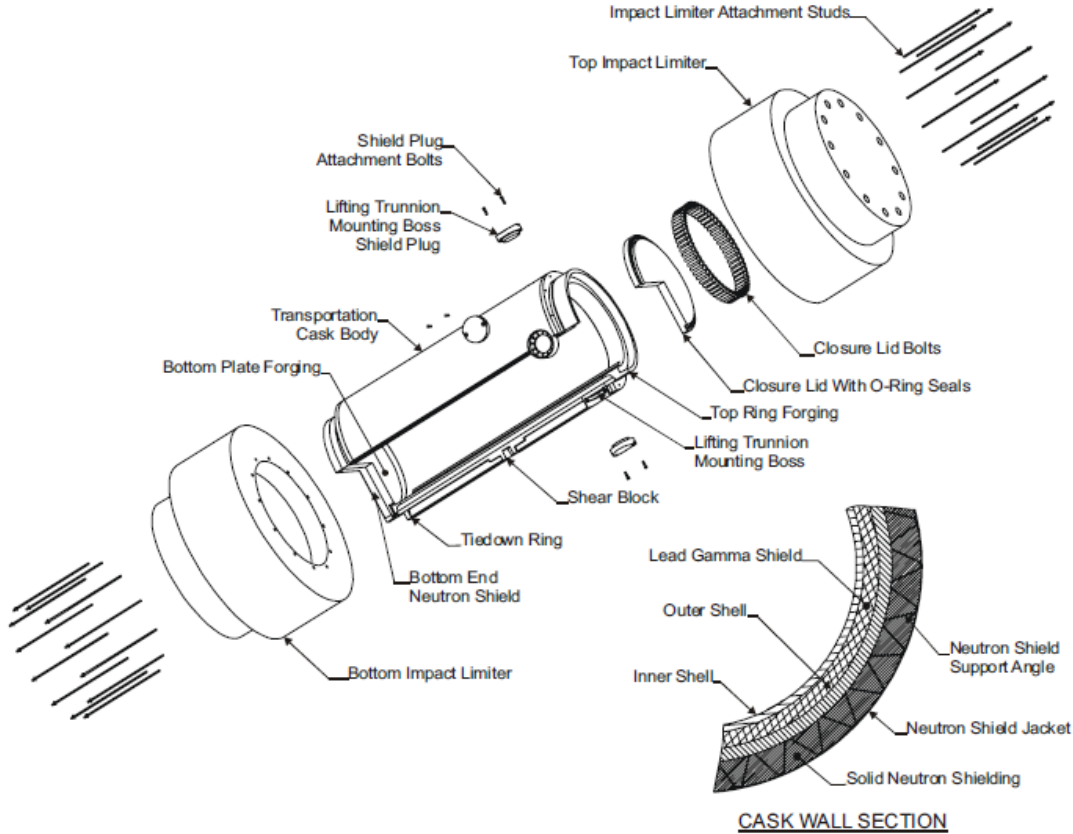


Figure 3-8 Expanded Cutaway View of FuelSolutions TS125 Transportation Package<sup>15</sup>

The TS125 cask cavity is 67 inches in diameter and 193 inches in length. The external dimensions of the cask body include an overall length of 324.4 inches and overall diameter of 143.5 inches diameter with impact limiters (210.4 inches long by 94.2 inches without the impact limiters). The maximum gross weight of the transport cask with the maximum payload is 285,000 pounds. The design basis decay heat load for the TS-125 transportation cask is 22kW.<sup>15</sup>

**Client Canisters:** The W21 and W274 FuelSolutions canisters consist of a steel shell assembly and an internal basket assembly. The canister shell assembly consists of a steel cylindrical shell, bottom end closure, bottom shield plug, bottom shell extension, bottom outer plate, top shield plug, top inner closure plate and top outer closure plate. All structural components of the canister shell assembly are constructed of austenitic stainless steel, with the exception of the shield plugs. The shield plug materials may be composed of lead, depleted uranium or carbon steel, depending on the specific canister variant.

The W21 TSC basket consists of 21 guide tubes that are positioned and supported by a series of circular spacer plates, which in turn are positioned and supported by support rod assemblies. The W21 guide tubes include neutron absorber sheets on all four sides. The W 74 canister includes two stackable basket assemblies with a capacity to accommodate up to 64 Big Rock Point Assemblies. Details on these canister designs are contained in References 29 and 30.

### **3.2.7 4.2.7 TN-FSV**

The TN-FSV is the smallest cask described in this report and is the only commercial used cask described that is designed primarily for road rather than rail transport. The cask body consists of two concentric shells of Type 304 Stainless Steel, welded to a bottom plate and a top closure flange. The inner shell has an inner diameter of approximately 18 inches, a typical wall thickness of 1.12 inches and an overall interior length of 199 inches. The inner cavity is capable of containing one fuel storage canister (FSC) which has exterior dimension of approximately 17.6 inches in diameter and 195 inches in overall length. The outer shell of the cask body has an outside diameter of 31 inches, a wall thickness of 1.5 inches and an overall exterior length of 247 inches. The annular space between the inner and outer shells is filled with lead. The maximum gross weight of the TN-FSV when transporting a FSC is 47,000 pounds.<sup>16</sup>

The TN-FSV does not include a variant for long-term storage of fuel and is sealed with butyl O-ring elastomer seals. The maximum heat load for the TN FSV with six HTGR fuel assemblies is 360 watts with an individual assembly heat load limit of 60 watts<sup>16</sup>.



Figure 3-9 TN-FSV Cask

## **4. Orphan Site Storage and Transport**

There are seven former commercial reactor sites in the U.S. which are considered by the NRC to be “ISFSI Only” sites where the plant license has been reduced to include only the spent fuel storage facility.<sup>e</sup> One of these sites stores fuel from a gas cooled reactor, Fort Saint Vrain, while the remaining

<sup>e</sup> Some of these sites are also storing Greater than Class C and Low Level Waste.

ISFSI sites contain the fuel of light water reactors. In addition to these sites, Humboldt Bay is a reactor site still being decommissioned and dismantled where all fuel has been placed into a below grade ISFSI. The Humboldt Bay spent fuel pool removal is scheduled for 2012. There are two more shutdown reactor sites, LaCrosse and Zion, where plans call for all spent fuel to be transferred to dry storage followed by decommissioning of all wet storage and transfer capabilities. As of the date of this report, three casks at LaCrosse have been loaded with two more planned. Collectively, these sites are often referred to as “orphan” sites, although sometimes this term is applied to only the first seven reactor sites listed in Table 4-1.

All fuel assemblies at “ISFSI Only” sites as well as those planned to become “ISFSI Only” sites in the near future, are stored in canisters that are dry, seal welded and purged with an inert gas. None of these sites use casks where the fuel is stored directly in a storage cask with a bolted closure and mechanical seal (“bare fuel” or “dual purpose” type cask).

Table 4-1 contains a listing of all the “ISFSI Only” sites as well as those planned to become “ISFSI Only” sites in the near future (Ft St Vrain is omitted from this list since it is a HTGR site). Although Table 4-1 is titled “Shutdown Reactor Site Inventory” it only refers to reactor sites where all reactors have been permanently shut down. It does not include reactor sites where one or more reactors have been permanently shutdown while others continue to operate<sup>f</sup>.

Table 4-1 lists the shutdown date of the last reactor shutdown at each site as well as the type of reactor. The third column lists the start and end dates of the loading of all fuel assemblies into dry storage or the planned load dates. The fourth column lists the cask system used at each site, the canister types used at that site, the transport cask model number and certificate number associated with the casks/canister system. If the storage technical specifications are publically available to check for consistency with the transport certificate, this is listed in column 4. Other comments or details associated with the site inventory are also listed in column 4. The fifth column gives the expiration date of the certificate listed in column 4.

The sixth column contains the number of fuel cask canisters as well as canisters with GTCC waste in storage at the ISFSI while column seven lists the number of assemblies in dry storage.<sup>1</sup> the eighth column lists the Metric Tons Initial Heavy Metal included in the dry stored fuel at each reactor. The ninth column contains information on the number of damaged fuel assemblies or cans at the ISFSI or the number damaged fuel assemblies or cans allowed per cask. The remaining columns list the specific fuel types and classifications as well as the associated limits for maximum burnup initial enrichment and heat load. The information in columns nine through 13 are generally taken from the cask or ISFSI technical specification listed except for the case of the Trojan and Zion ISFSI sites. The Trojan fuel details come from a report by the State of Oregon referenced in the table while the Zion information is mostly TBD.

<sup>f</sup> See Appendix A, such sites include Dresden, Indian Point, Millstone, Peach Bottom, and the San Onofre Nuclear Generating Station (SONGS)

Table 4-1 Shutdown Reactor Site Inventory

Reactor Site (Shutdown Date) (1)	Type (2)	ISFSI Load Dates (3)	Cask System/Canister(s)/ Transport Cask (4)	Transport Cask Status (5)	Total Casks Fuel/GTCC (6)	Total Assemblies (7)	MTHM (8)	Damaged Fuel Assemblies or Cans (9)	Fuel Types(Cladding) (10)	Max Burnup GWD/MTU(12)	Maximum Enrichment wt.% <sup>235</sup> U (13)	Heat Load Limit Assembly/Cask (14)
Big Rock Point 8/97	BWR	12/02-03/03	Fuel Solutions W150 Storage Overpack/W74 Canister/TS-125 71- 9276. BRG Tech Spec. contents match transport CoC contents including MOX fuel. -96 upgrade needed.	TS-125 Certificate Expires 10/31/2012 Timely Renewal Expected. Cask Never Fabricated	8/1	441	58	8 Maximum per Cask <sup>18</sup>	GE 9x9,(Zircaloy) <sup>18</sup> ANF 9x9 (Zircaloy) ANF 11x11 (Zircaloy) J2(9X9) MOX (Zircaloy) DA (11x11) MOX (Zircaloy) G-Pu (11x11) MOX (Zircaloy)	40 40 40 22.82 21.85 34.22	4.10 4.10 4.10 4.50/3.65 PuO <sub>2</sub> 2.40/2.45 PuO <sub>2</sub> 4.60/5.45 PuO <sub>2</sub>	338W/26.4kW 338W/26.4kW 338W/26.4kW 338W/26.4kW 338W/26.4kW 338W/26.4kW
Connecticut Yankee 12/96	PWR	05/04-03/05	NAC MPC/MPC-26 & MPC-24/ NAC-STC Cask 71-9235. CY Tech. Spec. contents match transport CoC contents including Reconfigured Fuel and Damaged Fuel cans.	NAC-STC Certificate Expires 05/31/2014. Foreign use versions of Cask have been fabricated. No domestic units fabricated.	40/3	1019	412	4 Maximum per Cask <sup>19</sup>	West. 15x15 (SS) <sup>19</sup> NUMEC 15x15(SS) B&W(GUNF) 15x15(SS) B&W 15x15 (SS) G A 15x15(Zircaloy) NUMEC 15x 15 (Zircaloy) B&W 15x15, (Zircaloy) B&W 15x15 (Zircaloy) Vantage 15x15(Zircaloy)	38 30 38 38 30 30 40 43 30	4.03 4.03 4.03 4.03 3.42 3.42 3.42 3.93 4.61	264W/17.5kW 264W/17.5kW 264W/17.5kW 264W/17.5kW 347W/17.5kW 347W/17.5kW 347W/17.5kW 347W/17.5kW 347W/17.5kW
Maine Yankee 8/97	PWR	08/02-03/04	NAC UMS/UMS-24/NAC-UMS Cask 71-9270. MY Tech. Spec. contents match transport CoC including High Burnup and Damaged Fuel. One Assembly cannot be transported until 2015	NAC-UMS Certificate Expires 10/31/2012 Timely Renewal Expected Cask Never Fabricated	60/4	1434	483	14 initial, Some of the 90 High Burnup Assemblies are Likely in MYFCs <sup>20</sup>	CE 14x14 (Zircaloy) <sup>20</sup> CE 14x14 High Burnup (Zircaloy) CE 14x14 w/SS Repl. Rods (Zr&SS)	45 50 50	4.2 4.2 4.2	830W/20kW 830W/20kW 830W/20kW
Yankee Rowe 9/91	PWR	06/02-06/03	NAC MPC/MPC-36/ NAC-STC Cask 71-9235. YR fuels called out in transport CoC including Reconfigured Fuel and Damaged Fuel cans.	NAC-STC Certificate Expires 05/31/2014. (See CY above)	15/1	533	127	4 max per canister <sup>19</sup>	CE Types A&B (Zircaloy), <sup>19</sup> ExxonTypes A&B (Zircaloy), Westinghouse Types A&B (SS) UN Types A&B (Zircaloy) Reconfigured Fuel (Zr or SS)	36 36 32 32	3.93 4.03 4.97 4.03	320W/12.5kW 320W/12.5kW 264W/12.5kW 320W/12.5kW 102W/12.5kW
Ranco Seco 6/89	PWR	04/01-08/02	TN/FO,FC,FF-DSCs/MP187 71-9255 RS fuels included in Transport CoC. Canister and fuel in RS TS match CoC	NUHOMS MP-187 Certificate Expires 11/30/2013 Timely Renewal Expected. One Cask has been Fabricated. No impact limiters Fabricated	21/1	493	228	13 in single FF DSC, 6 in FC DSC <sup>21</sup>	B&W 15x15 (Zircaloy-4) <sup>21</sup>	38.268	3.43	N.L./13.5kW
Trojan 11/92	PWR	12/02-9/03	HOLTEC MPC /MPC-24E/24EF /HISTAR 100 71-9261.	HISTAR 100 Certificate Expires 03/31/2014. Units Fabricated but not impact limiters	34/?	780	359	22 failed fuel cans <sup>22</sup>	17x17B (Zircaloy) <sup>22</sup>	42	3.7	725W/20kW
Humboldt Bay 7/76	BWR	08/08-12/08	HOLTEC HISTAR HB/ MPC-HB (MPC-80)/HISTAR HB 71-9261 HB Contents in TS match transport certificate	HISTAR HB Certificate Expires 03/31/2014. Fuel in Fabricated Casks. Impact Limiters not Fabricated	5/1	390	29	28 max per canister <sup>23</sup>	GE TYPE II 7x7 (Zircaloy) <sup>23</sup> GE TYPE III, 6x6 (Zircaloy) Exxon Types III 6x6 (Zircaloy) Exxon Type IV 6x6 (Zircaloy)	23 23 23 23	2.60 2.60 2.60 2.60	50W/2kW 50W/2kW 50W/2kW 50W/2kW
LaCrosse 4/87	BWR	07/12-Ongoing	NAC MPC-LACBWR/MPC- LACBWR 68 positions/ NAC-STC 71-9235 Contents described to right are included in current transport cert.	NAC-STC Certificate Expires 05/31/2014. (See CY above)	5(estimated)	333	38	155 (preliminary) <sup>19</sup>	Allis Chalmers (SS) <sup>19</sup> Allis Chalmers (SS) Exxon (SS)	22 22 21	3.64 3.94 3.71	63W/4.5kW 63W/4.5kW 62W/4.5kW
Zion 1 and 2 7/98	PWR	Planned 2013	NAC MAGNATRAN/TSC- 37/MAGNATRAN 71-9356 UNDER REVIEW.	NAC MAGNATRAN License under review. Never Fabricated	61(estimated)	2,226	1018	10 damaged or reconsolidated fuel cans (preliminary) <sup>1</sup>	LOPAR (Zircaloy) OFA (Zircaloy-4) VANTAGE 5(Zircaloy-4) VANTAGE 5 w/ IFMs (Zircaloy-4)	TBD TBD TBD TBD	TBD TBD TBD TBD	TBD TBD TBD TBD

## 5. Transfer Cask Designs

Transfer casks are lead and steel casks used for handling of fuel canisters during loading, drying, welding and transfer operations. Transfer casks provide biological (gamma and neutron) shielding during canister closure, drying, welding and transfer but do not provide containment or criticality control features. Unlike the Canister Transport Casks described in Section 3.2, the transfer casks described in this section do not meet 10CFR 71 requirements for shipment of used fuel in commerce. In general, transfer casks are not pressure vessels and do not consist of a pressure boundary. Some transfer casks are designed to ASME Section III Subsection NF or NC, and other aspects of the ASME Boiler & Pressure Vessel code such as welding and weld inspections may apply to their fabrication and inspection. Each transfer cask in use at U.S. ISFSIs is designed to transfer and handle a single canister at a time. Transfer casks are a heavy lift device designed, fabricated and proof load tested to the requirements of NUREG-0612 and ANSI N14.6 (withdrawn ANSI standard still cited by the industry). Transfer casks are fabricated predominantly of carbon steel meeting ASTM specification.

Neutron shielding is provided by either water jacket or solid neutron absorber material. Water jackets often contain ethylene glycol or another agent to prevent freezing.

### 5.1 NAC Transfer Casks

There are four NAC transfer cask designs, three of which have been used for canister loading and transfer operations and the fourth planned for use at Zion. There are two different cask designs originally designed for interface with the MPC canister systems used at Connecticut Yankee and Yankee Rowe respectively. The transfer cask for Connecticut Yankee has a slightly thicker gamma shield and neutron shield. The inner and outer shells of both these cask designs consisted of ASTM A588 Low alloy steel. The transfer cask from Yankee Rowe has been purchased by Dairyland power for transfer of fuel into dry storage at Lacrosse.

Table 5-1 NAC Transfer Cask Models (NEI 2010)<sup>24</sup>

Transfer Cask	NAC MPC YR	NAC MPC CY	NAC UMS	MAGNASTOR
<b>Number of Fabricated Casks</b>	1	2	4	2
<b>Transfer Cask Dimensions</b>				
Length [m] (in)	3.39(133.4)	4.8(189)	4.6(181.2)	4.79(188.4)
Outer Diameter [m](in)	2.20(86.5)	2.26(89)	2.4(94.8)	2.71(106.8)
Loaded Weight with water [t.] (lbs.)	61.45 135,473	78.34 172,708	90.6-97.2 199,800- 214,300	104.1 229,500

NAC prefers to use machined bricks which are curved at interface surfaces to reduce shine paths rather than pouring monolithic shield assemblies (Figure 5-1). Between the lead brick and the transfer cask outer shell is an annulus filled with a solid synthetic polymer neutron shield material. The solid neutron shield material placement stabilizes the lead brick structure although neither is a credited structural component. Shielding at the bottom of the transfer cask is provided by thick (~9 inch) sliding shield

doors. The top of the transfer cask is essentially open except for a retaining ring which bolts to the cask body preventing a loaded canister from being inadvertently removed through the top of the transfer cask. Shielding at the top of the transfer cask is provided by the canister shield lid while loaded.<sup>24</sup>



Figure 5-1 NAC Transfer Cask Fabrication

The transfer cask has retractable bottom shield doors which slide in rails incorporated in the transfer cask bottom. During loading operations, the doors are closed and secured by lock bolts/lock pins, so they cannot inadvertently open. During unloading, the doors are retracted using hydraulic cylinders to allow the canister to be lowered into the storage or transport cask. During transfer of the cask with a loaded canister, only the doors held in place by two door rails and the lock bolts/lock pins. The hydraulic actuators are integrated into an adaptor plate that attaches to a storage overpack or to a transport cask. With NAC systems, the transfer of the loaded canister to the storage overpack usually occurs inside the 10CFR50 facility. The storage overpack is then moved from the 10CFR50 facility to the ISFSI pad using either a heavy haul trailer or cask transporter. The transfer cask and adaptor plate are designed to also be capable of directly loading the storage overpack at the ISFSI pad.

To minimize potential contamination of the canister and transfer cask during loading operations in the spent fuel pool, clean water is circulated in the gap between the transfer cask interior surface and the canister exterior surface using fill and drain lines in the wall of the transfer cask. Clean water is injected into the annular space during the entire time the transfer cask is submerged. No seals are used on the bottom door interface or at the top of the canister. This design and process has been adequate in ensuring acceptable contamination levels on the canister exterior. Each of the fill and drain ports are offset to minimize shine paths from the unshielded fuel canister sidewall.<sup>24</sup>

Figure 5-2 shows a picture of the basic transfer cask body without the bottom doors in place. Figure 5-3 shows the adaptor plate mechanism with the doors in the open position



Figure 5-2 NAC Transfer Cask Body (NAC SNFDS Seminar)



Figure 5-3 NAC Adaptor Plate Door Operation (NAC SNFDS Seminar)

## 5.2 HOLTEC Transfer Casks

HI-TRAC is an acronym for Holtec International Transfer Cask. There are four basic HI-TRAC cask designs, the 125-ton standard design (HI-TRAC-125), the 125-ton dual-purpose lid design (HI-TRAC-125D), the 100 ton standard design (HI-TRAC -100) and the 100-ton dual purpose lid design (HI-TRAC-100D). The 100 ton HI-TRAC is used at sites with a maximum crane capacity less than 125 tons. All the HI-TRAC design variations use lead for gamma shielding and a water jacket for neutron shielding, the configuration of layers from interior to exterior being steel, lead, steel, water space, steel. Each of the transfer casks listed in Table 5-2 is designed and constructed in accordance with ASME Section III, Subsection NF, with certain NRC approved alternatives. Since all HOLTEC canisters have the same exterior dimensions, the basic internal diameter of all HI-TRAC transfer casks is the same.

Table 5-2 HOLTEC Transfer Cask Models<sup>25</sup>

<b>Transfer Cask</b>	HI-TRAC 100	HI-TRAC 100D	HI-TRAC 125	HI-TRAC 125D
<b>Number of Fabricated Casks</b>	2	4	5	11
<b>Transfer Cask Dimensions</b>				
Length (in)	191.25	191.25	201.5	201.5
Outer Diameter (in)	89	91.25	Water J. 93.75	Water J. 93.75
Inner Diameter (in)	68.75	68.75	Base Plate 104	Base Plate 104
Loaded Weight with water(lbs.)	192,000- 199,999	192,000- 199,000	228,500- 236,000	228,500- 236,000

### 5.2.1 HI-TRAC Standard Design

The standard design HI-TRAC transfer casks are heavy-walled cylindrical vessel composed of carbon steel and lead with an exterior water jacket. The top lid of the HI-TRAC 125 has additional neutron shielding to provide neutron attenuation of neutrons from the top of the MPC. The MPC access hole through the HI-TRAC top lid allows the lowering and raising of the MPC between the HI-TRAC transfer cask and the HI-STORM or HI-STAR overpacks. The standard design HI-TRAC (comprised of HI-TRAC 100 and HI-TRAC 125) is provided with two bottom lids, each used separately. The pool lid is bolted to the bottom flange of the HI-TRAC and is utilized during MPC fuel loading and sealing operations. In addition to providing shielding in the axial direction, the pool lid incorporates a seal that is designed to hold clean water in the HI-TRAC inner cavity preventing contamination of the MPC exterior from fuel pool water. After the MPC has been drained, dried and sealed, the pool lid is removed and the HI-TRAC transfer lid is attached (standard design only). The transfer lid incorporates two sliding doors that allow the opening of the HI-TRAC bottom for the MPC to be raised and lowered. Figure 5-4 shows the cross section of a HI-TRAC 125 standard cask with both a pool lid and a transfer lid attached. Both

lid types are attached to the cask body bottom flange with 36 1" diameter bolts in the case of the HI-TRAC 100. Both lid types are blind drilled and tapped to accept the 36 attachment bolts.<sup>25</sup>

There are two standard designs HI-TRAC transfer casks classified by total gross weight of the loaded cask. The HI-TRAC-125 weight does not exceed 125 tons during any loading or transfer operation while the HI-TRAC-100 weight does not exceed 100 tons during any loading or transfer operation. The internal cylindrical cavities of the two standard design HI-TRACs are identical while the exterior dimensions vary. The HI-TRAC 100 has a reduced thickness of lead and water shielding leading to reduction of the outside diameter at several locations, the thickness of the structural steel of the two standard HI-TRAC is identical such that most structural analyses of the HI-TRAC 125 bound the HI-TRAC 100 design.<sup>25</sup>

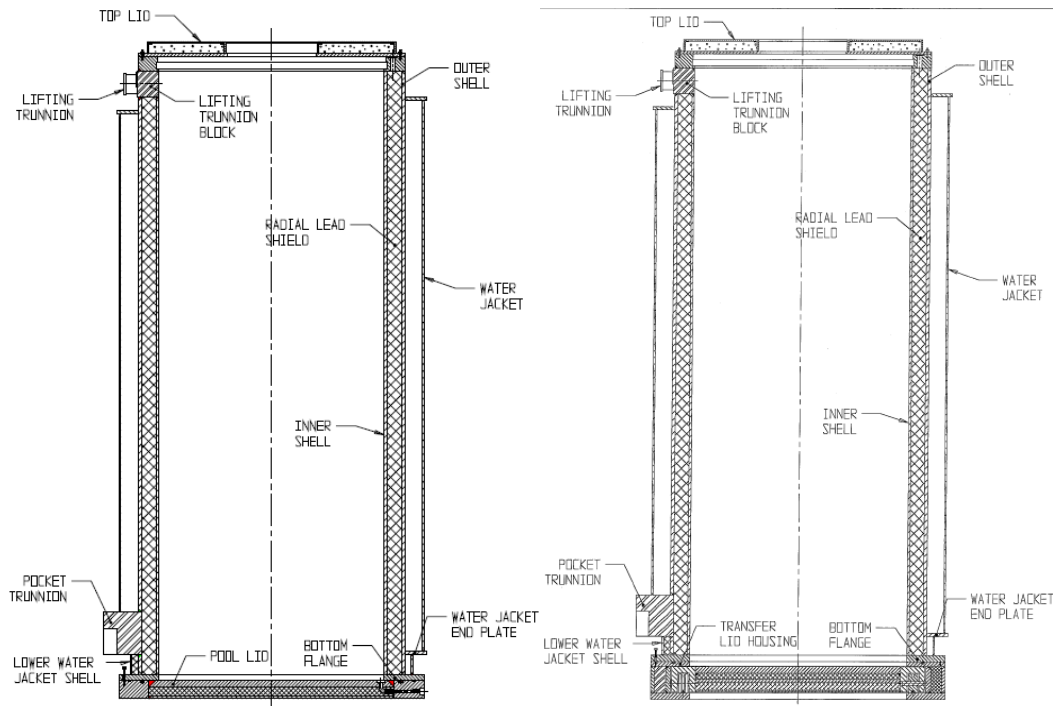


Figure 5-4 HI-TRAC 125 Pool Lid (Left) Transfer lid (Right)<sup>25</sup>

### 5.2.2 HI-TRAC 100D and 125D Transfer Casks

The HI-TRAC 100D and 125D designs are functionally equivalent to the standard design variants but have the following primary differences.

- No pocket trunnions
- No transfer lid (not required)
- HI-STORM mating device is required during MPC transfer operations
- A wider baseplate with attachment points for the mating device is included
- The baseplate incorporates gussets for added structural strength

Unlike the standard transfer cask variants, the 100D and 125D HI-TRAC transfer casks do not require swapping the pool lid for a transfer lid to facilitate transfer of the MPC. The HI-STORM mating device is located between the HI-TRAC and HI-STORM and secured with bolting to both. Figure 5-5 shows the lower assembly detail of a 125 D HI-TRAC. This patented<sup>26</sup> design allows for removal of the pool lid by loosening the inner bolts on the bottom flange lowering it into the cask mating device assembly shown in Figure 5-6.

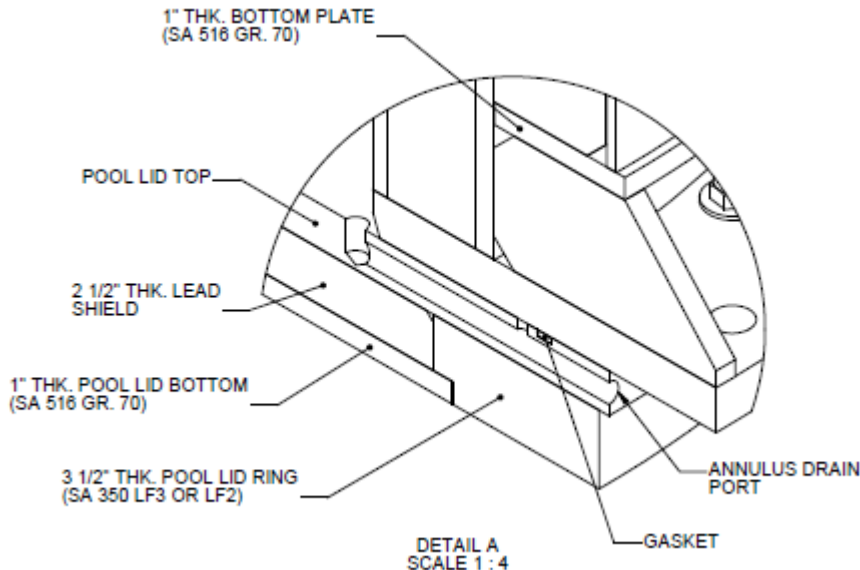


Figure 5-5 HI-TRAC 125D Lower Assembly Detail<sup>25,26</sup>

The patented design incorporates two gasket seals, one between the pool lid top and the bottom flange (Figure 5-5) and the other between the canister outer wall and the transfer cask inner wall close to the top lid of the transfer cask. These seals provide a barrier from pool water contamination while the transfer cask is submerged in the pool.

### 5.2.3 TN/NUHOMS Transfer Casks

TN/NUHOMS systems are unique in that the canister transfer from the transfer cask to the storage module is performed while the transfer cask is in the horizontal position. This transfer to the horizontal storage usually occurs at the ISFSI site such that the transfer cask carries the fuel canister between the 10CFR50 facility and the ISFSI pad vs. the storage overpack being heavy hauled to the storage sites in other systems. The TN systems are also unique in that the TN canister transport casks described in sections 3.2.1 and 3.2.2. above can also be used as transfer casks if desired. They can also be used to directly remove and transport canisters from the Horizontal Storage Modules without the need to an intermediary cask required by other systems. The TN transfer casks listed in Table 5-3 are fabricated and designed to ASME Section III, Division I, Subsection NC, Class 2 (non-pressure retaining components).

Table 5-3 TN Transfer Cask Designs<sup>2,27</sup>

Transfer Cask	OS187H <sup>c</sup>	0S197	OS197L	OS200
<b>Number of Fabricated Casks</b>	2	4	1	1
<b>Transfer Cask Dimensions</b>				
Length (in)	207.22 <sup>c</sup>	207.22	<sup>a</sup>	206.72
Outer Diameter (in)	85.5 <sup>c</sup>	85.5	<sup>a</sup>	92.11
Inner Diameter (in)	68	68	<sup>a</sup>	68
Payload limit(dry) (lbs.) <sup>b</sup>	80,000	97,250	<sup>a</sup>	116,000
Loaded Weight with water (lbs.)	<200,000 <sup>c</sup>	<200,000	<150,000	<250,000

<sup>a</sup>Proprietary Information withheld in accordance with 10 CFR 2.390

<sup>b</sup> Payload limit for analysis. Actual payload depends on as built cask weight and configuration

<sup>c</sup> Values from Reference 2. Reference 27 reports OS187H length of 197.1 in, outer diameter of 92.2in and a gross weight of 114.5 tons or 229,000 pounds.

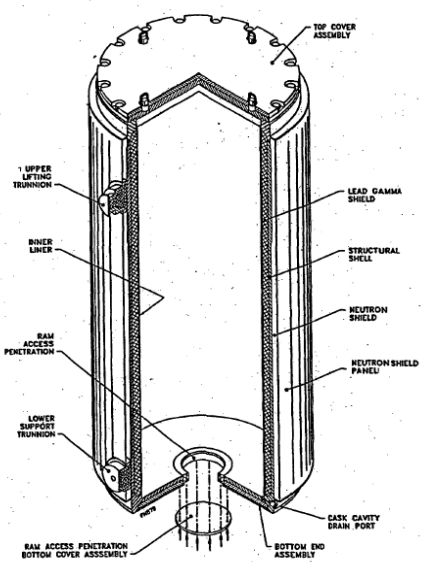


Figure 5-6 OS187H On-Site Transfer Cask<sup>27</sup>

#### 5.2.4 Fuel Solutions Transfer Casks

Fuel Solutions have two transfer cask designs for use with Fuel Solutions systems. The W100 transfer cask used with the W21 and W74 Dual Purpose Canisters<sup>13</sup> and the MTC (Multi-assembly Sealed Basket Transfer Cask) used with the VSC 24 canister system<sup>12</sup>. Details of these cask designs have been redacted

under 10 CFR 2.390. From the canister specifications, the W100 transfer cask must have a cavity capable of accepting a canister 66 inches in outer diameter, 192.25inches in length with a gross weight of 85,000 pounds. Likewise, the MTC must have a cavity capable of accepting a canister 62.5 inches in outer diameter, 192.5 inches long with a gross weight of 69,000pounds. Per available information both casks are capable of horizontal transfer to the TS-125 transport Cask. Actual number of each cask type fabricated are not reported in licensing documents but current storage conditions indicate that at least one W100 and MTC have been fabricated with possibly more than one MTC given two utility use of the VSC 24..

## 6. References

1. StoreFUEL Newsletter, August 07 2012 Vol. 13, No. 168
2. EPRI Industry Spent Fuel Storage Handbook, John Kessler, 1021048, Final Report July 2010
3. Hanson, Stockman, Alsaed, Enos, Gap Analysis to Support Extended Storage of Used Nuclear Fuel, FCRD-USED-2011-000XXX
4. American National Standard for Radioactive Materials- *Leakage Tests on Packages for Shipments*. ANSI N14.5, American National Standards Institute, INC. , New York, NY,(1997)
5. TN 68 Transport Packaging Safety Analysis Report, Revision 0, April 1999
6. TN-40 Transportation Packaging, Safety Analysis Report, E-23861, Revision 0, August 2006
7. Extended Drop Tests of DCI Casks with Artificial Flaws Demonstrating the Existing Safety Margins, B. Droste et. al., RAMTRANS, Volume 6, Nos 2/3 pp 177-182, 1995
8. Surry Independent Spent Fuel Storage Installation, Final Safety Analysis Report, Revision 18, SNM-2501, June 2008
9. Safety Analysis Report, NUHOMS-MP187 Multi-Purpose Cask Transportation Package Document No. NUH-05-151
10. NUHOMS-MP197 Transport Packaging Safety Analysis Report, Revision 4.
11. Certificate of Compliance Model Nos NUHOMS-MP197-MP197HB, USA/9302/B(U)F-96, Revision 4.
12. Safety Analysis Report on The HI-STAR 100 Cask System, Revision 15, HI-951251, October 2010
13. Safety Analysis Report, NAC Storage Transport Cask, Revision 16, September 2006, 71-9235
14. Safety Analysis Report for the Universal Transport Cask, Revision UMST-01D, November 2001, 71-9270
15. FuelSolutions TS125 Transportation Cask Safety Analysis Report, Revision 6, September 2006, WSNF-120
16. Certificate of Compliance Model No TN-FSV, USA/9253/B(U)F-96, Revision 12.
17. Halim Reference Document for MTIHM for Orphans
18. Technical Specification for the FuelSolutions<sup>TM</sup> W74 Canister NRC ML011210170
19. Technical Specifications for the NAC-MPC System Amendment 3 COC No. 1025 ML031340571
20. Technical Specifications for the NAC-UMS System Amendment 2 COC No. 1015 ML020250599
21. Technical Specifications for Rancho Seco Independent Fuel Storage Installation 72-11 ML003689836

22. Staff Evaluation of Holtec Design for Portland General Electric's Independent Spent Nuclear Fuel Storage Installation (ISFSI), Oregon Office of Energy, September 10,2002
23. Technical Specifications for Humboldt Bay Independent Fuel Storage Installation 72-27 ML053140032
24. NAC-MPC, Final Safety Analysis Report, Docket No. 72-1025, April 2012
25. Holtec International Final Safety Analysis Report for the HI-STORM 100 Cask System, 72-1014, HI-2002444, Revision 9, February 2010.
26. Unites States Patent, Singh, US 6,625,246 B1, September 23, 2003
27. Transnuclear Safety Analysis Report (Non-Proprietary), NUHOMS HD, Horizontal Modular Storage System for Irradiated Nuclear Fuel
28. VSC-24 Multi-Assembly Sealed Basket Transportation Safety Analysis Report, 0000-0632, Revision 0, September 2006
29. FuelSolutions W74 Canister Transportation Safety Analysis Report, WSNF-123, Revision 10, September 2006
30. FuelSolutions W21 Canister Transportation Safety Analysis Report, WSNF-121, Revision 6, September 2006

## **Appendix A**

Transportation Matrix for Commercial Power Reactor Fuel (Dry Storage, and  
Away from Reactor Wet Storage)

The accompanying chart details each cask or canister system in dry storage in the U.S. and cross-references these to a transportation pathway. Each row in the chart represents a cask system type at a certain reactor site listed by name of generating station (e.g. if the reactor ISFSI or ISFSIs contains three cask types in total, the chart contains three rows, one for each canister or cask type).

The first entry contains the utility name followed by the reactor name, reactor type (PWR or BWR), ISFSI license type (general or site specific), and year of first load. Next comes the Cask vendor followed by the Cask/Canister System and the specific canister/cask type employed. Generally the canister cask type includes a number that represents the number of assembly storage positions in that cask or canister type. The next column contains the total canisters or casks loaded followed by the assemblies stored in these canisters or casks. After the number of assemblies at each site, a rough estimate of the Metric Tons Initial Heavy metal of the fuel stored in each cask type is provided. (**NOTE: These numbers are based on an average value for PWR and BWR fuel. Actual MTIHM at each site can vary greatly from the number reported here depending on fuel type**)

Column 12 describes the storage configuration (fuel is stored directly in a bare fuel cask, in a canister in a concrete overpack (this includes NUHOMS storage modules and HISTORM concrete overpacks which have a metal skin), in a canister in a metal overpack (HISTAR 100) or in a canister inside a vault (Ft. St.Vrain is the only instance). If the storage configuration is a canister in a metal or concrete storage overpack, column 13 lists the primary transport cask currently licensed to transport the canister (if any) as well as any license applications for transportation casks which include the canister as a licensed content. Column 14 lists whether working units of the primary cask have been fabricated. For canister casks, only models of the NUHOMS MP187, HISTAR 100 and the TN-FSV have been fabricated. There are versions of the NAC-STC that have been fabricated for use overseas which are not available or licensable in the U.S. The NUHOMS MP197 cask has yet to be built as of the date of this report and will likely be replaced by the MP 197HB variant by the time working units are needed. The only domestic HISTAR 100 working transport casks are the 12 used for storage at Humboldt Bay, Dresden and Hatch. No production or full scale prototype units of the Fuel Solutions TS-125 cask have been fabricated as of the date of this report.

Column 15 lists any alternate transport casks which may be licensed for the same canister type or under application or even being considered for licensing of the canister type. If a certificate number is listed along with the cask name in columns 13 or 15, this signifies that that canister is included in the transport certificate. If the cask name is listed but no number is listed, this signifies that either the canister is under application for transport in the cask type named or is considered licensable for transport in the named cask by the cask vendor. Column 16 lists whether working units of the alternate cask in column 15 have been fabricated.

Column 17 applies to bare fuel casks and lists whether a transport license exists for the bare fuel cask with footnotes providing details.

For those systems which employ a fuel canister, Column 18 delineates whether the canister has been classified by the cask vendor as “storage only” canister. Storage only canisters may lack neutron absorbing material or may have simply not been evaluated in the 10 CFR71 accident sequence in a transportation overpack. By definition, each of the canisters listed in this column are not included in any transportation cask license. These canisters may still ultimately be shipped without repackaging of the fuel depending on the reasons for classification as “storage only”.

The final column of the chart contains the minimum lead time for shipment for canisters and casks at each reactor location. The lead time listed in this column only includes the time to prepare existing casks for shipment, time to fabricate casks and the time to obtain transportation licenses. It does not include factors such as approval of routing, security requirements, requirements for special rolling stock or the

implementation of “smart train” technology, or most importantly the time to make available a repository or interim storage site.

The wet storage table on the following page contains most of the same columns as the dry storage stable except that there are no references to bare fuel casks or “storage only” canisters. There are only two shutdown site currently transitioning into “ISFSI Only” status; LaCrosse and Zion. Both these sites have selected cask systems and in the case of LaCrosse, three casks have already been loaded as of August 2012 and the remaining two are expected to be completed in the coming weeks.

GE Morris is an away from reactor used fuel storage facility. There are no announced plans to transition fuel at GE Morris into dry cask storage as of the date of this report.

The final table in Appendix A is a storage summary table that gives a breakdown of the % of assemblies in each category of cask/vault storage listed.

Table A-1 Transportation Matrix for Commercial Reactor Fuel (Dry Storage, and Away from Reactor Wet Storage)

**U.S. Dry Storage Details (08/01/2012)**

Utility	Reactor	Type	License Type	Year of First Load <sup>14</sup>	Vendor	Cask System	Canister or Cask Type	Total Canisters or Casks Loaded	Assemblies Stored	MTIHM (Based on Average Assembly)	Storage Configuration	Primary Canister Transportation Cask (License Num.)	Primary Transport Cask Fabricated?	Alternative Canister Transportation Cask	Alternate Transport Cask Fabricated?	Bare Fuel Cask Transportation License (License Number)	"Storage Only" Canisters or Casks	Minimum Lead Time for Shipment	
AEP	D.C.Cook	PWR	GL	2012	Holtec	HI-STORM	MPC-32	1	32	13.9	Canister in Vertical Concrete Overpack	HI-STAR100 (71-9261)	Yes <sup>1</sup>		No			14 Months <sup>8</sup>	
APS	Palo Verde	PWR	GL	2003	NAC	NAC-UMS	UMS-24	94	2256	982.5	Canister in Vertical Concrete Overpack	NAC-UMS (71-9270)	No	NAC-MAGNASTOR	No			24 Months <sup>8</sup>	
Constellation	Calvert Cliffs	PWR	SS	1992	TN	NUHOMS	24P	48	1152	501.7	Canister in Horizontal Concrete Overpack		No		No		24P	36 Months <sup>10</sup>	
Constellation	Calvert Cliffs	PWR	SS	1992	TN	NUHOMS	32P	21	672	292.7	Canister in Horizontal Concrete Overpack		No		No		32P	36 Months <sup>10</sup>	
Constellation	Ginna	PWR	GL	2010		NUHOMS	32PT	6	192	83.6	Canister in Horizontal Concrete Overpack		No		No			24 Months <sup>8</sup>	
Consumers	Big Rock Point <sup>12</sup>	BWR	GL	2002	BFS/ES	FuelSolutions	W150	8	441	78.8	Canister in Vertical Concrete Overpack	TS-125 (71-9276)	No		No			24 Months <sup>8</sup>	
Ct.Yankee	Conn Yankee <sup>12</sup>	PWR	GL	2004	NAC	NAC-MPC	MPC-26	43	1019	443.8	Canister in Vertical Concrete Overpack	NAC-STC (71-9235)	No	NAC-MAGNASTOR	No			24 Months <sup>8</sup>	
Dairyland Power	Lacrosse	BWR	GL	2012	NAC	NAC	LACBWR	3	204	36.4	Canister in Horizontal Concrete Overpack	NAC-STC (71-9235)	No	NAC-MAGNASTOR	No			24 Months <sup>8</sup>	
DOE	INEEL	PWR	SS	TN	NUHOMS	12T		29	177	77.1	Canister in Horizontal Concrete Overpack		No		No		12T	36 Months <sup>10</sup>	
Dominion	Keweenaw	PWR	GL	2009	TN	NUHOMS	32PT	8	256	111.5	Canister in Horizontal Concrete Overpack		No	MP197HB	No			24 Months <sup>8</sup>	
Dominion	Millstone	PWR	GL	2005	TN	NUHOMS	32PT	18	576	250.8	Canister in Horizontal Concrete Overpack		No	MP197HB	No			24 Months <sup>8</sup>	
Dominion	North Anna	PWR	SS	1998	TN	TN Metal Casks	TN-32	27	864	376.3	Bare Fuel	-	-	-	-	No <sup>3</sup>		24 Months <sup>8</sup>	
Dominion	North Anna	PWR	GL	2008	TN	NUHOMS	32PTH	13	416	181.2	Canister in Horizontal Concrete Overpack		No	MP197HB	No			24 Months <sup>8</sup>	
Dominion	Surry	PWR	SS	1986	GNB	Castor	V/21 and X33	26	558	243.0	Bare Fuel		-	-	-	No <sup>4</sup>		36 Months <sup>10</sup>	
Dominion	Surry	PWR	SS	1986	NAC	NAC-128	NAC-128	2	56	24.4	Bare Fuel		-	-	-	No <sup>5</sup>		24 Months <sup>8</sup>	
Dominion	Surry	PWR	GL	2007	TN	NUHOMS	32PTH	18	576	250.8	Canister in Horizontal Concrete Overpack		No	MP197HB	No			24 Months <sup>8</sup>	
Dominion	Surry	PWR	SS	1986	TN	TN Metal Casks	TN-32	26	832	362.3	Bare Fuel		-	-	-	No <sup>3</sup>		24 Months <sup>8</sup>	
Dominion	Surry	PWR	SS	1986	W	MC-10	MC-10	1	24	10.5	Bare Fuel		-	-	-	No <sup>6</sup>		24 Months <sup>7</sup>	
Duke	Catawba	PWR	GL	2007	NAC	NAC-UMS	UMS-24	24	576	250.8	Canister in Vertical Concrete Overpack		No	NAC-MAGNASTOR	No				24 Months <sup>8</sup>
Duke	McGuire	PWR	GL	2001	NAC	NAC-UMS	UMS-24	28	672	292.7	Canister in Vertical Concrete Overpack	NAC-UMS (71-9270)	No	NAC-MAGNASTOR	No			24 Months <sup>8</sup>	
Duke	McGuire	PWR	GL	2001	TN	TN Metal Casks	TN-32	10	320	139.4	Bare Fuel		-	-	-	No <sup>3</sup>		24 Months <sup>7</sup>	
Duke	Oconee	PWR	GL/SS	1990	TN	NUHOMS	24P	84	2016	878.0	Canister in Horizontal Concrete Overpack		No		No		24P	36 Months <sup>10</sup>	
Duke	Oconee	PWR	GL	2000	TN	NUHOMS	24PHB	38	912	397.2	Canister in Horizontal Concrete Overpack		No		No		24PHB	36 Months <sup>10</sup>	
Energy Northwest	Columbia	BWR	GL	2002	Holtec	HI-STORM	MPC-68	27	1836	327.9	Canister in Vertical Concrete Overpack	HI-STAR100 (71-9261)	Yes <sup>1</sup>		No			14 Months <sup>8</sup>	
Entergy	ANO	PWR	GL	1996	BFS/ES	FuelSolutions	VSC-24	24	576	250.8	Canister in Vertical Concrete Overpack		No		No		VSC-24	36 Months <sup>10</sup>	
Entergy	ANO	PWR	GL	1996	Holtec	HI-STORM	MPC-24	22	528	229.9	Canister in Vertical Concrete Overpack	HI-STAR100 (71-9261)	Yes <sup>1</sup>		No			14 Months <sup>8</sup>	
Entergy	ANO	PWR	GL	1996	Holtec	HI-STORM	MPC-32	16	512	223.0	Canister in Vertical Concrete Overpack	HI-STAR100 (71-9261)	Yes <sup>1</sup>		No			14 Months <sup>8</sup>	
Entergy	Fitzpatrick	BWR	GL	2002	Holtec	HI-STORM	MPC-68	15	1020	182.2	Canister in Vertical Concrete Overpack	HI-STAR100 (71-9261)	Yes <sup>1</sup>		No			14 Months <sup>8</sup>	
Entergy	Grand Gulf	BWR	GL	2006	Holtec	HI-STORM	MPC-68	17	1156	206.5	Canister in Vertical Concrete Overpack	HI-STAR100 (71-9261)	Yes <sup>1</sup>		No			14 Months <sup>8</sup>	
Entergy	Indian Point 1	PWR	GL	2008	Holtec	HI-STORM	MPC-32	5	160	69.7	Canister in Vertical Concrete Overpack	HI-STAR100 (71-9261)	Yes <sup>1</sup>		No			14 Months <sup>8</sup>	
Entergy	Indian Point 2	PWR	GL	2008	Holtec	HI-STORM	MPC-32	14	448	195.1	Canister in Vertical Concrete Overpack	HI-STAR100 (71-9261)	Yes <sup>1</sup>		No			14 Months <sup>8</sup>	
Entergy	Palisades	PWR	GL	1993	BFS/ES	FuelSolutions	VSC-24	18	432	188.1	Canister in Vertical Concrete Overpack		No		No		VSC-24	36 Months <sup>10</sup>	
Entergy	Palisades	PWR	GL	1993	TN	NUHOMS	24PTH	13	312	135.9	Canister in Horizontal Concrete Overpack		No	MP197HB	No			24 Months <sup>8</sup>	
Entergy	Palisades	PWR	GL	1993	TN	NUHOMS	32PT	11	352	153.3	Canister in Horizontal Concrete Overpack		No	MP197HB	No			24 Months <sup>8</sup>	
Entergy	River Bend	BWR	GL	2005	Holtec	HI-STORM	MPC-68	15	1020	182.2	Canister in Vertical Concrete Overpack	HI-STAR100 (71-9261)	Yes <sup>1</sup>		No			14 Months <sup>8</sup>	
Entergy	Vermont Yankee	BWR	GL	2008	Holtec	HI-STORM	MPC-68	14	952	170.0	Canister in Vertical Concrete Overpack	HI-STAR100 (71-9261)	Yes <sup>1</sup>		No			14 Months <sup>8</sup>	
Exelon	Waterford	PWR	GL	2011	Holtec	HI-STORM	MPC-32	9	288	125.4	Canister in Vertical Concrete Overpack	HI-STAR100 (71-9261)	Yes <sup>1</sup>		No			14 Months <sup>8</sup>	
Exelon	Braidwood	PWR	GL	2011	Holtec	HI-STORM	MPC-32	3	96	41.8	Canister in Vertical Concrete Overpack	HI-STAR100 (71-9261)	Yes <sup>1</sup>		No			14 Months <sup>8</sup>	
Exelon	Byron	PWR	GL	2010	Holtec	HI-STORM	MPC-32	14	448	195.1	Canister in Vertical Concrete Overpack	HI-STAR100 (71-9261)	Yes <sup>1</sup>		No			14 Months <sup>8</sup>	
Exelon	Dresden	BWR	GL	2000	Holtec	HI-STORM	MPC-68	49	3332	595.1	Canister in Vertical Concrete Overpack	HI-STAR100 (71-9261)	Yes <sup>1</sup>		No			14 Months <sup>8</sup>	
Exelon	Dresden	BWR	GL	2000	Holtec	HI-STAR	MPC-68	4	272	48.6	Canister in Metal Cask	HI-STAR100 (71-9261)	Yes <sup>1</sup>		No			12 Months <sup>11</sup>	
Exelon	LaSalle	BWR	GL	2010	Holtec	HI-STORM	MPC-68	6	408	72.9	Canister in Vertical Concrete Overpack	HI-STAR100 (71-9261)	Yes <sup>1</sup>		No			14 Months <sup>8</sup>	
Exelon	Limerick	BWR	GL	2008	TN	NUHOMS	61BT	19	1159	207.0	Canister in Horizontal Concrete Overpack	MP197 (71-9302)	No	MP197HB (71-9302)	No			24 Months <sup>8</sup>	
Exelon	Oyster Creek	BWR	GL	2002	TN	NUHOMS	61BT	23	1403	250.6	Canister in Horizontal Concrete Overpack	MP197 (71-9302)	No	MP197HB (71-9302)	No			24 Months <sup>8</sup>	
Exelon	Peach Bottom	BWR	GL	2000	TN	TN Metal Casks	TN-68	59	4012	716.5	Bare Fuel		-	-	-	Yes (71-9293)		12 Months <sup>11</sup>	
Exelon	Quad Cities	BWR	GL	20															

Table Appendix A-1 (Continued) Transportation Matrix for Commercial Power Reactor Fuel (Dry Storage, and Away from Reactor Wet Storage)

Portland	GE Trojan	PWR	GL	2002	Holtec	TranStor Cask	MPC-24E/EF	34	780	339.7	Canister in Vertical Concrete Overpack	HISTAR 100 (71-9261)	Yes <sup>1</sup>	No	14 Months <sup>v</sup>	
PPL	Susquehanna	BWR	GL	1999	TN	NUHOMS	52B	27	1404	250.8	Canister in Horizontal Concrete Overpack		No	No	52B	36 Months <sup>10</sup>
PPL	Susquehanna	BWR	GL	1999	TN	NUHOMS	61BT	40	2440	435.8	Canister in Horizontal Concrete Overpack	MP197 (71-9302)	No	MP197HB(71-9302)	No	24 Months <sup>8</sup>
Progress	Brunswick	BWR		2010	TN	NUHOMS	61BTH	8	488	87.2	Canister in Horizontal Concrete Overpack	MP197HB (71-9302)	No	MP197HB(71-9302)	No	24 Months <sup>8</sup>
Progress	Robinson	PWR	SS	1989	TN	NUHOMS	7P	8	56	24.4	Canister in Horizontal Concrete Overpack		No	No	7P	36 Months <sup>10</sup>
Progress	Robinson	PWR	GL	2007	TN	NUHOMS	24PTH	14	336	146.3	Canister in Horizontal Concrete Overpack		No	MP197HB	No	24 Months <sup>9</sup>
PS Colorado	Ft. St. Vrain <sup>11</sup>	HTGR	SS	1991	DOE	Foster Wheeler	MVDS		1464	1,023.3	Canister in Vault	TN-FSV (71-9253)	Yes <sup>2</sup>	No		12 Months <sup>v</sup>
PSE&G	Hope Creek	BWR	GL	2006	Holtec	HI-STORM	MPC-68	16	1088	194.3	Canister in Vertical Concrete Overpack	HI-STAR100 (71-9261)	Yes <sup>1</sup>	No		14 Months <sup>8</sup>
PSE&G	Salem	PWR	GL	2010	Holtec	HI-STORM	MPC-32	14	448	195.1	Canister in Vertical Concrete Overpack	HI-STAR100 (71-9261)	Yes <sup>1</sup>	No		14 Months <sup>8</sup>
PG&E	Diablo Canyon	PWR	SS	2009	Holtec	HI-STORM	MPC-32	23	736	320.5	Canister in Vertical Concrete Overpack	HI-STAR100 (71-9261)	Yes <sup>1</sup>	No		14 Months <sup>9</sup>
PG&E	Humboldt Bay <sup>12</sup>	BWR	SS	2008	Holtec	HI-STAR	MPC-80	5	390	69.7	Canister in Metal Cask	HI-STAR100 (71-9261)	Yes <sup>1</sup>	No		12 Months <sup>11</sup>
SMUD	Rancho Seco <sup>12</sup>	PWR	SS	2001	TN	NUHOMS	24PT	22	493	214.7	Canister in Horizontal Concrete Overpack	MP187 (71-9255)	Yes <sup>2</sup>	MP197HB	No	12 Months <sup>v</sup>
Southern Cal Edison	SONGS 1 <sup>13</sup>	PWR	GL	2003	TN	NUHOMS	24PT1	18	395	172.0	Canister in Horizontal Concrete Overpack	MP187 (71-9255)	Yes	MP197HB	No	24 Months <sup>v</sup>
Southern Cal Edison	SONGS 2	PWR	GL	2003	TN	NUHOMS	24PT4	29	696	303.1	Canister in Horizontal Concrete Overpack		No	MP197HB (71-9302)	No	24 Months <sup>9</sup>
Southern Nuclear	Farley	PWR	GL	2005	Holtec	HI-STORM	MPC-32	15	480	209.0	Canister in Vertical Concrete Overpack	HI-STAR100 (71-9261)	Yes <sup>1</sup>	No		24 Months <sup>8</sup>
Southern Nuclear	Hatch	BWR	GL	2000	Holtec	HI-STORM	MPC-68	47	3196	570.8	Canister in Vertical Concrete Overpack	HI-STAR100 (71-9261)	Yes <sup>1</sup>	No		24 Months <sup>8</sup>
Southern Nuclear	Hatch	BWR	GL	2000	Holtec	HI-STAR	MPC-68	3	204	36.4	Canister in Metal Cask	HI-STAR100 (71-9261)	Yes <sup>1</sup>	No		12 Months <sup>11</sup>
TVA	Browns Ferry	BWR	GL	2005	Holtec	HI-STORM	MPC-68	37	2516	449.4	Canister in Vertical Concrete Overpack	HI-STAR100 (71-9261)	Yes <sup>1</sup>	No		14 Months <sup>8</sup>
TVA	Sequoyah	PWR	GL	2004	Holtec	HI-STORM	MPC-32	32	1024	446.0	Canister in Vertical Concrete Overpack	HI-STAR100 (71-9261)	Yes <sup>1</sup>	No		14 Months <sup>8</sup>
Xcel Energy	Prairie Island	PWR	SS	1993	TN	TN Metal Casks	TN-40	29	1160	505.2	Bare Fuel	-	-	-	Yes (71-9313)	12 Months <sup>9</sup>
Xcel Energy	Monticello	BWR	GL	2008	TN	NUHOMS	61BT	10	610	108.9	Canister in Horizontal Concrete Overpack	MP197 (MP197HB)	No	No		24 Months <sup>9</sup>
YAEC	Yankee Rowe <sup>13</sup>	PWR	GL	2002	NAC	NAC-MPC	MPC-36	16	533	232.1	Canister in Vertical Concrete Overpack	NAC-STC (71-9235)	No			24 Months <sup>v</sup>
Totals:								1640	64804	19,966.0						

Table A-2 Storage Summary – U.S. Wet Storage at Shutdown Reactor Sites

**U.S. Wet Storage at Shutdown Reactor Sites**

Utility	Reactor / Storage Facility	Reactor Type	ISFSI License Type	Planned Load Date	Vendor	Cask System	Canister or Cask Type	Estimated Canisters or Casks to be Loaded	Assemblies in Wet Storage	Future Dry Storage Configuration	Primary Canister Transportation Cask	Primary Transport Cask Fabricated?	Alternative Canister Transportation Cask	Alternate Transport Cask Fabricated?
Dairyland Power	Lacrosse	BWR	SS	2012	NAC	MPC-LACBWR	MPC-LACBWR	2	129	Canister in Vertical Concrete Overpack	NAC-STC (71-9235)	No	NAC-MAGNATRAN	No
Zion Solutions	Zion	PWR	SS	2013	NAC	MAGNASTOR	TSC-37	61	2,226	Canister in Vertical Concrete Overpack	NAC-MAGNATRAN	No	-	-
General Electric	GE Morris	NA	SS	NA	NA	NA	NA		3,217	Storage System not Selected	NA	NA	NA	NA
							<b>Totals:</b>		<b>63 5572</b>					

**Storage Summary**

	Number of Casks	Number of Assemblies	% of Dry Stored Assemblies
Bare Fuel Casks	180	7826	12.1 %
Canisters in Concrete Overpacks	1447	54648	84.3 %
Canisters in Transport Casks	12	866.0	1.3 %
Vault Storage	NA	1464	2.3 %
			100 %



Red Border indicates "ISFSI Only Site"

Orange border indicates a Site with a Shutdown Reactor but One or More Operating Reactors Remaining

<sup>1</sup>12 units actively storing fuel are the only HISTAR 100 Casks available in U.S. 7 of these can accommodate standard size MPCs

<sup>2</sup>One MP187 staged empty at Rancho Seco Site; one TN-FSV staged empty at INL.(Only one canister per shipment possible)

<sup>3</sup>No TN-32 Transportation License under review

<sup>4</sup>Castor Casks not licensed for shipment in the U.S.

<sup>5</sup>No NAC-128 Transportation License under review

<sup>6</sup>No MC-10 Transportation License under review

<sup>7</sup>Lead time mostly cask license application and review

<sup>8</sup>Lead time due to primary cask not yet fabricated

<sup>9</sup>TN-40 Certificate issued June 2011, TN-40HT Submittal which includes High Burnup Fuel as Content to follow in 2011

<sup>10</sup>Lead time addresses "Storage Only" canister issue, and cast iron bare-fuel

casks. Repackaging might be required.

<sup>11</sup>Designates Shortest Lead Time for Shipment of Fuel in Dry Storage. Fuel is Already in Cask

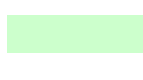
Licensed for Transportation. 6 Months Includes Cask Preparation Time, Leak Tests, Impact Limiter Mounting, etc.

<sup>12</sup>includes GTCC waste

<sup>13</sup>All the spent fuel from the shuttered Unit 1

<sup>14</sup>For multiple cask ISFSI sites the earliest load date applies to all casks

<sup>15</sup>Ft St Vrain Initial Heavy Metal does not include Thorium



Green shading indicates shortest lead time of 12 months -- fuel is already in casks licensed (Impact Limiter Fabrication Required) for transportation.



Red shading indicates indefinite lead time to first shipment -- canisters are "storage only" and casks are not licensed, or fuel is in cast iron bare-fuel casks that are not licensable.



Unshaded indicates intermediate lead time -- cask is licensed but not fabricated (or available), or cask license is in progress but not fabricated, or fuel is in (bare-fuel) cask but cask not licensed.

Filename: Dry Storage of Used Fuel\_Transition to Transport\_20120913FINAL.doc  
Directory: C:\Documents and Settings\l4184\Desktop  
Template: C:\Documents and Settings\l4184\Application Data\Microsoft\Templates\Normal.dotm  
Title: DOE/ID-Number  
Subject:  
Author: Bates  
Keywords:  
Comments:  
Creation Date: 9/13/2012 3:46:00 PM  
Change Number: 18  
Last Saved On: 9/25/2012 10:56:00 AM  
Last Saved By: SMITH, PATRICIA ANN  
Total Editing Time: 316 Minutes  
Last Printed On: 9/25/2012 10:57:00 AM  
As of Last Complete Printing  
Number of Pages: 46  
Number of Words: 12,385 (approx.)  
Number of Characters: 70,596 (approx.)

## **APPENDIX H**

### **Fuel-Assembly Shaker Test Plan Tests for Determining Loads on Used Nuclear Fuel under Normal Conditions of Transport**

# FUEL-ASSEMBLY SHAKER TEST PLAN

Tests for Determining Loads on Used Nuclear  
Fuel under Normal Conditions of Transport

**Fuel Cycle Research & Development**

*Prepared for  
US Department of Energy  
UFD Campaign  
Paul McConnell  
Sandia National Laboratories  
September 30, 2012  
FCRD-UFD-2012-000341*



**DISCLAIMER**

This information was prepared as an account of work sponsored by an agency of the U.S. Government. Neither the U.S. Government nor any agency thereof, nor any of their employees, makes any warranty, expressed or implied, or assumes any legal liability or responsibility for the accuracy, completeness, or usefulness, of any information, apparatus, product, or process disclosed, or represents that its use would not infringe privately owned rights. References herein to any specific commercial product, process, or service by trade name, trade mark, manufacturer, or otherwise, does not necessarily constitute or imply its endorsement, recommendation, or favoring by the U.S. Government or any agency thereof. The views and opinions of authors expressed herein do not necessarily state or reflect those of the U.S. Government or any agency thereof.



**Sandia National Laboratories**

Sandia National Laboratories is a multi-program laboratory managed and operated by Sandia Corporation, a wholly owned subsidiary of Lockheed Martin Corporation, for the U.S. Department of Energy's National Nuclear Security Administration under contract DE-AC04-94AL85000.

## FCT Quality Assurance Program Document

### Appendix E FCT Document Cover Sheet

Name/Title of Deliverable/Milestone  
Work Package Title and Number  
Work Package WBS Number  
Responsible Work Package Manager

Fuel-Assembly Shaker Test. Tests for Determining Loads on  
Used Nuclear Fuel under Normal Conditions of Transport  
ST Transportation – SNL / FT-12SN081305 (Rev. 1)  
**1.02.08.13**  
Paul McConnell  
(Name/Signature) 

Date Submitted

Quality Rigor Level for Deliverable/Milestone	<input checked="" type="checkbox"/> QRL-3	<input type="checkbox"/> QRL-2	<input type="checkbox"/> QRL-1	<input type="checkbox"/> N/A*
--	---	--------------------------------	--------------------------------	-------------------------------

This deliverable was prepared in accordance with

Sandia National Laboratories  
(Participant/National Laboratory Name)

QA program which meets the requirements of

DOE Order 414.1       NQA-1-2000

This Deliverable was subjected to:

Technical Review

Peer Review

**Technical Review (TR)**

**Peer Review (PR)**

**Review Documentation Provided**

**Review Documentation Provided**

Signed TR Report or,

Signed PR Report or,

Signed TR Concurrence Sheet or,

Signed PR Concurrence Sheet or,

Signature of TR Reviewer(s) below

Signature of PR Reviewer(s) below

**Name and Signature of Reviewers**

Gregg Flores



\*Note: In some cases there may be a milestone where an item is being fabricated, maintenance is being performed on a facility, or a document is being issued through a formal document control process where it specifically calls out a formal review of the document. In these cases, documentation (e.g., inspection report, maintenance request, work planning package documentation or the documented review of the issued document through the document control process) of the completion of the activity along with the Document Cover Sheet is sufficient to demonstrate achieving the milestone. QRL for such milestones may be also be marked N/A in the work package provided the work package clearly specifies the requirement to use the Document Cover Sheet and provide supporting documentation.

## SUMMARY

This report is the Sandia National Laboratories milestone (M3FT-12SN0813055) “Normal transport test report” for the Used Fuel Disposition Campaign Storage and Transportation (ST) Work Package.

This test plan defines a test designed to capture the response of a representative fuel assembly in its representative transportation configuration (i.e., *in-an-assembly-within-a-basket-within-a-cask-tied-to-a-transport-conveyance*) to actual loadings imposed during normal conditions of transport.

The representative assembly planned for the test is a 17x17 pressurized water reactor (PWR) assembly.

The assembly rods to be used for the tests will not be actual irradiated zirconium alloy/UO<sub>2</sub>-pellet rods. Surrogate rods shall be selected that have similar mass and stiffness as the actual irradiated rods. Due to the cost and availability, copper B280 alloy tubes filled with lead rods approximately meet the criteria for simulating Zircaloy-4/UO<sub>2</sub>-pellet rods. They shall be used for most of the positions within the assembly; Zircaloy-4/Pb rods shall be used for those assembly positions which will be instrumented for the test.

Finite-element modeling before the test shall provide information on which rod locations within the assembly should be instrumented and on which locations on those rods the instrumentation for measuring strains and accelerations should be placed. Finite-element modeling after the simulated normal transport tests will allow an estimate of the response all the rods may experience during normal transport based upon the test data from the surrogate rods. The test data will also allow the finite element model to be benchmarked.

The test results will allow for an analytic assessment of the ability of aged, high burnup cladding to withstand normal transport loads by assessing the strength of the aged, high burnup cladding relative to the stresses imposed on the cladding during normal transport.

## CONTENTS

SUMMARY .....	iv
CONTENTS.....	v
FIGURES .....	vii
TABLES .....	viii
ACRONYMS .....	ix
1 INTRODUCTION .....	1
2 BACKGROUND .....	3
2.1 Regulations.....	3
2.2 Shock and Vibration.....	4
3 NORMAL CONDITIONS OF TRANSPORT TEST PLAN .....	6
3.1 Introduction .....	6
3.1.1 Basis of test .....	6
3.1.2 General description of test .....	7
3.2 Purpose of Test Plan .....	7
3.3 Test Description .....	8
3.3.1 Acquisition of an unirradiated fuel assembly.....	8
3.3.2 Instrumentation .....	9
3.3.3 The 0.3-meter drop test .....	10
4 SCOPE.....	11
4.1 Test Parameters .....	11
4.1.1 Vibration facility .....	19
4.2 Instrumentation Installation Tables.....	23
4.3 Vibration Test Procedure .....	28
4.3.1 Test preparation.....	28
4.3.2 Test set-up .....	28
4.3.3 Post-test activities .....	28
5 TEST INPUT SPECIFICATIONS: RECOMMENDED VIBRATION AND SHOCK TRANSPORTATION TEST SPECIFICATIONS FOR THE REACTOR FUEL ASSEMBLY <sup>10</sup> .....	29
5.1 Introduction.....	29
5.2 Instrumentation .....	29
5.3 Random Vibration Test Specifications .....	31
5.4 Shock – Decayed Sine Specifications and Time Histories .....	33
5.5 Derivation of Test Specifications.....	44
5.5.1 Derivation of random vibration test specification.....	44

5.5.2	Derivation of shock test specification .....	45
6	PREVIOUS OVER-THE-ROAD TEST PROGRAMS.....	55
6.1	“Over-the-road testing of radioactive materials packagings” .....	55
6.1.1	Instrumentation .....	56
6.1.2	Test results .....	56
6.2	“Test specification for TRUPACT-I vibration assessment” .....	56
6.2.1	Instrumentation .....	57
7	KEY BACKGROUND INFORMATION.....	59
7.1	Souce of Vibration and Shock Data for Test.....	59
7.2	Related Documents .....	62
7.2.1	“Approach for the Use of Acceleration Values for Packages of Radioactive Material under Routine Conditions of Transport,” Andreas Apel, Viktor Ballheimer, Christian Kuschke, Sven Schubert, Frank Wille, Proceedings of the 9th International Conference on the Radioactive Materials Transport and Storage, May 2012, London.....	62
7.2.2	“Transportation Activities for BWR Fuels at NFI,” S. Uchikawa, H. Kishita, H. Ide, M. Owaki, K. Ohira, Nuclear Fuel Industries, LTD., Proceedings of Global 2009, Paris, September 2009.....	62
7.2.3	“High Burn-up Used Nuclear Fuel Vibration Integrity Study - Out-of-Cell Fatigue Testing Development,” , Jy-An John Wang, Hong Wang, Yong Yan, Rob Howard, Bruce Bevard, January 2011, Oak Ridge National Laboratory.....	62
7.2.4	Other documents related to this work include.....	65
8	REFERENCES .....	66

## **FIGURES**

Figure 1. Used nuclear fuel transportation modes, transportation vibration spectra (which result in loads applied to cladding), and material property data .....	2
Figure 2. Bounding acceleration shock response spectrum for a truck cask at 3% damping .....	5
Figure 3. Bounding truck vibration data for all three axes .....	5
Figure 4. Fuel assembly .....	8
Figure 5. Placement of assembly with rods, basket, and support beams on shaker .....	12
Figure 6. Differences between an actual test in a truck cask and the shaker test.....	12
Figure 7. Technical data used to select copper tubes as surrogate rods.....	13
Figure 8. Location of Zircaloy rods within the assembly which will be instrumented.....	14
Figure 9. Shock data from the 1978 truck cask transportation report.....	17
Figure 10. Data derived from the truck cask transportation report to be used as input to the shaker.....	18
Figure 11. Vibration facility. ....	19
Figure 12. Shaker to be used for test.....	20
Figure 13. Copper tube containing a lead rod to be used as a surrogate Zircaloy/UO <sub>2</sub> rod.....	21
Figure 14. Dimensions of basket to be used to contain the assembly on the shaker (Safety Analysis Report for the NAC-LWT, Revision 27, June 1999, Docket No. 9925 T-88004). ....	22
Figure 15. Fuel reactor assembly on shaker table.....	30
Figure 16. Cross-section of fuel reactor assembly.....	31
Figure 17. Recommended random vibration test specification.....	32
Figure 18. Recommended shock test specification.....	33
Figure 19. Recommended test specification & underlying ASDs. ....	45
Figure 20. Recommended test specification & underlying shock spectra. ....	46
Figure 21. Range of frequencies. ....	46
Figure 22. Decayed sine initial realization.....	47
Figure 23. Decayed sine second realization.....	47

---

Figure 24. Decayed sine third realization.....	48
Figure 25. Decayed sine fourth realization.....	48
Figure 26. Decayed sine fifth realization.....	49
Figure 27. Representative normal transport load data. ....	58

## TABLES

Table 1. Instrumentation Installation Data.....	23
Table 3: Response Accelerometers & Strain Gages. ....	30
Table 4: Vibration Breakpoints.....	32
Table 5: Reference Shock Breakpoints. ....	33
Table 6: Initial Realization of Decayed Sine Parameters.....	34
Table 7: Second Realization of Decayed Sine Parameters. ....	36
Table 8: Third Realization of Decayed Sine Parameters. ....	38
Table 9: Fourth Realization of Decayed Sine Parameters. ....	40
Table 10: Fifth Realization of Decayed Sine Parameters. ....	42
Table 11: Input to Cargo (g) – Vertical Axis. ....	44

## **ACRONYMS**

BWR	Boiling Water Reactor
CFR	Code of Federal Regulations
FAST	Facility for Accelerated Service Testing
IAEA	International Atomic Energy Agency
NEPA	National Environmental Policy Act
NRC	Nuclear Regulatory Commission
PNNL	Pacific Northwest National Laboratory
PWR	Pressurized Water Reactor
QA	Quality Assurance
SNL	Sandia National Laboratories
ST	Storage and Transportation
TRUPACT	Transuranic Package Transporter
TTC	Transportation Technology Center
US	United States



# FUEL-ASSEMBLY SHAKER TEST PLAN

## Tests for Determining Loads on Used Nuclear Fuel under Normal Conditions of Transport

### 1 INTRODUCTION

There is an international issue concerning storage and subsequent transportation of used nuclear fuel that requires quantitative knowledge of used nuclear fuel material properties and response to mechanical loadings during transport.

Many countries are in the position of having to store their used nuclear fuel longer than originally expected. For example, the closing of Yucca Mountain in the United States (US) and the German response to Fukushima will result in the need for extended storage times in these countries. Other countries are still in the planning stages for disposition of their used nuclear fuel, but they will also require extended storage times to accommodate deliberations on fuel disposition.

There are legitimate concerns for long-term storage associated with the degradation of material properties over time for the entire storage system: fuel, canister, overpack, and pad. An understanding of how degraded materials affect their safety functions over time is important to licensing these systems past their original design life. In addition, degradation of used nuclear fuel may adversely affect cladding integrity during transport after storage. Of the storage system components mentioned above, fuel clad integrity is the first line of defense for containment of the used nuclear fuel and so there is a high priority for better understanding of how its material properties may degrade over time, and if these degraded properties are sufficient to maintain fuel integrity during transportation.

This test program is designed to better understand fuel response to *normal* conditions of transport loadings and to estimate the ability of used nuclear fuel with degraded properties to withstand these loadings. This will be done with a combination of experimental data collection and numerical analyses. The experimental work will focus on using full-scale test articles that are subjected to realistic normal conditions of transport loadings. The test unit will be appropriately instrumented to capture the data needed to conduct numerical analyses. The numerical analyses will be used to augment the experimental data set to a more comprehensive set of conditions that will enable a better understanding of used nuclear fuel behavior under normal conditions of transport. The numerical analyses shall also provide the means to extend the test results from a specific package and assembly to other package/assembly configurations.

The data from the tests described herein shall also be compared to data to be generated in other Department of Energy Used Nuclear Fuel Disposition Campaign activities that will measure mechanical properties of both high burnup and aged used nuclear fuel. By comparing the loads applied to fuel cladding during normal transportation to the strength of used nuclear fuel, an assessment can be made of the ability of the cladding to withstand post-storage transportation environments (Figure 1).

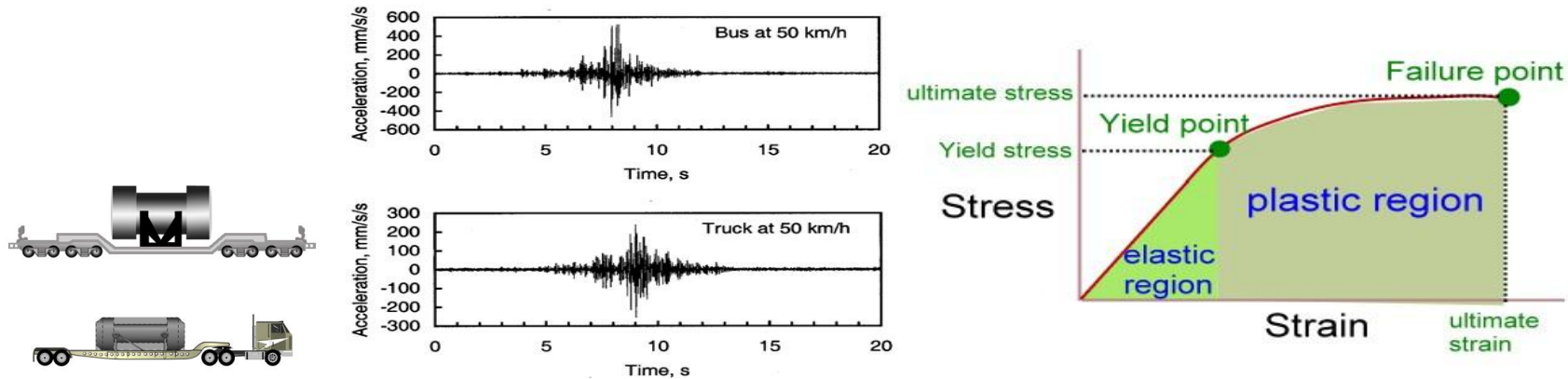


Figure 1. Used nuclear fuel transportation modes, transportation vibration spectra (which result in loads applied to cladding), and material property data.

## 2 BACKGROUND

### 2.1 Regulations

US regulations are harmonized with the International Atomic Energy Agency (IAEA) regulations. In the US, the design of casks and performance of the fuel within the casks is governed by 10 CFR Part 71 in the US Code of Federal Regulations. The regulations cover two loading conditions that are important to assure the integrity of used nuclear fuel and are, therefore, important to this test proposal.

- Incident-free transportation: Nuclear fuel must have sufficient strength to sustain its integrity during normal operations. For truck transport, this basically means that the fuel must be strong enough to withstand loadings imposed from driving on roads with various road conditions. For rail, the fuel must be strong enough to withstand loading from over the rail transport as well as longitudinal coupling loads that are imposed. Loading forces and vibrations are the primary loads that need to be obtained for both truck and rail.
- 0.3 meter drop tests: The 0.3 meter drop represents an in-plant accident that may occur while transferring the payload from its storage to its transport configuration. This drop test must be performed (or analyzed) with the package in an orientation that would cause maximum damage.<sup>1</sup> Numerical methods are more easily applied to the analysis of the effects on transport packages and their contents due to a 0.3-meter drop than they are for analysis of the vibrational loading inherent to normal transport conditions.<sup>2</sup>

The loads, to which the used nuclear fuel cladding is subjected during normal conditions of transport, either by truck or by rail, are the result of the induced vibrations and intermittent shock loads. There are virtually no known data for the loads to which used nuclear fuel – the individual pins, the assemblies, the baskets – is subjected during normal transport conditions.

Without mechanical property data for high burnup fuel cladding and knowledge of the loads to which that cladding would experience in a transport environment, predictions of the integrity of the used nuclear fuel during normal transport are speculative and possibly inexact. Mechanical property data for high burnup used nuclear fuel cladding alone is not sufficient for accurate predictions of the behavior of the cladding during normal transport – the applied loads to the cladding during normal transport are also required. Hence this test

---

<sup>1</sup> The regulations are silent regarding the presence of impact limiters on the cask for the 0.3-meter drop. The definition of a transport package in 10 CFR 71.4 “means the packaging together with its radioactive contents *as presented for transport*” and “Packaging means the assembly of components necessary to ensure compliance with the packaging requirements of this part [and]...*may consist of...devices for...absorbing mechanical shocks.*” Furthermore, 10 CFR 71.71(a) Normal Conditions of Transport states that this section is an “[e]valuation of [the] package design.”

<sup>2</sup> A detailed discussion of the US Nuclear Regulatory Commission (NRC) intent regarding the analysis necessary for the drop test may be gleaned from NUREG-1536, Revision 1A, “Standard Review Plan for Used Nuclear Fuel Dry Storage Systems at a General License Facility.” But, note that this document addresses used nuclear fuel casks used for dry storage, not transport.

proposal for obtaining load data applied to used nuclear fuel cladding residing within a transport package during normal transport.<sup>3</sup>

## 2.2 Shock and Vibration

Normal transport loads can be divided into two categories:

- Shock and vibration loading caused by normal over-the-road operations. (A fuel assembly is subjected to cyclic loading conditions as a result of random shock and vibration loading during normal transport conditions.<sup>4</sup>)
- The 0.3-m normal regulatory drop event, which is intended to be an initial condition before entering the accident environments.

A large quantity of experimental data has been derived from various sources to quantify the shock and vibration environment of cargo during truck and rail transport. The data usually were collected from instrumentation located at the interface between the packaging or cargo and the transporter, and generally consist of acceleration-response spectra as a function of frequency. The total acceleration response measured for a cargo includes response to superimposed shock and vibration. The vibration component is usually identified as a continuous excitation comprising all responses lower than or equal to 99% of the peaks in the acceleration response records. The remaining higher intensity, infrequently occurring acceleration peaks, correspond to sporadic shock events.

The bounding acceleration shock response spectrum for used nuclear fuel in truck casks for this test program is based on the union of triaxial data (longitudinal, transverse, and vertical axis accelerations) for 20- and 25-tonne cargoes reported in [2-4]. These data are shown in Figure 2. The suggested bilinear curve (in the log-log plane) that bounds these data from above consists of a linearly increasing portion up to a frequency of approximately 3.5 Hz, followed by a constant segment at 4.4-g acceleration, up to a maximum frequency of 300 Hz. For even greater simplicity, the dashed line indicated on the figure could be used at low frequencies, but this may be overly conservative because low-frequency response may be of dominant importance for the fuel assembly system. The data from [2] have been analyzed in a more detailed manner for this test as described in Section 5.

---

<sup>3</sup> Sandia National Laboratories conducted many tests in the late 1980s – early 1990s to establish the loading on transport packages during normal transport (summarized in a later section). This test campaign measured loading on the external surface of the transport package, not on the contents, which experience a somewhat different loading profile. The methodology for measuring the loads in the previous Sandia National Laboratories program has some analogies to the current test proposal, so pertinent aspects of the previous work can be applied to the current test proposal.

<sup>4</sup> The sensitivity of fuel rod failure due to fatigue was investigated in [1]. Analyses indicate that the magnitudes of the cyclic loads are such that the stresses induced in the cladding are below the endurance limit of the Zircaloy cladding. Even an infinite number of cyclic loads apparently would not propagate existing cracks into fuel rod failures. But, the fatigue strength of high burnup cladding – currently unknown – may require reanalysis of the fatigue issue.

The bounding rail shock spectrum is based on the union of measured triaxial data for a 45-tonne cargo reported by Magnuson [4-5]. The measured data include responses to typical shock generating events, e.g., crossing of bridges and switches, and coupling event shocks.

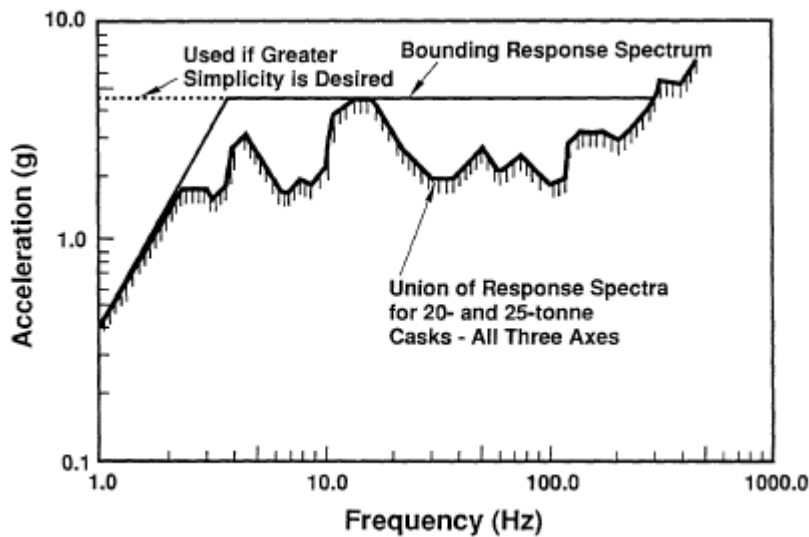


**Figure 2. Bounding acceleration shock response spectrum for a truck cask at 3% damping [1].**

The bounding truck vibration data for all three response directions are shown in Figure 3.

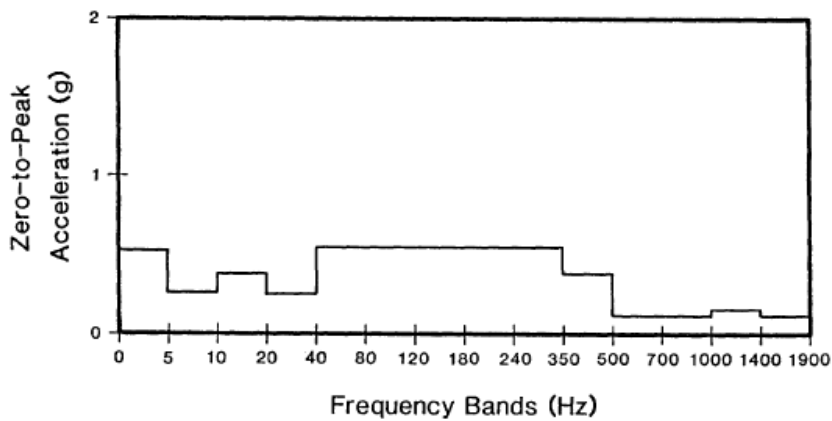


**Figure 3. Bounding truck vibration data for all three axes [1].**

The analyses in [1] showed that an unirradiated assembly will remain elastic under normal transportation shock and vibration loading conditions. The maximum tensile stress is 155 MPa and occurs at the bottom of the rod adjacent to the end plate. The corresponding maximum spacer grid pinch force is 80.1 N.

### 3 NORMAL CONDITIONS OF TRANSPORT TEST PLAN

#### 3.1 Introduction

The test is designed to capture the response of used nuclear fuel in its representative configuration to actual loadings imposed during normal conditions of transport. The normal conditions of transport are those defined within the US NRC regulations in 10 Code of Federal Regulations Part 71 [6].

Fuel rods are required to meet conditions defined in 10 CFR Part 71, Subpart F, ¶71.71 during normal transport. In particular, the rods must withstand vibrations and shocks associated with normal transport (while in a transport cask which is tied down to the transport conveyance). NRC guidance is also found in §2.5.6.5 *Vibration* in the “Standard Review Plan for Transportation Packages for Radioactive Material” (US Nuclear Regulatory Commission NUREG-1609 which cites NUREG/CR-2146 and NUREG/CR-0128). [2, 7-8]

To date, licensees have made the technical argument that unirradiated fuel rods and rods irradiated to relatively low burnup levels can withstand the loads imposed upon them by normal transport.

However, fuel is being irradiated to higher burnup levels – which further degrades the cladding – and shall be stored (aged) for longer periods of time. Both of these conditions – high burnup levels and aging during storage – may lead to a situation where the cladding is degraded to such an extent that it may not withstand normal transport loads. There are no data to justify the technical basis for asserting that aged, high burnup fuel can withstand normal transport conditions. The NRC has expressed concerns about approving transport of aged, high burnup fuel without such information.

The data needed to fill this technical gap falls in two categories: 1) the loads imposed directly on rods during normal transport; and 2) the material properties of aged, high burnup cladding. (See Figure 1.)

The goals of this test program are to expand understanding of used nuclear fuel loading environments and subsequent response to these environments. Given a quantitative understanding of fuel rod response, material properties of high burnup, degraded fuel can be coupled with realistic loadings to analytically estimate degraded fuel response to these transport conditions.

The objectives of this test program are to

- Simulate over-the-road tests on a full-scale fuel assembly by applying loadings that used nuclear fuel cladding would experience during normal conditions of transport.
- Instrument the cladding to capture mechanical load, strain, vibration, and shock inputs imposed by the mechanical loadings resulting from the normal condition of transport loading.

##### 3.1.1 Basis of test

The ideal test would be to place an *irradiated* fuel assembly in an actual cask and do over-the-road/rail tests to measure the vibrational loads on the rods. But, doing such a test with an irradiated assembly would be extremely difficult and expensive.

So, an alternative solution is to use an *unirradiated* assembly with surrogate rods (no UO<sub>2</sub> pellets) in an actual cask. However, the only casks available are truck casks and all of those are contaminated on the inside - the

casks have all been in pools - a major detriment for performing the tests due to Environmental, Safety, & Health considerations. In addition, the lease price for such a truck cask is significant.

The practical alternative is to place a representative, surrogate fuel assembly on a shaker and subject the assembly to vibrations and shocks simulating normal transport via a truck (or rail) cask. That is the basis of this test plan.

### 3.1.2 General description of test

This test proposal is designed to capture the response of cladding in its representative configuration (i.e., in-an-assembly-within-a-basket-within-a-cask-tied-to-a-transport-conveyance) to actual loadings imposed during normal conditions of transport. Finite-element modeling after the normal transport tests, coupled with degraded material property data from other UFD experimental work, will allow an estimate of the response irradiated rods would have experienced during the road tests based upon the test data from the surrogate rods.

The assembly planned for the test will represent a 17x17 PWR assembly.

The rods to be used for the tests will not be actual irradiated zirconium-alloy/UO<sub>2</sub>-pellet rods. Surrogate rods shall be selected that have similar mass and stiffness as the actual irradiated rods. Copper B280 alloy tubes filled with lead rods approximately meet the criteria for simulating Zircaloy-4/UO<sub>2</sub>-pellet rods. They shall be used for most of the positions with the assembly; Zircaloy-4/Pb rods shall be used for those assembly positions which will be instrumented for the test.

Finite-element modeling before the test shall provide information on which rod locations within the assembly should be instrumented and on which locations on those rods the instrumentation for measuring strains and accelerations should be placed. Finite-element modeling after the normal transport tests are conducted will allow an estimate of the response all the rods would have experienced during the road tests based upon the test data from the surrogate rods. The test data will also allow the finite element model to be benchmarked.

The test results will allow for an analytic assessment of the ability of aged, high burnup cladding to withstand normal transport loads by comparing the strength of the aged, high burnup cladding to the stresses imposed on the cladding during normal transport.

This test proposal provides data for the mechanical loads to which fuel rods are subjected during normal transport conditions. The integrity of the cladding is a function of its 1) material properties – yield and tensile strength, elastic modulus, fatigue strength, fracture toughness – all of which may degrade with high burnup and long aging times - and 2) the mechanical loads to which the cladding may be subjected. This test proposal addresses only the latter – the mechanical loads applied to the cladding during normal transport conditions.

## 3.2 Purpose of Test Plan

This document defines the testing of a 17x17 pressurized water reactor (PWR) assembly (Figure 4) containing surrogate fuel rods placed upon a shaker to simulate vibrational and shock loading associated with a normal

transport of an assembly within a truck (or rail) cask on a trailer. This test series will be performed by implementing plans and procedures identified in this document.

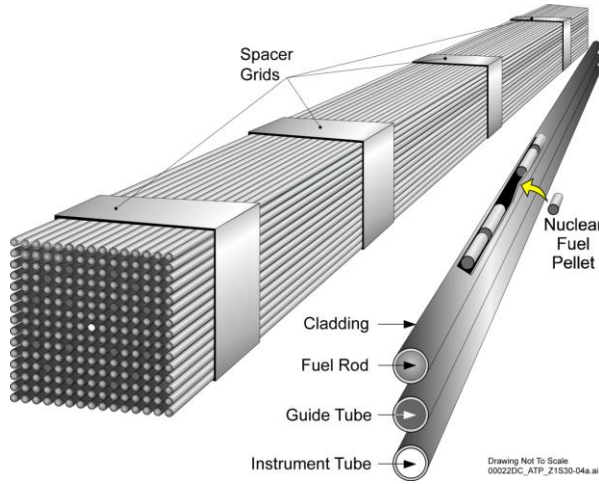


**Figure 4. Fuel assembly.**

### 3.3 Test Description

#### 3.3.1 Acquisition of an unirradiated fuel assembly

The most important requirement for the tests is to have available an actual fuel assembly. The assembly could be either PWR or boiling water reactor (BWR).

Both PWR and BWR fuel components have recently been procured by Sandia National Laboratories for an unrelated test program. It is proposed that a PWR assembly be used for the tests described in this plan. PWR fuel is more common than BWR fuel.

Ideally, irradiated, high burnup, aged fuel rods would be used for the tests. Actual fuel, let alone irradiated cladding and fuel, is not an option for the tests, so a surrogate material for the fuel pellets is required.<sup>5</sup> The vibration tests will be conducted with new hollow clad pins (Zircaloy-4 and copper tubing). For the over-the-road test simulation, these pins will be filled with a lead surrogate to represent the mass of the fuel.

The ideal surrogate rod for testing would have the same mass and flexibility as an irradiated rod. Unirradiated fuel has a gap between the fuel pellets and the cladding; irradiated fuel swells closing that gap. Thus, unirradiated fuel rods are not an exact surrogate for irradiated rods. A solid rod of some metal may be appropriate, but a survey indicated that the cost is prohibitive in the lengths necessary to match that of the PWR rods (e.g., thirteen-foot molybdenum rods). It is necessary to attempt to match the properties of surrogate rods with those of irradiated rods, although differences in the rod response can be accounted for by numerical analysis post-test. Using estimated properties of irradiated rods allowed selection of a surrogate rod of appropriate stiffness and mass.

<sup>5</sup> The cost is significant – approximately \$100k for a 17X17-PWR assembly with Zircaloy rods (sans fuel).

### 3.3.2 Instrumentation

#### 3.3.2.1 Placement of the instruments on the test unit

Strain gages must be placed on the assembly and cladding to obtain the maximum peak loads to which those components are subjected during normal transport.<sup>6</sup> Triaxial accelerometers will be placed at strategic locations on the assembly and rods. A total of thirty-two to forty-eight channels of data (strain gages plus accelerometers) are reasonable based on experience from previous test programs (the number of gages is to be determined based upon finite element analyses).

Modeling of an assembly will be employed to identify the optimum locations for the instrumentation. But, it is intuitive that placing strain gages on the cladding at the mid-point between spacer grid supports and adjacent to the grids would provide a representative profile of the loading on the rods. The strain gages should be placed on rods at both the top and the bottom of the assembly. Gauges will be placed in such locations along one-half of the length of the assembly.

#### 3.3.2.2 Data reduction and analysis

The protocol for processing the data shall be established using the example of previous test programs at Sandia National Laboratories. The results shall be collated in such a manner as to facilitate future modeling that could estimate loading on other assembly configurations not directly subjected to the transport tests.

The results shall be assessed relative to known or estimated properties of cladding to judge the effect of the normal transport conditions on the integrity of the cladding. Cladding properties of interest, likely available for unirradiated or low burnup conditions, are the yield strength and elastic modulus. The fracture toughness and fatigue strength of cladding, although relevant, are not available.

A LS-DYNA structural model of a detailed 17x17 assembly will be refined and modified at Pacific Northwest National Laboratory (PNNL) to include specific details for the test assembly and basket that will be utilized to impose the loading time history during the actual shaker testing.

Scoping pre-test evaluations will be performed to identify appropriate data collection sites within and about the test assembly. This information will help finalize the test design and provide baseline analyses for future benchmarking and validation of modeling techniques involving LS-DYNA.

A script will be written that converts LS-DYNA fuel assembly specific geometric data and shall port it to Sandia's PRESTO Structural Dynamics code. This tool will help provide baseline analyses for future benchmarking and validation of modeling techniques involving PRESTO as well as cross-comparison between LS-DYNA and PRESTO.

---

<sup>6</sup> Piezo-electric strain gauges are recommended. Piezo-electric sensors are able to achieve a better resolution than piezo-resistors, while piezo-resistors can be built in much smaller areas. Both types of the strain sensors are capable of high sensitivity measurements, however, and could be used for the tests.

### 3.3.2.3 Rail Tests

The simulated rail cask tests may be performed at Sandia National Laboratories using vibration and shock inputs from [5].<sup>7</sup>

### 3.3.3 The 0.3-meter drop test

It is proposed that the 0.3-meter drop test be conducted in a subsequent phase of the test program. The same assembly could be used for the drop tests after the vibrational tests, but not vice versa due to possible damage to the assembly resulting from the drop. It is also proposed that only one cask type, truck or rail, be used for the 0.3-meter drop test.

The 0.3-meter drop represents an accident that may occur while transferring the loaded cask *in its transport configuration* from one position to another, such as, the transfer of the cask from a trailer to a pad. This drop test must be performed (or analyzed) with the package in an orientation that would cause maximum damage.<sup>8,9</sup>

The US regulations are silent regarding the presence of impact limiters on the cask for the 0.3-meter drop. The definition of a transport package in 10 CFR 71.4 is “...the *packaging* together with its radioactive contents as presented for transport” and “*Packaging* means the assembly of components necessary to ensure compliance with the packaging requirements of this part [and]...may consist of...devices for...absorbing mechanical shocks.” Furthermore, 10 CFR 71.71(a) Normal Conditions of Transport states that this section is an “[e]valuation of [the] package design.” Thus, this test proposal interprets the regulations to allow for the use of “absorbing mechanical shocks” on the cask for the 0.3-meter drop test.

Regardless of whether impact limiters are used for the 0.3-meter drop test, the larger issue is procuring a cask for the test. Owners of existing casks would be reluctant to allow the cask to be dropped, with or without impact limiters. An option is to construct a surrogate cask – a cylinder – into which the fuel assembly can be placed for the drop test.

---

<sup>7</sup> Access to the rail car and transport system (although not a rail cask) may be possible through the US Federal Railroad Administration which has test tracks and has expressed a willingness to participate in such tests. Per the FRA website:

“There are 48 miles of railroad track available for testing locomotives, vehicles, track components, and signaling devices at the Transportation Technology Center’s (TTC) Facility for Accelerated Service Testing (FAST), Pueblo, Colorado. Specialized tracks are used to evaluate vehicle stability, safety, endurance, reliability, and ride comfort. The TTC’s tracks eliminate the interferences, delays, and safety issues encountered on an operating rail system (<http://www.aar.com/tracks.php>).”

<sup>8</sup> Numerical methods are more easily applied to the analysis of the effects on transport packages and their contents due to a 0.3-meter drop than they are for analysis of the vibrational loading inherent to normal transport conditions and they may be an option to an actual drop test.

<sup>9</sup> A detailed discussion of the US NRC intent regarding the analysis necessary for the drop test may be gleaned from NUREG-1536, Revision 1A, “Standard Review Plan for Used nuclear fuel Dry Storage Systems at a General License Facility.” But, note that this document addresses used nuclear fuel casks used for dry storage, not transport.

## 4 SCOPE

This test procedure

- Defines instrumentation requirements
- Defines pre-test and post-test inspection and construction tasks
- Describes steps required to perform the shaker tests
- Identifies applicable supporting and controlling documents
- Defines information, documentation, and data required to document the tests

This procedure, in conjunction with the Sandia National Laboratories (SNL) Job Safety Analysis, Work Control – Level of Rigor, National Environmental Policy Act (NEPA) Review Information, Accept Work, and the Quality Assurance (QA) Program Plan documents, are the planning package for the test program.

Any changes to this procedure will be documented in accordance with the instructions in the SNL Quality Assurance Program Plan.

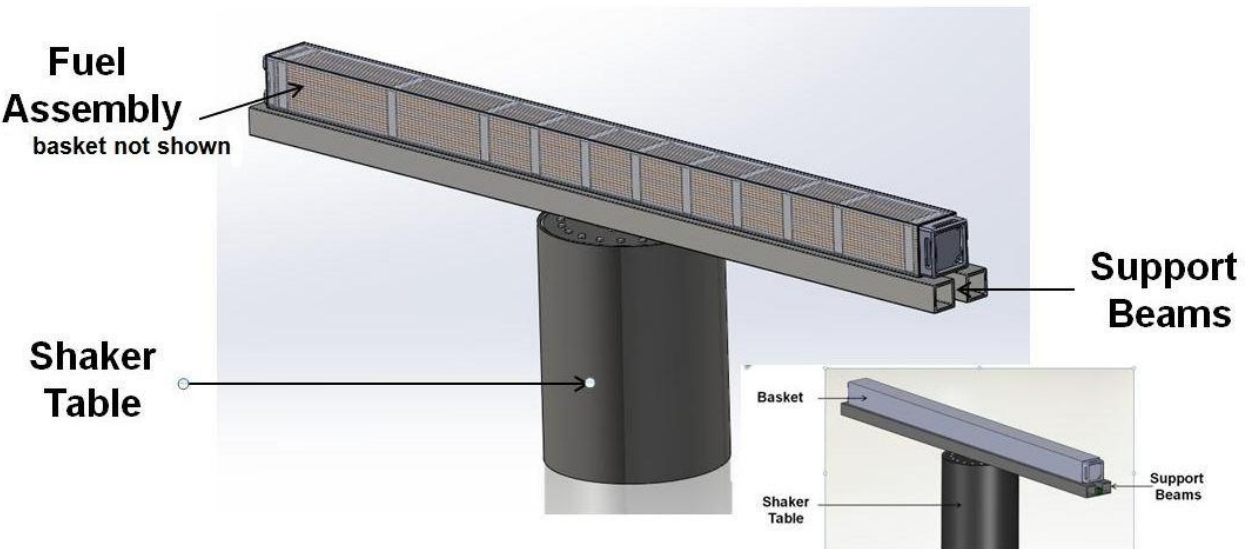
All supplementary information and test data (calibrations, inspections, change reports, etc.) for this test will be logged and attached to the test results report.

### 4.1 Test Parameters

The instrumented fuel assembly within its surrogate basket shall be securely affixed upon the shaker. Using the inputs from the analyses of the vibration and shock data from Section 5 the shaker shall impart loads to the assembly and the shaker data acquisition system shall record the responses from the accelerometers on the strain gages attached to the selected fuel rods.

The vibration facility in Excitation Equipment Building 6610 Area III at Sandia National Laboratories supports a wide spectrum of activities for the US Department of Energy Nuclear Weapons Complex. These capabilities provide the versatile and controllable simulation of vibration, acceleration, and shock environments, as well as tailored excitations for the development and validation of analytical models. The facility is used extensively for system level tests of full-scale assemblies or items requiring high vibration levels.

The following Figures 5 – 8 describe the test in more detail.



**Note:** Shaker table not long enough to support entire assembly. Beams used to simulate rigidity of an assembly-within-a-basket-within-a-cask-affixed-to-a-trailer under normal transport conditions.

Figure 5. Placement of assembly with rods, basket, and support beams on shaker.

Experimental Problem	Solution
Actual truck casks too costly (NAC-LWT)	Perform test without a cask
Available truck casks are contaminated	Simulate truck transport with shaker table*
Using UO <sub>2</sub> pellets not feasible	Use Pb rods as surrogate
Availability of Zircaloy tubes limited	Use Cu tubes as surrogate
Surrogates possess material properties dissimilar to Zircaloy	Adjust wall thickness of Cu tubes so that $EI_{Cu} = EI_{Zirc}$ Adjust amount of Pb in tubes to that total assembly weight is that of actual assembly
Assembly is in a basket in a truck cask	Construct basket to NAC-LWT specifications. Place assembly on "stiffeners" to ensure unrealistic bending does not occur about assembly midpoint

\*U.S. Nuclear Regulatory Commission, "Shock and Vibration Environments for a Large Shipping Container During Truck Transport (Part II)," NUREG/CR-0128 (SAND Report 78-0337), August 1978.  
(Referenced in Section 2.5.6.5 Vibration in NUREG-1609, "Standard Review Plan for Transportation Packages for Radioactive Material")

Figure 6. Differences between an actual test in a truck cask and the shaker test.

Zirc and Surrogate Material Properties (Based on equivalent thickness and variable EI)									
Zirc		Aluminum		Brass		Carbon Steel		Copper	
$E_{\text{Zirc}}$ (GPa)	99	$E_{\text{Al}}$ (GPa)	70	$E_{\text{Brass}}$ (GPa)	110	$E_{\text{SS}}$ (GPa)	205	$E_{\text{Cu}}$ (GPa)	115
$E_{\text{Zirc}}$ (ksi)	14359	$E_{\text{Al}}$ (ksi)	10153	$E_{\text{Brass}}$ (ksi)	15954	$E_{\text{SS}}$ (ksi)	29733	$E_{\text{Cu}}$ (ksi)	16679
$\rho_{\text{Zirc}}$ (g/cm <sup>3</sup> )	6.55	$\rho_{\text{Al}}$ (g/cm <sup>3</sup> )	2.7	$\rho_{\text{Brass}}$ (g/cm <sup>3</sup> )	8.5	$\rho_{\text{SS}}$ (g/cm <sup>3</sup> )	7.85	$\rho_{\text{Cu}}$ (g/cm <sup>3</sup> )	8.94
$\rho_{\text{Zirc}}$ (g/in <sup>3</sup> )	107	$\rho_{\text{Al}}$ (g/in <sup>3</sup> )	44	$\rho_{\text{Brass}}$ (g/in <sup>3</sup> )	139	$\rho_{\text{SS}}$ (g/in <sup>3</sup> )	129	$\rho_{\text{Cu}}$ (g/in <sup>3</sup> )	147
$h$ (in)	151.79	$h$ (in)	144	$h$ (in)	151.79	$h$ (in)	151.79	$h$ (in)	151.79
$\text{Vol}_{\text{Zirc}}$ (in <sup>3</sup> )	3.77	$\text{Vol}_{\text{Al}}$ (in <sup>3</sup> )	5.38	$\text{Vol}_{\text{Brass}}$ (in <sup>3</sup> )	5.67	$\text{Vol}_{\text{SS}}$ (in <sup>3</sup> )	5.67	$\text{Vol}_{\text{Cu}}$ (in <sup>3</sup> )	5.67
Mass (g)	404.80	Mass (g)	238.19	Mass (g)	790.42	Mass (g)	729.98	Mass (g)	831.34
$t$ (in)	0.0225	$t$ (in)	0.03500	$t$ (in)	0.03500	$t$ (in)	0.03500	$t$ (in)	0.03500
$D_{\text{Zirc}}$ (in)	0.374	$D_{\text{Al}}$ (in)	0.375	$D_{\text{Brass}}$ (in)	0.375	$D_{\text{SS}}$ (in)	0.375	$D_{\text{Cu}}$ (in)	0.375
$d_{\text{Zirc}}$ (in)	0.329	$d_{\text{Al}}$ (in)	0.305	$d_{\text{Brass}}$ (in)	0.305	$d_{\text{SS}}$ (in)	0.305	$d_{\text{Cu}}$ (in)	0.305
$EI$ (k <sup>4</sup> in <sup>2</sup> )	5.532	$EI$ (k <sup>4</sup> in <sup>2</sup> )	5.543	$EI$ (k <sup>4</sup> in <sup>2</sup> )	8.710	$EI$ (k <sup>4</sup> in <sup>2</sup> )	16.232	$EI$ (k <sup>4</sup> in <sup>2</sup> )	9.106
Zirc Rod (lbs)	0.891	Al Rod (lbs)	0.525	Brass Rod (lbs)	1.739	CS Rod (lbs)	1.606	Cu Rod (lbs)	1.829

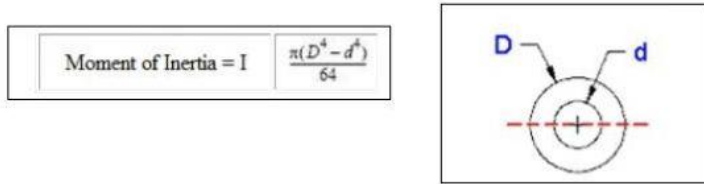


Figure 7. Technical data used to select copper tubes as surrogate rods.

The most important parameter for the test assembly is that its mass be close to the mass of a real assembly. Stiffness of the rods is a secondary but important parameter. This is a non-sequiterA SOLIDWORKSTM simulation predicts a bending response difference of less than 5% between the Cu-Pb rod and Zircaloy-Pb rods.

The combined Modulus / Moment of Inertia properties were checked in order to get an idea on the combined stiffness of each rod:

- $EI_{\text{Cu}} = 9.106 \text{ K-in}^2$
- $EI_{\text{Zirc}} = 5.53 \text{ K-in}^2$

The conclusion is that Cu tubing is slightly stiffer than Zircaloy.

Although the material surrogates do not mimic the true material properties exactly, they are the best as far as availability, constructability, and cost. UO<sub>2</sub> and lead share very similar densities but UO<sub>2</sub> is considerably stiffer than Pb. Zircaloy is 30% less dense than copper but Zircaloy shares a similar stiffness with Cu. An actual assembly weighs approximately 1404 lbs. The experimental assembly weighs approximately 1446 lbs. The difference in weight between the actual and experimental assemblies is 42 lbs (3% difference). Although the stiffness of the actual and experimental rods are not the same (mostly due to properties of the UO<sub>2</sub> v. Pb), the weights are nearly exact and weight is considered the most important parameter to simulate. Thus, dynamic response of the surrogate test assembly is expected to represent that of a real fuel assembly.

Figure 8 shows the locations of the Zircaloy rods within the assembly (locations are tentative pending finite element analyses).

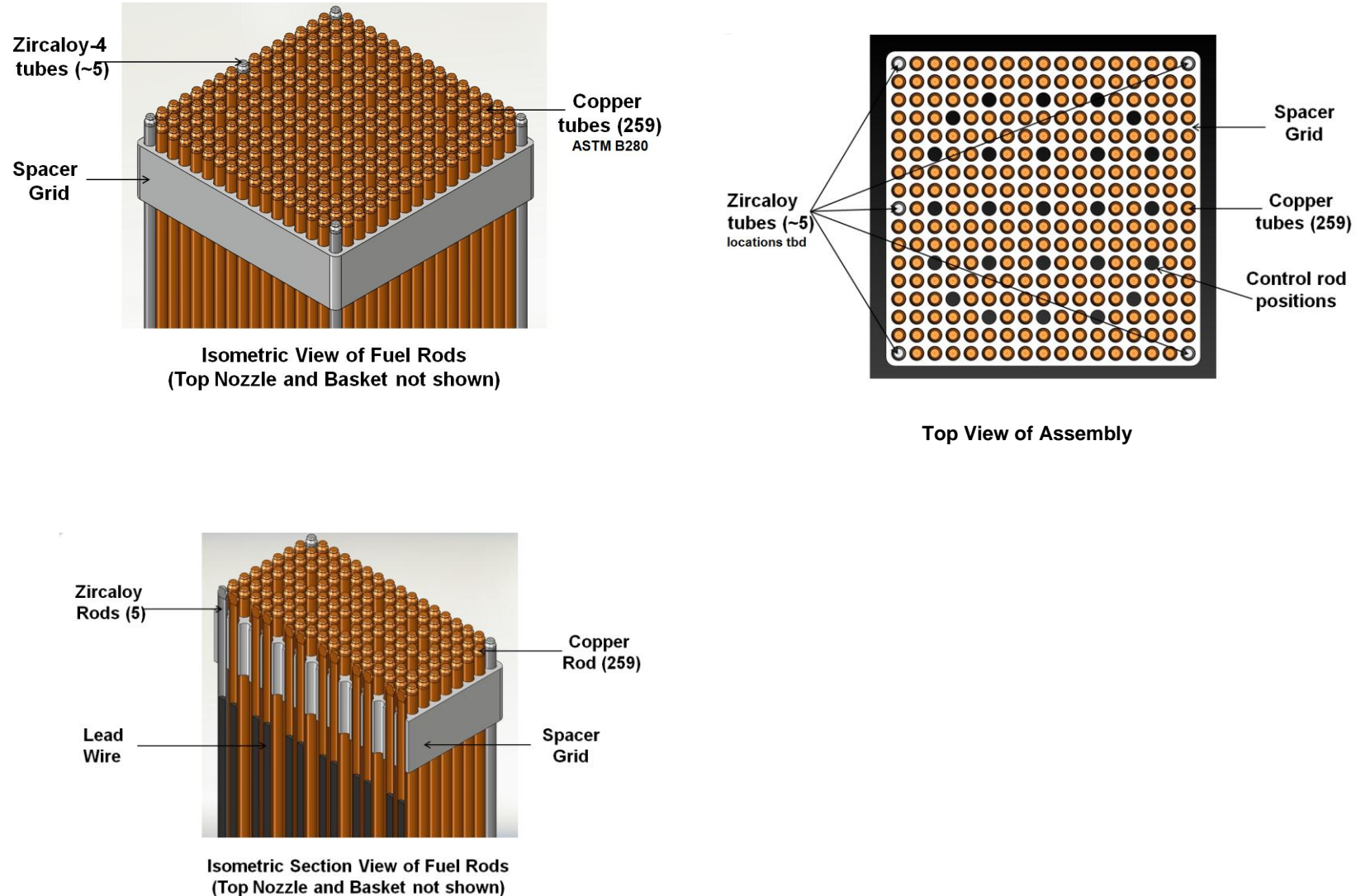


Figure 8. Location of Zircaloy rods within the assembly which will be instrumented.



Input for the shaker table was taken from US Nuclear Regulatory Commission, “Shock and Vibration Environments for a Large Shipping Container During Truck Transport (Part II),” NUREG/CR-0128, August 1978 [2] (referenced in *Section 2.5.6.5 Vibration* in NUREG-1609, “Standard Review Plan for Transportation Packages for Radioactive Material”). Key details from this report are

- Vibration and shock data were measured by accelerometers over a 700 mile journey
- 56,000 lb load for test 1 and 44000 lb for test 2
- Speeds ranged from 0 to 55 mph

Figure 9 shows data from this report.

Using the most conservative data from the 1978 report, the shaker table will simulate the vibration and shock experienced by the cask during transport.

Accelerometers will be placed along the length of the Zircaloy rods in order to measure shock and vertical vibration. Strain gauges will be placed along the length of the rods in order to measure strain. The stress state of the fuel rods will be calculated based on the strain gauge readings.

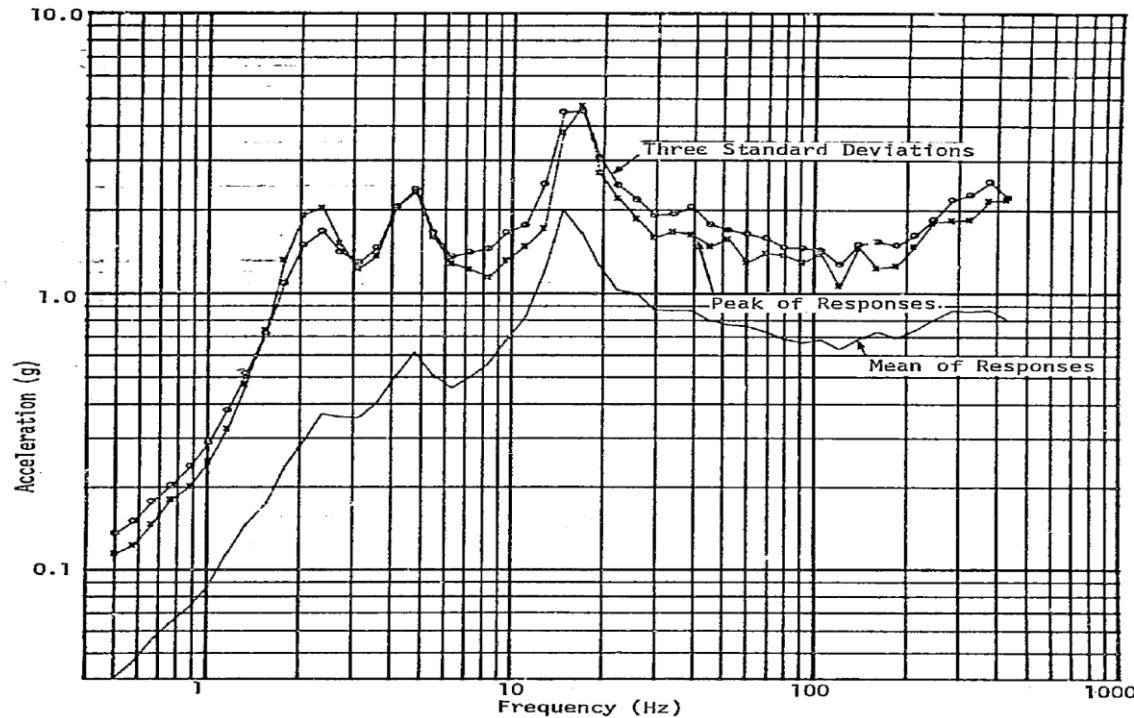


Figure 5. Superimposed Shock Response Spectra,  
3% Damping, Vertical Axis

20

Figure 9. Shock data from the 1978 truck cask transportation report [2].

The following Figure 10 shows data derived from the vibration and shock measured on the truck cask and are the inputs to the shaker as described in Section 5.

Figure 3.0-1.: Recommended Random Vibration Test Specification

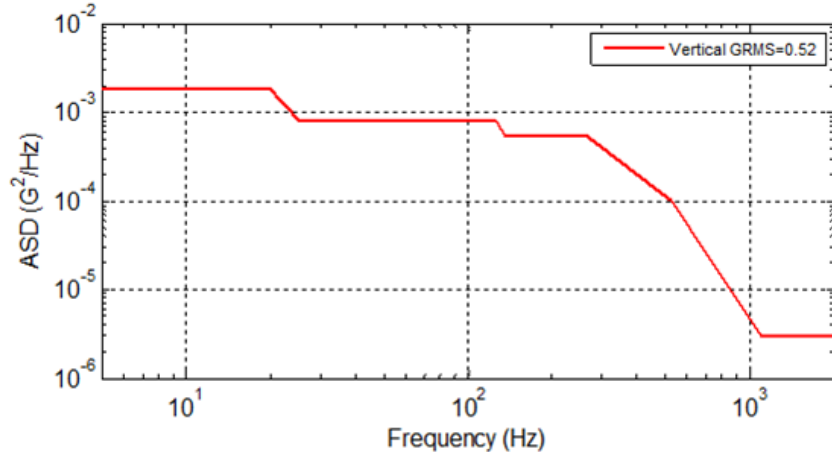


Figure 4.0-1.: Recommended Shock Test Specification

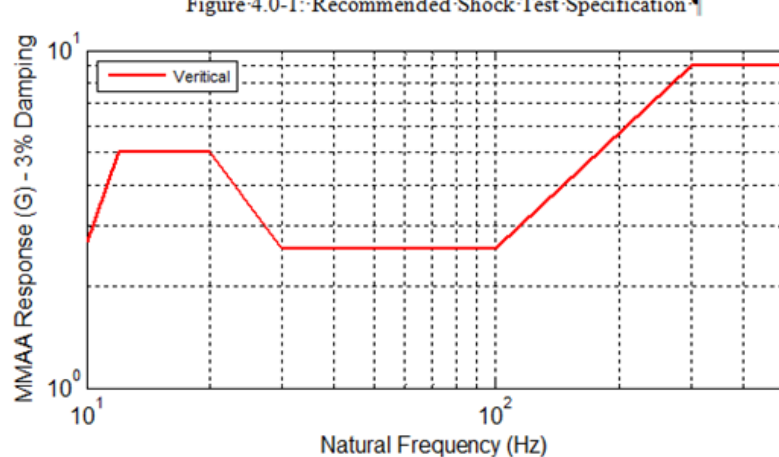


Table 3.0-1.: Vibration Breakpoints

Frequency (Hz)	ASD ( $G^2/Hz$ )
5	1.8e-3
20	1.8e-3
25	8.0e-4
125	8.0e-4
135	5.5e-4
265	5.5e-4
530	1.0e-4
1100	3.0e-6
2000	3.0e-6

Table 4.0-1.: Reference Shock Breakpoints

Frequency (Hz)	MMAA 3% (G)
10	2.7
12	5.0
20	5.0
30	2.6
100	2.6
300	9.0
600	9.0

Figure 10. Data derived from the truck cask transportation report to be used as input to the shaker.

The following Figures 11 and 12 show the vibration facility and the capabilities of the facility.

#### 4.1.1 Vibration facility



**Figure 11. Vibration facility.**

##### 4.1.1.1 Vibration facility capabilities

A vertical UD T4000 electrodynamic shaker shall be used for the testing. The system includes

- Control and data acquisition state-of-the-art digital vibration controller
  - 38 input channels available for control, limiting, or real-time monitoring
  - average, maximum, or minimum spectrum control options
- Computer controlled signal conditioning system
  - over 200 channels
  - conditions various types of sensors (e.g., strain gage, force, displacement)
- Data acquisition and analysis system
  - 208 channels
  - 102.4 kilo-samples/s, 24bit resolution
  - data streaming to disk array for long duration recording

Shakers at Sandia used for system level tests of full-scale assemblies or items requiring high vibration levels.

Shown is the Unholtz-Dickie Corporation T4000 electrodynamic shaker for vertical testing

[<http://www.udco.com/largetseries.shtml>](http://www.udco.com/largetseries.shtml)



**Vertical Shaker**

Figure 12. Shaker to be used for test.

The following photograph shows a lead rod inserted in to a copper tube which shall be used as a surrogate Zircaloy/UO<sub>2</sub> rod.



Initial Dimensions for Simulated Copper Fuel Rod Mock-up

OD (in.)	0.3750
ID (in.)	0.3120
Thickness (in.)	0.0315
Sample Length (in.)	24.0000
Clearance Between Cu & Pb	0.0300

**Figure 13. Copper tube containing a lead rod to be used as a surrogate Zircaloy/UO<sub>2</sub> rod.**

The following figure shows the dimensions of the simulated basket that will support the assembly on the shaker table (as a basket supports an assembly in a truck cask).

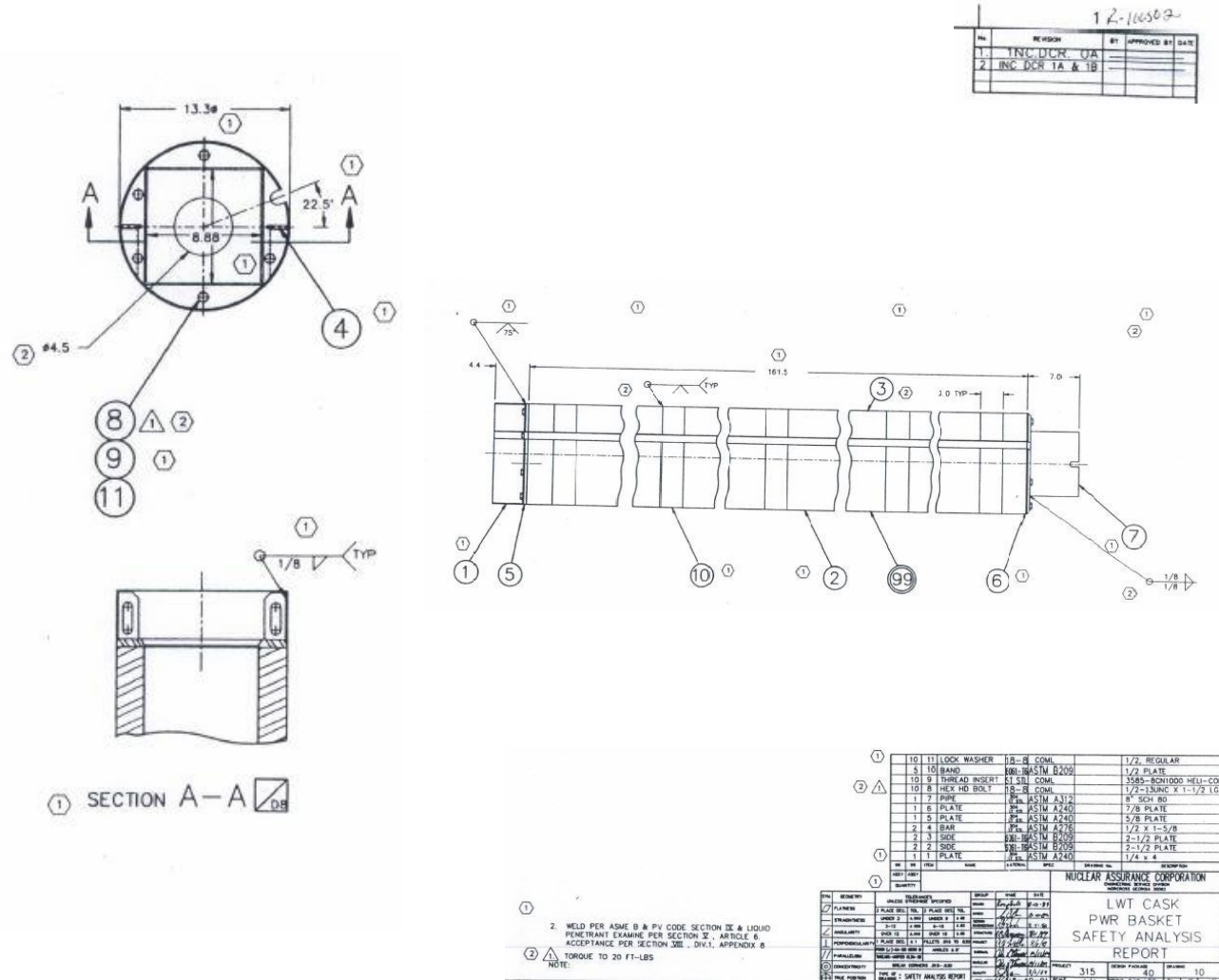


**Figure 14. Dimensions of basket to be used to contain the assembly on the shaker (Safety Analysis Report for the NAC-LWT, Revision 27, June 1999, Docket No. 9925 T-88004).**

## 4.2 Instrumentation Installation Tables

Each rod to be instrumented shall have the gauges recorded per the following tables. The strain gages and accelerometers are identified in the figures following the table.

**Table 1. Instrumentation Installation Data.  
Accelerometers and Strain Gages**

Gage ID	Range	Serial Number	Input Resistance (ohms)	Output Resistance (ohms)	Insulation Resistance (ohms)	Field Wire No.	Interface Panel No.	Check OK	Rod Location
A1-1X	20K								
SG1-1X	20K								
A1-2X	20K								
SG1-2X	20K								
A1-3X	20K								
SG1-3X	20K								
A1-4X	20K								
SG1-4X	20K								

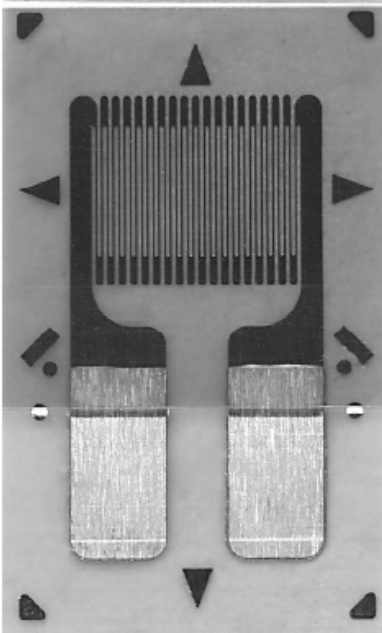
ROD #1 (SAME TABLE FOR EACH ROD TO BE INSTRUMENTED)

Accelerometer model #: Model 25 Isotron

Strain gage model #: Vishay Micro-Measurements CEA-03-062UW-350

Installed by \_\_\_\_\_

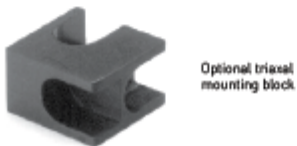
Witnessed by \_\_\_\_\_

<b>GAGE PATTERN DATA</b>		<b>GAGE DESIGNATION</b>	<b>RESISTANCE (OHMS)</b>	<b>OPTIONS AVAILABLE</b>
	 actual size	See Note 1		See Note 2
		CEA-XX-062UW-120 CEA-XX-062UW-350	120 ± 0.3% 350 ± 0.3%	P2 P2
<b>DESCRIPTION</b>				
<p>General-purpose gage. Exposed solder tab area is 0.07 x 0.04 in [1.8 x 1.0 mm].</p>				
<b>GAGE DIMENSIONS</b>		Legend:	ES = Each Section S = Section (S1 = Sec 1)	CP = Complete Pattern M = Matrix
Gage Length	Overall Length	Grid Width	Overall Width	Matrix Length
0.062	0.220	0.120	0.120	0.31
1.57	5.59	3.05	3.05	7.9
<b>GAGE SERIES DATA</b>		See Gage Series data sheet for complete specifications.		
Series	Description		Strain Range	Temperature Range
CEA	Universal general-purpose strain gages.		±3%	-100° to +350°F [-75° to +175°C]

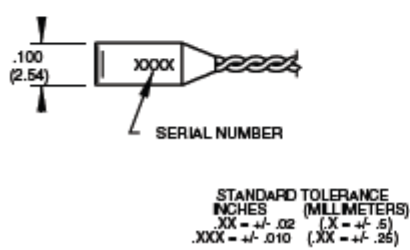
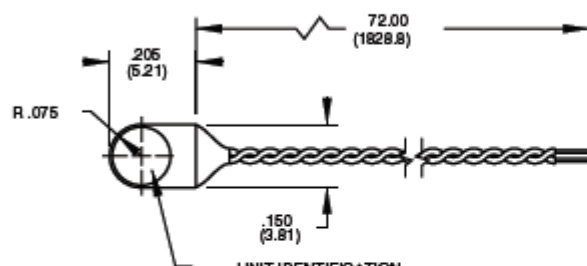
## Model 25A Isotron® accelerometer

### Features

- World's smallest Isotron®
- Light weight (0.2 gm)
- Flexible cable
- Low impedance output
- Excellent for printed circuit board and disk drive testing



Optional triaxial  
mounting block

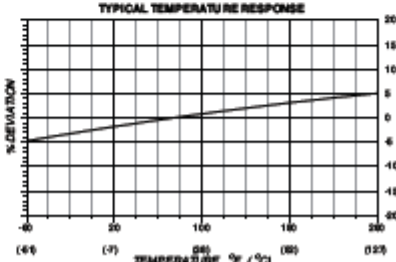
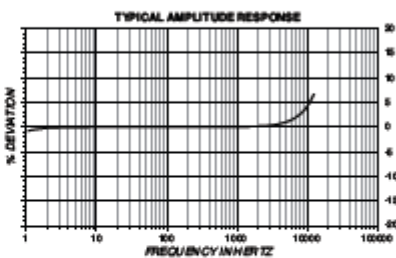


### Description

The Endevco® model 25A Isomin™ is an extremely small, adhesive mounted piezoelectric accelerometer with integral electronics, designed specifically for measuring vibration on very small objects. The unit weighs only 0.2 gm, reducing unwanted mass loading effects. The unit comes with two pre-installed fine gage (34 AWG) wires as output leads. These leads can be easily repaired in the field, or a new lead assembly may be reinstalled at the factory. A heavier gage (28 AWG) cable is also provided for extension purpose. The model 25A is ideal for measuring vibration in scaled models, small electronic components, and biomedical research. An optional triaxial mounting block (model 2950M16) is available for setting up three-axis measurement. If a detachable coaxial cable, which can be replaced by the user in the field, is desired, model 25B is available.

The model 25A features Endevco's Piezite® Type sensing element operating in shear mode. The internal electronics inside the accelerometer converts high impedance input into low impedance voltage output through the same cable that supplies the required 4 mA constant current power. Signal ground is isolated from the mounting surface of the unit by a hard anodized surface. A removal tool is included for proper removal in the field.

Endevco signal conditioner models 133, 4416B, 2793, 2776B, 4999, 6634C or Oaxis 2000 (4998A-X with cards 428 and/or 433) computer controlled system are recommended for use with this accelerometer.



## Model 25A Isotron® accelerometer



### Specifications

The following performance specifications conform to ISA-RP-37.2 (1964) and are typical values, referenced at +75°F (+24°C), 4 mA and 100 Hz, unless otherwise noted. Calibration data, traceable to National Institute of Standards and Technology (NIST), is supplied.

#### Dynamic characteristics

	Units	
Range	g	±740
Voltage sensitivity		
Typical	mV/g	5
Minimum	mV/g	4
Frequency response		See typical amplitude response
Resonance frequency		
Typical	kHz	50
Minimum	kHz	45
Amplitude response		
±5%	Hz	2 to 8000
±1 dB	Hz	1 to 12 000
Temperature response		See typical curve
Transverse sensitivity	%	≤ 5
Amplitude linearity	%	< 2 to full scale

#### Output characteristics

Output polarity		Acceleration directed into base of unit produces positive output
DC output bias voltage	Vdc	+8.5 to +11.5
-67°F to +257°F (-55°C to +125°C)	%	±5 typical
Output impedance	Ω	≤ 600
Full scale output voltage	V	±3.7
Residual noise	equiv. g rms	≤ 0.007
Grounding		Signal ground isolated from mounting surface
Load		See load diagram

#### Power requirement

Supply current [1]	mA	+3.5 to +4.5
Voltage	Vdc	+18 to +24
Warm-up time	sec	< 3

#### Environmental characteristics

Temperature range		-67°F to +257°F (-55°C to +125°C)
Humidity		Epoxy sealed, non-hermetic
Sinusoidal vibration limit (survival)	g pk	1000
Shock limit (survival) [2]	g pk	2000
Base strain sensitivity	equiv. g pk/strain	0.002
Electromagnetic sensitivity	equiv. g rms/gauss	0.09
Acoustic sensitivity at 140 dB SPL	equiv. g	0.008

#### Physical characteristics

Dimensions		See outline drawing
Weight without cable	oz (gm)	0.01 [0.2]
Case material		Aluminum alloy, hard anodized
Mounting [3]		Adhesive

#### Calibration

Supplied:		
Sensitivity	mV/g	
Transverse sensitivity	%	
Frequency response	%	20 Hz to 12 kHz

#### Included accessories

3024-120 [10 ft]	cable assembly, twisted pair [4]
31275	removal tool
32279	mounting wax

#### Optional accessories

2950M16	triaxial mounting block
133	Signal conditioner
2775B	Signal conditioner
2793	Isotron signal conditioner
4416B	Signal conditioner
4999	Signal conditioner
6634C	Signal conditioner
4990A-X	Oasis 2000 computer-controlled system with cards 428 and/or 433

#### Notes:

1. Excessive current supply may cause permanent damage to accelerometer.
2. Short duration shock pulses, such as those generated by metal-to-metal impacts, may excite transducer resonance and cause linearity errors. See Tech Paper 290 for more details.
3. Depending on the dynamic and environmental requirements, adhesives such as petro-wax, hot-melt glue, and cyanoacrylate epoxy (super glue) may be used to mount the accelerometer temporarily to the test structure. When removing an epoxy mounted accelerometer, first soften the epoxy with an appropriate solvent, then twist the unit off with the supplied removal tool. Failure to heed this caution may cause permanent damage to the transducer, which is not covered under warranty.
4. Small gage wires are soldered to the terminals at the factory. They are to be spliced together with the supplied cable assembly in the field for extension purpose.
5. Maintain high levels of precision and accuracy using Meggitt's factory calibration services. Call Meggitt's inside sales force at 800-982-6732 for recommended intervals, pricing and turnaround time for these services as well as for quotations on our standard products.

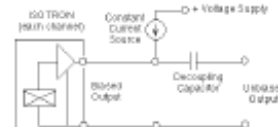


**Table 1. Instrumentation Installation Data. (Continued)**  
**Ambient Air Thermocouples**

TC ID	TC Type	Serial No.	Loop Resistance (ohms)	Sheath Resistance (ohms)	Location
TC-1 ID TC-1					

Installed by \_\_\_\_\_

Witnessed by \_\_\_\_\_

Multimeter:

Manufacturer/Model \_\_\_\_\_

Serial Number \_\_\_\_\_

Calibration Expiration Date \_\_\_\_\_

## 4.3 Vibration Test Procedure

### 4.3.1 Test preparation

Construct basket by welding four plates of steel per dimensions indicated in Figure 14. Provide cutouts of instrumentation wires.

Insert lead rods into the surrogate copper tubes and the Zircaloy tubes.

Insert all rods into the assembly.

Construct support beams from two square tubes by welding cross-bars along the length of the tubes.

Attach strain gages and accelerometers onto the rods selected for instrumentation.

Complete instrumentation installation forms.

### 4.3.2 Test set-up

Place support tubes onto shaker. Bolt to shaker.

Place basket/assembly onto support tubes. Bolt to support tubes.

Attach instrumentation from rods, assembly, and shaker surface to the vibration facility recording equipment. Calibrate instrumentation.

Apply vibration input to the shaker.

Apply shock input to the shaker.

Photograph shaker and test unit.

### 4.3.3 Post-test activities

Disassemble test unit.

Collect test data for post-test analyses.

## 5 TEST INPUT SPECIFICATIONS: RECOMMENDED VIBRATION AND SHOCK TRANSPORTATION TEST SPECIFICATIONS FOR THE REACTOR FUEL ASSEMBLY<sup>10</sup>

### 5.1 Introduction

The Environments Engineering Group at SNL was asked to derive a set of random vibration and shock test specifications for a laboratory test of a reactor fuel assembly. These specifications were derived from the vibration and shocks presented in references [2,8]. The purpose of the laboratory test is to measure loads during normal highway transportation. This memo presents test specifications for the vertical axis only since it is believed that is the direction which will affect the loading.

At this time the instrumentation has not been optimized and is subject to change. Section 5.2 presents the instrumentation.

Section 5.3 presents the random vibration specification. Section 4 presents the decayed sine specifications.

### 5.2 Instrumentation

The placement of instrumentation is designed to obtain the peak strain and has not been optimized. Therefore it is subject to change after further discussion with the model group. The accelerometers are used to get insight into what the structure is doing.

Table 2 presents the input accelerometers and their locations. Table 3 presents the response accelerometer and strain gage locations. The first few node shapes will determine where on the tube sections the strain gages are placed. Figure 15 shows the fuel reactor assembly on the shaker table and the input and response locations. Figure 16 shows a cross section of the fuel reactor assembly and the location of Tubes 1 thru 5.

---

<sup>10</sup> Letter report from Melissa C de Baca to Paul McConnell, April 30, 2012.

**Table 2: Response Accelerometers & Strain Gages.**

Location	Tube 1	Tube 2	Tube 3	Tube 4	Tube 5
End Spacer	A		A	A	
End Tube Section	A, S				
Mid Span Spacer	A		A	A	
Mid Span Tube Section	A, S				

Note: A – denotes accelerometer; S – denotes strain gage

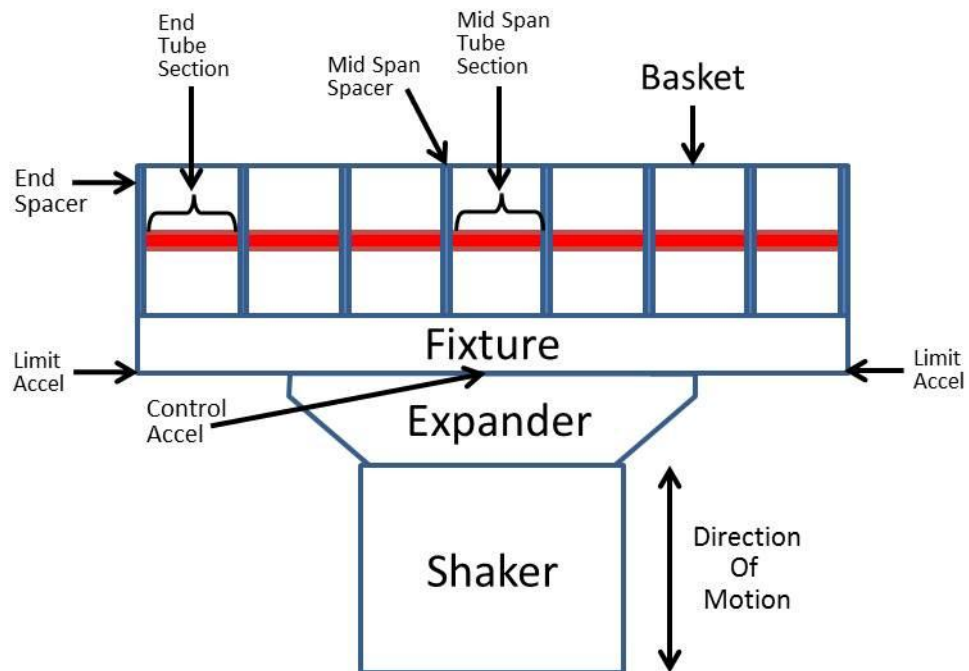


**Figure 15. Fuel reactor assembly on shaker table.**

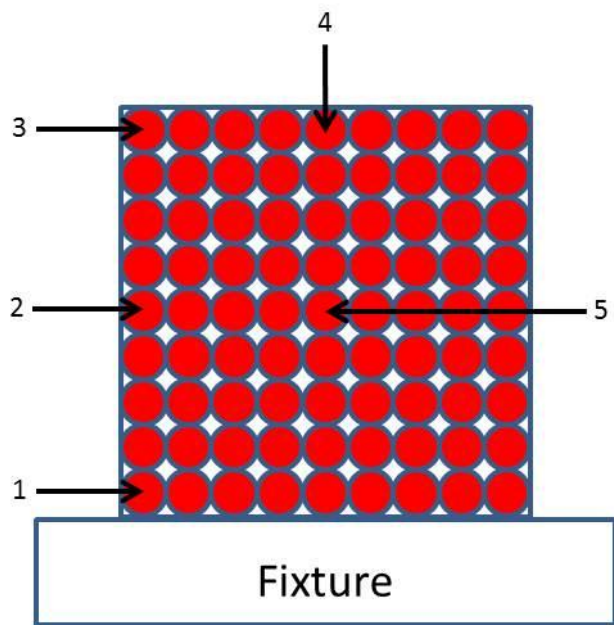
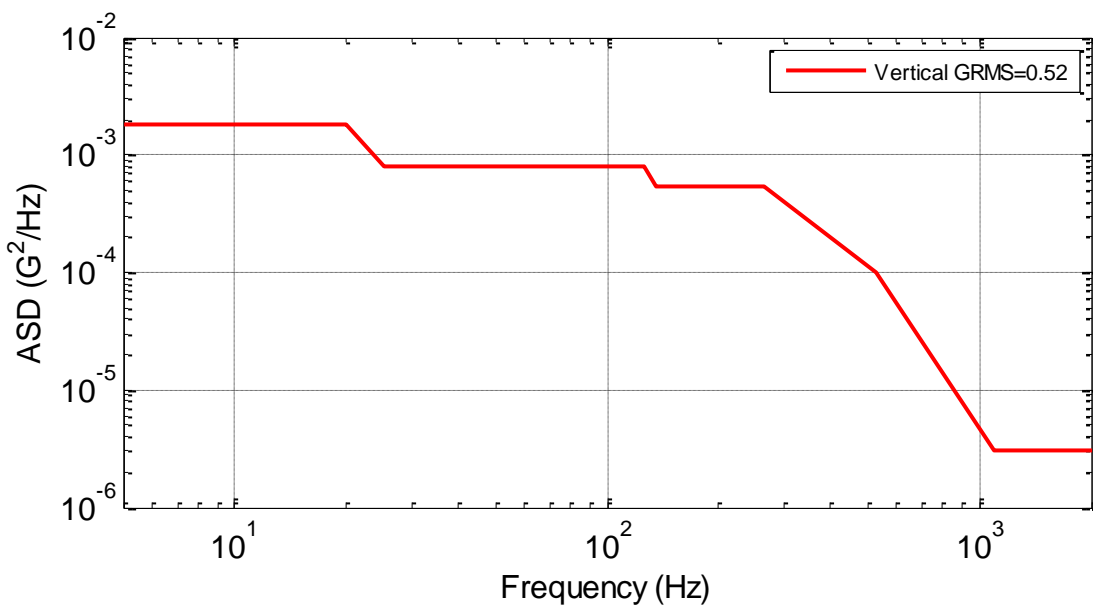


Figure 16. Cross-section of fuel reactor assembly.

### 5.3 Random Vibration Test Specifications

Figure 17 shows the recommended random vibration test specification to be applied at the midpoint of the fixture. Table 4 presents the corresponding breakpoints. The test should be run for a duration of one minute or long enough to obtain good data. Section 5.5 shows the derivation of this test specification.

We do not know what shape the limit channels should have; therefore they will be a scaled version of the control channel applied at the left and right ends of the fixture. The scaling will be determined at the time of the test.



**Figure 17. Recommended random vibration test specification.**

**Table 3: Vibration Breakpoints.**

Frequency (HZ)	ASD (G <sup>2</sup> /Hz)
5	1.8e-3
20	1.8e-3
25	8.0e-4
125	8.0e-4
135	5.5e-4
265	5.5e-4
530	1.0e-4
1100	3.0e-6
2000	3.0e-6

## 5.4 Shock – Decayed Sine Specifications and Time Histories

Figure 18 shows the recommended shock test specification. Table 5 lists the corresponding breakpoints. Appendix A shows the derivation of the test specification.

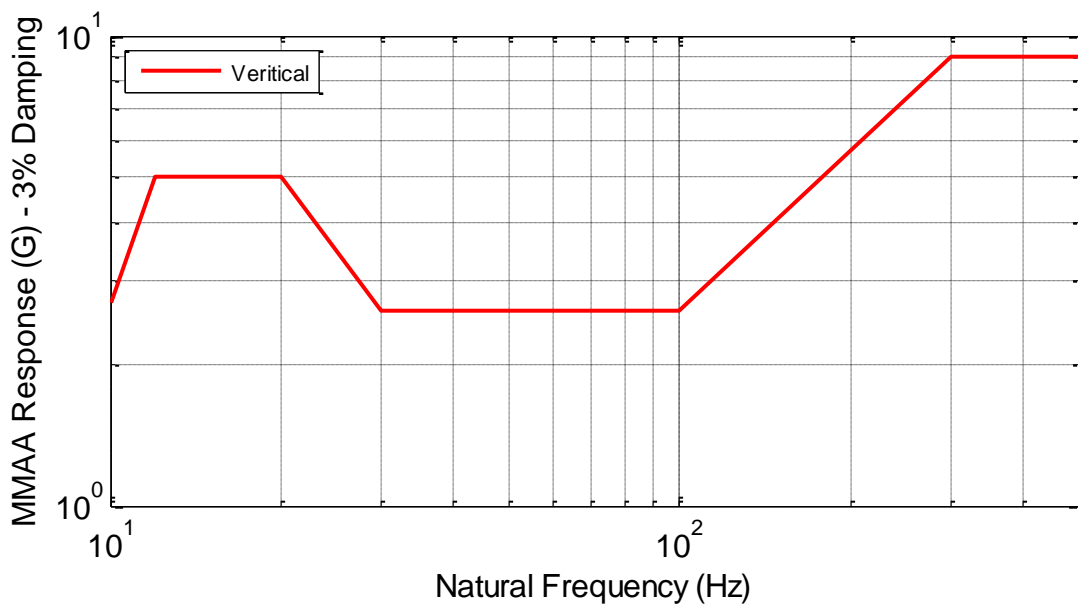


**Figure 18. Recommended shock test specification.**

**Table 4: Reference Shock Breakpoints.**

Frequency (HZ)	MMAA 3% (G)
10	2.7
12	5.0
20	5.0
30	2.6
100	2.6
300	9.0
600	9.0

Tables 6 thru 10 list the parameters for the five decayed sine realizations. Shown in these tables are the SRS parameters, the acceleration parameters, and the decayed sine parameters.

**Table 5: Initial Realization of Decayed Sine Parameters.**

SRS Parameters				
fmin	fmax	pts/oct	Damp	SRS Type
10.00	600.00	8.00	0.03	MMAA
Acceleration History Parameters				
Sample Rate	Frame Size	Gravity Constant	Ptype	
5120	8192	386.00	1	
Value	Acceleration (G)	Velocity (in/sec)	Displacement (in)	
Min	-2.28	-4.51	-0.0530	
Max	2.41	4.65	0.0592	
Res	-0.18	-0.06	0.0063	
Decayed Sine Parameters				
Frequency (Hz)	Accel (G)	Decay Rate	Delay	Frequency (Hz)
10.4	-0.359	0.0286	0.0000	82.6
11.4	0.487	0.0262	0.0000	90.1
12.4	-0.440	0.0241	0.0000	98.2
13.5	0.353	0.0221	0.0000	107.0
14.7	-0.300	0.0202	0.0000	116.7
16.1	0.265	0.0186	0.0000	127.2

17.5	-0.252	0.0170	0.0000	138.6	-0.149	0.0022	0.0000
19.1	0.237	0.0156	0.0000	151.1	0.144	0.0020	0.0000
20.8	-0.218	0.0143	0.0000	164.7	-0.165	0.0018	0.0000
22.7	0.201	0.0132	0.0000	179.5	0.183	0.0017	0.0000
24.7	-0.186	0.0121	0.0000	195.7	-0.193	0.0015	0.0000
26.9	0.120	0.0111	0.0000	213.3	0.219	0.0014	0.0000
29.4	-0.063	0.0102	0.0000	232.5	-0.221	0.0013	0.0000
32.0	0.082	0.0093	0.0000	253.4	0.271	0.0012	0.0000
34.9	-0.122	0.0086	0.0000	276.2	-0.270	0.0011	0.0000
38.0	0.087	0.0078	0.0000	301.1	0.324	0.0010	0.0000
41.5	-0.092	0.0072	0.0000	328.2	-0.294	0.0009	0.0000
45.2	0.114	0.0066	0.0000	357.7	0.283	0.0008	0.0000
49.3	-0.105	0.0061	0.0000	389.9	-0.295	0.0008	0.0000
53.7	0.101	0.0056	0.0000	425.0	0.225	0.0007	0.0000
58.5	-0.067	0.0051	0.0000	463.3	-0.350	0.0006	0.0000
63.8	0.083	0.0047	0.0000	505.0	0.243	0.0006	0.0000
69.5	-0.100	0.0043	0.0000	550.4	-0.259	0.0005	0.0000
75.8	0.093	0.0039	0.0000	600.0	0.393	0.0005	0.0000
				3.5	0.087	0.9500	-0.0457

**Table 6: Second Realization of Decayed Sine Parameters.**

SRS Parameters				
fmin	fmax	pts/oct	Damp	SRS Type
10.00	600.00	8.00	0.03	MMAA
Acceleration History Parameters				
Sample Rate	Frame Size	Gravity Constant	Ptype	
5120	8192	386.00	1	
Value	Acceleration (G)	Velocity (in/sec)	Displacement (in)	
Min	-2.40	-4.47	-0.0544	
Max	2.04	4.25	0.0530	
Res	0.01	-0.04	0.0057	
Decayed Sine Parameters				
Frequency (Hz)	Accel (G)	Decay Rate	Delay	Frequency (Hz)
10.4	-0.360	0.0286	0.0000	81.5
11.4	0.483	0.0263	0.0000	88.6
12.4	-0.496	0.0241	0.0000	96.9
13.4	0.354	0.0223	0.0000	106.8
14.8	-0.300	0.0202	0.0000	115.6
16.1	0.300	0.0185	0.0000	130.1
17.8	-0.210	0.0168	0.0000	138.2
19.4	0.242	0.0154	0.0000	148.8

21.0	-0.242	0.0142	0.0000	168.3	-0.135	0.0018	0.0000
22.6	0.210	0.0132	0.0000	184.1	0.184	0.0016	0.0000
25.1	-0.122	0.0119	0.0000	195.2	-0.206	0.0015	0.0000
27.0	0.147	0.0110	0.0000	209.2	0.207	0.0014	0.0000
29.2	-0.122	0.0102	0.0000	229.8	-0.295	0.0013	0.0000
32.8	0.074	0.0091	0.0000	252.4	0.223	0.0012	0.0000
35.6	-0.119	0.0084	0.0000	277.8	-0.277	0.0011	0.0000
38.2	0.104	0.0078	0.0000	297.6	0.423	0.0010	0.0000
41.8	-0.075	0.0071	0.0000	330.2	-0.244	0.0009	0.0000
45.4	0.061	0.0066	0.0000	362.0	0.243	0.0008	0.0000
48.6	-0.119	0.0061	0.0000	384.7	-0.315	0.0008	0.0000
53.2	0.081	0.0056	0.0000	417.0	0.244	0.0007	0.0000
58.5	-0.100	0.0051	0.0000	458.8	-0.280	0.0007	0.0000
63.0	0.108	0.0047	0.0000	500.7	0.254	0.0006	0.0000
70.9	-0.116	0.0042	0.0000	548.8	-0.320	0.0005	0.0000
74.7	0.096	0.0040	0.0000	574.7	0.358	0.0005	0.0000
				3.5	0.084	0.9500	-0.0457

**Table 7: Third Realization of Decayed Sine Parameters.**

SRS Parameters				
fmin	fmax	pts/oct	Damp	SRS Type
10.00	600.00	8.00	0.03	MMAA
Acceleration History Parameters				
Sample Rate		Frame Size	Gravity Constant	Ptype
5120		8192	386.00	1
Value		Accel (G)	Velocity (in/sec)	Disp (in)
Min		-2.13	-5.18	-0.0644
Max		2.36	5.06	0.0561
Res		0.03	0.15	-0.0017
Decayed Sine Parameters				
Frequency (Hz)	Accel (G)	Decay Rate	Delay	Frequency (Hz)
10.2	-0.311	0.0292	0.0000	81.0
11.3	0.399	0.0265	0.0000	89.0
12.6	-0.675	0.0237	0.0000	97.4
13.2	0.600	0.0226	0.0000	108.1
15.1	-0.267	0.0198	0.0000	114.6
16.3	0.300	0.0183	0.0000	128.7
17.5	-0.225	0.0170	0.0000	135.9
19.2	0.212	0.0156	0.0000	152.4

20.5	-0.246	0.0145	0.0000	164.8	-0.108	0.0018	0.0000
22.7	0.228	0.0132	0.0000	182.3	0.257	0.0016	0.0000
25.3	-0.191	0.0118	0.0000	198.0	-0.167	0.0015	0.0000
27.0	0.136	0.0110	0.0000	217.9	0.191	0.0014	0.0000
29.4	-0.069	0.0101	0.0000	237.4	-0.283	0.0013	0.0000
31.6	0.093	0.0094	0.0000	251.5	0.256	0.0012	0.0000
34.9	-0.107	0.0085	0.0000	279.3	-0.154	0.0011	0.0000
38.3	0.094	0.0078	0.0000	296.6	0.298	0.0010	0.0000
41.9	-0.061	0.0071	0.0000	320.5	-0.393	0.0009	0.0000
45.0	0.114	0.0066	0.0000	362.6	0.323	0.0008	0.0000
49.0	-0.134	0.0061	0.0000	390.3	-0.359	0.0008	0.0000
55.1	0.116	0.0054	0.0000	425.0	0.347	0.0007	0.0000
57.2	-0.070	0.0052	0.0000	473.4	-0.189	0.0006	0.0000
65.1	0.130	0.0046	0.0000	508.3	0.318	0.0006	0.0000
71.1	-0.086	0.0042	0.0000	554.3	-0.262	0.0005	0.0000
77.0	0.082	0.0039	0.0000	574.7	0.281	0.0005	0.0000
				3.4	0.040	0.9500	-0.0466

**Table 8: Fourth Realization of Decayed Sine Parameters.**

SRS Parameters				
fmin	fmax	pts/oct	Damp	SRS Type
10.00	600.00	8.00	0.03	MMAA
Acceleration History Parameters				
Sample Rate	Frame Size	Gravity Constant	Ptype	
5120	8192	386.00	1	
Value	Accel (G)	Velocity (in/sec)	Disp (in)	
Min	-2.26	-4.52	-0.0492	
Max	2.28	4.23	0.0572	
Res	-0.03	-0.01	0.0041	
Decayed Sine Parameters				
Frequency (Hz)	Accel (G)	Decay Rate	Delay	Frequency (Hz)
10.6	-0.364	0.0281	0.0000	84.7
11.4	0.522	0.0261	0.0000	90.8
12.2	-0.535	0.0244	0.0000	99.8
13.4	0.353	0.0223	0.0000	106.9
15.0	-0.412	0.0198	0.0000	116.4
15.7	0.405	0.0190	0.0000	129.4
17.5	-0.236	0.0170	0.0000	135.7
18.8	0.375	0.0159	0.0000	148.3
				0.171
				0.0020
				0.0000

21.3	-0.239	0.0140	0.0000	162.0	-0.160	0.0018	0.0000
22.9	0.232	0.0130	0.0000	178.7	0.203	0.0017	0.0000
24.7	-0.157	0.0121	0.0000	199.2	-0.208	0.0015	0.0000
26.9	0.153	0.0111	0.0000	216.8	0.237	0.0014	0.0000
28.7	-0.050	0.0104	0.0000	227.4	-0.199	0.0013	0.0000
32.3	0.078	0.0092	0.0000	252.3	0.238	0.0012	0.0000
34.1	-0.103	0.0088	0.0000	276.8	-0.295	0.0011	0.0000
37.2	0.114	0.0080	0.0000	300.1	0.342	0.0010	0.0000
41.5	-0.126	0.0072	0.0000	331.1	-0.308	0.0009	0.0000
44.3	0.074	0.0067	0.0000	360.4	0.281	0.0008	0.0000
50.1	-0.114	0.0060	0.0000	386.1	-0.195	0.0008	0.0000
54.6	0.100	0.0055	0.0000	423.9	0.260	0.0007	0.0000
59.3	-0.114	0.0050	0.0000	452.1	-0.418	0.0007	0.0000
62.7	0.086	0.0048	0.0000	518.1	0.265	0.0006	0.0000
70.2	-0.096	0.0043	0.0000	541.5	-0.170	0.0006	0.0000
76.0	0.081	0.0039	0.0000	574.7	0.350	0.0005	0.0000
				3.5	0.030	0.9500	-0.0449

**Table 9: Fifth Realization of Decayed Sine Parameters.**

SRS Parameters				
fmin	fmax	pts/oct	Damp	SRS Type
10.00	600.00	8.00	0.03	MMAA
Acceleration History Parameters				
Sample Rate	Frame Size	Gravity Constant	Ptype	
5120	8192	386.00	1	
Value	Acceleration (G)	Velocity (in/sec)	Displacement (in)	
Min	-1.99	-4.91	-0.0592	
Max	2.11	5.18	0.0631	
Res	-0.04	-0.01	0.0035	
Decayed Sine Parameters				
Frequency (Hz)	Accel (G)	Decay Rate	Delay	Frequency (Hz)
10.4	-0.360	0.0287	0.0000	80.7
11.2	0.438	0.0266	0.0000	90.4
12.4	-0.508	0.0240	0.0000	100.2
13.4	0.344	0.0222	0.0000	108.1
15.1	-0.296	0.0198	0.0000	114.9
16.4	0.464	0.0182	0.0000	126.4
17.1	-0.494	0.0174	0.0000	138.4
19.3	0.224	0.0154	0.0000	155.0
				0.131
				0.0019
				0.0000

20.6	-0.197	0.0145	0.0000	161.9	-0.148	0.0018	0.0000
22.6	0.218	0.0132	0.0000	183.0	0.194	0.0016	0.0000
24.8	-0.193	0.0120	0.0000	197.3	-0.185	0.0015	0.0000
27.6	0.127	0.0108	0.0000	212.1	0.167	0.0014	0.0000
29.3	-0.125	0.0102	0.0000	229.0	-0.293	0.0013	0.0000
32.8	0.093	0.0091	0.0000	252.7	0.166	0.0012	0.0000
34.6	-0.059	0.0086	0.0000	276.2	-0.372	0.0011	0.0000
38.5	0.080	0.0078	0.0000	295.4	0.327	0.0010	0.0000
41.9	-0.124	0.0071	0.0000	330.0	-0.307	0.0009	0.0000
45.3	0.111	0.0066	0.0000	353.0	0.297	0.0008	0.0000
49.8	-0.088	0.0060	0.0000	388.0	-0.241	0.0008	0.0000
54.2	0.075	0.0055	0.0000	427.2	0.326	0.0007	0.0000
57.6	-0.086	0.0052	0.0000	457.8	-0.306	0.0007	0.0000
62.6	0.110	0.0048	0.0000	500.0	0.182	0.0006	0.0000
71.4	-0.128	0.0042	0.0000	554.3	-0.266	0.0005	0.0000
74.6	0.077	0.0040	0.0000	574.7	0.329	0.0005	0.0000
				3.5	0.171	0.9500	-0.0459

## 5.5 Derivation of Test Specifications

The initial plan of the customer was to have a reactor fuel assembly in a large truck cast with the fuel rods instrumented within the cast to measure loads during normal highway transport. The cask was to be placed upon a trailer in a horizontal position for the test. However, procuring a cask was not realistic and plans were made to use the shaker.

The only data available to derive the laboratory test specifications are from two shock and vibration tests for large shipping containers during truck transport performed in the late 70's [2,8]. Section 5.5.1 describes the derivation of the random vibration test specification. Section 5.5.2 describes the derivation of the shock test specification.

### 5.5.1 Derivation of random vibration test specification

The two documents presented the random vibration data as VIBRAN data which was the 99% level of 0 to peak amplitudes over a frequency band. Table 11 shows the VIBRAN data for the vertical axis.

**Table 10: Input to Cargo (g) – Vertical Axis.**  
99% Level of 0 to Peak Amplitude

Frequency Range	44,000 lb.	56,000 lb.
0 – 5	0.27	0.52
5 – 10	0.19	0.27
10 – 20	0.27	0.37
20 – 40	0.27	0.19
40 – 80	0.52	0.37
80 – 120	0.52	0.37
120 – 180	0.52	0.52
180 – 240	0.52	0.52
240 – 350	0.52	0.52
350 – 500	0.14	0.37
500 – 700	0.07	0.10
700 – 1000	0.07	0.10
1000 – 1400	0.05	0.10
1400 – 1900	0.05	0.10

The first step was to convert the data into an ASD. This is shown in {Eq. A.1-1} where ZPA is the zero to peak amplitude and FR is the frequency band.

$$ASD = (ZPA \div 3)^2 \div (FR(2) - FR(1)) \quad \{Eq. A.1-1\}$$

Once the ASDs were generated the straight line test specification was created. The actual weight of the fuel reactor assembly falls between 44,000 lbs. and 56,000 lbs. therefore it was decided that enveloping the two ASDs would be conservative. Figure 19 shows the recommended test specification and the underlying ASDs.

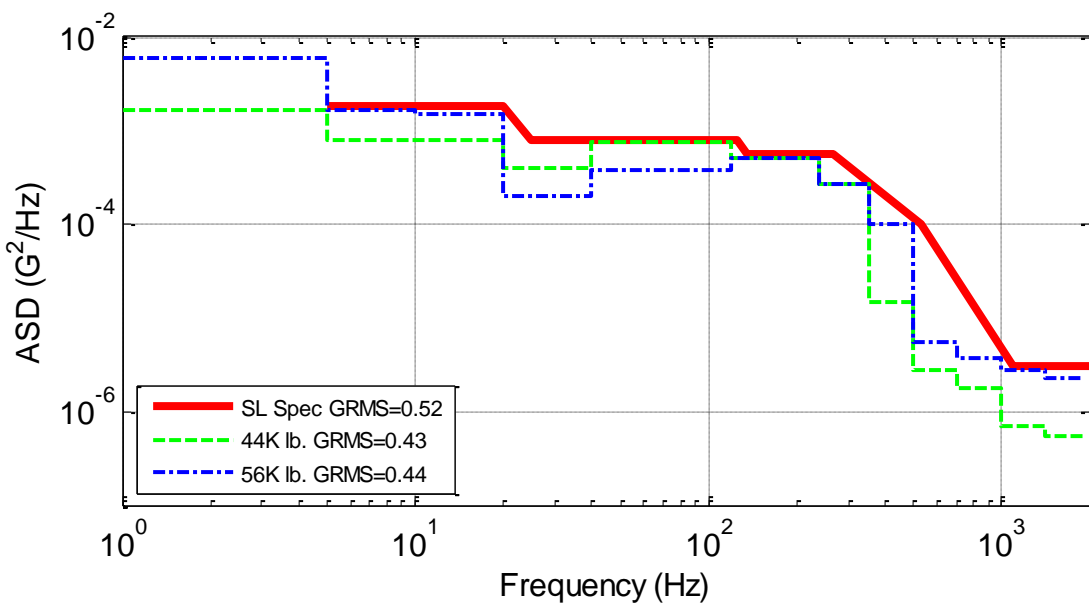


**Figure 19. Recommended test specification & underlying ASDs.**

### 5.5.2 Derivation of shock test specification

The shock response spectra were displayed as plots in References 8 and 9. Therefore before being able to use them the data had to be digitized to obtain electronic data. There were three shock responses displayed; the  $3\sigma$ , the peak of responses, and the mean of responses. Due to the quality of the plot it was decided to envelope the three shock responses when digitizing. Shock response spectra for the 44,000 lb. cargo and the 56,000 lb. cargo were obtained.

The straight line shock test specification was created to envelope the 44,000 lb. shock spectra and the 56,000 lb. shock spectra. Figure 20 shows the recommended test specification and the underlying shock response spectra.

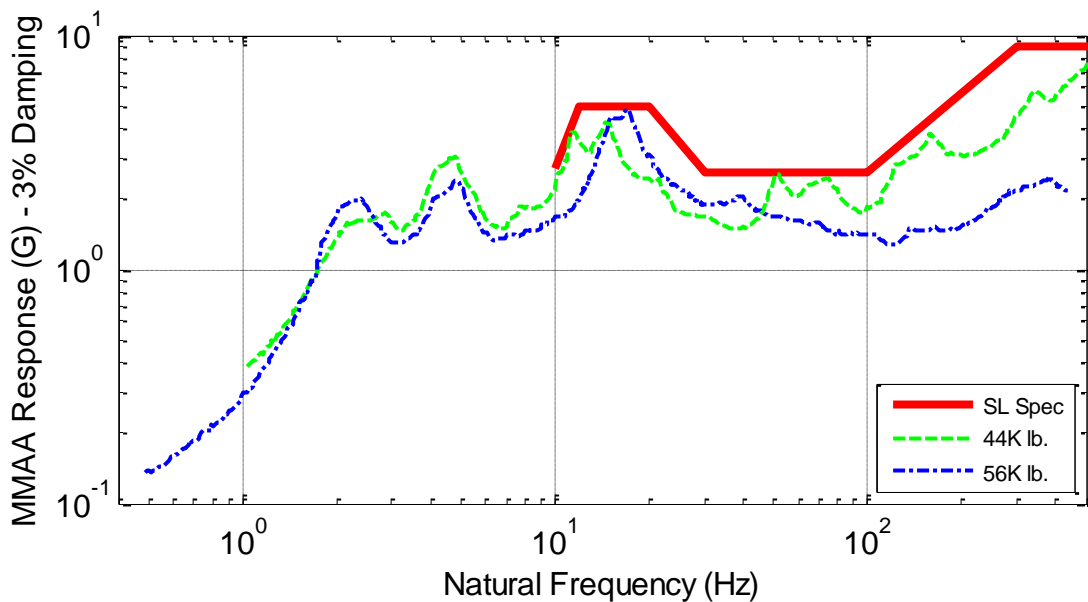


**Figure 20. Recommended test specification & underlying shock spectra.**

The next step was to obtain the five decayed sine realizations. The transients synthesized are composed of sum of decaying sinusoids which match the specified shock response spectrum. The pulse is compensated for velocity and displacement by adding a delayed decayed sinusoid.

In order to obtain five unique transients, “jitter” was added to the frequencies of the specified shock response spectrums. Figure 21 shows the range a given frequency was allowed to vary. The frequencies were allowed to vary a maximum of 80% from the midpoint (i.e.,  $F_1$ ) in the positive and negative direction (i.e.,  $F_{1\text{low}}$  and  $F_{1\text{high}}$ ). A uniform random distribution was used to determine the amount each frequency varied within its specified range.

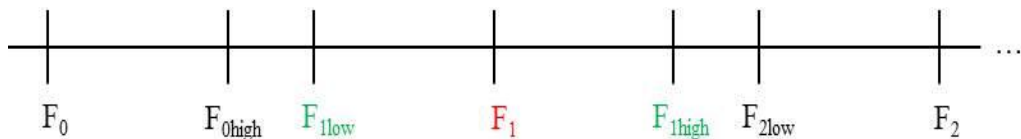


**Figure 21. Range of frequencies.**

Figures 22 through 26 show the acceleration history, velocity, displacement, and the decayed sine shock spectra versus the reference shock spectra for the five realizations.

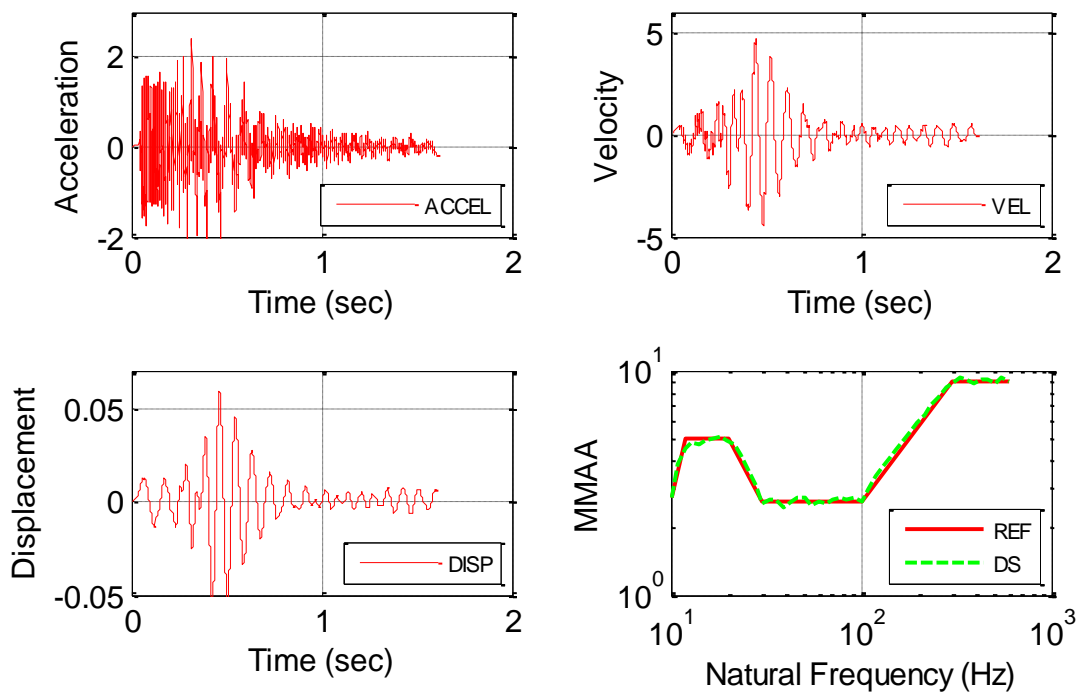


**Figure 22. Decayed sine initial realization.**

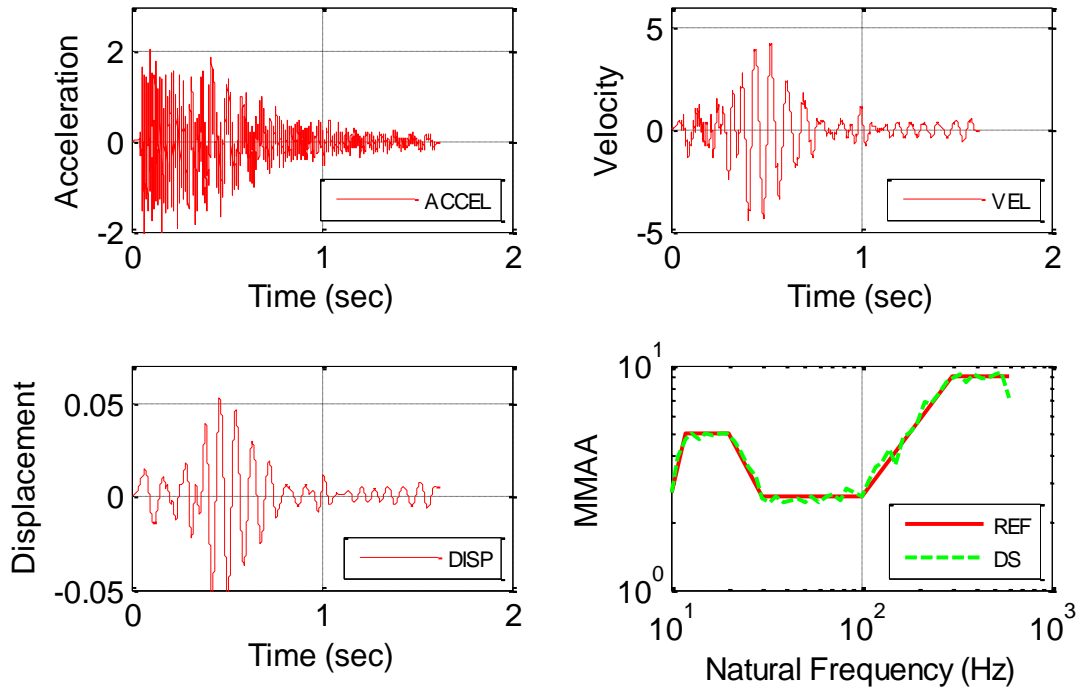


**Figure 23. Decayed sine second realization.**

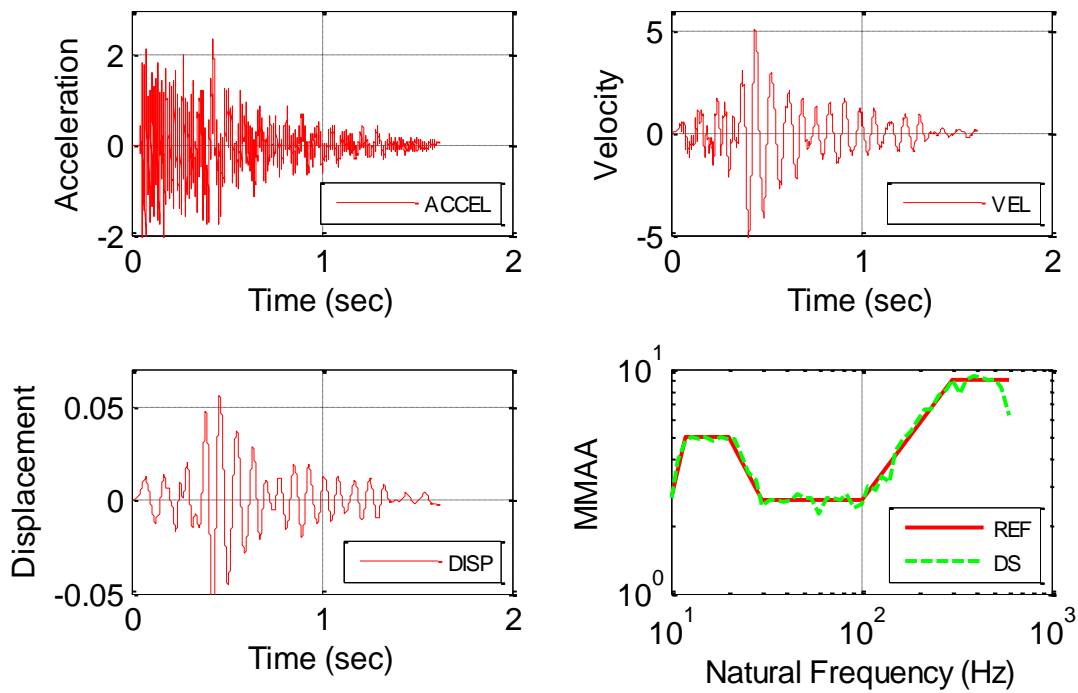


**Figure 24. Decayed sine third realization.**

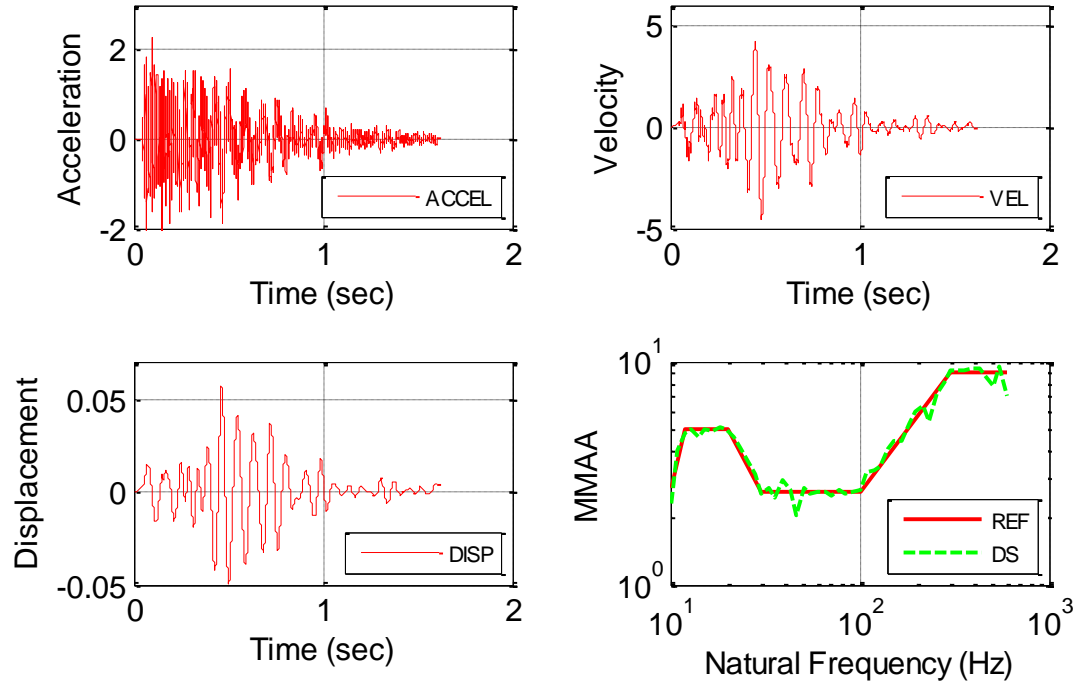


**Figure 25. Decayed sine fourth realization.**

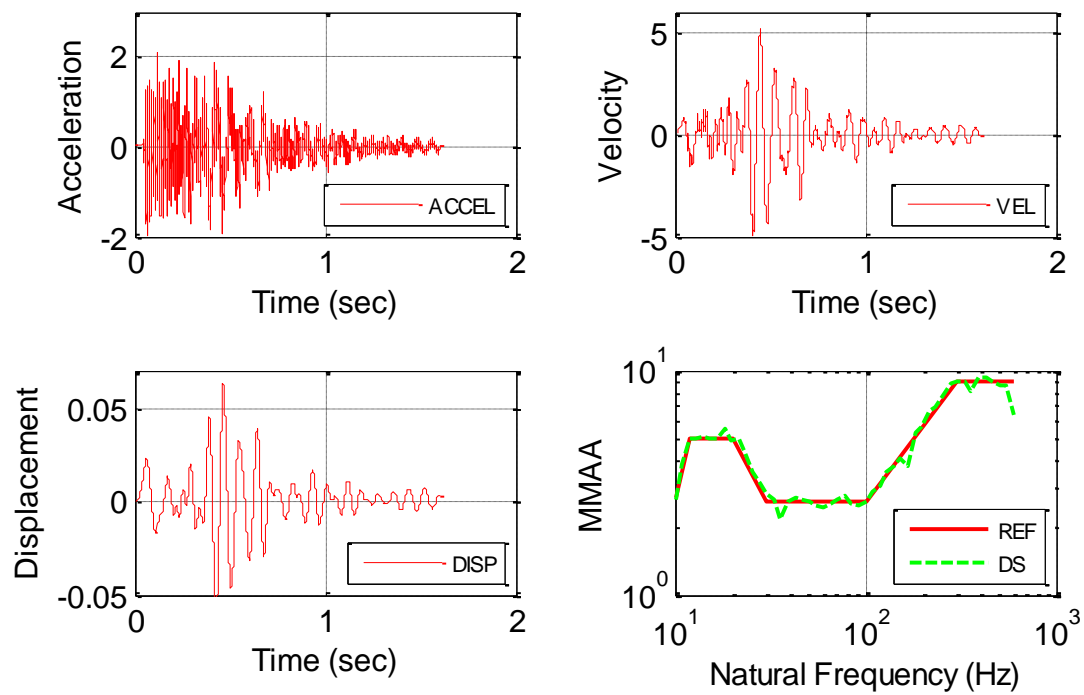


Figure 26. Decayed sine fifth realization.



## 6 PREVIOUS OVER-THE-ROAD TEST PROGRAMS

Note: The following describes testing where the instrumentation for measuring loads was on the transport package, not on the contents. For the current test proposal, some instruments may be placed on the external package, but the primary objective is to place instruments on the package internals – the basket, fuel assembly and fuel cladding.

### 6.1 “Over-the-road testing of radioactive materials packagings”<sup>11</sup>

Sandia National Laboratories had a program to characterize the normal environments encountered during the transport of radioactive materials. This effort consisted of obtaining experimental data from the external surface of the transport package and the transport bed during both road simulator and over-the-road tests and of analyzing the data to obtain numerical models to simulate those environments.

Test activities included 1) over-the-road testing, 2) hard braking, and 3) hard turning. Package response during any given test is specific to that package and trailer. The trailer and packaging were subjected to nine separate events to determine both the acceleration and tiedown loads experienced during normal transport. Five types of roads were used: 1) smooth asphalt primary; 2) rough asphalt primary; 3) rough concrete primary; 4) rough asphalt secondary; and 5) spalled asphalt secondary. The roads provided a vibrational environment for the packaging. To subject the packaging to a shock environment, a railroad crossing and bridge approach were selected. Finally, to determine the package’s response to maneuvering, a hard turn and a stop were executed. The speed driven for each event was the lesser of either the posted legal speed limit or the fastest speed consistent with safe operation of the tractor.

For each event, approximately 15 seconds of data were recorded. This provides 15,000 samples per data channel. This was adequate time to capture shock events, such as the rail crossing plus damping back to the random vibration state. For the random vibration events, such as smooth asphalt roads, it provided a representative sampling.

---

<sup>11</sup> R.E. Glass & K.W. Gwinn, “Over-the-Road Tests of Nuclear Materials Package Response to Normal Environments,” SAND91-0079, Sandia National Laboratories, December 1991.

### 6.1.1 Instrumentation

The primary role of the instrumentation was to obtain the acceleration at various points on the trailer and package. A total of nine instruments were used in each test. A *triaxial accelerometer* was placed on the package's center top to measure the package response along each axis. The stiffness of the package made this measurement representative of the entire package. At the same longitudinal location, an accelerometer measured the trailer's vertical acceleration. The maximum accelerations on a trailer were obtained at its front and rear. Longitudinal and vertical accelerometers were placed on the trailer bed over the rear axle, and a vertical accelerometer placed on the trailer over the kingpin. The combination of vertical accelerometer sat these three trailer locations allowed the bounce, pitch, and bending modes to be detected. The longitudinal and transverse accelerometers were useful in detecting the effects of braking and turning.

The response of the tiedown systems was determined from *load cells* in the links between attachment points and with *strain gages* mounted on the cradle straps.

### 6.1.2 Test results

A large volume of information is acquired from tests of this type, the actual time histories and resultant power spectral densities for each transducer. The time histories provide the mean-to-peak response at the different locations. From these time histories, the power spectral densities are generated. The power spectral densities transform the time history data into the frequency domain to relate how the response energy varies as a function of frequency. From this data, it is determined which modes of vibration are contributing to the overall response, and the root-mean square response can also be calculated. The mean squared response is the area under the power spectral densities response curve. The root mean square is the square root of this value. The root mean square relates the probability of a certain level of response occurring, and is equal to the standard deviation since the mean is zero. Three times the root mean square will envelope 99.9 percent of all expected responses. The transform magnitude plots are discrete Fourier transforms of the measured response and provide the frequency content of the transient record.

## 6.2 “Test specification for TRUPACT-I vibration assessment”<sup>12</sup>

This specification establishes the requirements for the vibration testing of a production unit Transuranic Package Transporter (TRUPACT-I). The in-service tests determined the normal transport shock and vibration environment. The purpose of the in-service tests was to determine the vibration and shock

---

<sup>12</sup> K.W. Gwinn, R.E. Glass, and L.E. Romesberg, “Test Specification for TRUPACT-I Vibration Assessment,” SAND85-1369, Sandia National Laboratories, February 1986

environments encountered by the TRUPACT-I during normal service conditions. The tests will consist of monitoring vibration and shock levels of an instrumented TRUPACT-I under normal operating conditions. The monitoring was accomplished using accelerometers located at the attachment points of the trailer.

A digital recorder was mounted on the trailer during the tests. Specific shock events of interest included railroad grade crossings, bridge approaches, potholes, raised bumps, and diagonal bumps. Vibration test events included normal primary asphaltic and concrete pavements, rough primary asphaltic and concrete surfaces, and rough secondary surfaces at a range of operating speeds. These shock and vibration events include most of the normal operating environments that would be experienced by a transport package.

### 6.2.1 Instrumentation

Six uniaxial piezoresistive accelerometers were attached. An accelerometer was used at each corner to measure the vertical accelerations, and the remaining two were used at the forward castings to measure longitudinal accelerations. The wiring was constrained to prevent straining during the tests. The recorder was mounted on shock isolating material to prevent recording errors and damage. All accelerometers were calibrated for a range of  $\pm 20$  g.

All road simulator and over-the-road tests were instrumented to determine the loads acting on the packages. Accelerometers were used to obtain vertical, longitudinal, and transverse accelerations. Load cells were used to directly monitor tie-down loads. Strain gages were used so that tie-down loads could be calculated.

A sample of the Normal transport transducer data is given in the table below.

Peak Response for Road Surface Events

Transducer <u>Location</u>	Event				
	Smooth <u>Asphalt</u>	Rough <u>Asphalt</u>	Rough <u>Concrete</u>	Secondary <u>Asphalt</u>	Spalled <u>Asphalt</u>
Cask top					
Transverse (g)	0.17	0.21	0.12	0.13	0.22
Vertical (g)	0.23	0.32	0.20	0.35	0.58
Longitudinal (g)	0.17	0.38	0.22	0.65	0.88
Trailer, mid					
Vertical (g)	0.21	0.37	0.07	0.07	0.08
Trailer, rear					
Vertical (g)	0.46	1.4	0.95	1.68	3.1
Longitudinal (g)	0.14	0.37	0.22	0.43	0.85
Trailer, front					
Vertical (g)	0.73	1.7	1.3	2.7	4.5
Front tiedown (lb) (N)	430 1900	580 2600	220 980	350 1600	460 2000
Rear tiedown (lb) (N)	220 980	360 1600	150 670	280 1200	650 2900

Both peak and root mean square values that the cask response was less than 1 g.

The representative time history is shown in Figure 27 (Figure 9a) - the measured vertical acceleration of the rear trailer bed in response to the spalled asphalt event. This figure shows a fairly severe vibrational environment, with two large transient events occurring 3 and 9 seconds into the run. Figure 27 (Figure 9b) shows the same response in the frequency domain in power spectral density form. The response is shown as  $\text{g}^2/\text{Hz}$  on a log-log plot. The larger response at 1.5 Hz is due to the first bounce mode of the tractor/trailer combination. This bounce mode of the vehicle is caused by the structure bouncing in unison on the suspension system of the trailer. The next feature seen is the response at 4 Hz. This is the frequency of the vehicle's first pitching mode. This is caused by the kingpin/rear tractor suspension deflecting down while the trailer rear suspension and tractor front suspension deflect up. The high-frequency modes, from 10 to 20 Hz, are combinations of the trailer bending with the tractor pitching and bending. The first bending mode occurs at approximately 11 Hz.

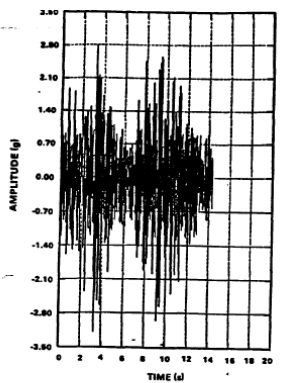


Figure 9a. Representative Time History

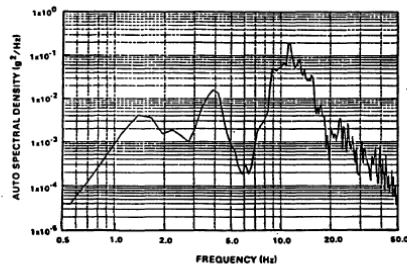


Figure 9b. Representative PSD

**Figure 27. Representative normal transport load data.**

## 7 KEY BACKGROUND INFORMATION

### 7.1 Source of Vibration and Shock Data for Test

EDB #A2164  
EXTRACTED FROM

SAND77-1110  
Unlimited Release  
Printed September 1977

NRC-12

#### SHOCK AND VIBRATION ENVIRONMENTS FOR LARGE SHIPPING CONTAINER DURING TRUCK TRANSPORT (PART I)

Cliff F. Magnuson  
Applied Mechanics Division K 1282  
Sandia Laboratories, Albuquerque, NM 87115

[3]

#### ABSTRACT

The purpose of this study was to obtain vibration and shock data during truck shipment of heavy cargo. Currently available data were taken on trucks bearing lighter loads than the loads of current interest. In addition, the new data are expected to be useful in the determination of any trends of vibration and shock environments with increased cargo weight. These new data were obtained on a "piggyback" basis during truck transport of 195 700 N (44,000 lb) cargo which consisted of a spent fuel container and its supporting structure from Mercury, Nevada, to Albuquerque, New Mexico. The routes traveled were US 95 from Mercury, Nevada, to Las Vegas, Nevada; US 93 from Las Vegas to Kingman, Arizona; and I-40/US 66 from Kingman to Albuquerque, New Mexico. Speeds varied from very slow during hill climbs to 101 km/hr (63 mph). A comparison of these data with a collectively reduced set of data for cargo weights varying from no-load to 133 400 N (30,000 lb) showed that the zero to peak amplitude levels of vibration were significantly lower for frequencies less than 40 Hz in the vertical axis and that there was a reduction in the vibration amplitude levels in all axes for frequencies greater than 500 Hz. The shock response amplitude was less severe for the entire frequency spectrum in the vertical axis, but it was not significantly different in the other axes. Data measurements were made on a truck shipment of a 249 100 N (56,000 lb) container over the same routes as were used for the shipment discussed in this report. These data will be presented in a subsequent report along with any additional data trends that result from studies of trucks carrying increased cargo weight.

EDB #A2165  
EXTRACTED FROM

NUREG/CR-0128  
SAND78-0337  
RT

SHOCK AND VIBRATION ENVIRONMENTS  
FOR A LARGE SHIPPING CONTAINER  
DURING TRUCK TRANSPORT (PART II)

Clifford F. Magnuson

Manuscript Submitted: February 13, 1978  
Date Published: May 1978

[2]

Manuscript Submitted: February 13, 1978  
Date Published: May 1978

Sandia Laboratories  
Albuquerque, New Mexico 87185  
operated by  
Sandia Corporation  
for the  
U.S. Department of Energy

Prepared for  
Division of Safeguards, Fuel Cycle and Environmental Research  
Office of Nuclear Regulatory Research  
U.S. Nuclear Regulatory Commission  
Washington, DC 20555  
Under Interagency Agreement DOE 40-550-75  
NRC FIN No. A-1049-6

#### ABSTRACT

The purpose of this study was to obtain vibration and shock data during truck shipment of heavy cargo. These data were for use in determining any trends of vibration and shock environments with increased cargo weight. The new data were obtained on a "piggyback" basis during truck transport of 249 100N (56,000-pound) cargo which consisted of a spent fuel container and its supporting structure. The truck was driven from Mercury, Nevada, to Albuquerque, New Mexico. The routes traveled were US 95 from Mercury, Nevada, to Las Vegas, Nevada; US 93 from Las Vegas to Kingman, Arizona; and I-40/US 66 from Kingman to Albuquerque, New Mexico. Speeds varied from very slow to 88 km/hr (55 mph). A comparison of data from similar experiments with cargo weights varying from no-load to this load shows that the zero-to-peak acceleration amplitude levels of vibration are highest when trucks carry relatively light loads. This is true for the longitudinal and vertical axes of the vehicles in most frequency bands and for the transverse axis above 700 Hz. The shock response acceleration amplitudes for heavier cargo weights were less severe above 3 Hz in the vertical axis and higher between 8 and 20 Hz in the transverse axis. The highest acceleration amplitude of shock response in the longitudinal axis below about 20 Hz was produced in a trailer having a spring suspension system and carrying the 249 100N (56,000 pounds) load.

## 7.2 Related Documents

- 7.2.1 “Approach for the Use of Acceleration Values for Packages of Radioactive Material under Routine Conditions of Transport,” Andreas Apel, Viktor Ballheimer, Christian Kuschke, Sven Schubert, Frank Wille, Proceedings of the 9th International Conference on the Radioactive Materials Transport and Storage, May 2012, London.**
- 7.2.2 “Transportation Activities for BWR Fuels at NFI,” S. Uchikawa, H. Kishita, H. Ide, M. Owaki, K. Ohira, Nuclear Fuel Industries, LTD., Proceedings of Global 2009, Paris, September 2009.**

Nuclear Fuel Industries, LTD. (NFI) supplies fuel assemblies for both PWR and BWR nuclear power plants in Japan. We also are involved in the field of nuclear fuel recycling and we manage transportation of the fuel assemblies from our fabrication facilities to the Japanese nuclear power plants. The NT-XII transportation container was developed by NFI for fresh BWR fuel assemblies. The foremost design priorities for this NT-XII container were transportation efficiency and ensuring fuel integrity during transportation. In addition to the design of new containers, we also develop improved packaging methods. Recently, NFI performed tests intended to determine the need for packing separators to mitigate vibration induced wear during fuel transportation. The transportation test was performed using dummy fuel assemblies and included wear data analysis and post-disassembly inspections. The fretting wear on the surface of fuel rods and spacer spring force degradation were measured. Results from these evaluations indicated that there was no significant difference in the vibration induced wear on the fuel between the packaging methods with and without packing separators. As a result, NFI developed a new packaging method which improves the packing and unpacking efficiency for fuel rods transported from the fuel fabrication facility to another facility. This method also enables the fuel assembly container to be used without the need for modifications to the design of container.

- 7.2.3 “High Burn-up Used Nuclear Fuel Vibration Integrity Study - Out-of-Cell Fatigue Testing Development,”, Jy-An John Wang, Hong Wang, Yong Yan, Rob Howard, Bruce Bevard, January 2011, Oak Ridge National Laboratory.**

For high burn-up spent nuclear fuel (SNF), it is expected that the used nuclear fuel cladding will have a high population of microcracks and hydrides, including macro-hydrides and micro-hydrides. This will reduce the stress intensity required to advance the crack growth. The linking of these microcracks during vibration loading may also reduce the fatigue threshold/incubation period, accelerating fatigue failure. In addition to the cladding damage, the microstructure of comprising fuel pellets and the interfaces of fuel rod have changed dramatically after high burn-up in the reactor. These changes may have a direct impact on the structural integrity and vibration response of SNF rods in transportation.

As a result, vibration has been included as a mandatory test condition for the structural evaluation of package that is used in transporting spent nuclear fuel by US NRC (Nuclear Regulatory Commission) in 10 CFR §71.71. Currently, no testing system is available to test the spent nuclear fuel and evaluate the

performance of fuel rods during transportation. It is the aim of this research project to develop a system that can appropriately test the response of high burn-up SNF rods under simulated loading conditions.

The SNF rods lie horizontally in a transportation cask and are supported by the spacers within fuel rod assembly. These rods are subjected to oscillatory bending due to inertia effects. This oscillatory bending is the major vibrational load of SNF rods as mentioned in 10 CFR §71.71 and its effect on integrity of the SNF rods needs to be captured by the designed testing system. The SNF rods include various burn-induced damage (pores and micro cracks), oxide and hydride layers, residual stresses, altered interfaces, and trapped fission products. They are highly radioactive. These factors complicate conventional cyclic bending testing and need to be considered in the development of the test apparatus.

An extensive literature survey revealed that a variety of bending fatigue testing methods have been developed including cantilever beam bending, three-point/ four-point bending, and pure bending, as well as their variants considering environmental factors, particularly temperature. Bending fatigue testing approaches also account for rotation based on if the rotation is introduced to carry out the reverse bending. However, the vibration of SNF rods during transportation usually involves deflection instead of rotation, and at the same time, the dominant frequencies involved with these dynamical events are generally less than 100 Hz. Therefore, the non-rotating reverse bending that can be accomplished by a universal material testing machine or its equivalent is the focus of this report.

Currently, bending cyclic fatigue test methods are used in testing and characterizing various engineering materials and their components including concrete, composites, ceramics, metal alloys, metallic glasses, and so forth. Available approaches include unipolar mode without reversal, and bipolar mode with full reversal. Mechanical support/ contact techniques to enable the designed beam bending boundary condition have been advanced significantly. But most of the bending fatigue tests are application-based. The following conclusions can be drawn from the literature survey:

- Among the bending fatigue testing methods reviewed, four-point bending fatigue testing is a mature experimental technology in testing materials and components that have a limited deformation before failure. Demonstration of this technology includes asphalt beam and the development of a self-aligning test rig.
- The above-mentioned techniques are mainly used in fatigue tests without bending reversal.
- A variety of supports were developed in bending fatigue testing including rotary joints, slide connection, and flexures. They either deviate from a true fixed boundary condition or involve contact damage.
- Four-point/ three-point bending and cantilever bending all suffer from an inherent drawback related to shear in the beam that has a non-uniform bending moment. This has a significant impact on testing materials that are sensitive to the shear.
- Pure bending fatigue has been used for high strain fatigue testing of metal alloys and composites. The implementation of the pure bending concept is application-based and has been partially successful.
- Environmental chambers and/or high temperature furnaces are currently incorporated into some critical bending fatigue tests. Specimen setup is usually manual and therefore insufficient for testing materials that are radioactive.

A bending fatigue testing system has been proposed and developed in this report to test high burn-up SNF rods. Pure bending is adopted as the bending mode of testing system. The use of a pure bending method in which a uniform bending moment is exerted on the gage length of the specimen should eliminate the effect of shear. The shear can eventually lead to a failure mode that is not relevant to the fatigue failure of concern. Two implementation concepts are presented with emphasis on bending fatigue testing on rod specimens in reversal bending.

The first implementation relates to an approach in which the specimen is setup horizontally. Some important features are

- It is based on the principle of four-point bending, but the gage length of the specimen is arranged in the part of beam that has a uniform bending moment. The driving mechanisms in conventional four-point testing can be applied to the horizontal setup.
- Rigid sleeves are introduced to reinforce the extensional parts of specimen and to convert external force couples into the bending moments.
- It accommodates various connections to loading contacts and supports. These connection options enable the free rotation and horizontal translation of beam boundary condition as required by reversal bending and can best fit into the different applications.

The second implementation concerns the design with the specimen setup vertically. The main features are

- Bending moments are applied through two horizontal rigid arms of a U-frame structure. The arms are equipped with two co-axial holes that accommodate the test specimen.
- Roller bearings or equivalent bearing sets in the arms of the U-frame allow the release of any axial load related to the loading of specimen and, at the same time, transfer the bending moments from the rigid arms to the specimen.
- The initial setup of a test specimen can be accomplished by a simple insertion of the specimen into the holes. This is advantageous for a hot-cell environment because most of the operations can be adapted for this testing environment.
- The U-frame has fewer components, which would result in a test system with enhanced reliability and controllability.
- Versatile designs in the vertical member and joints or corners of the U-frame provide options for different experimental studies.

Overall, the proposed test system has the following unique characteristics in comparison with the conventional bending fatigue testing methods:

- Bending fatigue testing is carried out under pure bending, eliminating the effect of the shearing force encountered in three-point bend and four-point bend testing.
- The bending fatigue is conducted in a reversal mode and the system approaches the loading condition of used nuclear fuel in transportation more closely than repeated three-point or four-point bending testing.
- Compliant layers are incorporated into the rigid sleeve to control the effect of contact on the fatigue failure in the specimen retaining areas.

- The system can test and examine specimens in very hostile or radioactive environments.

#### **7.2.4 Other documents related to this work include**

- 7.2.4.1 “Mechanical Behaviour of High Burn-Up SNF under Normal and Accident Transport Conditions – Present Approaches and Perspectives,” Fanke Wille, Viktor Ballheimer, Annette Rolle, Berhard Droste, Bundesanstalt für Materialforschung und –prüfung (BAM).**
- 7.2.4.2 “CANDU Irradiated Fuel Transportation: The Shock and Vibration Program,” B.P. Dalziel, M.A. Elbestawi, J.W. Forest, Ontario Hydro, Research Agreement Report No. 2715/R1/CF.**
- 7.2.4.3 “Transportation Shock and Vibration Descriptions for Package Designers,” J.T. Foley, Sandia National Laboratories Report SC-M-72 0076, July 1972.**
- 7.2.4.4 “Design Basis for Resistance to Shock and Vibration,” SAND89-0937C, R.E. Glass, K.W. Gwinn, Sandia National Laboratories.**
- 7.2.4.5 “Over-the-Road Testing of Radioactive Materials Packaging” SAND91-2709C, R.E. Glass and K.W. Gwinn, Sandia National Laboratories.**

## 8 REFERENCES

- [1] "A Method for Determining the Spent-Fuel Contribution to Transport Cask Containment Requirements," Thomas L. Sanders, Kevin D. Seager, Sandia National Laboratories; Yusef R. Rashid, Peter R. Barrett, ANATECH Research Corporation; Anthony P. Malinauskas, Oak Ridge National Laboratory; Robert E. Einziger, Pacific Northwest Laboratory; Hans Jordan, EG&G Rocky Flats Inc.; Thomas A. Duffey, Stephen H. Sutherland, APTEK Incorporated; Philip C. Reardon, GRAM Incorporated, SAND90-2406, November 1992.
- [2] "Shock and Vibration Environments for a Large Shipping Container during Truck Transport (Part II)," Clifford F. Magnuson, Extracted from NUREG/CR-0128, SAND78-0337, Sandia National Laboratories, May 1978.
- [3] "Shock and Vibration Environments for a Large Shipping Container during Truck Transport (Part I), Clifford F. Magnuson, SAND77-1110, Sandia National Laboratories, September 1977.
- [4] "Shock and Vibration Environments Encountered During Normal Rail Transportation of Highway Cargo," Magnuson, C.F., Sandia National Laboratories, Albuquerque, NM, SAND82-0819, August 1982.
- [5] "Shock Environments for Large Transport Containers during Rail-Coupling Operations," Magnuson, C.F., Sandia National Laboratories, Albuquerque, NM, SAND79-2168, NUREG/CR-1277, June 1980.
- [6] US Code of Federal Regulations, Title 10-Energy, Part 71 (10 CFR 71), "Packaging and Transportation of Radioactive Material."
- [7] "Standard Review Plan for Transportation Packages for Radioactive Material," NUREG-1609, US Nuclear Regulatory Commission, March 1999.
- [8] "Dynamic Analysis to Establish Normal Shock and Vibration of Radioactive Material Shipping Packages, Volumes 1-3," S.R. Fields, NUREG/CR-2146, US Nuclear Regulatory Commission, 1983.